Distribution Agreement

In presenting this thesis or dissertation as a partial fulfillment of the requirements for an advanced degree from Emory University, I hereby grant to Emory University and its agents the non-exclusive license to archive, make accessible, and display my thesis or dissertation in whole or in part in all forms of media, now or hereafter known, including display on the world wide web. I understand that I may select some access restrictions as part of the online submission of this thesis or dissertation. I retain all ownership rights to the copyright of the thesis or dissertation. I also retain the right to use in future works (such as articles or books) all or part of this thesis or dissertation.

Signature

_____ _____

Andrew D. Steele **Date**

Natural and Synthetic Compounds as Tools to Overcome Antibiotic Resistance

By

Andrew D. Steele

Doctor of Philosophy

Chemistry

_____

William M. Wuest, PhD

Advisor

_____

Huw M. L. Davies, PhD

Committee Member

_____

Dennis C. Liotta, PhD

Committee Member

Accepted:

_____

Lisa A. Tedesco, PhD

Dean of the James T. Laney School of Graduate Studies

_____

Date

Natural and Synthetic Compounds as Tools to Overcome Antibiotic Resistance

By

Andrew D. Steele

B.S., Messiah College, 2012

Advisor: William M. Wuest, PhD

An abstract of

A dissertation submitted to the Faculty of the James T. Laney of Graduate Studies of Emory University in partial fulfillment of the requirements for the degree of Doctor of Philosophy in Chemistry

2018

Abstract

Natural and Synthetic Compounds as Tools to Overcome Antibiotic Resistance

By: Andrew D. Steele

Antibiotic resistance is a pressing challenge that chemists have invested significant resources on. Current antibiotic development has slowed in recent years due to fewer compounds that operate via new mechanisms of action. To this end, we have looked to natural products with unknown, presumably new, mechanisms of action, as well as known scaffolds with newly discovered antibiotic activity to solve this problem. In each of these projects, diverted total synthesis was utilized to access not only the original target compounds, but also analogs in a highly efficient manner. Specifically, promysalin, a Gram-negative selective antibiotic, was synthesized for the first time, and its structure was elucidated. From there, a series of analogs was synthesized to determine preliminary structure-activity data. Utilizing these findings, an analog suitable for affinity-based protein profiling was synthesized and subsequent experiments allowed the discovery of the protein target of promysalin. Further experiments shed light on promysalin's specificity as well as structural mode of action. CD437 and nTZDpa were known synthetic compounds that received new attention in the laboratory of a collaborator (Mylonakis lab, Brown University) when they were shown to be membrane-disrupting compounds with potent activity against pathogenic Gram-positive bacteria. Through our synthetic studies, we optimized both the potency and toxicity of each compound. Finally, baulamycin A and B were discovered in a high-throughput screen effort to find new inhibitors of siderophore biosynthesis in pathogenic bacteria. However, their activity profile seemed to indicate multiple mechanisms were at play. The originally proposed structure was shown to be incorrect by others working on these molecules. We were the second laboratory to synthesize the corrected structures of baulamycins A and B, and the first to leverage baulamycin analogs in whole-cell assays. These assays allowed us to elucidate the baulamycins' alternative mechanism of action, which gratifyingly complemented the biological data previously disclosed. These projects attest to the power of total synthesis in new antibiotic discovery and development, and future work could open the door for new therapeutics and tools for further biological discoveries.

Natural and Synthetic Compounds as Tools to Overcome Antibiotic Resistance

By

Andrew D. Steele

B.S., Messiah College, 2012

Advisor: William M. Wuest, PhD

A dissertation submitted to the Faculty of the James T. Laney of Graduate Studies of Emory University in partial fulfillment of the requirements for the degree of Doctor of Philosophy in Chemistry

2018

Acknowledgements

I am extremely thankful to my family for constant love and support throughout the process of earning my PhD. Their support before and during my schooling has been essential for my success. My advisor, William Wuest, has been an exceptional mentor for both my personal and professional growth. In addition, I have had the privilege of working with many mentors both in the Wuest laboratory and neighboring labs, especially at Temple University. There are too many helpful conversations that helped me save a great deal of time and effort learning from senior students and post-doctoral researchers, especially in my first two years when I was very inexperienced. As I grew more experienced, I assumed a leadership role in our group.

As I became more of a leader in the group, I was given the opportunity to work with a great deal of talented graduate students and undergraduates, and later, post-doctoral researchers. Every attempt has been made to give credit where credit is due in terms of who performed what chemistry, and where intellectual contributions were made. However, especially in the case of the promysalin synthesis and analog campaign, the lines of the division of work become blurry. Colleen Keohane, Kyle Knouse, and myself were a highly effective and efficient team, and would very often hand material off to one another. Hence, it is sometimes impossible to say that one person alone synthesized an analog, as it was common for one person to do the same reaction on two different analogs, then hand it off to someone else for the subsequent step. Alternatively, one member of the team would commonly synthesize the same compound that someone else had made once before, for material throughput and/or for characterization data to be collected.

I also interacted a great deal and worked with two more undergraduate researchers: Sierra Williams and Isabelle Sinitsa. Sierra worked with me for one semester, and synthesized one promysalin analog, which I made one additional time to gather all the required characterization data. Isabelle began working with me with no prior organic chemistry experience, where she started off by synthesizing several batches of nTZDpa. From there, she synthesized one analog, which I made one additional time for characterization data.

On the baulamycin project, I worked closely with two post-doctoral researchers: Dr. Young Eun Lee and Dr. Guillaume Ernouf. The former was a researcher at Temple University and optimized the originally proposed baulamycin left half structure fragment herself. I repeated her optimized reaction procedure for material throughput and to gather characterization data. The latter was a researcher at Emory who helped me optimize reactions *en route* to the corrected structure.

All attempts to give sole credit where it was due has been made, however there are cases where a clear division cannot be made. These interactions give credence to the notion that science has and always will be a highly collaborative team effort, and the work presented in this thesis is certainly no exception.

Table of Contents

List of Illustrations

Figures

Tables

Schemes

List of Abbreviations

Table of Contents

Chapter 1: Introduction 1

1.1 The Discovery and Rise of Modern Antibiotics 1

1.2 Antibiotic Resistance 2

1.2.1 Introduction 2

1.2.2 Drug-Inactivating Enzymes 3

1.2.3 Modification of Drug Target 5

1.2.4 Prevention of Access to Target 7

1.3 Chemical Approaches to Antibiotic Resistance 8

1.3.1 Semisynthesis 8

1.3.2 Diverted Total Synthesis 11

1.3.3 Conclusions 13

1.4 References 13

Chapter 2: Synthesis, Structure Elucidation, and Target Identification of the Gram-negative Selective Antibiotic Promysalin 16

2.1 Promysalin background 16

2.1.1 Gram-negative and *Pseudomonas* Clinical Infections 16

2.1.2 Narrow-spectrum Therapeutics 17

2.1.3 Promysalin Background 19

2.2 Synthesis of Promysalin 21

2.2.1 Retrosynthesis 21

2.2.2 Synthesis of Promysalin Acid Fragment 22

2.2.3 Synthesis of alcohol fragment diastereomers 23
2.2.4 Completion of Promysalin Synthesis 24
2.3 Structure Elucidation of Promysalin 25
2.3.1 NMR Analysis of Promysalin Diastereomers 25
2.3.2 Biological Testing of Promysalin Diastereomers **(–)-2.1a** – **(–)-2.1d** 27
2.3.3 Observation of Novel Promysalin-Induced Phenotypes 30
2.3.4 Conclusions 30
2.4 Synthesis of Promysalin Analogs 32
2.4.1 Promysalin Analog Design 32
2.4.2 Promysalin Proline Analog Synthesis 34
2.4.3 Promysalin Salicylate Analog Synthesis 38
2.4.4 Promysalin Side Chain Analog Synthesis 43
2.4.5 Synthesis of "Pro-drug" Analogs 47
2.5 Promysalin Analog Results and Conclusions 47
2.5.1 Promysalin Analog Inhibitory Data 47
2.5.2 CAS Assay and Iron-binding 49
2.5.3 Conclusions 51
2.6 Synthesis of Promysalin Photoprobe and Affinity-based Protein Profiling 51
2.6.1 Affinity-based Protein Profiling in Natural Product Target Identification 51
2.6.2 Promysalin Photoaffinity Probe Design and Synthesis 54
2.6.3 Biological Evaluation of Promysalin Photoprobe and Proteomic Experiments 55
2.6.4 Succinate Dehydrogenase and its Role in *Pseudomonas* Metabolism 57
2.7 References 60
Chapter 3: Diverted Total Synthesis of CD437 and nTZDpa Analogs – Effective Membrane Disrupting Agents Against Gram-positive Pathogens 64
3.1 Introduction and Background 64
3.1.1 *Staphylococcus aureus* – Resistance and Clinical Relevance 64
3.1.2 Persister Cells 65
3.2 The Discovery of New Antibiotic Activity of CD437 and nTZDpa 67
3.2.1 *C. elegans*-MRSA High-throughput Screen 67
3.2.2 Biological Activity of CD437 and nTZDpa 68
3.2.3 CD437 Simulations and Proposed Mechanism of Action 70
3.3 Diverted total synthesis of CD437 and analogs 71

3.3.1 First-generation CD437 analogs from adapalene 71
3.3.2 Retrosynthetic Analysis and CD437 Analog Design 73
3.3.3 Synthesis of Boronic Acid Building Blocks 73
3.3.4 Synthesis of Unsubstituted Naphthalene CD437 Analogs 74
3.3.5 Unsuccessful attempts at accessing oxidized naphthalene analogs of CD437 75
3.3.6 Synthesis of oxidized naphthalene analogs of CD437 78
3.3.7 SAR data of CD437 analogs 80
3.3.8 Conclusions 82
3.4 Synthetic and Biological Studies of nTZDpa 82
3.4.1 Synthetic Route Design and Prior Art 82
3.4.2 Optimized Synthesis of nTZDpa and Analogs 83
3.4.2 SAR data of nTZDpa analogs 90
3.5 Conclusions 92
3.6 References 94
Chapter 4: Diverted Total Synthesis of Baulamycin A, B, and Analogs Provides Evidence to a Newly Identified Mechanism of Action 96
4.1 Introduction and background 96
4.1.1 Bacterial Iron Acquisition 96
4.1.2 Siderophores of Gram-positive and Gram-negative Bacteria 98
4.1.3 Biosynthesis of Citrate-containing Siderophores 99
4.1.4 Baulamycin A & B Isolation and Structural Ambiguity 101
4.1.5 Hypothesized Model of Binding and Absolute Configuration 103
4.2 Other Syntheses of Baulamycin A 107
4.2.1 Total Synthesis of Originally Reported Structure of Baulamycin A by Goswami *et al.* 107
4.2.2 Synthesis of the Proposed Baulamycin Carbon Framework by Chandrasekhar, *et al.* ... 111
4.2.3 Total Synthesis and Stereochemical Assignment of the Baulamycins by Aggarwal and Co-workers 113
4.2.4 Synthesis and *in vitro* SAR of Baulamycin Structures by Sim and Co-workers 118
4.3 Total Synthesis of Baulamycin A and B 122
4.3.1 Retrosynthesis 122
4.3.2 Synthesis of Originally Proposed Left Half Fragment 123
4.3.3 Synthesis of Corrected Structure 124
4.3.4 Completion of the Total Synthesis of Baulamycin A, Baulamycin B, and Analogs 127
4.4 Biological evaluation of Baulamycin A, B, and Analogs 131

4.4.1 *S. aureus* Inhibition 131
4.4.2 Hemolysis and SYTOX Uptake Assay Results 133
4.5 Conclusions 134
4.6 References 136
5.1 Experimental Details 140
5.1.1 Chemistry: Instrumentation and General Notes 140
5.1.2 Chemistry: Experimental Procedures and Characterization Data 141
5.1.3 Biology: Bacterial Strains and Culture Conditions 319
5.1.4 Biology: Assay Procedures 319
5.1.5 SYTOX Uptake Assay Data 322
Appendix: NMR Spectra 328

List of Illustrations

List of Figures **Page**

Chapter 1

Figure 1. A representative from each of the three major classes of antibiotics based on their mechanism of action. 2
Figure 2. Structures of aminoglycosides relevant to this discussion. (left) Structure of kanamycin B, **1.7,** with all known sites of possible enzymatic modification listed with each respective enzyme as well as its class. (right) Structure of plazomicin, **1.8,** with all its analogous sites of possible enzyme modification as compared to **1.7** labeled. Dotted arrows indicate the enzymes can no longer modify these positions. 5
Figure 3. Schematic representation of the mechanism of transpeptidation, the substrate of PBP, and the homology between the PBP substrate, penicillins, and cephalosporins. "xx" represents variable amino acids between bacterial species, R groups vary among various medicinal penicillin and cephalosporin antibiotics. 6
Figure 4. Clinically used tetracycline derivatives: natural product demeclocycline (**1.15**), and semisynthetic derivatives minocycline (**1.16**) and tigecycline (**1.16**). 11
Figure 5. Schematic representation of linear, convergent, and diverted total synthesis. 12
Figure 6. Epoxomicin (**1.17**), YU-101 (**1.18**), and carfilzomib (**1.19**). Changes from each round of optimization are highlighted in red. 13

Chapter 2

Figure 7. Summary of results from isolation report by De Mot *et al.* and the three key questions that we set out to answer in our studies. The red and green fonts for PA indicate strong and moderate antagonism, respectively. 19
Figure 8. Droplet assay showing that the synthetic compounds are all surfactants. Numbers at the top indicate concentrations in μM diluted in water from a 10% DMSO/H2O v/v 1 mM stock solution, and "CTL" refers to negative control solutions with the same DMSO concentration as test solutions. 28
Figure 9. Swarming motility induced by synthetic promysalin **(–)-2.1a.** The same 29

swarming phenotypes were also observed for **(–)-2.1b, (–)-2.1c,** and **(–)-2.1d** (data not shown).
Figure 10. Newly observed phenotypes induced by promysalin in our studies. (top row) *P. putida* WCS358 swarming plates visualized after two days at 30 °C. (bottom row) *P. putida* KT2440 UV fluorescent phenotypes visualized after two days at 30 °C. 30
Figure 11. Minimized structure of **(–)-2.1a** from Spartan. Red arrows indicate key hydrogen bond interactions we sought to probe via analog synthesis. 33
Figure 12. Analog design and grouping according to structural motif that was modified in each series. Key questions that were addressed with specific analogs are listed on the left, grouped by analog series. 34
Figure 13. Structures of proline analog targets. 35
Figure 14. Structures of salicylate analog targets. 38
Figure 15. Structures of side chain analog targets. 44
Figure 16. Promysalin prodrug hypotheses. Under acidic conditions, we found that promysalin forms diastereomeric products **(–)-2.128a** and **(+)-2.128b.** To test our esterase hypothesis, methyl ester **(–)-2.87** and diol **(+)-2.129** were synthesized. 47
Figure 17. All analog structures and PAO1 and PA14 IC50 values. Red numbers indicate inactive up to 250 μM, numbers are given as IC50: PAO1/PA14. 49
Figure 18. Photographs of CAS assay with agar (left) and solution (right). 50
Figure 19. Examples of salicylate-containing Gram-negative siderophores. The salicylate moiety of each structure is colored in red. 51
Figure 20. Background for proteomics. (a) Electrophilic functional groups used in ABPP and/or AfBPP. (b) Photoreactive functional groups and their respective reactions utilized in AfBPP. (c) General workflow of AfBPP, where "NP" denotes natural product of interest, the blue shape is a hypothetical protein target, with a generic amide bond showing for simplicity. The left pathway indicates biotin attachment via copper catalyzed azide alkyne cycloaddition (CuAAC), which can then be enriched, digested, and analyzed with LC-MS/MS. The right pathway indicates fluorophore appendage, which can then be analyzed via SDS-page and fluorescent imaging. 53
Figure 21. Examples of "minimalist" alkyne-diazirine probes reported by Yao and co-workers which allow installation onto a variety of functional groups. 54
Figure 22. Schematic of the three proteomic experiments in this work. Top row: typical proteomic run with natural product probe. Middle row: competition experiment where the natural product itself is first introduced into the system, then the probe compound is introduced and will only have false positives left to interact with. Bottom row: an inactive, but structurally similar, probe compound is used to identify further false positives. 56
Figure 23. Volcano plots from proteomic experiments with *P. aeruginosa* PA14. 57
Figure 24. TCA cycle/electron transport chain overview. Blue box indicates succinate dehydrogenase (complex II), and pink box represents cytochrome C (complex III). 59

Chapter 3
Figure 25. Schematic showing the difference between resistance and persistence. (a) typical antibiotic mechanism, where the antibiotic engages its target, and toxic products are formed, ultimately leading to cell death. (b) Resistance arises by an altered target, for example an amino acid mutation in an active site, whereby the antibiotic can no longer bind to the target. (c) Persistence occurs when the antibiotic can still engage its target, but it is dormant, so the binding has no effect. 66
Figure 26. (left) Images from *C. elegans* high-throughput screen and (right) structures of lead compounds from the *C. elegans-MRSA* screen. 68
Figure 27. Killing kinetics of retinoids (left) and nTZDpa (right) against MRSA. 69
Figure 28. Schematic of the molecular dynamics simulation results. 71

Figure 29. Goals of the CD437 analog campaign and general building block structures **3.15** and **3.16.** 73
Figure 30. Compiled MIC data results from CD437 analog biological testing. 81
Figure 31. Toxicity assay results with the two most potent CD437 analogs. "Analog 2" refers to **3.14,** while "Analog 9" refers to **3.34.** (a) Hemolysis assay results with Triton X-100 as the positive control. (b) Cytotoxicity assay results. (c) Hepatocyte (liver cell) toxicity of **3.14** vs. CD437 and bexarotene, a cytotoxic retinoid used in cancer therapy. 81
Figure 32. Results of initial screen of analogs **3.70, 3.71,** and **3.72.** 90
Figure 33. SAR data for the initial round of nTZDpa analogs, with MIC (MRSA) and HC50 (hemolysis) values given. 91
Figure 34. Potency and toxicity data for analogs **3.103, 3.108,** and **3.106.** 92

Chapter 4
Figure 35. Enterobactin/salmochelin uptake system in *E. coli*, as well as their chemical structures. Iron-chelating functionalities are highlighted in red. 98
Figure 36. Representative siderophore structures. 99
Figure 37. Summary of baulamycin A (**4.13a**) and baulamycin B (**4.14a**) isolation report initial findings. 102
Figure 38. Sequence alignment of AsbA (top row), SbnE (middle row), and IucA. The boxed residues are in the active site of IucA and contact ATP in the crystal structure. Green boxes indicate an exact match between the enzymes, and red indicates a mismatch. 104
Figure 39. Crystal structures and models used to rationalize the hypothesized absolute configuration. (a) Active site of IucA with ATP outlined in green (oxygen = red, carbon = gray, phosphorus = orange, nitrogen = blue). (b) View showing histidine 425 (orange) which π-stacks with adenine. (c) "Tunnel" with hydrophobic residues in red and hydrophilic in blue, ATP is green and Mg pink, and distance showing length of the tunnel. (d) Model of **4.13b** made in Spartan with important distances shown. (e) Model of **4.13c** showing the projection of the aromatic moiety. 106
Figure 40. Chemical structures of the diastereomeric isomers produced by Goswami, *et al.*, with key discrepancies involving the benzylic C-H highlighted. 111
Figure 41. Structures and IC50 values of analogs synthesized by Sim and co-workers. 121
Figure 42. Baulamycin A, B, and analog results of *S. aureus* inhibition. (a) structures of natural products and analogs. (b) MIC data of active compounds against SH1000, highlighting the minimal differences between IRM and IDM. ***(–)-4.146** had an MIC of >500 μM in IRM, but is shown as 500 μM for visual clarity. (c) Full set of MIC data for all compounds against all strains tested in IRM and IDM (values are in μM, except for vancomycin, which is given in μg/mL**)**. 132
Figure 43. Table of HC20 and SYTOX assay results. The four graphs show examples of positive/negative controls, and compounds that tested positive and negative for membrane permeabilization. 134

Chapter 5
Figure 44. Mosher ester analysis 298

List of Tables

Chapter 1
Table 1. NMR comparison between the four synthetic promysalin diastereomers and the spectral data from the isolation report by De Mot, *et al.* Δδ1H values greater than 0.02 ppm and Δδ13C values greater than 0.3 ppm are shown in red font. 27

Table 2. Inhibitory activity of the four synthetic diastereomers against *Pseudomonas* strains. Values are IC50 values calculated using curve-fitting software with OD600 values. "–" refers to no observation of growth inhibition. 27

Chapter 2

Chapter 3

List of Schemes

Chapter 1

Scheme 1. Mechanism of β-lactamase inactivation of penicillin, and structure of β-lactamase inhibitor clavulanic acid, **1.6.** 4
Scheme 2. Degradation products of erythromycin, **1.2.** 9
Scheme 3. Semisynthesis of roxithromycin, **1.12,** and azithromycin, **1.14.** 10

Chapter 2

Scheme 4. Biosynthesis of promysalin elucidated by De Mot, *et al.* 20
Scheme 5. Retrosynthesis of **2.1**. 22
Scheme 6. Synthesis of acid fragment **(–)-2.12.** 23
Scheme 7. Synthesis of four diastereomeric alcohols **2.15a – 2.15d.** 24
Scheme 8. Esterification and final deprotection steps yielding four promysalin diastereomers **2.1a – 2.1d.** 25
Scheme 9. Synthesis of fluorine analog **(+)-2.33.** 36
Scheme 10. Synthesis of 4-methyldehydroproline analog **(–)-2.34**. 36
Scheme 11. Synthesis of hydroxyproline analog **(–)-2.35.** 37
Scheme 12. Synthesis of proline analog **(–)-2.36** and piperidine analog **(+)-2.37.** 38
Scheme 13. Synthesis of analogs **(+)-2.57** and **(+)-2.58.** 39
Scheme 14. Synthesis of trimethoxy analog **(–)-2.59.** 40
Scheme 15. Synthesis of benzoyl analog **(–)-2.60.** 40
Scheme 16. Synthesis of methyl ether analog **(–)-2.61.** 41
Scheme 17. Synthesis of methoxy-substituted analog **(–)-2.62.** 42
Scheme 18. Synthesis of nitro analog **(–)-2.63.** 43
Scheme 19. Synthesis of deshydroxyl analog **(–)-2.106.** 44
Scheme 20. Synthesis of methyl ether analog **(–)-2.107.** 45
Scheme 21. Synthesis of alkene analog **(–)-2.108.** 45
Scheme 22. Synthesis of amide analog **(–)-2.109.** 46
Scheme 23. Synthesis of propargyl analog **(–)-2.110.** 46
Scheme 24. Synthesis of probe compound **(–)-2.135,** and inactive probe **(–)-2.137.** 55

Chapter 3

Scheme 25. Synthesis of first-generation retinoid analogs from adapalene (**3.6**). 72
Scheme 26. Synthesis of the two isomeric boronic acid precursors **3.21** and **3.25.** 74
Scheme 27. Synthesis of benzyl analog precursor **3.29.** 74
Scheme 28. Final steps in the synthesis of CD437 phenol isomer **3.32** and benzyl analog **3.34.** 75
Scheme 29. First attempt at synthesis of oxidized naphthalene Suzuki precursor **3.38.** 76
Scheme 30. Successful synthesis of bromo-naphthalene fragment **3.44.** 76
Scheme 31. Suzuki reaction and attempted deprotection. Highlighted in red are the sites of possible methylation and below are the resonance structures that rationalize them. 77
Scheme 32. Synthesis of oxidized naphthalene Suzuki precursors **3.48** and **3.49.** 78
Scheme 33. Synthesis of singly oxidized naphthalene analogs **3.56, 3.58,** and **3.60.** 79

Scheme 34. Synthesis of naphthalene analogs with two additional phenol substituents, **3.62, 3.64,** and **3.66.** 80
Scheme 35. Patent route to nTZDpa with highlighted issues we aimed to address. 83
Scheme 36. Synthesis of nTZDpa (**3.5**). 84
Scheme 37. Synthesis of analogs **3.70, 3.71,** and **3.72.** 85
Scheme 38. Synthesis of nTZDpa analogs **3.73, 3.75,** and **3.77.** 86
Scheme 39. Synthesis of analogs **3.79** and **3.81** and demonstration of the importance of indole nitrogen acidity. 87
Scheme 40. Synthesis of **3.84** and **3.86** with the generalized alkylation conditions. 88
Scheme 41. Synthesis of three indole nTZDpa analogs **3.90, 3.94,** and **3.98.** 88
Scheme 42. Synthesis of ether analogs **3.103** and **3.106.** 89
Scheme 43. Synthesis of methylene analog **3.108.** 90

Chapter 4

Scheme 44. General types of reactions catalyzed by each type of NIS synthetase. 100
Scheme 45. Reactions catalyzed by SbnE and AsbA. 101
Scheme 46. Retrosynthesis of Goswami and co-workers reported in 2017. 107
Scheme 47. Goswami and co-workers' synthesis of fragment 4.15. 108
Scheme 48. Synthesis of fragment **(–)-4.16** by Goswami and co-workers. 109
Scheme 49. Goswami and co-workers' revised route to the originally reported structure of baulamycin A, **(+)-4.13c.** 110
Scheme 50. Synthesis of fragment **(+)-4.50** as reported by Chandrasekhar and co-workers. 112
Scheme 51. Synthesis of right hand fragment and successful cross-metathesis leading to late stage intermediate **(–)-4.62** reported by Chandrasekhar and co-workers. 113
Scheme 52. Strategy reported by Aggarwal, *et al.* in 2016 to access 1,3-diols via lithiation/borylation. 114
Scheme 53. Retrosynthetic strategy of Aggarwal and co-workers. 115
Scheme 54. Synthesis of left half fragment **(–)-4.70** by Aggarwal and co-workers. 116
Scheme 55. Completion of the synthesis of **(+)-4.13a** by Aggarwal and co-workers, and the correct structure **(–)-4.13d.** 117
Scheme 56. Synthesis of originally reported left fragment **(+)-4.90** by Sim and co-workers. 118
Scheme 57. Synthesis of alkyne right half fragment **(+)-4.98** by Sim and co-workers. 119
Scheme 58. Completion of the synthesis of **(+)-4.13c** by Sim and co-workers. 120
Scheme 59. Retrosynthesis of **4.13b.** 122
Scheme 60. Synthesis of left fragment **(–)-4.15.** 123
Scheme 61. Synthesis of revised left half **(–)-4.124.** 124
Scheme 62. Synthesis of fragments used for the right half of the baulamycins and analogs: **(–)-4.131** and **(+)-4.133.** 127
Scheme 63. Completion of the synthesis of baulamycin A (**(–)-4.13d**) and analogs **(–)-4.126** and **(–)-4.127.** 128
Scheme 64. Synthesis of baulamycin B (**(–)-4.140**), **(–)-4.141,** and **(–)-4.142.** 129
Scheme 65. Synthesis of simplified analogs **(–)-4.146** and **(–)-4.147.** 130
Scheme 66. Synthesis of analogs **(–)-4.149** and **(–)-4.151.** 131

Chapter 5

List of Abbreviations

ABPP: activity-based protein profiling

AcCl: acetyl chloride

AfBPP: affinity-based protein profiling

ATP: adenosine triphosphate

Bn: benzyl

CAS: chrome azurol S

CSA: camphorsulfonic acid

DMF: dimethylformamide

DMAP: 4-dimethylaminopyridine

DMPU: 1,3-Dimethyl-3,4,5,6-tetrahydro-2(1H)-pyrimidinone

DMSO: dimethyl sulfoxide

DPPA: diphenylphosphoryl azide

DTS: diverted total synthesis

EDC: 1-ethyl-3-(3-dimethylaminopropyl)carbodiimide

EDTA: ethylenediaminetetraacetic acid

Et: ethyl

EtOAc: ethyl acetate

$FAD^+/FADH_2$: flavin adenine dinucleotide

GDP: guanosine diphosphate

GTP: guanosine triphosphate

HATU: 1-[Bis(dimethylamino)methylene]-1H-1,2,3-triazolo[4,5-b]pyridinium 3-oxid hexafluorophosphate)

HMPA: hexamethylphosphoramide

HOBt: hydroxybenzotriazole

HPLC: high-performance liquid chromatography

*i*Bu: isobutyl

IDM: iron-depleted media

*i*Pr: isopropyl

IRM: iron-rich media

KOH: potassium hydroxide

LC-MS and LC-MS/MS: Liquid Chromatography with tandem mass spectrometry

LiHMDS: lithium bis(trimethylsilyl)amide

Me: methyl

MEM: 2-methoxyethoxymethyl

MeOH: methanol

MIC: minimum inhibitory concentration

MOM: methoxymethyl

$NAD^+/NADH_2$: Nicotinamide adenine dinucleotide

NaHMDS: sodium bis(trimethylsilyl)amide

NaOH: sodium hydroxide

NMO: 4-methylmorpholine N-oxide

NMR: nuclear magnetic resonance

PCC: pyridinium chlorochromate

Q/QH_2: coenzyme Q, or ubiquinone/ubiquinol

SAR: structure-activity relationship

SEM: [2-(Trimethylsilyl)ethoxy]methyl acetal

TASF: trissulfonium difluorotrimethylsilicate

TBAF: tetrabutylammonium fluoride

TBAI: tetrabutylammonium iodide

TBS: tert-butyldimethylsilyl

TCA: tricarboxylic acid

THF: tetrahydrofuran

TBS: *tert*-butyldimethylsilyl

TMS: trimethylsilyl

$TMSCHN_2$: (trimethylsilyl)diazomethane

TPAP: tetrapropylammonium perruthenate

UV: ultraviolet

UV-vis: ultraviolet-visible

Chapter 1: Introduction

1.1 The Discovery and Rise of Modern Antibiotics

The modern age of antibiotics began with Sir Alexander Fleming's discovery of penicillin, a metabolite produced by a fungus with antagonistic activity against *Staphylococcus*.[1] After his discovery, Fleming himself warned the world that bacteria exposed to sub-lethal concentrations of antibiotics had the potential to develop antibiotic resistance under this type of selection pressure. After penicillin's introduction into the market in the 1940s, a surge of antibiotic research brought the discoveries of a breadth of natural products with impressive antibiotic activity. As such, many refer to the 1940s-1960s as the "golden era" of antibiotics. However, this wave of discovery was short-lived, and the number of new antibiotics has been steadily declining. Complicating the issue further, discovery of new antibiotics with new mechanisms of action has slowed even further. Since the 1960s, oxazolidinones and lipopeptides are the only new classes of antibiotics to have been discovered.[2]

Figure 1 highlights the major classes of antibiotics, with each class represented by a well-known example. Penicillin, **1.1**, inhibits cell wall biosynthesis via inhibition of penicillin-binding protein (PBP). Ciprofloxacin, **1.2**, disrupts DNA synthesis by inhibiting DNA gyrase and topoisomerase IV.[3] Erythromycin, **1.3**, inhibits the function of the 50s subunit of the bacterial ribosome by blocking the elongation cycle of a growing peptide chain during protein synthesis. More recent studies have suggested **1.3** is also capable of inhibiting ribosome formation.[4] Figure 1 includes many other examples of clinically prescribed antibiotics that operate via similar mechanisms as described above. There are certainly intricacies within each class, i.e. the mechanism of penicillin involves inhibiting a transpeptidase covalently, but vancomycin binds to the D-alanine residues on the end of the backbone peptide strands and prevents them from being

cross-linked.[5] The details of each antibiotic mechanism are outside the scope of this work, and for simplistic sake the three mechanisms presented here will provide sufficient classification.

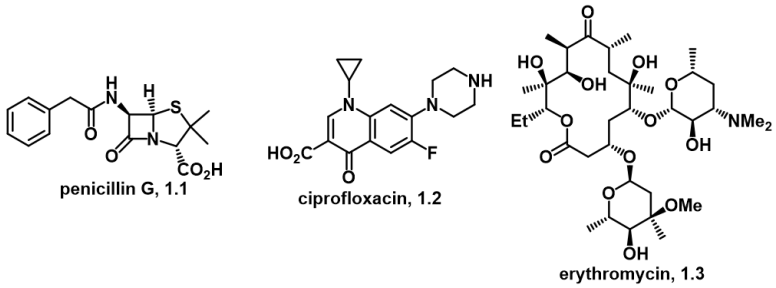

Cell wall/membrane	DNA synthesis	Protein synthesis
penicillins	quinolones	erythromycin
cephalosporins	rifampin	tetracyclines
carbapenems	nitrofurantoins	chloramphenicol
monobactams	nitroimidazoles	aminoglycosides
bacitracin		clindamycin
vancomycin		spectinomycin
cycloserine		mupirocin
fosfomycin		
polymyxins		

Figure 1. A representative from each of the three major classes of antibiotics based on their mechanism of action.

1.2 Antibiotic Resistance

1.2.1 Introduction

The initial discovery and subsequent commercialization of penicillin coincided with World War II. One of the scientists involved in the isolation/characterization of penicillin, Howard Walter Florey, traveled from England to the United States and successfully convinced the U.S. government to sponsor a penicillin mass-production effort. This led to penicillin saving the lives of countless soldiers during the war. However, this massive surge in antibiotic use caused penicillin resistance to become a widespread issue. In 1944, penicillin resistance among clinical isolates was a rare phenomenon, however, in 1948 a study of 100 patients showed that over half of their infections contained penicillin-resistant bacteria.[6] Since then, this pattern of

commercialization and resistance development has continued with each new antibiotic that enters the market.

In the United States alone, over two million drug-resistant infections occur per year, and 23,000 of those patients die as a direct result of bacterial infection. In addition, antibiotic-resistant infections have been estimated to cost society as much as $35 billion annually when healthcare costs are combined with lost productivity as a result of sickness.[7] The number one cause of increased cases of antibiotic-resistant bacteria is the use of antibiotics themselves. It has been estimated that half of all antibiotic prescriptions to humans are unnecessary or not optimally prescribed. This over- and mis-use is exacerbated by agriculture, where antibiotics are used preventatively to avoid infection and promote growth in livestock. This causes sublethal concentrations of antibiotics to build up in the environment, providing a selection pressure for bacteria to mutate and harbor antibiotic resistance.

In addition, bacteria can spread resistance in an intra- or inter-species manner, via DNA exchange, transduction with bacteriophages, conjugation with plasmids, and transposon transfer.[8] This transfer has even been shown to occur across distantly related bacteria. For example, erythromycin resistance genes (*erm*) in enterobacteria (Gram-negative) are thought to be of Gram-positive bacterial origin.[9] Once resistance genes are part of the bacterial population, antibiotic treatment will enrich this subpopulation until it takes over. These genes each typically encode one of three possible types of antibiotic resistance, which will be reviewed briefly here.

1.2.2 Drug-Inactivating Enzymes

Among all the drug-inactivating enzymes, β-lactamases are the most well-characterized and clinically relevant. They all function via the same mechanism (Scheme 1) whereby the β-lactam, the active pharmacophore of the drug, is hydrolyzed. Intermediate **1.4** is formed, which undergoes decarboxylation to the inactive metabolite **1.5**. The first characterized β-lactamase, named penicillinase, was discovered in 1940, before penicillin entered clinical use.[10] To

circumvent this issue, β-lactamase inhibitors can be used in conjunction with β-lactam antibiotics to restore their efficacy. The classic β-lactamase inhibitor, which itself is a natural product, is clavulanic acid, **1.6**. β-lactamases were first characterized in Gram-negative organisms and were very rare in Gram-positives. However, widespread use of penicillin and its derivatives have encouraged horizontal gene transfer across bacteria, making β-lactamases common among a wide variety of modern bacterial isolates.

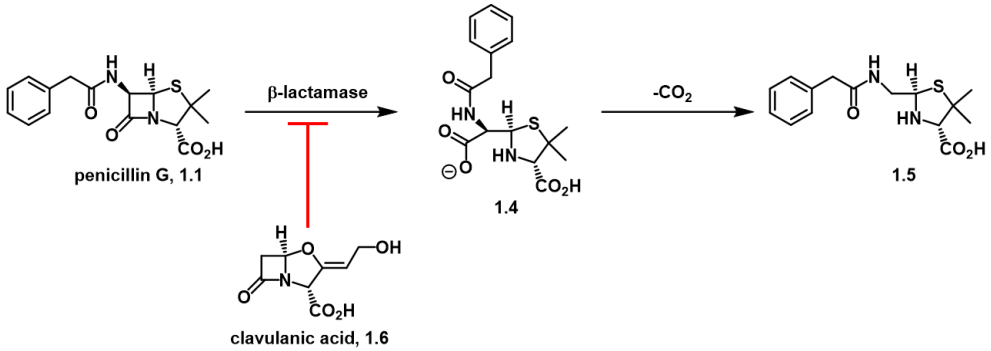

Scheme 1. Mechanism of β-lactamase inactivation of penicillin, and structure of β-lactamase inhibitor clavulanic acid, **1.6**.

Aminoglycosides are another class of antibiotics that commonly undergo enzymatic inactivation. Kanamycin B, **1.7**, is a well-studied aminoglycoside antibiotic, and many enzymes are known to modify and inactivate this drug. The structure, characterized sites of enzymatic modification, and the respective enzymes that do so are shown in Figure 2.[11-12] The sheer number of possible alterations demonstrates the need for creative solutions to this problem. Researchers in this area have attempted to design inhibitors of the modification enzymes themselves, akin to β-lactamase inhibitors. However, the plethora of possible modification enzymes that require inhibition makes this tactic extremely difficult.[13] Instead, modification of the drug molecule itself has been successful in evading drug-modifying enzymes. This is exemplified by plazomicin, **1.8**, which is currently undergoing phase 3 clinical trials, sponsored by Achaogen. Figure 2 shows how the design of this compound enables it to evade all but one kanamycin-modifying enzyme, AAC(2').

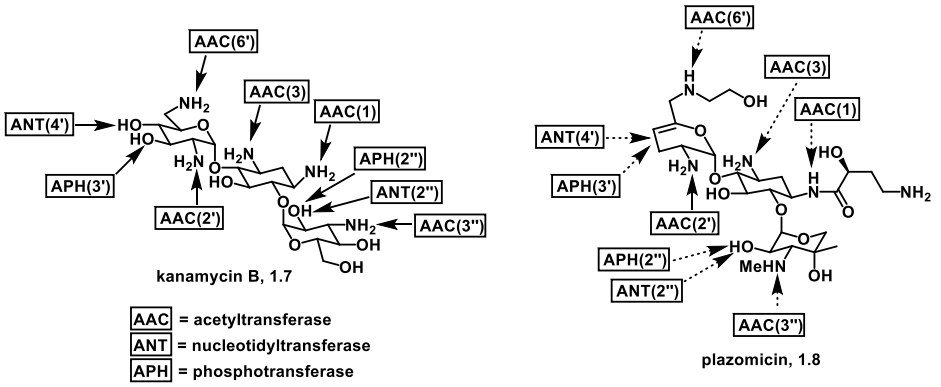

Figure 2. Structures of aminoglycosides relevant to this discussion. (left) Structure of kanamycin B, **1.7**, with all known sites of possible enzymatic modification listed with each respective enzyme as well as its class. (right) Structure of plazomicin, **1.8**, with all its analogous sites of possible enzyme modification as compared to **1.7** labeled. Dotted arrows indicate the enzymes can no longer modify these positions.

The penicillin and kanamycin examples demonstrate the potential to overcome antibiotic resistance when the mechanisms are well characterized and has been an inspiration for some of the discoveries within this work. However, the strategies outlined here are not sufficient to overcome the resistance mechanism discussed in the next section (drug target modification). For example, if a penicillin antibiotic being administered no longer engages its target, β-lactamase inhibitors will not restore efficacy.

1.2.3 Modification of Drug Target

Modification of an antibiotic's target is the simplest method by which bacteria can acquire resistance from an evolutionary standpoint. Many times, a single nucleotide and/or amino acid mutation is enough to confer resistance to a chemical moiety. This was the case in our studies with the natural product promysalin (*vida infra*). Beyond single mutations, homologous recombination and horizontal gene transfers can confer massive structural changes to a drug target in short order. During a medicinal chemistry campaign, these can cause significant setbacks and require a complete overhaul of the lead optimization process. One caveat of this mode of resistance is that the antibiotic target must still recognize its native substrate to maintain its

natural function, highlighting the value of mechanism-based inhibitors. These include compounds that mimic the antibiotic target's natural substrate structure or transition state.

The penicillin class of antibiotics offers a great deal of insight into drug design and resistance via target modification, both by Nature and mankind. The penicillin compounds are mechanism-based inhibitors, tailored by evolution. Figure 3 depicts the mechanism of transpeptidation, and how penicillin is a mimic of the substrate of its target PBP. The transpeptidation reaction forms cross-links that are essential for cell wall integrity.

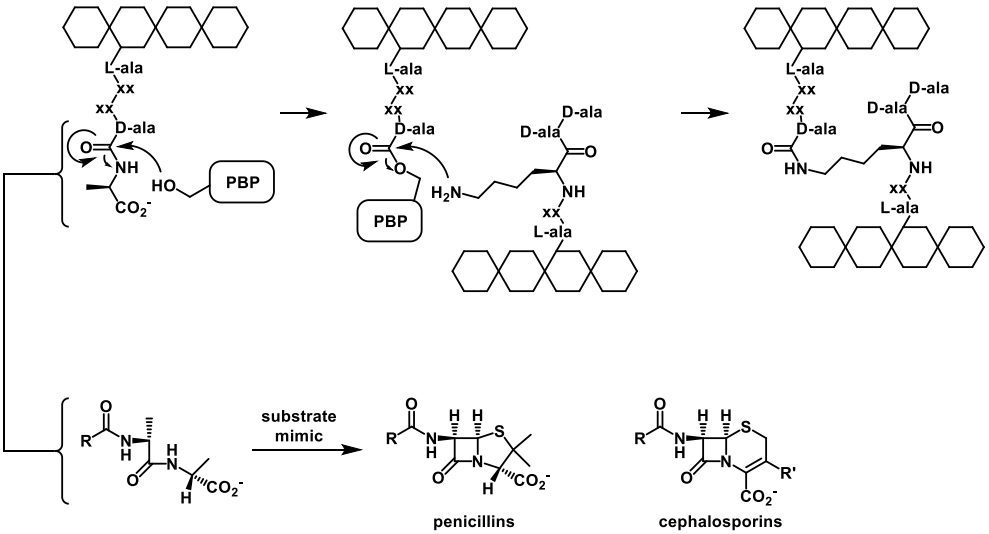

Figure 3. Schematic representation of the mechanism of transpeptidation, the substrate of PBP, and the homology between the PBP substrate, penicillins, and cephalosporins. "xx" represents variable amino acids between bacterial species, R groups vary among various medicinal penicillin and cephalosporin antibiotics.

Streptococcus pneumoniae has been heavily studied regarding penicillin resistance via PBP protein modifications. *S. pneumoniae* produces six PBPs, and up to four of these (PBP1a, PBP2b, PBP2x, and PBP2a) have been shown to be modified in resistant isolates.[14] Sequencing of isolates revealed that the altered PBP genes are mosaic. Mosaic genes have undergone multiple recombination events between the same, or closely related, species. This shows that a large gene pool of resistance-inducing elements exists, and the assessment of the relevant PBP for each situation is challenging.

In addition to complex mosaic genetic changes, PBP enzymes have been shown in both laboratory and clinical settings to undergo point mutations to confer antibiotic resistance. One example in *S. pneumoniae* is the PBP2x point mutation T550A. This mutation confers resistance to cephalosporins, but also susceptibility to penicillin.[15-18] A different mosaic version of PBP2x contains the analogous mutation along with another, T338A/M339F, and this phenotype is enhanced even further. The double mutant is even less susceptible to cephalosporin and efficacy of penicillin is almost completely restored.[19]

Another well-known example of a target modification conferring antibiotic resistance is methylation of the ribosome in response to protein synthesis inhibiting antibiotics. The erythromycin ribosomal methylation (Erm) methyltransferases transfer methyl groups to an adenine in the ribosome, which significantly perturbs the antibiotic binding site and causes resistance to macrolides, lincosamides, and streptogramin B.[20] Two other well-studied methyltransferases that methylate a different region of the ribosome are Cfr and RlmM.[21]

While target modification is a mechanism of antibiotic resistance that causes problems in medicinal and clinical settings, it can be taken advantage of in the laboratory to make important discoveries. Resistance generation followed by genome sequencing is a powerful technique that has been successfully utilized to discover the biological target(s) of compounds, and molecular mechanisms of resistance development simultaneously.[22-24] In our work, resistant mutant generation was used to both validate proteomic results and identify molecular mechanisms of resistance development in response to the natural product promysalin.[25]

1.2.4 Prevention of Access to Target

Bacteria's first line of defense against chemical attack is the cell wall. This is particularly challenging in Gram-negative pathogens; whose cell envelope consists of two membranes. The outer membrane (OM) is an asymmetric bilayer that is more rigid than a typical cell membrane, and its structural hallmark is lipopolysaccharide (LPS).

The outer membrane by nature of the LPS allows access of hydrophobic antibiotics (aminoglycosides, macrolides, novobiocin, etc.) via passive diffusion.[26] The LPS building blocks of the OM are each held together by divalent cations (Mg^{2+} or Ca^{2+}), forming a stable, rigid, "quasicrystalline" structure.[27] An antibiotic that cannot passively diffuse through the LPS of a Gram-negative organism must traverse nonspecific porins and/or uptake channels. Porins are meant to facilitate the uptake of nutrients into a bacterial cell, but small, hydrophilic antibiotics are also allowed passage. In the presence of antibiotics, porin loss can confer resistance to antibiotics. *E. coli* porin mutations and decreased expression levels have been shown to confer β-lactam resistance both in the laboratory and in clinical isolates.[28-29] Multi-drug resistance in *Serratia marcescens* (β-lactams and aminoglycosides) has been attributed to with porin mutations both *in vitro* and *in vivo*.[30] Further, clinical isolates of *Klebsiella pneumoniae* have been shown to resist β-lactam treatment with a combination of β-lactamase production and decreased porin expression.[31] This final example demonstrates how complicated the problem of resistance can become, when multiple modes (efflux and drug inactivation) are working together.

1.3 Chemical Approaches to Antibiotic Resistance

1.3.1 Semisynthesis

Natural products serve as lead scaffolds for a majority of clinically used antibiotics. However, Nature does not always select molecules with the best "drug-like" properties. Characteristics such as oral bioavailability and stability in the human gut are not typical selection pressures. Hence, chemists must optimize the leads that Nature has provided. Semisynthesis offers a direct approach to new compounds with potentially improved properties from a natural product directly. Advantages over total synthesis include lower step count, higher yields, and a high chance of obtaining an active derivative, since the scaffold is itself already "privileged", compared to designing a compound *de novo*. This latter point is also a drawback, however, since

altering an established elaborate chemical scaffold drastically is typically not feasible. Semisynthesis is completely dictated by intrinsic reactivity of the molecule, which can add many tedious steps *en route* to one simple manipulation. However, when the starting material is readily available via fermentation, the efficiency can still be favorable.

One of the classical examples of the success and power of semisynthesis is development of azithromycin from erythromycin. Under acidic conditions, such as in the human gut, erythromycin (**1.2**) has been shown to undergo the decomposition pathway shown in Scheme 2. The ketone moiety undergoes intramolecular attack by the indicated hydroxyl group, and subsequent dehydration leads to dihydrofuran **1.9**. Acid-mediated attack of another hydroxyl group onto the alkene of the dihydrofuran then leads to **1.10**.[32] Both degradation products are significantly less potent than **1.2**.

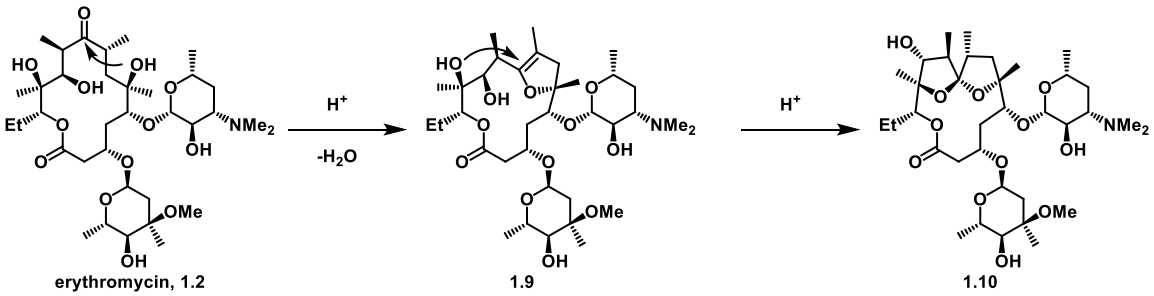

Scheme 2. Degradation products of erythromycin, **1.2**.

To overcome this acidic degradation pathway, chemists employed a creative approach to convert the ketone to a more stable functional group, while retaining potency. Erythromycin was converted to the corresponding oxime, **1.11** and derivatized to dozens of different oxime derivatives. This led to the discovery of roxithromycin, **1.12** (Scheme 3) which has significantly improved acidic stability while retaining the potency of erythromycin.[33] Another group of researchers subjected oxime intermediate **1.11** to a Beckmann rearrangement, yielding **1.13**, which was hydrogenated and methylated, yielding azithromycin, **1.14**.[34] Importantly, this compound not only has improved stability relative to erythromycin, but also lower toxicity and

improved potency against Gram-negative pathogens. Roxithromycin and azithromycin find extensive use in the clinic today, and semisynthesis remains the most efficient means of accessing these important medicines.

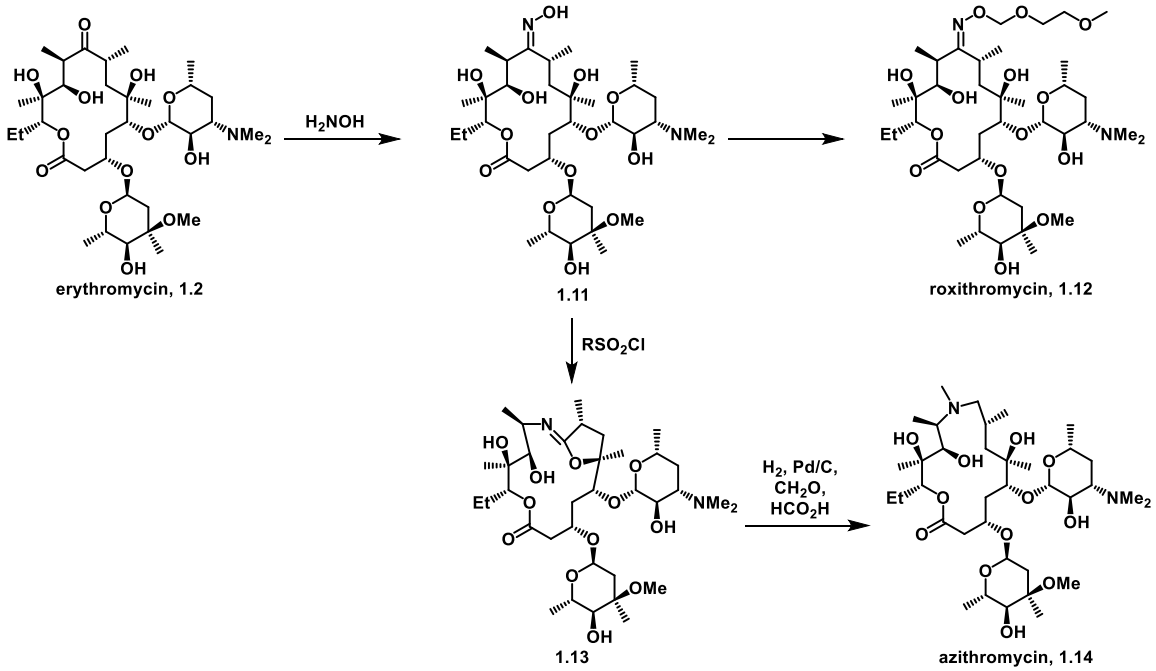

Scheme 3. Semisynthesis of roxithromycin, **1.12**, and azithromycin, **1.14**.

The tetracyclines offer a rich history of semisynthesis breakthroughs. Tetracycline resistance has been known since the 1950s, with several prevailing mechanisms, and semisynthetic tactics have been employed to discover solutions. Figure 4 shows demeclocycline, **1.15**, which is a natural product closely related to tetracycline and was approved by the FDA in 1960. This lead was converted in a few steps to minocycline, **1.16**, which gained FDA approval in 1971.[35] Further optimization and semisynthetic efforts then led to the discovery of tigecycline, **1.17**, decades later. This compound is used in the clinic today, but only for last-resort cases due to toxicity issues. This effort over the span of half a century demonstrates the power of semisynthesis for developing usable drugs consistently. However, it also demonstrates the limitations: chemical modifications are inherently limited to the reactive sites of the molecule.

Therefore, total synthesis remains the only means to access analogs where unreactive sites are altered.

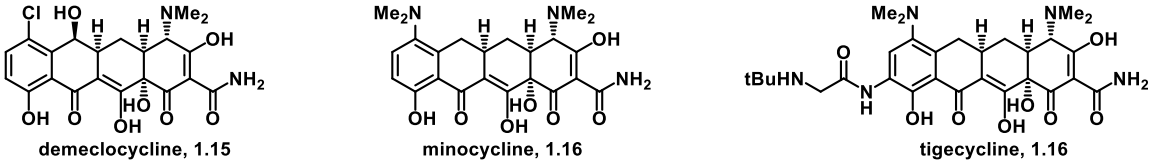

Figure 4. Clinically used tetracycline derivatives: natural product demeclocycline (**1.15**), and semisynthetic derivatives minocycline (**1.16**) and tigecycline (**1.16**).

1.3.2 Diverted Total Synthesis

Given the limits of biosynthesis and semi-synthesis, total synthesis remains the only way to modify natural products in an exhaustive and systematic manner. A convergent synthesis will always be more efficient, in terms of waste, cost, etc. compared to its linear counterpart. Figure 5 has a simple schematic, with both a linear and convergent synthesis both resulting in the same number of overall steps. Since yields are multiplicative, if all individual step yields are the same, the convergent synthesis will have a higher yield. Additionally, if one were to repeat the synthesis to change the "R" group, the linear synthesis would require four entirely new synthetic operations. In contrast, the convergent route would only require two new steps. Taking this concept one step farther, if advanced intermediate "A" is diverted, new targets with very different scaffolds can be accessed without a complete overhaul of the synthetic route. This approach was named diverted total synthesis by Danishefsky.[36-37]

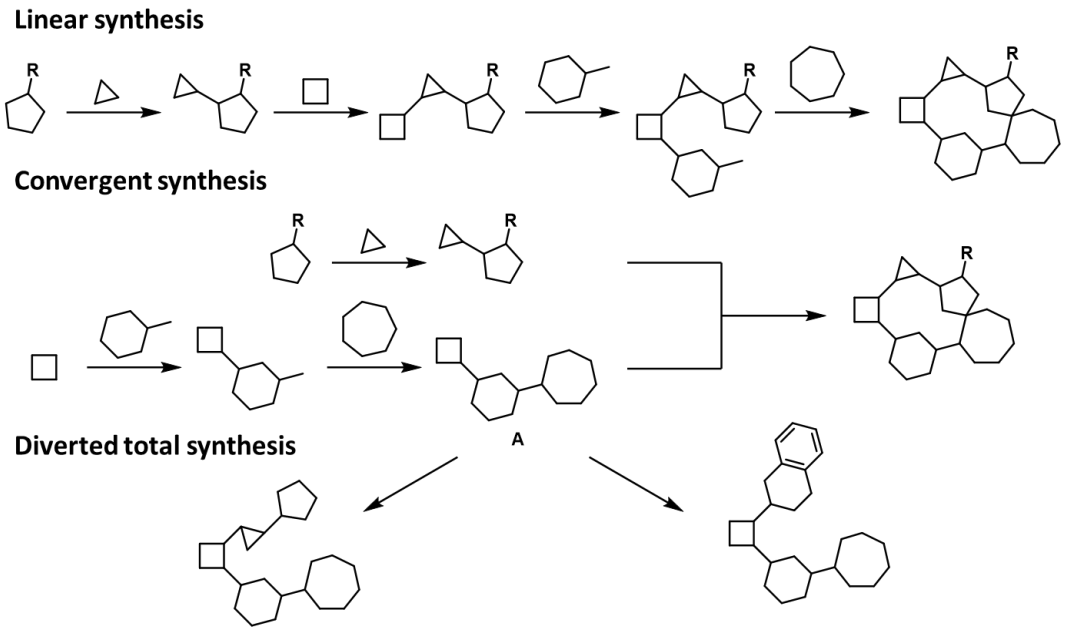

Figure 5. Schematic representation of linear, convergent, and diverted total synthesis.

The field of medicinal chemistry contains many examples of successful diverted total synthesis efforts leading to drug molecules. One success story is the development of carfilzomib (brand name Kyprolis), from the natural product epoxomicin, **1.17** (Figure 6). The compound was originally isolated by a group at Bristol Myers Squibb in Tokyo and shown to have potent antitumor activity.[38] However, the project was abandoned because the mechanism of action was unknown, and researchers worried that FDA approval would be troublesome for this reason. Crews *et al.* developed a total synthesis to access epoxomicin, whereby a biotinylated derivative was also prepared and used in target identification studies, which revealed that the compound targets the proteasome.[39] Subsequent optimization and medicinal chemistry efforts led to the discovery of YU-101 (**1.18**), which had increased potency. After starting a company and additional optimization, carfilzomib (**1.19**) was discovered.[40] This compound is the FDA-approved treatment for multiple myeloma, and is a success story enabled by diverted total synthesis and the answering of biological questions, which served as great inspiration for the work reported in this thesis.

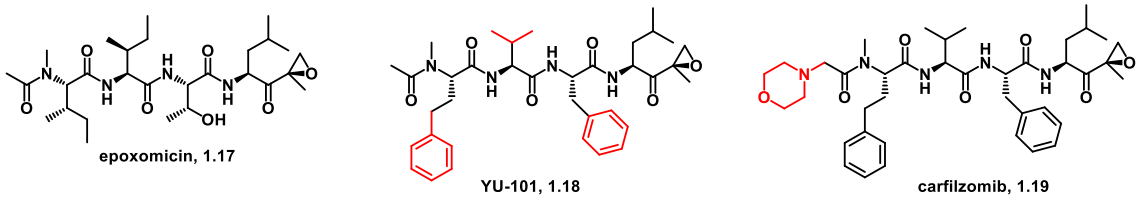

Figure 6. Epoxomicin (**1.17**), YU-101 (**1.18**), and carfilzomib (**1.19**). Changes from each round of optimization are highlighted in red.

1.3.3 Conclusions

While antibiotic resistance cannot be avoided altogether, it can be mediated by being responsible patrons of the powerful medicines currently available. Current treatments need to be used with more care, as mis- and over-use of antibiotics are much to blame for the modern antibiotic resistance issue. While the work presented in this thesis is centered on antibiotic discovery, existing treatments need to be cherished if they are to remain efficacious in the future.[11]

1.4 References

1) Fleming, A. *Br. J. Exp. Pathol.* **1929**, *10*, 226.

2) Conly, J. M.; Johnston, B. L. *Can. J. Infect. Dis. Med. Microbiol.* **2005**, *16*,

3) Drlica, A.; Zhao, X. *Microbiol. Mol. Biol. Rev.* **1997**, *61*, 377.

4) Champney, W. S.; Burdine, R. *Antimicrob. Agents Chemother*. **1995**, *39*, 2141.

5) Courvalin, P. *Clin. Infect. Dis.* **2006**, *42*, S25.

6) Barber, M.; Rozwadowska-Dowzenko, M. *Lancet* **1948**, *252*, 641.

7) U.S. Department of Health and Human Services (Centers for Disease Control and Prevention). Antibiotic Resistance Threats in the United States, 2013. https://www.cdc.gov/drugresistance/threat-report-2013/index.html (accessed March 12, 2018).

8) Neu, H. C. *Science* **1992**, *257,* 1064.

9) Arthur, M.; Brisson-Noël, A.; Courvalin, P. *J. Antimicrob. Chemother.* **1987**, *20*, 783.

10) Abraham, E. P.; Chain, E. *Nature* **1940**, *146,* 837.

11) Ramirez, M. S.; Tolmasky, M. E. *Drug Resist. Updat.* **2010**, *13,* 151.

12) Kotra, L. P.; Haddad, J.; Mobashery, S. *Antimicrob. Agents Chemother.* **2000**, *44,* 3249.

13) Labby, K. J.; Garneau-Tsodikova, S. *Future Med. Chem.* **2013**, *5*, 1285.

14) Zapun, A.; Contreras-Martel, C.; Vernet, T. *FEMS Microbiol. Rev.* **2008**, *32,* 361.

15) Grebe, T.; Hakenbeck, R. *Antimicrob. Agents Chemother.* **1996**, *40,*

16) Sifaoui, F.; Kitzis, M.-D.; Gutman, L. *Antimicrob. Agents Chemother.* **1996**, *40*, 152.

17) Krauss, J.; van der Linden, M.; Grebe, T.; Hakenbeck, R. *Microb. Drug Resist.* **1996**, *2,* 183.

18) Asahi, Y.; Ubukata, K. *Antimicrob. Agents Chemother.* **1998**, *42,* 2267.

19) Coffey, T. J.; Daniels, M.; McDougal, L. K.; Dowson, C. G.; Tenover, F. C.; Spratt, B. G. *Antimicrob. Agents Chemother.* **1995**, *39,* 1306.

20) Munita, J. M.; Arias, C. A. *Microbiol. Spectr.* **2016**, *4,* 1.

21) Stojkovic, V.; Noda-Garcia, L.; Tawfik, D. S.; Fujimori, D. G. *Nucleic Acids Res.* **2016**, *44,* 8897.

22) Ioerger, T. R.; O'Malley, T.; Liao, R.; Guinn, K. M.; Hickey, M. J.; Mohaideen, N.; Murphy, K. C.; Boshoff, H. I.; Mizrahi, V.; Rubin, E. J.; Sassetti, C. M.; Barry, C. E., 3rd; Sherman, D. R.; Parish, T.; Sacchettini, J. C. *PLoS One* **2013**, *8,* e75245.

23) Fujimoto-Nakamura, M.; Ito, H.; Oyamada, Y.; Nishino, T.; Yamagishi, J. *Antimicrob. Agents Chemother.* **2005**, *49,* 3810.

24) Telenti, A.; Imboden, P.; Marchesi, F.; Lowrie, D.; Cole, S.; Colston, M. J.; Matter, L.; Schopfer, K.; Bodmer, T. *Lancet* **1993**, *341,* 647.

25) Keohane, C. E.; Steele, A. D.; Fetzer, C.; Khowsathit, J.; Van Tyne, D.; Moynie, L.; Gilmore, M. S.; Karanicolas, J.; Sieber, S. A.; Wuest, W. M. *J. Am. Chem. Soc.* **2018**, *140*, 1774.

26) Delcour, A. H. *Biochimica et Biophysica Acta* **2009**, *1794*, 808.

27) Vaara, M. *Microbiol. Rev.* **1992**, *56*, 395.

28) Harder, K. J.; Nikaido, H.; Matsuhashi, M. *Antimicrob. Agents Chemother.* **1981**, *20*,

29) Bakken, J. S.; Sanders, C. C.; Thomson, K. S. *J. Infect. Dis.* **1987**, *155*, 1220.

30) W., G. F.; Gutmann, L.; Williamson, R.; Collatz, E.; Acar, J. F. *Ann. Microbiol. (Paris)* **1983**, *134A*, 329.

31) Pangon, B.; Bizet, C.; Bure, A.; Pichon, F.; Philippon, A.; Regnier, B.; Gutmann, L. *J. Infect. Dis.* **1989**, *159*,

32) Kirst, H. A. *Prog. Med. Chem.* **1993**, *30*,

33) Gasc, J. C.; d'Ambrieres, S. G.; Lutz, A.; Chantot, J. F. *J. Antibiotics (Tokyo)* **1991**, *44*,

34) Jelic, D.; Antolovic, R. *Antibiotics (Basel)* **2016**, *5*, 29.

35) Church, R. F. R.; Schaub, R. E.; Weiss, M. J. *J. Org. Chem.* **1971**, *36*, 723.

36) Njardarson, J. n. T.; Gaul, C.; Shan, D.; Huang, X.-Y.; Danishefsky, S. J. *J. Am. Chem. Soc.* **2004**, *126*, 1038.

37) Wilson, R. M.; Danishefsky, S. J. *J. Org. Chem.* **2006**, *71*, 8329.

38) Hanada, M.; Sugawara, K.; Kaneta, K.; Toda, S. N., Y.; Tomita, K.; Yamamoto, H.; Konishi, M.; Oki, T. *J. Antibiot.* **1992**, *45*,

39) Sin, N.; Bo Kim, K.; Elofsson, M.; Meng, L.; Auth, H.; Kwok, B. H. B.; Crews, C. M. *Bioorg. Med. Chem. Lett.* **1999**, *9*, 2283.

40) Kim, K. B.; Crews, C. M. *Nat. Prod. Rep.* **2013**, *30*, 600.

Chapter 2: Synthesis, Structure Elucidation, and Target Identification of the Gram-negative Selective Antibiotic Promysalin

2.1 Promysalin background

2.1.1 Gram-negative and *Pseudomonas* Clinical Infections

Gram-negative pathogens are versatile and known to infect lungs, indwelling medical devices, the blood stream, and soft tissues. They are notorious for resistance development and to cause recurrent, persistent infections.[1] The most highly represented in clinical isolates are *Pseudomonas aeruginosa*, *Acinetobacter baumannii*, and *Klebsiella pneumoniae*, which historically were highly susceptible to β-lactam antibiotics. However, problems with mis- and overuse of antibiotics for several decades have rendered these pathogens to be multi-drug resistant (MDR). *P. aeruginosa* is an opportunistic pathogen that is of particular concern to immunocompromised hospital patients, and multi-drug resistant strains are easily prepared in laboratory settings.[2] *P. aeruginosa* infections are the causative agent of hospital-acquired and ventilator-associated pneumonia. They also cause deadly infections in cystic fibrosis patients: over 90% of deaths are a direct result of *P. aeruginosa* infection.[3] In addition, *P. aeruginosa* represents the seventh most common blood-borne pathogen.[4] The issue of *P. aeruginosa* prevalence and resistance in the clinic is exacerbated by its plethora of virulence factors and its ability to thrive in and on a variety of aerobic/anaerobic environments and nutrient sources.

P. aeruginosa drug resistance can operate by many complementary mechanisms, making the issue a multi-faceted problem. Porin mutations, drug-inactivating enzymes, efflux pumps, and biofilm formation all represent drug resistance mechanisms exhibited by this bacterium. These work together to inactivate, pump out, and/or provide a physical barrier to evade antibiotic effects. *P. aeruginosa* can overexpress its resistance-nodulation-cell division (RND) transporters

in response to stressors such as antibiotics. A well-characterized multi-drug efflux pump is MexAB-OprM, which confers resistance to β-lactams, cephalosporins, tetracyclines, and fluoroquinolines.[5] Porins operate in the opposite fashion as efflux, and serve as selective or non-selective membrane channels that small molecules can pass through. Once inside the cell, drug inactivation enzymes also play a role when an antibiotic overcomes the aforementioned challenges. β-lactamase enzyme production is also a well-known resistance mechanism across many families of bacteria, and *P. aeruginosa* is no exception. The most notable enzymes of this type for this bacterium are the inducible AmpC, class A PER-1, and class D OXA β-lactamases.[6-7] Complicating the problem further, β-lactamase genes have been observed adjacent to 6'-N acetyltransferase genes, which inactivate aminoglycosides.[8] These highly transferrable and mobile genes mean that MDR phenotypes can spread throughout populations via horizontal gene transfer. Biofilms offer another physical and chemical line of defense for *P. aeruginosa*, which can provide up to 1000-fold increase in drug resistance.[9]

Taken in sum, the drug resistance mechanisms exhibited by *P. aeruginosa* listed above allow the pathogen to evade treatment by every known class of antibiotic. While modifying the same scaffolds can occasionally provide temporary relief from drug resistance, the same resistance mechanisms appear time and time again. Classes of molecules that operate via novel mechanisms of action would provide a valuable tool to combat *P. aeruginosa* infections and offer a complement to current treatment options.

2.1.2 Narrow-spectrum Therapeutics

With the advent of the human microbiome project in 2008, research into complex microbial communities increased exponentially. Studying these communities has proven challenging, but pioneering research has begun to shed light on the interactions in these complex communities in the context of wound infections, disease states, and the gut, to name a few. For

instance, *P. aeruginosa* has been shown to co-infect wounds with *Staphylococcus aureus*.[10] In mouse models, wounds co-infected with the two bacteria together healed significantly slower than wounds infected with either species alone.[11] Co-infection with these two bacteria have been linked with poor clinical outcomes in cystic fibrosis patients.[12] Narrow-spectrum tool compounds to manipulate one species in the presence of another would provide a new opportunity to study these types of interactions in a controlled, laboratory environment.

In addition to allowing fundamental scientific questions to be answered, narrow-spectrum antibiotics offer an opportunity for improved clinical outcomes. Treatment of an infection with a broad-spectrum antibiotic causes a significant amount of "collateral damage" whereby both the pathogenic and commensal bacteria killed. When treatment ceases, the environment can be freely re-colonized by pathogens. In the case of children with acute upper respiratory infections, broad-spectrum antibiotics were more likely to have a higher rate of adverse effects after treatment, compared to narrow-spectrum.[13]

One application of narrow-spectrum antibiotics that has been fruitful is in the fight against *Clostridium difficile* infections. *C. difficile* causes severe life-threatening diarrheal illness and has a high rate of reoccurrence when traditional antibiotics are used. The emergence of a "hypervirulent" strain has been attributed to a recent increase in number and severity of *C. difficile* infections, making this pathogen ever more challenging and relevant to treat[14] Fidaxomicin is a narrow-spectrum antibiotic with potent activity against *C. difficile*, and is currently on the market to treat this pathogen. Fidaxomicin does not harm intestinal flora, and phase 3 clinical trials showed that the compound gave patients a significantly lower recurrence rate, when compared to vancomycin, presumably due to its potent and narrow-spectrum activity.[15] This success story shows translational value of a potent, narrow-spectrum therapeutic, and has served as inspiration for the work reported herein.

2.1.3 Promysalin Background

Due to unmet medical clinical needs mentioned previously, we were interested in antibiotics that harbored selectivity against Gram-negative pathogens, specifically the *Pseudomonas*. In 2011, a compound was isolated and characterized from a strain of *Pseudomonas putida* named RW10S1 (promysalin) by De Mot and co-workers.[16] The compound showed selectivity against *Pseudomonas* bacteria compared to many other Gram-negative genera and species, and no activity against Gram-positive bacteria was observed. The two most notable antagonistic partners were *Pseudomonas aeruginosa* (see chapter 2.1.1) and *Pseudomonas stutzeri*, a plant pathogen with agricultural significance. Even more interestingly, promysalin showed higher potency against *P. aeruginosa* strain PA14 compared to PAO1. The genomes of these two strains are remarkably similar, and the fact that promysalin displays selectivity for PA14, the more virulent strain of the two, suggests that the compound's mechanism of action could have anti-virulence implications.[17] Hence, a long-term goal of the project would be to determine not only promysalin's mechanism of action, but also its selectivity (Figure 7).

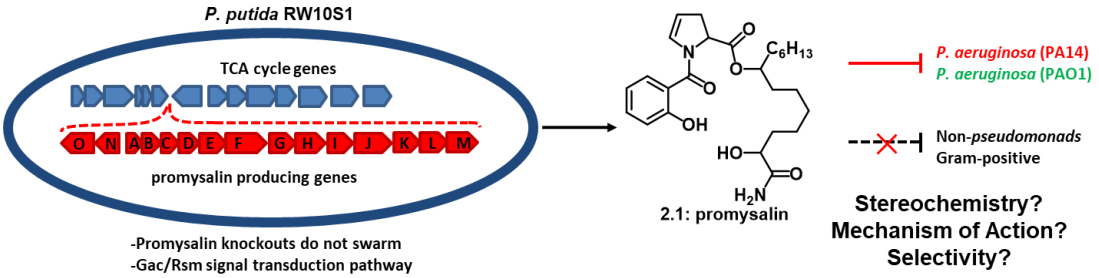

Figure 7. Summary of results from isolation report by De Mot *et al.* and the three key questions that we set out to answer in our studies. The red and green fonts for PA indicate strong and moderate antagonism, respectively.

De Mot and co-workers performed typical fermentation and bioactivity guided fractionation of *P. putida* RW10S1, followed by structural elucidation. They then turned to the bacterial genome to answer questions about promysalin's production and role in the producing strain.[16] A transposon mutant library of RW10S1 was screened for antagonistic activity against *P.*

stutzeri, and the biosynthetic gene cluster of promysalin was identified. Further, De Mot, *et al.* observed that the biosynthetic knockouts were incapable of swarming. In addition, transposon mutants of the gacS gene lacked antagonistic activity as well as swarming capabilities. These results indicated that promysalin is produced under regulation by the Gac/Rsm signal transduction pathway. Sequencing showed that the promysalin gene cluster was located adjacent to the tricarboxylic acid cycle genes, and that this gene cluster was an insertion unique to this strain.[16] Figure 7 depicts a summary of the initial isolation results, and the key questions that we aimed to address with our studies.

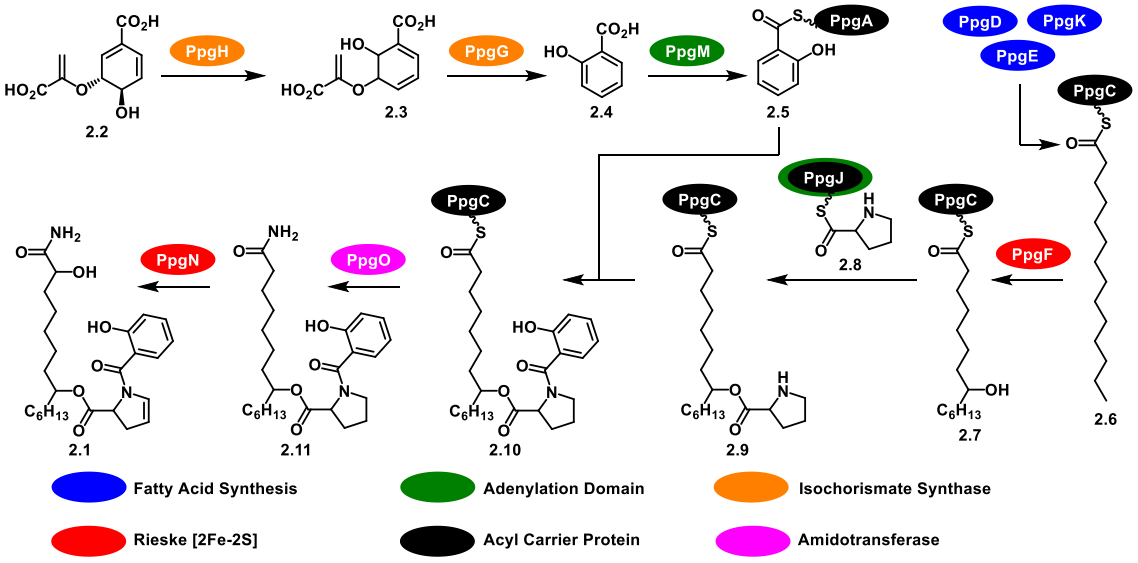

Scheme 4. Biosynthesis of promysalin elucidated by De Mot, *et al.*

In addition to the data presented above, the biosynthesis of promysalin was partially annotated by De Mot and co-workers (Scheme 4). The salicylate precursor, chorismate (**2.2**) undergoes standard biosynthetic transformations to yield salicylate (**2.4**), which is loaded onto an acyl carrier protein, ppgA, via an adenylation domain, ppgM. Concomitantly, typical fatty acid synthesis by ppgD, ppgE, and ppgK yields the myristic acid intermediate loaded onto the acyl carrier protein ppgC (**2.6**). **2.6** then undergoes a hydroxylation by Rieske [2Fe-2S] ppgF, yielding alcohol **2.7**. From there, an activated proline intermediate **2.8**, loaded onto an acyl carrier protein

ppgJ, is condensed with **2.7**, yielding ester **2.9**. Activated salicyl intermediate **2.5** then undergoes a condensation with **2.9**, yielding **2.10**. An amidotransferase, ppgO, then cleaves **2.10** from ppgC, yielding **2.11**, and the final step is a hydroxylation by ppgN. At some point between **2.10** and **2.1**, oxidation of proline occurs; however, the exact timing of this step could not be elucidated. The 4,5-dehydroproline heterocycle is rare among natural products, so enzymes that catalyze proline oxidations at the 4-5 positions are not well-characterized.

While the structure and connectivity of promysalin was identified, the stereochemistry about its three stereogenic centers remained undetermined. From a synthetic standpoint, synthesis of all possible diastereomers/enantiomers, followed by analysis of the spectroscopic and biological data would allow assignment of promysalin's absolute configuration. However, no optical rotation value was reported. The synthetic workload could be simplified while circumventing the issue of the unknown optical rotation by analyzing the biosynthesis. Specifically, ppgJ, which contains an adenylation domain and an acyl carrier domain, is responsible for activating and acylating a proline starting material. By bioinformatic analysis of ppgJ, we identified the Stachelhaus code of DVQFVAHV, which codes for L-proline.[18] This observation, along with no identifiable epimerase domains within the promysalin gene cluster, allowed us to infer that the stereochemistry in the hetereocyclic portion of promysalin was derived from L-proline. This allowed us to confidently synthesize one enantiomeric series of four compounds instead of all eight possibilities.

2.2 Synthesis of Promysalin

2.2.1 Retrosynthesis

At the outset, we knew that we would have to synthesize four diastereomers of the final product, so a retrosynthesis was designed to be as convergent as possible. The retrosynthesis of

promysalin is depicted in Scheme 5. A late-stage esterification reaction gave two equally complex fragments **2.12** and **2.15**. For the heterocyclic fragment **2.12**, the amide bond was created via standard peptide coupling reaction conditions, and the alkene was set from a dehydration reaction sequence, stemming from commercially available *trans*-4-hydroxyproline methyl ester **2.13**, and SEM-protected methyl salicylate **2.14**. Looking to the alkyl alcohol **2.15**, four diastereomers of the compound would need to be synthesized. Therefore, the molecule was broken in half via a metathesis and hydrogenation sequence. Ammonolysis of Evan's chiral auxiliary and stereoselective Davis oxidation yielded precursor **2.16**. Alcohol **2.17** contained another stereocenter, which could be set by a well-known allylation reaction.[19] Using this strategy, varying the stereocenters in fragments **2.16** and **2.17** would provide quick access to all four desired diastereomers of **2.1**.

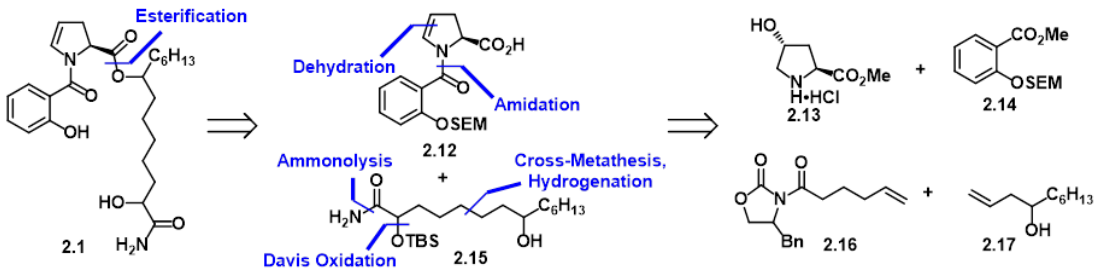

Scheme 5. Retrosynthesis of **2.1**.

2.2.2 Synthesis of Promysalin Acid Fragment

The forward synthesis of acid fragment **(–)-2.12** is depicted in Scheme 6. The phenol of commercially available methyl salicylate (**2.18**) was protected as the corresponding SEM ether (**2.14**) and the methyl ester moiety was then hydrolyzed, yielding unstable acid **2.19**, which had to be carried immediately on to the next step. The amine group of commercially available *trans*-4-hydroxyproline methyl ester hydrochloride **(–)-2.13** was coupled with acid **2.19**, yielding alcohol **(–)-2.20**. Oxidation and purification yielded ketone **(+)-2.21**. The ketone was converted regioselectively to the enol triflate **(–)-2.22**, with no detectable trace of the undesired alkene

regioisomer. Removal of the triflate moiety under palladium catalysis with tributyltin hydride yielded methyl ester **(–)-2.23**. Hydrolysis of the methyl ester yielded acid fragment **(–)-2.12**. This sequence allowed gram-quantities of **(–)-2.12** to be synthesized on demand, which was valuable for future studies.

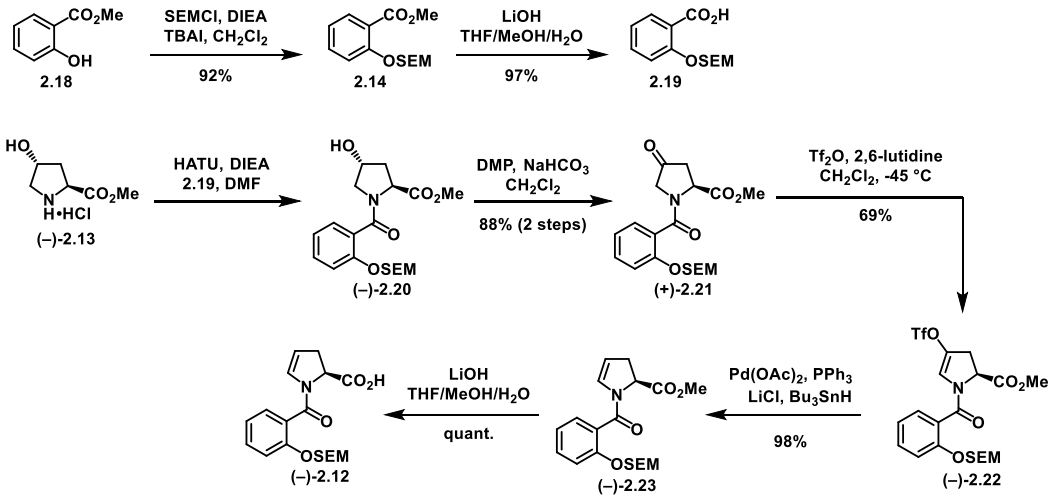

Scheme 6. Synthesis of acid fragment **(–)-2.12**.

2.2.3 Synthesis of alcohol fragment diastereomers

The synthesis of the four requisite alcohol fragments began with commercially available 5-hexenoic acid **2.24** (Scheme 7). Acylation of the two enantiomers of phenylalanine-derived oxazolidinones **(–)-2.25** and **(+)-2.25** yielded **(–)-2.16** and **(+)-2.16**, respectively. Subsequently, Davis oxidation of the sodium enolates, formed with NaHMDS using racemic oxaziridine **(±)-2.26**, yielded enantiomeric compounds **(–)-2.27** and **(+)-2.27** with complete stereocontrol. TBS protection of the resultant alcohols yielded silyl ethers **(–)-2.28** and **(+)-2.28**. The pair of enantiomeric alcohols **(–)-2.17** and **(+)-2.17** were prepared separately by using (*S*) or (*R*)-BINOL in an asymmetric allylation reaction with heptanal.[19] Cross metathesis with a modified Hoveyda-Grubbs catalyst **2.29** (Materia, C711) between **(–)-2.28** or **(+)-2.28** with **(–)-2.17** or **(+)-2.17** yielded the four diastereomeric alcohols **2.30a** – **2.30d**. Hydrogenation of the resultant alkenes

yielded the diastereomeric compounds **2.31a** – **2.31d**, which after ammonolysis with ammonium hydroxide and THF yielded the esterification precursors **2.15a** – **2.15d** (Colleen Keohane, Kyle Knouse, and myself shared material throughout this route to access all four diastereomers).

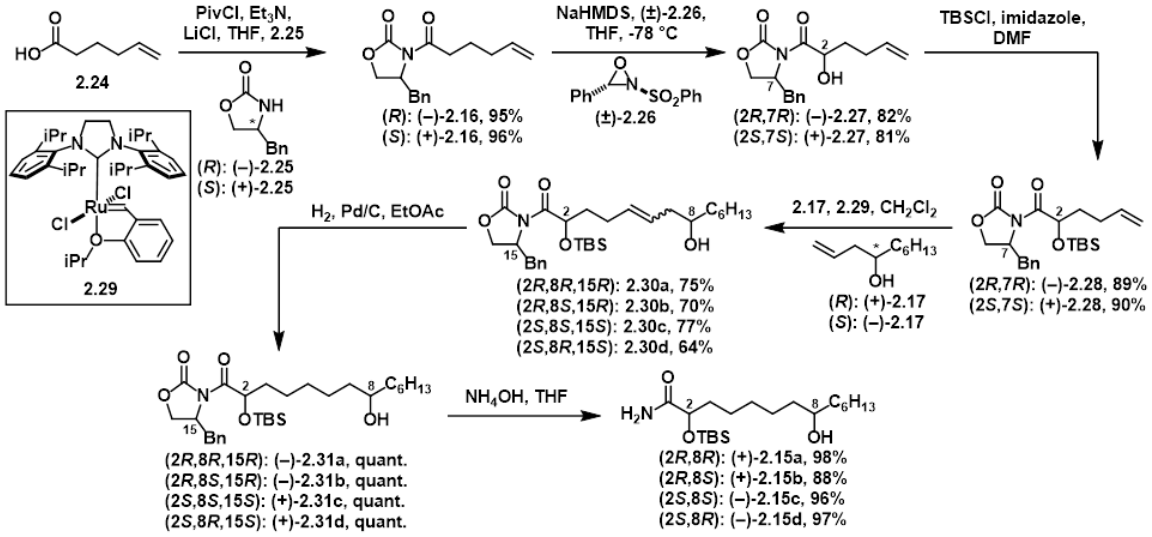

Scheme 7. Synthesis of four diastereomeric alcohols **2.15a** – **2.15d**.

2.2.4 Completion of Promysalin Synthesis

With heterocyclic acid fragment **(–)-2.12** and alcohol diastereomers **2.15a** – **2.15d** in hand, we turned to the fragment coupling esterification step. High and consistent yields for this step were achieved with EDC and DMAP in CH_2Cl_2 and an excess of acid (1.2 – 2.0 equiv.). At this stage we were poised to attempt the final global deprotection of esters **2.32a** – **2.32d**. Literature precedent for SEM removal typically involved acids (Lewis or Bronsted) or a fluoride source (TASF) both requiring long reaction times and/or heat.[20-21] Under these conditions, trace quantities of product were observed and isolated, and decomposition was the major reaction pathway. After many attempts, we found that the SEM and TBS protecting groups could be simultaneously removed with TBAF that was rigorously dried over 3 Å molecular sieves, with anhydrous HMPA as co-solvent, although removal of the co-solvent could never fully be

achieved. Gratifyingly, we then found that DMPU could be used in place of HMPA, which was much easier to remove using standard extraction and chromatography methods and is significantly less toxic (optimization of the deprotection step was carried out by Kyle Knouse, Colleen Keohane, and me. Material was shared and divided for deprotections).

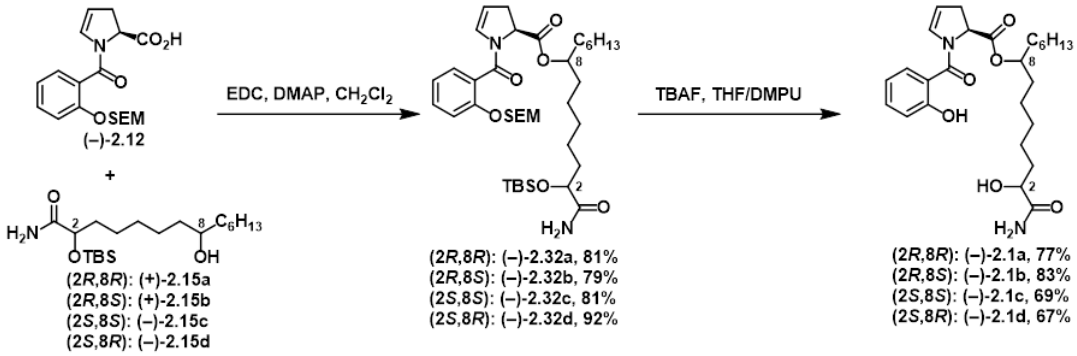

Scheme 8. Esterification and final deprotection steps yielding four promysalin diastereomers **2.1a** – **2.1d**.

2.3 Structure Elucidation of Promysalin

2.3.1 NMR Analysis of Promysalin Diastereomers

With the four promysalin diastereomers **2.1a** – **2.1d** in hand, we first looked to NMR spectroscopy to determine which structure matched the natural product. The NMR peaks were all assigned and mapped onto the same numbering convention utilized by De Mot and co-workers from their initial isolation report.[16] From here, we calculated $\Delta\delta^{1}H$ and $\Delta\delta^{13}C$ for each resonance, the results of which are shown in Table 1. **(–)-2.1a** is by far the best match by NMR. Minor discrepancies can be attributed to differences in resolution between instruments, as well as differences in reference ppm (De Mot *et al.* $CDCl_3$ solvent ^{13}C signal was 77.00 ppm instead of the standard 77.16 ppm value). With no optical rotation reported in the literature, we looked to biological assays to further verify that we synthesized the natural enantiomer. Eventually, private

correspondence with the isolation group confirmed the negative optical rotation sign for the natural product.

		$\delta\Delta^{1}H$					$\delta\Delta^{13}C$			
	Promysalin	**(–)-2.1a**	**(–)-2.1b**	**(–)-2.1c**	**(–)-2.1d**	Promysalin	**(–)-2.1a**	**(–)-2.1b**	**(–)-2.1c**	**(–)-2.1d**
C1	-	-	-	-	-	177.1	-0.2	-0.3	0	0
C2	4.10	0.00	0.00	-0.02	-0.01	71.1	0.1	**0.4**	**0.4**	**0.4**
C3A	1.80	0.00	**-0.03**	**-0.04**	**0.04**	34	0	-0.1	-0.2	0
C3B	1.65	-0.02	0.00	**-0.13**	**-0.06**	-	-	-	-	-
C4	1.43	0.00	**-0.05**	**-0.08**	0.01	24.4	0	0.1	0.1	0.1
C5	1.27	-0.01	-0.01	-0.01	-0.01	28.1	0.1	**0.6**	**0.6**	0.3
C6A	1.43	0.01	**-0.05**	**-0.08**	0.01	24.7	0	0.1	0.1	0
C6B	1.27	-0.01	-0.01	-0.01	-0.01	-	-	-	-	-
C7	1.60	-0.02	**-0.07**	**-0.08**	-0.02	34.1	0	0	-0.1	0.1
C8	5.00	0.00	**-0.04**	**-0.05**	0.01	75.8	0	0	0.1	0.2
C9	1.60	-0.02	**-0.07**	**-0.08**	-0.02	34.4	0	-0.1	-0.1	-0.1
C10A	1.43	0.00	**-0.05**	-0.05	0.01	25.4	0	-0.3	-0.3	-0.1
C10B	1.27	-0.01	-0.01	-0.02	-0.01	-	-	-	-	-
C11	1.27	-0.01	-0.01	-0.02	-0.01	29.1	0	0	-0.1	0
C12	1.27	-0.01	-0.01	-0.02	-0.01	31.7	0	0	0	0
C13	1.27	-0.01	-0.01	-0.02	-0.01	22.5	0	0	0	0
C14	0.87	0.00	0.01	0.00	0.00	14.1	-0.1	-0.1	-0.1	-0.1
C15	-	-	-	-	-	171.2	-0.1	**-0.4**	**-0.4**	-0.1
C16	5.01	0.00	0.00	-0.01	0.00	59.1	0.1	**0.6**	**0.5**	0.1
C17A	3.14	0.00	0.00	-0.01	0.00	33.5	0	0.1	0.1	0
C17B	2.70	0.00	0.01	0.00	0.00	-	-	-	-	-
C18	5.29	0.00	0.01	0.00	0.00	111	-0.1	-0.1	-0.2	-0.1

C19	6.71	0.01	**0.10**	**0.07**	0.01	130.7	0	0.1	0	0
C20	-	-	-	-	-	167.2	0	0.1	0.1	0
C21	-	-	-	-	-	117.6	0	**-0.7**	**-0.6**	0
C22	-	-	-	-	-	157.7	0.1	**1.2**	**1**	0.2
C23	6.99	0.00	0.02	0.01	0.01	117.8	0	0.1	0.1	0.1
C24	7.38	0.00	-0.01	-0.01	-0.02	133.3	0	0.2	0.1	0
C25	6.91	0.00	-0.01	0.00	0.00	119.3	-0.3	-0.3	-0.1	-0.1

Table 1. NMR comparison between the four synthetic promysalin diastereomers and the spectral data from the isolation report by De Mot, *et al.* $\Delta\delta^{1}$H values greater than 0.02 ppm and $\Delta\delta^{13}$C values greater than 0.3 ppm are shown in red font.

2.3.2 Biological Testing of Promysalin Diastereomers **(–)-2.1a** – **(–)-2.1d**

To further validate **(–)-2.1a** as the proposed structure, we turned to biological assays. To this end, inhibitory assays in liquid culture against a panel of *Pseudomonas* strains was undertaken. The compound was bacteriostatic at lower concentrations, so IC_{50} experiments were employed to test the potency of our synthetic material. We found that all synthetic promysalin diastereomers showed no antibiotic activity against *Pseudomonas putida* strains RW10S1 (the producing strain) and KT2440, or *P. fluorescens* WCS365. We found that all promysalin diastereomers showed inhibitory activity against *Pseudmonas aeruginosa* PAO1 and enhanced inhibitory activity against PA14, which was in line with the isolation report. Gratifyingly, the strongest inhibition against *P. aeruginosa* was exhibited by **(–)-2.1a** (Table 2).

	PAO1	PA14	KT2440	RW10S1	WCS365
(–)-2.1a	4.1 µM	0.067 µM	–	–	–
(–)-2.1b	46 µM	6.6 µM	–	–	–
(–)-2.1c	90 µM	22 µM	–	–	–
(–)-2.1d	33 µM	4.3 µM	–	–	–

Table 2. Inhibitory activity of the four synthetic diastereomers against *Pseudomonas* strains. Values are IC_{50} values calculated using curve-fitting software with OD_{600} values. "–" refers to no observation of growth inhibition.

With a growing amount of evidence for **(–)-2.1a** as the structure of promysalin, we next chose to look at other biological phenotypes that the compound elicits and its physical properties. With this information we hoped to gain an appreciation for the compound's role in the rhizosphere, from where it was isolated.

During our inhibition assays, we noticed that aqueous promysalin solutions altered the physical properties of the solvent, and seemed to decrease the surface tension. We dispensed 20 µL drops of compound solutions onto a petri dish and were able to observe a decrease in surface tension, demonstrating that not only **(–)-2.1a**, but all synthetic diastereomers, behaved as surfactants in DMSO/H_2O solution (Figure 8).

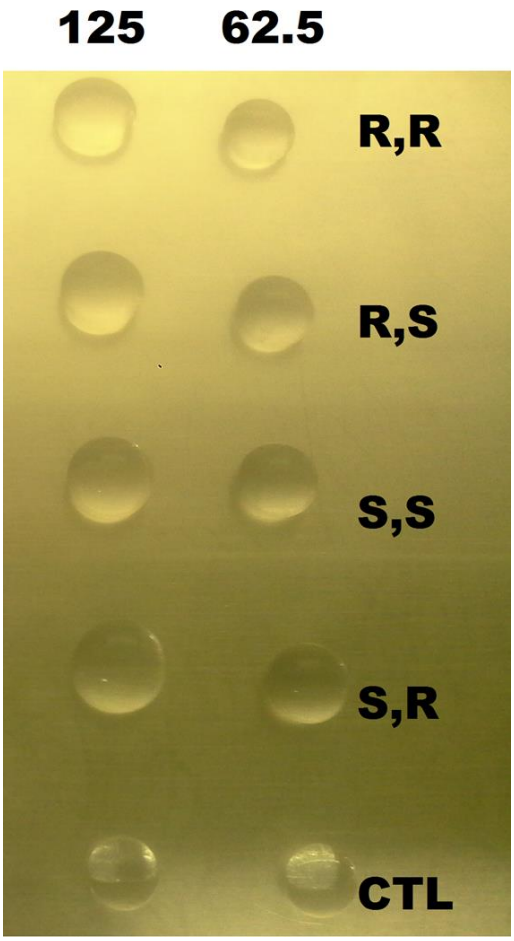

Figure 8. Droplet assay showing that the synthetic compounds are all surfactants. Numbers at the top indicate concentrations in µM diluted in water from a 10% DMSO/H_2O v/v 1 mM stock

solution, and "CTL" refers to negative control solutions with the same DMSO concentration as test solutions.

The physical surfactant property of the compounds was not surprising, considering their ampiphilic structure. Additionally, De Mot *et al.* demonstrated that biosynthetic mutants lacking the ability to produce promysalin were incapable of swarming on solid agar.[16] Swarming bacteria typically produce surfactants when they are exhibiting this phenotype.[22] In light of these results, we next wondered if our synthetic compounds would induce swarming in producing and non-producing *P. putida* strains.

We innoculated 1.0% agar with bacterial overnight culture, covered the spot with a sterile disk containing compound solution and visualized swarming after 24 hours. In all but one case, **(–)-2.1a** – **(–)-2.1d** induced swarming in *P. putida* and *Pseudomonas fluorescens* (Figure 9). The one exception, *P. putida* OUS82, has demonstrated the ability to break down a diverse array of aromatic hydrocarbons, including salicylic acid, which may explain the absence of the swarming phenotype.[23]

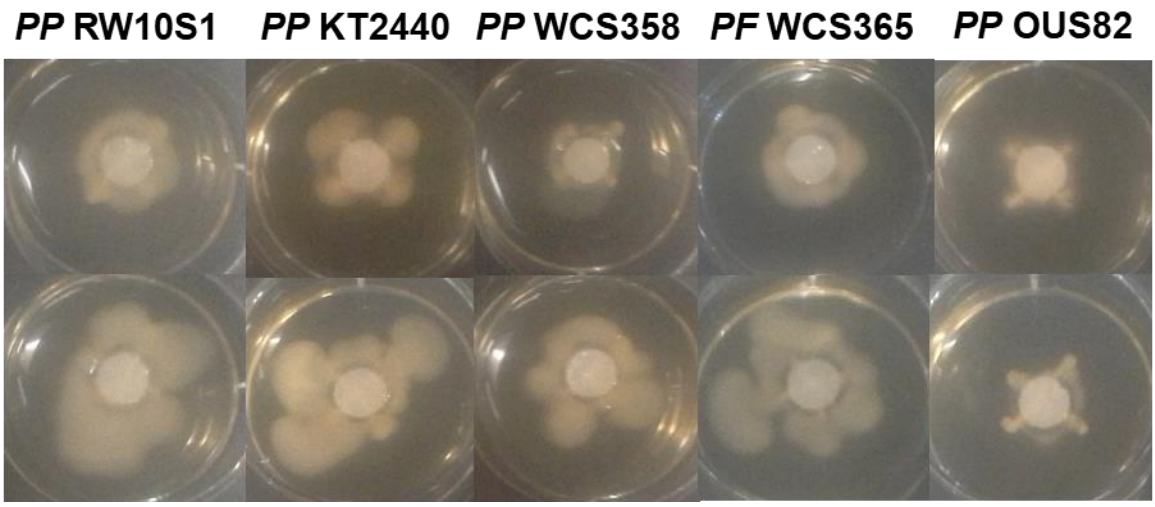

Figure 9. Swarming motility induced by synthetic promysalin **(–)-2.1a**. The same swarming phenotypes were also observed for **(–)-2.1b**, **(–)-2.1c**, and **(–)-2.1d** (data not shown).

2.3.3 Observation of Novel Promysalin-Induced Phenotypes

During our swarming experiments, we noticed a green phenotype developing in the agar plates of *P. putida* strain WCS358 when they were left at room temperature for two days. This green phenotype was abolished stereospecifically by **(–)-2.1a**, and not any of the other synthetic diastereomers. We next visualized the plates under UV light, and did not observe any fluorescence. However, *P. putida* KT2440 exhibited a UV-fluorescent phenotype, which was inhibited stereospecifically by **(–)-2.1a** (Figure 10). These new phenotypes seem to be more than just a consequence of promysalin's surfactant nature. If that were the case, all diastereomers would elicit the same phenotype inhibition.

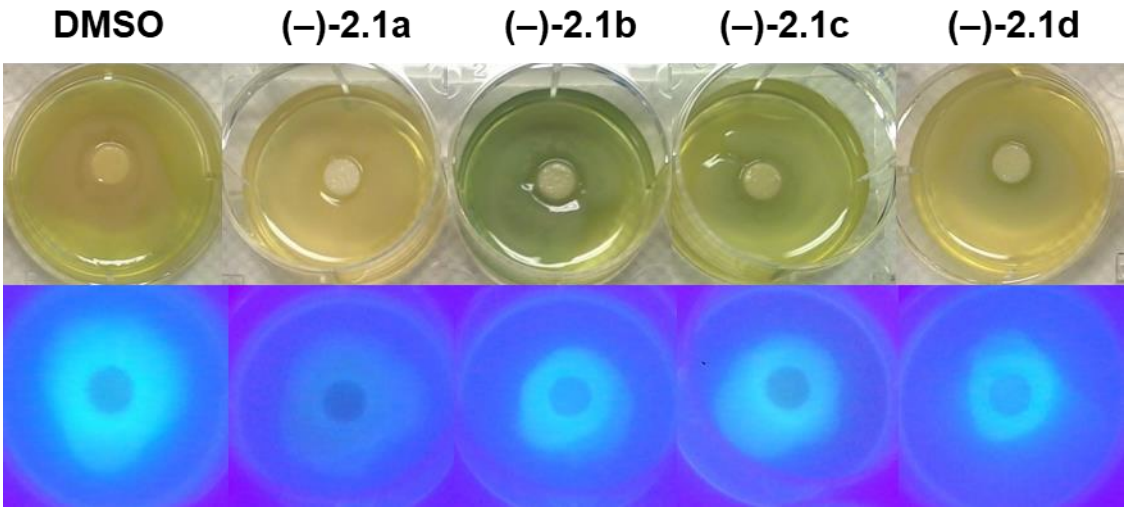

Figure 10. Newly observed phenotypes induced by promysalin in our studies. (top row) *P. putida* WCS358 swarming plates visualized after two days at 30 °C. (bottom row) *P. putida* KT2440 UV fluorescent phenotypes visualized after two days at 30 °C.

2.3.4 Conclusions

Our work in elucidating the structure of promysalin demonstrates the power of diverted total synthesis in a biological frame of mind. Without an optical rotation value, synthesis alone would have required us to synthesize all eight possible diastereomers of promysalin and isolate the material from the producing strain. However, our bioinformatic analysis at the outset allowed

us to cut the amount of synthetic workload in half and make an educated hypothesis about one of promysalin's stereogenic centers. Biological testing then allowed us to confirm this structural hypothesis.

In addition to elucidating the structure of promysalin, our synthetic route allowed us access to quantities of material to test further hypotheses about the compound's role in the rhizosphere. The diastereomers that did not match the natural product served as important negative control compounds, which possess similar physical and chemical properties to the natural product but lack the potency of **(–)-2.1a** against *P. aeruginosa*.

We demonstrated this first by showing that all synthetic diastereomers behave as surfactants in solution and are capable of inducing swarming motility in all but one strain of *P. putida* and *P. fluorescens* tested. This unambiguously showed that promysalin itself is directly responsible for the induction of swarming motility in the producing strain, and not a down- or upstream effect caused by genetic manipulations.

In addition to our swarming results, our experiments led us to discover new phenotypes elicited by promysalin for the first time: the inhibition of a green phenotype in one strain of *P. putida* (WCS358) and a UV fluorescent phenotype in another (KT2440). While a fluorescent yellow-green phenotype in strain WCS358 is typically associated with the production of pseudobactin 358, the phenotype in our case was not fluorescent.[24] In the case of KT2440, a fluorescent phenotype was abolished in the presence of promysalin, only with the natural stereochemistry. This strain produces pyoverdine as its only siderophore, to which we attribute the fluorescent phenotype.[25]

These results, taken in sum, allowed us to make more hypotheses about promysalin's mode of action, which set the stage for the next phase of the project. The inhibition of pyoverdine made us wonder if promysalin itself was behaving as a siderophore. The stereospecificity of the

newly elicited phenotypes in *P. putida* as well as *P. aeruginosa* inhibition made us hypothesize how promysalin's structure was tailored for its bioactivity. Finally, our synthetic route made us confident that we could efficiently access analogs to test our hypotheses.

2.4 Synthesis of Promysalin Analogs

2.4.1 Promysalin Analog Design

Our results from the first phase of the project generated new questions that synthesis could answer. First, we wondered how promysalin's structure and conformation influenced its bioactivity. Since we saw inhibition of siderophore production in *P. putida* KT2440, we hypothesized that promysalin may be acting as a siderophore itself, or a mimic of an iron-chelated small molecule. To this end, we turned to molecular modeling to see if this could offer a glimpse into the lowest-energy conformations of our synthetic promysalin diastereomers. When the correct stereochemistry of promysalin was modeled and minimized, we consistently observed the conformation depicted in Figure 11. This conformation was not observed when any of the other diastereomers **2.1b** – **2.1d** were modeled in the same fashion. This, in line with our previous results, demonstrated that the stereochemical array matching the natural product had unique structural features with biological implications. We hypothesized that a key hydrogen bond between the hydroxyl, phenol, and ester moieties had biological importance, and turned to synthesis to perturb these interactions.

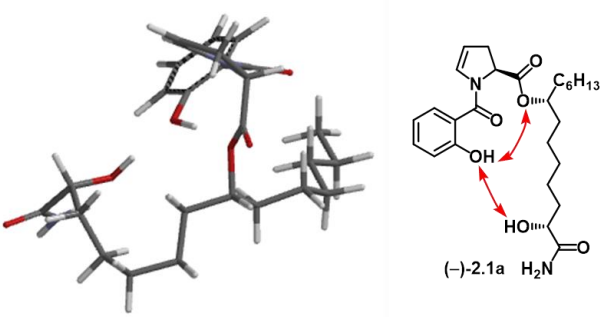

Figure 11. Minimized structure of **(–)-2.1a** from Spartan. Red arrows indicate key hydrogen bond interactions we sought to probe via analog synthesis.

In addition to perturbing the interactions suggested by modeling, we sought to probe key structural features of promysalin that make the molecule unique. We were interested in the importance of the 4,5-dehydroproline heterocycle, which is rare among natural products. We wondered if the ene-amide moiety was a covalent trap for promysalin's target, in which case saturation should remove all inhibitory activity. We divided our analog synthetic campaign into three groups, whereby each of promysalin's structural motifs were targeted: salicylate, proline, and myristic acid. Figure 12 details the analog design as well as more specific questions we set out to answer.

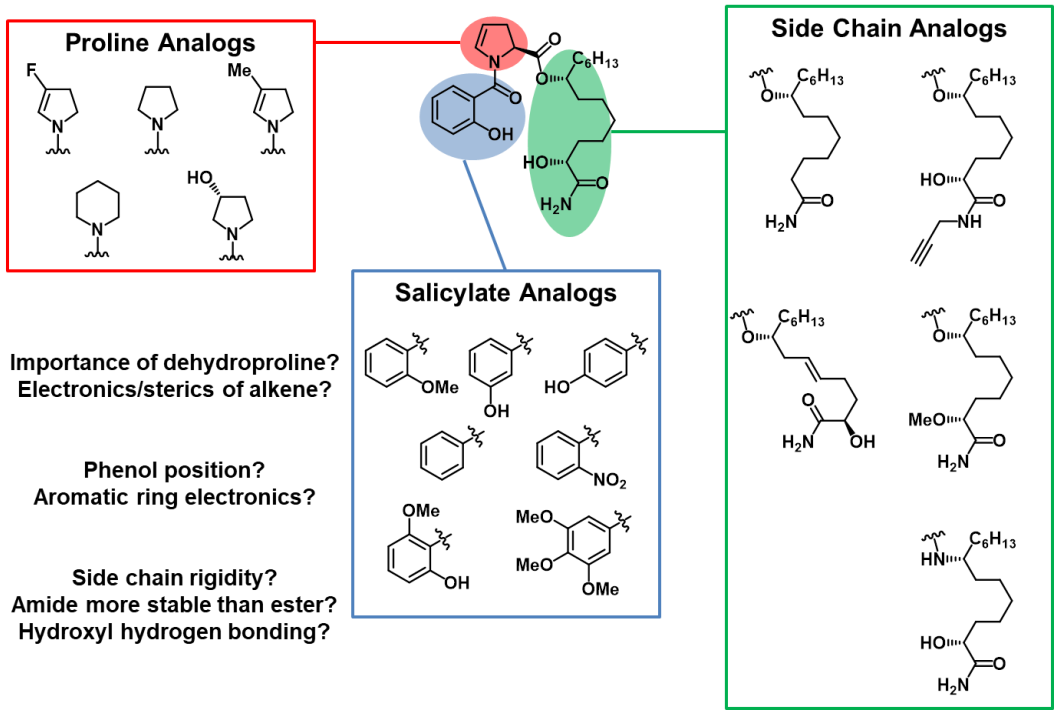

Figure 12. Analog design and grouping according to structural motif that was modified in each series. Key questions that were addressed with specific analogs are listed on the left, grouped by analog series.

One more key question that we sought to answer through our analog synthetic studies was where a photoaffinity handle could be installed without sacrificing potency. The three key places we thought this could be appended were onto the phenol or hydroxyl oxygens, or the primary amide nitrogen. Hence, by methylating the phenol or hydroxyl oxygen, and adding a propargyl group to the primary amide, this question could be answered.

2.4.2 Promysalin Proline Analog Synthesis

The proline analog series manifested itself in two different approaches. First, synthetic handles from our route were taken advantage of wherever possible. The enol triflate from our synthesis was utilized in cross-coupling reactions to install substituents at the 4-position of the proline ring (**(+)-2.33** and **(–)-2.34**). The hydroxyl group from hydroxyproline could be protected and maintained for hydroxy analog **(–)-2.35**. Additionally, by utilizing simplified building blocks

in lieu of hydroxyproline from the outset of the synthesis, we could access saturated versions of heterocylces, such as proline **(–)-2.36** and piperidine **(+)-2.37**.

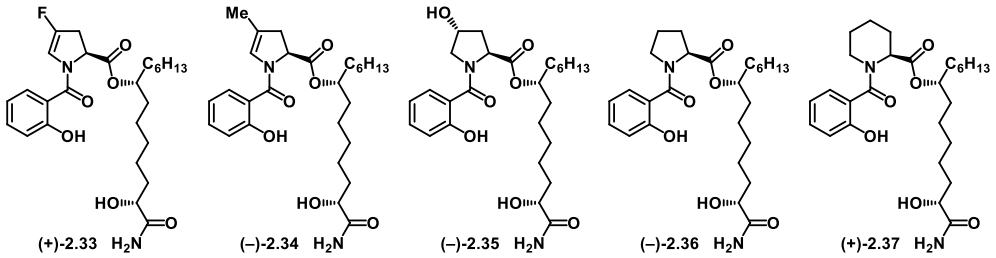

Figure 13. Structures of proline analog targets.

The synthesis of fluorine analog **(+)-2.33** is depicted in Scheme 9. Enol triflate **(–)-2.22** (see page 23) was converted to stannane **(–)-2.38**. Fluorination of stannane **(–)-2.38** was first attempted with xenon difluoride, silver triflate, and catalytic 2,6-di-*tert*-butyl-4-methylpyridine.[26] This reaction, while successful in forming desired product **(–)-2.39**, only did so in 29% yield, along with a myriad of side-products. This reaction is proposed to proceed by radical intermediates, which can easily lead to many undesirable side reactions. Alternatively, the much simpler reaction with Selectfluor in acetonitrile cleanly yielded fluoride **(–)-2.39** in good yield (59%). From there, hydrolysis of the methyl ester yielded **(–)-2.40**. Esterification of the resultant acid with our previous synthetic intermediate **(+)-2.15a** with EDC/DMAP yielded **(–)-2.41**, which after our previously developed deprotection conditions, gave fluorine analog **(+)-2.33**.

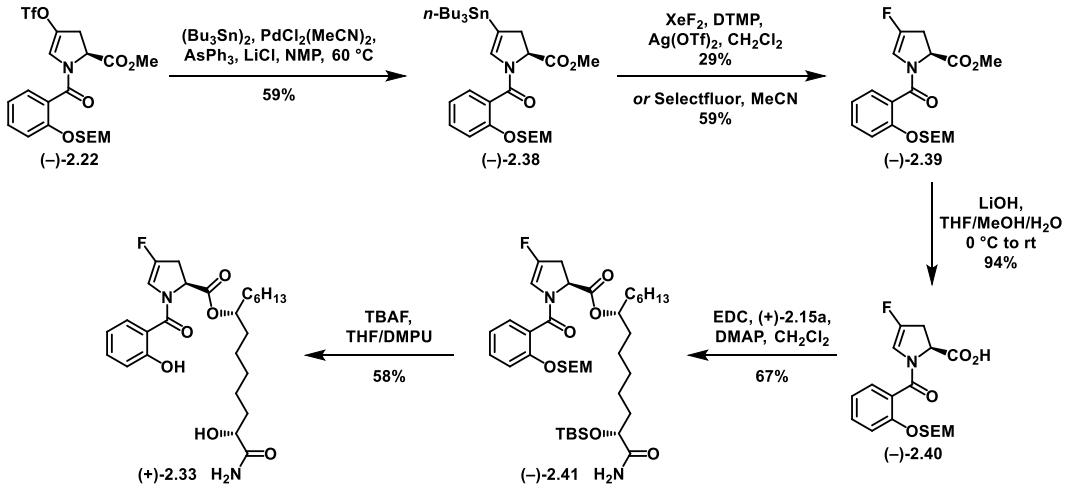

Scheme 9. Synthesis of fluorine analog **(+)-2.33**.

The synthesis of methyl analog is depicted in Scheme 10, and began from triflate intermediate **(–)-2.22**, which was methylated via a Suzuki reaction with methylboronic acid, yielding **(–)-2.42**. Hydrolysis, esterification (Shiina conditions), and deprotection yielded 4-methyldehydroproline analog **(–)-2.34**.

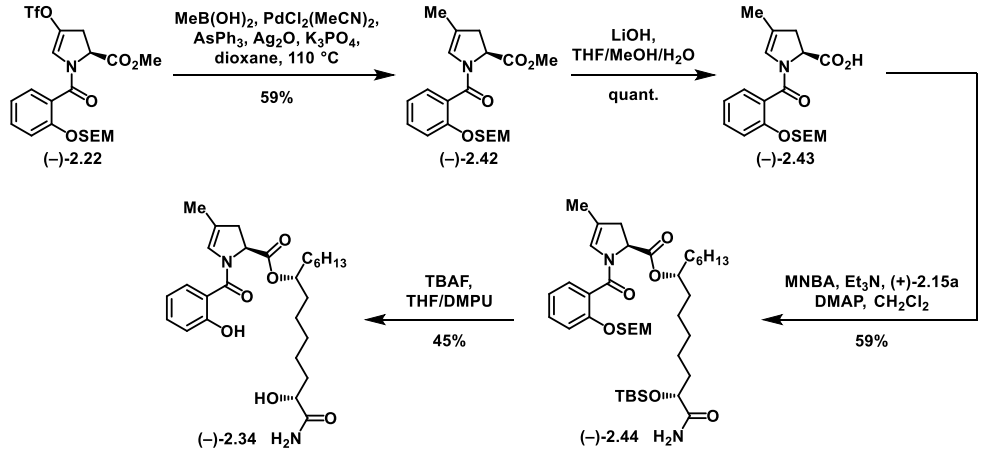

Scheme 10. Synthesis of 4-methyldehydroproline analog **(–)-2.34**.

Next, we leveraged another synthetic intermediate, **(–)-2.20**, to access 4-hydroxyproline analog **(–)-2.35**, the synthesis of which is shown in Scheme 11. TBS protection of the hydroxyl group of **(–)-2.20** yielded silyl ether **(–)-2.45**, which was then subjected to the typical hydrolysis, esterification, and deprotection conditions, leading to hydroxyproline analog **(–)-2.35**. The final

deprotection reaction required five extra equivalents of TBAF for the additional silyl group to proceed to completion.

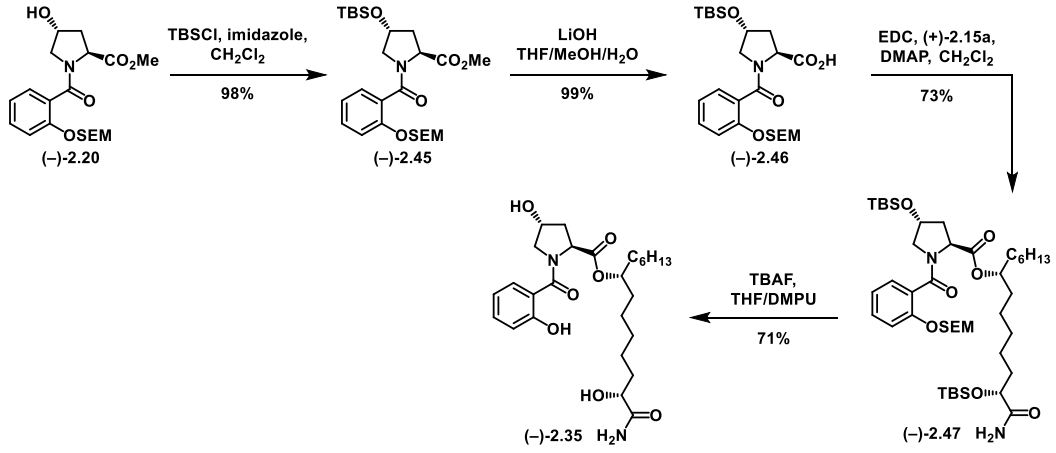

Scheme 11. Synthesis of hydroxyproline analog **(–)-2.35**.

We next targeted the saturated proline and piperidine analogs **(–)-2.36** and **(+)-2.37**, respectively, the details of which are depicted in Scheme 12 (piperidine analog was synthesized by Colleen Keohane). Commercially available proline methyl ester hydrochloride **(–)-2.48** and piperidine methyl ester hydrochloride **2.53** were each coupled with MOM-protected salicylic acid (**2.49**) via HATU-mediated peptide coupling. The typical hydrolysis and esterification conditions were then performed, yielding protected analogs **(–)-2.52** and **(+)-2.56**. At this stage, we utilized acidic global deprotection conditions (AcCl, MeOH) to cleave both the MOM and TBS ethers, yielding analogs **(–)-2.36** and **(+)-2.37**.

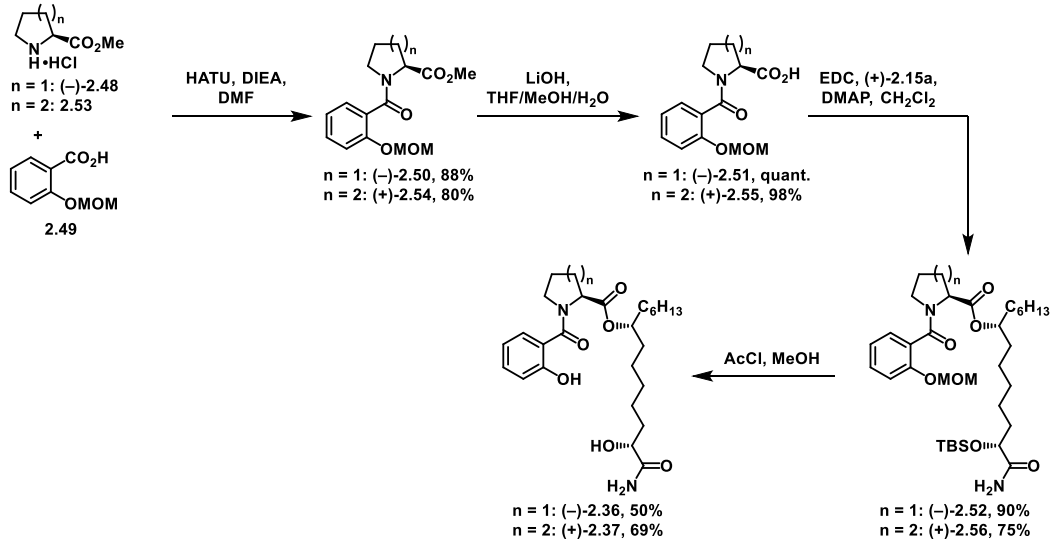

Scheme 12. Synthesis of proline analog **(–)-2.36** and piperidine analog **(+)-2.37**.

2.4.3 Promysalin Salicylate Analog Synthesis

The next analog series involved modifying the salicylate portion of promysalin. The full list of the salicylate analog series is depicted in Figure 14.

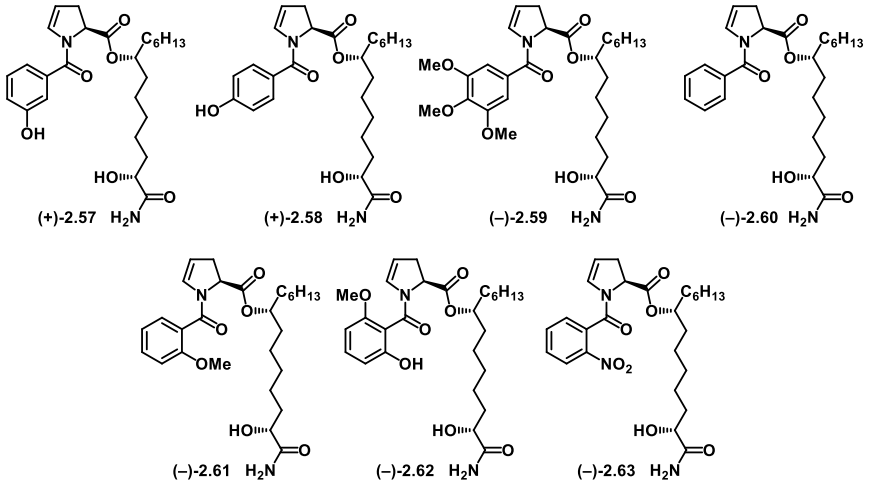

Figure 14. Structures of salicylate analog targets.

The synthesis of the first two analogs, **(+)-2.57** and **(+)-2.58**, began by protecting the two possible regioisomers of methyl salicylate **2.64** and **2.70** as their corresponding SEM ethers, **2.65**

and **2.71**, respectively. From here, the same steps were implemented as in our original synthesis, except for the final esterification, where Shiina esterification was employed instead of EDC, culminating in analogs **(+)-2.57** and **(+)-2.58** (Colleen synthesized analog **(+)-2.57** and I synthesized **(+)-2.58**).

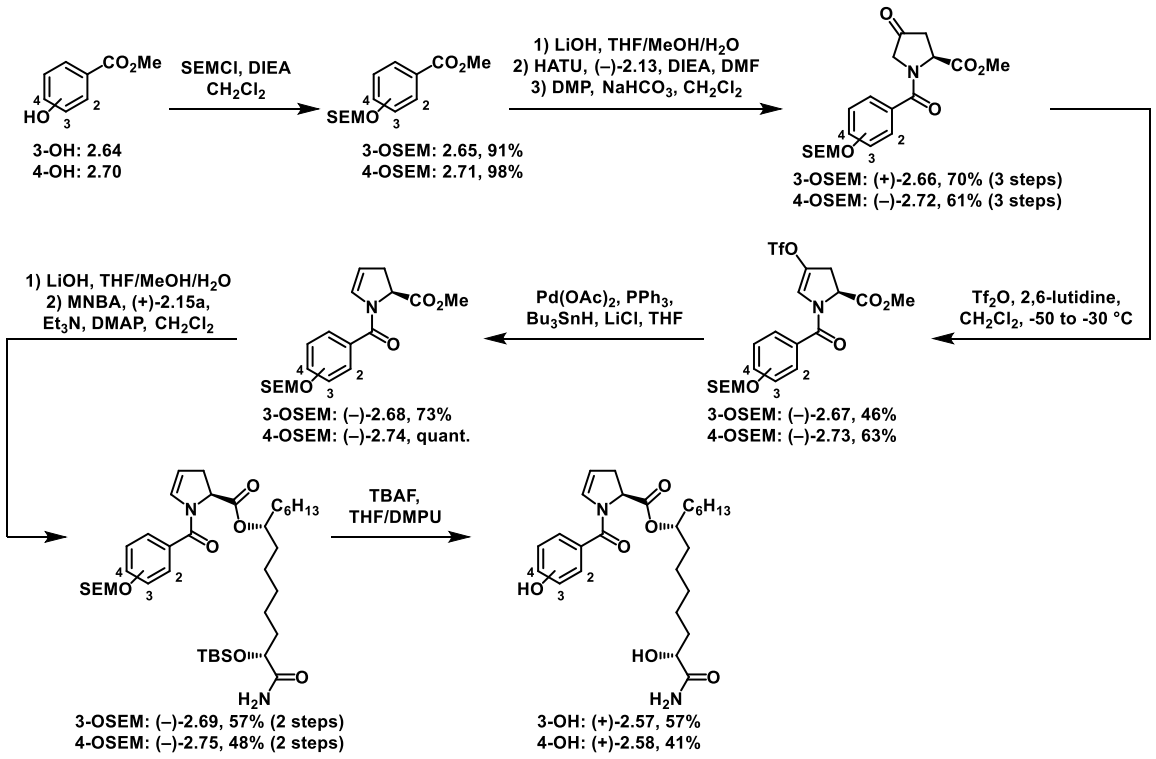

Scheme 13. Synthesis of analogs **(+)-2.57** and **(+)-2.58**.

The synthesis of the next two analogs, **(–)-2.59** and **(–)-2.60**, were simplified due to the lack of a phenol in the final products. Trimethoxy analog **(–)-2.59** (synthesized by Kyle Knouse) began from known alcohol **(–)-2.76**, and benzoyl analog **(–)-2.60** began from known ketone **(–)-2.82**.[27] The same synthetic steps as promysalin were then followed, except the final deprotection step required no DMPU, due to the absence of SEM (see Scheme 14 and Scheme 15).

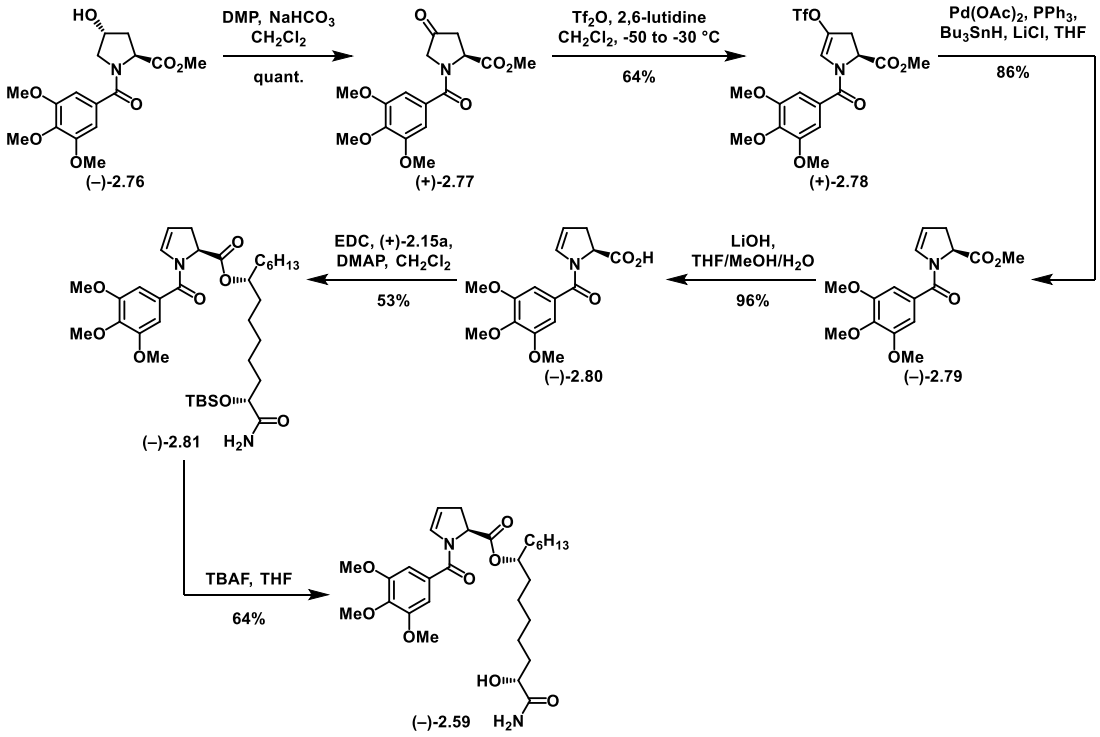

Scheme 14. Synthesis of trimethoxy analog **(–)-2.59**.

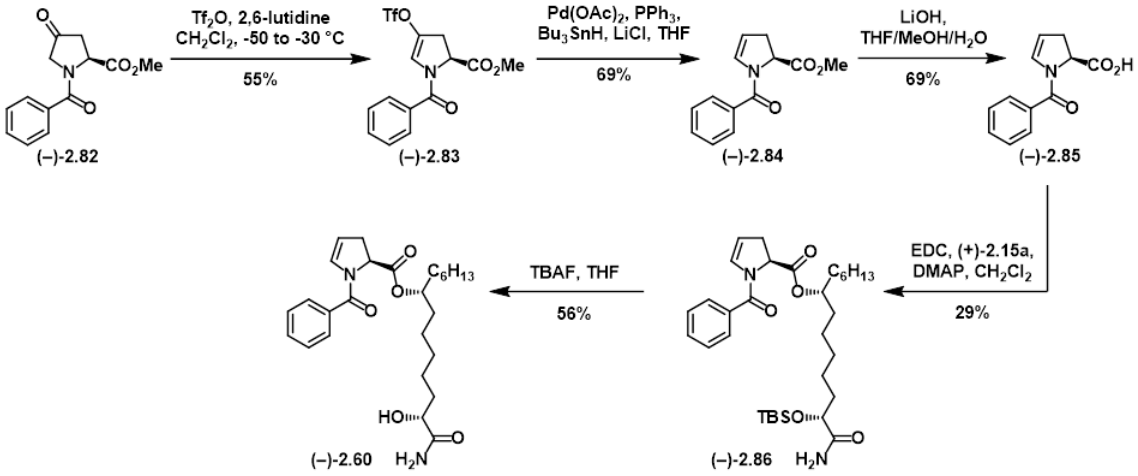

Scheme 15. Synthesis of benzoyl analog **(–)-2.60**.

We next turned to methoxy analog **(–)-2.61**. To be more convergent, this analog was accessed from previous intermediate **(–)-2.23**. Deprotection of the SEM ether yielded **(–)-2.86**, which was methylated to give **(–)-2.87**. Typical hydrolysis and esterification yielded **(–)-2.89**,

which was deprotected with TBAF in THF, yielding methyl ether analog **(–)-2.61** (see Scheme 16).

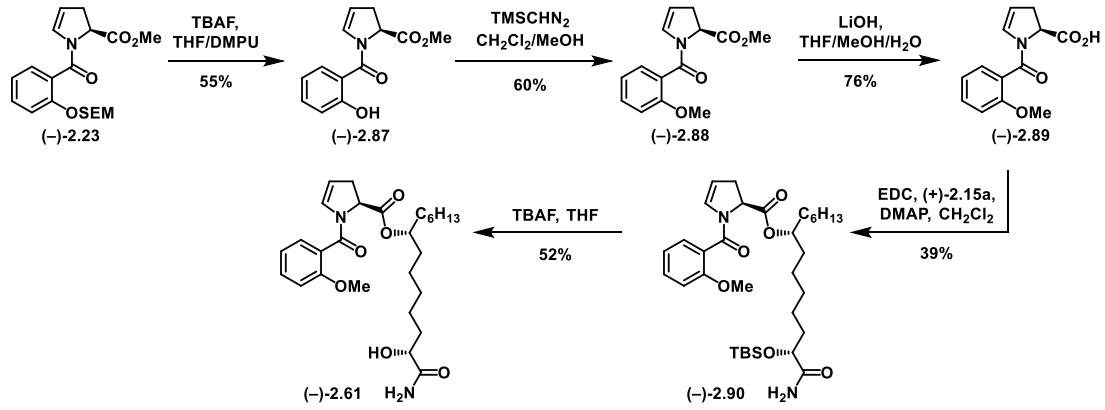

Scheme 16. Synthesis of methyl ether analog **(–)-2.61**.

We next synthesized a salicylate analog with an additional methoxy substituent, **(–)-2.62**, to increase electron density on the aromatic ring and potentially increase the phenol's hydrogen bond donor capabilities. This began with the double SEM-protection of commercially available methyl 2,6-dihydroxybenzoate (**2.91**, Scheme 17), yielding **2.92**. Hydrolysis of this intermediate required KOH and elevated temperatures, due to steric hinderance. From there, the typical promysalin synthesis steps led to acid intermediate **(–)-2.96**. Shiina esterification yielded protected ester **(–)-2.97**. Our SEM deprotection conditions then yielded the mono-protected intermediate **(–)-2.98**. The resultant phenol was selectively methylated in the presence of the hydroxyl using $TMSCHN_2$/MeOH, yielding methyl ether **(–)-2.99**. Another round of deprotection then yielded methoxy-substituted analog **(–)-2.61**.

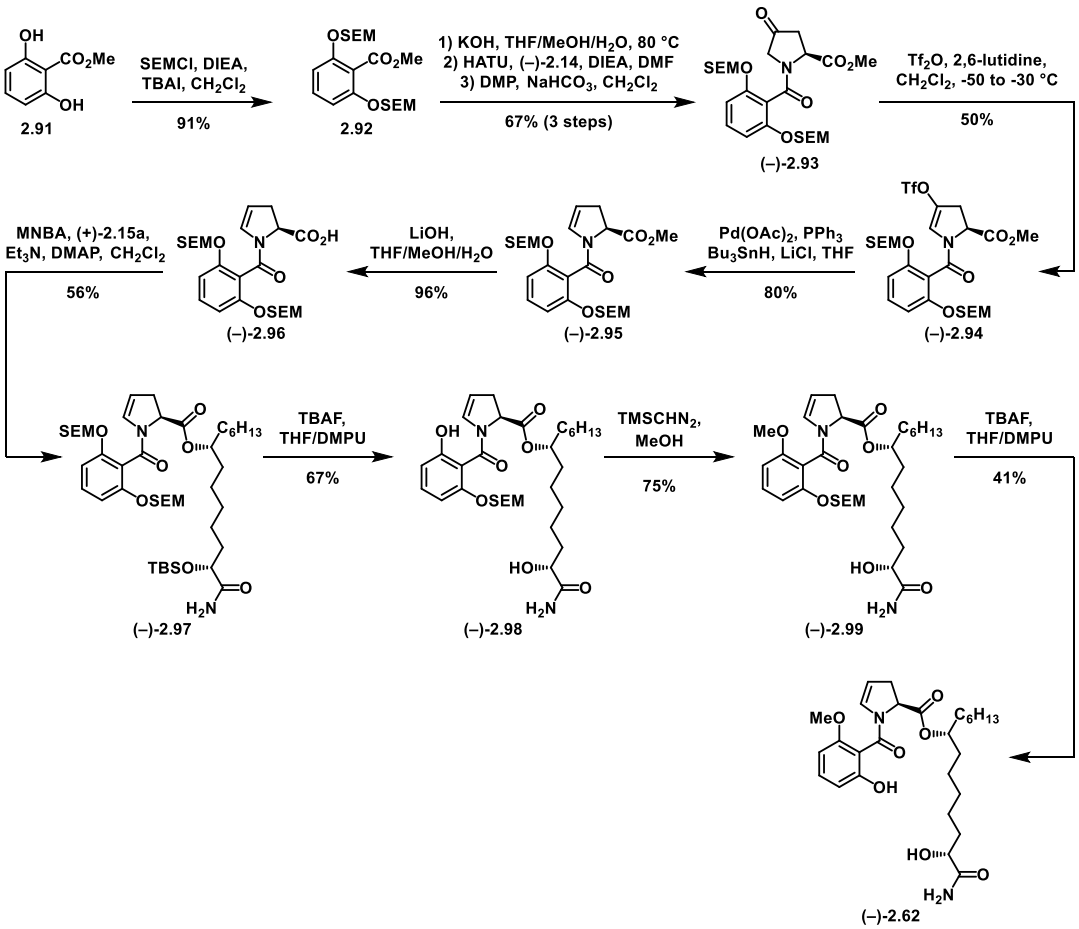

Scheme 17. Synthesis of methoxy-substituted analog **(–)-2.62**.

The final salicylate analog was nitro compound **(–)-2.63**, the synthesis of which is shown in Scheme 18. This compound required a different approach, as the electron poor *ortho*-nitro aryl carbonyl moiety was not stable to base hydrolysis. Therefore, the acid precursor to esterification had to be accessed via oxidation of an alcohol, instead of methyl ester hydrolysis. The synthesis proceeded from known pyrrolidone **(+)-2.100**.[28] Deprotonation with sodium hydride followed by acylation with potassium iodide and 2-nitrobenzoyl chloride yielded amide **(–)-2.101**. The lithium enolate formed by LiHMDS was trapped with Comins' reagent to form an unstable enol triflate, which was immediately removed with palladium and tributyltin hydride, yielding dehydroproline **(–)-2.102**. Removal of the TBS ether with CSA yielded primary alcohol **(–)-2.103** in quantitative yield. The oxidation of the resultant alcohol to carboxylic acid was non-trivial. Chromium

oxidants (PCC, Jones) led to rapid decomposition, and a 2-step Perikh-Doering Pinnick oxidation sequence occasionally gave product, but in very low yield (<15%). A multitude of products were observed in the Pinnick oxidation, likely due to side reactions with the generated hypochlorous acid. Undeterred, we found that oxidation with TPAP-NMO•H_2O consistently yielded acid **(–)-2.104** in modest yield.[29] From there, Shiina esterification yielded ester **(–)-2.105**, and deprotection under acidic conditions (AcCl, MeOH) yielded nitro analog **(–)-2.63**.

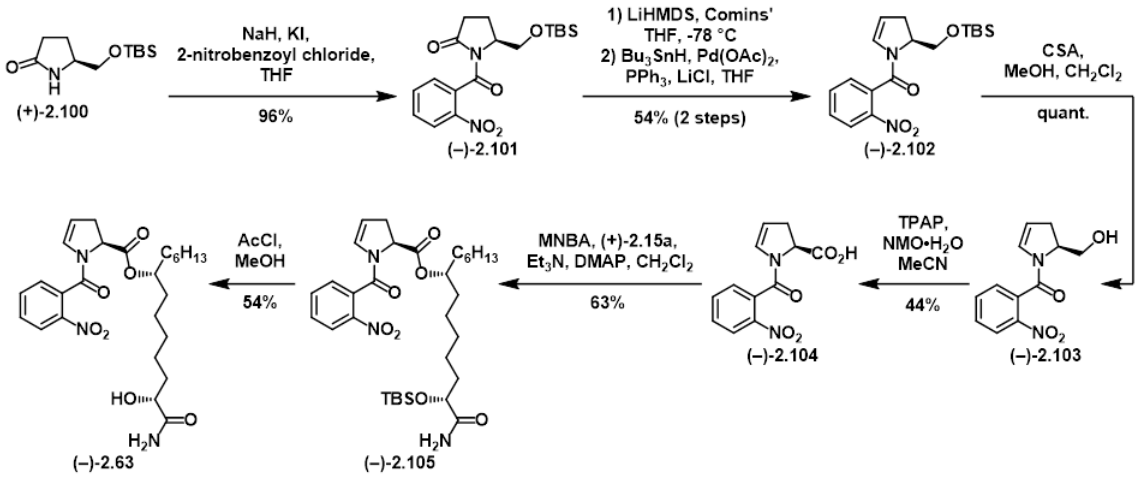

Scheme 18. Synthesis of nitro analog **(–)-2.63**.

2.4.4 Promysalin Side Chain Analog Synthesis

The next series of analogs involved modifications to the myristic acid side chain of promysalin. The structures of the analogs are depicted in Figure 15. All analogs except the simplified **(–)-2.106** deshydroxyl analog stemmed from previously synthesized promysalin intermediates and utilized our reliable synthetic steps whenever possible.

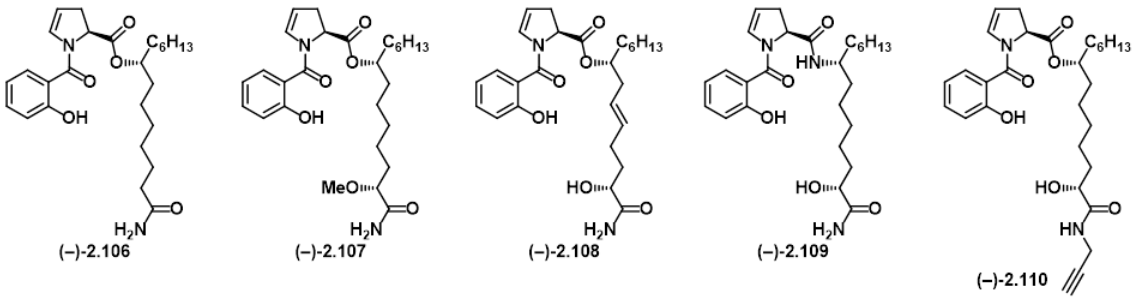

Figure 15. Structures of side chain analog targets.

The synthesis of deshydroxyl analog **(–)-2.106** is shown in Scheme 19. 5-hexenoic acid (**2.24**) was converted to hex-5-enamide (**2.111**), and from there the same synthetic steps as promysalin were followed.

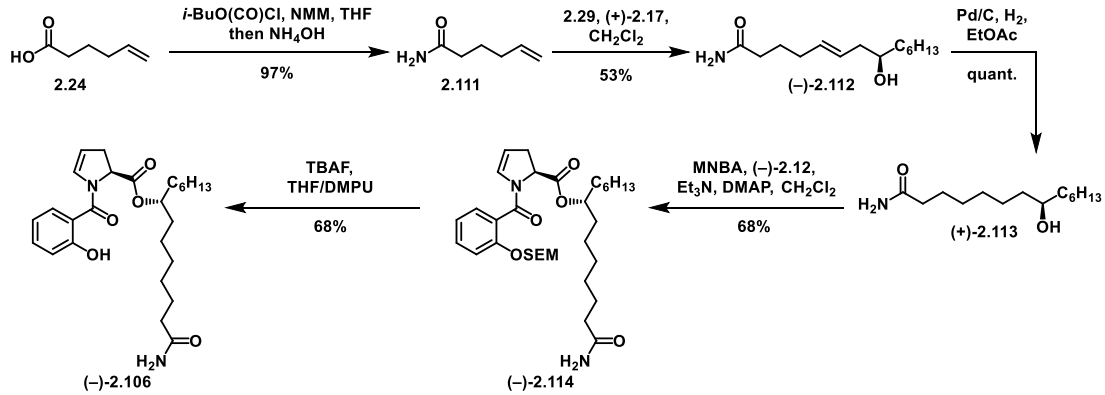

Scheme 19. Synthesis of deshydroxyl analog **(–)-2.106**.

The next analog contained a methyl ether in place of the side chain hydroxyl, and the synthesis of which is depicted in Scheme 20. Starting from previous intermediate **(–)-2.27**, methylation was accomplished with Me_3OBF_4, yielding **(–)-2.115**. From there, typical steps yielded alcohol **(+)-2.118**, which underwent esterification under Shiina conditions, yielding **(–)-2.119**, followed by deprotection to methyl ether analog **(–)-2.107** (synthesized by myself with the help of Sierra Williams).

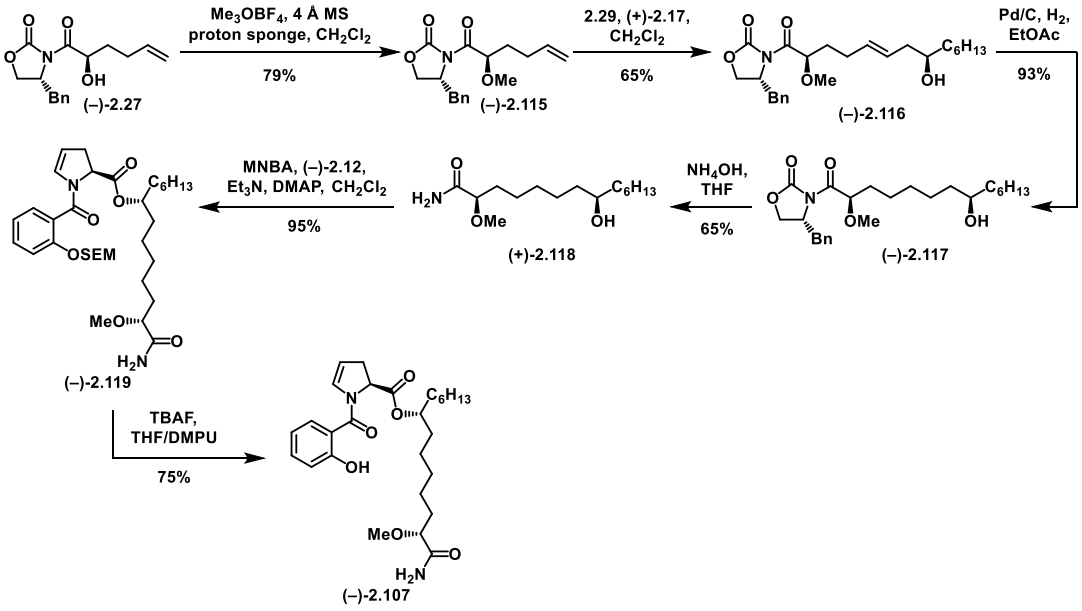

Scheme 20. Synthesis of methyl ether analog **(–)-2.107**.

The synthesis of alkene analog **(–)-2.108** was straightforward (Scheme 21), which involved simply skipping the hydrogenation step of the promysalin synthesis, and Shiina esterification in place of EDC.

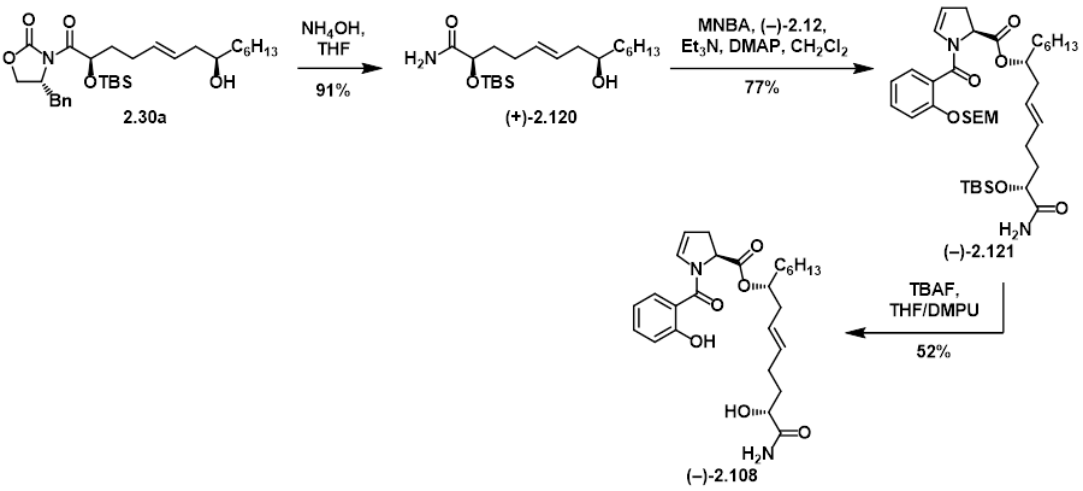

Scheme 21. Synthesis of alkene analog **(–)-2.108**.

The synthesis of amide analog **(–)-2.109** is depicted in Scheme 22, and commenced from promysalin intermediate **2.30b**. Mitsunobu reaction with DPPA as an azide source inverted the

alcohol stereocenter, yielding azide **(–)-2.122**. Hydrogenation reduced both the alkene and azide, yielding amine **(–)-2.123**. Ammonolysis yielded primary amide **(+)-2.124**. Amide coupling with EDC and HOBt yielded protected amide **(–)-2.125**, and global deprotection then provided amide analog **(–)-2.109**.

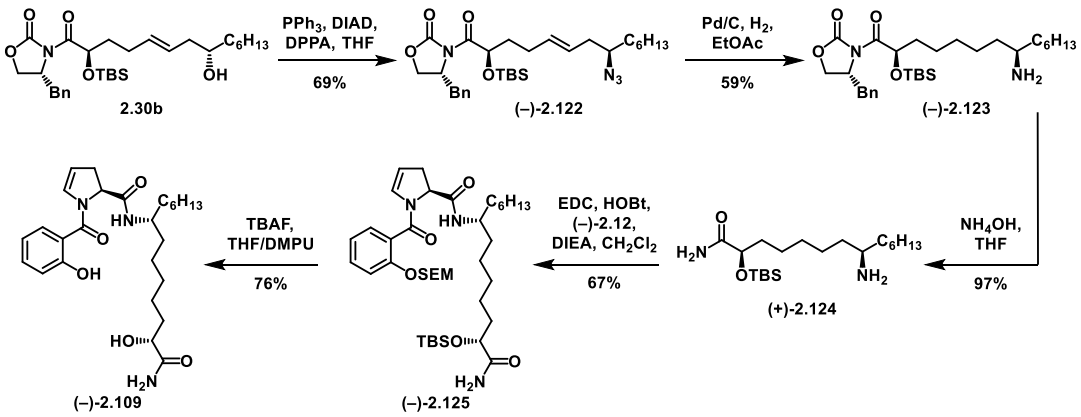

Scheme 22. Synthesis of amide analog **(–)-2.109**.

The synthesis of propargyl analog **(–)-2.110** is depicted in Scheme 23 and began with promysalin intermediate **(–)-2.31a**. Transamidation with propargylamine and trimethylaluminum yielded propargylamide **(+)-2.126**. Shiina esterification with acid **(–)-2.12** followed by global deprotection yielded propargyl analog **(–)-2.110**.

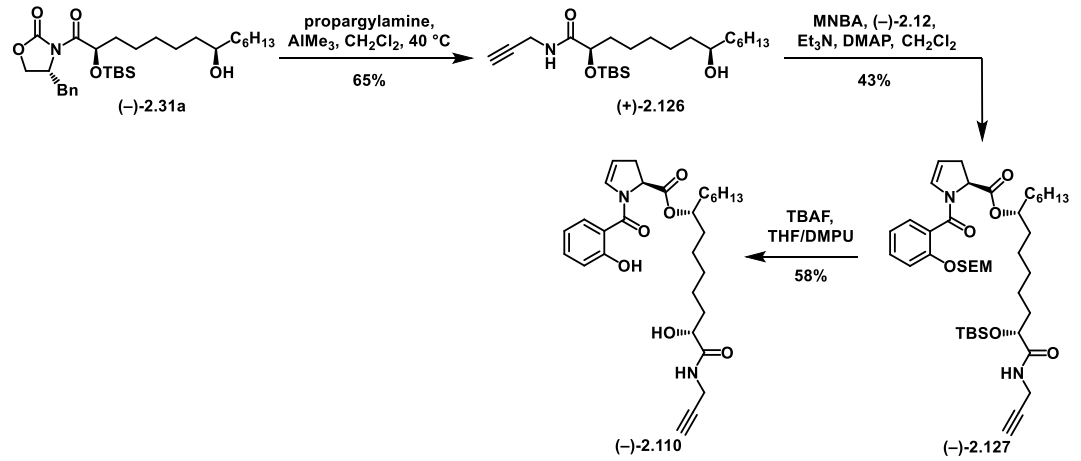

Scheme 23. Synthesis of propargyl analog **(–)-2.110**.

2.4.5 Synthesis of "Pro-drug" Analogs

During our initial synthetic studies of promysalin, we noticed that the final compound was not stable under acidic conditions. After careful chromatographic separation of the degradation products and spectroscopic analysis, we discovered that promysalin underwent a cyclization reaction, depicted in Figure 16. This made us question if the isolated structure of promysalin was a pro-drug, and if the cyclized products were active *in vivo*. This hypothesis was supported by the observation that *P. aeruginosa* biofilms are acidic.[30] We also postulated that an esterase enzyme harbored by *P. aeruginosa* could hydrolyze the ester moiety and release the corresponding acid and alcohol. To this aim, we synthesized diol **(+)-2.129** and methyl ester **(–)-2.87** (in lieu of the acid for cell permeability purposes). Methyl ester **(–)-2.87** was available from an earlier analog synthesis and diol **(+)-2.129** was prepared in one step from promysalin synthesis intermediate **(+)-2.15a** (Figure 16).

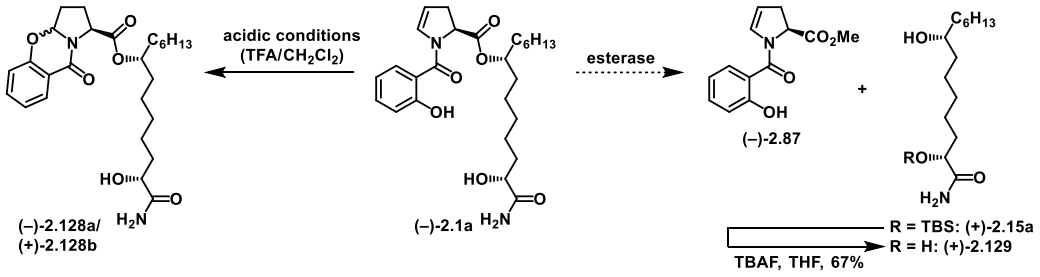

Figure 16. Promysalin prodrug hypotheses. Under acidic conditions, we found that promysalin forms diastereomeric products **(–)-2.128a** and **(+)-2.128b**. To test our esterase hypothesis, methyl ester **(–)-2.87** and diol **(+)-2.129** were synthesized.

2.5 Promysalin Analog Results and Conclusions

2.5.1 Promysalin Analog Inhibitory Data

With our library of promysalin analogs in hand, we evaluated each for its inhibitory activity against *P. aeruginosa*, using IC_{50} measurements, the results of which are shown in Figure

17 (biological assays were run by Colleen Keohane). The prodrug hypothesis did not prove to be biologically relevant, and the cyclization event is most likely a synthetic artifact. Most of the dehydroproline modifications were tolerated, except for hydroxyproline **(–)-2.35** and piperidine **(–)-2.37**. Saturated analog **(–)-2.36** and methyl-dehydroproline **(–)-2.34** were each 10-100-fold less potent, and the fluorine analog **(+)-2.33** displayed a small boost in potency. Taken in sum these results indicate that the dehydroproline motif is not a electrophilic trap for promysalin's target, and that the alkene serves to orient the heterocycle into a specific flatter conformation than proline. Salicylate modifications were almost all completely inactive, and the methyl ether analog **(–)-2.61** was 100-fold less active than promysalin. This shows that the orientation of the phenol is crucial for activity, and the hydrogen bond donor capabilities and size of the phenol are also important. Side chain modifications were all tolerated, except for amide **(–)-2.109**. This indicated that the ester's hydrogen bonding and/or orientation were crucial for promysalin's biologically active conformation. Removal of the hydroxyl group in analog **(–)-2.106** yielded an equipotent compound as promysalin. This result was surprising, but satisfying from a synthetic standpoint, as this compound required three less total steps to synthesize. However, this result, along with the great loss in potency of methyl ether **(–)-2.107** indicated that the hydroxyl group of promysalin was in a sterically demanding environment, either directly with its target or in an intramolecular hydrogen bonding structure. The rigidified alkene analog **(–)-2.108** was equipotent with promysalin which was not surprising, and the propargyl analog **(–)-2.110** was only 2-3-fold less active than promysalin. This result hinted at the possibility of synthesizing promysalin probe compounds by building off the amide nitrogen and paved the way for the next stage of this project.

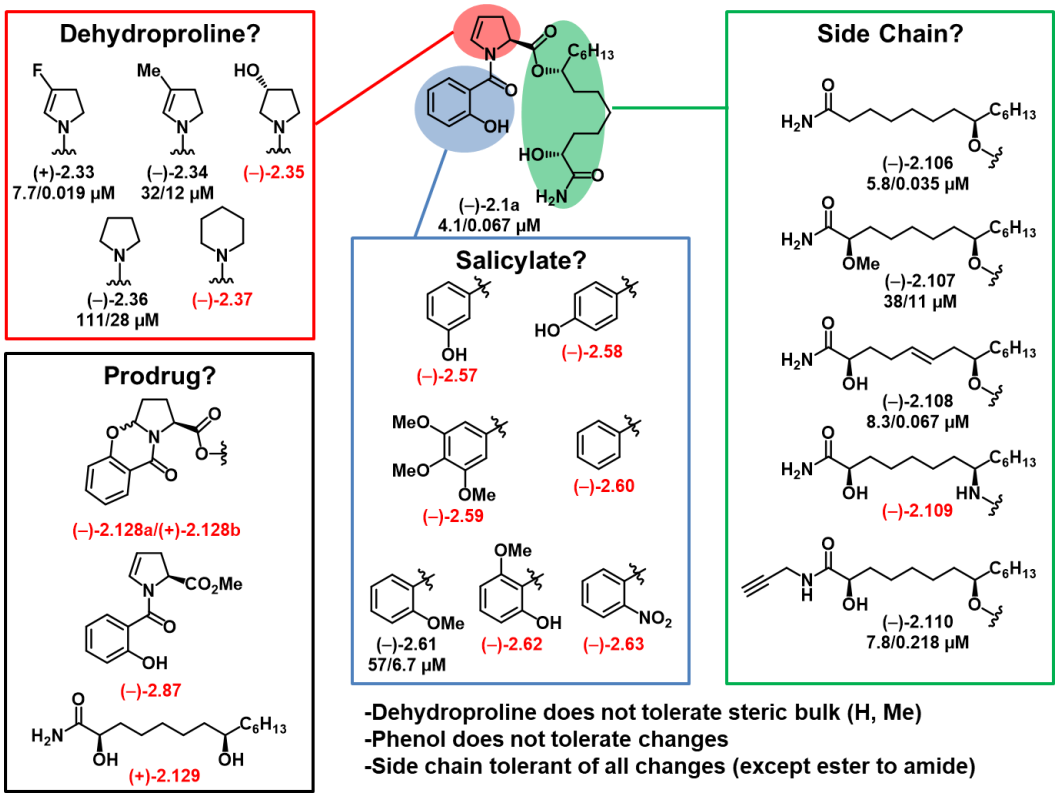

Figure 17. All analog structures and PAO1 and PA14 IC_{50} values. Red numbers indicate inactive up to 250 µM, numbers are given as IC_{50}: PAO1/PA14.

2.5.2 CAS Assay and Iron-binding

With our combined analog results, along with some structural similarities between promysalin and known siderophores (salicylate), we next postulated that promysalin itself may bind iron. Our modeling data suggested that promysalin could form a chelate complex with a metal ion. Additionally, our experimental observations of pyoverdine inhibition and swarming induction suggested promysalin itself would be capable of binding iron. Accordingly, we performed a CAS assay with promysalin solutions, which is a well-known colorimetric method of detecting iron-complexing agents.[31] We first prepared CAS agar and tested promysalin solutions ranging from 6-100 µM, and saw a positive result at high concentrations (Figure 18, left), albeit with much less intensity than EDTA, a high-affinity iron-chelator. Our results with liquid CAS

solution were similar, with promysalin causing a minor discoloration in solution, much less so than the positive EDTA control (CAS assays were run by Colleen Keohane).

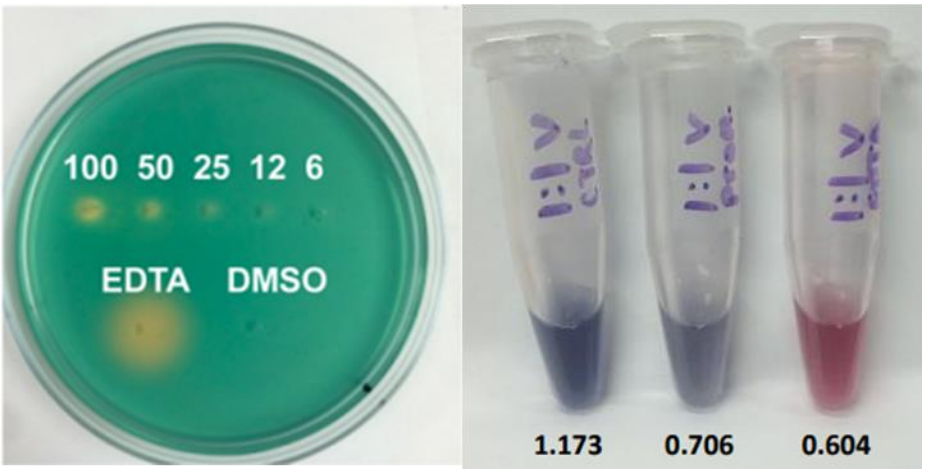

Figure 18. Photographs of CAS assay with agar (left) and solution (right).

With this positive CAS result, we then attempted to form a promysalin-iron complex and characterize it via typical methods. Unfortunately, mixing promysalin and iron in standard ratios for iron complexes (2:1 or 1:1 promysalin:iron) and across typical pH ranges (4-10) gave no detectable change in the UV-vis spectrum, mass spectrum, or NMR spectrum. Typical iron-siderophore complexes give distinct visible complexes that can be seen with the naked eye.[32] This led us to conclude that promysalin is not a siderophore.

Taken in sum, our results indicate that promysalin can form an iron complex. However, it was unclear whether this result was biologically relevant. The CAS assay seemed to indicate that promysalin forms a low-affinity iron complex. Siderophores typically bind iron with extremely high affinity, and it was possible that our positive result was simply due to the salicylate moiety of promysalin, which is a common siderophore structural motif.[33-34] Some examples of salicylate containing siderophores from Gram-negative organisms are shown in Figure 19. The role of iron in promysalin's mechanism of action would be a question that we would continue to address in future experiments.

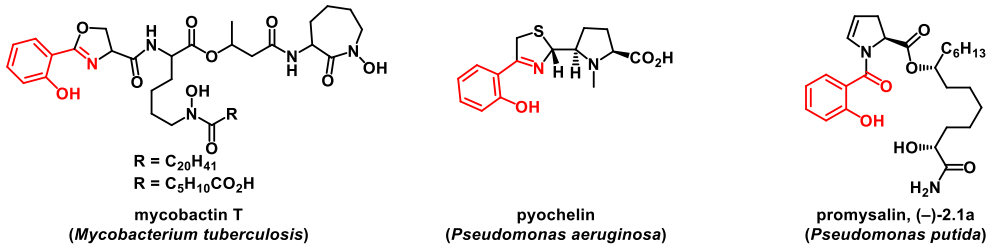

Figure 19. Examples of salicylate-containing Gram-negative siderophores. The salicylate moiety of each structure is colored in red.

2.5.3 Conclusions

Our analog studies gave us a great deal of insight about promysalin's SAR data in relation to inhibitory activity against *P. aeruginosa*. We also learned a great deal about promysalin's hydrogen bond donor/acceptor arrangement in relation to its inhibitory activity and had a computational model to rationalize many of these results. This model then led us to hypothesize that promysalin could bind metal ions, and we found that it forms a weakly-bound iron complex. We then wondered if promysalin elicits its species selectivity by mimicking siderophore-iron structures, which have specialized uptake system and can be very selective for the bacteria that sense them. Hence, the next logical direction for the project would be to identify promysalin's target in *P. aeruginosa* and utilize this information to do follow-up studies in *P. putida* to answer questions about selectivity.

2.6 Synthesis of Promysalin Photoprobe and Affinity-based Protein Profiling

2.6.1 Affinity-based Protein Profiling in Natural Product Target Identification

At this stage of the project, we had a reliable synthetic route to access promysalin, a breadth of SAR data around each of its key structural features, and several questions about the compound's mode of action: (1) What is promysalin's target in *P. aeruginosa*? (2) Is this target specific and only expressed in *P. aeruginosa*, but not other *Pseudomonads*? (3) Why is

promysalin more active against PA14 than PAO1? (4) What is the role of iron in promysalin's mode of action? These questions could all be addressed by first identifying promysalin's target in *P. aeruginosa*. Up to this point, all biological work was done in whole-cell assays, and based on phenotypes (growth/inhibition, swarming, etc.). Therefore, we had no chemical basis to make a hypothesis about promysalin's target. However, with the valuable SAR data that we obtained up to this point, we were well-poised to leverage affinity-based protein profiling (AfBPP) to determine promysalin's molecular target.

AfBPP is a modern extension of activity-based protein profiling (ABPP). In ABPP, a functional group with tailored reactivity is used to covalently capture enzymes (typically with an electrophile, Figure 20A) of a certain class, followed by some sort of enrichment/target identification. This work was pioneered by the inspirational work from the Cravatt laboratory, where several types of probes were developed, each selective for different classes of enzymes, such as serine hydrolases, proteases, and glycosidases, to name a few.[35] One disadvantage to this type of technique is that some knowledge of the enzyme target needs to be known before the experiment is carried out. AfBPP takes advantage of non-covalent interactions between a molecule and its protein target, by appending a photoreactive functional group to the molecule of interest (Figure 20B), which is then covalently captured. This molecule also typically contains a bioorthogonal group, such as an alkyne, which can be reacted with an azide appended to a fluorophore or affinity label for subsequent SDS-PAGE/fluorescence or enrichment/LC-MS/MS analysis, respectively (Figure 20C).

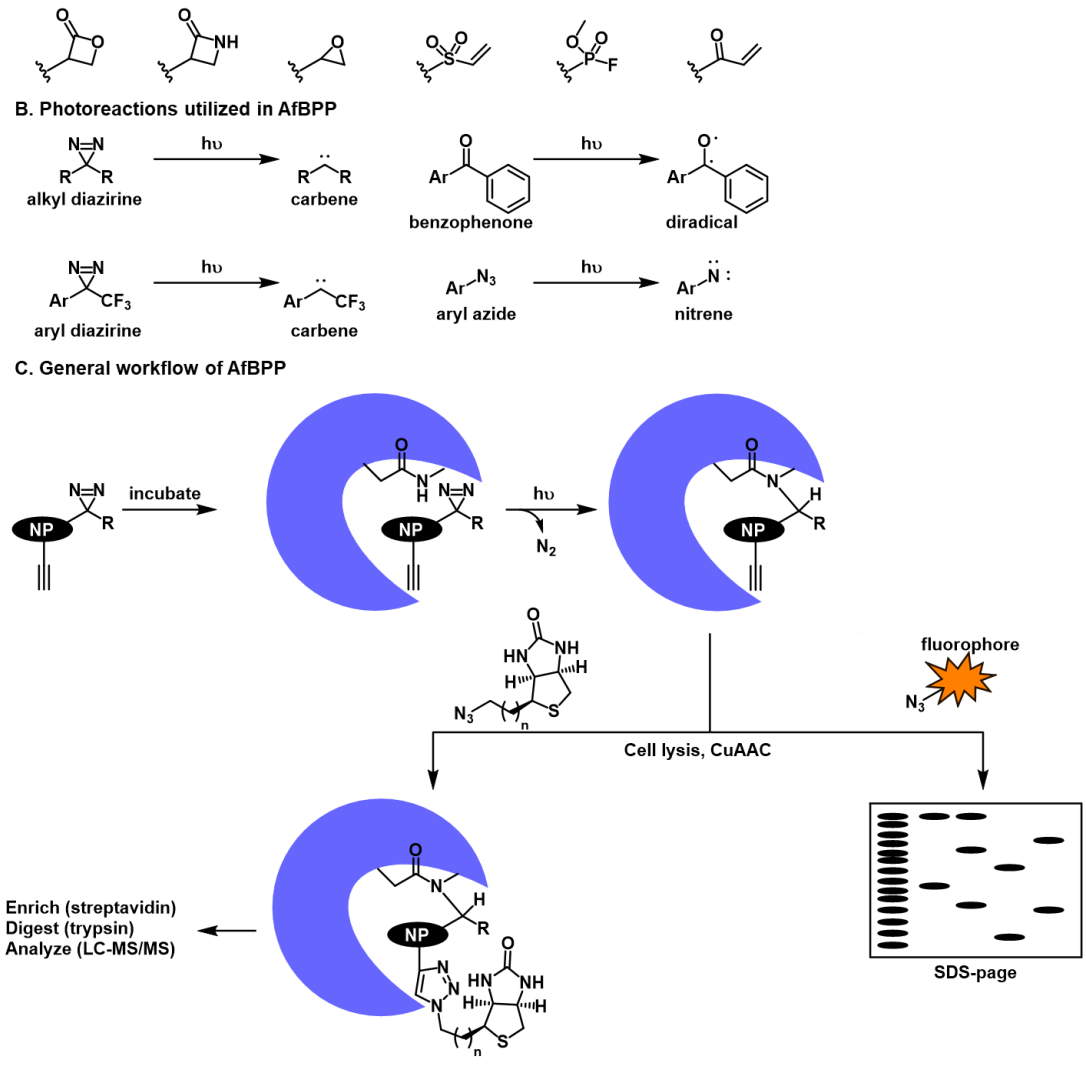

Figure 20. Background for proteomics. (a) Electrophilic functional groups used in ABPP and/or AfBPP. (b) Photoreactive functional groups and their respective reactions utilized in AfBPP. (c) General workflow of AfBPP, where "NP" denotes natural product of interest, the blue shape is a hypothetical protein target, with a generic amide bond showing for simplicity. The left pathway indicates biotin attachment via copper catalyzed azide alkyne cycloaddition (CuAAC), which can then be enriched, digested, and analyzed with LC-MS/MS. The right pathway indicates fluorophore appendage, which can then be analyzed via SDS-page and fluorescent imaging.

There are a wide variety of probe functional groups and bioorthogonal handles to choose from, Figure 20 gives a small sample of the large number of options. However, our AfBPP studies had a few requirements due to our limited knowledge of what promysalin's target could be: (1) The probe should be as small as possible, to not alter promysalin's interaction with its target. (2) The synthesis and installation of the probe should utilize our synthetic route and ideally

stem from a later stage intermediate to maintain synthetic feasibility. (3) The photoreactive and handle groups should be installed at the same time, to cut down on the number of extra synthetic operations. The "minimalist" alkyne-diazirine designed by Yao and co-workers meets these criteria, and can be easily synthesized with several different functional groups appended, to allow incorporation onto a variety of functional groups in the target molecule, shown in Figure 21.[36]

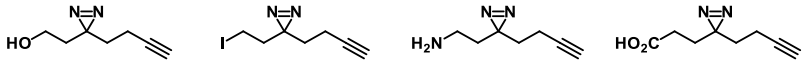

Figure 21. Examples of "minimalist" alkyne-diazirine probes reported by Yao and co-workers which allow installation onto a variety of functional groups.

2.6.2 Promysalin Photoaffinity Probe Design and Synthesis

Based on our previous SAR studies, we knew that functionalization on the amide carbon of **(–)-2.1a** was tolerated in terms of *P. aeruginosa* inhibition. We therefore set out to install the probe via the amine diazirine-alkyne **2.130**, the details of which are described in Scheme 24. This required conversion of our previously disclosed oxazolidinone intermediate (–**)-2.31a** to the corresponding acid **2.131**. Typical hydrolysis conditions for this type of transformation (LiOH, H_2O_2) caused very rapid cleavage of the silyl group, even at low temperatures. Therefore, a two-step procedure was performed instead, by displacement of the oxazolidinone with *n*-butyllithium and benzyl alcohol, yielding the corresponding benzyl ester **(+)-2.132**, which was hydrogenated to yield acid **2.131**. Not surprisingly, cleavage of the silyl group occurred very rapidly if this intermediate was isolated and stored. Amidation of acid **2.131** with the diazirine-alkyne amine **2.130** yielded amide **(+)-2.133**. This was then esterified with acid **(–)-2.12**, yielding ester **(–)-2.134**. Typical SEM/TBS deprotection then gave the probe compound **(–)-2.135**. A similar reaction sequence was employed to synthesize the negative control compound **(–)-2.137**, which lacked the phenol functional group that is essential for biological activity (synthesis of probe compounds was performed by myself with the help of Colleen Keohane).

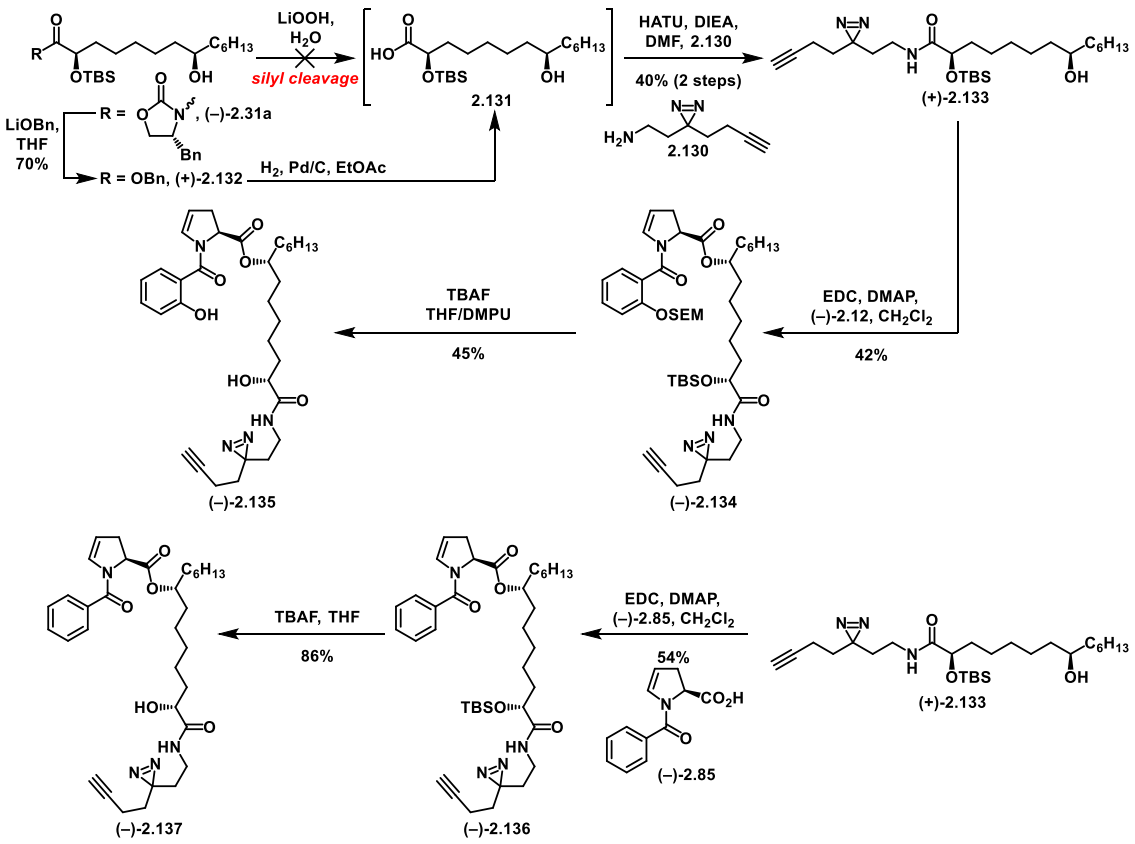

Scheme 24. Synthesis of probe compound **(–)-2.135**, and inactive probe **(–)-2.137**.

2.6.3 Biological Evaluation of Promysalin Photoprobe and Proteomic Experiments

With an efficient route to the probe compound in hand, we next had to evaluate its bioactivity to ensure it was still active against *P. aeruginosa*. We conducted the typical IC_{50} inhibitory assay as for promysalin, and gratifyingly found that probe **(–)-2.135** was about 20-fold less active against PA14 than promysalin (1.69 μM vs. 67 nM, biological assays conducted by Colleen Keohane). Even with this modest drop in potency, we were confident that the photoprobe would allow for proteomic target identification by using the proper control experiments in order to rule out false positives.

The proteomic experiments that we carried out are shown schematically in Figure 22. There were three distinct sample preparation procedures that were followed. The first is the "standard" workflow of a proteomic experiment, where probe compound **(–)-2.135** was incubated with *P. aeruginosa* cells and irradiated with UV light. The crosslinked probe-protein molecules were "clicked" with CuAAC onto an azide-functionalized biotin followed by streptavadin enrichment. The second set of experiments was the same as the first, except a 10-fold excess of promysalin was first introduced, which presumably used up all of the binding partners first. Thereforre, anything left for the probe to modify and enrich would be a false positive. Finally, the third experiment involved inactive probe compound **(–)-2.137**, with the typical workflow, whereby any enriched proteins would also be false positives. All three samples were differentially labeled then mixed, digested with trypsin, and analyzed by LC-MS/MS.

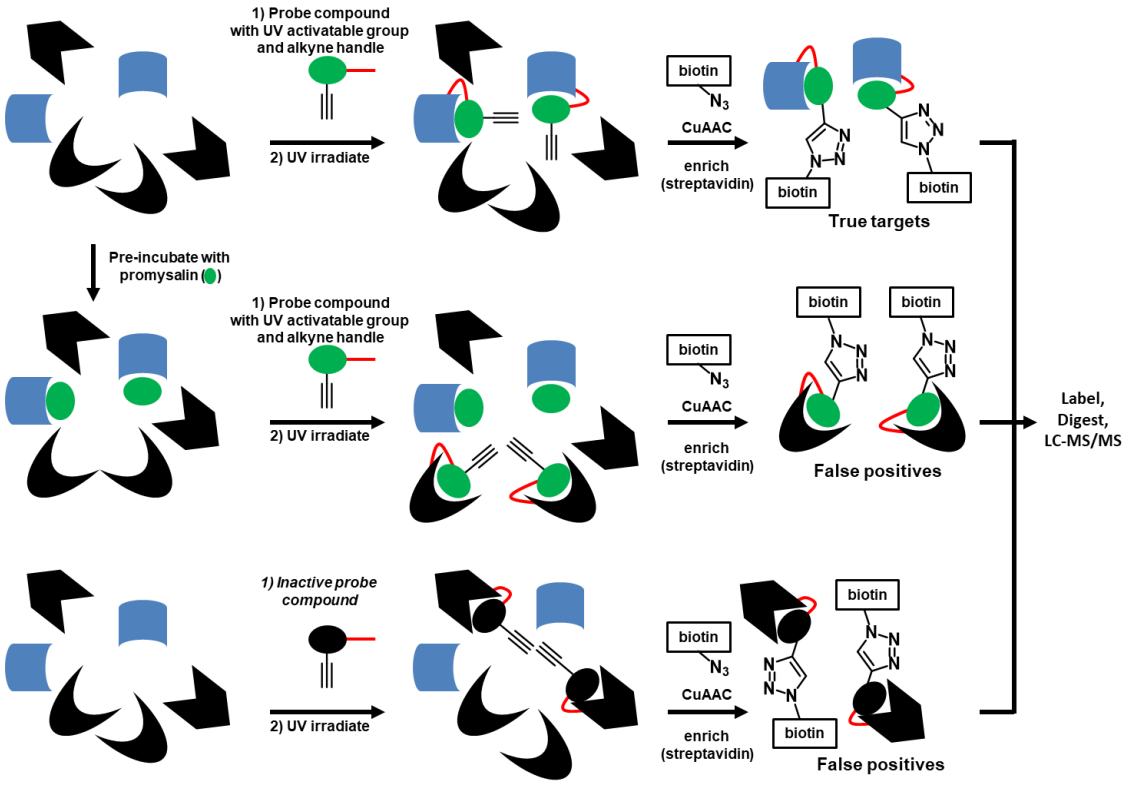

Figure 22. Schematic of the three proteomic experiments in this work. Top row: typical proteomic run with natural product probe. Middle row: competition experiment where the natural product itself is first introduced into the system, then the probe compound is introduced and will

only have false positives left to interact with. Bottom row: an inactive, but structurally similar, probe compound is used to identify further false positives.

The data for the experiments are typically plotted in volcano plot format, where each dot corresponds to a protein that was identified by LC-MS/MS. The plot is divided into four quadrants, where the upper half represents the statistically significantly enriched hits, and the right half represents the most reproducible between trials. Therefore, the best hits are located in the upper right quadrant. Each plot is a comparison between two experiments, in Figure 23, the left plot is promysalin vs. competition (top row, Figure 22 vs. middle row, Figure 22). In Figure 23, the right plot is promysalin vs. inactive probe (top row, Figure 22 vs. bottom row, Figure 22) (proteomic experiments were conducted by Colleen Keohane in the lab of our collaborator, Stephan Sieber, under the direct guidance of Christian Fetzer).

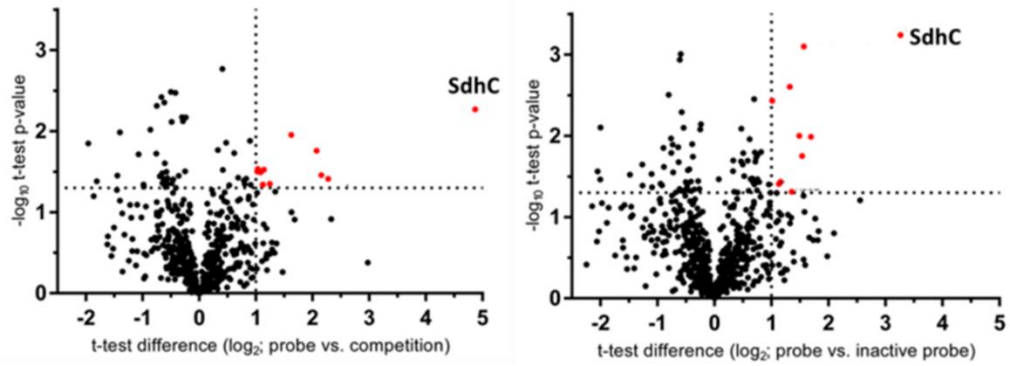

Figure 23. Volcano plots from proteomic experiments with *P. aeruginosa* PA14.

From the plots in Figure 23, it is easy to see that one protein in particular is enriched the most substantially and reproducibly in both sets of data: succinate dehydrogenase, subunit C (sdhC).

2.6.4 Succinate Dehydrogenase and its Role in *Pseudomonas* Metabolism

Our initial proteomic hit seemed counterintuitive, due to promysalin's selectivity. We expected to find a protein that *P. aeruginosa*, but not *P. putida* possessed. Instead, we found an enzyme that is found not only in both species of *Pseudomonas* mentioned here, but in all

kingdoms of life – even humans. To understand how this compound works in *Pseudomonas* and in Nature, we first took a look at the enzyme itself and its role in metabolism.

Succinate dehydrogenase is unique in that it operates in both the TCA cycle (also known as the Krebs Cycle) and the electron transport chain. The cycle is shown in Figure 24. The cycle begins with acetyl CoA (**2.138**), in the case of *Pseudomonas*, this is typically from the Entner-Doudoroff pathway. Acetyl CoA is converted to citric acid (**2.139**), which begins the cycle. A dehydration reaction then forms *cis*-aconitate (**2.140**). From there, hydration of the alkene yields D-isocitrate (**2.141**). Decarboxylative oxidation then yields α-ketoglutarate (**2.142**), with concommitant release of a molecule of CO_2 and reduction of NAD^+ to NADH. **2.142** is then converted to succinyl CoA (**2.143**) via a decarboxylation reaction which also yields CO_2 and NADH. Succinyl CoA (**2.143**) is then converted to succinate (**2.144**) while also converting a molecule of GDP to GTP. Succinate dehydrogenase then oxidizes succinate (**2.144**) to fumarate (**2.145**), with simultaneous reduction of FAD^+ to $FADH_2$. The resultant alkene is hydrated, to form malate (**2.146**). The alcohol is oxidized to yield oxaloacetate (**2.147**), with simultaneous reduction of NAD^+ to NADH. Oxaloacetate (**2.147**) is then condensed with acetyl CoA (**2.138**) to yield citric acid, and completing the cycle. Several steps in the TCA cycle can be circumvented, which is also shown in Figure 24. This is known as the glyoxylate cycle, and D-isocitrate (**2.141**) undergoes a retro-aldol reaction, yielding glyoxylate (**2.145**), and succinate (**2.144**). However, this process is endergonic, and is not a part of primary metabolism. The glyoxylate pathway typically dominates when bacteria are producing secondary metabolites from succinate, typically carbohydrates.[37]

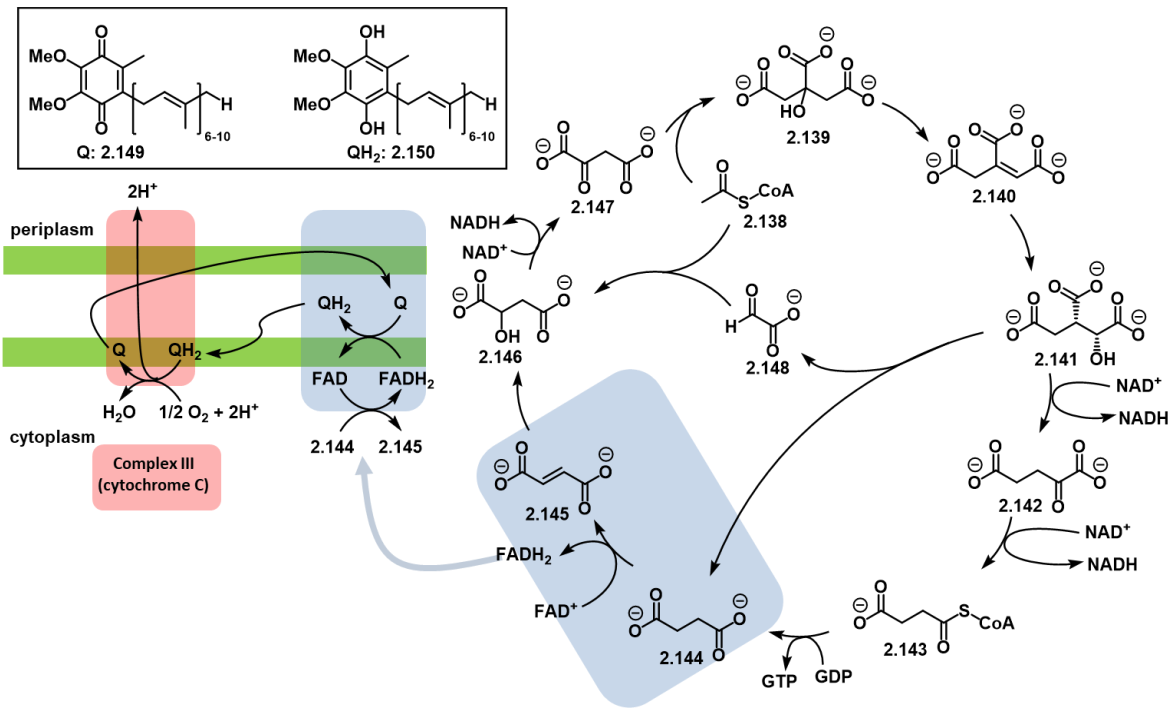

Figure 24. TCA cycle/electron transport chain overview. Blue box indicates succinate dehydrogenase (complex II), and pink box represents cytochrome C (complex III).

While only one actual unit of chemical energy is directly produced in the TCA cycle (GTP), all of the molecules of $FADH_2$ and $NADH_2$ are converted to chemical energy via the electron transport chain. A simplified version is shown in Figure 24, with a focus on succinate dehydrogenase. As **2.144** is oxidized to **2.145**, a molecule of FAD^+ is converted to $FADH_2$. The electrons from $FADH_2$ are then transferred to coenzyme Q (ubiquinone, **2.149**), and reduction forms QH_2 (ubiquinol, **2.150**). The hydrophobic QH_2 serves as an electron shuttle throughout the membrane, where it travels to electron transport chain enzymes, such as a cytochrome (pink square, Figure 24). These enzymes transfer electrons from QH_2 to an electron acceptor, for example O_2, which forms H_2O. At the same time, protons are pumped against their concentration gradient across the membrane. This potential energy is then converted to chemical energy by ATP synthase, which pumps protons down their concentration gradient across the membrane, and synthesizes ATP from ADP. Hence, the reducing equivalents ($FADH_2$, $NADH_2$, and QH_2) produced in the TCA cycle serve as important energy carriers for primary metabolism.

Our results in *P. aeruginosa* were in full agreement with succinate dehydrogenase inhibition. Others have shown that many of the TCA cycle genes (succinate dehydrogenase included) are essential in *P. aeruginosa*, but not *E. coli*.[38] This observation highlights the importance of the TCA cycle in particular for *Pseudomonas* and begins to shed light on the reason promysalin is selective between genera. We next performed a series of follow-up studies in order to verify the validity of our proteomic results. A multidisciplinary approach involving bioinorganic, *in vitro*, *in silico*, and resistance development experiments all verified succinate dehydrogenase as promysalin's protein target. These studies were spearheaded by my co-worker, Colleen Keohane, and will be fully disclosed in her dissertation, and are also published in the literature.[39]

2.7 References

1) Slama, T. G. *Crit. Care* **2008**, *12*, S4.

2) Sekiya, H.; Mima, T.; Morita, Y.; Kuroda, T.; Mizushima, T.; Tsuchiya, T. *Antimicrob. Agents Chemother.* **2003**, *47*, 2990.

3) Davies, J. C. *Paediatr. Respir. Rev.* **2002**, *3*, 128.

4) Wisplinghoff, H.; Bischoff, T.; Tallent, S. M.; Seifert, H.; Edmond, M. B. *Clin. Infect. Dis.* **2004**, *39*, 309.

5) Li, X. Z.; Zhang, L.; Poole, K. *J. Antimicrob. Chemother.* **2000**, *45*, 433.

6) Livermore, D. M. *Clin. Microbiol. Rev.* **1995**, *8*, 557.

7) Livermore, D. M. *Clin. Infect. Dis.* **2002**, *34*, 634.

8) Arakawa, Y.; Murakami, M.; Suzuki, K.; Ito, H.; Wacharotayankun, R.; Ohsuka, S.; Kato, N.; Ohta, M. *Antimicrob. Agents Chemother.* **1995**, *39*, 1612.

9) Drenkard, E. *Microbes Infect.* **2003**, *5*, 1213.

10) Fazli, M.; Bjarnsholt, T.; Kirketerp-Moller, K.; Jorgensen, B.; Andersen, A. S.; Krogfelt, K. A.; Givskov, M.; Tolker-Nielsen, T. *J Clin Microbiol* **2009**, *47*, 4084.

11) Pastar, I.; Nusbaum, A. G.; Gil, J.; Patel, S. B.; Chen, J.; Valdes, J.; Stojadinovic, O.; Plano, L. R.; Tomic-Canic, M.; Davis, S. C. *PLoS One* **2013**, *8*, e56846.

12) Limoli, D. H.; Yang, J.; Khansaheb, M. K.; Helfman, B.; Peng, L.; Stecenko, A. A.; Goldberg, J. B. *Eur. J. Clin. Microbiol. Infect. Dis.* **2016**, *35*, 947.

13) Gerber, J. S.; Ross, R. K.; Bryan, M.; Localio, A. R.; Szymczak, J. E.; Wasserman, R.; Barkman, D.; Odeniyi, F.; Conaboy, K.; Bell, L.; Zaoutis, T. E.; Fiks, A. G. *JAMA* **2017**, *318*, 2325.

14) Kelly, C. P.; LaMont, J. T. *N. Engl. J. Med.* **2008**, *359*, 1932.

15) Louie, T. J.; Miller, M. A.; Mullane, K. M.; Weiss, K.; Lentnek, A.; Golan, Y.; Gorbach, S.; Sears, P.; Shue, Y.-K. *N. Engl. J. Med.* **2011**, *364*, 422.

16) Li, W.; Estrada-de los Santos, P.; Matthijs, S.; Xie, G. L.; Busson, R.; Cornelis, P.; Rozenski, J.; De Mot, R. *Chem. Biol.* **2011**, *18*, 1320.

17) Lee, D. G.; Urbach, J. M.; Wu, G.; Liberati, N. T.; Feinbaum, R. L.; Miyata, S.; Diggins, L. T.; He, J.; Saucier, M.; Deziel, E.; Friedman, L.; Li, L.; Grills, G.; Montgomery, K.; Kucherlapati, R.; Rahme, L. G.; Ausubel, F. M. *Genome Biol.* **2006**, *7*, R90.

18) Stachelhaus, T.; Mootz, H. D.; Marahiel, M. A. *Chem. Biol.* **1999**, *6*, 493.

19) Hanawa, H.; Hashimoto, T.; Maruoka, K. *J. Am. Chem. Soc.* **2003**, *125*, 1708.

20) An, C.; Hoye, A. T.; Smith, A. B., III *Org. Lett.* **2012**, *14*, 4350.

21) Smith, A. B., III; Jurica, J. A.; Walsh, S. P. *Org. Lett.* **2008**, *10*, 5625.

22) Kearns, D. B. *Nat. Rev. Microbiol.* **2010**, *8*, 634.

23) Kiyohara, H.; Torigoe, S.; Kaida, N.; Asaki, T.; Iida, T.; Hayashi, H.; Takizawa, N. *J. Bacteriol.* **1994**, *176*, 2439.

24) Marugg, J. D.; De Weger, L. A.; Nielander, H. B.; Oorthuizen, M.; Recourt, K.; Lugtenberg, B.; Van Der Hofstad, G. A. J. M.; Weisbeek, P. J. *J. Bacteriol.* **1989**, *171*, 2819.

25) Matthijs, S.; Laus, G.; Meyer, J. M.; Abbaspour-Tehrani, K.; Schafer, M.; Budzikiewicz, H.; Cornelis, P. *Biometals* **2009**, *22*, 951.

26) Tius, M. A.; Kawakami, J. K. *Tetrahedron* **1995**, *51*, 3997.

27) Li, X.; Li, Y.; Xu, W. *Bioorg. Med. Chem.* **2006**, *14*, 1287.

28) Torssell, S.; Wanngren, E.; Somfai, P. *J. Org. Chem.* **2007**, *72*, 4246.

29) Schmidt, A.-K. C.; Stark, C. B. W. *Org. Lett.* **2011**, *13*, 4164.

30) Hunter, R. C.; Beveridge, T. J. *Appl Environ Microbiol* **2005**, *71*, 2501.

31) Bernhard, S.; Neilands, J. B. *Anal. Biochem.* **1987**, *160*, 47.

32) Shapiro, J. A.; Wencewicz, T. A. *ACS Infect. Dis.* **2016**, *2*, 157.

33) Ankenbauer, R. G.; Toyokuni, T.; Staley, A.; Rinehart, K. L. J.; Cox, C. D. *J. Bacteriol.* **1988**, *170*, 5344.

34) De Voss, J. J.; Rutter, K.; Schroeder, B. G.; Su, H.; Zhu, Y.; Barry, C. E. *PNAS* **2000**, *97*, 1252.

35) Evans, M. J.; Cravatt, B. F. *Chem. Rev.* **2006**, *106*, 3279.

36) Li, Z.; Hao, P.; Li, L.; Tan, C. Y.; Cheng, X.; Chen, G. Y.; Sze, S. K.; Shen, H. M.; Yao, S. Q. *Angew. Chem. Int. Ed.* **2013**, *52*, 8551.

37) Kondrashov, F. A.; Koonin, E. V.; Morgunov, I. G.; Finogenova, T. V.; Kondrashova, M. N. *Biol. Direct* **2006**, *1*, 31.

38) Lee, S. A.; Gallagher, L. A.; Thongdee, M.; Staudinger, B. J.; Lippman, S.; Singh, P. K.; Manoil, C. *PNAS* **2015**, *112*, 5189.

39) Keohane, C. E.; Steele, A. D.; Fetzer, C.; Khowsathit, J.; Van Tyne, D.; Moynie, L.; Gilmore, M. S.; Karanicolas, J.; Sieber, S. A.; Wuest, W. M. *J. Am. Chem. Soc.* **2018**, *140*, 1774.

Chapter 3: Diverted Total Synthesis of CD437 and nTZDpa Analogs – Effective Membrane Disrupting Agents Against Gram-positive Pathogens

3.1 Introduction and Background

3.1.1 *Staphylococcus aureus* – Resistance and Clinical Relevance

Staphylococcus aureus is a devastating infective pathogen, with mortality rates estimated between 20 and 40%.[1] This pathogen has been attributed to 18,000 deaths and $3 – $4 billion of healthcare costs in the United States per year.[2] When penicillin was first discovered, it was highly effective against *S. aureus*. However, resistant strains were isolated as early as 1942, and within two decades, over 80% of all community and hospital-associated strains of *S. aureus* were resistant to this antibiotic. The prevailing mechanism of penicillin resistance is the expression of *blaZ*, which encodes a β-lactamase (see section 1.2.2 Drug-Inactivating Enzymes, page 3).

After penicillin resistance emerged, the development of methicillin in 1961 offered a glimmer of hope, since this compound was not a viable substrate for β-lactamase enzymes. The emergence of methicillin-resistant *S. aureus* (MRSA) showed the community that the fight was far from over. Methicillin resistance is conferred by the expression of PBP2a, a homolog of the typical penicillin-binding protein that methicillin is unable to inhibit.[3] While the β-lactam resistance is the most problematic issue in MRSA infection treatment, resistance to other antibiotics like vancomycin is becoming commonplace and limits current alternative treatment options.[4]

An additional challenging aspect of pathogenic *S. aureus* treatment is the microbe's prevalence within the human population. 20% of the population carries *S. aureus* indefinitely and asymptomatically. Another 60% of the population carries the microbe intermittently, usually without incident. These carriers are typically less susceptible to pathogenic *S. aureus* than non-

carriers, however, once antibiotics are administered, this protective effect disappears.[5] The prevalence of *S. aureus* presents a challenging issue with respect to antibiotic resistance, as the genes that confer antibiotic resistance are typically highly susceptible to horizontal gene transfer, whereby the resistance can quickly spread throughout a microbial population.

3.1.2 Persister Cells

An additional challenge that is complementary to antibiotic resistance is the problem of persister cells within a bacterial population. This phenomenon was first described in the context of a *S. aureus* population by Hobby and co-workers, where researchers observed that 1% of the bacterial population was left behind after treatment with penicillin.[6] Since the discovery of this phenotype, it is well-known that persisters are a metabolically dormant subset of a bacterial population genetically indistinguishable from its antibiotic-susceptible cohorts.[7] This is in stark contrast to resistance, where mobile genetic elements are transferred and copied within a population, and/or mutations arise. In some cases, the antibiotic is able to engage its target, but its dormancy allows it to survive, since the toxic products usually introduced by an antibiotic do not form. Alternatively, persister cell survival can be a result of decreased drug uptake. These phenomena are depicted schematically in Figure 25.

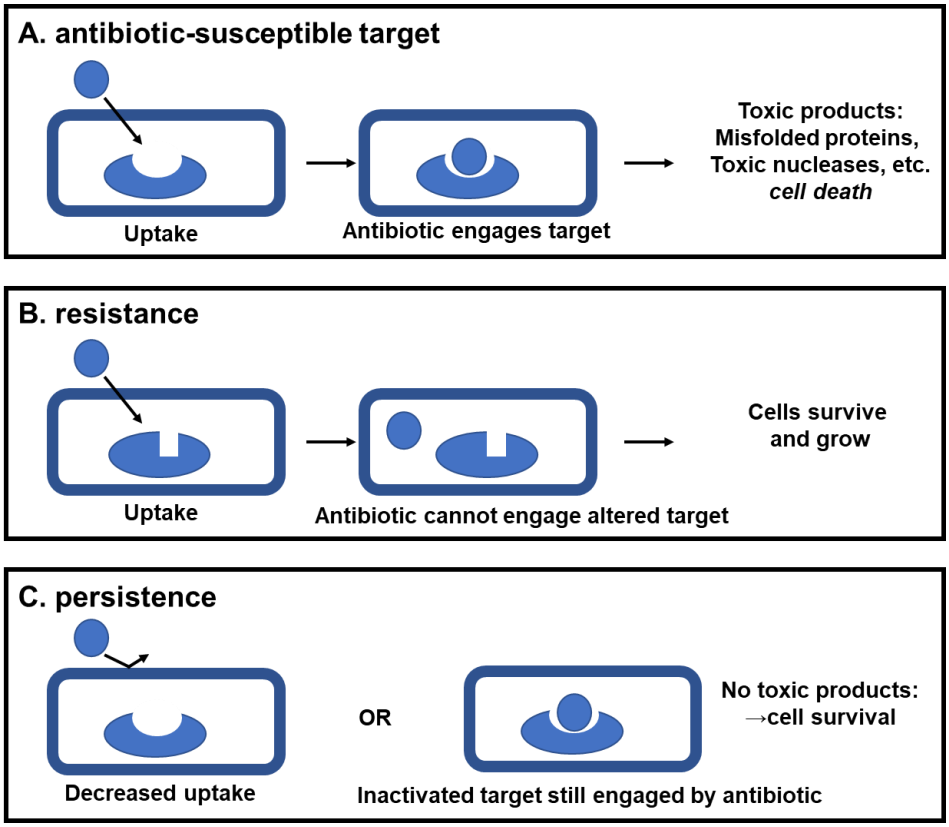

Figure 25. Schematic showing the difference between resistance and persistence. (a) typical antibiotic mechanism, where the antibiotic engages its target, and toxic products are formed, ultimately leading to cell death. (b) Resistance arises by an altered target, for example an amino acid mutation in an active site, whereby the antibiotic can no longer bind to the target. (c) Persistence occurs when the antibiotic can still engage its target, but it is dormant, so the binding has no effect.

Persister cells on their own do not cause any kind of immediate threat, as removal of 99% of a bacterial population is typically enough to allow a patient to recover. However, this becomes an issue during a chronic infection, and is exemplified by biofilm populations. In these environments, antibiotics wipe out the bacterial population, leaving the persisters within the biofilm behind. Once treatment ceases, the persisters within the biofilm can begin to divide, proliferate, and recolonize the infected area. Therefore, compounds that either “wake” persister cells from their dormant state, or directly kill them, would be greatly beneficial to patients with chronic bacterial infections.

3.2 The Discovery of New Antibiotic Activity of CD437 and nTZDpa

3.2.1 *C. elegans*-MRSA High-throughput Screen

In 2017, our collaborators (Mylonakis lab, Brown University - Rhode Island Hospital) developed a high-throughput screen to search for new antibiotics with activity against *S. aureus* (all biological experiments in this chapter were performed by Wooseong Kim in the Mylonakis laboratory). Hits from the screen rescue the nematode *Caenorhabditis elegans* (*C. elegans*) from infection by MRSA.[8] *C. elegans* are infected with MRSA in the presence of test compounds in 384-well plates, then treated with a fluorescent dye (SYTOX). Dead worms stain with SYTOX and display a fluorescent signal (see DMSO image, Figure 26), and living worms give no signal. The assay is highly automated and can be conducted in a high-throughput fashion, properties such as solubility and stability are already accounted for, and toxicity is assayed at the same time as antibiotic activity (i.e. *C. elegans* must survive both the infection and antibiotic treatment). The assay was conducted in 384-well plates, and 82,000 compounds were screened, which resulted in 185 positive hits. These included three vitamin A (**3.4**) analogs (which will be referred to as retinoids) CD437 (**3.1**), CD1530 (**3.2**), and adarotene (**3.3**), as well as a structurally unrelated molecule nTZDpa (**3.5**). Figure 26 depicts photographs from the high-throughput experiment as well as chemical structures of compounds **3.1** – **3.5**.

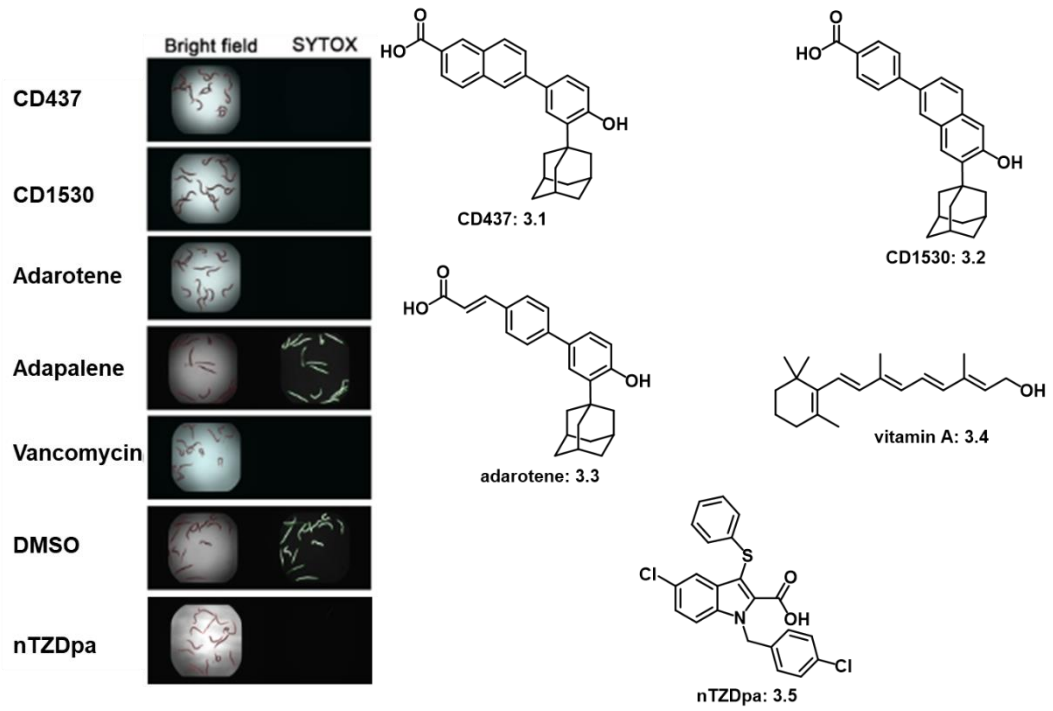

Figure 26. (left) Images from *C. elegans* high-throughput screen and (right) structures of lead compounds from the *C. elegans*-MRSA screen.

CD437 (**3.1**), CD1530 (**3.2**), and adarotene (**3.3**, also known as ST1926) have been studied previously as possible cancer therapeutic leads.[9-10] nTZDpa (**3.5**) has gained considerable interest as a selective agonist of PPARγ, which is an enzyme involved in glucose metabolism, and consequently, the pathology of diseases such as obesity, diabetes, and atherosclerosis.[11] The fact that these compounds have seen use *in vivo* means that many toxicity issues have already been addressed.

3.2.2 Biological Activity of CD437 and nTZDpa

CD437 (**3.1**), CD1530 (**3.2**), adarotene (**3.3**), and nTZDpa (**3.5**) all displayed inhibitory activity against MRSA (1, 1, 2, and 4 μg/mL, respectively) comparable to vancomycin (1 μg/mL). They were also active against another Gram-positive organism, *Enterococcus faecium*, and no antibiotic activity was observed against Gram-negative organisms. The active retinoids and nTZDpa killed MRSA within 2 hours, significantly faster than vancomycin (Figure 27).

Additionally, plating MRSA on agar containing 2.5-fold and higher concentrations of compounds did not give rise to any resistant mutants. However, serial passage of MRSA for 100 days in CD437, CD1530, or adarotene yielded mutants that were two-fold less susceptible to treatment. Whole-genome sequencing showed that the slightly resistant mutants contained mutations in the *graS*, *yjbH*, and *manA* genes. Others have shown mutations in these genes result in cell membrane abnormalities.[12-14] This pointed to cell membrane damage as the mechanism of action. In a series of follow-up experiments published elsewhere, the mechanism of action of the compounds was shown to be membrane damage, but not cell lysis. The compounds were also shown to display synergy with gentamicin both in whole-cell *in vitro* assays, and *in vivo* mouse models.

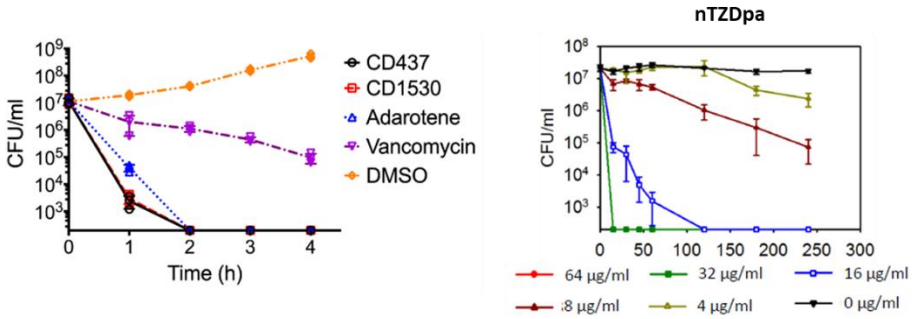

Figure 27. Killing kinetics of retinoids (left) and nTZDpa (right) against MRSA.

One pressing issue with MRSA infections is their persistence (see section 3.1.2 Persister Cells, page 65). Since these compounds operate via membrane damage, they do not require a metabolically active cell to elicit their inhibitory effect. Therefore, our collaborators hypothesized that they should maintain activity against persister cells. Gratifyingly, active retinoids, with the exception of adarotene, eradicated MRSA persister cells at ten times their MIC within four hours. Traditional antibiotics (vancomycin, gentamicin, and ciprofloxacin) could not accomplish this at 100 times their MIC. nTZDpa also eradicated persister cells, and all active persister-eradicating compounds still operated via membrane damage.

The compounds also behaved well *in vivo* in a mouse model and were shown to significantly decrease the bacterial cell counts in an infection model. However, each set of compounds had toxicity issues. In the case of the retinoids, hepatocyte (liver cell) toxicity was observed at as little as 15 μg/mL, which is 15 times higher than the MIC. This is an overwhelming concern, as liver toxicity is one of the three most common safety reasons that drugs are pulled from the market.[15] In the case of nTZDpa, hemolysis was observed with a HC_{50} of 50 μg/mL, and cytotoxicity (HepG2 cell) was observed at and above 20 μg/mL. While the antibacterial profile and mechanism of action of the retinoids and nTZDpa seemed promising, these toxicity issues had to first be addressed if the compounds were to ever find clinical use. Toward this end, we first developed synthetic routes to each compound with the goal of finding new analogs with improved toxicity profiles and potency.

3.2.3 CD437 Simulations and Proposed Mechanism of Action

In addition to the experimental investigation into the mechanism of action of CD437, molecular simulations were also carried out. These were performed to verify the mechanism of CD437 with membranes, and gain insight into the molecular interactions responsible for it. The simulations were run over a 500-nanosecond timescale, and the result of the CD437 simulation is shown schematically in Figure 28. When the compound approaches the phospholipid bilayer, the polar acid group interacts electrostatically with the phosphate polar head group of the membrane. Then, the rest of the compound approaches the membrane and the non-polar adamantane moiety begins intercalating. The compound then lays down almost vertical into the membrane, and then the whole compound flattens out with the adamantane facing down into the non-polar interior of the membrane, with the acid and phenol functional groups anchored to the polar phospholipid head groups. We developed a synthetic plan that would allow us to test the hypothesis of this model while also addressing the issues of toxicity mentioned in the previous section.

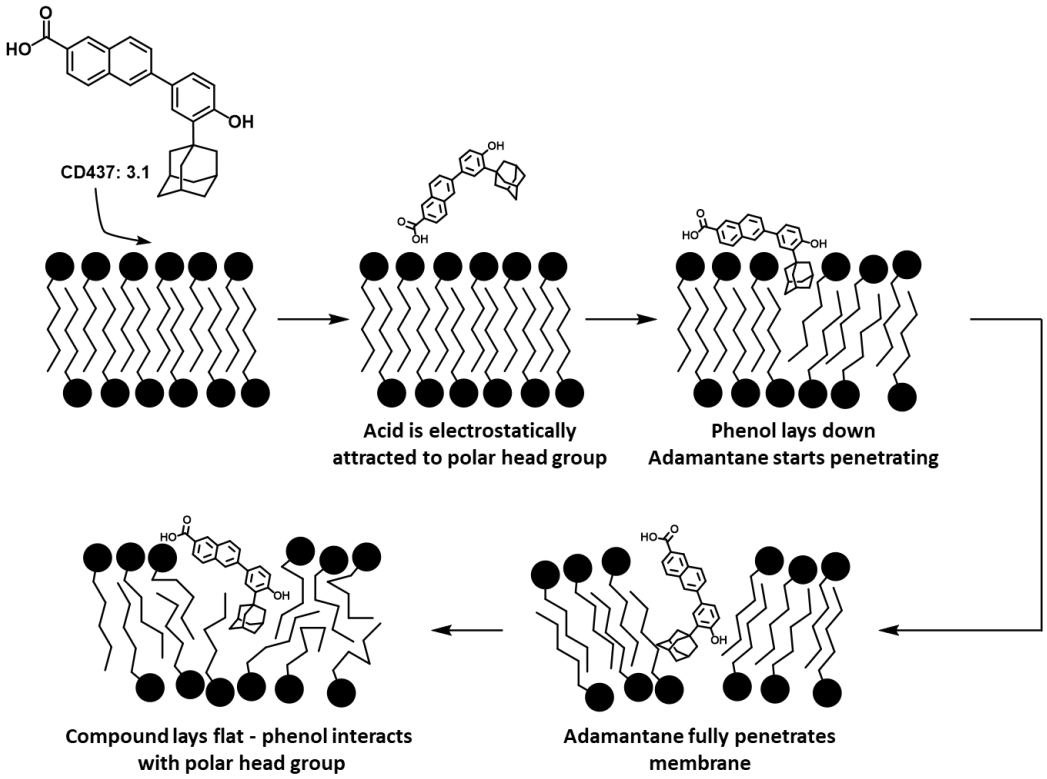

Figure 28. Schematic of the molecular dynamics simulation results.

3.3 Diverted total synthesis of CD437 and analogs

3.3.1 First-generation CD437 analogs from adapalene

To gain an initial glimpse into CD437 SAR, we took advantage of the commercially available adapalene (**3.6**), which is the active ingredient in several acne medications. Preliminary biological testing showed that this compound does not possess antimicrobial activity. However, we sought to use this starting material to access various functional groups in place of the carboxylic acid to test its importance, along with the phenol moiety present in CD437. The modeling results (section 3.2.3 CD437 Simulations and Proposed Mechanism of Action) indicated that both the acid and phenol groups were important for the hypothesized mode of action, which we set out to test.

Scheme 25 details the synthesis of the first-generation CD437 analogs. From adapalene (**3.6**), analogs retaining the methyl ether with changes at the acid moiety could be accessed in one step. We synthesized a methyl ester (**3.7**), ethyl amide (**3.8**), primary amide (**3.9**), and alcohol (**3.10**) with standard transformations. The ethyl and primary amides were demethylated with BBr_3 to yield the corresponding phenols **3.11** and **3.12**, respectively. CD437 was accessed from adapalene via BBr_3 demethylation then converted to the corresponding methyl ester (**3.13**) and alcohol (**3.14**) (first generation analogs were synthesized by Colleen Keohane).

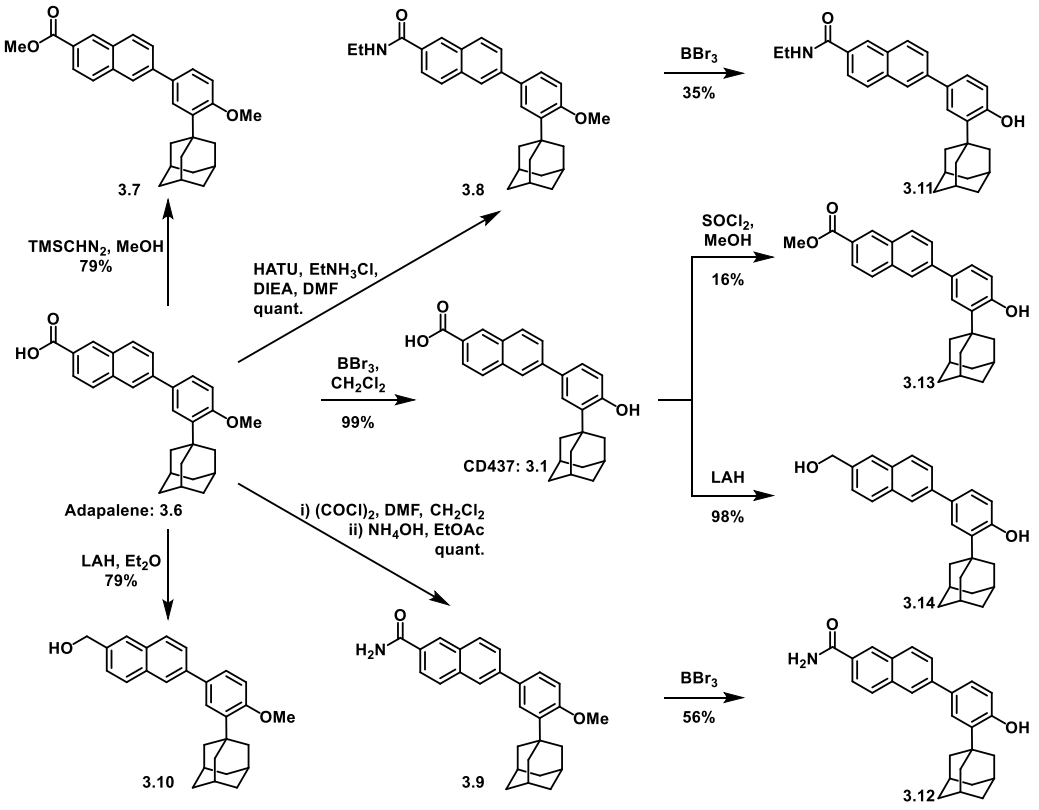

Scheme 25. Synthesis of first-generation retinoid analogs from adapalene (**3.6**).

These analogs allowed a quick test of the importance of the acid and phenol functionalities. The methyl ether proved to be essential for bioactivity (*vida infra*). The acid could also not be severely altered, however the alcohol analog (**3.14**) did improve the toxicity profile

while marginally affecting potency. We next looked to more drastic changes to the molecule, specifically the naphthalene, phenol, and adamantane functionalities.

3.3.2 Retrosynthetic Analysis and CD437 Analog Design

With the data from our first-generation analogs, we next looked to alterations on the rest of the lead compound. We knew that alterations to the acid were not tolerated, as well as phenol. Retrosynthetically, CD437 was split in half, which meant we would need appropriately brominated naphthalene precursors with the general structure **3.15** (Figure 29). We hoped to add extra phenols to this precursor such that R_2 would be a suitably protected phenol (MEM or acetyl) at any of the available positions 1, 3, 4, 5, 7, and/or 8. The complementary Suzuki partner, boronic acid **3.16**, would involve moving the phenol moiety to another position (ortho to boronic acid), and altering R_1 from adamantane to benzyl. The modeling results indicated that the isomeric phenol may give the adamantane moiety a better projection into the membrane, and benzyl is much more flexible, which could make membrane binding more favorable.

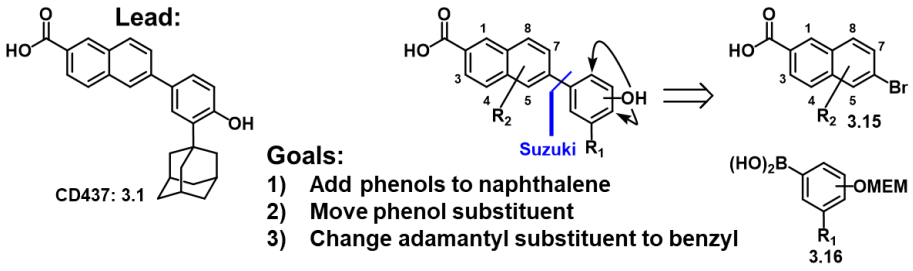

Figure 29. Goals of the CD437 analog campaign and general building block structures **3.15** and **3.16**.

3.3.3 Synthesis of Boronic Acid Building Blocks

We first targeted the boronic acid coupling fragment in our synthetic studies. There has been much work done to optimize the synthesis of adapalene, **3.6**. To this end, a large-scale procedure is available for the Friedel-Crafts reaction between 4-bromophenol **3.17** and 1-adamantol **3.18**, which gave a modest yield of 42% in our hands (Scheme 26).[16] The phenol was

protected as the corresponding MEM ether, providing **3.20**. Lithiation and borylation followed by hydrolysis provided boronic acid **3.21** as a mixture of acid and borate oligomers. This route was applied starting from 2-bromophenol **3.22**, to provide the isomeric boronic acid **3.25**. The issue of the boronic acid oligomer mixture was not an issue since the compounds all reacted in the following step. However, recent follow-up work has involved using boronic esters instead of acids to allow characterization of the borate intermediates (**3.25** and subsequent analog synthesis was performed by me, **3.21** and resultant analogs were synthesized by Colleen Keohane).

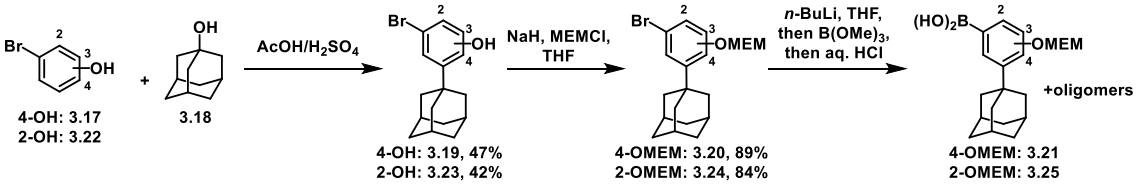

Scheme 26. Synthesis of the two isomeric boronic acid precursors **3.21** and **3.25**.

The synthesis of the precursor for the benzyl analogs was very similar to the adamantane compounds and is depicted in Scheme 27. Bromination of commercially available *ortho*-cresol **3.26** was carried out according to literature precedent, yielding **3.27** in quantitative yield.[17] From there, the same sequence was followed as shown for the adamantane precursors above, yielding boronic acid **3.29** as a mixture of monomer and oligomers.

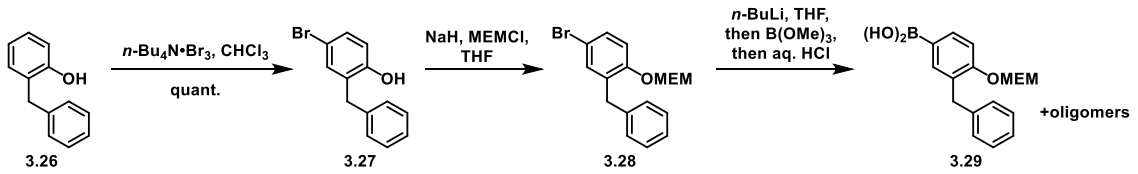

Scheme 27. Synthesis of benzyl analog precursor **3.29**.

3.3.4 Synthesis of Unsubstituted Naphthalene CD437 Analogs

With boronic acids in hand, we first synthesized CD437 analogs containing the original naphthalene fragment. The Suzuki reactions and deprotections were very reliable, and the results

are shown in Scheme 28. Yields for the Suzuki reaction are reported over two steps, due to the boronic acid being a mixture of monomer and oligomers.

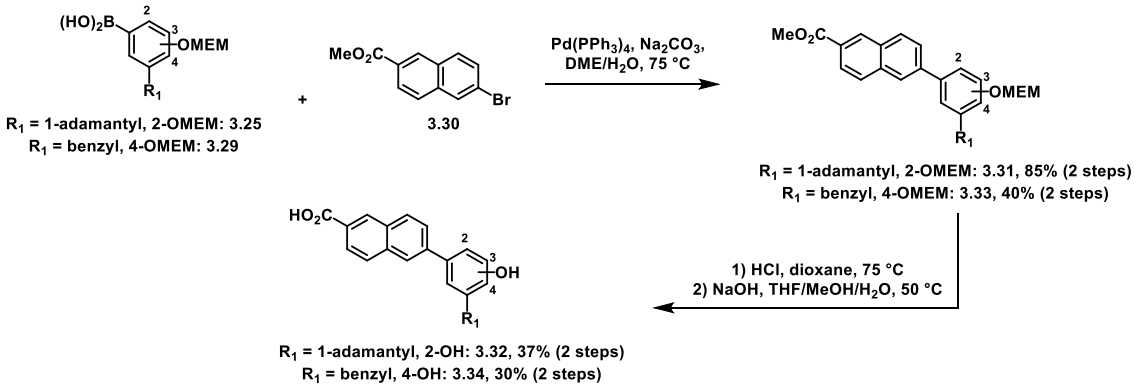

Scheme 28. Final steps in the synthesis of CD437 phenol isomer **3.32** and benzyl analog **3.34**.

3.3.5 Unsuccessful attempts at accessing oxidized naphthalene analogs of CD437

Looking toward the naphthalene fragment, we were curious if oxidation of the C-H bonds in the naphthalene ring would yield less toxic and/or more potent analogs. We first attempted a published procedure to access naphthalene derivatives with a phenol at the 4-position, which is shown in Scheme 29 (carried out by Colleen Keohane).[18] The precedent did not include any examples with a bromine substituent, which proved to be an important distinction. The first step was an aldol reaction between 4-bromobenzaldehyde (**3.35**) and dimethyl succinate (**3.36**) and subsequent elimination, followed by hydrolysis. This yielded dicarboxylic acid **3.37** in quantitative yield. Next the Friedel-Crafts acylation/cyclization was attempted to access naphthalene **3.38**. Exposure of **3.37** to concentrated sulfuric acid yielded no product, only recovered starting material. Extended reaction times and heat also yielded no product. This was most likely due to the electron-withdrawing bromine, which destabilizes the carbocation intermediate of the Friedel-Crafts reaction relative to its unsubstituted counterpart.

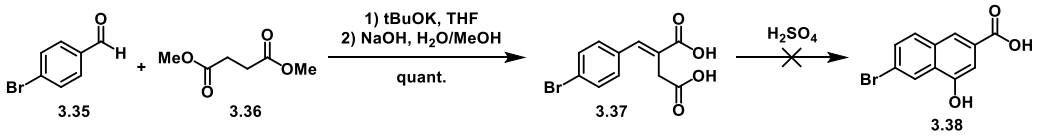

Scheme 29. First attempt at synthesis of oxidized naphthalene Suzuki precursor **3.38**.

With this temporary set-back in mind, we turned to literature precedent containing all of the desired functionalities. The Kozlowski lab synthesizes many oxidized naphthalene derivatives to explore biaryl coupling reactions. We sought to utilize their well-established syntheses to generate oxidized naphthalene derivatives containing the requisite bromine and acid/ester moieties.[19] The synthesis of the precursor is shown in Scheme 30. Commercially available acid **3.39** was brominated to yield compound **3.40** in good yield. From there, the acid was converted to the corresponding acid chloride and alkylated with the sodium enolate of dimethyl malonate (**3.41**). The resultant diester **3.42** was cyclized upon treatment with concentrated sulfuric acid, yielding naphthalene **3.43**, which was acetylated to yield Suzuki precursor **3.44**. The crude intermediates were carried directly between steps to avoid any decomposition, and yielded gram quantities of material with 60% over the three steps from **3.40** to **3.44** (naphthalene fragment was synthesized by me, Colleen Keohane and I both used this material for the subsequent chemistry).

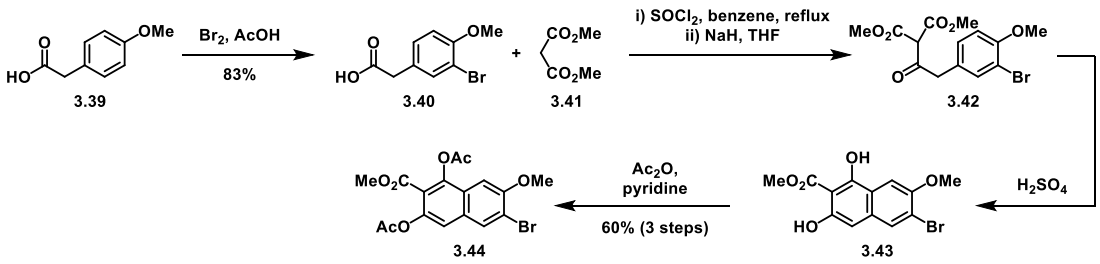

Scheme 30. Successful synthesis of bromo-naphthalene fragment **3.44**.

With boronic acids **3.21**, **3.25**, and **3.29** in hand, as well as naphthalene **3.44**, we next looked to the Suzuki reaction and deprotection steps to access our desired oxidized analogs, the details of which are shown in Scheme 31. The Suzuki reactions were all successful, but in many cases mixtures of phenols were isolated, due to partial hydrolysis of one or both acetates. This

was not an issue, since the next step was deprotection, which proved to be non-trivial. MEM ethers could be easily removed with HCl and dioxane, however saponification or demethylation (BBr_3) were not successful. The final step resulted in unstable materials that underwent decomposition within a few hours or a day. Extra methyl signals in many of the NMR spectra of the isolated materials as well as the disappearance of an aromatic signal indicated that the naphthalene ring, once the phenols were revealed, was becoming methylated. This was most likely from reaction solvents (dichloromethane or methanol) and/or purification solvents (acetonitrile) when HPLC was attempted (Colleen Keohane and I each attempted several deprotections with the depicted compounds).

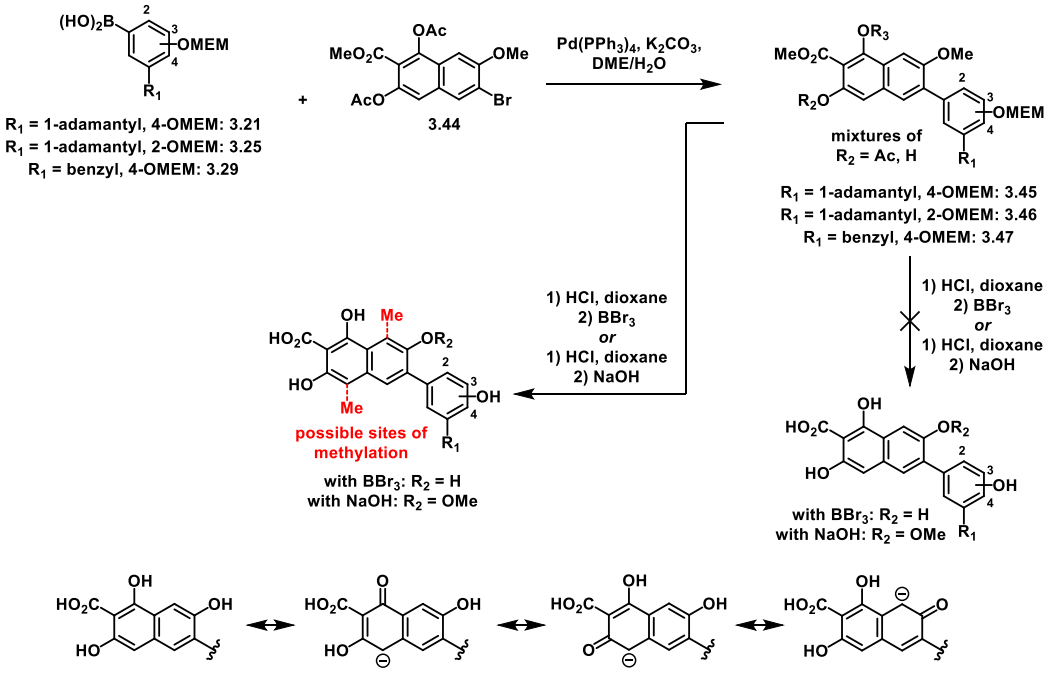

Scheme 31. Suzuki reaction and attempted deprotection. Highlighted in red are the sites of possible methylation and below are the resonance structures that rationalize them.

From our observations, it appeared that the attempted sites of oxidation were not feasible, due to the reactivity of the naphthalene system. We next looked to a different pattern of oxidation to avoid this issue, specifically at the 3 and 7 positions of the naphthalene ring.

3.3.6 Synthesis of oxidized naphthalene analogs of CD437

We next strategically chose a substrate to avoid the reactivity issues encountered with the previous set of analogs. We took advantage of a previously published procedure to access naphthalene **3.48** and used this chemistry to construct another naphthalene with an additional methoxy substituent, **3.49**.[20] The sequence began with commercially available benzaldehydes **3.50** and **3.53** and is shown in Scheme 32. The aldehydes were subjected to Horner-Wadsworth Emmons (HWE) olefinations with phosphonate **3.51**, yielding mixed esters **3.52** and **3.54**. The *tert*-butyl esters were selectively hydrolyzed with TFA/water and the crude acid was subjected to cyclization/acetylation with acetic anhydride and sodium acetate, yielding oxidized Suzuki precursors **3.48** and **3.49** in modest yield (synthesized by Colleen Keohane and me).

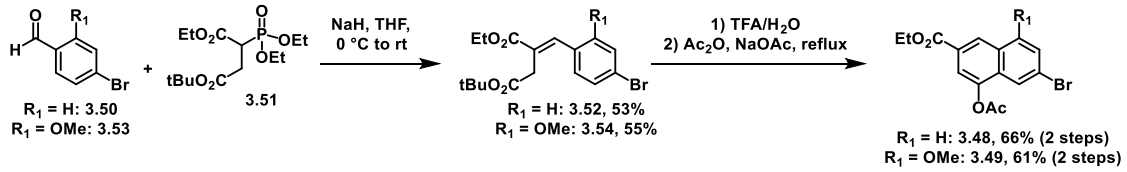

Scheme 32. Synthesis of oxidized naphthalene Suzuki precursors **3.48** and **3.49**.

We next looked toward Suzuki couplings and deprotections with the three boronic acids **3.21**, **3.25**, and **3.29** and oxidized naphthyl bromides **3.48** and **3.49**. First, the singly oxidized naphthyl bromide **3.48** was coupled with each of the boronic acids shown in Scheme 33. We switched to sodium hydroxide from sodium carbonate as previously shown, as this change led to consistent hydrolysis of the acetates during the Suzuki reaction. This yielded protected analogs **3.55**, **3.57**, and **3.59**. From there, acid-mediated cleavage of the MEM ethers followed by saponification provided analogs **3.56**, **3.58**, and **3.60**.

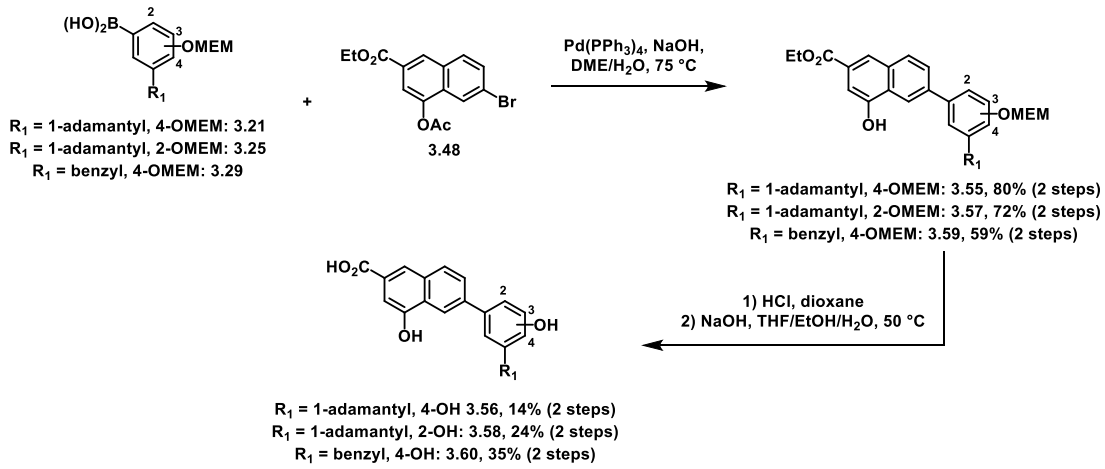

Scheme 33. Synthesis of singly oxidized naphthalene analogs **3.56**, **3.58**, and **3.60.**

The synthesis of bisphenol naphthalene analogs was analogous to the monophenols, apart from the deprotection step, which is shown in Scheme 34. Suzuki reaction yielded protected analogs **3.61**, **3.63**, and **3.65**. One of the Suzuki reaction products, **3.61**, retained the acetate over the course of the reaction, while the others were hydrolyzed. In all cases, excess BBr_3 at room temperature overnight was sufficient to remove all protecting groups, including MEM, acetate, methyl ether, and ethyl ester. This sequence yielded analogs **3.62**, **3.64**, and **3.66** all containing two extra phenol substituents compared to CD437. Gratifyingly, we did not observe decomposition of any of the analogs after purification as was the case with the previous set of compounds.

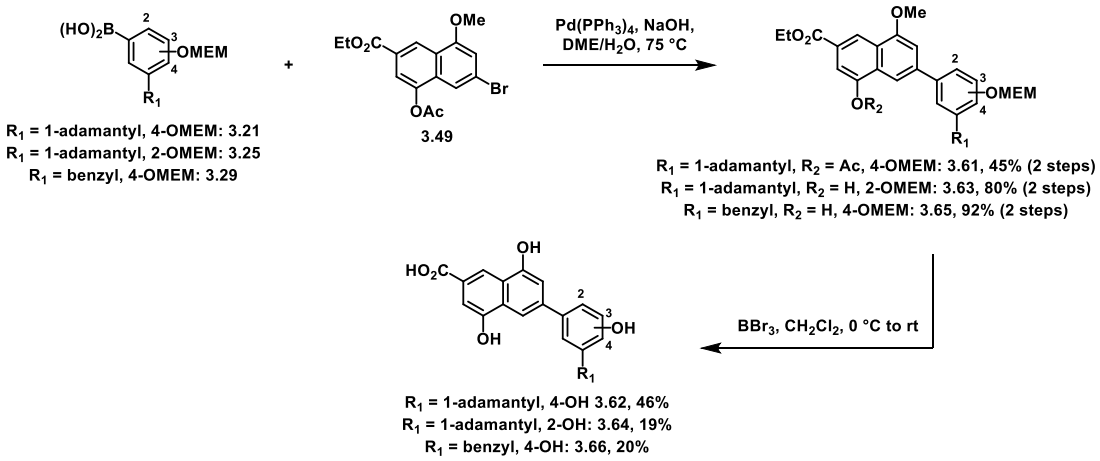

Scheme 34. Synthesis of naphthalene analogs with two additional phenol substituents, **3.62**, **3.64**, and **3.66**.

3.3.7 SAR data of CD437 analogs

With the library of analogs in hand, we next sent the compounds to our collaborators for biological testing. All compounds were tested for inhibitory activity and membrane polarization against MRSA. The structures and MIC values are shown in Figure 30. Our initial analog results (left column) showed that the acid could only be replaced by an alcohol to maintain biological activity, with a modest (2-fold) drop in potency, while the phenol was essential for any bioactivity. For the adamantane analogs (middle column), addition of a phenol to the naphthalene core decreased activity, and even further when a second phenol was added. The benzyl analogs (right column) retained activity compared to adamantane, but also decreased potency as phenols were added to naphthalene. Our two most active analogs, **3.14** and **3.34**, were merely two-fold less active than CD437. We then wondered if their toxicity was greatly reduced, which would be an important discovery going forward into a clinical setting.

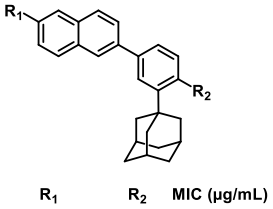

#	R_1	R_2	MIC (μg/mL)
3.1 (CD437)	CO_2H	OH	1
3.7	CO_2Me	OMe	>64
3.8	CONHEt	OMe	>64
3.9	$CONH_2$	OMe	>64
3.10	CH_2OH	OMe	>64
3.11	CONHEt	OH	>64
3.12	$CONH_2$	OH	>64
3.13	CO_2Me	OH	>64
3.14	CH_2OH	OH	2

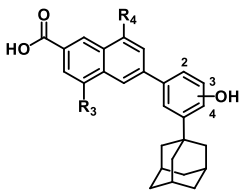

#	R_3	R_4	x-OH	MIC (μg/mL)
3.1 (CD437)	H	H	4	1
3.56	OH	H	4	4
3.62	OH	OH	4	16
3.32	H	H	2	32
3.58	OH	H	2	4
3.64	OH	OH	2	8

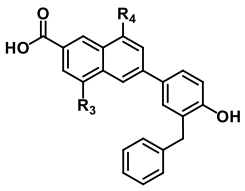

#	R_3	R_4	MIC (μg/mL)
3.34	H	H	2
3.60	OH	H	16
3.66	OH	OH	64

Figure 30. Compiled MIC data results from CD437 analog biological testing.

The two most potent compounds **3.14** and **3.34** were then subjected to toxicity experiments, both for hemolysis and cytotoxicity. Unfortunately, **3.34** caused hemolysis beginning around 20 μg/mL and cytotoxicity at 15 μg/mL (see Figure 31a/b). Gratifyingly, **3.14** caused no significant hemolysis and minimal cytotoxicity at 30 μg/mL, which are significant improvements from CD437. Additionally, **3.14** showed significantly less hepatotoxicity than CD437, which was one of the main problems we wished to solve at the outset of this project (see Figure 31c).

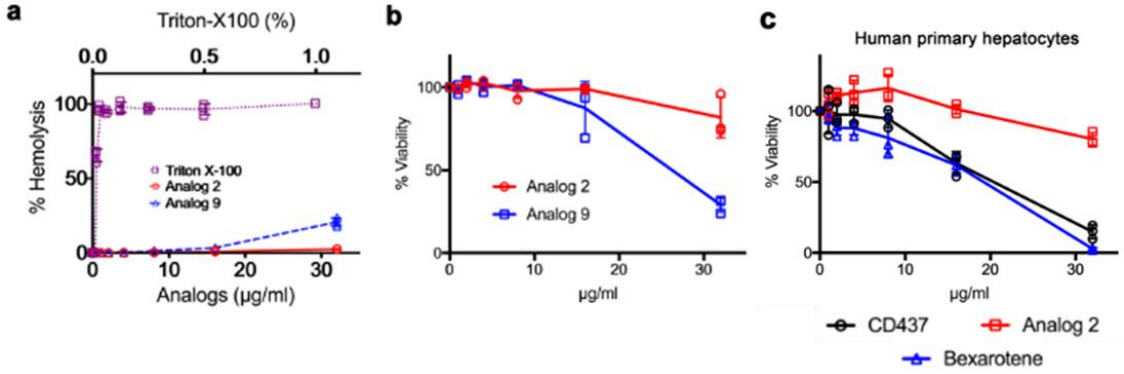

Figure 31. Toxicity assay results with the two most potent CD437 analogs. "Analog 2" refers to **3.14**, while "Analog 9" refers to **3.34**. (a) Hemolysis assay results with Triton X-100 as the positive control. (b) Cytotoxicity assay results. (c) Hepatocyte (liver cell) toxicity of **3.14** vs. CD437 and bexarotene, a cytotoxic retinoid used in cancer therapy.

3.3.8 Conclusions

Our studies have laid the groundwork for a new class of MRSA planktonic/persister cell eradicating retinoids with potential clinical use. CD437 was an initial hit with promising activity, and our synthetic studies led to the discovery of a compound with less toxicity issues, while still maintaining CD437's favorable medicinal potential. Since our initial discovery, we have begun sending **3.14** to other laboratories for preclinical trials, after our collaborators completed many pharmacodynamic/pharmacokinetic experiments in mouse models. We have synthesized over a gram of **3.14** to date from adapalene and will further scale up the route from simpler starting materials. Current results have shown that **3.14** is very safe and mice were able to safely tolerate doses of 200 mg/kg.

In addition to the discovery of **3.14**, our synthetic work also helped shed light on the compounds' mechanism of action. Our data showed that additional phenol substituents on the naphthalene ring decreased the potency of analogs, the importance of the phenol's position on the benzene ring, as well as the importance of adamantane for maintaining selectivity for bacterial membrane damage. Since our analogs all lend credence to the computational simulations/modeling, we have been able to leverage this data in designing another generation of CD437 analogs, which have the potential to increase potency/selectivity even further. These efforts will be fueled by the work shown here, as our synthetic procedures and routes are very flexible and efficient.

3.4 Synthetic and Biological Studies of nTZDpa

3.4.1 Synthetic Route Design and Prior Art

Our goals at the outset of the nTZDpa project were very similar to the CD437 project: make more potent and selective (less toxic) analogs. The literature precedent for the synthesis of nTZDpa was limited to one patent, the relevant chemistry from which is shown in Scheme 35,

with the issues we aimed to address.[21] First, no yields were reported. Second, treatment of **3.67** with a Grignard reagent with the intent of deprotonation of the indole nitrogen is unlikely to be successful in the presence of an ester. This functional group is well-known to undergo single and double addition with Grignard reagents, yielding ketone and alcohol products, respectively. Additionally, the thiosulfonate reagent for the subsequent sulfenylation leading to **3.68** requires an additional step to synthesize. This is not compatible with our desire to make many derivatives involving changes to the thiophenyl substituent. Finally, the use of HMPA is problematic from a practical standpoint, as it is difficult to remove from crude reaction mixtures and is highly toxic.

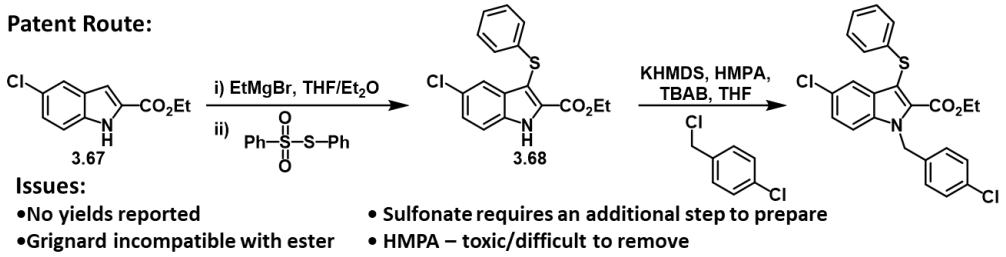

Scheme 35. Patent route to nTZDpa with highlighted issues we aimed to address.

The patent route did, however, show the most logical bond disconnections in our synthetic approach to nTZDpa analogs. We adopted a versatile sulfenylation strategy for addition of thiophenol derivatives to the 3-position of indoles in our synthesis, and optimized alkylation conditions to add benzyl derivatives to the indole nitrogen.[22] Using this strategy, we were able to quickly and efficiently assemble a library of nTZDpa analogs to gain insight into SAR data for the first time.

3.4.2 Optimized Synthesis of nTZDpa and Analogs

Our synthesis of nTZDpa is detailed in Scheme 36. While the corresponding indole (**3.67**) is commercially available, our goal was to find a general method to synthesize a library of indole starting materials. We leveraged a palladium-catalyzed annulation of 4-chloro-2-

iodoaniline with pyruvic acid, to yield the corresponding indole-2-carboxylic acid.[23] The purification of this intermediate proved difficult: its polarity made the polar byproducts from the reaction elute with the product during chromatography, and residual DMF along with the byproducts made crystallization not feasible. We eventually found that subjecting the crude reaction mixture after aqueous workup to esterification ($SOCl_2$, EtOH, reflux) allowed isolation of ethyl ester **3.67** in high yield and purity after filtering over a short plug of silica gel. From there, sulfenylation as reported in the literature precedent commenced without incident, except a small amount of acetonitrile was needed to fully solubilize the starting material.[22] Alkylation of the indole nitrogen was then accomplished with 4-chlorobenzyl chloride, K_2CO_3, and TBAB in DMF at elevated temperatures. The polarity of the solvent proved crucial for this step, as only trace amounts of product were observed with acetone as a reaction solvent. NaH in DMF caused significant hydrolysis of the ester, leading to a mixture of ethyl and benzyl esters. From the benzylated product, saponification yielded nTZDpa, with an overall yield of 40% (several batches of nTZDpa were prepared by both myself and Isabelle Sinitsa).

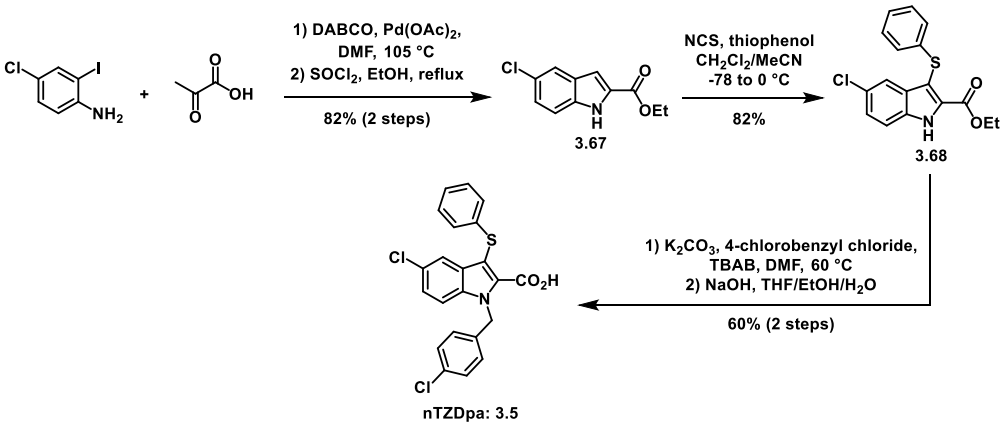

Scheme 36. Synthesis of nTZDpa (**3.5**).

After the synthesis of nTZDpa, we constructed three analogs to test the importance of the benzyl and carboxylic acid functionalities (Scheme 37). From previous intermediate **3.68**, methylation followed by hydrolysis yielded the simplified analog **3.70**. Akin to CD437, nTZDpa

was also converted to its corresponding primary and ethyl amide analogs, **3.71** and **3.72**, respectively.

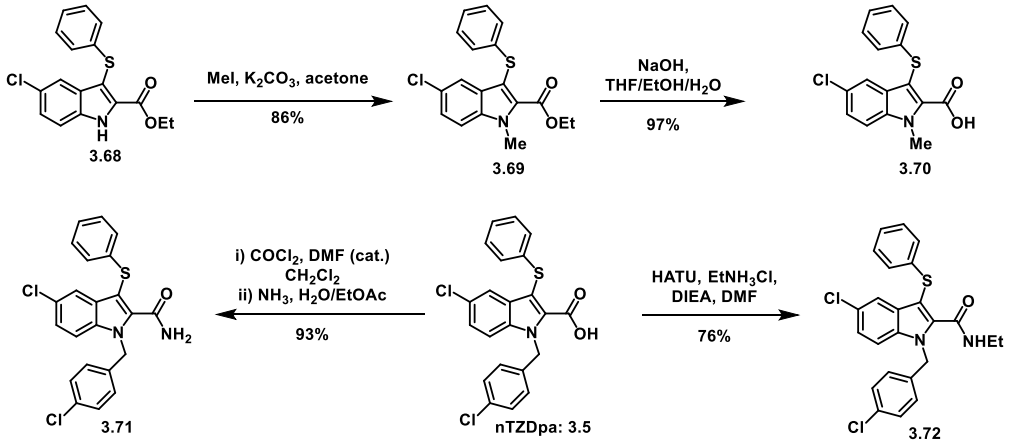

Scheme 37. Synthesis of analogs **3.70**, **3.71**, and **3.72**.

Next, we targeted a series of benzyl analogs, the synthesis of which are shown in Scheme 38. Benzyl analog **3.73** was first made via alkylation with BnBr and NaH. The intermediate was isolated as a mixture of ethyl and benzyl esters, due to trace amounts of water in DMF, which would in turn form hydroxide *in situ*. The mixture was then hydrolyzed directly to analog **3.73**, in 80% yield over two steps. Next, we attempted alkylation of indole **3.68** with PMBCl and NaH in DMF and observed only trace amounts of product. Relative to BnBr, PMBCl is less reactive due to both its less stable leaving group (chloride) and electron-donating substituent (methoxy). Alternatively, alkylation of indole **3.68** with PMBCl, K_2CO_3, and NaI in acetone yielded alkylated product **3.74** in 80% yield, which was hydrolyzed to yield benzyl analog **3.75**. These conditions were favorable compared to NaH/DMF, in that they did not result in any trans-esterified product mixtures. Alkylation of **3.68** with 3-chlorobenzyl chloride was successful with these conditions as well, providing product **3.76** in 65% yield, which was hydrolyzed to nTZDpa analog **3.77** (synthesized first by me and another batch was synthesized by Isabelle Sinitsa). These alkylation conditions seemed reliable going forward, as they were successful with benzyl chlorides containing both electron-donating and electron-withdrawing substituents.

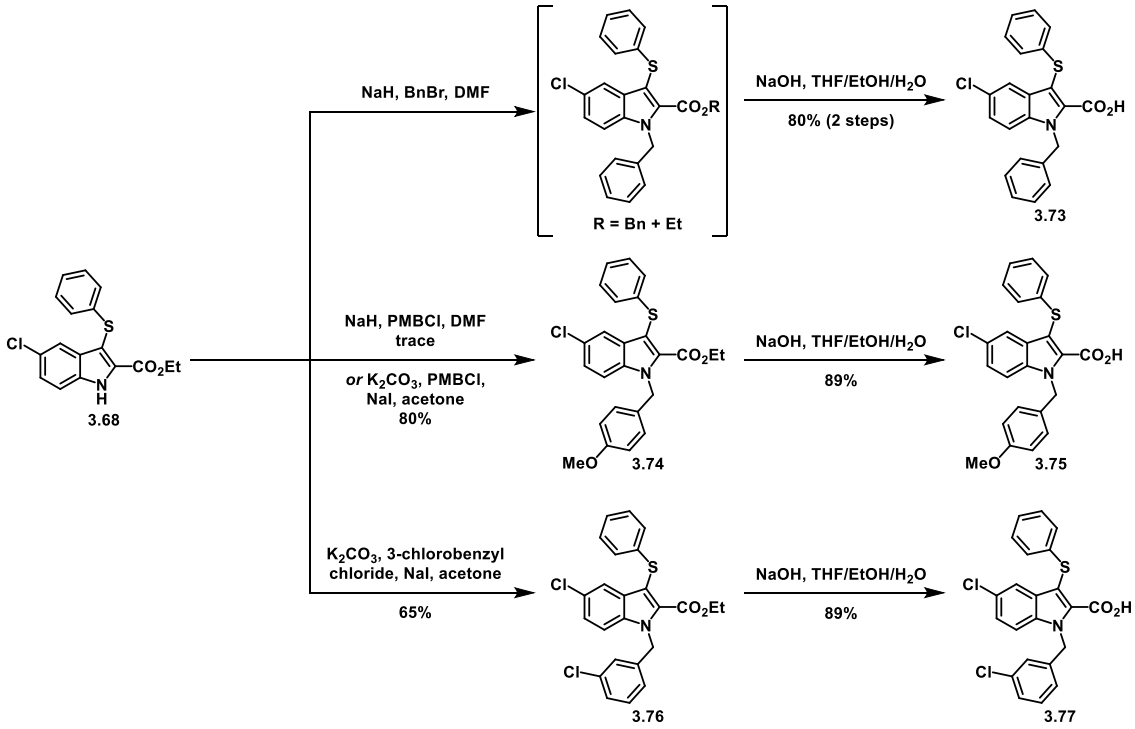

Scheme 38. Synthesis of nTZDpa analogs **3.73**, **3.75**, and **3.77**.

After the first three benzyl analogs, we next looked at varying the substituents on 4-position of the phenyl thioether moiety. We began with three substituents of similar size, but drastically different electronic properties: chlorine, methyl, and methoxy. The initial results of these studies are shown in Scheme 39. From nTZDpa intermediate **3.67**, sulfenylation with 4-chlorothiophenol yielded thioether **3.78**. Alkylation with 4-chlorobenzyl chloride, K_2CO_3, and NaI in acetone and subsequent hydrolysis yielded analog **3.79** in good yield. Similarly, sulfenylation of **3.67** with 4-methylthiophenol yielded thioether **3.80**, followed by the same alkylation/hydrolysis conditions as above provided **3.81** in 44% yield over two steps. When the same sequence was adopted starting with **3.67** and 4-methoxythiophenol, the alkylation yield fell to 15%. The alkylation yields were clearly correlated with the acidity of the indole nitrogen, as ring systems with more electron density (methoxy vs. chloro) provided lower yields.

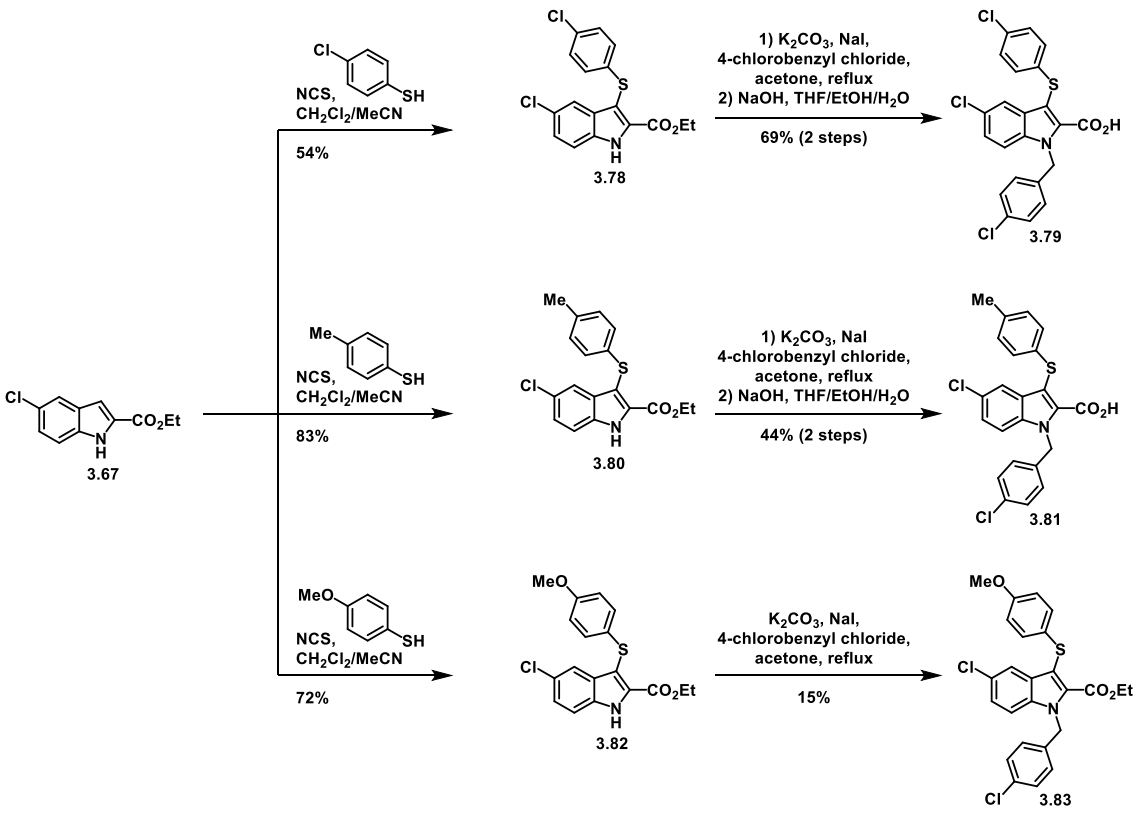

Scheme 39. Synthesis of analogs **3.79** and **3.81** and demonstration of the importance of indole nitrogen acidity.

To solve this issue, we reverted to NaH in DMF as the base and solvent, which was successful in our initial studies, with the caveat that mixtures of benzyl and ethyl esters were isolated. We found that NaH, 4-chlorobenzyl chloride, and TBAI in DMF followed by saponification of the benzyl/ethyl ester mixture yielded methoxy-phenyl thioether analog **3.84** in 59% yield over two steps (Scheme 40). We next carried out a sulfenylation reaction between **3.67** and 4-*tert*-butylthiophenol, yielding **3.85**. The same alkylation/hydrolysis conditions as above provided **3.86** in 64% yield. This analog contains another electron-donating group (*tert*-butyl), highlighting the generality of the alkylation procedure.

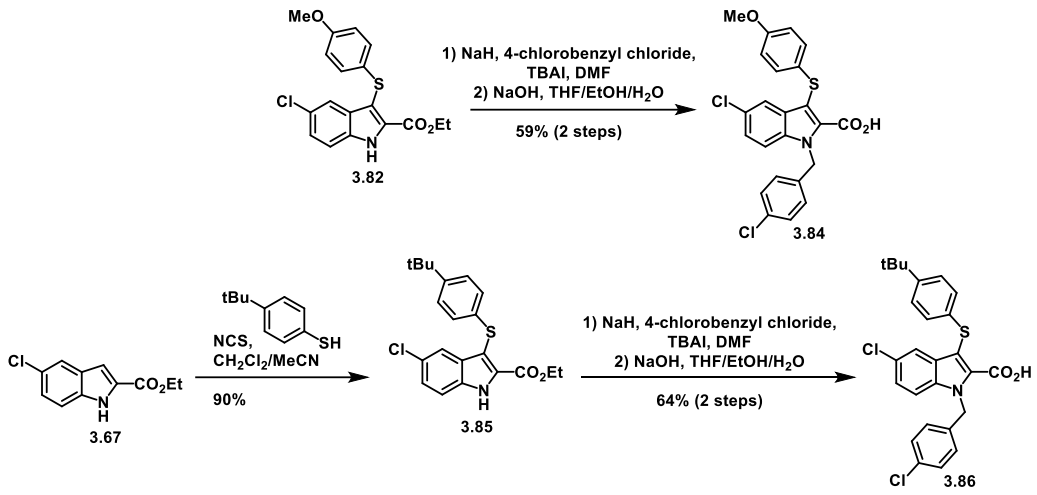

Scheme 40. Synthesis of **3.84** and **3.86** with the generalized alkylation conditions.

We next applied our synthetic route to a series of indole analogs, whereby the chlorine substituent of the indole ring was replaced with more electron withdrawing groups: fluorine and trifluoromethyl, yielding analogs **3.90** and **3.94**, respectively. We also synthesized the chlorine isomer to test the importance of the location of the substituent, leading to nTZDpa isomer **3.98** (see Scheme 41 for details, one batch was synthesized by me and another by Isabelle Sinitsa).

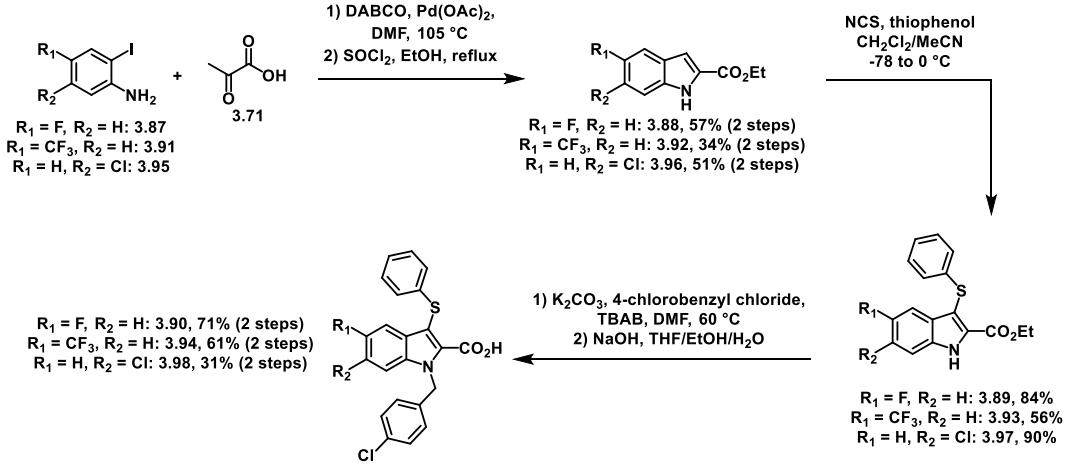

Scheme 41. Synthesis of three indole nTZDpa analogs **3.90**, **3.94**, and **3.98**.

We next aimed to test the importance of the thioether moiety of nTZDpa, by first altering it to a more electron-withdrawing oxygen. The synthesis of this analog, as well as a simplified methyl ether analog, **3.103**, is detailed in Scheme 42. Methyl 2-amino-5-chlorobenzoate (**3.99**)

was alkylated with methyl bromoacetate, followed by cyclization with NaOMe, providing indole **3.100**. Selective methylation of the resultant phenol was accomplished with K_2CO_3 and dimethyl sulfate, providing **3.101**.[24] The methoxyindole was then alkylated with our generalized conditions, yielding **3.102**. Notably, no transesterification products were observed. **3.102** was diverted via hydrolysis to yield analog **3.103**. Additionally, **3.102** was carried forward and deprotected with BBr_3, yielding phenol **3.104**. Chan-Lam coupling with phenylboronic acid provided ether **3.105**, which was subsequently hydrolyzed, providing ether analog **3.106**.[25]

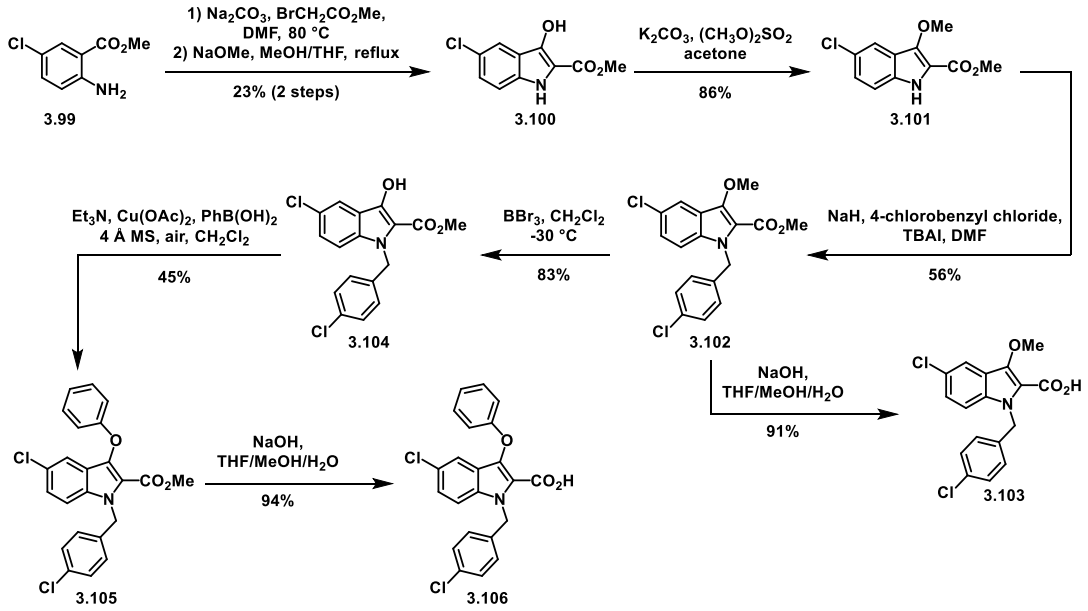

Scheme 42. Synthesis of ether analogs **3.103** and **3.106**.

We next targeted another thioether analog, where the sulfur was replaced by a methylene functional group. The synthesis of this analog is shown in Scheme 43. A published procedure was followed that involved Friedel-Crafts acylation with benzoyl chloride followed by reduction with Et_3SiH/TFA to provide indole **3.107**, which was benzylated at the 3-position.[26] From there, our standard alkylation/hydrolysis conditions yielded methylene analog **3.108**, which was the final analog synthesized over the course of this study.

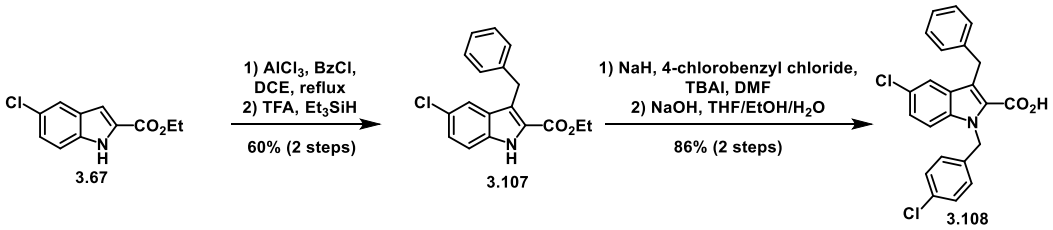

Scheme 43. Synthesis of methylene analog **3.108**.

3.4.2 SAR data of nTZDpa analogs

With our library of compounds in hand, we enlisted the help of collaborators for biological testing. MIC assays were performed against MRSA to evaluate each compound's potency. A membrane permeabilization assay showed if the mechanism of action was still the same as nTZDpa. This assay involved the monitoring of the uptake of SYTOX, which a compound that forms a fluorescent complex with DNA. Damaged membranes allow passage of the dye, and subsequent fluorescent signal. A hemolysis assay was used to gauge toxicity, whereby raising the HC_{50} meant a less toxic compound. Our first group of three analogs were quickly synthesized from nTZDpa itself or intermediates along the way, which gave a quick glimpse into the importance of two key structural features of the molecule: the benzyl substituent on nitrogen and the carboxylic acid. Figure 32 shows the results of this initial screen. Both structural features proved crucial for biological activity, as the three analogs maintained either little (**3.70**) or no biological activity (**3.71** and **3.72**).

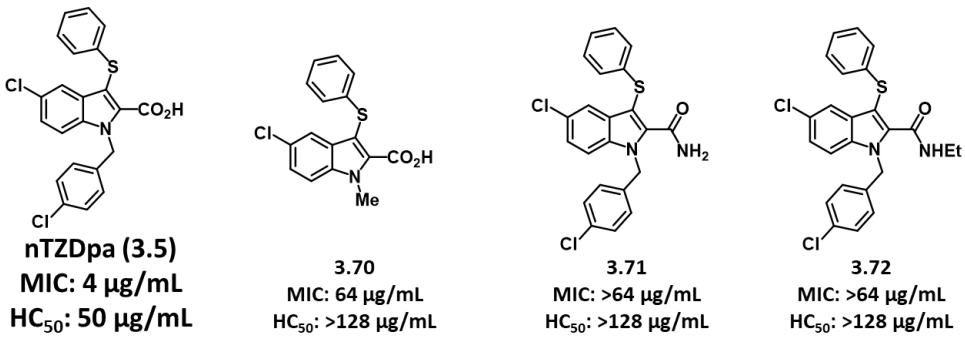

Figure 32. Results of initial screen of analogs **3.70**, **3.71**, and **3.72**.

After the initial screen of analogs, the next series was synthesized and tested. The MIC and HC_{50} values for the first series of analogs that vary the substituents on each portion of nTZDpa (without changing thioether) are shown in Figure 33. Of this first series of 10 analogs, two (**3.80** and **3.88**) were more potent than nTZDpa, however each of these compounds was also significantly more toxic (HC_{50} reduced from 50 μg/mL).

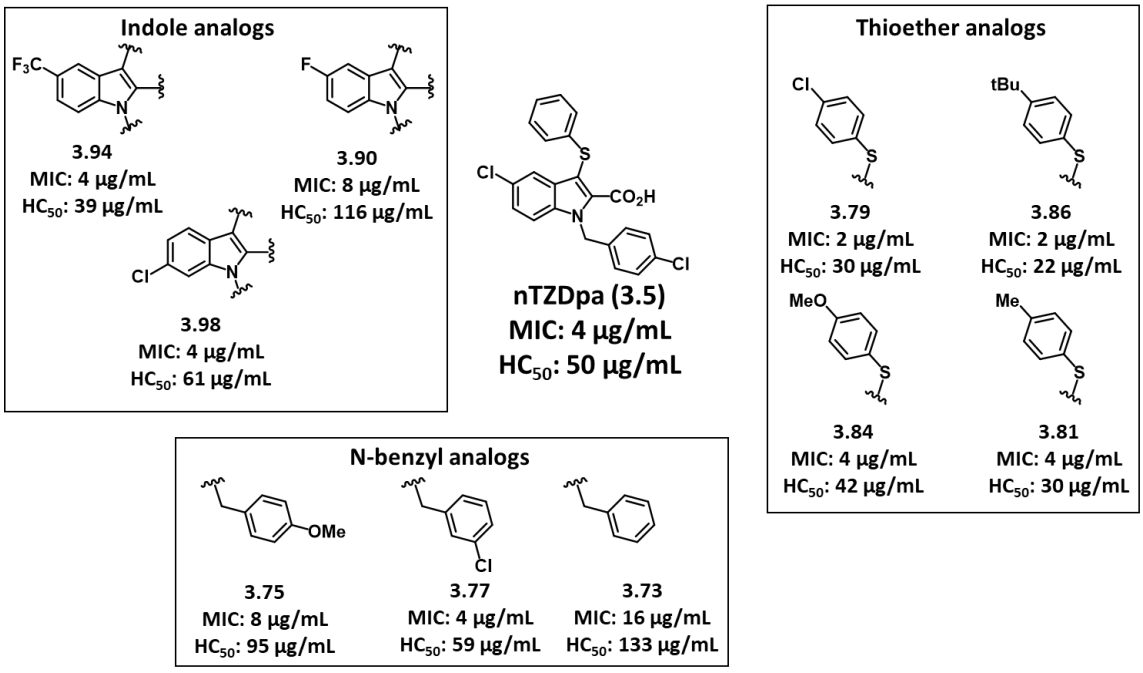

Figure 33. SAR data for the initial round of nTZDpa analogs, with MIC (MRSA) and HC_{50} (hemolysis) values given.

The ether and methylene analogs had interesting results from the initial biological testing, summarized in Figure 34. All three analogs exhibited *no toxicity against red blood cells*, revealing that replacement of the sulfur atom had a positive effect on selectivity. Additionally, ether analog **3.106** was equipotent with nTZDpa and is the new lead compound. Changes that increased the original scaffold's potency and toxicity are currently being implemented alongside the successful switch of thioether to ether and may provide non-toxic analogs with increased potency.

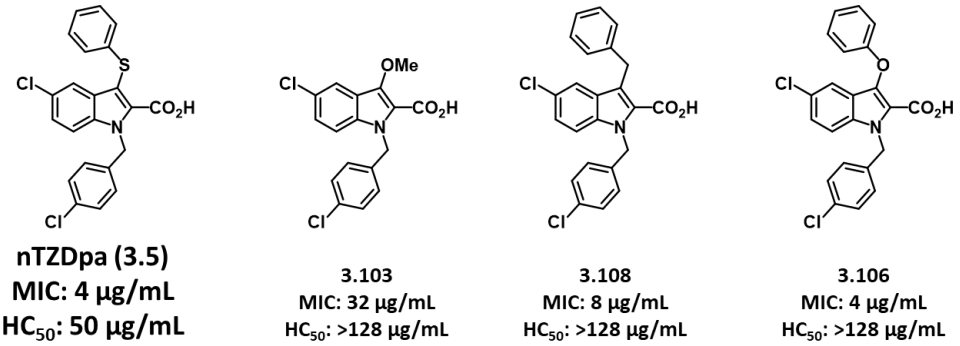

Figure 34. Potency and toxicity data for analogs **3.103**, **3.108**, and **3.106**.

3.5 Conclusions

The goals of both the CD437 and nTZDpa projects were very similar: develop a high-yielding, efficient, and flexible synthetic route to access the lead compound as well as a variety of analogs to test specific hypotheses about the compound's mechanism of action. Concurrently, apply this synthetic strategy to discover less toxic and more potent compounds that are effective killers of MRSA planktonic and persister cells, a clinically relevant and challenging problem.

Persister cells itself are not an easily manageable problem, as these cells are metabolically dormant, and evade typical drug treatments. Two examples of compounds with activity against persister cells are the potent DNA-crosslinking agents mitomycin C and cisplatin.[27-28] Both compounds are FDA-approved for use in oncology. DNA-crosslinking has the potential to cause undesirable toxicity effects, and it is unlikely that these types of treatments will find use as antibiotics due to their myriad of side effects. In contrast, our membrane-damaging compounds have the potential to be extremely selective for bacterial cells, demonstrated by the results presented here.

We accomplished many of the goals for each project in short order. In the case of CD437, we assembled eight structurally unique analogs in 1-2 steps from commercially available

adapalene, which gave preliminary results into SAR of this molecule. Additionally, the discovery of analog **3.14** with greatly reduced toxicity has brought forth a new generation of analogs currently, and intense follow-up studies in mouse models and preclinical testing have begun. From this initial library, we designed an additional series of analogs with stepwise oxidation of the naphthalene portion of CD437, phenol isomers, as well as adamantyl replaced with benzyl. Unfortunately, all analogs in this series had an unfavorable potency/toxicity profile in relation to CD437. However, these compounds were important in that they lend credence to the proposed mechanism of action that combines both experimental and computational data. With our increasing confidence in the mechanism, new generations of CD437 analogs are currently being designed and synthesized.

In a similar fashion to CD437, nTZDpa analogs were quickly synthesized from a reliable route after applying it to the initial lead compound. We first showed that adding chlorine or *tert*-butyl substituents to the thioether portion of the molecule increased potency, but also toxicity. All other changes caused reductions in potency as well as toxicity. From there, we tested the importance of the sulfur atom of the thioether moiety, by changing it to a methylene or ether functional group. All the analogs with these changes were completely selective for bacterial cells over red blood cells. Gratifyingly, ether analog **3.106** retained the same potency level as nTZDpa vs. MRSA cells. This new scaffold has been further probed for biological activity by other students in this lab, and new, more potent compounds have since been discovered.

Both concurrent projects have been delivered from their infancy to a more mature state by the work reported here and have the potential to cause significant clinical impact. This is exemplified by CD437, where analog **3.14** has been sent out for preclinical screening, and extensive mouse model work has already been done, demonstrating the compound's potential. The less potent of the two original lead compounds, nTZDpa, has been optimized regarding its

toxicity. Improvements to the potency will unfold by continually utilizing the SAR data from the work shown here along with future studies.

3.6 References

1) Mylotte, J. M.; McDermott, C.; Spooner, J. A. *Rev. Infect. Dis.* **1987**, *9*, 891.

2) Fischbach, M. A.; Walsh, C. T. *Science* **2009**, *325*, 1089.

3) Lowy, F. D. *J. Clin. Invest.* **2003**, *111*, 1265.

4) David, M. Z.; Daum, R. S. *Clin. Microbiol. Rev.* **2010**, *23*, 616.

5) Kluytmans, J.; van Belkum, A.; Verbrugh, H. *Clin. Microbiol. Rev.* **1997**, *10*, 505.

6) Hobby, G. L.; Meyer, K.; Chaffee, E. *Proc. Soc. Exp. Biol. Med.* **1942**, *50*, 281.

7) Lewis, K. *Annu. Rev. Microbiol.* **2010**, *64*, 357.

8) Rajamuthiah, R.; Fuchs, B. B.; Jayamani, E.; Kim, Y.; Larkins-Ford, J.; Conery, A.; Ausubel, F. M.; Mylonakis, E. *PLoS One* **2014**, *9*, e89189.

9) Valli, C.; Paroni, G.; Di Francesco, A. M.; Riccardi, R.; Tavecchio, M.; Erba, E.; Boldetti, A.; Gianni, M.; Fratelli, M.; Pisano, C.; Merlini, L.; Antoccia, A.; Cenciarelli, C.; Terao, M.; Garattini, E. *Mol. Cancer Ther.* **2008**, *7*, 2941.

10) Tang, X. H.; Osei-Sarfo, K.; Urvalek, A. M.; Zhang, T.; Scognamiglio, T.; Gudas, L. J. *PNAS* **2014**, *111*, 8907.

11) Berger, J. P.; Petro, A. E.; Macnaul, K. L.; Kelly, L. J.; Zhang, B. B.; Richards, K.; Elbrecht, A.; Johnson, B. A.; Zhou, G.; Doebber, T. W.; Biswas, C.; Parikh, M.; Sharma, N.; Tanen, M. R.; Thompson, G. M.; Ventre, J.; Adams, A. D.; Mosley, R.; Surwit, R. S.; Moller, D. E. *Mol. Endocrinol.* **2003**, *17*, 662.

12) Meehl, M.; Herbert, S.; Gotz, F.; Cheung, A. *Antimicrob. Agents Chemother.* **2007**, *51*, 2679.

13) Yang, S. J.; Bayer, A. S.; Mishra, N. N.; Meehl, M.; Ledala, N.; Yeaman, M. R.; Xiong, Y. Q.; Cheung, A. L. *Infect. Immun.* **2012**, *80,* 74.

14) Elbaz, M.; Ben-Yehuda, S. *PLoS Genet.* **2010**, *6*, e1001119.

15) Bakke, O. M.; Manocchia, M.; de Abajo, F.; Kaitin, K. I.; Lasagna, L. *Clin. Pharmacol. Ther.* **1995**, *58*, 108.

16) Liu, Z.; Xiang, J. *Org. Process Res. Dev.* **2006**, *10*, 285.

17) Williams, A. B.; Hanson, R. N. *Tetrahedron* **2012**, *68,* 5406.

18) Liang, J. L.; Javed, U.; Lee, S. H.; Park, J. G.; Jahng, Y. *Arch. Pharm. Res.* **2014**, *37,* 862.

19) Morgan, B. J.; Xie, X.; Phuan, P.-W.; Kozlowski, M. C. *J. Org. Chem.* **2007**, *72*, 6171.

20) Tietze, L. F.; Panknin, O.; Major, F.; Krewer, B. *Chem. Eur. J.* **2008**, *14*, 2811.

21) Gillard, J. W.; Morton, H. E.; Fortin, R.; Guindon, Y. 3-hetero-substituted-n-benzyl-indoles and prevention of leucotriene synthesis therewith. 1992.

22) Schlosser, K. M.; Krasutsky, A. P.; Hamilton, H. W.; Reed, J. E.; Sexton, K. *Org. Lett.* **2004**, *6*, 819.

23) Chen, C.; Lieberman, D. R.; Larsen, R. D.; Verhoeven, T. R.; Reider, P. J. *J. Org. Chem.* **1997**, *62*, 2676.

24) Ngernmeesri, P.; Soonkit, S.; Konkhum, A.; Kongkathip, B. *Tet. Lett.* **2014**, *55*, 1621.

25) Chan, D. M. T.; Monaco, K. L.; Wang, R.-P.; Winters, M. P. *Tet. Lett.* **1998**, *39,* 2933.

26) Mahmoud, M. M.; Ali, H. I.; Ahn, K. H.; Damaraju, A.; Samala, S.; Pulipati, V. K.; Kolluru, S.; Kendall, D. A.; Lu, D. *J. Med. Chem.* **2013**, *56*, 7975.

27) Kwan, B. W.; Chowdhury, N.; Wood, T. K. *Environ. Microbiol.* **2015**, *17,* 4406.

28) Chowdhury, N.; Wood, T. L.; Martinez-Vazquez, M.; Garcia-Contreras, R.; Wood, T. K. *Biotechnol. Bioeng.* **2016**, *113*, 1984.

Chapter 4: Diverted Total Synthesis of Baulamycin A, B, and Analogs Provides Evidence to a Newly Identified Mechanism of Action

4.1 Introduction and background

4.1.1 Bacterial Iron Acquisition

Iron, an essential nutrient for all forms of life, is an ecological paradox. As the 4th most abundant element in the earth's crust, the fact that organisms compete for this resource seems counterintuitive. Iron is typically encountered in one of its two most common oxidation states: 2+ or 3+. Fe^{2+} is very water-soluble, however, in an aerobic environment; it can be spontaneously oxidized to Fe^{3+}. Fe^{3+}, due to its poor solubility, cannot exceed a concentration of 10^{-18} M at physiological pH.[1] Furthermore, ferric (3+) iron is toxic below this concentration, due to the propensity of it to form reactive oxygen species (ROS) via Fenton and Haber-Weiss reactions. As such, humans have evolved systems to store and transport iron in various proteins to keep the free iron concentration at approximately 10^{-24} M.

When a pathogen invades a human host, it must compete for Fe^{3+} with one of several established transport/storage systems. There are four main strategies/sources that bacteria utilize: (1) acquisition and subsequent decomposition of heme (2) competition with ferritin, lactoferrin, and transferrin (3) ferrous (2+) iron uptake (4) siderophore-mediated iron acquisition. Each of these strategies will be discussed briefly below.

Heme can be obtained by both Gram-positive and Gram-negative bacteria via specialized uptake systems. *P. aeruginosa* has a well-characterized heme uptake system, which is encoded by the genes *phuR-phuSTUVW*, and is regulated by TonB. PhuR is an outer-membrane receptor that removes heme from hemoglobin, which is then transported by the heme transport protein PhuT.

PhuUVW transports heme across the inner membrane, and handed off to PhuS, the intracellular heme trafficking protein, whereby it is ultimately delivered to one of many heme oxygenases.[2-3] These proteins degrade heme, and reduce the iron to the ferrous (2+) state, which can then be utilized and/or stored within the bacterial cell.[4] In *S. aureus*, the uptake system is very similar and encoded by Isd (iron-regulated surface determinant) and Srt (cell wall sortase) genes, which are regulated by Fur.[5]

Transferrins and lactoferrins are proteins capable of binding two Fe^{3+} atoms per protein, with each K_A value exceeding 10^{19}.[6] These proteins facilitate iron transport throughout the host, and iron within cells is stored in large storage proteins called ferritins. Some bacteria have been shown to possess systems that can scavenge iron from these protein sources directly.[7-9] Others utilize catecholamine to facilitate the liberation of iron from transferrins and acquire the nutrient in an indirect manner.[10]

Under acidic anaerobic conditions, the ferrous (2+) form of iron is stable and can freely diffuse through the outer membrane of Gram-negative bacteria. While many bacteria harbor specialized uptake systems, a well-known and conserved system that facilitates ferrous iron transport across the inner membrane of Gram-negative bacteria is FeoABC, which was first discovered in *E. coli*.[11] The specialized strategies that certain bacteria utilize to acquire ferrous iron is outside the scope of this work.

The final bacterial iron uptake system, and most relevant to the work herein, is siderophore-mediated iron acquisition. Siderophores are small molecule high-affinity chelators of iron that bacteria secrete to sequester it from their environment. The first siderophore discovered was enterobactin (**4.1**), in 1970.[12-13] Since its discovery, the uptake of enterobactin has been well-characterized in *E. coli*, and the pathway is shown schematically in Figure 35. Iron-loaded enterobactin is recognized by and transported through the outer membrane by FepA.[14] FepB then

facilitates transport of the complex through the periplasm, whereby the cargo is transported through the inner membrane via the ABC transporter FepCDG.[15] Once inside the cytoplasm, the iron-enterobactin complex must be degraded, due to the extremely high affinity that enterobactin has for iron. This degradation is accomplished by ferric enterobactin esterase (Fes), which releases hydrolyzed enterobactin fragments to be recycled along with its iron payload.[16]

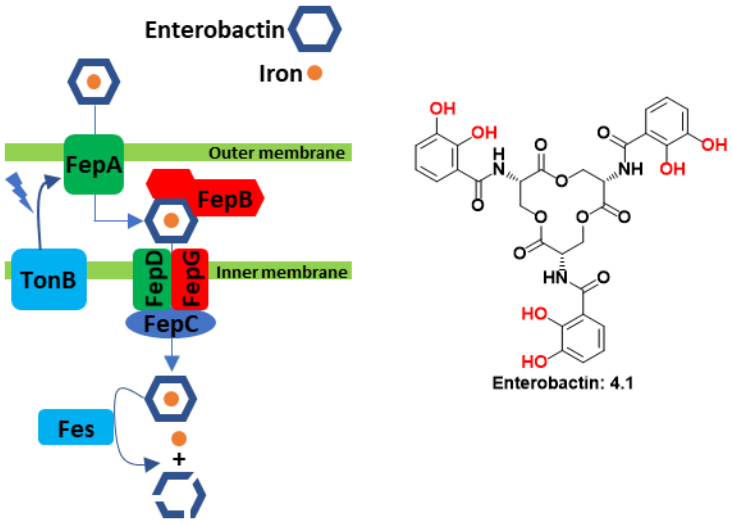

Figure 35. Enterobactin/salmochelin uptake system in *E. coli*, as well as their chemical structures. Iron-chelating functionalities are highlighted in red.

The catechol moieties of **4.1**, highlighted in Figure 35, are the functionalities responsible for iron chelation. Since the discovery of enterobactin, many other siderophores have been characterized from a wide variety of organisms. The common siderophore structural motifs, as well as siderophore biosynthesis, will be covered in the next section.

4.1.2 Siderophores of Gram-positive and Gram-negative Bacteria

While siderophores are diverse, they typically harbor one to four key structural features that are ubiquitous: catecholates, phenolates, hydroxamates, and carboxylates. These functionalities all contain Lewis bases (oxygen) that coordinate with iron in iron-siderophore complexes. Some representative structures of siderophores are shown in Figure 36 with their

respective bacterial counterparts denoted. Petrobactin (**4.2**) is utilized by various species of *Bacillus* and contains citrate and catecholate functionalities. Staphyloferrin B (**4.3**) is synthesized by *S. aureus* and exists as an equilibrium between an α-keto acid and cyclic hemiamidal, and contains citrate, carboxylic acid, and amine functionalities. Pyochelin (**4.4**) and similar structures are utilized by *Pseudomonas*, this compound is typically associated with *P. aeruginosa*. Pyochelin contains one chelating phenolate and a carboxylate. Aerobactin (**4.5**) is synthesized by the Gram-negative bacteria *E. coli* and *Shigella flexneri*, and contains hydroxamate, citrate, and carboxylate moieties. Mycobactin-T (**4.6**) is one example from a family of structures collectively known as the mycobactins, which are produced by *Mycobacterium tuberculosis*, and contain phenolate and hydroxamate functionalities. Petrobactin (**4.2**), staphyloferrin B (**4.3**), and aerobactin (**4.5**) all contain citrate moieties, which stem from similar biosynthetic enzymes, and are of relevance to the work presented here.

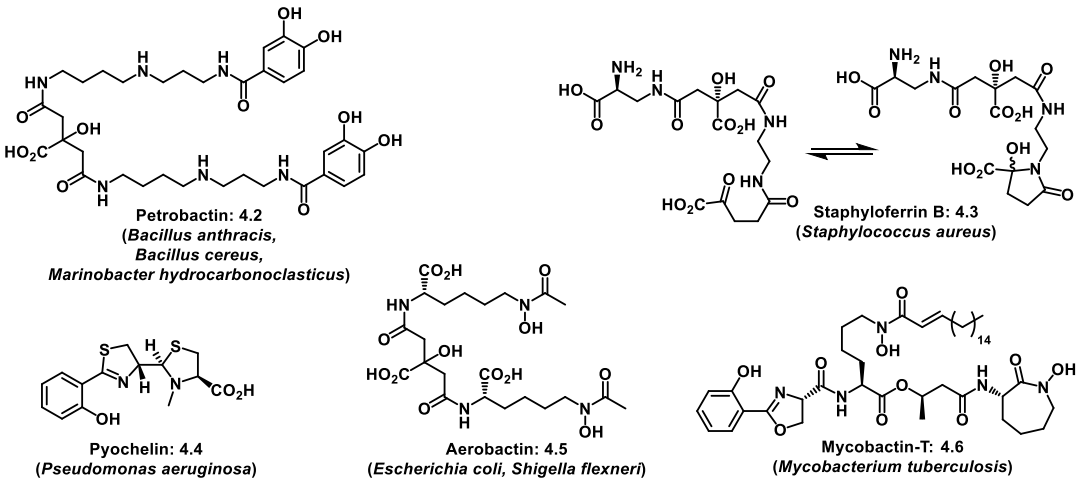

Figure 36. Representative siderophore structures.

4.1.3 Biosynthesis of Citrate-containing Siderophores

From the previous overview, it is evident that citrate is a functionality present in many different siderophore structures. In fact, citrate itself has been shown to be utilized by certain bacteria as a siderophore.[17] This affinity for iron, along with its ubiquitous presence in nature as a

TCA cycle substrate makes its utilization as a starting material for siderophore biosynthesis not surprising. Accordingly, specialized enzymes have been tailored by evolution to utilize citrate as a starting material for various amide and ester-forming reactions. Collectively they are known as NRPS-independent siderophore (NIS) synthetases. In 2005, Challis performed sequence alignments of 88 homologs of two well-characterized NIS synthetases, IucA and IucC.[18] This analysis revealed three distinct clades, which Challis denoted type A, B, and C. From there, he proposed two possible models of classifications within the three types. Model 1 proposed that the enzymes were specific for the acid substrate, with type A enzymes having specificity for citrate (**4.7**), type B for α-ketoglutarate (**4.8**), and type C for monosubstituted citrate amide or ester derivatives. Model 2 proposed the enzyme specificities were based upon the nucleophile types. Since this proposal, studies have shown that model 1 is correct, and that these enzymes are promiscuous in the types of nucleophiles they can accept as substrates, which is depicted in Scheme 44.[19]

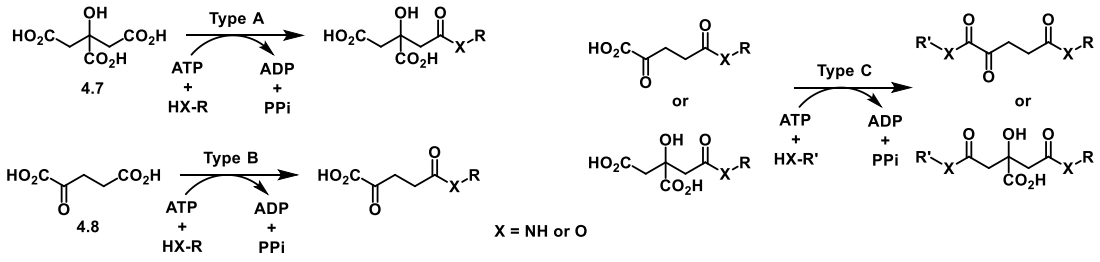

Scheme 44. General types of reactions catalyzed by each type of NIS synthetase.

Siderophore production has been directly correlated with pathogenicity, for example, *S. aureus* knockouts unable to produce staphyloferrin A and B have attenuated virulence.[20] As such, inhibition of bacterial siderophore-mediated iron acquisition via chemical inhibition of siderophore biosynthesis has been pursued as a new avenue for antibiotic development.[21]

4.1.4 Baulamycin A & B Isolation and Structural Ambiguity

In pursuit of NIS synthetase inhibitors (see section 4.1.3), the Sherman laboratory (Michigan State) designed a high-throughput screen.[22] Specifically, the authors were interested in SbnE and AsbA, which are from *S. aureus* and *B. anthracis*, respectively. Each NIS synthatase is type A and catalyzes the first step of the biosynthesis of each natural product (Scheme 45). In staphyloferrin B (**4.3**) biosynthesis, SbnE catalyzes the condensation of citrate (**4.7**) with L-2,3-diamino propionic acid (**4.9**), yielding intermediate **4.11**. Similarly, in petrobactin (**4.2**) biosynthesis, AsbA catalyzes the condensation of citrate (**4.7**) with spermidine (**4.10**) to provide amide intermediate **4.12**.

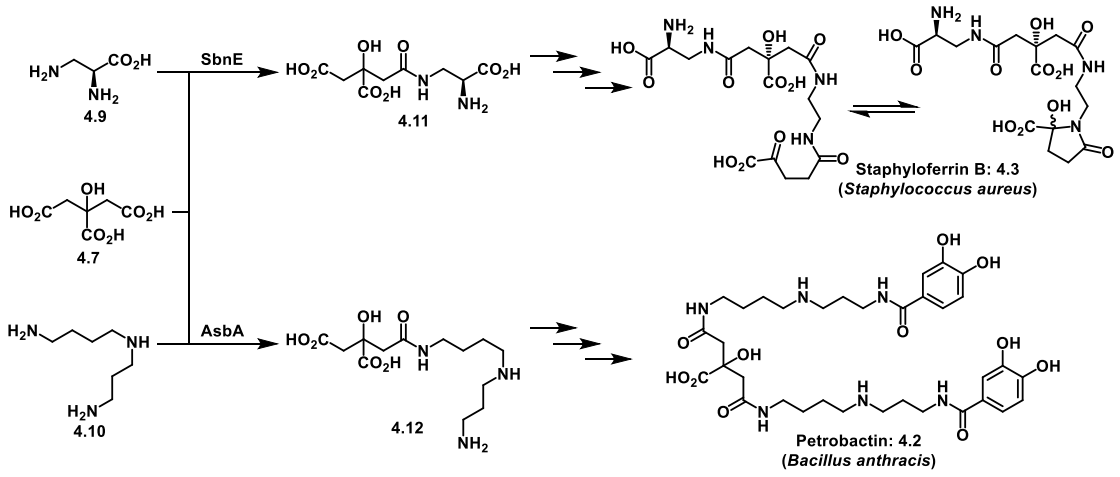

Scheme 45. Reactions catalyzed by SbnE and AsbA.

Sherman and co-workers screened for inhibitors of *both* SbnE and AsbA simultaneously, to find compounds useful against both pathogens, and rule out false positives. A previously developed malachite green assay was modified to permit the screening of natural product extracts.[23] Starting from 19,855 natural product extracts, the hits were narrowed down to a few hundred extracts, and another round of screening led to the discovery of 33 strains that inhibited SbnE and 22 strains that inhibited AsbA. The most potent extract, from *Streptomyces*

tempiquensis, showed high activity against both enzymes (95.9% and 90.2% inhibition against SbnE and AsbA, respectively), and was taken on further for activity-based fractionation.

After two rounds of purification, the isolation effort yielded two bioactive compounds: baulamycin A (**4.13a**) and baulamycin B (**4.14a**). Extensive NMR experiment analysis allowed elucidation of the molecules' connectivity, and a J-based configuration analysis was carried out.[24] This initial analysis led to the proposed structures with the depicted relative configurations in Figure 37, which also shows the *in vitro* and whole-cell assay results. Both baulamycin A and B showed *in vitro* activity against SbnE and AsbA, with baulamycin B displaying a slightly lower potency against each enzyme. Both compounds were not active against a type C NIS synthetase, AsbB, which showed that they were selective for this type of NIS synthetase.

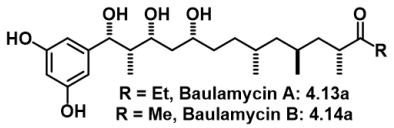

in vitro

Enzyme	NIS type	Bacterium	BmcA IC_{50} (μM)	BmcB IC_{50} (μM)
SbnE	A	*S. aureus*	4.8	19
AsbA	A	*B. anthracis*	180	200
AsbB	C	*B. anthracis*	>1000	>1000

whole cell

Strain	NIS synthetase	BmcA IRM IC_{50} (μM)	BmcA IDM IC_{50} (μM)
S. aureus Newman	SbnE	86	69
MRSA USA 300	SbnE	130	130
B. anthracis Sterne $34F_2$	AsbA	120	110
S. typhimurium	IucA	>1000	>1000
E. coli MC1061	IucA	150	4.2
S. flexneri BS103	IucA	46	20

Figure 37. Summary of baulamycin A (**4.13a**) and baulamycin B (**4.14a**) isolation report initial findings.

Due to low isolation yields of baulamycin B, whole-cell inhibition assays were only performed with baulamycin A. These were done in both iron-rich media (IRM) and iron-depleted media (IDM). Siderophore biosynthesis inhibitors typically display a large differential in potency between these two growth conditions. In most cases, baulamycin A displayed a very minimal difference in its potency between iron-rich and iron-depleted media. The authors did note a large difference in potency between iron-rich and iron-depleted media in the case of *E. coli*. However, large error bars in the IC_{50} plots in this data set makes the results questionable. Nonetheless, it seemed that multiple mechanisms were at play. A compound that solely inhibiting siderophore

biosynthesis should display a large difference in potency between IRM and IDM. In addition, a follow-up report to the isolation brought about ambiguity about the stereochemical assignments.[25] We sought to resolve these structural and mechanistic discrepancies through the use of total synthesis.

4.1.5 Hypothesized Model of Binding and Absolute Configuration

From the outset, we were aware of ambiguity surrounding the structure of the baulamycins, specifically, the configuration of its seven stereogenic centers. J-based configurational analyses have been successful in many structural elucidations, but in some cases, misassignments have occurred.[26-27] These are typically minimized if the analysis is conducted in parallel with other computational or experimental methods, i.e. simulations, Mosher's ester, etc. which were not performed in this case.

The isolation report showed that the baulamycins were competitive inhibitors of AsbA and SbnE with respect to both citrate and ATP. While the crystal structure of AsbA and SbnE have yet to be solved, a homologous enzyme, IucA, has been crystalized and characterized both with and without ATP in the active site.[28] Accordingly, analysis of the active site of IucA would allow us to make a hypothesis about the baulamycins' mode of binding and structure. Before any structural analysis was done, a sequence alignment of SbnE, AsbA, and IucA was carried out, the results of which are shown in Figure 38. The active site residues of the three proteins (boxed in Figure 38) share a great deal of homology, and the residues that make contacts with citrate and ATP are identical. Therefore, the structure of IucA will serve as a representative model for SbnE and AsbA.

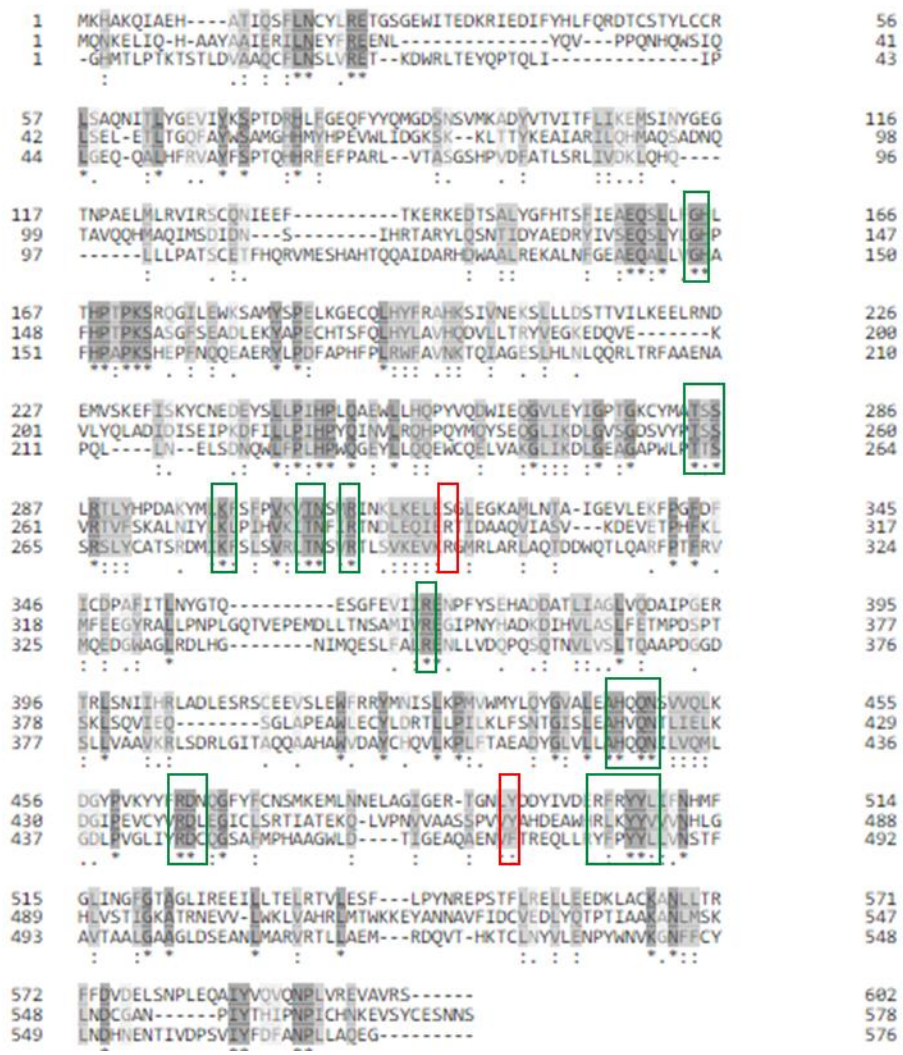

Figure 38. Sequence alignment of AsbA (top row), SbnE (middle row), and IucA. The boxed residues are in the active site of IucA and contact ATP in the crystal structure. Green boxes indicate an exact match between the enzymes, and red indicates a mismatch.

Since the baulamycins are competitive inhibitors with respect to ATP, and ATP was co-crystallized with IucA, the conformation of bound ATP may be analogous to the baulamycins. The images in Figure 39 depict the co-crystal structure of ATP with IucA and offer a great deal of insight. The distance between the two phosphate oxygens farthest apart that coordinate Mg^{2+} (Figure 39A) is 4.55 Å. The structure of baulamycin A was modeled in Spartan and minimized, then the structure was reoriented to mimic the coordination geometry of ATP (Figure 39D). It is worth emphasizing that the minimized structure of a potential ligand does not necessarily reflect

its conformation when docked to a protein, whereby favorable binding interactions between a ligand and protein may outweigh entropic factors involved in the minimization process. The 1,5-diol that is highlighted in Figure 39D has a distance of 3.89 Å between the two oxygen atoms. This distance is in close agreement with the native substrate, which indicates that baulamycin A may coordinate Mg^{2+} in the active site of IucA via the two indicated hydroxyl groups, or at least has the potential to orient itself in a similar fashion. This orientation of baulamycin A also projects the aromatic moiety of the natural product in proximity to where the adenine of ATP is in IucA. Figure 39B shows the important residue histidine 425, which interacts with adenine via π-stacking. This same residue can interact analogously with the aromatic group of baulamycin A. Figure 39C shows the back pocket of the active site, where there is a "tunnel" that pyrophosphate is ejected from ATP into during catalysis. In Figure 39C, hydrophobic residues are red and hydrophilic are blue. The tunnel contains many hydrophobic (red) residues, and the crystal structure shows that the pocket is 13.09 Å long. The model indicates that the hydrophobic portion of BmcA is 12.40 Å long, starting from the C5-hydroxyl, giving enough room for the compound to fit into the tunnel and make hydrophobic contacts with the protein.

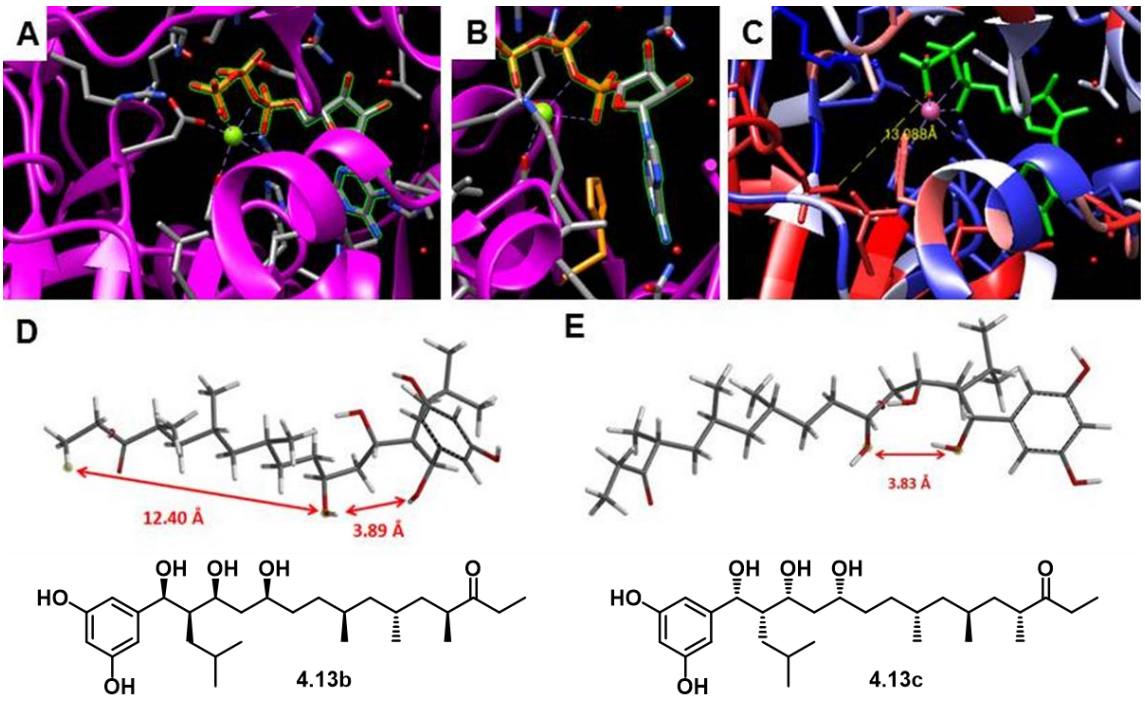

Figure 39. Crystal structures and models used to rationalize the hypothesized absolute configuration. (a) Active site of IucA with ATP outlined in green (oxygen = red, carbon = gray, phosphorus = orange, nitrogen = blue). (b) View showing histidine 425 (orange) which π-stacks with adenine. (c) "Tunnel" with hydrophobic residues in red and hydrophilic in blue, ATP is green and Mg pink, and distance showing length of the tunnel. (d) Model of **4.13b** made in Spartan with important distances shown. (e) Model of **4.13c** showing the projection of the aromatic moiety.

The model presented herein also allows rationalization of only one enantiomer's synthesis. Figure 39E shows a computational model of **4.13c**. The 1,5-diol has been arranged to match Figure 39D after minimization, and the projection of the aromatic moiety is strikingly different than its enantiomer. The aromatic residue is projected straight to the right, which in the protein puts it far away from histidine 425. Without this important contact, it is likely that **4.13c** would be a much less potent inhibitor, if at all, of IucA; and consequently, SbnE and AsbA.

This structural analysis of IucA made **4.13b** our first synthetic target. While no attempt was made in the isolation report to claim absolute stereochemistry, this gave us a reasonable starting point to hypothesize an absolute configuration, rather than pick one ambiguously.

4.2 Other Syntheses of Baulamycin A

4.2.1 Total Synthesis of Originally Reported Structure of Baulamycin A by Goswami *et al.*

In 2017, Goswami and co-workers reported the first total synthesis of the originally reported structure of baulamycin A.[29] The retrosynthesis is shown in Scheme 46, and the route revolved around a penultimate cross-metathesis between fragments **4.15** and **4.16**. The left half, **4.15**, was envisioned to be derived from primary alcohol **4.17** via a Crimmins acetate aldol reaction. The right half, **4.16**, would result in an Evans methylation and standard functional group manipulations, from known compound **4.18**.

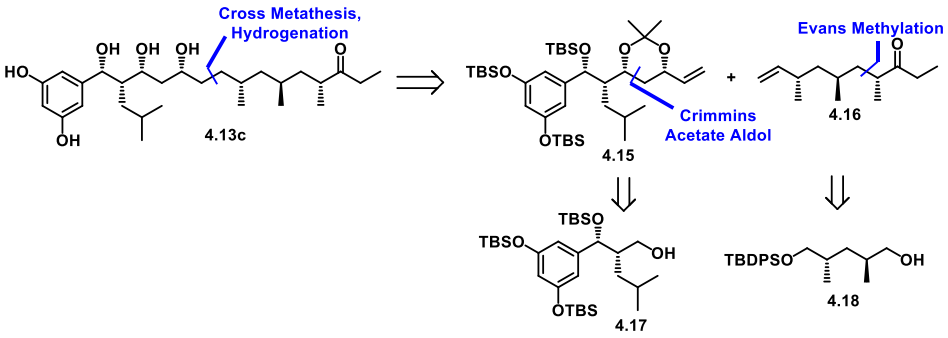

Scheme 46. Retrosynthesis of Goswami and co-workers reported in 2017.

The forward synthesis of the left fragment, **4.15** is detailed in Scheme 47. The synthesis began with a Crimmins aldol reaction between **4.19** and **4.20**, yielding **(+)-4.21** as a single diastereomer in high yield. TBS protection of the resultant secondary alcohol followed by reductive removal of the chiral auxiliary yielded alcohol **(+)-4.17**. Next, Swern oxidation followed by a Crimmins acetate aldol between the resultant aldehyde and thiazolidinedione **4.22** yielded aldol adduct **(+)-4.23** with 5:1 diastereoselectivity. The resultant secondary alcohol was then protected as a TES ether and reduction with DIBAL-H yielded aldehyde **4.24**. Treatment of this aldehyde with vinylmagnesium bromide yielded alcohol **4.25** with a 5:4 ratio of diastereomers in slight favor of the desired stereoisomer. From there, treatment with CSA yielded

a mixture of diastereomeric diols, which could be separated after subsequent acetonide protection, yielding pure **(+)-4.15**.

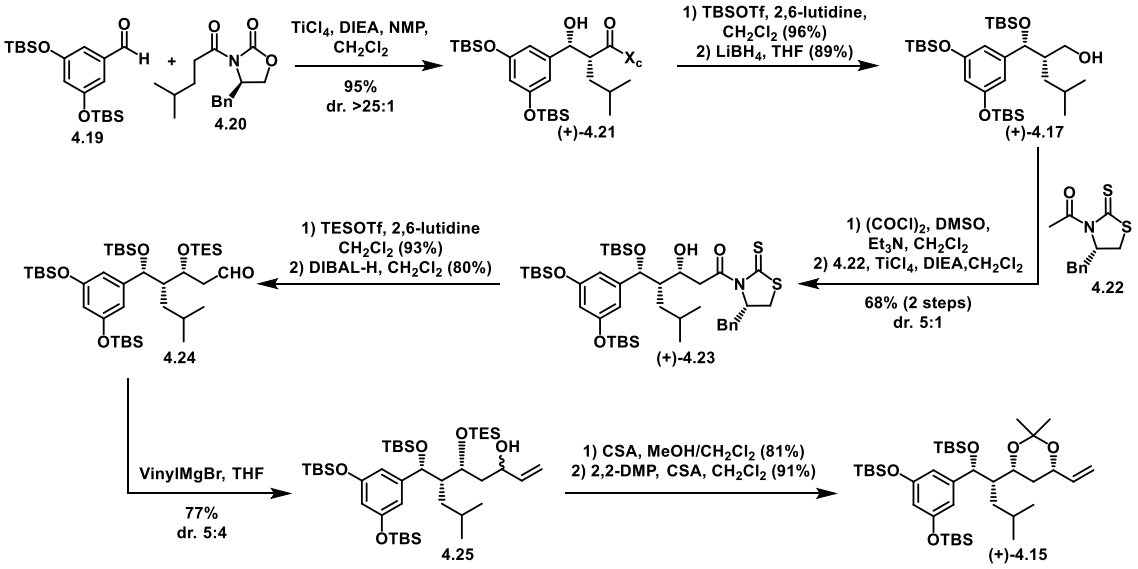

Scheme 47. Goswami and co-workers' synthesis of fragment **4.15**.

The synthesis of the right half fragment began from known alcohol **(–)-4.18**, and is detailed in Scheme 48.[30] Oxidation of **(–)-4.18** under Swern conditions yielded aldehyde **(+)-4.26**, which was then subjected to a Horner-Wadsworth Emmons olefination with phosphonate **4.27**, yielding olefin **(–)-4.28**, then hydrogenated to give **(–)-4.29**. Treatment of this intermediate with NaHMDS gave the corresponding sodium enolate which was methylated upon treatment with methyl iodide, yielding **(–)-4.30** as a single diastereomer. Reductive removal of the chiral auxiliary yielded alcohol **(+)-4.31**, which was then benzyl protected, followed by removal of the silyl protecting group, providing benzyl alcohol **(–)-4.32**. Swern oxidation of this alcohol yielded aldehyde **(+)-4.33**, with a small amount of epimerization observed at the α-methyl stereocenter (dr. 9.4:1). After trying many oxidation conditions, the authors showed that the Swern oxidation led to the smallest amount of epimerization, which was a useful observation for our work. Olefination of the resultant aldehyde via a Wittig reaction yielded alkene **(+)-4.34**, and selective debenzylation in the presence of the alkene was accomplished with Li/naphthalene, providing

alcohol **(+)-4.35**. Swern oxidation of this alcohol followed by a Grignard reaction with ethylmagnesium bromide yielded **4.36** as an inconsequential mixture of diastereomers at the resultant secondary alcohol, which were oxidized together to yield ketone fragment **(–)-4.16**.

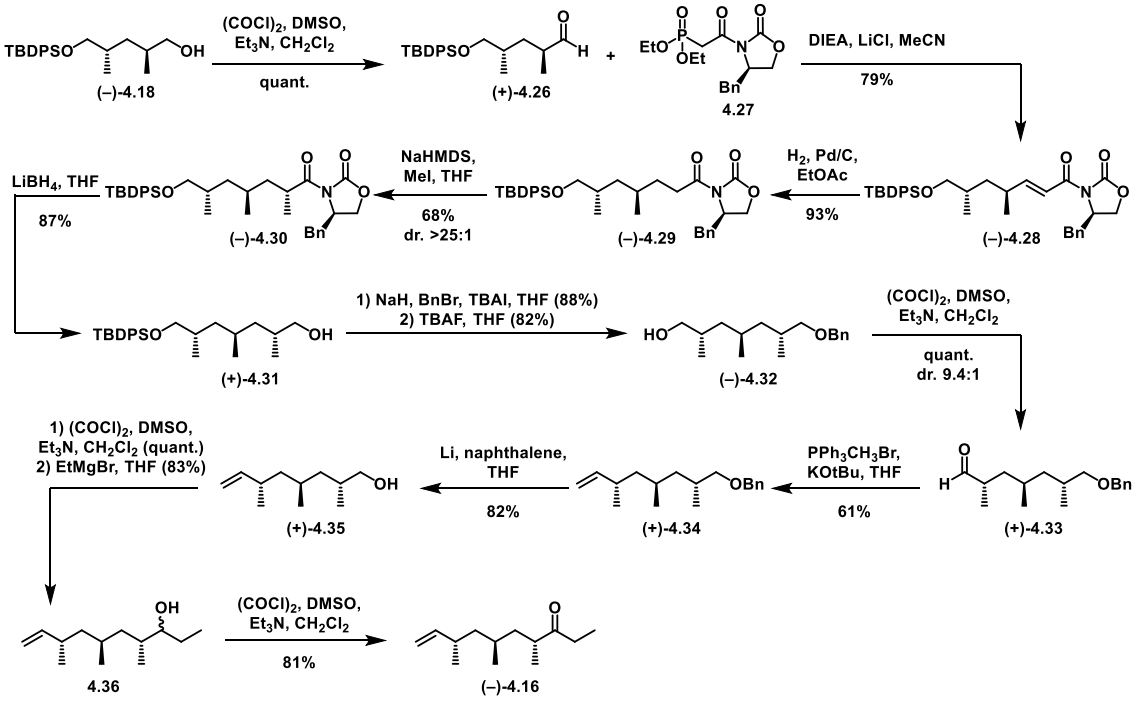

Scheme 48. Synthesis of fragment **(–)-4.16** by Goswami and co-workers.

With both fragments in hand, Goswami and co-workers then reported the failure of the cross-metathesis reaction between **(+)-4.15** and **(–)-4.16**. Four sets of conditions were reported: Grubbs I, Grubbs II, Grubbs II with catalytic copper (I) iodide, and Hoveyda-Grubbs II. The authors stated that "under none of these conditions could a cross-coupled product be obtained". However, no additional experimental information was given such as solvent, temperature, reaction time, catalyst loading, or equivalents.

Undeterred, the authors adopted an alternative route based upon a Honrer-Wadsworth Emmons olefination instead of metathesis. The revised route is shown in Scheme 49. Beginning from previously shown aldol adduct **(+)-4.23**, displacement of the thiazolidinedione with methanol and imidazole provided the corresponding methyl ester, which upon TES protection

yielded **(+)-4.37**. From there, deprotonation of dimethyl methyl phosphonate with *n*-butyllithium followed by displacement of the methyl ester yielded ketophosphonate **(+)-4.38**. HWE olefination was then accomplished between **(+)-4.38** and aldehyde **(+)-4.34** and barium hydroxide to yield **(+)-4.39**. Hydrogenation then removed both the benzyl ether and alkene functionalities, providing **(+)-4.40** in high yield. From there, deprotection of the TES ether followed by reduction of the ketone with DIBAL-H yielded diol **(+)-4.41** with a dr of 3:1 in favor of the desired *syn* isomer. Acetonide protection then provided **(+)-4.42**. From there, a 3-step conversion of the primary alcohol to the ketone was carried out (oxidation, then Grignard, then oxidation), followed by global deprotection with HF•pyridine to yield **(+)-4.13c**.

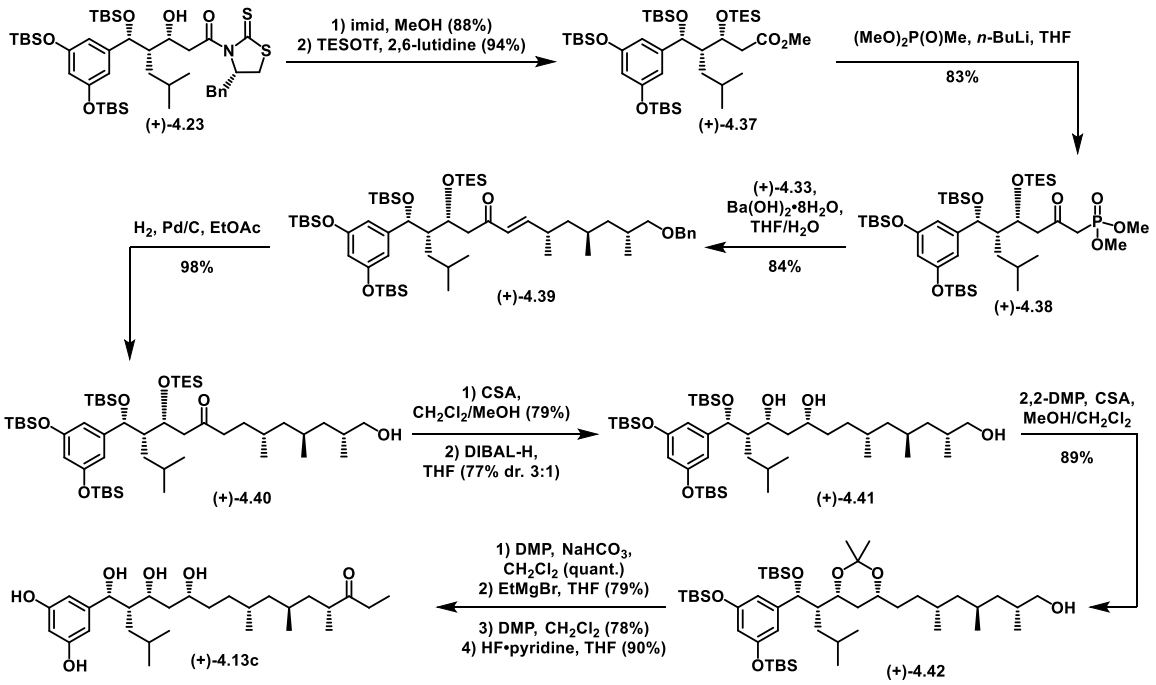

Scheme 49. Goswami and co-workers' revised route to the originally reported structure of baulamycin A, **(+)-4.13c**.

Upon completion of their synthesis, Goswami *et al.* reported major discrepancies between their synthetic material and the isolation data. The optical rotation was not of the correct sign, and although the connectivity seemed to be assigned correctly, misassigned stereochemistry appeared to be the cause of differences in the NMR spectra. The authors next synthesized two

more diastereomeric isomers of **(+)-4.13c** which were accessed via the same chemistry described above. The structures of **(–)-4.13d** and **(–)-4.13e**, shown in Figure 40, correspond to the other diastereomers synthesized by Goswami and co-workers. While the optical rotation did become negative, which matches the natural product, the NMR discrepancies did not improve with the structural changes introduced by the authors. The benzylic chemical shift of all the synthetic compounds differed significantly from the isolated material by about 0.5 ppm, and their associated J-values were too low (3-4 Hz vs. 7.0 for baulamycin A). This suggested that the relative stereochemistry around the benzylic position was not correctly assigned in the isolation report.

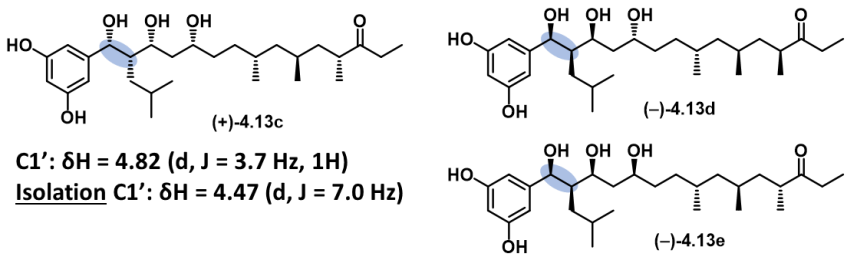

Figure 40. Chemical structures of the diastereomeric isomers produced by Goswami, *et al.*, with key discrepancies involving the benzylic C-H highlighted.

4.2.2 Synthesis of the Proposed Baulamycin Carbon Framework by Chandrasekhar, *et al.*

Within two months of the publication of Goswami and co-workers' synthetic work, Chandrasekhar, *et al.* submitted a report about their pursuit of the same structure.[31] Their retrosynthetic approach was almost identical to that previously shown, and they proposed a very similar cross-metathesis/hydrogenation approach that Goswami, *et al.* deemed unsuccessful.

The synthesis of left fragment by Chandrasekhar and co-workers is shown in Scheme 50, also began with a Crimmins aldol reaction between methoxy-protected benzaldehyde **4.43** and oxazolidinone **4.20**, yielding aldol adduct **(–)-4.44** as a single diastereomer. From there, TBS protection afforded **(–)-4.45**, followed by reductive removal of the chiral auxiliary to provide

alcohol **(+)-4.46**. Swern oxidation yielded an aldehyde which was reacted without purification in a Mukaiyama aldol with silyl enol ether **4.47**, which yielded aldol adduct **(+)-4.48** in 75% yield with 85:15 diastereomeric ratio in favor of the desired *syn* isomer. From there, *syn*-selective reduction with Et_2OMe and $NaBH_4$ yielded diol **(+)-4.49** in a 91:9 diastereomeric ratio. Acetonide protection then yielded left fragment **(+)-4.50**.

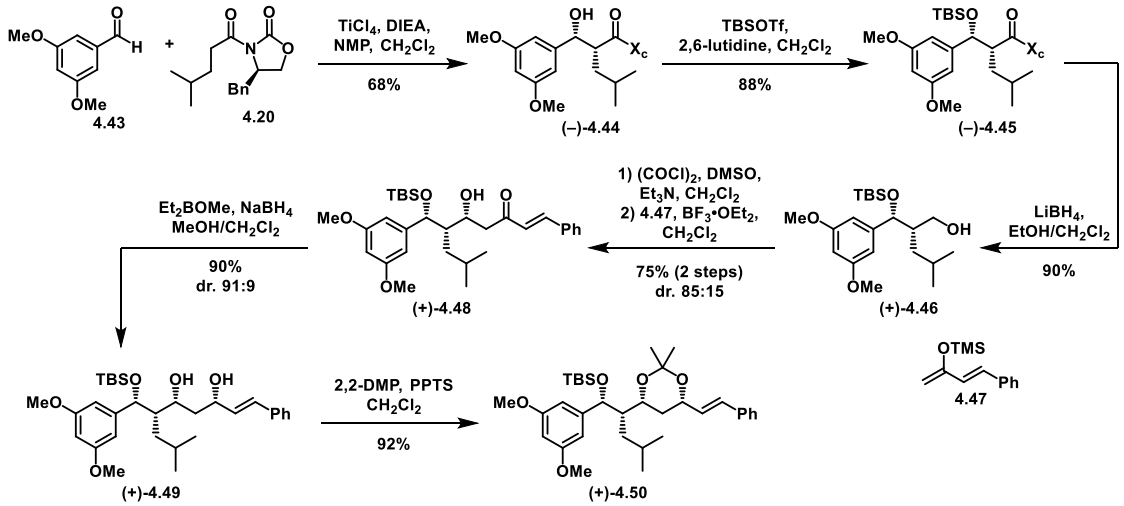

Scheme 50. Synthesis of fragment **(+)-4.50** as reported by Chandrasekhar and co-workers.

The rest of the reported synthesis by Chandrasekhar, *et al.* is depicted in Scheme 51, and begins from known compound **(+)-4.51**.[32] Reduction of the α,β-unsaturated ester with $NiCl_2$ and $NaBH_4$ yielded ester **(+)-4.52**. Hydrolysis to the corresponding acid yielded **(+)-4.53**, which was amidated with Evans oxazolidinone **4.54** to yield **(+)-4.55**. Stereoselective methylation of the lithium enolate formed with LiHMDS yielded **(+)-4.56**, followed by reductive removal of the auxiliary to provide alcohol **(–)-4.57**. Swern oxidation followed by Crimmins aldol with the titanium enolate of 3-pentanone yielded anti-Felkin product **(–)-4.58** as the major product in a 72% isolated yield and 4.8:1 diastereoselectivity. Two-step Barton-McCombie deoxygenation then provided **(–)-4.59**. Oxidation followed by Wittig homologation then yielded metathesis precursor **(–)-4.61**. Cross-metathesis was then accomplished between **(–)-4.61** and **(+)-4.50**. This

contrasts with what was reported by Goswami, and co-workers, who claimed a very similar transformation would not proceed. In this successful metathesis, 20 mol % catalyst was used, along with high reaction temperatures (90 °C, sealed tube), and long reaction times (48 hours). It is likely that Goswami and co-workers did not attempt such forcing reaction conditions, which would explain the discrepancy between the reports. The synthesis of Chandrasekhar and co-workers ceased here, due to Goswami, *et al.* demonstrating that the stereochemical array of **(–)-4.62** did not match the natural product. Nevertheless, this report was important to demonstrate that the metathesis strategy was feasible, and that the synthesis of right hand fragment **(–)-4.61** could be much more efficient than the previously shown.

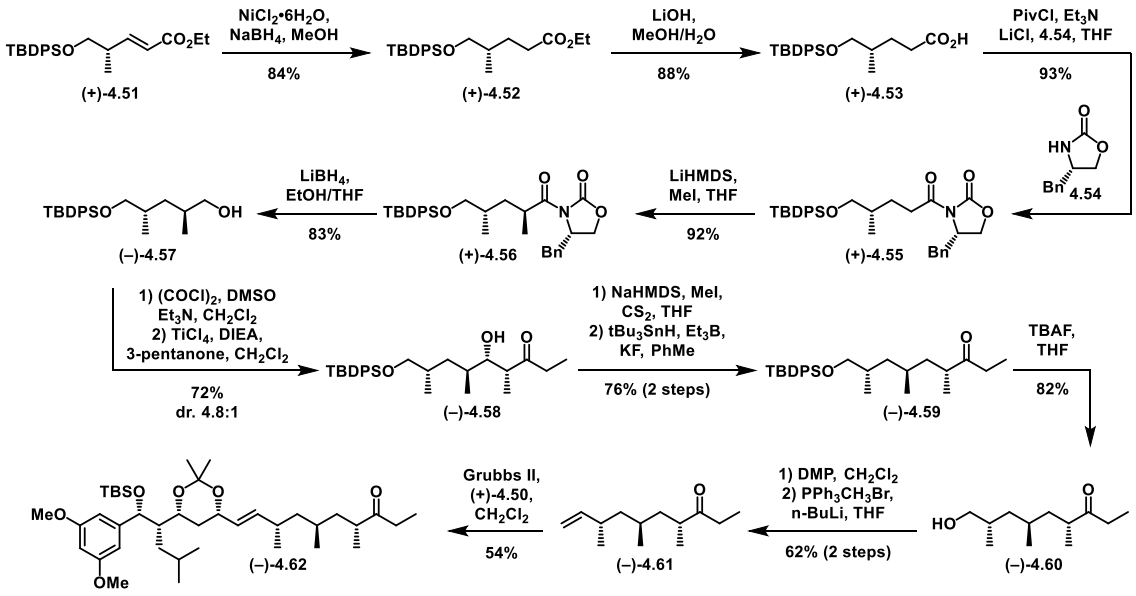

Scheme 51. Synthesis of right hand fragment and successful cross-metathesis leading to late stage intermediate **(–)-4.62** reported by Chandrasekhar and co-workers.

4.2.3 Total Synthesis and Stereochemical Assignment of the Baulamycins by Aggarwal and Co-workers

A few months after the report from Chandrasekhar, *et al.*, another publication finally settled the dispute on the structure of the baulamycins, which was the culmination of a valiant effort by Aggarwal and co-workers.[33] Prior to their work on the baulamycins, Aggarwal *et al.*

published a powerful approach to 1,3-diol synthesis enabled by a borylation-lithiation strategy, which was applied in the same report to the synthesis of a macrolactone containing a 1,3-diol motif. The general approach is shown in Scheme 52. A borylated substrate, **4.63** is reacted with lithiated species **4.65**, which was derived in the original report from an asymmetric deprotonation by *s*-butyl lithium and spartiene, neighboring the triisopropylbenzoyl (TIB) group. Intermediate **4.65** is then formed, which undergoes a 1,2-migration of the "R_1" group to yield **4.66**. This reaction pathway competes with β-elimination, especially when "R_1" contains electron-withdrawing groups. To circumvent this issue, Aggarwal and co-workers used diborylated substrates such as **4.67**, which result in 1,3-diborylated compounds **4.68**. These borylated compounds serve as "masked alcohols", which can be carried through more synthetic steps and oxidized later, in this case forming 1,3-diols **4.69**.

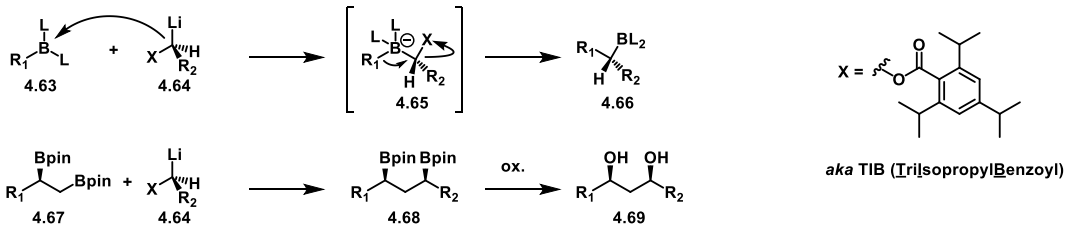

Scheme 52. Strategy reported by Aggarwal, *et al.* in 2016 to access 1,3-diols via lithiation/borylation.

The strategy of Aggarwal's lithiation/borylation approach to 1,3-diols is very advantageous over traditional methods. An example is aldol reaction to form a β-hydroxy ketone, then reduction. While the aldol reaction can often be highly selective and fruitful, substrates typically dictate the stereochemical outcome, and matched vs. mismatched cases can greatly complicate certain pairs of substrates. The method of Aggarwal *et al.* is reagent-controlled, which allows the manipulation of complex substrates no matter what the desired stereochemical outcome.

With this strategy in hand, it is not surprising that Aggarwal, *et al.* took an interest in the baulamycins. The structural ambiguity of the natural products provided the perfect platform to demonstrate how this method could be applied to deoxypropionate and 1,3-diol synthesis and provide access to any stereochemical array. Their retrosynthesis is shown in Scheme 53. From originally reported structure **4.13c**, the molecule was divided into two halves via lithiation/borylation: **4.70** and **4.71**. The left half, **4.70** was envisioned to arise from an asymmetric diborylation of alkene **4.72**, which comes from an allylboration between **4.73** and **4.74**. The protected ketone moiety of the right fragment **4.71** would come from a Zweifel olefination of **4.75**.[34] This fragment would be assembled from iterative lithiation/borylation reactions with methyl-bearing stereocenters arising from building blocks **4.76** and **4.77**, methylene fragments from **4.78**, and the terminal propyl-OTIB moeity from **4.79**. Due to the reagent-controlled selectivity of lithiation/borylation reactions, this strategy allows construction of any possible stereoisomer.

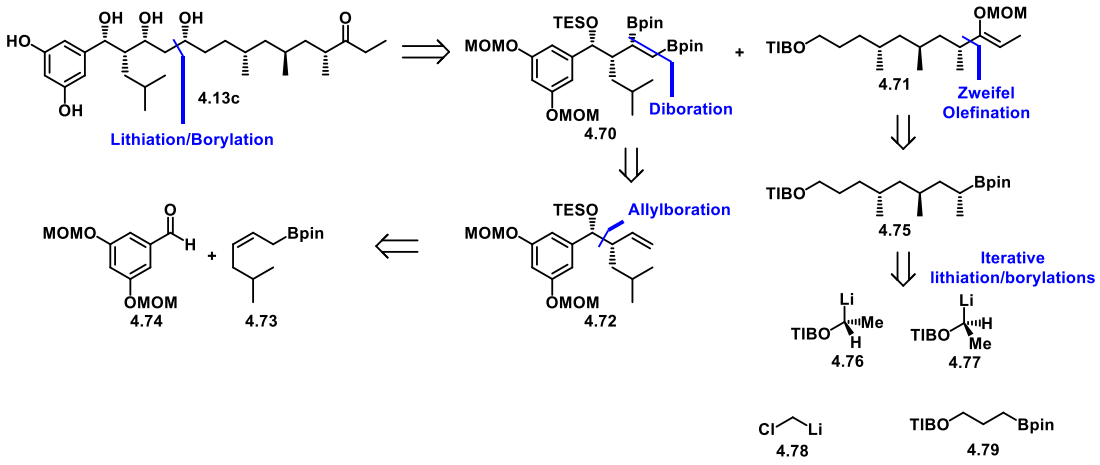

Scheme 53. Retrosynthetic strategy of Aggarwal and co-workers.

The forward synthesis of the left fragment is detailed in Scheme 54. From alkyne **4.80**, rhodium-catalyzed hydroboration yielded *Z*-vinyl boronic ester **4.81**, which was homologated with reagent **4.78** to yield **4.73**. This intermediate then underwent an asymmetric allylboration with aldehyde **4.74** catalyzed by chiral phosphoric acid **4.82** (also known as (*R*)-TRIP-PA), to

yield *syn* product **(+)-4.72** in high yield, diastereo- and enantioselectivity.[35] The newly formed hydroxyl group was then used to direct a stereoselective diboration reaction, which was subsequently transformed to the corresponding TBS ether **(–)-4.70**

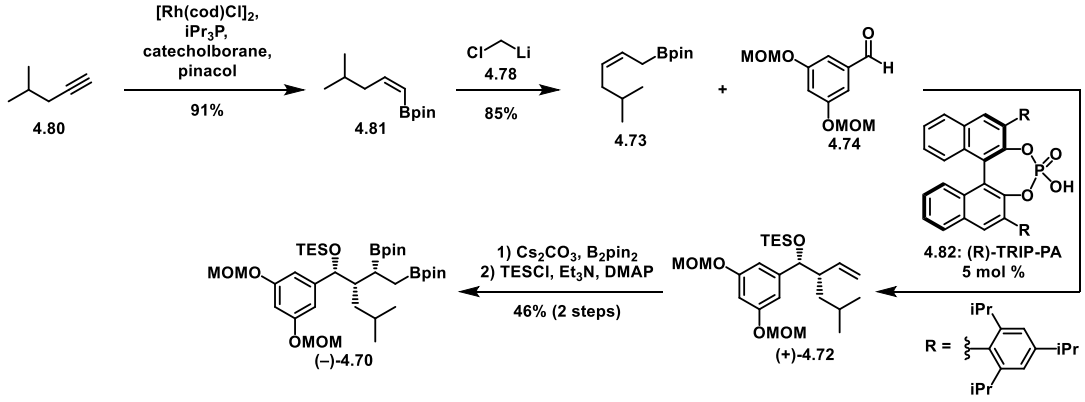

Scheme 54. Synthesis of left half fragment **(–)-4.70** by Aggarwal and co-workers.

With fragment **(–)-4.70** in hand, Aggarwal *et al.* next looked to the synthesis of the right half fragment, which is shown in Scheme 55. 2,4,6-triisopropylbenzoic acid (**4.83**) was first allylated to yield **4.84**, then rhodium-catalyzed hydroboration provided **4.79**. Next, five iterative lithiation/borylation reactions were carried out. By choosing **4.77** or **4.76**, which are prepared *in situ* via lithiation of the corresponding stannane, the methyl stereogenic centers can be easily chosen, and **4.78** was used to install each methylene group. This process provided the three stereocenters of the deoxypropionate chain, in **(–)-4.75**. Next, Zweifel olefination was performed with **4.85** generated *in situ*, followed by iodine, then an ethyl vinyl ether and sodium methoxide quench, yielded right fragment **(–)-4.71**. From there, lithiation/borylation reaction between the two fragments **(–)-4.70** and **(–)-4.71** was carried out with subsequent oxidation followed by global deprotection with hydrochloric acid.

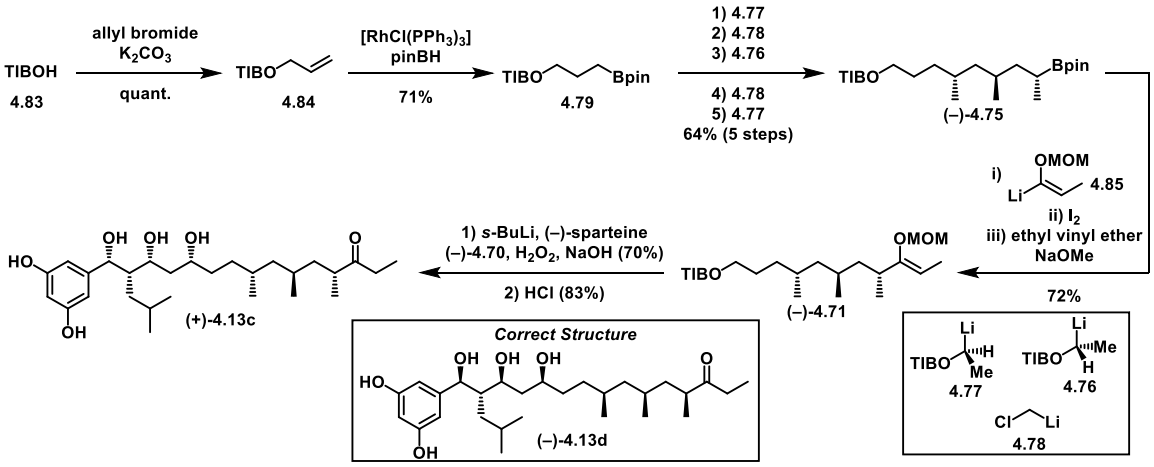

Scheme 55. Completion of the synthesis of **(+)-4.13a** by Aggarwal and co-workers, and the correct structure **(–)-4.13d**.

With the wrong structure synthesized, Aggarwal and co-workers next carried out an analysis of the NMR spectra of their synthetic compound compared to the natural product and hypothesized the *anti*-configuration between the benzylic hydroxyl and isobutyl-bearing stereocenters. They synthesized the remaining possible diastereomer fragments and used NMR-based calculations to infer the correct stereochemical array of the left half. Next, the right half was assigned in a relative fashion by synthesizing an "encoded mix" of the possible diastereomers. By making known ratios of each possible diastereomer in a single flask in one synthetic operation, then finishing the synthesis, HPLC peak areas revealed which diastereomer of the "encoded mix" corresponded to which peak. From there, isolation and characterization of each compound in the mixture was compared with the natural product. This analysis allowed them to narrow down the possible absolute configurations to only four, corresponding to each possible enantiomer of left and right half fragments. Hence, Aggarwal, *et al.* were very elegantly able to unequivocally assign the stereochemistry of baulamycin A (**(–)-4.13d**, Scheme 55) without having to synthesize all 128 stereochemical possibilities.

4.2.4 Synthesis and *in vitro* SAR of Baulamycin Structures by Sim and Co-workers

A report by Sim and co-workers concerning the baulamycins was published after the Aggarwal *et al.* publication, but was in review during the disclosure.[36] They first synthesized the originally proposed structure **4.13a**, and their approach was unique in that they joined the two fragments of the molecule together via an asymmetric Carriera alkynylation. The Sim *et al.* synthesis of the originally reported left half fragment is shown in Scheme 56. Beginning from the same intermediate reported by Chandrasekhar, **(+)-4.45** (each report provided conflicting optical rotation signs, the reported signs are shown in the respective schemes), DIBAL-H reduction provided aldehyde **(+)-4.86**, which was subjected to a Brown allylation, yielding **(+)-4.87** (diastereomeric ratio 92:8). Deprotection with TBAF provided diol **(+)-4.88**, which was converted to the corresponding acetonide **(+)-4.89**. Dihydroxylation followed by oxidative cleavage then provided aldehyde **(+)-4.90**.

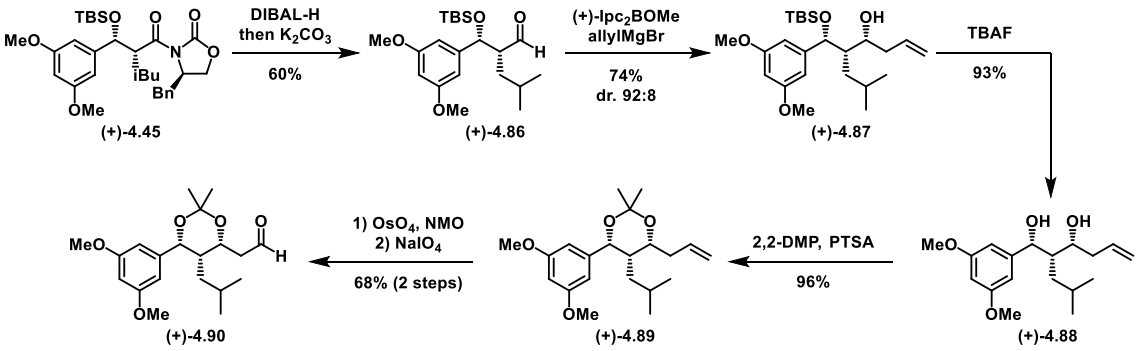

Scheme 56. Synthesis of originally reported left fragment **(+)-4.90** by Sim and co-workers.

The synthesis of the right half by Sim and co-workers was more efficient than Goswami and Chandrasekhar, and took advantage of prolinol-derived chiral auxiliaries developed by Evans.[37] The synthesis is shown in Scheme 57 and begins from known iodide **(+)-4.91**. Alkylation of acyl prolinol **(–)-4.92** yielded alkylation product **4.93** (no optical rotation given). Removal of the chiral auxiliary by acidic hydrolysis, followed by reduction yielded **(+)-4.94**. Iodination of the resultant alcohol yielded **4.95**, and this crude material was alkylated with acyl

prolinol **(+)-4.92**, yielding **(+)-4.96**. Acidic hydrolysis and subsequent reduction again yielded the corresponding alcohol, **(–)-4.97**. Swern oxidation followed by Seyferth-Gilbert homologation yielded alkyne right half fragment **(+)-4.98**.

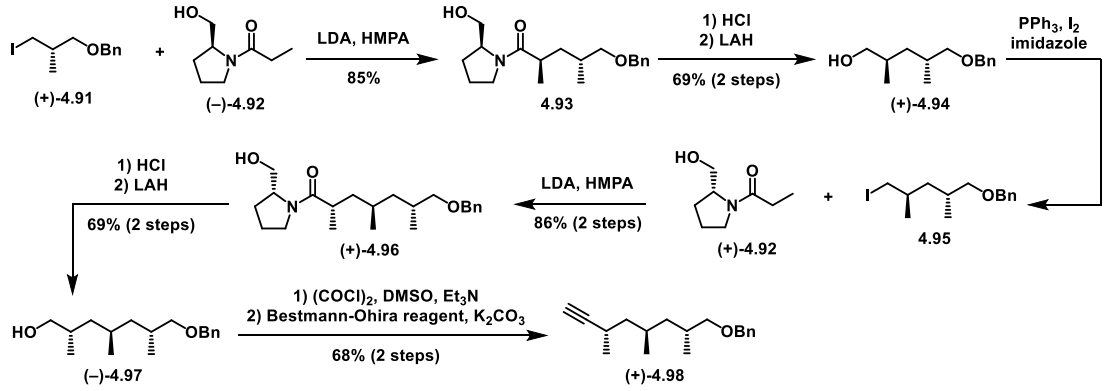

Scheme 57. Synthesis of alkyne right half fragment **(+)-4.98** by Sim and co-workers.

With each coupling partner in hand, next Sim, *et al.* performed the Carriera alkynylation coupling step between fragments **(+)-4.90** and **(+)-4.98**, which proceeded in good yield (72%) and high selectivity (diastereomeric ratio 96:4), yielding **(+)-4.99** (Scheme 58). TBS protection and hydrogenation then provided **(+)-4.100**. A 3-step conversion of the alcohol to ethyl ketone then yielded **(+)-4.101**. TBS and acetonide removal under acidic conditions yielded **(+)-4.102**, and the methyl ethers could only be removed with aluminum triiodide treatment for two days, with very poor yields. In subsequent syntheses, the authors used MOM ethers instead of methyl, and could accomplish global deprotection with good yields.

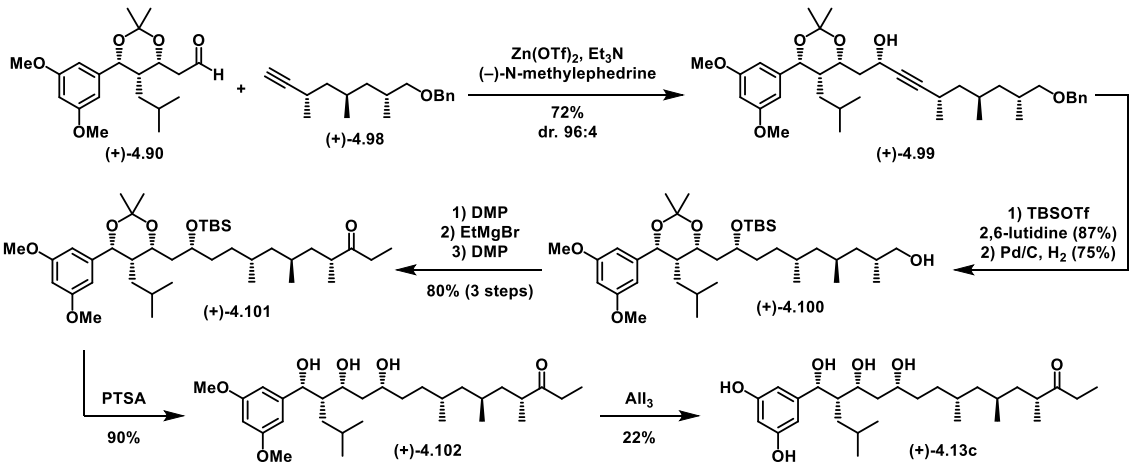

Scheme 58. Completion of the synthesis of **(+)-4.13c** by Sim and co-workers.

After realizing the stereochemical misassignment, Sim *et al.* determined the correct stereochemistry through a series of NMR and synthetic experiments. They first re-evaluated the JBCA analysis used by the isolation authors to determine the stereochemistry of the left half. Then they synthesized a series of deoxypropionate precursors to match J-values and chemical shifts to the natural product to assign the right half. They were then able to leverage their synthetic route to make the relative configuration corresponding to the natural product. However, it was the enantiomer of natural baulamycin A. Nevertheless, they also synthesized a library of analogs based off easily accessible synthetic intermediates, which is shown in Figure 41. Each compound was tested *in vitro* in accordance with the isolation report against SbnE. Originally proposed structure **(+)-4.13c** showed no activity against SbnE. **(+)-4.13d**, the enantiomer of baulamycin A, exhibited an IC_{50} of 14.40 μM. This is just 4-fold higher than the natural product, which was reported to be 4.8 μM. When 3 of the methyl stereocenters were altered in **(+)-4.13e**, a significant drop in potency was observed (47.27 μM). Compound **4.103** was active with an IC_{50} of 10.16 μM, which differs from **(+)-4.13c** only by the removal of one hydroxyl group. Similarly, inactive analog **4.104** was rendered active by deletion of one hydroxyl group, reflected by the activity of **4.105**. **(+)-4.106** and **(+)-4.107** were both inactive, highlighting the importance of the phenol and methyl functional groups. Diols **4.108** and **4.109** were both active at similar potencies,

however, many stereocenters were altered between them, as well as their triol counterparts **4.103** and **(+)-4.13d**, making SAR analysis convoluted. Suprisingly, simplified alkyne analog **(+)-4.110** was almost as potent as the natural product (7.16 μM vs. 4.8 μM reported for baulamycin A). Additional methyl groups to this simplified compound (**4.111**) caused a mild drop in potency, and the IC_{50} increased from 7.16 μM to 11.07 μM. While this SAR study provided a great deal of new data, interpretation is difficult, as the natural product was never synthesized, and none of the analogs were a result of systematic alterations. Since no analogs were more potent than the natural product, it is unclear how this information could be used to design further analogs stemming from the natural product itself, and not its enantiomer, **(+)-4.13d**.

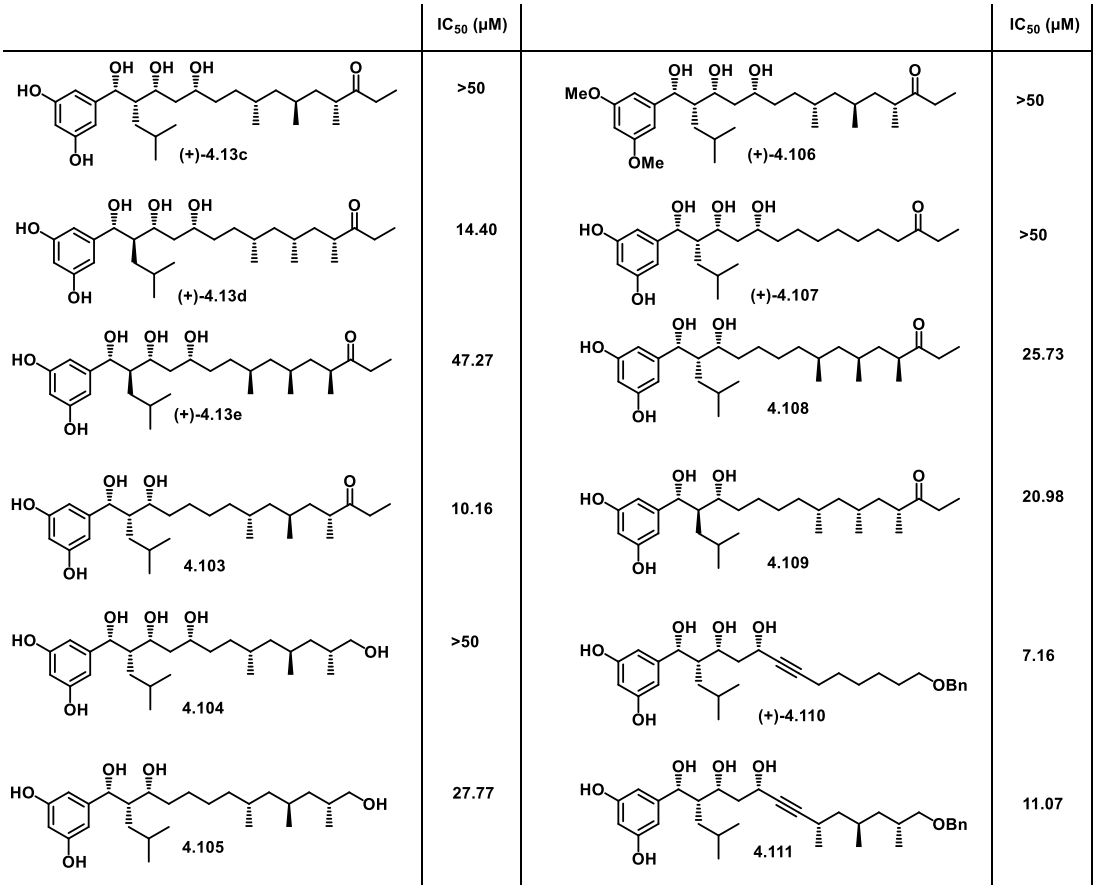

Figure 41. Structures and IC_{50} values of analogs synthesized by Sim and co-workers.

4.3 Total Synthesis of Baulamycin A and B

4.3.1 Retrosynthesis

At the outset of this project, we sought a flexible and convergent synthetic strategy. At the time this project began, no synthesis had been reported. In our approach, similar to others, late-stage cross-metathesis was envisioned to be the key fragment coupling step, giving the two advanced intermediates **(–)-4.15** and **4.112** (Scheme 59), and due to the structural analysis shown previously in this work (see 4.1.5 Hypothesized Model of Binding and Absolute Configuration, page 103), we targeted the absolute configuration depicted as **4.13b**.

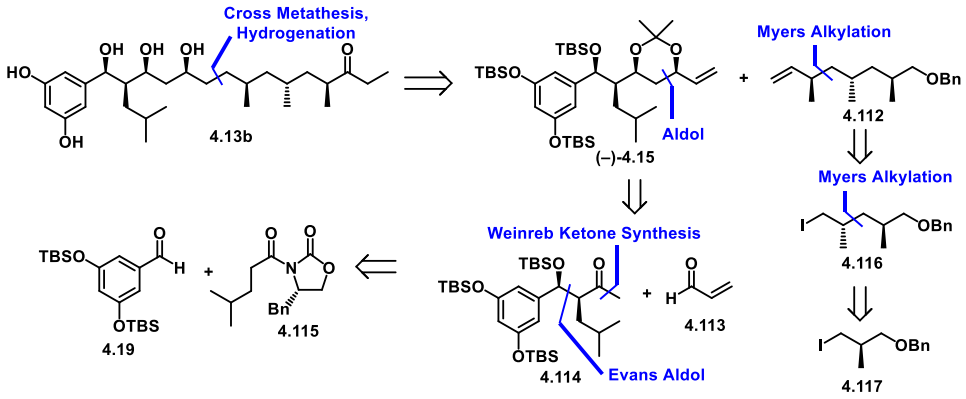

Scheme 59. Retrosynthesis of **4.13b**.

Left fragment **(–)-4.15** would arise from an asymmetric aldol between acrolein (**4.113**) and an enolate derived from methyl ketone **4.114**. Weinreb ketone synthesis and an Evans aldol breaks **4.114** down to acylated oxazolidinone **4.115** and known aldehyde **4.19**. For the right half, **4.112**, a Myers alkylation and standard functional group manipulations breaks this molecule down to **4.116**, and iteratively the same sequence back to iodide **4.117**. These disconnections

were chosen based on the most precedented chemistry available, as aldols and alkylations are well-established and reliable.

4.3.2 Synthesis of Originally Proposed Left Half Fragment

The synthesis of left half fragment **(–)-4.15** began with known benzaldehyde **4.19**, and the synthesis is shown in Scheme 60.[38] An Evans aldol reaction between **4.19** and **4.115** yielded aldol adduct **(–)-4.21** with full diastereoselectivity (>25:1). Weinreb amide formation followed by TBS protection yielded **(–)-4.118** in 76% yield over two steps. From there, ketone formation via MeMgBr yielded **(–)-4.114** in 83% yield. A large excess of Grignard reagent was required to obtain acceptable yields. Alternatively, methyllithium yielded product without a large excess of reagent, but also resulted in a significant amounts of aromatic silyl ether cleavage. Next, **(–)-4.114** was converted to the corresponding (–)-$(Ipc)_2$ boron enolate and reacted with acrolein, which yielded aldol adduct **(–)-4.119** in high yield (91%) and as a single diastereomer. From there, a *syn*-reduction of the β-hydroxy ketone via treatment with Et_2BOMe and $NaBH_4$, with subsequent acetonide protection, provided **(–)-4.15** in 52% yield over two steps and as a single diastereomer (original synthesis and optimization of this fragment was performed by Dr. Young Eun Lee, I repeated reactions to push material forward and for characterization).

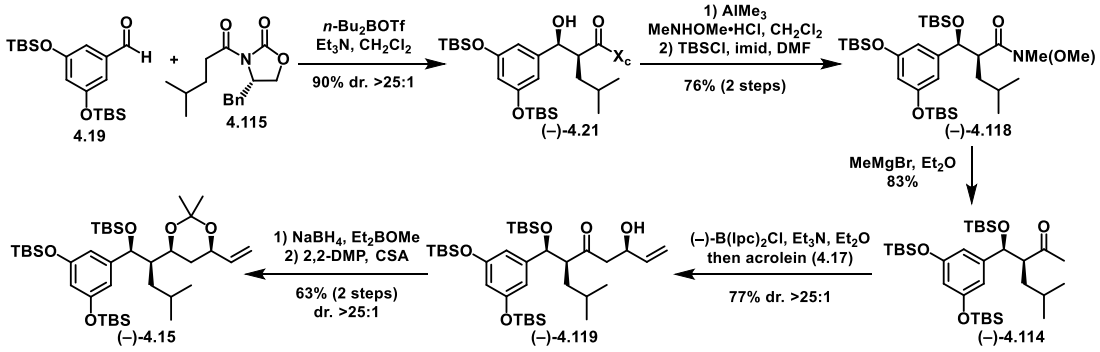

Scheme 60. Synthesis of left fragment **(–)-4.15**.

This route allowed us access to appreciable quantitites of **(–)-4.15** for not only natural product synthesis, but analogs as well. However, it was around this time that the report by Goswami *et al.* was published and showed that our target **4.13b** was not the natural product.[29]

4.3.3 Synthesis of Corrected Structure

After seeing the report from Goswami, *et al.* and realizing our synthetic target did not match the natural product, we analyzed NMR data from benzaldehyde aldol adducts in the literature, along with studies on deoxypropionate chains to rationalize the correct relative configuration.[39-40] Consequently, we were well on our way to the correct stereochemical array when the publication by Aggarwal was disclosed.[33] Our revised synthesis of the left fragment is shown in Scheme 61.

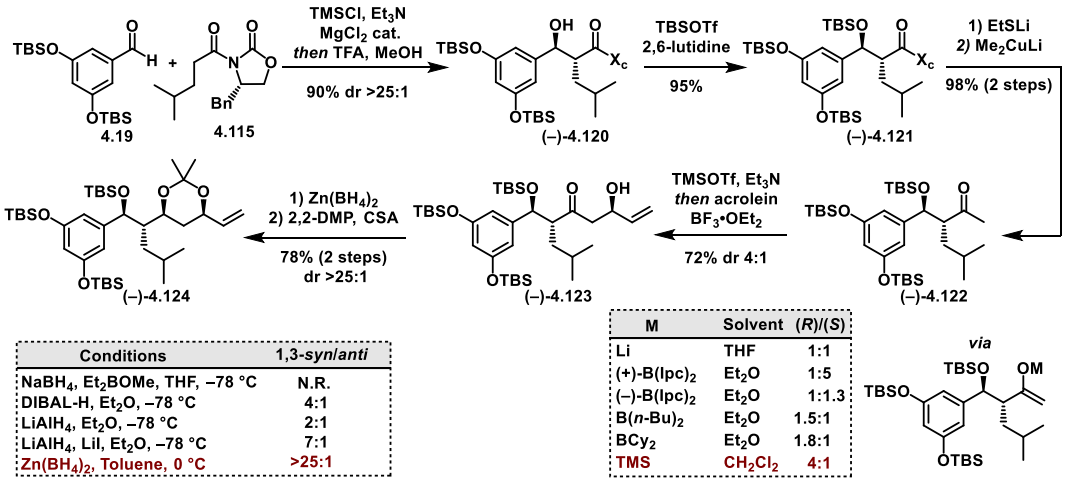

Scheme 61. Synthesis of revised left half **(–)-4.124**.

Our revised synthesis began with a $MgCl_2$-catalyzed *anti*-aldol between the same starting materials as before, **4.19** and **4.115**, yielding **(–)-4.120** in high yield as a single diastereomer (Dr. Guillaume Ernouf and myself each ran this reaction).[41] From there, we attempted to synthesize the corresponding Weinreb amide via transamidation, to no avail. The previously successful conditions provided no trace amount of product, and warming the reaction only caused retro-aldol

reaction under the Lewis acidic conditions, whereby we detected significant quantities of **4.19** forming in the reaction. Instead, we protected the secondary alcohol as the corresponding TBS ether, yielding **(–)-4.121**. From there, we found that displacement of the chiral auxiliary was possible with lithium ethyl thiolate (generated *in situ* with EtSH and *n*-BuLi), which yielded a crude thioester. The crude thioester was then exposed to Me_2CuLi overnight, generating **(–)-4.122** in nearly quantitative yield over two steps (initial optimization of this 2-step sequence was carried out by myelf, and Dr. Guillaume Ernouf performed scale-up).

The aldol reaction of methyl ketone **(–)-4.122** with acrolein was then investigated. We first attempted reaction with the lithium enolate, to gain an understanding of substrate bias, which gave an equimolar mixture of possible products (ratio by crude NMR). Enolates derived from both (+)-$(Ipc)_2BCl$ and (–)-$(Ipc)_2BCl$ provided predominantly the undesired stereoisomer, in a diastereomeric ratio of 1:5, and 1:1.3, respectively. The enolates derived from achiral boron reagents B(*n*-Bu)$_2$OTf and B(cyclohexyl)$_2$Cl gave some selectivity in favor of the desired product in a 1.5:1 and 1.8:1 ratio, respectively. We next attempted a Mukaiyama aldol of the corresponding TMS silyl enol ether, and gratifyingly obtained the desired stereoisomer in a 4:1 diastereomeric ratio. The absolute configuration of the newly created stereocenter in **(–)-4.123** was also unequivocally assigned by Mosher's ester derivatization and analysis (see Figure 44, page 298, carried out by Dr. Guillaume Ernouf). While the separation of the diastereomers was not trivial, this ratio made the process much simpler, and we were able to isolate several hundred milligrams of **(–)-4.123** after one reaction and purification. Next, the reduction of the β-hydroxy ketone to provide the *syn* 1,3-diol was investigated. The originally successful conditions (Et_2BOMe, $NaBH_4$), delivered no product, even upon warming to room temperature. Since this reaction is known to proceed via a 6-membered chelated intermediate, the steric bulk of the neighboring isobutyl group was undoubtedly blocking the approach of the reductant from the desired face. We next looked at aluminum-based reducing agents (DIBAL-H and $LiAlH_4$) and

found the desired product to be formed preferentially, but the diastereomers were inseparable with typical column chromatography. We then attempted reduction with $Zn(BH_4)_2$, and gratifyingly found, after acetonide protection, **(–)-4.124** to be the only detectable diastereomer (optimized and performed by Dr. Guillaume Ernouf).

The stereochemical reassignment had little bearing on the synthesis of the right half fragment of the revised structure of the baulamycins, which is shown in Scheme 62. Starting from (*R*)-Roche ester **(–)-4.125**, benzylation was carried out under acidic conditions with reagent **4.126** and catalytic triflic acid, followed by $LiAlH_4$ reduction and iodination, to give iodide **(–)-4.117**. Myers alkylation with propionate **(+)-4.127** was then carried out to give **4.128**.[42] The NMR spectra of this compound was a complex mixture of rotamers. The material was subjected to lithium amidotrihydroborate reduction to give **(+)-4.129** as a single diastereomer. From there, the same 3-reaction sequence as before was carried out: iodination, Myers alkylation, and lithium amidotrihydroborate reduction, which provided **(+)-4.130** as a single diastereomer. Swern oxidation followed by Wittig reaction of the resultant alcohol then yielded **(–)-4.131** in high yield, with no detectable epimerization of the α-methyl stereocenter in the aldehyde intermediate. Fragment **(–)-4.131** was used for baulamycin B, along with any other analogs that contained alterations to the ethyl ketone moiety. For baulamycin A, and analogs retaining the ethyl ketone, the benzyl ether was converted to the ethyl ketone prior to metathesis. Removal of the benzyl ether of **(–)-4.131** with lithium/naphthalene provided **(–)-4.132**, which was converted to ethyl ketone **(+)-4.133** in three simple operations: oxidation, Grignard reaction, and oxidation.

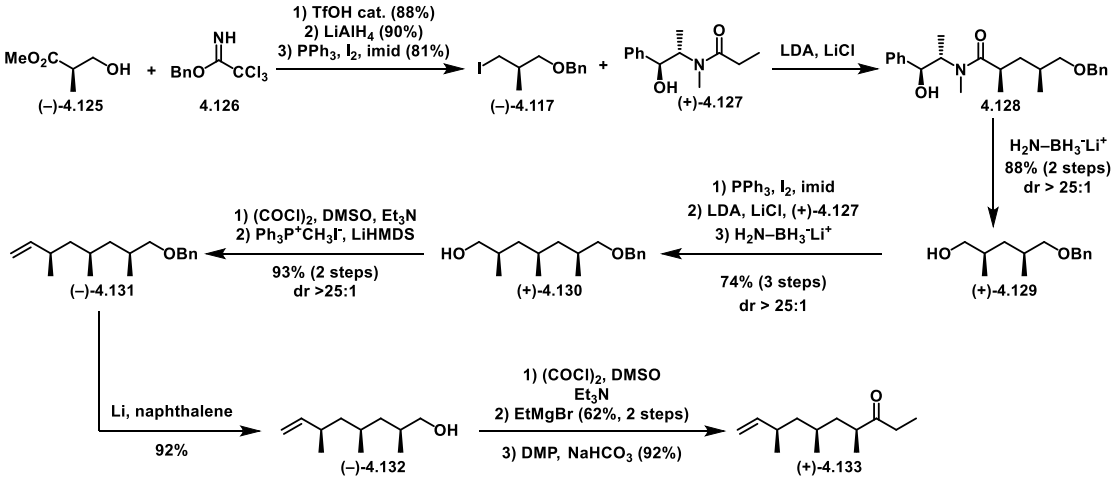

Scheme 62. Synthesis of fragments used for the right half of the baulamycins and analogs: **(–)-4.131** and **(+)-4.133**.

4.3.4 Completion of the Total Synthesis of Baulamycin A, Baulamycin B, and Analogs

With the necessary fragments in hand, we next looked to complete not only the total synthesis of baulamycin A & B, but also analogs. Scheme 63 shows the synthesis of baulamycin A, baulamycin B, and three analogs that were synthesized *en route* to them. Fragment **(–)-4.124** was coupled with **(+)-4.133** via cross-metathesis with Grubbs II catalyst. Several portions of Grubbs II had to be added during the reaction for this transformation to be successful, providing **(–)-4.134** in high yield. From there, hydrogenation (Pd/C, H_2) and global deprotection (HF•pyridine) provided baulamycin A, **(–)-4.13d**, in 56% yield over two steps. The natural product was methylated directly with K_2CO_3 and MeI to provide methyl ether analog **(–)-4.135** (reaction ran by Dr. Guillaume Ernouf). We were also able to use fragment **(–)-4.124** to yield a greatly simplified analog, whereby the compound was first hydrogenated and then deprotected, yielding analog **(–)-4.136**.

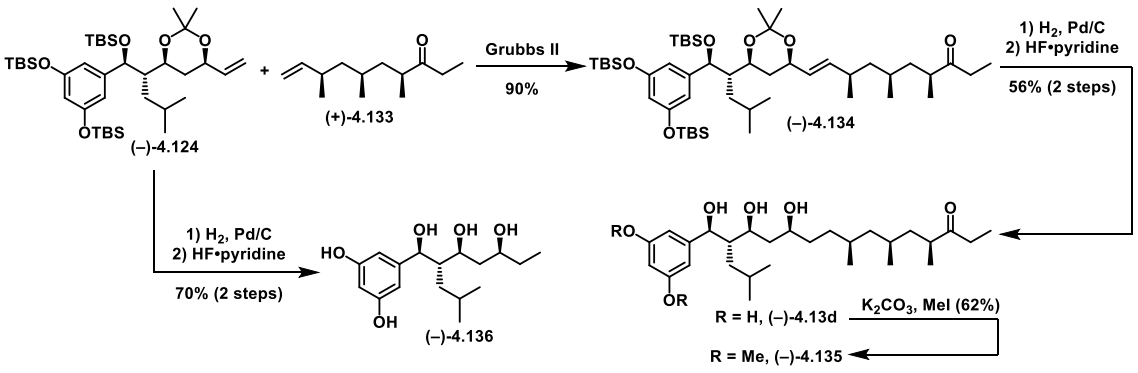

Scheme 63. Completion of the synthesis of baulamycin A (**(–)-4.13d**) and analogs **(–)-4.126** and **(–)-4.127**.

To access baulamycin B, and analogs where the ketone moiety was modified, a slightly different strategy was employed, which is shown in Scheme 64. Fragments **(–)-4.124** and **(–)-4.131** were coupled via cross-metathesis. The product, starting materials, and dimerized starting material **(–)-4.131** were all extremely difficult to separate by column chromatography, as they had very similar R_f values in many solvent eluents, and were extremely non-polar. However, the partially purified mixture could be hydrogenated, which formed the primary alcohol of **(–)-4.137** and made it very easily separable from the mixture. From **(–)-4.137**, protected baulamycin B (**(–)-4.138**) and propyl analog **(–)-4.139** were both accessed by oxidation, Grignard reaction, and oxidation. Global deprotection then yielded the final products baulamycin B and propyl analog, **(–)-4.140** and **(–)-4.141**, respectively. Along the way, alcohol intermediate **(–)-4.137** was also subjected to global deprotection, yielding alcohol analog **(–)-4.142**.

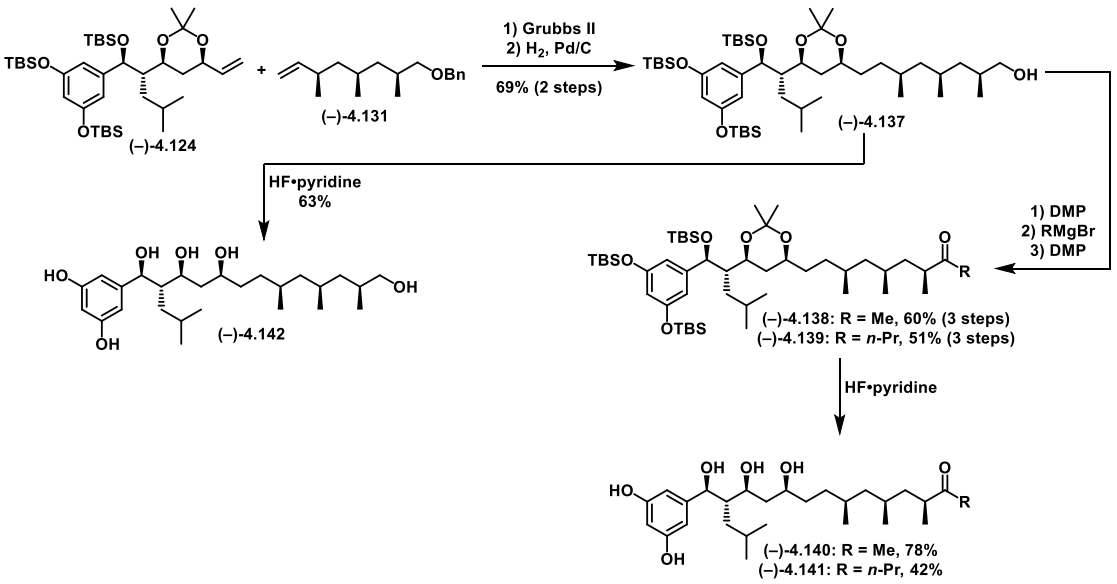

Scheme 64. Synthesis of baulamycin B (**(–)-4.140**), **(–)-4.141**, and **(–)-4.142**.

Two simplified analogs with the same carbon chain length as baulamycin A were synthesized, which are shown in Scheme 65. Left half fragment **(–)-4.124** was first coupled with metathesis partner **4.143**, the ketone of which made separation of the product from the reaction mixture very feasible, yielding product **4.144** in good yield. In contrast, when **(–)-4.124** was subjected to metathesis with 1-decene, the product was very difficult to separate from the reaction mixture. Subsequent hydrogenation made the resultant product, **(–)-4.145**, more polar and more easily separable. Global deprotection of these intermediates yielded the simplified analogs **(–)-4.146** (synthesized by Guillaume Ernouf) and **(–)-4.147**.

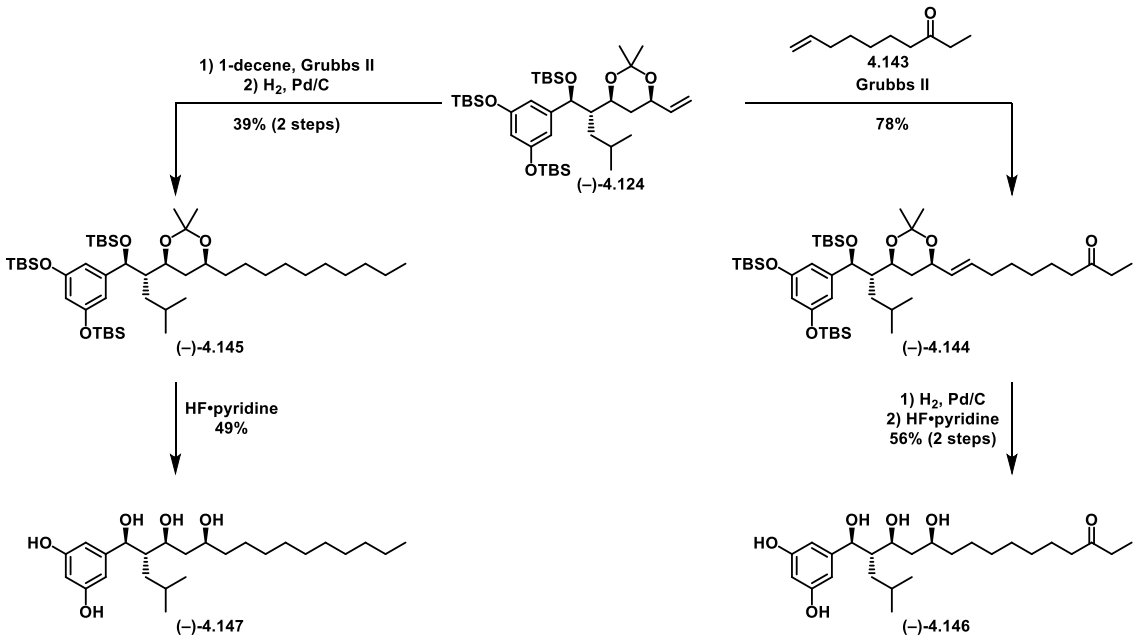

Scheme 65. Synthesis of simplified analogs **(–)-4.146** and **(–)-4.147**.

Finally, two previously disclosed synthetic intermediates were used to access analogs with changes to the left half, each starting from ketone **(+)-4.133**, shown in Scheme 66. We subjected the originally reported structure left half **(–)-4.15** to metathesis with ketone **(+)-4.133**, which after hydrogenation, yielded **(–)-4.148**. Global deprotection then afforded all *syn* analog **(–)-4.149**. A previous synthetic intermediate, ketone **(–)-4.123** was similarly coupled with **(+)-4.133** to provide **(–)-4.150**, which afforded ketone **(–)-4.151** (synthesized by Guillaume Ernouf) after global deprotection.

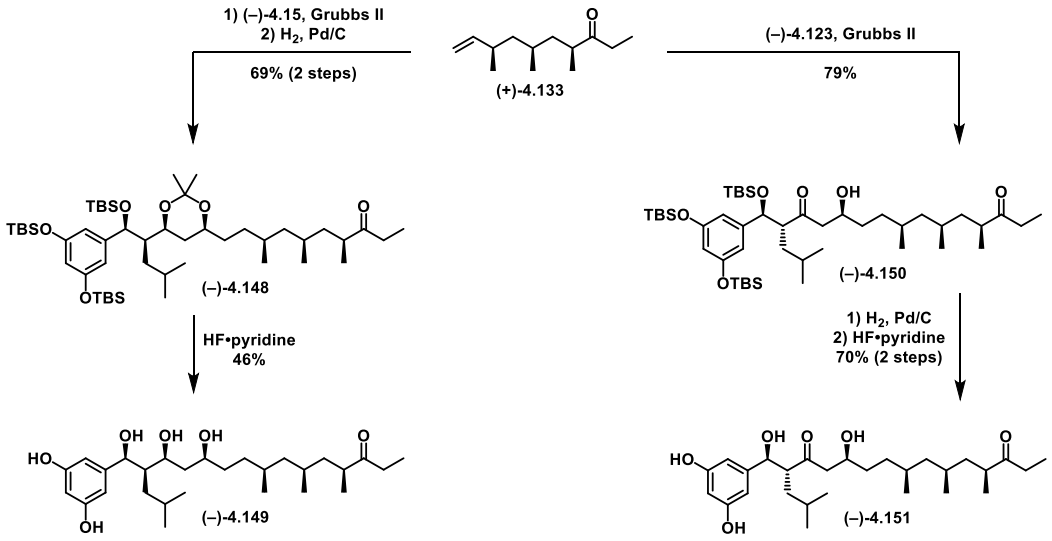

Scheme 66. Synthesis of analogs **(–)-4.149** and **(–)-4.151**.

4.4 Biological evaluation of Baulamycin A, B, and Analogs

4.4.1 *S. aureus* Inhibition

With the natural products, baulamycin A and B, and eight analogs, we investigated growth inhibition of *S. aureus* with a standard MIC assay. These were run in both iron-rich (LB media) and iron-depleted (LB media supplemented with 2,2'-bipyridyl) growth conditions and against methicillin-sensitive (SH1000), community-acquired methicillin-resistant (USA300), and hospital-acquired methicillin resistant (ATCC 33591) *S. aureus*. The structures and results are shown in Figure 42. The graph of SH1000 inhibition data (Figure 42B) makes it abundantly clear that the differences between iron-rich and iron-limited media are minimal, which is in accordance with the isolation publication data. In that report, the IC_{50} of baulamycin A against *S. aureus* strain USA300 was 130 μM in both IRM and IDM. Of the synthetic analogs, four showed equal or improved potency relative to the natural product. The propyl ketone, **(–)-4.141** exhibited two-fold increased potency, which was expected since ethyl ketone (baulamycin A) was already more potent than methyl ketone (baulamycin B). The unnatural diastereomer of baulamyin A, **(–)-4.149**

was equipotent with the natural baulamycin A. We were surprised that this compound was equipotent, since epimerizing the stereogenic center with the very large isobutyl group would likely cause a drastic structural change, especially if engaging with a protein active site. Ketone analog, **(–)-4.151** was equipotent with the natural product, which is likely a subtle change in overall compound structure. Finally, simplified analog **(–)-4.147** showed a 100-fold boost in potency relative to the natural product and was consistent across strain and iron availability in media. The fact that this compound showed no semblance of selectivity across all strains tested, and a very structurally similar compound, **(–)-4.146**, was completely inactive, made us question whether this improved activity was simply a result of increased general toxicity, which was the focus of the next round of biological experiments.

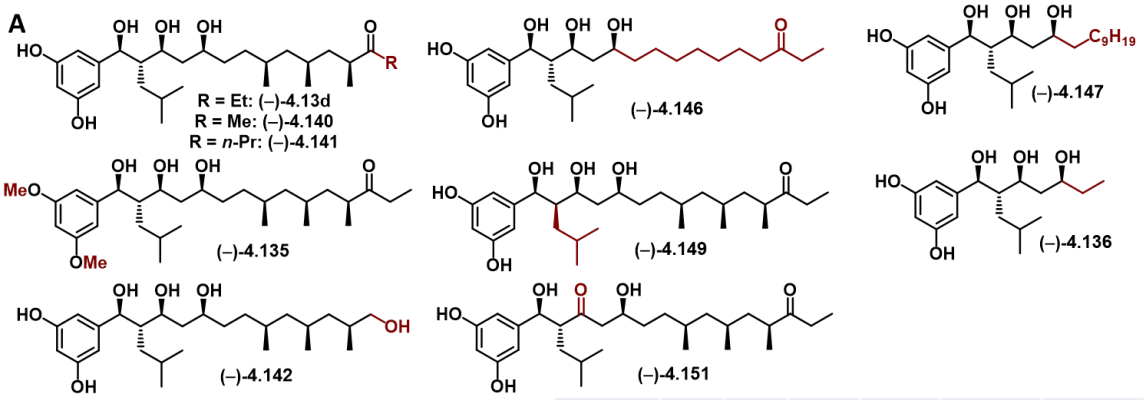

C

cmpd	SH1000 IRM	SH1000 IDM	USA300 IRM	USA300 IDM	ATCC 33591 IRM	ATCC 33591 IDM
(–)-4.13d	125	125	500	>500	500	250
(–)-4.140	250	250	>500	>500	>500	500
(–)-4.141	63	63	125	125	250	63
(–)-4.135	>500	>500	>500	>500	>500	>500
(–)-4.142	500	250	>500	>500	500	500
(–)-4.146	>500	250	>500	>500	>500	>500
(–)-4.149	125	125	250	250	250	250
(–)-4.151	63	63	125	125	125	63
(–)-4.147	8	8	8	8	8	8
(–)-4.136	>500	>500	>500	>500	>500	>500
vanco	3	1.5	6	6	3	3

Figure 42. Baulamycin A, B, and analog results of *S. aureus* inhibition. (a) structures of natural products and analogs. (b) MIC data of active compounds against SH1000, highlighting the minimal differences between IRM and IDM. ***(–)-4.146** had an MIC of >500 μM in IRM, but is shown as 500 μM for visual clarity. (c) Full set of MIC data for all compounds against all strains tested in IRM and IDM (values are in μM, except for vancomycin, which is given in μg/mL)

4.4.2 Hemolysis and SYTOX Uptake Assay Results

We next tested each compound for hemolytic activity, and quantified the hemolysis concentration 20%, HC_{20}, as the concentration that caused 20% hemolysis (red blood cells were from sheep's blood). The hemolysis data is presented in the table in Figure 43. The natural products, as well as the propyl analog **(–)-4.141** did not cause hemolysis. The inactive methoxy analog **(–)-4.135** caused hemolysis at high concentrations with an HC_{20} of 250 μM. Alcohol analog **(–)-4.142** and simplified ketone analog **(–)-4.146** did not cause detectable hemolysis, both of which were inactive against *S. aureus*. Unnatural baulamycin diastereomer **(–)-4.151** also caused no hemolysis. Ketone analog **(–)-4.151** caused hemolysis near its MIC value, with an HC_{20} value of 125 μM compared to its MIC of 63 μM against *S. aureus* SH1000. Not surprisingly, our most active compound **(–)-4.147** caused significant hemolysis on par with its MIC value, indicating that its increased potency was a result of general toxicity. Finally, simplified analog **(–)-4.136** showed no hemolytic activity, which indicated that the activity of **(–)-4.147** could be related to its amphiphilic structure and acting like a detergent since half of the molecule is very hydrophobic and the other half hydrophilic. This would mean that the compounds elicit their inhibitory effect via membrane damage.

To test our hypothesis concerning membrane damage directly on *S. aureus*, we performed SYTOX uptake experiments. SYTOX is a commonly used dye which exhibits a large increase in its fluorescence upon complexation with DNA. Cells were extensively washed and then incubated with SYTOX for 30 minutes in the dark. The cells were then treated with test compounds and fluorescence readings were immediately taken and repeated every 10 minutes for an hour. Figure 43 shows examples of experiments with both positive (QAC and **(–)-4.13d**) and negative (vancomycin and **(–)-4.136**) results (see 5.1.5 SYTOX Uptake Assay Data for full presentation of

graphs of each experiment, each run in triplicate). In all case but one (**(–)-4.140**), each compound that was active against *S. aureus* tested positive for membrane damage via this assay. We believe that baulamycin B did not test positive for membrane damage due to its very modest MIC value.

cmpd	HC20	SYTOX
(–)-4.13d	>500	+
(–)-4.140	>500	-
(–)-4.141	>500	+
(–)-4.135	250	-
(–)-4.142	>500	+
(–)-4.146	>500	-
(–)-4.149	>500	+
(–)-4.151	125	+
(–)-4.147	31	+
(–)-4.136	>500	+

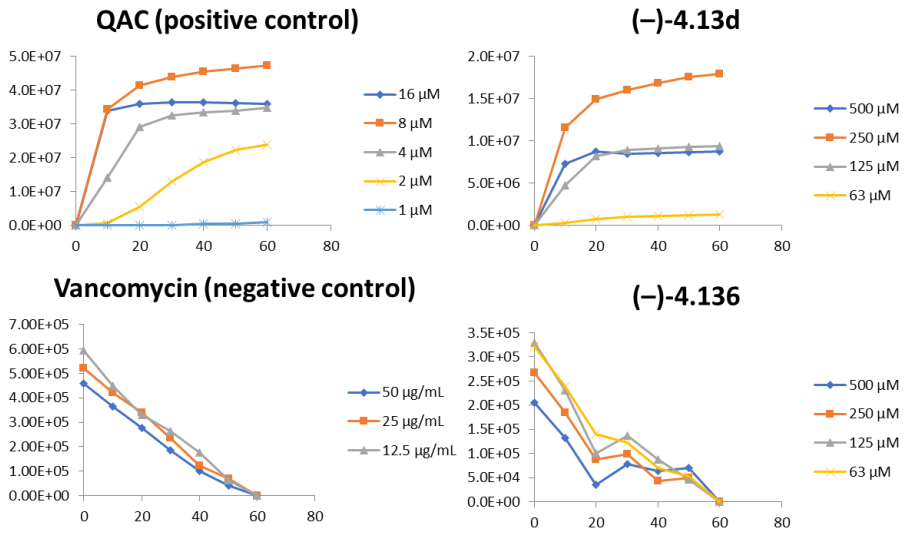

Figure 43. Table of HC_{20} and SYTOX assay results. The four graphs show examples of positive/negative controls, and compounds that tested positive and negative for membrane permeabilization.

4.5 Conclusions

The baulamycins are broad-spectrum growth inhibitors of many species of bacteria, with *in vitro* activity against the siderophore biosynthetic enzymes SbnE and AsbA. The *in vitro* activity was not sufficient in explaining the observed broad-spectrum activity, which in the case of *S. aureus*, did not change between iron-rich and -limited growth conditions. These mechanistic questions, as well as the question of the stereochemistry of the natural products' seven stereocenters are what inspired this work.

During our initial synthetic work, several reports emerged showing that the originally proposed relative stereochemistry of the baulamycins was not correct. The discrepancies were

finally resolved by Aggarwal *et al.* who unequivocally proved the correct relative and absolute stereochemistry of the molecules' seven stereogenic centers. Luckily, we were well on our way to this stereochemical array at the time, which was the result of analyzing NMR data from similar stereochemical arrays.

With complete confirmation that the structure we were pursuing was correct, we synthesized the natural products, as well as eight analogs, in short order. We performed a series of MIC assays against *S. aureus* due to its relevance as a clinical pathogen, and very minimal differences reported in iron-rich and -limited media. This led to the discovery of analog **(–)-4.147**, which was 100-fold more potent than baulamycin A. However, removal of the unfunctionalized alkane chain to analog **(–)-4.136**, abolished all inhibitory activity. Therefore, the alkyl chain of **(–)-4.147** was the reason for its inhibition, which made us hypothesize that non-selective membrane lysis was occurring.

To test this hypothesis, we performed hemolysis assays to see if the active compounds exhibited broad toxicity. Many of the analogs, **(–)-4.147** in particular, caused significant hemolysis near their MIC value. This made us directly test whether the compounds were inducing membrane damage in *S. aureus*, via a SYTOX uptake assay. All active compounds, except for baulamycin B, tested positive for membrane damage with this assay. This allowed us to say, in the case of baulamycin A and active analogs, membrane damage was the main mechanism of action in *S. aureus*, not siderophore biosynthesis inhibition.

This work shows the importance in drug discovery of testing compounds in many different assays, and not relying on *in vitro* data alone. Supplementing MIC data with hemolysis data is extremely helpful to gauge whether improved activity relative to a lead is due to non-selective toxicity or productive, selective antagonism. Additionally, *in vitro* data alone does not

take parameters such as permeability into account, and can lead to pursuit of compounds that do not function as intended in a whole-cell environment.

Considering the toxicity and mechanism data presented here, it is unlikely that **(–)-4.147** is a useful antibiotic lead. However, propyl analog **(–)-4.141** displayed a 2-fold increase in potency relative to the natural product, with no evidence of hemolytic activity. Whether this compound, and the natural products, are acting solely via this newly discovered membrane-disruption mechanism remains to be seen. Further alternative mechanisms could also be at play in other bacteria. Specifically, the baulamycins were reported to have much stronger antagonism against *E. coli* in iron-limited compared to iron-rich conditions, suggesting that IucA or another protein involved in iron acquisition may be a more relevant biological target in this bacterium. Future work will be focused on validation of the mechanism presented here, discovery of new phenotypes elicited by the compounds, and new analogs with improved potency and selectivity.

4.6 References

1) Raymond, K. N.; Carrano, C. J. *Acc. Chem. Res.* **1979**, *12*, 183.

2) Ochsner, U. A.; Johnson, Z.; Vasil, M. L. *Microbiology* **2000**, *146*, 185.

3) Lansky, I. B.; Lukat-Rodgers, G. S.; Block, D.; Rodgers, K. R.; Ratliff, M.; Wilks, A. *J. Biol. Chem.* **2006**, *281*, 13652.

4) Ratliff, M.; Zhu, W.; Deshmukh, R.; Wilks, A.; Stojiljkovic, I. *J. Bacteriol.* **2001**, *183*, 6394.

5) Mazmanian, S. K.; Skaar, E. P.; Gaspar, A. H.; Humayun, M.; Gornicki, P.; Jelenska, J.; Joachimiak, A.; Missiakas, D. M.; Schneewind, O. *Science* **2003**, *299*, 906.

6) Aisen, P.; Leibman, A.; Zweier, J. *J. Biol. Chem.* **1978**, *253*, 1930.

7) Cornelissen, C. N.; Biswas, G. D.; Tsai, J.; Paruchuri, D. K.; Thompson, S. A.; Sparling, P. F. *J. Bacteriol.* **1992**, *174*, 5788.

8) Biswas, G. D.; Sparling, P. F. *Infect. Immun.* **1995**, *63*, 2958.

9) Larson, J. A.; Howie, H. L.; So, M. *Mol. Microbiol.* **2004**, *53*, 807.

10) Sandrini, S. M.; Shergill, R.; Woodward, J.; Muralikuttan, R.; Haigh, R. D.; Lyte, M.; Freestone, P. P. *J. Bacteriol.* **2010**, *192*, 587.

11) Kammler, M.; Schon, C.; Hantke, K. *J. Bacteriol.* **1993**, *175*, 6212.

12) O'Brien, I. G.; Gibson, F. *Biochim. Biophys. Acta* **1970**, *215*, 393.

13) Pollack, J. R.; Neilands, J. B. *Biochem. Biophys. Res. Commun.* **1970**, *38*, 989.

14) Pierce, J. R.; Pickett, C. L.; Earhart, C. F. *J. Bacteriol.* **1983**, *155*, 330.

15) Shea, C. M.; McIntosh, M. A. *Mol. Microbiol.* **1991**, *5*, 1415.

16) Brickman, T. J.; McIntosh, M. A. *J. Biol. Chem.* **1992**, *267*, 12350.

17) Guerinot, M. L.; Meidl, E. J.; Plessner, O. *J. Bacteriol.* **1990**, *172*, 3298.

18) Challis, G. L. *Chembiochem* **2005**, *6*, 601.

19) Schmelz, S.; Botting, C. H.; Song, L.; Kadi, N. F.; Challis, G. L.; Naismith, J. H. *J. Mol. Biol.* **2011**, *412*, 495.

20) Dale, S. E.; Doherty-Kirby, A.; Lajoie, G.; Heinrichs, D. E. *Infect. Immun.* **2003**, *72*, 29.

21) Lamb, A. L. *Biochim. Biophys. Acta* **2015**, *1854*, 1054.

22) Tripathi, A.; Schofield, M. M.; Chlipala, G. E.; Schultz, P. J.; Yim, I.; Newmister, S. A.; Nusca, T. D.; Scaglione, J. B.; Hanna, P. C.; Tamayo-Castillo, G.; Sherman, D. H. *J. Am. Chem. Soc.* **2014**, *136*,

23) McQuade, T. J.; Shallop, A. D.; Sheoran, A.; Delproposto, J. E.; Tsodikov, O. V.; Garneau-Tsodikova, S. *Anal. Biochem.* **2009**, *386*, 244.

24) Matsumori, N.; Kaneno, D.; Murata, M.; Nakamura, H.; Tachibana, K. *J. Org. Chem.* **1999**, *64*, 866.

25) Tripathi, A.; Schofield, M. M.; Chlipala, G. E.; Schultz, P. J.; Yim, I.; Newmister, S. A.; Nusca, T. D.; Scaglione, J. B.; Hanna, P. C.; Tamayo-Castillo, G.; Sherman, D. H. *J. Am. Chem. Soc.* **2014**, *136*, 10541.

26) Peng, J.; Place, A. R.; Yoshida, W.; Anklin, C.; Hamann, M. T. *J. Am. Chem. Soc.* **2010**, *132*, 3277.

27) Waters, A. L.; Oh, J.; Place, A. R.; Hamann, M. T. *Angew. Chem. Int. Ed.* **2015**, *54*, 15705.

28) Bailey, D. C.; Drake, E. J.; Grant, T. D.; Gulick, A. M. *Biochemistry* **2016**, *55*, 3559.

29) Guchhait, S.; Chatterjee, S.; Ampapathi, R. S.; Goswami, R. K. *J. Org. Chem.* **2017**, *82*, 2414.

30) Pichlmair, S.; Marques, M. M. B.; Green, M. P.; Martin, H. J.; Mulzer, J. *Org. Lett.* **2003**, *5*, 4657.

31) Paladugu, S.; Mainkar, P. S.; Chandrasekhar, S. *Tet. Lett.* **2017**, *58*, 2784.

32) Pasqua, A. E.; Ferrari, F. D.; Crawford, J. J.; Marquez, R. *Tet. Lett.* **2012**, *53*, 2114.

33) Wu, J.; Lorenzo, P.; Zhong, S.; Ali, M.; Butts, C. P.; Myers, E. L.; Aggarwal, V. K. *Nature* **2017**, *547*, 436.

34) Zweifel, G.; Arzoumanian, H.; Whitney, C. C. *J. Am. Chem. Soc.* **1967**, *89*, 3652.

35) Jain, P.; Antilla, J. C. *J. Am. Chem. Soc.* **2010**, *132*, 11884.

36) Sengupta, S.; Bae, M.; Oh, D. C.; Dash, U.; Kim, H. J.; Song, W. Y.; Shin, I.; Sim, T. *J. Org. Chem.* **2017**, *82*, 12947.

37) Evans, D. A.; Dow, R. L.; Shih, T. L.; Takacs, J. M.; Zahler, R. *J. Am. Chem. Soc.* **1990**, *112*, 5290.

38) Naduthambi, D.; Bhor, S.; Elbaum, M. B.; Zondlo, N. J. *Org. Lett.* **2013**, *15*, 4892.

39) Harada, K.; Kubo, M.; Horiuchi, H.; Ishii, A.; Esumi, T.; Hioki, H.; Fukuyama, Y. *J. Org. Chem.* **2015**, *80*, 7076.

40) Schmidt, Y.; Lehr, K.; Colas, L.; Breit, B. *Chem. Eur. J.* **2012**, *18*, 7071.

41) Evans, D. A.; Tedrow, J. S.; Shaw, J. T.; Downey, C. W. *J. Am. Chem. Soc.* **2002**, *124,* 392.

42) Myers, A. G.; Yang, B. H.; Chen, H.; McKinstry, L.; Kopecky, D. J.; Gleason, J. L. *J. Am. Chem. Soc.* **1997**, *119,* 6496.

5.1 Experimental Details

5.1.1 Chemistry: Instrumentation and General Notes

NMR spectra were recorded using the following spectrometers: Bruker Advance 500 (500/125 MHz, Temple University), Bruker Advance 400 (400/100 MHz, Temple University), Varian Inova 500 (500/125 MHz, Emory University), Bruker Avance 600 (600/150 MHz, Emory University), Varian Inova 400 (400/100 MHz, Emory University), or VNMR 400 (400/100 MHz, Emory University). Chemical shifts are quoted in ppm relative to tetramethylsilane and with the indicated solvent as an internal reference. The following abbreviations are used to describe signal multiplicities: s (singlet), d (doublet), t (triplet), q (quartet), m (multiplet), br (broad), dd (doublet of doublets), dt (doublet of triplets), etc. Accurate mass spectra were recorded on an Agilent 6520 Accurate-Mass Q-TOF LC/MS. Some accurate mass measurement data were acquired on a Waters LCT Premier XE by use of electrospray ionization with an internal lock mass reference of leucine enkephalin. Waters instruments are calibrated and report by use of neutral atom masses. Alternatively, a Thermo LTQ-FTMS using a nanospray source for ESI mode or an ion max source with an APCI probe was used, with ionization mode indicated for each compound.

Infrared spectra were obtained using a Thermo Nicolet Nexus 670 FTIR spectrophotometer and specific rotation measurements were made with a 1 dm path length using a Perkin Elmer 341 Polarimeter. Non-aqueous reactions were performed under an atmosphere of argon, in flame-dried glassware, with HPLC-grade solvents purified on a Pure Process Technology purification system. Amine bases were freshly distilled from CaH_2 prior to use. Brine refers to a saturated aqueous solution of sodium chloride. “Column chromatography”, unless otherwise indicated, refers to purification on a Biotage Isolera One Automated system in a gradient of ethyl acetate in hexanes. Reactions were monitored via thin-layer chromatography

(TLC) using EMD Millipore® TLC silica gel glass plates with $KMnO_4$, vanillin, *p*-anisaldehyde, or PMA stain.

5.1.2 Chemistry: Experimental Procedures and Characterization Data

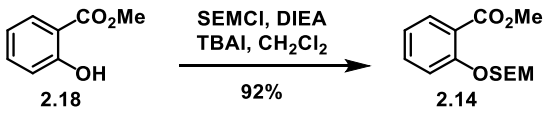

Methyl 2-{[2-(trimethylsilyl)ethoxy]methoxy}benzoate 2.14. To a solution of methyl salicylate (0.51 mL, 3.94 mmol) in CH_2Cl_2 (10 mL) was added SEMCl (1.40 mL, 7.89 mmol) and TBAI (146 mg, 0.40 mmol) at room temperature. The mixture was cooled to 0 °C and diisopropylethylamine (2.80 mL, 15.77 mmol) was slowly added, after which the reaction was warmed to room temperature and stirred for 16 hours. The color of the reaction went from pink to orange to a burgundy red. The reaction was poured into H_2O and extracted with CH_2Cl_2 3x. The combined organics were washed with brine, dried over $MgSO_4$, filtered, concentrated, and purified by column chromatography to yield the title compound as a clear oil (1.023 g, 92% yield). $\mathbf{R_f}$ (9:1 hexanes:EtOAc) = 0.34; **^{1}H NMR** (500 MHz, $CDCl_3$) δ = 7.77 (dd, J = 7.8, 1.7 Hz, 1H), 7.43 (ddd, J = 8.4, 7.3, 1.8 Hz, 1H), 7.22 (dd, J = 8.4, 0.9 Hz, 1H), 7.02 (td, J = 7.7, 1.0 Hz, 1H), 5.30 (s, 2H), 3.88 (s, 3H), 3.83 – 3.78 (m, 2H), 0.99 – 0.91 (m, 2H), -0.01 (s, 9H); **^{13}C NMR** (125 MHz, $CDCl_3$) δ = 166.8, 157.0, 133.4, 131.5, 121.5, 121.4, 116.5, 93.7, 66.7, 52.1, 18.2, 1.3; **IR** (film) 2952, 1731 (C=O), 1601, 1583, 1489, 1454, 1297, 1247, 1188, 1048, 985, 938, 755, 694, 659; **HRMS** Accurate mass (ES+): Found 305.1183, $C_{14}H_{22}O_4SiNa$ (M+Na+) requires 305.1180.

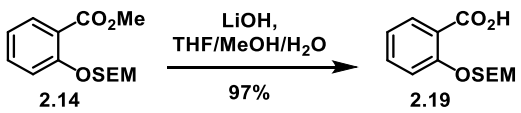

2-{[2-(trimethylsilyl)ethoxy]methoxy}benzoic acid 2.19. To a solution of compound **2.14** (2.217 g, 7.849 mmol) dissolved in 3:1:1 THF:MeOH:H_2O (80 mL) was added LiOH·H_2O (1.180 g, 28.124 mmol), and the solution was stirred at room temperature for 16 hours. After the reaction was complete, it was acidified (pH 5-6) with 5% (v/v) aqueous AcOH solution and extracted with CH_2Cl_2 3x. The combined organic extracts were washed with brine, dried over $MgSO_4$, filtered, and concentrated yielding the title compound as a yellow oil (2.036 g, 97% yield). **^{1}H NMR** (500 MHz, $CDCl_3$) δ = 10.82 (br s, 1H), 8.19 (dd, J = 7.9, 1.8 Hz, 1H), 7.55 (ddd, J = 8.4, 7.3, 1.9 Hz, 1H), 7.30 (dd, J = 8.4, 0.8 Hz, 1H), 7.17 (ddd, J = 7.9, 7.4, 1.0 Hz, 1H), 5.47 (s, 2H), 3.85 – 3.77 (m, 2H), 1.03 – 0.93 (m, 2H), 0.01 (s, 9H); **^{13}C NMR** (500 MHz, $CDCl_3$) δ = 165.5, 156.4, 135.1, 133.8, 123.1, 118.3, 115.2, 94.6, 68.1, 18.2, 1.3; **IR** (film) 3300 (br O-H), 2953, 2870, 1738, 1694, 1602, 1581, 1486, 1458, 1411, 1381, 1301, 1248, 1232, 1154, 1083, 938, 856, 833, 755, 692, 650; **HRMS** Accurate mass (ES+): Found 291.1037, $C_{13}H_{20}O_4SiNa$ (M+Na+) requires 291.1023.

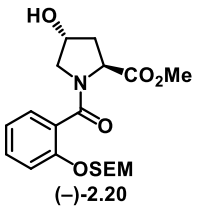

(–)-2.20

Methyl (2S,4R)-4-hydroxy-1-(2-((2-(trimethylsilyl)ethoxy)methoxy)benzoyl)pyrrolidine-2-carboxylate (–)-2.20. The intermediate from the next reaction sequence was purified by preparative TLC (2:1:1 EtOAc:CH_2Cl_2:Et_2O) yielding a pure sample of the title compound. **^{1}H NMR** (500 MHz, $CDCl_3$, mixture of rotamers/conformers) δ 7.34 (ddt, J = 7.6, 3.2, 1.8 Hz, 1.50H), 7.32 – 7.29 (m, 0.25H), 7.20 (dd, J = 7.5, 1.7 Hz, 0.25H), 7.16 (d, J = 7.9 Hz, 1H), 7.05 (td, J = 7.5, 0.9 Hz, 0.75H), 6.99 (td, J = 7.5, 0.9 Hz, 0.25H), 5.24 (dt, J = 13.7, 5.1 Hz, 2H), 4.80 (t, J = 8.2 Hz, 0.75H), 4.56 (br s, 0.25H), 4.48 – 4.41 (m, 1H), 3.99 (d, J = 12.9 Hz, 0.25H), 3.82 – 3.72 (m, 4.50H), 3.62 (d, J = 8.4 Hz, 0.75H), 3.42 (s, 0.75H), 3.39 – 3.31 (m, 1H), 2.44 – 2.28

(m, 1H), 2.17 – 2.09 (m, 2H), 1.62 (br s, 1H), 0.95 (ddd, J = 8.3, 7.5, 4.2 Hz, 2H), 0.01 – -0.01 (m, 9H); **^{13}C NMR** (100 MHz, CDCl3) δ 172.74, 168.37, 153.34, 130.99, 130.93, 128.36, 127.03, 126.18, 122.23, 121.82, 115.72, 115.10, 93.87, 69.94, 68.81, 66.74, 60.52, 58.73, 57.31, 56.22, 54.71, 52.38, 52.14, 39.49, 38.17, 18.07, 14.25, -1.33; **$[\alpha]^{25}_{D}$** –62.5 (c = 2.14 in $CHCl_3$); **IR** (film) 3390 (br, O-H), 2951, 2944, 2360, 2160, 2028, 1979, 1747 (C=O), 1616 (C=O), 1601, 1491, 1455, 1432, 1359, 1248, 1229, 1248, 1201, 1175, 1148, 1084, 1042, 984, 916, 857, 834, 755; **HRMS** Accurate mass (ES^+): Found 418.1656, $C_{29}H_{29}NO_6SiNa$ ($M+Na^+$) requires 418.1662.

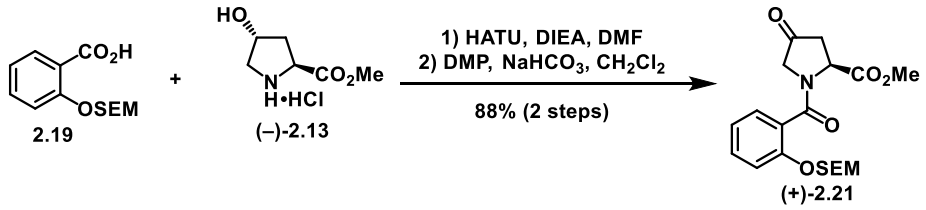

Methyl (2S)-4-oxo-1-(2-{[2-(trimethylsilyl)ethoxy]methoxy}benzoyl)pyrrolidine-2-carboxylate (+)-2.21. To a solution of **2.19** (660 mg, 2.460 mmol) in DMF (12 mL) was added HATU (1.122 g, 2.952 mmol). In a separate vessel, L-4-hydroxyproline methyl ester hydrochloride (574 mg, 2.952 mmol) was dissolved in DMF (12 mL) and diisopropylethylamine (0.64 mL, 3.69 mmol) was added. The amine solution was then added to the acid/HATU solution via syringe, followed by diisopropylethylamine (1.30 mL, 7.38 mmol). The resulting yellow solution was stirred for 16 hours, and upon completion turned orange. The reaction was diluted with EtOAc and saturated aqueous NH_4Cl solution and H_2O until the solids dissolved then extracted 3x with EtOAc. The combined organics were washed with H_2O, 5% LiCl solution 2x, and brine then dried over $MgSO_4$, filtered, concentrated, and purified by column chromatography R_f (5% MeOH/EtOAc) = 0.71. The amide intermediate (orange oil, 1.184 g) was not of sufficient purity for characterization. The intermediate was dissolved in CH_2Cl_2 (50 mL), and $NaHCO_3$ (4.133 g, 49.196 mmol) was added, forming a slurry. DMP (2.087 g, 4.920 mmol) was then added in one portion. After 16 hours, H_2O (44 μL, 2.460 mmol) was added to the vigorously stirring

bright yellow solution very slowly over 20 minutes. After 1 additional hour of reaction time, the starting material was consumed by TLC. 2:1:1 H_2O:sat. $Na_2S_2O_3$:sat. $NaHCO_3$ (60 mL) was added and stirred for 16 hours. The mixture was filtered and extracted 3x with CH_2Cl_2, the combined organics were washed with sat. $Na_2S_2O_3$, sat. $NaHCO_3$, water, and brine; then dried over Na_2SO_4, filtered, concentrated, and purified by column chromatography yielding the title compound as a yellow oil (851 mg, 88% yield over 2 steps). $\mathbf{R_f}$ (1:1 hexanes:EtOAc) = 0.46; **^{1}H NMR** (500 MHz, $CDCl_3$, mixture of conformers) δ = 7.40 – 7.30 (m, 1.75H), 7.25 – 7.24 (m, 0.25H), 7.19 (d, J = 8.4 Hz, 1H), 7.08 – 7.03 (m, 1H), 5.29 – 5.22 (m, 2.56H), 4.67 (d, J = 9.1 Hz, 0.30H), 4.38 (d, J = 19.8 Hz, 0.30H), 3.98 (dd, J = 35.3, 19.2 Hz, 1H), 3.81 (s, J = 4.6 Hz, 2.51H), 3.79 – 3.69 (m, 2.49H), 3.61 (s, 0.76H), 2.99 (dd, J = 19.1, 10.7 Hz, 0.83H), 2.93 (d, J = 10.1 Hz, 0.17H), 2.69 (dd, J = 19.0, 2.7 Hz, 0.70H), 2.61 (d, J = 18.3 Hz, 0.31H), 0.97 – 0.90 (m, 2H), -0.00 (s, 2.47H), -0.01 (s, 6.18H); **^{13}C NMR** (125 MHz, $CDCl_3$) δ = 207.4, 207.3, 171.4, 171.2, 168.4, 153.1, 131.3, 131.3, 128.6, 128.1, 126.1, 125.0, 122.2, 115.3, 115.1, 66.7, 57.4, 55.0, 53.7, 53.5, 52.6, 52.6, 52.0, 41.7, 40.2, 17.9, -1.5; **$[\alpha]^{25}_D$** +1.53 (c = 1.43 in $CHCl_3$); **IR** (film) 2953, 1764 (C=O), 1747 (C=O), 1646, 1601, 1488, 1455, 1406, 1359, 1228, 1177, 1142, 1086, 1033, 981, 937, 918, 834, 753, 694, 657; **HRMS** Accurate mass (ES+): Found 416.1503, $C_{19}H_{27}NO_6SiNa$ (M+Na+) requires 416.1500.

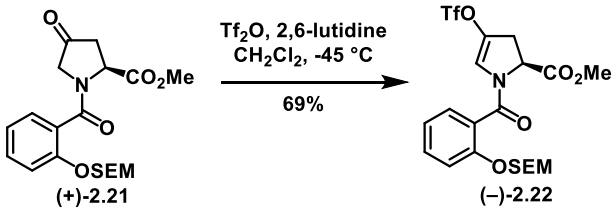

Methyl (2S)-4-(trifluoromethanesulfonyloxy)-1-(2-{[2-(trimethylsilyl)ethoxy]methoxy}benzoyl)-2,3-dihydro-1H-pyrrole-2-carboxylate (–)-2.22. To a solution of ketone **(+)-2.21** (293 mg, 0.745 mmol) in CH_2Cl_2 (10 mL) was added 2,6-lutidine (0.10 mL, 0.894 mmol) at room temperature. The solution was cooled to -40 °C and Tf_2O (0.14

mL, 0.819 mmol) was added very slowly, over which time the solution turned from pink to deep orange/red. After an hour stirring at -40 °C, the reaction was quenched with sat. $NaHCO_3$ and extracted with CH_2Cl_2 3x. The combined organics were washed with sat. NH_4Cl, water, and brine, dried over Na_2SO_4, filtered, concentrated, and purified by column chromatography yielding the title compound as an orange oil (269 mg, 69% yield). $\mathbf{R_f}$ (3:1 hexanes:EtOAc) = 0.54; **^{1}H NMR** (400 MHz, $CDCl_3$) δ = 7.45 – 7.33 (m, 2H), 7.26 – 7.15 (m, 1H), 7.11 – 6.99 (m, 1H), 6.43 (t, J = 1.9 Hz, 1H), 5.26 – 5.21 (m, 2H), 5.09 (dd, J = 11.9, 4.8 Hz, 1H), 3.83 (s, 3H), 3.81 – 3.69 (m, 2H), 3.41 (ddd, J = 16.4, 11.9, 2.3 Hz, 1H), 2.95 (ddd, J = 16.4, 4.8, 1.6 Hz, 1H), 0.98 – 0.88 (m, 2H), -0.01 (s, J = 3.2 Hz, 9H); **^{13}C NMR** (100 MHz, $CDCl_3$) δ = 169.7, 165.7, 154.0, 134.1, 132.3, 129.4, 124.1, 123.5, 122.3, 115.5, 93.6, 66.9, 57.1, 53.0, 33.4, 18.1, -1.3; $\mathbf{[\alpha]^{25}_D}$ –51.6 (c = 1.13 in $CHCl_3$); **IR** (film) 2955, 1751 (C=O), 1652 (C=O), 1601, 1488, 1456, 1407, 1306, 1218, 1136, 1088, 1029, 981, 936, 910, 834, 754, 665, 604; **HRMS** Accurate mass (ES+): Found 548.1001, $C_{20}H_{26}F_3NO_8SSiNa$ (M+Na+) requires 548.0993.

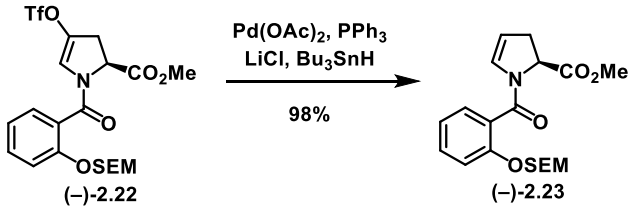

Methyl (2S)-1-(2-{[2-(trimethylsilyl)ethoxy]methoxy}benzoyl)-2,3-dihydro-1H-pyrrole-2-carboxylate (–)-2.23. A solution of **(–)-2.22** (931 mg, 1.771 mmol) dissolved in THF (5 mL) in a glass vial was degassed. At the same time, a flask containing 10 mL of THF was also degassed for 30 mins at which time $Pd(OAc)_2$ (40 mg, 0.177 mmol) was added to the flask, which turned orange. Then PPh_3 (139 mg, 0.531 mmol) and LiCl (225 mg, 5.314 mmol) were added to the flask, and the solution turned into a bright yellow slurry. The solution of **(–)-2.22** was transferred to the flask via syringe, followed by Bu_3SnH (0.52 mL, 1.948 mmol) dropwise. After an hour, 1M aqueous KF (2 mL) and EtOAc were added, and the resulting solution was filtered through Celite

followed by a plug of silica, and purification by column chromatography yielded the title compound as an orange oil (658 mg, 98% yield). **R_f** (3:1 hexanes:EtOAc) = 0.26; **^{1}H NMR** (500 MHz, $CDCl_3$) δ = 7.39 – 7.34 (m, 2H), 7.19 (dd, J = 8.9, 0.9 Hz, 1H), 7.05 (td, J = 7.5, 1.0 Hz, 1H), 6.17 (dt, J = 4.4, 2.2 Hz, 1H), 5.27 – 5.19 (m, 2H), 5.07 – 4.99 (m, 2H), 3.81 (s, 3H), 3.78 – 3.73 (m, 2H), 3.52 – 3.44 (m, 1H), 3.11 (ddt, J = 16.6, 11.6, 2.4 Hz, 1H), 2.71 (dddd, J = 17.0, 4.8, 2.7, 2.0 Hz, 1H), 0.96 – 0.92 (m, 2H), -0.01 (s, 9H); **^{13}C NMR** (125 MHz, $CDCl_3$) δ = 171.3, 164.9, 153.6, 131.1, 130.8, 128.8, 125.7, 121.8, 115.0, 108.3, 93.1, 66.4, 57.7, 52.3, 34.0, 17.9, -1.5; **$[\alpha]^{25}_D$** –91.3 (c = 1.12 in $CHCl_3$); IR (film) 2952, 1750 (C=O), 1650 (C=O), 1618, 1600, 1487, 1405, 1363, 1290, 1248, 1229, 1200, 1179, 1151, 1016, 1006, 983, 940, 857 755, 696, 656, 613; **HRMS** Accurate mass (ES+): Found 400.1543, $C_{19}H_{27}NO_5Si$ (M+Na+) requires 400.1551.

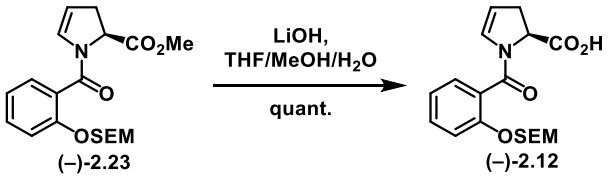

(2S)-1-(2-{[2-(trimethylsilyl)ethoxy]methoxy}benzoyl)-2,3-dihydro-1H-pyrrole-2-carboxylic acid (–)-2.12. To a solution of ester **(–)-2.23** (255 mg, 0.675 mmol) in 4:1 THF:H_2O (5 mL) was added LiOH·H_2O (283 mg, 6.75 mmol). After 4 hours the mixture was acidified (pH 5) with 5% aq. AcOH and extracted with CH_2Cl_2 3x. The combined organic layers were washed with brine, dried over Na_2SO_4, filtered, and concentrated, yielding the title compound as a yellow oil (260 mg, quant. yield). **^{1}H NMR** (400 MHz, $CDCl_3$) δ = 7.45 – 7.34 (m, 2H), 7.23 (d, J = 8.4 Hz, 1H), 7.08 (t, J = 7.5 Hz, 1H), 6.07 (dt, J = 4.4, 2.3 Hz, 1H), 5.26 (dd, J = 4.2, 1.8 Hz, 1H), 5.23 (d, J = 1.5 Hz, 2H), 5.17 (dd, J = 10.9, 4.1 Hz, 1H), 3.76 – 3.69 (m, 2H), 3.38 – 3.28 (m, 1H), 3.01 (ddd, J = 14.8, 10.9, 2.5 Hz, 1H), 0.98 – 0.89 (m, 2H), -0.01 (s, 9H); **^{13}C NMR** (100 MHz, $CDCl_3$) δ = 173.2, 167.2, 153.8, 131.9, 130.0, 129.0, 124.7, 122.0, 115.1, 111.1, 93.3, 66.77, 58.9, 33.2, 18.1, -1.3; **$[\alpha]^{25}_D$** –69.5 (c = 1.13 in $CHCl_3$); IR (film) 2952, 1748 (C=O), 1599 (C=O), 1456, 1410,

1230, 1152, 1086, 984, 834, 752, 729, 650, 613; **HRMS** Accurate mass (ES+): Found 386.1401, $C_{18}H_{25}NO_5Si$ (M+Na+) requires 386.1394.

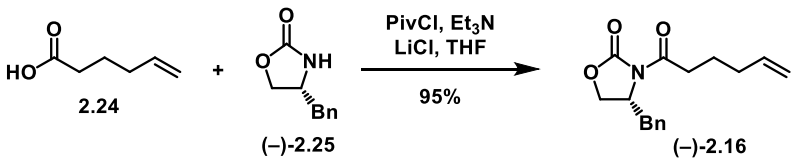

(4R)-4-benzyl-3-(hex-5-enoyl)-1,3-oxazolidin-2-one (–)-2.16. To a solution of 5-hexenoic acid (1.75 ml, 14.8 mmol) and triethylamine (5.4 mL, 38.7 mmol) in THF (80 mL) at -10 °C was added pivaloyl chloride (1.82 mL, 14.8 mmol) dropwise, and the reaction was stirred at this temperature for an hour. LiCl (687 mg, 16.21 mmol) and (*R*)-4-(phenylmethyl)-2-oxazolidinone (2.5 g, 14.1 mmol) were each quickly added in one portion. The reaction was allowed to warm to room temperature and stirred for 16 hours. The reaction was quenched with saturated $NaHCO_3$ and extracted with EtOAc 3x. The combined organic layers were washed with brine, dried over Na_2SO_4, concentrated, and purified by column chromatography, yielding the title compound as a clear oil (3.67 g, 95% yield), with spectroscopic data identical to that previously described: Ghosh, A. K.; Gong, G. J. Org. Chem. **2006**, *71*, 1085.

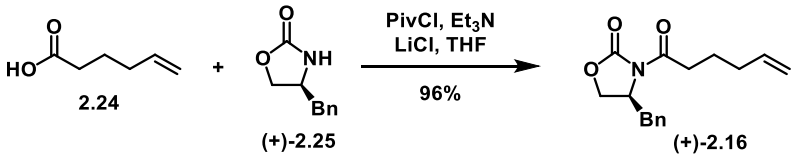

(4S)-4-benzyl-3-(hex-5-enoyl)-1,3-oxazolidin-2-one (+)-2.16. Prepared following the same procedure as **(–)-2.16**. 5-hexenoic acid (1.37 g, 11.99 mmol), triethylamine (4.38 mL, 31.4 mmol), pivaloyl chloride (1.48 mL, 12.0 mmol), LiCl (557 mg, 13.127 mmol), and (*S*)-4-(phenylmethyl)-2-oxazolidinone (2.023 g, 11.415 mmol) yielded the title compound (3.00 g, 96% yield) as a clear oil, with spectroscopic data identical to that previously described: Ghosh, A. K.; Gong, G. J. Org. Chem. **2006**, *71*, 1085.

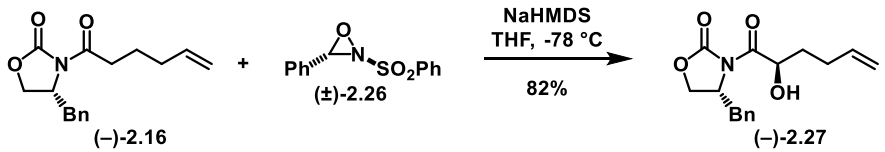

(4R)-4-benzyl-3-[(2R)-2-hydroxyhex-5-enoyl]-1,3-oxazolidin-2-one (–)-2.27. NaHMDS (16.20 mL, 1M in THF, 16.20 mmol) was diluted with THF (100 mL), and cooled to -78 °C. **(–)-2.16** (3.70 g, 13.53 mmol) was dissolved in THF (20 mL), cooled to -78 °C, and slowly added to the NaHMDS solution via cannula. The resulting solution was stirred for an hour at -78 °C. Davis oxaziridine (5.30 g, 20.3 mmol) was dissolved in THF (20 mL) and added via syringe pump to the reaction over a 25-minute period. The reaction was stirred for an additional hour at -78 °C. (±)-Camphorsulfonic acid (CSA) (15.7 g, 67.8 mmol) dissolved in THF (135 mL) was added, and the reaction was warmed up to room temperature. H_2O was added, and the solution was extracted 3x EtOAc. The combined organic layers were washed with brine, dried over $MgSO_4$, filtered, concentrated, and purified by column chromatography to yield the title compound as a yellow oil (3.20 g, 82% yield). $\mathbf{R_f}$ (2:1 hexanes:EtOAc) = 0.36; **^{1}H NMR** (400 MHz, $CDCl_3$) δ = 7.37 – 7.26 (m, 3H), 7.23 – 7.19 (m, 2H), 5.84 (ddt, J = 17.0, 10.2, 6.7 Hz, 1H), 5.08 (ddd, J = 17.1, 3.5, 1.6 Hz, 1H), 5.03 – 4.96 (m, 2H), 4.67 (ddt, J = 9.5, 6.9, 3.2 Hz, 1H), 4.31 – 4.22 (m, 2H), 3.52 (d, J = 7.8 Hz, 1H), 3.31 (dd, J = 13.5, 3.2 Hz, 1H), 2.84 (dd, J = 13.5, 9.3 Hz, 1H), 2.38 – 2.18 (m, 2H), 1.92 (dddd, J = 13.8, 9.1, 7.1, 3.5 Hz, 1H), 1.69 (dtd, J = 14.3, 8.5, 5.9 Hz, 1H); **^{13}C NMR** (125 MHz, $CDCl_3$) δ = 174.9, 153.3, 137.6, 134.9, 129.6, 129.1, 127.6, 115.4, 70.3, 67.1, 55.6, 37.6, 33.3, 29.5; $\mathbf{[\alpha]^{25}_D}$ –59.1 (c = 1.75 in $CHCl_3$); **IR (**film) 3502 (br O-H) 2925, 1778 (C=O), 1695 (C=O), 1497, 1455, 1397, 1351, 1289, 1210, 1197, 1109, 1074, 1051, 980, 914, 751, 701; **HRMS** Accurate mass (ES^+): Found 290.1393, $C_{16}H_{19}NO_4$ ($M+H^+$) requires 290.1387.

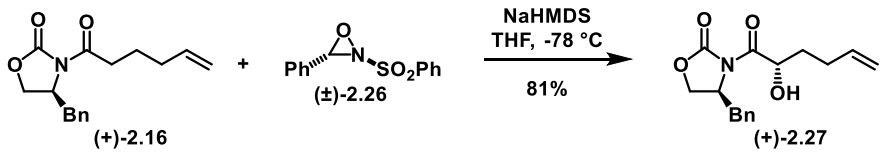

(4S)-4-benzyl-3-[(2S)-2-hydroxyhex-5-enoyl]-1,3-oxazolidin-2-one (+)-2.27. Following the same procedure as **(–)-2.27**; NaHMDS (6.22 mL, 1M in THF, 6.218 mmol), diluted with THF (35 mL), compound **(+)-2.16** (1.416 g, 5.181 mmol) dissolved in THF (10 mL), Davis oxaziridine (2.031 g, 7.772 mmol) dissolved in THF (10 mL), and CSA (6.018 g, 25.907 mmol) dissolved in THF (50 mL) yielded the title compound as a yellow oil (1.211 g, 81% yield). **^{1}H NMR** (500 MHz, $CDCl_3$) δ = 7.35 (tt, J = 8.1, 1.7 Hz, 2H), 7.31 – 7.27 (m, 1H), 7.23 – 7.19 (m, 2H), 5.84 (ddt, J = 17.0, 10.2, 6.7 Hz, 1H), 5.08 (ddd, J = 17.1, 3.5, 1.6 Hz, 1H), 5.03 – 4.96 (m, 2H), 4.73 – 4.62 (m, 1H), 4.32 – 4.22 (m, 2H), 3.50 (d, J = 7.8 Hz, 1H), 3.31 (dd, J = 13.5, 3.3 Hz, 1H), 2.85 (dd, J = 13.5, 9.4 Hz, 1H), 2.35 – 2.22 (m, 2H), 1.92 (dddd, J = 13.8, 9.1, 7.0, 3.5 Hz, 1H), 1.70 (dtd, J = 14.2, 8.6, 5.7 Hz, 1H); **^{13}C NMR** (100 MHz, $CDCl_3$) δ = 174.9, 153.4, 137.7, 134.9, 129.6, 129.2, 127.7, 115.5, 70.4, 67.1, 55.7, 37.6, 33.4, 29.5; **$[\alpha]^{25}_{D}$** +62.1 (c = 1.47 in $CHCl_3$); **IR** (film) 3502 (br O-H), 2922 (C-H), 1778 (C=O), 1695 (C=O), 1640, 1498, 1387, 1351, 1288, 1255, 1211, 1197, 1109, 1074, 1051, 980, 913, 814, 752, 733, 701, 634, 592; **HRMS** Accurate mass (ES^+): Found 290.1385, $C_{16}H_{19}NO_4$ ($M+H^+$) requires 290.1387.

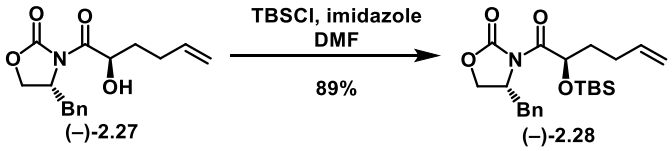

(4R)-4-benzyl-3-[(2R)-2-hydroxyhex-5-enoyl]-1,3-oxazolidin-2-one (–)-2.28. To a solution of **(–)-2.27** (3.16 g, 10.92 mmol) in DMF (60 mL) at 0 °C was added TBSCl (2.47 g, 16.38 mmol) and imidazole (0.966 g, 14.19 mmol). The solution was then allowed to warm to room temperature and stirred overnight. The following day, the reaction was poured into H_2O (60 mL) and extracted with 1:1 EtOAc:hexanes (4x50 mL). The combined organic layers were washed with H_2O then brine, dried over Na_2SO_4, filtered, concentrated, and purified by column chromatography to give the title compound as a clear oil (3.90 g, 89% yield). **R_f** (2:1 hexanes:EtOAc) = 0.78; **^{1}H NMR** (400 MHz, $CDCl_3$) δ 7.37 – 7.27 (m, 3H), 7.26 – 7.21 (m, 2H),

5.83 (ddt, J = 16.9, 10.2, 6.6 Hz, 1H), 5.39 (dd, J = 8.2, 3.5 Hz, 1H), 5.04 (ddd, J = 17.1, 3.3, 1.7 Hz, 1H), 4.98 (dd, J = 10.2, 1.6 Hz, 1H), 4.62 (ddt, J = 9.9, 6.5, 3.4 Hz, 1H), 4.28 – 4.12 (m, 2H), 3.41 (dd, J = 13.3, 3.3 Hz, 1H), 2.70 (dd, J = 13.2, 10.2 Hz, 1H), 2.34 – 2.13 (m, 2H), 1.85 – 1.66 (m, 2H), 0.96 – 0.93 (m, 9H), 0.11 (s, 3H), 0.09 (s, 3H); **^{13}C NMR** (100 MHz, $CDCl_3$) δ = 174.4, 153.2, 137.9, 135.4, 129.6, 129.2, 127.5, 115.2, 71.0, 66.7, 55.8, 37.8, 34.7, 29.8, 26.0, 18.5, -4.5, -4.9; **$[\alpha]^{25}_D$** –5.8 (c = 1.10 in $CHCl_3$); **IR** (film) 2953, 2929, 2857, 1779 (C=O), 1713 (C=O), 1456, 1472, 1387, 1348, 1250, 1209, 1196, 1142, 1106, 1050, 1011, 983, 913, 814, 777, 700; **HRMS** Accurate mass (ES^+): Found 404.2262, $C_{22}H_{33}NO_4Si$ ($M+H^+$) requires 404.2252.

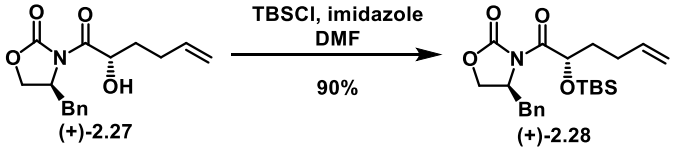

(4S)-4-benzyl-3-[(2S)-2-[(tert-butyldimethylsilyl)oxy]hex-5-enoyl]-1,3-oxazolidin-2-one (+)-2.28. Following the same procedure as **(–)-2.28**; compound **(+)-2.27** (599 mg, 2.069 mmol) in DMF (12 mL), tertbutyldimethylsilyl chloride (526 mg, 3.489 mmol), and imidazole (206 mg, 3.024 mmol), yielded **(+)-2.28** as a clear oil (751 mg, 90% yield). **^{1}H NMR** (500 MHz, CDCl3) δ = 7.36 – 7.31 (m, 2H), 7.30 – 7.26 (m, 1H), 7.26 – 7.23 (m, 2H), 5.83 (ddt, J = 17.0, 10.2, 6.6 Hz, 1H), 5.39 (dd, J = 8.3, 3.4 Hz, 1H), 5.04 (ddd, J = 17.1, 3.5, 1.6 Hz, 1H), 4.98 (ddd, J = 10.2, 3.2, 1.3 Hz, 1H), 4.62 (ddt, J = 10.1, 6.6, 3.3 Hz, 1H), 4.24 – 4.16 (m, 2H), 3.41 (dd, J = 13.3, 3.2 Hz, 1H), 2.70 (dd, J = 13.3, 10.2 Hz, 1H), 2.31 – 2.16 (m, 2H), 1.85 – 1.68 (m, 2H), 0.94 (s, 9H), 0.11 (s, 3H), 0.09 (s, 3H); **^{13}C NMR** (100 MHz, $CDCl_3$) δ = 174.4, 153.2, 137.9, 135.4, 129.6, 129.1, 127.5, 115.2, 71.0, 66.7, 55.8, 37.8, 34.7, 29.8, 26.0, 18.5, -4.5, -4.9; **$[\alpha]^{25}_D$** +9.12 (c = 1.25 in $CHCl_3$); **IR** (film) 2953, 2928, 2856, 1779 (C=O), 1711 (C=O), 1455, 1387, 1348, 1250, 1209, 1195, 1143, 1106, 982, 913, 814, 777, 700; **HRMS** Accurate mass (ES^+): Found 404.2272, $C_{22}H_{33}NO_4Si$ ($M+H^+$) requires 404.2252.

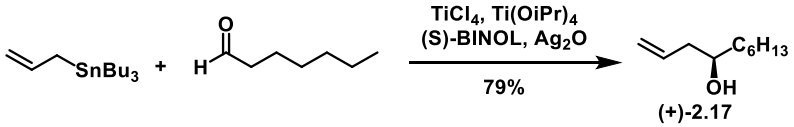

(4R)-dec-1-en-4-ol (+)-2.17. Prepared as previously described (Hanawa, H.; Hashimoto, T.; Maruoka, K. *J. Am. Chem. Soc.* **2003**, *125*, 1708). $TiCl_4$ (1M in DCM, 0.66 mL, 0.66 mmol), $Ti(OiPr)_4$ (0.36 mL, 1.200 mmol), Ag_2O (306 mg, 1.32 mmol), S-BINOL (756 mg, 2.64 mmol), heptanal (1.86 mL, 13.140 mmol), and allyltributylstannane (5.28 mL, 17.100 mmol) yielded the title compound as a yellow oil (1.617g, 79% yield). Spectroscopic data was identical to that previously described: Ortega, N.; Martín, V. S.; Martín, T. *J. Org. Chem.* **2010**, 75, 6660-6672.

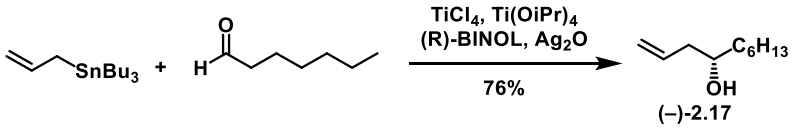

(4S)-dec-1-en-4-ol (–)-2.17. Following the same procedure as **(+)-2.17**; $TiCl_4$ (1M in DCM, 0.66 mL, 0.66 mmol), $Ti(OiPr)_4$ (0.36 mL, 1.200 mmol), Ag_2O (306 mg, 1.32 mmol), R-BINOL (756 mg, 2.64 mmol), heptanal (1.86 mL, 13.140 mmol), and allyltributylstannane (5.28 mL, 17.100 mmol) yielded the title compound as a yellow oil (1.590g, 76% yield).

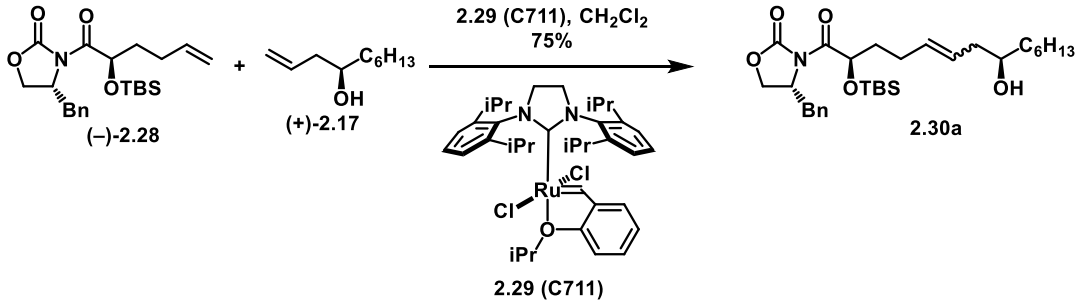

(4R)-4-benzyl-3-[(2R,8R)-2-[(tert-butyldimethylsilyl)oxy]-8-hydroxytetradec-5-enoyl]-1,3-oxazolidin-2-one 2.30a. To a solution of compound **(–)-2.28** (52 mg, 0.128 mmol), and **(+)-2.17** (99 mg, 0.644 mmol) in CH_2Cl_2 (5 mL) was added catalyst **2.29** (catalyst C711, Materia, CAS [635679-24-2]) (9 mg, 0.0128 mmol), and the reaction was stirred overnight. The solution was

purified column chromatography, yielding the title compound as a brown oil and mixture of *E*/*Z* isomers (66 mg, 75% yield). **R_f** (9:1 DCM:EtOAc) = 0.73; **^{1}H NMR** (400 MHz, $CDCl_3$) δ = 7.37 – 7.27 (m, 3H), 7.26 – 7.22 (m, 2H), 5.64 – 5.41 (m, 2H), 5.37 (dd, J = 8.3, 3.4 Hz, 1H), 4.62 (ddt, J = 10.1, 6.5, 3.2 Hz, 1H), 4.24 – 4.16 (m, 2H), 3.59 (br s, 1H), 3.41 (dd, J = 13.2, 3.3 Hz, 1H), 2.68 (dd, J = 13.3, 10.2 Hz, 1H), 2.28 – 2.17 (m, 3H), 2.10 – 1.97 (m, 1H), 1.82 – 1.67 (m, 3H), 1.48 – 1.39 (m, 3H), 1.34 – 1.26 (m, 6H), 0.94 (s, 9H), 0.88 (t, J = 6.8 Hz, 3H), 0.12 (s, 0.44H), 0.11 (s, 2.24H), 0.10 (s, 0.64H), 0.09 (s, 2.29H); **^{13}C NMR** (100 MHz, $CDCl_3$) δ = 174.5, 153.3, 135.4, 133.1, 129.6, 129.2, 127.6, 127.4, 71.0, 70.8, 66.7, 55.8, 53.6, 40.9, 37.9, 37.0, 35.2, 32.0, 29.5, 28.6, 26.0, 25.8, 22.8, 18.5, 14.3, -4.4, -4.9; **IR** (film) 3545 (br O-H), 2927, 2856, 1780 (C=O), 1714 (C=O), 1471, 1387, 1348, 1249, 1210, 1196, 1111, 1012 ,971, 814, 777, 700; **HRMS** Accurate mass (ES^+): Found 532.3438, $C_{30}H_{49}NO_5Si$ ($M+H^+$) requires 532.3453.

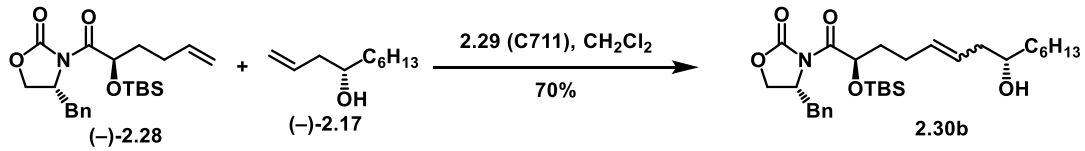

(4R)-4-benzyl-3-[(2R,8S)-2-[(tert-butyldimethylsilyl)oxy]-8-hydroxytetradec-5-enoyl]-1,3-oxazolidin-2-one 2.30b. Following the same procedure as **2.30a**; compound **(–)-2.28** (100 mg, 0.247 mmol) and **(–)-2.17** (173 mg, 1.23 mmol) in CH_2Cl_2 (5 mL) with catalyst **2.29** (17 mg, 0.0247 mmol), yielded the title compound as a brown oil (92 mg, 70% yield). **^{1}H NMR** (400 MHz, $CDCl_3$) δ = 7.37 – 7.27 (m, 3H), 7.26 – 7.22 (m, 2H), 5.51 (tdd, J = 22.0, 15.2, 6.6 Hz, 2H), 5.37 (dd, J = 8.3, 3.3 Hz, 1H), 4.62 (qd, J = 6.6, 3.1 Hz, 1H), 4.23 – 4.15 (m, 2H), 3.58 (br s, 1H), 3.41 (dd, J = 13.0, 3.1 Hz, 1H), 2.68 (dd, J = 13.2, 10.2 Hz, 1H), 2.30 – 2.15 (m, 3H), 1.85 – 1.66 (m, 3H), 1.49 – 1.38 (m, 3H), 1.33 – 1.24 (m, 8H), 0.94 (s, 9H), 0.88 (t, J = 6.8 Hz, 3H), 0.11 (s, 3H), 0.09 (s, 3H); **^{13}C NMR** (125 MHz, $CDCl_3$) δ 174.5, 153.2, 135.4, 133.1, 129.6, 129.1, 127.5, 127.4, 71.1, 70.8, 66.7, 55.7, 40.9, 37.8, 37.0, 35.2, 32.0, 29.8, 29.5, 28.6, 26.0, 25.8, 22.8, 18.5, 14.2, -4.4, -4.9; **IR** (film) 3545 (br O-H), 2927, 2855, 1780 (C=O), 1713 (C=O), 1455, 1388,

1348, 1249, 1210, 1196, 1111, 1012, 971, 814, 777, 700; **HRMS** Accurate mass (ES^+): Found 532.3438, $C_{30}H_{49}NO_5Si$ ($M+H^+$) requires 532.3453.

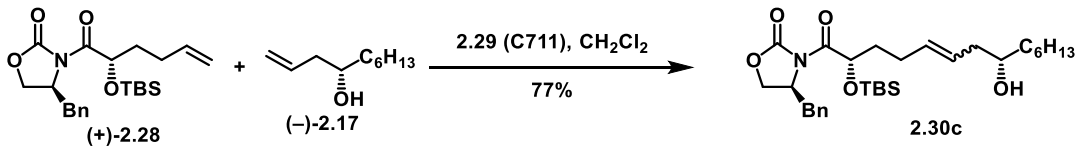

(4S)-4-benzyl-3-[(2S,8S)-2-[(tert-butyldimethylsilyl)oxy]-8-hydroxytetradec-5-enoyl]-1,3-oxazolidin-2-one 2.30c. Following the same procedure as **2.30a**; compound **(+)-2.28** (207 mg, 0.512 mmol) and **(–)-2.17** (400 mg, 2.56 mmol) in CH_2Cl_2 (10 mL) with catalyst **2.29** (37 mg, 0.052 mmol), yielded the title compound as a brown oil (210 mg, 77% yield). **^{1}H NMR** (400 MHz, $CDCl_3$) δ = 7.37 – 7.27 (m, 3H), 7.26 – 7.22 (m, 2H), 5.61 – 5.42 (m, 2H), 5.37 (dd, J = 8.3, 3.4 Hz, 1H), 4.62 (ddt, J = 10.2, 6.6, 3.3 Hz, 1H), 4.24 – 4.15 (m, 2H), 3.65 – 3.54 (m, 1H), 3.41 (dd, J = 13.3, 3.1 Hz, 1H), 2.70 (dt, J = 13.2, 9.1 Hz, 1H), 2.32 – 2.13 (m, 3H), 1.83 – 1.66 (m, 3H), 1.50 – 1.37 (m, 3H), 1.36 – 1.20 (m, 8H), 0.94 (s, J = 5.0 Hz, 9H), 0.88 (t, J = 6.7 Hz, 3H), 0.12 (s, 0.44H), 0.11 (s, 2.19H), 0.10 (s, 0.67H), 0.09 (s, J = 3.8 Hz, 2.43H); **^{13}C NMR** (125 MHz, $CDCl_3$) δ = 174.4, 153.2, 135.3, 132.9, 129.5, 129.1, 127.5, 127.3, 66.7, 55.7, 40.8, 37.8, 36.9, 35.2, 31.9, 29.5, 28.5, 25.9, 25.9, 22.7, 18.4, 14.2, -4.5, -4.9; **IR** (film) 3545 (br O-H) 2927, 2856, 1779 (C=O), 1712 (C=O), 1456, 1387, 1348, 1249, 1210, 1195, 111, 1012, 971, 814, 777, 700; **HRMS** Accurate mass (ES^+): Found 532.3443, $C_{30}H_{49}NO_5Si$ ($M+H^+$) requires 532.3453.

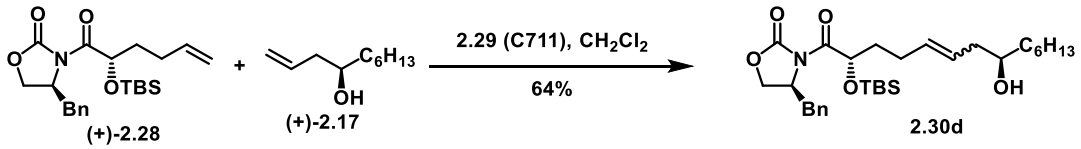

(4S)-4-benzyl-3-[(2S,8R)-2-[(tert-butyldimethylsilyl)oxy]-8-hydroxytetradec-5-enoyl]-1,3-oxazolidin-2-one. 2.30d. Following the same procedure as **2.30a**; compound **(+)-2.28** (89 mg, 0.221 mmol) and **(+)-2.17** (154 mg, 0.996 mmol) in CH_2Cl_2 (0.5 mL) with catalyst **2.29** (16 mg, 0.022 mmol), yielded the title compound as a brown oil (75 mg, 64%). **^{1}H NMR** (500 MHz,

$CDCl_3$) δ = 7.36 – 7.31 (m, 2H), 7.31 – 7.26 (m, 1H), 7.25 – 7.22 (m, 2H), 5.58 – 5.43 (m, 2H), 5.37 (dd, J = 8.4, 3.3 Hz, 1H), 4.61 (qd, J = 6.5, 3.1 Hz, 1H), 4.22 – 4.15 (m, 2H), 3.62 – 3.53 (m, 1H), 3.41 (dd, J = 13.2, 3.2 Hz, 1H), 2.72 – 2.62 (m, 1H), 2.29 – 2.16 (m, 3H), 2.08 – 2.01 (m, 1H), 1.79 – 1.66 (m, 2H), 1.48 – 1.37 (m, 3H), 1.33 – 1.25 (m, 6H), 0.94 (s, 9H), 0.88 (t, J = 6.9 Hz, 3H), 0.10 (s, 3H), 0.09 (s, 3H); **^{13}C NMR** (125 MHz, $CDCl_3$) δ = 174.4, 153.2, 135.4, 133.1, 129.6, 129.1, 127.5, 127.4, 71.0, 70.8, 66.7, 55.7, 40.9, 37.8, 37.0, 35.2, 32.0, 29.5, 28.6, 26.0, 25.8, 22.8, 18.5, 14.2, -4.4, -4.9; **IR** (film) 3526 (br O-H), 2954, 2927, 2856, 1779 (C=O), 1711 (C=O), 1455, 1387, 1348, 1289, 1249, 1210, 1111, 971, 836, 777, 701; **HRMS** Accurate mass (ES^+): Found 532.3472, $C_{30}H_{49}NO_5Si$ ($M+H^+$) requires 532.3453.

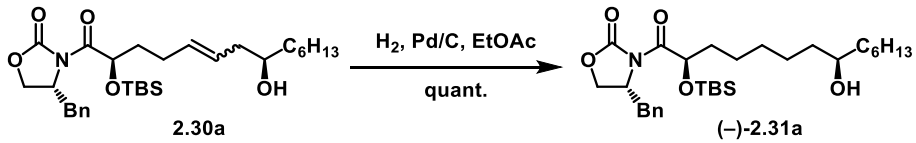

(4R)-4-benzyl-3-[(2R,8R)-2-[(tert-butyldimethylsilyl)oxy]-8-hydroxytetradecanoyl]-1,3-oxazolidin-2-one (–)-2.31a. To a solution of compound **2.30a** (139 mg, 0.260 mmol) in EtOAc (5 mL) was added 5% Pd/C (100 mg) and stirred under a H_2 atmosphere for 16 hours. The reaction was filtered through Celite and concentrated, yielding the title compound as a clear oil (136 mg, quant.). **^{1}H NMR** (500 MHz, $CDCl_3$) δ = 7.36 – 7.31 (m, 2H), 7.31 – 7.26 (m, 1H), 7.25 – 7.23 (m, 2H), 5.37 (dd, J = 8.4, 3.3 Hz, 1H), 4.62 (ddt, J = 6.9, 6.3, 3.0 Hz, 1H), 4.25 – 4.14 (m, 2H), 3.58 (br s, 1H), 3.41 (dd, J = 13.2, 3.1 Hz, 1H), 2.69 (dd, J = 13.3, 10.2 Hz, 1H), 1.74 – 1.58 (m, 2H), 1.53 – 1.22 (m, 19H), 0.94 (s, 9H), 0.88 (t, J = 7.0 Hz, 3H), 0.11 (s, 3H), 0.09 (s, 3H); **^{13}C NMR** (125 MHz, $CDCl_3$) δ = 174.6, 153.3, 135.4, 129.6, 129.2, 127.5, 77.2, 72.0, 71.4, 66.7, 55.8, 37.9, 37.6, 37.5, 35.2, 32.0, 29.5, 29.2, 26.0, 25.8, 25.6, 25.5, 22.8, 18.5, 14.2, -4.5, -4.9; **$[\alpha]^{25}_D$** –2.5 (c = 0.72 in $CHCl_3$); **IR** (film) 3545 (br O-H), 2927, 2856, 1780 (C=O), 1714 (C=O), 1456, 1472, 1387, 1348, 1289, 1249, 1210, 1195, 1106, 1012, 975, 836, 777, 701; **HRMS** Accurate mass (ES^+): Found 534.3616, $C_{30}H_{51}NO_5Si$ ($M+H^+$) requires 534.3609.

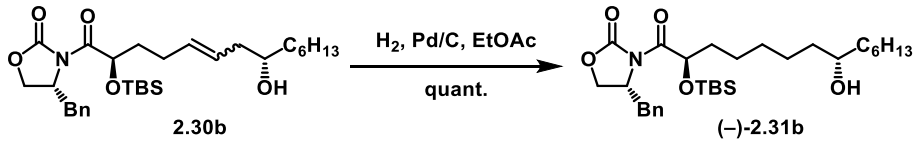

(4R)-4-benzyl-3-[(2R,8S)-2-[(tert-butyldimethylsilyl)oxy]-8-hydroxytetradecanoyl]-1,3-oxazolidin-2-one (–)-2.31b. Following the same procedure as **(–)-2.31a**; **2.30b** (105 mg, 0.197 mmol) in EtOAc (5 mL) with 5% Pd/C (105 mg) yielded the title compound as a clear oil (105 mg, quant.) **^{1}H NMR** (400 MHz, $CDCl_3$) δ 7.37 – 7.31 (m, 2H), 7.31 – 7.27 (m, 1H), 7.26 – 7.22 (m, 2H), 5.36 (dd, J = 8.3, 3.4 Hz, 1H), 4.62 (qd, J = 6.6, 3.2 Hz, 1H), 4.26 – 4.16 (m, 2H), 3.58 (br s, 1H), 3.41 (dd, J = 13.2, 3.2 Hz, 1H), 2.69 (dd, J = 13.2, 10.2 Hz, 1H), 1.76 – 1.60 (m, 2H), 1.53 – 1.24 (m, 19H), 0.94 (s, J = 2.9 Hz, 9H), 0.88 (t, J = 6.8 Hz, 3H), 0.11 (s, J = 3.1 Hz, 3H), 0.09 (s, J = 7.8 Hz, 3H); **$[\alpha]^{25}_D$** –9.5 (c = 0.21 in $CHCl_3$); **IR** (film) 3545 (br O-H), 2927, 2856, 1781 (C=O), 1712 (C=O), 1456, 1387, 1348, 1249, 1210, 1195, 1106, 1051, 1012, 975, 834, 777, 700; **HRMS** Accurate mass (ES^+): Found 534.3598, $C_{30}H_{51}NO_5Si$ ($M+H^+$) requires 534.3609.

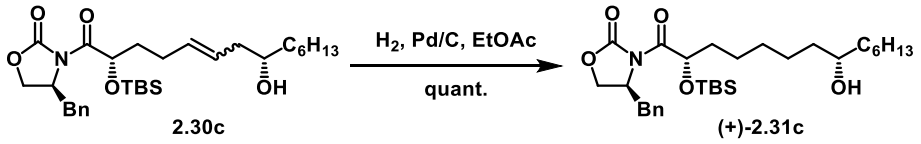

(4S)-4-benzyl-3-[(2S,8S)-2-[(tert-butyldimethylsilyl)oxy]-8-hydroxytetradecanoyl]-1,3-oxazolidin-2-one (+)-2.31c. Following the same procedure as **(–)-2.31a**; **2.30c** (198 mg, 0.371 mmol) in EtOAc (5 mL) with 5% Pd/C (150 mg) yielded **(+)-2.31c** as a clear oil (198 mg, quant.). **^{1}H NMR** (400 MHz, $CDCl_3$) δ = 7.37 – 7.31 (m, 2H), 7.31 – 7.27 (m, 1H), 7.26 – 7.22 (m, 2H), 5.36 (dd, J = 8.3, 3.4 Hz, 1H), 4.62 (ddd, J = 10.2, 6.8, 3.3 Hz, 1H), 4.24 – 4.15 (m, 2H), 3.57 (br s, 1H), 3.40 (dd, J = 13.1, 3.1 Hz, 1H), 2.70 (dd, J = 13.2, 10.2 Hz, 1H), 1.77 – 1.59 (m, 2H), 1.53 – 1.34 (m, 8H), 1.34 – 1.19 (m, 11H), 0.94 (s, J = 2.6 Hz, 9H), 0.90 – 0.86 (m, 3H), 0.11 (s, 3H), 0.09 (s, 3H); **^{13}C NMR** (100 MHz, $CDCl_3$) δ = 174.6, 153.3, 135.4, 129.6, 129.1, 127.5, 72.1, 71.5, 66.6, 55.7, 37.8, 37.7, 37.5, 35.3, 32.0, 29.5, 29.3, 25.9, 25.7, 25.6, 25.6, 22.8, 18.5, 14.2, -

4.5, -5.0; **[α]$^{25}_{D}$** +4.96 (c = 1.6 in $CHCl_3$); **IR** (film) 3545 (br O-H), 2928, 2856, 1780 (C=O), 1712 (C=O), 1456, 1387, 1348, 1249, 1210, 1195, 1106,1051, 1012, 975, 939, 836, 776, 753, 700; **HRMS** Accurate mass (ES^+): Found 534.3625, $C_{30}H_{51}NO_5Si$ ($M+H^+$) requires 534.3609.

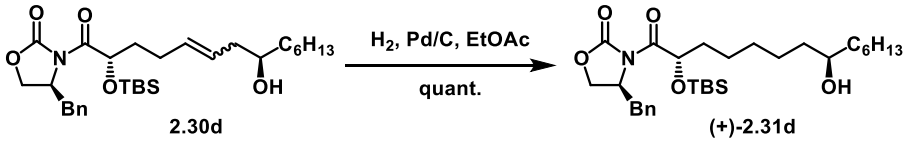

(4S)-4-benzyl-3-[(2S,8R)-2-[(tert-butyldimethylsilyl)oxy]-8-hydroxytetradecanoyl]-1,3-oxazolidin-2-one (+)-2.31d. Following the same procedure as **(–)-2.31a**; **2.30d** (302 mg, 0.569 mmol) in EtOAc (20 mL) with 5% Pd/C (300 mg) yielded the title compound as a clear oil (309 mg, quant.). **^{1}H NMR** (500 MHz, $CDCl_3$) δ = 7.36 – 7.31 (m, 2H), 7.30 – 7.27 (m, 1H), 7.26 – 7.22 (m, 2H), 5.36 (dt, J = 6.6, 3.2 Hz, 1H), 4.62 (qd, J = 6.4, 2.9 Hz, 1H), 4.27 – 4.13 (m, 2H), 3.58 (br s, 1H), 3.40 (dd, J = 13.2, 3.0 Hz, 1H), 2.70 (dd, J = 13.2, 10.2 Hz, 1H), 1.74 – 1.20 (m, 19H), 0.94 (s, 9H), 0.90 – 0.86 (m, 3H), 0.11 (s, 3H), 0.09 (s, 3H); **^{13}C NMR** (125 MHz, $CDCl_3$) δ = 174.6, 153.3, 135.4, 129.6, 129.1, 127.5, 71.9, 71.4, 66.7, 55.7, 37.8, 37.61, 37.4, 35.2, 32.0, 29.5, 29.2, 25.9, 25.8, 25.5, 25.5, 22.8, 18.5, 14.2, -4.5, -5.0; **[α]$^{25}_{D}$** +3.6 (c = 1.03 in $CHCl_3$); **IR** (film) 3545 (br O-H), 2929, 2857, 1781 (C=O), 1712 (C=O), 1456, 1387, 1349, 1214, 1195, 1108, 1014, 975, 939, 836, 776, 753, 701, 667; **HRMS** Accurate mass (ES^+): Found 534.3609, $C_{30}H_{51}NO_5Si$ ($M+H^+$) requires 534.3609.

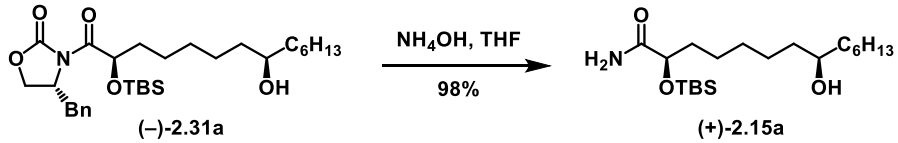

(2R,8R)-2-[(tert-butyldimethylsilyl)oxy]-8-hydroxytetradecanamide (+)-2.15a. To a tightly sealed flask with compound **(–)-2.31a** (136 mg, 0.255 mmol) dissolved in THF (6 mL) was added ammonium hydroxide solution (30% NH_3, 3 mL). The biphasic mixture was vigorously stirred for 48 hours. The reaction was carefully vented, concentrated, and co-evaporated with methanol 3

times to remove residual water. To the residue was added hexanes, the solution was cooled in a freezer, and then filtered to remove precipitated oxazolidinone. The process was repeated (typically 3x) until white solids no longer appeared. Concentration of the filtrate yielded the title compound crude material as a clear oil (95 mg, contains *ca.* 11 % w/w oxazolidinone by NMR analysis, 98% yield). The crude mixture could be carried through to the next step directly without purification. An analytically pure sample was prepared by purification with column chromatography (0→30% Et_2O/CH_2Cl_2→5%MeOH/30%Et_2O/65%CH_2Cl_2). **R_f** (2:1 DCM:Et_2O) = 0.23; **^{1}H NMR** (500 MHz, $CDCl_3$) δ = 6.52 (d, J = 3.4 Hz, 1H), 5.74 (d, J = 3.0 Hz, 1H), 4.13 (t, J = 5.1 Hz, 1H), 3.57 (br s, 1H), 1.76 (ddd, J = 16.2, 10.9, 5.5 Hz, 1H), 1.67 (ddd, J = 14.6, 10.1, 4.9 Hz, 2H), 1.50 – 1.13 (m, 19H), 0.92 (s, 9H), 0.90 – 0.82 (m, 3H), 0.10 (s, 3H), 0.08 (s, 3H); **^{13}C NMR** (125 MHz, $CDCl_3$) δ = 177.2, 73.6, 72.0, 37.6, 37.5, 35.2, 32.0, 29.8, 29.7, 29.5, 25.9, 25.8, 25.6, 24.3, 22.8, 18.2, 14.2, -4.7, -5.1; **$[\alpha]^{25}_D$** +12.1 (c = 1.36 in $CHCl_3$); **IR** (film) 3480 (N-H), 3297 (br O-H), 2927, 2856, 1693 (C=O), 1558, 1463, 1389, 1362, 1339, 1253, 1098, 836, 778, 723, 668; **HRMS** Accurate mass (ES^+): Found 374.3091, $C_{20}H_{43}NO_3Si$ ($M+H^+$) requires 374.3085.

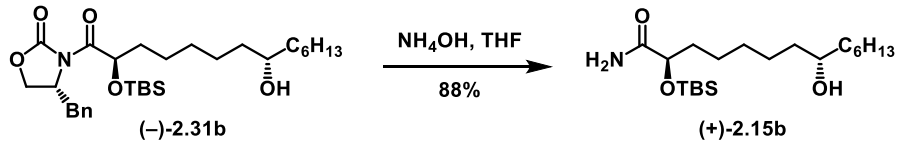

(2R,8S)-2-[(tert-butyldimethylsilyl)oxy]-8-hydroxytetradecanamide (+)-2.15b. Using the procedure given for the preparation of compound **(+)-2.15a**; compound **(–)-2.31b** (154 mg, 0.2885 mmol), THF (6 mL), and NH_4OH (3 mL) yielded the title compound as a clear oil (107 mg, contains *ca.* 7 % w/w oxazolidinone, 88% yield). **^{1}H NMR** (500 MHz, $CDCl_3$) δ = 6.52 (br s, 1H), 5.90 (br s, 1H), 4.13 (t, J = 5.0 Hz, 1H), 3.56 (br s, 1H), 1.80 – 1.71 (m, 1H), 1.71 – 1.61 (m, 1H), 1.50 – 1.15 (m, 19H), 0.92 (s, 9H), 0.87 (t, J = 5.8 Hz, 3H), 0.09 (s, 3H), 0.08 (s, 3H); **^{13}C NMR** (100 MHz, $CDCl_3$) δ = 177.3, 73.6, 72.0, 37.6, 37.5, 35.2, 32.0, 29.8, 29.7, 29.5, 25.9,

25.8, 25.7, 24.2, 22.8, 18.1, 14.2, -4.7, -5.1; **[α]$^{25}_{D}$** +14.9 (c = 0.96 in $CHCl_3$); **IR** (film) 3480 (N-H), 3297 (br O-H), 2927, 2856, 1683 (C=O), 1577, 1436, 1253, 1099, 836, 778, 730, 668, 599; **HRMS** Accurate mass (ES^+): Found 374.3084, $C_{20}H_{43}NO_3Si$ ($M+H^+$) requires 374.3085.

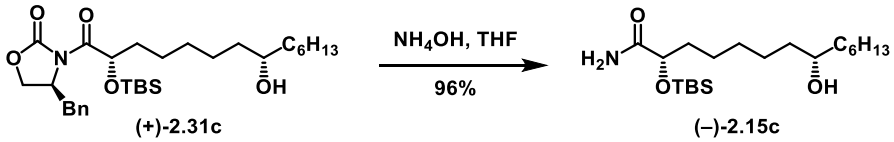

(2S,8S)-2-[(tert-butyldimethylsilyl)oxy]-8-hydroxytetradecanamide (–)-2.15c. Using the procedure given for the preparation of **(+)-2.15a**; compound **(+)-2.31c** (100 mg, 0.187 mmol), THF (3 mL), and NH_4OH (2 mL) yielded the title compound as a clear oil (76 mg, contains *ca.* 9 % w/w oxazolidinone, 96% yield). **^{1}H NMR** (400 MHz, $CDCl_3$) δ = 6.50 (br s, 1H), 6.41 (br s, 1H), 4.09 (t, J = 4.8 Hz, 1H), 3.53 (br s, 1H), 1.71 (dd, J = 10.2, 4.8 Hz, 1H), 1.69 – 1.57 (m, 1H), 1.47 – 1.16 (m, 19H), 0.89 (s, 9H), 0.85 (t, J = 6.4 Hz, 3H), 0.07 (s, 3H), 0.06 (s, 3H); **^{13}C NMR** (100 MHz, $CDCl_3$) δ = 177.5, 73.4, 71.9, 37.5, 37.4, 35.1, 31.9, 29.7, 29.5, 25.8, 25.7, 25.6, 24.2, 22.7, 18.1, 14.2, -4.8, -5.2; **[α]$^{25}_{D}$** –14.4 (c = 1.12 in $CHCl_3$); **IR** (film) 3480 (N-H), 3292 (br O-H), 2927, 2856, 1683 (C=O), 1582, 1463, 1389, 1361, 1339, 1253, 1098, 1005, 938, 835, 778, 755, 667, 577; **HRMS** Accurate mass (ES^+): Found 374.3078, $C_{20}H_{43}NO_3Si$ ($M+H^+$) requires 374.3085.

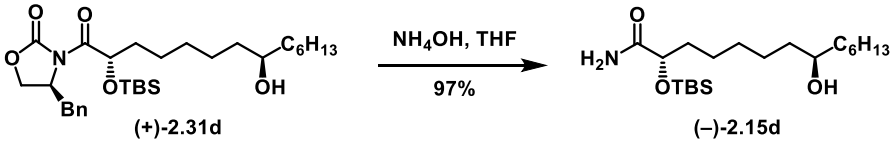

(2S,8R)-2-[(tert-butyldimethylsilyl)oxy]-8-hydroxytetradecanamide (–)-2.15d. Following the procedure given for the preparation of compound **(+)-2.15a**; compound **(+)-2.31d** (97 mg, 0.182 mmol), THF (3 mL), and NH_4OH (3 mL) yielded the title compound as a clear oil (76 mg, contains *ca.* 13 % w/w oxazolidinone, 97% yield). **^{1}H NMR** (500 MHz, $CDCl_3$) δ = 6.53 (br s, 1H), 5.37 (br s, 1H), 4.14 (t, J = 5.1 Hz, 1H), 3.57 (br s, 1H), 1.81 – 1.73 (m, 1H), 1.71 – 1.64 (m,

1H), 1.47 – 1.26 (m, 19H), 0.93 (s, 9H), 0.88 (t, J = 6.9 Hz, 3H), 0.11 (s, 3H), 0.09 (s, 3H).; **^{13}C NMR** (125 MHz, $CDCl_3$) δ = 177.4, 73.5, 71.9, 37.6, 37.4, 35.1, 31.9, 29.7, 29.5, 25.8, 25.7, 25.6, 24.2, 22.7, 18.1, 14.2, -4.7, -5.2; **$[\alpha]^{25}_D$** –14.8 (c = 1.05 in $CHCl_3$); **IR** (film) 3480 (N-H), 3292 (br O-H), 2927, 2856, 1683 (C=O), 1584, 1463, 1389, 1361, 1339, 1253, 1098, 1005, 938, 835, 778, 724, 668, 591; **HRMS** Accurate mass (ES^+): Found 374.3078, $C_{20}H_{43}NO_3Si$ ($M+H^+$) requires 374.3085.

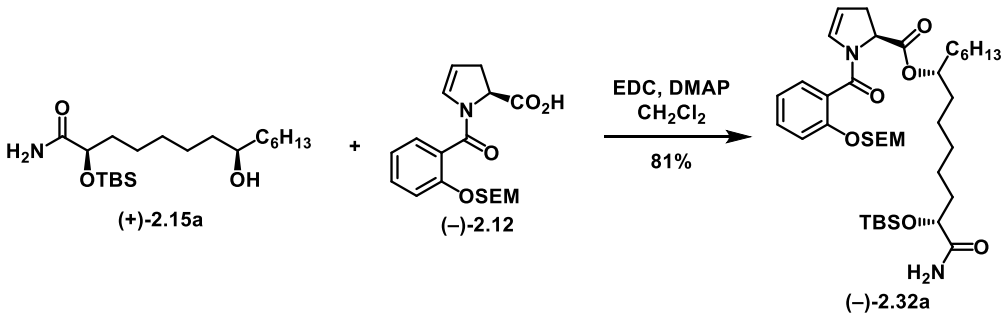

(1R,7R)-1-[(tert-butyldimethylsilyl)oxy]-1-carbamoyltridecan-7-yl(2S)-1-(2-{[2-(trimethylsilyl)ethoxy]methoxy}benzoyl)-2,3-dihydro-1H-pyrrole-2-carboxylate (–)-2.32a. To a solution of **(–)-2.12** (104.8 mg, 0.2882 mmol) in CH_2Cl_2 (8 mL) at 0 °C was added EDC (67 mg, 0.351 mmol), followed by DMAP (10.7 mg, 0.0878 mmol), then a solution of **(+)-2.15a** (74 mg containing 11% w/w oxazolidinone, corrected mass = 66 mg, 0.176 mmol) dissolved in CH_2Cl_2 (2 mL) was added dropwise. The solution was warmed to room temperature and stirred for 16 hours. The reaction was then poured into water and extracted with CH_2Cl_2 3x. The combined organic layers were washed with brine, dried over Na_2SO_4, filtered, concentrated, and purified by column chromatography, yielding the title compound as a yellow oil (102 mg, 81% yield). **R_f** (1:1 hexanes:EtOAc) = 0.39; **^{1}H NMR** (500 MHz, $CDCl_3$, mixture of conformers) δ 7.40 – 7.28 (m, 2H), 7.23 – 7.12 (m, 1H), 7.07 – 6.94 (m, 1H), 6.51 (br s, 1H), 6.15 (br s, 1H), 5.74 (br s, 1H), 5.22 (dd, J = 16.8, 7.0 Hz, 2H), 5.05 – 4.93 (m, 2H), 4.17 – 4.07 (m, 1H), 3.73 (t, J = 8.3 Hz, 2H), 3.16 – 3.07 (m, 1H), 2.66 (d, J = 17.0 Hz, 1H), 1.82 – 1.70 (m, 1H), 1.70 – 1.60 (m, 1H), 1.60 – 1.47 (m, 5H), 1.41 – 1.15 (m, 14H), 0.97 – 0.91 (m, 11H), 0.87 – 0.83 (m, 3H),

0.08 (s, 3H), 0.07 (s, 3H), -0.02 (s, 9H); **^{13}C NMR** (100 MHz, $CDCl_3$) δ = 176.9, 170.8, 165.0, 153.9, 131.2, 131.1, 129.0, 126.0, 122.0, 115.2, 108.4, 93.4, 75.5, 73.6, 66.6, 58.2, 35.1, 34.4, 34.1, 31.9, 29.5, 29.3, 25.9, 25.3, 25.1, 24.1, 22.7, 18.2, 14.2, -1.3, -4.7, -5.1; **$[\alpha]^{25}_D$** –17.7 (c = 0.78 in $CHCl_3$); **IR** (film) 3481 (N-H), 2927, 2857, 1739 (C=O), 1690 (C=O), 1651 (C=O), 1620, 1601, 1488, 1455, 1406, 1249, 1230, 1194, 1151, 1087, 990, 939, 824, 778, 754, 697, 666, 613; **HRMS** Accurate mass (ES^+): Found 719.4503, $C_{38}H_{66}N_2O_7Si_2$ ($M+H^+$) requires 719.4481.

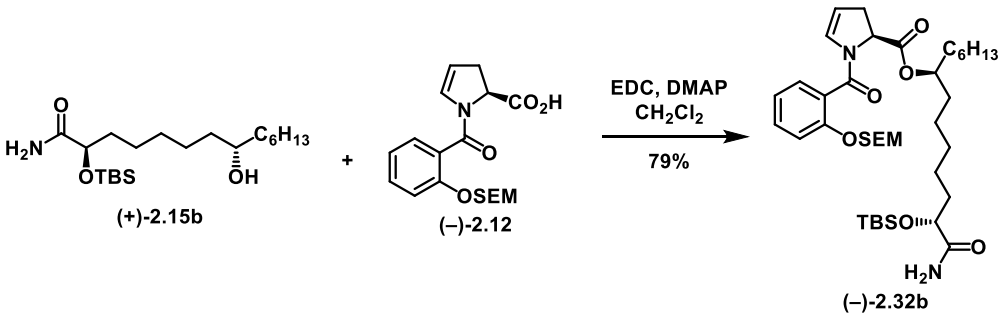

(1R,7S)-1-[(tert-butyldimethylsilyl)oxy]-1-carbamoyltridecan-7-yl(2S)-1-[1-(2-{[2-(trimethylsilyl)ethoxy]methoxy}phenyl)ethenyl]-2,3-dihydro-1H-pyrrole-2-carboxylate (–)-2.32b. Following the same procedure as **(–)-2.32a**; **(–)-2.12** (105 mg, 0.288 mmol) in CH_2Cl_2 (10 mL), EDC (65 mg, 0.388 mmol), DMAP (10 mg, 0.085 mmol), and **(+)-2.15b** (68 mg, containing 7% w/w oxazolidinone, corrected mass = 63 mg, 0.169 mmol) yielded the title compound as a yellow oil (85 mg, 79% yield). **^{1}H NMR** (400 MHz, $CDCl_3$) δ = 7.39 – 7.27 (m, 2H), 7.22 – 7.12 (m, 1H), 7.07 – 6.95 (m, 1H), 6.52 (d, J = 3.9 Hz, 1H), 6.16 (br s, 1H), 5.63 (br s, 1H), 5.22 (q, J = 7.1 Hz, 2H), 5.05 – 4.90 (m, 3H), 4.12 (t, J = 5.0 Hz, 1H), 3.79 – 3.69 (m, 2H), 3.19 – 3.05 (m, 1H), 2.73 – 2.61 (m, 1H), 1.82 – 1.70 (m, 1H), 1.70 – 1.62 (s, 1H), 1.62 – 1.50 (m, 5H), 1.34 – 1.03 (m, 14H), 0.96 – 0.89 (m, 11H), 0.89 – 0.83 (m, 3H), 0.09 (s, 3H), 0.08 (s, 3H), -0.02 (s, 9H); **^{13}C NMR** (100 MHz, $CDCl_3$) δ = 177.0, 170.8, 165.0, 153.8, 131.2, 131.0, 129.0, 126.0, 122.0, 115.2, 108.3, 93.3, 75.5, 73.5, 66.6, 58.2, 35.2, 34.4, 34.1, 34.0, 31.8, 29.5, 29.3, 25.8, 25.2, 24.1, 22.7, 18.1, 14.2, -1.3, -4.7, -5.1; **$[\alpha]^{25}_D$** –28.9 (c = 1.0 in $CHCl_3$); **IR** (film) 3481 (N-H), 2927, 2857, 1744 (C=O), 1690 (C=O), 1652 (C=O), 1620, 1601, 1488, 1455, 1406, 1249,

1230, 1194, 1151, 1087, 990, 939, 824, 778, 754, 697, 666, 613; **HRMS** Accurate mass (ES^+): Found 719.4478, $C_{38}H_{66}N_2O_7Si_2$ ($M+H^+$) requires 719.4481.

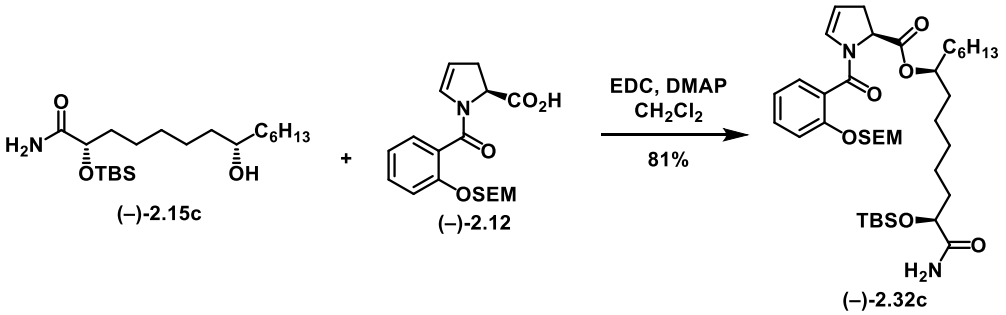

(1S,7S)-1-[(tert-butyldimethylsilyl)oxy]-1-carbamoyltridecan-7-yl(2S)-1-(2-{[2-(trimethylsilyl)ethoxy]methoxy}benzoyl)-2,3-dihydro-1H-pyrrole-2-carboxylate (–)-2.32c. Following the same procedure as **(–)-2.32a**; **(–)-2.12** (75 mg, 0.206 mmol) in CH_2Cl_2 (10 mL), EDC (43 mg, 0.223 mmol), DMAP (11 mg, 0.086 mmol), and **(–)-2.15c** (70 mg, containing 9% w/w oxazolidinone, corrected mass = 64 mg, 0.171 mmol) yielded the title compound as a yellow oil (100 mg, 81% yield). **^{1}H NMR** (500 MHz, $CDCl_3$) δ = 7.40 – 7.29 (m, 2H), 7.23 – 7.15 (m, 1H), 7.08 – 6.98 (m, 1H), 6.52 (br s, 1H), 6.19 – 6.14 (m, 1H), 5.34 – 5.28 (m, 1H), 5.27 – 5.19 (m, 2H), 5.04 – 4.92 (m, 2H), 4.17 – 4.07 (m, 1H), 3.78 – 3.71 (m, 2H), 3.16 – 3.08 (m, 1H), 2.71 – 2.62 (m, 1H), 1.80 – 1.71 (m, 1H), 1.71 – 1.61 (m, 1H), 1.61 – 1.50 (m, 5H), 1.43 – 1.15 (m, 14H), 0.97 – 0.89 (m, 11H), 0.86 (t, J = 6.9 Hz, 3H), 0.09 (s, 3H), 0.09 (s, 3H), -0.01 (s, 9H); **^{13}C NMR** (125 MHz, $CDCl_3$) δ = 177.0, 170.8, 165.0, 153.8, 131.2, 131.0, 129.0, 126.0, 122.0, 115.2, 108.3, 93.3, 75.4, 73.5, 66.6, 58.2, 35.2, 34.4, 34.2, 34.1, 31.8, 29.5, 29.3, 25.8, 25.3, 25.2, 24.2, 22.7, 18.1, 18.1, 14.2, -1.3, -4.7, -5.1; **$[\alpha]^{25}_D$** –42.6 (c = 0.98 in $CHCl_3$); **IR** (film) 3481 (N-H), 2928, 2857, 1734 (C=O), 1689 (C=O), 1652 (C=O), 1620, 1601, 1488, 1455, 1406, 1249, 1230, 1194, 1151, 1087, 990, 939, 824, 778, 753, 697, 676, 606 ; **HRMS** Accurate mass (ES^+): Found 719.4503, $C_{38}H_{66}N_2O_7Si_2$ ($M+H^+$) requires 719.4481.

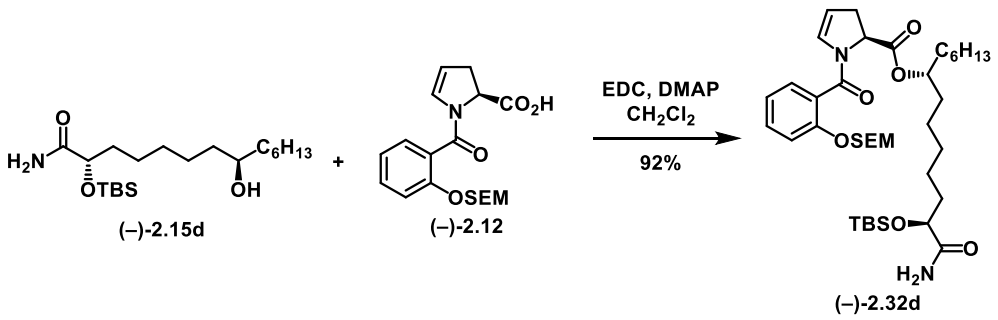

(1S,7R)-1-[(tert-butyldimethylsilyl)oxy]-1-carbamoyltridecan-7-yl(2S)-1-(2-{[2-(trimethylsilyl)ethoxy]methoxy}benzoyl)-2,3-dihydro-1H-pyrrole-2-carboxylate (–)-2.32d. Following the same procedure as **(–)-2.32a**; **(–)-2.12** (138 mg, 0.378 mmol) in CH_2Cl_2 (10 mL), EDC (65 mg, 0.337 mmol), DMAP (10 mg, 0.084 mmol), and **(–)-2.15d** (63 mg, 0.168 mmol) yielded the title compound as a yellow oil (111 mg, 92% yield). **^{1}H NMR** (500 MHz, $CDCl_3$) δ = 7.39 – 7.30 (m, 2H), 7.23 – 7.15 (m, 1H), 7.07 – 7.00 (m, 1H), 6.53 (d, J = 4.8 Hz, 1H), 6.16 (dt, J = 4.3, 2.1 Hz, 1H), 5.38 – 5.29 (m, 1H), 5.27 – 5.18 (m, 2H), 5.05 – 4.90 (m, 2H), 4.17 – 4.09 (m, 1H), 3.78 – 3.70 (m, 1H), 3.18 – 3.06 (m, 1H), 2.74 – 2.63 (m, 1H), 1.81 – 1.71 (m, 1H), 1.69 – 1.63 (m, 1H), 1.62 – 1.51 (m, 5H), 1.42 – 1.18 (m, 14H), 0.96 – 0.93 (m, 2H), 0.91 (s, 9H), 0.86 (t, J = 6.8 Hz, 3H), 0.09 (s, 3H), 0.07 (s, 3H), -0.01 (s, 9H); **^{13}C NMR** (125 MHz, $CDCl_3$) δ = 177.0, 170.8, 165.0, 153.8, 131.2, 131.1, 129.0, 126.0, 122.0, 115.2, 108.3, 93.4, 75.5, 73.6, 66.6, 58.2, 35.2, 34.4, 34.1, 34.1, 31.9, 29.5, 29.3, 25.9, 25.3, 25.1, 24.1, 22.7, 18.2, 18.1, 14.2, -1.3, -4.7, -5.1; **$[\alpha]^{25}_D$** –44.0 (c = 1.21 in $CHCl_3$); **IR** (film) 3481 (N-H), 2927, 2857, 1739 (C=O), 1690 (C=O), 1651 (C=O), 1620, 1601, 1488, 1455, 1406, 1249, 1230, 1194, 1151, 1087, 990, 939, 824, 778, 754, 697, 666, 613; **HRMS** Accurate mass (ES^+): Found 719.4492, $C_{38}H_{66}N_2O_7Si_2$ ($M+H^+$) requires 719.4481.

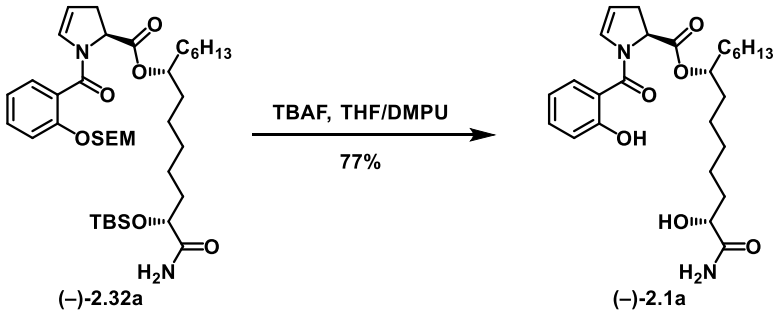

(1R,7R)-1-carbamoyl-1-hydroxytridecan-7-yl(2S)-1-(2-hydroxybenzoyl)-2,3-dihydro-1H-pyrrole-2-carboxylate (–)-2.1a. To a solution of compound **(–)-2.32a** (25.2 mg, 0.0350 mmol) dissolved in DMPU (0.7 mL, dried over 3Å molecular sieves for at least 24 hours prior to use) was added TBAF (0.7 mL 1M solution in THF, 0.70 mmol, dried over 3Å molecular sieves for 1-3 days) dropwise. The reaction was stirred at room temperature until LC-MS analysis (non-polar phase 95% acetonitrile/5% water/0.1% formic acid, 15 minute gradient 40→90% non-polar phase, product retention time = 5.6 minutes, SEM-protected/TBS-deprotected intermediate retention time = 12.6 minutes) indicated consumption of the mono-protected SEM ether intermediate (TBS deprotection occurred in <1 minute by TLC analysis), which was typically complete in 30 minutes. After completion, the reaction was quenched with sat. NH_4Cl solution (6 mL) and water (6 mL), and extracted with Et_2O (12 mL). The organic layer was separated and washed 5x with 1M NH_4Cl solution (10 mL), water, and brine. The organic layer was dried over Na_2SO_4, filtered, concentrated, and purified by column chromatography (0→3% MeOH/CH_2Cl_2) to yield the title compound as a white translucent oil (13 mg, 77% yield). $\mathbf{R_f}$ (19:1 EtOAc:MeOH) = 0.44; **^{1}H NMR** (500 MHz, $CDCl_3$) δ = 9.53 (s, 1H), 7.47 – 7.31 (m, 2H), 6.98 (d, J = 8.1 Hz, 1H), 6.90 (t, J = 7.5 Hz, 1H), 6.71 (s, 1H), 6.62 (s, 1H), 5.46 (s, 1H), 5.35 – 5.24 (m, 1H), 5.01 (dd, J = 11.1, 4.6 Hz, 2H), 4.09 (s, 1H), 3.48 (s, 1H), 3.21 – 3.08 (m, 1H), 2.69 (d, J = 17.0 Hz, 1H), 1.80 (m, 1H), 1.76 – 1.48 (m, 6H), 1.48 – 1.33 (m, 5H), 1.32 – 1.17 (m, 21H), 0.87 (t, J = 6.9 Hz, 3H); **^{13}C NMR** (100 MHz, $CDCl_3$) δ = 177.0, 171.3, 167.4, 158.0, 133.5, 130.8, 128.3, 119.4, 118.0, 117.8, 111.1, 76.0, 71.4, 59.3, 34.5, 34.3, 34.2, 33.7, 31.8, 29.2, 28.3, 25.5, 24.8,

24.6, 22.7, 14.2; **[α]$^{25}_{D}$** –32.2 (c = 1.06 in $CHCl_3$); **IR** (film) 3338 (br O-H), 2926, 2857, 1733 (C=O), 1667 (C=O), 1592 (C=O), 1457, 1429, 1376, 1294, 1252, 1197, 1152, 1098, 1017, 945, 859, 817, 761, 665, 614; **HRMS** Accurate mass (ES^+): Found 475.2806, $C_{26}H_{38}N_2O_6$ ($M+H^+$) requires 475.2803.

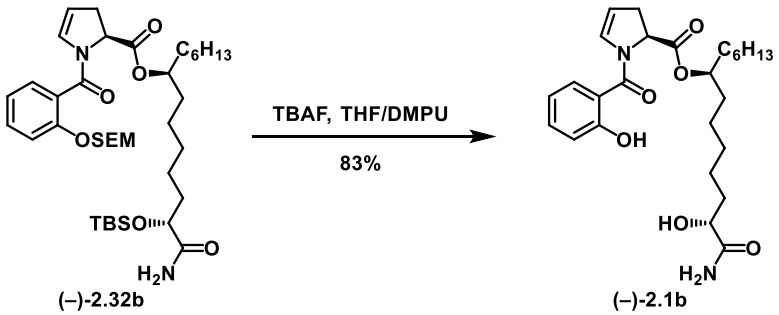

(1R,7S)-1-carbamoyl-1-hydroxytridecan-7-yl(2S)-1-(2-hydroxybenzoyl)-2,3-dihydro-1H-pyrrole-2-carboxylate (–)-2.1b. Following the same procedure as **(–)-2.1a**; **(–)-2.32b** (16 mg, 0.023 mmol), DMPU (0.46 mL), and TBAF (0.46 mL 1M solution in THF, 0.46 mmol) yielded the title compound as a white translucent oil (9 mg, 83% yield). **^{1}H NMR** (500 MHz, $CDCl_3$) δ = 9.94 (s, 1H), 7.45 – 7.33 (m, 2H), 7.00 (d, J = 8.0 Hz, 1H), 6.90 (t, J = 7.5 Hz, 1H), 6.80 (s, 1H), 6.53 (s, 1H), 5.54 (s, 1H), 5.29 (d, J = 4.1 Hz, 1H), 5.05 – 4.99 (m, 1H), 4.99 – 4.90 (m, 1H), 4.09 (d, J = 4.5 Hz, 1H), 3.18 – 3.09 (m, 1H), 3.06 (s, 1H), 2.70 (d, J = 17.1 Hz, 1H), 1.81 – 1.72 (m, 1H), 1.68 – 1.46 (m, 9H), 1.37 (s, 4H), 1.35 – 1.17 (m, 18H), 0.87 (t, J = 6.9 Hz, 3H); **^{13}C NMR** (125 MHz, $CDCl_3$) δ = 177.0, 170.9, 167.5, 159.0, 133.7, 130.9, 128.5, 119.2, 118.1, 117.0, 111.0, 76.0, 71.7, 59.8, 34.5, 34.3, 34.0, 33.8, 31.8, 29.2, 28.8, 25.2, 25.0, 24.7, 22.7, 14.2; **[α]$^{20}_{D}$** –29.1 (c = 1.00 in $CHCl_3$); **IR** (film) 3339 (br O-H), 2927, 2857, 1733 (C=O), 1667 (C=O), 1592 (C=O), 1457, 1429, 1376, 1294, 1252, 1197, 1152, 1098, 1017, 945, 859, 817, 761, 665, 614; **HRMS** Accurate mass (ES^+): Found 475.2806, $C_{26}H_{38}N_2O_6$ ($M+H^+$) requires 475.2803.

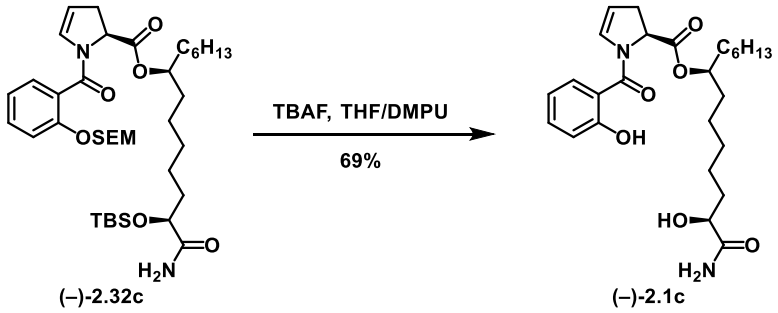

(1S,7S)-1-carbamoyl-1-hydroxytridecan-7-yl(2S)-1-(2-hydroxybenzoyl)-2,3-dihydro-1H-pyrrole-2-carboxylate (–)-2.1c. Following the same procedure as **(–)-2.1a**; **(–)-2.32c** (63 mg, 0.087 mmol), DMPU (1.74 mL), and TBAF (1.74 mL 1M solution in THF, 1.74 mmol) yielded the title compound as a white translucent oil (28 mg, 69% yield). **^{1}H NMR** (500 MHz, $CDCl_3$) δ = 9.87 (s, 1H), 7.44 – 7.33 (m, 2H), 6.99 (d, J = 8.2 Hz, 1H), 6.89 (t, J = 7.5 Hz, 1H), 6.77 (s, 1H), 6.65 (s, 1H), 5.79 (s, 1H), 5.32 – 5.20 (m, 1H), 4.99 (dd, J = 11.2, 4.8 Hz, 1H), 4.94 (s, 1H), 4.07 (d, J = 4.1 Hz, 1H), 3.43 (s, 1H), 3.21 – 3.04 (m, 1H), 2.69 (d, J = 17.1 Hz, 1H), 1.80 – 1.69 (m, 1H), 1.64 – 1.43 (m, 6H), 1.43 – 1.09 (m, 17H), 0.86 (t, J = 6.8 Hz, 3H); **^{13}C NMR** (125 MHz, $CDCl_3$) δ = 177.2, 170.9, 167.5, 158.9, 133.6, 130.9, 128.5, 119.2, 118.0, 117.2, 111.0, 76.0, 71.6, 59.8, 34.5, 34.2, 33.9, 33.8, 31.8, 29.2, 28.8, 25.2, 25.0, 24.7, 22.7, 14.2; **$[\alpha]^{20}_{D}$** –41.5 (c = 0.26 in $CHCl_3$); **IR** (film) 3339 (br O-H), 2927, 2857, 1733 (C=O), 1667 (C=O), 1592 (C=O), 1457, 1429, 1376, 1294, 1252, 1197, 1152, 1098, 1017, 945, 859, 817, 761, 665, 614; **HRMS** Accurate mass (ES^+): Found 475.2815, $C_{26}H_{38}N_2O_6$ ($M+H^+$) requires 475.2803.

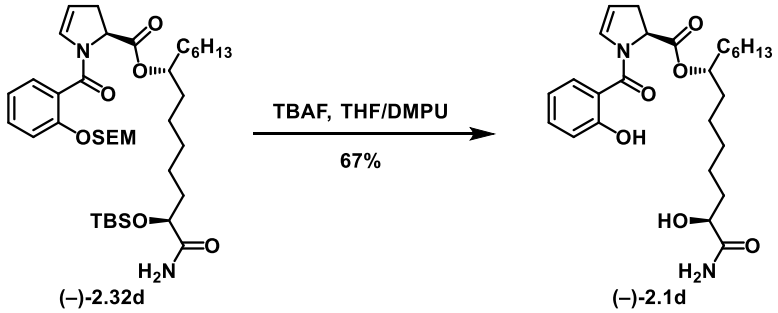

(1S,7R)-1-carbamoyl-1-hydroxytridecan-7-yl(2S)-1-(2-hydroxybenzoyl)-2,3-dihydro-1H-pyrrole-2-carboxylate (–)-2.1d. Following the same procedure as **(–)-2.1a**, **(–)-2.32d** (11 mg, 0.015 mmol), DMPU (0.61 mL), and TBAF (0.30 mL 1M solution in THF, 0.30 mmol) yielded the title compound as a white translucent oil (5 mg, 67% yield). **^{1}H NMR** (500 MHz, $CDCl_3$) δ = 9.54 (s, 1H), 7.37 (dd, J = 16.8, 7.7 Hz, 1H), 6.98 (d, J = 8.2 Hz, 1H), 6.90 (t, J = 7.5 Hz, 1H), 6.71 (s, 1H), 6.61 (s, 1H), 5.61 (s, 1H), 5.30 – 5.24 (m, 1H), 5.00 (dd, J = 11.2, 4.6 Hz, 1H), 4.08 (d, J = 4.2 Hz, 1H), 3.54 – 3.33 (m, 1H), 3.19 – 3.08 (m, 1H), 2.69 (d, J = 17.0 Hz, 1H), 1.89 – 1.72 (m, 1H), 1.69 – 1.49 (m, 6H), 1.47 – 1.16 (m, 18H), 0.86 (t, J = 7.0 Hz, 1H); **^{13}C NMR** (100 MHz, $CDCl_3$) δ = 177.3, 171.3, 167.4, 158.1, 133.5, 130.9, 128.4, 119.4, 118.0, 117.8, 111.0, 76.2, 71.7, 59.4, 34.5, 34.3, 34.2, 33.7, 31.8, 29.2, 28.6, 25.5, 24.8, 24.7, 22.7, 14.2; **$[\alpha]^{20}_{D}$** –65.1 (c = 1.29 in $CHCl_3$); **IR** (film) 3339 (br O-H), 2927, 2857, 1733 (C=O), 1667 (C=O), 1592 (C=O), 1457, 1429, 1376, 1294, 1252, 1197, 1152, 1098, 1017, 945, 859, 817, 761, 665, 614; **HRMS** Accurate mass (ES^+): Found 475.2806, $C_{26}H_{38}N_2O_6$ ($M+H^+$) requires 475.2803.

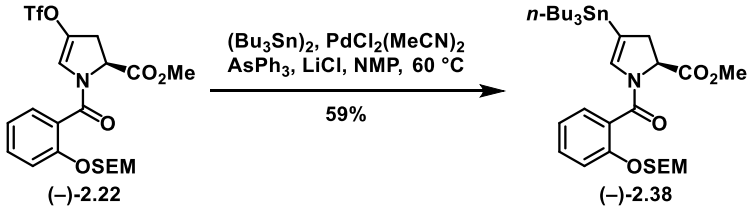

Methyl (S)-4-(tributylstannyl)-1-(2-((2-(trimethylsilyl)ethoxy)methoxy)benzoyl)-2,3-dihydro-1H-pyrrole-2-carboxylate (–)-2.38. To a solution of triflate **(–)-2.22** (559 mg, 1.064 mmol) in NMP (6 mL) was added $PdCl_2(MeCN)_2$ (14 mg, 0.053 mmol), $AsPh_3$ (65 mg, 0.213 mmol), LiCl (135 mg, 3.191 mmol), and bis(tributyltin) (0.56 mL, 1.117 mmol). The solution was heated to 60 °C for 1 hour, after which time the reaction turned from orange to brown/black. The reaction was cooled to room temperature, quenched with 1M aq. KF, and extracted 2x with Et_2O. The combined organic layers were washed with 1M aq. KF, and brine 2x, then dried over $MgSO_4$, filtered, concentrated and purified by column chromatography, yielding the title

compound as a yellow oil (416 mg, 59% yield). **^{1}H NMR** (400 MHz, $CDCl_3$) δ 7.41 – 7.35 (m, 2H), 7.22 (dd, J = 8.8, 0.9 Hz, 1H), 7.09 – 7.03 (m, 1H), 5.97 (t, J = 2.1 Hz, 1H), 5.26 – 5.19 (m, 2H), 4.96 (dd, J = 11.4, 5.0 Hz, 1H), 3.84 – 3.72 (m, 5H), 3.15 (ddd, J = 16.8, 11.3, 2.3 Hz, 1H), 2.76 (ddd, J = 16.8, 5.0, 1.9 Hz, 1H), 1.52 – 1.38 (m, 6H), 1.33 – 1.20 (m, 8H), 0.98 – 0.82 (m, 18H), 0.00 (s, 9H); **^{13}C NMR** (125 MHz, $CDCl_3$) δ 171.83, 164.19, 154.01, 135.61, 131.09, 128.90, 126.25, 121.93, 118.43, 93.64, 66.39, 58.29, 52.28, 40.55, 29.08, 29.00, 27.24, 27.16, 17.92, 13.67, 13.63, 9.52 (J = 309 Hz, ^{13}C-^{117}Sn; J = 355 Hz, ^{13}C-^{119}Sn), -1.36; **$[\alpha]^{25}_D$** –41.5 (c = 1.63 in $CHCl_3$); **IR** (film) 2953, 2923, 2869, 2852, 1754 (C=O), 1651 (C=O), 1584, 1488, 1454, 1399, 1283, 1247, 1228, 1198, 1176, 1152, 1087, 1019, 989, 917, 856, 834, 753, 731, 692, 658, 599, 561; **HRMS** Accurate mass (ES^+): Found 668.2798, $C_{31}H_{54}NO_5SiSn$ ($M+H^+$) requires 668.2793.

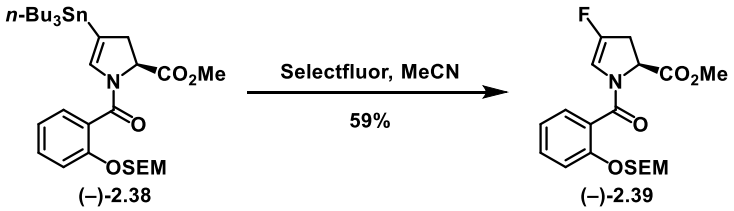

Methyl (S)-4-fluoro-1-(2-((2-(trimethylsilyl)ethoxy)methoxy)benzoyl)-2,3-dihydro-1H-pyrrole-2-carboxylate (–)-2.39. To a solution of stannane **(–)-2.38** (400 mg, 0.6001 mmol) in MeCN (5 mL) was added Selectfluor® (234 mg, 0.6601 mmol). After 5 minutes, solids crashed out and the solution was filtered into water. The layers were separated and the aqueous layer was extracted with CH_2Cl_2 2x. The combined organic layers were washed with brine, dried over $MgSO_4$, filtered, concentrated, and purified by column chromatography, yielding the title compound as a clear oil (140 mg, 59% yield). **^{1}H NMR** (500 MHz, $CDCl_3$) δ 7.40 – 7.34 (m, 2H), 7.21 (t, J = 7.2 Hz, 1H), 7.05 (td, J = 7.5, 0.9 Hz, 1H), 6.06 (dd, J = 4.1, 2.2 Hz, 1H), 5.24 (q, J = 7.1 Hz, 2H), 5.05 (dd, J = 11.7, 4.7 Hz, 1H), 3.83 (s, 3H), 3.79 – 3.73 (m, 2H), 3.32 (dddd, J = 16.4, 11.8, 4.3, 2.3 Hz, 1H), 2.89 – 2.83 (m, 1H), 0.99 – 0.91 (m, 2H), -0.01 (s, 9H); **^{13}C NMR**

(125 MHz, $CDCl_3$) δ 170.10, 165.21, 153.60, 151.05, 148.92, 131.45, 128.93, 124.94, 121.95, 115.07, 111.54 (d, J = 30 Hz ^{13}C-^{19}F), 93.20, 66.66, 56.30, 56.26, 52.70, 32.07, 31.91, 18.04, -1.47; **[α]$^{25}_D$** –56.1 (c = 1.08 in $CHCl_3$; **IR** (film) 2953, 2924, 1749 (C=O), 1644 (C=O), 1600, 1488, 1456, 1417, 1356, 1229, 1306, 1247, 1231, 1201, 1179, 1144, 1086, 1028, 982, 934, 914, 857, 834, 754, 693, 658, 577; **HRMS** Accurate mass (ES^+): Found 418.1427, $C_{19}H_{26}FNO_5SiNa$ ($M+Na^+$) requires 418.1462.

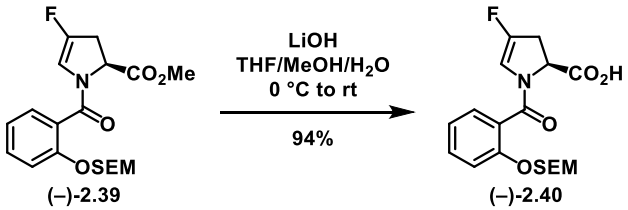

(S)-4-fluoro-1-(2-((2-(trimethylsilyl)ethoxy)methoxy)benzoyl)-2,3-dihydro-1H-pyrrole-2-carboxylic acid (–)-2.40. To a solution of methyl ester **(–)-2.39** (128 mg, 0.324 mmol) in 3:1:1 THF:MeOH:H_2O (3 mL) was added LiOH•H_2O (14 mg) dissolved in water (0.5 mL) at 0 °C. The reaction was stirred for 15 minutes then warmed to room temperature and stirred for 2 hours. The reaction was acidified (pH 5-6) with 5% aq. AcOH, and extracted with CH_2Cl_2 3x. The combined organic layers were washed with brine, dried over $MgSO_4$, filtered, concentrated and purified by column chromatography (0 → 5% MeOH/0.1% AcOH/CH_2Cl_2), yielding the title compound as a clear oil (116 mg, 94% yield). *Note:* While the acids in this study prepared by ester hydrolysis generally did not require chromatography, this one required purification for acceptable yields in the next step. **R_f** (10% MeOH/0.1% AcOH/CH_2Cl_2) = 0.29; **^{1}H NMR** (400 MHz, $CDCl_3$) δ 7.47 – 7.42 (m, 1H), 7.36 (dd, J = 7.5, 1.5 Hz, 1H), 7.24 (d, J = 8.5 Hz, 1H), 7.09 (td, J = 7.5, 0.7 Hz, 1H), 5.96 (d, J = 1.9 Hz, 1H), 5.28 – 5.20 (m, 3H), 3.76 – 3.70 (m, 2H), 3.62 – 3.54 (m, 1H), 3.27 – 3.14 (m, 1H), 0.97 – 0.91 (m, 2H), 0.00 (s, 9H); **^{13}C NMR** (100 MHz, $CDCl_3$) δ 171.19, 167.47, 153.70, 153.26, 150.58, 132.17, 129.05, 123.85, 122.08, 115.05, 110.80 (d, J = 31 Hz, ^{13}C-^{19}F), 93.26, 66.93, 57.71, 18.13, -1.39; **[α]$^{25}_D$** –62.7 (c = 0.72 in $CHCl_3$); **IR** (film) 2954, 2923, 2853,

1742 (C=O), 1600 (C=O), 1458, 1425, 1354, 1315, 1248, 1231, 1144, 1086, 983, 916, 857, 834, 753, 693, 658; **HRMS** Accurate mass (ES^+): Found 404.1291, $C_{18}H_{24}FNO_5SiNa$ ($M+Na^+$) requires 404.1305.

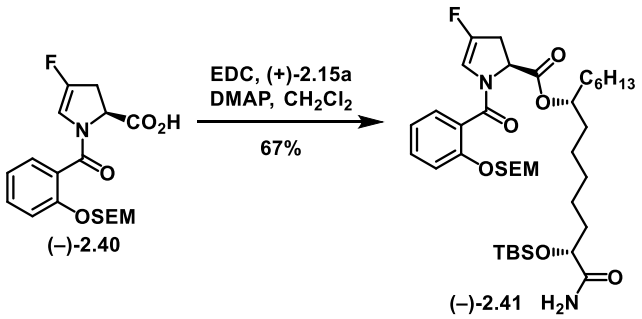

(7R,13R)-14-amino-13-((tert-butyldimethylsilyl)oxy)-14-oxotetradecan-7-yl (S)-4-fluoro-1-(2-((2-(trimethylsilyl)ethoxy)methoxy)benzoyl)-2,3-dihydro-1H-pyrrole-2-carboxylate (–)-2.41. Acid **(–)-2.40** (39 mg, 0.102 mmol) was dissolved in CH_2Cl_2 (0.5 mL) and cooled to 0°C and EDC (28 mg, 0.146 mmol) was added. A solution of alcohol **(+)-2.15a** (27 mg, 0.073 mmol) and DMAP (4 mg, 0.036 mmol) in CH_2Cl_2 (0.5 mL) was added to the first solution, and allowed to stir overnight. The resulting mixture was poured into water and extracted with CH_2Cl_2 3x. The combined organic layers were washed with brine, dried over $MgSO_4$, concentrated, and purified by column chromatography (0 → 30% Et_2O/CH_2Cl_2), yielding the title compound as a clear oil (36 mg, 67% yield). $\mathbf{R_f}$ (2:1 CH_2Cl_2:Et_2O) = 0.60; **^{1}H NMR** (400 MHz, $CDCl_3$) δ 7.40 – 7.30 (m, 2H), 7.20 (d, J = 8.2 Hz, 1H), 7.04 (t, J = 7.1 Hz, 1H), 6.57 – 6.48 (m, 1H), 6.05 (d, J = 1.8 Hz, 1H), 5.57 – 5.43 (m, 1H), 5.24 (q, J = 7.1 Hz, 2H), 5.08 – 4.91 (m, 2H), 4.13 (t, J = 5.1 Hz, 1H), 3.80 – 3.71 (m, 2H), 3.38 – 3.27 (m, 1H), 2.85 – 2.75 (m, 1H), 1.82 – 1.70 (m, 1H), 1.69 – 1.50 (m, 6H), 1.41 – 1.19 (m, 20H), 0.97 – 0.89 (m, 12H), 0.89 – 0.85 (m, 3H), 0.13 – 0.06 (m, 6H), -0.01 (s, 9H); **^{13}C NMR** (125 MHz, $CDCl_3$) δ 177.10, 169.48, 165.13, 153.75, 151.09, 148.97, 131.45, 129.02, 125.18, 122.02, 115.20, 111.72 (d, J = 31 Hz, ^{13}C-^{19}F), 93.33, 76.00, 73.52, 66.76, 56.71, 35.16, 35.06, 34.00, 33.95, 32.39, 32.23, 31.81, 29.80, 29.44, 29.27, 25.84, 25.31, 25.19, 25.00, 24.14, 24.07, 22.68, 18.17, 18.11, 14.16, -1.30, -1.35, -4.74, -5.16; $\mathbf{[\alpha]^{25}_D}$ –12.5 (c =

1.18 in $CHCl_3$); **IR** (film) 3480, 2951, 2927, 2856, 2242, 1742 (C=O), 1688 (C=O), 1645 (C=O), 1601, 1488, 1456, 1419, 1353, 1249, 1189, 1142, 1088, 988, 916, 835, 778, 754, 730, 659, 577; **HRMS** Accurate mass (ES^+): Found 759.4182, $C_{38}H_{65}FN_2O_7Si_2Na$ ($M+Na^+$) requires 759.4212.

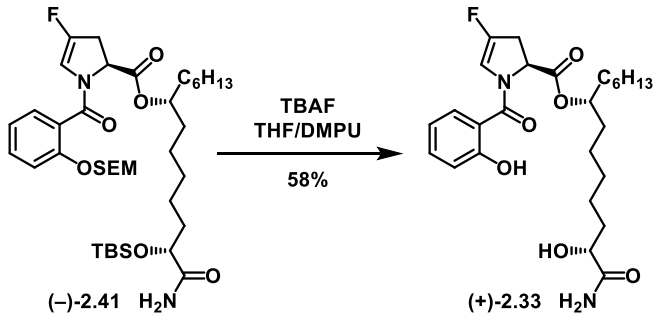

(7R,13R)-14-amino-13-hydroxy-14-oxotetradecan-7-yl (S)-4-fluoro-1-(2-hydroxybenzoyl)-2,3-dihydro-1H-pyrrole-2-carboxylate (+)-2.33. Silyl ether **(–)-S17** (21 mg, 0.029 mmol) was dissolved in DMPU (0.58 mL, dried over 3Å molecular sieves), and TBAF (1M solution in THF, 0.58 mL, 0.58 mmol, dried over 3Å molecular sieves for 1 - 5 days) was added dropwise. After 30 minutes, the reaction was quenched with sat. NH_4Cl. The mixture was extracted with Et_2O 5x, and the combined organic layers were washed with aq. 1M NH_4Cl 5x followed by brine, dried over Na_2SO_4, concentrated, and purified by column chromatography (0 → 5% MeOH/CH_2Cl_2), yielding the title compound as a clear oil (8 mg, 58% yield). **^{1}H NMR** (500 MHz, $CDCl_3$) δ 9.67 (br d, 1H), 7.41 – 7.33 (m, 2H), 7.02 – 6.96 (m, 1H), 6.91 (t, J = 7.6 Hz, 1H), 6.70 (d, J = 38.0 Hz, 1H), 6.55 (d, J = 28.6 Hz, 1H), 5.49 (d, J = 44.7 Hz, 1H), 5.07 – 4.92 (m, 2H), 4.09 (dd, J = 7.9, 3.5 Hz, 1H), 3.35 (t, J = 14.0 Hz, 1H), 3.03 (br s, 1H), 2.88 – 2.80 (m, 1H), 1.84 – 1.72 (m, 1H), 1.72 – 1.50 (m, 6H), 1.50 – 1.18 (m, 14H), 0.87 (t, J = 7.0 Hz, 3H); **^{13}C NMR** (125 MHz, $CDCl_3$) δ 176.96, 176.73, 169.87, 169.56, 167.43, 159.01, 158.10, 152.93, 152.82, 150.67, 133.80, 133.63, 127.97, 119.49, 119.28, 118.22, 118.13, 117.08, 116.43, 112.12, 111.87, 76.58, 71.68, 71.48, 58.34, 57.83, 34.53, 34.45, 34.37, 34.14, 33.86, 31.82, 29.21, 28.81, 28.43, 25.52, 25.27, 24.95, 24.84, 24.61, 22.68, 14.19; **$[\alpha]^{25}_D$** +12.0 (c = 0.45 in $CHCl_3$); **IR** (film) 3308 (br, O-H), 2929, 2858, 1734 (C=O), 1669 (C=O), 1653, 1623, 1594, 1521, 1457, 1436, 1354, 1337,

1300, 1192, 1142, 1097, 1037, 1004, 919, 859, 804, 755, 655; **HRMS** Accurate mass (ES^+): Found 493.2738, $C_{26}H_{38}FN_2O_6$ ($M+H^+$) requires 493.2714.

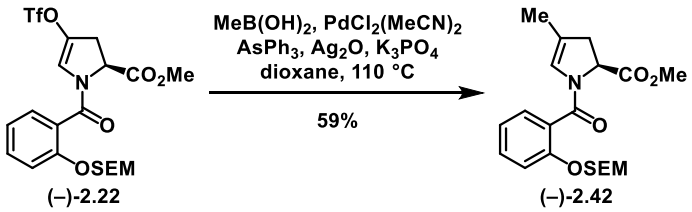

Methyl (S)-4-methyl-1-(2-((2-(trimethylsilyl)ethoxy)methoxy)benzoyl)-2,3-dihydro-1H-pyrrole-2-carboxylate (–)-2.42. Triflate **(–)-2.22** (75 mg, 0.143 mmol) was dissolved in dioxane (1.5 mL), and triphenylarsine (18 mg, 0.057 mmol), methylboronic acid (30 mg, 0.501 mmol), silver oxide (133 mg, 0.572 mmol) and K_3PO_4 (182 mg, 0.858 mmol) were added, and the reaction flask was covered in foil. The flask was vacuumed and back-filled with argon 3x, then $PdCl_2(MeCN)_2$ (4 mg, 0.014 mmol) was added, and the reaction was heated to 110 °C. Upon heating, the reaction turned from green to dark red, and TLC analysis indicated the starting material was consumed. The reaction was filtered through Celite, concentrated, and purified by column chromatography, yielding the title compound as an orange oil (39 mg, 71% yield). **^{1}H NMR** (400 MHz, $CDCl_3$, mixture of rotamers/conformers) δ 7.39 – 7.28 (m, 2H), 7.20 (d, J = 8.1 Hz, 0.91H), 7.15 (d, J = 7.9 Hz, 0.15H), 7.04 (td, J = 7.5, 1.0 Hz, 0.92H), 6.99 (td, J = 7.5, 1.0 Hz, 0.14H), 5.88 (dd, J = 3.5, 1.7 Hz, 1H), 5.26 – 5.19 (m, 2H), 5.01 (dd, J = 11.6, 4.9 Hz, 1H), 3.80 (s, 3H), 3.78 – 3.71 (m, 2H), 3.06 – 2.96 (m, 1H), 2.61 – 2.53 (m, 1H), 1.64 (d, J = 1.4 Hz, 3H), 0.98 – 0.89 (m, 2H), 0.01 – -0.03 (m, 9H); **^{13}C NMR** (100 MHz, $CDCl_3$) δ 171.70, 164.44, 153.83, 131.11, 128.90, 126.23, 125.30, 122.04, 119.42, 115.48, 93.48, 66.58, 58.32, 52.59, 38.23, 18.16, 13.54, -1.27; **$[\alpha]^{25}_D$** –18.5 (c = 0.43 in $CHCl_3$); **IR** (film) 2951, 2919, 2850, 2102, 1747 (C=O), 1670 (C=O), 1600, 1486, 1454, 1409, 1345, 1247, 1230, 1144, 1088, 1052, 976, 916, 857, 834, 755, 694, 664, 605; **HRMS** Accurate mass (ES^+): Found 414.1684, $C_{20}H_{29}NO_5SiNa$ ($M+Na^+$) requires 414.1713.

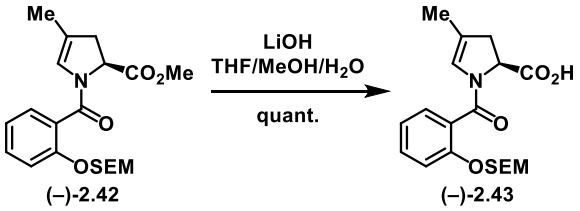

(S)-4-methyl-1-(2-((2-(trimethylsilyl)ethoxy)methoxy)benzoyl)-2,3-dihydro-1H-pyrrole-2-carboxylic acid (–)-2.43. Methyl ester **(–)-2.42** (19 mg, 0.049 mmol) was dissolved in 3:1:1 THF:MeOH:H_2O (2 mL) and LiOH•H_2O (10 mg, 0.245 mmol) was added as a solution in a minimal volume of water. After completion by TLC the reaction was carefully acidified with 5% AcOH (pH 5-6). The solution was extracted with CH_2Cl_2 3x, and the combined organic layers were washed with brine, dried over $MgSO_4$, filtered, and concentrated, yielding the title compound as a clear oil (20 mg, quant. yield). **^{1}H NMR** (500 MHz, $CDCl_3$) δ 7.41 (t, J = 7.7 Hz, 1H), 7.33 (d, J = 6.5 Hz, 1H), 7.23 (d, J = 8.3 Hz, 1H), 7.07 (t, J = 7.5 Hz, 1H), 5.78 (s, 1H), 5.22 (s, 2H), 5.20 – 5.11 (m, 1H), 3.75 – 3.69 (m, 2H), 3.22 (d, J = 16.4 Hz, 1H), 2.97 – 2.85 (m, 1H), 1.70 (s, 3H), 0.99 – 0.87 (m, 2H), -0.01 (s, 9H); **^{13}C NMR** (100 MHz, $CDCl_3$) δ 170.97, 167.90, 153.86, 132.11, 124.43, 124.15, 123.55, 122.09, 115.25, 93.38, 66.87, 60.45, 36.19, 18.17, 13.61, -1.27; **$[\alpha]^{25}_D$** –80.6 (c = 0.70 in $CHCl_3$); **IR** (film) 2954, 2921, 2857, 1743, 1598, 1489, 1457, 1427, 1378, 1303, 1232, 1143, 1086, 1043, 983, 916, 856, 834, 754, 694, 658; **HRMS** Accurate mass (ES^+): Found 400.1573, $C_{19}H_{27}NO_5SiNa$ ($M+Na^+$) requires 400.1556.

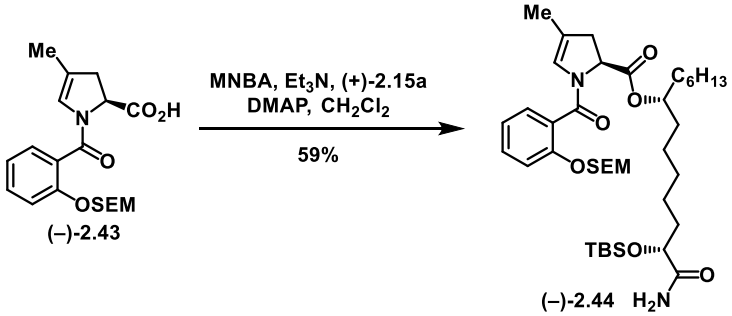

(7R,13R)-14-amino-13-((tert-butyldimethylsilyl)oxy)-14-oxotetradecan-7-yl (S)-4-methyl-1-(2-((2-(trimethylsilyl)ethoxy)methoxy)benzoyl)-2,3-dihydro-1H-pyrrole-2-carboxylate (–)-

2.44). To a solution of acid **(–)-2.43** (25 mg, 0.066 mmol) dissolved in CH_2Cl_2 (2 mL) was added MNBA (23 mg, 0.066 mmol) and Et_3N (0.025 mL, 0.182 mmol) and the solution was stirred for 10 minutes. Then alcohol **(+)-2.15a** (21 mg, 0.055 mmol) and DMAP (0.6 mg, 0.005 mmol) dissolved in CH_2Cl_2 (2 mL) was added, and the reaction was stirred overnight. The reaction was poured into sat. NH_4Cl, extracted with CH_2Cl_2 3x, washed with brine, dried over $MgSO_4$, filtered, concentrated, and purified by column chromatography (0 → 30% Et_2O/CH_2Cl_2), yielding the title compound as a yellow oil (24 mg, 59% yield). **^{1}H NMR** (500 MHz, $CDCl_3$) δ 7.37 – 7.31 (m, 2H), 7.19 (t, J = 9.5 Hz, 1H), 7.03 (td, J = 7.5, 0.9 Hz, 1H), 6.53 (t, J = 8.5 Hz, 1H), 5.87 (d, J = 1.6 Hz, 1H), 5.58 – 5.46 (m, 1H), 5.22 (dd, J = 17.5, 7.1 Hz, 2H), 5.03 – 4.91 (m, 2H), 4.16 – 4.09 (m, 1H), 3.79 – 3.70 (m, 2H), 3.08 – 2.96 (m, 1H), 2.51 (dd, J = 16.7, 4.8 Hz, 1H), 1.79 – 1.66 (m, 3H), 1.64 (s, 3H), 1.60 – 1.51 (m, 4H), 1.41 – 1.19 (m, 18H), 0.96 – 0.89 (m, 12H), 0.88 – 0.84 (m, 3H), 0.09 – 0.05 (m, 6H), 0.01 – -0.03 (m, 9H); **^{13}C NMR** (100 MHz, $CDCl_3$) δ 176.96, 170.93, 164.26, 153.87, 131.01, 128.89, 126.36, 125.41, 121.99, 119.19, 115.47, 93.48, 75.41, 73.57, 66.56, 58.63, 38.46, 35.12, 34.08, 31.87, 29.52, 29.32, 25.88, 25.34, 25.05, 24.12, 22.73, 18.17, 14.22, 13.58, -1.26, -4.69, -5.13; **$[\alpha]^{25}_D$** –18.3 (c = 0.69 in $CHCl_3$); **IR** (film) 2927, 2856, 2359, 2341, 1733 (C=O), 1683 (C=O), 1645 (C=O), 1601, 1506, 1488, 1456, 1419, 1377, 1248, 1188, 1141, 1086, 989, 834, 778, 754, 692, 667, 561; **HRMS** Accurate mass (ES^+): Found 733.4666, $C_{39}H_{69}N_2O_7Si_2$ ($M+H^+$) requires 733.4643.

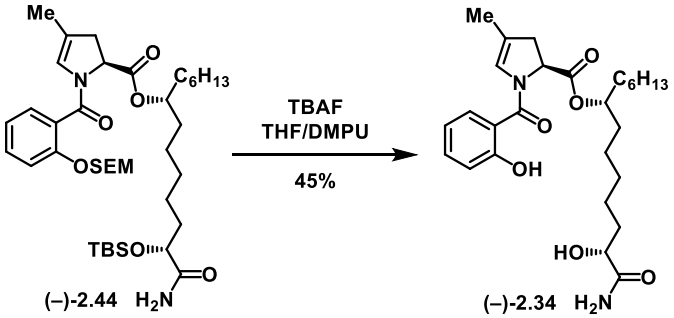

(7R,13R)-14-amino-13-hydroxy-14-oxotetradecan-7-yl (S)-1-(2-hydroxybenzoyl)-4-methyl-2,3-dihydro-1H-pyrrole-2-carboxylate (–)-2.34. Silyl ether **(–)-2.44** (11 mg, 0.015 mmol) was

dissolved in DMPU (0.03 mL, dried over 3Å molecular sieves), and TBAF (1M solution in THF, 0.03 mL, 0.030 mmol, dried over 3Å molecular sieves for 1 - 5 days) was added dropwise. The reaction was quenched with sat. NH_4Cl after 30 minutes. The mixture was extracted with Et_2O 5x, and the combined organic layers were washed with aq. 1M NH_4Cl 5x followed by brine, dried over Na_2SO_4, concentrated, and purified by column chromatography (0 → 5% MeOH/CH_2Cl_2), yielding the title compound as a clear oil (3.2 mg, 45% yield). **^{1}H NMR** (500 MHz, $CDCl_3$) δ 9.53 (s, 1H), 7.44 – 7.32 (m, 2H), 7.01 – 6.96 (m, 1H), 6.90 (t, J = 7.4 Hz, 1H), 6.61 (s, 0.68H), 6.55 (s, 0.46H), 6.44 (s, 1H), 5.32 (s, 1H), 5.05 – 4.94 (m, 2H), 4.13 – 4.05 (m, 1H), 3.47 (s, 1H), 3.09 – 3.00 (m, 1H), 2.59 – 2.51 (m, 1H), 1.84 – 1.77 (m, 1H), 1.75 (s, J = 8.0 Hz, 3H), 1.68 – 1.49 (m, 12H), 1.48 – 1.36 (m, 4H), 1.36 – 1.22 (m, 12H), 0.87 (t, J = 7.0 Hz, 3H); **^{13}C NMR** (125 MHz, $CDCl_3$) δ 176.97, 171.46, 166.42, 157.88, 133.25, 128.21, 125.19, 122.31, 119.35, 117.98, 117.92, 75.91, 71.33, 59.76, 56.13, 37.72, 34.59, 34.27, 34.20, 31.84, 29.85, 29.22, 28.26, 25.53, 24.81, 24.54, 22.69, 14.20, 13.70; **$[\alpha]^{25}_D$** –21.8 (c = 0.27 in $CHCl_3$); **IR** (film) 3306 (br O-H), 2921, 2855, 2493, 2361, 2159, 2031, 1978, 1734 (C=O), 1669 (C=O), 1591 (C=O), 1457, 1378, 1298, 1202, 1157, 1096, 1020, 867, 806, 756, 667; **HRMS** Accurate mass (ES^+): Found 489.2937, $C_{27}H_{41}N_2O_6$ ($M+H^+$) requires 489.2965.

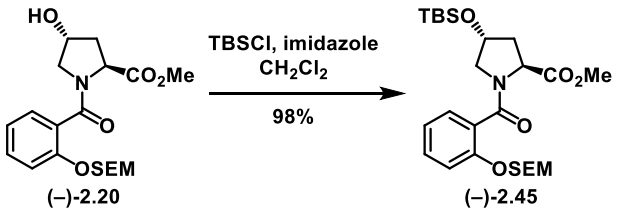

Methyl (2S,4R)-4-[(tert-butyldimethylsilyl)oxy]-1-(2-{[2-(trimethylsilyl)ethoxy]methoxy}benzoyl)pyrrolidine-2-carboxylate (–)-2.45. (originally synthesized by Kyle Knouse and repeated by me) To a solution of compound **(–)-2.20** (64 mg, 0.162 mmol, purified before use) in CH_2Cl_2 (1 mL) was added imidazole (22 mg, 0.324 mmol) followed by TBSCl (49 mg, 0.324 mmol), and the reaction was stirred for 24 hours. Another

portion of imidazole (22 mg, 0.324 mmol) and TBSCl (49 mg, 0.324) were added, and the reaction was stirred at room temperature for an additional 24 hours. The reaction was quenched with water and extracted with CH_2Cl_2 3x. The combined organic layers were washed with water then brine, dried over $MgSO_4$, filtered, concentrated and purified by column chromatography, yielding the title compound as a clear oil (80 mg, 98% yield). **^{1}H NMR** (500 MHz, $CDCl_3$, mixture of rotamers/conformers) δ 7.36 – 7.27 (m, 1.36H), 7.20 – 7.17 (m, 1.31H), 7.03 (td, J = 7.5, 1.0 Hz, 0.68H), 6.98 (td, J = 7.5, 0.9 Hz, 0.33H), 5.25 – 5.19 (m, 2H), 4.75 (t, J = 7.8 Hz, 0.67H), 4.52 – 4.44 (m, 0.59H), 4.43 – 4.38 (m, 0.69H), 3.82 – 3.72 (m, 4.53H), 3.59 (dd, J = 10.9, 4.5 Hz, 0.68H), 3.37 (s, 0.89H), 3.18 (dd, J = 11.0, 1.7 Hz, 0.68H), 2.28 – 2.19 (m, 1H), 2.14 – 2.05 (m, 1H), 0.95 (td, J = 8.3, 2.5 Hz, 2H), 0.90 (s, J = 2.9 Hz, 2.84H), 0.82 (s, J = 2.9 Hz, 6H), 0.10 (s, J = 3.1 Hz, 0.85H), 0.09 (s, J = 3.0 Hz, 0.86H), 0.02 (s, J = 2.8 Hz, 1.79H), 0.00 – -0.01 (m, 8.25H), -0.04 (s, 2H); **^{13}C NMR** (125 MHz, $CDCl_3$) δ 172.74, 168.16, 153.74, 130.77, 130.73, 128.24, 127.33, 122.04, 121.71, 115.89, 93.86, 93.47, 70.45, 69.40, 66.47, 57.47, 56.28, 54.78, 52.26, 51.98, 40.39, 38.58, 25.78, 25.65, 18.12, 18.02, 17.87, -1.32, -1.36, -4.81, -4.92; **$[\alpha]^{25}_D$** –65.9 (c = 0.72 in $CHCl_3$); **IR** (film) 2952, 2924, 2893, 2856, 1746 (C=O), 1644 (C=O), 1601 (C=O), 1489, 1455, 1412, 1359, 1317, 1249, 1227, 1197, 1175, 1144, 1086, 1023, 986, 920, 833, 775, 753, 693, 653; **HRMS** Accurate mass (ES^+): Found 532.2485, $C_{25}H_{43}NO_6Si_2Na$ ($M+Na^+$) requires 532.2527.

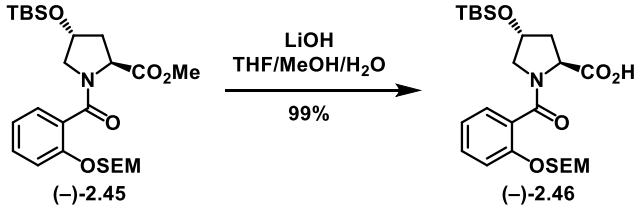

(2S,4R)-4-[(tert-butyldimethylsilyl)oxy]-1-(2-{[2-(trimethylsilyl)ethoxy]methoxy}benzoyl)pyrrolidine-2-carboxylic acid (–)-2.46. (originally synthesized by Kyle Knouse and repeated by me) Methyl ester **(–)-2.45** (166 mg, 0.325 mmol)

was dissolved in 3:1:1 THF:MeOH:H_2O (1 mL) and LiOH•H_2O (68 mg, 1.625 mmol) was added as a solution in a minimal volume of water. The reaction was monitored by TLC and upon completion was carefully acidified (pH 5-6) by addition of 1M HCl. The solution was extracted with CH_2Cl_2 3x, washed with brine, dried over $MgSO_4$, filtered, and concentrated, yielding the title compound as a clear oil (160 mg, 99% yield). **^{1}H NMR** (400 MHz, $CDCl_3$) δ 7.57 (br s, 1H), 7.38 (t, J = 7.9 Hz, 1H), 7.30 (d, J = 7.5 Hz, 1H), 7.22 (d, J = 8.4 Hz, 1H), 7.16 (d, J = 8.5 Hz, 1H), 7.05 (t, J = 7.5 Hz, 1H), 6.99 – 6.93 (m, 1H), 5.26 – 5.18 (m, 2H), 4.87 (t, J = 7.7 Hz, 1H), 4.36 (s, 1H), 3.49 (dd, J = 11.2, 4.1 Hz, 1H), 3.20 (t, J = 17.9 Hz, 1H), 2.53 – 2.44 (m, 1H), 2.25 – 2.12 (m, 1H), 0.98 – 0.87 (m, 3H), 0.82 (s, 9H), 0.03 (s, 3H), -0.01 (s, 9H), -0.06 (s, 3H); **^{13}C NMR** (125 MHz, $CDCl_3$) δ 172.72, 171.48, 153.73, 131.57, 128.02, 125.78, 122.12, 115.57, 93.64, 69.84, 66.80, 58.79, 57.12, 37.22, 25.72, 18.10, 17.95, -1.27, -4.73, -4.89; **$[\alpha]^{25}_D$** –86.6 (c = 1.75 in $CHCl_3$); **IR** (film) 2952, 2856, 2359, 2341, 1743 (C=O), 1595 (C=O), 1489, 1462, 1434, 1361, 1249, 1024, 988, 921, 754, 693, 667, 611; **HRMS** Accurate mass (ES^+): Found 518.2330, $C_{24}H_{41}NO_6Si_2Na$ ($M+Na^+$) requires 518.2370.

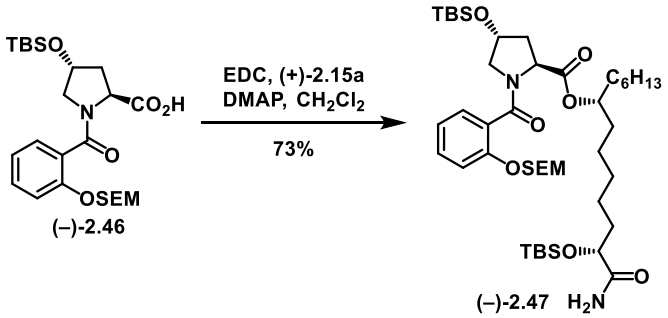

(1R,7R)-1-[(tert-butyldimethylsilyl)oxy]-1-carbamoyltridecan-7-yl (2S,4R)-4-[(tert-butyldimethylsilyl)oxy]-1-(2-{[2-(trimethylsilyl)ethoxy]methoxy}benzoyl)pyrrolidine-2-carboxylate (–)-2.47. (originally synthesized by Kyle Knouse and repeated by me) Acid **(–)-2.46** (125 mg, 0.252 mmol) was dissolved in CH_2Cl_2 (1 mL) and cooled to 0°C. EDC (64 mg, 0.336 mmol) was added, followed by a solution of alcohol **(+)-2.15a** (63 mg, 0.168 mmol) and DMAP (0.084 mmol) in CH_2Cl_2 (1 mL), and the reaction was stirred at room temperature overnight. The

reaction was poured into water and extracted with CH_2Cl_2 3x. The combined organic layers were washed with brine, dried over $MgSO_4$, concentrated, and purified by column chromatography (0 → 30% Et_2O/CH_2Cl_2), yielding the title compound as a clear oil (103 mg, 73% yield). **^{1}H NMR** (500 MHz, $CDCl_3$, mixture of rotamers/conformers) δ 7.34 – 7.27 (m, 1.35H), 7.25 – 7.17 (m, 1.35H), 7.14 (d, J = 8.1 Hz, 0.33H), 7.02 (td, J = 7.5, 0.9 Hz, 0.65H), 6.93 (td, J = 7.5, 0.9 Hz, 0.32H), 6.60 – 6.48 (m, 1H), 5.73 (s, 0.40H), 5.68 (s, 0.60H), 5.24 – 5.19 (m, 2H), 4.97 – 4.90 (m, 0.63H), 4.72 (t, J = 7.6 Hz, 0.63H), 4.60 – 4.54 (m, 0.32H), 4.50 – 4.45 (m, 0.32H), 4.45 – 4.37 (m, 1H), 4.13 (dt, J = 13.1, 5.2 Hz, 1H), 3.87 – 3.69 (m, 2.72H), 3.57 (dd, J = 10.7, 4.3 Hz, 0.63H), 3.16 (dd, J = 10.9, 2.7 Hz, 0.63H), 2.24 (ddd, J = 12.8, 8.2, 4.7 Hz, 1H), 2.14 – 2.03 (m, 1H), 1.81 – 1.70 (m, 1H), 1.70 – 1.46 (m, 4H), 1.46 – 1.09 (m, 16H), 0.95 – 0.93 (m, 4H), 0.91 – 0.89 (m, 8.54H), 0.83 – 0.81 (m, 5.72H), 0.12 – 0.06 (m, 8.34H), 0.01 – -0.02 (m, 10.78H), -0.05 (s, 1.77H); **^{13}C NMR** (125 MHz, $CDCl_3$) δ 177.18, 171.97, 168.48, 168.01, 153.83, 130.67, 128.29, 127.45, 126.67, 122.04, 121.88, 115.88, 93.92, 93.43, 75.48, 75.11, 73.49, 70.42, 69.34, 66.48, 58.74, 57.83, 56.18, 54.35, 40.40, 38.72, 35.25, 35.12, 34.09, 33.74, 33.69, 31.82, 31.75, 29.55, 29.49, 29.24, 29.13, 25.82, 25.71, 25.31, 25.24, 25.10, 24.79, 24.08, 22.66, 22.61, 18.20, 18.08, 17.93, 14.15, -1.27, -4.76, -4.80, -4.90, -5.19; **$[\alpha]^{25}_D$** –20.8 (c = 0.86 in $CHCl_3$); **IR** (film) 3480 (N-H), 2927, 2856, 1739 (C=O), 1691 (C=O), 1644 (C=O), 1455, 1412, 1250, 1189, 1088, 991, 937, 897, 834, 754, 574; **HRMS** Accurate mass (ES^+): Found 873.5226, $C_{44}H_{82}N_2O_8Si_3Na$ ($M+Na^+$) requires 873.5277.

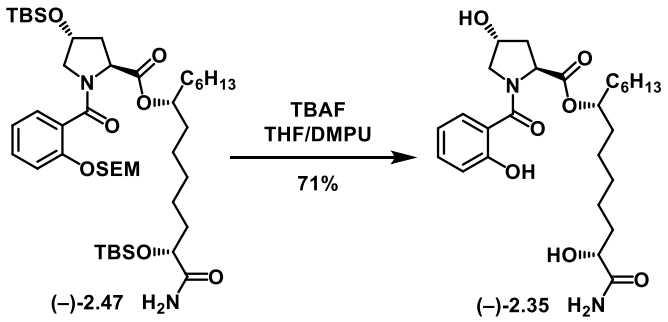

(1R,7R)-1-carbamoyl-1-hydroxytridecan-7-yl (2S,4R)-4-hydroxy-1-(2-hydroxybenzoyl)pyrrolidine-2-carboxylate (–)-2.35. (originally synthesized by Kyle Knouse and repeated by me) Silyl ether **(–)-2.47** (25 mg, 0.029 mmol) was dissolved in DMPU (0.58 mL, dried over 3Å molecular sieves) and TBAF (1M solution in THF, 0.58 mL, 0.580 mmol, dried over 3Å molecular sieves for 1 - 5 days) was added dropwise. The reaction was quenched with sat. NH_4Cl after 30 minutes. The mixture was extracted with Et_2O 5x, and the combined organic layers were washed with aq. 1M NH_4Cl 5x followed by brine, dried over Na_2SO_4, concentrated, and purified by column chromatography (0 → 5% MeOH/CH_2Cl_2), yielding the title compound as a clear oil (10 mg, 71% yield). $\mathbf{R_f}$ (9:1 CH_2Cl_2:MeOH) = 0.34; **^{1}H NMR** (500 MHz, $CDCl_3$) δ 10.50 (br s, 1H), 7.41 (d, J = 7.2 Hz, 1H), 7.32 (t, J = 7.7 Hz, 1H), 6.93 (d, J = 8.3 Hz, 1H), 6.86 (t, J = 7.5 Hz, 1H), 6.74 (br s, 1H), 5.69 (br s, 1H), 4.97 (br s, 1H), 4.81 (t, J = 8.2 Hz, 1H), 4.53 (s, 1H), 4.05 (dd, J = 7.7, 3.4 Hz, 1H), 3.95 (d, J = 8.7 Hz, 1H), 3.82 – 3.61 (m, 2H), 3.15 (br s, 1H), 2.43 – 2.30 (m, 1H), 2.09 (ddd, J = 13.0, 8.7, 4.4 Hz, 1H), 1.85 – 1.72 (m, 1H), 1.65 – 1.32 (m, 9H), 1.30 – 1.12 (m, 10H), 0.86 (t, J = 7.1 Hz, 3H); **^{13}C NMR** (125 MHz, $CDCl_3$) δ 177.57, 172.31, 170.88, 158.86, 133.28, 128.30, 118.98, 117.88, 75.73, 71.58, 70.44, 59.12, 58.36, 37.40, 34.48, 34.17, 34.04, 31.84, 29.23, 28.42, 25.46, 24.70, 24.50, 22.69, 14.21; $\mathbf{[\alpha]^{25}_D}$ –43.4 (c = 0.71 in $CHCl_3$); **IR** (film) 3303 (br O-H), 2928, 2857, 1732 (C=O), 1666 (C=O), 1586 (C=O), 1434, 1376, 1298, 1193, 1082, 1001, 958, 911, 878, 754, 728, 651, 609; **HRMS** Accurate mass (ES^+): Found 515.2691, $C_{26}H_{40}N_2O_7Na$ ($M+Na^+$) requires 515.2733.

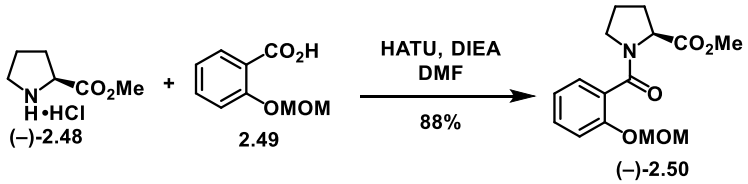

Methyl (2S)-1-[2-(methoxymethoxy)benzoyl]pyrrolidine-2-carboxylate (–)-2.50. Using general procedure C, 2-methoxymethyloxybenzoic acid (248 mg, 1.364 mmol) and L-proline methyl ester hydrochloride (271 mg, 1.636 mmol) yielded the title compound as a clear oil (352

mg, 88% yield). **^{1}H NMR** (400 MHz, MeOD, mixture of rotamers/conformers) δ 7.43 – 7.34 (m, 1H), 7.28 (dd, J = 7.5, 1.7 Hz, 0.73H), 7.23 (d, J = 8.4 Hz, 0.71H), 7.20 (d, J = 8.3 Hz, 0.30H), 7.15 (d, J = 7.6 Hz, 0.26H), 7.09 (td, J = 7.5, 0.9 Hz, 0.74H), 7.04 (dd, J = 11.2, 3.8 Hz, 0.29H), 5.26 – 5.20 (m, 2H), 4.59 (dd, J = 8.7, 4.7 Hz, 0.72H), 4.30 (dd, J = 8.6, 2.8 Hz, 0.28H), 3.77 (s, 1.52H), 3.75 – 3.69 (m, 0.54H), 3.48 (s, 0.63H), 3.47 (s, 1.88H), 3.46 (s, 1.18H), 3.41 (dt, J = 17.4, 5.3 Hz, 1.40H), 3.35 (s, 1.28H), 2.44 – 2.25 (m, 1H), 2.09 – 1.86 (m, 3H); **^{13}C NMR** (100 MHz, MeOD) δ 173.83, 170.08, 169.82, 154.26, 131.97, 129.18, 128.65, 128.30, 127.93, 123.08, 122.81, 116.41, 116.07, 95.98, 61.55, 59.94, 56.67, 52.73, 49.54, 47.42, 31.87, 30.48, 25.55, 23.76; **$[\alpha]^{25}_{D}$** –18.3 (c = 0.66 in $CHCl_3$) **IR** (film) 2054, 2359, 1741 (C=O), 1625 (C=O), 1601, 1489, 1455, 1418, 1362, 1281, 1234, 1198, 1152, 1107, 1078, 1041, 989, 922, 844, 747, 666; **HRMS** Accurate mass (ES^+): Found 316.1134, $C_{15}H_{19}NO_5Na$ ($M+Na^+$) requires 316.1161.

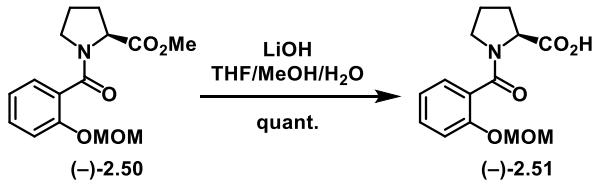

(2S)-1-[2-(methoxymethoxy)benzoyl]pyrrolidine-2-carboxylic acid (–)-2.51. Methyl ester **(–)-2.50** (117 mg, 0.399 mmol) was dissolved in 3:1:1 THF:MeOH:H_2O (1 mL) and LiOH•H_2O (84 mg, 1.995 mmol) was added as a solution in a minimal volume of water. The reaction was monitored by TLC and upon completion was carefully acidified by addition of 1M HCl (pH 5-6). The solution was extracted with CH_2Cl_2 3x, washed with brine, dried over $MgSO_4$, filtered, and concentrated, yielding the title compound as a clear oil (115 mg, quant. yield). **^{1}H NMR** (400 MHz, MeOD, mixture of rotamers/conformers) δ 7.91 (s, 0.55H), 7.43 – 7.34 (m, 1.06H), 7.31 (dd, J = 7.5, 1.6 Hz, 0.66H), 7.26 – 7.18 (m, 1.29H), 7.09 (td, J = 7.5, 0.9 Hz, 0.64H), 7.03 (t, J = 7.5 Hz, 0.31H), 5.26 – 5.19 (m, 2H), 4.57 (dd, J = 8.5, 4.5 Hz, 0.60H), 4.23 (d, J = 6.6 Hz, 0.31H), 3.80 – 3.67 (m, 0.66H), 3.47 (s, 3H), 3.45 – 3.35 (m, 1H), 2.44 – 2.22 (m, 1H), 2.14 – 1.84 (m, 3H); **^{13}C NMR** (100 MHz, MeOD) δ 175.57, 170.59, 170.23, 154.43, 132.01, 128.76,

128.55, 123.19, 122.97, 116.54, 116.05, 96.13, 96.01, 79.48, 56.66, 49.74, 47.41, 32.11, 30.81, 25.64, 23.78; **[α]$^{25}_{D}$** –71.4 (c = 1.28 in $CHCl_3$); **IR** (film) 2956, 2359, 1733 (C=O), 1592 (C=O), 1490, 1456, 1234, 1198, 1152, 1107, 1078, 1042, 979, 921, 845, 748, 665; **HRMS** Accurate mass (ES^+): Found 302.1012, $C_{14}H_{17}NO_5$ ($M+Na^+$) requires 302.1004.

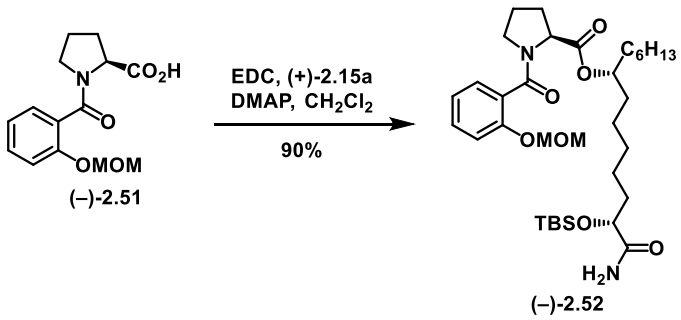

(1R,7R)-1-[(tert-butyldimethylsilyl)oxy]-1-carbamoyltridecan-7-yl (2S)-1-[2-(methoxymethoxy)benzoyl]pyrrolidine-2-carboxylate (–)-2.52. Acid **(–)-2.51** (43 mg, 0.154 mmol) was dissolved in CH_2Cl_2 (1 mL) and cooled to 0 °C. EDC (30 mg, 0.154 mmol) was added followed by a solution of alcohol **(+)-2.15a** (29 mg, 0.077 mmol) and DMAP (1 mg, 0.008 mmol) dissolved in CH_2Cl_2 (1 mL), and the reaction was stirred at room temperature overnight. The reaction was poured into water and extracted with CH_2Cl_2 3x. The combined organic layers were washed with brine, dried over $MgSO_4$, concentrated, and purified by column chromatography (0 → 30% Et_2O/CH_2Cl_2), yielding the title compound as a clear oil (43 mg, 90% yield). **^{1}H NMR** (500 MHz, $CDCl_3$, mixture of rotamers/conformers) δ 7.29 (tdd, J = 9.8, 8.2, 1.4 Hz, 1.36H), 7.25 – 7.20 (m, 0.86H), 7.14 (d, J = 8.2 Hz, 0.69H), 7.08 (d, J = 8.4 Hz, 0.41H), 7.03 (t, J = 7.4 Hz, 0.68H), 6.94 (t, J = 7.5 Hz, 0.39H), 6.53 (dd, J = 10.1, 4.3 Hz, 1H), 5.77 (s, 0.39H), 5.74 (s, 0.58H), 5.21 – 5.14 (m, 2H), 4.92 (dt, J = 12.2, 6.2 Hz, 0.62H), 4.69 – 4.60 (m, 1H), 4.27 – 4.21 (m, 0.34H), 4.12 (dt, J = 10.4, 5.0 Hz, 1H), 3.81 – 3.73 (m, 0.63H), 3.50 – 3.38 (m, 3.66H), 3.33 (dt, J = 10.6, 6.7 Hz, 1H), 2.34 – 2.17 (m, 1H), 2.06 – 1.79 (m, 4H), 1.79 – 1.47 (m, 5H), 1.42 – 1.16 (m, 18H), 0.94 – 0.88 (m, 9H), 0.85 (t, J = 6.8 Hz, 3H), 0.10 (d, J = 5.6 Hz, 1.78H), 0.06 (d, J = 6.1 Hz, 3.81H); **^{13}C NMR** (125 MHz, $CDCl_3$) δ 177.06, 172.01, 167.68, 153.19, 130.57,

128.16, 127.98, 122.31, 115.60, 95.22, 95.09, 75.56, 75.15, 73.54, 60.47, 58.90, 56.36, 48.31, 46.18, 35.23, 35.11, 34.10, 33.98, 33.77, 31.85, 31.78, 31.43, 29.92, 29.49, 29.29, 29.18, 25.85, 25.31, 25.11, 24.86, 24.10, 22.89, 22.69, 22.64, 18.12, 14.17, -4.73, -5.16; **[α]$^{25}_{D}$** –21.4 (c = 0.95 in $CHCl_3$); **IR** (film) 3477 (N-H), 3307 (br O-H); 2927, 2856, 1738 (C=O), 1683 (C=O), 1626, 1601, 1558, 1489, 1456, 1417, 1338, 1281, 1235, 1194, 1153, 1079, 1042, 989, 922, 837, 755, 652; **HRMS** Accurate mass (ES^+): Found 635.4109, $C_{34}H_{59}N_2O_7Si$ ($M+H^+$) requires 635.4092.

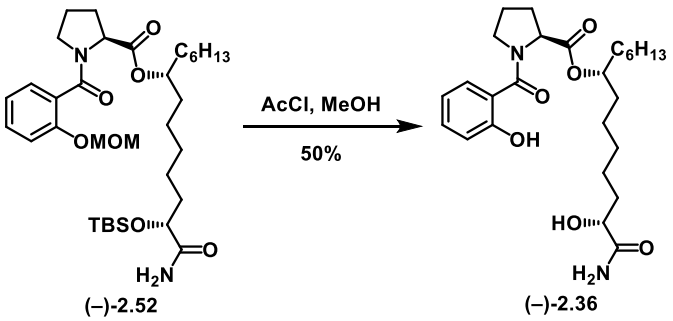

(1R,7R)-1-carbamoyl-1-hydroxytridecan-7-yl (2S)-1-(2-hydroxybenzoyl)pyrrolidine-2-carboxylate (–)-2.36. To a solution of protected ester **(–)-2.52** (43 mg, 0.068 mmol) in MeOH (1 mL) was added acetyl chloride (*ca.* 1 μL, 1 drop) at room temperature. After 1 hour, the reaction was quenched with sat. $NaHCO_3$ and extracted with CH_2Cl_2 3x. The combined organic layers were washed with water, dried over Na_2SO_4, filtered, concentrated, and purified by column chromatography (0 → 10% MeOH/CH_2Cl_2), yielding the title compound as a clear oil (16 mg, 50% yield). **^{1}H NMR** (500 MHz, $CDCl_3$) δ 10.64 (s, 1H), 7.49 (d, J = 6.9 Hz, 1H), 7.33 (t, J = 7.6 Hz, 1H), 6.96 (t, J = 8.6 Hz, 1H), 6.86 (t, J = 7.3 Hz, 1H), 6.66 (s, 1H), 5.52 (s, 1H), 4.98 (s, 1H), 4.71 – 4.60 (m, 1H), 4.08 (s, J = 19.6 Hz, 1H), 3.93 – 3.83 (m, 1H), 3.83 – 3.73 (m, 1H), 3.66 (s, 1H), 2.40 – 2.28 (m, 1H), 2.15 – 2.05 (m, 1H), 2.05 – 1.90 (m, 2H), 1.87 – 1.76 (m, 3H), 1.68 – 1.48 (m, 5H), 1.48 – 1.33 (m, 6H), 1.33 – 1.16 (m, 11H), 0.86 (t, J = 7.0 Hz, 3H); **^{13}C NMR** (125 MHz, $CDCl_3$) δ 177.22, 172.37, 170.30, 159.04, 133.20, 128.10, 118.83, 117.85, 117.73, 75.42, 71.48, 60.56, 50.78, 34.58, 34.39, 34.29, 31.84, 29.21, 28.52, 25.82, 25.49, 24.87, 24.65, 22.67, 14.19; **[α]$^{25}_{D}$** –28.0 (c = 1.51 in $CHCl_3$); **IR** (film) 3189 (br O-H), 2928, 2857, 2360, 1736 (C=O),

1667 (C=O), 1583 (C=O), 1434, 1374, 1186, 1089, 1025, 877, 754, 651, 609, 563; **HRMS** Accurate mass (ES^+): Found 477.2935, $C_{26}H_{41}N_2O_6$ ($M+H^+$) requires 477.2965.

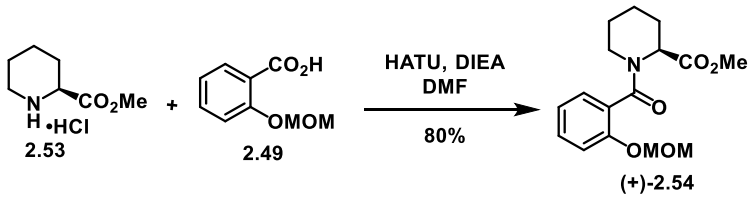

Methyl (2S)-1-[2-(methoxymethoxy)benzoyl]piperidine-2-carboxylate (+)-2.54. (synthesized by Colleen Keohane) To a solution of 2-methoxymethyloxybenzoic acid (200 mg, 1.101 mmol) in DMF (5 mL) was added HATU (502 mg, 1.321 mmol). A solution of methyl 2-piperidinecarboxylate hydrochloride (237 mg, 1.321 mmol) and diisopropylethylamine (0.23 mL, 1.652 mmol) in DMF (5 mL) was added to the acid/HATU solution. Another portion of diisopropylethylamine (0.46 mL, 3.304 mmol) was added and the reaction was allowed to stir overnight. The reaction was poured into water and extracted with EtOAc 3x. The combined organic layers were washed with sat. NH_4Cl, sat. $NaHCO_3$, water 2x and brine 2x, then dried over $MgSO_4$, filtered, concentrated, and purified by column chromatography (0 → 50% EtOAc/CH_2Cl_2), yielding the title compound as a clear oil (248 mg, 80% yield). **^{1}H NMR** (500 MHz, $CDCl_3$, mixture of rotamers/conformers) δ 7.42 – 7.26 (m, 2.67H), 7.25 – 7.17 (m, 1.16H), 7.14 – 7.03 (m, 1.23H), 5.67 (s, 0.73H), 5.27 (dt, J = 11.7, 6.9 Hz, 2H), 5.15 (dd, J = 39.3, 6.6 Hz, 0.32H), 4.81 (d, J = 13.7 Hz, 0.31H), 4.43 (d, J = 5.1 Hz, 0.08H), 4.36 (d, J = 4.3 Hz, 0.22H), 3.85 (s, 2.22H), 3.76 (s, J = 4.4 Hz, 1.08H), 3.59 – 3.46 (m, 4.22H), 3.41 – 3.33 (m, 0.55H), 3.18 (td, J = 13.0, 2.4 Hz, 0.57H), 2.92 – 2.84 (m, 0.23H), 2.41 (t, J = 13.5 Hz, 0.75H), 2.28 (d, J = 12.8 Hz, 0.32H), 1.87 – 1.73 (m, 2.52H), 1.68 – 1.51 (m, 2.08H), 1.51 – 1.35 (m, 1.49H); **^{13}C NMR** (125 MHz, $CDCl_3$) δ 171.53, 171.34, 171.26, 168.93, 168.85, 168.72, 153.19, 152.82, 152.62, 130.27, 130.24, 127.98, 127.81, 127.42, 126.70, 126.65, 126.53, 122.28, 122.11, 122.05, 115.15, 114.77, 114.72, 94.85, 94.78, 94.70, 77.36, 60.27, 57.86, 56.17, 56.11, 52.28, 52.24,

52.07, 51.82, 51.60, 45.34, 44.53, 39.40, 39.05, 27.38, 26.87, 26.59, 25.49, 25.33, 24.64, 21.16, 21.10, 20.95, 14.12; **[α]$^{25}_{D}$** –28.6 (c = 2.15 in $CHCl_3$); **IR** (film) 1076, 2945, 1737 (C=O), 1633 (C=O), 1599, 1488, 1452, 1422, 1339, 1286, 1232, 1199, 1143, 985, 921, 756, 645; **HRMS** Accurate mass (ES^+): Found 308.1502 (+1.3 ppm), $C_{16}H_{21}NO_5Na$ ($M+Na^+$) requires 308.1498.

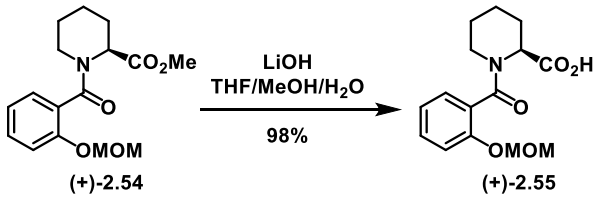

(2S)-1-[2-(methoxymethoxy)benzoyl]piperidine-2-carboxylic acid (+)-2.55. (synthesized by Colleen Keohane) Using the LiOH hydrolysis procedure described above, methyl ester **(–)-2.54** (215 mg, 0.700 mmol) yielded the title compound as a clear oil (200 mg, 98% yield). **^{1}H NMR** (500 MHz, $CDCl_3$, mixture of rotamers/conformers) δ 9.53 (br s, 1H), 7.36 – 7.23 (m, 2.16H), 7.16 (dt, J = 18.2, 8.0 Hz, 1.56H), 7.04 (t, J = 7.3 Hz, 0.91H), 6.99 (t, J = 7.6 Hz, 0.37H), 5.64 – 5.56 (m, 0.75H), 5.18 (ddd, J = 14.8, 13.8, 7.3 Hz, 2H), 5.06 (dd, J = 40.1, 6.7 Hz, 0.40H), 4.72 (d, J = 10.5 Hz, 0.31H), 4.35 (d, J = 4.9 Hz, 0.09H), 4.27 (d, J = 4.0 Hz, 0.20H), 3.76 (t, J = 6.0 Hz, 0.60H), 3.49 – 3.40 (m, 3.74H), 3.32 – 3.22 (m, 0.61H), 3.12 (t, J = 12.0 Hz, 0.57H), 2.86 – 2.77 (m, 0.28H), 2.37 (d, J = 13.2 Hz, 0.77H), 2.19 (d, J = 13.3 Hz, 0.26H), 2.07 (d, J = 11.4 Hz, 0.12H), 1.89 – 1.82 (m, 0.62H), 1.82 – 1.63 (m, 2.67H), 1.56 (dd, J = 32.8, 13.9 Hz, 1.35H), 1.51 – 1.32 (m, 2.57H); **^{13}C NMR** (125 MHz, $CDCl_3$) δ 175.19, 174.99, 174.14, 169.79, 169.58, 169.27, 153.31, 152.97, 152.77, 130.68, 130.58, 128.22, 128.01, 127.59, 126.13, 122.40, 122.18, 115.15, 114.79, 94.92, 94.78, 67.95, 57.89, 56.29, 56.26, 52.02, 51.92, 45.59, 44.84, 39.64, 27.51, 26.73, 26.55, 25.61, 25.53, 25.36, 24.75, 21.17; **[α]$^{25}_{D}$** –59.8 (c = 0.85 in $CHCl_3$); **IR** (film) 2941, 1731 (C=O), 1587 (C=O), 1442, 1286, 1233, 1199, 1151, 1077, 1041, 983, 921, 864, 755, 732, 700, 641; **HRMS** Accurate mass (ES^+): Found 316.1173, $C_{15}H_{19}NO_5Na$ ($M+Na^+$) requires 316.1161.

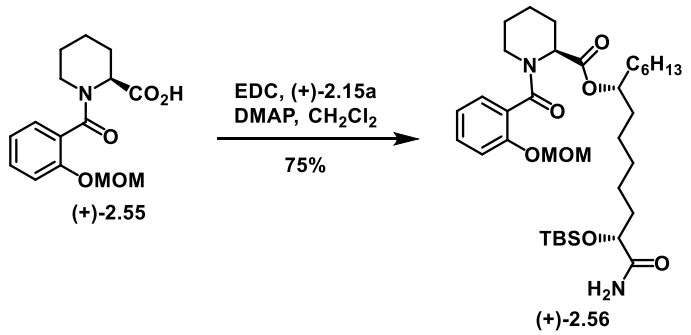

(1R,7R)-1-[(tert-butyldimethylsilyl)oxy]-1-carbamoyltridecan-7-yl (2S)-1-[2-(methoxymethoxy)benzoyl]piperidine-2-carboxylate (+)-2.56. (synthesized by Colleen Keohane) Using the EDC esterification procedure described above (1.5 eq acid, 1.7 eq EDC, 0.5 eq DMAP, 1.0 eq alcohol); acid **(+)-2.55** (85 mg, 0.291 mmol) yielded the title compound as a clear oil (94 mg, 75% yield). **^{1}H NMR** (500 MHz, $CDCl_3$, mixture of rotamers/conformers) δ 7.34 – 7.27 (m, 1.42H), 7.25 – 7.10 (m, 2.47H), 7.04 (t, J = 7.5 Hz, 0.82H), 6.96 (t, J = 6.9 Hz, 0.45H), 6.52 (s, 1.13H), 5.56 (s, 0.88H), 5.49 – 5.33 (m, 1.49H), 5.25 – 5.16 (m, 2.13H), 4.94 (s, 0.77H), 4.75 (d, J = 13.9 Hz, 0.71H), 4.16 – 4.07 (m, 1.93H), 3.48 (d, J = 3.8 Hz, 3H), 3.45 – 3.37 (m, 1.45H), 3.12 (t, J = 12.7 Hz, 0.59H), 2.90 – 2.80 (m, 0.48H), 2.39 – 2.29 (m, 0.81H), 2.23 – 2.15 (m, 0.51H), 1.82 – 1.68 (m, 4.11H), 1.60 – 1.45 (m, 9.21H), 1.45 – 1.11 (m, 17.89H), 0.93 (d, J = 6.7 Hz, 9.57H), 0.87 (t, J = 7.0 Hz, 4.95H), 0.11 – 0.06 (m, 6H); **^{13}C NMR** (100 MHz, $CDCl_3$) δ 176.93, 170.95, 170.77, 168.84, 153.37, 152.84, 130.34, 128.13, 127.04, 125.65, 122.31, 114.92, 94.96, 75.69, 73.53, 58.07, 56.43, 56.32, 52.06, 45.55, 35.20, 34.05, 31.83, 30.43, 29.55, 29.31, 25.86, 25.43, 25.32, 24.19, 22.70, 21.39, 18.14, 14.20, -4.71, -5.12; **$[\alpha]^{25}_{D}$** +13.9 (c = 2.42 in $CHCl_3$); **IR** (film) 3480, 2928, 2857, 1732 (C=O), 1687 (C=O), 1634 (C=O), 1600, 1489, 1455, 1424, 1286, 1251, 1233, 1198, 1153, 1096, 1078, 1042, 991, 922, 836, 778, 755, 730, 668, 645; **HRMS** Accurate mass (ES^+): Found 649.4264, $C_{35}H_{61}N_2O_7Si$ ($M+H^+$) requires 649.4249.

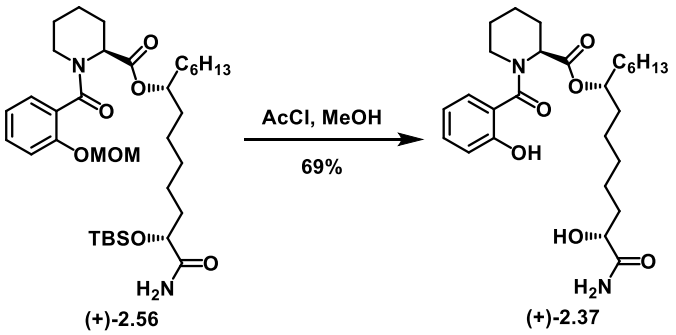

(1R,7R)-1-carbamoyl-1-hydroxytridecan-7-yl (2S)-1-(2-hydroxybenzoyl)piperidine-2-carboxylate (+)-2.37. (synthesized by Colleen Keohane) To a solution of protected ester **(+)-2.56** (25 mg, 0.038 mmol) dissolved in MeOH (1 mL) was added acetyl chloride (5 μL, 0.006 mmol) at 0 °C. The reaction was stirred at this temperature for 45 minutes then warmed to room temperature and stirred for 2 hours. The reaction was quenched with sat. $NaHCO_3$, and extracted with CH_2Cl_2 3x. The combined organic layers were washed with brine, dried over $MgSO_4$, filtered, concentrated, and purified by preparative TLC (100% EtOAc), yielding the title compound as a clear oil (12 mg, 69% yield). *Note:* High temperature ^{1}H NMR was possible, but extended heating times caused decomposition. **^{1}H NMR** (500 MHz, $CDCl_3$, 328K) δ 8.67 (br s, 0.39H), 8.54 (br s, 0.47H), 7.37 – 7.27 (m, 1H), 6.99 (d, J = 8.1 Hz, 1H), 6.87 (s, 1H), 5.21 (d, J = 34.3 Hz, 1H), 5.05 – 4.96 (m, 1H), 4.16 – 3.98 (m, 2H), 3.36 – 3.22 (m, 1H), 2.39 – 2.26 (m, 1H), 1.80 (d, J = 11.5 Hz, 3H), 1.60 (s, 10H), 1.30 (s, 15H), 0.90 (t, J = 6.6 Hz, 3H); **^{13}C NMR** (125 MHz, $CDCl_3$, room temp) δ 171.55, 171.12, 157.86, 132.52, 132.41, 130.70, 128.11, 128.03, 119.41, 119.26, 118.08, 118.01, 60.41, 34.83, 34.56, 34.46, 34.23, 34.10, 31.88, 29.86, 29.29, 29.24, 29.03, 28.80, 26.95, 26.79, 25.58, 25.54, 25.36, 25.21, 25.14, 24.80, 22.66, 21.38, 21.24, 14.33, 14.03; **$[\alpha]^{25}_D$** +21.5 (c = 1.3 in $CHCl_3$); **IR** (film) 3291 (br O-H), 2928, 2857, 1731 (C=O), 1692 (C=O), 1624 (C=O), 1454, 1373, 1207, 1142, 1007, 935, 911, 847, 827, 753, 645, 602; **HRMS** Accurate mass (ES^+): Found 491.3097, $C_{27}H_{43}N_2O_6$ ($M+H^+$) requires 491.3121.

Methyl 3-((2-(trimethylsilyl)ethoxy)methoxy)benzoate 2.65. (synthesized by Colleen Keohane) Using the procedure given for the preparation of compound **2.14**, methyl 3-hydroxybenzoate (250 mg, 1.640 mmol) yielded the title compound as a clear oil (421 mg, 91% yield). **^{1}H NMR** (500 MHz, $CDCl_3$) δ 7.71 – 7.66 (m, 2H), 7.34 (dd, J = 11.9, 4.2 Hz, 1H), 7.23 (ddd, J = 8.2, 2.6, 1.1 Hz, 1H), 5.26 (s, 2H), 3.91 (s, J = 2.9 Hz, 3H), 3.80 – 3.73 (m, 2H), 0.98 – 0.93 (m, 2H), -0.01 (s, J = 3.3 Hz, 9H); **^{13}C NMR** (125 MHz, $CDCl_3$) δ 166.58, 157.34, 131.42, 129.27, 122.79, 120.89, 116.93, 92.73, 77.16, 66.22, 51.93, 17.91, -1.51; **IR** (film) 2952, 2897, 1723 (C=O), 1586, 1488, 1447, 1380, 1274, 1248, 1211, 1153, 1106, 1083, 1009, 994, 918, 857, 833, 783, 755, 683; **HRMS** Accurate mass (ES^+): Found 305.1195 (+3.3 ppm), $C_{14}H_{22}O_4SiNa$ ($M+Na^+$) requires 305.1185.

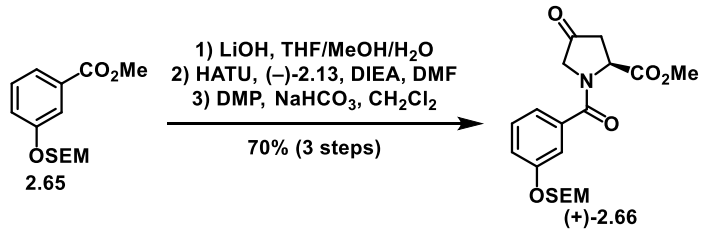

Methyl (S)-4-oxo-1-(3-((2-(trimethylsilyl)ethoxy)methoxy)benzoyl)pyrrolidine-2-carboxylate (+)-2.66. (synthesized by Colleen Keohane) Using the procedure given for the preparation of compound **2.19**, methyl ester **2.65** (264 mg, 0.934 mmol) yielded the corresponding acid, which was used directly in the next step. Using the procedure given for the preparation of compound **(–)-2.20**, the acid yielded the corresponding acylhydroxyproline methyl ester compound, whose purity made it unsuitable for characterization. Using the procedure given for the preparation of compound **(+)-2.21** on this intermediate then yielded the title compound as a yellow oil (254 mg, 70% over 3 steps). **^{1}H NMR** (500 MHz, $CDCl_3$) δ 7.37 – 7.32 (m, 1H), 7.19 – 7.11 (m, 3H), 5.37

– 5.27 (m, 1H), 5.24 (s, 2H), 3.85 – 3.70 (m, 5H), 2.97 (dd, J = 18.8, 10.6 Hz, 1H), 2.70 (d, J = 20.3 Hz, 1H), 0.98 – 0.91 (m, 2H), -0.00 (s, J = 3.4 Hz, 9H); **^{13}C NMR** (100 MHz, $CDCl_3$) δ 207.21, 171.60, 170.18, 157.50, 136.18, 129.90, 120.19, 118.61, 114.92, 92.81, 66.44, 55.37, 52.90, 40.02, 18.04, -1.39; **$[\alpha]^{25}_D$** +25.3 (c = 0.91 in $CHCl_3$); **IR** (film) 2950, 2395, 2342, 1757 (C=O), 1635 (C=O), 1575 (C=O), 1445, 1393, 1296, 1264, 1250, 1228, 1186, 1151, 1122, 1078, 1030, 1008, 990, 950, 862, 833, 817, 774, 753, 694, 600, 562; **HRMS** Accurate mass (ES^+): Found 394.1700 (+3.6 ppm), $C_{19}H_{28}NO_6Si$ ($M+H^+$) requires 394.1686.

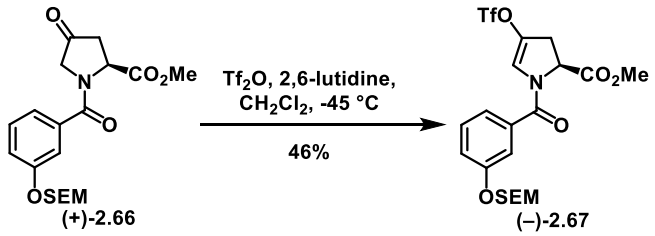

Methyl (S)-4-(((trifluoromethyl)sulfonyl)oxy)-1-(3-((2-(trimethylsilyl)ethoxy)methoxy)benzoyl)-2,3-dihydro-1H-pyrrole-2-carboxylate (–)-2.67. (synthesized by Colleen Keohane) Using the procedure given for the preparation of compound **(–)-2.22**, ketone **(+)-2.66** (150 mg, 0.388 mmol) yielded the title compound as an orange oil (95 mg, 46% yield). **^{1}H NMR** (500 MHz, $CDCl_3$) δ 7.37 (t, J = 7.9 Hz, 1H), 7.18 (dt, J = 24.8, 8.2 Hz, 3H), 6.81 (s, 1H), 5.24 (s, 2H), 5.08 (d, J = 6.5 Hz, 1H), 3.83 (s, 3H), 3.78 – 3.72 (m, 2H), 3.46 – 3.36 (m, 1H), 2.97 (ddd, J = 16.4, 4.8, 1.5 Hz, 1H), 0.99 – 0.92 (m, 2H), 0.00 (s, 9H); **^{13}C NMR** (125 MHz, $CDCl_3$) δ 169.70, 167.12, 159.69, 157.65, 144.29, 137.47, 134.65, 134.45, 130.04, 124.14, 123.29, 123.07, 120.90, 119.79, 119.45, 117.23, 115.61, 92.84, 66.56, 58.33, 57.60, 53.02, 33.18, 24.36, 18.09, -1.42; **$[\alpha]^{25}_D$** –56.4 (c = 0.45 in $CHCl_3$); **IR** (film) 2954, 2359, 2341, 1749 (C=O), 1652 (C=O), 1581 (C=O), 1488, 1427, 1398, 1207, 1137, 1086, 1005, 990, 917, 857, 832, 744, 693, 667, 605; **HRMS** Accurate mass (ES^+): Found 548.1028, $C_{20}H_{26}NO_8SSiNa$ ($M+Na^+$) requires 548.0998.

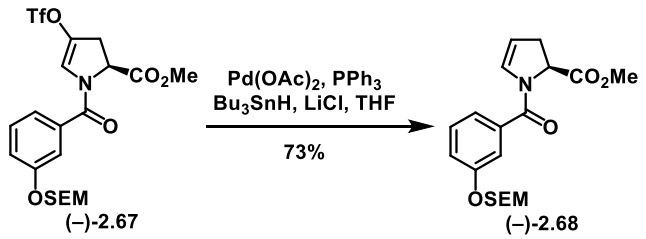

Methyl (S)-1-(3-((2-(trimethylsilyl)ethoxy)methoxy)benzoyl)-2,3-dihydro-1H-pyrrole-2-carboxylate (–)-2.68. (synthesized by Colleen Keohane) Using the procedure given for the preparation of compound **(–)-2.23**, triflate **(–)-2.67** (90 mg, 0.171 mmol) yielded the title compound as a yellow oil (47 mg, 73% yield). **^{1}H NMR** (500 MHz, $CDCl_3$) δ 7.33 (t, J = 7.9 Hz, 1H), 7.23 (s, 1H), 7.18 (d, J = 7.6 Hz, 1H), 7.14 (d, J = 8.4 Hz, 1H), 6.58 – 6.52 (m, 1H), 5.23 (s, 2H), 5.11 (d, J = 5.1 Hz, 1H), 5.01 (dd, J = 11.6, 5.0 Hz, 1H), 3.80 (s, 3H), 3.77 – 3.72 (m, 2H), 3.15 – 3.06 (m, 1H), 2.76 – 2.67 (m, 1H), 0.98 – 0.93 (m, 2H), 0.00 (s, 9H); **^{13}C NMR** (100 MHz, $CDCl_3$) δ 171.56, 166.75, 157.46, 136.25, 130.97, 129.71, 121.15, 118.65, 115.86, 109.05, 92.95, 66.49, 58.51, 52.64, 33.87, 18.14, -1.31; **$[\alpha]^{25}_D$** –44.0 (c = 0.31 in $CHCl_3$); **IR** (film) 2953, 2359, 2341, 1749 (C=O), 1646, 1617, 1488, 1446, 1398, 1362, 1317, 1086, 1005, 989, 858, 834, 694, 668; **HRMS** Accurate mass (ES^+): Found 378.1706, $C_{19}H_{28}NO_5Si$ ($M+H^+$) requires 378.1737.

(7R,13R)-14-amino-13-((tert-butyldimethylsilyl)oxy)-14-oxotetradecan-7-yl (S)-1-(3-((2-(trimethylsilyl)ethoxy)methoxy)benzoyl)-2,3-dihydro-1H-pyrrole-2-carboxylate (–)-2.69. (synthesized by Colleen Keohane) Using the procedure given above for LiOH hydrolysis, methyl ester **(–)-2.68** (26 mg, 0.069 mmol) was converted to the corresponding acid, which was unstable

and carried directly to the next step. To a solution of the acid intermediate (25 mg, 0.069 mmol) dissolved in CH_2Cl_2 (2 mL) was added MNBA (24 mg, 0.069 mmol) and Et_3N (0.03 mL, 0.190 mmol), and the solution was stirred for 10 minutes. Then alcohol **(+)-2.15** (21 mg, 0.057 mmol) and DMAP (1 mg, 0.057 mmol) dissolved in CH_2Cl_2 (2 mL) was added, and the reaction was stirred overnight. The reaction was poured into sat. NH_4Cl, extracted with CH_2Cl_2 3x, washed with brine, dried over $MgSO_4$, filtered, concentrated, and purified by column chromatography (0 → 30% Et_2O/CH_2Cl_2), yielding the title compound as a yellow oil (24 mg, 57% yield, 2 steps). **^{1}H NMR** (500 MHz, $CDCl_3$) δ 7.32 (q, J = 7.8 Hz, 1H), 7.20 (s, J = 11.1 Hz, 1H), 7.15 (dd, J = 15.5, 7.9 Hz, 2H), 6.52 (s, 2H), 5.54 – 5.44 (m, 1H), 5.23 (s, 2H), 5.08 (d, J = 1.9 Hz, 1H), 5.01 – 4.90 (m, 2H), 4.17 – 4.08 (m, 1H), 3.80 – 3.67 (m, 2H), 3.15 – 3.06 (m, 1H), 2.67 (d, J = 16.9 Hz, 1H), 1.81 – 1.70 (m, 1H), 1.69 – 1.47 (m, 7H), 1.26 (dd, J = 14.1, 6.9 Hz, 17H), 0.97 – 0.89 (m, 12H), 0.85 (t, J = 6.9 Hz, 3H), 0.10 – 0.06 (m, 6H), -0.01 (s, J = 3.2 Hz, 9H); **13C NMR** (100 MHz, $CDCl_3$) δ 176.94, 170.86, 166.62, 157.49, 136.52, 131.08, 129.70, 121.13, 118.46, 115.85, 108.87, 92.97, 75.62, 73.60, 66.51, 58.80, 35.13, 34.05, 31.85, 29.85, 29.51, 29.32, 25.89, 25.31, 25.08, 24.11, 22.72, 18.17, 14.22, -1.28, -4.68, -5.12; **$[\alpha]^{25}_D$** –16.1 (c = 1.18 in $CHCl_3$); **IR (**film) 3480, 2927, 2867, 1739 (C=O), 1689 (C=O), 1651 (C=O), 1618, 1579, 1488, 1446, 1397, 1248, 1192, 1088, 1029, 1005, 991, 938, 857, 834, 778, 745, 694, 668; **HRMS** Accurate mass (ES^+): Found 719.4445, $C_{38}H_{67}N_2O_7Si_2$ ($M+H^+$) requires 719.4487.

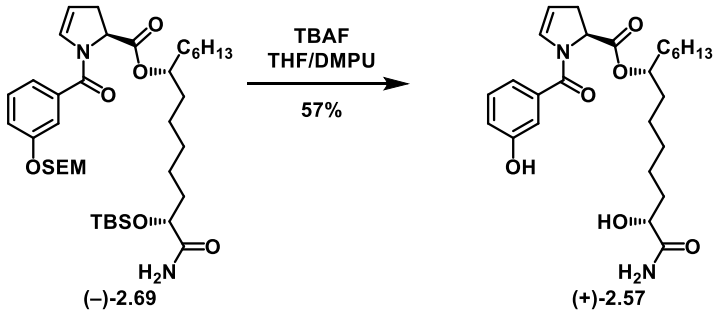

(7R,13R)-14-amino-13-hydroxy-14-oxotetradecan-7-yl (S)-1-(3-hydroxybenzoyl)-2,3-dihydro-1H-pyrrole-2-carboxylate (+)-2.57. (synthesized by Colleen Keohane) Using the

procedure given for the preparation of compound **(–)-2.1a**, silyl ether **(–)-2.69** (24 mg, 0.033 mmol) yielded the title compound as a clear oil (9 mg, 57% yield) after purification by column chromatography (50 → 100% EtOAc/hexanes). **^{1}H NMR** (400 MHz, $CDCl_3$) δ 7.22 (d, J = 7.8 Hz, 1H), 7.05 – 6.87 (m, 5H), 6.57 (s, 1H), 5.91 (s, 1H), 5.16 (s, 1H), 5.09 – 5.01 (m, 1H), 4.93 (dd, J = 11.4, 5.1 Hz, 1H), 4.12 – 4.02 (m, 1H), 3.18 – 3.07 (m, 1H), 2.67 (d, J = 17.3 Hz, 1H), 1.87 – 1.76 (m, 1H), 1.61 – 1.23 (m, 27H) 0.88 (t, J = 5.6 Hz, 3H); **^{13}C NMR** (100 MHz, $CDCl_3$) δ 178.78, 171.03, 167.83, 167.38, 157.46, 157.32, 135.46, 130.94, 129.78, 118.82, 115.06, 110.10, 75.42, 71.04, 58.70, 34.90, 34.43, 33.97, 33.75, 31.85, 29.84, 29.24, 27.91, 25.63, 24.83, 24.60, 22.70, 14.21; **$[\alpha]^{25}_D$** +14.4 (c = 0.90 in $CHCl_3$); **IR** (film) 3195 (br, O-H), 2925, 2856, 1732 (C=O), 1662 (C=O), 1579, 1416, 1273, 1196, 998, 880, 746; **HRMS** Accurate mass (ES^+): Found 475.2838 (+6.3 ppm), $C_{26}H_{39}N_2O_6$ ($M+H^+$) requires 475.2808.

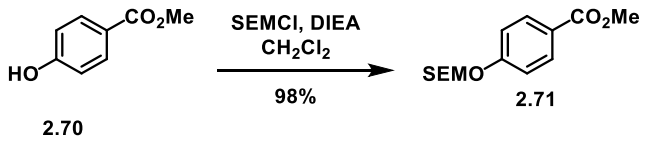

2.70 **2.71**

Methyl 4-((2-(trimethylsilyl)ethoxy)methoxy)benzoate 2.71. Using the procedure given for the preparation of **2.14**, methyl 4-hydroxybenzoate (250 mg, 1.640 mmol) yielded the title compound as a clear oil (454 mg, 98% yield). **^{1}H NMR** (500 MHz, $CDCl_3$) δ 7.99 (dd, J = 8.9, 1.9 Hz, 2H), 7.05 (dd, J = 8.8, 1.9 Hz, 2H), 5.27 (s, J = 1.8 Hz, 2H), 3.89 (s, 3H), 3.78 – 3.73 (m, 2H), 0.95 (s, 2H), -0.01 (s, 9H); **^{13}C NMR** (125 MHz, $CDCl_3$) δ 166.96, 161.32, 131.63, 123.55, 115.75, 92.71, 66.73, 52.02, 18.17, -1.28, -1.31; **IR** (film) 2952, 2896, 1717 (C=O), 1605, 1580, 1510, 1435, 1381, 1315, 1276, 1234, 1191, 1168, 1090, 1013, 986, 938, 917, 851, 834, 770, 696, 668, 610; **HRMS** Accurate mass (ES^+): Found 283.1373, $C_{14}H_{23}O_4Si$ ($M+H^+$) requires 283.1366.

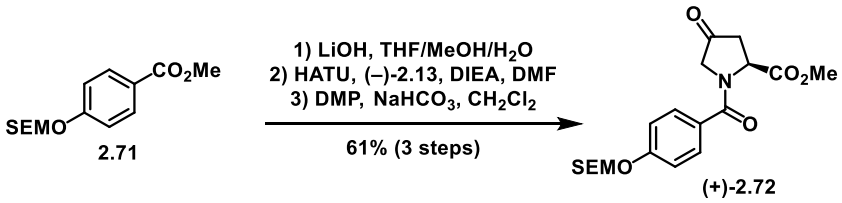

Methyl (2S)-4-oxo-1-(4-{[2-(trimethylsilyl)ethoxy]methoxy}benzoyl)pyrrolidine-2-carboxylate (+)-2.72. Using the procedure given for the preparation of compound **2.19**, methyl ester **2.71** (445 mg, 1.577 mmol) yielded the corresponding acid, which was used directly in the next step. Using the procedure given for the preparation of compound **(–)-2.20**, the acid yielded the corresponding acylhydroxyproline methyl ester compound, whose purity made it unsuitable for characterization. Using the procedure given for the preparation of compound **(+)-2.21** on this intermediate then yielded the title compound as a yellow oil (394 mg, 61% over 3 steps). **^{1}H NMR** (500 MHz, $CDCl_3$) δ 7.49 (br s, J = 12.1 Hz, 2H), 7.12 – 7.06 (m, 2H), 5.25 (s, 2H), 3.83 – 3.72 (m, 5H), 2.96 (dd, J = 18.8, 10.5 Hz, 1H), 2.69 (dd, J = 18.8, 2.2 Hz, 1H), 1.03 – 0.91 (m, 2H), -0.00 (s, J = 3.3 Hz, 9H); **^{13}C NMR** (100 MHz, $CDCl_3$) δ 207.52, 207.36, 171.78, 171.05, 170.65, 159.54, 129.46, 129.22, 127.41, 125.35, 116.02, 115.53, 92.59, 66.57, 65.02, 52.91, 18.00, -1.42; **$[\alpha]^{25}_{D}$** –24.2 (c = 1.39 in $CHCl_3$); **IR** (film) 2953, 1764 (C=O), 1745 (C=O), 1606 (C=O), 1513, 1404, 1230, 1168, 1090, 1025, 986, 918, 834, 764, 692, 612; **HRMS** Accurate mass (ES^+): Found 394.1698, $C_{19}H_{28}NO_6Si$ ($M+H^+$) requires 394.1686.

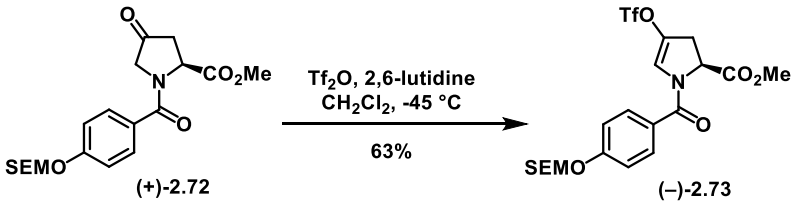

Methyl (2S)-4-(trifluoromethanesulfonyloxy)-1-(4-{[2-(trimethylsilyl)ethoxy]methoxy}benzoyl)-2,3-dihydro-1H-pyrrole-2-carboxylate (–)-2.73. Using the procedure given for the preparation of compound **(–)-2.22**, ketone **(+)-2.72** (100 mg,

0.254 mmol) yielded the title compound as a yellow oil (85 mg, 63% yield). **^{1}H NMR** (400 MHz, $CDCl_3$) δ 7.52 (d, J = 8.7 Hz, 2H), 7.10 (d, J = 8.7 Hz, 2H), 6.87 (s, 1H), 5.27 (s, 2H), 5.08 (dd, J = 11.6, 5.1 Hz, 1H), 3.82 (s, 3H), 3.80 – 3.72 (m, 2H), 3.44 – 3.35 (m, 1H), 2.97 (ddd, J = 16.4, 5.1, 1.6 Hz, 1H), 1.00 – 0.91 (m, 2H), 0.00 (s, 9H); **^{13}C NMR** (125 MHz, $CDCl_3$) δ 169.86, 167.25, 160.10, 134.28, 129.89, 126.40, 123.58, 119.82, 117.26, 116.24, 92.72, 66.71, 57.83, 53.01, 33.25, 29.79, 18.12, -1.36; **$[\alpha]^{25}_D$** –18.5 (c = 0.20 in 2:1 $CHCl_3$/MeOH); **IR** (film) 2954, 2899, 1750 (C=O), 1644, 1606, 1512, 1424, 1398, 1306, 1280, 1208, 1170, 1136, 1091, 1027, 987, 935, 910, 833, 759, 694, 644, 607; **HRMS** Accurate mass (ES^+): Found 526.1148, $C_{20}H_{27}F_3NO_8SSi$ ($M+H^+$) requires 526.1179.

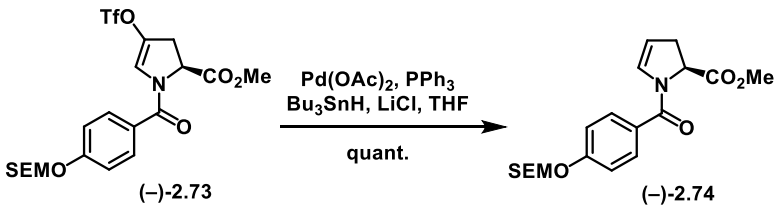

Methyl (2S)-1-(4-{[2-(trimethylsilyl)ethoxy]methoxy}benzoyl)-2,3-dihydro-1H-pyrrole-2-carboxylate (–)-2.74. Using the procedure given for the preparation of compound **(–)-2.23**, triflate **(–)-2.73** (62 mg, 0.117 mmol) yielded the title compound as a yellow oil (47 mg, quant. yield). **R_f** (3:1 hexanes:EtOAc) = 0.20; **^{1}H NMR** (400 MHz, $CDCl_3$) δ 7.53 (d, J = 8.5 Hz, 2H), 7.08 – 7.03 (m, 2H), 6.60 (s, 1H), 5.25 (s, 2H), 5.11 (s, 1H), 5.04 – 4.95 (m, 1H), 3.84 – 3.71 (m, 5H), 3.17 – 3.03 (m, 1H), 2.77 – 2.66 (m, 1H), 0.97 – 0.90 (m, 2H), -0.01 (s, J = 3.3 Hz, 9H); **^{13}C NMR** (125 MHz, $CDCl_3$) δ 171.72, 166.83, 159.49, 131.22, 129.91, 128.10, 115.94, 108.69, 92.76, 66.60, 58.70, 52.59, 33.82, 18.16, -1.31; **$[\alpha]^{25}_D$** –60.2 (c = 1.22 in MeOH); **IR** (film) 2952, 2924, 2872, 1749 (C=O), 1644 (C=O), 1606, 1574, 1511, 1396, 1362, 1291, 1231, 1201, 1170, 1089, 1023, 985, 917, 834, 759, 694, 582; **HRMS** Accurate mass (ES^+): Found 378.1710, $C_{19}H_{28}NO_5Si$ ($M+H^+$) requires 378.1737.

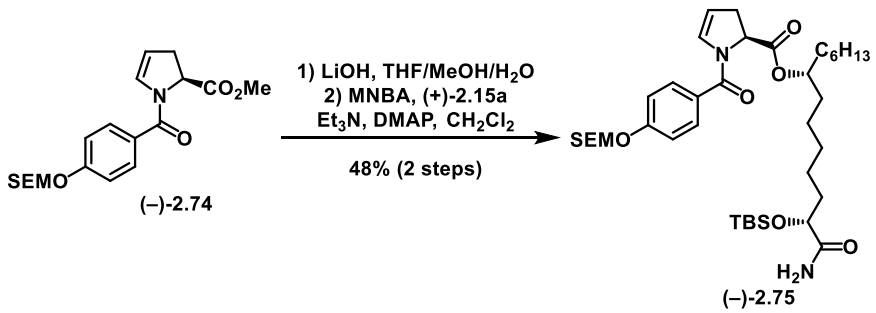

(1R,7R)-1-[(tert-butyldimethylsilyl)oxy]-1-carbamoyltridecan-7-yl (2S)-1-(4-{[2-(trimethylsilyl)ethoxy]methoxy}benzoyl)-2,3-dihydro-1H-pyrrole-2-carboxylate (–)-2.75. Using the procedure given above for LiOH hydrolysis, methyl ester **(–)-2.74** (22 mg, 0.055 mmol) was converted to the corresponding acid, which was unstable and carried directly to the next step. To a solution of the acid intermediate (21 mg, 0.055 mmol) dissolved in CH_2Cl_2 (2 mL) was added MNBA (19 mg, 0.055 mmol) and Et_3N (0.02 mL, 0.152 mmol), and the solution was stirred for 10 minutes. Then alcohol **(+)-2.15** (17 mg, 0.046 mmol) and DMAP (1 mg, 0.005 mmol) dissolved in CH_2Cl_2 (2 mL) was added, and the reaction was stirred overnight. The reaction was poured into sat. NH_4Cl, extracted with CH_2Cl_2 3x, washed with brine, dried over $MgSO_4$, filtered, concentrated, and purified by column chromatography (0 → 30% Et_2O/CH_2Cl_2), yielding the title compound as a yellow oil (19 mg, 48% yield, 2 steps). **^{1}H NMR** (500 MHz, $CDCl_3$) δ 7.52 (d, J = 8.6 Hz, 2H), 7.05 (d, J = 8.6 Hz, 2H), 6.60 – 6.51 (m, 2H), 5.45 (m, 2H), 5.25 (s, 2H), 5.09 (s, 1H), 5.01 – 4.89 (m, 2H), 4.88 – 4.81 (m, 1H), 4.15 – 4.12 (m, 2H), 3.78 – 3.72 (m, 2H), 3.14 – 3.06 (m, 1H), 2.71 – 2.64 (m, 1H), 1.80 – 1.70 (m, 1H), 1.69 – 1.65 (m, 1H), 1.61 – 1.47 (m, 7H), 1.40 – 1.17 (m, 27H), 0.91 (s, 9H), 0.86 (t, J = 8.0 Hz, 3H), 0.08 (d, J = 6.0 Hz, 6H), -0.00 (s, 9H); **^{13}C NMR** (125 MHz, $CDCl_3$) δ 176.97, 171.07, 166.70, 159.41, 131.32, 129.85, 128.40, 115.93, 108.50, 92.80, 75.56, 74.45, 73.60, 66.61, 58.98, 35.20, 35.15, 34.26, 34.18, 34.02, 31.84, 29.56, 29.51, 29.32, 25.88, 25.40, 25.33, 25.28, 25.07, 24.18, 24.12, 22.71, 21.42, 18.18, 14.20, -1.30, -4.69, -5.12; **$[\alpha]^{25}_D$** –16.8 (c = 0.95 in $CHCl_3$); **IR** (film) 2926, 2856, 1733 (C=O), 1688 (C=O), 1645 (C=O), 1607, 1510, 1463, 1396, 1248, 1195, 1169, 1089, 991,

939, 760, 713, 580; **HRMS** Accurate mass (ES^+): Found 719.4447 (-5.6 ppm), $C_{38}H_{67}N_2O_7Si_2$ ($M+H^+$) requires 719.4487.

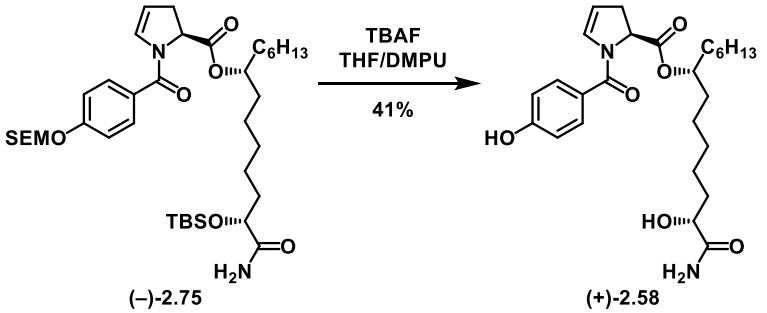

(1R,7R)-1-carbamoyl-1-hydroxytridecan-7-yl (2S)-1-(4-hydroxybenzoyl)-2,3-dihydro-1H-pyrrole-2-carboxylate (+)-2.58. Using the procedure given for the preparation of compound **(–)-2.1a**, silyl ether **(–)-2.75** (19 mg, 0.026 mmol) yielded the title compound as a clear oil (5.3 mg, 41% yield). **^{1}H NMR** (500 MHz, $CDCl_3$) δ 8.11 (s, 1H), 7.38 (d, J = 7.9 Hz, 2H), 6.94 (s, 1H), 6.79 (d, J = 8.1 Hz, 2H), 6.53 (d, J = 45.0 Hz, 1H), 5.63 (s, 1H), 5.17 (s, 1H), 4.96 (s, 2H), 4.03 (s, 2H), 3.18 – 3.09 (m, 1H), 2.69 (d, J = 16.8 Hz, 1H), 1.77 – 1.12 (m, 37H), 0.87 (t, J = 6.8 Hz, 3H); **^{13}C NMR** (125 MHz, $CDCl_3$) δ 171.12, 168.20, 159.37, 131.12, 129.98, 115.68, 109.85, 74.51, 70.77, 60.57, 58.82, 34.80, 34.27, 34.21, 34.06, 31.85, 29.85, 29.32, 29.25, 28.97, 27.62, 25.60, 25.45, 25.23, 24.78, 24.32, 22.70, 21.47, 14.34, 14.21; **$[\alpha]^{25}_D$** +17.9 (c = 0.24 in $CHCl_3$); **IR** (film) 3300 (br O-H), 2956, 2923, 2853, 2361, 2341, 2159, 2028, 1976, 1733, 1669, 1653, 1609, 1558, 1516, 1507, 1467, 1436, 1378, 1260, 1198, 1165, 1093, 1021, 948, 847, 798, 761, 721, 667; **HRMS** Accurate mass (ES^+): Found 475.2804 (-0.8 ppm), $C_{26}H_{39}N_2O_6$ ($M+H^+$) requires 475.2808.

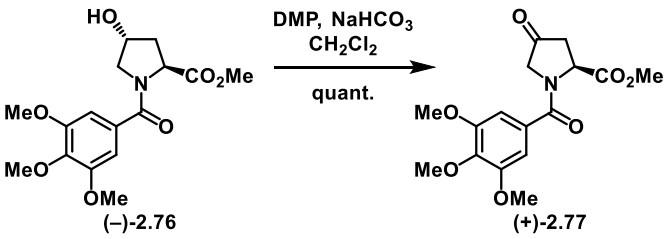

Methyl (2S)-4-oxo-1-(3,4,5-trimethoxybenzoyl)pyrrolidine-2-carboxylate (+)-2.77. (synthesized by Kyle Knouse) Using the procedure given for the preparation of compound **(+)-2.21**, alcohol **(–)-2.76** (prepared as previously described: Li, X.; Li, Y.; Xu, W. *Bioorg. & Med. Chem.* **2006**, *14*, 1287) (1.34 g, 3.950 mmol) yielded the title compound as a white foam (1.33 g, quant. yield). **^{1}H NMR** (400 MHz, $CDCl_3$) δ 6.66 (s, 2H), 5.19 (br s, 1H), 3.97 (br s, 1H), 3.83 – 3.67 (m, 12H), 2.91 (dd, J = 18.8, 10.5 Hz, 1H), 2.59 (d, J = 18.6 Hz, 1H); **^{13}C NMR** (100 MHz, CDCl3) δ 207.11, 171.59, 170.16, 153.24, 139.94, 129.95, 104.43, 77.36, 60.80, 56.19, 52.80; **$[\alpha]^{25}_D$** +4.4 (c = 0.45 in 2:1 $CHCl_3$/MeOH); **IR** (film) 3451, 2953, 2360, 1728 (C=O), 1633 (C=O), 1580, 1506, 1448, 1414, 1324, 1238, 1179, 1119, 998, 922, 879, 840, 763, 723, 691, 603; **HRMS** Accurate mass (ES^+): Found 360.1072, $C_{16}H_{19}NO_7Na$ ($M+Na^+$) requires 360.1059.

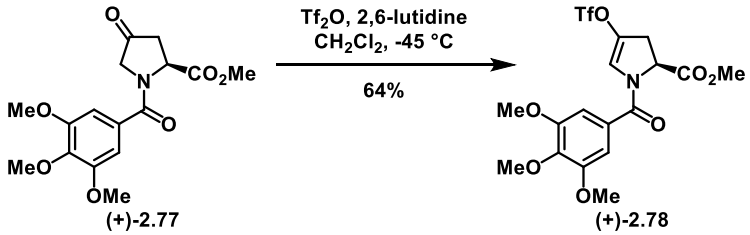

Methyl (2S)-4-(trifluoromethanesulfonyloxy)-1-(3,4,5-trimethoxybenzoyl)-2,3-dihydro-1H-pyrrole-2-carboxylate (+)-2.78. (synthesized by Kyle Knouse) Using the procedure given for the preparation of compound **(–)-2.22**, ketone **(+)-2.77** (145 mg, 0.431 mmol) yielded the title compound as an orange oil (129 mg, 64% yield). **^{1}H NMR** (500 MHz, $CDCl_3$) δ 6.90 (s, 1H), 6.75 (s, 2H), 5.10 – 5.00 (m, 1H), 3.88 – 3.78 (m, 12H), 3.40 (dd, J = 15.2, 13.1 Hz, 1H), 3.00 – 2.90 (m, 1H); **^{13}C NMR** (125 MHz, $CDCl_3$) δ 169.72, 167.22, 153.49, 140.84, 134.51, 128.35, 123.32, 105.35, 61.03, 56.37, 53.10; **$[\alpha]^{25}_D$** +7.3 (c = 0.26 in $CHCl_3$); **IR** (film) 2953, 2359, 1745 (C=O), 1636 (C=O), 1582, 1413, 1326, 1234, 1120, 999, 924, 819, 760, 725, 637, 605; **HRMS** Accurate mass (ES^+): Found 470.0756, $C_{17}H_{19}F_3NO_9S$ ($M+H^+$) requires 470.0733.

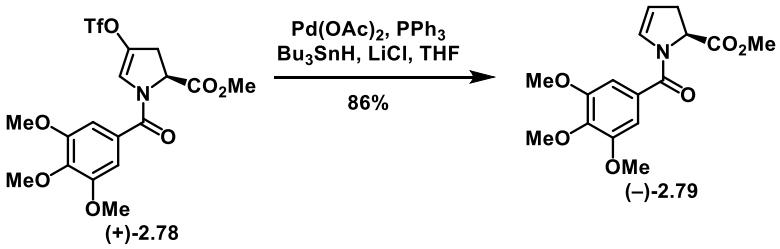

Methyl (2S)-1-(3,4,5-trimethoxybenzoyl)-2,3-dihydro-1H-pyrrole-2-carboxylate (–)-2.79. (synthesized by Kyle Knouse) Using the procedure given for the preparation of compound **(–)-2.23**, triflate **(+)-2.78** (110 mg, 0.234 mmol) yielded the title compound as a yellow oil (61 mg, 86% yield). **^{1}H NMR** (500 MHz, $CDCl_3$) δ 6.78 (s, 2H), 6.60 (s, 1H), 5.13 (s, 1H), 4.98 (dd, J = 11.2, 4.6 Hz, 1H), 3.91 – 3.76 (m, 12H), 3.16 – 3.07 (m, 1H), 2.71 (ddd, J = 17.0, 4.7, 2.3 Hz, 1H); **[α]$^{25}_{D}$** –48.3 (c = 0.40 in $CHCl_3$); **^{13}C NMR** (125 MHz, $CDCl_3$) δ 171.56, 166.79, 153.30, 140.20, 131.00, 130.21, 109.13, 105.39, 61.02, 58.61, 56.43, 52.65, 33.81; **IR** (film) 2997, 2950, 2832, 1751 (C=O), 1642 (C=O), 1619, 1582, 1506, 1462, 1404, 1361, 1315, 1235, 1196, 1177, 1143, 1119, 1000, 964, 895, 850, 810, 754, 734, 675, 570; **HRMS** Accurate mass (ES^+): Found 344.1087(-6.7 ppm), $C_{16}H_{19}NO_6Na$ ($M+Na^+$) requires 344.1110.

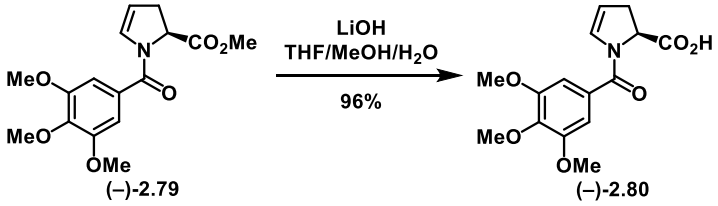

(2S)-1-(3,4,5-trimethoxybenzoyl)-2,3-dihydro-1H-pyrrole-2-carboxylic acid (–)-2.80. (synthesized by Kyle Knouse) Using the procedure for LiOH hydrolysis given above, methyl ester **(–)-2.79** (55 mg, 0.180 mmol) yielded the title compound as a yellow oil (50 mg, 96% yield). **^{1}H NMR** (400 MHz, $CDCl_3$) δ 6.83 – 6.76 (m, 2H), 6.55 (s, 1H), 5.28 (d, J = 11.1 Hz, 1H), 5.06 (d, J = 6.1 Hz, 1H), 3.92 – 3.83 (m, 12H), 3.14 – 3.00 (m, 2H); **^{13}C NMR (**100 MHz, $CDCl_3$) δ 173.49, 167.90, 153.29, 140.45, 132.30, 132.20, 130.28, 129.39, 128.76, 128.64, 110.99, 105.54, 68.02, 61.02, 59.25, 56.42; **[α]$^{25}_{D}$** –104.3 (c = 0.29 in $CHCl_3$); **IR** (film) 3269,

2954, 2899, 1747 (C=O), 1631 (C=O), 1605, 1467, 1425, 1363, 1311, 1208, 1136, 1028, 912, 833, 755, 693, 665, 605; **HRMS** Accurate mass (ES^+): Found 308.1148, $C_{15}H_{18}NO_6$ ($M+H^+$) requires 308.1134.

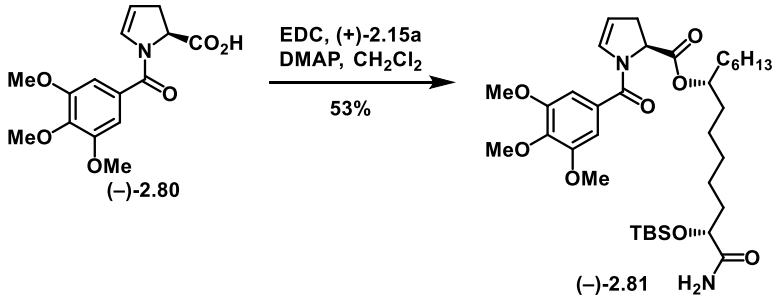

(1R,7R)-1-[(tert-butyldimethylsilyl)oxy]-1-carbamoyltridecan-7-yl (2S)-1-(3,4,5-trimethoxybenzoyl)-2,3-dihydro-1H-pyrrole-2-carboxylate (–)-2.81. (synthesized by Kyle Knouse) Using the procedure given for the preparation of compound **(–)-2.32a**, acid **(–)-2.80** (26 mg, 0.085 mmol) yielded the title compound as a yellow oil (21 mg, 53% yield). **^{1}H NMR** (500 MHz, $CDCl_3$) δ 6.78 (s, 2H), 6.58 (s, 1H), 6.53 (d, J = 4.1 Hz, 1H), 5.47 (d, J = 4.1 Hz, 1H), 5.12 (s, 1H), 5.01 – 4.91 (m, 2H), 4.13 (t, J = 5.1 Hz, 1H), 3.87 (s, 9H), 3.16 – 3.06 (m, 1H), 2.68 (d, J = 16.5 Hz, 1H), 1.80 – 1.71 (m, 1H), 1.68 – 1.46 (m, 10H), 1.39 – 1.16 (m, 20H), 0.91 (s, J = 6.5 Hz, 9H), 0.86 (t, J = 7.0 Hz, 3H), 0.08 (d, J = 5.8 Hz, 6H); **^{13}C NMR** (100 MHz, $CDCl_3$) δ 177.02, 170.84, 166.66, 153.28, 140.01, 131.08, 130.50, 129.10, 108.95, 105.25, 75.67, 73.52, 61.03, 58.84, 56.39, 35.10, 34.01, 31.83, 29.49, 29.31, 25.85, 25.30, 25.03, 24.06, 22.69, 18.13, 14.18, -4.72, -5.15; **$[\alpha]^{25}_D$** –34.7 (c = 0.86 in $CHCl_3$); **IR** (film) 3480, 2927, 2856, 1738 (C=O), 1687 (C=O), 1645 (C=O), 1616, 1582, 1506, 1456, 1414, 1358, 1236, 1192, 1126, 1004, 951, 836, 810, 778, 720, 671; **HRMS** Accurate mass (ES^+): Found 663.4066, $C_{35}H_{59}N_2O_8Si$ ($M+H^+$) requires 663.4041.

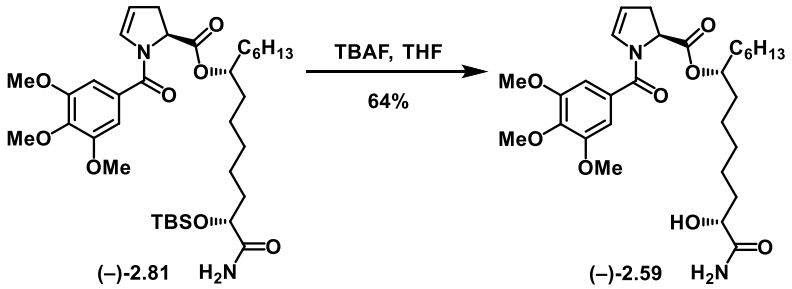

(1R,7R)-1-carbamoyl-1-hydroxytridecan-7-yl (2S)-1-(3,4,5-trimethoxybenzoyl)-2,3-dihydro-1H-pyrrole-2-carboxylate (–)-2.59. (synthesized by Kyle Knouse) To a solution of silyl ether **(–)-2.81** (12.5 mg, 0.0189 mmol) dissolved in THF (0.5 mL) was added TBAF (0.094 mL, 1M in THF, 0.094 mmol). After 20 minutes, the reaction was diluted with Et_2O, and washed with sat. NH_4Cl 4x, dried over Na_2SO_4, filtered, concentrated, and purified by preparative TLC (100% EtOAc), yielding the title compound as a clear oil (6.7 mg, 64% yield). **^{1}H NMR** (500 MHz, $CDCl_3$) δ 6.96 – 6.66 (t, J = 14.9 Hz, 2H), 6.57 (s, 1H), 5.20 (dd, J = 64.4, 27.8 Hz, 2H), 5.11 – 4.96 (m, 1H), 4.96 – 4.85 (m, 1H), 4.28 (d, J = 25.3 Hz, 1H), 4.05 (d, J = 39.2 Hz, 1H), 3.87 (s, J = 6.2 Hz, 9H), 3.13 (s, 1H), 2.69 (d, J = 16.0 Hz, 1H), 1.82 (s, 1H), 1.75 – 1.40 (m, 12H), 1.35 – 1.16 (m, 10H), 0.87 (s, J = 6.3 Hz, 3H); **^{13}C NMR** (125 MHz, $CDCl_3$) δ 177.45, 170.66, 167.47, 153.39, 140.28, 130.92, 129.85, 110.16, 109.95, 105.18, 75.30, 70.81, 61.09, 58.71, 56.48, 34.77, 34.04, 33.98, 33.81, 31.85, 29.25, 27.53, 25.59, 24.67, 24.28, 22.69, 14.20; **$[\alpha]^{25}_D$** –32.4 (c = 0.67 in $CHCl_3$); **IR** (film) 3337 (br O-H), 2927, 2856, 1733 (C=O), 1668 (C=O), 1614 (C=O), 1581, 1506, 1414, 1318, 1236,1194, 1124, 1002, 951, 853, 810, 756, 722, 674**; HRMS** Accurate mass (ES^+): Found 549.3152, $C_{29}H_{45}N_2O_8$ ($M+H^+$) requires 283.1366.

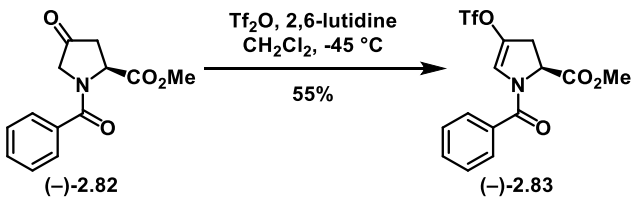

Methyl (2S)-1-benzoyl-4-(trifluoromethanesulfonyloxy)-2,3-dihydro-1H-pyrrole-2-carboxylate (–)-2.83. Using the procedure given for the preparation of compound **(–)-2.22**, ketone **(–)-2.82** (prepared as previously described: Yoshifuji, S.; Kaname, M. *Chem. Pharm. Bull.* **1995**, *43*, 1302 with the procedure given for the preparation of compound **(+)-2.21** used in place of Swern oxidation) (50 mg, 0.202 mmol) yielded the title compound as an orange oil (44 mg, 55% yield). **^{1}H NMR** (500 MHz, $CDCl_3$) δ 7.59 – 7.43 (m, 5H), 6.79 (s, 1H), 5.16 – 5.05 (m, 1H), 3.83 (s, 3H), 3.45 – 3.37 (m, 1H), 2.98 (ddd, J = 16.5, 4.9, 1.6 Hz, 1H); **^{13}C NMR** (100 MHz, $CDCl_3$) δ 169.78, 167.56, 134.52, 133.50, 131.67, 128.95, 127.93, 123.31, 120.14, 116.95, 77.16, 57.65, 53.12, 33.26; **$[\alpha]^{25}_D$** –47.6 (c = 1.49 in $CHCl_3$); **IR** (film) 2957, 2921, 2851, 2361, 2160, 2031, 1979, 1749 (C=O), 1648 (C=O), 1578, 1495, 1448, 1426, 1404, 1306, 1208, 1135, 1029, 937, 909, 843, 752, 721, 702, 669; **HRMS** Accurate mass (ES^+): Found 402.0244, $C_{14}H_{12}F_3NO_6SNa$ ($M+Na^+$) requires 402.0235.

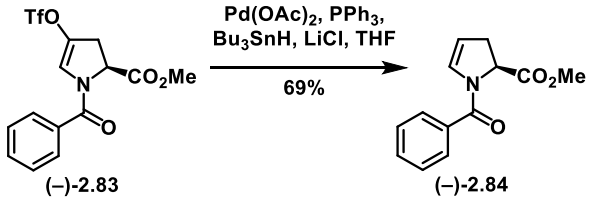

Methyl (2S)-1-benzoyl-2,3-dihydro-1H-pyrrole-2-carboxylate (–)-2.84. Using the procedure given for the preparation of compound **(–)2.23**, triflate **(–)-2.83** (100 mg, 0.252 mmol) yielded the title compound as a yellow oil (40 mg, 69% yield). **^{1}H NMR** (500 MHz, $CDCl_3$) δ 7.57 (d, J = 7.3 Hz, 2H), 7.50 – 7.37 (m, 3H), 6.53 (s, 1H), 5.12 (s, 1H), 5.02 (dd, J = 11.5, 5.0 Hz, 1H), 3.81 (s, 3H), 3.15 – 3.07 (m, 1H), 2.72 (d, J = 16.9 Hz, 1H); **^{13}C NMR** (125 MHz, $CDCl_3$) δ 171.6, 167.2, 135.1, 131.0, 130.9, 128.6, 128.0, 109.1, 58.5, 52.7, 33.9; **$[\alpha]^{25}_D$** –110.8 (c = 1.00 in $CHCl_3$); **IR** (film) 2953, 2923, 2160, 2029, 1979, 1747 (C=O), 1641, 1615, 1576, 1496, 1447, 1403, 1362, 1290, 1201, 1179, 1106, 1016, 936, 841, 790, 724, 700, 662; **HRMS** Accurate mass (ES^+): Found 254.0813, $C_{13}H_{13}NO_3Na$ ($M+Na^+$) requires 254.0793.

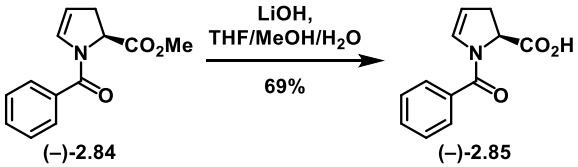

(2S)-1-benzoyl-2,3-dihydro-1H-pyrrole-2-carboxylic acid (–)-2.85. Using the procedure for LiOH hydrolysis given above, methyl ester **(–)-2.84** (37 mg, 0.160 mmol) yielded the title compound as a yellow oil (24 mg, 69% yield). **^{1}H NMR** (500 MHz, $CDCl_3$) δ 7.61 – 7.43 (m, 5H), 6.47 (s, 1H), 5.30 (s, 1H), 5.12 (d, J = 7.5 Hz, 1H), 3.19 (d, J = 17.1 Hz, 1H), 3.10 – 3.02 (m, 1H); **^{13}C NMR** (100 MHz, $CDCl_3$) δ 173.24, 168.67, 131.41, 130.06, 128.71, 128.56, 128.23, 111.50, 59.52, 32.97, 29.83; **$[\alpha]^{25}_{D}$** –85.3 (c = 1.20 in $CHCl_3$); **IR** (film) 3061 (br, CO_2-H), 2953, 2924, 2918, 1716 (C=O), 1596 (C=O), 1573, 1497, 1448, 1408, 1352, 1315, 1289, 1195, 1106, 1017, 941, 846, 787, 753, 719, 700, 660; **HRMS** Accurate mass (ES^+): Found 218.0825 (+3.2 ppm), $C_{12}H_{12}NO_3$ ($M+H^+$) requires 218.0818.

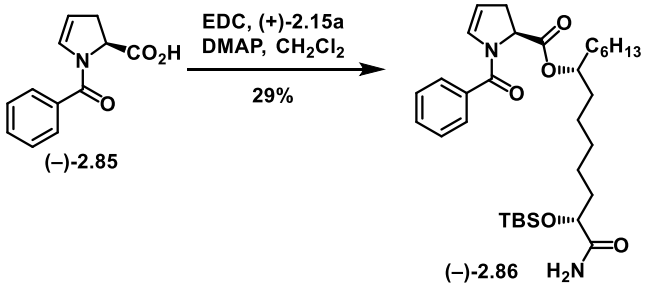

(1R,7R)-1-[(tert-butyldimethylsilyl)oxy]-1-carbamoyltridecan-7-yl (2S)-1-benzoyl-2,3-dihydro-1H-pyrrole-2-carboxylate (–)-2.86. Using the EDC procedure given above (1.2 eq acid, 1.5 eq EDC, 1.0 eq alcohol, 0.5 eq DMAP), acid **(–)-2.85** (24 mg, 0.111 mmol) after purification by preparative TLC (2:1 CH_2Cl_2:Et_2O), yielded the title compound as a clear oil (15 mg, 29% yield). **R_f** (2:1 CH_2Cl_2:Et_2O) = 0.70; **^{1}H NMR** (500 MHz, CDCl3) δ 7.57 (d, J = 7.5 Hz, 2H), 7.45 (dt, J = 14.5, 7.1 Hz, 3H), 6.53 (s, 2H), 5.58 (s, 1H), 5.02 (dd, J = 11.5, 4.7 Hz, 1H), 4.98 – 4.94 (m, 1H), 3.18 – 3.08 (m, 1H), 2.70 (d, J = 17.1 Hz, 1H), 1.85 – 1.16 (m, 10H), 0.92 (s, 9H), 0.87 (t, J = 6.6 Hz, 3H), 0.10 (s, 3H), 0.09 (s, 3H); **^{13}C NMR** (100 MHz, $CDCl_3$) δ 177.0,

170.9, 167.0, 135.3, 131.1, 130.7, 128.6, 127.9, 108.9, 75.6, 73.6, 58.8, 35.1, 34.0, 31.8, 29.8, 29.5, 29.3, 25.9, 25.3, 25.1, 24.1, 22.7, 18.2, 14.2, -4.7, -5.1; **$[\alpha]^{25}_{D}$** –38.6 (c = 1.43 in $CHCl_3$); **IR** (film) 3480, 2927, 2856, 1738 (C=O), 1688 (C=O), 1645 (C=O), 1618, 1577, 1463, 1495, 1402, 1360, 1253, 1195, 1100, 1004, 940, 836, 779, 723, 699, 666; **HRMS** Accurate mass (ES^+): Found 573.3695 (-5.1 ppm), $C_{32}H_{53}N_2O_5Si$ ($M+H^+$) requires 573.3724.

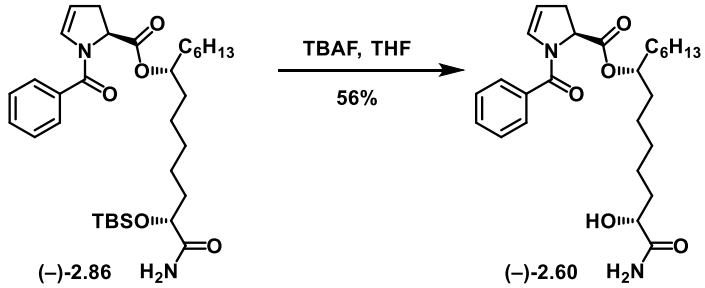

(1R,7R)-1-carbamoyl-1-hydroxytridecan-7-yl (2S)-1-benzoyl-2,3-dihydro-1H-pyrrole-2-carboxylate (–)-2.60. To a solution of silyl ether **(–)-2.86** (14 mg, 0.025 mmol) dissolved in THF (0.5 mL) was added TBAF (0.25 mL, 1M in THF, 0.250 mmol) at room temperature. After 5 minutes, the reaction was quenched with 1M aq. NH_4Cl and extracted with Et_2O 3x. The combined organic layers were washed with brine, dried over Na_2SO_4, filtered, concentrated, and purified by preparative TLC (2% MeOH/EtOAc), yielding the title compound as a clear oil (6.4 mg, 56% yield). **R_f** (2% MeOH/EtOAc) = 0.50; **^{1}H NMR** (500 MHz, $CDCl_3$) δ 7.61 – 7.36 (m, 5H), 6.95 (s, 0.16H), 6.91 (s, 0.45H), 6.83 (s, 0.67H), 6.52 – 6.47 (m, 1H), 5.47 (s, 0.37H), 5.27 (s, 1H), 5.16 (d, J = 4.0 Hz, 1H), 5.08 – 5.02 (m, 1H), 5.02 – 4.94 (m, 1H), 4.35 (s, 0.55H), 4.14 – 3.99 (m, 1H), 3.18 – 3.08 (m, 1H), 2.76 – 2.66 (m, 1H), 1.87 – 1.79 (m, 1H), 1.77 – 1.48 (m, 11H), 1.48 – 1.16 (m, 22H), 0.87 (t, J = 6.8 Hz, 3H); **^{13}C NMR** (125 MHz, CDCl3) δ 177.59, 170.92, 170.62, 167.88, 167.49, 134.93, 134.69, 131.09, 130.80, 128.81, 128.76, 127.78, 127.69, 110.01, 109.84, 75.54, 75.24, 70.64, 59.14, 58.60, 34.84, 34.53, 34.39, 34.15, 34.02, 33.78, 33.61, 31.85, 29.84, 29.25, 27.73, 27.49, 25.60, 25.31, 24.68, 24.50, 24.24, 24.00, 22.70, 14.20; **$[\alpha]^{25}_{D}$** – 5.3 (c = 0.62 in $CHCl_3$); **IR** (film) 3325 (br, O-H), 2925, 2856, 2360, 1733 (C=O), 1668 (C=O),

1615 (C=O), 1576, 1496, 1448, 1406, 1197, 1153, 1082, 1017, 1001, 944, 844, 788, 724, 699, 660; **HRMS** Accurate mass (ES^+): Found 481.2650, $C_{26}H_{38}N_2O_5Na$ ($M+Na^+$) requires 481.2678.

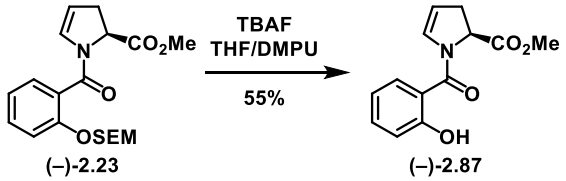

(–)-2.23 (–)-2.87

Methyl (2S)-1-(2-hydroxybenzoyl)-2,3-dihydro-1H-pyrrole-2-carboxylate (–)-2.87. Using the TBAF/DMPU procedure given above (10 eq TBAF, 0.10 M DMPU), SEM-ether **(–)-2.23** (23 mg, 0.061 mmol) yielded the title compound as a clear oil (8.2 mg, 55% yield). **^{1}H NMR** (500 MHz, $CDCl_3$) δ 9.80 (s, 1H), 7.43 (dd, J = 7.8, 1.5 Hz, 1H), 7.41 – 7.35 (m, 1H), 7.01 (dd, J = 8.3, 0.8 Hz, 1H), 6.89 (td, J = 7.8, 1.1 Hz, 1H), 6.83 (s, 1H), 5.28 (dt, J = 4.4, 2.7 Hz, 1H), 5.04 (dd, J = 11.3, 5.2 Hz, 1H), 3.80 (s, 3H), 3.11 (ddt, J = 16.4, 11.3, 2.4 Hz, 1H), 2.73 (ddt, J = 17.1, 5.0, 2.5 Hz, 1H); **^{13}C NMR** (100 MHz, $CDCl_3$) δ 171.45, 167.75, 159.36, 133.70, 130.99, 128.49, 118.98, 118.15, 110.85, 77.16, 59.29, 52.85, 33.49, 29.83. **$[\alpha]^{25}_D$** –104.5 (c = 1.00 in $CHCl_3$); **IR** (film) 3119 (br, O-H), 2954, 2918, 2850, 2360, 2341, 2160, 2031, 1979, 1746 (C=O), 1616, 1590 (C=O), 1487, 1434, 1362, 1295, 1250, 1202, 1179, 1153, 1098, 1017, 984, 944, 855, 817, 757, 721, 667; **HRMS** Accurate mass (ES^+): Found 270.0751, $C_{13}H_{13}NO_4Na$ ($M+Na^+$) requires 270.0742.

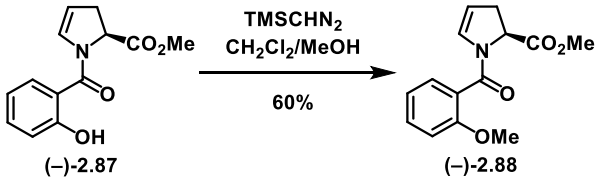

(–)-2.87 (–)-2.88

Methyl (2S)-1-(2-methoxybenzoyl)-2,3-dihydro-1H-pyrrole-2-carboxylate (–)-2.88. To a solution of phenol **(–)-2.87** (45 mg, 0.182 mmol) in 3:1 CH_2Cl_2:MeOH (2 mL) was added $TMSCHN_2$ (0.46 mL, 2M in hexanes, 0.920 mmol), and the reaction went from a clear to yellow color, with effervescence. After 2 hours, TLC analysis indicated remaining starting material, and

more MeOH (0.5 mL) was added, after another 30 minutes the starting material was consumed. The reaction was concentrated and purified by column chromatography, yielding the title compound as a yellow oil (28 mg, 60% yield). **^{1}H NMR** (500 MHz, $CDCl_3$) δ 7.41 – 7.34 (m, 2H), 7.00 (t, J = 7.5 Hz, 1H), 6.94 (d, J = 8.3 Hz, 1H), 6.17 – 6.13 (m, 1H), 5.07 – 5.00 (m, 2H), 3.84 (s, 3H), 3.81 (s, 3H), 3.16 – 3.07 (m, 1H), 2.75 – 2.67 (m, 1H); **^{13}C NMR** (100 MHz, $CDCl_3$) δ 171.61, 165.22, 155.94, 131.42, 130.91, 129.11, 124.94, 120.92, 111.44, 108.60, 57.88, 55.90, 52.59, 34.17; **$[\alpha]^{25}_{D}$** –85.9 (c = 1.27 in $CHCl_3$); **IR** (film) 2951, 2923, 2851, 2160, 2032, 1979, 1746 (C=O), 1643 (C=O), 1618, 1600, 1491, 1461, 1436, 1406, 1363, 1280, 1249, 1201, 1179, 1103, 1046, 1016, 843, 754, 654; **HRMS** Accurate mass (ES^+): Found 284.0875, $C_{14}H_{15}NO_4Na$ ($M+Na^+$) requires 284.0899.

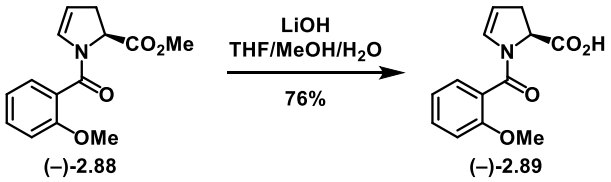

(2S)-1-(2-methoxybenzoyl)-2,3-dihydro-1H-pyrrole-2-carboxylic acid (–)-2.89. Using the LiOH hydrolysis procedure given above, methyl ester **(–)-2.88** (27 mg, 0.103 mmol) yielded the title compound as a yellow oil (19 mg, 76% yield). **^{1}H NMR** (500 MHz, $CDCl_3$) δ 8.03 (s, 1H), 7.46 – 7.41 (m, 1H), 7.38 (d, J = 7.5 Hz, 1H), 7.03 (t, J = 7.5 Hz, 1H), 6.96 (d, J = 8.4 Hz, 1H), 6.06 (dt, J = 4.3, 2.2 Hz, 1H), 5.23 (dd, J = 4.3, 2.4 Hz, 1H), 5.13 (dd, J = 11.0, 4.2 Hz, 1H), 3.84 (s, 3H), 3.19 (d, J = 17.1 Hz, 1H), 3.09 – 3.00 (m, 1H); **^{13}C NMR** (125 MHz, $CDCl_3$) δ 172.39, 167.64, 155.96, 132.16, 129.76, 129.23, 123.82, 121.07, 111.58, 111.51, 59.25, 55.89, 32.89, 29.82; **$[\alpha]^{25}_{D}$** –82.1 (c = 1.80 in $CHCl_3$); **IR** (film) 3444 (br, CO_2-H), 2930, 1738 (C=O), 1598 (C=O), 1492, 1464, 1437, 1412, 1356, 1282, 1249, 1185, 1163, 1104, 1047, 1018, 941, 848, 754, 723, 652; **HRMS** Accurate mass (ES^+): Found 270.0721, $C_{13}H_{13}NO_4Na$ ($M+Na^+$) requires 270.0742.

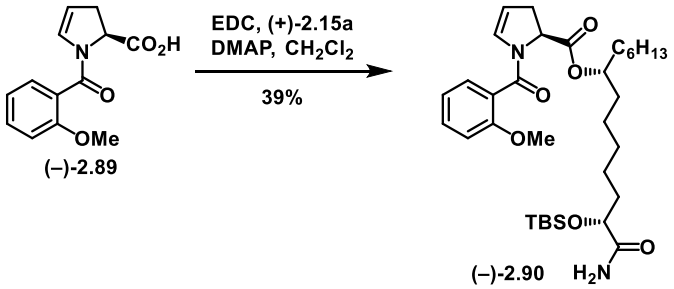

(1R,7R)-1-[(tert-butyldimethylsilyl)oxy]-1-carbamoyltridecan-7-yl (2S)-1-(2-methoxybenzoyl)-2,3-dihydro-1H-pyrrole-2-carboxylate (–)-2.90. Using the EDC esterification procedure given above (1.2 eq acid, 1.5 eq EDC, 1.0 eq alcohol, 0.1 eq DMAP), acid **(–)-2.89** (18 mg, 0.073 mmol), after purification by column chromatography (0 → 2% MeOH/CH_2Cl_2) yielded the title compound as a clear oil (14 mg, 39% yield). $\mathbf{R_f}$ (2:1 CH_2Cl_2:Et_2O) = 0.60; **^{1}H NMR** (500 MHz, $CDCl_3$) δ 7.40 – 7.31 (m, 2H), 7.17 (d, J = 7.2 Hz, 1H), 6.99 (s, 1H), 6.93 (d, J = 8.2 Hz, 1H), 6.54 (s, 1H), 6.14 (dd, J = 4.1, 1.9 Hz, 1H), 5.71 – 5.59 (m, 1H), 5.05 – 4.95 (m, 2H), 4.17 – 4.06 (m, 2H), 3.83 (s, 3H), 3.12 (ddd, J = 14.1, 11.6, 2.0 Hz, 1H), 2.91 – 2.85 (m, 1H), 2.66 (ddd, J = 17.1, 4.3, 2.1 Hz, 1H), 1.76 – 1.54 (m, 6H), 1.39 – 1.19 (m, 20H), 0.91 (s, 9H), 0.89 – 0.83 (m, 3H), 0.08 (d, J = 6.2 Hz, 6H); **^{13}C NMR** (100 MHz, $CDCl_3$) δ 177.11, 170.92, 165.02, 155.98, 131.32, 131.01, 129.17, 129.11, 127.43, 125.11, 120.89, 111.42, 108.46, 75.50, 73.55, 69.78, 58.23, 55.86, 53.93, 41.65, 35.11, 34.39, 34.08, 34.02, 31.85, 29.83, 29.51, 29.33, 25.87, 25.31, 25.05, 24.11, 22.72, 18.15, 14.21, -4.70, -5.13; $\mathbf{[\alpha]^{25}_D}$ –27.2 (c = 1.11 in $CHCl_3$); **IR** (film) 3481, 2927, 2856, 1745, 1683, 1646, 1619, 1601, 1491, 1463, 1437, 1406, 1360, 1280, 1251, 1194, 1101, 1048, 1019, 939, 837, 778, 754, 701, 655; **HRMS** Accurate mass (ES^+): Found 603.3802, $C_{33}H_{55}N_2O_6Si$ ($M+H^+$) requires 603.3829.

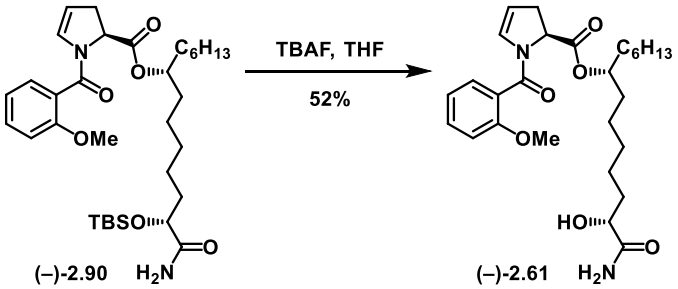

(1R,7R)-1-carbamoyl-1-hydroxytridecan-7-yl (2S)-1-(2-methoxybenzoyl)-2,3-dihydro-1H-pyrrole-2-carboxylate (–)-2.61. To a solution of protected ester **(–)-2.90** (11 mg, 0.018 mmol) dissolved in THF (0.5 mL) was added TBAF (0.18 mL, 1M in THF, 0.180 mmol). After 5 minutes the reaction was poured into 1M aq. NH_4Cl and extracted with Et_2O 3x. The combined organic layers were washed with brine, dried over Na_2SO_4, filtered, concentrated and purified by preparative TLC (2% MeOH/EtOAc), yielding the title compound as a clear oil (4.6 mg, 52% yield). $\mathbf{R_f}$ (2% MeOH/EtOAc) = 0.45; **^{1}H NMR** (500 MHz, $CDCl_3$) δ 7.43 – 7.38 (m, 1H), 7.33 (d, J = 7.3 Hz, 1H), 7.00 (t, J = 7.5 Hz, 1H), 6.97 – 6.91 (m, 2H), 6.19 – 6.12 (m, 1H), 5.15 – 5.02 (m, 3H), 4.95 (dd, J = 11.6, 4.8 Hz, 1H), 4.43 (s, 1H), 4.06 (d, J = 4.4 Hz, 1H), 3.83 (s, 3H), 3.18 – 3.09 (m, 1H), 2.68 (ddd, J = 14.7, 4.5, 2.2 Hz, 1H), 1.87 – 1.77 (m, 1H), 1.69 – 1.35 (m, 17H), 1.35 – 1.16 (m, 21H), 0.88 (t, J = 6.8 Hz, 4H); **^{13}C NMR** (100 MHz, $CDCl_3$) δ 177.75, 170.61, 165.90, 155.96, 131.80, 130.74, 128.96, 124.24, 120.99, 111.52, 109.73, 74.99, 70.35, 58.07, 55.92, 34.99, 34.27, 33.52, 31.86, 29.85, 29.26, 27.29, 25.65, 24.65, 24.22, 22.71, 14.22; $\mathbf{[\alpha]^{25}_D}$ – 8.9 (c = 0.45 in $CHCl_3$); **IR** (film) 2920, 2850, 1740 (C=O), 1668 (C=O), 1618 (C=O), 1492, 1463, 1439, 1412, 1377, 1280, 1253, 1196, 1102, 1047, 1021, 847, 803, 755, 720; **HRMS** Accurate mass (ES^+): Found 489.2941, $C_{27}H_{41}N_2O_6$ ($M+H^+$) requires 489.2965.

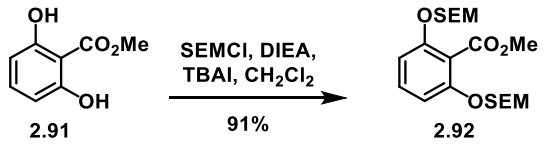

Methyl 2,6-bis((2-(trimethylsilyl)ethoxy)methoxy)benzoate 2.92. Using a modified procedure given for the preparation of compound **2.14** (double equivalents of SEMCl and DIEA, and 0.1 eq tetrabutylammonium iodide), 2,6-dihydroxy methyl benzoate (563 mg, 3.348 mmol) yielded the title compound as a yellow oil (1.308 g, 91% yield). $\mathbf{R_f}$ (7:1 hexanes:EtOAc) = 0.34; **^{1}H NMR** (500 MHz, $CDCl_3$) δ 7.24 (t, J = 8.4 Hz, 1H), 6.82 (d, J = 8.4 Hz, 2H), 5.21 (s, 4H), 3.90 (s, J = 2.6 Hz, 3H), 3.76 – 3.71 (m, 4H), 0.96 – 0.92 (m, 4H), 0.01 – -0.02 (m, 18H); **^{13}C NMR** (125 MHz, $CDCl_3$) δ 166.89, 155.07, 130.98, 115.47, 108.36, 93.22, 66.55, 52.41, 18.12, -1.30; **IR** (film) 2951, 2897, 2359, 2341, 1738 (C=O), 1599, 1469, 1272, 1245, 1145, 1111, 1038, 936, 917, 895, 856, 831, 757, 692, 667, 609**; HRMS** Accurate mass (ES^+): Found 451.1915, $C_{20}H_{36}O_6Si_2Na$ ($M+Na^+$) requires 451.1948.

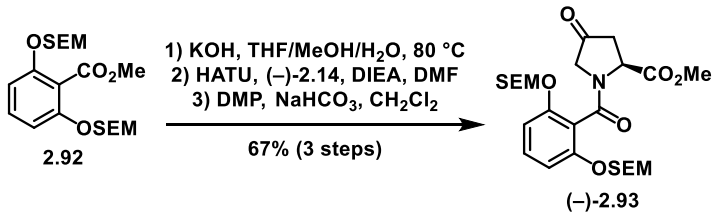

Methyl (S)-1-(2,6-bis((2-(trimethylsilyl)ethoxy)methoxy)benzoyl)-4-oxopyrrolidine-2-carboxylate (–)-2.93. Methyl ester **2.92** (1.283 g, 2.993 mmol) was dissolved in 9:1:1 MeOH:THF:H_2O (11 mL), and KOH (1.914 g, 34.117 mmol) was added as a solid. The reaction was heated to reflux (80 °C) overnight. The following day, the reaction was cooled to room temperature, acidified (pH 5-6) with 5% aq. AcOH, and extracted with CH_2Cl_2 3x. The combined organic layers were washed with brine, dried over $MgSO_4$, filtered and concentrated. The crude acid was unstable and used directly in the next step. Using the procedure given for the preparation of compound **(–)-2.20**, the acid yielded the corresponding acylhydroxyproline methyl ester compound, whose purity made it unsuitable for characterization. Using the procedure given for the preparation of compound **(+)-2.21**, the alcohol intermediate yielded the title compound as a yellow oil (1.075 g, 67% over 3 steps). $\mathbf{R_f}$ (3:1 hexanes:EtOAc) = 0.25; **^{1}H NMR** (500 MHz,

$CDCl_3$, mixture of rotamers/conformers) δ 7.29 – 7.24 (m, 1H), 6.86 (tt, J = 7.4, 4.3 Hz, 2H), 5.32 – 5.15 (m, 4.56H), 5.11 (t, J = 5.8 Hz, 0.35H), 4.64 – 4.59 (m, 0.33H), 4.43 (d, J = 19.7 Hz, 0.34H), 4.07 – 4.03 (m, 0.18H), 4.03 – 3.99 (m, 0.16), 3.93 – 3.90 (m, 0.30), 3.90 – 3.86 (m, 0.41H), 3.82 – 3.66 (m, 6.48H), 3.63 – 3.59 (m, 0.83H), 3.03 – 2.93 (m, 0.73H), 2.90 – 2.82 (m, 0.38H), 2.72 – 2.62 (m, 0.73H), 2.57 (d, J = 18.1 Hz, 0.35H), 0.98 – 0.88 (m, 4H), 0.05 – -0.06 (m, 18H); **^{13}C NMR** (125 MHz, $CDCl_3$) δ 207.70, 170.94, 165.99, 154.92, 154.16, 131.50, 131.17, 116.27, 109.11, 108.75, 108.54, 108.23, 93.81, 93.63, 93.47, 93.31, 66.84, 66.73, 66.68, 57.33, 54.73, 52.69, 52.55, 51.82, 41.95, 40.69, 18.10, 14.31, -1.27, -1.30, -1.31; **$[\alpha]^{25}_D$** –1.8 (c = 1.41 in $CHCl_3$); **IR** (film) 2952, 2896, 1765 (C=O), 1747 (C=O), 1658 (C=O), 1596, 1467, 1404, 1245, 1177, 1142, 1094, 1035, 918, 893, 856, 832, 790, 751, 693, 664; **HRMS** Accurate mass (ES^+): Found 562.2232, $C_{25}H_{41}NO_8Si_2Na$ ($M+Na^+$) requires 562.2268.

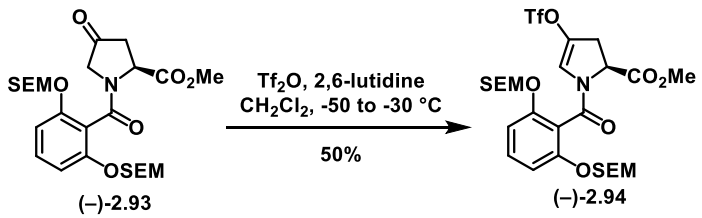

Methyl (S)-1-(2,6-bis((2-(trimethylsilyl)ethoxy)methoxy)benzoyl)-4-(((trifluoromethyl)sulfonyl)oxy)-2,3-dihydro-1H-pyrrole-2-carboxylate (–)-2.94. Using the procedure given for the preparation of **(–)-2.22**, ketone **(–)-2.93** (238 mg, 0.440 mmol) yielded the title compound as an orange oil (149 mg, 50% yield). **R_f** (3:1 hexanes:EtOAc) = 0.48; **^{1}H NMR** (400 MHz, $CDCl_3$) δ 7.37 – 7.28 (m, 1H), 6.87 (t, J = 8.2 Hz, 2H), 6.35 (s, 1H), 5.28 – 5.16 (m, 4H), 5.10 (dd, J = 11.8, 5.0 Hz, 1H), 3.82 (s, 3H), 3.74 (dt, J = 21.8, 8.0 Hz, 4H), 3.45 – 3.34 (m, 1H), 2.95 (dd, J = 16.5, 4.9 Hz, 1H), 0.93 (dd, J = 16.0, 7.7 Hz, 4H), -0.01 (s, J = 7.4 Hz, 18H); **^{13}C NMR** (125 MHz, $CDCl_3$) δ 169.52, 163.25, 155.19, 133.94, 131.84, 123.14, 114.23, 108.67, 108.37, 93.48, 93.16, 66.69, 66.64, 56.77, 52.81, 33.66, 18.04, -1.34, -1.38; **$[\alpha]^{25}_D$** –41.3 (c = 1.04 in $CHCl_3$); **IR** (film) 3269, 2954, 2899, 1747 (C=O), 1605 (C=O), 1425, 1363, 1311,

1208, 1136, 1028, 912, 833, 755, 693, 605; **HRMS** Accurate mass (ES^+): Found 694.1727, $C_{26}H_{40}F_3NO_{10}SSi_2Na$ ($M+Na^+$) requires 694.1761.

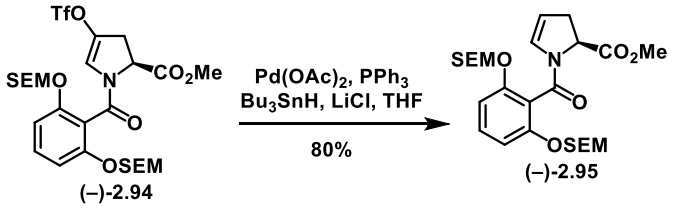

Methyl (S)-1-(2,6-bis((2-(trimethylsilyl)ethoxy)methoxy)benzoyl)-2,3-dihydro-1H-pyrrole-2-carboxylate (–)-2.95. Using the procedure given for the preparation of compound **(–)-2.23**, triflate **(–)-2.94** (130 mg, 0.194 mmol) yielded the title compound as a yellow oil (82 mg, 80% yield). **^{1}H NMR** (500 MHz, $CDCl_3$) δ 7.25 – 7.20 (m, 1H), 6.83 (dt, J = 12.5, 6.2 Hz, 2H), 6.11 (dt, J = 4.4, 2.2 Hz, 1H), 5.29 (d, J = 7.1 Hz, 1H), 5.24 – 5.13 (m, 3H), 5.01 (ddd, J = 8.3, 6.9, 3.8 Hz, 2H), 3.86 – 3.64 (m, 7H), 3.12 (ddt, J = 16.7, 11.6, 2.3 Hz, 1H), 2.74 – 2.68 (m, 1H), 0.99 – 0.87 (m, 4H), 0.02 – -0.06 (m, 18H); **^{13}C NMR** (100 MHz, $CDCl_3$) δ 171.27, 162.64, 154.96, 154.81, 130.92, 130.58, 115.96, 108.57, 108.29, 108.10, 93.02, 92.96, 66.43, 57.50, 52.35, 34.42, 18.05, -1.36; **$[\alpha]^{25}_D$** –55.9 (c = 1.49 in $CHCl_3$); **IR** (film) 2952, 2921, 2899, 1744 (C=O), 1656 (C=O), 1620, 1596, 1468, 1404, 1245, 1199, 1178, 1151, 1094, 1038, 917, 895, 857, 832, 741, 694, 608; **HRMS** Accurate mass (ES^+): Found 546.2288, $C_{25}H_{41}NO_7Si_2Na$ ($M+Na^+$) requires 546.2319.

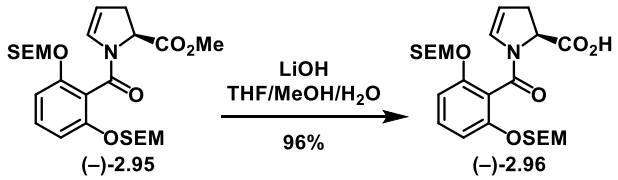

(S)-1-(2,6-bis((2-(trimethylsilyl)ethoxy)methoxy)benzoyl)-2,3-dihydro-1H-pyrrole-2-carboxylic acid (–)-2.96. Using the LiOH hydrolysis procedure given above, methyl ester **(–)-2.95** (73 mg, 0.139 mmol) yielded the title compound as a yellow oil (68 mg, 96% yield). **^{1}H**

NMR (400 MHz, $CDCl_3$) δ 7.31 (t, J = 8.4 Hz, 1H), 6.85 (dd, J = 8.5, 0.8 Hz, 2H), 6.02 (dt, J = 4.4, 2.2 Hz, 1H), 5.28 – 5.16 (m, 6H), 3.74 – 3.67 (m, 4H), 3.48 – 3.40 (m, 1H), 2.98 (ddt, J = 17.4, 11.0, 2.5 Hz, 1H), 0.95 – 0.89 (m, 4H), -0.01 (d, J = 1.7 Hz, 18H); **^{13}C NMR** (100 MHz, $CDCl_3$) δ 171.36, 166.43, 154.97, 154.62, 131.84, 129.07, 114.45, 112.17, 108.27, 107.97, 93.08, 92.94, 77.36, 66.75, 66.67, 59.24, 32.64, 30.43, 29.81, 18.10, -1.30, -1.33; **$[\alpha]^{25}_D$** –66.4 (c = 1.38 in $CHCl_3$); **IR** (film) 2952, 2924, 2896, 1748 (C=O), 1652 (C=O), 1619, 1595, 1468, 1405, 1245, 1183, 1150, 1093, 1039, 832, 738, 693, 664; **HRMS** Accurate mass (ES^+): Found 532.2130, $C_{24}H_{39}NO_7Si_2Na$ ($M+Na^+$) requires 532.2163.

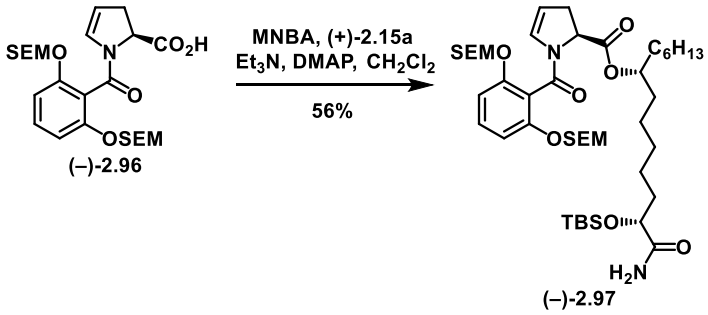

(7R,13R)-14-amino-13-((tert-butyldimethylsilyl)oxy)-14-oxotetradecan-7-yl (S)-1-(2,6-bis((2-(trimethylsilyl)ethoxy)methoxy)benzoyl)-2,3-dihydro-1H-pyrrole-2-carboxylate (–)-2.97. To a solution of acid **(–)-2.96** (81 mg, 0.158 mmol) dissolved in CH_2Cl_2 (2 mL) was added MNBA (101 mg, 0.294 mmol) and Et_3N (0.05 mL, 0.373 mmol), and the solution was stirred for 10 minutes. Then alcohol **(+)-2.15a** (42 mg, 0.113 mmol 1 eq) and DMAP (1 mg, 0.011 mmol) dissolved in CH_2Cl_2 (2 mL) was added, and the reaction was stirred overnight. The reaction was poured into sat. NH_4Cl, extracted with CH_2Cl_2 3x, washed with brine, dried over $MgSO_4$, filtered, concentrated, and purified by column chromatography (0 → 30% Et_2O/CH_2Cl_2), yielding the title compound as a yellow oil (55 mg, 56% yield). **R_f** (4:1 CH_2Cl_2:Et_2O) = 0.67; **^{1}H NMR** (500 MHz, $CDCl_3$) δ 7.23 (d, J = 8.4 Hz, 1H), 6.92 – 6.75 (m, 2H), 6.57 – 6.48 (m, 1H), 6.10 (dt, J = 4.2, 2.0 Hz, 1H), 5.46 – 5.35 (m, 1H), 5.30 – 5.12 (m, 5H), 4.98 (dt, J = 8.7, 5.3 Hz, 2H), 4.13 (t, J = 5.1 Hz, 1H), 3.83 – 3.64 (m, 4H), 3.17 – 3.07 (m, 1H), 2.70 – 2.62 (m, 1H), 1.81 – 1.70 (m, 1H), 1.70

– 1.62 (m, 1H), 1.43 – 1.17 (m, 16H), 0.98 – 0.89 (m, 12H), 0.87 (t, J = 6.3 Hz, 3H), 0.14 – 0.04 (m, 6H), 0.03 – -0.06 (m, 18H); **^{13}C NMR** (125 MHz, $CDCl_3$) δ 177.02, 170.41, 162.48, 155.04, 154.97, 130.87, 130.79, 116.20, 108.76, 108.22, 108.10, 93.11, 93.03, 75.01, 73.54, 66.43, 57.85, 35.10, 34.67, 34.07, 34.02, 31.85, 29.48, 29.30, 25.85, 25.28, 25.06, 24.11, 22.68, 18.16, 18.10, 14.17, -1.30, -4.73, -5.15; **$[\alpha]^{25}_D$** –25.4 (c = 1.27 in $CHCl_3$); **IR** (film) 2927, 2857, 1749 (C=O), 1689 (C=O), 1657 (C=O), 1621, 1596, 1467, 1404, 1247, 1188, 1151, 1095, 1040, 937, 896, 833, 778, 751, 694, 665, 580, 554; **HRMS** Accurate mass (ES^+): Found 865.5290, $C_{44}H_{81}N_2O_9Si_3$ ($M+H^+$) requires 865.5250.

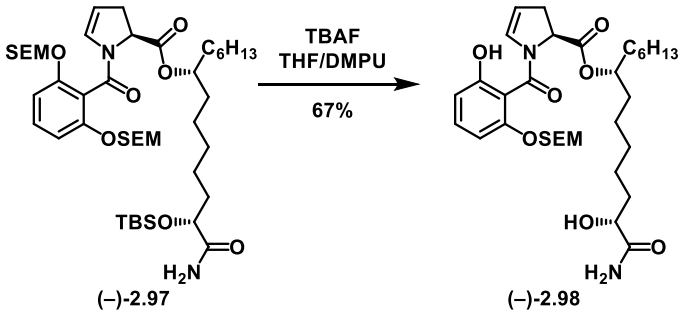

(7R,13R)-14-amino-13-hydroxy-14-oxotetradecan-7-yl (S)-1-(2-hydroxy-6-((2-(trimethylsilyl)ethoxy)methoxy)benzoyl)-2,3-dihydro-1H-pyrrole-2-carboxylate (–)-2.98. Using the procedure given for the preparation of compound **(–)-2.1a**, compound **(–)-2.97** (37 mg, 0.043 mmol) yielded the title compound, after purification by preparative TLC (4% MeOH/EtOAc), as a yellow oil (18 mg, 67% yield). **^{1}H NMR** (400 MHz, $CDCl_3$) δ 8.13 – 7.89 (m, 1H), 7.22 (t, J = 8.3 Hz, 1H), 6.81 (s, 1H), 6.71 (t, J = 7.2 Hz, 1H), 6.62 (d, J = 8.3 Hz, 1H), 6.31 – 6.25 (m, 1H), 5.33 – 5.02 (m, 6H), 4.14 – 3.99 (m, 2H), 3.77 – 3.68 (m, 2H), 3.23 – 3.10 (m, 1H), 2.70 (d, J = 17.5 Hz, 1H), 1.86 – 1.74 (m, 1H), 1.73 – 1.15 (m, 22H), 0.99 – 0.81 (m, 5H), -0.01 (d, J = 2.9 Hz, 9H); **^{13}C NMR** (125 MHz, $CDCl_3$) δ 177.79, 172.11, 164.33, 155.46, 154.76, 132.20, 130.96, 130.57, 111.63, 110.73, 110.27, 106.20, 93.42, 76.45, 70.80, 66.78, 58.28, 34.75, 34.29, 34.13, 33.84, 31.81, 29.17, 27.77, 25.59, 24.78, 24.40, 22.66, 18.13, 14.18, -1.29; **$[\alpha]^{25}_D$** –1.7 (c = 0.93 in $CHCl_3$); **IR** (film) 3338 (br, O-H), 2927, 2858, 1748 (C=O), 1661,

1616, 1601, 1466, 1432, 1378, 1292, 1247, 1193, 1153, 1102, 1038, 941, 835, 792, 721; **HRMS** Accurate mass (ES^+): Found 643.3417, $C_{32}H_{52}N_2O_8SiNa$ ($M+Na^+$) requires 643.3391.

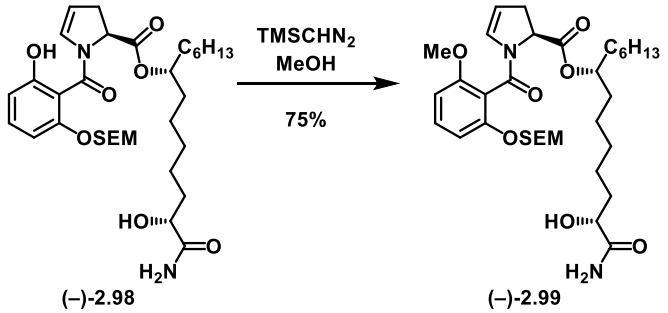

(7R,13R)-14-amino-13-hydroxy-14-oxotetradecan-7-yl (S)-1-(2-methoxy-6-((2-(trimethylsilyl)ethoxy)methoxy)benzoyl)-2,3-dihydro-1H-pyrrole-2-carboxylate (–)-2.99. To a solution of compound **(–)-2.98** (19 mg, 0.031 mmol) in MeOH (1 mL) was added $TMSCHN_2$ (0.070 mL, 2M in hexanes, 0.140 mmol). The reaction was stirred overnight at room temperature, over which time the reaction turned from yellow to clear. The reaction was concentrated and purified by preparative TLC (5% MeOH/EtOAc), yielding the title compound as a yellow oil (15 mg, 75% yield). **^{1}H NMR** (500 MHz, $CDCl_3$, mixture of rotamers/conformers) δ 8.00 (dd, J = 8.3, 1.3 Hz, 1H), 7.61 – 7.56 (m, 0.39H), 7.45 (t, J = 7.8 Hz, 1H), 7.28 (td, J = 8.0, 1.9 Hz, 1H), 6.97 (d, J = 26.7 Hz, 1H), 6.78 (dd, J = 8.2, 6.7 Hz, 1H), 6.58 (dd, J = 8.3, 2.7 Hz, 1H), 6.43 (s, 0.37H), 6.10 (ddq, J = 12.7, 6.4, 2.2 Hz, 1H), 5.32 – 5.03 (m, 5H), 4.98 – 4.88 (m, 2H), 4.26 (dd, J = 7.0, 3.2 Hz, 0.38H), 4.16 – 4.11 (m, 0.42H), 4.06 (d, J = 6.6 Hz, 0.62H), 3.84 – 3.80 (m, 1.84H), 3.80 – 3.76 (m, 2.25H), 3.75 – 3.66 (m, 1.59H), 3.18 – 3.08 (m, 1H), 2.74 – 2.63 (m, 1H), 1.89 – 1.68 (m, 2H), 1.68 – 1.37 (m, 12H), 1.36 – 1.14 (m, 24H), 0.98 – 0.77 (m, 9H), -0.02 (d, J = 5.9 Hz, 9H); **^{13}C NMR** (100 MHz, $CDCl_3$) δ 178.21, 178.09, 170.41, 170.07, 165.15, 163.64, 157.65, 157.10, 155.01, 154.80, 133.70, 131.56, 131.47, 130.53, 129.95, 128.63, 113.96, 113.59, 109.58, 107.87, 107.12, 104.95, 104.55, 101.07, 93.07, 92.78, 82.51, 79.60, 77.16, 74.43, 74.34, 70.81, 70.12, 69.95, 66.72, 66.65, 63.15, 57.71, 56.30, 56.06, 35.11, 34.57, 34.35, 33.50, 32.06, 31.87, 29.84, 29.50, 29.29, 27.22, 27.04, 26.15, 25.66, 24.80, 24.63, 24.23, 24.15, 22.83, 22.71,

18.15, 18.10, 14.22, -1.28; **[α]$^{25}_{D}$** –19.8 (c = 1.72 in $CHCl_3$); **IR** (film) 3329 (br, O-H), 2924, 2854, 1721, 1658, 1619, 1595, 1472, 1409, 1379, 1291, 1247, 1190, 1107, 1073, 1002, 951, 898, 858, 835, 789, 716; 668, 604; **HRMS** Accurate mass (ES^+): Found 657.3570 (+3.5 ppm), $C_{33}H_{54}N_2O_8SiNa$ ($M+Na^+$) requires 657.3547.

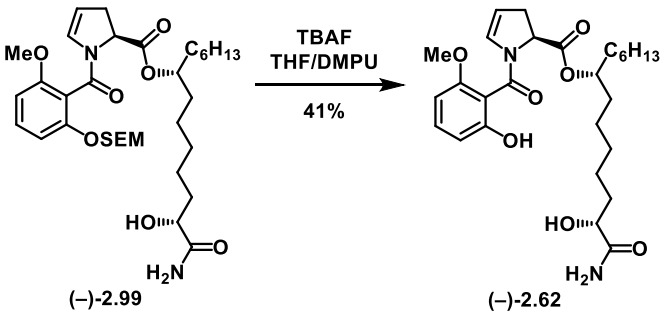

(–)-2.99 (–)-2.62

(7R,13R)-14-amino-13-hydroxy-14-oxotetradecan-7-yl (S)-1-(2-hydroxy-6-methoxybenzoyl)-2,3-dihydro-1H-pyrrole-2-carboxylate (–)-2.62. Using the procedure given above for TBAF/DMPU deprotection (10 eq TBAF, 0.1M DMPU), silyl ether **(–)-2.99** (17 mg, 0.027 mmol) after purification by column chromatography (0 → 3% MeOH/CH_2Cl_2), yielded the title compound as a clear oil (5.6 mg, 41% yield). **^{1}H NMR** (500 MHz, $CDCl_3$) δ 7.98 (s, 1H), 7.28 – 7.23 (m, 1H), 6.83 (s, 1H), 6.60 (dd, J = 8.3, 4.8 Hz, 1H), 6.47 (t, J = 8.7 Hz, 1H), 6.25 (dt, J = 4.4, 2.2 Hz, 1H), 5.19 (dt, J = 4.6, 2.4 Hz, 1H), 5.14 – 5.04 (m, 2H), 4.60 (d, J = 5.9 Hz, 1H), 4.08 – 4.00 (m, 1H), 3.83 – 3.79 (m, 3H), 3.21 – 3.12 (m, 1H), 2.69 (d, J = 18.6 Hz, 1H), 1.84 – 1.74 (m, 1H), 1.71 – 1.19 (m, 22H), 0.88 (t, J = 6.9 Hz, 3H); **^{13}C NMR** (125 MHz, $CDCl_3$) δ 177.47, 176.57, 172.39, 172.24, 164.48, 164.39, 157.00, 155.68, 132.38, 130.55, 110.52, 110.44, 110.14, 110.10, 102.72, 102.63, 76.66, 76.46, 70.77, 70.70, 64.51, 58.37, 58.33, 56.07, 56.02, 34.79, 34.35, 34.21, 34.07, 33.81, 33.58, 31.83, 29.84, 29.18, 27.72, 27.53, 25.63, 24.75, 24.69, 24.33, 24.14, 22.68, 14.20; **[α]$^{25}_{D}$** –10.5 (c = 0.56 in $CHCl_3$); **IR** (film) 3307 (br, O-H), 2926, 2856, 1733 (C=O), 1653, 1592, 1470, 1435, 1250, 1194, 1088, 1016, 947, 847, 791, 720, 601; **HRMS** Accurate mass (ES^+): Found 527.2751, $C_{27}H_{40}N_2O_7Na$ ($M+Na^+$) requires 527.2733.

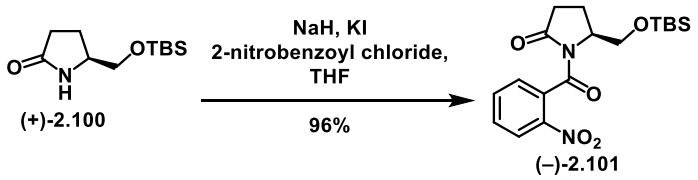

(S)-5-(((tert-butyldimethylsilyl)oxy)methyl)-1-(2-nitrobenzoyl)pyrrolidin-2-one (–)-2.101. To a suspension of NaH (60% in mineral oil, 74 mg, 1.852 mmol) and KI (307 mg, 1.852 mmol) in THF (4 mL) at 0°C was added a solution of (S)-5-(((tert-butyldimethylsilyl)oxy)methyl)pyrrolidin-2-one (prepared as previously described: Torssell, S., Wanngren, E., Somfai, P. *J. Org. Chem.* **2007**, *72*, 4246) (386 mg, 1.683 mmol) dropwise in THF (2 mL). The solution was allowed to warm to room temperature and stir for 90 minutes. Then 2-nitrobenzoyl chloride (0.27 mL, 2.020 mmol) was added as a solution in THF (2 mL). After 10 minutes, the reaction was quenched with sat. NH_4Cl (10 mL) and extracted 3x with EtOAc. The combined organic layers were washed 2x with sat. Na_2CO_3, water, and brine, dried over $MgSO_4$, filtered, concentrated, and filtered through a plug of silica gel, which was washed with 3:1 hexanes:EtOAc. The filtrate was concentrated then triturated with MeOH, yielding the title compound as a white solid (609 mg, 96% yield). **^{1}H NMR** (500 MHz, $CDCl_3$) δ 8.23 (dd, J = 8.3, 0.9 Hz, 1H), 7.71 (td, J = 7.5, 1.2 Hz, 1H), 7.58 (ddd, J = 8.3, 7.5, 1.4 Hz, 1H), 7.32 (dt, J = 6.7, 3.4 Hz, 1H), 4.69 – 4.62 (m, 1H), 4.14 (dd, J = 10.4, 3.7 Hz, 1H), 3.85 (d, J = 10.6 Hz, 1H), 2.75 (dt, J = 17.8, 10.3 Hz, 1H), 2.36 (ddd, J = 17.8, 9.8, 2.0 Hz, 1H), 2.21 (ddd, J = 34.5, 22.6, 11.4 Hz, 2H), 0.90 (s, 9H), 0.11 (s, 3H), 0.11 (s, 3H); **^{13}C NMR** (125 MHz, $CDCl_3$) δ 175.70, 166.50, 145.21, 134.37, 133.47, 129.94, 127.72, 124.17, 63.52, 58.18, 32.27, 25.94, 21.33, 18.29, -5.39, -5.50; **$[\alpha]^{25}_D$** –76.1 (c = 0.77 in $CHCl_3$); **IR** (film) 2925, 2891, 2853, 1743 (C=O), 1668 (C=O), 1533, 1471, 1353, 1319, 1264, 1226, 1193, 1104, 1087, 1028, 1005, 986, 967, 872, 837, 776, 744, 703, 640, 560; **HRMS** Accurate mass (ES^+): Found 401.1536, $C_{18}H_{26}N_2O_5SiNa$ ($M+Na^+$) requires 401.1509; **MP** 121.5 – 124.0°C.

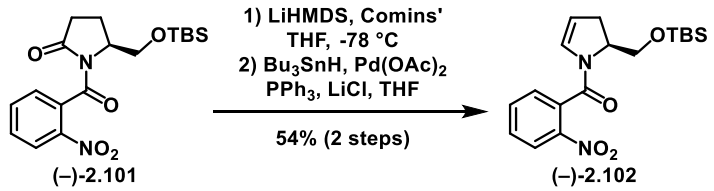

(S)-(2-(((tert-butyldimethylsilyl)oxy)methyl)-2,3-dihydro-1H-pyrrol-1-yl)(2-nitrophenyl)methanone (–)-2.102. LiHMDS (1M in THF, 2.83 mL, 2.83 mmol) was diluted with THF (12 mL) and cooled to -78°C. A solution of compound **(–)-2.101** (713 mg, 1.884 mmol) was added dropwise as a solution in THF (6 mL), and the reaction turned a deep purple color. After 1 hour, Comins' reagent (1.849g, 4.710 mmol) was added dropwise as a solution in THF (5 mL), and the reaction was stirred for 2 hours at -78°C, quenched with sat. NH_4Cl, warmed to room temperature, and extracted 3x with EtOAc. The combined organic layers were washed with sat $NaHCO_3$ and brine, then purified by column chromatography [triflate R_f (4:1 hexanes:EtOAc) = 0.49], which yielded the triflate intermediate as a yellow oil, which was highly unstable (decomposed overnight in a freezer). The triflate was immediately taken up in THF (15 mL) and to the resulting solution was added LiCl (240 mg, 5.651 mmol), $Pd(OAc)_2$ (42 mg, 0.188 mmol), PPh_3 (148 mg, 0.565 mmol), and Bu_3SnH (0.40 mL, 1.484 mmol) dropwise; during addition of the stannane the solution turned from a yellow suspension to a clear orange/brown solution. After 10 minutes, the reaction was quenched with aqueous 1M KF and extracted 3x with EtOAc. The combined organic layers were washed with aqueous 1M KF, water, and brine, dried over $MgSO_4$, filtered, concentrated, and purified by column chromatography, yielding the title compound as a yellow solid (366 mg, 54% over two steps). **^{1}H NMR** (500 MHz, $CDCl_3$) δ 8.20 (dd, J = 8.3, 1.0 Hz, 1H), 7.72 (td, J = 7.5, 1.2 Hz, 1H), 7.63 – 7.57 (m, 1H), 7.45 (dd, J = 7.6, 1.4 Hz, 1H), 5.87 – 5.83 (m, 1H), 5.15 – 5.10 (m, 1H), 4.70 (qd, J = 7.1, 3.7 Hz, 1H), 4.09 – 3.95 (m, 1H), 3.90 – 3.80 (m, 1H), 2.86 (ddt, J = 12.3, 9.9, 2.6 Hz, 1H), 2.73 (ddd, J = 17.0, 5.0, 3.3 Hz, 1H), 0.91 (s, J = 2.8 Hz, 9H), 0.11 (s, 3H), 0.10 (s, 3H); **^{13}C NMR** (125 MHz, $CDCl_3$) δ 163.35, 145.47, 134.47, 132.51, 130.27, 128.78, 128.71, 124.75, 112.36, 58.64, 32.34, 25.86, 18.23, -

5.31, -5.32; **[α]$^{25}_{D}$** –144.6 (c = 0.81 in $CHCl_3$); **IR** (film) 2952, 2929, 2856, 1633 (C=O), 1615, 1571, 1528, 1480, 1471, 1422, 1388, 1345, 1286, 1248, 1205, 1179, 1104, 1077, 1060, 1006, 969,941, 832, 775, 763, 740, 723, 701, 687, 666, 642, 607; **HRMS** Accurate mass (ES^+): Found 363.1754, $C_{18}H_{27}N_2O_4Si$ ($M+H^+$) requires 363.1740. **MP** 90.1 – 94.7°C.

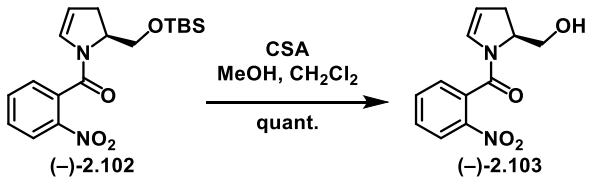

(S)-(2-(hydroxymethyl)-2,3-dihydro-1H-pyrrol-1-yl)(2-nitrophenyl)methanone (–)-2.103. To a solution of compound **(–)-2.102** (285 mg, 0.786 mmol) in 1:1 MeOH:CH_2Cl_2 (8 mL) was added CSA (183 mg, 0.786 mmol). The reaction was stirred for 1 hour at rt then quenched with sat. $NaHCO_3$ and extracted 3x with CH_2Cl_2. The combined organic layers were washed with water and brine, dried over $MgSO_4$, filtered, concentrated, and purified by column chromatography, yielding the title compound as a yellow oil (209 mg, quant. yield). **^{1}H NMR** (500 MHz, $CDCl_3$) δ 8.24 (dd, J = 8.3, 0.9 Hz, 1H), 7.77 (td, J = 7.5, 1.1 Hz, 1H), 7.67 – 7.62 (m, 1H), 7.52 – 7.49 (m, 1H), 5.88 (dt, J = 4.4, 2.2 Hz, 1H), 5.18 (dt, J = 4.4, 2.7 Hz, 1H), 4.78 (td, J = 10.0, 4.9 Hz, 1H), 3.92 (d, J = 4.5 Hz, 2H), 3.01 (ddt, J = 17.1, 10.5, 2.5 Hz, 1H), 2.44 (d, J = 16.8 Hz, 1H); **^{13}C NMR** (100 MHz, $CDCl_3$) δ 165.39, 145.33, 134.82, 132.02, 130.72, 128.81, 128.69, 124.98, 113.00, 66.05, 61.30, 33.25; **[α]$^{25}_{D}$** –105.2 (c = 1.23 in $CHCl_3$); **IR** (film) 3392 (br O-H), 2928, 2359, 2341, 1610 (C=O), 1574, 1526, 1482, 1418, 1343, 1240, 1046, 967, 789, 761, 687, 668, 643; **HRMS** Accurate mass (ES^+): Found 271.0715, $C_{12}H_{12}N_2O_4Na$ ($M+Na^+$) requires 271.0695.

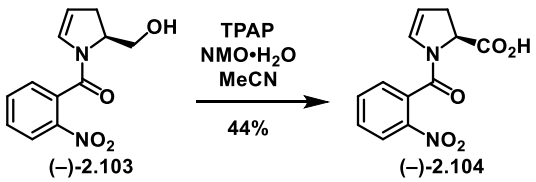

(S)-1-(2-nitrobenzoyl)-2,3-dihydro-1H-pyrrole-2-carboxylic acid (–)-2.104. To a solution of compound **(–)-2.103** (52 mg, 0.210 mmol) in MeCN (2 mL) was added NMO•H2O (294 mg, 2.096 mmol), and the solution was stirred until complete dissolution. Then TPAP (7 mg, 0.021 mmol) was added, and the reaction was stirred for 1 hour, quenched with IPA, concentrated, and filtered over a plug of silica gel, which was washed with 1% AcOH/MeCN. The filtrate was concentrated and purified by column chromatography (0 → 3% MeOH/0.1% AcOH/CH_2Cl_2) yielding the title compound as a brown residue (24 mg, 44% yield). **^{1}H NMR** (400 MHz, $CDCl_3$) δ 8.15 (d, J = 8.1 Hz, 1H), 7.73 (t, J = 7.0 Hz, 1H), 7.64 – 7.55 (m, 2H), 5.92 (s, 1H), 5.17 (s, 1H), 5.02 (s, 1H), 3.17 – 3.01 (m, 1H), 2.97 – 2.85 (m, 1H); **^{13}C NMR** (100 MHz, $CDCl_3$) δ 174.39, 164.60, 145.33, 134.98, 131.34, 130.80, 129.52, 128.51, 124.76, 112.48, 99.77, 59.21, 53.58, 33.98; **$[\alpha]^{25}_D$** –127.8 (c = 0.94 in $CHCl_3$); **IR** (film) 3446, 3098, 2921, 2851, 1733 (C=O), 1615 (C=O), 1526, 1485, 1417, 1344, 1200, 1119, 1080, 1018, 941, 860, 840, 790, 762, 737, 704, 642; **HRMS** Accurate mass (ES^+): Found 263.683, $C_{12}H_{11}N_2O_5$ ($M+H^+$) requires 263.0668.

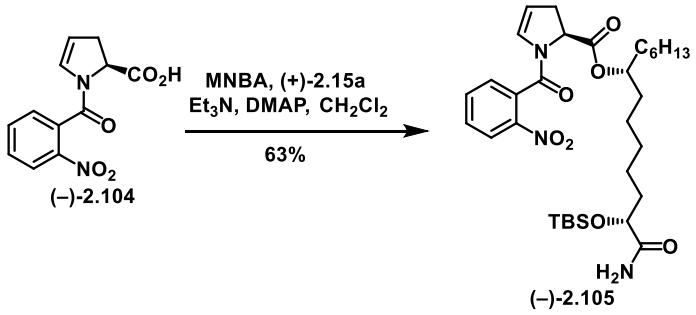

(7R,13R)-14-amino-13-((tert-butyldimethylsilyl)oxy)-14-oxotetradecan-7-yl (S)-1-(2-nitrobenzoyl)-2,3-dihydro-1H-pyrrole-2-carboxylate (–)-2.105. To a solution of acid **(–)-2.104** (19 mg, 0.073 mmol) dissolved in CH_2Cl_2 (2 mL) was added MNBA (47 mg, 0.135 mmol) and Et_3N (0.02mL, 0.172 mmol), and the solution was stirred for 10 minutes. Then alcohol **(+)-2.15a** (19 mg, 0.052 mmol) and DMAP (1 mg, 0.005 mmol) dissolved in CH_2Cl_2 (2 mL) was added, and the reaction was stirred overnight. The reaction was poured into sat. NH_4Cl, extracted with CH_2Cl_2 3x, washed with brine, dried over $MgSO_4$, filtered, concentrated, and purified by

preparative TLC (2:1 CH_2Cl_2: Et_2O) yielding the title compound as a clear oil (24 mg, 63% yield). **^{1}H NMR** (500 MHz, $CDCl_3$) δ 8.20 (d, J = 8.2 Hz, 1H), 7.74 (td, J = 7.5, 1.0 Hz, 1H), 7.64 – 7.55 (m, 2H), 6.52 (d, J = 3.9 Hz, 1H), 6.01 (dt, J = 4.2, 2.1 Hz, 1H), 5.49 (s, 1H), 5.14 – 5.11 (m, 1H), 5.07 (dd, J = 11.7, 5.0 Hz, 1H), 5.02 – 4.95 (m, 1H), 4.14 – 4.09 (m, 1H), 3.23 – 3.15 (m, 1H), 2.72 (ddd, J = 19.5, 4.8, 2.4 Hz, 1H), 1.74 (dd, J = 14.9, 9.5 Hz, 1H), 1.69 – 1.51 (m, 6H), 1.37 – 1.21 (m, 16H), 0.90 (s, J = 3.0 Hz, 9H), 0.87 (t, J = 6.8 Hz, 3H), 0.12 – 0.04 (m, 9H); **^{13}C NMR** (125 MHz, $CDCl_3$) δ 177.07, 170.65, 163.28, 145.61, 134.56, 131.99, 130.59, 129.38, 129.26, 124.80, 110.35, 75.99, 73.59, 58.19, 35.15, 34.45, 34.14, 34.09, 31.86, 29.48, 29.29, 25.87, 25.41, 25.08, 24.11, 22.71, 18.14, 14.20, -4.70, -5.14; **$[\alpha]^{25}_D$** –71.1 (c = 1.21 in $CHCl_3$); **IR** (film) 3480, 2927, 2856, 1739 (C=O), 1658 (C=O), 1622 (C=O), 1574, 1531, 1463, 1413, 1347, 1252, 1198, 1098, 1005, 940, 836, 779, 739, 705, 669, 642, 582; **HRMS** Accurate mass (ES^+): Found 618.3548, $C_{32}H_{52}N_3O_7Si$ ($M+H^+$) requires 618.3575.

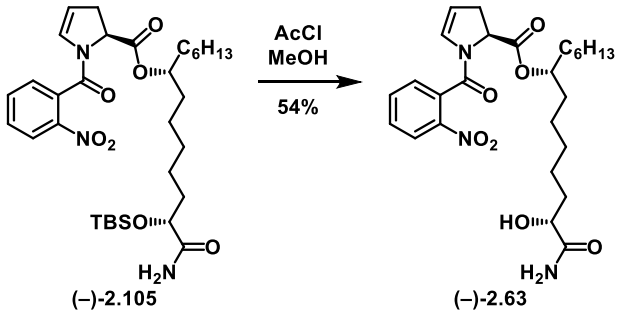

(7R,13R)-14-amino-13-hydroxy-14-oxotetradecan-7-yl (S)-1-(2-nitrobenzoyl)-2,3-dihydro-1H-pyrrole-2-carboxylate (–)-2.63. To a solution of silyl ether **(–)-2.105** (13 mg, 0.021 mmol) dissolved in MeOH (0.5 mL) was added acetyl chloride (ca. 1 μL, 1 drop). After 10 minutes, the reaction was diluted with EtOAc and quenched with sat. $NaHCO_3$, then extracted with EtOAc 3x. The combined organic layers were washed with water and brine, dried over $MgSO_4$, filtered, concentrated, and purified by preparative TLC (10% MeOH/CH_2Cl_2), yielding the title compound as a yellow oil (7 mg, 54% yield). **^{1}H NMR** (500 MHz, $CDCl_3$) δ 8.21 (dd, J = 8.3, 0.9 Hz, 1H), 7.76 (tt, J = 4.0, 2.0 Hz, 1H), 7.67 – 7.60 (m, 2H), 6.64 (s, 1H), 6.03 (dt, J = 4.4, 2.2 Hz, 1H),

5.26 – 5.21 (m, 1H), 5.20 – 5.17 (m, 1H), 5.11 – 5.02 (m, 2H), 4.04 – 3.99 (m, 1H), 3.90 (t, J = 7.0 Hz, 1H), 3.21 (ddt, J = 16.8, 11.7, 2.4 Hz, 1H), 2.76 – 2.69 (m, 1H), 1.85 – 1.76 (m, 1H), 1.68 – 1.36 (m, 16H), 1.36 – 1.20 (m, 14H), 0.88 (t, J = 7.0 Hz, 3H); **$[\alpha]^{25}_{D}$** –64.6 (c = 0.22 in $CHCl_3$); **IR** (film) 3350 (br, O-H), 2926, 2856, 1733 (C=O), 1652 (C=O), 1621, 1530, 1483, 1417, 1346. 1197, 1079, 840, 791, 763, 740, 705; **HRMS** Accurate mass (ES^+): Found 526.2540, $C_{26}H_{37}N_3O_7Na$ ($M+Na^+$) requires 526.2529.

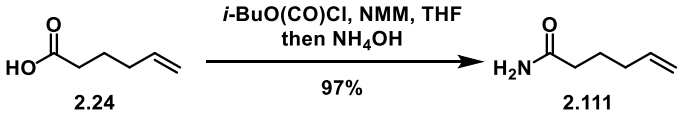

Hex-5-enamide 2.111. To a solution of 5-hexenoic acid (0.44 mL, 3.701 mmol) dissolved in THF (5 mL) was added N-methylmorpholine (0.45 mL, 4.071 mmol) and the solution was cooled to 0 °C. Isobutyl chloroformate (0.53 mL, 4.071 mmol) was added dropwise and the reaction was stirred at 0 °C for 30 minutes, then ammonium hydroxide (28% NH_3 in H_2O, 0.64 mL) was added and the reaction was allowed to warm to room temperature and stir overnight. The reaction was quenched with sat. NH_4Cl and extracted with EtOAc 3x. The combined organic layers were washed with 1M HCl and brine, dried over $MgSO_4$, filtered and concentrated, yielding the title compound as a white solid (407 mg, 97% yield). **^{1}H NMR** (400 MHz, $CDCl_3$) δ 5.79 (ddt, J = 17.0, 10.2, 6.7 Hz, 1H), 5.34 (br s, 2H), 5.10 – 4.95 (m, 2H), 2.28 – 2.21 (m, 1H), 2.12 (dd, J = 14.2, 7.1 Hz, 2H), 1.82 – 1.70 (m, 1H); **^{13}C NMR** (101 MHz, CDCl3) δ 175.73, 137.90, 115.51, 35.16, 33.16, 24.57; **IR** (film) 3361 (br N-H), 3184 (br N-H), 2944, 2359, 2342, 1633 (C=O), 1415, 1229, 1135, 1077, 991, 908, 775, 667; **HRMS** Accurate mass (ES^+): Found 114.0917, $C_6H_{12}NO$ ($M+H^+$) requires 114.0919; **MP** 70.0 – 75.1°C.

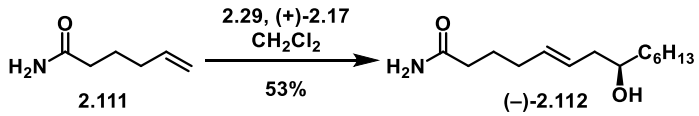

(R,E)-8-hydroxytetradec-5-enamide (–)-2.112. To a solution of **2.111** (41 mg, 0.362 mmol) and alcohol **(+)-2.17** (283 mg, 1.812 mmol) in CH_2Cl_2 (1 mL) was added catalyst **2.29** (13 mg, 0.018 mmol, Materia, C711, CAS #635679-24-2). The reaction was stirred for overnight at room temperature, concentrated and purified by column chromatography (0 → 5% MeOH/CH_2Cl_2) yielding the title compound as a tan solid (46 mg, 53% yield). $\mathbf{R_f}$ (5% MeOH/CH_2Cl_2) = 0.23; **^{1}H NMR** (400 MHz, $CDCl_3$) δ 5.52 – 5.44 (m, 2H), 5.30 (br s, 1H), 3.59 (br s, 1H), 2.23 (dd, J = 13.6, 6.1 Hz, 2H), 2.08 (dt, J = 14.3, 6.8 Hz, 2H), 1.74 (dt, J = 14.3, 7.2 Hz, 2H), 1.66 – 1.54 (m, 3H), 1.50 – 1.38 (m, 3H), 1.29 (t, J = 15.3 Hz, 7H), 0.93 – 0.84 (m, 10H); **^{13}C NMR** (100 MHz, $CDCl_3$) δ 176.13, 132.67, 127.69, 71.13, 40.68, 37.00, 35.02, 31.95, 31.90, 29.41, 25.83, 25.76, 24.93, 22.67, 14.15; $\mathbf{[\alpha]^{25}_D}$ –1.8 (c = 1.69 in $CHCl_3$); **IR** (film) 3361, 3183,2954, 2921, 2850, 2359, 1650 (C=O), 1416, 1349, 1268, 1202, 1126, 1068, 1040, 1008, 966, 940, 863, 647, 598, 559; **HRMS** Accurate mass (ES^+): Found 264.1950, $C_{14}H_{27}NO_2Na$ ($M+Na^+$) requires 264.1940; **MP** 54.6 – 56.8°C.

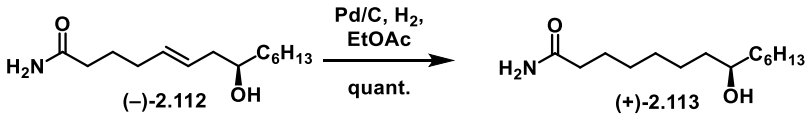

(R)-8-hydroxytetradecanamide (+)-2.113. To a solution of alkene **(–)-2.112** (89 mg, 0.168 mmol) dissolved in EtOAc (5 mL) was added 10% Pd/C (50 mg), then the reaction flask was vacuum and backfilled with H_2 5x and stirred under a H_2 balloon overnight. The reaction was filtered over Celite and concentrated, yielding the title compound as a white solid (91 mg, quant. yield). **^{1}H NMR (**400 MHz, $CDCl_3$) δ 5.24 (br d, 2H), 3.58 (br s, 1H), 2.38 (td, J = 7.4, 4.2 Hz, 1H), 2.27 – 2.16 (m, 2H), 1.69 – 1.60 (m, 2H), 1.48 – 1.21 (m, 18H), 0.90 – 0.85 (m, 3H); **^{13}C NMR** (100 MHz, $CDCl_3$) δ 175.89, 72.02, 37.65, 37.46, 35.99, 35.87, 31.96, 29.49, 29.45, 29.27, 25.75, 25.56, 22.74, 14.22; $\mathbf{[\alpha]^{25}_D}$ +7.0 (c = 1.34 in $CHCl_3$); **IR** (film) 3207 (br O-H), 2922, 2849, 1651 (C=O), 1614, 1467, 1413, 1129, 1066, 1012, 913, 850, 793, 720, 655; **HRMS** Accurate mass (ES^+): Found 266.2102, $C_{14}H_{29}NO_2Na$ ($M+Na^+$) requires 266.2096; **MP** 95.4 – 98.7 °C.

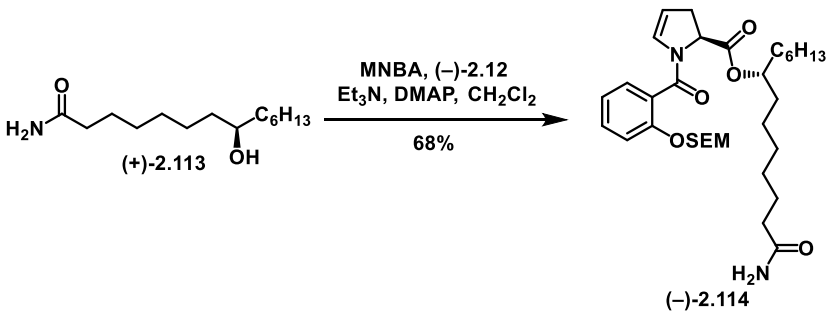

(R)-14-amino-14-oxotetradecan-7-yl (S)-1-(2-((2-(trimethylsilyl)ethoxy)methoxy)benzoyl)-2,3-dihydro-1H-pyrrole-2-carboxylate (–)-2.114. To a solution of acid **(–)-2.12** (18 mg, 0.050 mmol) dissolved in CH_2Cl_2 (2 mL) was added MNBA (17 mg, 0.050 mmol) and Et_3N (0.02 mL, 0.139 mmol), and the solution was stirred for 10 minutes. Then alcohol **(+)-2.113** (9.7 mg, 0.042 mmol) and DMAP (1 mg, 0.004 mmol) dissolved in CH_2Cl_2 (2 mL) was added, and the reaction was stirred overnight. The reaction was poured into sat. NH_4Cl, extracted with CH_2Cl_2 3x, washed with brine, dried over $MgSO_4$, filtered, concentrated, and purified by column chromatography (0 → 30% Et_2O/CH_2Cl_2), yielding the title compound as a yellow oil (16 mg, 68% yield). **^{1}H NMR** (500 MHz, $CDCl_3$) δ 7.40 – 7.28 (m, 2H), 7.19 (t, J = 8.0 Hz, 1H), 7.04 (td, J = 7.5, 0.8 Hz, 1H), 6.31 (s, 1H), 6.19 – 6.12 (m, 1H), 5.22 (ddd, J = 16.3, 7.1, 2.9 Hz, 2H), 5.11 (s, 1H), 5.04 (td, J = 5.4, 2.9 Hz, 1H), 5.03 – 4.93 (m, 2H), 3.79 – 3.69 (m, 2H), 3.19 – 3.10 (m, 1H), 2.72 – 2.64 (m, 1H), 2.23 – 2.11 (m, 1H), 1.66 – 1.52 (m, 6H), 1.45 – 1.16 (m, 16H), 0.97 – 0.90 (m, 2H), 0.90 – 0.83 (m, 3H), 0.03 – -0.05 (m, 9H); **^{13}C NMR** (125 MHz, $CDCl_3$) δ 170.73, 165.29, 153.74, 131.43, 130.96, 128.89, 125.67, 122.05, 115.33, 108.77, 93.34, 75.35, 66.70, 58.08, 35.99, 34.60, 34.37, 31.85, 29.27, 28.83, 28.55, 25.48, 25.09, 24.70, 22.70, 18.15, 14.19, -1.28; **$[\alpha]^{25}_D$** –27.2 (c = 0.79 in $CHCl_3$); **IR** (film) 2925, 2856, 1738 (C=O), 1645 (C=O), 1618 (C=O), 1600, 1487, 1455, 1406, 1355, 1277, 1229, 1193, 1150, 1085, 1043, 987, 938, 917, 857, 834, 754, 696, 655; **HRMS** Accurate mass (ES^+): Found 611.3533, $C_{32}H_{52}N_2O_6SiNa$ ($M+Na^+$) requires 611.3492.

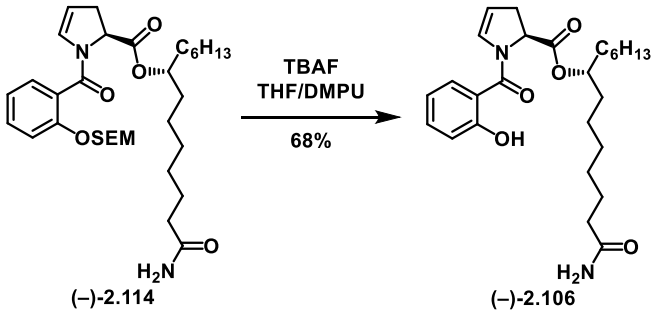

(R)-14-amino-14-oxotetradecan-7-yl (S)-1-(2-hydroxybenzoyl)-2,3-dihydro-1H-pyrrole-2-carboxylate (–)-2.106. Using the procedure for TBAF/DMPU deprotection given above (10 eq TBAF, 0.1M DMPU), SEM ether **(–)-2.114** (7.5 mg, 0.013 mmol) yielded the title compound as a clear oil (4.1 mg, 68% yield). **^{1}H NMR** (500 MHz, $CDCl_3$) δ 9.83 (d, J = 46.9 Hz, 1H), 7.44 – 7.34 (m, 2H), 6.99 (dd, J = 7.4, 3.5 Hz, 1H), 6.89 (t, J = 7.8 Hz, 1H), 6.79 (s, 1H), 5.60 (br d, 1H), 5.29 (d, J = 10.2 Hz, 2H), 5.05 – 4.90 (m, 2H), 3.17 – 3.08 (m, 1H), 2.70 (d, J = 18.0 Hz, 1H), 2.23 – 2.16 (m, 2H), 1.66 – 1.48 (m, 8H), 1.39 – 1.16 (m, 15H), 0.86 (t, J = 7.0 Hz, 3H); **^{13}C NMR** (125 MHz, $CDCl_3$) δ 175.77, 171.03, 167.50, 159.30, 158.93, 133.56, 131.00, 128.41, 119.11, 118.06, 110.79, 75.99, 74.40, 59.54, 36.00, 35.90, 34.33, 34.19, 31.82, 29.25, 29.08, 29.02, 28.91, 25.41, 25.24, 24.90, 22.69, 14.20; **$[\alpha]^{25}_D$** –20.8 (c = 0.24 in $CHCl_3$); **IR** (film) 3190 (br O-H), 2926, 2856, 1733 (C=O), 1660 (C=O), 1593, 1456, 1414, 1294, 1252, 1194, 1152, 1098, 1016, 945, 912, 859, 816, 755, 723, 654, 617, 567; **HRMS** Accurate mass (ES^+): Found 481.2700, $C_{26}H_{38}N_2O_5Na$ ($M+Na^+$) requires 481.2678.

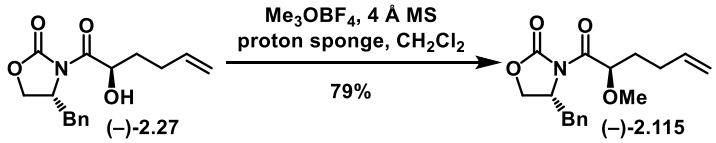

(R)-4-benzyl-3-((R)-2-methoxyhex-5-enoyl)oxazolidin-2-one (–)-2.115. (synthesized with the help of Sierra Williams) 4 Å molecular sieves were flame-dried in a round-bottom flask, and alcohol **(–)-2.27** (121 mg, 0.418 mmol) was added to the flask as a solution in CH_2Cl_2 (2 mL) followed by trimethyloxonium tetrafluoroborate (493 mg, 3.333 mmol) and 1,8-

Bis(dimethylamino)naphthalene (714 mg, 3.333 mmol). The reaction was stirred at room temperature for 48 hours, then quenched with isopropanol and filtered. The solution was diluted with Et_2O and washed with 1M HCl, sat. $NaHCO_3$, and brine, dried over Na_2SO_4, filtered, concentrated, and purified by column chromatography, yielding the title compound as a yellow oil (100 mg, 79% yield). **^{1}H NMR** (400 MHz, $CDCl_3$) δ 7.38 – 7.27 (m, 3H), 7.25 – 7.20 (m, 2H), 5.82 (ddt, J = 16.9, 10.1, 6.7 Hz, 1H), 5.09 – 4.97 (m, 2H), 4.91 (dd, J = 8.3, 3.5 Hz, 1H), 4.68 (ddt, J = 10.1, 6.7, 3.3 Hz, 1H), 4.28 – 4.21 (m, 2H), 3.42 (s, 3H), 3.36 (dd, J = 13.3, 3.1 Hz, 1H), 2.87 – 2.80 (m, 1H), 2.26 (dt, J = 14.0, 6.9 Hz, 2H), 1.88 – 1.68 (m, 2H); **^{13}C NMR** (100 MHz, $CDCl_3$) δ 173.15, 153.22, 137.59, 135.13, 129.54, 129.11, 127.57, 115.42, 79.27, 66.87, 58.17, 55.61, 37.93, 32.13, 29.67; **$[\alpha]^{25}_D$** –6.0 (c = 0.63 in $CHCl_3$); **IR** (film) 2923, 2854, 1723 (C=O), 1583, 1452, 1376, 1313, 1271, 1109, 1070, 1028, 967, 817, 743, 710; **HRMS** Accurate mass (ES^+): Found 326.1381, $C_{17}H_{21}NO_4Na$ ($M+Na^+$) requires 326.1368.

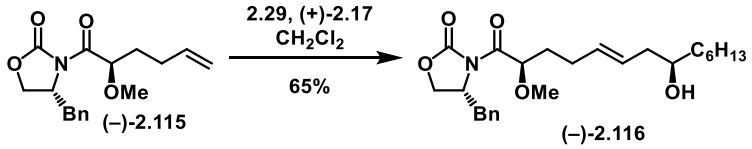

(R)-4-benzyl-3-((2R,8R,E)-8-hydroxy-2-methoxytetradec-5-enoyl)oxazolidin-2-one (–)-2.116. (synthesized with the help of Sierra Williams) Catalyst **2.29** (13 mg, 0.017 mmol, C711, Materia, CAS #635679-24-2) was added to a solution of alcohol **(+)-2.17** (258 mg, 1.651 mmol) and methyl ether **(–)-2.115** (100 mg, 0.330 mmol) dissolved in CH_2Cl_2 (2 mL) and stirred at room temperature overnight. The reaction was concentrated and purified by column chromatography yielding the title compound as a yellow oil (95 mg, 65% yield). **^{1}H NMR** (400 MHz, $CDCl_3$) δ 7.37 – 7.27 (m, 3H), 7.23 (d, J = 6.9 Hz, 2H), 5.52 (dt, J = 13.2, 8.3 Hz, 3H), 4.91 (dd, J = 8.1, 3.6 Hz, 1H), 4.73 – 4.65 (m, 1H), 4.27 – 4.20 (m, 2H), 3.60 (br s, 2H), 3.41 (s, J = 3.4 Hz, 3H), 3.39 – 3.33 (m, 1H), 2.87 – 2.78 (m, 1H), 2.32 – 2.20 (m, 3H), 2.14 – 2.07 (m, 1H), 1.85 – 1.70 (m, 2H), 1.64 – 1.56 (m, 2H), 1.51 – 1.39 (m, 6H), 1.34 – 1.24 (m, 14H), 0.88 (t, J = 6.4 Hz, 3H); **^{13}C**

NMR (100 MHz, $CDCl_3$) δ 173.25, 153.23, 135.11, 132.69, 130.09, 129.53, 129.11, 127.56, 79.13, 70.95, 70.84, 66.91, 58.18, 55.61, 40.85, 40.72, 37.94, 37.03, 36.86, 32.68, 31.93, 29.44, 28.51, 25.80, 25.76, 22.72, 14.19; **[α]$^{25}_{D}$** –17.5 (c = 0.83 in $CHCl_3$); **IR** (film) 3500 (br, O-H), 2925, 2854, 1778 (C=O), 1705 (C=O), 1455, 1387, 1349, 1290, 1252, 1211, 1113, 1073, 1049, 971, 814, 761, 732, 700; **HRMS** Accurate mass (ES^+): Found 454.2585, $C_{25}H_{37}NO_5Na$ ($M+Na^+$) requires 454.2569.

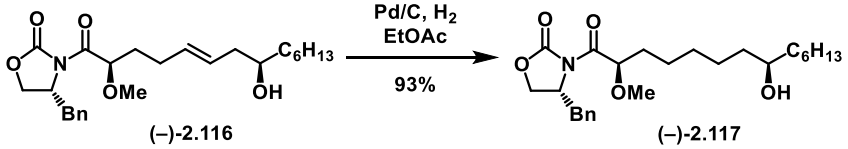

(R)-4-benzyl-3-((2R,8R)-8-hydroxy-2-methoxytetradecanoyl)oxazolidin-2-one (–)-2.117. (synthesized with the help of Sierra Williams) To a solution of alkene **(–)-2.116** (95 mg, 0.220 mmol) dissolved in EtOAc (10 mL) in a round-bottom flask was added 10% Pd/C (50 mg), and the flask was vacuum and backfilled with H_2 5x then stirred under a balloon of H_2 overnight. The reaction was filtered over Celite and concentrated, yielding the title compound as a clear oil (89 mg, 93% yield). **^{1}H NMR** (400 MHz, $CDCl_3$) δ 7.36 – 7.27 (m, 3H), 7.24 – 7.20 (m, 2H), 4.90 (dd, J = 7.9, 3.5 Hz, 1H), 4.72 – 4.66 (m, 1H), 4.28 – 4.22 (m, 2H), 3.59 (br s, 2H), 3.41 (s, 3H), 3.34 (dd, J = 7.3, 4.2 Hz, 1H), 2.83 (dd, J = 13.4, 9.5 Hz, 1H), 2.39 (dt, J = 10.8, 7.4 Hz, 1H), 1.70 – 1.59 (m, 2H), 1.50 – 1.37 (m, 10H), 1.32 – 1.23 (m, 12H), 0.88 – 0.85 (m, 3H); **^{13}C NMR** (100 MHz, $CDCl_3$) δ 173.14, 153.17, 135.05, 129.43, 128.97, 127.42, 79.81, 71.80, 71.69, 66.76, 58.04, 55.46, 37.80, 37.52, 37.47, 37.35, 37.31, 32.79, 31.85, 29.39, 29.24, 25.62, 25.39, 22.62, 14.10; **[α]$^{25}_{D}$** –12.0 (c = 0.93 in $CHCl_3$); **IR** (film) 2924, 2855, 1781 (C=O), 1705, 1456, 1387, 1349, 1211, 1107, 1019, 814, 754, 700, 667; **HRMS** Accurate mass (ES^+): Found 434.2911, $C_{25}H_{40}NO_5$ ($M+H^+$) requires 434.2906.

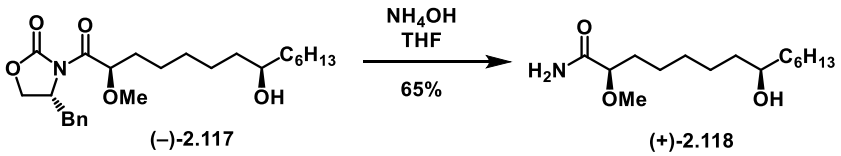

(2R,8R)-8-hydroxy-2-methoxytetradecanamide (+)-2.118. (synthesized with the help of Sierra Williams) To a solution of oxazolidinone **(–)-2.117** (88 mg, 0.203 mmol) in THF (3 mL) was added ammonium hydroxide (28% NH_3 in H_2O, 2 mL), and the reaction was tightly sealed and stirred for 48 hours. The reaction was diluted with MeOH and concentrated, and this process was repeated 2x. Purification by column chromatography (0 → 8% MeOH/CH_2Cl_2) yielded the title compound as a white solid (36 mg, 65% yield). $\mathbf{R_f}$ (8% MeOH/CH_2Cl_2) = 0.36; **^{1}H NMR** (500 MHz, $CDCl_3$) δ 6.46 (br s, 1H), 5.57 (br s, 1H), 3.62 (dd, J = 6.9, 4.4 Hz, 1H), 3.57 (br s, 1H), 3.41 (s, 3H), 1.82 – 1.74 (m, 1H), 1.73 – 1.63 (m, 2H), 1.47 – 1.35 (m, 9H), 1.35 – 1.22 (m, 10H), 0.88 (t, J = 6.9 Hz, 3H); **^{13}C NMR** (100 MHz, $CDCl_3$) δ 175.75, 99.78, 82.49, 72.06, 58.47, 37.62, 37.47, 32.44, 31.99, 29.58, 29.51, 25.76, 25.59, 24.85, 22.76, 14.24; $\mathbf{[\alpha]^{25}_D}$ +21.0 (c = 0.67 in $CHCl_3$); **IR** (film) 3366 (br, N-H), 3189 (br, N-H), 2916, 2852, 1636 (C=O), 1532, 1462, 1431, 1340, 1221, 1207, 1133, 1112, 1067, 1050, 1001, 926, 859, 806, 726, 682, 617; **HRMS** Accurate mass (ES^+): Found 274.2385, $C_{15}H_{32}NO_3$ ($M+H^+$) requires 274.2382; **MP** 106 – 110 °C.

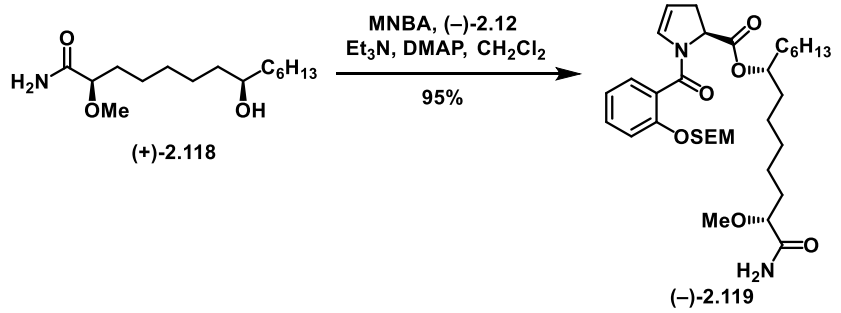

(7R,13R)-14-amino-13-methoxy-14-oxotetradecan-7-yl (S)-1-(2-((2-(trimethylsilyl)ethoxy)methoxy)benzoyl)-2,3-dihydro-1H-pyrrole-2-carboxylate (–)-2.119. (synthesized with the help of Sierra Williams) To a solution of acid **(–)-2.12** (17 mg, 0.047 mmol)

dissolved in CH_2Cl_2 (1 mL) was added MNBA (30 mg, 0.086 mmol) and Et_3N (0.015 mL, 0.109 mmol), and the solution was stirred for 10 minutes. Then alcohol **(+)-2.118** (9 mg, 0.033 mmol) and DMAP (1 mg, 0.003 mmol) dissolved in CH_2Cl_2 (1 mL) was added, and the reaction was stirred overnight. The reaction was poured into sat. NH_4Cl, extracted with CH_2Cl_2 3x, washed with brine, dried over $MgSO_4$, filtered, concentrated, and purified by column chromatography (0 → 30% Et_2O/CH_2Cl_2), yielding the title compound as a yellow oil (19 mg, 95% yield). **^{1}H NMR** (400 MHz, $CDCl_3$) δ 7.40 – 7.28 (m, 2H), 7.21 – 7.16 (m, 1H), 7.03 (td, J = 7.5, 0.8 Hz, 1H), 6.52 (br s, 1H), 6.20 – 6.11 (m, 1H), 5.60 (br s, 1H), 5.25 – 5.18 (m, 1H), 5.04 – 5.00 (m, 1H), 5.01 – 4.93 (m, 2H), 3.74 (dd, J = 16.0, 7.6 Hz, 2H), 3.60 (dd, J = 6.8, 4.5 Hz, 1H), 3.37 (s, 3H), 3.12 (ddd, J = 14.2, 10.4, 5.8 Hz, 1H), 2.70 – 2.62 (m, 1H), 1.77 – 1.64 (m, 2H), 1.62 – 1.48 (m, 4H), 1.41 – 1.17 (m, 17H), 0.93 (dd, J = 10.6, 6.2 Hz, 2H), 0.85 (t, J = 5.8 Hz, 3H), -0.02 (s, 9H); **^{13}C NMR** (100 MHz, $CDCl_3$) δ 175.79, 170.79, 165.03, 153.82, 131.26, 131.02, 129.01, 125.91, 121.98, 115.24, 108.45, 99.74, 93.34, 82.37, 75.46, 66.63, 58.33, 58.16, 34.40, 34.18, 34.09, 32.33, 31.85, 29.30, 25.35, 25.01, 24.68, 22.71, 18.15, 14.20, -1.28; **$[\alpha]^{25}_D$** –10.0 (c = 0.24 in $CHCl_3$); **IR** (film) 2927, 2858, 1733 (C=O), 1652 (C=O), 1619, 1601, 1488, 1456, 1278, 1407, 1248, 1230, 1194, 1153, 1087, 988, 836, 754, 697, 656, 609; **HRMS** Accurate mass (ES^+): Found 641.3621, $C_{33}H_{54}N_2O_7SiNa$ ($M+Na^+$) requires 641.3598.

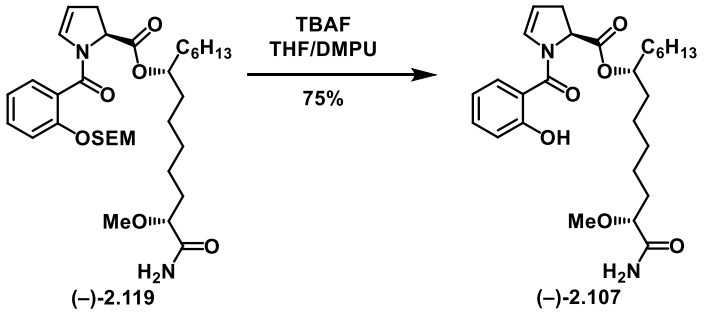

(7R,13R)-14-amino-13-methoxy-14-oxotetradecan-7-yl (S)-1-(2-hydroxybenzoyl)-2,3-dihydro-1H-pyrrole-2-carboxylate (–)-2.107. (synthesized with the help of Sierra Williams) Using the procedure for TBAF/DMPU deprotection given above (10 eq TBAF, 0.1 M DMPU),

SEM-ether **(–)-2.119** (14 mg, 0.022 mmol) yielded the title compound as a clear oil (8 mg, 75% yield). **^{1}H NMR** (400 MHz, $CDCl_3$) δ 9.87 (s, 1H), 7.42 (dd, J = 7.8, 1.4 Hz, 1H), 7.39 – 7.34 (m, 1H), 6.99 (dd, J = 8.3, 0.9 Hz, 1H), 6.93 – 6.86 (m, 1H), 6.81 (br s, 1H), 6.47 (br s, 1H), 5.40 (br s, 1H), 5.27 (d, J = 4.2 Hz, 1H), 5.06 – 4.91 (m, 2H), 3.61 (dd, J = 6.7, 4.5 Hz, 1H), 3.38 (s, 3H), 3.18 – 3.07 (m, 1H), 2.70 (d, J = 17.0 Hz, 1H), 1.79 – 1.62 (m, 2H), 1.61 – 1.46 (m, 5H), 1.43 – 1.17 (m, 15H), 0.85 (t, J = 6.9 Hz, 3H); **^{13}C NMR** (100 MHz, $CDCl_3$) δ 175.68, 170.88, 167.53, 159.28, 133.54, 131.05, 128.48, 118.96, 118.09, 117.03, 110.68, 82.44, 75.98, 59.61, 58.39, 34.16, 34.09, 33.66, 32.34, 31.82, 29.27, 25.35, 25.05, 24.71, 22.69, 14.21; **$[\alpha]^{25}_D$** –21.3 (c = 0.39 in $CHCl_3$); **IR** (film) 3386 (N-H), 3348 (N-H), 3144 (br, O-H), 2927, 2858, 1719 (C=O), 1688 (C=O), 1672, 1619, 1567, 1487, 1445, 1431, 1355, 1303, 1281, 1252, 1230, 1191, 1147, 1120, 1095, 1070, 1039, 1020, 1003, 992, 954, 943, 905, 857, 822, 796, 759, 730, 699, 667, 643; **HRMS** Accurate mass (ES^+): Found 489.2979, $C_{27}H_{41}N_2O_6$ ($M+H^+$) requires 308.1498.

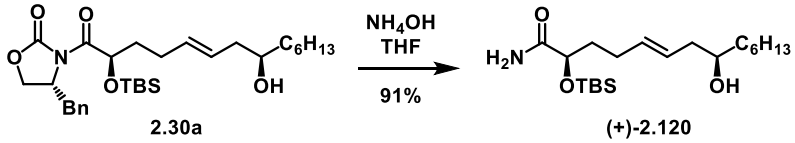

(2R,8R,E)-2-((tert-butyldimethylsilyl)oxy)-8-hydroxytetradec-5-enamide (+)-2.120. To a solution of oxazolidinone **2.30a** (50 mg, 0.094 mmol) dissolved in THF (3 mL) was added ammonium hydroxide (28% in H_2O, 2 mL). The reaction was tightly sealed and stirred for 24 hours. Another portion of ammonium hydroxide (1 mL) was added after this time, and the reaction was stirred for another 24 hours. The reaction was diluted with MeOH and concentrated. This process was repeated another 2x, and the crude product was purified by column chromatography (0 → 30% Et_2O/CH_2Cl_2 → 5% MeOH/30% Et_2O/65% CH_2Cl_2), yielding the title compound as a yellow oil (32 mg, 91% yield). **R_f** (2:1 CH_2Cl_2:Et_2O) = 0.25; **^{1}H NMR (**400 MHz, $CDCl_3$) δ 6.63 – 6.46 (m, 1H), 5.60 – 5.40 (m, 3H), 4.21 – 4.12 (m, 1H), 3.55 (d, J = 16.1 Hz, 1H), 2.28 – 1.99 (m, 4H), 1.95 – 1.80 (m, 1H), 1.80 – 1.71 (m, 3H), 1.47 – 1.39 (m, 2H), 1.33 –

1.23 (m, 6H), 0.93 (s, J = 2.9 Hz, 9H), 0.88 (t, J = 6.7 Hz, 3H), 0.13 – 0.07 (m, 6H); **^{13}C NMR** (100 MHz, $CDCl_3$) δ 177.15, 133.16, 126.95, 72.95, 71.03, 56.05, 40.79, 36.87, 34.91, 31.92, 29.44, 27.36, 25.82, 22.70, 18.09, 14.18, -4.73, -5.15; **$[\alpha]^{25}_D$** +9.3 (c = 1.64 in $CHCl_3$); **IR** (film) 3479, 2954, 2927, 2855, 1682 (C=O), 1556, 1463, 1388, 1361, 1253, 1101, 1005, 967, 912, 836, 778, 722, 669, 578; **HRMS** Accurate mass (ES^+): Found 394.2757, $C_{20}H_{41}NO_3SiNa$ ($M+Na^+$) requires 394.2753.

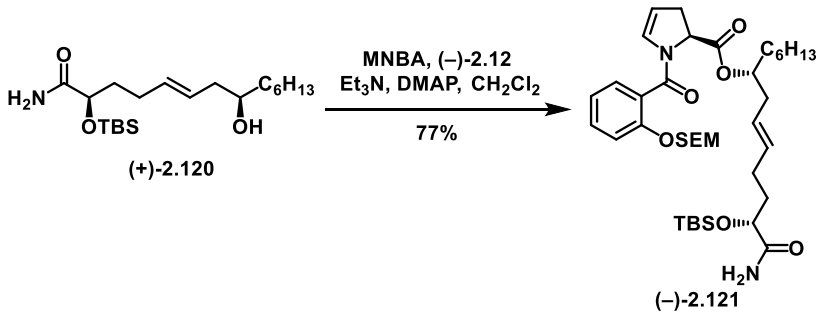

(7R,13R,E)-14-amino-13-((tert-butyldimethylsilyl)oxy)-14-oxotetradec-9-en-7-yl (S)-1-(2-((2-(trimethylsilyl)ethoxy)methoxy)benzoyl)-2,3-dihydro-1H-pyrrole-2-carboxylate (–)-2.121. To a solution of acid **(–)-2.12** (22 mg, 0.060 mmol) dissolved in CH_2Cl_2 (1 mL) was added MNBA (38 mg, 0.112 mmol) and Et_3N (0.02 mL, 0.132 mmol), and the solution was stirred for 10 minutes. Then alcohol **(+)-2.120** (16 mg, 0.043 mmol) and DMAP (1 mg, 0.004 mmol) dissolved in CH_2Cl_2 (1 mL) was added, and the reaction was stirred overnight. The reaction was poured into sat. NH_4Cl, extracted with CH_2Cl_2 3x, washed with brine, dried over $MgSO_4$, filtered, concentrated, and purified by column chromatography (0 → 30% Et_2O/CH_2Cl_2), yielding the title compound as a yellow oil (24 mg, 77% yield). **R_f** (2:1 CH_2Cl_2:Et_2O) = 0.76; **^{1}H NMR** (500 MHz, CDCl3) δ 7.38 – 7.31 (m, 2H), 7.20 (d, J = 8.2 Hz, 1H), 7.03 (td, J = 7.5, 0.8 Hz, 1H), 7.00 – 6.92 (m, 1H), 6.53 (d, J = 4.2 Hz, 1H), 6.15 (dd, J = 4.2, 2.1 Hz, 1H), 5.70 (s, 1H), 5.44 (dtd, J = 22.1, 15.3, 6.6 Hz, 2H), 5.27 – 5.19 (m, 2H), 5.06 – 4.90 (m, 3H), 4.19 – 4.09 (m, 1H), 3.79 – 3.69 (m, 2H), 3.16 – 3.06 (m, 1H), 2.70 – 2.63 (m, 1H), 2.33 – 2.26 (m, 2H), 2.14 – 2.02 (m, 3H), 1.89 – 1.78 (m, 2H), 1.77 – 1.68 (m, 2H), 1.61 – 1.51 (m, 3H), 1.35 – 1.17 (m, 12H), 0.96 – 0.89 (m,

9H), 0.86 (t, J = 6.9 Hz, 3H), 0.11 – 0.06 (m, 6H), -0.02 (s, 9H); **^{13}C NMR** (100 MHz, $CDCl_3$) δ 176.80, 170.68, 164.99, 153.84, 132.90, 131.25, 131.00, 128.99, 125.92, 125.52, 121.97, 115.21, 108.43, 93.33, 74.91, 73.13, 66.63, 58.24, 37.36, 34.89, 34.39, 33.45, 31.84, 30.43, 29.82, 29.26, 27.44, 25.86, 25.28, 22.70, 18.15, 14.19, -1.28, -4.70, -5.12; **$[\alpha]^{25}_D$** –19.8 (c = 1.20 in $CHCl_3$); **IR** (film) 3479, 2952, 2926, 2856, 1736 (C=O), 1689, 1650, 1619, 1600, 1488, 1455, 1406, 1359, 1249, 1230, 1191, 1151, 1087, 1043, 988, 917, 778, 754; **HRMS** Accurate mass (ES^+): Found 717.4299, $C_{38}H_{65}N_2O_7Si_2$ ($M+H^+$) requires 717.4330.

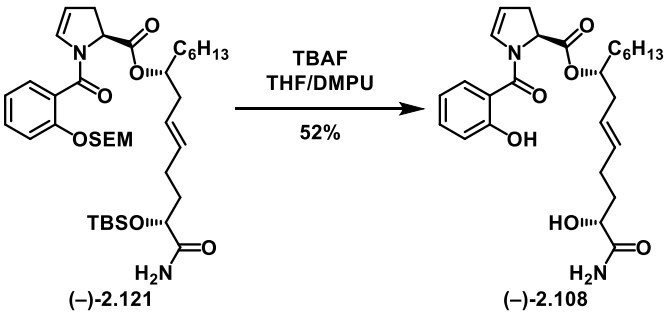

(7R,13R,E)-14-amino-13-hydroxy-14-oxotetradec-9-en-7-yl (S)-1-(2-hydroxybenzoyl)-2,3-dihydro-1H-pyrrole-2-carboxylate (–)-2.108. Using procedure given above for TBAF/DMPU deprotection, silyl ether **(–)-2.121** (24 mg, 0.034 mmol) yielded the title compound as a clear oil (8.3 mg, 52% yield). **^{1}H NMR** (500 MHz, CDCl3) δ 9.06 (s, 1H), 7.42 – 7.34 (m, 2H), 7.03 – 6.95 (m, 1H), 6.95 – 6.87 (m, 1H), 6.62 (d, J = 17.8 Hz, 2H), 5.52 (s, 2H), 5.35 – 5.29 (m, 1H), 5.29 – 5.23 (m, 1H), 5.03 (dd, J = 11.5, 4.6 Hz, 2H), 4.08 – 4.00 (m, 1H), 3.90 (s, 1H), 3.20 – 3.08 (m, 1H), 2.70 (d, J = 17.2 Hz, 1H), 2.34 – 2.11 (m, 2H), 1.96 – 1.87 (m, 1H), 1.72 – 1.49 (m, 5H), 1.34 – 1.18 (m, 10H), 0.87 (t, J = 7.0 Hz, 3H); **^{13}C NMR** (100 MHz, $CDCl_3$) δ 177.53, 171.32, 167.40, 157.36, 133.41, 132.37, 130.76, 128.36, 126.87, 119.55, 118.26, 118.03, 111.07, 70.14, 59.13, 37.82, 34.65, 33.75, 33.34, 31.79, 29.16, 27.87, 25.45, 22.66, 14.20; **$[\alpha]^{25}_D$** –40.3 (c = 0.83 in $CHCl_3$); **IR** (film) 3200 (br, O-H), 2926, 2855, 1733 (C=O), 1662 (C=O), 1592, 1487, 1430,1194, 1152, 1097, 1017, 969, 860, 755; **HRMS** Accurate mass (ES^+): Found 473.2689, $C_{26}H_{37}N_2O_6$ ($M+H^+$) requires 473.2652.

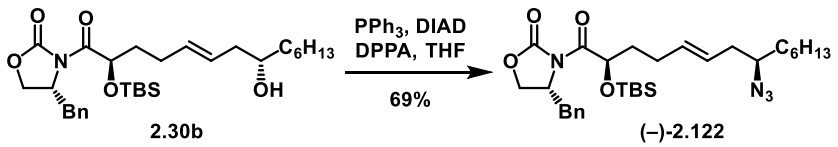

(R)-3-((2R,8R,E)-8-azido-2-((tert-butyldimethylsilyl)oxy)tetradec-5-enoyl)-4-benzyloxazolidin-2-one (–)-2.122. To a solution of compound **2.30b** (153 mg, 0.288 mmol) in THF (2 mL) was added PPh_3 (302 mg, 1.153 mmol), diisopropyl azodicarboxylate (DIAD) (0.23 mL, 1.153 mmol), and diphenylphosphoryl azide (DPPA) (0.25 mL, 1.153 mmol). After 30 minutes, the reaction was concentrated and purified by prep TLC (100% CH_2Cl_2), yielding the title compound as a yellow oil (111 mg, 69% yield). **^{1}H NMR** (400 MHz, $CDCl_3$) δ 7.26 – 7.16 (m, 3H), 7.15 – 7.11 (m, 2H), 5.48 – 5.29 (m, 2H), 5.27 (dd, J = 8.2, 3.4 Hz, 1H), 4.55 – 4.47 (m, 1H), 4.12 – 4.04 (m, 2H), 3.30 (dd, J = 13.3, 3.0 Hz, 1H), 2.58 (dd, J = 13.2, 10.2 Hz, 1H), 2.19 – 2.01 (m, 2H), 1.72 – 1.52 (m, 2H), 1.42 – 1.26 (m, 3H), 1.26 – 1.10 (m, 8H), 0.86 – 0.82 (m, 9H), 0.77 (t, J = 6.7 Hz, 3H), 0.02 – -0.03 (m, 6H); **^{13}C NMR** (125 MHz, $CDCl_3$) δ 174.33, 153.18, 135.34, 132.97, 129.56, 129.11, 127.51, 126.26, 71.01, 66.62, 62.84, 55.71, 37.79, 35.00, 33.98, 31.82, 29.17, 28.68, 26.15, 25.93, 22.69, 18.44, 14.18, 1.13, -4.49, -4.95; **$[\alpha]^{25}_D$** –5.0 (c = 0.42 in $CHCl_3$); **IR** (film) 2927, 2856, 2097, 1780 (C=O), 1712 (C=O), 1455, 1386, 1347, 1249, 1209, 1194, 1106, 1012, 969, 835, 777, 749, 700, 663, 593; **HRMS** Accurate mass (ES^+): Found 579.3367, $C_{30}H_{48}N_4O_4SiNa$ ($M+Na^+$) requires 579.3343.

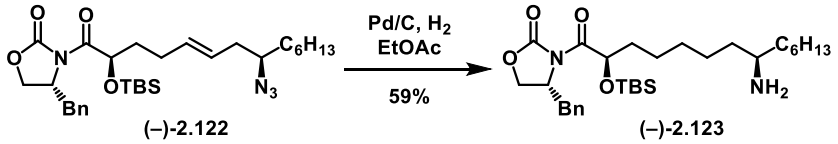

(R)-3-((2R,8R)-8-amino-2-((tert-butyldimethylsilyl)oxy)tetradecanoyl)-4-benzyloxazolidin-2-one (–)-2.123. To a solution of compound **(–)-2.122** (111 mg, 0.199 mmol) in EtOAc (10 mL) was added Pd/C (10% by wt., 100 mg), and stirred for 16 hours under a balloon of H_2. The reaction was filtered through Celite and purified by column chromatography, (50% → 0%

hexanes/CH_2Cl_2 then 0 → 20% MeOH/CH_2Cl_2), yielding the title compound as a clear oil (63 mg, 59% yield). **R_f** (9:1 CH_2Cl_2:MeOH) = 0.18, stains brown in ninhydrin; **^{1}H NMR** (400 MHz, $CDCl_3$) δ 7.36 – 7.29 (m, 3H), 7.25 – 7.22 (m, 2H), 5.40 – 5.34 (m, 1H), 4.70 – 4.59 (m, 1H), 4.32 – 4.24 (m, 1H), 4.15 (dd, J = 9.0, 2.2 Hz, 1H), 3.42 – 3.35 (m, 1H), 3.15 – 3.07 (m, 1H), 2.70 (dd, J = 13.3, 10.1 Hz, 1H), 1.74 – 1.57 (m, 10H), 1.52 – 1.19 (m, 20H), 0.93 (s, 9H), 0.86 (t, J = 6.1 Hz, 3H), 0.10 (s, 3H), 0.08 (s, 3H); **^{13}C NMR** (125 MHz, $CDCl_3$) δ 174.56, 153.26, 135.40, 129.58, 129.12, 127.51, 71.45, 66.64, 55.72, 37.83, 35.33, 31.98, 29.58, 29.48, 26.15, 26.04, 25.95, 25.63, 22.77, 18.48, 14.22, -4.50, -4.95; **$[\alpha]^{25}_D$** –9.3 (c = 0.45 in $CHCl_3$); **IR** (film) 2927, 2856, 1779 (C=O), 1711 (C=O), 1605, 1519, 1455, 1387, 1348, 1248, 1210, 1145, 1109, 1051, 1007, 977, 939, 835, 776, 762, 700, 663, 593; **HRMS** Accurate mass (ES^+): Found 533.3745, $C_{30}H_{53}N_2O_4Si$ ($M+H^+$) requires 533.3775.

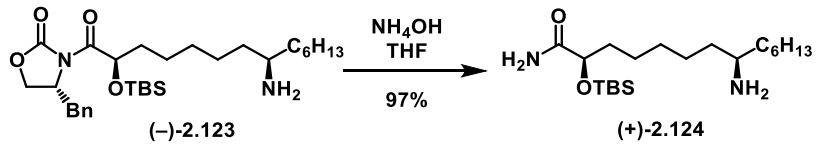

(2R,8R)-8-amino-2-((tert-butyldimethylsilyl)oxy)tetradecanamide (+)-2.124. Compound **(–)-2.123** (44 mg, 0.083 mmol) was dissolved in THF (3 mL) and 28% ammonium hydroxide (2 mL), sealed tightly and stirred for 48 hours. MeOH was added and the reaction was concentrated, and this process was repeated two more times. The resulting mixture was purified by column chromatography, eluting in 0 → 15% MeOH/0.1% NH_4OH/CH_2Cl_2, yielding the title compound as a clear oil (29 mg, 97% yield). **R_f** (0.1% NH_4OH/10% MeOH/90% CH_2Cl_2) = 0.18; **^{1}H NMR** (500 MHz, $CDCl_3$) δ 6.64 – 6.50 (m, 2H), 4.15 – 4.09 (m, 1H), 3.12 (dt, J = 14.7, 7.4 Hz, 2H), 1.79 (ddd, J = 15.1, 10.2, 4.9 Hz, 1H), 1.75 – 1.57 (m, 6H), 1.45 – 1.23 (m, 22H), 0.91 (s, 9H), 0.86 (t, J = 6.6 Hz, 3H), 0.09 (s, 3H), 0.08 (s, 3H); **^{13}C NMR** (125 MHz, $CDCl_3$) δ 177.56, 73.20, 52.12, 34.60, 33.25, 32.94, 31.71, 29.78, 29.20, 29.04, 25.84, 25.40, 24.94, 23.51, 22.68, 18.11, 14.16, -4.73, -5.16; **$[\alpha]^{25}_D$** +5.8 (c = 1.47 in $CHCl_3$); **IR** (film) 3477, 2925, 2854, 1672 (C=O),

1557, 1462, 1388, 1361, 1337, 1252, 1101, 1005, 938, 836, 778, 721, 668, 588; **HRMS** Accurate mass (ES^+): Found 373.3264, $C_{20}H_{45}N_2O_2Si$ ($M+H^+$) requires 373.3250.

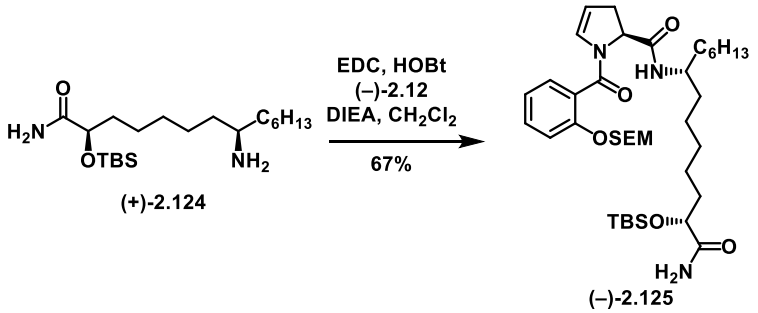

(S)-N-((7R,13R)-14-amino-13-((tert-butyldimethylsilyl)oxy)-14-oxotetradecan-7-yl)-1-(2-((2-(trimethylsilyl)ethoxy)methoxy)benzoyl)-2,3-dihydro-1H-pyrrole-2-carboxamide (–)-2.125. To a solution of acid **(–)-2.12** (19 mg, 0.053 mmol) dissolved in CH_2Cl_2 (1 mL), was added EDC (9 mg, 0.056 mmol), HOBt•H_2O (9 mg, 0.056 mmol), DIEA (0.02 mL, 0.113 mmol), and amine **(+)-2.124** (14 mg, 0.038 mmol) dissolved in CH_2Cl_2 (1 mL). The reaction was stirred overnight, then poured into water, extracted 3x with CH_2Cl_2, washed with water and brine, dried over $MgSO_4$ and purified by column chromatography (0 → 20% Et_2O/CH_2Cl_2), yielding the title compound as a yellow oil (18 mg, 67% yield). **R_f** (1:1 Et_2O:CH_2Cl_2) = 0.51; **^{1}H NMR** (500 MHz, $CDCl_3$) δ 7.41 – 7.36 (m, 1H), 7.25 (d, J = 8.5 Hz, 1H), 7.07 (t, J = 7.5 Hz, 1H), 6.98 (s, 1H), 6.52 (d, J = 4.3 Hz, 1H), 6.11 – 6.02 (m, 1H), 5.52 (s, 1H), 5.23 (t, J = 7.2 Hz, 2H), 5.19 – 5.14 (m, 1H), 5.09 (dd, J = 15.0, 5.4 Hz, 1H), 4.18 – 4.08 (m, 1H), 3.93 (s, 1H), 3.77 – 3.69 (m, 2H), 3.18 – 2.89 (m, 2H), 1.80 – 1.45 (m, 6H), 1.40 – 1.17 (m, 22H), 0.96 – 0.89 (m, 12H), 0.88 – 0.81 (m, 3H), 0.08 (s, 3H), 0.08 (s, 3H), -0.01 (s, 9H); **^{13}C NMR** (100 MHz, $CDCl_3$) δ 176.95, 169.89, 153.58, 131.57, 129.66, 128.59, 125.53, 122.27, 114.83, 111.81, 93.28, 73.55, 66.95, 59.47, 56.12, 49.30, 35.34, 35.07, 31.87, 29.84, 29.58, 29.36, 25.87, 24.17, 22.74, 18.22, 18.15, 14.21, 1.16, -1.25, -4.69, -5.12; **$[\alpha]^{25}_D$** –46.4 (c = 0.74 in $CHCl_3$); **IR** (film) 3480, 3295, 2926, 2855, 1662, 1618, 1551, 1487, 1455, 1404, 1249, 1228, 1087, 985, 938, 778, 754, 730, 667, 506; **HRMS** Accurate mass (ES^+): Found 740.4447, $C_{38}H_{67}N_3O_6Si_2Na$ ($M+Na^+$) requires 740.4466.

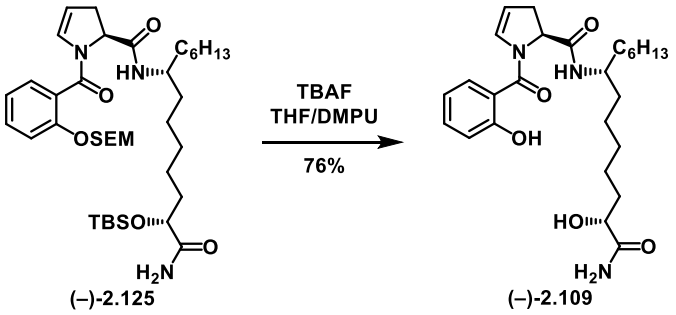

(S)-N-((7R,13R)-14-amino-13-hydroxy-14-oxotetradecan-7-yl)-1-(2-hydroxybenzoyl)-2,3-dihydro-1H-pyrrole-2-carboxamide (–)-2.109. Using the procedure given for the preparation of compound **(–)-2.1a**, silyl ether **(–)-2.125** (15 mg, 0.021 mmol) yielded the title compound as translucent oil (7.6 mg, 76% yield). $\mathbf{R_f}$ (5% MeOH/ 95% CH_2Cl_2) = 0.23; **^{1}H NMR** (500 MHz, $CDCl_3$) δ 9.68 (s, 1H), 7.33 (t, J = 7.2 Hz, 2H), 6.97 (d, J = 8.2 Hz, 1H), 6.89 (t, J = 7.3 Hz, 1H), 6.82 (s, 1H), 6.61 (s, 1H), 6.45 (s, 1H), 5.74 (s, 1H), 5.26 (s, 1H), 5.08 – 4.99 (m, 1H), 4.14 (s, 1H), 4.03 (s, 1H), 3.92 (s, 1H), 3.07 – 2.96 (m, 1H), 2.90 (d, J = 15.2 Hz, 1H), 1.81 (d, J = 69.1 Hz, 2H), 1.64 – 1.11 (m, 22H), 0.86 (t, J = 6.5 Hz, 3H); **^{13}C NMR** (100 MHz, $CDCl_3$) δ 177.87, 170.68, 167.49, 156.12, 132.93, 130.44, 128.40, 119.71, 117.58, 112.13, 71.27, 60.12, 49.71, 35.65, 34.89, 33.89, 31.89, 29.32, 28.13, 26.13, 25.18, 24.29, 22.73, 14.22; **$[\alpha]^{25}_D$** –57.5 (c = 0.76 in $CHCl_3$); **IR** (film) 3287 (br, O-H), 2927, 2856, 1653 (C=O), 1616 (C=O), 1558, 1540, 1507, 1489, 1457, 1398, 1295, 1235, 1155, 1096, 1016, 944, 855, 817, 754, 723, 653, 620, 566; **HRMS** Accurate mass (ES^+): Found 496.2817, $C_{26}H_{39}N_3O_5Na$ ($M+Na^+$) requires 496.2787.

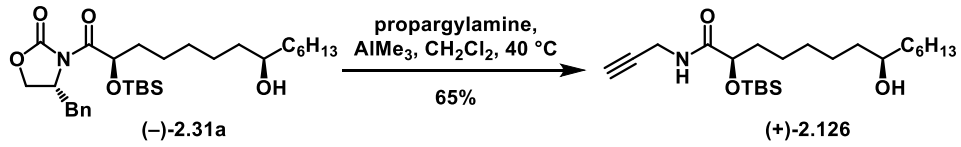

(2R,8R)-2-((tert-butyldimethylsilyl)oxy)-8-hydroxy-N-(prop-2-yn-1-yl)tetradecanamide (+)-2.126. To a solution of propargylamine (0.020 mL, 0.310 mmol) dissolved in CH_2Cl_2 (1 mL) at 0 °C was added trimethylaluminum (2M in CH_2Cl_2, 0.155 mL, 0.310 mmol), and the solution was allowed to warm to room temperature. Oxazolidinone **(–)-2.31a** (33 mg, 0.062 mmol) was added

as a solution in CH_2Cl_2 (1 mL) and the reaction was heated to reflux overnight. The reaction was then quenched with water and filtered through Celite. The layers were separated and the aqueous was extracted further (2x) with CH_2Cl_2. The combined organic layers were washed with water and brine, dried over $MgSO_4$, filtered, concentrated, and purified by column chromatography, yielding the title compound as a clear oil (17 mg, 65% yield). $\mathbf{R_f}$ (2:1 hexanes:EtOAc) = 0.44; **^{1}H NMR** (500 MHz, $CDCl_3$) δ 6.74 (t, J = 5.2 Hz, 1H), 4.17 – 4.08 (m, 2H), 3.97 (ddd, J = 17.6, 4.8, 2.5 Hz, 1H), 3.61 – 3.50 (m, 1H), 2.22 (t, J = 2.5 Hz, 1H), 1.74 – 1.65 (m, 2H), 1.46 – 1.16 (m, 28H), 0.93 (s, 9H), 0.87 (t, J = 6.8 Hz, 3H), 0.09 (s, J = 2.9 Hz, 3H), 0.08 (s, 3H); **^{13}C NMR** (101 MHz, $CDCl_3$) δ 173.73, 125.65, 79.37, 73.59, 72.02, 71.73, 37.61, 37.47, 35.25, 31.97, 30.44, 29.66, 29.50, 28.76, 25.89, 25.75, 25.60, 24.28, 22.75, 18.17, 14.23, -4.68, -5.13; $\mathbf{[\alpha]^{25}_D}$ +21.8 (c = 1.00 in $CHCl_3$); **IR** (film) 3430, 3313, 2927, 2856, 2123, 1668 (C=O), 1513, 1463, 1361, 1253, 1106, 1004, 937, 836, 779, 732, 666, 625; **HRMS** Accurate mass (ES^+): Found 434.3085, $C_{23}H_{45}NO_3SiNa$ ($M+Na^+$) requires 434.3066.

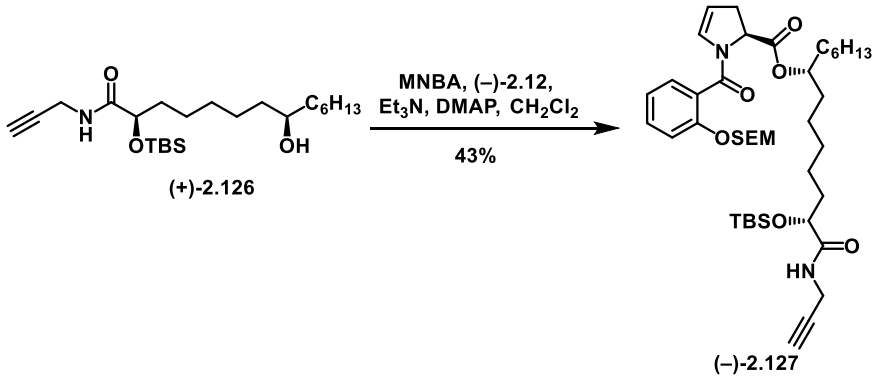

(7R,13R)-13-((tert-butyldimethylsilyl)oxy)-14-oxo-14-(prop-2-yn-1-ylamino)tetradecan-7-yl (S)-1-(2-((2-(trimethylsilyl)ethoxy)methoxy)benzoyl)-2,3-dihydro-1H-pyrrole-2-carboxylate (–)-2.127. To a solution of acid **(–)-2.12** (25 mg, 0.068 mmol) in CH_2Cl_2 (1 mL) was added MNBA (44 mg, 0.126 mmol) and Et_3N (0.022 mL, 0.160 mmol). The solution was stirred at room temperature for 10 minutes, then a solution of alcohol **(+)-2.126** (20 mg, 0.049 mmol) and DMAP (1 mg, 0.012 mmol) in CH_2Cl_2 (1 mL) was added and the reaction was stirred at room

temperature overnight. The following day, the reaction was poured into sat. NH_4Cl and extracted with CH_2Cl_2 3x. The combined organic layers were washed with brine, dried over $MgSO_4$, filtered, concentrated, and purified by column chromatography, yielding the title compound as a yellow oil (16 mg, 43% yield). **^{1}H NMR** (500 MHz, $CDCl_3$) δ 7.36 (dd, J = 12.2, 4.6 Hz, 2H), 7.20 (d, J = 8.0 Hz, 1H), 7.07 – 7.00 (m, 1H), 6.74 (t, J = 5.4 Hz, 1H), 6.16 (dt, J = 4.2, 2.1 Hz, 1H), 5.22 (dd, J = 17.4, 7.1 Hz, 2H), 5.02 (dt, J = 4.8, 2.5 Hz, 1H), 4.99 – 4.91 (m, 2H), 4.16 – 4.08 (m, 2H), 3.97 (tt, J = 4.9, 3.5 Hz, 1H), 3.75 (dd, J = 16.5, 8.1 Hz, 2H), 3.11 (ddt, J = 16.7, 11.6, 2.3 Hz, 1H), 2.69 – 2.63 (m, 1H), 2.23 (t, J = 2.6 Hz, 1H), 1.76 – 1.48 (m, 7H), 1.41 – 1.19 (m, 17H), 0.96 – 0.90 (m, 11H), 0.86 (t, J = 6.8 Hz, 3H), 0.09 – 0.05 (m, 6H), -0.01 (s, 9H); **^{13}C NMR** (101 MHz, $CDCl_3$) δ 173.69, 170.79, 164.95, 153.85, 131.22, 131.06, 129.03, 125.96, 121.97, 115.21, 108.31, 93.34, 79.42, 75.50, 73.59, 71.72, 66.62, 58.19, 35.29, 34.41, 34.10, 31.86, 29.56, 29.33, 28.71, 25.90, 25.31, 25.13, 24.16, 22.72, 18.17, 14.21, -1.27, -4.68, -5.15; **$[\alpha]^{25}_D$** –17.7 (c = 1.00 in $CHCl_3$); **IR** (film) 3435, 3314, 2950, 2927, 2856, 1745 (C=O), 1651 (C=O), 1620 (C=O), 1601, 1488, 1455, 1407, 1355, 1249, 1230, 1193, 1151, 1086, 989, 938, 917, 835, 779, 754, 730, 696, 667; **HRMS** Accurate mass (ES^+): Found 757.4687, $C_{41}H_{69}N_2O_7Si_2$ ($M+H^+$) requires 757.4643.

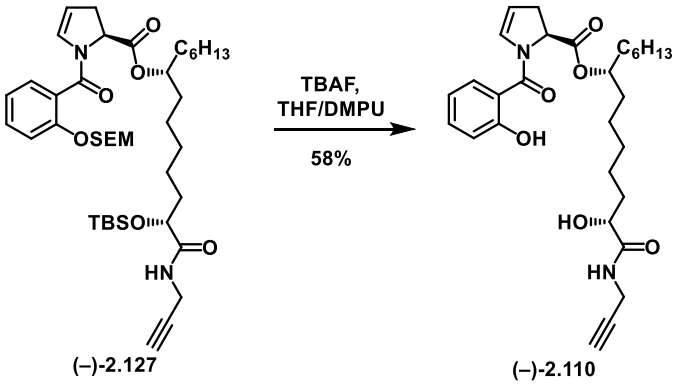

(–)-2.127 (–)-2.110

(7R,13R)-13-hydroxy-14-oxo-14-(prop-2-yn-1-ylamino)tetradecan-7-yl (S)-1-(2-hydroxybenzoyl)-2,3-dihydro-1H-pyrrole-2-carboxylate (–)-2.110. To a solution of silyl ether **(–)-2.127** (15 mg, 0.020 mmol) dissolved in DMPU (0.39 mL) was added TBAF (1M in THF,

0.39 mL, 0.390 mmol). After 30 minutes, the reaction was quenched with sat. NH_4Cl, and the mixture was extracted with Et_2O 5x. The combined organic layers were washed with 1M NH_4Cl 5x and brine, dried over $MgSO_4$, filtered, concentrated, and purified by column chromatography (3:1 EtOAc:hexanes), yielding the title compound as a clear oil (5.9 mg, 58% yield). **R_f** (3:1 EtOAc:hexanes) = 0.20; **^{1}H NMR** (500 MHz, $CDCl_3$) δ 9.53 (br s, 1H), 7.44 – 7.35 (m, 2H), 7.03 – 6.98 (m, 1H), 6.94 – 6.87 (m, 1H), 6.73 (s, 1H), 5.33 – 5.25 (m, 1H), 5.01 (dd, J = 11.3, 4.6 Hz, 2H), 4.13 – 3.94 (m, 3H), 3.35 (br s, 1H), 3.19 – 3.08 (m, 1H), 2.70 (d, J = 17.3 Hz, 1H), 2.19 (t, J = 2.5 Hz, 1H), 1.87 – 1.76 (m, 1H), 1.71 – 1.48 (m, 6H), 1.32 (ddd, J = 28.0, 17.2, 10.1 Hz, 15H), 0.87 (t, J = 7.0 Hz, 3H); **^{13}C NMR** (126 MHz, CDCl3) δ 173.87, 171.31, 167.45, 158.09, 133.52, 130.86, 128.33, 119.42, 118.06, 117.70, 111.12, 79.64, 75.98, 71.62, 71.53, 59.39, 34.54, 34.31, 34.11, 31.83, 29.22, 28.86, 28.27, 25.52, 24.84, 24.56, 22.68, 14.20; **$[\alpha]^{25}_D$** –32.4 (c = 0.38 in $CHCl_3$); **IR** (film) 3305 (br O-H), 2927, 2856, 1733 (C=O), 1681 (C=O) 1592, 1487, 1430, 1354, 1195, 1152, 1098, 1017, 859, 755, 720, 655; **HRMS** Accurate mass (ES^+): Found 513.2991 (+5.3 ppm), $C_{29}H_{41}N_2O_6$ ($M+H^+$) requires 513.2964.

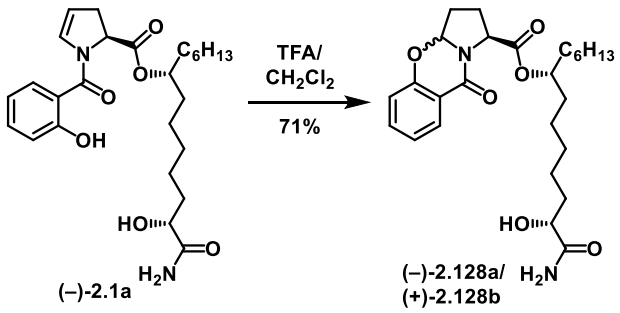

(7R,13R)-14-amino-13-hydroxy-14-oxotetradecan-7-yl (1S,3aS)-9-oxo-1,2,3,3a-tetrahydro-9H-benzo[e]pyrrolo[2,1-b][1,3]oxazine-1-carboxylate (2a), **(7R,13R)-14-amino-13-hydroxy-14-oxotetradecan-7-yl (1S,3aR)-9-oxo-1,2,3,3a-tetrahydro-9H-benzo[e]pyrrolo[2,1-b][1,3]oxazine-1-carboxylate (–)-2.128a/(+)-2.128b.** To a solution of **(–)-2.1a** (12 mg, 0.025 mmol) dissolved in CH_2Cl_2 (1 mL) was added trifluoroacetic acid (1 mL), and the reaction was stirred for 30 minutes at room temperature. The reaction was slowly quenched with sat. Na_2CO_3

solution until the pH was greater than 8, then extracted with CH_2Cl_2 3x, washed with brine, dried over $MgSO_4$, filtered, concentrated, and purified by preparative TLC (2% MeOH/EtOAc), yielding the diastereomeric title compounds (configurations were not assigned) (8.5 mg total, 71% yield). *Less polar isomer* (5.0 mg, 42% yield): **R_f** (2% MeOH/EtOAc) = 0.37; **^{1}H NMR** (500 MHz, $CDCl_3$) δ 7.88 – 7.81 (m, 1H), 7.49 – 7.43 (m, 1H), 7.12 (td, J = 7.7, 0.9 Hz, 1H), 7.01 – 6.70 (m, 2H), 5.78 – 5.73 (m, 1H), 5.42 (s, 1H), 5.04 – 4.97 (m, 1H), 4.82 – 4.71 (m, 1H), 4.28 – 4.17 (m, 2H), 2.59 – 2.46 (m, 2H), 2.36 – 2.27 (m, 1H), 2.03 – 1.96 (m, 1H), 1.95 – 1.87 (m, 1H), 1.80 – 1.70 (m, 1H), 1.68 – 1.43 (m, 7H), 1.42 – 1.20 (m, 12H), 0.88 (t, J = 6.9 Hz, 3H); **^{13}C NMR** (125 MHz, $CDCl_3$) δ 177.48, 171.59, 171.49, 161.36, 157.42, 134.64, 128.18, 128.04, 123.12, 119.04, 116.94, 88.82, 75.73, 71.17, 58.31, 34.64, 33.98, 33.86, 31.87, 30.96, 29.84, 29.22, 27.73, 26.36, 25.56, 24.62, 24.28, 22.70, 14.21; **$[\alpha]^{25}_D$** +63.8 (c = 0.13 in $CHCl_3$); **IR** (film) 3326 (br, O-H), 2928, 2858, 2360, 1733 (C=O), 1660 (C=O), 1597, 1507, 1468, 1431, 1351, 1197, 1166, 1099, 1019, 959, 860, 822, 788, 758, 651, 608, 585; **HRMS** Accurate mass (ES^+): Found 475.2781, $C_{26}H_{39}N_2O_6$ ($M+H^+$) requires 475.2808. *More polar isomer* (3.5 mg, 29% yield): **R_f** (2% MeOH/EtOAc) = 0.29; **^{1}H NMR** (500 MHz, $CDCl_3$) δ 7.91 – 7.79 (m, 1H), 7.49 – 7.44 (m, 1H), 7.12 (td, J = 7.7, 1.0 Hz, 1H), 7.01 (dd, J = 8.2, 4.2 Hz, 1H), 6.94 – 6.73 (m, 1H), 5.58 (dt, J = 9.8, 4.9 Hz, 1H), 5.39 (s, 1H), 5.05 – 4.94 (m, 1H), 4.68 – 4.59 (m, 1H), 4.28 (d, J = 17.5 Hz, 1H), 4.17 – 4.09 (m, 1H), 2.53 – 2.47 (m, 1H), 2.44 – 2.25 (m, 2H), 2.19 (dd, J = 13.4, 7.8 Hz, 1H), 1.87 – 1.79 (m, 1H), 1.77 – 1.68 (m, 1H), 1.59 – 1.35 (m, 7H), 1.30 – 1.20 (m, 12H), 0.87 (t, J = 7.0 Hz, 3H); **^{13}C NMR** (100 MHz, $CDCl_3$) δ 177.36, 170.73, 161.68, 158.00, 134.67, 127.96, 123.01, 119.04, 117.12, 88.70, 75.62, 71.05, 57.27, 34.68, 33.93, 33.71, 31.85, 30.33, 29.84, 29.21, 27.61, 26.19, 25.57, 24.60, 24.05, 22.69, 14.22; **$[\alpha]^{25}_D$** –28.1 (c = 0.11 in $CHCl_3$); **IR** (film) 3326 (br, O-H), 2927, 2856, 2360, 1734 (C=O), 1659 (C=O), 1613, 1578, 1469, 1432, 1351, 1225, 1196, 1079, 1024, 954, 907, 856, 785, 759, 732, 700, 652, 606, 584; **HRMS** Accurate mass (ES^+): Found 475.2783, $C_{26}H_{39}N_2O_6$ ($M+H^+$) requires 475.2808.

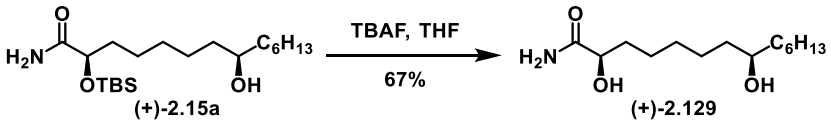

(2R,8R)-2,8-dihydroxytetradecanamide (+)-2.129. To a solution of silyl ether **(+)-2.15a** (25 mg, 0.069 mmol) in THF (0.5 mL) was added TBAF (1M in THF, 0.34 mL, 0.34 mmol), and the reaction was stirred for 30 minutes, poured into sat. NH_4Cl, and extracted with Et_2O 3x. The combined organic layers were washed with 1M NH_4Cl 5x, dried over $MgSO_4$, filtered, concentrated, and purified by column chromatography (2:1 CH_2Cl_2:Et_2O) yielding the title compound as a white solid (12 mg, 67% yield). **^{1}H NMR** (500 MHz, MeOD) δ 3.98 (dd, J = 7.9, 3.9 Hz, 1H), 3.53 – 3.46 (m, 1H), 1.80 – 1.72 (m, 1H), 1.64 – 1.55 (m, 1H), 1.50 – 1.26 (m, 18H), 0.91 (t, J = 7.0 Hz, 3H); **^{13}C NMR** (125 MHz, MeOD) δ 180.66, 72.68, 72.42, 38.47, 38.36, 35.64, 33.07, 30.63, 30.57, 26.80, 26.72, 26.13, 23.71, 14.43; **$[\alpha]^{25}_D$** +14.8 (c = 0.59 in MeOH); **IR** (film) 3232 (br, O-H), 2953, 2922, 2852, 2545, 2410, 2361, 2342, 2159, 2027, 1978, 1734, 1622 (C=O), 1591, 1558, 1465, 1452, 1436, 1378, 1363, 1345, 1227, 1169, 1133, 1090, 1065, 1024, 957, 923, 906, 857, 803, 721, 668, 609; **HRMS** Accurate mass (ES^+): Found 282.2041, $C_{14}H_{29}NO_3Na$ ($M+Na^+$) requires 282.2045; **MP** 99.2 – 101.7 °C.

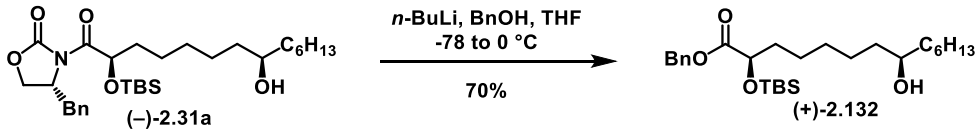

Benzyl (2R,8R)-2-((tert-butyldimethylsilyl)oxy)-8-hydroxytetradecanoate (+)-2.132. (synthesized once by Colleen Keohane and once by me) To a solution of benzyl alcohol (0.040 mL, 0.388 mmol) dissolved in THF (3 mL) at -78 °C was added *n*-BuLi (2.25 M in hexanes, 0.140 mL, 0.323 mmol) dropwise. After 5 minutes, a solution of oxazolidinone **(–)-2.31a** (69 mg, 0.129 mmol) in THF (1 mL) was added dropwise to the reaction. The reaction was warmed to 0 °C, after which time TLC indicated the consumption of starting material. The reaction was

quenched with sat. NH_4Cl, extracted with EtOAc 3x, and the combined organic layers were washed with brine, dried over $MgSO_4$, filtered, concentrated, and purified by column chromatography, yielding the title compound as a clear oil (42 mg, 70% yield). **^{1}H NMR** (500 MHz, $CDCl_3$) δ 7.37 – 7.30 (m, 5H), 5.15 (dd, J = 27.9, 12.2 Hz, 2H), 4.22 (dd, J = 6.7, 5.5 Hz, 1H), 3.56 (s, 1H), 1.74 – 1.67 (m, 2H), 1.46 – 1.22 (m, 22H), 0.88 (s, J = 9H), 0.03 (s, 3H), 0.02 (s, 3H); **^{13}C NMR** (125 MHz, $CDCl_3$) δ 173.85, 135.86, 128.63, 128.54, 128.41, 72.38, 72.03, 66.54, 37.62, 37.46, 35.23, 31.97, 29.50, 25.83, 25.73, 25.60, 25.20, 22.75, 18.41, 14.22, -4.80, -5.24; **$[\alpha]^{25}_D$** +20.3 (c = 1.00 in $CHCl_3$); **HRMS** Accurate mass (ES^+): Found 465.3413, $C_{27}H_{49}O_4Si$ ($M+H^+$) requires 465.3400.

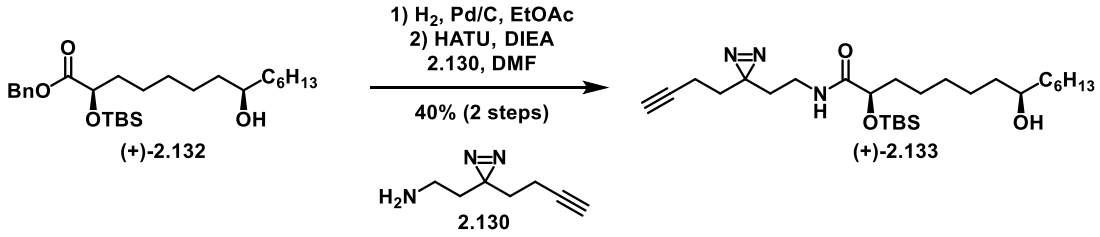

(2R,8R)-N-(2-(3-(but-3-yn-1-yl)-3H-diazirin-3-yl)ethyl)-2-((tert-butyldimethylsilyl)oxy)-8-hydroxytetradecanamide (+)-2.133. (synthesized once by Colleen Keohane and once by me) To a solution of benzyl ester **(+)-2.132** (43 mg, 0.093 mmol) dissolved in EtOAc (2 mL) was added 10% Pd/C (20 mg), and the reaction flask was vacuumed and backfilled 5x with a balloon of H_2. The reaction was closely monitored by TLC, and after 2 hours, the starting material was consumed. The reaction was filtered over Celite and concentrated (*the acid intermediate, in particular the silyl ether moiety, was highly unstable, and cleavage was observed in as little as an hour)* and immediately used in the next step. The acid was dissolved in DMF (1 mL), and HATU (42 mg, 0.112 mmol) was added as a solid, followed by a solution of amine **2.130** (prepared as previously described: Li, Z.; Hao, P.; Li, L.; Tan, C. Y.; Cheng, X.; Chen, G. Y.; Sze, S. K.; Shen, H. M.; Yao, S. Q. *Angew. Chem. Int. Ed.* **2013**, *52*, 8551.) (14 mg, 0.102 mmol) dissolved in DMF (1 mL), then DIEA (0.05 mL, 0.279 mmol) was added, and the reaction was stirred at

room temperature overnight. The following day, the reaction was poured into water and EtOAc, and the layers were separated. The aqueous layer was extracted 2x more with EtOAc and the combined organic layers were washed with water and brine, concentrated, and purified by column chromatography, yielding the title compound as a yellow oil (18 mg, 40% over 2 steps). **^{1}H NMR** (500 MHz, $CDCl_3$) δ 6.63 (t, J = 5.5 Hz, 1H), 4.15 – 4.09 (m, 1H), 3.56 (s, 1H), 3.16 – 3.06 (m, 2H), 2.06 – 1.95 (m, 3H), 1.79 – 1.61 (m, 6H), 1.47 – 1.21 (m, 19H), 0.94 (s, 9H), 0.88 (t, J = 6.7 Hz, 3H), 0.10 (d, J = 7.0 Hz, 6H); **$[\alpha]^{25}_D$** +12.2 (c = 0.81 in $CHCl_3$); **^{13}C NMR** (100 MHz, $CDCl_3$) δ 173.99, 82.62, 73.48, 72.00, 69.49, 37.60, 37.48, 35.18, 33.80, 32.79, 32.35, 31.96, 29.70, 29.49, 26.84, 25.90, 25.74, 25.60, 24.13, 22.74, 18.16, 14.21, 13.38, -4.66, -5.04; **HRMS** Accurate mass (ES^+): Found 494.3801, $C_{27}H_{52}N_3O_3Si$ ($M+H^+$) requires 494.3778.

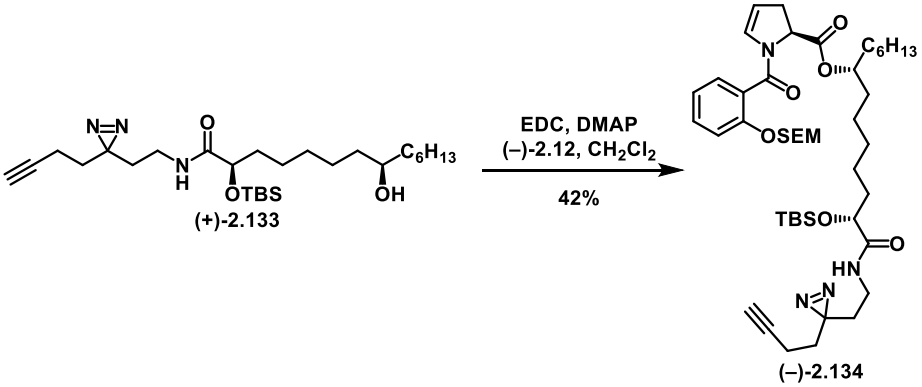

(7R,13R)-14-((2-(3-(but-3-yn-1-yl)-3H-diazirin-3-yl)ethyl)amino)-13-((tert-butyldimethylsilyl)oxy)-14-oxotetradecan-7-yl (S)-1-(2-((2-(trimethylsilyl)ethoxy)methoxy)benzoyl)-2,3-dihydro-1H-pyrrole-2-carboxylate (–)-2.134. (synthesized once by Colleen Keohane and once by me) To a solution of acid **(–)-2.12** (33 mg, 0.091 mmol), alcohol **(+)-2.133** (28 mg, 0.057 mmol), and EDC (20 mg, 0.114 mmol) in CH_2Cl_2 (2 mL) was added DMAP (3 mg, 0.029 mmol) and the reaction was stirred at room temperature overnight. The next day the reaction was poured into water and extracted with CH_2Cl_2 3x. The combined organic layers were washed with brine, dried over $MgSO_4$, filtered, concentrated, and

purified by column chromatography, yielding the title compound as a yellow oil (20 mg, 42% yield). **^{1}H NMR** (500 MHz, $CDCl_3$) δ 7.37 – 7.32 (m, 2H), 7.19 (d, J = 8.0 Hz, 1H), 7.03 (t, J = 7.5 Hz, 1H), 6.64 (t, J = 5.9 Hz, 1H), 6.16 (dt, J = 4.2, 2.0 Hz, 1H), 5.22 (dd, J = 18.2, 7.1 Hz, 2H), 5.01 (dt, J = 4.7, 2.5 Hz, 1H), 4.99 – 4.91 (m, 2H), 4.12 (t, J = 5.0 Hz, 1H), 3.76 – 3.70 (m, 2H), 3.18 – 3.02 (m, 3H), 2.70 – 2.61 (m, 1H), 2.02 – 1.96 (m, 3H), 1.78 – 1.16 (m, 26H), 0.92 (s, 9H), 0.86 (t, J = 6.7 Hz, 3H), 0.08 (s, 3H), 0.07 (s, 3H), -0.02 (s, J = 9H); **^{13}C NMR** (126 MHz, $CDCl_3$) δ 173.95, 170.78, 164.95, 153.86, 131.22, 131.08, 129.03, 126.02, 121.98, 115.25, 108.29, 93.37, 82.64, 75.50, 73.55, 69.49, 66.62, 58.22, 35.26, 34.42, 34.11, 33.82, 32.83, 32.35, 31.86, 29.82, 29.62, 29.33, 26.84, 25.93, 25.32, 25.14, 24.09, 22.72, 18.17, 14.20, 13.39, -1.27, -4.64, -5.03; **$[\alpha]^{25}_D$** −16.3 (c = 1.00 in $CHCl_3$); **HRMS** Accurate mass (ES^+): Found 839.5166, $C_{45}H_{76}N_4O_7Si_2$ ($M+H^+$) requires 839.5174.

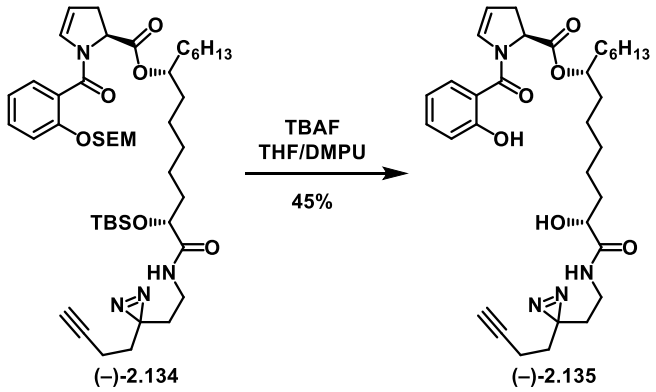

(7R,13R)-14-((2-(3-(but-3-yn-1-yl)-3H-diazirin-3-yl)ethyl)amino)-13-hydroxy-14-oxotetradecan-7-yl (S)-1-(2-hydroxybenzoyl)-2,3-dihydro-1H-pyrrole-2-carboxylate (–)-2.135. (synthesized once by Colleen Keohane and once by me) To a solution of silyl ether **(–)-2.134** (13 mg, 0.015 mmol) dissolved in DMPU (0.31 mL, dried over 3 Å molecular sieves prior to use) was added TBAF (1M in THF, 0.31 mL, 0.31 mmol, dried over 3 Å molecular sieves prior to use). After 30 minutes, the reaction was quenched with sat. NH_4Cl, and the mixture was extracted with Et_2O 5x. The combined organic layers were washed with 1M NH_4Cl 5x and brine,

dried over $MgSO_4$, filtered, concentrated, and purified by column chromatography yielding the title compound as a clear oil (4.0 mg, 45% yield). **^{1}H NMR** (500 MHz, $CDCl_3$) δ 9.54 (br s, 1H), 7.43 – 7.35 (m, 2H), 6.98 (t, J = 10.1 Hz, 1H), 6.91 (t, J = 7.5 Hz, 1H), 6.73 (s, 1H), 5.31 – 5.25 (m, 1H), 5.01 (dd, J = 11.2, 4.4 Hz, 1H), 4.07 (dd, J = 8.0, 3.4 Hz, 1H), 3.30 (br s, 1H), 3.18 – 3.03 (m, 3H), 2.70 (d, J = 17.0 Hz, 1H), 2.02 – 1.94 (m, 3H), 1.80 (s, 1H), 1.71 – 1.11 (m, 25H), 0.87 (t, J = 6.9 Hz, 3H); **^{13}C NMR** (100 MHz, $CDCl_3$) δ 174.21, 171.24, 167.42, 158.14, 133.54, 130.86, 128.34, 119.41, 118.03, 117.65, 111.14, 82.80, 75.98, 71.60, 69.49, 59.39, 34.52, 34.33, 34.09, 32.77, 32.21, 31.83, 29.84, 29.22, 28.30, 26.89, 25.51, 24.84, 24.57, 22.69, 14.21, 13.38; **$[\alpha]^{25}_D$** −28.4 (c = 0.52 in $CHCl_3$); **HRMS** Accurate mass (ES^+): Found 595.3523, $C_{33}H_{47}N_4O_6$ ($M+H^+$) requires 595.3496.

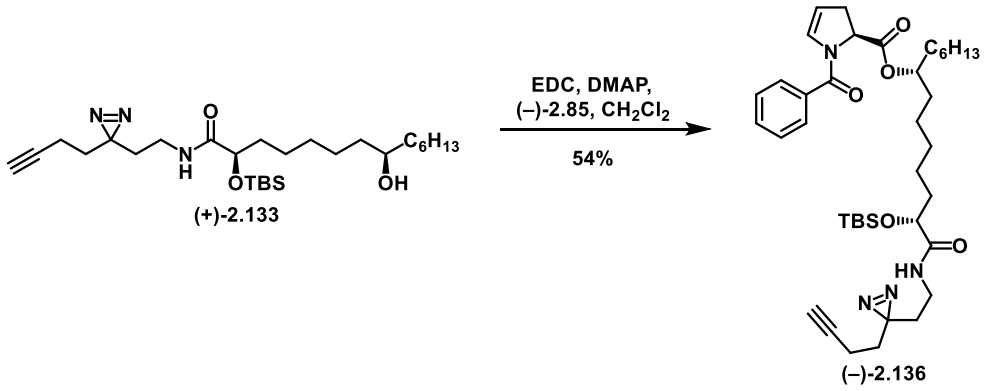

(7R,13R)-14-((2-(3-(but-3-yn-1-yl)-3H-diazirin-3-yl)ethyl)amino)-13-((tert-butyldimethylsilyl)oxy)-14-oxotetradecan-7-yl (S)-1-benzoyl-2,3-dihydro-1H-pyrrole-2-carboxylate (–)-2.136. (synthesized once by Colleen Keohane and once by me) To a solution of acid **(–)-2.85** (22 mg, 0.101 mmol), alcohol **(+)-2.133** (25 mg, 0.051 mmol), and EDC (19 mg, 0.101 mmol) dissolved in CH_2Cl_2 (2 mL) was added DMAP (3 mg, 0.026 mmol), and the reaction was stirred at room temperature overnight. Water was added and the aqueous layer was extracted with CH_2Cl_2 3x. The combined organic layers were washed with brine, dried over Na_2SO_4, filtered, concentrated, and purified by column chromatography, yielding the title compound as a

yellow oil (19 mg, 54% yield). **R_f** (9:1 CH_2Cl_2:Et_2O) = 0.50; **^{1}H NMR** (500 MHz, $CDCl_3$) δ 7.55 (d, J = 6.9 Hz, 2H), 7.48 – 7.39 (m, 3H), 6.65 (t, J = 6.0 Hz, 1H), 6.51 (s, 1H), 5.10 (s, 1H), 5.02 – 4.90 (m, 1H), 4.12 (t, J = 4.9 Hz, 1H), 3.17 – 3.02 (m, 3H), 2.75 – 2.63 (m, 1H), 2.04 – 1.96 (m, 2H), 1.74 – 1.50 (m, 12H), 1.41 – 1.15 (m, 14H), 0.93 (s, 9H), 0.85 (t, J = 6.8 Hz, 3H), 0.08 (d, J = 5.8 Hz, 6H); **^{13}C NMR** (125 MHz, $CDCl_3$) δ 173.97, 170.88, 166.96, 135.27, 131.05, 130.72, 128.55, 127.93, 108.84, 82.63, 75.64, 73.53, 69.49, 58.80, 35.23, 34.07, 33.81, 32.81, 32.33, 31.83, 29.60, 29.30, 26.84, 25.92, 25.27, 25.13, 24.07, 22.69, 18.17, 14.19, 13.39, -4.65, -5.04; **$[\alpha]^{25}_D$** −26.6 (c = 1.36 in $CHCl_3$); **HRMS** Accurate mass (ES^+): Found 693.4409, $C_{39}H_{61}N_4O_5Si$ ($M+H^+$) requires 693.4411.

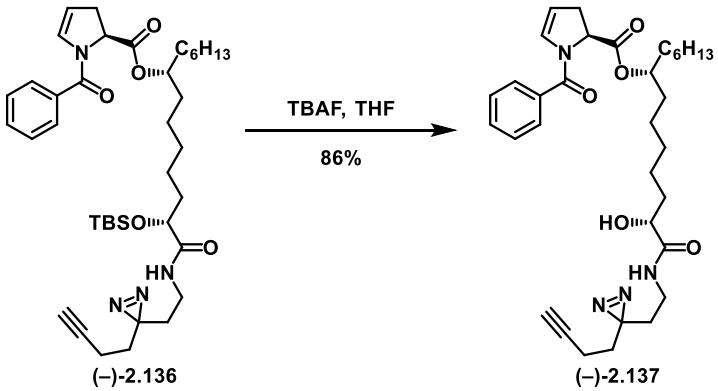

(7R,13R)-14-((2-(3-(but-3-yn-1-yl)-3H-diazirin-3-yl)ethyl)amino)-13-hydroxy-14-oxotetradecan-7-yl (S)-1-benzoyl-2,3-dihydro-1H-pyrrole-2-carboxylate (–)-2.137. (synthesized once by Colleen Keohane and once by me) To a solution of silyl ether **(–)-2.136** (18 mg, 0.026 mmol) in THF (1 mL) was added TBAF (1M in THF, 0.03 mL, 0.03 mmol). After 15 minutes the reaction was quenched with sat. NH_4Cl, and the mixture was extracted with EtOAc 3x, washed with brine, dried over Na_2SO_4, filtered, concentrated, and purified by column chromatography, yielding the title compound as a clear oil (13 mg, 86% yield). **^{1}H NMR** (500 MHz, $CDCl_3$) δ 7.56 – 7.42 (m, 5H), 6.89 (t, J = 5.9 Hz, 1H), 6.50 (dt, J = 4.3, 2.1 Hz, 1H), 5.18 – 5.14 (m, 1H), 5.04 (qd, J = 8.4, 4.2 Hz, 1H), 4.96 (dd, J = 11.6, 5.0 Hz, 1H), 4.02 (dd, J = 8.5, 3.3

Hz, 1H), 3.14 (ddt, J = 16.7, 11.6, 2.4 Hz, 2H), 2.92 (dd, J = 13.3, 7.1 Hz, 2H), 2.73 – 2.64 (m, 1H), 1.99 – 1.94 (m, 3H), 1.86 – 1.77 (m, 1H), 1.68 – 1.38 (m, 16H), 1.34 – 1.19 (m, 8H), 0.87 (t, J = 7.0 Hz, 3H); **^{13}C NMR** (125 MHz, $CDCl_3$) δ 174.74, 170.53, 167.80, 134.73, 131.12, 130.81, 128.78, 127.83, 125.66, 110.03, 82.77, 75.19, 70.85, 69.42, 58.61, 34.77, 34.00, 33.91, 33.67, 32.79, 32.20, 31.84, 30.44, 29.25, 27.50, 26.82, 25.59, 24.67, 24.26, 22.69, 14.20, 13.37; **$[\alpha]^{25}_D$** – 25.1 (c = 0.49 in $CHCl_3$); **HRMS** Accurate mass (ES^+): Found 579.3558, $C_{33}H_{47}N_4O_5$ ($M+H^+$) requires 579.3546.

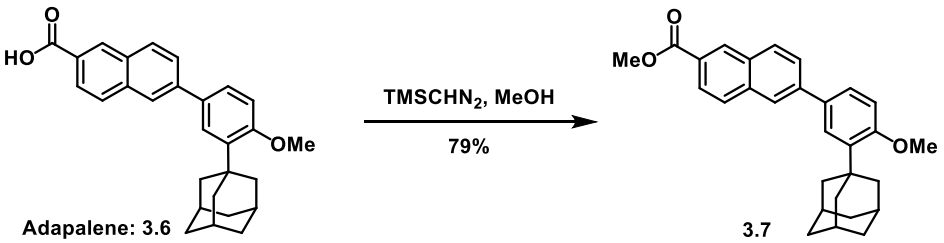

Methyl 6-(3-(adamantan-1-yl)-4-methoxyphenyl)-2-naphthoate (3.7). (synthesized by Colleen Keohane) To a solution of adapalene (50 mg, 0.121 mmol) in 4:1 THF/MeOH (0.4 mL) at 0 °C was added $TMSCH_2N_2$ (0.15 mL, 0.290 mmol) and the reaction was warmed to room temperature over 1 hour. The reaction mixture was concentrated, 1N HCl was added, and was extracted with EtOAc 3x. The combined organic layers were washed with water and brine, dried over Na_2SO_4, filtered, and concentrated; yielding the title compound as a white solid (41 mg, 79% yield). **^{1}H NMR** (500 MHz, $CDCl_3$) δ 8.61 (s, 1H), 8.07 (dd, J = 8.6, 1.7 Hz, 1H), 8.03 – 7.96 (m, 2H), 7.92 (d, J = 8.6 Hz, 1H), 7.80 (dd, J = 8.5, 1.8 Hz, 1H), 7.60 (d, J = 2.4 Hz, 1H), 7.55 (dd, J = 8.4, 2.4 Hz, 1H), 7.00 (d, J = 8.5 Hz, 1H), 3.99 (s, 3H), 3.91 (s, 3H), 2.19 (s, 6H), 2.10 (s, 3H), 1.80 (s, 6H); **^{13}C NMR** (125 MHz, $CDCl_3$) δ 167.44, 159.03, 141.51, 139.11, 136.06, 132.67, 131.35, 130.95, 129.82, 128.33, 127.02, 126.59, 126.09, 125.84, 125.68, 124.84, 112.21, 55.27, 52.31, 40.72, 37.25, 29.23; **HRMS** Accurate mass (ES+): Found 427.2268, $C_{29}H_{31}O_3$ (M+H+) requires 427.2273.

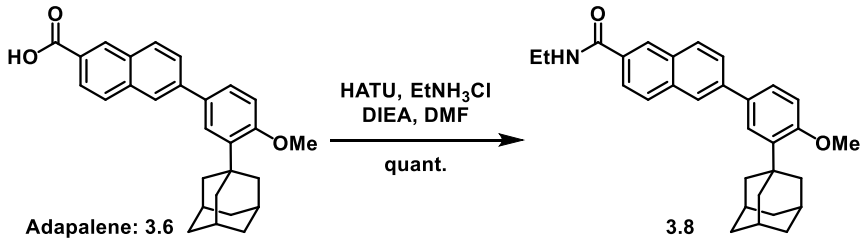

6-(3-(adamantan-1-yl)-4-methoxyphenyl)-N-ethyl-2-naphthamide (3.8). (synthesized by Colleen Keohane) To a slurry of adapalene (50 mg, 0.121 mmol) in DMF (3 mL) was added DIEA (0.13 mL, 0.726 mmol) followed by HATU (50.6 mg, 0.133 mmol) and $EtNH_3Cl$ (30 mg, 0.363 mmol) and the reaction was stirred at room temperature overnight. The reaction poured into water and quenched with sat. $NaHCO_3$, then extracted with CH_2Cl_2 3x. The combined organic layers were washed with water and brine, dried over Na_2SO_4, filtered, concentrated, and purified by prep TLC (neat EtOAc), yielding the title compound as a white solid (53 mg, quant. yield). **^{1}H NMR** (500 MHz, $CDCl_3$) δ 8.28 (s, 1H), 8.00 (s, 1H), 7.94 (dd, J = 13.3, 8.6 Hz, 2H), 7.83 (dd, J = 8.5, 1.7 Hz, 1H), 7.79 (dd, J = 8.5, 1.8 Hz, 1H), 7.59 (d, J = 2.4 Hz, 1H), 7.54 (dd, J = 8.4, 2.4 Hz, 1H), 7.00 (d, J = 8.5 Hz, 1H), 6.24 (br s, 1H), 3.91 (s, 3H), 3.58 (qd, J = 7.3, 5.9 Hz, 2H), 2.19 (s, 6H), 2.10 (s, 3H), 1.80 (s, 6H), 1.32 (t, J = 7.3 Hz, 3H); **^{13}C NMR** (125 MHz, $CDCl_3$) δ 167.64, 158.98, 140.85, 139.12, 135.23, 132.76, 131.65, 131.53, 129.36, 128.64, 127.15, 126.70, 126.08, 125.81, 124.86, 124.01, 112.24, 55.30, 40.75, 37.27, 35.20, 29.25, 15.13; **HRMS** Accurate mass (ES+): Found 462.2404, $C_{30}H_{33}NO_2Na$ (M+Na+) requires 462.2409.

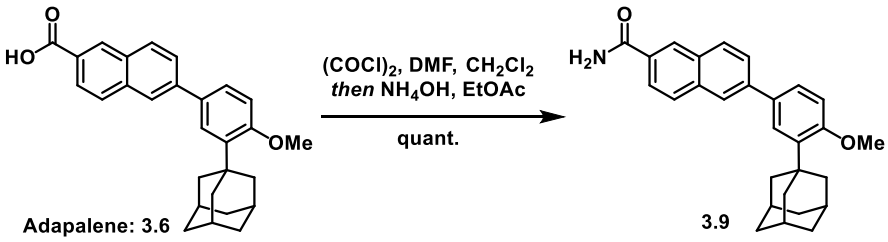

6-(3-(adamantan-1-yl)-4-methoxyphenyl)-2-naphthamide (3.9). (synthesized by Colleen Keohane) To a solution of adapalene (50 mg, 0.121 mmol) in CH_2Cl_2 (3 mL) and DMF (one

drop, cat.) was added oxalyl chloride (2M in CH_2Cl_2, 0.15 mL, 0.30 mmol), and the reaction was stirred at room temperature 2 hours. The reaction was concentrated and dissolved in 8:1 EtOAc/NH_4OH (5 mL) and stirred at 0 °C for 30 minutes. The reaction was diluted with EtOAc and water, and the aqueous layer was extracted with EtOAc 3x. The combined organic layers were washed with water and brine, dried over Na_2SO_4, filtered, and concentrated, yielding the title compound as a white solid (49 mg, quant.). **^{1}H NMR** (500 MHz, $CDCl_3$) δ 8.36 (s, 1H), 8.02 (s, 1H), 8.00 – 7.93 (m, 2H), 7.87 (dd, J = 8.5, 1.8 Hz, 1H), 7.81 (dd, J = 8.5, 1.8 Hz, 1H), 7.60 (d, J = 2.4 Hz, 1H), 7.55 (dd, J = 8.4, 2.4 Hz, 1H), 7.00 (d, J = 8.5 Hz, 1H), 3.91 (s, 3H), 2.19 (s, 6H), 2.11 (s, 3H), 1.80 (s, 6H); **^{13}C NMR** (125 MHz, $CDCl_3$) δ 170.04, 159.00, 141.20, 139.11, 135.53, 132.60, 131.39, 129.97, 129.49, 128.68, 128.09, 126.77, 126.03, 125.79, 124.79, 124.11, 112.22, 55.26, 40.69, 37.20, 29.19; **HRMS** Accurate mass (ES+): Found 434.2085, $C_{28}H_{29}NO_2Na$ (M+Na+) requires 434.2096.

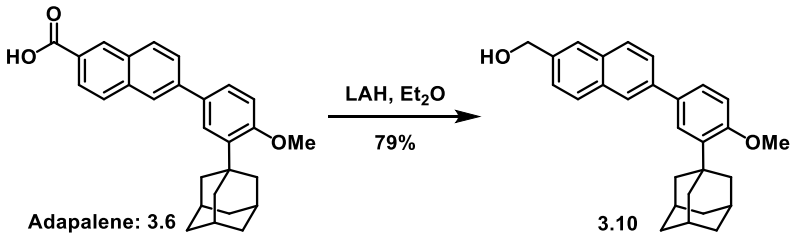

(6-(3-(adamantan-1-yl)-4-methoxyphenyl)naphthalen-2-yl)methanol (3.10). (synthesized by Colleen Keohane) To a solution of lithium aluminum hydride (LAH) (5 mg, 0.133 mmol) in Et_2O (1 mL) at 0 °C was added adapalene (50 mg, 0.121 mmol) in Et_2O (0.5 mL). The reaction was warmed to room temperature and stirred for 2 hours. The reaction was cooled to 0 °C and H_2O (1 mL) was added slowly followed by 1N NaOH (1 mL). The resulting slurry was filtered over Celite and washed with EtOAc. The aqueous layer was extracted with EtOAc 3x and the combined organic layers were washed with water and brine, dried over Na_2SO_4, filtered, and concentrated; yielding the title compound as a white solid (38 mg, 79% yield). **^{1}H NMR** (500 MHz, $CDCl_3$) δ 7.98 (d, J = 1.1 Hz, 1H), 7.88 (t, J = 8.5 Hz, 2H), 7.82 (s, 1H), 7.74 (dd, J = 8.5,

1.8 Hz, 1H), 7.60 (d, J = 2.3 Hz, 1H), 7.53 (dd, J = 8.4, 2.3 Hz, 1H), 7.50 (dd, J = 8.4, 1.6 Hz, 1H), 6.99 (d, J = 8.4 Hz, 1H), 4.87 (s, 2H), 3.90 (s, 3H), 2.20 (s, 6H), 2.11 (s, 3H), 1.81 (s, 6H); **^{13}C NMR** (125 MHz, $CDCl_3$) δ 158.72, 139.19, 139.01, 138.09, 133.44, 133.20, 132.29, 128.64, 128.36, 126.17, 126.01, 125.70, 125.65, 125.40, 124.98, 112.22, 65.69, 55.31, 40.76, 37.28, 29.26; **HRMS** Accurate mass (ES+): Found 421.2141, $C_{28}H_{31}O_2Na$ (M+Na+) requires 421.2143.

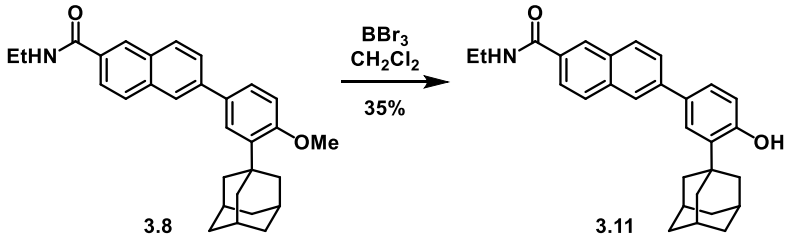

3.8 3.11

6-(3-(adamantan-1-yl)-4-hydroxyphenyl)-N-ethyl-2-naphthamide (3.11). (synthesized by Colleen Keohane) To a solution of amide **3.8** (25 mg, 0.061 mmol) in CH_2Cl_2 (2 mL) at 0°C was added BBr_3 (1M in CH_2Cl_2, 0.12 mL, 0.122 mmol). The reaction was warmed to room temperature and stirred overnight. The reaction was cooled to 0 °C then quenched with water and allowed to stir for 15 minutes, then extracted with EtOAc 3x. The combined organic layers were washed with water and brine, dried over Na_2SO_4, filtered, concentrated, and purified by HPLC, yielding the title compound as a white solid (5.3 mg, 35% yield). **^{1}H NMR** (500 MHz, $CDCl_3$) δ 8.29 (s, 1H), 8.06 (br s, 1H), 7.98 (s, 1H), 7.93 (dd, *J* = 12.3, 8.7 Hz, 2H), 7.82 (dd, *J* = 8.5, 1.8 Hz, 1H), 7.77 (dd, *J* = 8.5, 1.8 Hz, 1H), 7.58 (d, *J* = 2.3 Hz, 1H), 7.41 (dd, *J* = 8.1, 2.3 Hz, 1H), 6.81 (d, *J* = 8.1 Hz, 1H), 3.59 (qd, *J* = 7.3, 5.6 Hz, 2H), 2.22 (s, 6H), 2.12 (s, 3H), 1.81 (s, 6H), 1.32 (t, *J* = 7.3 Hz, 3H); **^{13}C NMR** (125 MHz, $CDCl_3$) δ 168.03, 154.86, 140.92, 137.04, 135.28, 133.01, 131.51, 131.41, 129.39, 128.71, 127.29, 126.74, 126.54, 125.81, 124.82, 123.94, 117.51, 40.70, 37.20, 37.06, 29.19, 15.08; **HRMS** Accurate mass (ES+): Found 448.2247, $C_{29}H_{31}NO_2Na$ (M+Na+) requires 448.2252.

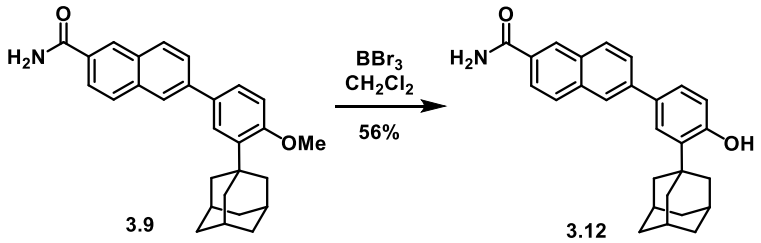

6-(3-(adamantan-1-yl)-4-hydroxyphenyl)-2-naphthamide (3.12). (synthesized by Colleen Keohane) To a solution of amide **3.9** (25 mg, 0.061 mmol) in CH_2Cl_2 (2 mL) at 0°C was added BBr_3 (1M in CH_2Cl_2, 0.06 mL, 0.06 mmol), the reaction was warmed to room temperature and stirred overnight. The reaction was cooled to 0 °C and quenched with water and allowed to stir for 15 minutes, then extracted with EtOAc 3x. The combined organic layers were washed with water and brine, dried over Na_2SO_4, filtered, concentrated, and purified by HPLC, yielding the title compound as a white solid (13 mg, 56% yield). **^{1}H NMR** (500 MHz, DMSO) δ 9.68 (br s, 1H), 8.47 (s, 1H), 8.12 (d, J = 9.5 Hz, 2H), 8.02 (d, J = 8.6 Hz, 2H), 7.94 (dd, J = 8.6, 1.7 Hz, 1H), 7.84 (dd, J = 8.6, 1.8 Hz, 1H), 7.54 – 7.40 (m, 1H), 7.44 (br s, 1H) 6.92 (d, J = 8.2 Hz, 1H), 2.17 (s, 6H), 2.07 (s, 3H), 1.76 (s, 6H); **^{13}C NMR** (125 MHz, DMSO) δ 168.36, 156.84, 140.29, 136.44, 135.14, 131.45, 131.15, 130.47, 129.75, 128.28, 127.95, 126.13, 125.71, 125.52, 125.06, 123.99, 117.43, 37.06, 36.77, 28.83; **HRMS** Accurate mass (ES+): Found 398.2127, $C_{27}H_{28}NO_2$ (M+H+) requires 398.2120.

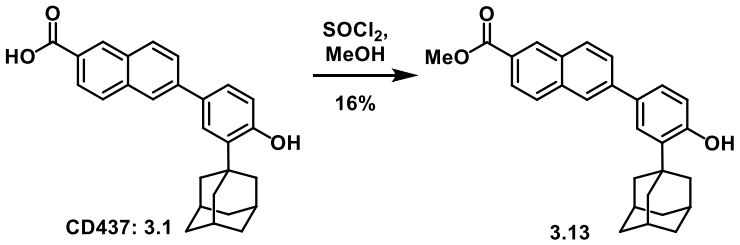

Methyl 6-(3-(adamantan-1-yl)-4-hydroxyphenyl)-2-naphthoate (3.13). (synthesized by Colleen Keohane) To a solution of CD437 (20 mg, 0.047 mmol) in MeOH (0.5 mL) was added $SOCl_2$ (0.01 mL, 0.12 mmol) at 0°C, the reaction was heated to reflux and stirred for 2 hours. The

reaction was cooled to room temperature and concentrated. The yellow solid was purified by HPLC, yielding the title compound as a white solid (3.1 mg, 16% yield). **^{1}H NMR** (500 MHz, DMSO) δ 9.60 (s, 1H), 8.62 (s, 1H), 8.22 – 8.12 (m, 2H), 8.08 (d, *J* = 8.8 Hz, 1H), 7.97 (dd, *J* = 8.6, 1.7 Hz, 1H), 7.88 (dd, *J* = 8.6, 1.8 Hz, 1H), 7.55 – 7.46 (m, 2H), 6.92 (d, *J* = 8.2 Hz, 1H), 3.92 (s, 3H), 2.17 (s, 6H), 2.07 (s, 3H), 1.76 (s, 6H); **^{13}C NMR** (125 MHz, DMSO) δ 166.39, 156.55, 140.89, 136.09, 135.66, 130.68, 130.27, 129.91, 129.83, 128.50, 126.24, 126.06, 125.44, 125.26, 125.03, 123.65, 117.02, 52.19, 36.64, 36.37, 28.41; **HRMS** Accurate mass (ES+): Found 413.2115, $C_{28}H_{29}O_3$ (M+H+) requires 413.2117.

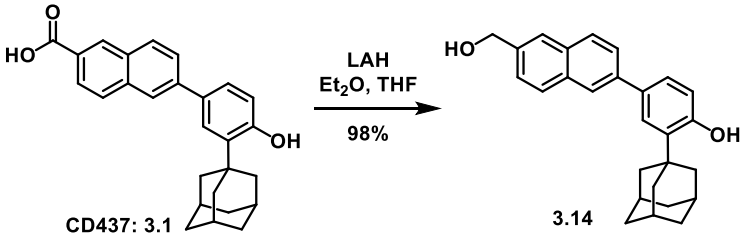

2-(adamantan-1-yl)-4-(6-(hydroxymethyl)naphthalen-2-yl)phenol (3.14). (synthesized by Colleen Keohane) Lithium aluminum hydride (LAH) (44 mg, 1.154 mmol) was added to a solution of CD437 (230 mg, 0.577 mmol) in 2:1 Et_2O:THF (15 mL) at 0 °C. The reaction was warmed to room temperature and stirred for 2 hours. The reaction was cooled to 0 °C and H_2O (10 mL) was added slowly followed by 2M NaOH (10 mL). The resulting slurry was filtered over Celite and washed with EtOAc. The aqueous layer was extracted with EtOAc 3x and the combined organics were washed with water and brine, dried over Na_2SO_4, filtered, and concentrated; yielding the title compound as a white solid (217 mg, 98% yield). **^{1}H NMR** (500 MHz, DMSO) δ 8.03 (s, 1H), 7.90 (t, J = 8.9 Hz, 2H), 7.79 (s, 1H), 7.73 (dd, J = 8.5, 1.8 Hz, 1H), 7.47 – 7.38 (m, 3H), 6.96 (d, J = 8.2 Hz, 1H), 4.66 (s, 2H), 2.17 (s, 6H), 2.06 (s, 3H), 1.76 (s, 6H); **^{13}C NMR** (150 MHz, $CDCl_3$) δ 154.33, 139.11, 138.11, 136.91, 133.67, 133.44, 132.30, 128.66, 128.39, 126.51, 126.14, 125.75, 125.69, 125.42, 124.97, 117.42, 65.73, 40.72, 37.20, 29.19; **HRMS** Accurate mass (ES+): Found 385.2177, $C_{27}H_{29}O_2$ (M+H+) requires 385.2168.

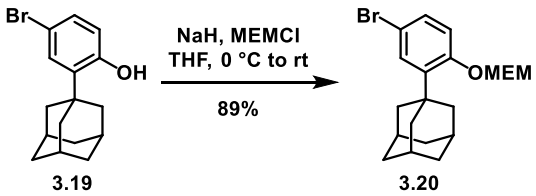

1-(5-bromo-2-((2-methoxyethoxy)methoxy)phenyl)adamantane (3.20). (synthesized by Colleen Keohane) To a suspension of sodium hydride (60% in mineral oil, 53 mg, 1.33 mmol) in THF (3 mL) at 0 °C was added phenol **3.19** (prepared as previously described: Liu, Z. & Xiang, J. *Org. Process Res. Dev.* **2006**, *10*, 285.) (314 mg, 1.02 mmol) dissolved in THF (2 mL). The solution was warmed to room temperature and stirred for one hour, at which time MEMCl (0.19 mL, 1.64 mmol) was added dropwise, and the reaction was stirred for two hours at room temperature. The reaction was quenched with water and extracted with EtOAc 3x. The combined organic layers were washed with water then brine, dried over Na_2SO_4, filtered, concentrated, and purified by column chromatography, yielding the title compound as a white solid (361 mg, 89% yield). **^{1}H NMR** (500 MHz, $CDCl_3$) δ 7.31 (d, J = 2.5 Hz, 1H), 7.23 (dd, J = 8.7, 2.5 Hz, 1H), 7.04 (d, J = 8.7 Hz, 1H), 5.28 (s, 2H), 3.87 – 3.79 (m, 2H), 3.59 – 3.56 (m, 2H), 3.39 (s, 3H), 2.06 (s, 9H), 1.76 (s, 6H); **^{13}C NMR** (125 MHz, $CDCl_3$) δ 155.68, 140.93, 129.95, 129.55, 116.49, 114.54, 93.51, 71.62, 67.91, 59.11, 40.52, 37.31, 37.02, 29.03; **HRMS** Accurate mass (ES+): Found 417.1036, $C_{20}H_{27}BrO_3Na$ (M+Na+) requires 417.1041.

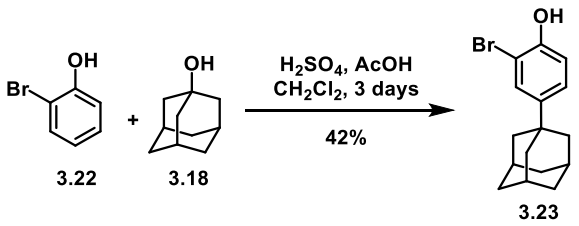

4-(adamantan-1-yl)-2-bromophenol (3.23). To a mixture of 2-bromophenol (1.475 g, 8.526 mmol) and 1-adamantol (1.298 g, 8.526 mmol) in CH_2Cl_2 (4 mL) was added 5:1 AcOH:H_2SO_4 (3 mL), and the reaction was stirred at room temperature for 3 days. The reaction poured into water

and quenched with sat. $NaHCO_3$, then extracted with CH_2Cl_2 3x. The combined organic layers were washed with water and brine, dried over Na_2SO_4, filtered, concentrated, and purified by column chromatography (loaded crude oil in hexanes, 0 → 2% EtOAc/hexanes), yielding the title compound as a white solid (1.100 g, 42% yield). **^{1}H NMR** (500 MHz, $CDCl_3$) δ 7.41 (d, J = 2.3 Hz, 1H), 7.21 (dd, J = 8.5, 2.3 Hz, 1H), 6.98 – 6.95 (m, 1H), 5.34 (s, 1H), 2.08 (s, 3H), 1.85 (d, J = 2.6 Hz, 6H), 1.81 – 1.70 (m, 6H); **^{13}C NMR** (125 MHz, $CDCl_3$) δ 150.10, 145.54, 128.70, 125.83, 115.68, 110.16, 68.11, 43.40, 36.78, 35.83, 29.02, 25.74; **HRMS** Accurate mass (ES+): Found 307.0711, $C_{16}H_{20}BrO$ (M+H+) requires 307.0698.

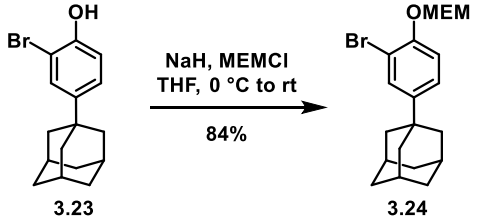

1-(3-bromo-4-((2-methoxyethoxy)methoxy)phenyl)adamantane (3.24). To a suspension of sodium hydride (60% in mineral oil, 258 mg, 6.453 mmol) in THF (5 mL) at 0 °C was added a solution of phenol **3.23** (1.525g, 4.964 mmol) in THF (3 mL) dropwise. The ice bath was removed and the reaction was stirred at room temperature for 30 minutes, at which time MEMCl (0.91 mL, 7.942 mmol) was added. After 2 hours at room temperature, the reaction was quenched with water and extracted with EtOAc 3x. The combined organic layers were washed with brine, dried over Na_2SO_4, filtered, concentrated, and purified by column chromatography, yielding the title compound as a clear oil (1.650g, 84% yield). **^{1}H NMR** (500 MHz, $CDCl_3$) δ 7.50 (d, J = 2.3 Hz, 1H), 7.22 (dd, J = 8.6, 2.3 Hz, 1H), 7.13 (d, J = 8.7 Hz, 1H), 5.30 (d, J = 5.2 Hz, 2H), 3.89 – 3.85 (m, 2H), 3.59 – 3.55 (m, 2H), 3.37 (s, 3H), 2.08 (s, 3H), 1.85 (d, J = 2.3 Hz, 6H), 1.75 (dd, J = 26.7, 12.1 Hz, 6H); **^{13}C NMR** (125 MHz, $CDCl_3$) δ 151.53, 146.85, 130.11, 125.04, 116.05, 112.65, 94.33, 71.62, 68.02, 59.12, 43.28, 36.74, 35.84, 28.96; **HRMS** Accurate mass (ES+): Found 417.1058, $C_{20}H_{27}BrO_3Na$ (M+Na+) requires 417.1041.

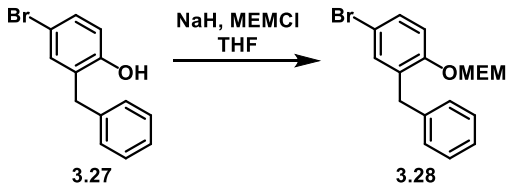

2-benzyl-4-bromo-1-((2-methoxyethoxy)methoxy)benzene (3.28). (synthesized by Colleen Keohane and me) Phenol **3.27** (prepared as previously described: Williams, A. B. & Hanson, R. N. *Tetrahedron* **2012**, *68*, 5406.) (1.500g, 5.701 mmol) dissolved in THF (5 mL) was added via cannula to a suspension of NaH (60% in mineral oil, 296 mg, 7.411 mmol) in THF (15 mL) at 0 °C. The solution was warmed to room temperature and stirred for 30 minutes, after which time MEMCl (1.04 mL, 9.12 mmol) was added, and the reaction was stirred for 2 hours at room temperature. The reaction was quenched with water and extracted with EtOAc 3x. The combined organic layers were washed with brine, dried over Na_2SO_4, filtered, concentrated, and purified by column chromatography, yielding the title compound as a clear oil (1.70g, 85% yield). **^{1}H NMR** (500 MHz, $CDCl_3$) δ 7.32 - 7.27 (m, 3H), 7.25 (d, J = 2.5 Hz, 1H), 7.21 (t, J = 6.6 Hz, 3H), 7.04 (d, J = 8.7 Hz, 1H), 5.25 (s, 2H), 3.96 (s, 2H), 3.66 (dd, J = 5.5, 3.7 Hz, 2H), 3.49 (dd, J = 5.5, 3.8 Hz, 2H), 3.37 (s, 3H); **^{13}C NMR** (125 MHz, $CDCl_3$) δ 153.91, 139.93, 132.99, 132.38, 130.09, 128.68, 128.22, 125.94, 115.60, 113.87, 93.04, 71.34, 67.49, 58.77, 35.92; **HRMS** Accurate mass (ES+): Found 375.0382, $C_{17}H_{19}BrO_3Na$ (M+Na+) requires 375.0382.

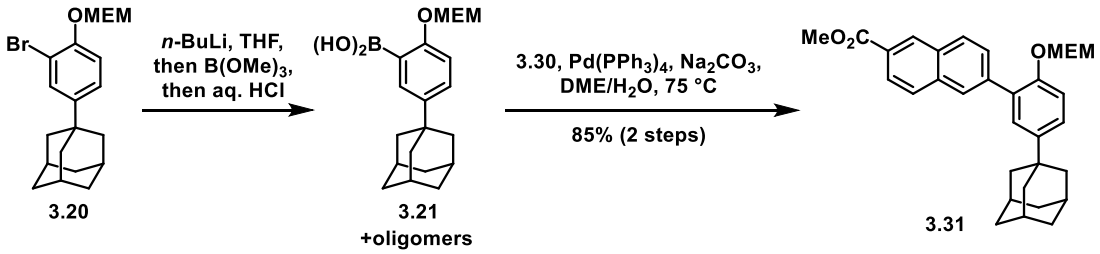

Methyl 6-(5-(adamantan-1-yl)-2-((2-methoxyethoxy)methoxy)phenyl)-2-naphthoate (3.31). To a solution of bromide **3.20** (31 mg, 0.079 mmol) in THF (2 mL) at -78 °C was added *n*-BuLi (2.40 M in hexanes, 0.036 mL, 0.087 mmol) dropwise and then stirred for 15 minutes at -78 °C,

over which time the reaction turned blue. $B(OMe)_3$ (0.013 mL, 0.119 mmol) was then added dropwise, and the reaction stirred for an additional hour at -78 °C, then warmed to room temperature, over which time the reaction turned maroon. After one hour at room temperature, 0.1 M HCl was added (2 mL) and the reaction was stirred for an additional 30 minutes. Water was added, and the solution was extracted with EtOAc 3x. The combined organic layers were washed with brine, dried over Na_2SO_4, filtered, concentrated and purified by column chromatography (EtOAc/hexanes then MeOH/CH_2Cl_2). The intended boronic acid product also contained another similar compound, presumably a borate oligomer of the material (Rf = 0.75 in 5% MeOH/ 95% CH_2Cl_2, stains red in vanillin), both of which reacted in the following step. The boronic acid mixture was then dissolved in 9:1 DME:H_2O (2 mL), then methyl 6-bromo-2-naphthoate (21 mg, 0.079 mmol), and Na_2CO_3 (17 mg, 0.158 mmol) were added, then argon was bubbled through the mixture for 5 minutes. After degassing, $Pd(PPh_3)_4$ (3 mg, 0.002 mmol) was added, and the reaction was heated to 75 °C for 6 hours. Water and EtOAc were added, and the aqueous layer was extracted with EtOAc 3x. The combined organic layers were washed with brine, dried over Na_2SO_4, filtered, concentrated, and purified by column chromatography, yielding the title compound as a white foam (34 mg, 85% yield with respect to naphthyl bromide). **^{1}H NMR** (500 MHz, $CDCl_3$) δ 8.63 (s, 1H), 8.07 (d, J = 8.6 Hz, 1H), 7.99 – 7.89 (m, 3H), 7.75 (d, J = 8.5 Hz, 1H), 7.40 (s, 1H), 7.34 (d, J = 8.6 Hz, 1H), 7.25 (d, J = 8.2 Hz, 1H), 5.21 (s, 2H), 3.99 (s, 3H), 3.72 – 3.65 (m, 2H), 3.49 – 3.42 (m, 2H), 3.32 (s, 3H), 2.10 (s, 3H), 1.95 (s, 6H), 1.77 (q, J = 12.2 Hz, 6H); **^{13}C NMR** (125 MHz, $CDCl_3$) δ 167.44, 152.34, 145.63, 139.61, 135.65, 131.47, 130.89, 130.71, 129.23, 128.68, 128.41, 127.99, 127.88, 127.31, 125.73, 125.46, 115.63, 94.46, 71.61, 67.82, 59.07, 52.32, 43.46, 36.87, 35.91, 29.07; **HRMS** Accurate mass (ES+): Found 523.2461, $C_{32}H_{36}O_5Na$ (M+Na+) requires 523.2460.

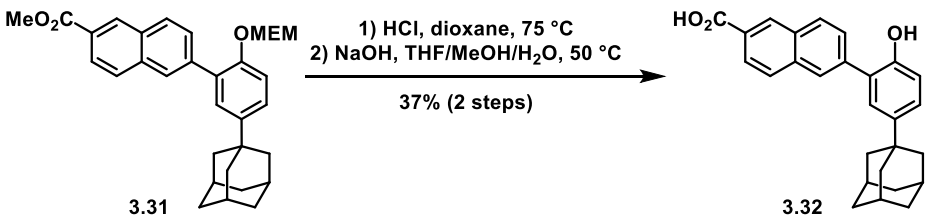

6-(5-(adamantan-1-yl)-2-hydroxyphenyl)-2-naphthoic acid (3.32). MEM ether **3.31** (34 mg, 0.068 mmol) was dissolved in 4M HCl in dioxane (1 mL), and stirred for 2 hours at room temperature. The solution was concentrated under reduced pressure, then dissolved in 1:1 THF:MeOH (2 mL) and 1M NaOH was added (0.34 mL, 0.34 mmol), and this reaction was heated to 50 °C overnight. The following day, the reaction was acidified with 1M HCl (pH 1) and extracted with EtOAc 3x. The combined organic layers were washed with brine, dried over Na_2SO_4, filtered, concentrated, and purified by column chromatography (0 to 3% MeOH/0.1% AcOH/CH_2Cl_2, loaded in EtOAc), yielding the title compound as a white solid (10 mg, 37% yield over two steps). **^{1}H NMR** (500 MHz, DMSO) δ 13.06 (br s, 1H), 9.47 (br s, 1H), 8.60 (d, J = 0.7 Hz, 1H), 8.13 – 8.07 (m, 2H), 8.04 (d, J = 8.8 Hz, 1H), 7.97 (dd, J = 8.5, 1.6 Hz, 1H), 7.82 (dd, J = 8.5, 1.7 Hz, 1H), 7.32 (d, J = 2.5 Hz, 1H), 7.20 (dd, J = 8.5, 2.5 Hz, 1H), 6.93 (d, J = 8.5 Hz, 1H), 2.04 (s, 3H), 1.88 (d, J = 2.7 Hz, 6H), 1.72 (s, 6H); **^{13}C NMR** (100 MHz, DMSO) δ 167.56, 152.33, 142.08, 139.35, 135.05, 130.83, 130.18, 128.88, 128.46, 128.32, 127.73, 127.14, 126.89, 126.48, 125.35, 125.18, 115.82, 42.88, 36.23, 35.11, 28.41; **HRMS** Accurate mass (ES+): Found 399.1957, $C_{27}H_{27}O_3$ (M+H+) requires 399.1960.

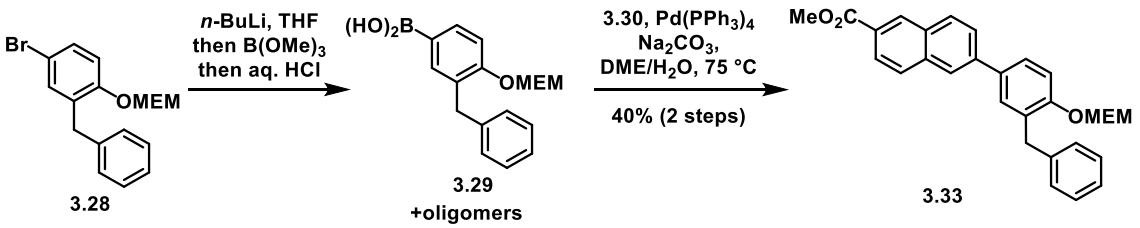

Methyl 6-(3-benzyl-4-((2-methoxyethoxy)methoxy)phenyl)-2-naphthoate (3.33). (synthesized by Colleen Keohane and me) To a solution of bromide **3.28** (198 mg, 0.56 mmol) in THF (5 mL)

at -78 °C was added *n*-BuLi (2.40 M in hexanes, 0.26 mL, 0.62 mmol) dropwise. The reaction was stirred for 15 minutes at -78 °C. $B(OMe)_3$ (0.09 mL, 0.840 mmol) was then added dropwise, and the reaction stirred for an additional hour at -78 °C, then warmed to room temperature. After one hour at room temperature, 0.1 M HCl was added (5 mL) and the reaction was stirred for an additional 30 minutes. Water was added, and the solution was extracted with EtOAc 3x. The combined organic layers were washed with brine, dried over Na_2SO_4, filtered, concentrated and purified by column chromatography (EtOAc/hexanes then MeOH/CH_2Cl_2). The intended boronic acid product also contained another similar compound, presumably a borate oligomer of the material (Rf = 0.75 in 5% MeOH/95% CH_2Cl_2, stains red in vanillin), both of which reacted in the following step. The boronic acid mixture was then dissolved in 9:1 DME:H_2O (5 mL), then methyl 6-bromo-2-naphthoate (126 mg, 0.47 mmol) and Na_2CO_3 (100 mg, 0.94 mmol) were added, then argon was bubbled through the mixture for 5 minutes. After degassing, $Pd(PPh_3)_4$ (16 mg, 0.014 mmol) was added, and the reaction was heated to 75 °C for 6 hours. Water and EtOAc were added, and the aqueous layer was extracted with EtOAc 3x. The combined organic layers were washed with brine, dried over Na_2SO_4, filtered, concentrated, and purified by column chromatography, yielding the title compound as a white foam (86 mg, 40% yield with respect to naphthalene). **^{1}H NMR** (500 MHz, $CDCl_3$) δ 8.60 (s, 1H), 8.06 (dd, J = 8.6, 1.7 Hz, 1H), 7.98 - 7.97 (m, 2H), 7.90 (d, J = 8.7 Hz, 1H), 7.75 (dd, J = 8.5, 1.8 Hz, 1H), 7.56 (dd, J = 8.5, 2.4 Hz, 1H), 7.52 (d, J = 2.3 Hz, 1H), 7.30 – 7.24 (m, 5H), 7.20 – 7.16 (m, 1H), 5.32 (s, 2H), 4.08 (s, 2H), 3.99 (s, 3H), 3.70 – 3.65 (m, 2H), 3.52 – 3.47 (m, 2H), 3.37 (s, 3H); **^{13}C NMR** (125 MHz, $CDCl_3$) δ 167.33, 155.09, 140.88, 140.64, 135.94, 133.96, 131.42, 130.88, 130.76, 129.85, 129.79, 128.91, 128.40, 128.33, 127.15, 126.67, 126.35, 126.02, 125.71, 124.94, 114.47, 93.22, 71.64, 67.71, 59.10, 52.29, 36.59; **HRMS** Accurate mass (ES+): Found 457.2028, $C_{29}H_{29}O_5$ (M+H+) requires 457.2015.

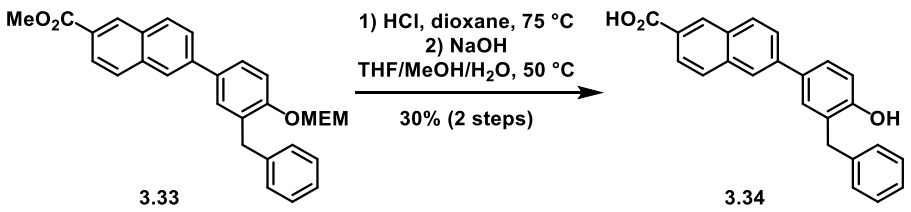

6-(3-benzyl-4-hydroxyphenyl)-2-naphthoic acid (3.34). (synthesized by Colleen Keohane and me) MEM ether **3.33** (78 mg, 0.17 mmol) was dissolved in dioxane (1.5 mL) and 4M HCl in dioxane (0.5 mL) was added. The reaction was heated to 75 °C for 2 hours. The solution was concentrated under reduced pressure, then dissolved in 1:1 THF:MeOH (2 mL) and 1M NaOH was added (0.34 mL, 0.34 mmol), and this reaction was heated to 50 °C overnight. The following day, the reaction was acidified with 1M HCl (pH 1) and filtered. The filter cake was washed with water, yielding the title compound as a white solid (20 mg, 30% yield over two steps). **^{1}H NMR** (500 MHz, CD_3CN) δ 9.51 (br s, 1H), 8.60 (s, 1H), 8.11 (s, 1H), 8.06 (d, J = 8.7 Hz, 1H), 8.02 (dd, J = 8.6, 1.6 Hz, 1H), 7.97 (d, J = 8.6 Hz, 1H), 7.83 (dd, J = 8.6, 1.8 Hz, 1H), 7.61 (d, J = 2.4 Hz, 1H), 7.53 (dd, J = 8.3, 2.4 Hz, 1H), 7.33 – 7.25 (m, 4H), 7.20 – 7.13 (m, 2H), 6.96 (d, J = 8.3 Hz, 1H), 4.03 (s, 2H); **^{13}C NMR** (125 MHz, DMSO) δ 167.51, 155.48, 141.24, 139.95, 135.49, 130.83, 130.30, 130.27, 129.81, 129.29, 128.67, 128.25, 128.22, 128.15, 127.56, 126.14, 125.71, 125.55, 123.65, 115.79, 35.53; **HRMS** Accurate mass (ES+): Found 355.1331, $C_{24}H_{19}O_3$ (M+H+) requires 355.1334.

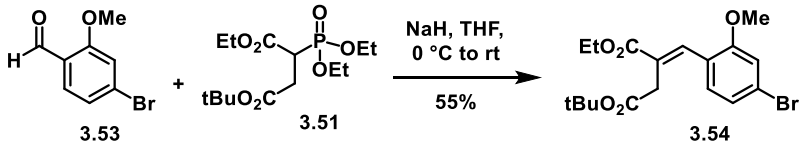

4-(tert-butyl) 1-ethyl (E)-2-(4-bromo-2-methoxybenzylidene)succinate (3.54). To a suspension of NaH (60% in mineral oil, 176 mg, 4.6 mmol) in THF (10 mL) at 0 °C was added phosphonate **3.51** (prepared as previously described: Owton, W. M.; Gallagher, P. T. & Juan-Montesinos, A. *Synth. Commun.* **1993**, *23*, 2119.) (1.56g, 4.6 mmol), and the solution was

warmed to room temperature and stirred for 1 hour. The solution was cooled back down to 0 °C and 4-bromo-2-methoxybenzaldehyde dissolved in THF (2 mL) was added dropwise. The resulting orange suspension was allowed to warm to room temperature and stirred overnight. The following day, the solvent was concentrated and diluted with EtOAc, then washed with water 3x and brine, dried over Na_2SO_4, filtered, concentrated, and purified by column chromatography, yielding the title compound as a clear oil (731 mg, 55% yield). **^{1}H NMR** (500 MHz, $CDCl_3$) δ 7.83 (s, 1H), 7.15 (dd, J = 8.1, 0.6 Hz, 1H), 7.10 (dd, J = 8.1, 1.7 Hz, 1H), 7.04 (d, J = 1.7 Hz, 1H), 4.27 (q, J = 7.1 Hz, 2H), 3.84 (s, 3H), 3.34 (d, J = 0.6 Hz, 2H), 1.46 (s, 9H), 1.33 (t, J = 7.1 Hz, 3H); **^{13}C NMR** (100 MHz, $CDCl_3$) δ 170.52, 167.38, 158.19, 136.60, 130.77, 127.51, 123.88, 123.65, 123.44, 114.42, 81.09, 61.16, 55.92, 35.37, 28.15, 14.40; **HRMS** Accurate mass (ES+): Found 365.0007, $C_{14}H_{15}BrO_5Na$ (M+Na+) requires 365.0001.

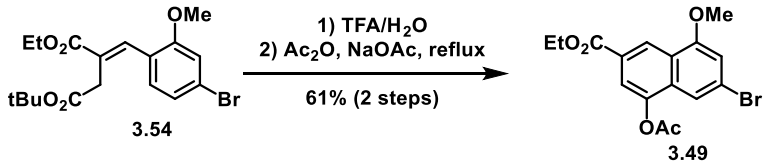

Ethyl 4-acetoxy-6-bromo-8-methoxy-2-naphthoate (3.49). Ester **3.54** (1.02g, 2.55 mmol) was dissolved in 9:1 TFA:H_2O (3 mL) and stirred at room temperature for 3.5 hours. The reaction was concentrated under reduced pressure and azeotropically dried twice with toluene. The crude oil was cooled to 0 °C and saturated $NaHCO_3$ was added (3 mL), then the mixture was acidified with 1M HCl (pH 1). The aqueous layer was extracted with EtOAc 3x, and the combined organic layers were washed with brine, dried over Na_2SO_4, filtered and concentrated, yielding the crude acid as a clear oil. The crude acid was dissolved in Ac_2O (13 mL) and sodium acetate (227 mg, 2.77 mmol) was added, and the mixture turned from pink to yellow. The reaction was refluxed for 2 hours, cooled to room temperature, and then poured into water. The yellow precipitate was filtered and washed with water. The solids were dissolved in CH_2Cl_2, washed with brine, and dried over Na_2SO_4, filtered and concentrated, yielding the title compound as a yellow solid (568

mg, 61% yield over two steps). **^{1}H NMR** (500 MHz, $CDCl_3$) δ 8.84 (dd, *J* = 1.5, 0.9 Hz, 1H), 7.86 (d, *J* = 1.6 Hz, 1H), 7.59 (dd, *J* = 1.5, 0.9 Hz, 1H), 6.97 (d, *J* = 1.6 Hz, 1H), 4.43 (q, *J* = 7.1 Hz, 1H), 4.03 (s, 1H), 2.48 (s, 1H), 1.43 (t, *J* = 7.1 Hz, 1H); **^{13}C NMR** (125 MHz, CDCl3) δ 169.12, 165.80, 157.05, 145.38, 130.60, 127.18, 124.77, 123.72, 123.23, 119.56, 115.85, 109.31, 61.41, 56.08, 21.01, 14.43; **HRMS** Accurate mass (ES+): Found 367.0162, $C_{16}H_{16}BrO_5$ (M+H+) requires 367.0181.

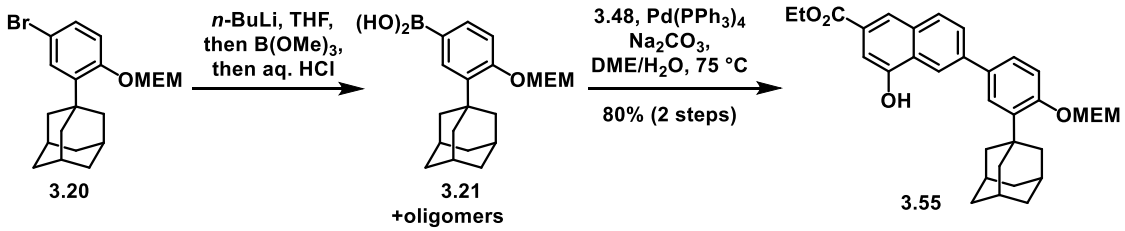

Ethyl 6-(3-(adamantan-1-yl)-4-((2-methoxyethoxy)methoxy)phenyl)-4-hydroxy-2-naphthoate (3.55). (synthesized by Colleen Keohane) To a solution of bromide **3.20** (68 mg, 0.172 mmol) in THF (2 mL) at -78 °C was added *n*-BuLi (2.40 M in hexanes, 0.036 mL, 0.087 mmol) dropwise and then stirred for 15 minutes at -78 °C, over which time the reaction turned blue. $B(OMe)_3$ was then added dropwise, and the reaction stirred for an additional hour at -78 °C, then warmed to room temperature, over which time the reaction turned maroon. After one hour at room temperature, 0.1 M HCl was added (2 mL) and the reaction was stirred for an additional 30 minutes. Water was added, and the solution was extracted with EtOAc 3x. The combined organic layers were washed with brine, dried over Na_2SO_4, filtered, concentrated and purified by column chromatography (EtOAc/hexanes then MeOH/CH_2Cl_2). The intended boronic acid product also contained another similar compound, presumably a borate oligomer of the material (Rf = 0.75 in 5% MeOH/ 95% CH_2Cl_2, stains red in vanillin), both of which reacted in the following step. The boronic acid mixture was then dissolved in DME (2 mL), then naphthyl bromide **3.48** (prepared as previously described: Tietze, L. F.; Panknin, O.; Major, F. & Krewer, B. *Chem. Eur. J.* **2008**, *14*, 2811.) (53 mg, 0.143 mmol), and 1M NaOH (0.72 mL, 0.72 mmol) were added, then argon

was bubbled through the mixture for 5 minutes. After degassing, $Pd(PPh_3)_4$ (5 mg, 0.004 mmol) was added, and the reaction was heated to 75 °C for 4 hours, at which time another portion of 1M NaOH (0.72 mL, 0.72 mmol) was added, to ensure complete acetate hydrolysis. After 2 additional hours, the reaction was complete by TLC. Water and EtOAc were added, and the aqueous layer was extracted with EtOAc 3x. The combined organic layers were washed with brine, dried over Na_2SO_4, filtered, concentrated, and purified by column chromatography, yielding the title compound as a white foam (64 mg, 80% yield with respect to **3.48**). **^{1}H NMR** (500 MHz, $CDCl_3$) δ 8.40 (s, 1H), 8.21 (s, 1H), 7.95 (d, J = 8.6 Hz, 1H), 7.79 (dd, J = 8.5, 1.8 Hz, 1H), 7.65 – 7.60 (m, 2H), 7.53 (dd, J = 8.5, 2.3 Hz, 1H), 7.27 (d, J = 8.4 Hz, 1H), 6.64 (br s, 1H), 5.38 (s, 2H), 4.46 (q, J = 7.1 Hz, 2H), 3.95 – 3.88 (m, 2H), 3.69 – 3.62 (m, 2H), 3.44 (s, 3H), 2.19 (d, J = 2.0 Hz, 6H), 2.10 (s, 3H), 1.80 (s, 6H), 1.46 (t, J = 7.1 Hz, 3H); **^{13}C NMR** (125 MHz, $CDCl_3$) δ 167.41, 156.59, 152.38, 140.70, 139.06, 134.07, 132.71, 129.68, 127.39, 126.96, 126.23, 126.08, 123.35, 119.37, 115.19, 108.12, 93.51, 71.80, 67.97, 61.48, 59.21, 40.85, 37.40, 37.23, 29.23, 14.51; **HRMS** Accurate mass (ES+): Found 531.2758, $C_{33}H_{39}O_6$ (M+H+) requires 531.2747.

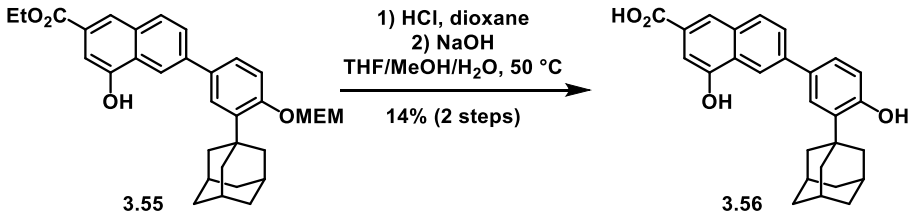

6-(3-(adamantan-1-yl)-4-hydroxyphenyl)-4-hydroxy-2-naphthoic acid (3.56). (synthesized by Colleen Keohane) MEM ether **3.55** (20 mg, 0.038 mmol) was dissolved in 4M HCl in dioxane (2 mL) and the reaction was stirred at room temperature overnight. The reaction was quenched with water and extracted with EtOAc 3x. The combined organic layers were washed with brine, dried over Na_2SO_4, filtered, and concentrated. The crude intermediate was dissolved in 2:1 EtOH/THF (1.5 mL) and 1N NaOH was added (0.2 mL), the mixture was heated to 50°C and stirred

overnight. The reaction was cooled to room temperature, acidified (pH 1) with 1M HCl and extracted with EtOAc 3x. The combined organic layers were washed with brine, dried over Na_2SO_4, filtered, concentrated, and purified by column chromatography (0→6% MeOH/0.1%AcOH/CH_2Cl_2) yielding the title compound as a white solid (2.1 mg, 14% over two steps). **^{1}H NMR** (500 MHz, CD_3CN) δ 8.33 (d, J = 1.9 Hz, 1H), 8.14 (s, 1H), 8.00 (d, J = 8.5 Hz, 1H), 7.84 (dd, J = 8.6, 1.9 Hz, 1H), 7.58 (d, J = 2.4 Hz, 1H), 7.47 (dd, J = 8.2, 2.4 Hz, 1H), 7.37 (d, J = 1.4 Hz, 1H), 6.88 (d, J = 8.2 Hz, 1H), 2.22 – 2.19 (m, 6H), 2.10 – 2.07 (m, 3H), 1.81 (t, J = 2.8 Hz, 6H); **^{13}C NMR** (100 MHz, CD_3CN) δ 167.87, 156.85, 153.83, 141.36, 137.78, 133.46, 132.88, 130.63, 128.30, 128.17, 127.45, 126.85, 126.61, 123.50, 119.26, 108.29, 41.05, 37.74, 30.04; **HRMS** Accurate mass (ES+): Found 415.1906, $C_{27}H_{27}O_4$ (M+H+) requires 415.1909.

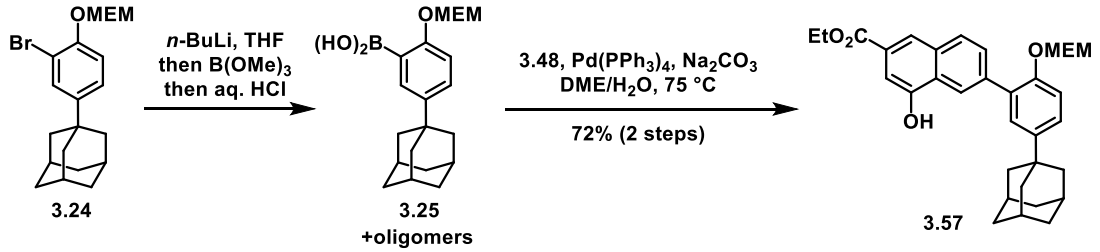

Ethyl 6-(5-(adamantan-1-yl)-2-((2-methoxyethoxy)methoxy)phenyl)-4-hydroxy-2-naphthoate (3.57). Using the procedure given for the preparation of compound **3.55**, bromide **3.24** (66 mg, 0.167 mmol) and naphthyl bromide **3.48** (47 mg, 0.139 mmol) yielded the title compound as a clear oil (53 mg, 72% yield with respect to **3.48**). **^{1}H NMR** (500 MHz, $CDCl_3$) δ 8.37 (s, 1H), 8.22 (s, 1H), 7.93 (d, J = 8.4 Hz, 1H), 7.75 (d, J = 8.2 Hz, 1H), 7.58 (s, 1H), 7.42 (s, 1H), 7.31 (t, J = 11.5 Hz, 1H), 7.23 (d, J = 8.6 Hz, 1H), 6.76 (br s, 1H), 5.22 (s, 2H), 4.46 (dd, J = 13.7, 6.7 Hz, 2H), 3.73 (s, 2H), 3.50 (s, 2H), 3.34 (s, 3H), 2.10 (s, 3H), 1.94 (s, 6H), 1.77 (q, J = 11.6 Hz, 6H), 1.46 (t, J = 7.0 Hz, 3H); **^{13}C NMR** (125 MHz, $CDCl_3$) δ 167.42, 152.23, 145.60, 138.77, 132.77, 131.05, 129.56, 128.60, 127.97, 127.64, 127.03, 125.61, 123.23, 122.38, 115.46, 108.00, 94.35, 71.70, 67.88, 61.49, 59.10, 43.45, 36.88, 35.90, 29.09, 14.51; **HRMS** Accurate mass (ES+): Found 553.2562, $C_{33}H_{38}O_6Na$ (M+Na+) requires 553.2566.

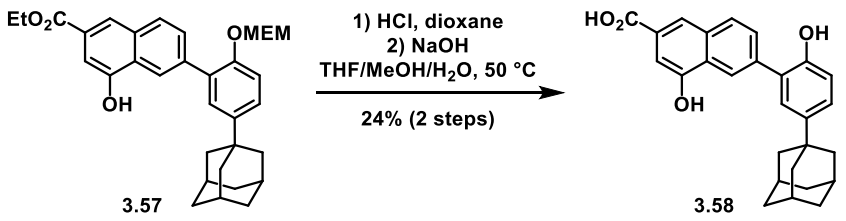

6-(5-(adamantan-1-yl)-2-hydroxyphenyl)-4-hydroxy-2-naphthoic acid (3.58). Using the procedure given for the preparation of compound **3.56**, MEM ether **3.57** (39 mg, .073 mmol) yielded the title compound as a yellow residue (7.2 mg, 24% yield over two steps). **^{1}H NMR** (500 MHz, CD_3CN) δ 8.31 (s, 1H), 8.17 (s, 1H), 7.98 (d, J = 8.5 Hz, 1H), 7.78 (dd, J = 8.5, 1.7 Hz, 1H), 7.40 – 7.35 (m, 2H), 7.24 (dd, J = 8.5, 2.5 Hz, 1H), 6.90 (d, J = 8.5 Hz, 1H), 1.97 – 1.95 (m, 6H), 1.93 – 1.90 (m, 3H), 1.81 – 1.75 (m, 6H); **^{13}C NMR** (125 MHz, CD_3CN) δ 172.64, 168.08, 153.93, 152.55, 144.70, 139.34, 133.62, 130.15, 129.69, 128.49, 128.44, 128.35, 127.93, 126.55, 123.48, 122.82, 116.84, 108.17, 44.04, 37.37, 30.04; **HRMS** Accurate mass (ES+): Found 415.1905, $C_{27}H_{27}O_4$ (M+H+) requires 415.1909.

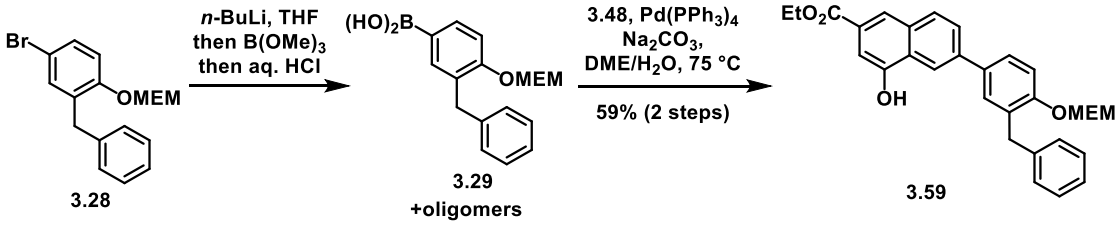

Ethyl 6-(3-benzyl-4-((2-methoxyethoxy)methoxy)phenyl)-4-hydroxy-2-naphthoate (3.59). (synthesized by Colleen Keohane and me) Using the procedure given for the preparation of compound **3.55**, bromide **3.28** (40 mg, 0.114 mmol) and naphthyl bromide **3.48** (32 mg, 0.095 mmol) yielded the title compound as a clear oil (26 mg, 59% yield with respect to **3.48**). **^{1}H NMR** (400 MHz, $CDCl_3$) δ 8.35 (s, 1H), 8.20 (s, 1H), 7.93 (d, J = 8.5 Hz, 1H), 7.75 (dd, J = 8.5, 1.8 Hz, 1H), 7.60 – 7.54 (m, 2H), 7.48 (d, J = 1.2 Hz, 1H), 7.26 – 7.23 (m, 5H), 7.20 – 7.14 (m, 1H), 5.80 (br s, 1H), 5.30 (s, 2H), 4.43 (q, J = 7.1 Hz, 2H), 4.07 (s, 2H), 3.69 – 3.61 (m, 2H), 3.53 – 3.45 (m, 2H), 3.36 (s, 3H), 1.44 (t, J = 7.1 Hz, 3H); **^{13}C NMR** (125 MHz, $CDCl_3$) δ 167.48,

155.01, 152.52, 141.04, 139.89, 134.27, 132.74, 130.62, 129.92, 129.71, 128.90, 128.39, 127.45, 126.79, 126.70, 125.98, 123.20, 119.40, 114.45, 108.12, 93.20, 71.70, 67.67, 61.52, 59.12, 36.70, 29.84, 14.49; **HRMS** Accurate mass (ES+): Found 487.2126, $C_{30}H_{31}O_6$ (M+H+) requires 487.2121.

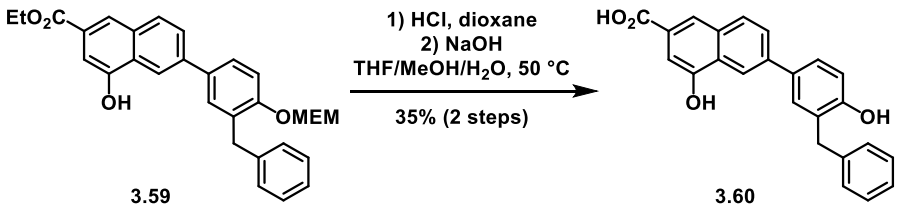

6-(3-benzyl-4-hydroxyphenyl)-4-hydroxy-2-naphthoic acid (3.60). (synthesized by Colleen Keohane and me) Using the procedure given for the preparation of compound **3.56**, MEM ether **3.59** (25 mg, .055 mmol) yielded the title compound as a yellow residue (7.0 mg, 35% yield over two steps). **^{1}H NMR** (500 MHz, CD_3CN) δ 8.31 (s, 1H), 8.15 (d, J = 14.7 Hz, 1H), 8.01 – 7.93 (m, 1H), 7.83 – 7.77 (m, 1H), 7.58 (d, J = 1.9 Hz, 1H), 7.54 – 7.50 (m, 1H), 7.37 (s, 1H), 7.28 (q, J = 8.1 Hz, 4H), 7.18 (t, J = 6.9 Hz, 1H), 6.95 (d, J = 8.3 Hz, 1H), 4.02 (s, 2H); **^{13}C NMR** (125 MHz, CD_3CN) δ 172.55, 167.98, 155.76, 153.85, 142.27, 140.70, 133.53, 133.20, 130.65, 129.69, 129.46, 129.31, 128.27, 127.40, 127.29, 126.85, 123.49, 119.33, 116.72, 108.35, 36.52; **HRMS** Accurate mass (ES+): Found 393.1093, $C_{24}H_{18}O_4Na$ (M+Na+) requires 393.1103.

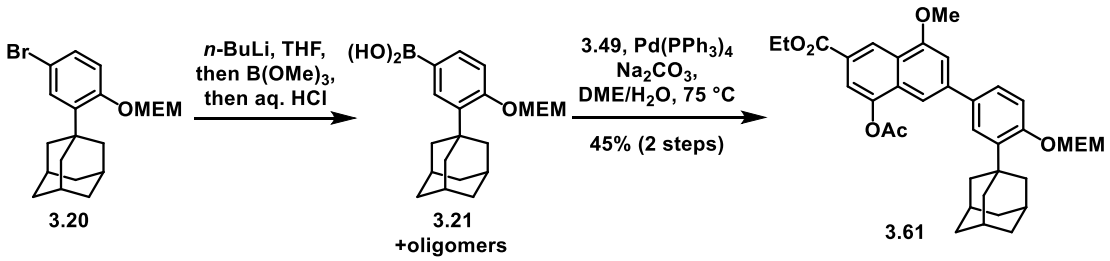

Ethyl 4-acetoxy-6-(3-(adamantan-1-yl)-4-((2-methoxyethoxy)methoxy)phenyl)-8-methoxy-2-naphthoate (3.61). (synthesized by Colleen Keohane) Using the procedure given for the preparation of compound **3.55**, bromide **3.20** (43 mg, 0.109 mmol) and naphthyl bromide **3.49**

(30 mg, 0.090 mmol) yielded the title compound as a clear oil (21 mg, 45% yield with respect to **3.49**). **^{1}H NMR** (500 MHz, $CDCl_3$) δ 8.92 (s, 1H), 7.86 (s, 1H), 7.53 (d, J = 8.4 Hz, 2H), 7.47 (d, J = 8.4 Hz, 1H), 7.29 (d, J = 8.4 Hz, 1H), 7.08 (s, 1H), 5.40 (s, 2H), 4.44 (q, J = 7.1 Hz, 2H), 4.10 (s, 3H), 3.94 – 3.86 (m, 2H), 3.67 – 3.60 (m, 2H), 3.42 (s, 3H), 2.47 (s, 3H), 2.19 (s, 6H), 2.11 (s, 3H), 1.81 (s, 6H), 1.45 (t, J = 7.1 Hz, 3H); **^{13}C NMR** (125 MHz, $CDCl_3$) δ 169.44, 166.29, 157.00, 156.80, 146.60, 143.00, 139.11, 134.51, 130.47, 126.45, 126.28, 126.18, 125.12, 123.43, 118.85, 115.16, 111.03, 105.42, 93.49, 71.74, 68.01, 61.31, 59.21, 55.94, 40.80, 37.39, 37.19, 29.82, 29.19, 21.11, 14.55; **HRMS** Accurate mass (ES+): Found 625.2781, $C_{36}H_{42}O_8Na$ (M+Na+) requires 625.2777.

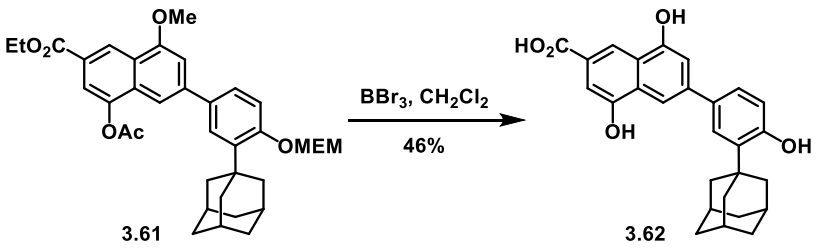

6-(3-(adamantan-1-yl)-4-hydroxyphenyl)-4,8-dihydroxy-2-naphthoic acid (3.62). (synthesized by Colleen Keohane) To a solution of MEM ether **3.61** (18 mg, 0.03 mmol) dissolved in CH_2Cl_2 (2 mL) at -78 °C was added BBr_3 (1M in CH_2Cl_2, 0.24 mL, 0.24 mmol) dropwise, and the mixture was allowed to warm to room temperature and stir overnight. The reaction was quenched with water and extracted with EtOAc 3x. The combined organic layers were washed with brine, dried over Na_2SO_4, filtered, concentrated, and purified by column chromatography (0→6% MeOH/0.1%AcOH/DCM) yielding the title compound as an orange oil (7 mg, 46% yield). **^{1}H NMR** (400 MHz, CD_3CN) δ 8.37 (s, 1H), 7.85 (s, 1H), 7.55 (d, J = 2.2 Hz, 1H), 7.43 (dd, J = 8.3, 2.3 Hz, 1H), 7.34 (s, 1H), 7.23 (s, 1H), 6.87 (d, J = 8.1 Hz, 1H), 2.22 – 2.17 (m, 6H), 2.11 – 2.05 (m, 3H), 1.83 – 1.79 (m, 6H); **^{13}C NMR** (125 MHz, CD_3CN) δ 168.03, 156.86, 155.13, 153.73, 142.15, 137.68, 133.00, 129.59, 126.92, 126.69, 126.44, 124.74, 111.14,

109.72, 108.71, 41.07, 37.75, 30.07; **HRMS** Accurate mass (ES+): Found 431.1856, $C_{27}H_{27}O_5$ (M+H+) requires 431.1859.

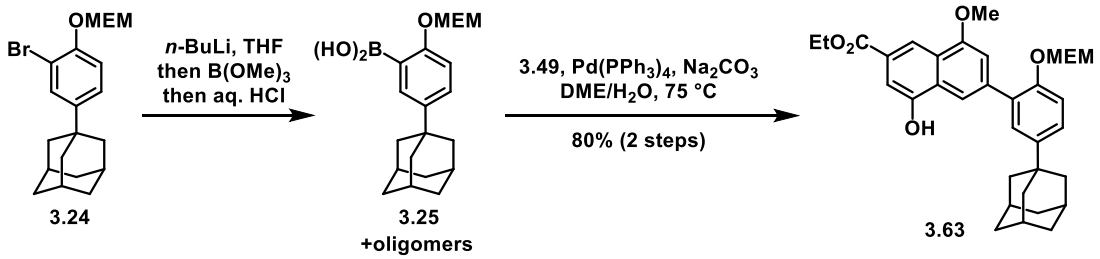

Ethyl 6-(5-(adamantan-1-yl)-2-((2-methoxyethoxy)methoxy)phenyl)-4-hydroxy-8-methoxy-2-naphthoate (3.63). Using the procedure given for the preparation of compound **3.55**, bromide **3.24** (68 mg, 0.172 mmol) and naphthyl bromide **3.49** (53 mg, 0.143 mmol) yielded the title compound as a white foam (64 mg, 80% yield with respect to **3.49**). **^{1}H NMR** (500 MHz, $CDCl_3$) δ 8.60 (s, 1H), 7.89 (s, 1H), 7.60 (s, 1H), 7.42 (d, J = 2.2 Hz, 1H), 7.33 (dd, J = 8.6, 2.1 Hz, 1H), 7.22 (d, J = 8.7 Hz, 1H), 7.10 (s, 1H), 6.49 (br s, 1H), 5.22 (s, 2H), 4.46 (q, J = 7.0 Hz, 2H), 4.03 (s, 3H), 3.75 – 3.70 (m, 2H), 3.52 – 3.48 (m, 2H), 3.34 (s, 3H), 2.10 (s, 3H), 1.94 (s, 6H), 1.77 (q, J = 12.2 Hz, 6H), 1.46 (t, J = 7.1 Hz, 3H); **^{13}C NMR** (125 MHz, $CDCl_3$) δ 167.74, 155.67, 152.48, 152.09, 145.57, 139.24, 131.66, 128.06, 127.79, 126.72, 125.54, 125.07, 117.40, 115.65, 114.67, 108.74, 107.83, 94.42, 71.65, 67.84, 61.41, 59.02, 55.73, 43.40, 36.84, 35.85, 29.05, 14.49; **HRMS** Accurate mass (ES+): Found 583.2653, $C_{34}H_{40}O_7Na$ (M+Na+) requires 583.2672.

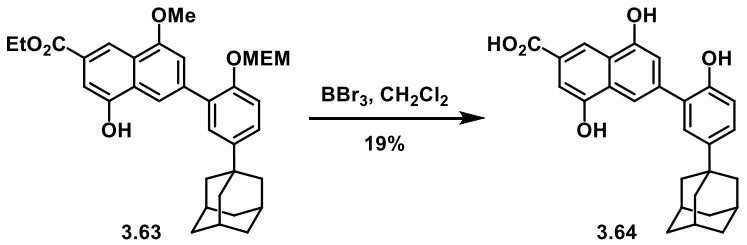

6-(5-(adamantan-1-yl)-2-hydroxyphenyl)-4,8-dihydroxy-2-naphthoic acid (3.64). Using the procedure given for the preparation of compound **3.62**, MEM ether **3.63** (19 mg, 0.034 mmol) yielded the title compound as an orange oil (2.8 mg, 19% yield). **^{1}H NMR** (500 MHz, CD_3CN) δ 8.40 (s, 1H), 7.80 (s, 1H), 7.74 (br s, 1H), 7.35 (s, 2H), 7.29 – 7.22 (m, 1H), 7.18 (s, 1H), 6.90 (d, J = 8.4 Hz, 1H), 6.74 (br s, 1H), 2.10 – 2.03 (m, 3H), 1.96 – 1.89 (m, 6H *overlaps with CD_3CN signal*), 1.83 – 1.75 (m, 6H); **^{13}C NMR** (125 MHz, CD_3CN) δ 168.06, 154.35, 153.77, 152.45, 144.59, 139.97, 129.19, 128.52, 128.12, 127.20, 126.50, 124.90, 117.85, 116.84, 114.63, 112.47, 108.54, 44.03, 37.35, 30.02; **HRMS** Accurate mass (ES+): Found 453.1673, $C_{27}H_{26}O_5Na$ (M+Na+) requires 453.1678.

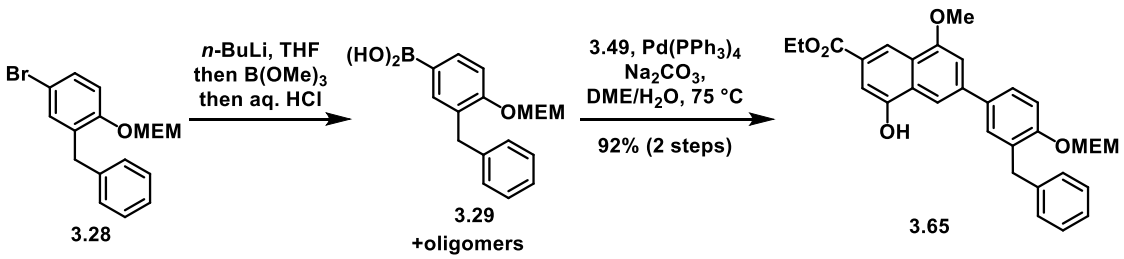

Ethyl 6-(3-benzyl-4-((2-methoxyethoxy)methoxy)phenyl)-4-hydroxy-8-methoxy-2-naphthoate (3.65). (synthesized by Colleen Keohane and me) Using the procedure given for the preparation of compound **3.55**, bromide **3.28** (60 mg, 0.171 mmol) and naphthyl bromide **3.49** (50 mg, 0.136 mmol) yielded the title compound as a clear oil (66 mg, 92% yield with respect to **3.49**). **^{1}H NMR** (500 MHz, $CDCl_3$) δ 8.72 (s, 1H), 8.11 (s, 1H), 7.80 (s, 1H), 7.70 (s, 2H), 7.45 – 7.36 (m, 5H), 7.31 (s, 1H), 7.18 (s, 1H), 6.98 (br s, 1H), 5.44 (s, 2H), 4.61 (dd, J = 13.9, 6.8 Hz, 2H), 4.23 (s, 2H), 4.20 (s, 3H), 3.81 (s, 2H), 3.65 (s, 2H), 3.53 (s, 3H), 1.60 (t, J = 6.9 Hz, 3H); **^{13}C NMR** (125 MHz, $CDCl_3$) δ 167.73, 156.74, 154.97, 152.42, 141.03, 140.46, 134.80, 130.48, 129.92, 128.85, 128.34, 126.74, 126.54, 125.93, 125.04, 117.50, 114.33, 111.85, 108.96, 104.82, 93.14, 71.69, 67.62, 61.46, 59.08, 55.74, 36.69, 29.82, 14.50; **HRMS** Accurate mass (ES+): Found 517.2227, $C_{31}H_{33}O_7$ (M+H+) requires 517.2226.

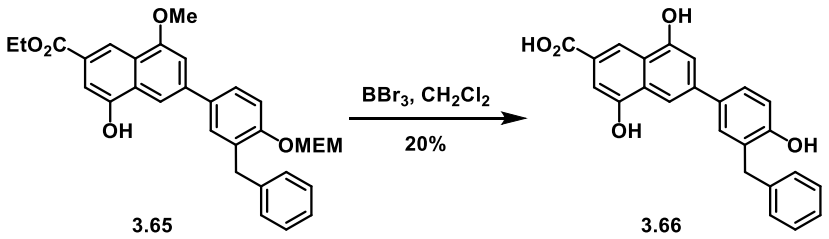

6-(3-benzyl-4-hydroxyphenyl)-4,8-dihydroxy-2-naphthoic acid (3.66). (synthesized by Colleen Keohane and me) Using the procedure given for the preparation of compound **3.62**, MEM ether **3.65** (20 mg, 0.039 mmol) yielded the title compound as an orange oil (3.0 mg, 20% yield). **^{1}H NMR** (400 MHz, CD_3CN) δ 8.36 (s, 1H), 7.82 (s, 1H), 7.76 (br s, 1H), 7.52 (d, J = 2.4 Hz, 1H), 7.47 (dd, J = 8.3, 2.4 Hz, 1H), 7.34 (d, J = 1.4 Hz, 1H), 7.33 – 7.25 (m, 5H), 7.22 – 7.11 (m, 2H), 6.94 (d, J = 8.3 Hz, 1H), 4.02 (s, 2H); **^{13}C NMR** (125 MHz, CD_3CN) δ 168.08, 155.74, 155.12, 153.74, 142.28, 141.51, 133.36, 130.48, 129.67, 129.52, 129.30, 127.26, 127.02, 126.84, 124.79, 117.86, 116.62, 111.23, 109.59, 108.71, 36.48; **HRMS** Accurate mass (ES+): Found 387.1241, $C_{24}H_{19}O_5$ (M+H+) requires 387.1233.

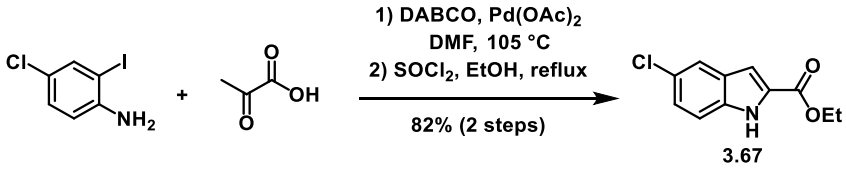

Ethyl 5-chloro-1H-indole-2-carboxylate (3.67). (several batches were prepared by myself and Isabelle Sinitsa) To a solution of 4-chloro-2-iodoaniline (4.99g, 19.69 mmol, purified on silica gel prior to use - from Oakwood Products, Inc.) in DMF (39 mL) was added DABCO (6.62 g, 59.06 mmol). After 30 minutes, pyruvic acid (4.16 mL, 59.06 mmol) was added over 10 minutes. The reaction flask was purged with argon, then $Pd(OAc)_2$ (221 mg, 0.984 mmol) was added and the reaction flask was purged with argon again. The reaction was heated to 105 °C for 1 hour then cooled to room temperature. After an hour at this temperature the reaction was acidified to a pH of 3 with 1M HCl. The total volume was doubled with water and the mixture was filtered. The

brown solid was washed with two portions of water, and the crude acid was carried directly to the next step. The acid was dissolved in EtOH (100 mL) and $SOCl_2$ (2.57 mL, 35.44 mmol) was slowly added. The mixture was heated to reflux overnight, and then concentrated to dryness. The solid was dissolved in acetone then dry-loaded onto silica gel and purified by column chromatography, yielding the title compound as a tan solid (3.60g, 82% yield over two steps) with spectral data matching that previously described (Koenig, S. G., Dankwardt, J. W., Liu, Y., Zhao, H. & Singh, S. P. *Tet. Lett.* **2010**, *51*, 6549).

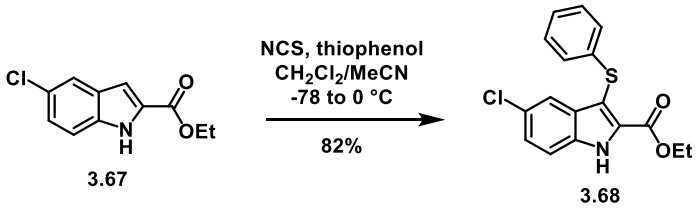

Ethyl 5-chloro-3-(phenylthio)-1H-indole-2-carboxylate (3.68). (several batches were prepared by myself and Isabelle Sinitsa) To a solution of N-chlorosuccinimide (297 mg, 2.221 mmol) in CH_2Cl_2 (10 mL) at -78 °C was added thiophenol (0.23 mL, 2.22 mmol). The reaction was warmed to 0 °C, over which time the reaction turned from clear to bright yellow. After 15 minutes at this temperature, ethyl 5-chloro-1H-indole-2-carboxylate (414 mg, 1.851 mmol) was added as a solution in 1:1 CH_2Cl_2:MeCN (8 mL). After stirring for 1 hour at 0 °C, the reaction was quenched with water and extracted with CH_2Cl_2 3x. The combined organic layers were washed with brine, dried over Na_2SO_4, filtered, concentrated and purified by column chromatography, yielding the title compound as a white solid (449 mg, 82% yield). **^{1}H NMR** (500 MHz, $CDCl_3$) δ 9.28 (br s, 1H), 7.60 (dd, J = 1.3, 0.7 Hz, 1H), 7.38 (dd, J = 8.7, 0.5 Hz, 1H), 7.31 (dd, J = 8.8, 2.0 Hz, 1H), 7.22 – 7.08 (m, 5H), 4.39 (q, J = 7.1 Hz, 2H), 1.30 (t, J = 7.1 Hz, 3H); **^{13}C NMR** (125 MHz, $CDCl_3$) δ 161.10, 137.52, 134.04, 131.39, 130.26, 128.98, 127.63, 127.43, 126.92, 125.71, 121.13, 113.40, 110.19, 61.83, 14.29; **HRMS** APCI (*m/z*): $[M-H]^-$ calcd for $C_{17}H_{13}ClNO_2S$ 330.0356, found 330.0362.

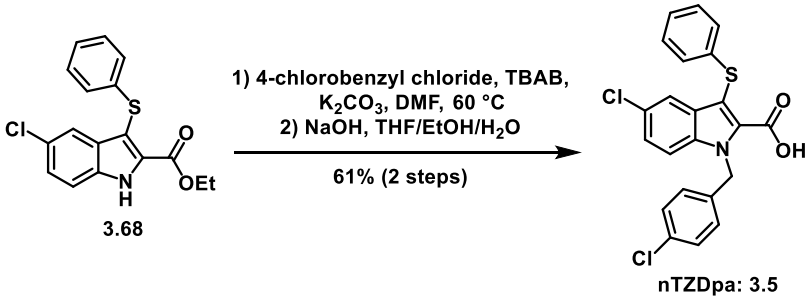

5-chloro-1-(4-chlorobenzyl)-3-(phenylthio)-1H-indole-2-carboxylic acid (nTZDpa, 3.5). (several batches were prepared by myself and Isabelle Sinitsa) To a solution of indole **3.68** (90 mg, 0.303 mmol) in DMF (2 mL) was added K_2CO_3 (84 mg, 0.605 mmol), TBAB (10 mg, 0.030 mmol), and 4-chlorobenzyl chloride (97 mg, 0.605 mmol), and the reaction was stirred at 60 °C overnight. The reaction was quenched with water and extracted with EtOAc 3x. The combined organic layers were washed with brine, dried over Na_2SO_4, filtered, concentrated, and purified by column chromatography. The intermediate was dissolved in 2:2:1 EtOH:THF:H_2O and NaOH (38 mg, 0.942 mmol) was added. The reaction was stirred at room temperature for 3 hours, then acidified with 1M HCl and extracted with CH_2Cl_2 3x. The combined organic layers were washed with brine, dried over Na_2SO_4, filtered, concentrated, and purified by column chromatography (0→5%/MeOH/0.1% AcOH/CH_2Cl_2), yielding the title compound as a white solid (75 mg, 61% over 2 steps). **^{1}H NMR** (500 MHz, DMSO) δ 13.89 (br s, 1H), 7.71 (dd, J = 8.6, 0.9 Hz, 1H), 7.41 – 7.33 (m, 4H), 7.29 – 7.23 (m, 2H), 7.17 – 7.11 (m, 1H), 7.11 – 7.05 (m, 4H), 5.83 (s, 2H); **^{13}C NMR** (125 MHz, DMSO) δ 162.00, 137.17, 136.77, 136.11, 134.32, 131.94, 129.14, 129.03, 128.65, 128.22, 126.56, 126.41, 125.59, 125.55, 119.32, 113.88, 107.17, 47.57; **HRMS** APCI (*m/z*): $[M-H]^-$ calcd for $C_{22}H_{14}Cl_2NO_2S$ 426.0122, found 222.0328.

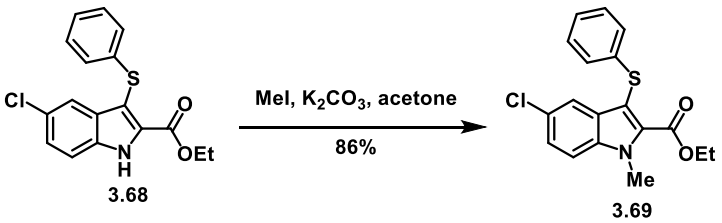

Ethyl 5-chloro-1-methyl-3-(phenylthio)-1H-indole-2-carboxylate (3.69). To a solution of indole **3.68** (42 mg, 0.127 mmol) in acetone (2 mL) was added K_2CO_3 (70 mg, 0.506 mmol) and iodomethane (0.016 mL, 0.254 mmol), and the reaction was stirred at room temperature overnight. The following day a large amount of white solids were visible in the reaction flask. The reaction was poured into water and extracted with EtOAc 3x. The combined organic layers were washed with brine, dried over Na_2SO_4, filtered, concentrated, and purified by column chromatography, yielding the title compound as a clear oil (38 mg, 86% yield). **^{1}H NMR** (500 MHz, $CDCl_3$) δ 7.64 (dd, J = 1.9, 0.6 Hz, 1H), 7.37 – 7.30 (m, 2H), 7.20 – 7.15 (m, 2H), 7.12 – 7.06 (m, 3H), 4.35 (q, J = 7.1 Hz, 2H), 4.05 (s, 3H), 1.26 (t, J = 7.1 Hz, 3H); **^{13}C NMR** (125 MHz, $CDCl_3$) δ 161.61, 138.34, 136.88, 132.81, 130.09, 128.87, 127.51, 126.76, 126.19, 125.31, 120.90, 111.79, 108.86, 61.63, 32.77, 14.13; **HRMS** APCI (*m/z*): $[M+H]^+$ calcd for $C_{18}H_{17}ClNO_2S$ 346.0669, found 346.0665.

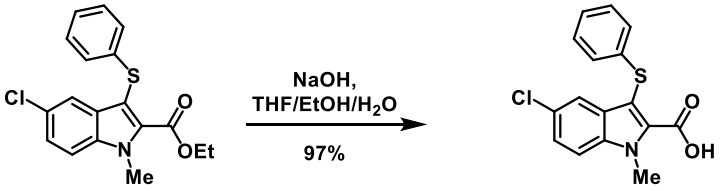

3.69 3.70

5-chloro-1-methyl-3-(phenylthio)-1H-indole-2-carboxylic acid (3.70). To a solution of **3.69** (38 mg, 0.110 mmol) in 1:1 THF:EtOH (2 mL) was added 1M NaOH (0.55 mL, 0.55 mmol). The reaction was stirred for 4 hours at room temperature, then acidified with 1M HCl and extracted with EtOAc 3x. The combined organic layers were washed with brine, dried over Na_2SO_4, filtered, concentrated, and purified by column chromatography (0→5% MeOH/0.1% AcOH/CH_2Cl_2), yielding the title compound as a white solid (34 mg, 97% yield). **^{1}H NMR** (500 MHz, DMSO) δ 7.75 (d, J = 8.8 Hz, 1H), 7.41 – 7.34 (m, 2H), 7.22 (dt, J = 20.2, 7.2 Hz, 2H), 7.11 (ddd, J = 6.9, 2.3, 1.2 Hz, 1H), 7.08 – 7.04 (m, 2H), 4.02 (s, 3H); **^{13}C NMR** (125 MHz, MeOD + drop of $CDCl_3$) δ 154.47, 129.76, 128.77, 125.52, 121.25, 120.29, 118.66, 118.57,

117.19, 116.88, 111.56, 103.89, 100.04, 23.57; **HRMS** APCI (*m/z*): $[M-H]^-$ calcd for $C_{16}H_{11}ClNO_2S$ 316.0199, found 316.0206.

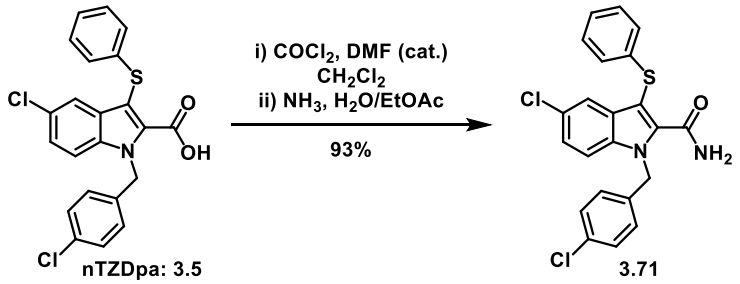

5-chloro-1-(4-chlorobenzyl)-3-(phenylthio)-1H-indole-2-carboxamide (3.71). To a solution of nTZDpa (15 mg, 0.035 mmol) dissolved in CH_2Cl_2 (2 mL) was added oxalyl chloride (2M in CH_2Cl_2, 0.04 mL, 0.08 mmol) and the reaction turned from clear to yellow color. A drop of DMF was then added, and the reaction was stirred at room temperature for 2 hours. The reaction was concentrated under reduced pressure and dried under vacuum for 5 minutes, after which time the crude acid chloride was cooled to 0 °C and 8:1 EtOAc:NH_4OH (5 mL) was added. After 30 minutes at 0 °C, the reaction was diluted with water and extracted with EtOAc 3x. The combined organic layers were washed with brine, dried over Na_2SO_4, filtered, concentrated, and purified by column chromatography, yielding the title compound as a white solid (14 mg, 93% yield). **^{1}H NMR** (500 MHz, Acetone) δ 7.72 (br s, 2H), 7.63 (d, J = 8.9 Hz, 1H), 7.58 (d, J = 2.1 Hz, 1H), 7.35 – 7.28 (m, 4H), 7.28 – 7.21 (m, 4H), 7.18 – 7.11 (m, 3H), 5.94 (s, 2H); **^{13}C NMR** (125 MHz, Acetone) δ 162.89, 138.79, 137.94, 137.77, 136.94, 133.53, 131.04, 130.12, 129.52, 129.46, 128.07, 127.23, 126.73, 125.99, 120.27, 114.11, 103.52, 48.69; **HRMS** APCI (*m/z*): $[M-H]^-$ calcd for $C_{22}H_{15}Cl_2N_2OS$ 425.0282, found 425.0288.

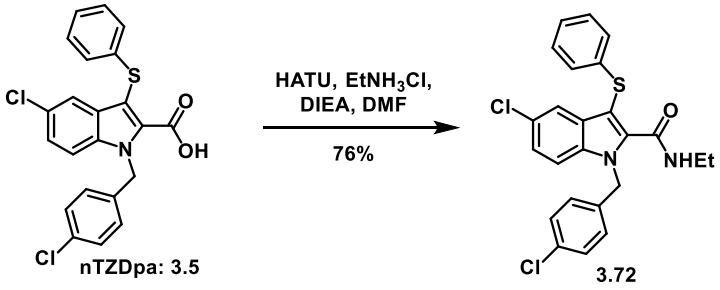

5-chloro-1-(4-chlorobenzyl)-N-ethyl-3-(phenylthio)-1H-indole-2-carboxamide (3.72). To a solution of nTZDpa (23 mg, 0.054 mmol) in DMF (1 mL) was added ethylamine hydrochloride (13 mg, 0.161 mmol), HATU (22 mg, 0.058 mmol) and DIEA (0.06 mL, 0.324 mmol), and the reaction was stirred at room temperature overnight. The following day, the reaction was poured into water and extracted with EtOAc 3x. The combined organic layers were washed with brine, dried over Na_2SO_4, filtered, concentrated, and purified by prep TLC (2:1 hexanes:EtOAc, R_f = 0.61), yielding the title compound as a white solid (19 mg, 76% yield). **^{1}H NMR** (500 MHz, $CDCl_3$) δ 7.71 (dd, J = 1.9, 0.6 Hz, 1H), 7.62 (br s, 1H), 7.32 - 7.19 (m, 6H), 7.17 – 7.12 (m, 1H), 7.08 – 7.02 (m, 4H), 5.87 (s, 2H), 3.42 – 3.33 (m, 2H), 1.07 (t, J = 7.3 Hz, 3H); **^{13}C NMR** (100 MHz, $CDCl_3$) δ 160.71, 136.55, 136.19, 136.11, 135.91, 133.37, 130.61, 129.50, 129.00, 128.04, 126.23, 125.98, 120.31, 112.30, 102.93, 48.63, 34.72, 14.52; **HRMS** APCI (*m/z*): $[M+H]^+$ calcd for $C_{24}H_{21}Cl_2N_2OS$ 455.0752, found 455.0753.

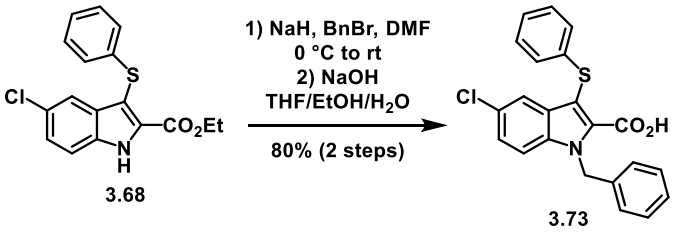

1-benzyl-5-chloro-3-(phenylthio)-1H-indole-2-carboxylic acid (3.73). To a suspension of sodium hydride (60% in mineral oil, 10 mg, 0.250 mmol) in DMF (1 mL) at 0 °C was added a solution of indole **3.68** (40 mg, 0.121 mmol) in DMF (1 mL). The solution was stirred at 0 °C for 30 minutes, and then held at room temperature for 30 minutes. The reaction was cooled to 0 °C

and benzyl bromide (0.03 mL, 0.270 mmol) was added, and the reaction was allowed to warm to room temperature and stirred overnight. The following day, the reaction was poured into water and extracted with EtOAc 3x. The combined organic layers were washed with brine, dried over Na_2SO_4, filtered, concentrated, and purified by column chromatography (*The N-alkylated product was an inseparable mixture of ethyl and chlorobenzyl esters, which was carried to the next step*). The intermediate was dissolved in 1:1 THF:EtOH (2 mL) and 1M NaOH solution (0.60 mL, 0.60 mmol) was added, and the reaction was stirred for 2 hours at room temperature. The reaction was acidified with 1M HCl and extracted with EtOAc 3x. The combined organic layers were washed with brine, dried over Na_2SO_4, filtered, and concentrated, yielding the title compound as a white solid (41 mg, 80% yield). **^{1}H NMR** (500 MHz, DMSO) δ 13.88 (br s, 1H), 7.71 (d, J = 8.8 Hz, 1H), 7.38 – 7.28 (m, 4H), 7.27 – 7.21 (m, 3H), 7.16 – 7.11 (m, 1H), 7.10 – 7.05 (m, 4H), 5.85 (s, 2H); **^{13}C NMR** (125 MHz, DMSO) δ 173.33, 162.07, 137.69, 137.27, 136.15, 134.61, 129.12, 129.04, 128.67, 127.37, 126.50, 126.30, 125.52, 125.45, 119.24, 113.96, 106.82, 48.10; **HRMS** APCI (*m/z*): $[M-H]^-$ calcd for $C_{22}H_{15}ClNO_2S$ 392.0512, found 392.0518.

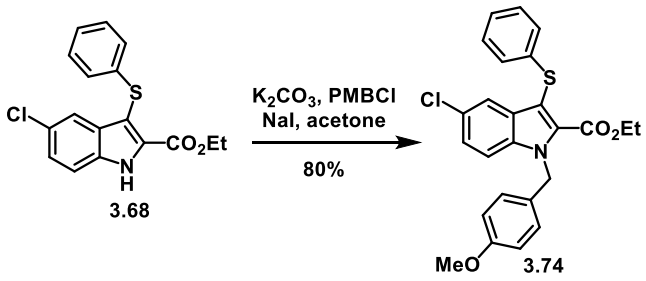

Ethyl 5-chloro-1-(4-methoxybenzyl)-3-(phenylthio)-1H-indole-2-carboxylate (3.74). To a solution of indole **3.68** (54 mg, 0.163 mmol) in acetone (2 mL) was added K_2CO_3 (90 mg, 0.651 mmol), NaI (42 mg, 0.277 mmol), and PMBCl (0.044 mL, 0.326 mmol). The reaction was stirred at room temperature overnight. The following day, yellow solids were observed in the reaction. Water was added, and the aqueous layer was extracted with EtOAc 3x. The combined organic layers were washed with brine, dried over Na_2SO_4, filtered, concentrated, and purified by column

chromatography, yielding the title compound as a clear oil (59 mg, 80% yield). **^{1}H NMR** (500 MHz, $CDCl_3$) δ 7.62 (dd, *J* = 2.0, 0.5 Hz, 1H), 7.33 (dd, *J* = 8.9, 0.4 Hz, 1H), 7.26 (dd, *J* = 8.8, 2.0 Hz, 1H), 7.23 – 7.16 (m, 2H), 7.12 – 7.08 (m, 3H), 7.03 – 6.99 (m, 2H), 6.83 – 6.79 (m, 2H), 5.70 (s, 2H), 4.29 (q, *J* = 7.1 Hz, 2H), 3.76 (s, 3H), 1.19 (t, *J* = 7.1 Hz, 3H); **^{13}C NMR** (125 MHz, $CDCl_3$) δ 161.47, 159.10, 138.09, 136.64, 132.66, 130.20, 129.34, 128.91, 127.75, 127.65, 126.78, 126.36, 125.36, 120.98, 114.23, 112.45, 109.63, 61.70, 55.36, 48.47, 14.05; **HRMS** APCI (*m/z*): $[M+H]^+$ calcd for $C_{25}H_{23}ClNO_3S$ 452.1087, found 452.1087.

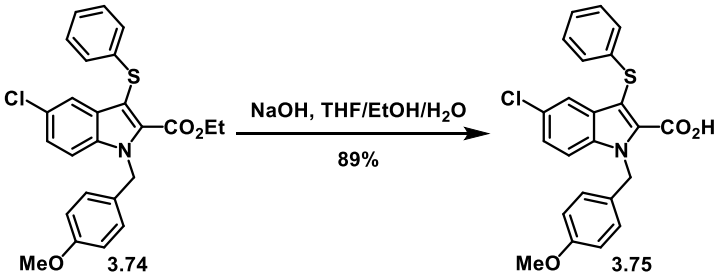

5-chloro-1-(4-methoxybenzyl)-3-(phenylthio)-1H-indole-2-carboxylic acid (3.75). Following the NaOH hydrolysis procedure given above, ester **3.74** (37 mg, 0.082 mmol) yielded the title compound as a white solid (31 mg, 89% yield). **^{1}H NMR** (600 MHz, Acetone) δ 7.66 (d, *J* = 8.9 Hz, 1H), 7.50 (d, *J* = 1.8 Hz, 1H), 7.32 (dd, *J* = 8.9, 2.0 Hz, 1H), 7.22 (t, *J* = 7.7 Hz, 2H), 7.17 – 7.07 (m, 5H), 6.84 (d, *J* = 8.5 Hz, 2H), 5.84 (s, 2H), 3.73 (s, 3H); **^{13}C NMR** (151 MHz, Acetone) δ 160.10, 138.80, 137.59, 130.70, 130.58, 129.81, 128.89, 127.78, 126.49, 126.32, 120.81, 114.84, 114.42, 55.49, 48.81; **HRMS** APCI (*m/z*): $[M+H]^+$ calcd for $C_{23}H_{17}ClNO_3S$ 422.0618, found 422.0623.

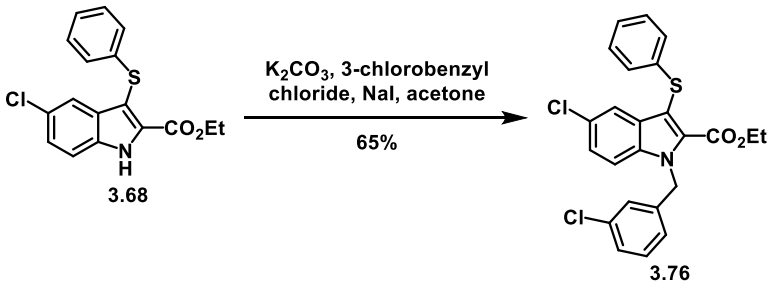

Ethyl 5-chloro-1-(3-chlorobenzyl)-3-(phenylthio)-1H-indole-2-carboxylate (3.76). Indole **3.68** (37 mg, 0.112 mmol) was dissolved in acetone (3 mL) and K_2CO_3 (62 mg, 0.446 mmol), NaI (29 mg, 0.190 mmol), and 3-chlorobenzyl chloride (0.028 mL, 0.224 mmol) were sequentially added to the solution and the reaction was stirred at room temperature overnight. The following day the reaction was heated to reflux for 2 hours and cooled back to room temperature. The reaction was poured into water and extracted with EtOAc 3x. The combined organic layers were washed with brine, dried over Na_2SO_4, filtered, concentrated, and purified by column chromatography, yielding the title compound as a clear oil (33 mg, 65% yield). **^{1}H NMR** (500 MHz, $CDCl_3$) δ 7.64 (dd, J = 1.8, 0.8 Hz, 1H), 7.31 – 7.27 (m, 2H), 7.23 – 7.17 (m, 4H), 7.14 – 7.08 (m, 3H), 7.04 (s, 1H), 6.93 – 6.89 (m, 1H), 5.75 (s, J = 6.9 Hz, 2H), 4.28 (q, J = 7.1 Hz, 2H), 1.18 (t, J = 7.1 Hz, 3H); **^{13}C NMR** (125 MHz, $CDCl_3$) δ 161.40, 139.44, 137.93, 136.67, 130.24, 129.00, 127.99, 126.95, 126.77, 126.51, 125.54, 124.48, 121.27, 112.16, 110.60, 61.81, 48.51, 14.03; **HRMS** APCI (*m/z*): $[M+H]^+$ calcd for $C_{24}H_{20}Cl_2NO_2S$ 456.0592, found 456.0590.

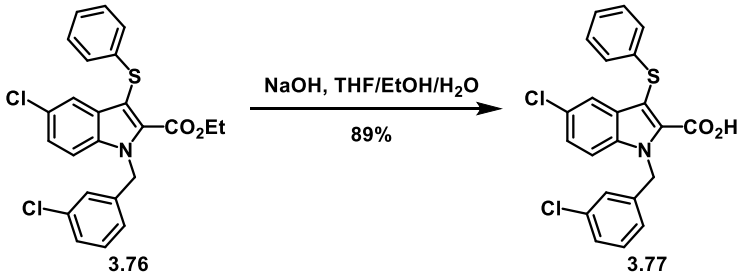

3.76 3.77

5-chloro-1-(3-chlorobenzyl)-3-(phenylthio)-1H-indole-2-carboxylic acid (3.77). To a solution of ester **3.76** (31 mg, 0.068 mmol) in 1:1 THF:EtOH (2 mL) was added 1M NaOH (0.34 mL, 0.34 mmol) and the reaction was stirred at room temperature for 2 hours. The reaction was acidified with 1M HCl and extracted with EtOAc 3x. The combined organic layers were washed with brine, dried over Na_2SO_4, filtered, and concentrated, yielding the title compound as a white solid (29 mg, 94% yield). **^{1}H NMR** (500 MHz, MeOD) δ 7.50 (d, J = 8.9 Hz, 1H), 7.45 (dd, J = 2.0, 0.4 Hz, 1H), 7.30 (dd, J = 8.9, 2.1 Hz, 1H), 7.27 – 7.17 (m, 4H), 7.13 – 7.08 (m, 3H), 7.06 (s,

1H), 6.98 (dt, J = 7.3, 1.6 Hz, 1H), 5.84 (s, 2H); **^{13}C NMR** (125 MHz, MeOD) δ 163.88, 141.60, 139.04, 138.05, 135.64, 134.77, 131.28, 131.00, 129.96, 128.62, 128.59, 128.25, 127.50, 127.16, 126.62, 125.82, 121.38, 113.92, 111.15; **HRMS** APCI (*m/z*): [M-H]$^-$ calcd for $C_{22}H_{14}Cl_2NO_2S$ 426.0122, found 426.0127.

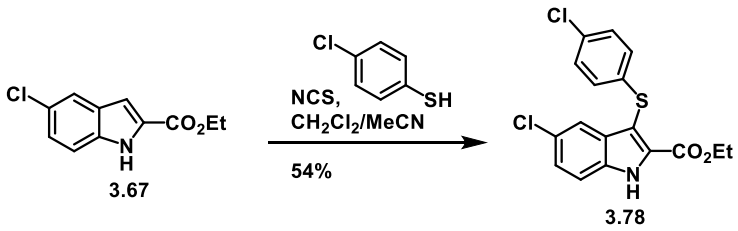

Ethyl 5-chloro-3-((4-chlorophenyl)thio)-1H-indole-2-carboxylate (3.78). To a solution of N-chlorosuccinimide (72 mg, 0.539 mmol) in CH_2Cl_2 (5 mL) at -78 °C was added 4-chlorothiophenol (78 mg, 0.539 mmol). The reaction was warmed to 0 °C, over which time the reaction turned from clear to bright yellow. After 15 minutes at this temperature, **3.67** (100 mg, 0.449 mmol) was added as a solution in 1:1 CH_2Cl_2:MeCN (4 mL). After stirring for 1 hour at 0 °C, the reaction was quenched with water and extracted with CH_2Cl_2 3x.The combined organic layers were washed with brine, dried over Na_2SO_4, filtered, concentrated and purified by column chromatography, yielding the title compound as a white solid (88 mg, 54% yield). **^{1}H NMR** (500 MHz, $CDCl_3$) δ 9.23 (s, 1H), 7.61 (dd, J = 1.3, 0.7 Hz, 1H), 7.39 (dd, J = 8.8, 0.5 Hz, 1H), 7.33 (dd, J = 8.8, 2.0 Hz, 1H), 7.18 – 7.13 (m, 2H), 7.10 – 7.04 (m, 2H), 4.39 (q, J = 7.1 Hz, 2H), 1.32 (t, J = 7.1 Hz, 3H); **^{13}C NMR** (125 MHz, $CDCl_3$) δ 161.17, 136.53, 134.31, 131.14, 130.99, 130.47, 128.89, 128.16, 127.46, 126.63, 120.46, 113.73, 108.57, 61.69, 14.11; **HRMS** APCI (*m/z*): [M-H]$^-$ calcd for $C_{17}H_{12}Cl_2NO_2S$ 363.9966, found 363.9976.

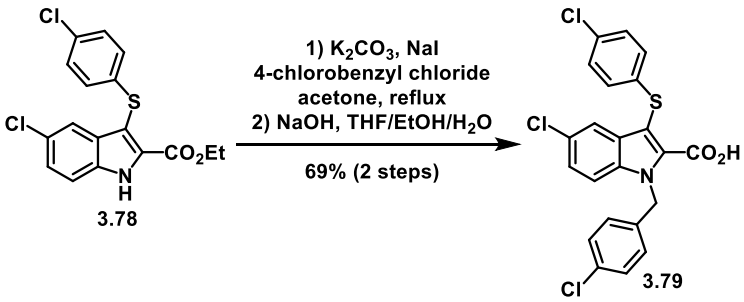

5-chloro-1-(4-chlorobenzyl)-3-((4-chlorophenyl)thio)-1H-indole-2-carboxylic acid (3.79). To a solution of indole **3.78** (75 mg, 0.205 mmol) in acetone (4 mL) was added K_2CO_3 (113 mg, 0.819 mmol), NaI (52 mg, 0.349 mmol), and 4-chlorobenzyl chloride (66 mg, 0.410 mmol). The reaction was refluxed for 6 hours then stirred at room temperature overnight. The reaction was poured into water and extracted with EtOAc 3x. The combined organic layers were washed with brine, dried over Na_2SO_4, filtered, concentrated, and purified by column chromatography. The alkylated intermediate was then dissolved in 1:1 THF:EtOH (2 mL), and 1M NaOH (1.10 mL, 1.10 mmol) was added. The reaction was stirred for 4 hours at room temperature and acidified with 1M HCl, then extracted with EtOAc 3x. The combined organic layers were washed with brine, dried over Na_2SO_4, filtered, and concentrated, yielding the title compound as a white solid (65 mg, 69% yield over 2 steps). **^{1}H NMR** (500 MHz, Acetone) δ 7.65 (d, J = 8.9 Hz, 1H), 7.56 (dd, J = 2.0, 0.4 Hz, 1H), 7.38 – 7.30 (m, 3H), 7.30 – 7.23 (m, 2H), 7.20 – 7.13 (m, 4H), 5.94 (s, 2H); **^{13}C NMR** (125 MHz, Acetone) δ 162.35, 137.87, 137.62, 134.58, 133.57, 131.59, 130.59, 129.80, 129.55, 129.17, 129.12, 128.24, 126.94, 120.77, 114.30, 109.13, 48.85; **HRMS** APCI (*m/z*): $[M-H]^-$ calcd for $C_{22}H_{13}Cl_3NO_2S$ 459.9733, found 459.9740.

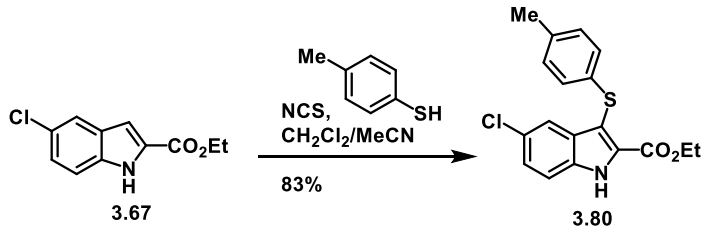

Ethyl 5-chloro-3-(p-tolylthio)-1H-indole-2-carboxylate (3.80). Using the procedure given for the preparation of **3.68**, indole **3.67** (100 mg, 0.447 mmol) and 4-methylthiophenol (67 mg, 0.537 mmol) yielded the title compound as a white solid (129 mg, 83%). **^{1}H NMR** (400 MHz, $CDCl_3$) δ 9.17 (s, 1H), 7.58 (s, 1H), 7.36 (d, *J* = 8.7 Hz, 1H), 7.30 (t, *J* = 8.8 Hz, 1H), 7.10 (d, *J* = 8.1 Hz, 2H), 7.01 (d, *J* = 8.0 Hz, 2H), 4.40 (q, *J* = 7.1 Hz, 2H), 2.27 (s, 3H), 1.34 (t, *J* = 7.1 Hz, 3H); **^{13}C NMR** (125 MHz, $CDCl_3$) δ 161.15, 135.81, 134.04, 133.67, 131.30, 129.92, 129.76, 128.12, 127.47, 126.83, 121.20, 113.34, 111.15, 61.79, 21.10, 14.35; **HRMS** APCI (*m/z*): $[M-H]^-$ calcd for $C_{18}H_{15}ClNO_2S$ 344.0512, found 344.0517.

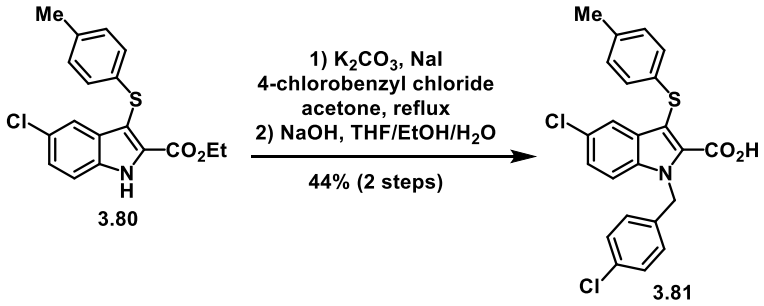

5-chloro-1-(4-chlorobenzyl)-3-(p-tolylthio)-1H-indole-2-carboxylic acid (3.81). To a solution of indole **3.80** (110 mg, 0.318 mmol) in acetone (5 mL) was added K_2CO_3 (176 mg, 1.272 mmol), NaI (81 mg, 0.541 mmol), and 4-chlorobenzyl chloride (102 mg, 0.636 mmol). The reaction was stirred overnight at room temperature, then refluxed for 2 hours. Water was added, and the aqueous layer was extracted with EtOAc 3x. The combined organic layers were washed with brine, dried over Na_2SO_4, filtered, concentrated, and purified by column chromatography. The intermediate was dissolved in 2:2:1 THF:EtOH:H_2O (3 mL) and 1M NaOH (0.52 mL) was added, and the reaction was stirred overnight at room temperature. The reaction was acidified with 1M HCl and extracted with EtOAc 3x. The combined organic layers were washed with water and brine, dried over Na_2SO_4, filtered, and concentrated, yielding the title compound as a white solid (45 mg, 44% yield over two steps). **^{1}H NMR** (500 MHz, Acetone) δ 7.65 – 7.58 (m, 1H), 7.52 (dd, *J* = 2.1, 0.4 Hz, 1H), 7.35 – 7.30 (m, 3H), 7.15 (d, *J* = 8.6 Hz, 2H), 7.13 – 7.09 (m, 2H), 7.06

(d, *J* = 8.1 Hz, 2H), 5.91 (s, 2H), 2.24 (s, 3H); **^{13}C NMR** (125 MHz, Acetone) δ 162.55, 137.75, 137.62, 136.39, 134.85, 133.54, 130.59, 130.54, 129.52, 129.12, 128.48, 127.87, 126.75, 121.06, 114.12, 110.92, 48.73, 29.84, 20.87; **HRMS** APCI (*m/z*): [M-H]$^-$ calcd for $C_{23}H_{16}Cl_2NO_2S$ 440.0279, found 440.0284.

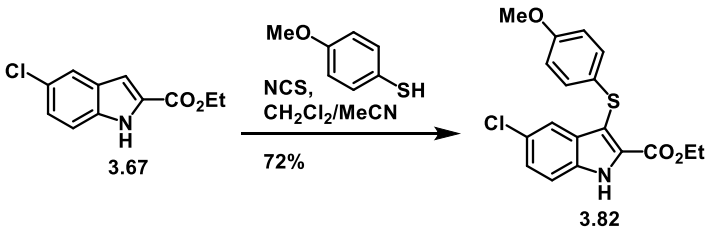

Ethyl 5-chloro-3-((4-methoxyphenyl)thio)-1H-indole-2-carboxylate (3.82). Using the procedure given for the preparation of compound **3.68**, indole **3.67** (207 mg, 0.926 mmol) and 4-methoxythiophenol (0.14 mL, 1.111 mmol) yielded the title compound as a white solid (308 mg, 92% yield). **^{1}H NMR** (500 MHz, $CDCl_3$) δ 9.12 (s, 1H), 7.55 (dd, *J* = 1.3, 0.7 Hz, 1H), 7.34 (dd, *J* = 8.7, 0.6 Hz, 1H), 7.28 (dd, *J* = 8.7, 2.0 Hz, 1H), 7.26 – 7.22 (m, 2H), 6.80 – 6.75 (m, 2H), 4.42 (q, *J* = 7.1 Hz, 2H), 3.76 (s, 3H), 1.38 (t, *J* = 7.1 Hz, 3H); **^{13}C NMR** (126 MHz, $CDCl_3$) δ 161.42, 158.45, 134.20, 130.89, 130.59, 129.27, 127.72, 127.08, 126.50, 120.92, 114.63, 113.44, 111.94, 61.66, 55.42, 14.30; **HRMS** APCI (*m/z*): [M-H]$^-$ calcd for $C_{18}H_{15}ClNO_3S$ 360.0461, found 360.0458.

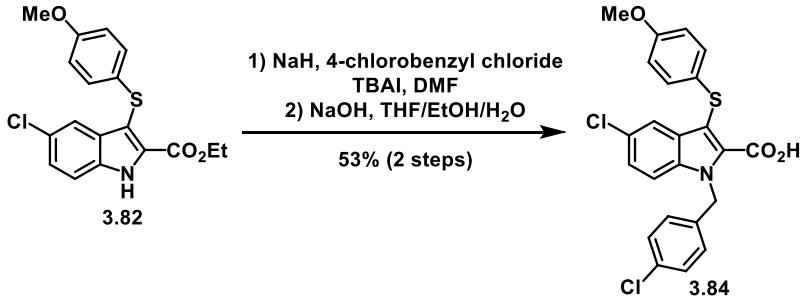

5-chloro-1-(4-chlorobenzyl)-3-((4-methoxyphenyl)thio)-1H-indole-2-carboxylic acid (3.84). To a suspension of sodium hydride (60% in mineral oil, 13 mg, 0.331 mmol) in DMF (2 mL) at 0

°C was added indole **3.82** (100 mg, 0.276 mmol) dissolved in DMF (2 mL). The reaction was warmed to room temperature and stirred for 30 minutes. 4-chlorobenzyl chloride (67 mg, 0.414 mmol) and TBAI (102 mg, 0.276 mmol) were added, and the reaction was stirred at room temperature overnight. The reaction was quenched with water and extracted with EtOAc 3x. The combined organic layers were washed with brine, dried over Na_2SO_4, filtered concentrated and purified by column chromatography, yielding the intermediate mixture of benzyl and ethyl esters. The intermediate was dissolved in 1:1 THF:EtOH (4 mL) and 1M NaOH (0.88 mL, 0.88 mmol) was added. The reaction was stirred until complete by TLC, acidified with 1M HCl, and extracted with EtOAc 3x. The combined organic layers were washed with brine, dried over Na_2SO_4, filtered and concentrated, yielding the title compound as a white solid (67 mg, 53% yield over two steps). **^{1}H NMR** (500 MHz, DMSO) δ 7.65 (d, *J* = 8.7 Hz, 1H), 7.39 – 7.35 (m, 2H), 7.34 – 7.29 (m, 2H), 7.20 – 7.16 (m, 2H), 7.06 (d, *J* = 8.5 Hz, 2H), 6.89 – 6.85 (m, 2H), 5.79 (s, 2H), 3.70 (s, 3H); **^{13}C NMR** (125 MHz, DMSO) δ 162.18, 158.08, 136.85, 135.99, 135.79, 131.91, 130.07, 128.80, 128.63, 128.23, 126.07, 119.43, 114.87, 113.70, 55.20, 47.43; **HRMS** APCI (*m/z*): [M-H]$^-$ calcd for $C_{23}H_{16}Cl_2NO_3S$ 456.0228, found 456.0233.

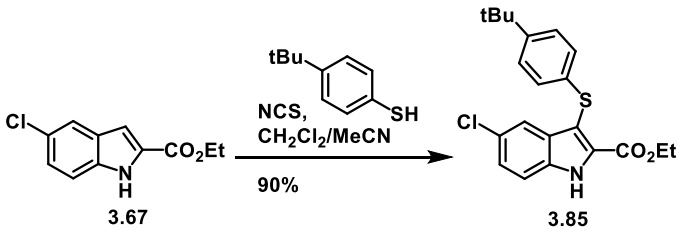

Ethyl 3-((4-(tert-butyl)phenyl)thio)-5-chloro-1H-indole-2-carboxylate (3.85). Using the procedure given for the preparation of compound **3.68**, indole **3.67** (218 mg, 0.975) and 4-tert-butylbenzenethiol (0.20 mL, 1.170 mmol) yielded the title compound as a white solid (341 mg, 90% yield). **^{1}H NMR** (500 MHz, Acetone) δ 11.52 (s, 1H), 7.61 (d, *J* = 8.8 Hz, 1H), 7.49 (s, *J* = 0.6 Hz, 1H), 7.34 – 7.30 (m, 1H), 7.28 (d, *J* = 8.0 Hz, 2H), 7.14 (d, *J* = 8.2 Hz, 2H), 4.35 (q, *J* = 7.1 Hz, 2H), 1.28 (t, *J* = 7.1 Hz, 3H), 1.25 (s, 9H); **^{13}C NMR** (125 MHz, Acetone) δ 161.12,

149.63, 135.69, 135.01, 131.77, 131.62, 128.34, 127.37, 126.75, 120.78, 115.41, 109.98, 61.79, 34.90, 31.52, 14.48; **HRMS** APCI (*m/z*): $[M-H]^-$ calcd for $C_{21}H_{21}ClNO_2S$ 386.0988, found 386.0988.

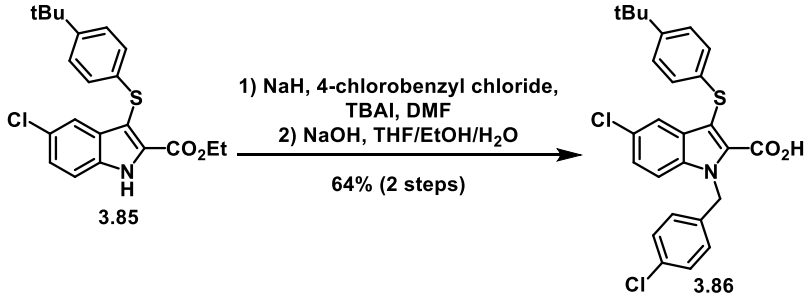

3-((4-(tert-butyl)phenyl)thio)-5-chloro-1-(4-chlorobenzyl)-1H-indole-2-carboxylic acid (3.86). Using the procedure given for the preparation of **3.84**, indole **3.85** (100 mg, 0.258 mmol) yielded the title compound as a white solid (80 mg, 64% yield over two steps). **^{1}H NMR** (500 MHz, DMSO) δ 13.87 (s, 1H), 7.69 (d, *J* = 9.5 Hz, 1H), 7.40 – 7.37 (m, 2H), 7.35 (td, *J* = 4.7, 2.1 Hz, 2H), 7.30 – 7.27 (m, 2H), 7.09 – 7.06 (m, 2H), 7.05 – 7.02 (m, 2H), 5.83 (s, 2H), 1.22 (s, 9H); **^{13}C NMR** (125 MHz, DMSO) δ 162.07, 148.37, 136.80, 136.10, 134.04, 133.58, 131.94, 129.08, 128.67, 128.59, 128.20, 128.11, 126.72, 126.35, 126.08, 125.57, 119.41, 113.82, 107.82, 47.54, 39.52, 34.14, 31.02; **HRMS** APCI (*m/z*): $[M-H]^-$ calcd for $C_{26}H_{22}Cl_2NO_2S$ 482.0748, found 482.0756.

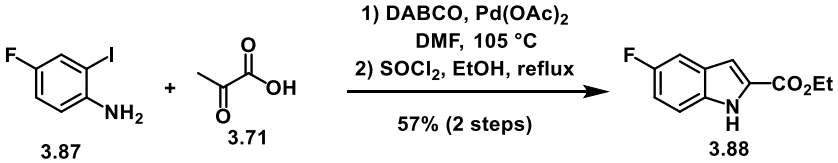

Ethyl 5-chloro-1H-indole-2-carboxylate (3.88). Using the procedure given for the preparation of compound **3.67**, aniline **3.87** (445 mg, 1.877 mmol) yielded the title compound as a brown solid (222 mg, 57% yield over two steps). Spectral data matched that previously described

(Sudhakara, A.; Jayadevappa, H.; Mahadevan, K. M.; Hulikal, V. *Synth Commun.* **2009**, *39*, 2506).

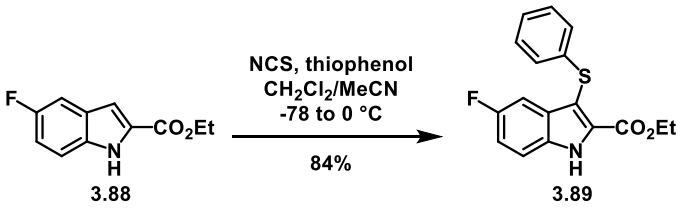

Ethyl 5-fluoro-3-(phenylthio)-1H-indole-2-carboxylate (3.89). Using the procedure given for the preparation of compound **3.68**, indole **3.88** (101 mg, 0.487 mmol) yielded the title compound as a white solid (129 mg, 84% yield). **^{1}H NMR** (500 MHz, $CDCl_3$) δ 9.24 (s, 1H), 7.41 – 7.37 (m, 1H), 7.23 (dd, J = 7.7, 5.2 Hz, 1H), 7.21 – 7.08 (m, 6H), 4.39 (q, J = 7.1 Hz, 2H), 1.31 (t, J = 7.1 Hz, 3H); **13C NMR** (125 MHz, $CDCl_3$) δ 161.14, 157.77, 137.54, 132.29, 130.91 (d, J = 10 Hz), 130.53, 128.95, 127.46, 125.67, 115.54 (d, J = 27.2 Hz), 113.32 (d, J = 9.5 Hz), 110.53 (d, J = 5.9 Hz), 106.36 (d, J = 24.4 Hz), 61.76, 14.30; **HRMS** APCI (*m/z*): $[M-H]^-$ calcd for $C_{17}H_{13}FNO_2S$ 314.0651, found 314.0660.

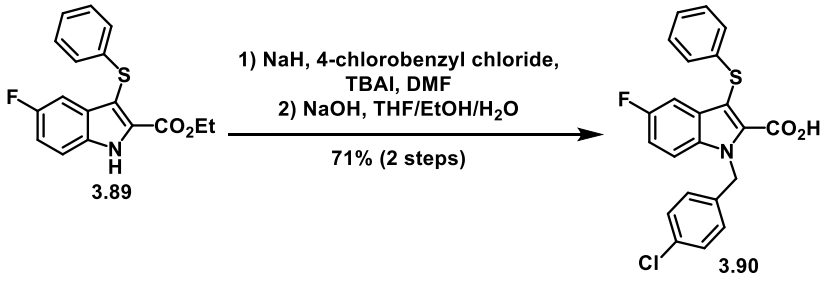

1-(4-chlorobenzyl)-5-fluoro-3-(phenylthio)-1H-indole-2-carboxylic acid (3.90). Using the procedure given for the preparation of compound **3.84**, indole **3.89** (58 mg, 0.184 mmol) yielded the title compound as a white solid (54 mg, 71% yield over two steps). **^{1}H NMR** (500 MHz, DMSO) δ 13.84 (s, 1H), 7.70 (dd, *J* = 9.2, 4.2 Hz, 1H), 7.40 – 7.36 (m, 2H), 7.27 – 7.20 (m, 3H), 7.15 – 7.06 (m, 6H), 5.84 (s, 2H); **^{13}C NMR** (100 MHz, DMSO) 162.10, 159.32, 156.97, 137.10 (d, J = 36.5 Hz), 134.34 (d, J = 8.1 Hz), 131.95, 129.13, 128.68, 128.52, 128.25, 126.57, 125.52,

114.35 (d, J = 26.5 Hz), 113.75 (d, J = 9.1 Hz), 107.56, 104.79 (d, J = 24.0 Hz), 47.62; **HRMS** APCI (*m/z*): $[M-H]^-$ calcd for $C_{22}H_{14}ClFNO_2S$ 410.0418, found 410.0424.

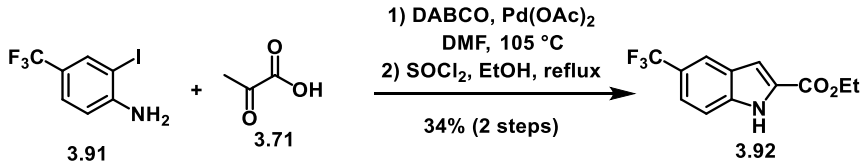

Ethyl 5-(trifluoromethyl)-1H-indole-2-carboxylate (3.92). Prepared using the procedure given for the preparation of compound **3.67**; **3.91** (2.30 g, 8.03 mmol) yielded the title compound as a white solid (1.57 g, 76% over two steps) with spectral data matching that previously described (Temple, K. J.; Duvernay, M. T.; Young, S. E.; Wen, W.; Wu, W.; Maeng, J.; Blobaum, A. L.; Stauffer, S. R.; Hamm, H. E. & Lindsley, C. W. *J. Med. Chem.* **2016**, *59*, 7690).

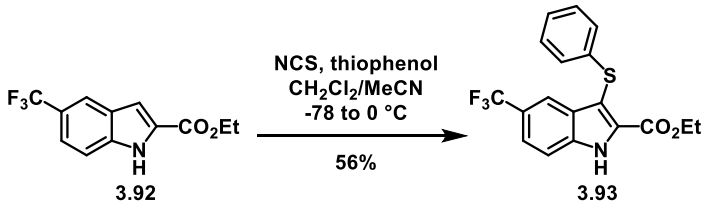

Ethyl 3-(phenylthio)-5-(trifluoromethyl)-1H-indole-2-carboxylate (3.93). Using the procedure given for the preparation of compound **3.68**, indole **3.92** (75 mg, 0.292 mmol) yielded the title compound as a white solid (60 mg, 56% yield) **^{1}H NMR** (500 MHz, $CDCl_3$) δ 9.65 (br s, 1H), 7.91 (d, J = 0.8 Hz, 1H), 7.59 – 7.52 (m, 2H), 7.23 – 7.17 (m, 4H), 7.15 – 7.11 (m, 1H), 4.42 (q, J = 7.1 Hz, 2H), 1.32 (t, J = 7.1 Hz, 3H); **^{13}C NMR** (125 MHz, $CDCl_3$) δ 161.47, 137.20, 137.15, 130.49, 129.03, 127.75, 125.97, 124.80 (q, J = 271.7 Hz), 124.10 (q, J = 32.2 Hz), 122.73 (d, J = 3.0 Hz), 119.83 (d, J = 4.2 Hz), 112.94, 112.18, 62.08, 14.21; **HRMS** APCI (*m/z*): $[M-H]^-$ calcd for $C_{18}H_{13}F_3NO_2S$ 364.0619, found 364.0625.

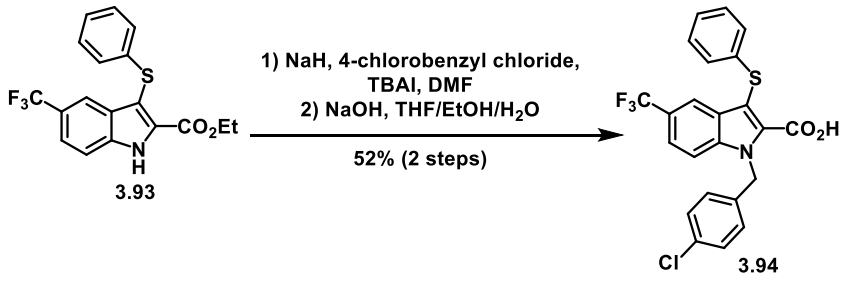

1-(4-chlorobenzyl)-5-fluoro-3-(phenylthio)-1H-indole-2-carboxylic acid (3.94). Using the procedure given for the preparation of compound **3.84**, indole **3.93** (45 mg, 0.123 mmol) yielded the title compound as a white solid (35 mg, 52% yield over two steps). **^{1}H NMR** (500 MHz, MeOD) δ 7.73 (s, 1H), 7.68 (d, J = 8.8 Hz, 1H), 7.55 (dd, J = 8.8, 1.6 Hz, 1H), 7.31 – 7.28 (m, 2H), 7.24 – 7.19 (m, 2H), 7.18 – 7.11 (m, 3H), 7.08 (d, J = 8.5 Hz, 2H), 5.87 (s, 2H); **^{13}C NMR** (100 MHz, Acetone) δ 162.37, 140.55, 138.25, 137.54, 133.62, 129.89, 129.57, 129.16, 128.86, 128.17, 126.62, 124.27 (q, J = 31.8 Hz) 122.73, 119.62 (d, J = 4.1 Hz), 113.62, 111.99, 48.89, 29.84. **HRMS** APCI (*m/z*): [M-H]$^{-}$ calcd for $C_{23}H_{14}ClF_3NO_2S$ 460.0386, found 460.0393.

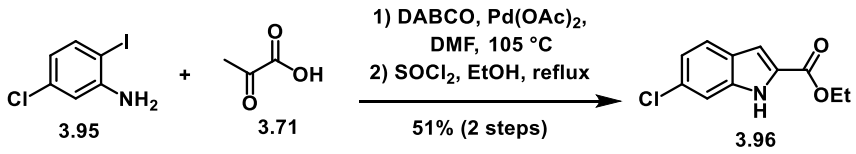

Ethyl 6-chloro-1H-indole-2-carboxylate (3.96). (one batch was prepared by me and another by Isabelle Sinitsa) Using the procedure given for the preparation of compound **3.67**, **3.95** (874 mg, 3.45 mmol) yielded the title compound as a tan solid (394 mg, 51% yield over two steps) **^{1}H NMR** (400 MHz, $CDCl_3$) δ 8.86 (br s, 1H), 7.60 (d, J = 8.6 Hz, 1H), 7.42 (s, 1H), 7.19 (s, 1H), 7.12 (d, J = 8.6 Hz, 1H), 4.41 (q, J = 7.1 Hz, 1H), 1.42 (t, J = 7.1 Hz, 2H); **^{13}C NMR** (100 MHz, $CDCl_3$) δ 161.92, 137.14, 131.42, 123.67, 122.01, 111.83, 108.75, 61.38, 14.52; **HRMS** APCI (*m/z*): [M-H]$^{-}$ calcd for $C_{11}H_9ClNO_2$ 222.0327, found 222.0328.

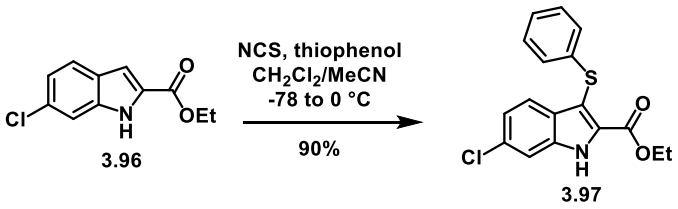

Ethyl 6-chloro-3-(phenylthio)-1H-indole-2-carboxylate (3.97). (one batch was prepared by me and another by Isabelle Sinitsa) Using the procedure given for the preparation of compound **3.68**, indole **3.96** (108 mg, 0.483 mmol) yielded the title compound as a white solid (137 mg, 90% yield). **^{1}H NMR** (500 MHz, $CDCl_3$) δ 9.18 (s, 1H), 7.48 (d, J = 8.6 Hz, 1H), 7.46 – 7.44 (m, 1H), 7.21 – 7.14 (m, 4H), 7.13 – 7.08 (m, 2H), 4.39 (q, J = 7.1 Hz, 2H), 1.32 (t, J = 7.1 Hz, 3H). **^{13}C NMR** (100 MHz, $CDCl_3$) δ 161.21, 137.46, 136.04, 132.29, 128.95, 127.62, 125.74, 122.96, 122.68, 112.04, 99.77, 61.80, 14.32; **HRMS** APCI (*m/z*): $[M-H]^-$ calcd for $C_{17}H_{13}ClNO_2S$ 330.0356, found 330.0361.

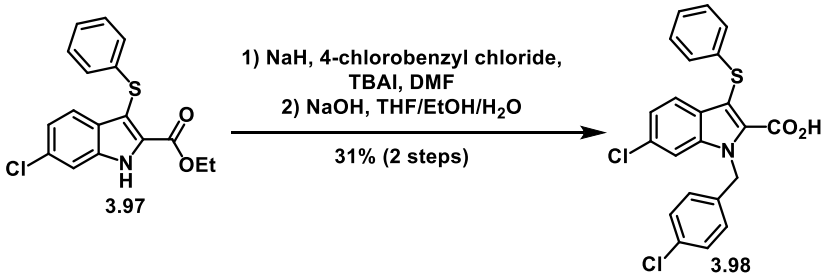

6-chloro-1-(4-chlorobenzyl)-3-(phenylthio)-1H-indole-2-carboxylic acid (3.98). (one batch was prepared by me and another by Isabelle Sinitsa) Using the procedure given for the preparation of compound **3.84**, indole **3.97** (115 mg, 0.365 mmol) yielded the title compound as a yellow solid (49 mg, 31% yield over two steps). **^{1}H NMR** (500 MHz, DMSO) δ 13.85 (br s, 1H), 7.84 (dd, J = 6.9, 1.6 Hz, 1H), 7.40 (dd, J = 14.5, 8.5 Hz, 3H), 7.27 – 7.19 (m, 2H), 7.17 – 7.05 (m, 6H), 5.89 – 5.80 (s, 2H); **^{13}C NMR** (125 MHz, DMSO) δ 162.06, 138.05, 137.32, 136.82, 133.79, 131.95, 130.31, 129.07, 128.65, 128.22, 126.63, 126.54, 125.46, 122.27, 122.08, 111.62, 108.24, 47.45; **HRMS** APCI (*m/z*): $[M+H]^+$ calcd for $C_{22}H_{16}Cl_2NO_2S$ 428.0279, found 428.0275.

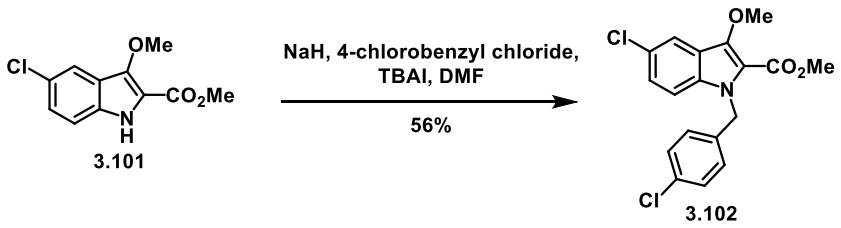

Ethyl 5-chloro-1-(4-chlorobenzyl)-3-methoxy-1H-indole-2-carboxylate (3.102). To a suspension of sodium hydride (60% in mineral oil, 81 mg, 2.033 mmol) in DMF (5 mL) at 0 °C was added **3.101** (prepared as previously described: Ngernmeesri, P.; Soonkit, S.; Konkhum, A. & Kongkathip, B. *Tet. Lett.* **2014**, *55*, 1621.) (406 mg, 1.694 mmol) dissolved in DMF (5 mL). The reaction was stirred for 30 minutes at 0 °C then warmed to room temperature for 30 minutes. The reaction was cooled back to 0 °C and 4-chlorobenzyl chloride (327 mg, 2.033 mmol) and TBAI (626 mg, 1.694 mmol) were sequentially added, and the reaction was stirred at room temperature overnight. The following day, the reaction was poured into water and extracted with EtOAc 3x. The combined organic layers were washed with brine, dried over Na_2SO_4, filtered, concentrated, and purified by column chromatography, yielding the title compound as a white solid (344 mg, 56% yield). **^{1}H NMR** (500 MHz, $CDCl_3$) δ 7.76 (dd, J = 2.0, 0.5 Hz, 1H), 7.26 – 7.16 (m, 4H), 6.95 – 6.90 (m, 2H), 5.65 (s, 2H), 4.05 (s, 3H), 3.90 (s, 3H); **^{13}C NMR** (125 MHz, $CDCl_3$) δ 161.84, 145.69, 136.55, 135.01, 133.14, 128.88, 127.64, 126.85, 126.16, 120.62, 119.54, 117.10, 111.92, 62.90, 51.93, 47.51; **HRMS** APCI (*m/z*): $[M+H]^+$ calcd for $C_{18}H_{16}Cl_2NO_3$ 364.0507, found 364.0501.

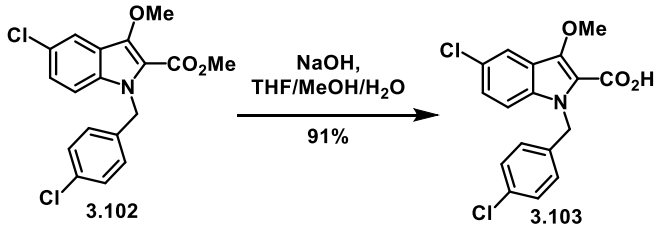

5-chloro-1-(4-chlorobenzyl)-3-methoxy-1H-indole-2-carboxylic acid (3.103). To a solution of ester **3.102** (34 mg, 0.093 mmol) in 1:1 THF:EtOH (2 mL) was added 1M NaOH (0.47 mL, 0.47

mmol), and the reaction was stirred for 4 hours at room temperature. The reaction was acidified with 1M HCl and extracted with EtOAc 3x. The combined organic layers were washed with brine, dried over Na_2SO_4, filtered, and concentrated, yielding the title compound as a white solid (30 mg, 91% yield). **^{1}H NMR** (500 MHz, MeOD) δ 7.73 (d, J = 1.6 Hz, 1H), 7.39 (d, J = 8.9 Hz, 1H), 7.26 (dd, J = 9.0, 2.1 Hz, 1H), 7.24 – 7.21 (m, 2H), 6.98 (d, J = 8.6 Hz, 2H), 5.74 (s, 2H), 4.04 (s, 3H); **^{13}C NMR** (125 MHz, MeOD) δ 163.79, 146.80, 138.64, 136.25, 133.95, 129.60, 129.01, 127.49, 127.10, 121.81, 119.94, 118.94, 113.54, 63.22, 48.08; **HRMS** APCI (*m/z*): [M-H]$^-$ calcd for $C_{17}H_{12}Cl_2NO_3$ 348.0194, found 348.0201.

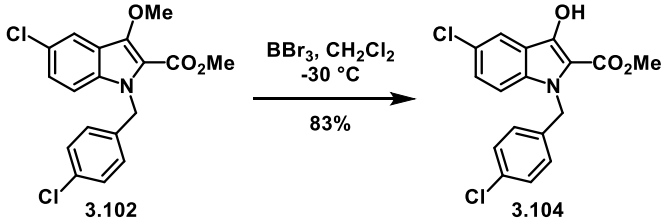

Methyl 5-chloro-1-(4-chlorobenzyl)-3-hydroxy-1H-indole-2-carboxylate (3.104). To a solution of methyl ether **3.102** (216 mg, 0.593 mmol) in CH_2Cl_2 (5 mL) at -30 °C was added BBr_3 (0.60 mL, 0.60 mmol, 1M in CH_2Cl_2) dropwise, and the reaction was stirred at this temperature for 30 minutes. The reaction was quenched with sat. $NaHCO_3$ and extracted with CH_2Cl_2 3x. The combined organic layers were washed with brine, dried over Na_2SO_4, filtered, concentrated, and purified by column chromatography, yielding the title compound as a yellow foam (172 mg, 83% yield). **^{1}H NMR** (500 MHz, $CDCl_3$) δ 8.46 (s, 1H), 7.76 (d, *J* = 1.9 Hz, 1H), 7.28 (dt, *J* = 7.1, 3.6 Hz, 1H), 7.24 – 7.20 (m, 2H), 7.14 (d, *J* = 9.0 Hz, 1H), 6.90 (d, *J* = 8.4 Hz, 2H), 5.52 (s, 2H), 3.90 (s, 3H); **^{13}C NMR** (126 MHz, $CDCl_3$) δ 163.90, 148.13, 136.65, 135.91, 133.30, 128.98, 128.31, 127.53, 125.51, 119.93, 117.80, 111.55, 109.87, 51.89, 47.72; **HRMS** APCI (*m/z*): [M-H]$^-$ calcd for $C_{17}H_{12}Cl_2NO_3$ 348.0194, found 348.0199.

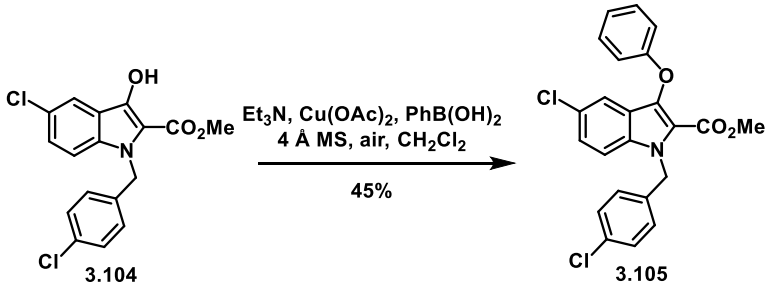

Methyl 5-chloro-1-(4-chlorobenzyl)-3-phenoxy-1H-indole-2-carboxylate (3.105). To a solution of phenol **3.104** (80 mg, 0.228 mmol) in CH_2Cl_2 was added activated 4 Å molecular sieves, Et_3N (0.16 mL, 1.140 mmol), $Cu(OAc)_2$ (41 mg, 0.228 mmol), and phenylboronic acid (55 mg, 0.457 mmol). The reaction was stirred in a flask open to air for 1 hour, after which time TLC indicated consumption of starting material. The reaction was filtered through Celite, concentrated, and purified by column chromatography, yielding the title compound as a tan solid (45 mg, 45% yield). **^{1}H NMR** (500 MHz, $CDCl_3$) δ 7.42 (t, *J* = 1.1 Hz, 1H), 7.32 – 7.23 (m, 7H), 7.05 (t, *J* = 7.4 Hz, 1H), 7.00 – 6.93 (m, 4H), 5.76 (s, 2H), 3.71 (s, 3H); **^{13}C NMR** (125 MHz, $CDCl_3$) δ 161.58, 158.89, 139.05, 136.34, 135.16, 133.41, 129.73, 129.07, 127.70, 127.22, 126.86, 122.55, 120.95, 119.63, 118.56, 115.69, 112.10, 52.03, 47.66; **HRMS** APCI (*m/z*): $[M-H]^-$ calcd for $C_{23}H_{16}Cl_2NO_3$ 424.0507, found 424.0511.

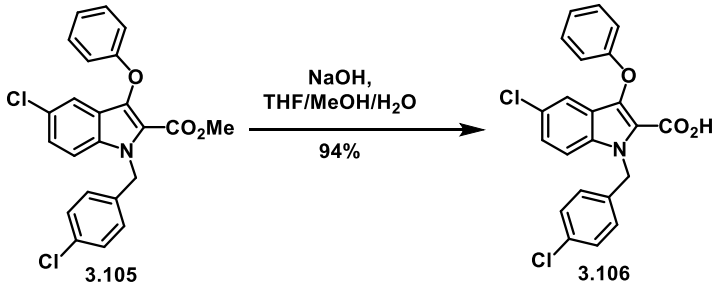

5-chloro-1-(4-chlorobenzyl)-3-phenoxy-1H-indole-2-carboxylic acid (3.106). To a solution of ester **3.105** (28 mg, 0.066 mmol) in 1:1 THF:MeOH:H_2O (3 mL) was added 1M NaOH (0.33 mL, 0.33 mmol), and the reaction was stirred at room temperature overnight. The reaction was acidified with 1M HCl and extracted with EtOAc 3x. The combined organic layers were washed

with water and brine, dried over Na_2SO_4, filtered and concentrated, yielding the title compound as a white solid (25 mg, 94% yield). **^{1}H NMR** (500 MHz, Acetone) δ 7.64 (dd, *J* = 8.6, 1.0 Hz, 1H), 7.36 – 7.28 (m, 6H), 7.17 (d, *J* = 8.6 Hz, 2H), 7.07 – 7.02 (m, 1H), 7.00 (dt, *J* = 9.1, 2.2 Hz, 2H), 5.94 (s, 2H); **^{13}C NMR** (125 MHz, Acetone) δ 162.16, 159.85, 139.19, 138.29, 135.99, 133.36, 130.45, 129.48, 129.08, 127.25, 126.92, 123.13, 121.53, 119.46, 116.48, 114.00, 47.88; **HRMS** APCI (*m/z*): $[M-H]^-$ calcd for $C_{22}H_{14}Cl_2NO_3$ 410.0351, found 410.0357.

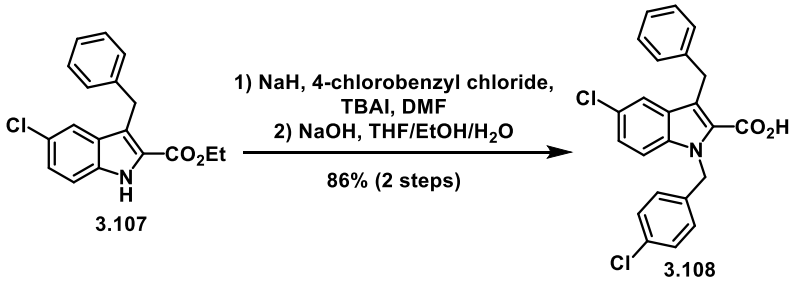

3-benzyl-5-chloro-1-(4-chlorobenzyl)-1H-indole-2-carboxylic acid (3.108). Using the procedure given for the preparation of compound **3.84**, indole **3.107** (prepared as previously described: Mahmoud, M. M.; Ali, H. I.; Ahn, K. H.; Damaraju, A.; Samala, S.; Pulipati, V. K.; Kolluru, S.; Kendall, D. A.; Lu, D. *J. Med. Chem.* **2013**, *56*, 7975.) (78 mg, 0.249 mmol) yielded the title compound as a white solid (88 mg, 86% yield over two steps). **^{1}H NMR** (500 MHz, DMSO) δ 13.49 (s, 1H), 7.69 (d, *J* = 2.0 Hz, 1H), 7.58 (d, *J* = 8.9 Hz, 1H), 7.37 – 7.31 (m, 2H), 7.28 (dd, *J* = 8.9, 2.1 Hz, 1H), 7.26 – 7.21 (m, 4H), 7.15 – 7.11 (m, 1H), 6.99 (d, *J* = 8.6 Hz, 2H), 5.82 (s, 2H), 4.45 (s, 2H); **^{13}C NMR** (125 MHz, DMSO) δ 163.16, 140.93, 137.65, 136.42, 131.61, 128.51, 128.30, 128.11, 128.03, 127.41, 125.79, 125.29, 124.92, 122.19, 119.97, 113.00, 46.99, 30.10; **HRMS** APCI (*m/z*): $[M-H]^-$ calcd for $C_{23}H_{16}Cl_2NO_2$ 408.0558, found 408.0565.

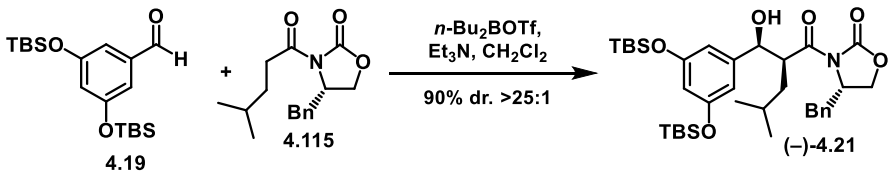

(*S*)-4-benzyl-3-((*S*)-2-((*S*)-(3,5-bis((*tert*-butyldimethylsilyl)oxy)phenyl)(hydroxy)methyl)-4-methylpentanoyl)oxazolidin-2-one (–)-4.21. (optimized by Dr. Young Eun Lee and repeated by me for characterization data) To a stirred solution of oxazolidinone **4.115** (1.09 g, 4.0 mmol) in dry CH_2Cl_2 (10 mL) at –78 °C was added *n*-Bu_2BOTf (4.4 mL, 4.4 mmol, 1M solution in CH_2Cl_2) and Et_3N (700 µL, 4.8 mmol) under argon atmosphere. The temperature was warmed to 0 °C, and 10 min later, cooled to –78 °C again. Aldehyde **4.19** (1.5 g, 4.0 mmol) in CH_2Cl_2 (10 mL) was then added. The mixture was stirred for 1 h and warmed to 0 °C. The reaction was then quenched with pH = 7 buffer (10 mL) and 30% H_2O_2 (10 mL) in MeOH (10 mL) and stirred at room temperature for 1 h. The CH_2Cl_2 was evaporated and the aqueous layer was extracted with EtOAc. The combined organic layers were dried over anhydrous $MgSO_4$, concentrated under reduced pressure, and purified by flash chromatography to afford the product **(–)-7** as a white foam (2.32 g, dr >25:1, 90% yield). Spectroscopic data was identical to that previously described: Guchhait, S.; Chatterjee, S.; Ampapathi, R. S.; Goswami, R. K. *J. Org. Chem.* **2017**, *82*, 2414.

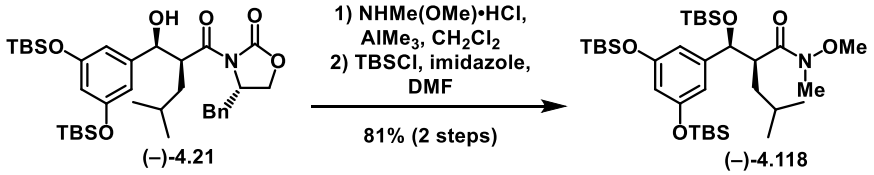

(*S*)-2-((*S*)-(3,5-bis((*tert*-butyldimethylsilyl)oxy)phenyl)((*tert*-butyldimethylsilyl)oxy)methyl)-*N*-methoxy-*N*,4-dimethylpentanamide (–)-4.118. (optimized by Dr. Young Eun Lee and repeated by me for characterization data) To a suspension of *N*,*O*-dimethylhydroxylamine hydrochloride (577 mg, 5.92 mmol) in CH_2Cl_2 (12 mL) was added a solution of trimethylaluminum (2 M in hexanes, 2.96 mL, 5.92 mmol) dropwise at 0 °C. After 15 minutes the reaction was warmed to room temperature. After 45 minutes at this temperature, the reaction was cooled to –20 °C and a solution of aldol adduct **(–)-4.21** (1.52 g, 2.37 mmol) was added as a solution in CH_2Cl_2 (5 mL) dropwise. The reaction was warmed to room temperature and stirred for 2 hours. The reaction was slowly added to an ice cold solution of aqueous DL-tartaric acid

(1M) and the biphasic mixture was stirred for an hour at room temperature. The aqueous layer was extracted with CH_2Cl_2 3x, and the combined organic layers were washed with brine, dried over Na_2SO_4, filtered and concentrated. The crude product was carried directly to the next step. The intermediate was dissolved in DMF (5 mL), and TBSCl (1.10 g, 7.58 mmol) was added followed by imidazole (650 mg, 9.48 mmol), and the reaction was stirred at room temperature overnight. The following day, the reaction was quenched with sat. aq NH_4Cl and extracted with EtOAc 3x. The combined organic layers were washed with brine, dried over Na_2SO_4, filtered, concentrated, and purified by column chromatography, yielding the title compound as a clear oil (1.62 g, 81% yield over 2 steps). **^{1}H NMR** (600 MHz, $CDCl_3$) δ 6.46 (d, J = 2.2 Hz, 2H), 6.18 (s, 1H), 4.65 (d, J = 8.2 Hz, 1H), 3.22 (s, 3H), 3.13 (t, J = 8.3 Hz, 1H), 2.99 (s, 3H), 1.72 (dd, J = 17.5, 6.9 Hz, 1H), 1.63 (dd, J = 16.4, 6.5 Hz, 1H), 1.42 (br s, 1H), 0.96 (s, 18H), 0.89 (s, 9H), 0.87–0.84 (m, 6H), 0.16 (s, 6H), 0.15 (s, 6H), 0.04 (s, 3H), -0.20 (s, 3H); **^{13}C NMR** (150 MHz, $CDCl_3$) δ 175.3, 156.2, 146.6, 112.1, 111.2, 76.1, 61.1, 49.2, 39.1, 32.0, 26.3, 26.0, 25.8, 24.1, 22.2, 18.35, 18.31, -4.24, -4.25, -4.4, -4.9; **$[\alpha]^{25}_D$** –175.0 (c = 1.00 in $CHCl_3$); **HRMS** ESI (*m/z*) calcd for $C_{33}H_{66}NO_5Si_3$ $[M+H^+]$: 640.4249, found 640.4254.

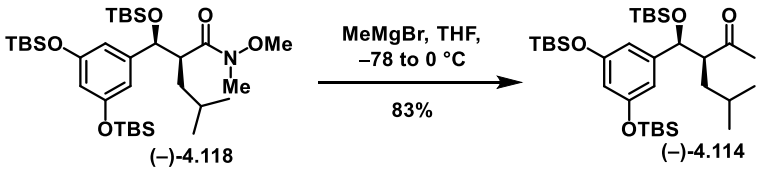

(*S*)-3-((*S*)-(3,5-bis((*tert*-butyldimethylsilyl)oxy)phenyl)((*tert*-butyldimethylsilyl)oxy)methyl)-5-methylhexan-2-one (–)-4.114. To a solution of Weinreb amide **(–)-4.118** (329 mg, 0.514 mmol) in THF (10 mL) at –78 °C was added MeMgBr (3M in Et_2O, 0.51 mL, 1.542 mmol) dropwise. After stirring for 30 minutes at –78 °C the reaction was warmed to 0 °C and stirred at this temperature for 7 hours. The reaction was cooled to –78 °C and another portion of MeMgBr (3M in Et_2O, 0.51 mL, 1.542 mmol) was added dropwise, and the reaction was stirred at –78 °C for 30 minutes, then warmed to 0 °C and stirred at this temperature overnight. The following day,

the reaction was carefully quenched with sat. aq NH_4Cl and extracted with Et_2O 3x. The combined organic layers were washed with brine, dried over $MgSO_4$, filtered, concentrated, and purified by column chromatography, yielding the title compound as a clear oil (254 mg, 83% yield). **^{1}H NMR** (600 MHz, $CDCl_3$) δ 6.37 (d, J = 2.2 Hz, 2H), 6.22 (t, J = 2.2 Hz, 1H), 4.41 (d, J = 8.1 Hz, 1H), 2.86 (ddd, J = 11.0, 8.1, 3.0 Hz, 1H), 1.74 (s, 3H), 1.68 (ddd, J = 13.4, 10.8, 4.5 Hz, 1H), 1.56–1.50 (m, 1H), 1.45–1.38 (m, 1H), 0.97 (s, 18H), 0.87–0.85 (m, 15H), 0.17 (s, 6H), 0.16 (s, 6H), 0.02 (s, 3H), -0.22 (s, 3H); **^{13}C NMR** (150 MHz, $CDCl_3$) δ 212.1, 156.5, 145.6, 112.2, 111.9, 76.7, 60.3, 38.7, 32.9, 26.5, 26.0, 25.8, 24.1, 22.0, 18.4, 18.2, -4.24, -4.25, -4.3, -5.0; **$[\alpha]_D^{20}$** –203.3 (c = 0.91 in $CHCl_3$); **HRMS** ESI (*m/z*) calcd for $C_{32}H_{63}O_4Si_3$ $[M+H^+]$: 595.4034, found 595.4040.

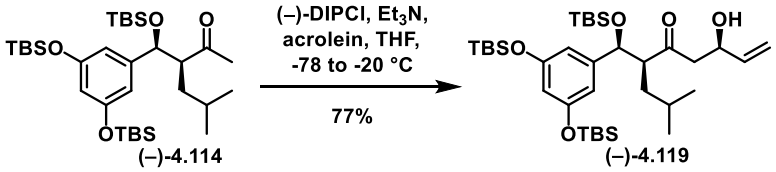

(3R,6S)-6-((S)-(3,5-bis((tert-butyldimethylsilyl)oxy)phenyl)((tert-butyldimethylsilyl)oxy)methyl)-3-hydroxy-8-methylnon-1-en-5-one (–)-4.119. (optimized by Dr. Young Eun Lee and repeated by me for characterization data) To a stirred solution of ketone **(–)-4.114** (440 mg, 0.739 mmol)) in Et_2O (5 mL) at 0 °C was added Et_3N (0.31 mL, 2.22 mmol) followed by (–)-DIPCl (617 mg, 1.924 mmol) dissolved in Et_2O (1 mL). The reaction was stirred for an hour at 0 °C and the white suspension was then cooled to –78 °C, then acrolein (0.099 mL, 1.48 mmol) dissolved in Et_2O (1 mL) was slowly added. The reaction was stirred for 1 hour at –78 °C then at –20 °C for 3 hours and stored in a –20 °C freezer overnight. The reaction was quenched with pH 7 buffer (25 mL), MeOH (10 mL), and 30% H_2O_2 (5 mL), and the biphasic solution was stirred for an hour at room temperature. The aqueous layer was extracted with Et_2O 3x, and the combined organic layers were washed with brine, dried over $MgSO_4$, filtered, concentrated, and purified by column chromatography, yielding the title compound as a clear oil

(372 mg, 77% yield). ^{1}H NMR (600 MHz, $CDCl_3$) δ 6.33 (d, J = 2.2 Hz, 2H), 6.21 (t, J = 2.2 Hz, 1H), 5.59 (ddd, J = 17.1, 10.6, 5.4 Hz, 1H), 5.13 (dt, J = 17.2, 1.5 Hz, 1H), 5.01 (dt, J = 10.6, 1.5 Hz, 1H), 4.40 (d, J = 8.2 Hz, 1H), 4.27–4.20 (m, 1H), 3.15 (d, J = 3.1 Hz, 1H), 2.91–2.82 (m, 1H), 2.30 (dd, J = 18.4, 9.4 Hz, 1H), 2.01 (dd, J = 18.4, 2.5 Hz, 1H), 1.70 (ddd, J = 13.3, 10.8, 4.4 Hz, 1H), 1.53 (ddd, J = 13.8, 8.5, 3.6 Hz, 1H), 1.47–1.40 (m, 1H), 0.97 (s, J = 3.1 Hz, 18H), 0.87–0.85 (m, 15H), 0.17 (s, J = 3.0 Hz, 6H), 0.17 (s, J = 3.0 Hz, 6H), 0.03 (s, J = 2.9 Hz, 3H), -0.21 (s, J = 3.0 Hz, 3H); ^{13}C NMR (150 MHz, $CDCl_3$) δ 214.9, 156.7, 145.2, 138.7, 114.8, 112.0, 111.8, 76.8, 68.2, 60.3, 52.1, 39.0, 26.3, 25.9, 25.8, 24.1, 21.99, 18.4, 18.2, -4.21, -4.23, -4.3, -4.9; $[\alpha]_D^{20}$ –48.3 (c = 1.20 in $CHCl_3$); HRMS ESI (*m/z*) calcd for $C_{35}H_{66}O_5Si_3Na$ [M+Na$^+$]: 673.4116, found 673.4123.

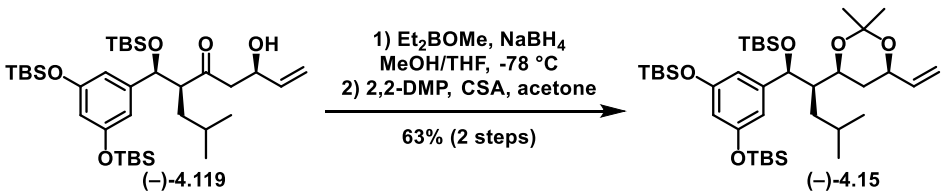

((5-((1*S*,2*R*)-1-((*tert*-butyldimethylsilyl)oxy)-2-((4*S*,6*R*)-2,2-dimethyl-6-vinyl-1,3-dioxan-4-yl)-4-methylpentyl)-1,3-phenylene)bis(oxy))bis(*tert*-butyldimethylsilane) (–)-4.15. (optimized by Dr. Young Eun Lee and repeated by me for characterization data) To a solution of β-hydroxy ketone **(–)-4.119** (151 mg, 0.232 mmol) in 10:1 THF:MeOH (3 mL) at –78 °C was added Et_2BOMe (1M in THF, 0.27 mL, 0.267 mmol) dropwise. After an hour, $NaBH_4$ (26 mg, 0.696 mmol) was added. After 2 hours at the same temperature, the reaction was warmed to 0 °C and quenched with a mixture of pH 7 phosphate buffer (6 mL), MeOH (6 mL) and 30% H_2O_2 (1 mL), and this solution was stirred for an hour and allowed to warm to room temperature. The solution was extracted with EtOAc 3x, and the combined organic layers were washed with brine, dried over Na_2SO_4, filtered, concentrated, and purified by column chromatography, yielding the diol as a clear oil (121 mg, 80% yield). The intermediate was dissolved in acetone (2 mL) then 2,2 dimethoxypropane (0.044 mL, 0.356 mmol) and CSA (4 mg, 0.018) were added. After 4 hours,

another portion of 2,2-dimethoxypropane (0.022 mL, 0.178 mmol) and CSA (1 mg, 0.004 mmol) were added, and the reaction was stirred at room temperature overnight. The following day, the reaction was quenched with sat. $NaHCO_3$ and extracted with EtOAc 3x. The combined organic layers were washed with brine, dried over Na_2SO_4, filtered, concentrated, and purified by column chromatography, yielding the title compound as a clear oil (97 mg, 63% yield over two steps). **^{1}H NMR** (600 MHz, $CDCl_3$) δ 6.39 (d, J = 2.2 Hz, 2H), 6.21 (t, J = 2.2 Hz, 1H), 5.85–5.74 (m, 1H), 5.20 (dt, J = 17.3, 1.3 Hz, 1H), 5.11–5.07 (m, 1H), 4.56 (d, J = 6.4 Hz, 1H), 4.17 (ddd, J = 10.2, 5.8, 1.1 Hz, 1H), 3.66–3.59 (m, 1H), 1.63–1.56 (m, 1H), 1.52–1.40 (m, 3H), 1.37 (s, 3H), 1.34–1.31 (m, 2H), 1.30 (s, 3H), 0.97 (s, 18H), 0.87 (s, 9H), 0.83 (d, J = 6.6 Hz, 3H), 0.79 (d, J = 6.6 Hz, 3H), 0.17 (s, 6H), 0.17 (s, 6H), 0.04 (s, 3H), -0.24 (s, 3H); **^{13}C NMR** (150 MHz, $CDCl_3$) δ 156.1, 147.0, 139.2, 115.3, 112.6, 110.9, 98.6, 75.8, 70.6, 68.9, 49.5, 34.9, 34.7, 30.3, 27.8, 26.1, 25.8, 23.1, 22.9, 19.8, 18.4, 18.2, -4.09, -4.15, -4.2, -4.6; **$[\alpha]_D^{20}$** –18.3 (c = 1.22 in $CHCl_3$); **HRMS** ESI (*m/z*) calcd for $C_{38}H_{73}O_5Si_3$ $[M+H^+]$: 693.4766, found 693.4775.

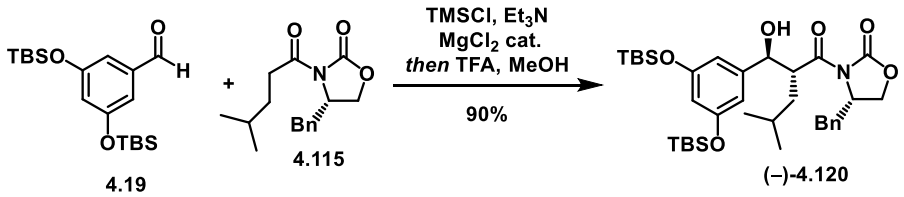

(*S*)-4-benzyl-3-((*S*)-2-((*S*)-(3,5-bis((*tert*-butyldimethylsilyl)oxy)phenyl)(hydroxy)methyl)-4-methylpentanoyl)oxazolidin-2-one (–)-4.120. (synthesized by me and Dr. Guillaume Ernouf) To a stirred solution of oxazolidinone **4.115** (1.71 g, 6.2 mmol) and aldehyde **4.19** (2.74 g, 7.5 mmol) in EtOAc (8 mL) at 0 °C was added $MgCl_2$ (119 mg, 1.24 mmol), Et_3N (1.26 mL, 12.5 mmol) and TMSCl (1.01 mL, 9.34 mmol). The reaction was warmed to room temperature and stirred overnight. The yellow slurry was pushed through a plug of silica with 300 mL of diethyl ether. The ether solution was concentrated *in vacuo*, and 20 mL of methanol was added along with 3 drops of trifluoroacetic acid. This solution was stirred at rt for 1 h, concentrated to a pale-yellow

oil and analysis of the residue by ^{1}H NMR spectroscopy *indicated the formation of a single detectable diastereomer*. The residue was purified by column chromatography, yielding title compound as a white foam (3.94 g, 90% yield). **^{1}H NMR** (400 MHz, $CDCl_3$) δ 7.31–7.14 (m, 5H), 6.54 (d, J = 2.2 Hz, 2H), 6.27 (t, J = 2.2 Hz, 1H), 4.64 (ddd, J = 9.7, 6.6, 3.2 Hz, 1H), 4.59 (t, J = 8.0 Hz, 1H), 4.51–4.42 (m, 1H), 4.15–4.06 (m, 2H), 3.24 (dd, J = 13.6, 3.2 Hz, 1H), 3.11 (d, J = 7.6 Hz, 1H), 2.60 (dd, J = 13.6, 9.8 Hz, 1H), 1.71 (ddd, J = 13.5, 9.6, 5.5 Hz, 1H), 1.56–1.42 (m, 1H), 1.14 (ddd, J = 14.2, 9.0, 5.1 Hz, 1H), 1.00–0.90 (m, 18H), 0.83 (d, J = 6.6 Hz, 3H), 0.79 (d, J = 6.6 Hz, 3H), 0.18 (s, 12H); **^{13}C NMR** (100 MHz, $CDCl_3$) δ 176.4, 156.8, 153.7, 144.8, 135.5, 129.5, 128.9, 127.2, 111.77, 111.68, 65.9, 55.8, 47.4, 38.6, 37.6, 26.2, 25.8, 23.1, 22.3, 18.3, -4.30, -4.33; **$[\alpha]_D^{20}$** –69.0 (c = 1.00 in $CHCl_3$); **HRMS** ESI (*m/z*) calcd for $C_{35}H_{56}NO_6Si_2$ $[M+H^+]$: 642.36407, found 642.36354.

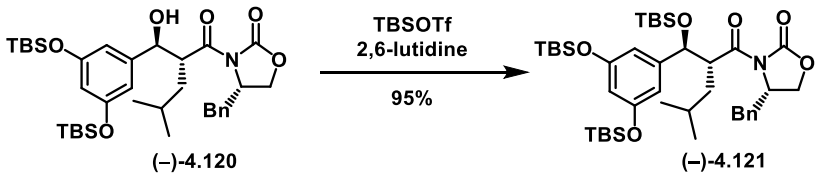

(*S*)-4-benzyl-3-((*R*)-2-((*S*)-(3,5-bis((*tert*-butyldimethylsilyl)oxy)phenyl)((*tert*-butyldimethylsilyl)oxy)methyl)-4-methylpentanoyl)oxazolidin-2-one (–)-4.121. (synthesized by me and Dr. Guillaume Ernouf) To a solution of alcohol **(–)-4.120** (2.11 g, 3.29 mmol) in CH_2Cl_2 (8 mL) was added 2,6-lutidine (766 µL, 6.57 mmol) and TBSOTf (906 µL, 3.94 mmol). After 30 minutes, the reaction mixture was diluted with EtOAc and washed with sat. aq NH_4Cl. The organic layer was washed with brine, dried over $MgSO_4$, filtered, concentrated, and purified by column chromatography, yielding the title compound as a white foam (2.34 g, 95% yield). **^{1}H NMR** (400 MHz, $CDCl_3$) δ 7.37–7.31 (m, 2H), 7.30–7.24 (m, 3H), 6.55 (d, J = 2.2 Hz, 2H), 6.29 (t, J = 2.2 Hz, 1H), 4.71–4.56 (m, 2H), 4.50 (t, J = 8.7 Hz, 1H), 4.16–4.02 (m, 2H), 3.61 (dd, J = 13.1, 2.7 Hz, 1H), 2.61 (dd, J = 13.0, 11.3 Hz, 1H), 1.68–1.51 (m, 1H), 1.34–1.20 (m, 1H), 0.97 (s, 18H), 0.90–0.79 (m, 1H), 0.83 (s, 9H), 0.76 (d, J = 6.6 Hz, 3H), 0.69 (d, J = 6.5 Hz, 3H), 0.20

(s, 6H), 0.19 (s, 6H), -0.04 (s, 3H), -0.29 (s, 3H); **^{13}C NMR** (100 MHz, $CDCl_3$) δ 176.4, 156.5, 153.1, 145.05, 136.2, 129.5, 129.1, 127.3, 113.0, 112.2, 78.5, 65.9, 56.5, 49.3, 39.2, 38.6, 26.4, 26.0, 25.9, 23.9, 21.9, 18.4, 18.1, -4.2, -4.3, -4.9; **$[\alpha]_D^{20}$** –57.1 (c = 0.35 in $CHCl_3$); **HRMS** ESI (*m/z*) calcd for $C_{41}H_{69}NO_6Si_3Na$ [M+Na^+]: 778.43249, found 778.43249

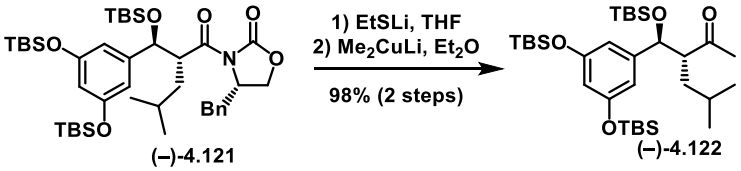

(*R*)-3-((*S*)-(3,5-bis((*tert*-butyldimethylsilyl)oxy)phenyl)((*tert*-butyldimethylsilyl)oxy)methyl)-5-methylhexan-2-one (–)-4.122. (originally optimized by me and scaled up by Dr. Guillaume Ernouf) To a solution of EtSH (400 μL, 5.4 mmol) in THF (45.0 mL) at 0 °C was added *n*-BuLi (2.05 mL, 5.1 mmol, 2.5 M in hexanes). After 20 min, a solution of compound **(–)-4.121** (2.04 g, 2.7 mmol) in THF (15 mL) was transferred via cannula dropwise. After 20 min, the reaction was quenched with sat. aq NH_4Cl (10 mL) and extracted with Et_2O (3 × 50 mL). The dried ($MgSO_4$) extract was concentrated in vacuo and purified by a plug of silica gel, eluting with 10% EtOAc/hexanes, to give the corresponding thioester intermediate as a slightly yellow oil. To a suspension of CuI (2.57 g, 13.5 mmol) in Et_2O (29.0 mL) at 0 °C was added MeLi (16.9 mL, 27 mmol, 1.6M in Et_2O). After 15 min, the colorless solution was cooled to −50 °C, and the solution of the above thioester intermediate in Et_2O (10 mL) was transferred into the reaction dropwise via cannula. The reaction was warmed to 0 °C and stirred at this temperature overnight. The following day, the reaction was quenched with sat. aq NH_4Cl at 0 °C, warmed to room temperature, and extracted with Et_2O. The dried ($MgSO_4$) extract was concentrated in vacuo and purified by chromatography over silica gel yielding the title compound as a clear oil (1.59 g, 98% yield). **^{1}H NMR** (400 MHz, $CDCl_3$) δ 6.40 (d, *J* = 2.2 Hz, 2H), 6.25 (t, *J* = 2.2 Hz, 1H), 4.44 (d, *J* = 9.4 Hz, 1H), 2.97–2.85 (m, 1H), 2.26 (s, 3H), 1.49–1.37 (m, 1H), 1.31–1.17 (m, 1H), 0.96 (s, 18H), 0.79 (s, 9H), 0.72 (d, *J* = 6.6 Hz, 3H), 0.70 (d, *J* = 6.6 Hz, 3H), 0.16 (s, 12H), -0.07 (s, 3H),

-0.30 (s, 3H); **^{13}C NMR** (100 MHz, $CDCl_3$) δ 213.2, 156.5, 145.1, 112.7, 112.2, 78.7, 58.9, 38.5, 33.3, 26.0, 25.9, 24.0, 21.5, 18.4, 18.1, -4.22, -4.18, -4.4, -5.3; **$[\alpha]_D^{20}$** –42.6 (c = 0.19 in $CHCl_3$); **HRMS** ESI (*m/z*) calcd for $C_{32}H_{63}O_4Si_3$ $[M+H^+]$: 595.40287, found 595.40350.

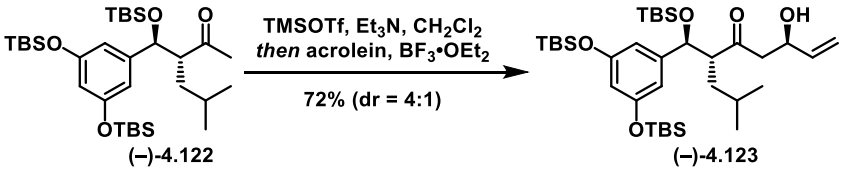

(3*R*,6*R*)-6-((*S*)-(3,5-bis((*tert*-butyldimethylsilyl)oxy)phenyl)((*tert*-butyldimethylsilyl)oxy)methyl)-3-hydroxy-8-methylnon-1-en-5-one (–)-4.123). To a stirred solution of ketone **(–)-4.122** (1.4 g, 2.3 mmol) was added Et_3N (796 µL, 5.9 mmol) and TMSOTf (853 µL, 4.7 mmol) in CH_2Cl_2 (23 mL) at 0 °C under argon atmosphere. The reaction was warmed to room temperature and stirred for 2 hours, then quenched with sat. $NaHCO_3$ and extracted with pentane (3 × 30 mL). The dried ($MgSO_4$) extract was concentrated in vacuo to give the crude silyl enol ether (1.6 g, quantitative), which was taken for the next step without further characterization. To a solution of silyl enol ether (1.6 g, 2.3 mmol) in CH_2Cl_2 (23 mL) at –78 °C was added acrolein (187 µL, 2.8 mmol) and $BF_3{\cdot}OEt_2$ (305 µL, 2.5 mmol). After stirring at –78 °C for 1 h, the reaction mixture was quenched with sat. aq NH_4Cl and extracted with EtOAc (x3) concentrated to a pale-yellow oil and *analysis of the residue by ^{1}H NMR spectroscopy indicated the formation of a 4:1 mixture of the diastereomeric alcohols,* (*R*)-**4.123** *and* (*S*)-**4.123'**. The residue was purified by flash chromatography to afford the desired pure product (*R*)-**4.123** as a colorless oil (726 mg, 48% yield) and a mixture of *major* and *minor* alcohols as a colorless oil (363 mg, 24% yield). **^{1}H NMR** (400 MHz, $CDCl_3$) δ 6.40 (d, *J* = 2.2 Hz, 2H), 6.26 (t, *J* = 2.1 Hz, 1H), 5.88 (app sept, 1H), 5.31 (d, *J* = 17.3 Hz, 1H), 5.13 (d, *J* = 10.4 Hz, 1H), 4.61–4.52 (m, 1H), 4.48 (d, *J* = 9.4 Hz, 1H), 3.40 (s, 1H), 2.89 (ddd, *J* = 10.5, 9.8, 4.1 Hz, 1H), 2.83–2.67 (m, 2H), 1.51–1.37 (m, 1H), 1.35–1.14 (m, 2H), 0.97 (s, 18H), 0.80 (s, 9H), 0.74 (d, *J* = 6.6 Hz, 3H), 0.71 (d, *J* = 6.5 Hz, 3H), 0.17 (s, 12H), -0.05 (s, 3H), -0.29 (s, 3H); **^{13}C NMR** (100 MHz, $CDCl_3$) δ

215.8, 156.6, 144.8, 139.1, 115.0, 112.7, 112.3, 78.4, 68.6, 59.1, 51.7, 38.6, 25.98, 25.90, 25.85, 24.0, 21.6, 18.4, 18.1, -4.17, -4.21, -4.4, -5.1; **[α]$_D^{20}$** –19.2 (c = 2.00 in $CHCl_3$); **HRMS** ESI (*m/z*) calcd for $C_{35}H_{66}O_5Si_3Na$ [M+Na^+]: 673.41103, found 673.41028.

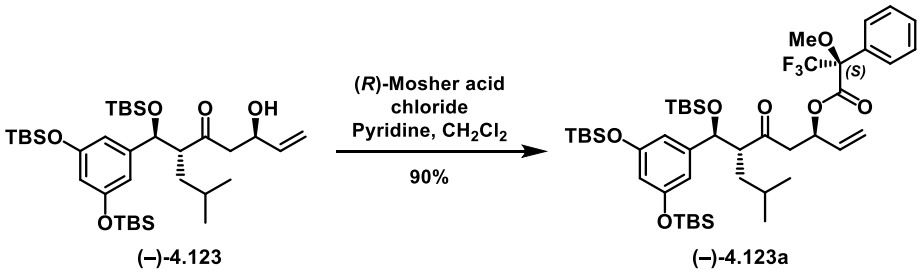

(3*R*,6*R*)-6-((*S*)-(3,5-bis((*tert*-butyldimethylsilyl)oxy)phenyl)((*tert*-butyldimethylsilyl)oxy)methyl)-8-methyl-5-oxonon-1-en-3-yl (*S*)-3,3,3-trifluoro-2-methoxy-2-phenylpropanoate (–)-4.123a. (synthesized by Dr. Guillaume Ernouf) To a solution of alcohol **(–)-4.123** (15 mg, 0.023 mmol) in CH_2Cl_2 (1 mL) at 0 °C was added pyridine (5.8 µL, 0.071 mmol) and (*R*)-MTPA-Cl (8.2 µL, 0.044 mmol). After 2 hours, the reaction was quenched with sat. aq NH_4Cl and extracted with Et_2O. The dried ($MgSO_4$) extract was concentrated in vacuo and purified by flash chromatography, yielding the (*S*)-Mosher ester **(–)-4.123a** (18 mg, 90% yield) as a colorless oil. **^{1}H NMR** (600 MHz, $CDCl_3$) δ 7.51 (d, *J* = 3.7 Hz, 2H), 7.39 (d, *J* = 2.0 Hz, 3H), 6.38 (d, *J* = 2.1 Hz, 2H), 6.26 (t, *J* = 2.1 Hz, 1H), 5.89 (q, *J* = 6.5 Hz, 1H), 5.83 (ddd, *J* = 17.1, 10.5, 6.6 Hz, 1H), 5.31 (d, *J* = 17.1 Hz, 1H), 5.22 (d, *J* = 10.5 Hz, 1H), 4.44 (d, *J* = 9.3 Hz, 1H), 3.56 (s, 3H), 3.14 (dd, *J* = 18.4, 6.0 Hz, 1H), 2.90 (dd, *J* = 18.4, 6.9 Hz, 1H), 2.86–2.80 (m, 1H), 1.49–1.39 (m, 1H), 1.21–1.10 (m, 1H), 0.97 (s, 18H), 0.90–0.83 (m, 1H), 0.77 (s, 9H), 0.66 (app t, *J* = 7.0 Hz, 6H), 0.17 (s, 12H), -0.07 (s, 3H), -0.32 (s, 3H); **^{13}C NMR** (150 MHz, $CDCl_3$) δ 209.7, 165.6, 156.6, 144.7, 134.6, 132.4, 129.7, 128.4, 127.6, 118.6, 112.7, 112.3, 78.2, 72.3, 59.0, 55.7, 48.8, 38.5, 25.9, 25.6, 23.9, 21.4, 18.4, 18.1, -4.18, -4.22, -4.4, -5.3; **^{19}F NMR** (375 MHz, $CDCl_3$) δ -71.6; **[α]$_D^{20}$** –45.9 (c = 1.52 in $CHCl_3$); **HRMS** ESI (*m/z*) calcd for $C_{45}H_{74}F_3O_7Si_3$ [M+H^+]: 867.46890, found 867.47108.

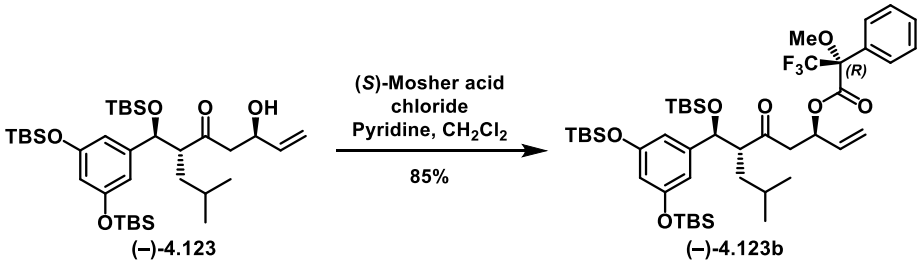

(3*R*,6*R*)-6-((*S*)-(3,5-bis((*tert*-butyldimethylsilyl)oxy)phenyl)((*tert*-butyldimethylsilyl)oxy)methyl)-8-methyl-5-oxonon-1-en-3-yl (*R*)-3,3,3-trifluoro-2-methoxy-2-phenylpropanoate (–)-4.123b. (synthesized by Dr. Guillaume Ernouf) To a solution of alcohol **(–)-4.123** (15 mg, 0.023 mmol) in CH_2Cl_2 (1.0 mL) at 0 °C was added pyridine (5.8 µL, 0.071 mmol) and (*S*)-MTPA-Cl (8.2 µL, 0.044 mmol). After 2 hours, the reaction was quenched with sat. aq NH_4Cl and extracted with Et_2O. The dried ($MgSO_4$) extract was concentrated in vacuo and purified by flash chromatography yielding the (*R*)-Mosher ester **(–)-4.123b** (17 mg, 85% yield) as a colorless oil. **^{1}H NMR** (300 MHz, $CDCl_3$) δ 7.55–7.50 (m, 2H), 7.44–7.36 (m, 3H), 6.37 (d, *J* = 2.1 Hz, 2H), 6.26 (t, *J* = 2.1 Hz, 1H), 5.98–5.89 (m, 2H), 5.44 (d, *J* = 16.0 Hz, 1H), 5.28 (d, *J* = 9.7 Hz, 1H), 4.42 (d, *J* = 9.3 Hz, 1H), 3.54 (s, 3H), 3.09 (dd, AB syst, *J* = 18.4, 4.6 Hz, 1H), 2.91 (dd, AB syst, *J* = 18.4, 7.6 Hz, 1H), 2.83–2.76 (m, 1H), 1.50–1.00 (2H) 0.97 (s, 18H), 0.91–0.82 (m, 1H), 0.78 (s, 9H), 0.67 (d, *J* = 6.5 Hz, 3H), 0.63 (d, *J* = 6.5 Hz, 3H), 0.17 (s, 12H), -0.08 (s, 3H), -0.31 (s, 3H); **^{13}C NMR** (150 MHz, $CDCl_3$) δ 209.5, 165.5, 156.6, 144.8, 134.7, 129.7, 128.8, 128.5, 127.6, 119.3, 112.7, 78.3, 72.5, 58.7, 55.6, 49.3, 38.5, 25.9, 25.6, 24.0, 21.5, 18.4, 18.1, -4.18, -4.22, -4.4, -5.3; **^{19}F NMR** (375 MHz, $CDCl_3$) δ -71.5; **$[\alpha]_D^{20}$** –13.9 (*c* 1.47, $CHCl_3$); **HRMS** ESI (*m/z*) calcd for $C_{45}H_{74}F_3O_7Si_3$ [M+H$^+$]: 867.46890, found 867.47137

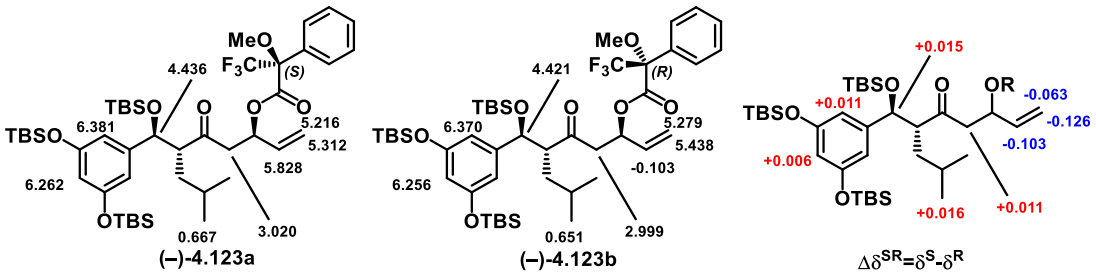

Figure 44. Mosher ester analysis (carried out by Dr. Guillaume Ernouf).

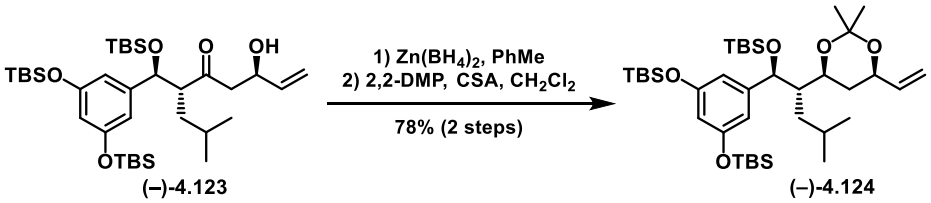

((5-((1*S*,2*S*)-1-((*tert*-butyldimethylsilyl)oxy)-2-((4*S*,6*R*)-2,2-dimethyl-6-vinyl-1,3-dioxan-4-yl)-4-methylpentyl)-1,3-phenylene)bis(oxy))bis(*tert*-butyldimethylsilane) (–)-4.124. (synthesized and optimized by Dr. Guillaume Ernouf) To a solution of ketone **(–)-4.123** (176 mg, 0.27 mmol) in toluene (25 mL) at –20 °C was added $Zn(BH_4)_2$ (Narasimhan, S.; Madhavan, S.; Prasad, K. G. *J. Org. Chem.* **1995**, *60*, 5314. $Zn(BH_4)_2$ solution stirred for at least 3 days at rt before use) (1.6 mL, 0.81 mmol, 0.5 M in THF). After stirring for 2 hours at –20 °C the reaction was warmed to 0 °C and stirred at this temperature for 12 hours. The reaction was poured into a sat. aq NH_4Cl and extracted with EtOAc. The combined organic layers were washed with brine, dried over $MgSO_4$, filtered and concentrated. Analysis of the crude residue by ^{1}H NMR spectroscopy *indicated the formation of a single detectable diastereomer*. The residue was filtered over a plug of silica gel, and carried to the next step. To a solution of the intermediate in CH_2Cl_2 (2 mL) was added 2,2-dimethoxypropane (53 µL, 0.43 mmol) and CSA (6 mg, 0.027 mmol). After 1 hour, the reaction was quenched with one drop of Et_3N, concentrated, and purified by column chromatography, yielding the title compound as a clear oil (145 mg, 78% yield over two steps). **^{1}H NMR** (400 MHz, $CDCl_3$) δ 6.41 (d, J = 2.1 Hz, 2H), 6.22 (t, J = 2.1 Hz, 1H), 5.88–5.78 (m, 1H), 5.24 (dd, J = 17.3, 1.1 Hz, 1H), 5.11 (dd, J = 10.5, 1.1 Hz, 1H), 4.64 (d, J =

5.8 Hz, 1H), 4.26 (dd, *J* = 10.2, 5.8 Hz, 1H), 3.95 (dd, *J* = 9.6, 5.4 Hz, 1H), 1.87 (app p, 1H), 1.75–1.46 (m, 2H), 1.46–1.32 (m, 1H), 1.42 (s, 3H), 1.39 (s, 3H), 1.16–1.00 (m, 2H), 0.97 (s, 18H), 0.89 (s, 9H), 0.80 (d, *J* = 6.5 Hz, 3H), 0.78 (d, *J* = 6.5 Hz, 3H), 0.17 (s, 12H), 0.01 (s, 3H), -0.22 (s, 3H); **^{13}C NMR** (100 MHz, $CDCl_3$) δ 156.1, 145.9, 139.3, 115.2, 112.6, 111.1, 98.5, 74.7, 70.4, 69.0, 48.4, 35.0, 33.4, 30.3, 26.3, 26.0, 25.9, 23.2, 22.8, 20.0, 18.4, 18.3, -4.2, -4.2, -4.4, -5.0; **$[\alpha]_D^{20}$** –12.0 (*c* 1.00, $CHCl_3$); **HRMS** ESI (*m/z*) calcd for $C_{38}H_{72}O_5Si_3Na$ $[M+Na^+]$: 715.45798, found 715.45843

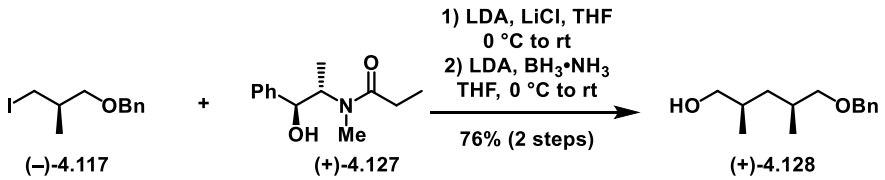

(2*R*,4*S*)-5-(benzyloxy)-2,4-dimethylpentan-1-ol (+)-4.128. Following the reported procedure (Myers, A. G.; Yang, B. H.; Chen, H.; McKinstry, L.; Kopecky, D. J. & Gleason, J. L. *J. Am. Chem. Soc.* **1997**, *119*, 6496.) (*S*,*S*)-pseudoephedrine propionate **(+)-4.127** (6.97 g, 31.48 mmol) was alkylated with iodide **(–)-4.117** (prepared as previously described: Kim, J.; Hewitt, G.; Carroll, P. & Sieburth, S. McN. *J. Org. Chem.* **2005**, *70*, 5781.) (4.35 g, 14.99 mmol) and the product was isolated after chromatography as a mixture with excess propionate. This mixture was then subjected to lithium amidotrihydroborate reduction as previously reported (Myers, A. G.; Yang, B. H.; Chen, H.; McKinstry, L.; Kopecky, D. J. & Gleason, J. L. *J. Am. Chem. Soc.* **1997**, *119*, 6496.) yielding the title compound as a clear oil (2.55 g, 76% over two steps). **^{1}H NMR** (300 MHz, $CDCl_3$) δ 7.38–7.27 (m, 5H), 4.50 (s, 2H), 3.44 (ddd, *J* = 16.9, 10.6, 5.7 Hz, 1H), 3.28 (ddd, *J* = 23.5, 9.0, 6.2 Hz, 1H), 1.88 (dt, *J* = 13.1, 6.6 Hz, 1H), 1.70 (td, *J* = 13.4, 6.7 Hz, 1H), 1.48 (dt, *J* = 13.7, 6.8 Hz, 1H), 1.00–0.90 (m, 6H); **^{13}C NMR** (75 MHz, $CDCl_3$) δ 138.7, 128.5, 127.7, 127.6, 76.0, 73.2, 68.0, 37.7, 33.3, 31.1, 18.3, 17.7; **$[\alpha]_D^{20}$** +8.3 (c = 1.1 in $CHCl_3$); **HRMS** ESI (*m/z*) calcd for $C_{14}H_{23}O_2$ $[M+H^+]$: 223.1698, found 223.1691.

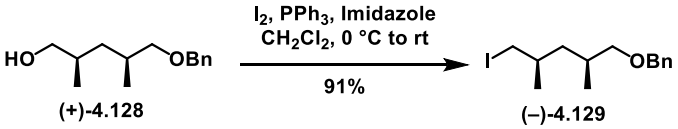

((((2*S*,4*R*)-5-iodo-2,4-dimethylpentyl)oxy)methyl)benzene (–)-4.129. To a solution of PPh_3 (3.22 g, 12.29 mmol) dissolved in CH_2Cl_2 (40 mL) was added imidazole (1.05 g, 15.38 mmol), and after complete dissolution, I_2 (3.50 g, 13.84 mmol) was added in one portion. The mixture was cooled to 0 °C and alcohol **(+)-4.128** (2.28 g, 10.25 mmol) was added as a solution in CH_2Cl_2 (10 mL). The reaction was warmed to room temperature and stirred for two hours. Half saturated $Na_2S_2O_3$ (100 mL) was added and the reaction was stirred until the color became clear. The layers were separated and the aqueous was extracted twice more with CH_2Cl_2. The combined organic layers were washed with half saturated $Na_2S_2O_3$ then brine, dried over Na_2SO_4, filtered, concentrated, and purified by column chromatography, yielding the title compound as a clear oil (3.21 g, 91% yield). **^{1}H NMR** (400 MHz, $CDCl_3$) δ 7.40–7.24 (m, 5H), 4.51 (s, 2H), 3.35 (dd, J = 9.1, 5.5 Hz, 1H), 3.28–3.22 (m, 2H), 3.13 (dd, J = 9.6, 6.1 Hz, 1H), 1.90–1.78 (m, 1H), 1.61–1.50 (m, 1H), 1.50–1.41 (m, 1H), 1.10–1.02 (m, 1H), 0.99 (d, J = 6.4 Hz, 3H), 0.97 (d, J = 6.7 Hz, 3H); **^{13}C NMR** (100 MHz, $CDCl_3$) δ 138.8, 128.4, 127.6, 127.6, 75.8, 73.1, 40.8, 32.0, 31.0, 21.5, 18.1, 17.7; **$[\alpha]_D^{20}$** –1.5 (c = 1.7 in $CHCl_3$); **HRMS** ESI (*m/z*) calcd for $C_{14}H_{22}IO$ $[M+H^+]$: 333.0715, found 333.0706.

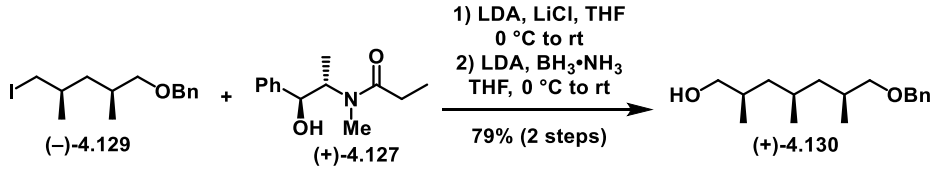

(2*R*,4*S*,6*S*)-7-(benzyloxy)-2,4,6-trimethylheptan-1-ol (+)-4.130. Using the procedure given for the preparation of compound **(+)-4.128**, (*S*,*S*)-pseudoephedrine propionate **(+)-4.127** (4.48 g, 20.23 mmol) was alkylated with iodide **(–)-4.129** (3.20 g, 9.63 mmol) and subjected to reduction, yielding the title compound as a clear oil (1.01 g, 90% yield). **^{1}H NMR** (600 MHz, $CDCl_3$) δ

7.36–7.32 (m, 4H), 7.31–7.27 (m, 1H), 4.51 (d, *J* = 12.1 Hz, 1H), 4.48 (d, *J* = 12.1 Hz, 1H), 3.56–3.49 (m, 1H), 3.39–3.33 (m, 2H), 3.21 (dd, *J* = 9.0, 6.9 Hz, 1H), 1.91–1.82 (m, 1H), 1.72 (dtd, *J* = 13.6, 6.8, 5.1 Hz, 1H), 1.62–1.55 (m, 2H), 1.39–1.27 (m, 2H), 1.26–1.22 (m, 1H), 0.95 (d, *J* = 6.7 Hz, 3H), 0.92 (d, *J* = 6.7 Hz, 3H), 0.90 (d, *J* = 6.6 Hz, 3H); **^{13}C NMR** (150 MHz, $CDCl_3$) δ 139.0, 128.4, 127.6, 127.5, 76.0, 73.2, 68.3, 41.7, 41.2, 33.2, 31.1, 27.8, 21.1, 18.5, 17.7; **$[\alpha]_D^{20}$** +116.3 (c = 3.10 in $CHCl_3$); **HRMS** ESI (*m/z*) calcd for $C_{17}H_{28}O_2Na$ [M+Na^+]: 287.1987, found 287.1979.

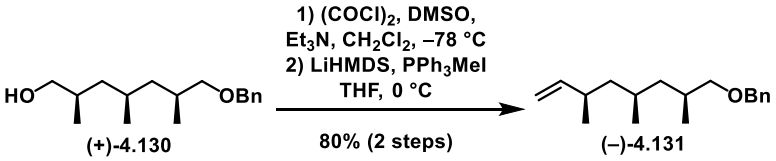

((((2*S*,4*S*,6*R*)-2,4,6-trimethyloct-7-en-1-yl)oxy)methyl)benzene (–)-4.131. Oxalyl chloride (2M in CH_2Cl_2, 3.80 mL, 7.596 mmol) at –78 °C was diluted with CH_2Cl_2 (30 mL) and then DMSO (1.08 mL, 4.24 mmol) dissolved in CH_2Cl_2 (10 mL) was added dropwise. After 15 minutes, alcohol **(+)-4.130** (1.339 g, 5.064 mmol) dissolved in CH_2Cl_2 (10 mL) was added dropwise. After 30 minutes, triethylamine (3.51 mL, 25.32 mmol) was added dropwise. After 15 minutes at –78 °C, the reaction was warmed to 0 °C, quenched with sat. aq NH_4Cl, and extracted with CH_2Cl_2 3x. The combined organic layers were washed with sat. aq NH_4Cl then brine, dried over Na_2SO_4, filtered, and concentrated to a minimal volume. The solution was loaded onto a plug of silica gel and eluted with 9:1 hexanes:EtOAc. ^{1}H NMR analysis of the crude aldehyde indicated no epimerization of the α-methyl stereocenter. LiHMDS (1M in THF, 9.62 mL, 9.62 mmol) was added to a suspension of methyltriphenylphosphonium iodide (4.09 g, 10.128 mmol) in THF (80 mL) at 0 °C. The suspension was warmed to room temperature and stirred for an hour. The solution was cooled back down to 0 °C and the crude aldehyde was added as a solution in THF (20 mL). The reaction was stirred at 0 °C for 2 hours, then quenched with water. The aqueous layer was extracted with Et_2O 3x, and the combined organic layers were washed with brine, dried

over $MgSO_4$, filtered, concentrated, and purified by column chromatography, yielding the title compound as a yellow oil (1.060 g, 80% over 2 steps). **^{1}H NMR** (400 MHz, $CDCl_3$) δ 7.38–7.25 (m, 5H), 5.67–5.53 (m, 1H), 5.02–4.85 (m, 2H), 4.55–4.44 (m, 2H), 3.32 (dd, *J* = 9.0, 5.4 Hz, 1H), 3.20 (dd, *J* = 9.0, 7.0 Hz, 1H), 2.30–2.15 (m, 1H), 1.93–1.79 (m, 1H), 1.58–1.48 (m, 1H), 1.35–1.23 (m, 2H), 0.96 (d, *J* = 6.7 Hz, 3H), 0.92 (d, *J* = 6.7 Hz, 3H), 0.85 (d, *J* = 6.5 Hz, 3H); **^{13}C NMR** (100 MHz, $CDCl_3$) δ 144.7, 138.9, 128.4, 127.6, 127.5, 112.8, 76.2, 73.1, 44.1, 42.2, 35.7, 30.9, 27.7, 21.7, 20.4, 18.0; **$[\alpha]_D^{20}$** –18.8 (c = 1.5 in $CHCl_3$); **HRMS** ESI (*m/z*) calcd for $C_{18}H_{29}O$ $[M+H^+]$: 261.2218, found 261.2212.

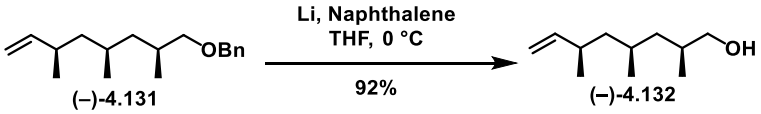

(2*S*,4*S*,6*R*)-2,4,6-trimethyloct-7-en-1-ol (–)-4.132. To a solution of naphthalene (1.54 g, 12.0 mmol) in THF (35 mL) under argon was added Li (83 mg, 12.0 mmol) as small pieces. After it was stirred for 3 h at room temperature, the reaction mixture was cooled to −40 °C and a solution of benzyl ether **(–)-4.131** (626 mg, 2.40 mmol), dissolved in 4 mL of anhydrous THF was cannulated into it. The reaction was continued further for 1 h at the same temperature and then quenched with a sat. aq NH_4Cl (15 mL). The resultant mixture was extracted with EtOAc (2 × 30 mL), washed with water and brine, dried over anhydrous $MgSO_4$, and concentrated under reduced pressure. The residue was purified by flash column chromatography yielding the title compound as a yellowish oil (375 mg, 92% yield). **^{1}H NMR** (400 MHz, $CDCl_3$) δ 5.57 (ddd, *J* = 17.2, 10.2, 8.2 Hz, 1H), 4.99–4.83 (m, 2H), 3.47 (dd, *J* = 10.5, 5.3 Hz, 1H), 3.32 (dd, *J* = 10.5, 6.8 Hz, 1H), 2.28–2.14 (m, 1H), 2.02 (s, 1H), 1.75–1.61 (m, 1H), 1.59–1.44 (m, 1H), 1.32–1.19 (m, 2H), 0.95 (d, *J* = 6.7 Hz, 3H), 0.99–0.89 (m, 2H), 0.87 (d, *J* = 6.7 Hz, 3H), 0.84 (d, *J* = 6.5 Hz, 3H); **^{13}C NMR** (100 MHz, $CDCl_3$) δ 144.7, 112.8, 68.4, 44.0, 41.6, 35.8, 33.1, 27.7, 21.7, 20.4, 17.3; **$[\alpha]_D^{20}$** –25.5 (c = 0.40 in $CHCl_3$); **HRMS** ESI (*m/z*) calcd for $C_{11}H_{23}O$ $[M+H^+]$: 171.1719, found 171.1744.

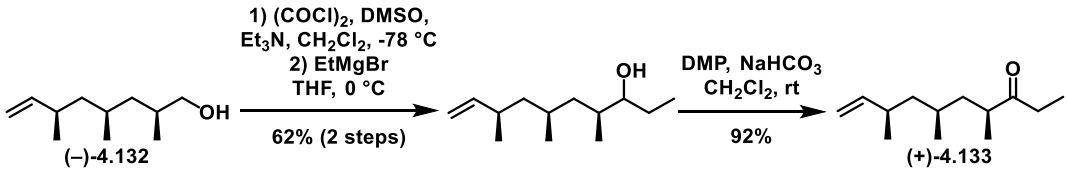

(4*S*,6*S*,8*R*)-4,6,8-trimethyldec-9-en-3-one (+)-4.133. Following the same Swern oxidation conditions described in the preparation of compound **(–)-4.131**, compound **(–)-4.132** (195 mg) was transformed to the corresponding aldehyde, purified by flash column chromatography using a short pad of silica and EtOAc as eluent as a yellowish oil (165 mg, 85% yield), which was taken for the next step without further characterization. To a stirred solution of the above aldehyde (165 mg, 0.86 mmol) in anhydrous THF (2 mL) at 0 °C under argon was added EtMgBr (0.54 mL, 1.5 mmol, 3.0 M in THF), and the reaction was continued for 10 min at the same temperature. The reaction was then quenched by a sat. aq NH_4Cl. The resultant mixture was then extracted with EtOAc, washed with water and brine, dried over $MgSO_4$, and concentrated in vacuo. Purification of the crude residue by flash column chromatography yielded an inseparable mixture of diastereomeric alcohols (140 mg, 73% yield) as a colorless oil which was taken for the next reaction without further characterization. To a solution of the alcohol intermediate (183 mg, 0.92 mmol) and $NaHCO_3$ (387 mg, 4.61 mmol) in CH_2Cl_2 (2 mL) at 0 °C was added DMP (785 mg, 1.85 mmol) and the reaction was stirred at room temperature for 1 hour. The reaction was quenched with 2:1:1 H_2O:sat. $Na_2S_2O_3$:sat. $NaHCO_3$ and extracted with CH_2Cl_2 3x. The combined organic extracts were washed with brine, dried over Na_2SO_4, filtered, concentrated and purified by column chromatography, yielding the title compound as a pale yellow oil (166 mg, 92% yield). **^{1}H NMR** (600 MHz, $CDCl_3$) δ 5.59 (ddd, J = 17.2, 10.2, 8.2 Hz, 1H), 4.94 (dd, J = 17.2, 1.9 Hz, 1H), 4.89 (dd, J = 10.2, 1.8 Hz, 1H), 2.67–2.60 (m, 1H), 2.47 (dq, AB syst, J = 17.6, 7.3 Hz, 1H), 2.41 (dq, AB syst, J = 17.7, 7.3 Hz, 1H), 2.27–2.18 (m, 1H), 1.67–1.57 (m, 1H), 1.43–1.35 (m, 1H), 1.27–1.21 (m, 1H), 1.03 (app p, 6H), 1.09–0.97 (m, 2H), 0.96 (d, J = 6.7 Hz, 3H), 0.85 (d, J = 6.5 Hz, 3H); **^{13}C NMR** (150 MHz, $CDCl_3$) δ 215.7, 144.6, 112.9, 44.3, 43.8,

41.2, 35.6, 34.3, 28.4, 21.4, 19.9, 17.4, 8.0; $[\alpha]_D^{20}$ +5.0 (c = 1.00 in $CHCl_3$); **HRMS** ESI (*m/z*) calcd for $C_{13}H_{25}O$ [$M+H^+$]: 197.18999, found 197.18995.

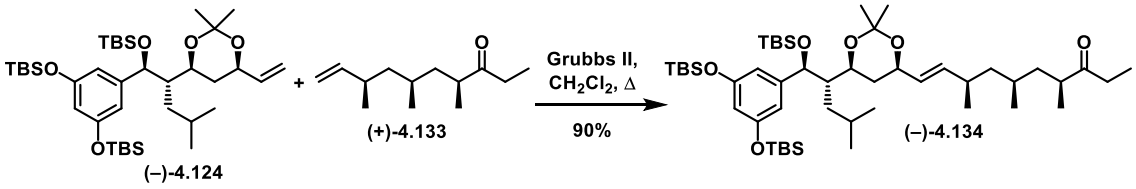

(4*S*,6*S*,8*R*,*E*)-10-((4*R*,6*S*)-6-((1*S*,2*S*)-1-(3,5-bis((*tert*-butyldimethylsilyl)oxy)phenyl)-1-((*tert*-butyldimethylsilyl)oxy)-4-methylpentan-2-yl)-2,2-dimethyl-1,3-dioxan-4-yl)-4,6,8-trimethyldec-9-en-3-one (–)-4.134. To a solution of alkene **(–)-4.124** (98 mg, 0.14 mmol) and ethyl ketone **(+)-4.133** (55 mg, 0.28 mmol) in CH_2Cl_2 (2 mL) was added Grubbs II (6 mg, 0.007 mmol) and the reaction was heated to 40 °C. After 3 hours, another portion of Grubbs II (6 mg, 0.007 mmol) was added. The reaction was then cooled to room temperature, concentrated and purified by column chromatography, yielding the title compound as a clear oil (105 mg, 90% yield). **^{1}H NMR** (600 MHz, $CDCl_3$) δ 6.41 (s, 2H), 6.21 (s, 1H), 5.47–5.36 (m, 2H), 4.63 (d, *J* = 5.7 Hz, 1H), 4.20 (dd, *J* = 8.7, 5.8 Hz, 1H), 3.97–3.90 (m, 1H), 2.63 (dd, *J* = 13.9, 6.9 Hz, 1H), 2.51–2.37 (m, 2H), 2.27–2.19 (m, 1H), 1.85 (s, 1H), 1.69–1.58 (m, 2H), 1.55–1.45 (m, 2H), 1.41 (s, 3H), 1.43–1.33 (m, 2H), 1.38 (s, 3H), 1.31–1.19 (m, 2H), 1.10–0.99 (m, 10H), 0.97 (s, 21H), 0.88 (s, 9H), 0.86 (d, *J* = 6.4 Hz, 3H), 0.79 (d, *J* = 6.5 Hz, 3H), 0.76 (d, *J* = 6.5 Hz, 3H), 0.17 (s, 12H), 0.01 (s, 3H), -0.23 (s, 3H); **^{13}C NMR** (150 MHz, $CDCl_3$) δ 215.6, 156.1, 145.9, 137.6, 129.8, 112.7, 111.1, 98.5, 74.7, 70.5, 69.0, 48.4, 44.2, 43.7, 40.9, 35.1, 34.3, 34.0, 33.9, 30.4, 28.2, 26.3, 26.07, 25.86, 23.2, 22.9, 21.2, 20.3, 20.1, 18.4, 18.3, 17.3, 8.1, -4.19, -4.24, -4.4, -5.0; $[\alpha]_D^{20}$ –7.0 (c = 0.5 in $CHCl_3$); **HRMS** ESI (*m/z*) calcd for $C_{49}H_{92}O_6Si_3Na$ [$M+Na^+$]: 883.60939, found 883.61094.

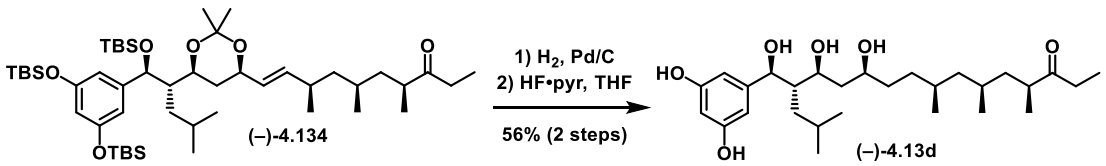

(4*S*,6*S*,8*S*,11*S*,13*S*,14*S*)-14-((*S*)-(3,5-dihydroxyphenyl)(hydroxy)methyl)-11,13-dihydroxy-4,6,8,16-tetramethylheptadecan-3-one (–)-4.13d. To a solution of alkene **(–)-4.134** (60 mg, 0.07 mmol) in EtOAc:MeOH (2/1, 5 mL) was added 10 % Pd/C (7.4 mg, 0.007 mmol, 10 mol %), and the reaction flask was purged and backfilled with H_2 (3x), then stirred under an atmosphere of H_2 (balloon) for 2 h. The reaction was filtered over Celite, and of the residue was dissolved in THF (1 mL) in a plastic tube and HF-pyridine (70%, 500 µL) was added. The reaction was allowed to warm to room temperature and stir overnight. The following day, the reaction was slowly poured into a stirring solution of sat. $NaHCO_3$ (10 mL). The solution was extracted with EtOAc 3x. The combined organic layers were washed with 1M HCl, and then washed with water repeatedly until the pH of the washes reached ~6. The organic layer was then washed with brine, dried over Na_2SO_4, filtered, concentrated, and purified by column chromatography, yielding the title compound as a clear oil (18.7 mg, 56% yield). **^{1}H NMR** (600 MHz, CD_3OD) δ 6.32 (d, J = 2.2 Hz, 2H), 6.14 (t, J = 2.2 Hz, 1H), 4.47 (d, J = 6.8 Hz, 1H), 4.00 (dt, J = 10.0, 3.3 Hz, 1H), 3.72–3.66 (m, 1H), 2.76 (dqd, J = 9.1, 7.0, 5.3 Hz, 1H), 2.58 (dq, J = 18.1, 7.3 Hz, 1H), 2.49 (dq, J = 18.1, 7.2 Hz, 1H), 1.88 (m, 1H), 1.78 (ddd, J = 14.1, 4.5, 3.2 Hz, 1H), 1.73 (ddd, J = 13.8, 9.1, 5.0 Hz, 1H), 1.54 (ddd, J = 14.1, 10.1, 8.2 Hz, 1H), 1.53 (m, 1H), 1.43–1.38 (m, 3H), 1.38 (m, 1H), 1.32 (m, 1H), 1.22 (ddd, J = 13.9, 7.0, 6.7 Hz, 1H), 1.21 (m, 2H), 1.19 (m, 1H), 1.00 (ddd, J = 13.8, 8.6, 5.4 Hz, 1H), 1.06 (d, J = 6.9 Hz, 3H), 1.02 (t, J = 7.3 Hz, 3H), 0.95 (dt, J = 13.6, 7.2 Hz, 1H), 0.89 (d, J = 6.6 Hz, 3H), 0.86 (d, J = 6.6 Hz, 3H), 0.83 (d, J = 6.6 Hz, 3H), 0.77 (d, J = 6.5 Hz, 3H); **^{13}C NMR** (150 MHz, CD_3OD) δ 218.5, 159.5, 148.3, 106.3, 102.3, 76.9, 73.7, 72.9, 48.8, 46.6, 45.0, 42.0, 41.0, 37.6, 35.7, 35.4, 33.4, 31.2, 29.5, 26.9, 23.6, 22.8, 20.9, 20.5, 18.2, 8.1; **$[\alpha]_D^{20}$** –15.1 (c = 0.44 in MeOH)

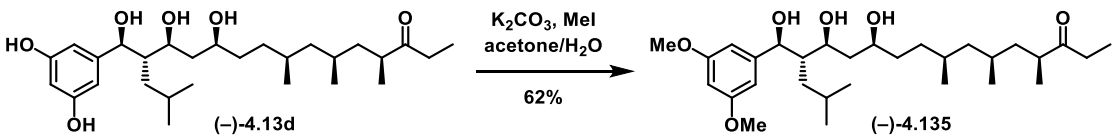

(4*S*,6*S*,8*S*,11*S*,13*S*,14*S*)-14-((*S*)-(3,5-dimethoxyphenyl)(hydroxy)methyl)-11,13-dihydroxy-4,6,8,16-tetramethylheptadecan-3-one (–)-4.135. To a solution of **(–)-4.13d** (3.8 mg, 8 μmol) in acetone/water (10:1, 1.0 mL) at room temperature was added K_2CO_3 (3.3 mg, 24 μmol) and MeI (1.25 μL, 20 μmol). After 3 days, the reaction mixture was concentrated in vacuo and purified by column chromatography, yielding the title compound as a clear oil (2.5 mg, 62% yield). **^{1}H NMR** (600 MHz, CD_3OD) δ 6.50 (d, J = 2.3 Hz, 2H), 6.33 (t, J = 2.2 Hz, 1H), 4.54 (d, J = 6.8 Hz, 1H), 3.94 (dt, J = 10.1, 3.4 Hz, 1H), 3.74 (s, 6H), 3.65 (s, 1H), 2.80–2.64 (m, 1H), 2.61–2.39 (m, 2H), 1.93–1.85 (m, 1H), 1.82–1.73 (m, 1H), 1.73–1.66 (m, 1H), 1.58–1.44 (m, 2H), 1.42–1.25 (m, 9H), 1.23–1.11 (m, 3H), 1.03 (d, J = 6.9 Hz, 3H), 1.04–0.99 (m, 1H), 0.98 (t, J = 7.3 Hz, 3H), 0.95–0.89 (m, 1H), 0.85 (d, J = 6.5 Hz, 3H), 0.82 (d, J = 6.6 Hz, 3H), 0.79 (d, J = 6.5 Hz, 3H), 0.73 (d, J = 6.4 Hz, 3H); **^{13}C NMR** (150 MHz, CD_3OD) δ 218.4, 162.2, 148.4, 105.8, 99.9, 76.7, 73.4, 72.8, 55.7, 49.0, 46.6, 44.9, 42.0, 40.9, 37.4, 35.7, 35.4, 33.4, 31.2, 29.5, 26.9, 23.6, 22.7, 20.9, 20.5, 18.2, 8.1; **$[\alpha]_D^{20}$** –138 (c = 0.03 in MeOH); **HRMS** ESI (*m/z*) calcd for $C_{30}H_{52}O_6Na$ [M+Na$^+$]: 531.36561, found 531.36539.

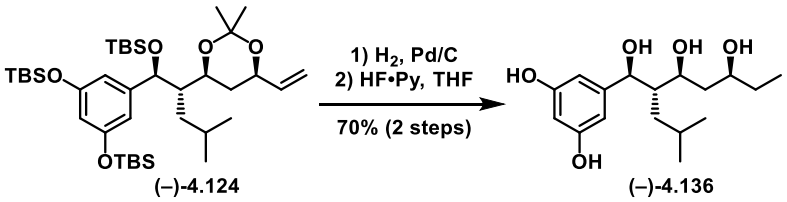

(1*S*,2*S*,3*S*,5*S*)-1-(3,5-dihydroxyphenyl)-2-isobutylheptane-1,3,5-triol (–)-4.136. Alkene **(–)-4.124** (19 mg, 0.027 mmol) was dissolved in 2:1 EtOAc:MeOH (4 mL) and 10 % Pd/C (15 mg) was added, and the reaction flask was purged and backfilled with H_2 3x, then stirred under an atmosphere of H_2 (balloon) overnight. The reaction was filtered over Celite, and carried directly

to the next step. The crude product was dissolved in THF (0.5 mL) in a plastic tube and cooled to 0 °C. HF-pyridine (70%, 0.25 mL) was added dropwise, and the reaction was warmed to room temperature and stirred overnight. The following day, the reaction was slowly poured into a stirring solution of sat. $NaHCO_3$ (10 mL). The solution was extracted with EtOAc 3x. The combined organic layers were washed with 1M HCl, and then washed with water repeatedly until the pH of the washes reached ~6. The organic layer was then washed with brine, dried over Na_2SO_4, filtered, concentrated, and purified by column chromatography, yielding the title compound as a clear oil (6.0 mg, 70% yield over 2 steps). **^{1}H NMR** (600 MHz, CD_3OD) δ 6.32 (d, J = 2.2 Hz, 2H), 6.15 (t, J = 2.1 Hz, 1H), 4.46 (d, J = 6.9 Hz, 1H), 4.01 (dt, J = 10.0, 3.3 Hz, 1H), 3.69–3.63 (m, 1H), 1.90–1.84 (m, 1H), 1.82–1.75 (m, 1H), 1.55–1.45 (m, 3H), 1.44–1.33 (m, 2H), 1.25–1.15 (m, 3H), 0.93 (t, J = 7.4 Hz, 3H), 0.82 (d, J = 6.6 Hz, 3H), 0.76 (d, J = 6.5 Hz, 3H); **^{13}C NMR** (150 MHz, CD_3OD) δ 159.3, 148.3, 106.3, 102.2, 76.9, 74.2, 73.7, 40.4, 37.5, 31.1, 26.9, 23.6, 22.7, 10.0; **$[\alpha]_D^{20}$** –52.5 (c = 0.40 in MeOH); **HRMS** ESI (*m/z*) calcd for ESI (m/z) calcd for $C_{17}H_{28}O_5Na$ [M+Na^+]: 335.1834, found 335.1837.

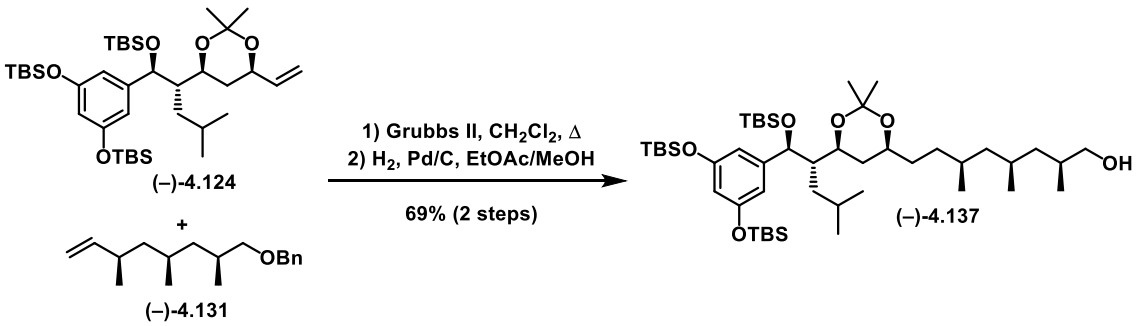

(2*S*,4*S*,6*S*)-8-((4*S*,6*S*)-6-((1*S*,2*S*)-1-(3,5-bis((*tert*-butyldimethylsilyl)oxy)phenyl)-1-((*tert*-butyldimethylsilyl)oxy)-4-methylpentan-2-yl)-2,2-dimethyl-1,3-dioxan-4-yl)-2,4,6-trimethyloctan-1-ol ((–)-4.137). To a solution of alkene **(–)-4.124** (100 mg, 0.144 mmol) and benzyl ether **(–)-4.131** (75 mg, 0.289 mmol) in CH_2Cl_2 (3 mL) was added Grubbs II (6 mg, 0.007 mmol) and the reaction was heated to 40 °C. After 3 hours, another portion of Grubbs II (2 mg, 0.002 mmol) was added. After another hour at the same temperature, another portion of Grubbs II

(2 mg, 0.002 mmol) was added. After another hour, the reaction was cooled to room temperature, and filtered through a plug of silica gel, which was washed with 9:1 hexanes:EtOAc. The mixture was concentrated and carried directly to the next step. To the crude metathesis mixture dissolved in 2:1 EtOAc:MeOH (5 mL) was added 10 % Pd/C (22 mg), and the reaction flask was purged and backfilled with H_2 3x, then stirred under an atmosphere of H_2 (balloon) overnight. The reaction was filtered over Celite, and of the residue was purified by column chromatography, yielding the title compound as a clear oil (83 mg, 69% yield over two steps). **^{1}H NMR** (600 MHz, $CDCl_3$) δ 6.41 (d, J = 2.1 Hz, 2H), 6.21 (t, J = 2.2 Hz, 1H), 4.62 (d, J = 5.9 Hz, 1H), 3.90 (ddd, J = 11.5, 5.3, 2.1 Hz, 1H), 3.69–3.63 (m, 1H), 3.53 (dd, J = 10.4, 5.0 Hz, 1H), 3.37 (dd, J = 10.4, 6.9 Hz, 1H), 1.88–1.82 (m, 1H), 1.76–1.69 (m, 1H), 1.64–1.46 (m, 5H), 1.38–1.19 (m, 11H), 1.11–1.01 (m, 3H), 0.97 (s, 18H), 0.93 (d, J = 6.7 Hz, 3H), 0.91–0.82 (m, 17H), 0.79 (d, J = 6.5 Hz, 3H), 0.77 (d, J = 6.5 Hz, 3H), 0.17 (s, 12H), 0.01 (s, 3H), -0.23 (s, 3H); **^{13}C NMR** (150 MHz, $CDCl_3$) δ 156.1, 146.0, 112.6, 111.0, 98.3, 74.8, 69.3, 69.2, 68.4, 48.4, 45.1, 41.3, 35.0, 34.0, 33.4, 33.2, 31.6, 30.4, 30.0, 27.6, 26.3, 26.1, 25.9, 23.2, 22.8, 21.1, 20.5, 20.0, 18.4, 18.3, 17.7, -4.2, -4.2, -4.4, -5.0; **$[\alpha]_D^{20}$** –38.7 (c = 1.00 in $CHCl_3$); **HRMS** ESI (*m/z*) calcd for $C_{47}H_{92}O_6Si_3Na$ [M+Na$^+$]: 859.6099, found 859.6094.

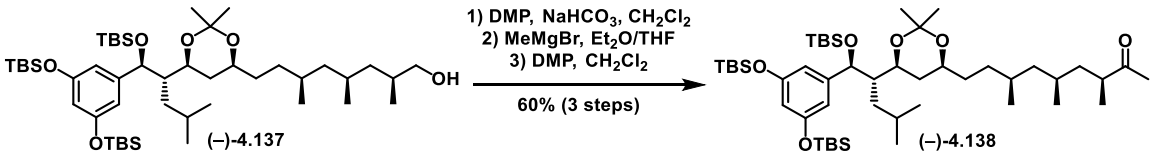

(3*S*,5*S*,7*S*)-9-((4*S*,6*S*)-6-((1*S*,2*S*)-1-(3,5-bis((*tert*-butyldimethylsilyl)oxy)phenyl)-1-((*tert*-butyldimethylsilyl)oxy)-4-methylpentan-2-yl)-2,2-dimethyl-1,3-dioxan-4-yl)-3,5,7-trimethylnonan-2-one (–)-4.138. To a solution of alcohol **(–)-4.137** (29 mg, 0.035 mmol) and $NaHCO_3$ (14 mg, 0.170 mmol) in CH_2Cl_2 (2 mL) at 0 °C was added DMP (19 mg, 0.046 mmol) and the reaction was stirred at room temperature for 1 hour, and another portion of DMP (5 mg, 0.012 mmol) was added. After an hour, the reaction was quenched with 2:1:1 H_2O:sat.

$Na_2S_2O_3$:sat. $NaHCO_3$ and extracted with CH_2Cl_2 3x. The combined organic extracts were washed with brine, dried over Na_2SO_4, filtered, concentrated, and filtered over a plug of silica gel, which was washed with 9:1 hexanes:EtOAc. To a solution of the crude aldehyde in THF (2 mL) at 0 °C was added MeMgBr (3.0 M in THF, 0.020 mL, 0.060 mmol) dropwise. After 10 minutes, the reaction was quenched with sat. aq NH_4Cl and extracted with EtOAc 3x. The combined organic layers were washed with brine, dried over Na_2SO_4, filtered, and concentrated. The crude alcohol was then dissolved in CH_2Cl_2 (2 mL) and DMP (19 mg, 0.045 mmol) was added. The reaction was stirred at room temperature for 30 minutes, then quenched with 2:1:1 H_2O:sat. $Na_2S_2O_3$:sat. $NaHCO_3$ and extracted with CH_2Cl_2 3x. The combined organic layers were washed with brine, dried over Na_2SO_4, filtered, concentrated, and purified by column chromatography, yielding the title compound as a clear oil (18 mg, 60% yield over 3 steps). **^{1}H NMR** (600 MHz, $CDCl_3$) δ 6.41 (d, J = 2.2 Hz, 2H), 6.21 (t, J = 2.2 Hz, 1H), 4.62 (d, J = 5.9 Hz, 1H), 3.93–3.86 (m, 1H), 3.69–3.62 (m, 1H), 2.68–2.57 (m, 1H), 2.12 (s, 3H), 1.88–1.81 (m, 1H), 1.73–1.64 (m, 1H), 1.58–1.42 (m, 5H), 1.36 (s, 3H), 1.35 (s, 3H), 1.32–1.26 (m, 2H), 1.24–1.17 (m, 2H), 1.09–1.04 (m, 7H), 0.97 (s, 18H), 0.90–0.84 (m, 16H), 0.79 (d, J = 6.6 Hz, 3H), 0.77 (d, J = 6.5 Hz, 3H), 0.17 (s, 12H), 0.01 (s, 3H), -0.23 (s, 3H); **^{13}C NMR** (150 MHz, $CDCl_3$) δ 213.2, 156.1, 146.0, 112.6, 111.0, 98.3, 74.8, 69.2, 69.2, 48.4, 45.1, 45.0, 40.6, 35.0, 34.1, 33.4, 31.9, 30.4, 29.9, 28.2, 27.99, 26.3, 26.1, 25.9, 23.2, 22.8, 20.7, 20.3, 20.0, 18.4, 18.3, 17.5, -4.19, -4.23, -4.4, -5.0; **$[\alpha]_D^{20}$** –21.4 (c = 0.90 in $CHCl_3$); **HRMS** ESI (*m/z*) calcd for $C_{48}H_{92}O_6Si_3Na$ [M+Na$^+$]: 871.6099, found 871.6102.

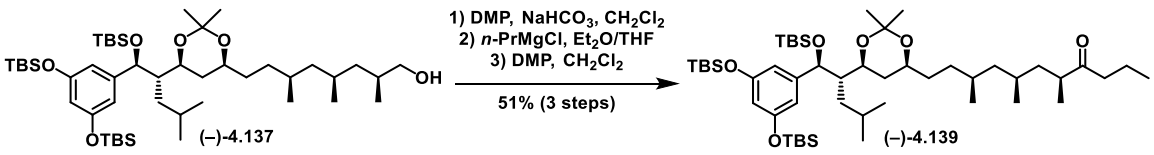

(5*S*,7*S*,9*S*)-11-((4*S*,6*S*)-6-((1*S*,2*S*)-1-(3,5-bis((*tert*-butyldimethylsilyl)oxy)phenyl)-1-((*tert*-butyldimethylsilyl)oxy)-4-methylpentan-2-yl)-2,2-dimethyl-1,3-dioxan-4-yl)-5,7,9-

trimethylundecan-4-one (–)-4.139. Following the procedure given for the preparation of compound **(–)-4.138**, with *n*-PrMgCl in place of MeMgBr, alcohol **(–)-4.137** (39 mg, 0.047 mmol) yielded the title compound as a clear oil (21 mg, 51% yield over 3 steps). **^{1}H NMR** (600 MHz, $CDCl_3$) δ 6.41 (d, J = 2.0 Hz, 2H), 6.21 (t, J = 2.0 Hz, 1H), 4.62 (d, J = 5.9 Hz, 1H), 3.93–3.87 (m, 1H), 3.71–3.62 (m, 1H), 2.68–2.60 (m, 1H), 2.46–2.34 (m, 2H), 1.89–1.81 (m, 1H), 1.70 (ddd, J = 20.1, 12.7, 8.4 Hz, 1H), 1.63–1.40 (m, 7H), 1.38–1.19 (m, 10H), 1.08–1.03 (m, 6H), 0.97 (s, 18H), 0.93–0.88 (m, 14H), 0.87–0.82 (m, 6H), 0.79 (d, J = 6.5 Hz, 3H), 0.77 (d, J = 6.5 Hz, 3H), 0.17 (s, 12H), 0.01 (s, 3H), -0.23 (s, 3H); **^{13}C NMR** (150 MHz, $CDCl_3$) δ 215.1, 156.1, 146.0, 112.6, 111.0, 98.3, 74.8, 69.3, 69.2, 48.4, 45.2, 44.1, 43.2, 40.7, 35.0, 34.1, 33.4, 31.9, 30.4, 29.9, 28.2, 26.3, 26.1, 25.9, 23.2, 22.8, 20.7, 20.3, 20.0, 18.4, 18.3, 17.7, 17.2, 14.0, -4.19, -4.24, -4.4, -5.0; **$[\alpha]_D^{20}$** –74.5 (*c* 1.10, $CHCl_3$); **HRMS** ESI (*m/z*) calcd for $C_{50}H_{96}O_6Si_3Na$ [M+Na^+]: 899.6412, found 899.6431.

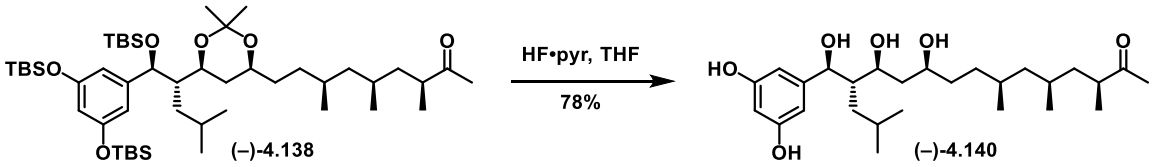

(3*S*,5*S*,7*S*,10*S*,12*S*,13*S*)-13-((*S*)-(3,5-dihydroxyphenyl)(hydroxy)methyl)-10,12-dihydroxy-3,5,7,15-tetramethylhexadecan-2-one (–)-4.140. Using the HF-pyridine procedure given for the preparation of **(–)-4.13d**, silyl ether **(–)-4.138** (17 mg, 0.020 mmol) yielded the title compound as a clear oil (7 mg, 78% yield). **^{1}H NMR** (600 MHz, CD_3OD) δ 6.32 (d, J = 2.2 Hz, 2H), 6.14 (t, J = 2.2 Hz, 1H), 4.47 (d, J = 6.8 Hz, 1H), 4.00 (dt, J = 9.9, 3.3 Hz, 1H), 3.73–3.67 (m, 1H), 2.76–2.68 (m, 1H), 2.15 (s, 3H), 1.92–1.86 (m, 1H), 1.81–1.76 (m, 1H), 1.72 (ddd, J = 13.8, 8.9, 5.1 Hz, 1H), 1.58–1.28 (m, 7H), 1.27–1.16 (m, 4H), 1.08 (d, J = 7.0 Hz, 3H), 1.06–0.92 (m, 2H), 0.89 (d, J = 6.6 Hz, 3H), 0.87 (d, J = 6.6 Hz, 3H), 0.83 (d, J = 6.6 Hz, 3H), 0.77 (d, J = 6.5 Hz, 3H); **^{13}C NMR** (150 MHz, CD_3OD) δ 216.1, 159.5, 148.3, 106.3, 102.3, 76.9, 73.7, 72.9, 46.6, 46.0, 41.8, 41.0, 37.6, 35.7, 33.3, 31.2, 29.4, 28.2, 26.9, 23.6, 22.8, 20.8, 20.6, 17.8; **$[\alpha]_D^{20}$** –12.2

(c = 0.39 in MeOH); **HRMS** ESI (*m/z*) calcd for $C_{27}H_{46}O_6Na$ [M+Na^+]: 489.3192, found 489.3188.

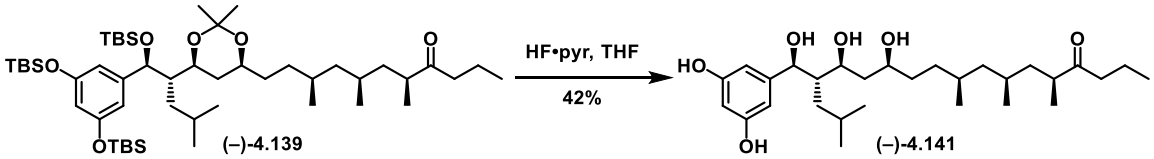

(5*S*,7*S*,9*S*,12*S*,14*S*,15*S*)-15-((*S*)-(3,5-dihydroxyphenyl)(hydroxy)methyl)-12,14-dihydroxy-5,7,9,17-tetramethyloctadecan-4-one (–)-4.141. Following the HF-pyridine deprotection procedure given for the preparation of compound **(–)-4.13d**, silyl ether **(–)-4.139** (21 mg, 0.024 mmol) yielded the title compound as a clear oil (5 mg, 42% yield). **^{1}H NMR** (600 MHz, CD_3OD) δ 6.33 (d, J = 2.2 Hz, 2H), 6.15 (t, J = 2.2 Hz, 1H), 4.47 (d, J = 6.8 Hz, 1H), 4.00 (dt, J = 9.9, 3.3 Hz, 1H), 3.73–3.66 (m, 1H), 2.78–2.70 (m, 1H), 2.57–2.42 (m, 2H), 1.92–1.84 (m, 1H), 1.81–1.71 (m, 2H), 1.61–1.49 (m, 5H), 1.48–1.26 (m, 4H), 1.26–1.15 (m, 4H), 1.05 (d, J = 6.9 Hz, 3H), 1.02–0.94 (m, 1H), 0.93–0.81 (m, 13H), 0.77 (d, J = 6.5 Hz, 3H); **^{13}C NMR** (150 MHz, CD_3OD) δ 217.9, 159.4, 148.3, 106.3, 102.2, 76.9, 73.7, 72.9, 46.6, 45.1, 44.2, 41.9, 41.0, 37.6, 35.7, 33.4, 31.2, 29.5, 26.9, 23.6, 22.8, 20.9, 20.6, 18.1, 18.0, 14.1; **$[\alpha]_D^{20}$** –10.2 (c = 0.48 in MeOH); **HRMS** ESI (*m/z*) calcd for $C_{29}H_{50}O_6Na$ [M+Na^+]: 517.3505, found 517.3500.

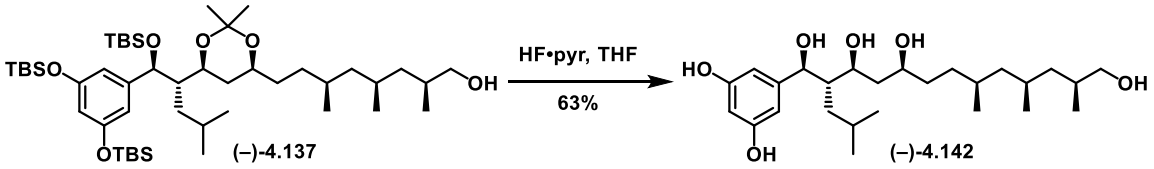

(1*S*,2*S*,3*S*,5*S*,8*S*,10*S*,12*S*)-1-(3,5-dihydroxyphenyl)-2-isobutyl-8,10,12-trimethyltridecane-1,3,5,13-tetraol (–)-4.142. Following the HF-pyridine procedure given for the preparation of compound **(–)-4.13d**, silyl ether **(–)-4.137** (36 mg, 0.043 mmol) yielded the title compound as a clear oil (12 mg, 63% yield). **^{1}H NMR** (600 MHz, CD_3OD) δ 6.33 (d, J = 2.1 Hz, 2H), 6.15 (t, J = 2.2 Hz, 1H), 4.46 (d, J = 6.9 Hz, 1H), 4.00 (dt, J = 10.0, 3.4 Hz, 1H), 3.73–3.66 (m, 1H), 3.46

(dd, *J* = 10.6, 5.1 Hz, 1H), 3.27 (dd, *J* = 10.6, 7.0 Hz, 1H), 1.92–1.85 (m, 1H), 1.78 (ddd, *J* = 14.1, 4.5, 3.2 Hz, 1H), 1.72–1.61 (m, 3H), 1.57–1.50 (m, 2H), 1.46–1.32 (m, 6H), 1.23–1.16 (m, 2H), 0.94–0.91 (m, 4H), 0.90 (d, *J* = 6.5 Hz, 3H), 0.89–0.87 (m, 4H), 0.83 (d, *J* = 6.6 Hz, 3H), 0.77 (dd, *J* = 6.5, 2.8 Hz, 3H); **^{13}C NMR** (150 MHz, CD_3OD) δ 159.3, 148.3, 106.3, 102.2, 76.9, 73.7, 72.9, 68.4, 46.5, 42.7, 41.0, 37.6, 35.7, 34.3, 33.1, 31.4, 28.8, 26.9, 23.6, 22.8, 21.3, 20.9, 18.2; **$[\alpha]_D^{20}$** –19.8 (c = 0.43 in MeOH); **HRMS** ESI (*m/z*) calcd for $C_{26}H_{46}O_6Na$ $[M+Na^+]$: 477.3192, found 477.3187.

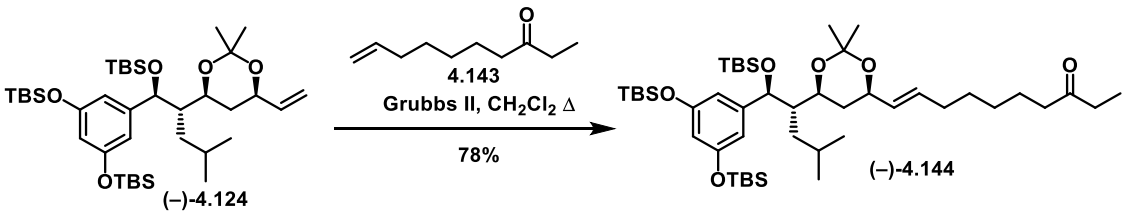

(*E*)-10-((4*R*,6*S*)-6-((1*S*,2*S*)-1-(3,5-bis((*tert*-butyldimethylsilyl)oxy)phenyl)-1-((*tert*-butyldimethylsilyl)oxy)-4-methylpentan-2-yl)-2,2-dimethyl-1,3-dioxan-4-yl)dec-9-en-3-one (–)-4.144. (synthesized by Dr. Guillaume Ernouf) To a solution of alkene **(–)-4.124** (34 mg, 0.047 mmol) and dec-9-en-3-one (15 mg, 0.094 mmol) in CH_2Cl_2 (2 mL) was added Grubbs II (2 mg, 0.002 mmol) and the reaction was heated to 40 °C. After 3 hours, another portion of Grubbs II (2 mg, 0.002 mmol) was added. The reaction was then cooled to room temperature, concentrated and purified by column chromatography, yielding the title compound as a clear oil (30 mg, 78% yield). **^{1}H NMR** (600 MHz, $CDCl_3$) δ 6.41 (d, *J* = 2.2 Hz, 2H), 6.21 (t, *J* = 2.2 Hz, 1H), 5.64 (dt, *J* = 13.3, 6.4 Hz, 1H), 5.44 (dd, *J* = 15.4, 6.5 Hz, 1H), 4.64 (d, *J* = 5.8 Hz, 1H), 4.20 (ddd, *J* = 11.0, 6.5, 1.9 Hz, 1H), 3.93 (ddd, *J* = 11.5, 5.5, 2.2 Hz, 1H), 2.41 (q, *J* = 7.3 Hz, 2H), 2.39 (t, *J* = 7.3 Hz, 2H), 2.06–1.98 (m, 2H), 1.86 (s, 1H), 1.63–1.54 (m, 2H), 1.50 (dt, *J* = 10.4, 2.5 Hz, 2H), 1.41 (s, 3H), 1.38 (s, 3H), 1.42–1.34 (m, 2H), 1.33–1.23 (m, 4H), 1.11–1.01 (m, 1H), 1.05 (t, *J* = 7.3 Hz, 3H), 0.97 (s, 18H), 0.88 (s, 9H), 0.80 (d, *J* = 6.5 Hz, 3H), 0.77 (d, *J* = 6.6 Hz, 3H), 0.17 (s, 12H), 0.01 (s, 3H), -0.22 (s, 3H); **^{13}C NMR** (150 MHz, $CDCl_3$) δ 212.0, 156.1, 145.9, 132.3,

131.2, 112.7, 111.1, 98.5, 74.7, 70.4, 69.0, 48.4, 42.5, 36.0, 35.0, 33.8, 32.2, 30.4, 29.0, 28.9, 26.3, 26.1, 25.9, 23.9, 23.2, 22.9, 20.1, 18.4, 18.3, 8.0, -4.2, -4.2, -4.4, -5.0; **$[\alpha]_D^{20}$** –9.5 (c = 1.00 in $CHCl_3$); **HRMS** ESI (*m/z*) calcd for $C_{46}H_{86}O_6Si_3Na$ $[M+Na^+]$: 841.56244, found 841.56299.

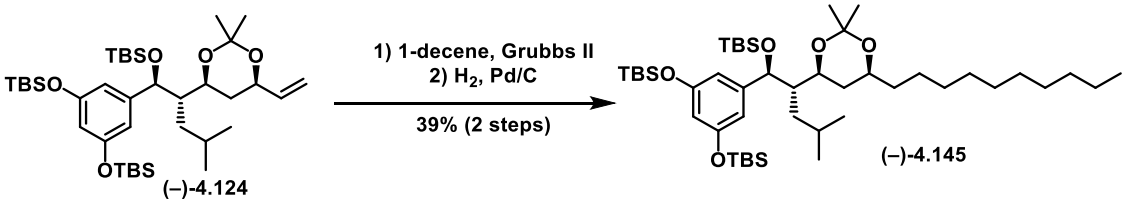

((5-((1*S*,2*S*)-1-((*tert*-butyldimethylsilyl)oxy)-2-((4*S*,6*S*)-6-decyl-2,2-dimethyl-1,3-dioxan-4-yl)-4-methylpentyl)-1,3-phenylene)bis(oxy))bis(*tert*-butyldimethylsilane) (–)-4.145. To a solution of alkene **(–)-4.124** (27 mg, 0.039 mmol) and 1-decene (0.015 mL, 0.078 mmol) in CH_2Cl_2 (2 mL) was added Grubbs II (2 mg, 0.002 mmol) and the reaction was heated to 40 °C. After 3 hours, another portion of Grubbs II (1 mg, 0.001 mmol) was added. After another hour at the same temperature, another portion of Grubbs II (1 mg, 0.001 mmol) was added. After another hour, the reaction was cooled to room temperature, and filtered through a plug of silica gel, which was washed with 9:1 hexanes:EtOAc. The mixture was concentrated and carried directly to the next step. To the crude metathesis mixture dissolved in 2:1 EtOAc:MeOH (4 mL) was added 10 % Pd/C (15 mg), and the reaction flask was purged and backfilled with H_2 3x, then stirred under an atmosphere of H_2 (balloon) overnight. The reaction was filtered over Celite, and of the residue was purified by column chromatography, yielding the title compound as a clear oil (12 mg, 39% yield over two steps). **^{1}H NMR** (600 MHz, $CDCl_3$) δ 6.41 (d, J = 2.2 Hz, 2H), 6.21 (t, J = 2.2 Hz, 1H), 4.62 (d, J = 5.9 Hz, 1H), 3.90 (ddd, J = 11.6, 5.3, 2.3 Hz, 1H), 3.73–3.66 (m, 1H), 1.87–1.82 (m, 1H), 1.54–1.48 (m, 2H), 1.36 (s, 3H), 1.35 (s, 3H), 1.31–1.22 (m, 18H), 1.11–1.00 (m, 3H), 0.97 (s, J = 3.0 Hz, 18H), 0.90–0.87 (m, 12H), 0.79 (d, J = 6.5 Hz, 3H), 0.77 (d, J = 6.5 Hz, 3H), 0.17 (s, 12H), 0.01 (s, 3H), -0.23 (s, 3H); **^{13}C NMR** (150 MHz, $CDCl_3$) δ 156.1, 146.0, 112.6, 111.0, 98.3, 74.9, 69.2, 69.1, 48.4, 36.8, 35.1, 33.3, 32.1, 30.4, 29.8, 29.8, 29.5, 26.3, 26.1, 25.9,

25.2, 23.2, 22.8, 22.8, 20.1, 18.4, 18.3, 14.3, -4.18, -4.24, -4.4, -5.0; **[α]$_D^{20}$** –10.2 (c = 1.20 in $CHCl_3$); **HRMS** ESI (*m/z*) calcd for $C_{46}H_{90}O_5Si_3Na$ [M+Na^+]: 829.5994, found 829.5988.

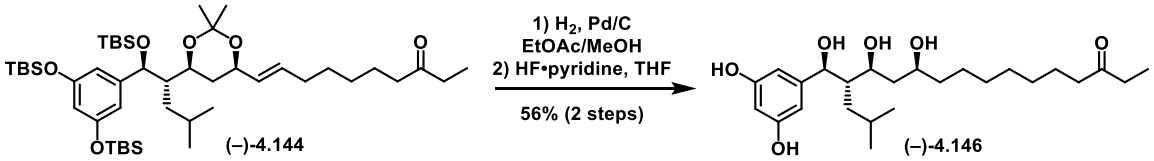

(11*S*,13*S*,14*S*)-14-((*S*)-(3,5-dihydroxyphenyl)(hydroxy)methyl)-11,13-dihydroxy-16-methylheptadecan-3-one (–)-4.146. (synthesized by Dr. Guillaume Ernouf) To a solution of alkene **(–)-4.144** (20 mg, 0.024 mmol) in EtOAc:MeOH (2/1, 5 mL) was added 10% Pd/C (2.6 mg, 0.002 mmol, 10 mol %), and the reaction flask was purged and backfilled with H_2 (3x), then stirred under an atmosphere of H_2 (balloon) for 2 hours. The reaction was filtered over Celite, and of the residue was dissolved in THF (1 mL) in a plastic tube and HF-pyridine (70%, 500 µL) was added. The reaction was allowed to warm to room temperature and stir overnight. The following day, the reaction was slowly poured into a stirring solution of sat. $NaHCO_3$ (10 mL). The solution was extracted with EtOAc 3x. The combined organic layers were washed with 1M HCl, and then washed with water repeatedly until the pH of the washes reached ~6. The organic layer was then washed with brine, dried over Na_2SO_4, filtered, concentrated, and purified by column chromatography, yielding the title compound as a clear oil (5.9 mg, 56% yield over two steps). **^{1}H NMR** (600 MHz, CD_3OD) δ 6.32 (s, 2H), 6.14 (s, 1H), 4.46 (d, *J* = 6.8 Hz, 1H), 3.99 (dt, *J* = 9.8, 3.1 Hz, 1H), 3.71 (s, 1H), 1.90–1.84 (m, 1H), 1.80–1.75 (m, 1H), 1.61–1.48 (m, 4H), 1.47–1.26 (m, 18H), 1.25–1.16 (m, 3H), 1.01 (t, *J* = 7.3 Hz, 3H), 0.83 (d, *J* = 6.5 Hz, 3H), 0.77 (d, *J* = 6.5 Hz, 3H); **^{13}C NMR** (150 MHz, CD_3OD) δ 214.2, 159.4, 148.3, 106.3, 102.2, 76.8, 73.7, 72.6, 43.1, 48.9, 40.9, 38.5, 37.6, 36.5, 30.7, 30.5, 30.3, 26.9, 26.4, 25.0, 23.6, 22.8, 8.1; **[α]$_D^{20}$** –10.0 (c = 0.16 in MeOH); **HRMS** ESI (*m/z*) calcd for $C_{25}H_{43}O_6Na$ [M+H^+]: 439.30542, found 439.30588.

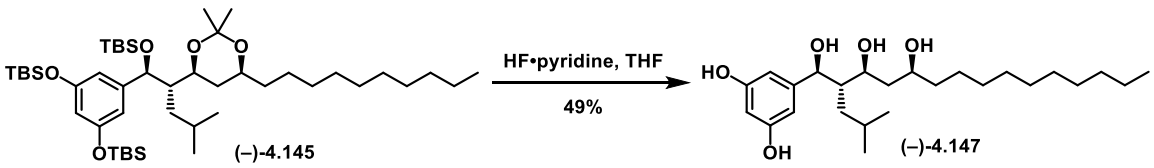

(1*S*,2*S*,3S,5*S*)-1-(3,5-dihydroxyphenyl)-2-isobutylpentadecane-1,3,5-triol (–)-4.147. Using the HF-pyridine deprotection procedure given for the preparation of compound **(–)-4.13d**, silyl ether **(–)-4.145** (18 mg, 0.022 mmol) yielded the title compound as a clear oil (4.6 mg, 49% yield). **^{1}H NMR** (600 MHz, CD_3OD) δ 6.22 (d, J = 2.1 Hz, 2H), 6.05 (t, J = 2.1 Hz, 1H), 4.36 (d, J = 6.9 Hz, 1H), 3.90 (dt, J = 9.9, 3.2 Hz, 1H), 3.65–3.58 (m, 1H), 1.80–1.74 (m, 1H), 1.71–1.64 (m, 1H), 1.46–1.38 (m, 1H), 1.37–1.25 (m, 4H), 1.20 (s, 20H), 1.15–1.05 (m, 2H), 0.80 (t, J = 7.0 Hz, 3H), 0.72 (d, J = 6.5 Hz, 3H), 0.66 (d, J = 6.5 Hz, 3H); **^{13}C NMR** (150 MHz, CD_3OD) δ 159.3, 148.3, 106.3, 102.2, 76.9, 73.7, 72.7, 48.9, 40.9, 38.6, 37.6, 33.1, 30.9, 30.8, 30.5, 26.9, 26.5, 23.8, 23.6, 22.8, 14.4; **$[\alpha]_D^{20}$** –5.4 (c = 0.17 in MeOH); **HRMS** ESI (*m/z*) calcd for $C_{25}H_{44}O_5Na$ [M+Na^+]: 447.30810, found 447.30850.

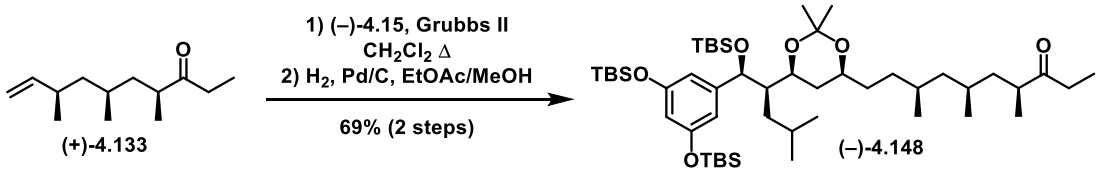

(4*S*,6*S*,8S)-10-((4*S*,6*S*)-6-((1S,2*R*)-1-(3,5-bis((*tert*-butyldimethylsilyl)oxy)phenyl)-1-((*tert*-butyldimethylsilyl)oxy)-4-methylpentan-2-yl)-2,2-dimethyl-1,3-dioxan-4-yl)-4,6,8-trimethyldecan-3-one (–)-4.148. To a solution of aromatic alkene **(–)-4.15** (40 mg, 0.058 mmol) and ethyl ketone **(+)-4.133** (23 mg, 0.115 mmol) in CH_2Cl_2 (3 mL) was added Grubbs II (2.5 mg, 0.003 mmol) and the reaction was heated to 40 °C. After 3 hours, another portion of Grubbs II (1 mg, 0.001 mmol) was added. After another hour at the same temperature, another portion of Grubbs II (1 mg, 0.001 mmol) was added. After another hour, the reaction was cooled to room temperature, and filtered through a plug of silica gel, which was washed with 9:1 hexanes:EtOAc.

The mixture was concentrated and carried directly to the next step. To the crude metathesis mixture dissolved in 2:1 EtOAc:MeOH (4 mL) was added 10% Pd/C (5 mg), and the reaction flask was purged and backfilled with H_2 3x, then stirred under an atmosphere of H_2 (balloon) overnight. The reaction was filtered over Celite, and the residue was purified by column chromatography, yielding the title compound as a clear oil (16 mg, 32% yield over two steps). **^{1}H NMR** (600 MHz, $CDCl_3$) δ 6.38 (d, J = 2.2 Hz, 2H), 6.20 (t, J = 2.0 Hz, 1H), 4.57 (d, J = 6.2 Hz, 1H), 3.61–3.53 (m, 2H), 2.69–2.63 (m, 1H), 2.51–2.37 (m, 2H), 1.73–1.66 (m, 1H), 1.60–1.55 (m, 2H), 1.52–1.45 (m, 3H), 1.41–1.37 (m, 3H), 1.35–1.32 (m, 4H), 1.32–1.27 (m, 4H), 1.26–1.23 (m, 5H), 1.07–1.00 (m, 6H), 0.97 (s, 18H), 0.87 (s, 9H), 0.85–0.81 (m, 9H), 0.78 (d, J = 6.5 Hz, 3H), 0.17 (s, 6H), 0.16 (s, 6H), 0.04 (s, 3H), -0.25 (s, 3H); **^{13}C NMR** (150 MHz, $CDCl_3$) δ 215.7, 156.0, 147.2, 112.6, 110.9, 98.3, 75.8, 69.4, 69.3, 49.6, 45.2, 43.9, 40.8, 34.9, 34.9, 34.3, 34.2, 33.9, 31.8, 30.4, 29.8, 28.2, 27.8, 26.1, 25.8, 23.1, 22.9, 20.7, 20.2, 19.8, 18.4, 18.2, 17.7, 8.0, -4.1, -4.1, -4.2, -4.6; **$[\alpha]_D^{20}$** –75.6 (c = 1.60 in $CHCl_3$); **HRMS** ESI (*m/z*) calcd for $C_{49}H_{94}O_6Si_3Na$ [$M+Na^+$]: 885.6256, found 885.6261.

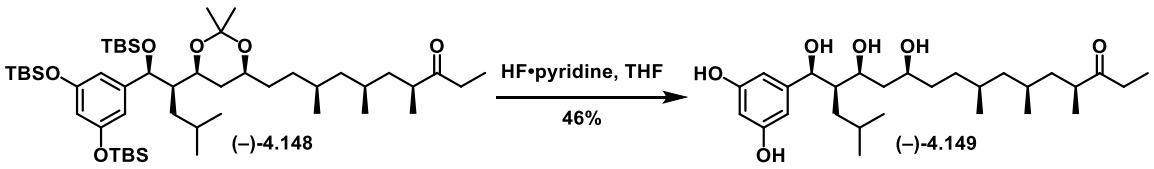

(4*S*,6*S*,8*S*,11*S*,13*S*,14*R*)-14-((*S*)-(3,5-dihydroxyphenyl)(hydroxy)methyl)-11,13-dihydroxy-4,6,8,16-tetramethylheptadecan-3-one (–)-4.149. Using the procedure given for the preparation of compound **(–)-4.13d**, silyl ether **(–)-4.418** (16 mg, 0.019 mmol) yielded the title compound as a clear oil (4.1 mg, 46% yield). **^{1}H NMR** (600 MHz, CD_3OD) δ 6.33 (d, J = 2.2 Hz, 2H), 6.13 (t, J = 2.1 Hz, 1H), 4.84 (d, J = 3.5 Hz, 1H), 4.02–3.94 (m, 1H), 3.71 (ddd, J = 11.2, 8.8, 4.1 Hz, 1H), 2.80–2.70 (m, 1H), 2.63–2.43 (m, 2H), 1.77–1.60 (m, 4H), 1.59–1.48 (m, 1H), 1.48–1.16 (m, 9H), 1.06 (d, J = 6.9 Hz, 3H), 1.03–0.92 (m, 5H), 0.88 (d, J = 6.6 Hz, 3H), 0.85 (d, J = 6.6 Hz, 3H), 0.78 (d, J = 6.0 Hz, 3H), 0.64 (d, J = 6.2 Hz, 3H); **^{13}C NMR** (150 MHz, CD_3OD) δ

218.4, 159.3, 148.6, 105.7, 101.9, 76.8, 75.0, 72.2, 46.6, 44.9, 42.3, 42.0, 35.8, 35.4, 33.3, 31.2, 29.4, 28.3, 23.4, 22.9, 20.8, 20.5, 18.2, 8.1; $[\alpha]_D^{20}$ –137.3 (c = 0.51 in MeOH); **HRMS** ESI (*m/z*) calcd for $C_{28}H_{49}O_6$ [M+H$^+$]: 481.3529, found 481.3524.

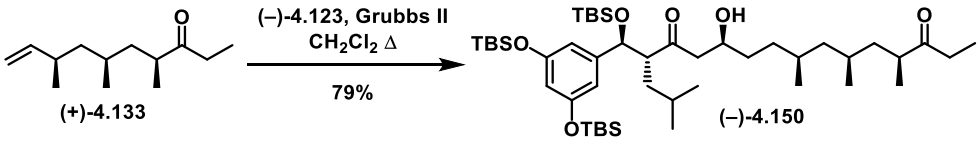

(4*S*,6*S*,8*R*,11*R*,14*R*,*E*)-14-((*S*)-(3,5-bis((*tert*-butyldimethylsilyl)oxy)phenyl)((*tert*-butyldimethylsilyl)oxy)methyl)-11-hydroxy-4,6,8,16-tetramethylheptadec-9-ene-3,13-dione (–)-4.150. (synthesized by Dr. Guillaume Ernouf) To a solution of alkene **(–)-4.123** (30 mg, 0.046 mmol) and ethyl ketone **(+)-4.133** (18 mg, 0.092 mmol) in CH_2Cl_2 (2 mL) was added Grubbs II (3 mg, 0.002 mmol, 5 mol %) and the reaction was heated to 40 °C. After 3 hours, another portion of Grubbs II (3 mg, 0.002 mmol, 5 mol %) was added. The reaction was then cooled to room temperature, concentrated and purified by column chromatography, yielding the title compound as a clear oil (29.6 mg, 79% yield). **^{1}H NMR** (600 MHz, $CDCl_3$) δ 6.40 (d, *J* = 2.1 Hz, 2H), 6.26 (t, *J* = 2.1 Hz, 1H), 5.51 (dd, *J* = 15.4, 7.9 Hz, 1H), 5.42 (dd, *J* = 15.4, 6.2 Hz, 1H), 4.56–4.46 (m, 1H), 4.49 (d, *J* = 9.4 Hz, 1H), 3.37 (s, 1H), 2.95–2.86 (m, 1H), 2.85–2.77 (m, 1H), 2.75–2.60 (m, 2H), 2.53–2.37 (m, 2H), 2.28–2.19 (m, 1H), 1.71–1.56 (m, 3H), 1.48–1.34 (m, 3H), 1.30–1.20 (m, 2H), 1.09–1.01 (m, 9H), 0.97 (s, 18H), 0.89–0.84 (m, 3H), 0.80 (s, 9H), 0.73 (d, *J* = 6.5 Hz, 3H), 0.71 (d, *J* = 6.5 Hz, 3H), 0.17 (s, 12H), -0.05 (s, 3H), -0.29 (s, 3H); **^{13}C NMR** (150 MHz, $CDCl_3$) δ 216.0, 215.6, 156.6, 144.9, 137.5, 129.5, 112.7, 112.2, 78.4, 68.5, 59.1, 52.3, 44.4, 43.7, 41.0, 38.6, 34.4, 34.0, 28.3, 26.0, 25.89, 25.85, 24.0, 21.6, 21.3, 20.2, 18.4, 18.1, 17.5, 8.0, -4.18, -4.22, -4.4, -5.1; $[\alpha]_D^{20}$ –50.0 (c = 0.5, $CHCl_3$); **HRMS** ESI (*m/z*) calcd for $C_{46}H_{86}O_6Si_3Na$ [M+Na$^+$]: 841.56244, found 841.56361.

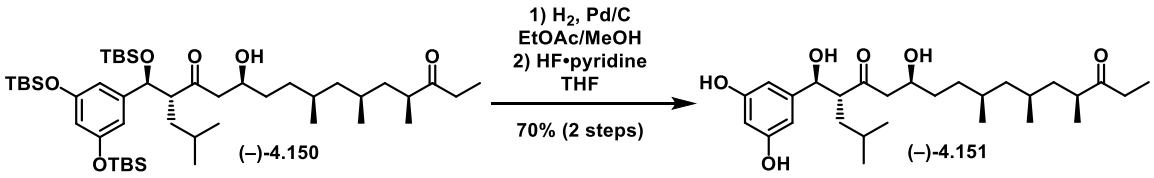

(4*S*,6*S*,8*S*,11*S*,14*R*)-14-((*S*)-(3,5-dihydroxyphenyl)(hydroxy)methyl)-11-hydroxy-4,6,8,16-tetramethylheptadecane-3,13-dione (–)-4.151. (synthesized by Dr. Guillaume Ernouf) To a solution of alkene **(–)-4.150** (20 mg, 0.024 mmol) in EtOAc/MeOH (2:1, 5 mL) was added 10 % Pd/C (2.5 mg, 0.002 mmol, 10 mol %), and the reaction flask was purged and backfilled with H_2 (3x), then stirred under an atmosphere of H_2 (balloon) for 2 h. The reaction was filtered over Celite, and of the residue was dissolved in THF (1 mL) in a plastic tube and HF-pyridine (70%, 500 µL) was added. The reaction was allowed to warm to room temperature and stir overnight. The following day, the reaction was slowly poured into a stirring solution of sat. $NaHCO_3$ (10 mL). The solution was extracted with EtOAc 3x. The combined organic layers were washed with 1M HCl, and then washed with water repeatedly until the pH of the washes reached ~6. The organic layer was then washed with brine, dried over Na_2SO_4, filtered, concentrated, and purified by column chromatography, yielding the title compound as a clear oil (8.0 mg, 70% yield over 2 steps). **^{1}H NMR** (600 MHz, CD_3OD) δ 6.30 (s, 2H), 6.19 (s, 1H), 4.45 (d, J = 9.3 Hz, 1H), 4.05 (dt, J = 11.8, 5.9 Hz, 1H), 2.93 (td, J = 10.0, 3.3 Hz, 1H), 2.81 (dd, J = 17.0, 7.1 Hz, 1H), 2.75 (dd, J = 14.3, 7.1 Hz, 1H), 2.65 (dd, J = 17.0, 4.8 Hz, 1H), 2.58 (dd, J = 17.9, 7.1 Hz, 1H), 2.48 (dd, J = 17.9, 7.3 Hz, 1H), 1.73 (ddd, J = 13.7, 9.1, 4.8 Hz, 1H), 1.60–1.34 (m, 8H), 1.34–1.26 (m, 4H), 1.26–1.17 (m, 2H), 1.06 (d, J = 6.7 Hz, 3H), 1.01 (t, J = 7.2 Hz, 3H), 0.99–0.92 (m, 2H), 0.89 (d, J = 6.6 Hz, 3H), 0.86 (d, J = 6.8 Hz, 3H), 0.78 (t, J = 7.2 Hz, 6H); **^{13}C NMR** (150 MHz, CD_3OD) δ 218.4, 215.7, 159.6, 146.6, 106.5, 103.0, 77.9, 68.7, 59.1, 51.9, 46.6, 44.9, 42.0, 39.4, 35.4, 33.6, 31.0, 29.5, 26.9, 24.1, 21.9, 20.8, 20.5, 18.2, 8.1; **$[\alpha]_D^{20}$** –8.6 (c = 0.25 in MeOH); **HRMS** ESI (*m/z*) calcd for $C_{28}H_{46}O_6Na$ [M+Na^+]: 501.31866, found 501.31865.

5.1.3 Biology: Bacterial Strains and Culture Conditions

Pseudomonas spp. were grown from freezer stocks overnight (16-24 hr) with shaking at 37°C in Tryptic Soy Broth (TSB) media (5 mL). All *S. aureus* strains were grown with the same procedure in LB. Growth curves were obtained to determine the OD of each strain in exponential growth; OD readings at 595 nm were taken every 10 minutes for 6 hours in a plate reader at 37°C with shaking and repeated in triplicate

5.1.4 Biology: Assay Procedures

IC_{50} Assay. Compounds were serially diluted in sterile DI water from a stock solution (1 mM in 10% DMSO/90% H_2O) to yield twenty-four test concentrations over the rows of two 96-well plates. Overnight cultures were diluted 1:100 in 5 mL fresh media and grown with shaking at 37 °C until exponential growth was reached. Bacteria were diluted to a concentration of 0.004 using the following equation: (x μL O/N)(OD reading) = (0.004)(volume needed) and 100 μL was inoculated into each well of a flat-bottom 96-well plate (Corning 3370) containing 100 μL of compound solution. Plates were incubated statically at 37°C for 24 hours, upon which time the OD at 595 nm was measured using a plate reader. IC_{50} values were calculated by fitting the OD readings vs. concentration with a 4 parameter logistic model. Controls were prepared by serially diluting a 10% DMSO/90% H_2O the same as the compound stock solution. Compounds were tested in triplicate from separate O/N cultures and results averaged (original inhibitory assays for promysalin were carried out by me, analogs were tested by Colleen Keohane).

Swarming Motility Assay. Hot TSB agar of the indicated concentration was poured into 6 well plates (~5 mL/well) and allowed to set open in a laminar flow hood for an hour after the surface became gelatinous (typically within 5 minutes). After the set time, a small cross was cut into the surface of the agar, and 5 μL of overnight bacterial culture was inoculated into the cross. Compound stock solution (30 μL) of the indicated concentration was absorbed into discs and

allowed to dry. Then the discs were carefully placed on top of the site of inoculation in the 6-well plate. The plates were statically incubated at 30°C, and the swarming phenotype was visualized after 20 hours. UV irradiation/visualization was performed after 48 hours of incubation.

CAS Agar Assay. CAS agar was prepared as described previously (Cordero, O. X.; Ventouras, L.; DeLong, E. F.; Polz, M. F., PNAS, **2012**, *109*, 49, 29059). 10 μL of solution at given concentration were dosed onto plates and imaged after 24 hours. Stock solutions were made in 10% DMSO/H_2O (assay performed by Colleen Keohane).

CAS Liquid Assay. To 100 μL of CAS-Fe-HDTMA dye was added 100 μL of water (control), 100 μL of 1 mM promysalin, or 100 μL 1mM EDTA with 2 μL shuttle solution (0.2 M 5-sulfosalicylic acid in water). Optical density measurements were taken at 630 nm (assay performed by Colleen Keohane).

MIC Assay Procedure. Overnight cultures of the indicated bacteria were diluted 1:100 in fresh LB media, and regrown at 37 °C with 200 rpm shaking. When the cultures reached mid-log phase, 100 μL was dosed into each well of a 96-well plate (Corning ® 96-well clear bottom plates), which contained 100 μL of serially diluted compound. Compound serial dilutions were done starting from a 10 mM stock solution in DMSO, which was diluted with LB media to arrive at the desired final concentration. 96-well plates were grown statically at 37 °C for 18 hours and growth was evaluated visually. The MIC value reflects the lowest concentration where no growth was visualized, and each assay was performed in triplicate.

For iron-depleted media, the same procedure was followed, except after cultures reached mid-log phase, they were centrifuged and the supernatant was discarded, and cells were washed 3x with LB supplemented with 750 μM of the iron chelator 2,2'-bipyridyl. The cells were suspended in the same volume as they were grown to mid-log phase in, then diluted 1:50 and

dosed into 96-well plates, all containing compounds serially diluted with chelator-supplemented media. Growth was evaluated visually as above.

Hemolysis Assay. Sheep's blood was centrifuged (0.5 mL per 10 mL of final cell volume needed) and washed with PBS until the supernatant was clear (2-3 runs typically). The washed cells were suspended in PBS (10 mL per initial 0.5 mL) and dosed into U-bottom 96-well plates (50 µL per well) which contained 10 mM DMSO stock solution of compound serially diluted with PBS, with each well containing 50 µL of compound solution, to a final volume of 100 µL. The positive control was a 1% w/v solution of Triton-X in PBS, which was diluted to a final concentration of 0.5% w/v in the highest concentration of the 96-well plate, and negative control was the DMSO corresponding to the amount for each compound test concentration. The 96-well plates were centrifuged, and 75 µL of the supernatant from each well was carefully transferred to a flat-bottom 96-well plate. The OD_{545} was recorded with a plate reader, and HC_{20} was calculated as follows: $OD_{HC20} = 0.2 * (OD_{pos} - OD_{neg}) + OD_{neg}$ where OD_{pos} refers to the OD_{545} of the 0.5% Triton-X positive control, and OD_{neg} refers to the OD_{545} in the well containing the smallest concentration of DMSO negative control. The highest concentration of compound before the OD_{545} reaches the value of OD_{HC20} is referred to as the HC_{20}.

SYTOX Uptake Assay. Bacterial overnight cultures were regrown to mid-log phase in LB media and the culture was centrifuged and washed with PBS three times. The cells were suspended in the same volume of PBS corresponding to the original regrow volume, and SYTOX green solution (5 mM in DMSO) was added to a final concentration of 5 µM, and the cells were incubated in the dark for 30 minutes. Black, clear bottom 96-well plates were serially diluted with test compounds from 10 mM DMSO stock solutions with PBS to 50 µL per well, and 50 µL of SYTOX-incubated cells were added to each well of the 96-well plate. Fluorescence readings (excitation wavelength 485 nm, emission wavelength 525 nm) were taken every 10 minutes with a plate reader. The lowest fluorescence value for each concentration of compound was subtracted

from all readings of the run to allow data to be viewed on a similar y-axis. Each graph is given with relative fluorescence units on y-axis and time in minutes on x-axis. The quaternary ammonium compound shown in the first set of data was used as the positive control. DMSO was used as a negative control for solvent, and vancomycin was used as a non-lysing negative control compound.

5.1.5 SYTOX Uptake Assay Data

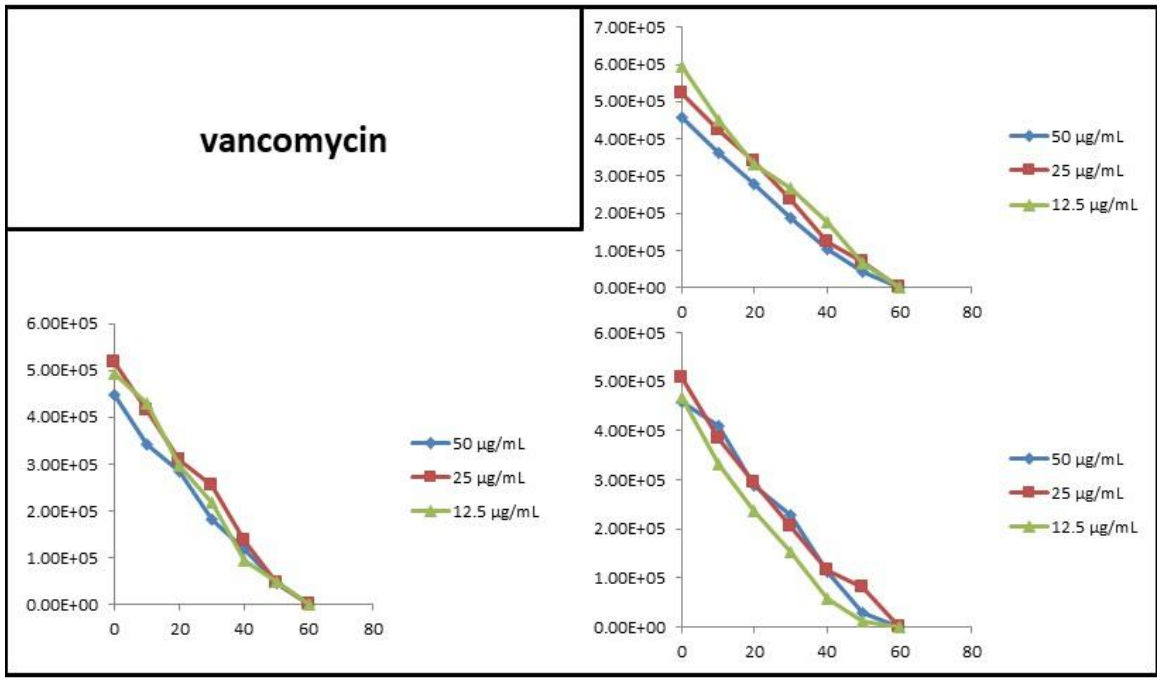

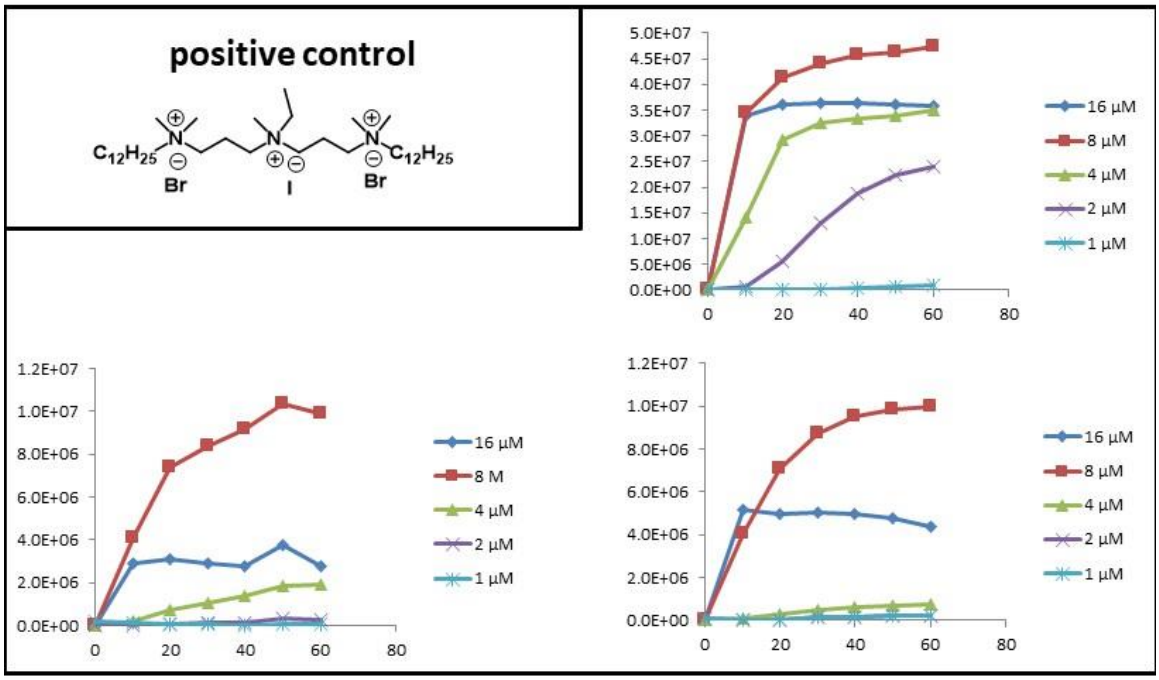
positive control
$C_{12}H_{25}$
Br
I
Br
$C_{12}H_{25}$
16 µM
8 µM
4 µM
2 µM
1 µM
16 µM
8 M
4 µM
2 µM
1 µM
16 µM
8 µM
4 µM
2 µM
1 µM

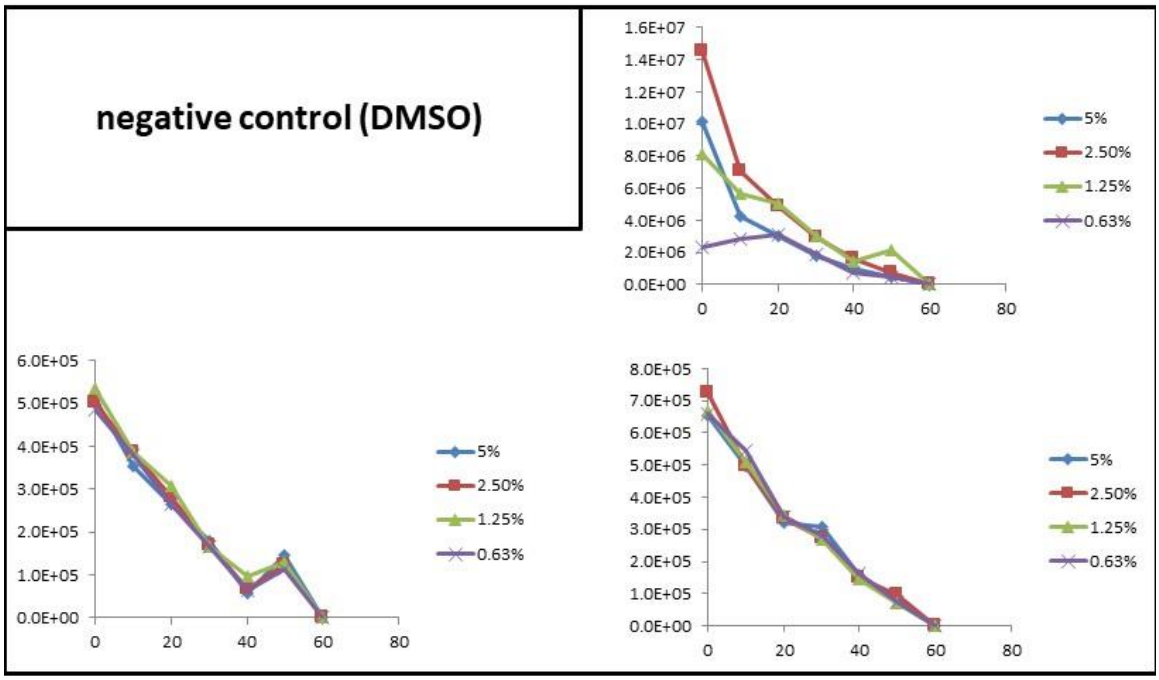
negative control (DMSO)
5%
2.50%
1.25%
0.63%
5%
2.50%
1.25%
0.63%
5%
2.50%
1.25%
0.63%

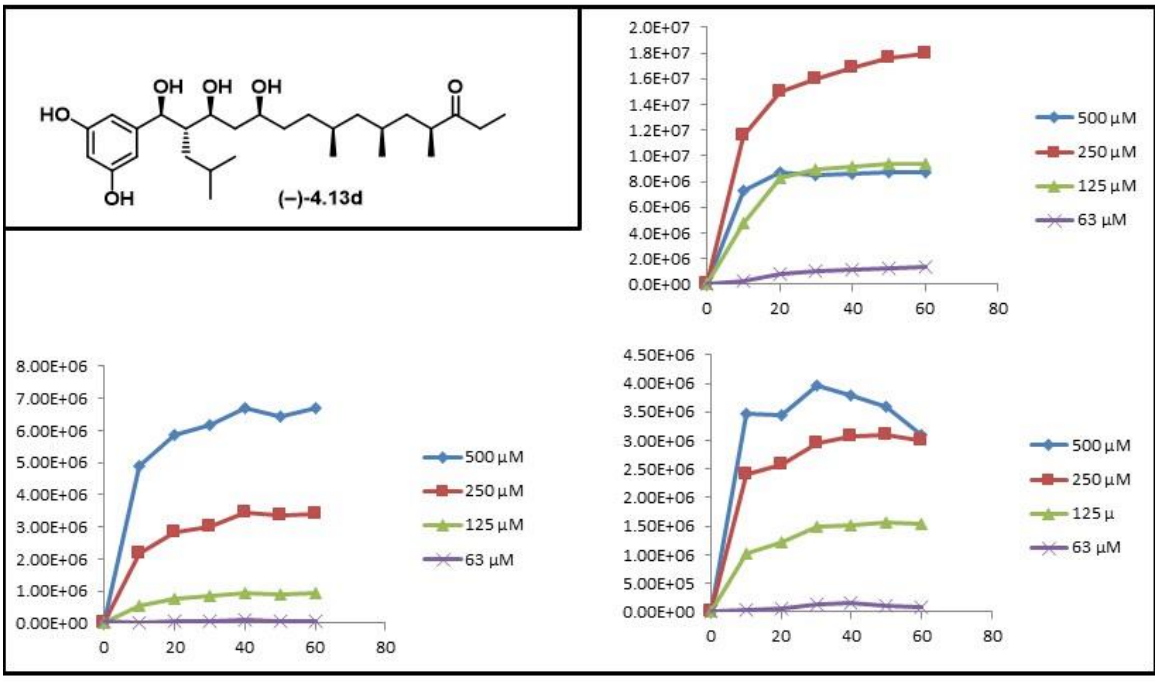
HO
OH
OH
OH
O
OH
(–)-4.13d
500 µM
250 µM
125 µM
63 µM
500 µM
250 µM
125 µ
63 µM

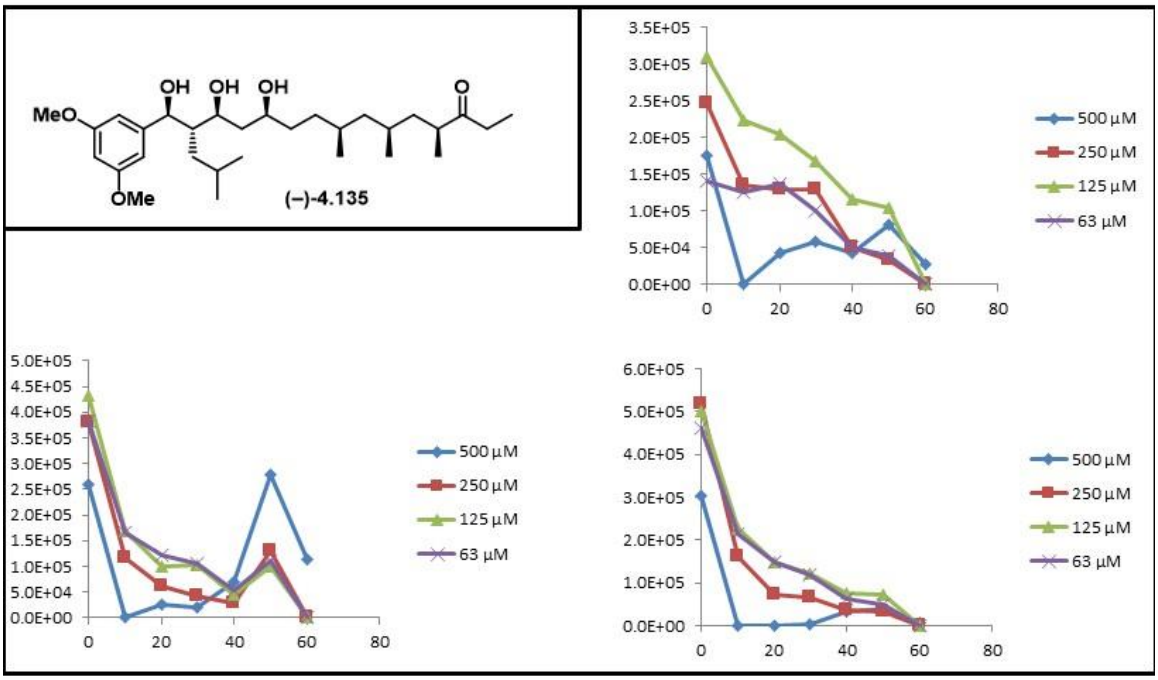
MeO
OH
OH
OH
O
OMe
(–)-4.135
500 µM
250 µM
125 µM
63 µM
500 µM
250 µM
125 µM
63 µM

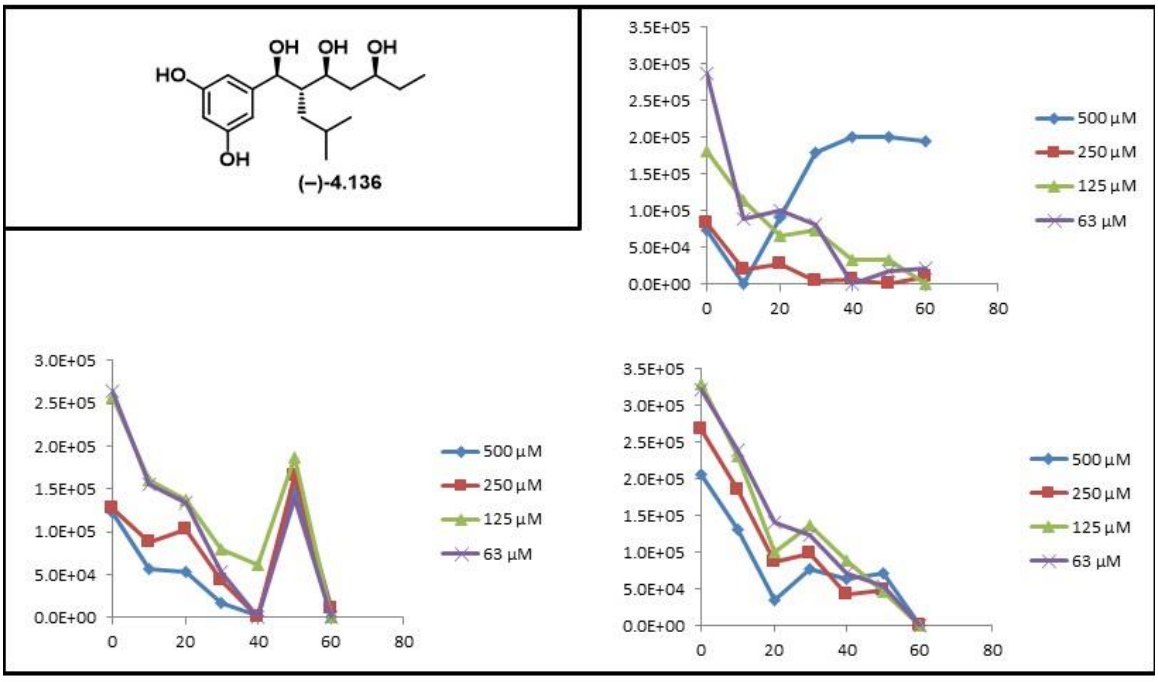
HO
OH
OH
OH
OH
(–)-4.136
3.5E+05
3.0E+05
2.5E+05
2.0E+05
1.5E+05
1.0E+05
5.0E+04
0.0E+00
0
20
40
60
80
500 µM
250 µM
125 µM
63 µM

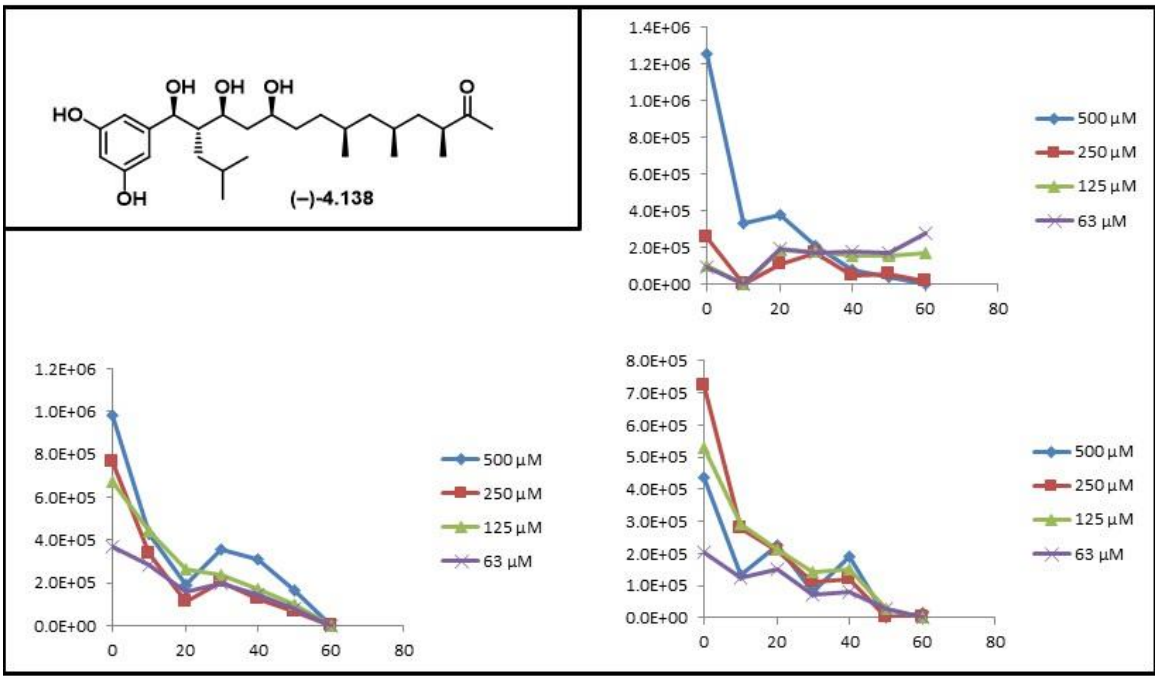
HO
OH
OH
OH
O
OH
(–)-4.138
1.4E+06
1.2E+06
1.0E+06
8.0E+05
6.0E+05
4.0E+05
2.0E+05
0.0E+00
0
20
40
60
80
500 µM
250 µM
125 µM
63 µM

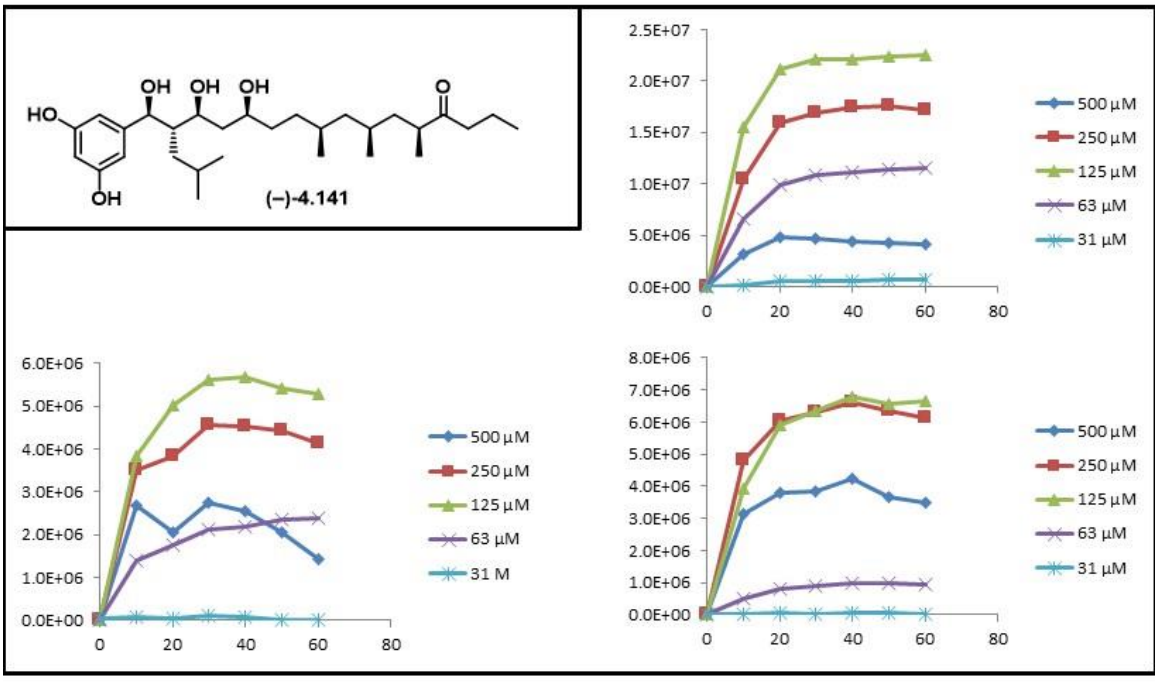
HO
OH
OH
OH
O
OH
(–)-4.141
500 µM
250 µM
125 µM
63 µM
31 µM
31 M

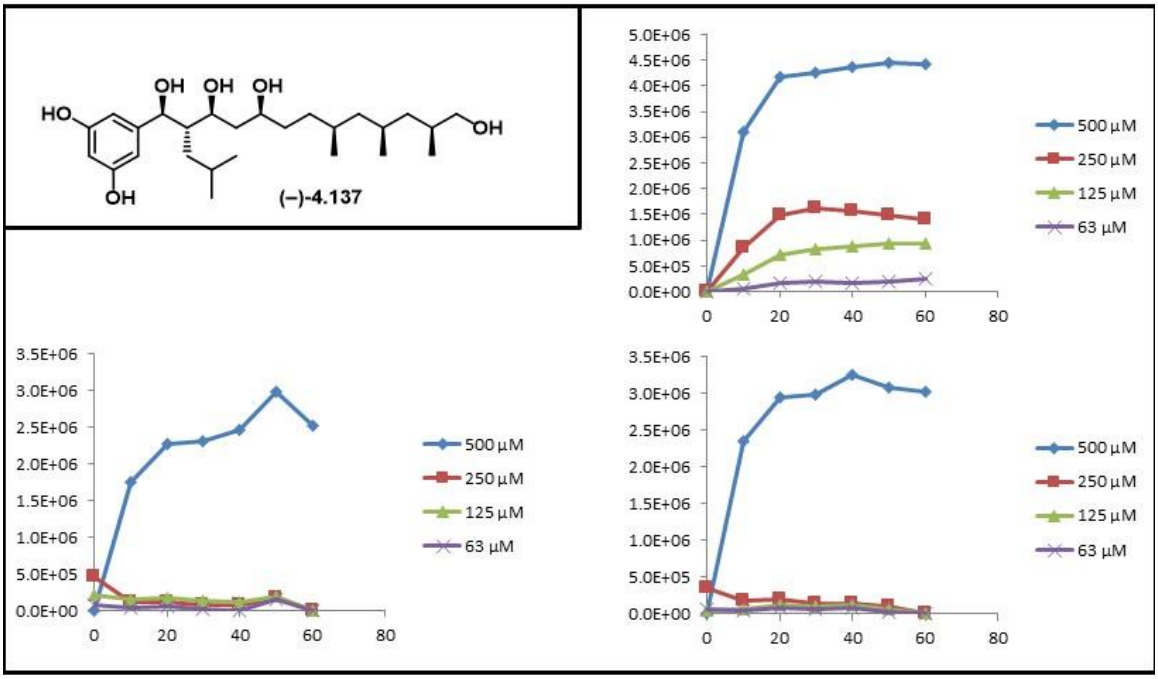
HO
OH
OH
OH
OH
OH
(–)-4.137
500 µM
250 µM
125 µM
63 µM

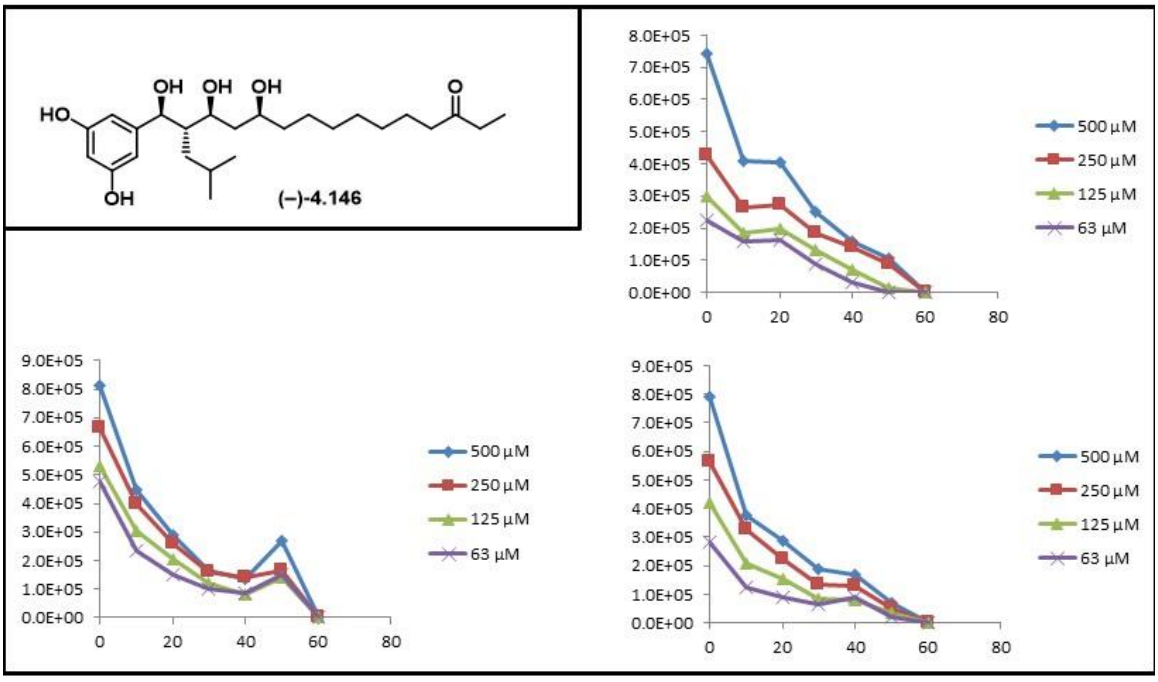
HO
OH
OH
OH
O
OH
(–)-4.146
8.0E+05
7.0E+05
6.0E+05
5.0E+05
4.0E+05
3.0E+05
2.0E+05
1.0E+05
0.0E+00
0
20
40
60
80
500 µM
250 µM
125 µM
63 µM
9.0E+05
8.0E+05
7.0E+05
6.0E+05
5.0E+05
4.0E+05
3.0E+05
2.0E+05
1.0E+05
0.0E+00
0
20
40
60
80
500 µM
250 µM
125 µM
63 µM
9.0E+05
8.0E+05
7.0E+05
6.0E+05
5.0E+05
4.0E+05
3.0E+05
2.0E+05
1.0E+05
0.0E+00
0
20
40
60
80
500 µM
250 µM
125 µM
63 µM

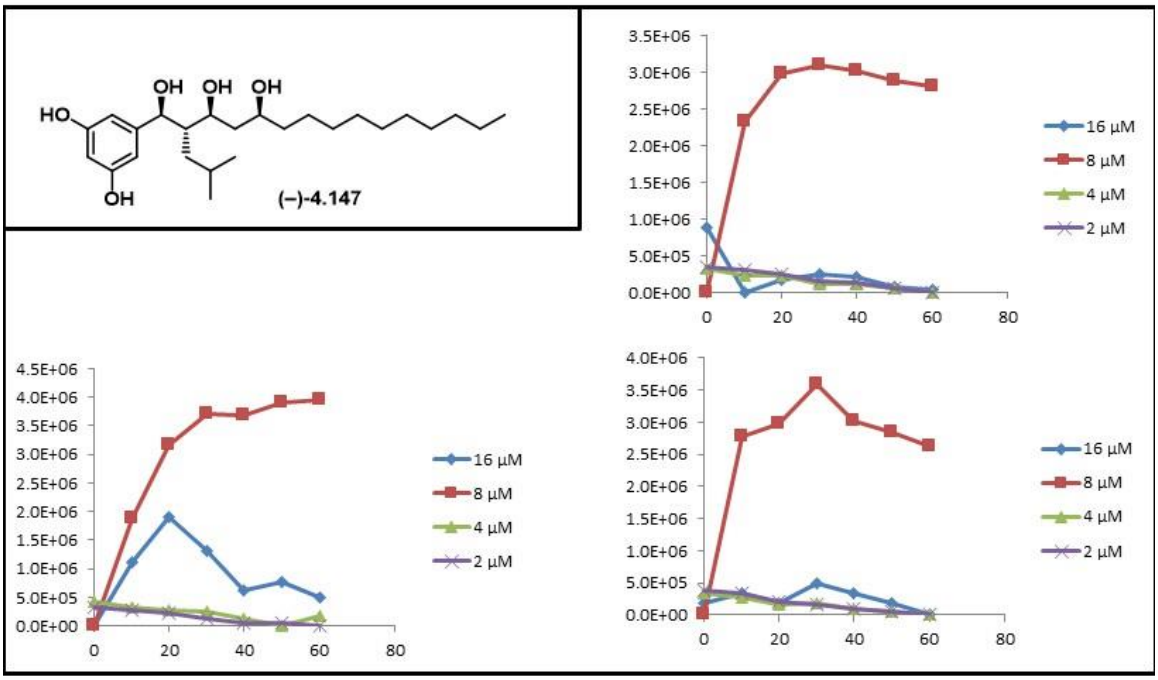
HO
OH
OH
OH
OH
(–)-4.147
3.5E+06
3.0E+06
2.5E+06
2.0E+06
1.5E+06
1.0E+06
5.0E+05
0.0E+00
0
20
40
60
80
16 µM
8 µM
4 µM
2 µM
4.5E+06
4.0E+06
3.5E+06
3.0E+06
2.5E+06
2.0E+06
1.5E+06
1.0E+06
5.0E+05
0.0E+00
0
20
40
60
80
16 µM
8 µM
4 µM
2 µM
4.0E+06
3.5E+06
3.0E+06
2.5E+06
2.0E+06
1.5E+06
1.0E+06
5.0E+05
0.0E+00
0
20
40
60
80
16 µM
8 µM
4 µM
2 µM

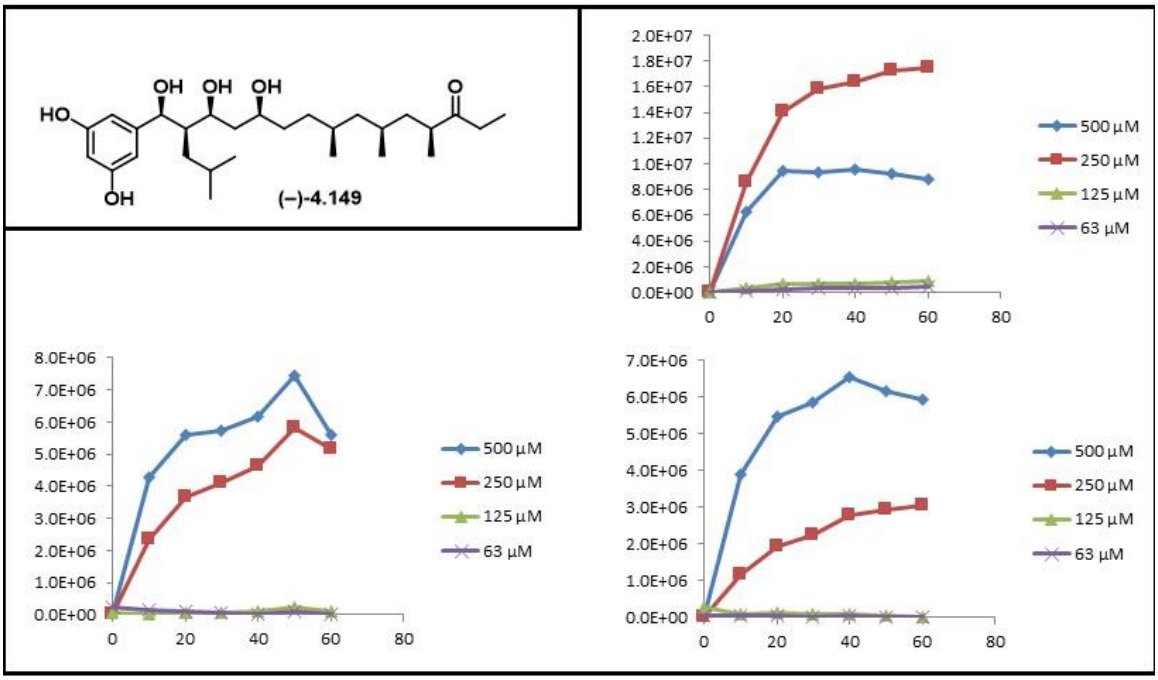

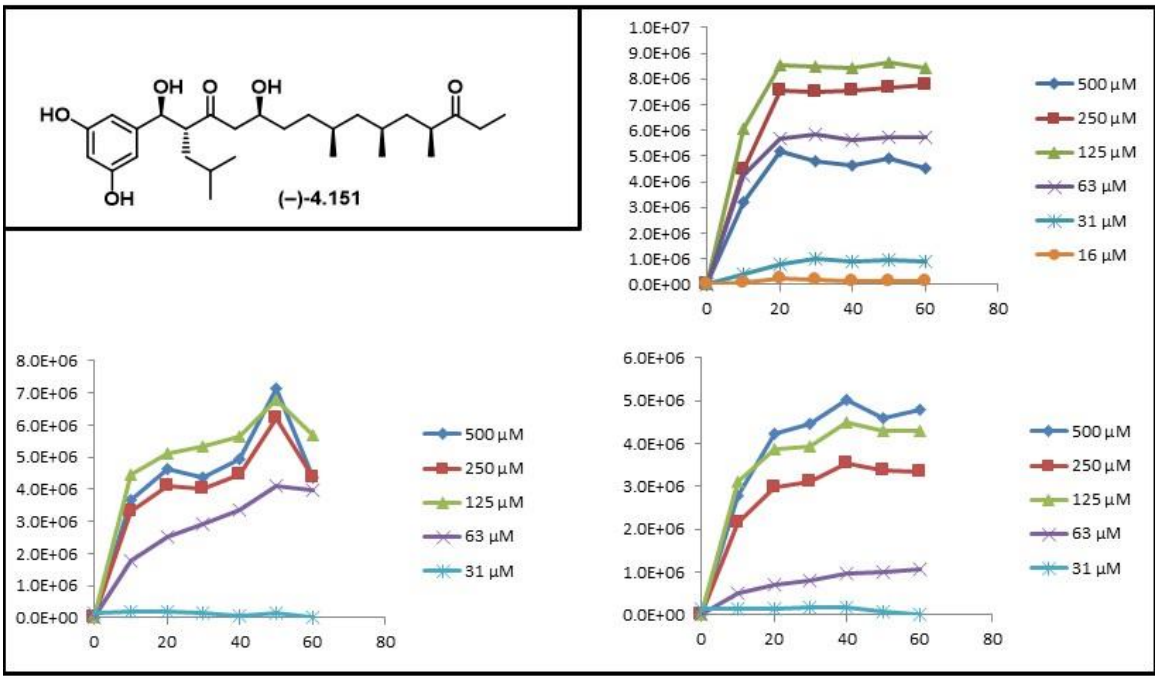

Appendix: NMR Spectra

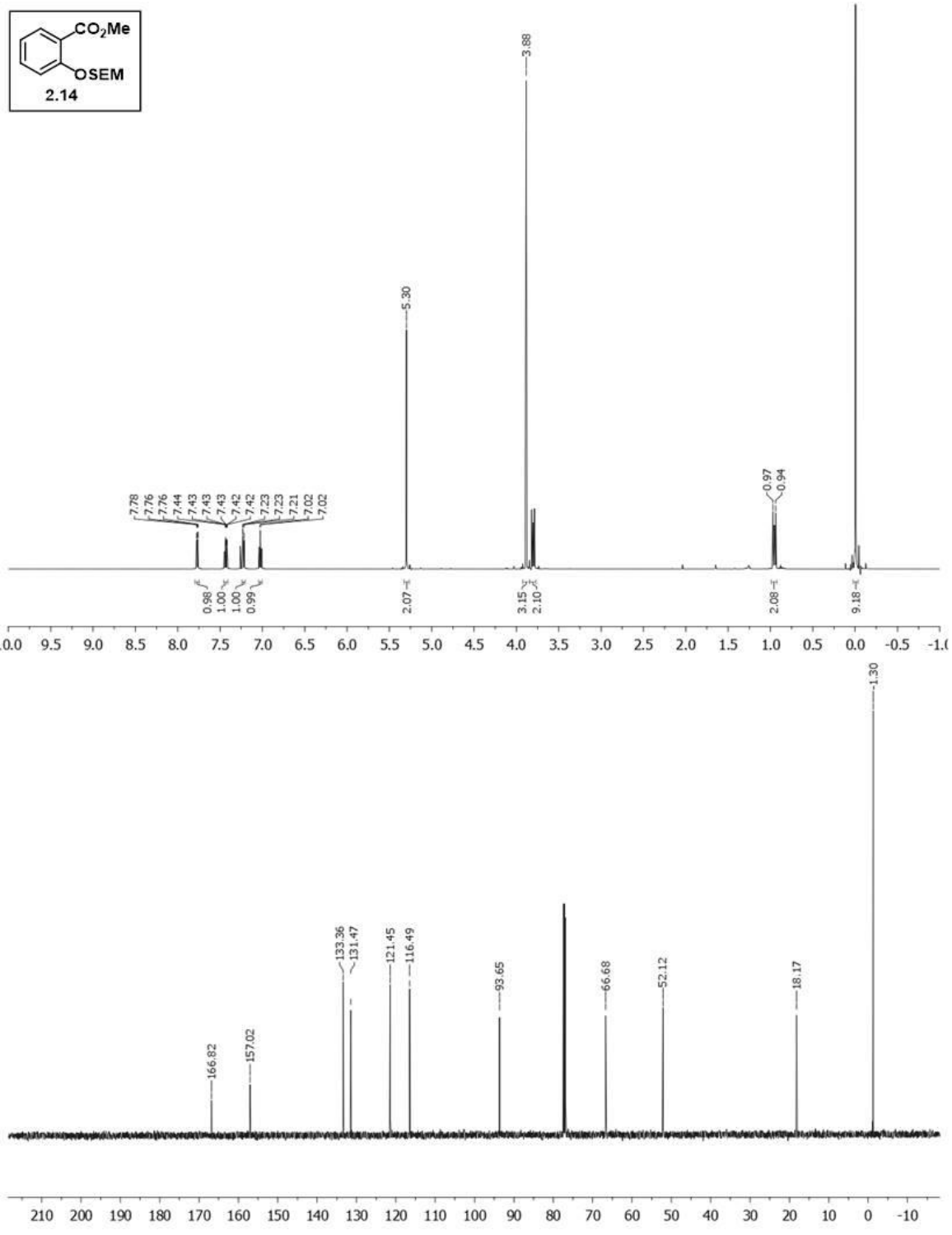
CO2Me
OSEM
2.14
7.78
7.76
7.76
7.44
7.43
7.43
7.43
7.42
7.42
7.23
7.23
7.21
7.02
7.02
5.30
3.88
0.97
0.94
0.98
1.00
1.00
0.99
2.07
3.15
2.10
2.08
9.18
1.30
166.82
157.02
133.36
131.47
121.45
116.49
93.65
66.68
52.12
18.17

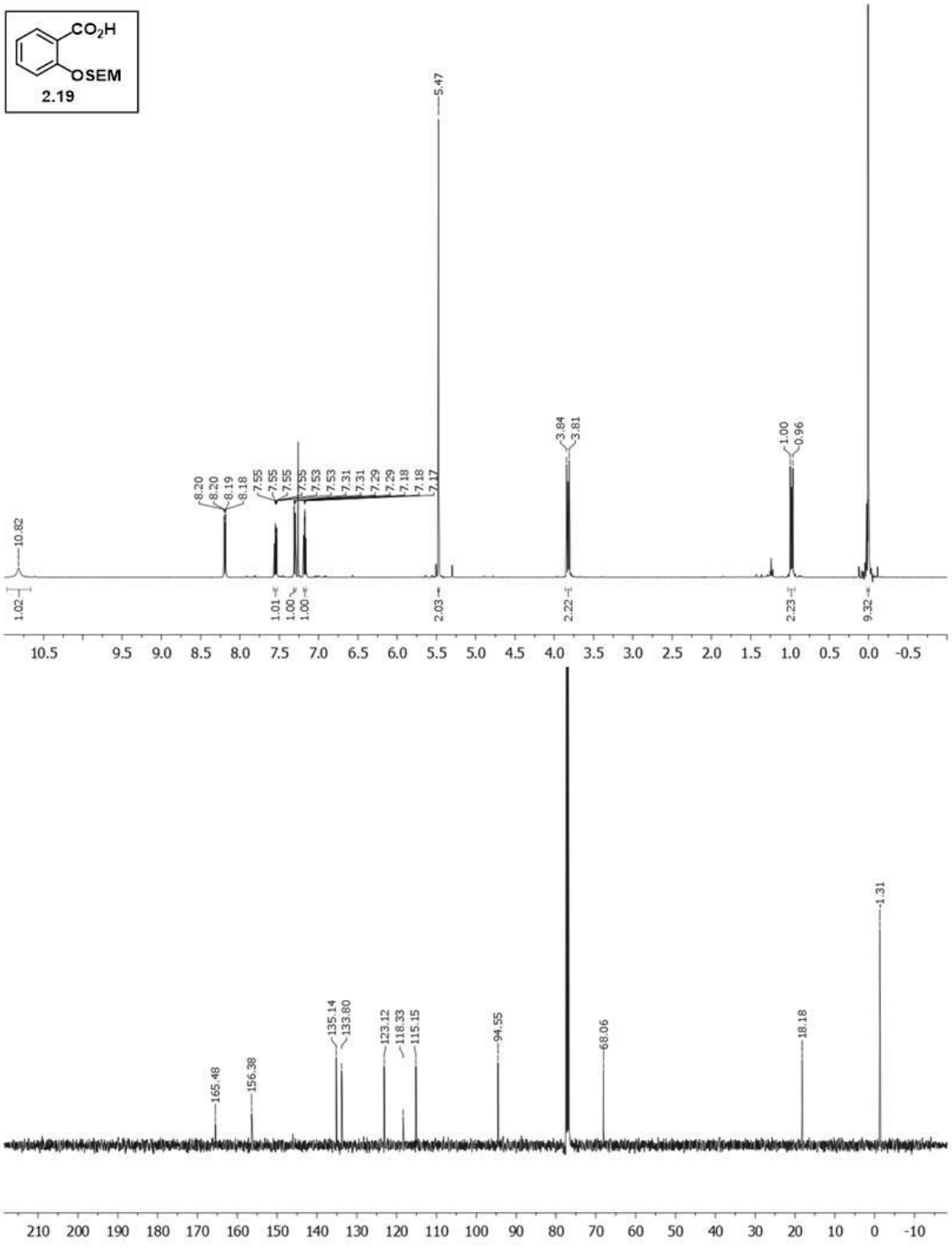
CO2H
OSEM
2.19
10.82
8.20
8.20
8.19
8.18
7.55
7.55
7.55
7.55
7.53
7.53
7.31
7.31
7.29
7.29
7.18
7.18
7.17
5.47
3.84
3.81
1.00
0.96
1.02
1.01
1.00
1.00
2.03
2.22
2.23
9.32
165.48
156.38
135.14
133.80
123.12
118.33
115.15
94.55
68.06
18.18
-1.31

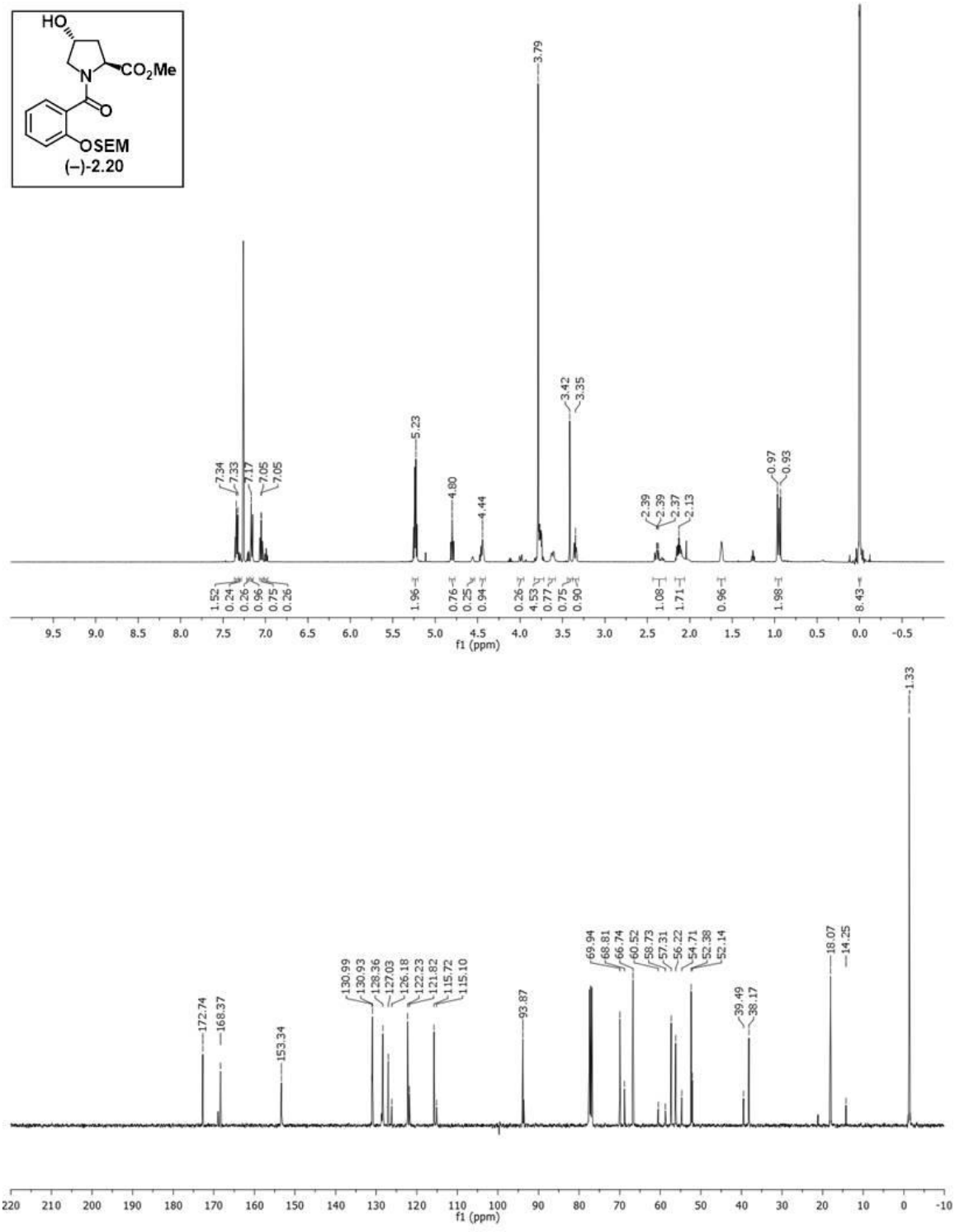
HO
CO2Me
N
O
OSEM
(–)-2.20
f1 (ppm)
f1 (ppm)

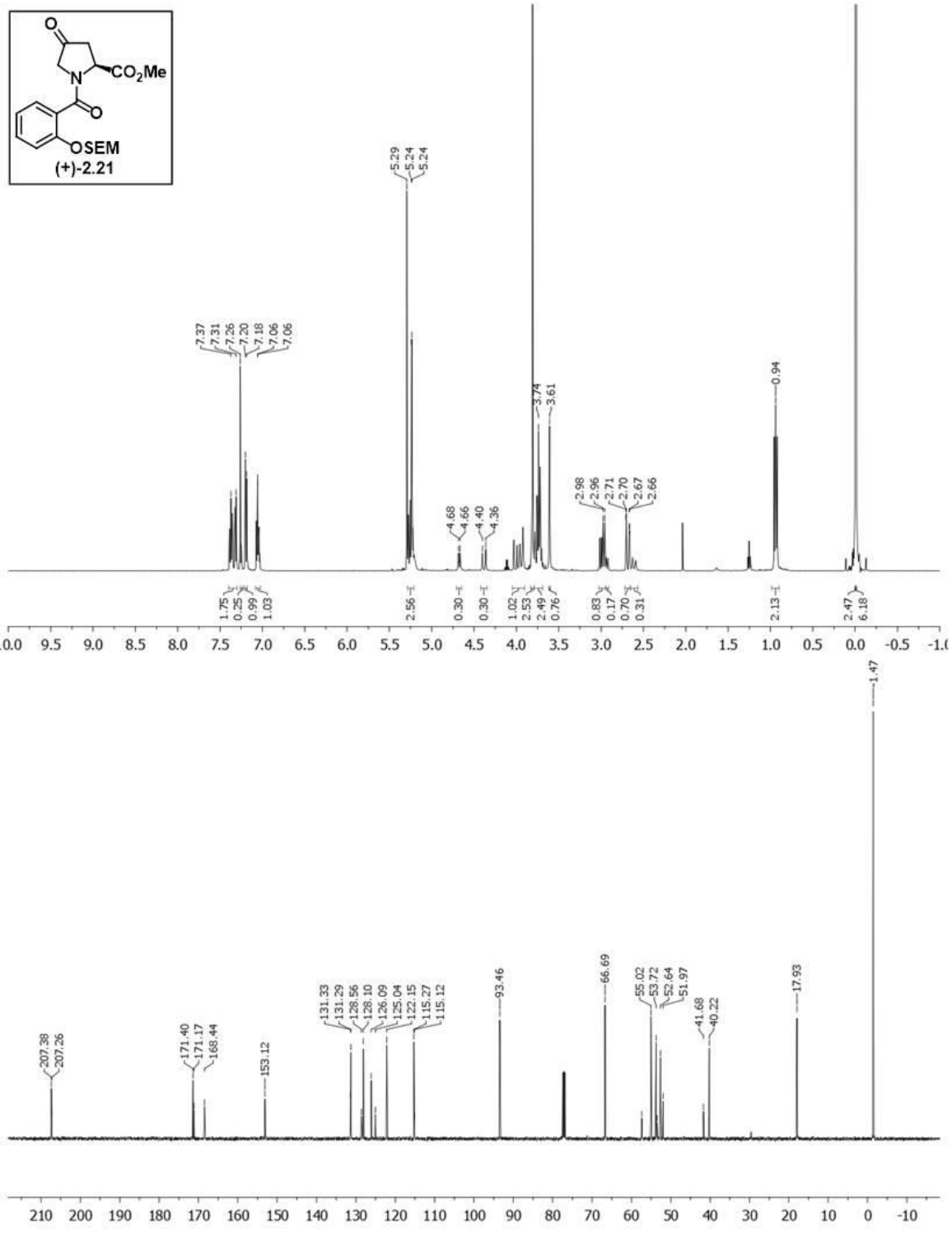
O
N
CO2Me
O
OSEM
(+)-2.21
7.37
7.31
7.26
7.20
7.18
7.06
7.06
5.29
5.24
5.24
4.68
4.66
4.40
4.36
3.74
3.61
2.98
2.96
2.71
2.70
2.67
2.66
0.94
1.75
0.25
0.99
1.03
2.56
0.30
0.30
1.02
2.53
2.49
0.76
0.83
0.17
0.70
0.31
2.13
2.47
6.18
207.38
207.26
171.40
171.17
168.44
153.12
131.33
131.29
128.56
128.10
126.09
125.04
122.15
115.27
115.12
93.46
66.69
55.02
53.72
52.64
51.97
41.68
40.22
17.93
1.47

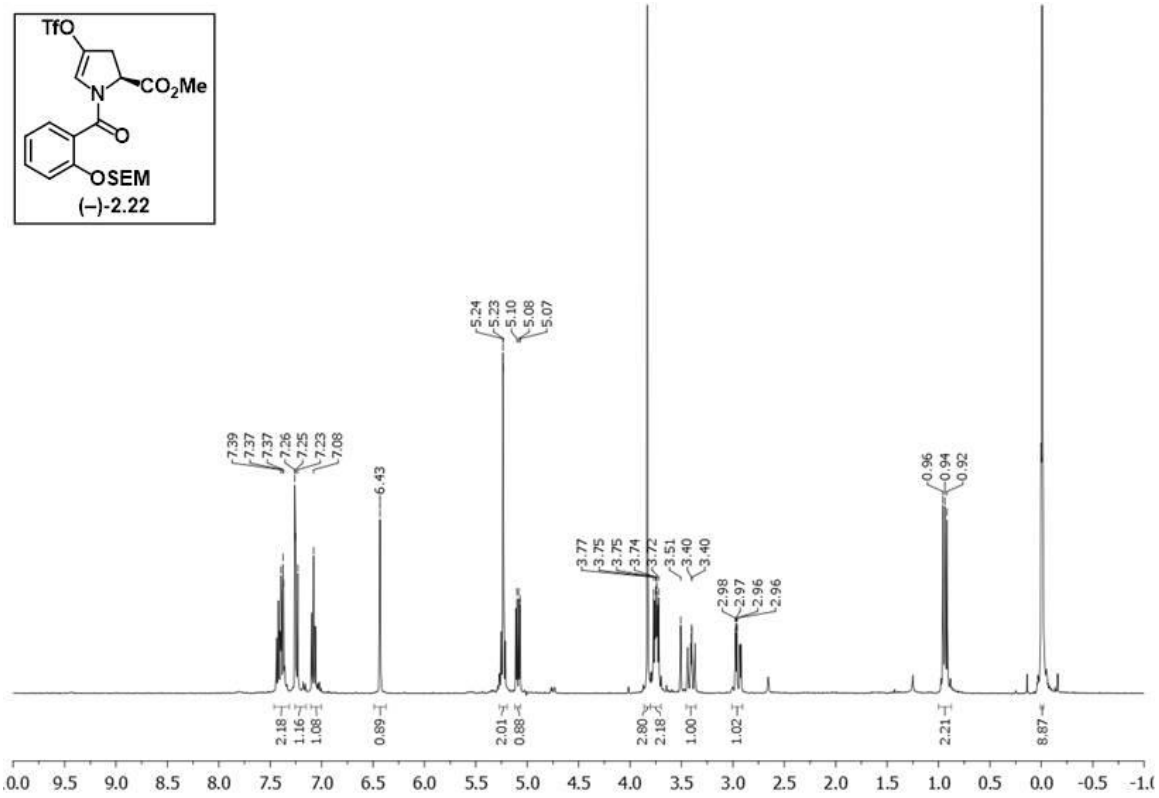
TfO
CO2Me
N
O
OSEM
(–)-2.22
7.39
7.37
7.37
7.26
7.25
7.23
7.08
6.43
5.24
5.23
5.10
5.08
5.07
3.77
3.75
3.75
3.74
3.72
3.51
3.40
3.40
2.98
2.97
2.96
2.96
0.96
0.94
0.92
2.18
1.16
1.08
0.89
2.01
0.88
2.80
2.18
1.00
1.02
2.21
8.87

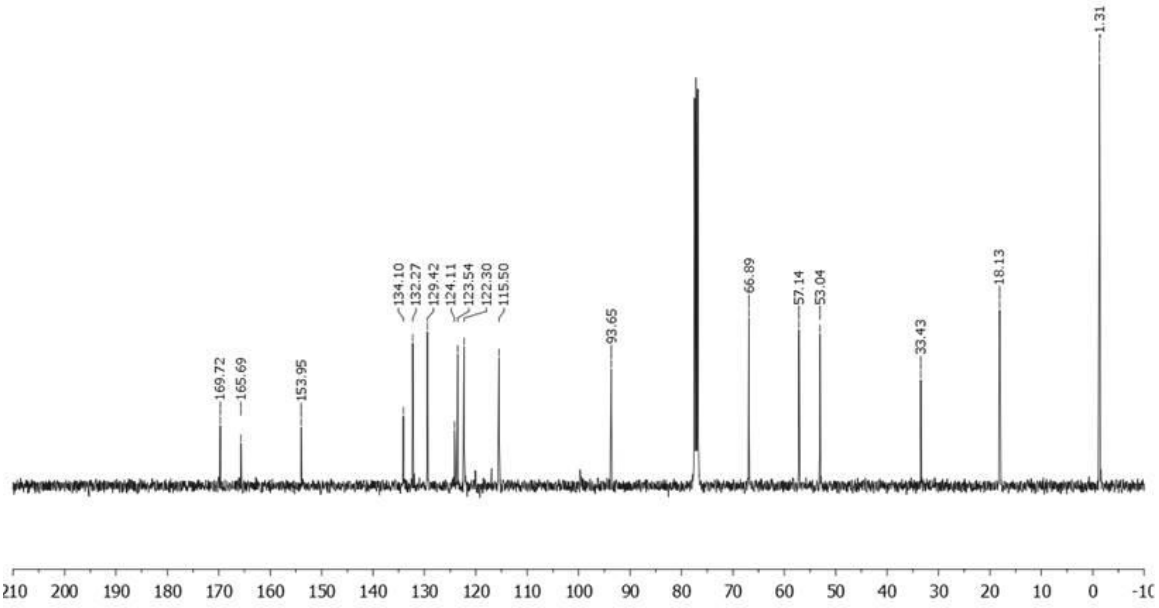
169.72
165.69
153.95
134.10
132.27
129.42
124.11
123.54
122.30
115.50
93.65
66.89
57.14
53.04
33.43
18.13
1.31

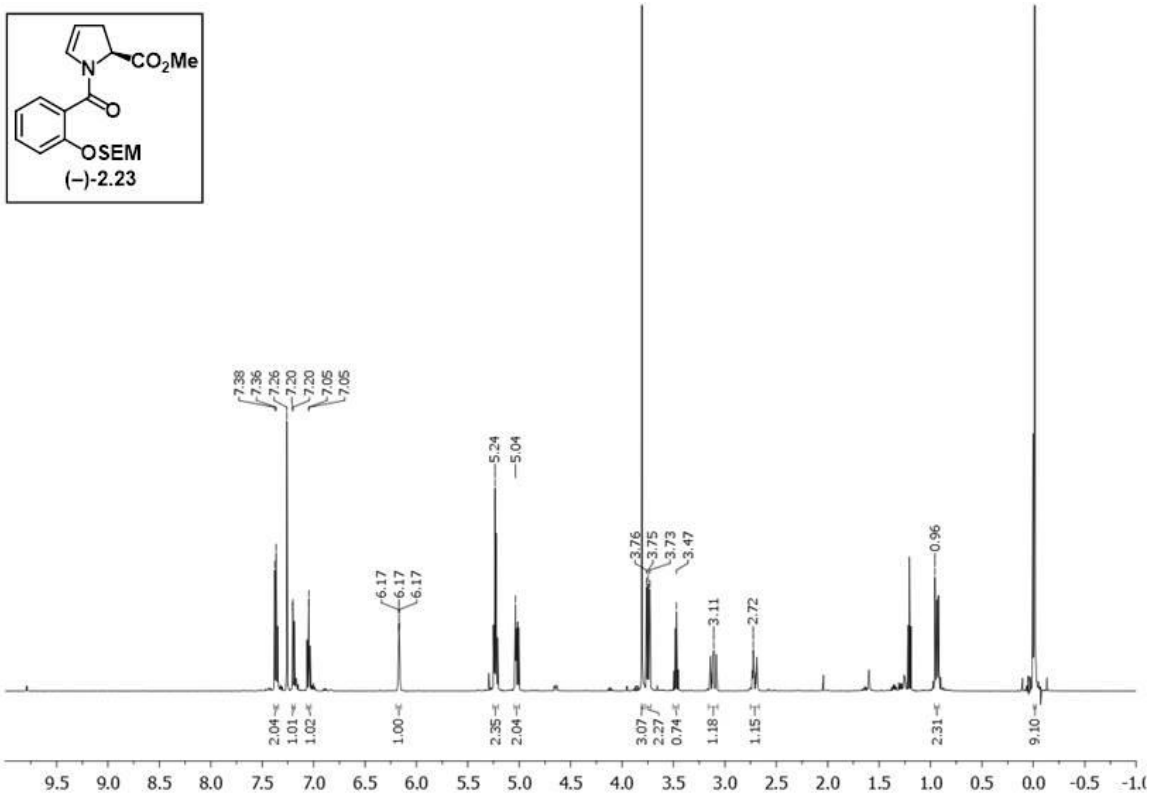
CO2Me
N
O
OSEM
(–)-2.23
7.38
7.36
7.26
7.20
7.20
7.05
7.05
6.17
6.17
6.17
5.24
5.04
3.76
3.75
3.73
3.47
3.11
2.72
0.96
2.04
1.01
1.02
1.00
2.35
2.04
3.07
2.27
0.74
1.18
1.15
2.31
9.10

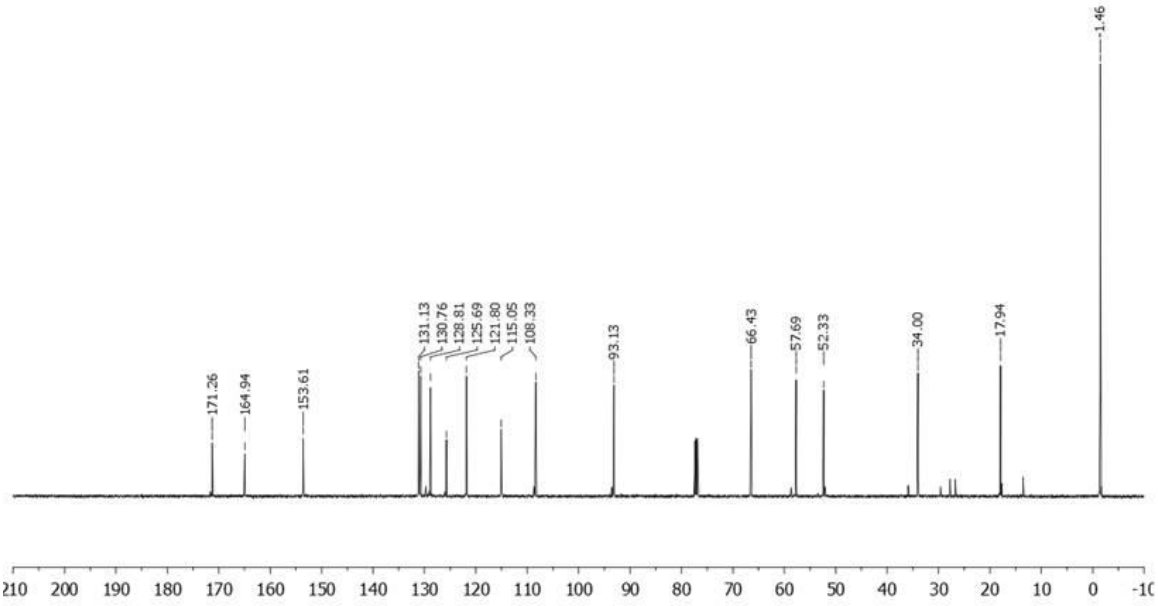
171.26
164.94
153.61
131.13
130.76
128.81
125.69
121.80
115.05
108.33
93.13
66.43
57.69
52.33
34.00
17.94
1.46

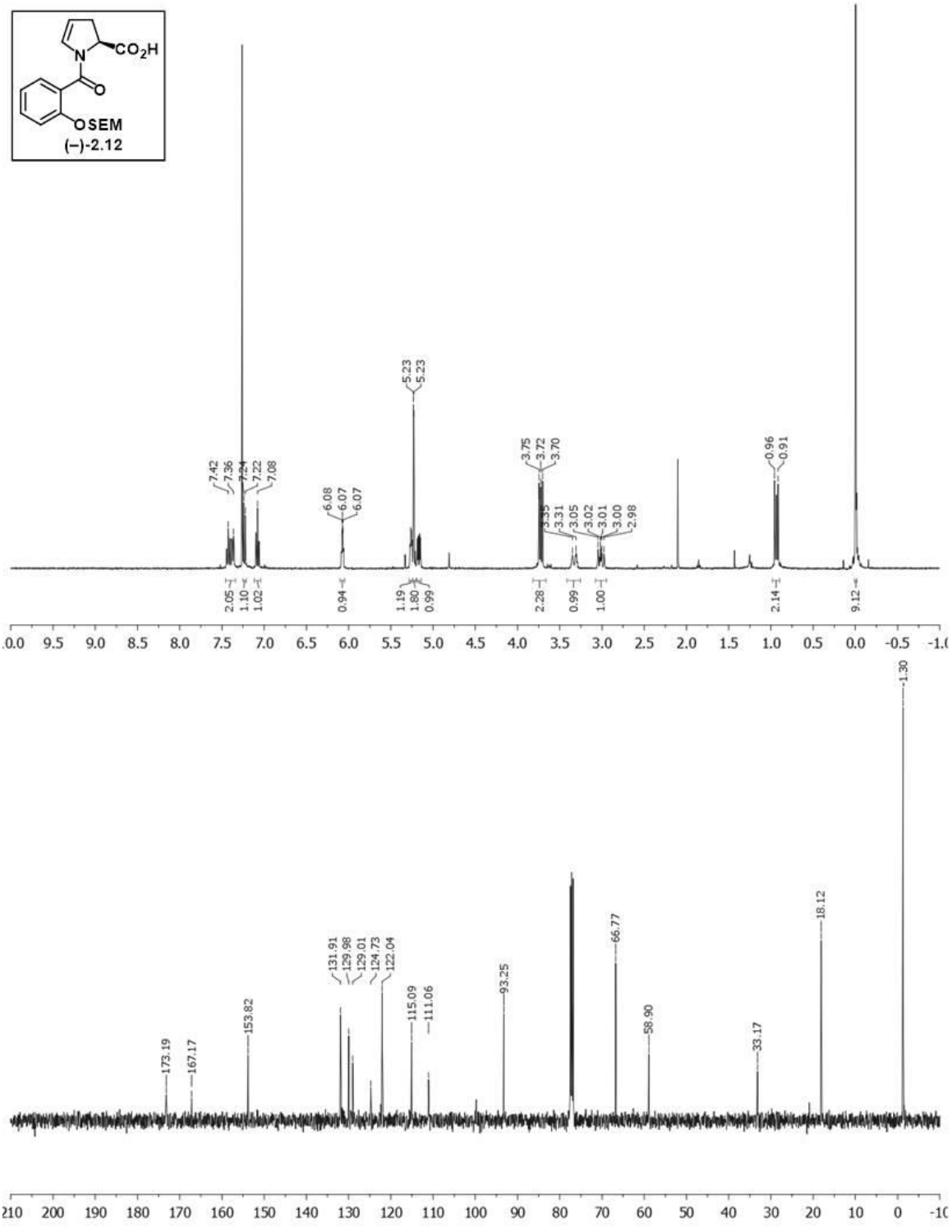
CO2H
N
O
OSEM
(–)-2.12
7.42
7.36
7.24
7.22
7.08
6.08
6.07
6.07
5.23
5.23
3.75
3.72
3.70
3.35
3.31
3.05
3.02
3.01
3.00
2.98
0.96
0.91
2.05
1.10
1.02
0.94
1.19
1.80
0.99
2.28
0.99
1.00
2.14
9.12
131.91
129.98
129.01
124.73
122.04
115.09
111.06
93.25
66.77
58.90
33.17
18.12
1.30
173.19
167.17
153.82

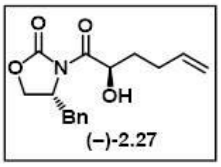
O
O
O
N
OH
Bn

(–)-2.27

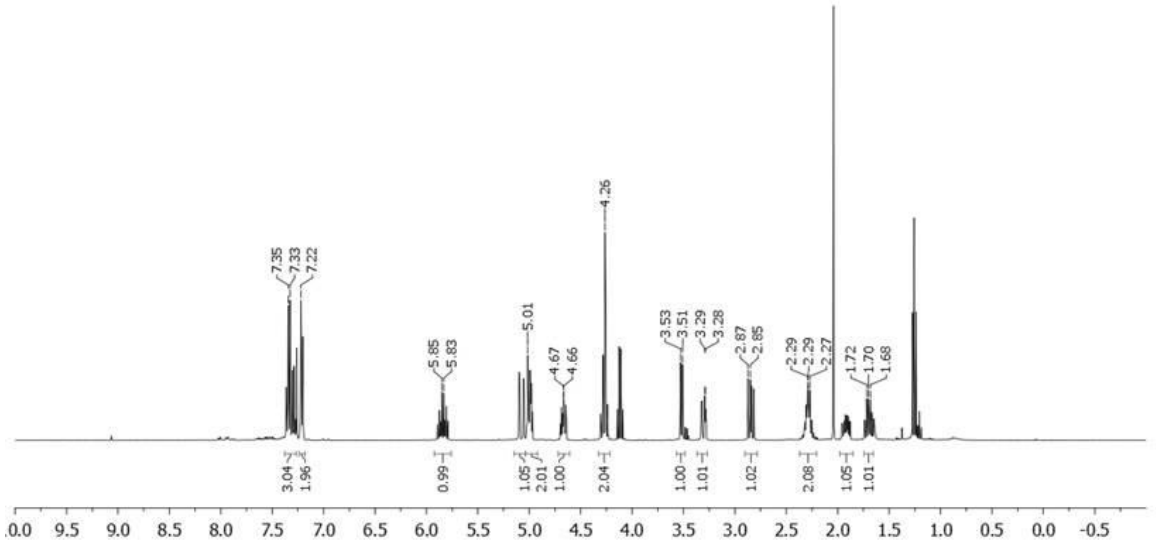
7.35
7.33
7.22
5.85
5.83
5.01
4.67
4.66
4.26
3.53
3.51
3.29
3.28
2.87
2.85
2.29
2.29
2.27
1.72
1.70
1.68
3.04
1.96
0.99
1.05
2.01
1.00
2.04
1.00
1.01
1.02
2.08
1.05
1.01

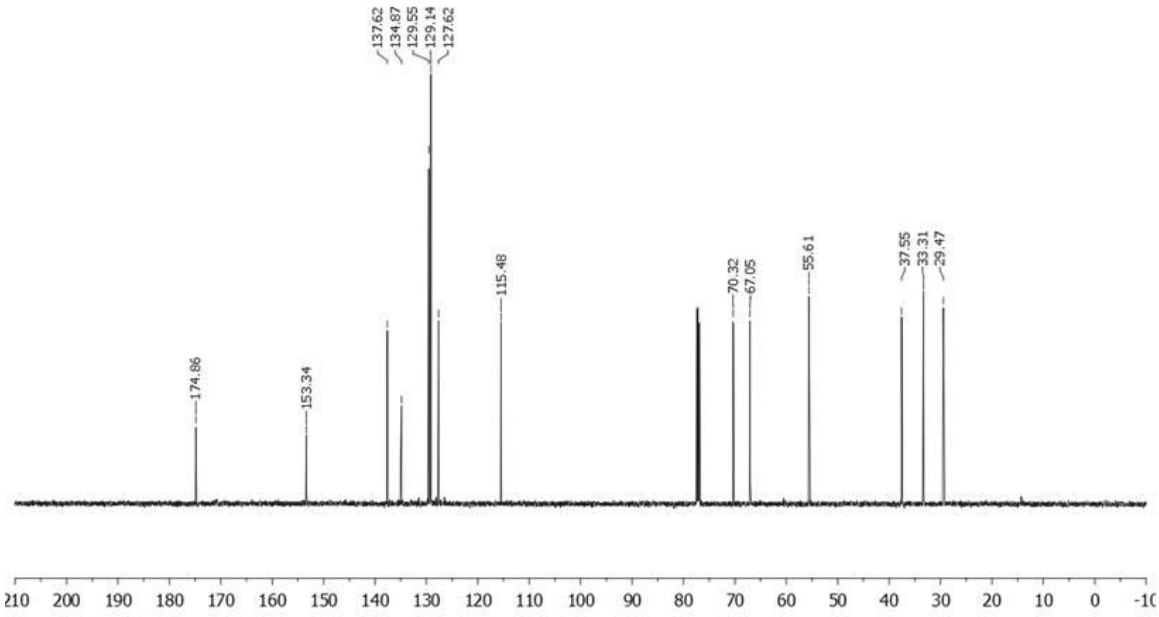
137.62
134.87
129.55
129.14
127.62
115.48
70.32
67.05
55.61
37.55
33.31
29.47
174.86
153.34

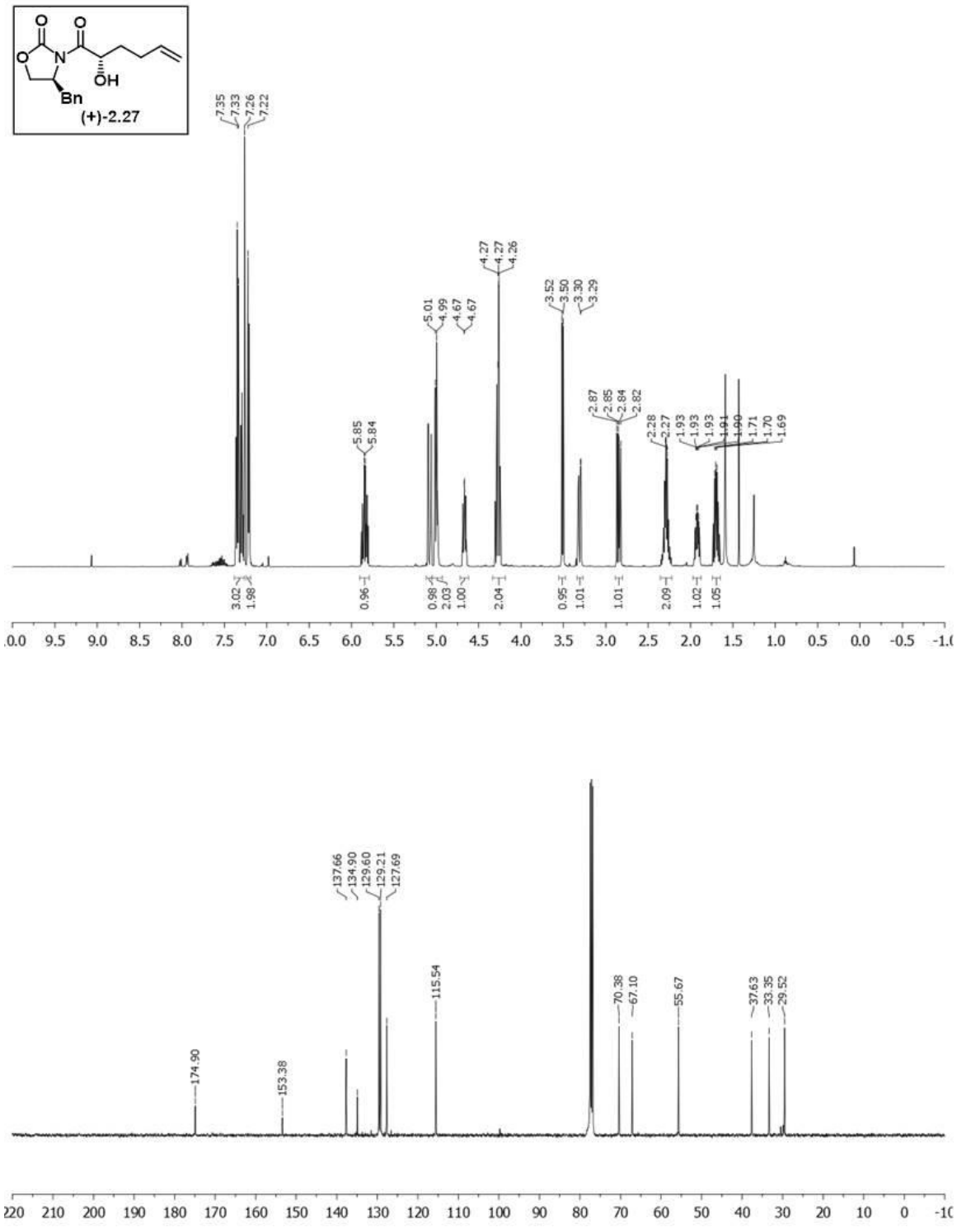
(+)-2.27
Bn
OH
7.35
7.33
7.26
7.22
5.85
5.84
5.01
4.99
4.67
4.67
4.27
4.27
4.26
3.52
3.50
3.30
3.29
2.87
2.85
2.84
2.82
2.28
2.27
1.93
1.93
1.93
1.91
1.90
1.71
1.70
1.69
3.02
1.98
0.96
0.98
2.03
1.00
2.04
0.95
1.01
1.01
2.09
1.02
1.05
137.66
134.90
129.60
129.21
127.69
115.54
174.90
153.38
70.38
67.10
55.67
37.63
33.35
29.52

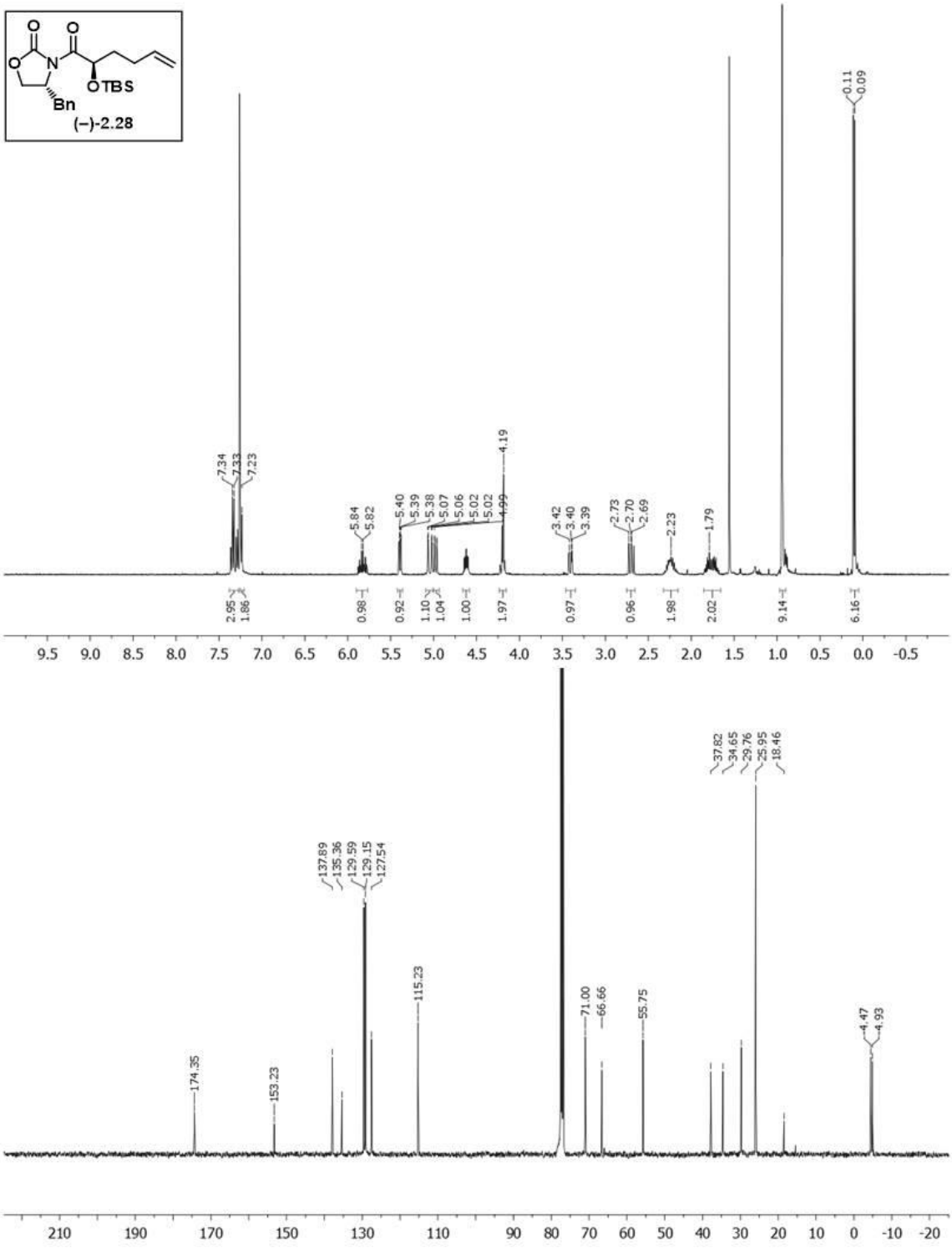
(−)-2.28
OTBS
Bn
7.34
7.33
7.23
5.84
5.82
5.40
5.39
5.38
5.07
5.06
5.02
5.02
4.99
4.19
3.42
3.40
3.39
2.73
2.70
2.69
2.23
1.79
0.11
0.09
2.95
1.86
0.98
0.92
1.10
1.04
1.00
1.97
0.97
0.96
1.98
2.02
9.14
6.16
174.35
153.23
137.89
135.36
129.59
129.15
127.54
115.23
71.00
66.66
55.75
37.82
34.65
29.76
25.95
18.46
-4.47
-4.93

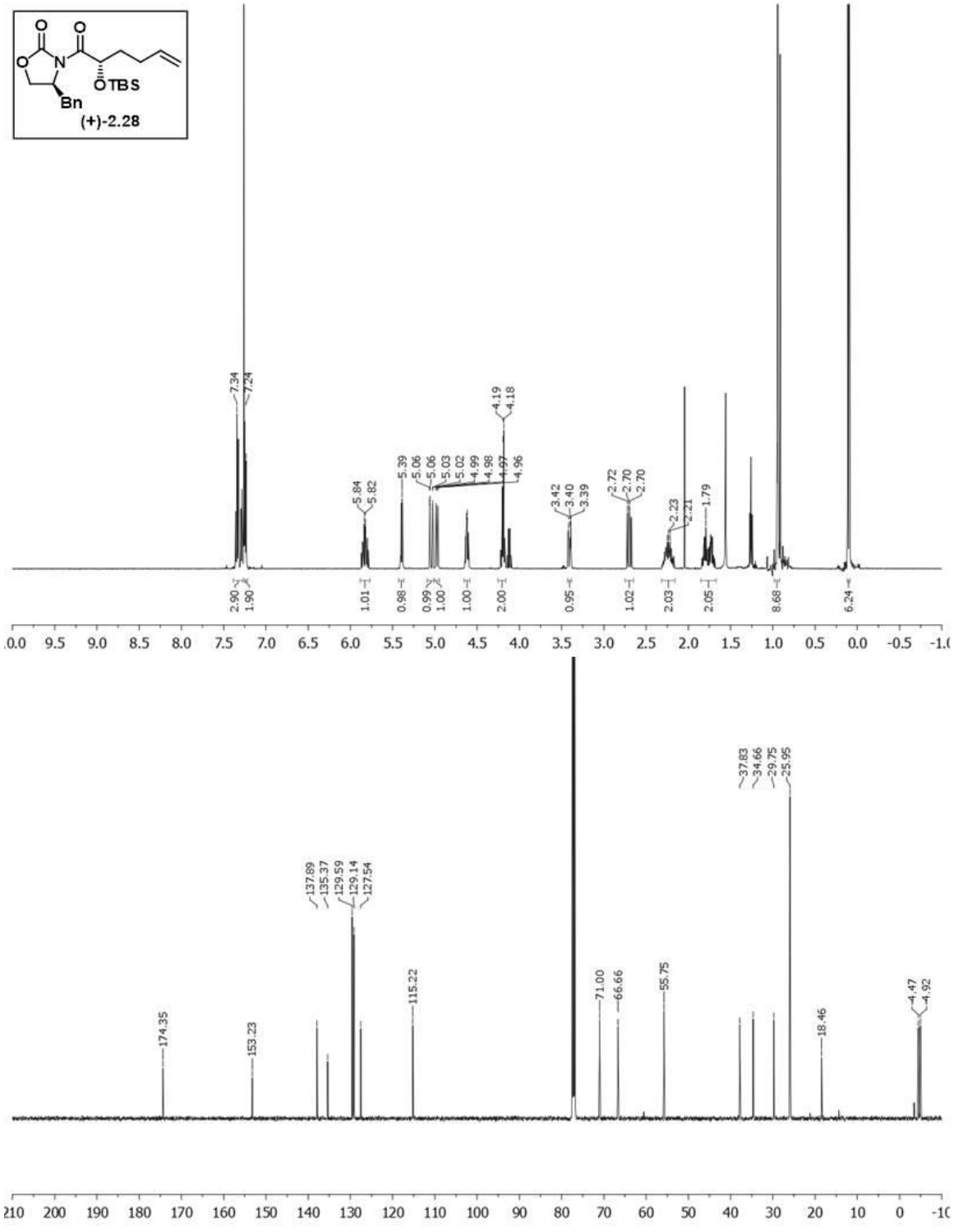
(+)-2.28
OTBS
Bn
7.34
7.24
5.84
5.82
5.39
5.06
5.06
5.03
5.02
4.99
4.98
4.97
4.96
4.19
4.18
3.42
3.40
3.39
2.72
2.70
2.70
2.23
2.21
1.79
2.90
1.90
1.01
0.98
0.99
1.00
1.00
2.00
0.95
1.02
2.03
2.05
8.68
6.24
174.35
153.23
137.89
135.37
129.59
129.14
127.54
115.22
71.00
66.66
55.75
37.83
34.66
29.75
25.95
18.46
14.47
14.92

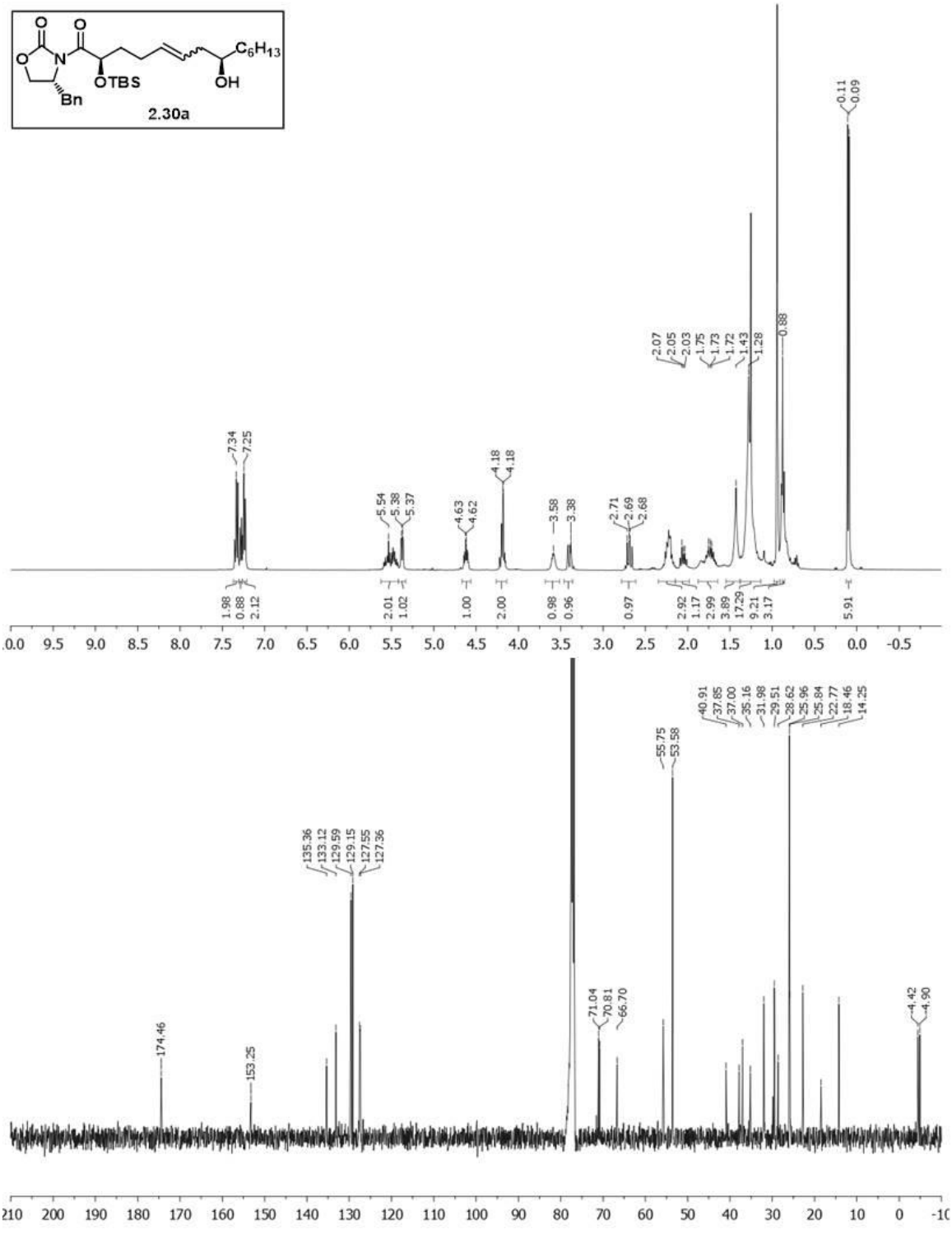
OTBS
OH
Bn
2.30a

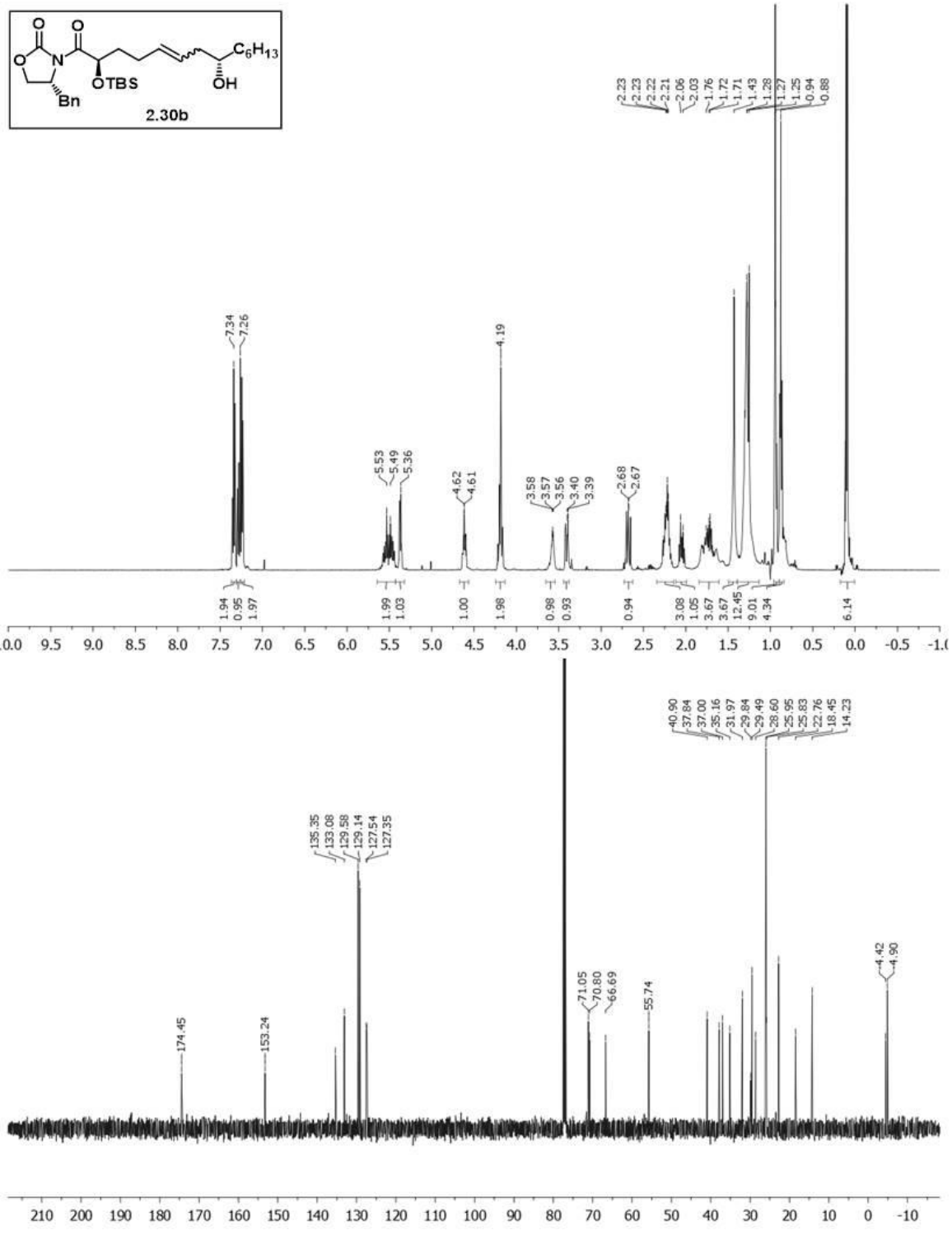
2.30b
OTBS
OH
Bn
C_6H_{13}

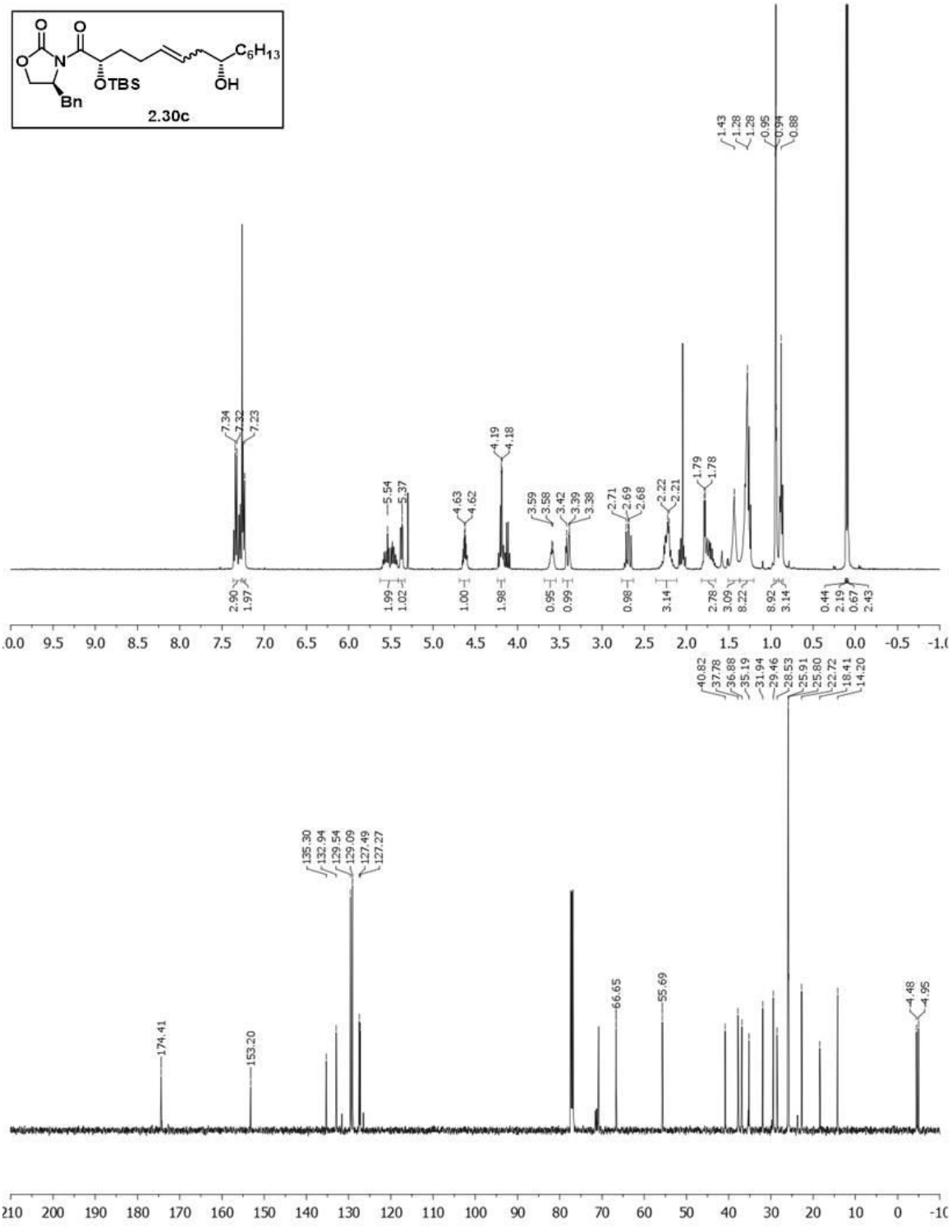
OTBS
OH
Bn
2.30c

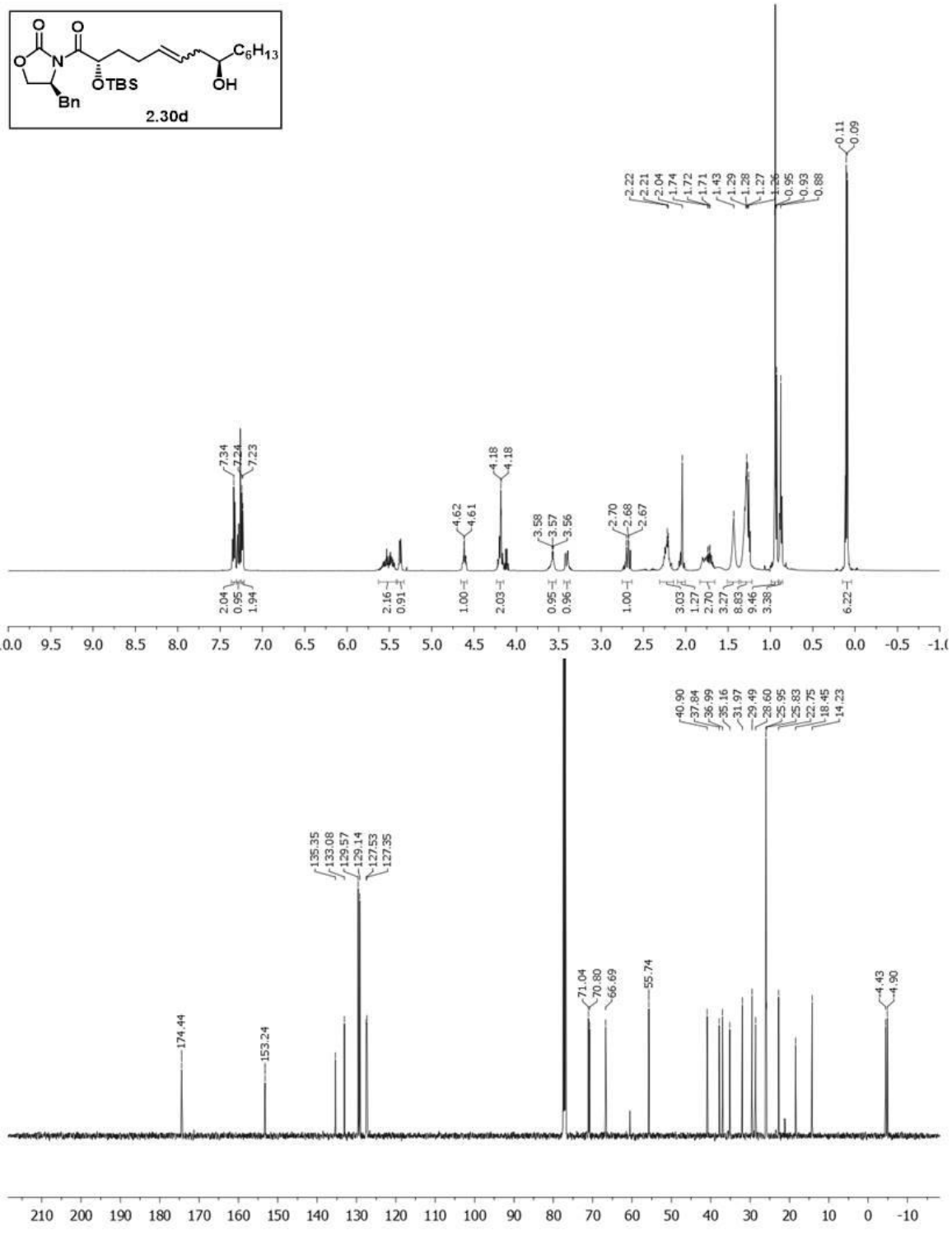
2.30d
OTBS
OH
Bn
C_6H_{13}
7.34
7.24
7.23
4.62
4.61
4.18
4.18
3.58
3.57
3.56
2.70
2.68
2.67
2.22
2.21
2.04
1.74
1.72
1.71
1.43
1.29
1.28
1.27
0.95
0.93
0.88
0.11
0.09
135.35
133.08
129.57
129.14
127.53
127.35
174.44
153.24
71.04
70.80
66.69
55.74
40.90
37.84
36.99
35.16
31.97
29.49
28.60
25.95
25.83
22.75
18.45
14.23
4.43
4.90

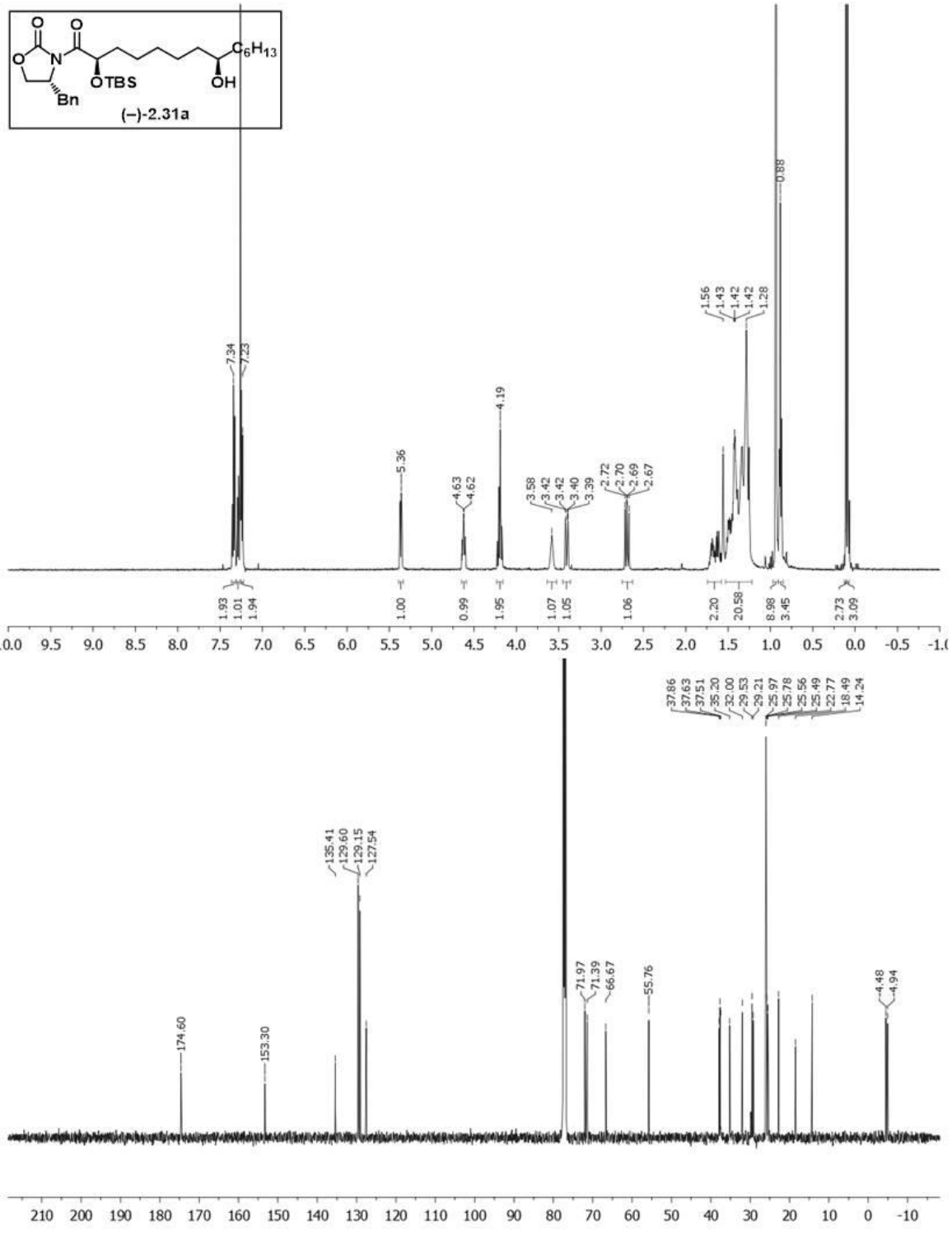
(–)-2.31a
OTBS
OH
Bn
C_6H_{13}
7.34
7.23
5.36
4.63
4.62
4.19
3.58
3.42
3.42
3.40
3.39
2.72
2.70
2.69
2.67
1.56
1.43
1.42
1.42
1.28
0.88
1.93
1.01
1.94
1.00
0.99
1.95
1.07
1.05
1.06
2.20
20.58
8.98
3.45
2.73
3.09
37.86
37.63
37.51
35.20
32.00
29.53
29.21
25.97
25.78
25.56
25.49
22.77
18.49
14.24
135.41
129.60
129.15
127.54
174.60
153.30
71.97
71.39
66.67
55.76
4.48
4.94

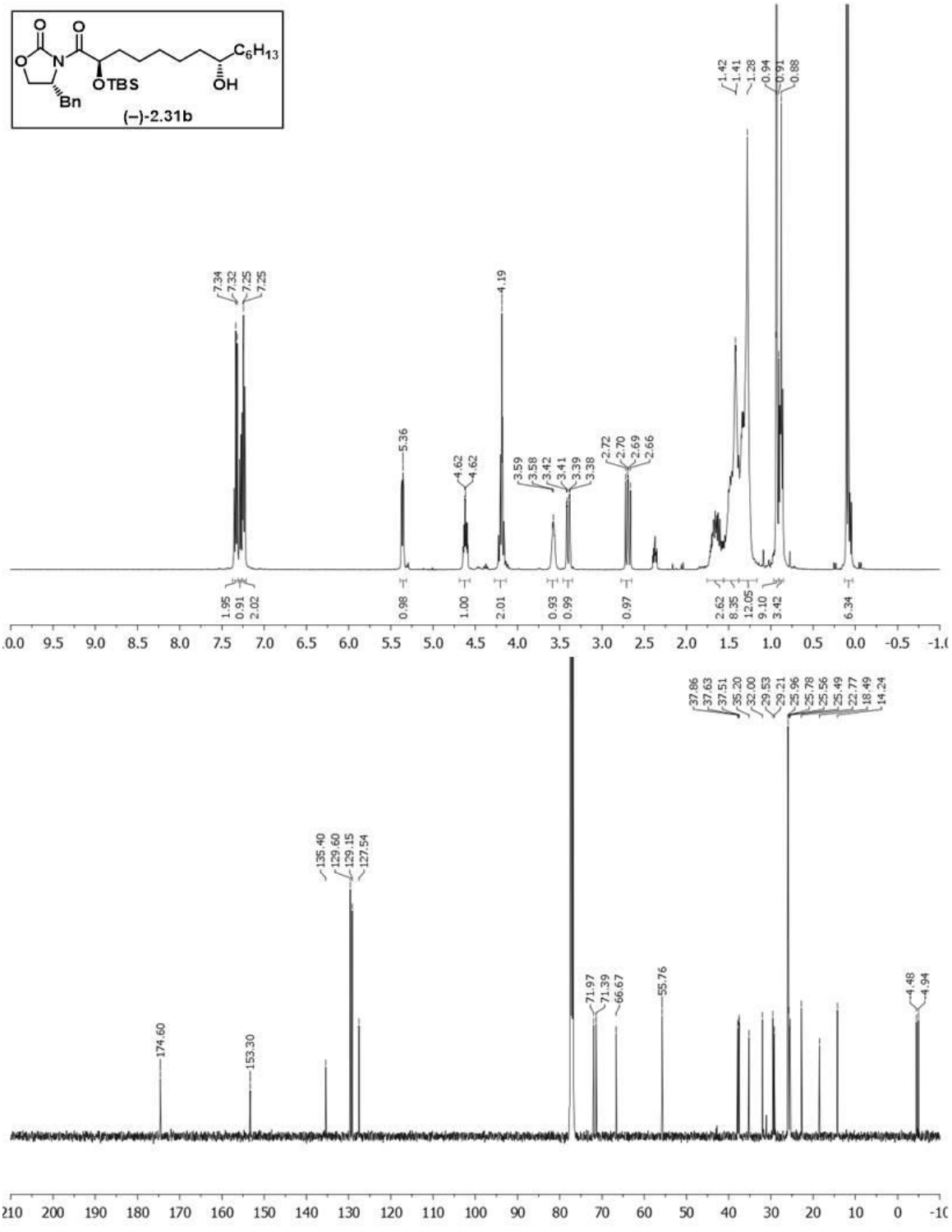
(–)-2.31b
OTBS
OH
Bn
C6H13
7.34
7.32
7.25
7.25
5.36
4.62
4.62
4.19
3.59
3.58
3.42
3.41
3.39
3.38
2.72
2.70
2.69
2.66
1.42
1.41
1.28
0.94
0.91
0.88
1.95
0.91
2.02
0.98
1.00
2.01
0.93
0.99
0.97
2.62
8.35
12.05
9.10
3.42
6.34
37.86
37.63
37.51
35.20
32.00
29.53
29.21
25.96
25.78
25.56
25.49
22.77
18.49
14.24
135.40
129.60
129.15
127.54
71.97
71.39
66.67
55.76
14.48
14.94
174.60
153.30

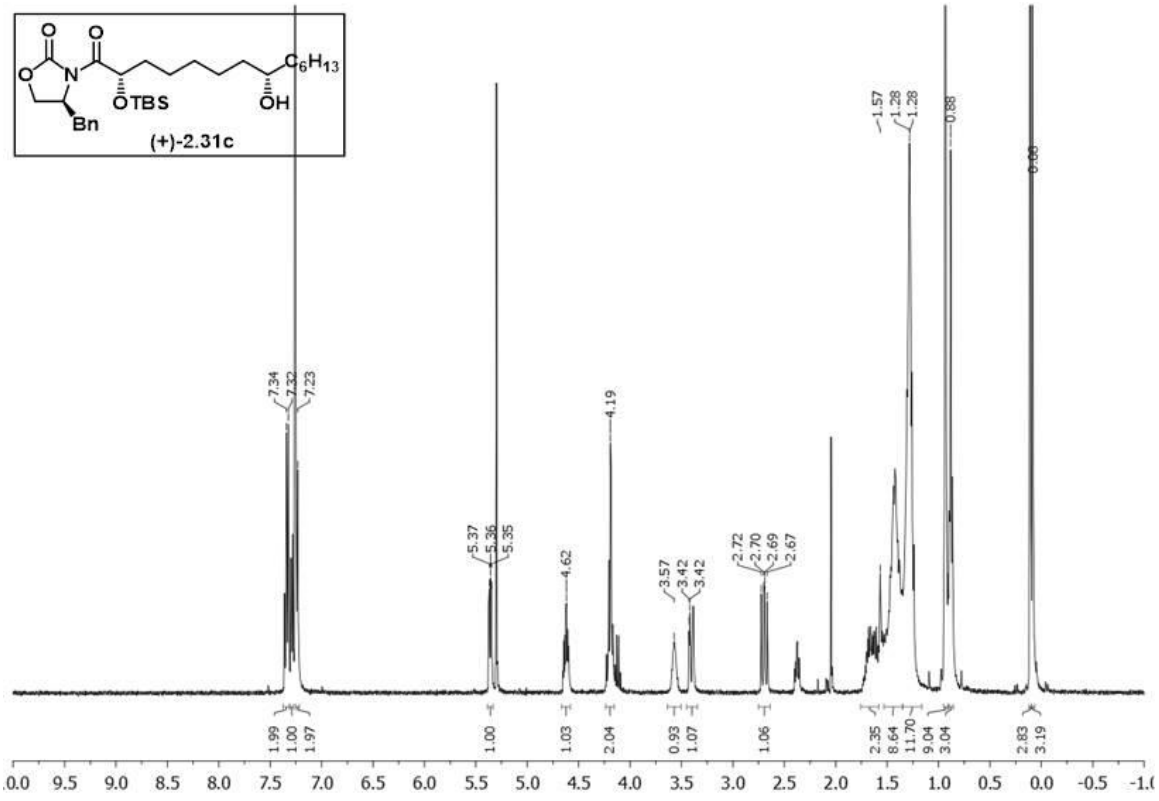
(+)-2.31c
OTBS
OH
Bn
C6H13
7.34
7.32
7.23
5.37
5.36
5.35
4.62
4.19
3.57
3.42
3.42
2.72
2.70
2.69
2.67
1.57
1.28
1.28
0.88
0.00
1.99
1.00
1.97
1.00
1.03
2.04
0.93
1.07
1.06
2.35
8.64
11.70
9.04
3.04
2.83
3.19

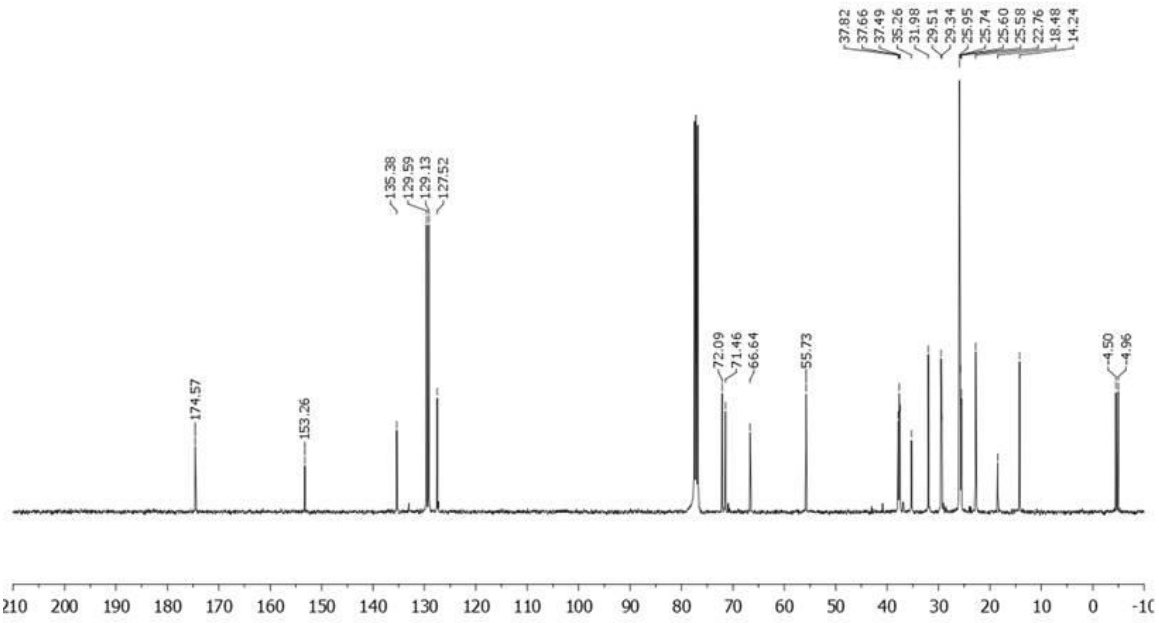
37.82
37.66
37.49
35.26
31.98
29.51
29.34
25.95
25.74
25.60
25.58
22.76
18.48
14.24
135.38
129.59
129.13
127.52
174.57
153.26
72.09
71.46
66.64
55.73
4.50
4.96

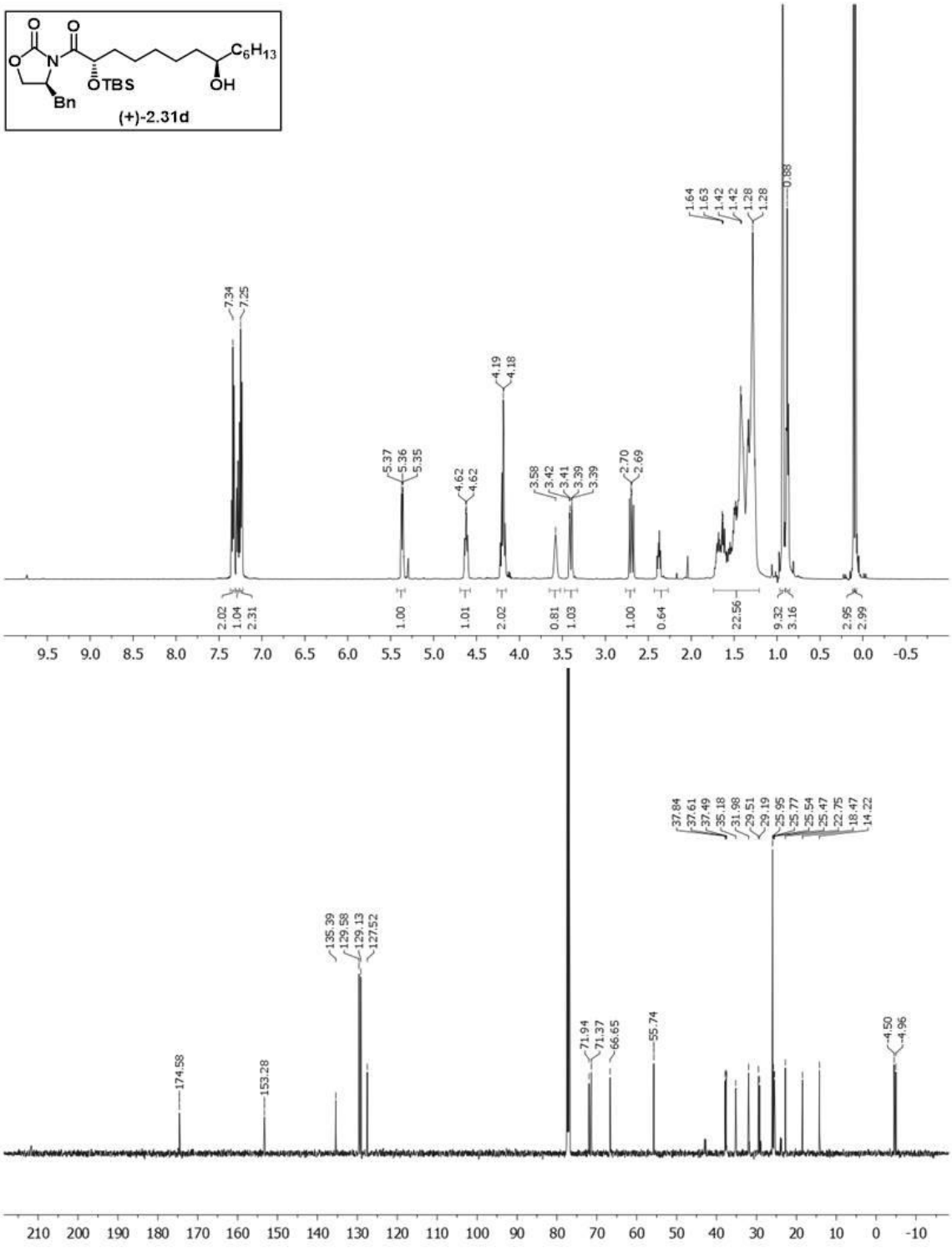
(+)-2.31d
OTBS
OH
Bn
C_6H_{13}
7.34
7.25
5.37
5.36
5.35
4.62
4.62
4.19
4.18
3.58
3.42
3.41
3.39
3.39
2.70
2.69
1.64
1.63
1.42
1.42
1.28
1.28
0.88
2.02
1.04
2.31
1.00
1.01
2.02
0.81
1.03
1.00
0.64
22.56
9.32
3.16
2.95
2.99
174.58
153.28
135.39
129.58
129.13
127.52
71.94
71.37
66.65
55.74
37.84
37.61
37.49
35.18
31.98
29.51
29.19
25.95
25.77
25.54
25.47
22.75
18.47
14.22
-4.50
-4.96

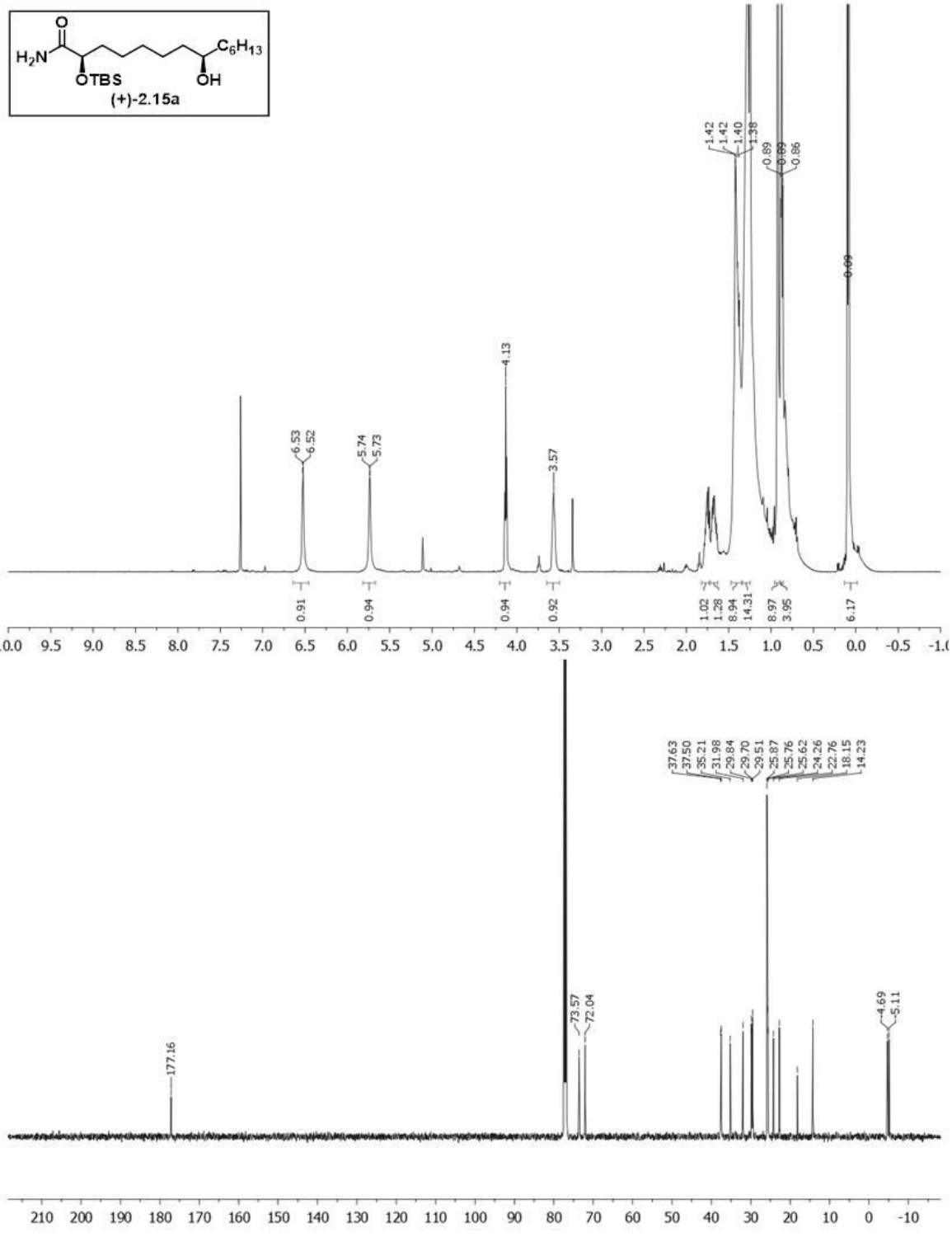
O
H2N
C6H13
OTBS
OH
(+)-2.15a
1.42
1.42
1.40
1.38
0.89
0.89
0.86
0.09
6.53
6.52
5.74
5.73
4.13
3.57
0.91
0.94
0.94
0.92
1.02
1.28
8.94
14.31
8.97
3.95
6.17
37.63
37.50
35.21
31.98
29.84
29.70
29.51
25.87
25.76
25.62
24.26
22.76
18.15
14.23
177.16
73.57
72.04
4.69
5.11

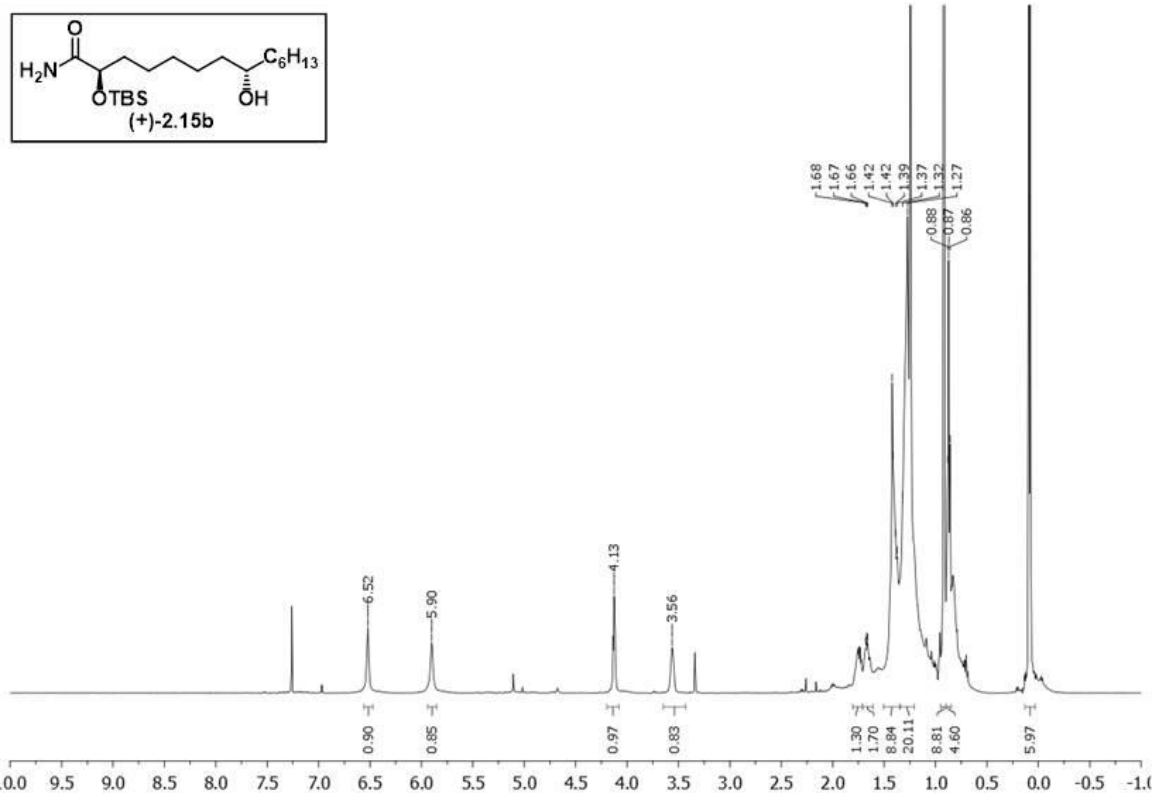
O
H2N
C6H13
OTBS
OH
(+)-2.15b
1.68
1.67
1.66
1.42
1.42
1.39
1.37
1.32
1.27
0.88
0.87
0.86
6.52
5.90
4.13
3.56
0.90
0.85
0.97
0.83
1.30
1.70
8.84
20.11
8.81
4.60
5.97

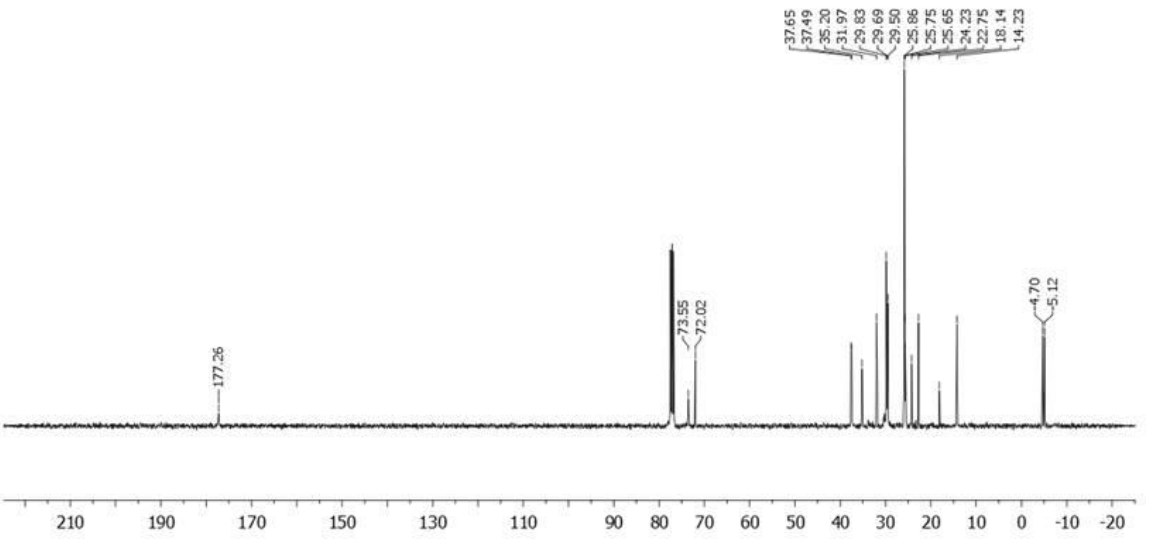
37.65
37.49
35.20
31.97
29.83
29.69
29.50
25.86
25.75
25.65
24.23
22.75
18.14
14.23
177.26
73.55
72.02
4.70
5.12

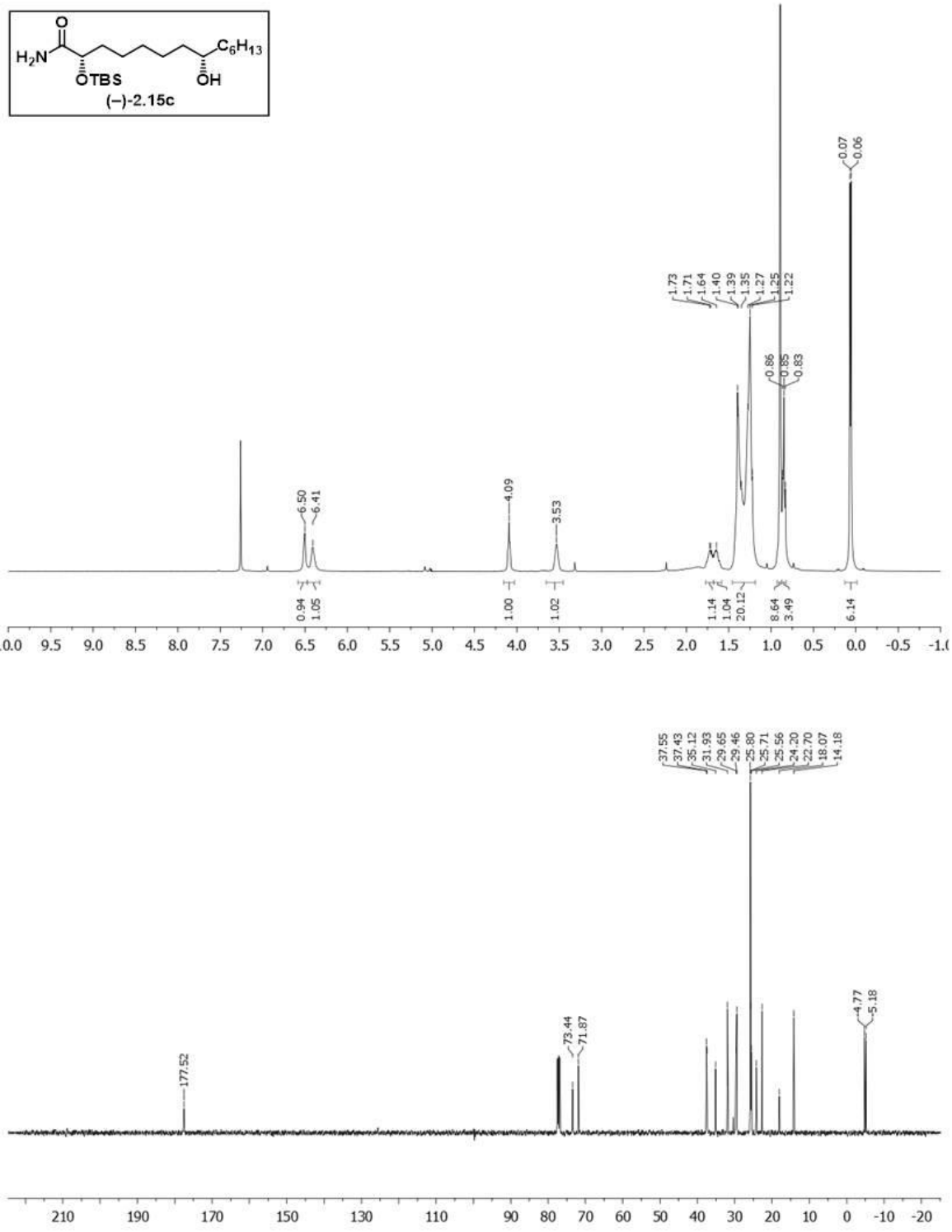
O
H2N
C6H13
OTBS
OH
(–)-2.15c
0.07
0.06
1.73
1.71
1.64
1.40
1.39
1.35
1.27
1.25
1.22
0.86
0.85
0.83
6.50
6.41
4.09
3.53
0.94
1.05
1.00
1.02
1.14
1.04
20.12
8.64
3.49
6.14
37.55
37.43
35.12
31.93
29.65
29.46
25.80
25.71
25.56
24.20
22.70
18.07
14.18
4.77
5.18
177.52
73.44
71.87

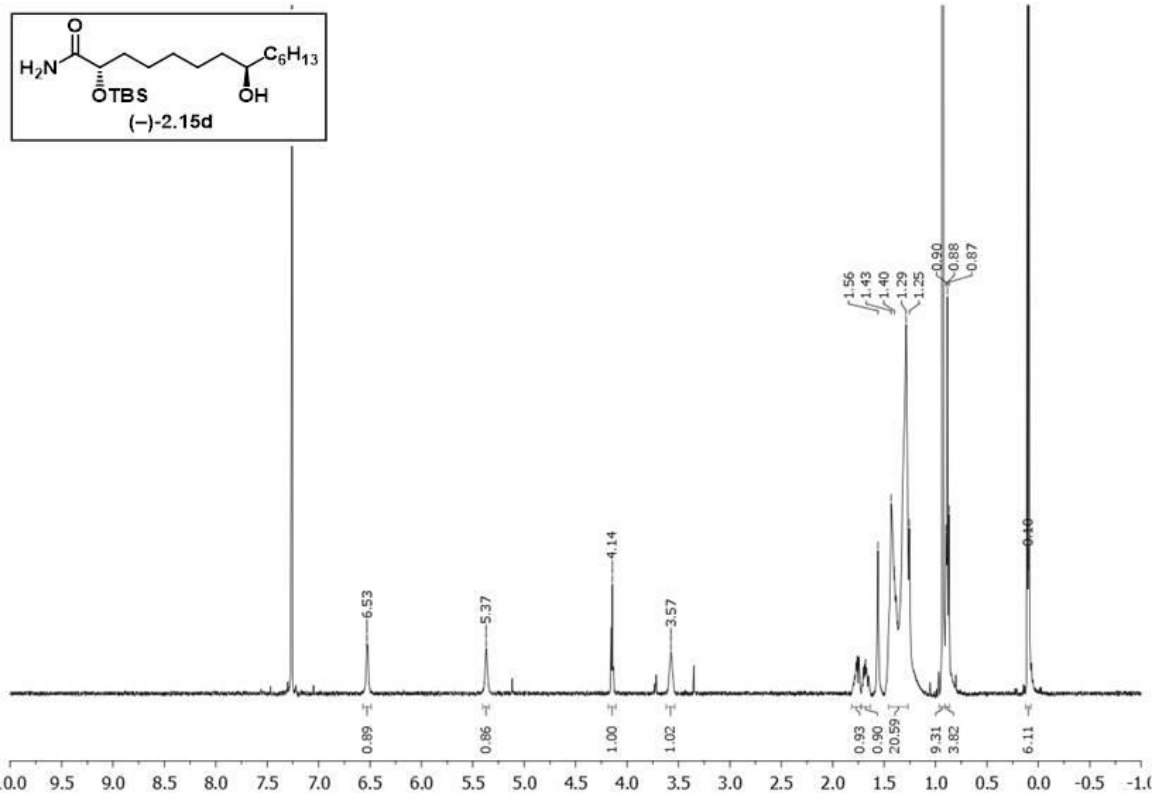
O
H2N
C6H13
OTBS
OH
(–)-2.15d
6.53
5.37
4.14
3.57
1.56
1.43
1.40
1.29
1.25
0.90
0.88
0.87
0.10
0.89
0.86
1.00
1.02
0.93
0.90
20.59
9.31
3.82
6.11

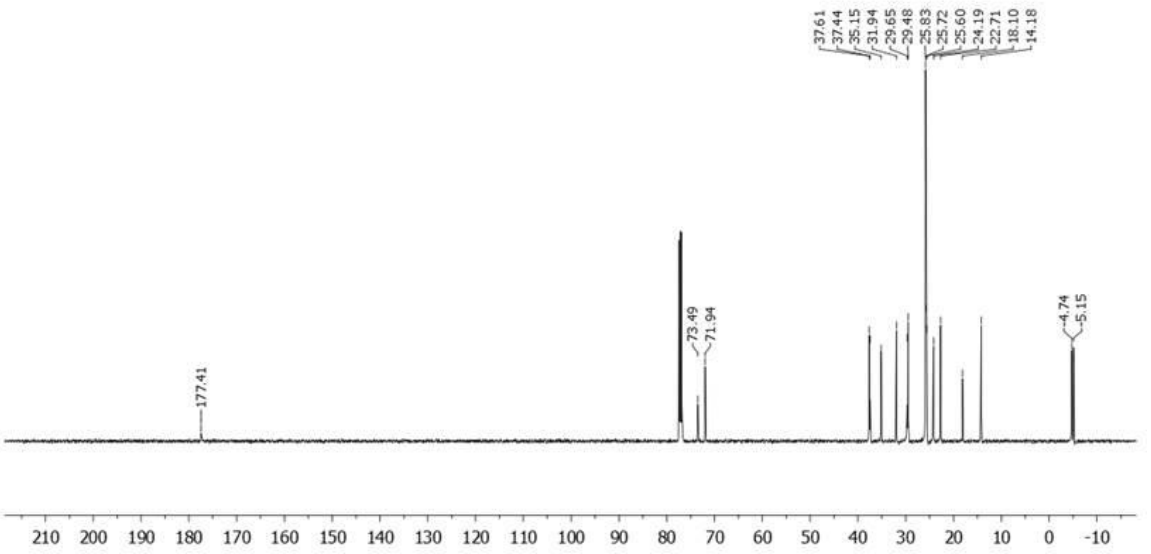
177.41
73.49
71.94
37.61
37.44
35.15
31.94
29.65
29.48
25.83
25.72
25.60
24.19
22.71
18.10
14.18
-4.74
-5.15

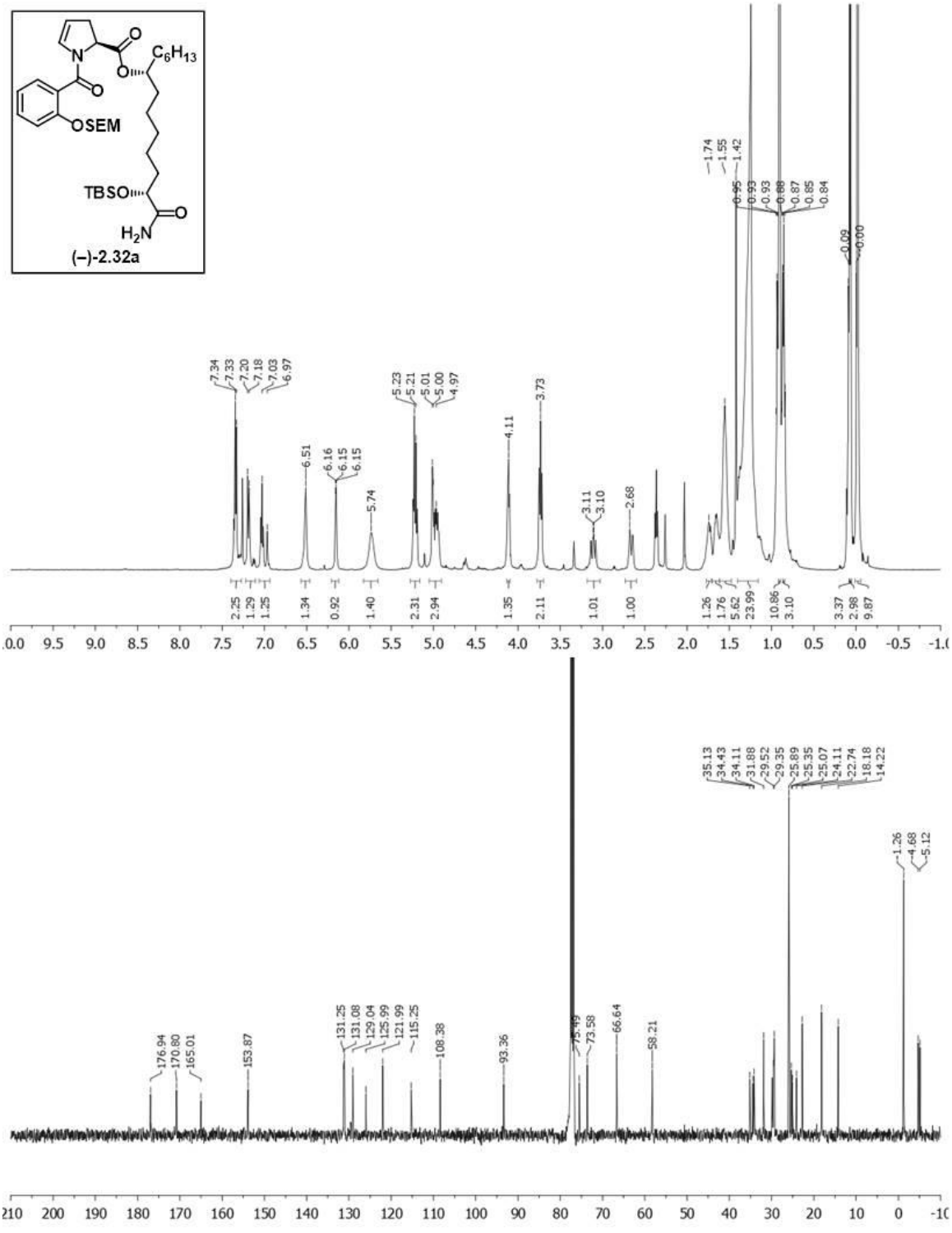
C6H13
OSEM
TBSO
H2N
(–)-2.32a
7.34
7.33
7.20
7.18
7.03
6.97
6.51
6.16
6.15
6.15
5.74
5.23
5.21
5.01
5.00
4.97
4.11
3.73
3.11
3.10
2.68
1.74
1.55
1.42
0.95
0.93
0.93
0.88
0.87
0.85
0.84
0.09
0.00
2.25
1.29
1.25
1.34
0.92
1.40
2.31
2.94
1.35
2.11
1.01
1.00
1.26
1.76
5.62
23.99
10.86
3.10
3.37
2.98
9.87
35.13
34.43
34.11
31.88
29.52
29.35
25.89
25.35
25.07
24.11
22.74
18.18
14.22
1.26
4.68
5.12
176.94
170.80
165.01
153.87
131.25
131.08
129.04
125.99
121.99
115.25
108.38
93.36
75.49
73.58
66.64
58.21

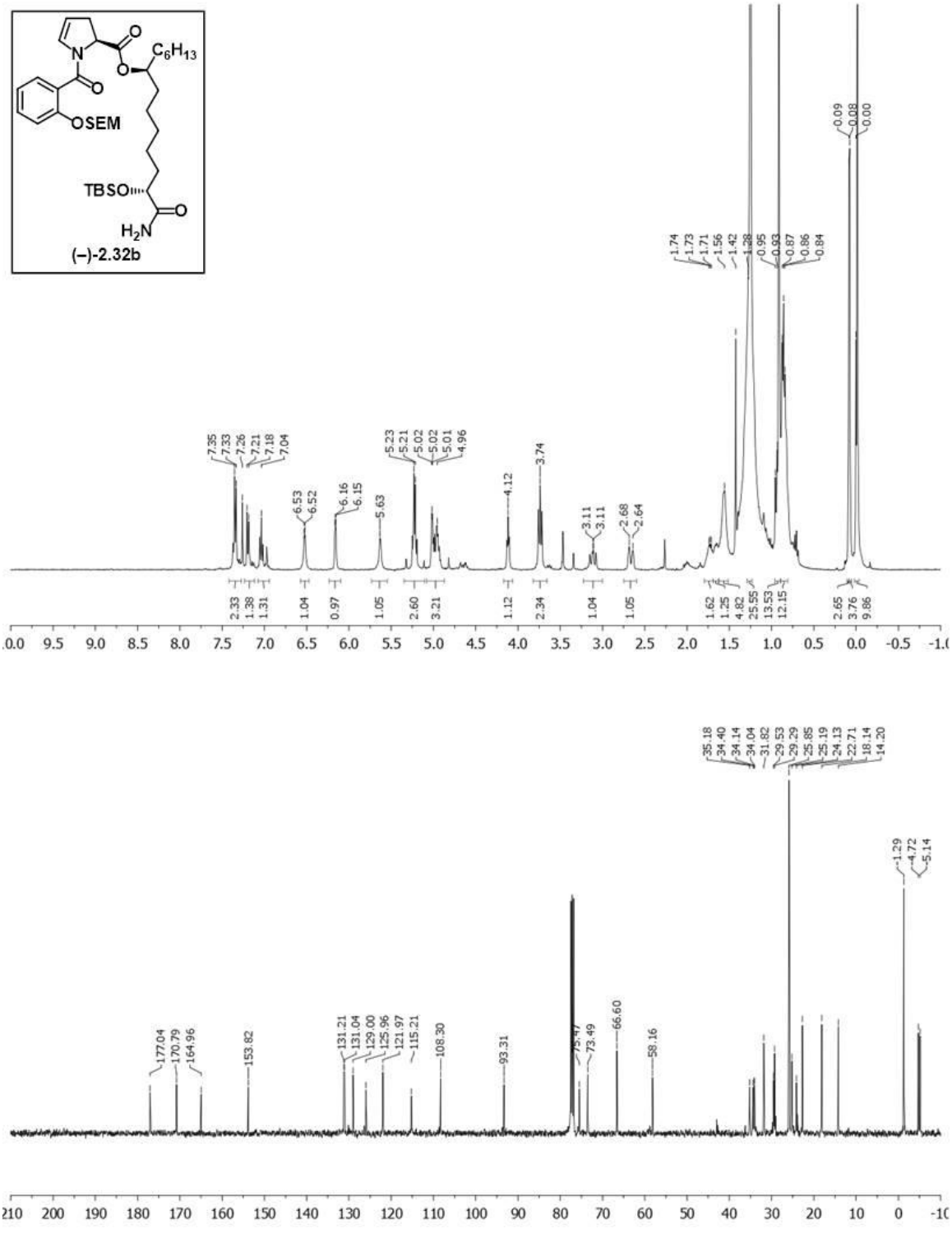
OSEM
TBSO
C_6H_{13}
H_2N
(–)-2.32b

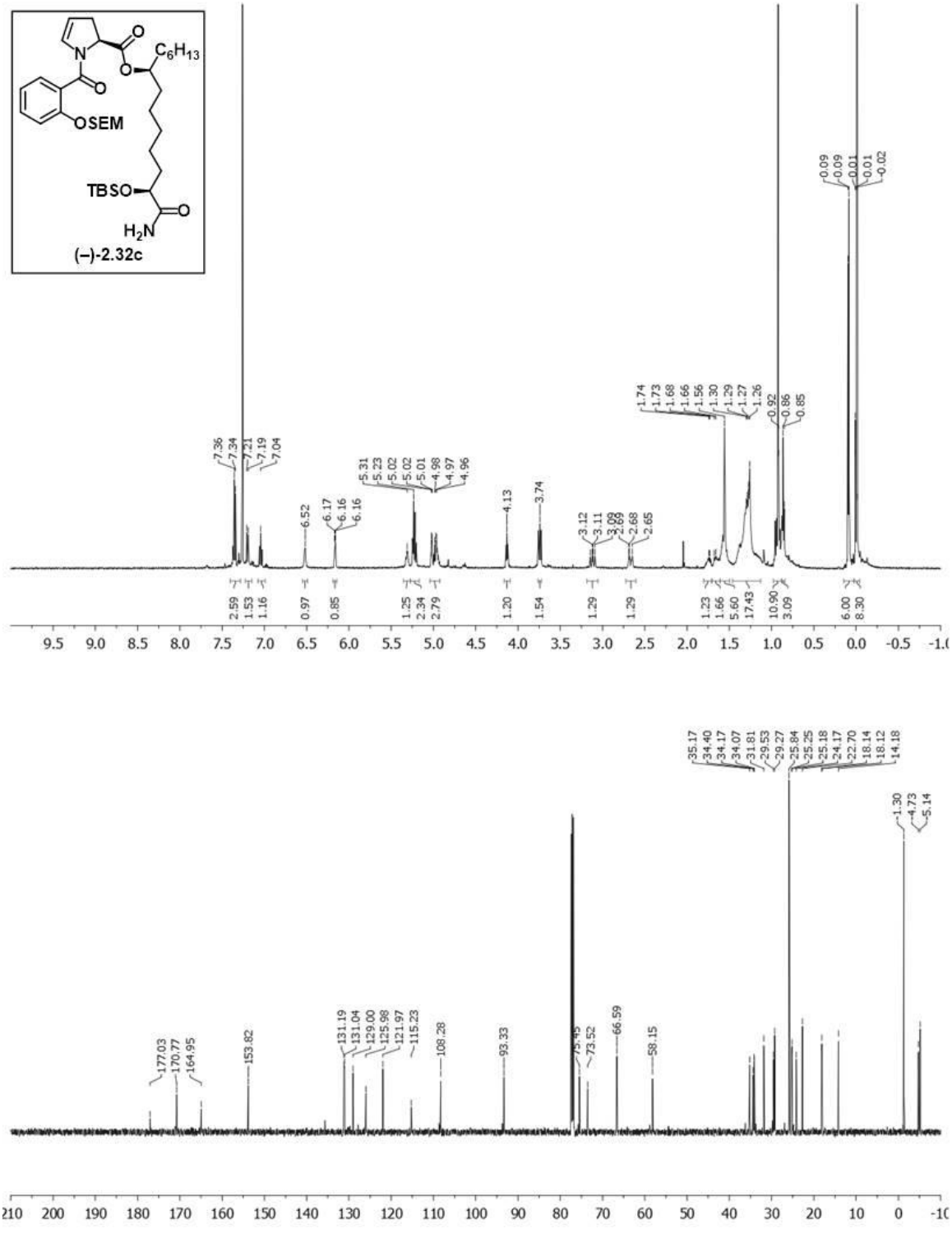
C6H13
OSEM
TBSO
H2N
(–)-2.32c

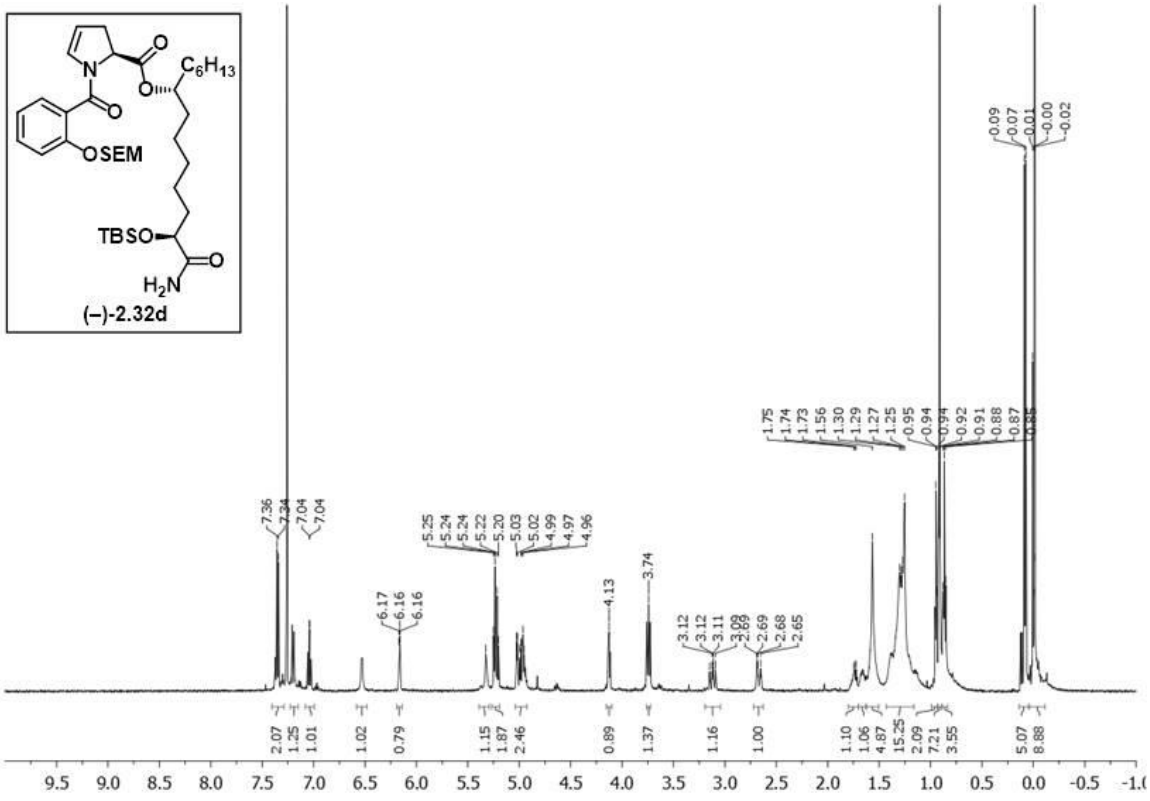
OSEM
TBSO
C_6H_{13}
H_2N
(–)-2.32d

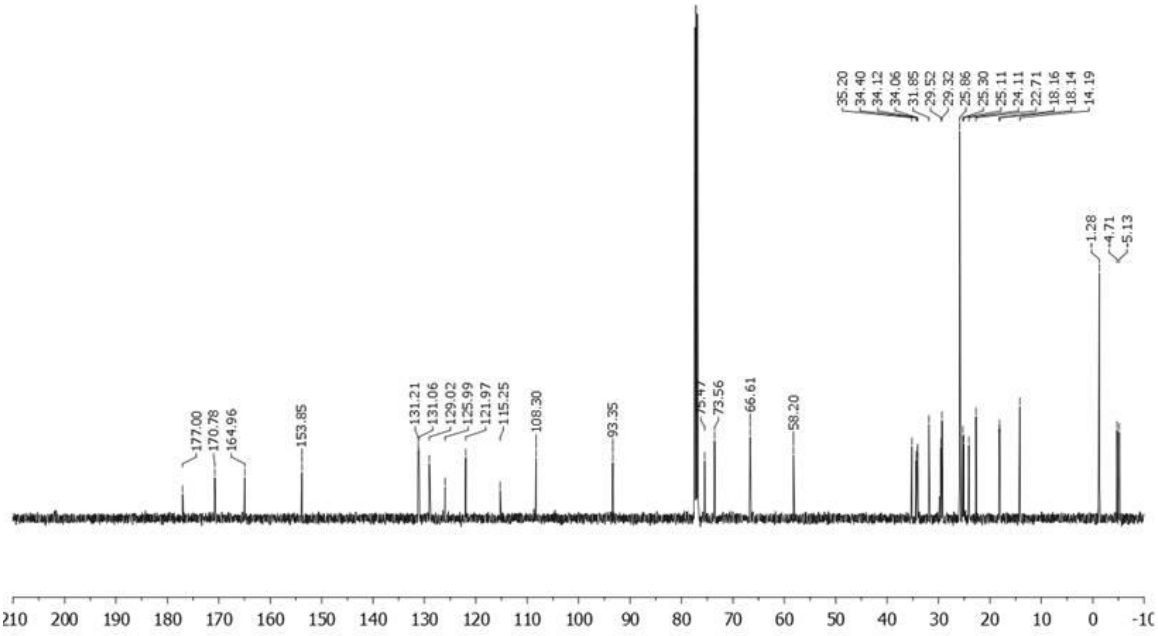

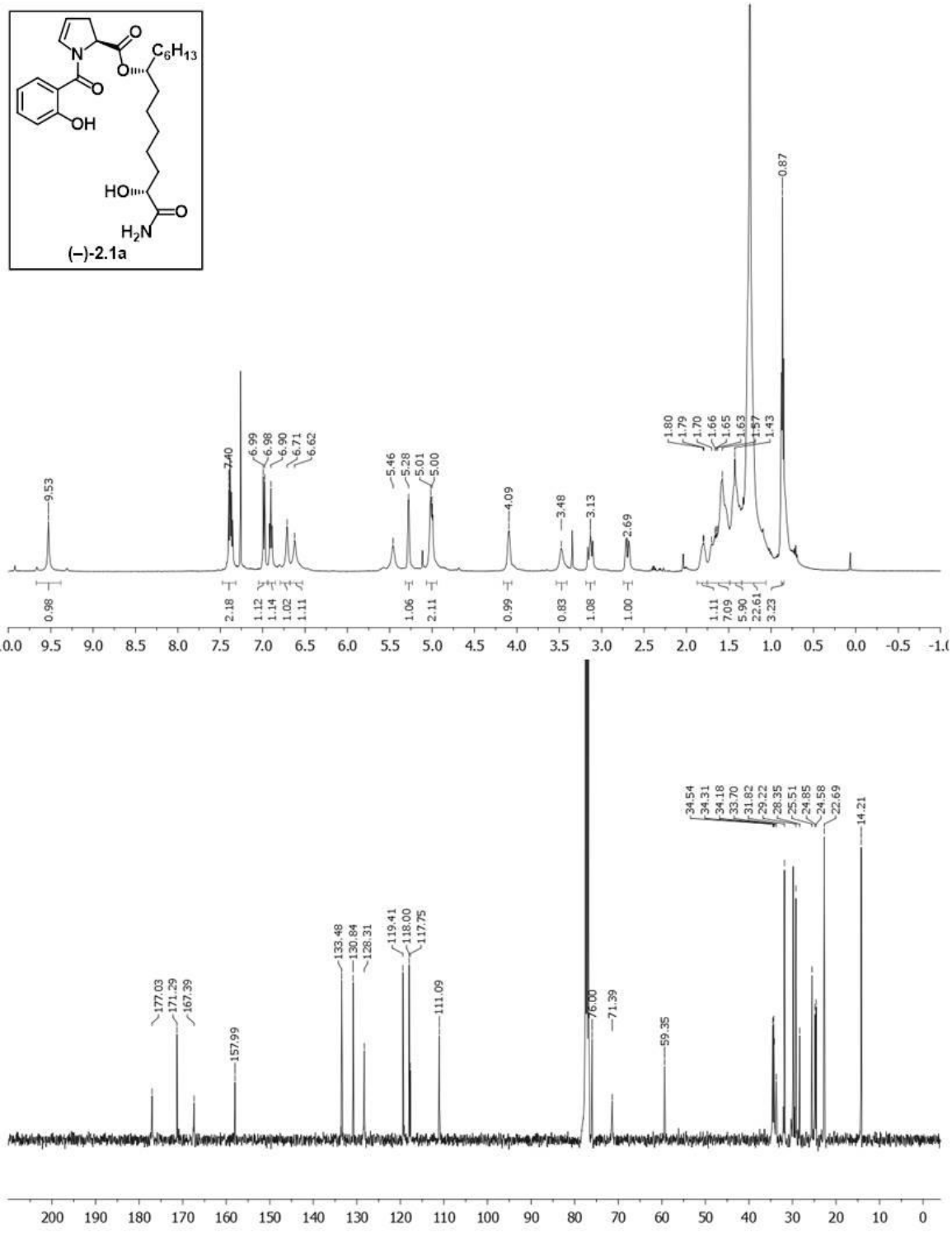
(–)-2.1a
9.53
7.40
6.99
6.98
6.90
6.71
6.62
5.46
5.28
5.01
5.00
4.09
3.48
3.13
2.69
1.80
1.79
1.70
1.66
1.65
1.63
1.57
1.43
0.87
0.98
2.18
1.12
1.14
1.02
1.11
1.06
2.11
0.99
0.83
1.08
1.00
1.11
7.09
5.90
22.61
3.23
177.03
171.29
167.39
157.99
133.48
130.84
128.31
119.41
118.00
117.75
111.09
76.00
71.39
59.35
34.54
34.31
34.18
33.70
31.82
29.22
28.35
25.51
24.85
24.58
22.69
14.21

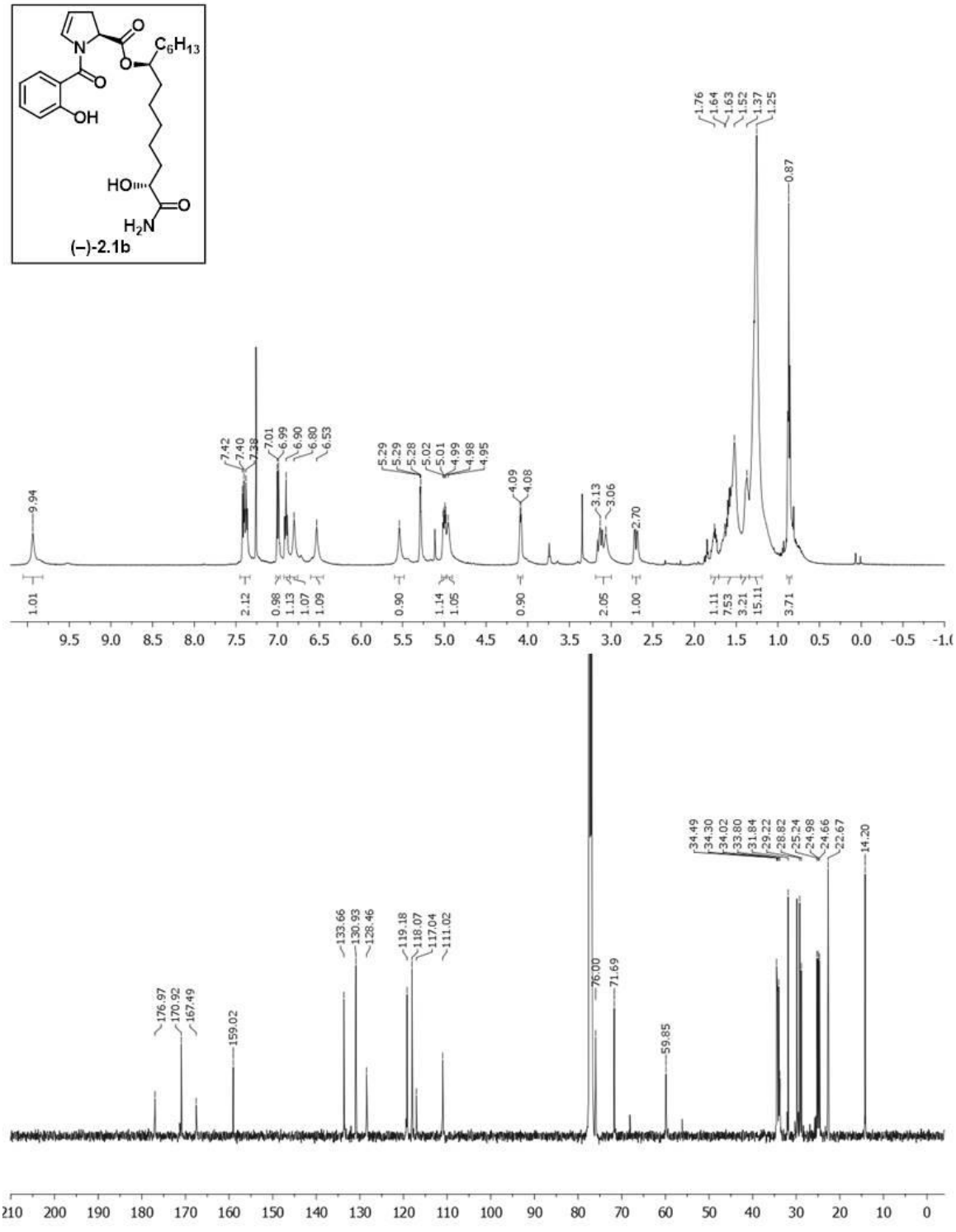
(–)-2.1b

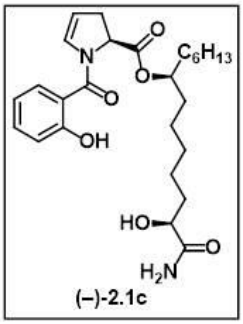
O
N
O
C6H13
O
OH
HO
O
H2N

(–)-2.1c

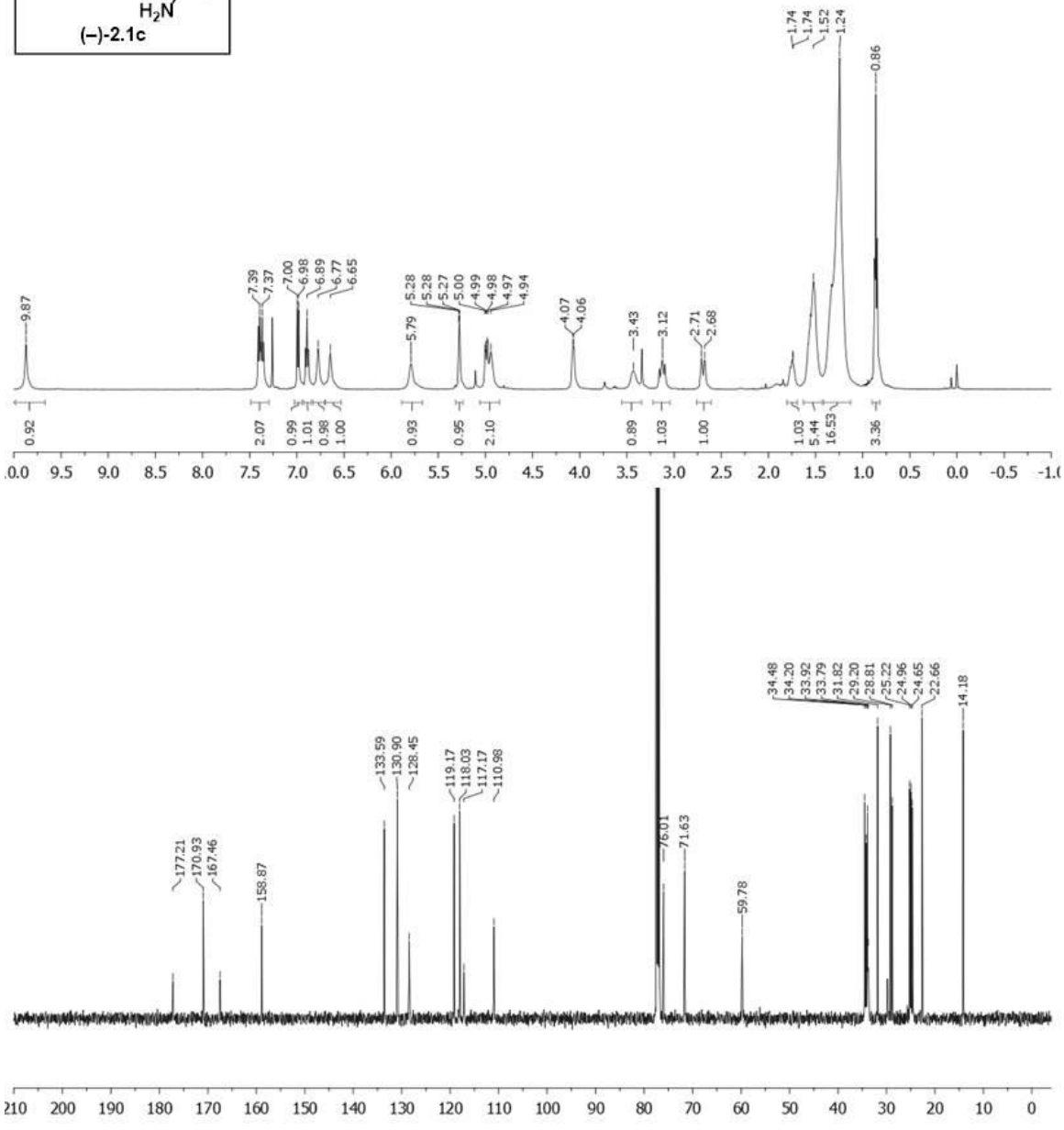
9.87
7.39
7.37
7.00
6.98
6.89
6.77
6.65
5.79
5.28
5.28
5.27
5.00
4.99
4.98
4.97
4.94
4.07
4.06
3.43
3.12
2.71
2.68
1.74
1.74
1.52
1.24
0.86
0.92
2.07
0.99
1.01
0.98
1.00
0.93
0.95
2.10
0.89
1.03
1.00
1.03
5.44
16.53
3.36
177.21
170.93
167.46
158.87
133.59
130.90
128.45
119.17
118.03
117.17
110.98
76.01
71.63
59.78
34.48
34.20
33.92
33.79
31.82
29.20
28.81
25.22
24.96
24.65
22.66
14.18

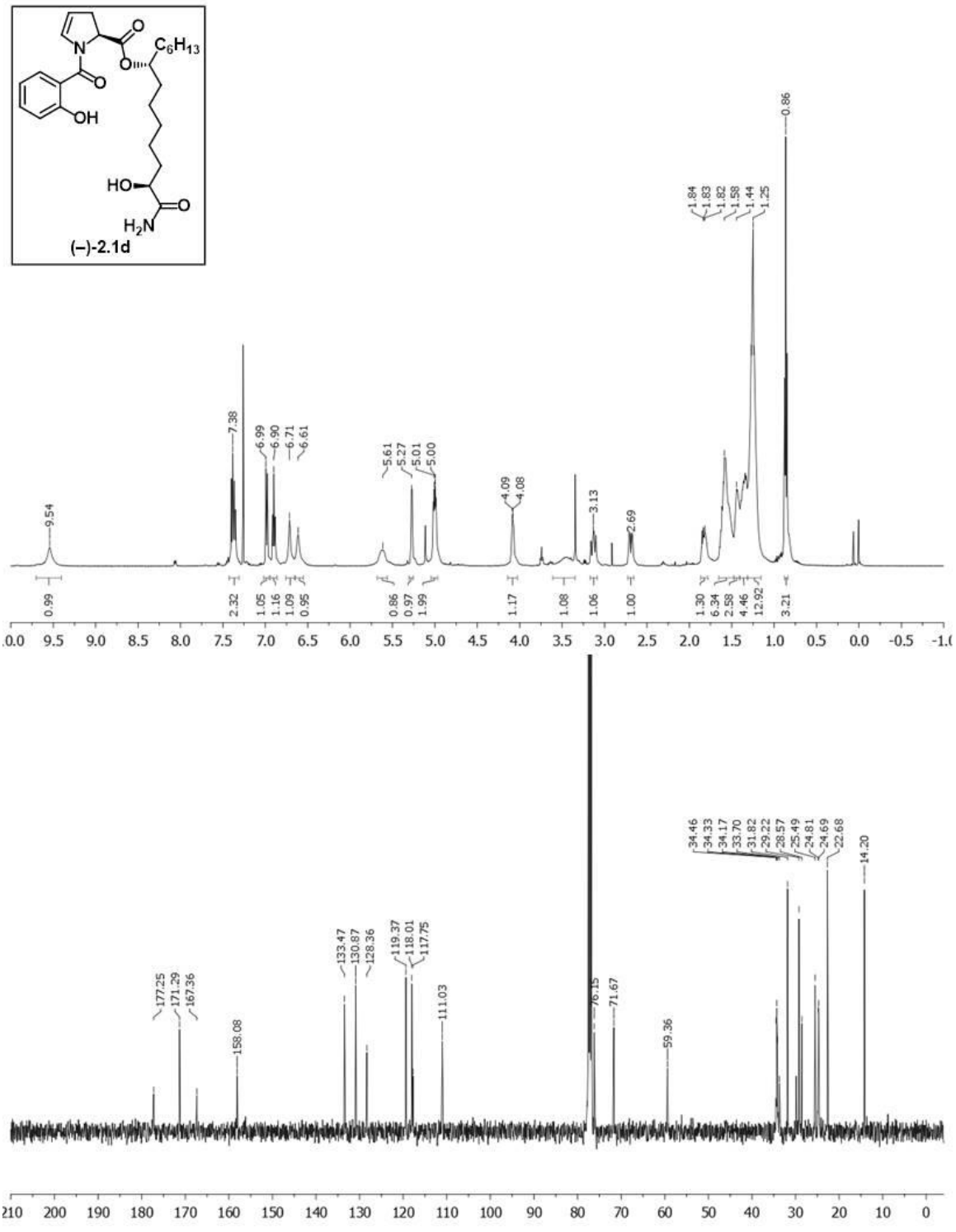
(–)-2.1d
9.54
7.38
6.99
6.90
6.71
6.61
5.61
5.27
5.01
5.00
4.09
4.08
3.13
2.69
1.84
1.83
1.82
1.58
1.44
1.25
0.86
177.25
171.29
167.36
158.08
133.47
130.87
128.36
119.37
118.01
117.75
111.03
76.15
71.67
59.36
34.46
34.33
34.17
33.70
31.82
29.22
28.57
25.49
24.81
24.69
22.68
14.20

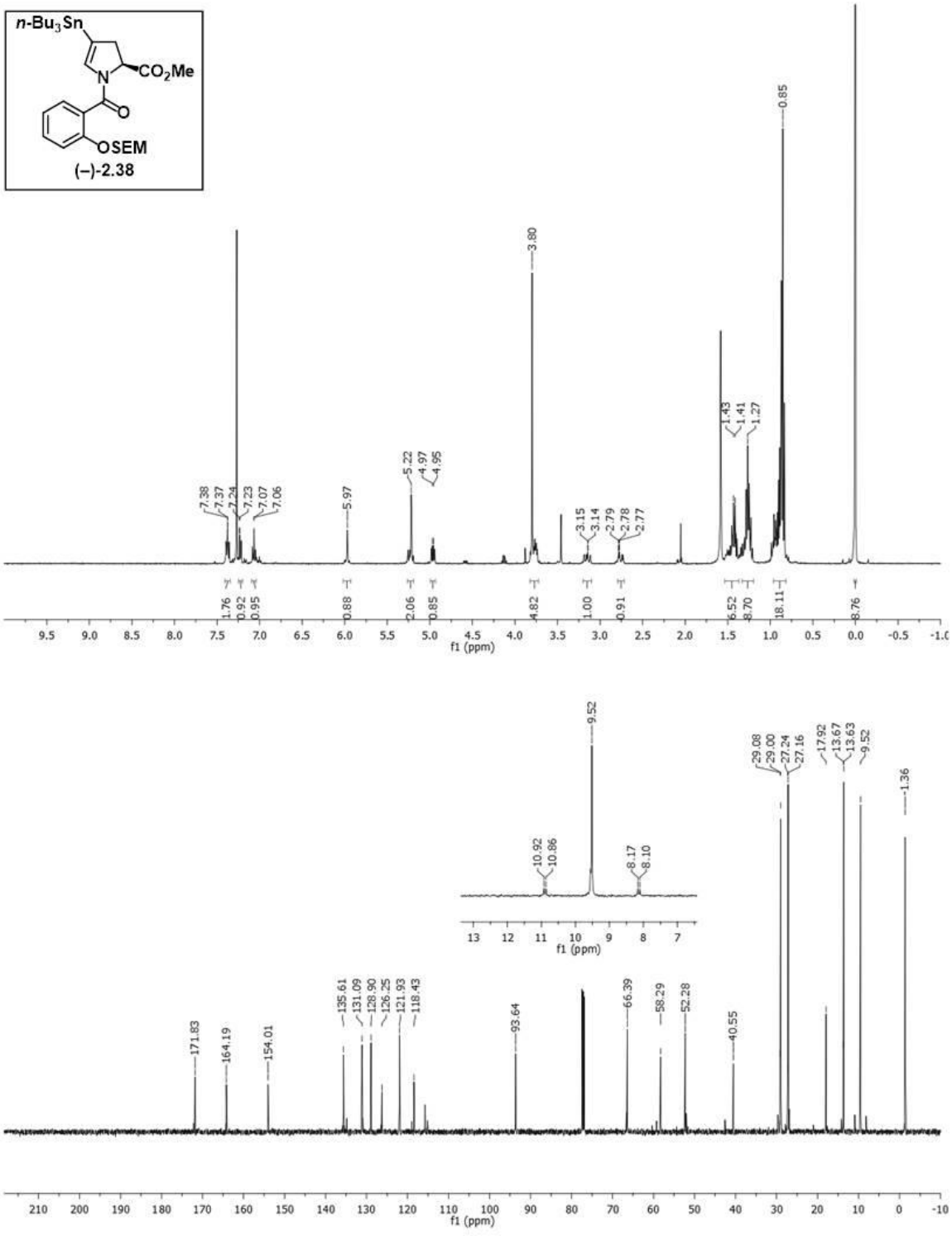
n-Bu3Sn
CO2Me
N
O
OSEM
(–)-2.38
f1 (ppm)

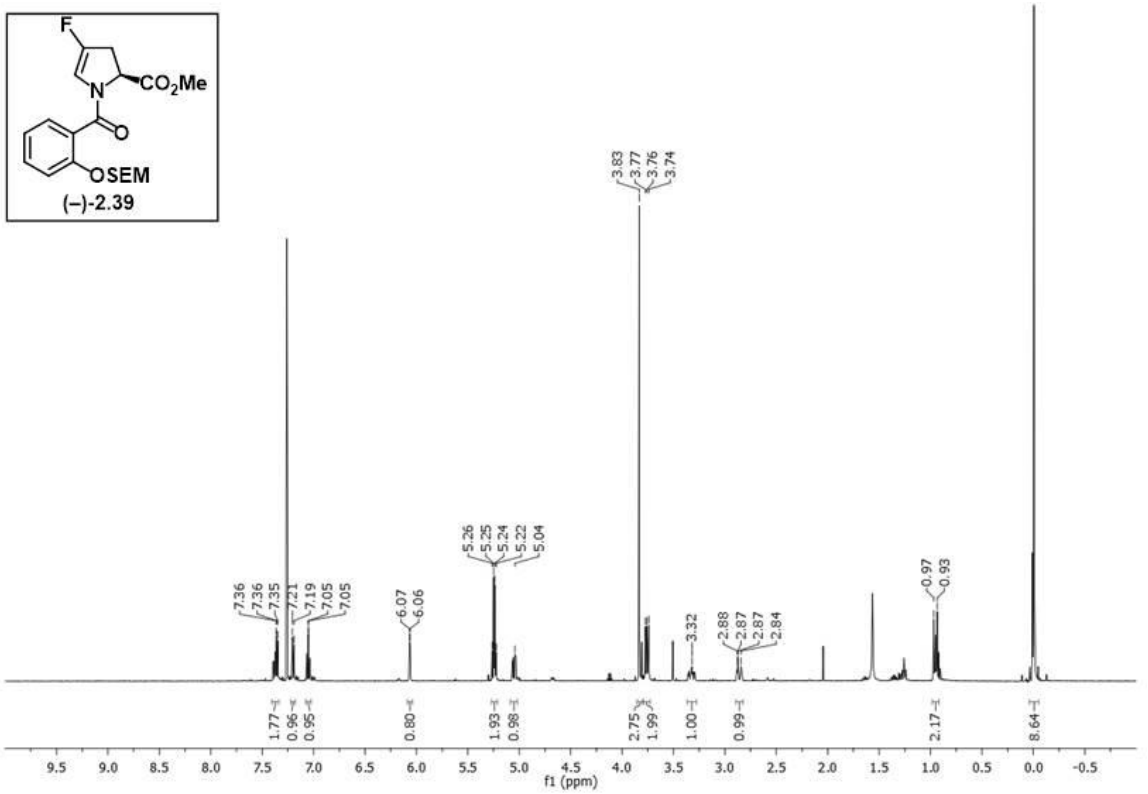
F
CO2Me
N
O
OSEM
(–)-2.39
7.36
7.36
7.35
7.21
7.19
7.05
7.05
6.07
6.06
5.26
5.25
5.24
5.22
5.04
3.83
3.77
3.76
3.74
3.32
2.88
2.87
2.87
2.84
0.97
0.93
1.77
0.96
0.95
0.80
1.93
0.98
2.75
1.99
1.00
0.99
2.17
8.64
f1 (ppm)

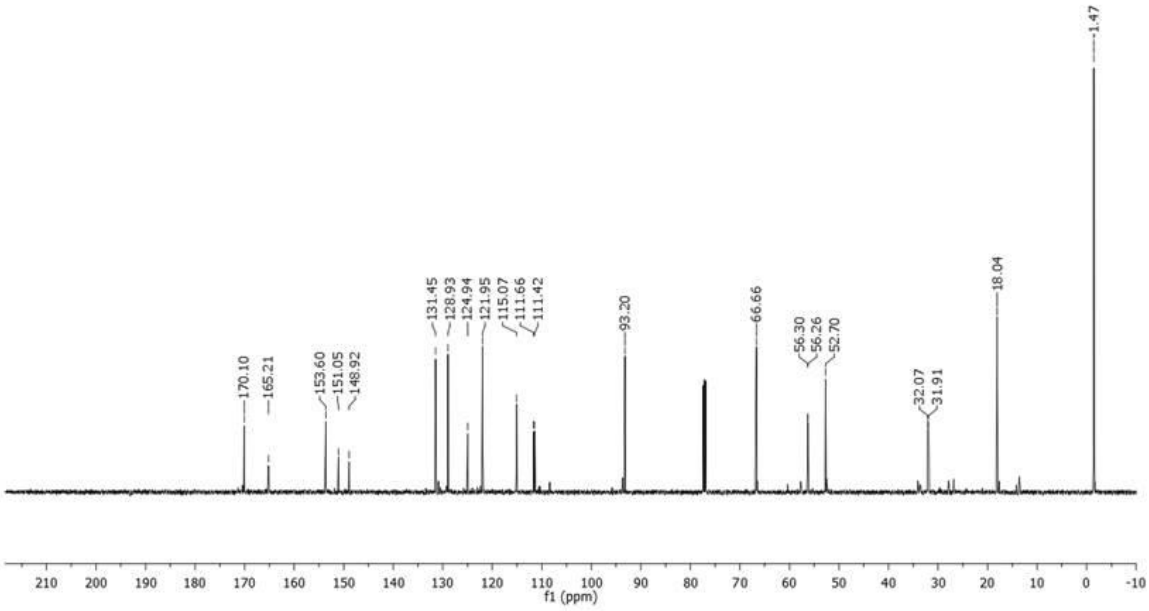
170.10
165.21
153.60
151.05
148.92
131.45
128.93
124.94
121.95
115.07
111.66
111.42
93.20
66.66
56.30
56.26
52.70
32.07
31.91
18.04
1.47
f1 (ppm)

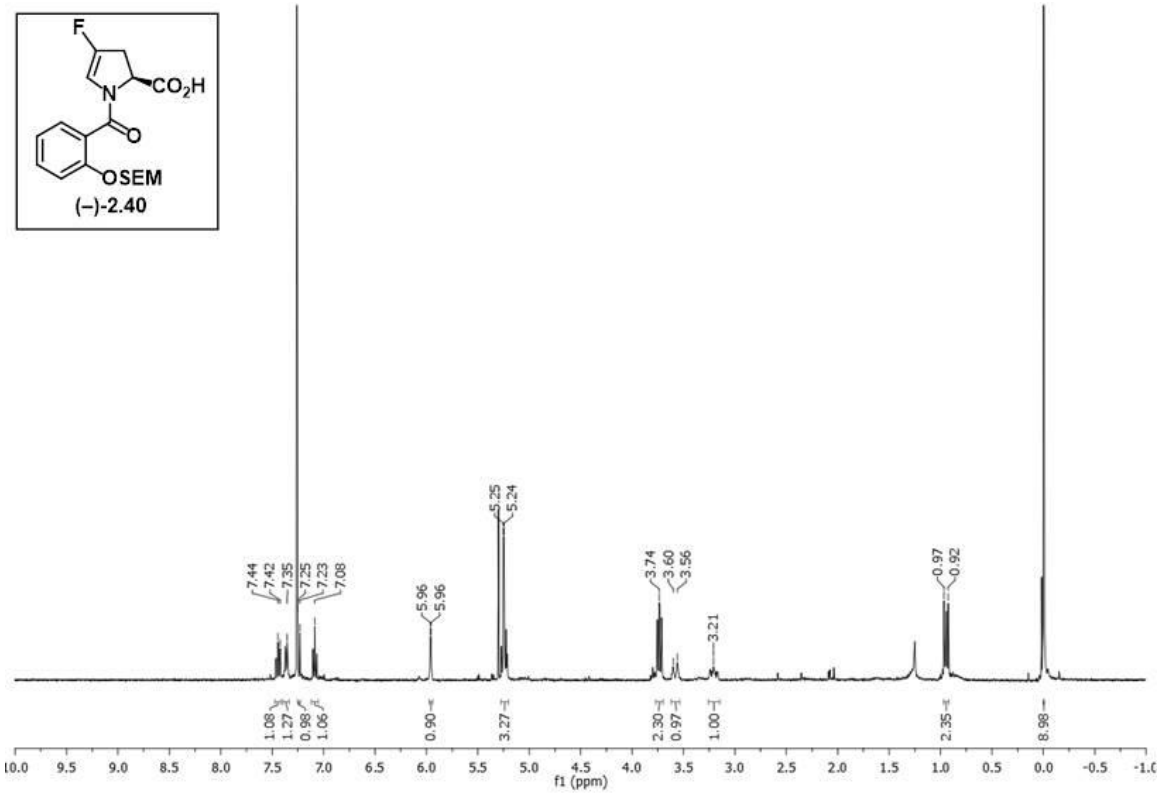
F
CO2H
N
O
OSEM
(–)-2.40
7.44
7.42
7.35
7.25
7.23
7.08
5.96
5.96
5.25
5.24
3.74
3.60
3.56
3.21
0.97
0.92
1.08
1.27
0.98
1.06
0.90
3.27
2.30
0.97
1.00
2.35
8.98
f1 (ppm)

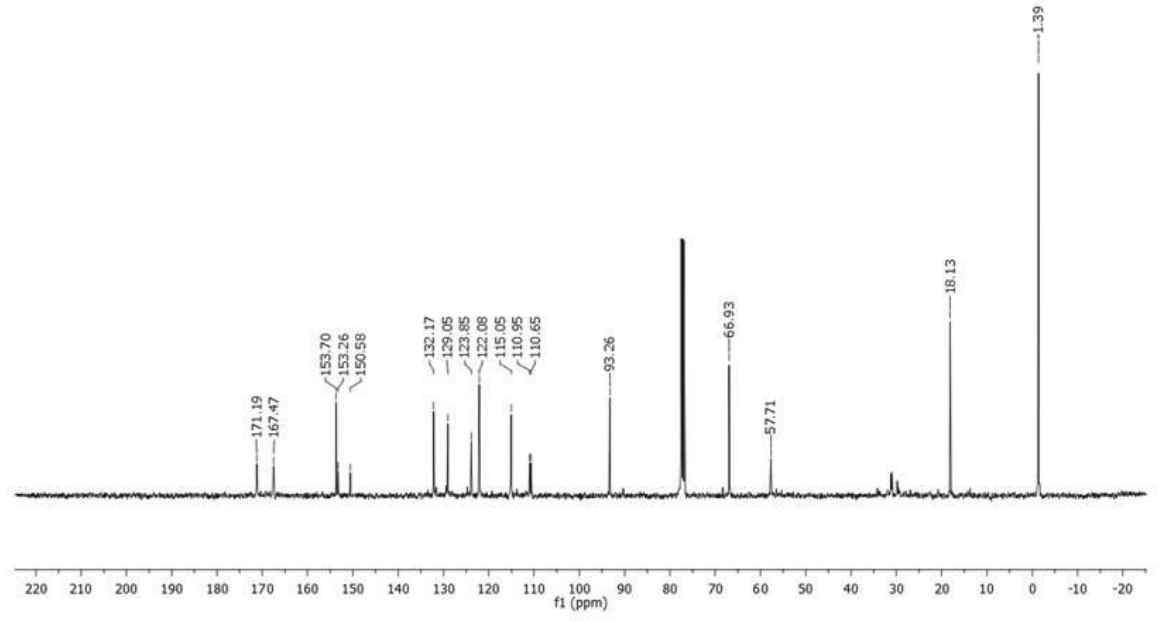
171.19
167.47
153.70
153.26
150.58
132.17
129.05
123.85
122.08
115.05
110.95
110.65
93.26
66.93
57.71
18.13
1.39
f1 (ppm)

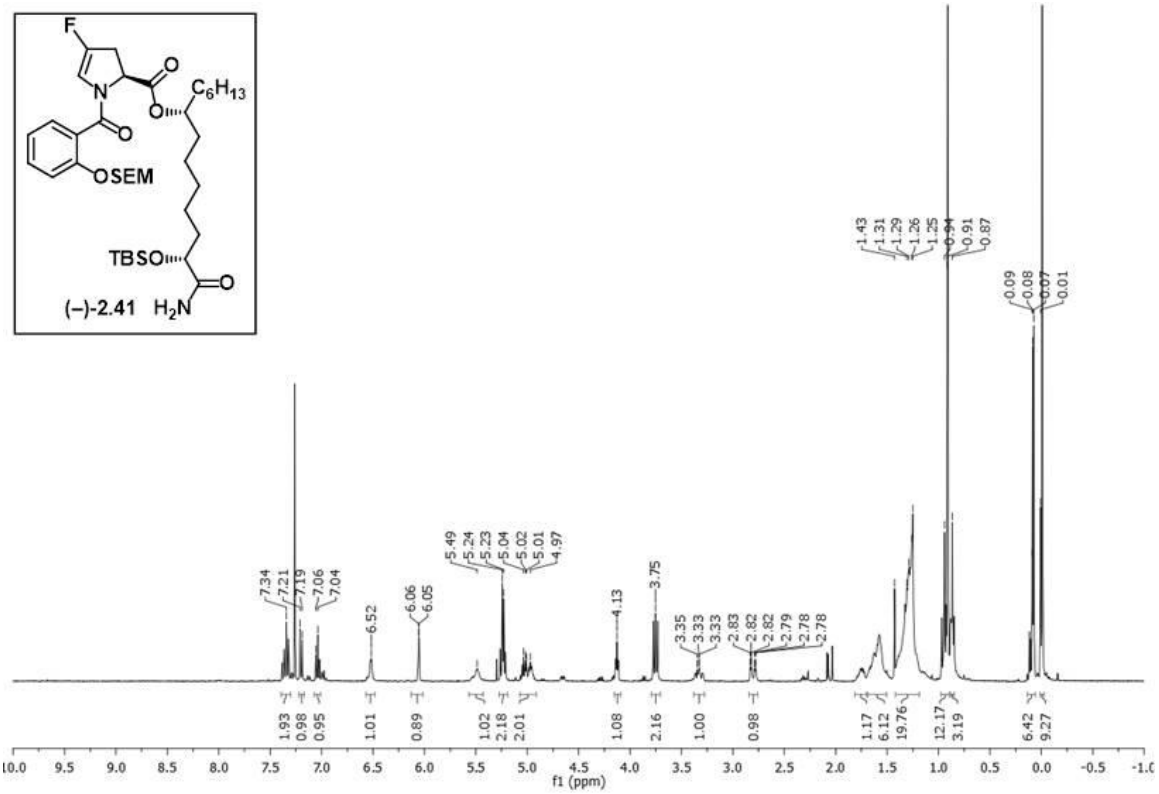
F
O
N
O
C_6H_{13}
O
OSEM
TBSO
O
(–)-2.41 H_2N
7.34
7.21
7.19
7.06
7.04
6.52
6.06
6.05
5.49
5.24
5.23
5.04
5.02
5.01
4.97
4.13
3.75
3.35
3.33
3.33
2.83
2.82
2.82
2.79
2.78
2.78
1.43
1.31
1.29
1.26
1.25
0.94
0.91
0.87
0.09
0.08
0.07
0.01
1.93
0.98
0.95
1.01
0.89
1.02
2.18
2.01
1.08
2.16
1.00
0.98
1.17
6.12
19.76
12.17
3.19
6.42
9.27
f1 (ppm)

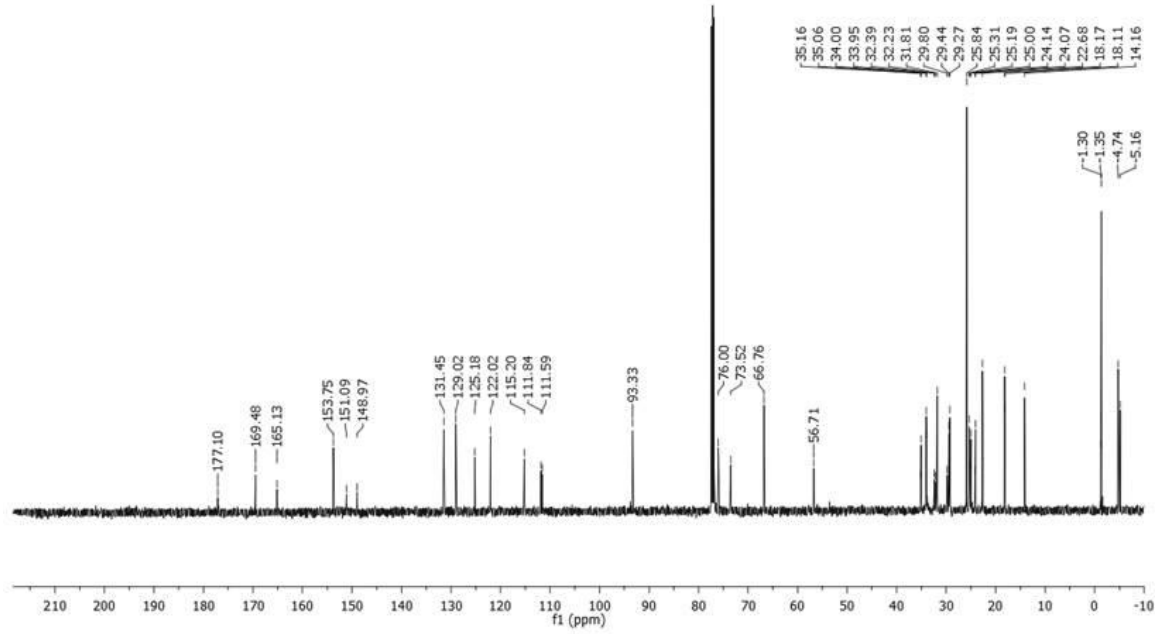
35.16
35.06
34.00
33.95
32.39
32.23
31.81
29.80
29.44
29.27
25.84
25.31
25.19
25.00
24.14
24.07
22.68
18.17
18.11
14.16
1.30
1.35
4.74
5.16
177.10
169.48
165.13
153.75
151.09
148.97
131.45
129.02
125.18
122.02
115.20
111.84
111.59
93.33
76.00
73.52
66.76
56.71
f1 (ppm)

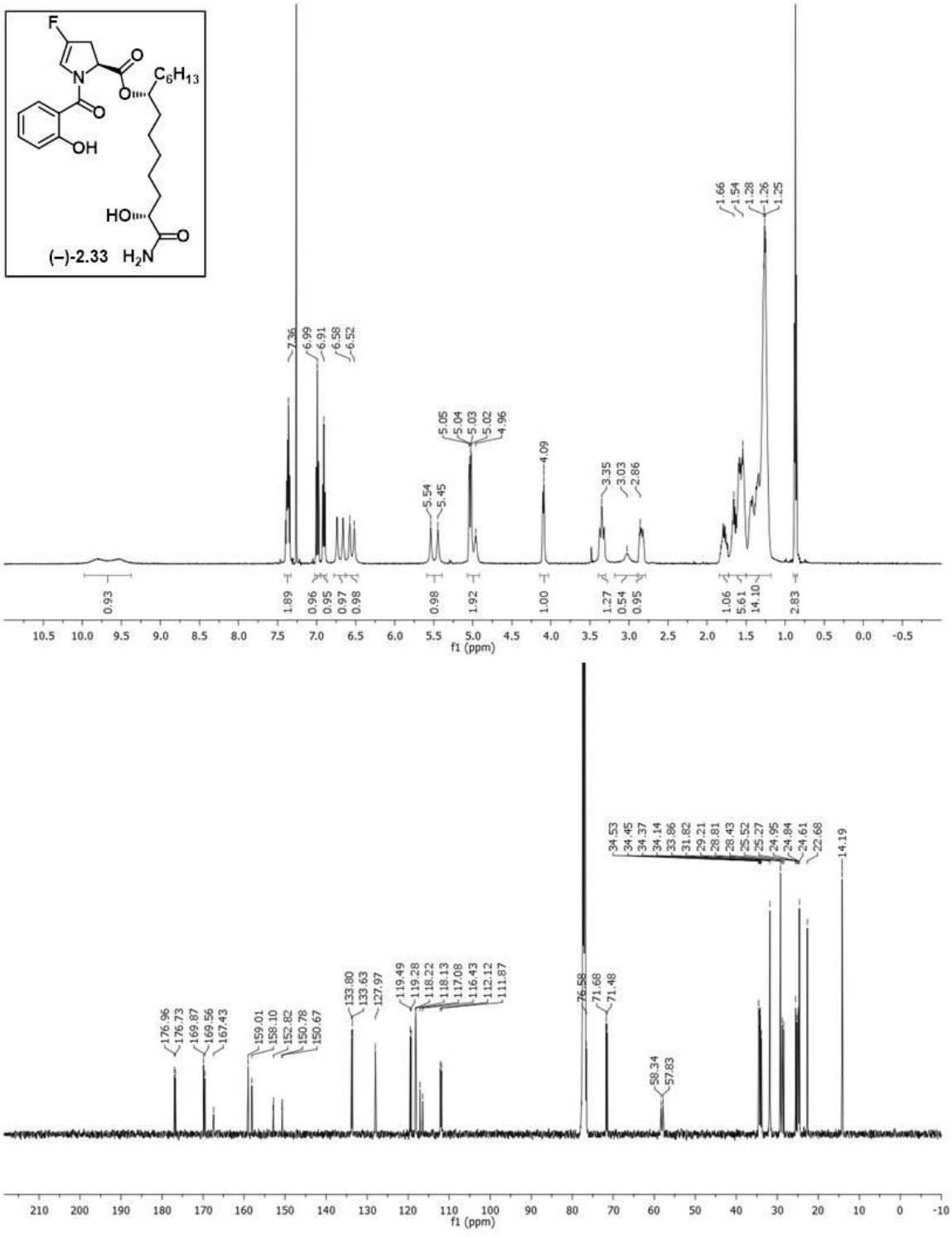
F
O
N
O
O
C_6H_{13}
OH
HO
O
(–)-2.33 H_2N
7.36
6.99
6.91
6.58
6.52
5.54
5.45
5.05
5.04
5.03
5.02
4.96
4.09
3.35
3.03
2.86
1.66
1.54
1.28
1.26
1.25
0.93
1.89
0.96
0.95
0.97
0.98
0.98
1.92
1.00
1.27
0.54
0.95
1.06
5.61
14.10
2.83
f1 (ppm)
176.96
176.73
169.87
169.56
167.43
159.01
158.10
152.82
150.78
150.67
133.80
133.63
127.97
119.49
119.28
118.22
118.13
117.08
116.43
112.12
111.87
76.58
71.68
71.48
58.34
57.83
34.53
34.45
34.37
34.14
33.86
31.82
29.21
28.81
28.43
25.52
25.27
24.95
24.84
24.61
22.68
14.19
f1 (ppm)

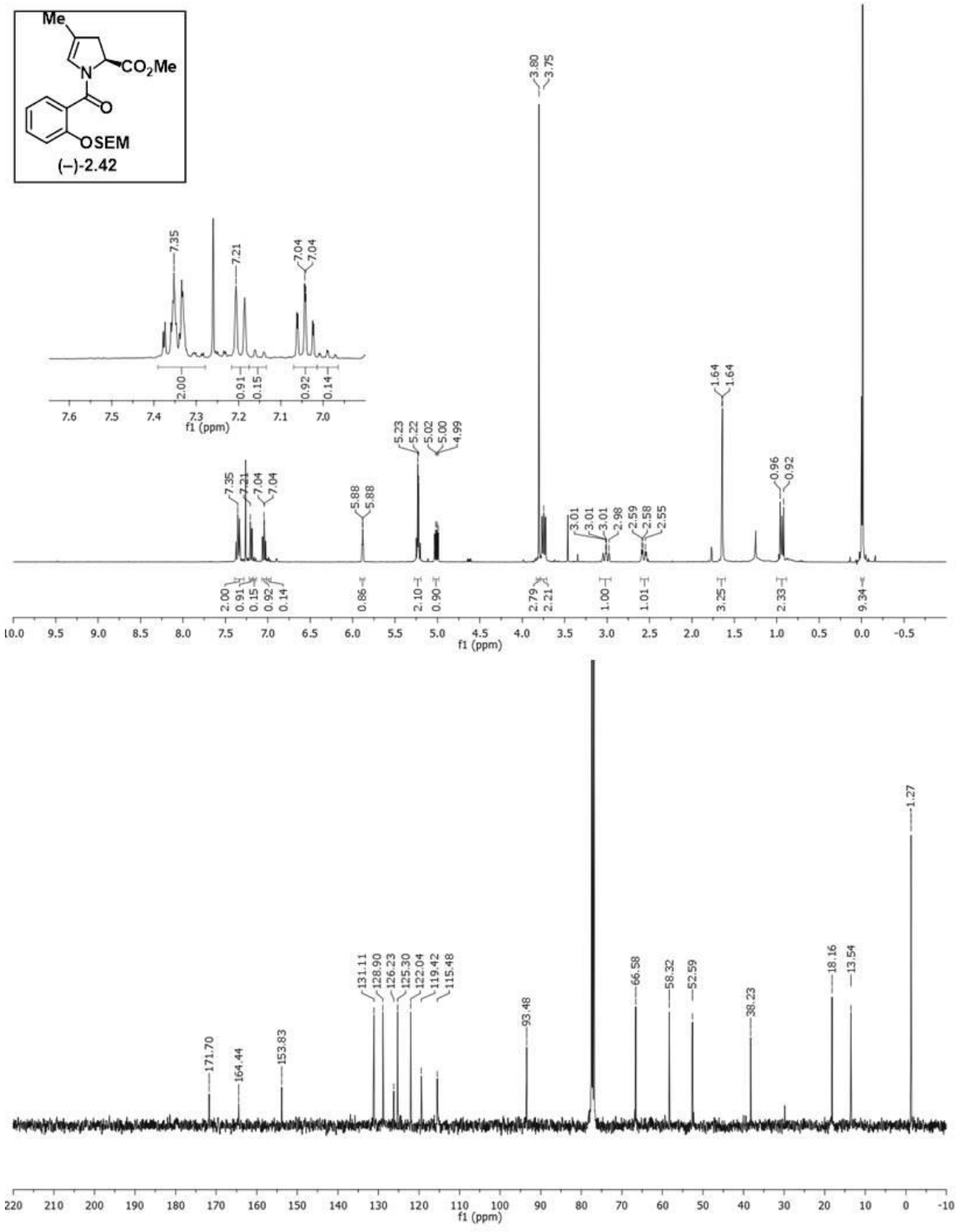
Me
CO2Me
N
O
OSEM
(–)-2.42
f1 (ppm)
f1 (ppm)

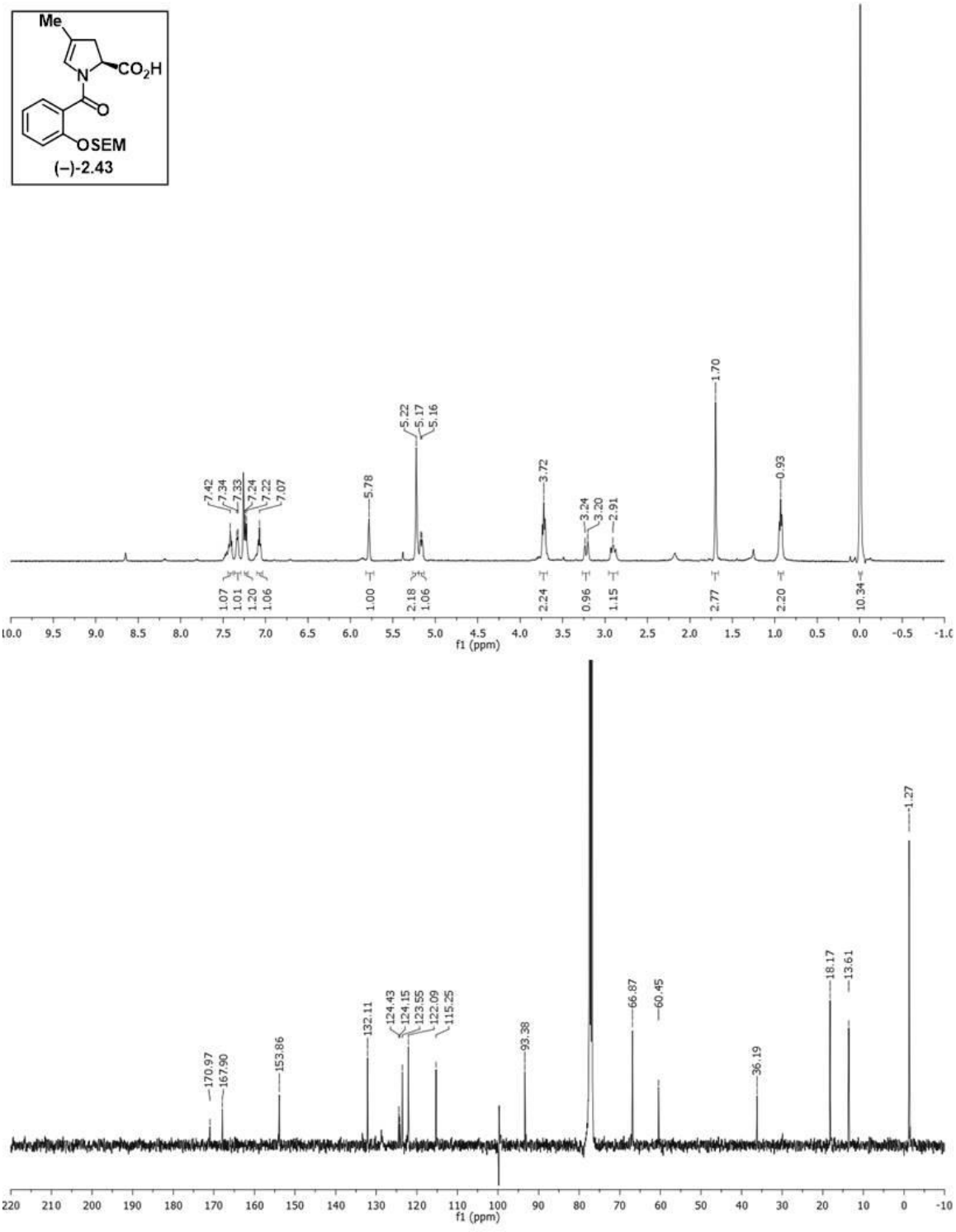
Me
CO2H
N
O
OSEM
(–)-2.43
7.42
7.34
7.33
7.24
7.22
7.07
5.78
5.22
5.17
5.16
3.72
3.24
3.20
2.91
1.70
0.93
1.07
1.01
1.20
1.06
1.00
2.18
1.06
2.24
0.96
1.15
2.77
2.20
10.34
f1 (ppm)
170.97
167.90
153.86
132.11
124.43
124.15
123.55
122.09
115.25
93.38
66.87
60.45
36.19
18.17
13.61
1.27
f1 (ppm)

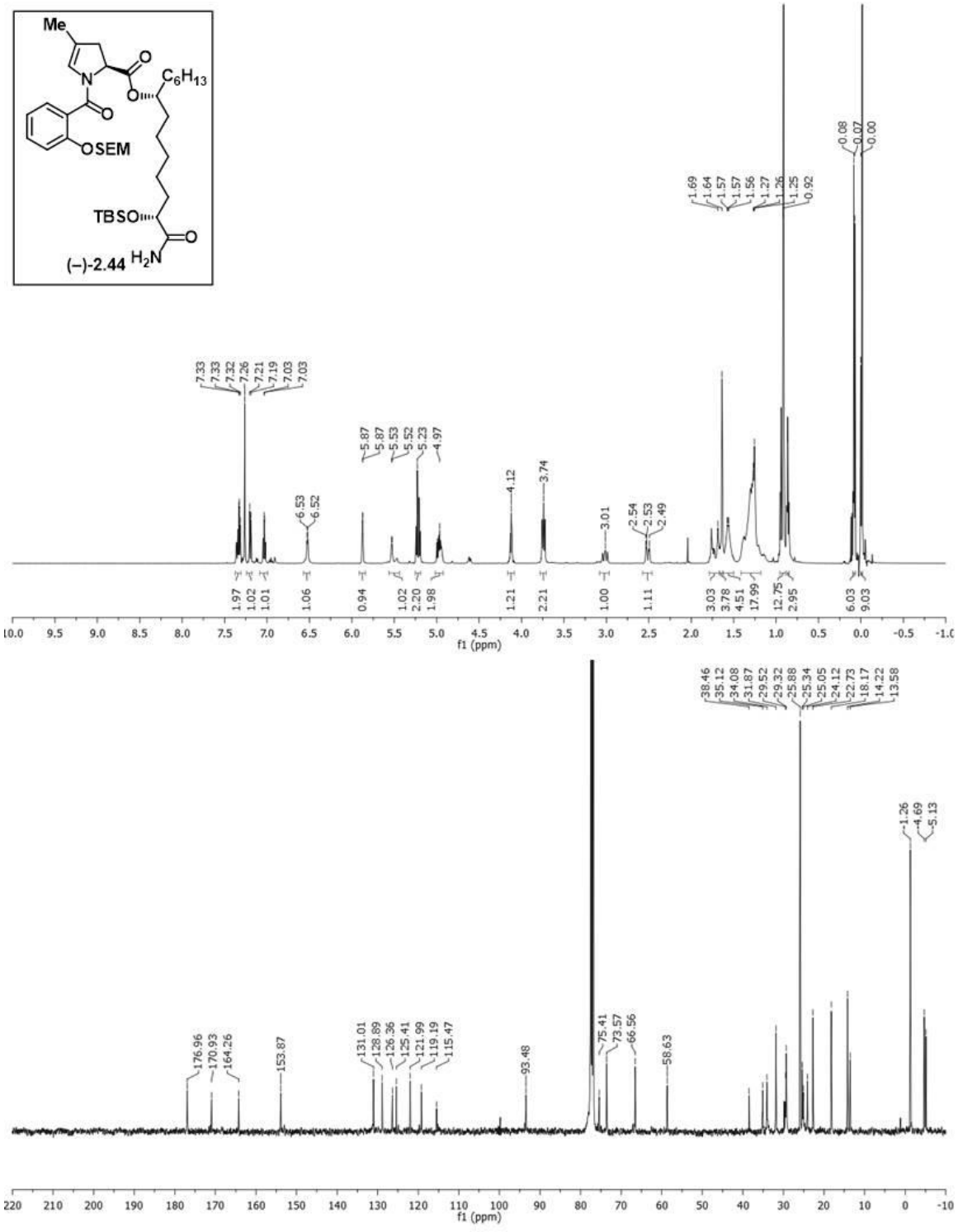
Me
C_6H_{13}
OSEM
TBSO
(–)-2.44 H_2N
f1 (ppm)
f1 (ppm)

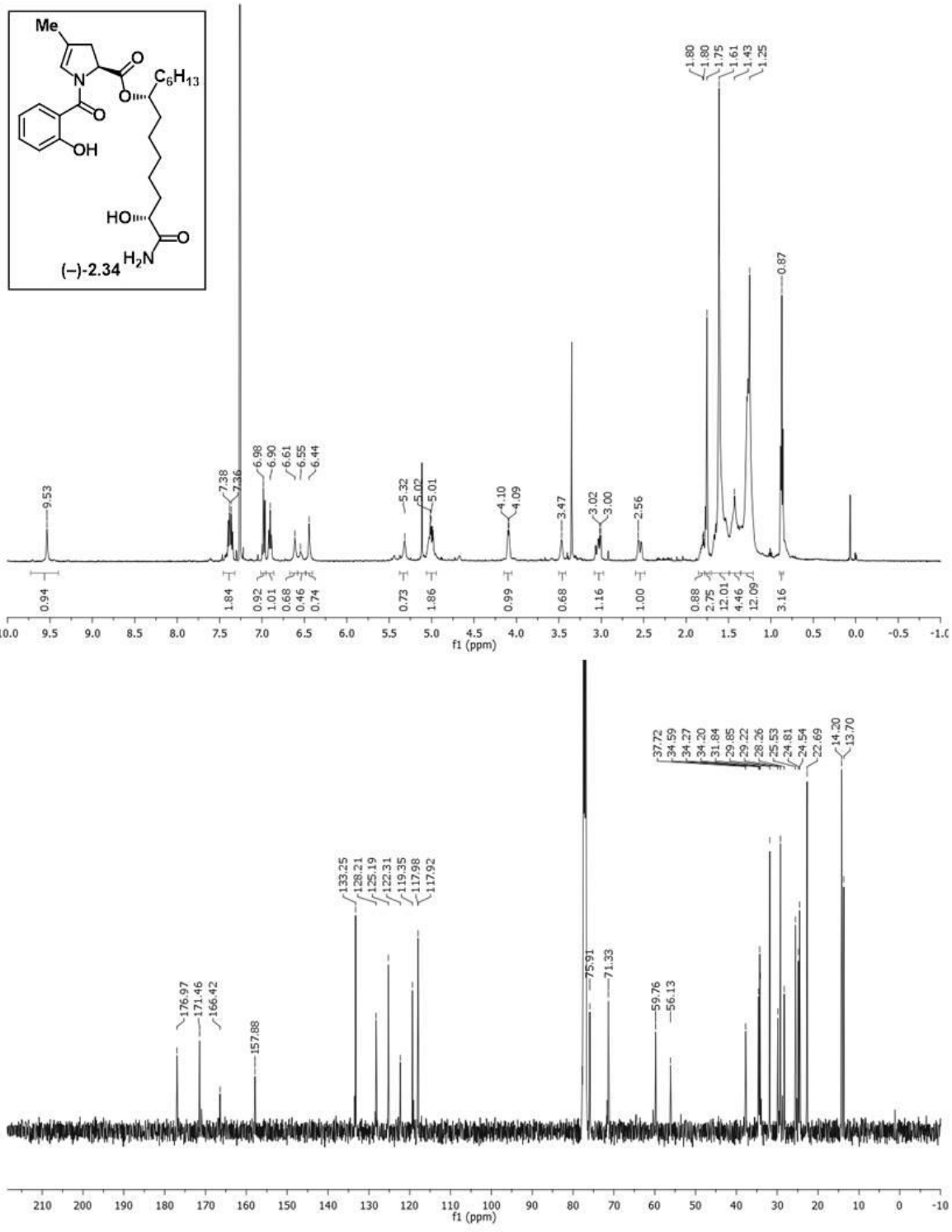
Me
O
N
O
C_6H_{13}
O
OH
HO
O
H_2N
(–)-2.34
9.53
7.38
7.36
6.98
6.90
6.61
6.55
6.44
5.32
5.02
5.01
4.10
4.09
3.47
3.02
3.00
2.56
1.80
1.80
1.75
1.61
1.43
1.25
0.87
0.94
1.84
0.92
1.01
0.68
0.46
0.74
0.73
1.86
0.99
0.68
1.16
1.00
0.88
2.75
12.01
4.46
12.09
3.16
f1 (ppm)
176.97
171.46
166.42
157.88
133.25
128.21
125.19
122.31
119.35
117.98
117.92
75.91
71.33
59.76
56.13
37.72
34.59
34.27
34.20
31.84
29.85
29.22
28.26
25.53
24.81
24.54
22.69
14.20
13.70
f1 (ppm)

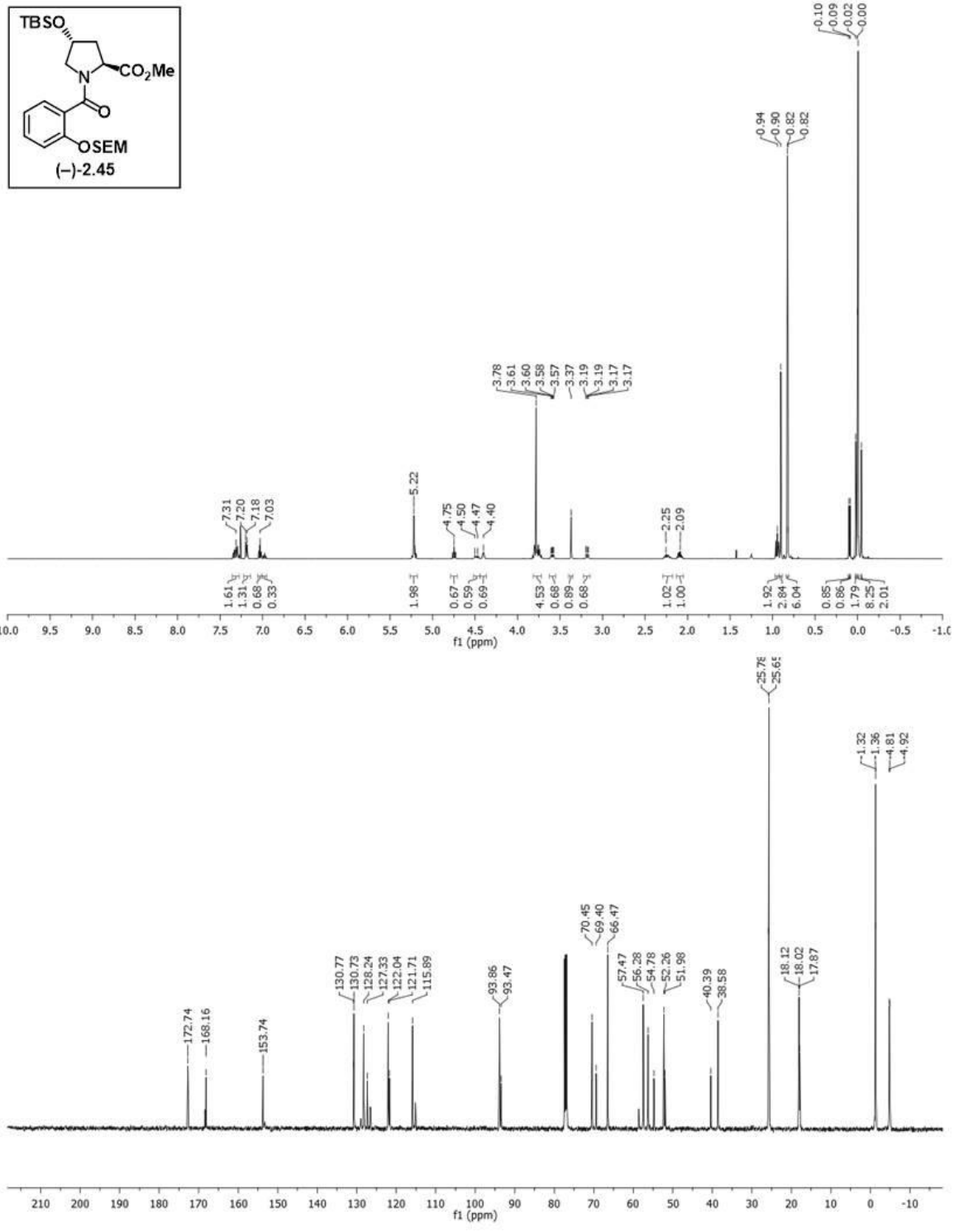
TBSO
CO2Me
N
O
OSEM
(–)-2.45
f1 (ppm)
f1 (ppm)

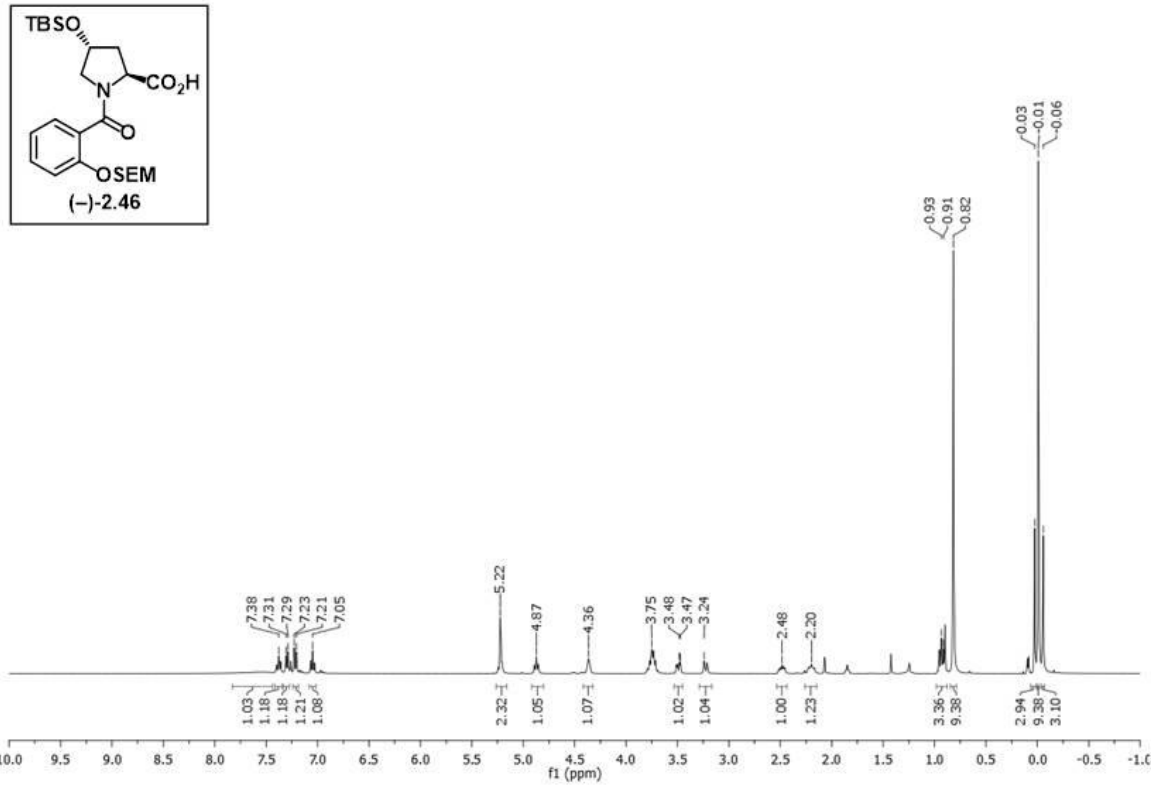
TBSO
CO2H
N
O
OSEM
(–)-2.46
0.03
0.01
0.06
0.93
0.91
0.82
7.38
7.31
7.29
7.23
7.21
7.05
5.22
4.87
4.36
3.75
3.48
3.47
3.24
2.48
2.20
1.03
1.18
1.18
1.21
1.08
2.32
1.05
1.07
1.02
1.04
1.00
1.23
3.36
9.38
2.94
9.38
3.10
f1 (ppm)

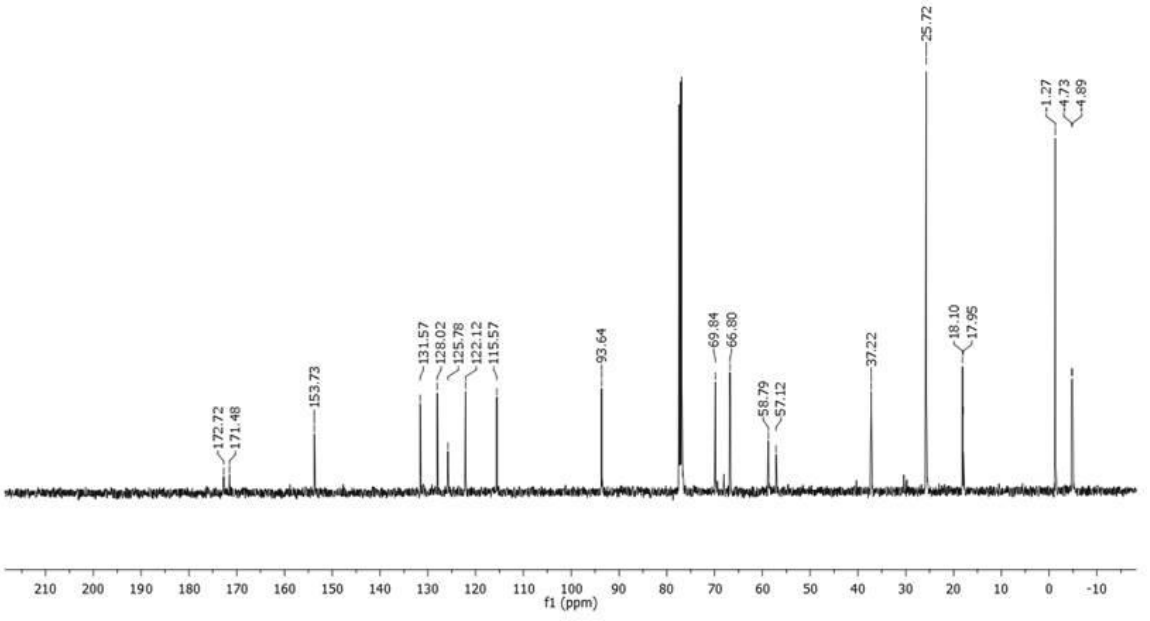
25.72
1.27
4.73
4.89
131.57
128.02
125.78
122.12
115.57
93.64
69.84
66.80
58.79
57.12
37.22
18.10
17.95
172.72
171.48
153.73
f1 (ppm)

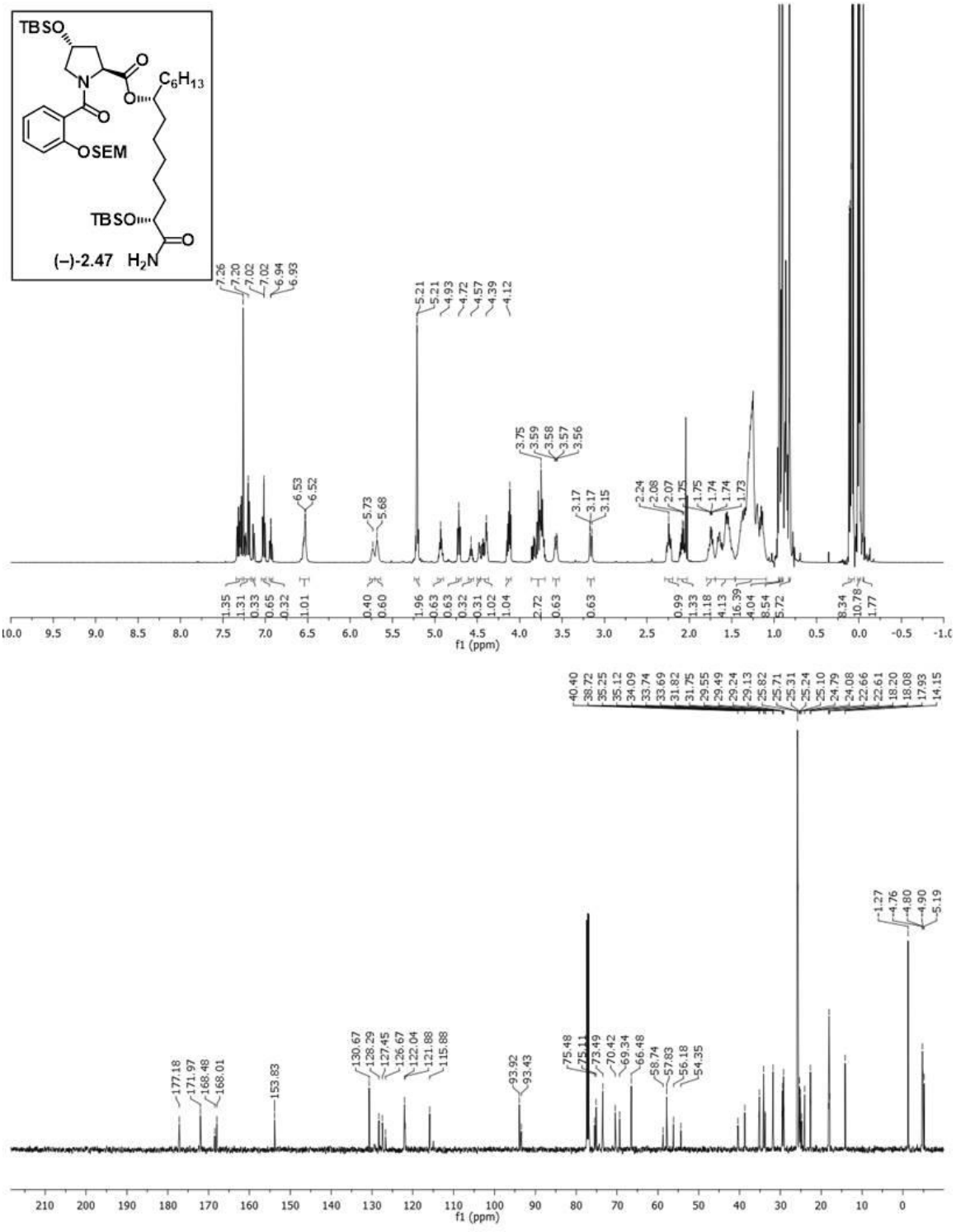
TBSO
C6H13
OSEM
TBSO
(–)-2.47 H2N
f1 (ppm)
f1 (ppm)

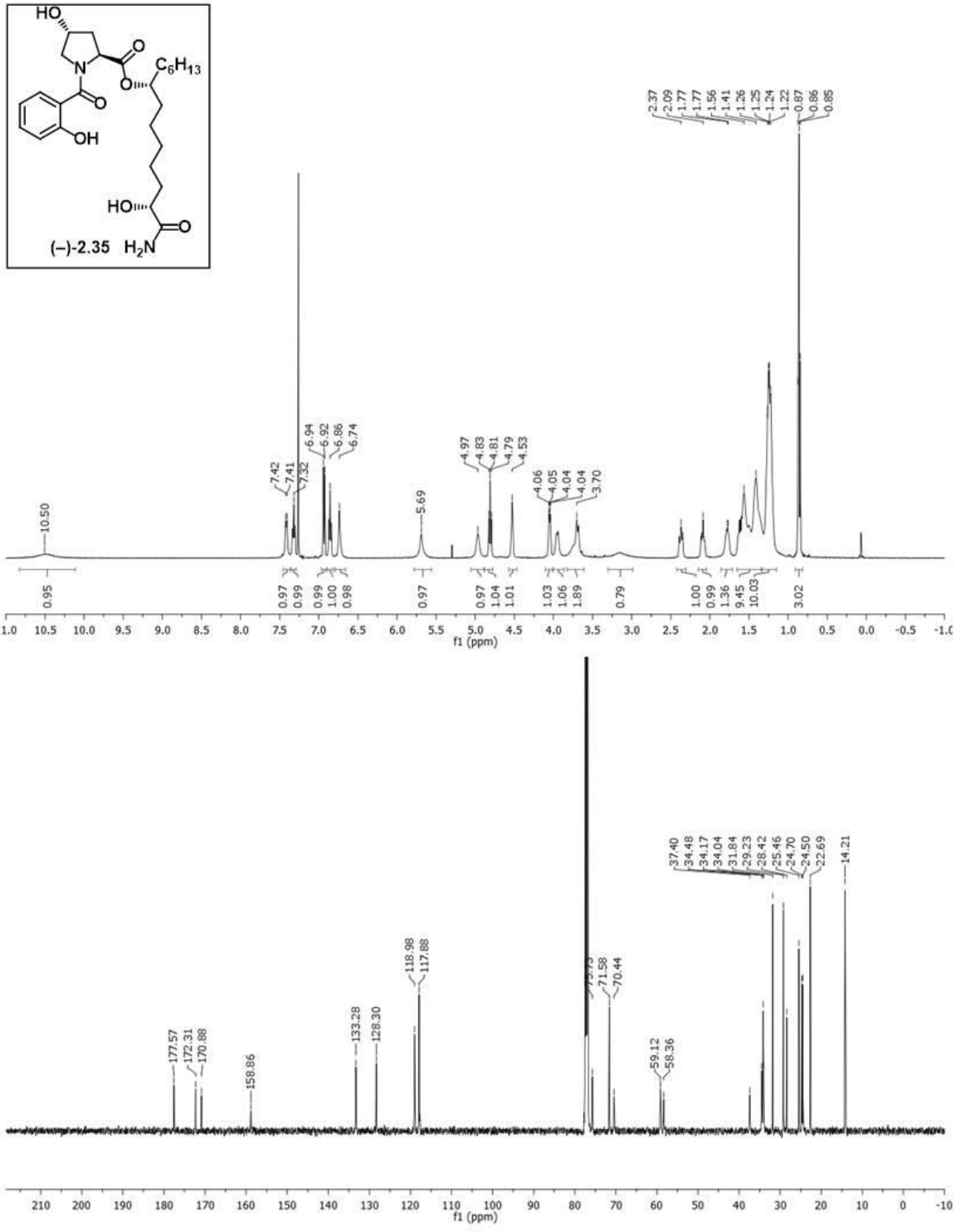
HO
N
O
O
C_6H_{13}
O
OH
HO
O
(–)-2.35 H_2N
2.37
2.09
1.77
1.77
1.56
1.41
1.26
1.25
1.24
1.22
0.87
0.86
0.85
7.42
7.41
7.32
6.94
6.92
6.86
6.74
5.69
4.97
4.83
4.81
4.79
4.53
4.06
4.05
4.04
4.04
3.70
10.50
0.95
0.97
0.99
0.99
1.00
0.98
0.97
0.97
1.04
1.01
1.03
1.06
1.89
0.79
1.00
0.99
1.36
9.45
10.03
3.02
f1 (ppm)
177.57
172.31
170.88
158.86
133.28
128.30
118.98
117.68
71.58
70.44
59.12
58.36
37.40
34.48
34.17
34.04
31.84
29.23
28.42
25.46
24.70
24.50
22.69
14.21
f1 (ppm)

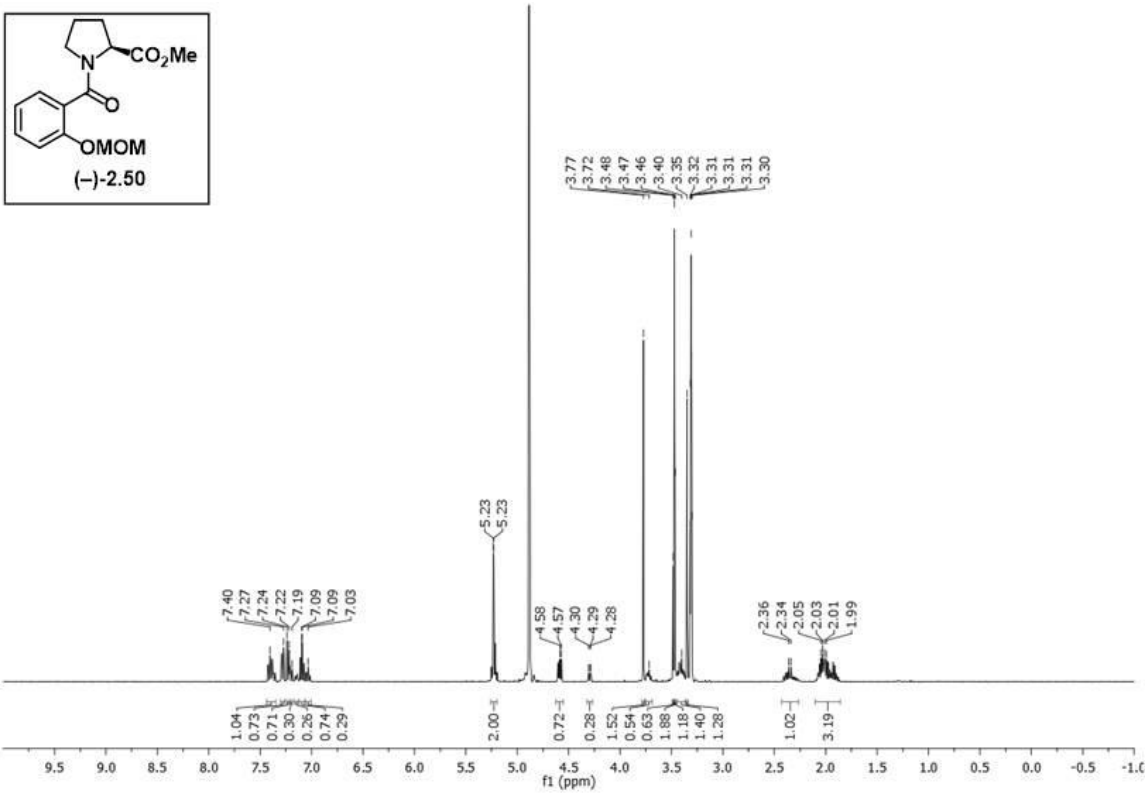
CO2Me
N
O
OMOM
(–)-2.50
7.40
7.27
7.24
7.22
7.19
7.09
7.09
7.03
5.23
5.23
4.58
4.57
4.30
4.29
4.28
3.77
3.72
3.48
3.47
3.46
3.40
3.35
3.32
3.31
3.31
3.31
3.30
2.36
2.34
2.05
2.03
2.01
1.99
1.04
0.73
0.71
0.30
0.26
0.74
0.29
2.00
0.72
0.28
1.52
0.54
0.63
1.88
1.18
1.40
1.28
1.02
3.19
f1 (ppm)

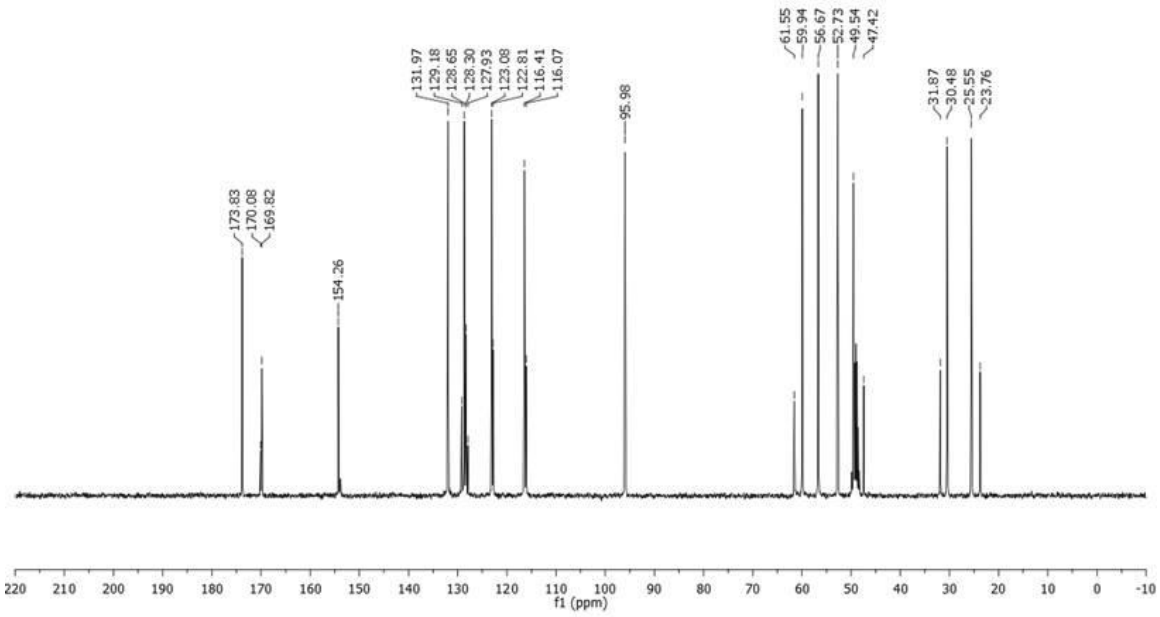
173.83
170.08
169.82
154.26
131.97
129.18
128.65
128.30
127.93
123.08
122.81
116.41
116.07
95.98
61.55
59.94
56.67
52.73
49.54
47.42
31.87
30.48
25.55
23.76
f1 (ppm)

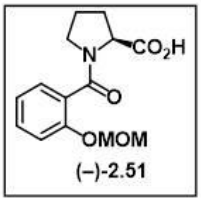
CO2H
N
O
OMOM

(–)-2.51

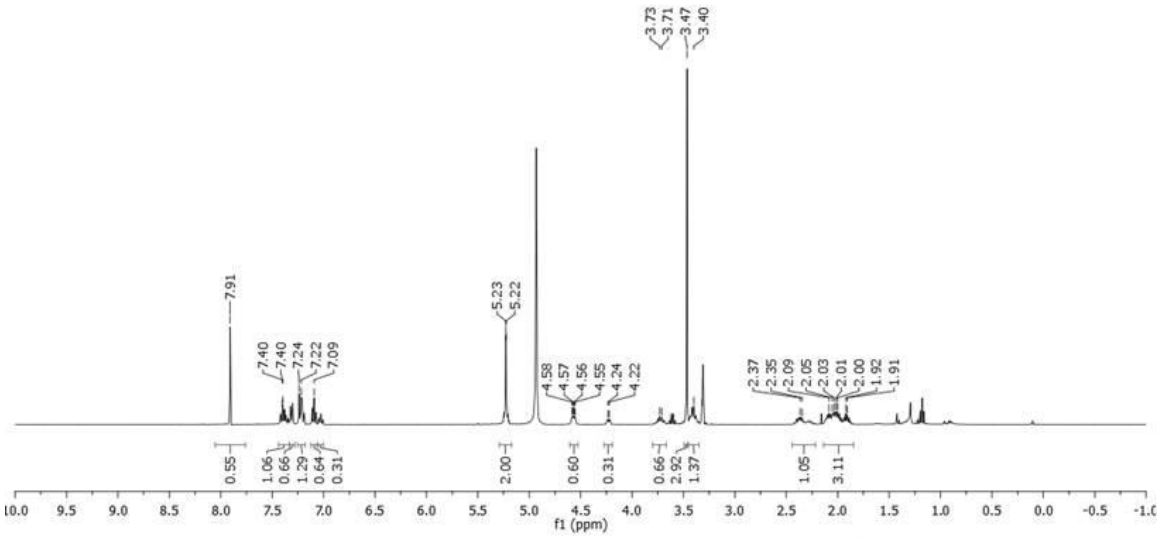
7.91
7.40
7.40
7.24
7.22
7.09
5.23
5.22
4.58
4.57
4.56
4.55
4.24
4.22
3.73
3.71
3.47
3.40
2.37
2.35
2.09
2.05
2.03
2.01
2.00
1.92
1.91
0.55
1.06
0.66
1.29
0.64
0.31
2.00
0.60
0.31
0.66
2.92
1.37
1.05
3.11
f1 (ppm)

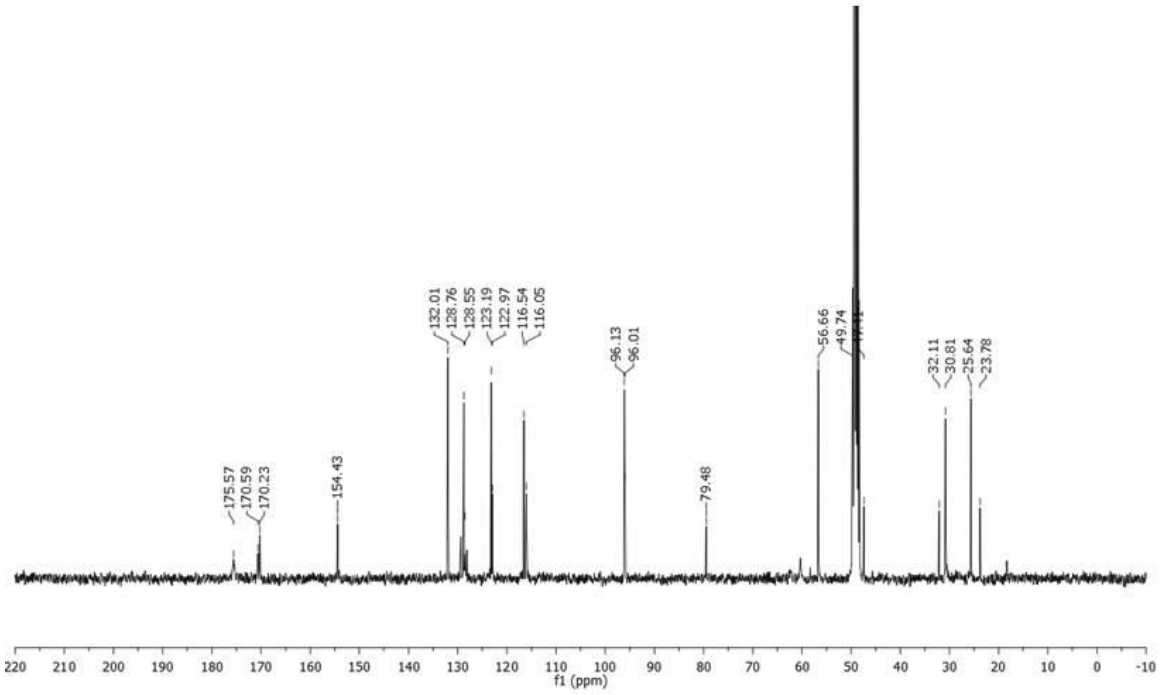
132.01
128.76
128.55
123.19
122.97
116.54
116.05
96.13
96.01
56.66
49.74
32.11
30.81
25.64
23.78
175.57
170.59
170.23
154.43
79.48
f1 (ppm)

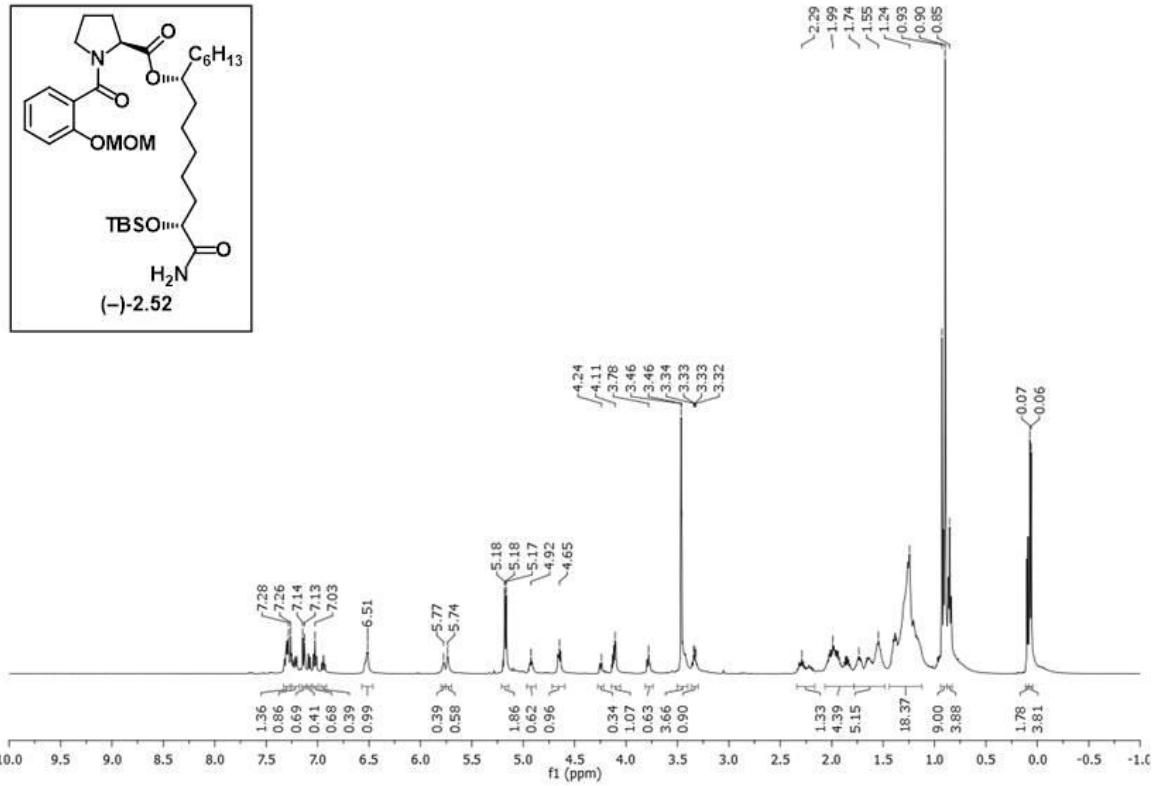
OMOM
TBSO
C_6H_{13}
H_2N
(–)-2.52
f1 (ppm)

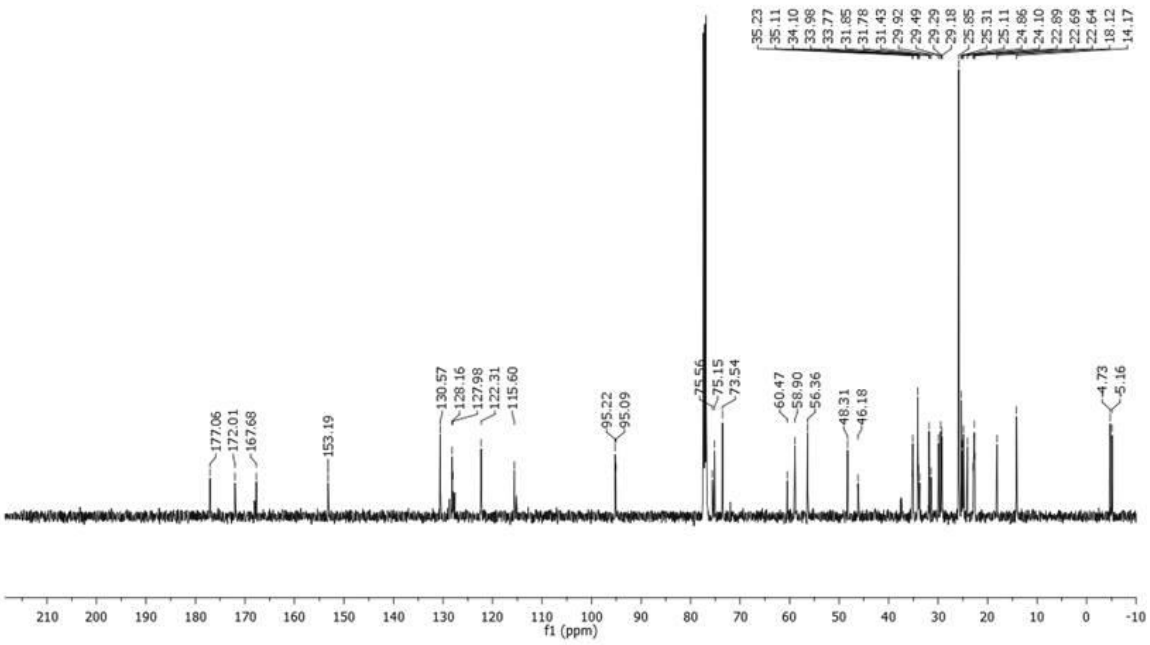
f1 (ppm)

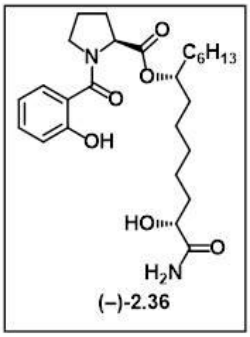
O
N
O
C_6H_{13}
O
OH
HO
O
H_2N

(–)-2.36

10.64
7.49
7.48
7.33
6.96
6.94
6.86
6.66
5.52
4.98
4.64
4.08
3.87
3.86
3.79
3.78
3.77
3.66
2.36
2.35
2.34
2.32
2.10
1.97
1.96
1.95
1.82
1.26
0.86
0.89
0.94
0.98
0.99
1.11
0.99
0.98
1.00
1.00
1.07
1.10
1.30
1.10
0.92
1.09
2.31
2.86
5.39
6.11
10.75
3.25
f1 (ppm)

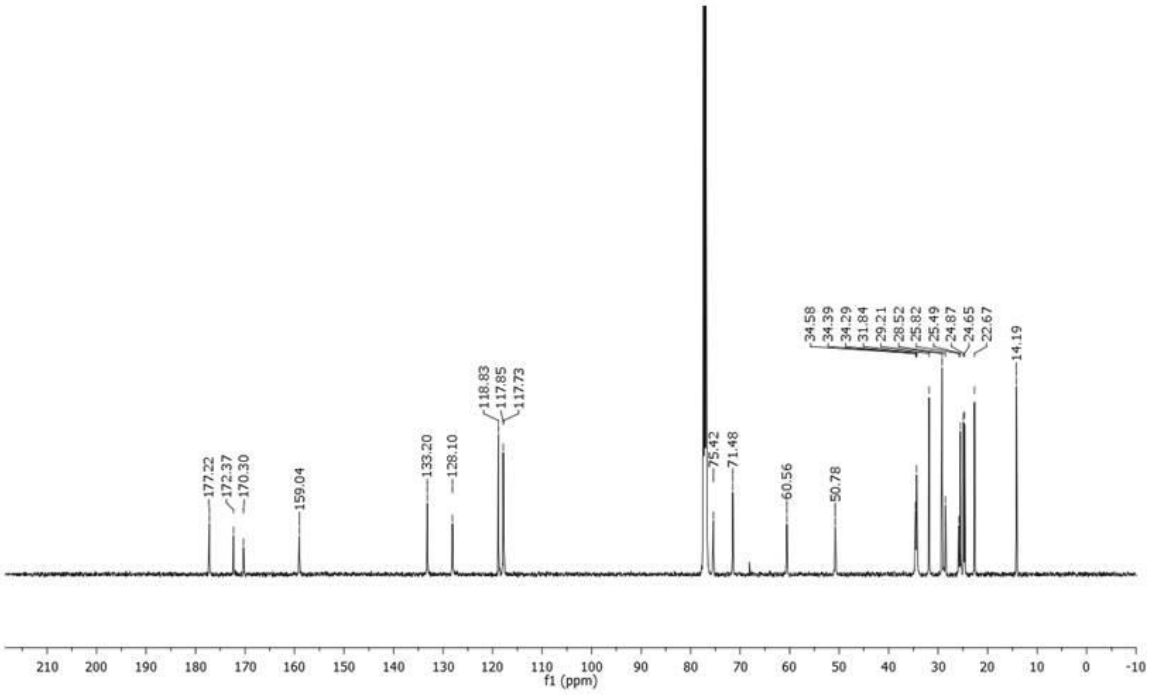
177.22
172.37
170.30
159.04
133.20
128.10
118.83
117.85
117.73
75.42
71.48
60.56
50.78
34.58
34.39
34.29
31.84
29.21
28.52
25.82
25.49
24.87
24.65
22.67
14.19
f1 (ppm)

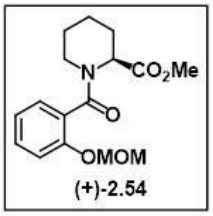
N
CO2Me
O
OMOM

(+)-2.54

7.39
7.39
7.35
7.34
7.24
7.22
7.11
5.29
5.28
5.26
5.26
5.24
5.67
4.83
4.80
4.36
4.35
3.85
3.54
3.19
3.18
2.88
2.88
2.41
2.30
2.27
2.10
2.10
2.10
1.83
1.80
1.64
1.59
1.42
2.67
1.16
1.23
0.73
2.00
0.32
0.31
0.08
0.22
2.22
1.08
4.22
0.55
0.57
0.23
0.75
0.32
2.52
2.08
1.49
f1 (ppm)

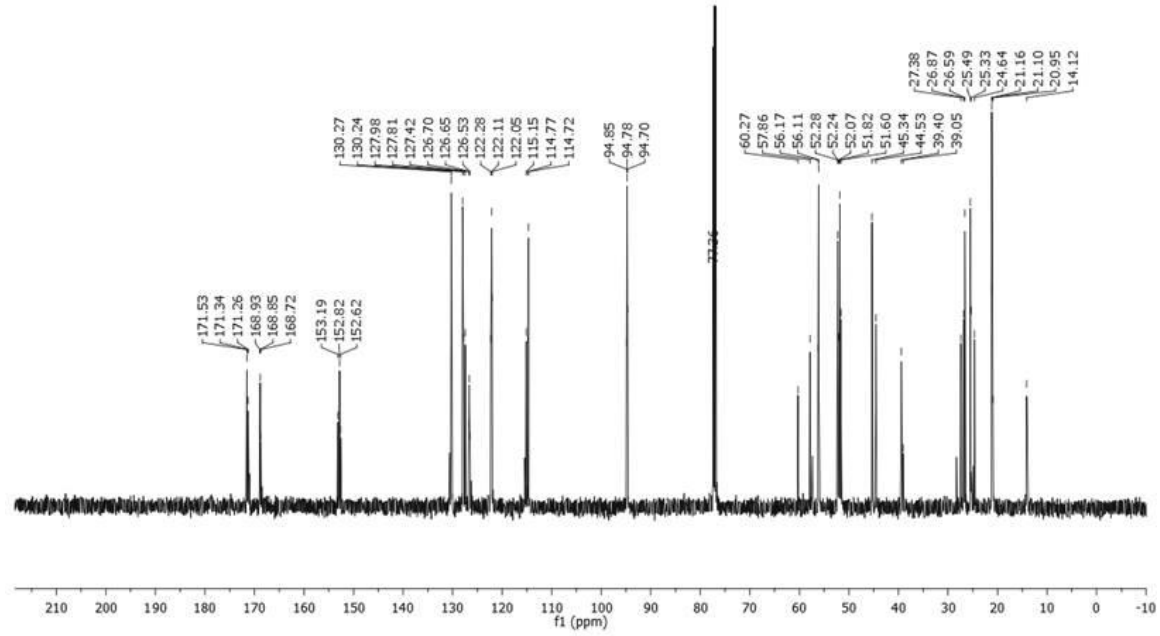
171.53
171.34
171.26
168.93
168.85
168.72
153.19
152.82
152.62
130.27
130.24
127.98
127.81
127.42
126.70
126.65
126.53
122.28
122.11
122.05
115.15
114.77
114.72
94.85
94.78
94.70
77.36
60.27
57.86
56.17
56.11
52.28
52.24
52.07
51.82
51.60
45.34
44.53
39.40
39.05
27.38
26.87
26.59
25.49
25.33
24.64
21.16
21.10
20.95
14.12
f1 (ppm)

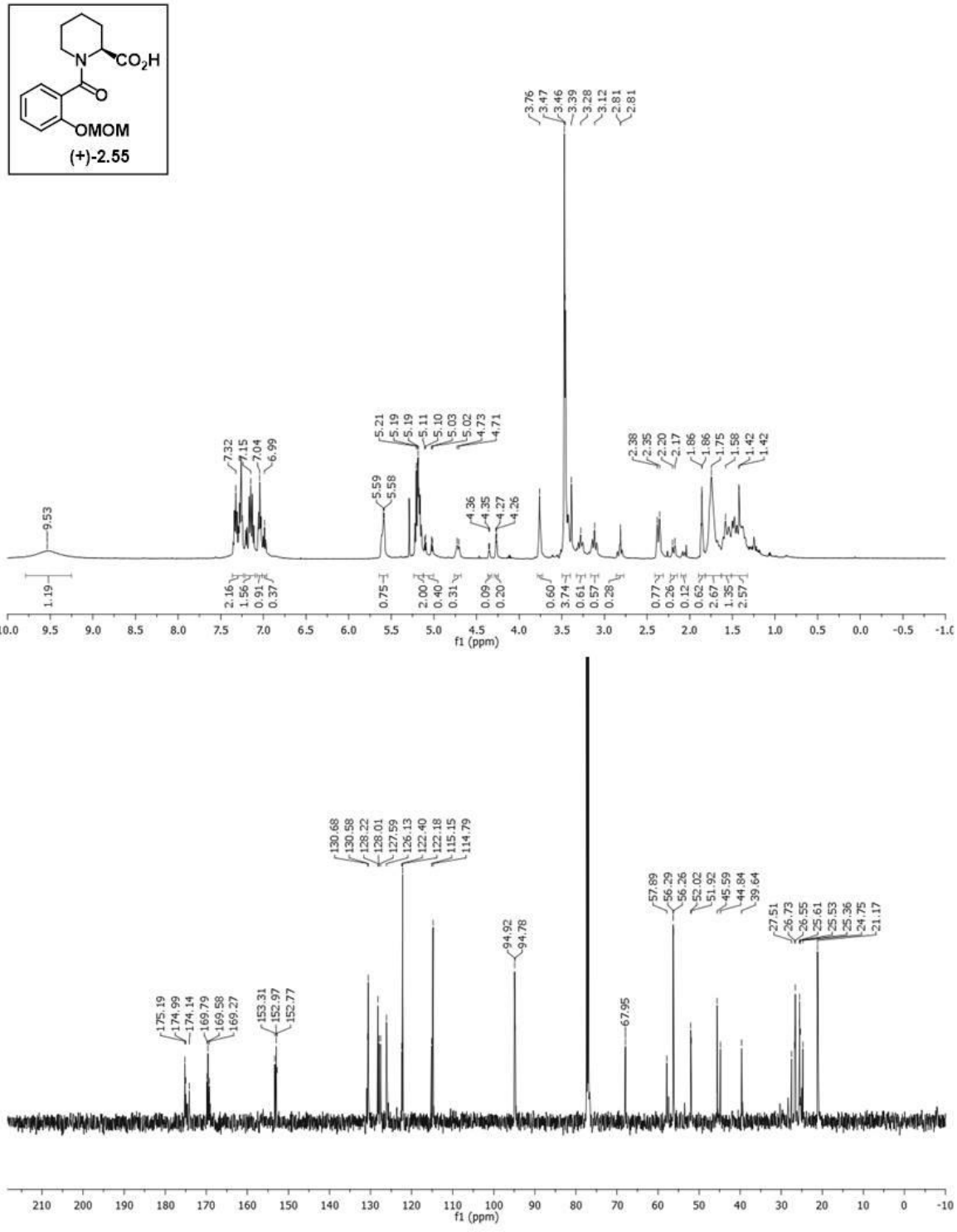
CO2H
N
O
OMOM
(+)-2.55
f1 (ppm)
f1 (ppm)

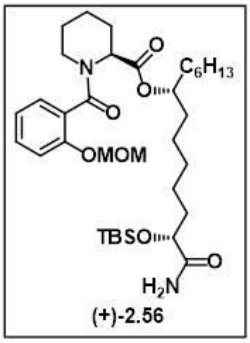
C6H13
OMOM
TBSO
H2N
(+)-2.56

f1 (ppm)

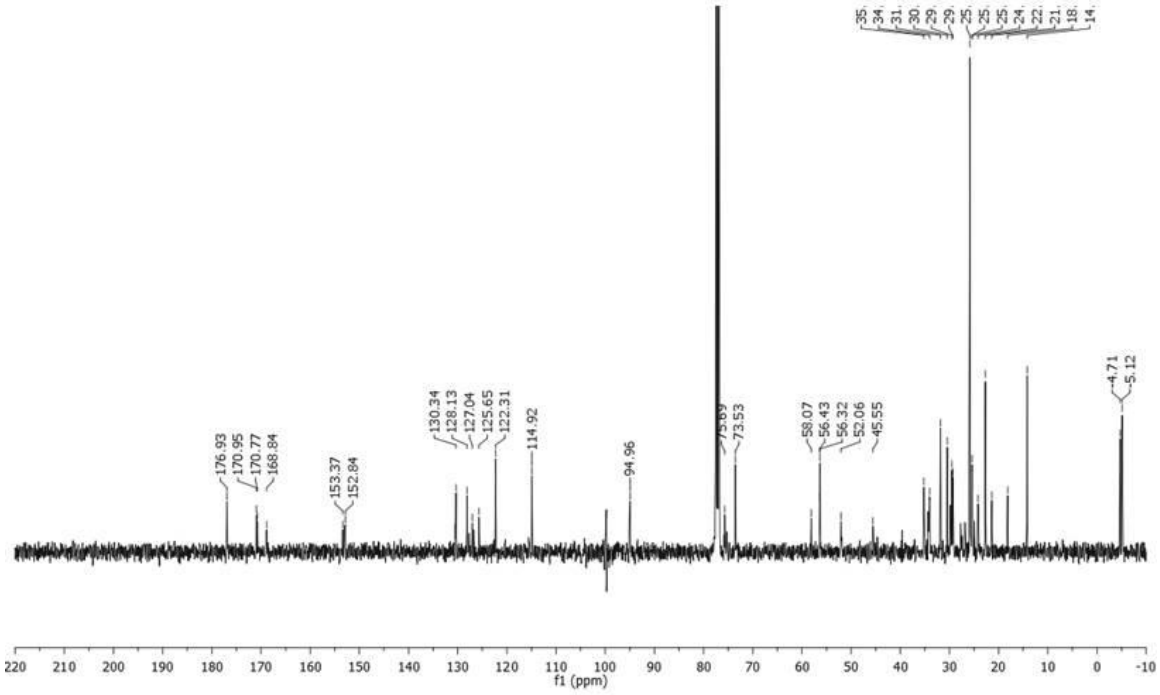
f1 (ppm)

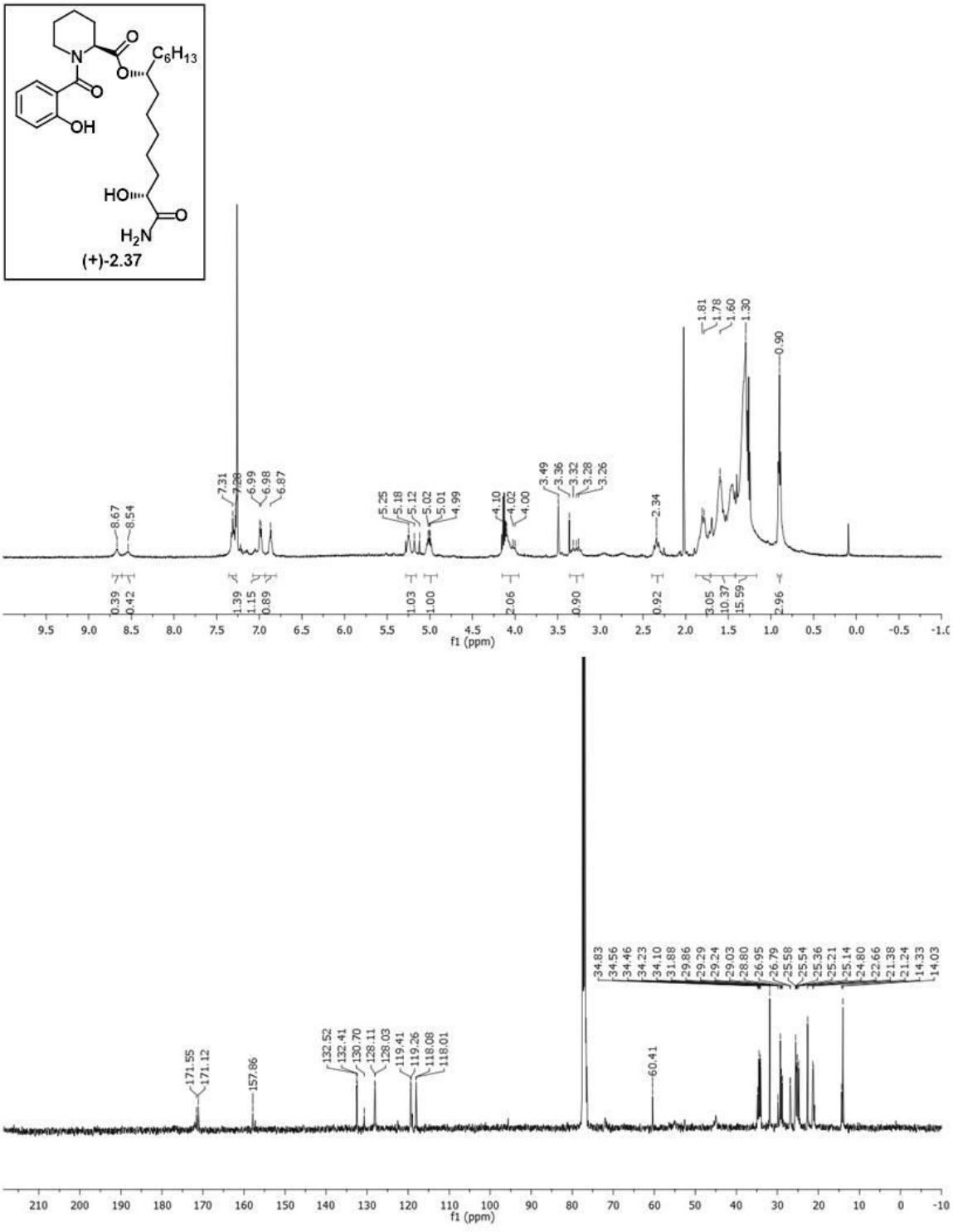
(+)-2.37
f1 (ppm)
f1 (ppm)

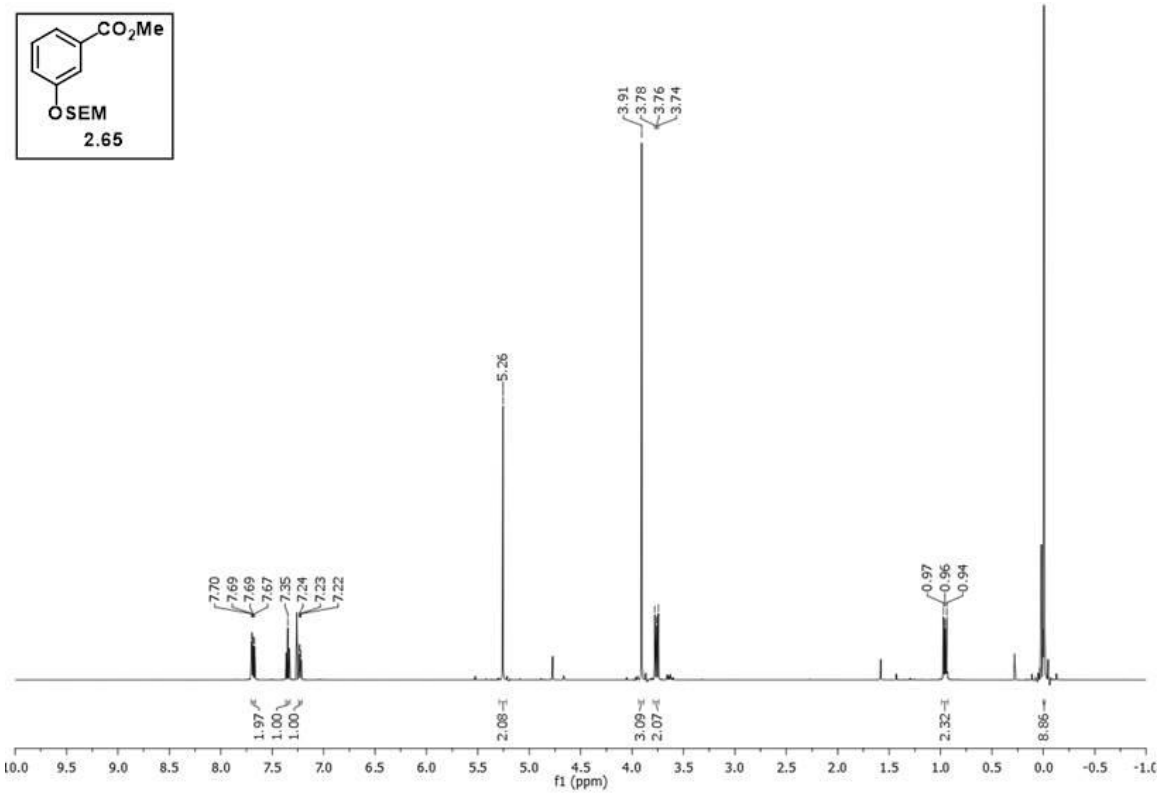
CO2Me
OSEM
2.65
7.70
7.69
7.69
7.67
7.35
7.24
7.23
7.22
5.26
3.91
3.78
3.76
3.74
0.97
0.96
0.94
1.97
1.00
1.00
2.08
3.09
2.07
2.32
8.86
f1 (ppm)

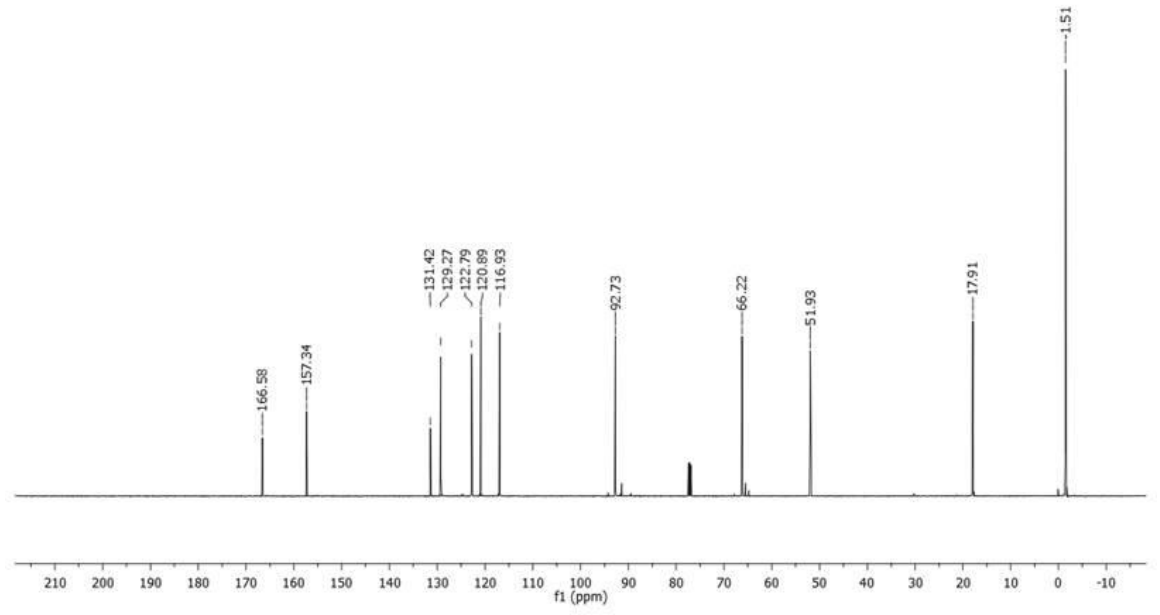
166.58
157.34
131.42
129.27
122.79
120.89
116.93
92.73
66.22
51.93
17.91
1.51
f1 (ppm)

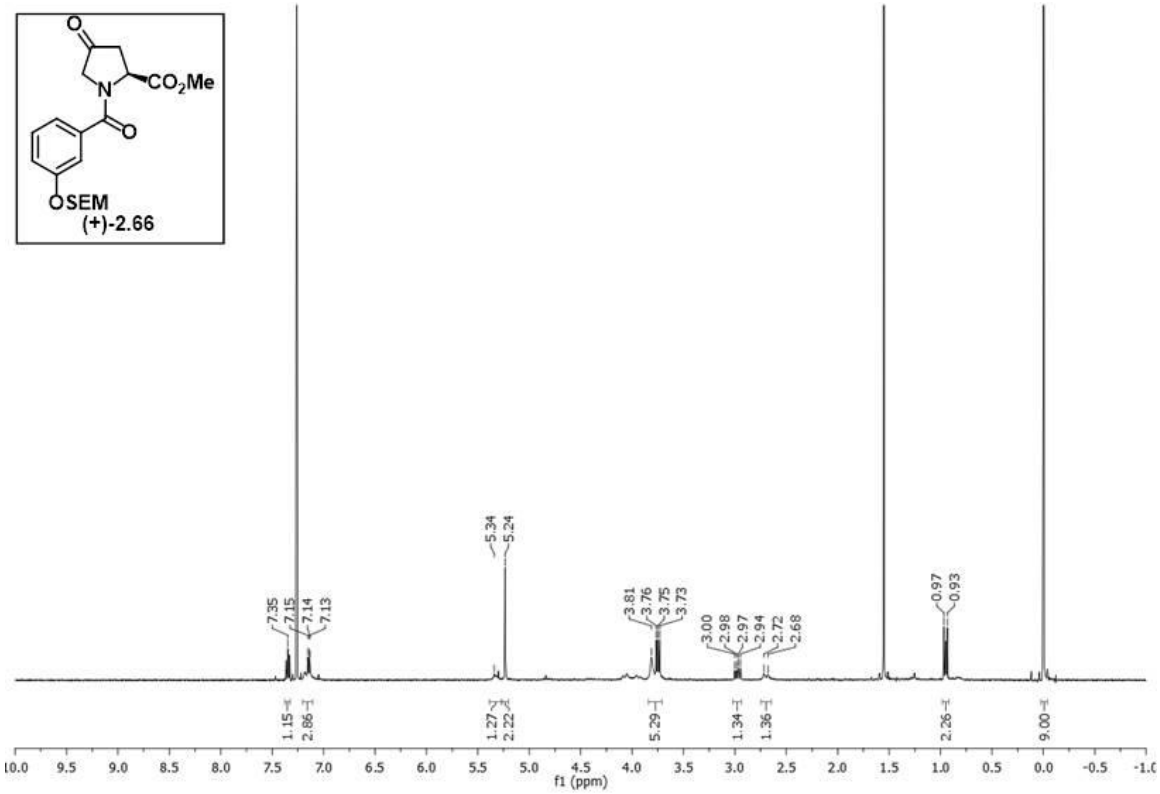
O
N
CO2Me
O
OSEM
(+)-2.66
7.35
7.15
7.14
7.13
5.34
5.24
3.81
3.76
3.75
3.73
3.00
2.98
2.97
2.94
2.72
2.68
0.97
0.93
1.15
2.86
1.27
2.22
5.29
1.34
1.36
2.26
9.00
f1 (ppm)

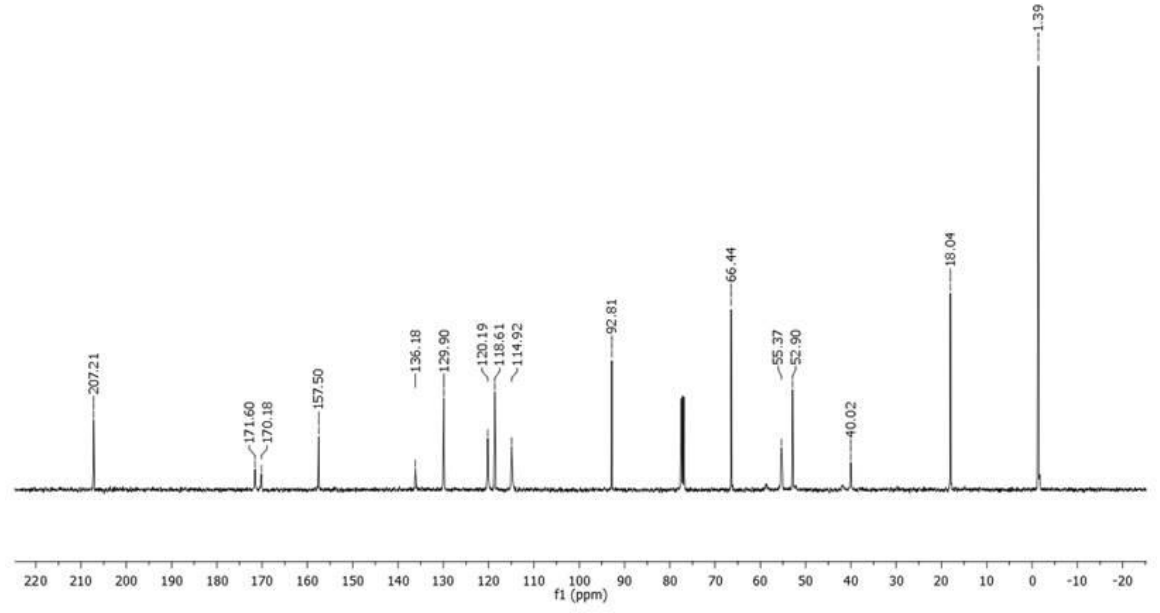
207.21
171.60
170.18
157.50
136.18
129.90
120.19
118.61
114.92
92.81
66.44
55.37
52.90
40.02
18.04
1.39
f1 (ppm)

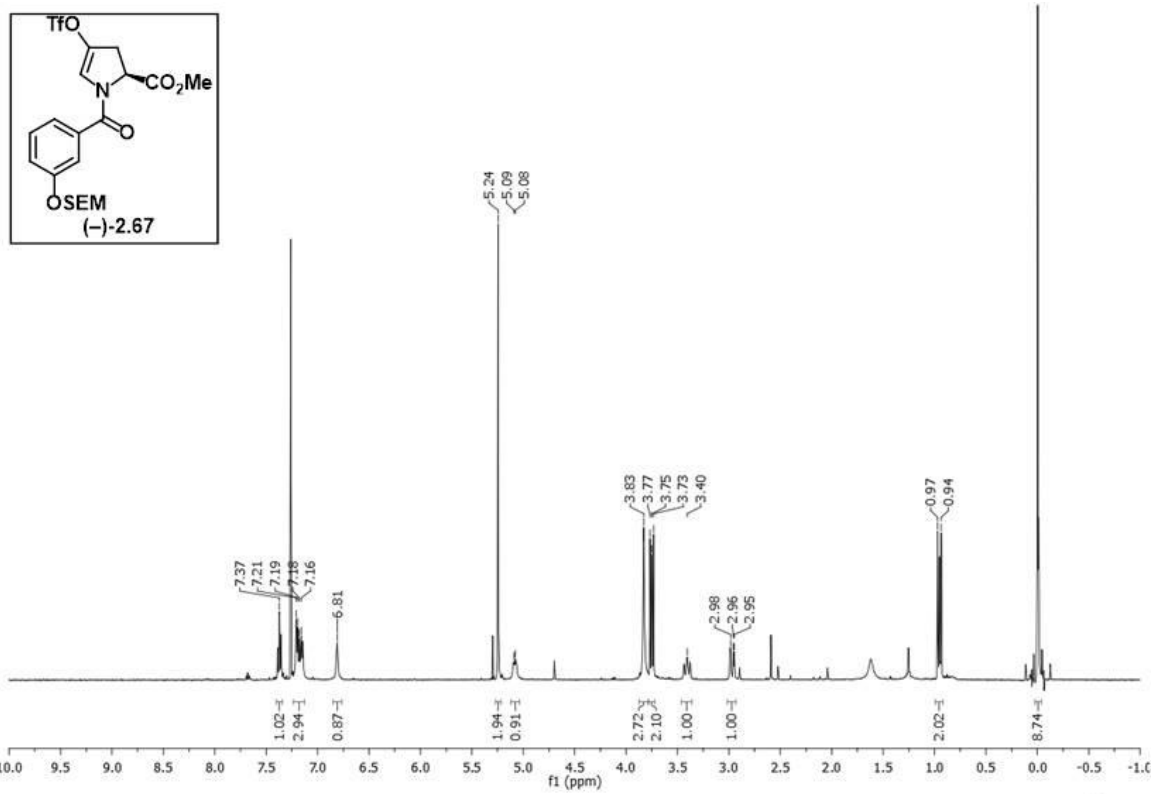
TfO
CO2Me
N
O
OSEM
(–)-2.67
7.37
7.21
7.19
7.18
7.16
6.81
5.24
5.09
5.08
3.83
3.77
3.75
3.73
3.40
2.98
2.96
2.95
0.97
0.94
1.02
2.94
0.87
1.94
0.91
2.72
2.10
1.00
1.00
2.02
8.74
f1 (ppm)

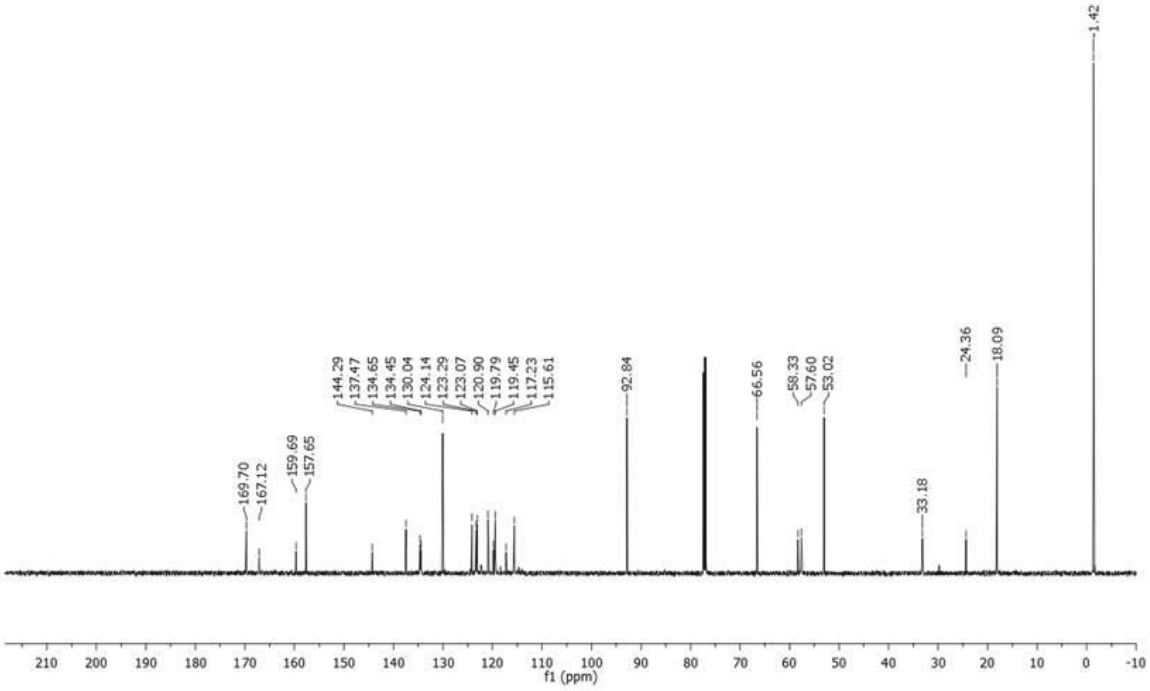
169.70
167.12
159.69
157.65
144.29
137.47
134.65
134.45
130.04
124.14
123.29
123.07
120.90
119.79
119.45
117.23
115.61
92.84
66.56
58.33
57.60
53.02
33.18
24.36
18.09
1.42
f1 (ppm)

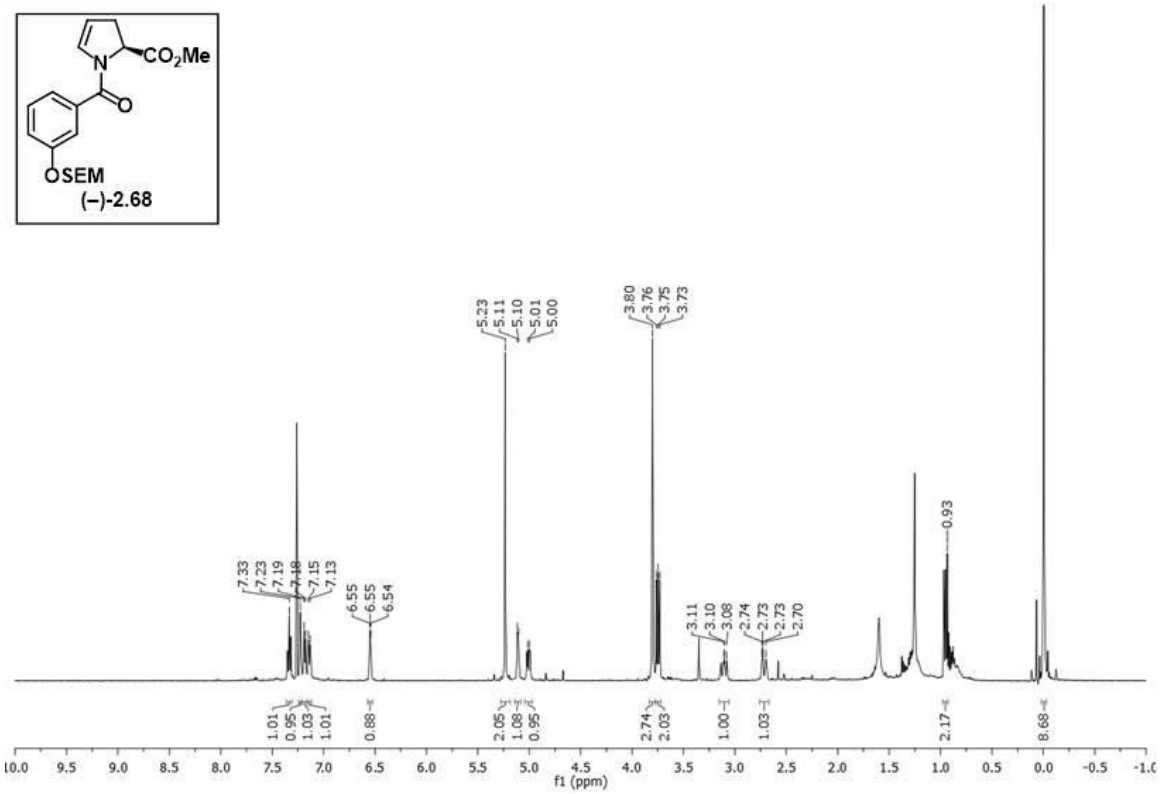
CO2Me
N
O
OSEM
(–)-2.68
7.33
7.23
7.19
7.18
7.15
7.13
6.55
6.55
6.54
5.23
5.11
5.10
5.01
5.00
3.80
3.76
3.75
3.73
3.11
3.10
3.08
2.74
2.73
2.73
2.70
0.93
1.01
0.95
1.03
1.01
0.88
2.05
1.08
0.95
2.74
2.03
1.00
1.03
2.17
8.68
f1 (ppm)

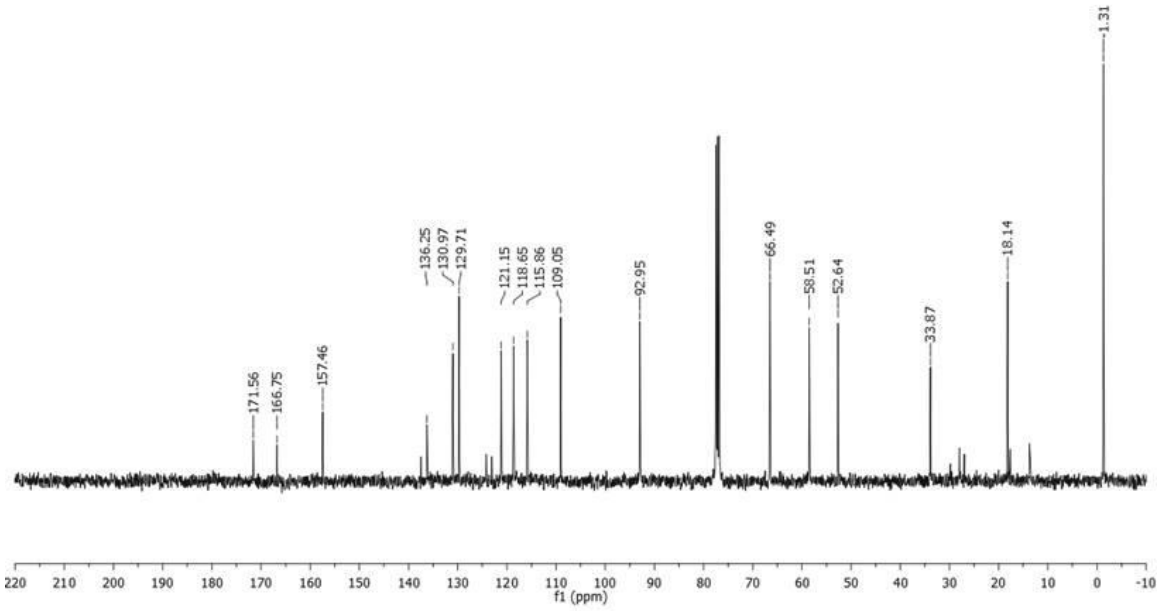
171.56
166.75
157.46
136.25
130.97
129.71
121.15
118.65
115.86
109.05
92.95
66.49
58.51
52.64
33.87
18.14
1.31
f1 (ppm)

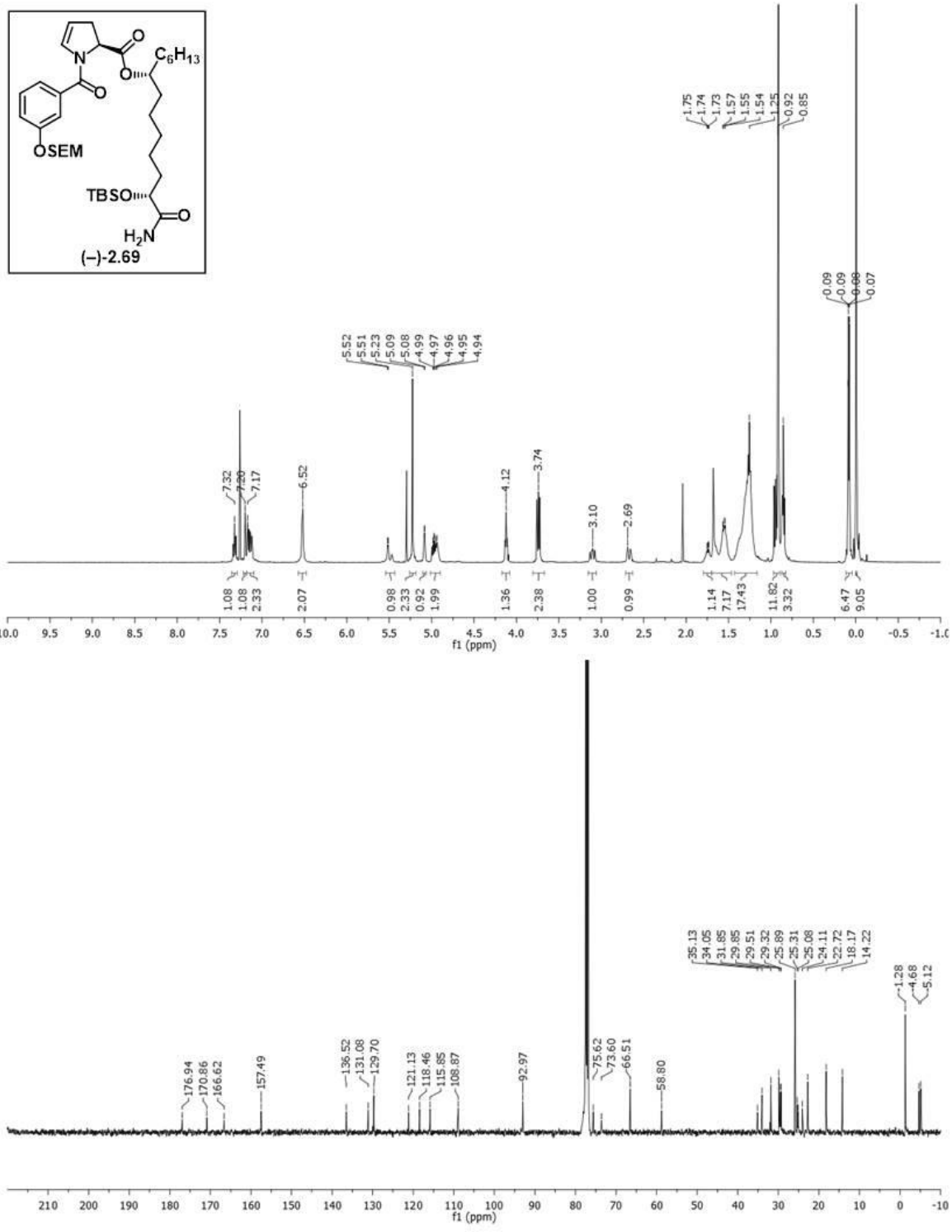
OSEM
TBSO
C_6H_{13}
H_2N
(–)-2.69
f1 (ppm)
f1 (ppm)

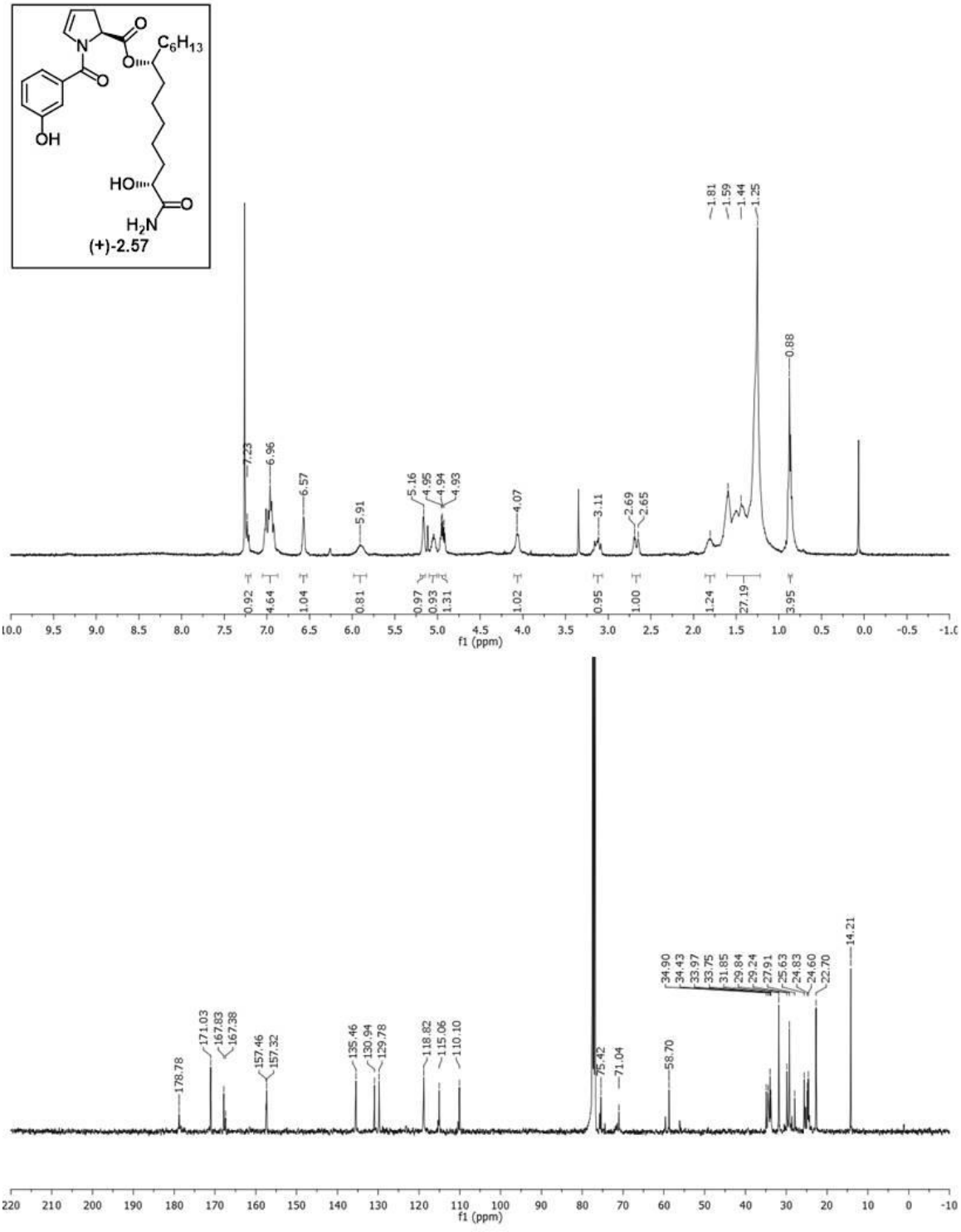
(+)-2.57
f1 (ppm)
f1 (ppm)

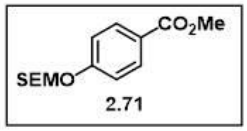
CO2Me
SEMO

2.71

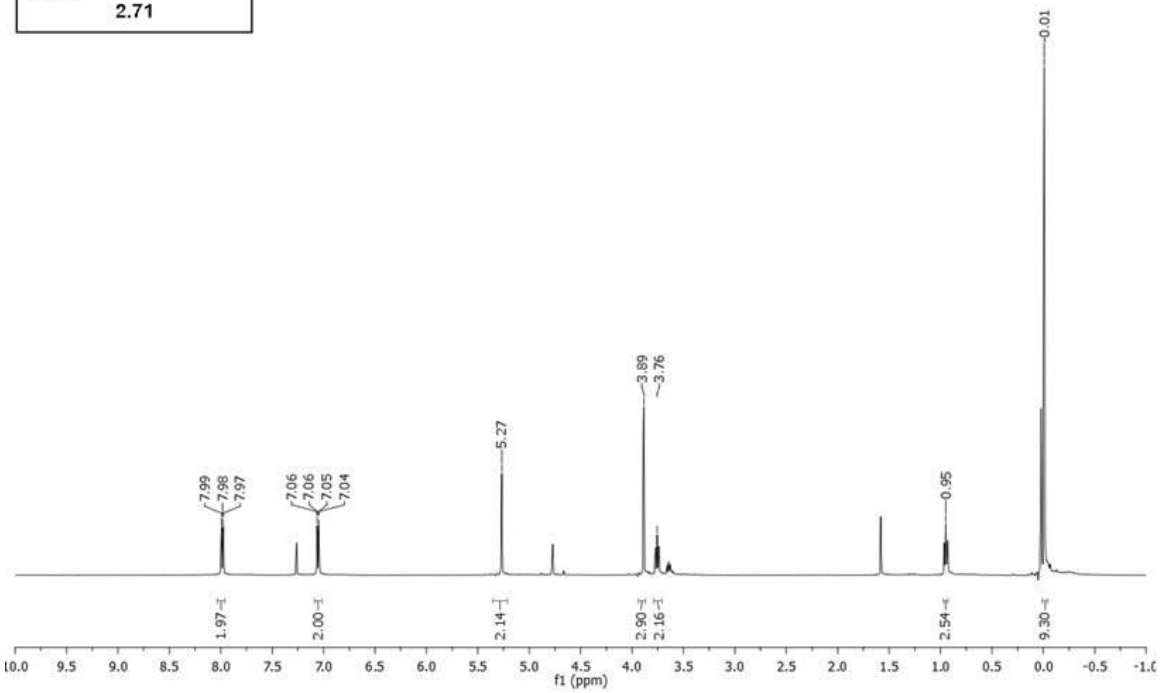
7.99
7.98
7.97
7.06
7.06
7.05
7.04
5.27
3.89
3.76
0.95
0.01
1.97
2.00
2.14
2.90
2.16
2.54
9.30
f1 (ppm)

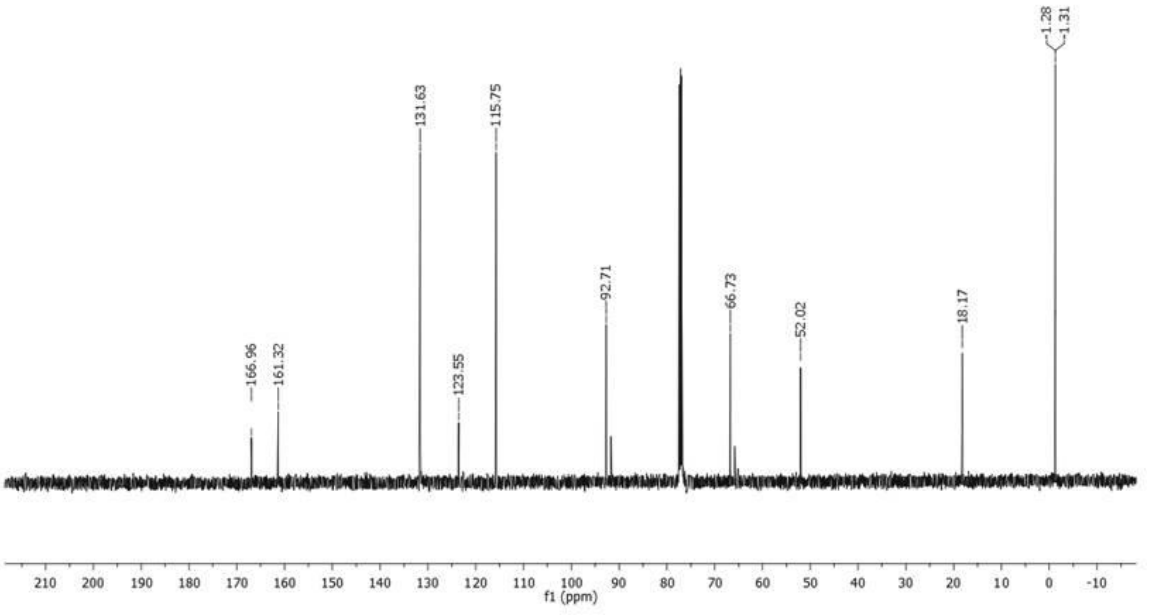
166.96
161.32
131.63
123.55
115.75
92.71
66.73
52.02
18.17
1.28
1.31
f1 (ppm)

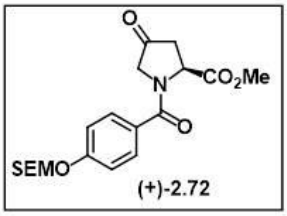
O
N
CO2Me
O
SEMO

(+)-2.72

7.49
7.08
7.06
5.25
3.77
3.73
2.95
2.93
2.71
2.70
0.97
0.93
0.00
1.88
1.82
1.96
5.05
1.00
1.03
1.97
9.08
f1 (ppm)

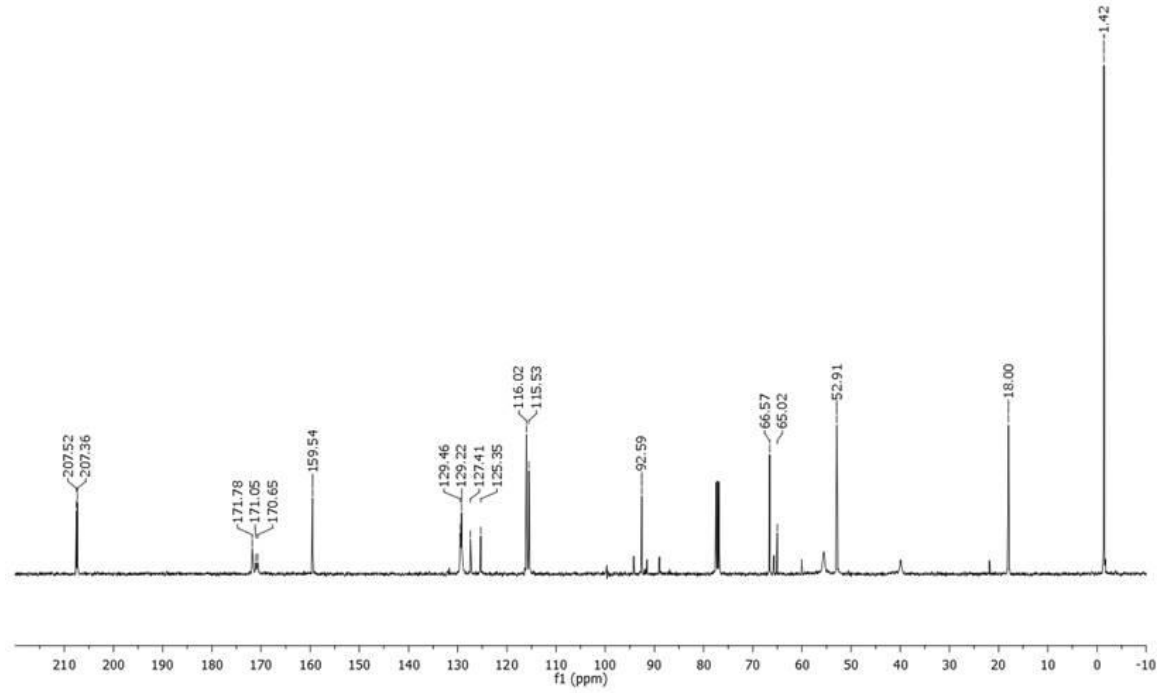
207.52
207.36
171.78
171.05
170.65
159.54
129.46
129.22
127.41
125.35
116.02
115.53
92.59
66.57
65.02
52.91
18.00
1.42
f1 (ppm)

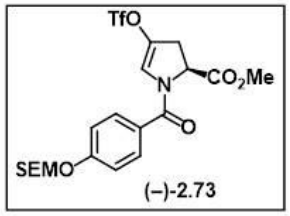
TfO
CO2Me
N
O
SEMO

(–)-2.73

7.53
7.51
7.11
7.09
6.87
5.27
5.08
5.07
3.82
3.78
3.76
3.74
3.40
2.98
2.96
0.98
0.95
0.93
0.00
2.00
2.08
0.95
2.01
0.95
2.85
2.22
1.02
1.00
2.03
9.04
f1 (ppm)

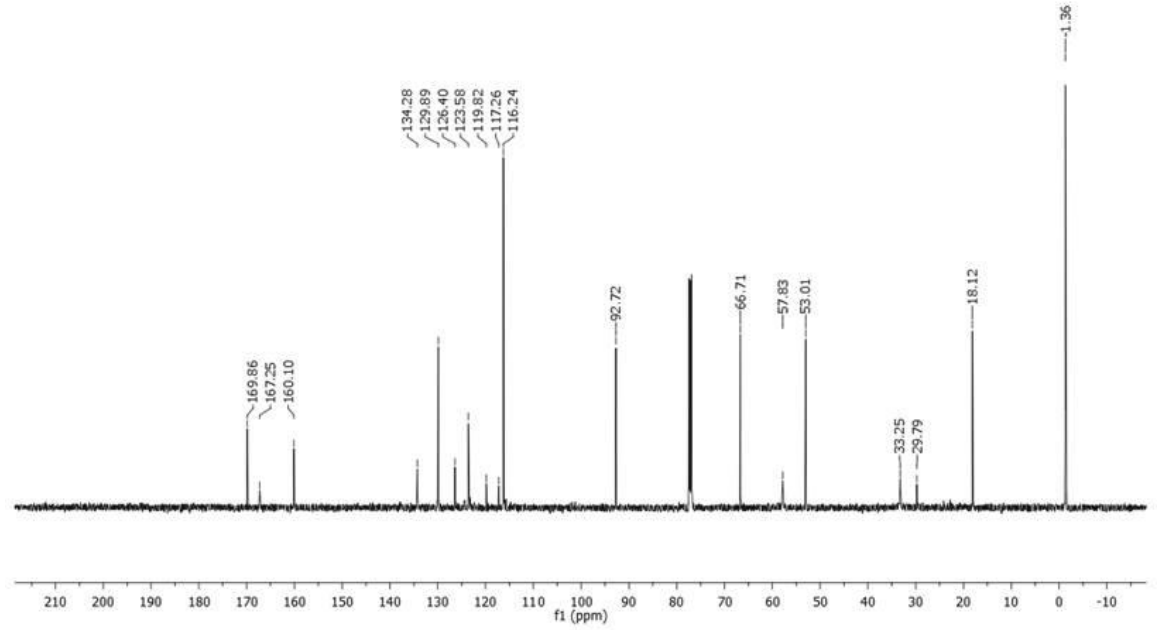
134.28
129.89
126.40
123.58
119.82
117.26
116.24
169.86
167.25
160.10
92.72
66.71
57.83
53.01
33.25
29.79
18.12
1.36
f1 (ppm)

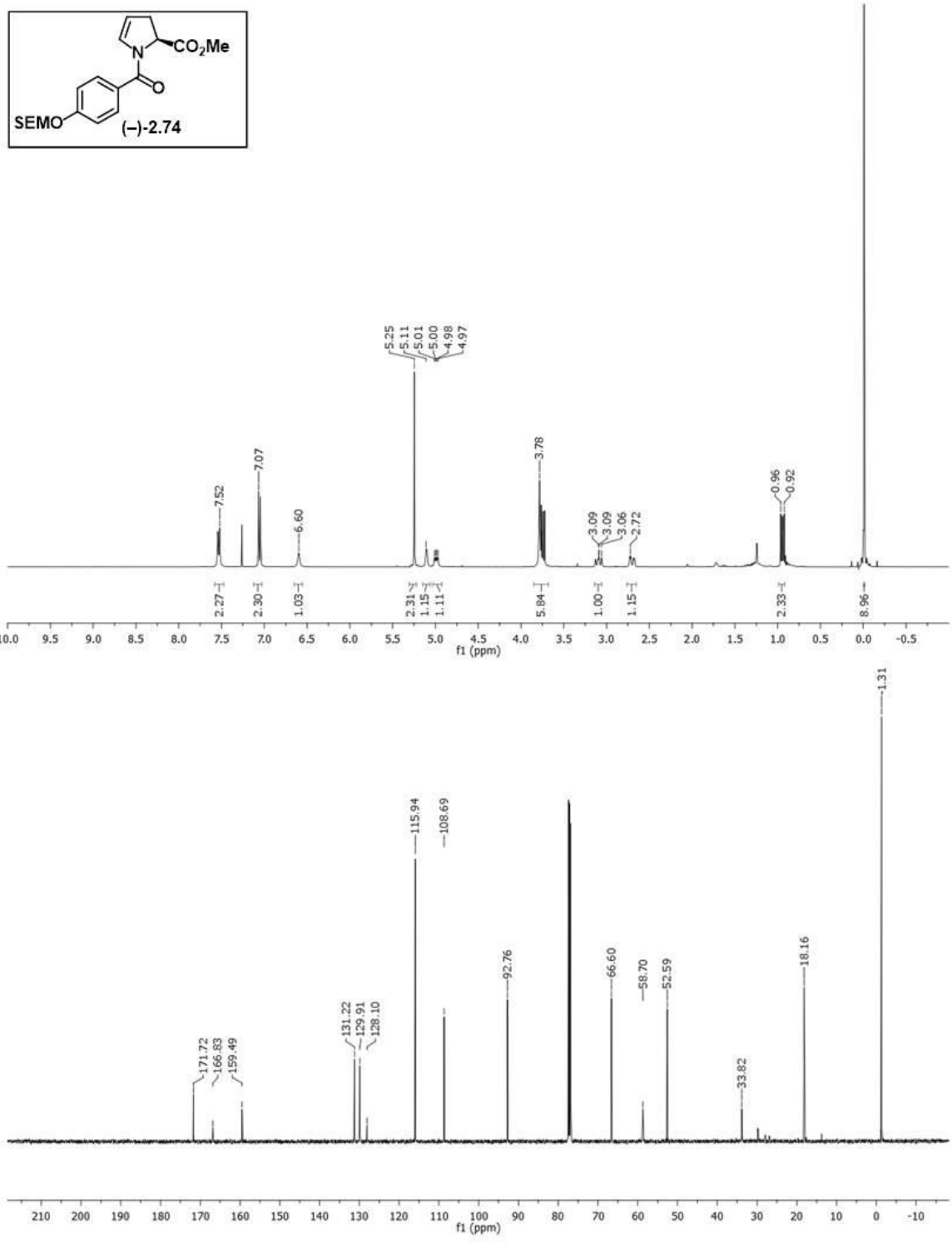
CO2Me
N
O
SEMO
(–)-2.74
7.52
7.07
6.60
5.25
5.11
5.01
5.00
4.98
4.97
3.78
3.09
3.09
3.06
2.72
0.96
0.92
2.27
2.30
1.03
2.31
1.15
1.11
5.84
1.00
1.15
2.33
8.96
f1 (ppm)
171.72
166.83
159.49
131.22
129.91
128.10
115.94
108.69
92.76
66.60
58.70
52.59
33.82
18.16
1.31
f1 (ppm)

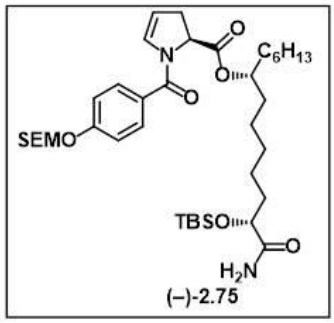
SEMO
TBSO
C_6H_{13}
H_2N
(–)-2.75

f1 (ppm)

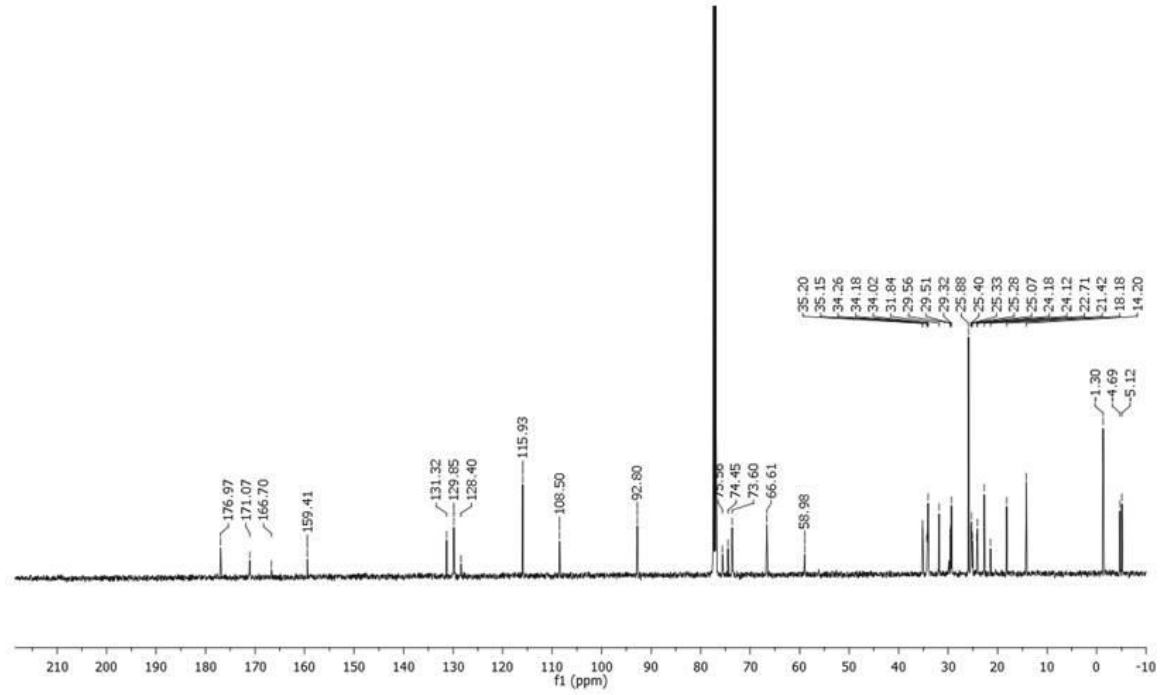
f1 (ppm)

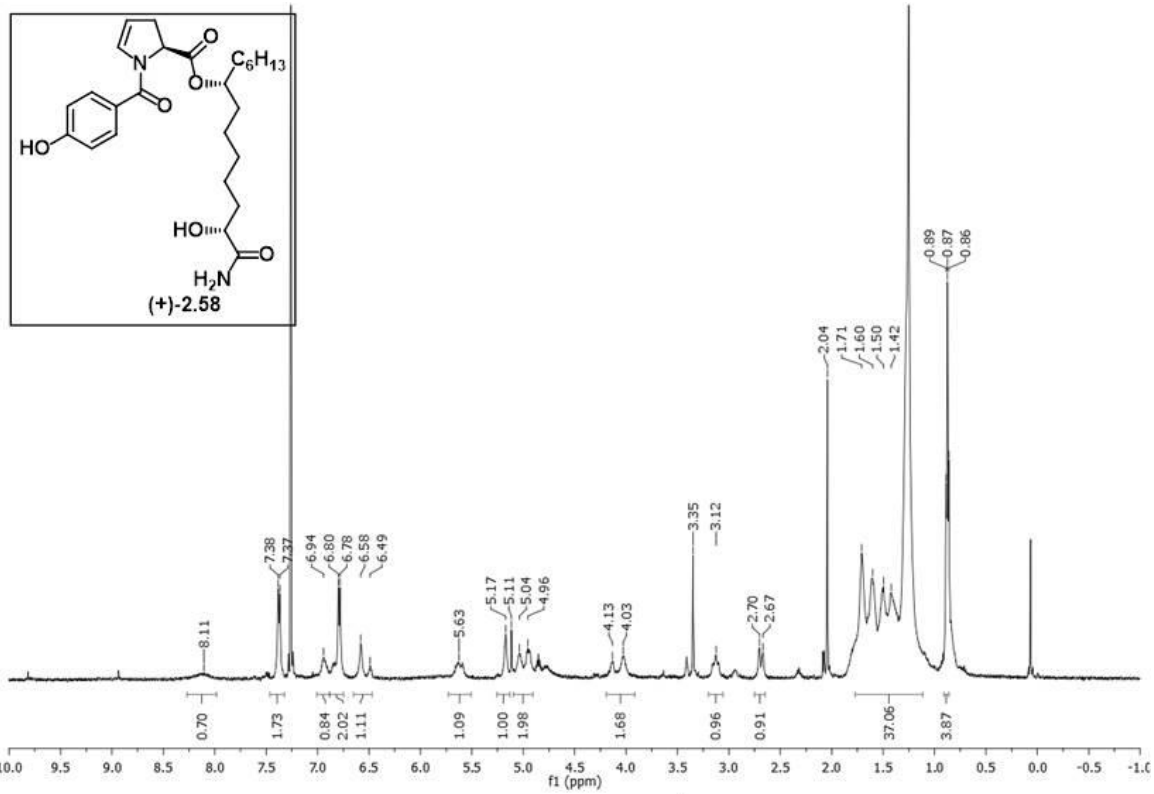
(+)-2.58
f1 (ppm)

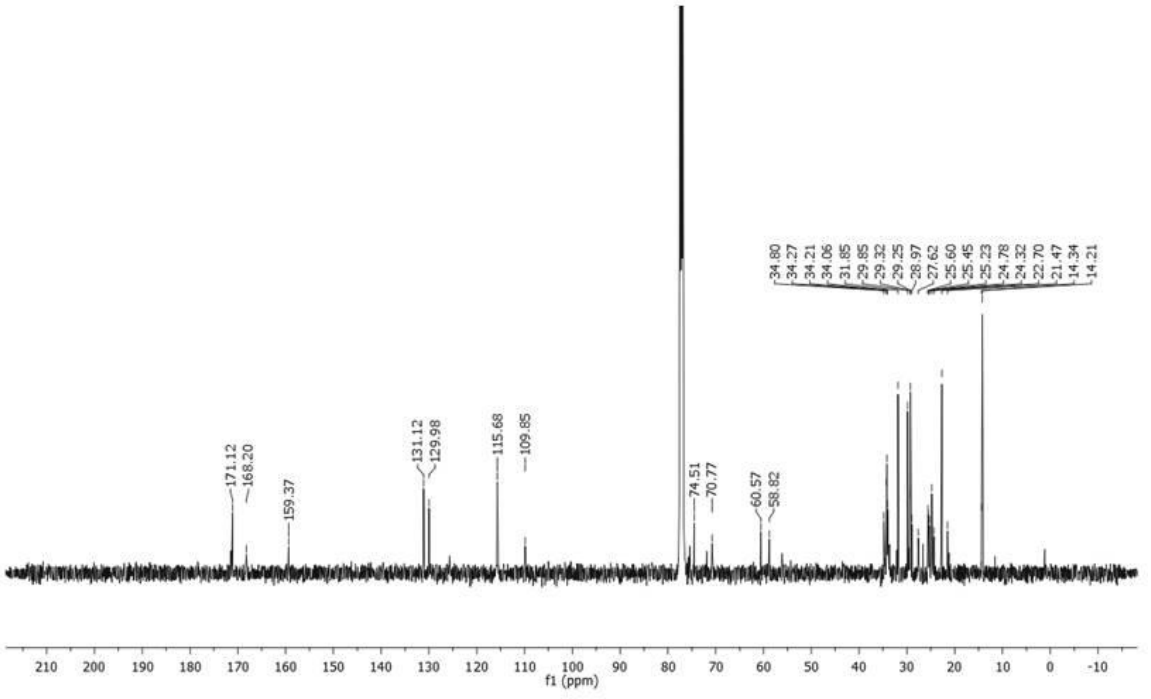
f1 (ppm)

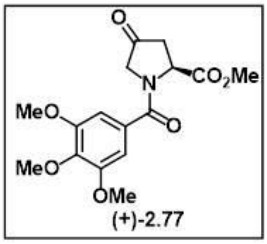
O
N
CO2Me
MeO
O
MeO
OMe

(+)-2.77

3.97
3.81
3.79
3.78
3.75
3.71
6.66
5.19
2.95
2.93
2.90
2.88
2.62
2.11
0.62
1.58
12.64
1.00
0.99
f1 (ppm)

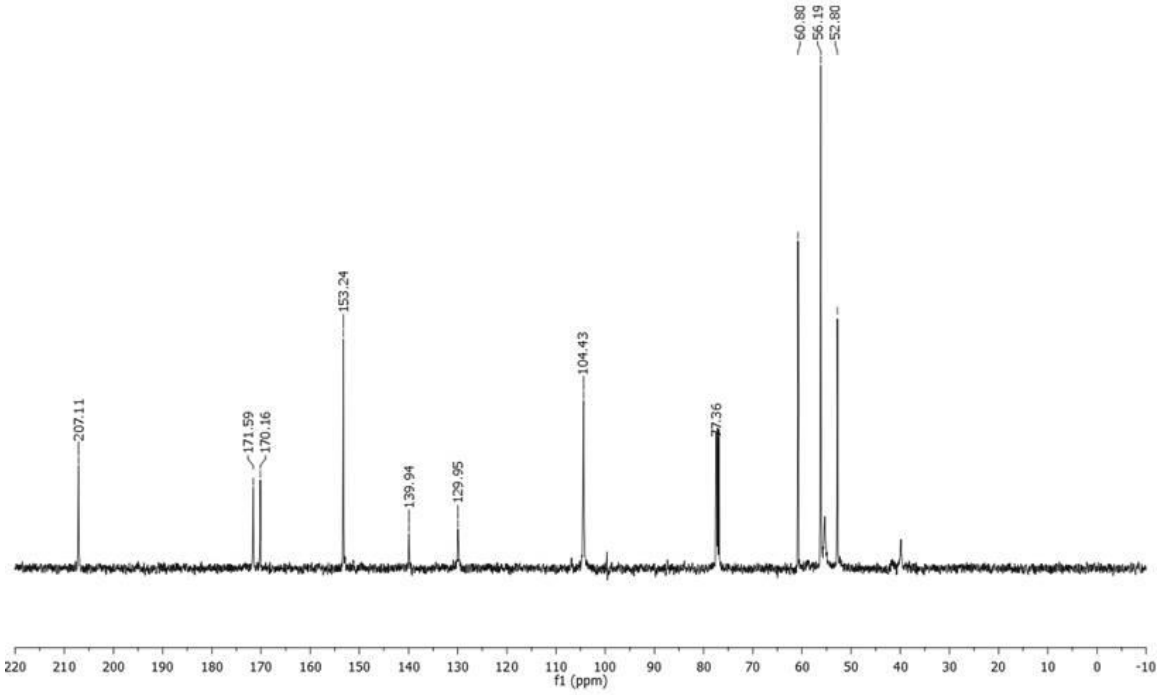
60.80
56.19
52.80
207.11
171.59
170.16
153.24
139.94
129.95
104.43
27.36
f1 (ppm)

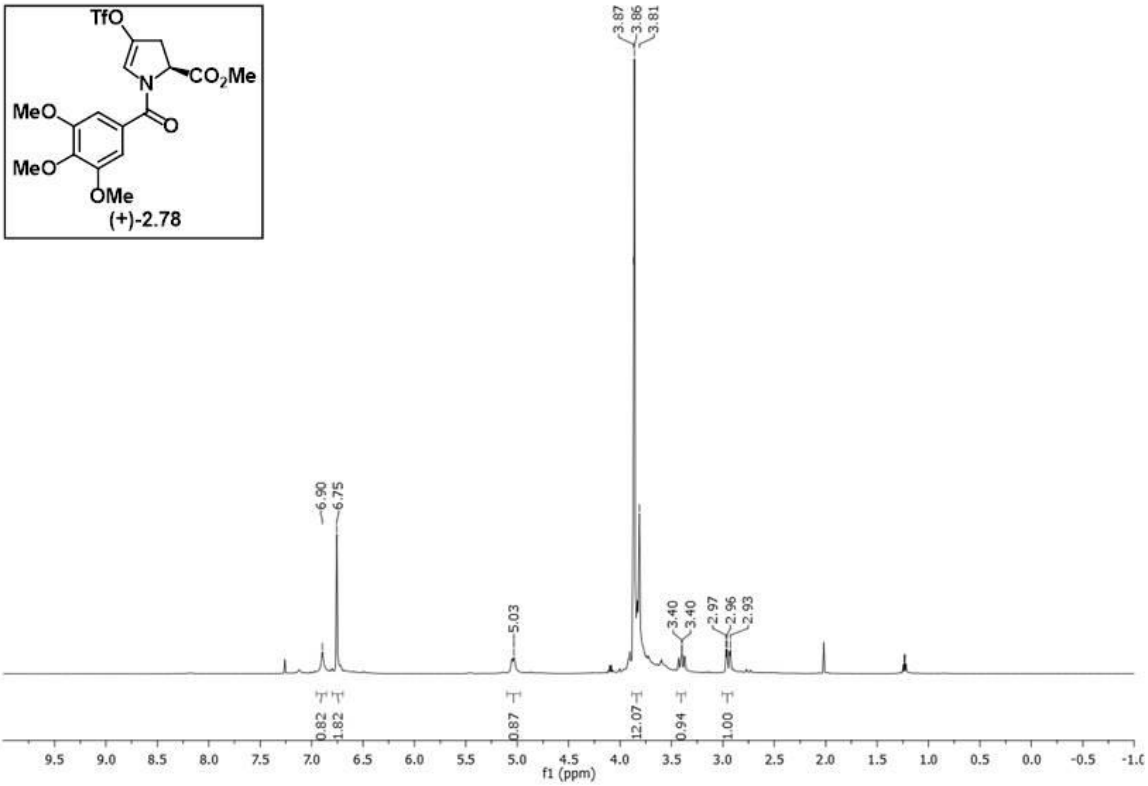
TfO
CO2Me
N
O
MeO
MeO
OMe
(+)-2.78
3.87
3.86
3.81
6.90
6.75
5.03
3.40
3.40
2.97
2.96
2.93
0.82
1.82
0.87
12.07
0.94
1.00
f1 (ppm)

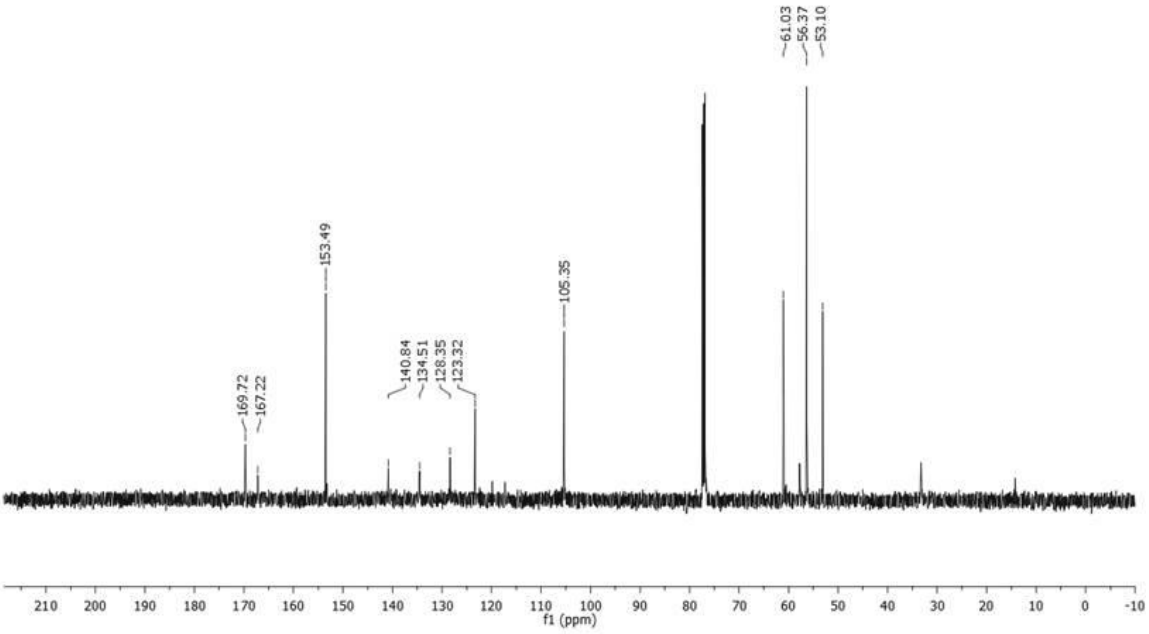
61.03
56.37
53.10
153.49
105.35
140.84
134.51
128.35
123.32
169.72
167.22
f1 (ppm)

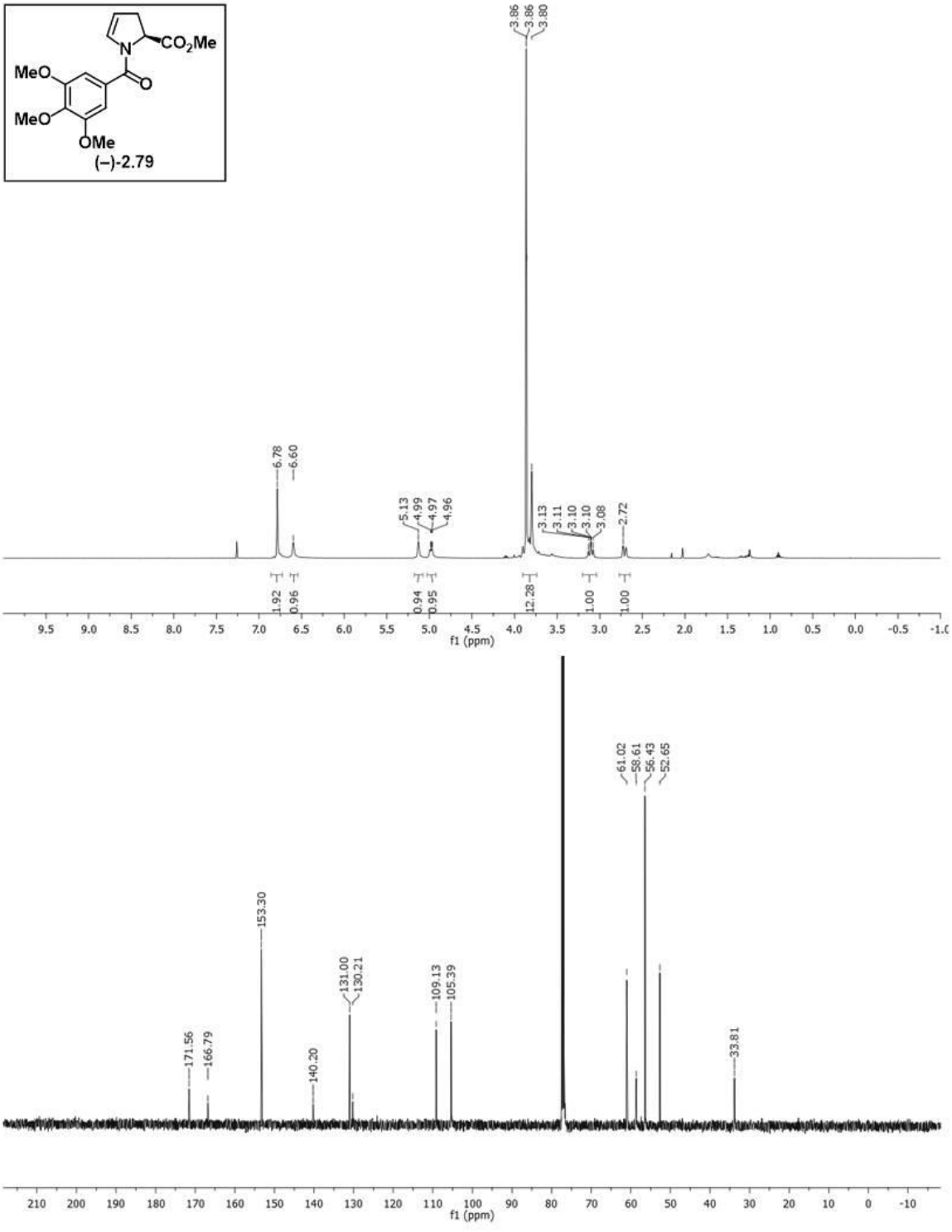
MeO
MeO
OMe
N
CO2Me
O
(–)-2.79
3.86
3.86
3.80
6.78
6.60
5.13
4.99
4.97
4.96
3.13
3.11
3.10
3.10
3.08
2.72
1.92
0.96
0.94
0.95
12.28
1.00
1.00
f1 (ppm)
61.02
58.61
56.43
52.65
153.30
131.00
130.21
109.13
105.39
171.56
166.79
140.20
33.81
f1 (ppm)

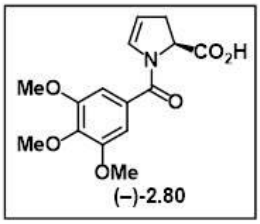
CO2H
N
O
MeO
MeO
OMe

(–)-2.80

3.87
6.80
6.55
5.26
5.06
3.06
2.45
1.53
0.94
1.12
9.95
2.00
f1 (ppm)

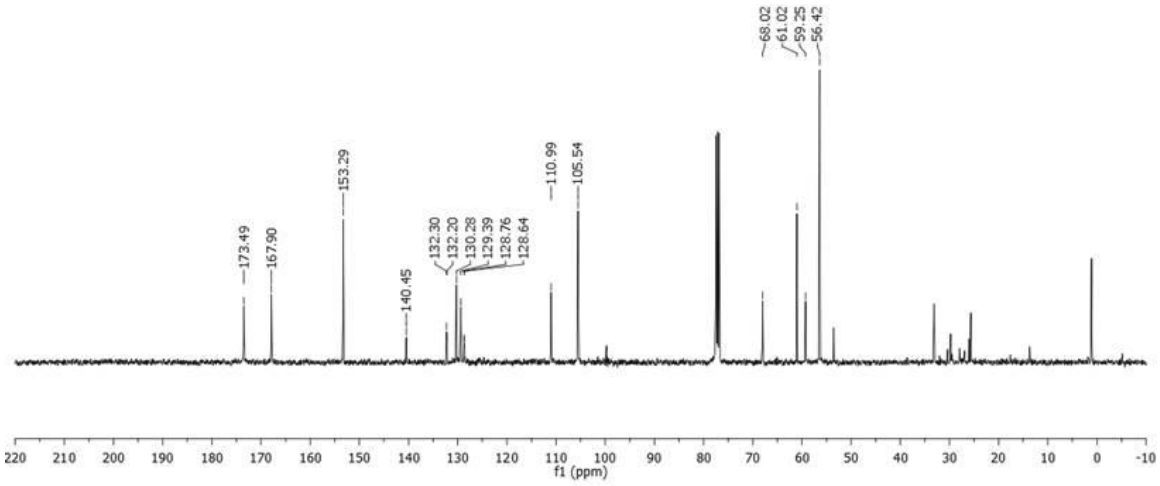
68.02
61.02
59.25
56.42
153.29
110.99
105.54
173.49
167.90
140.45
132.30
132.20
130.28
129.39
128.76
128.64
f1 (ppm)

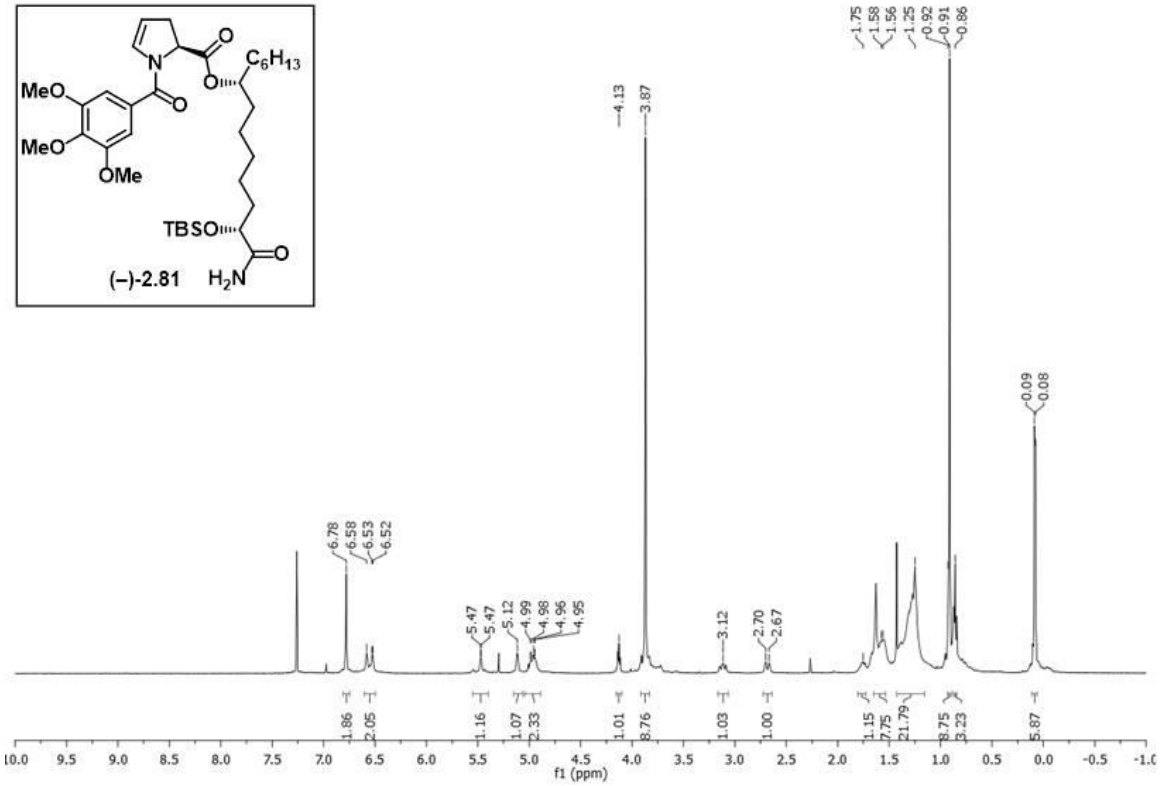
MeO
MeO
OMe
N
O
O
O
C6H13
TBSO
O
H2N
(–)-2.81
f1 (ppm)

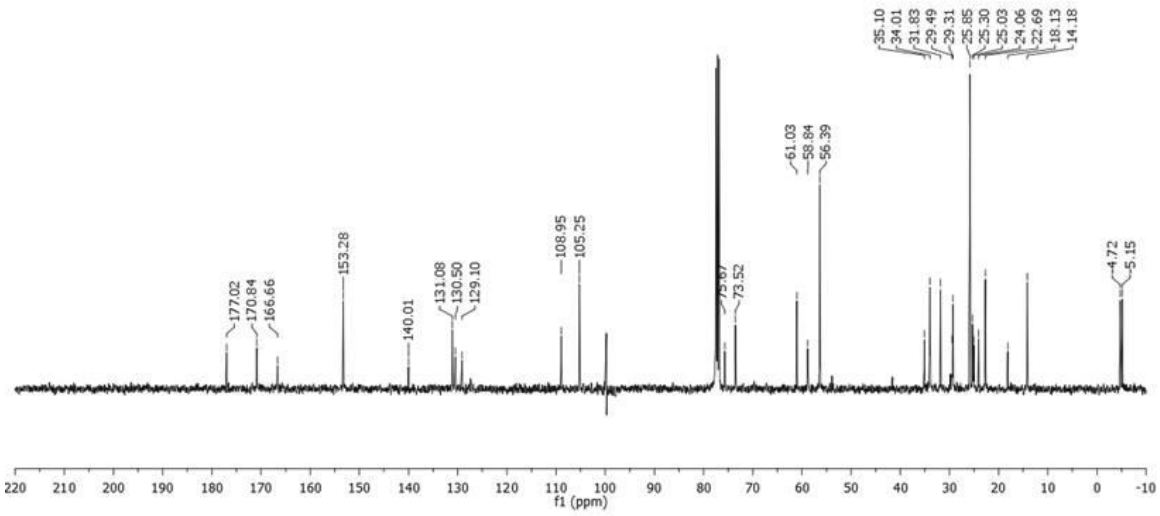
f1 (ppm)

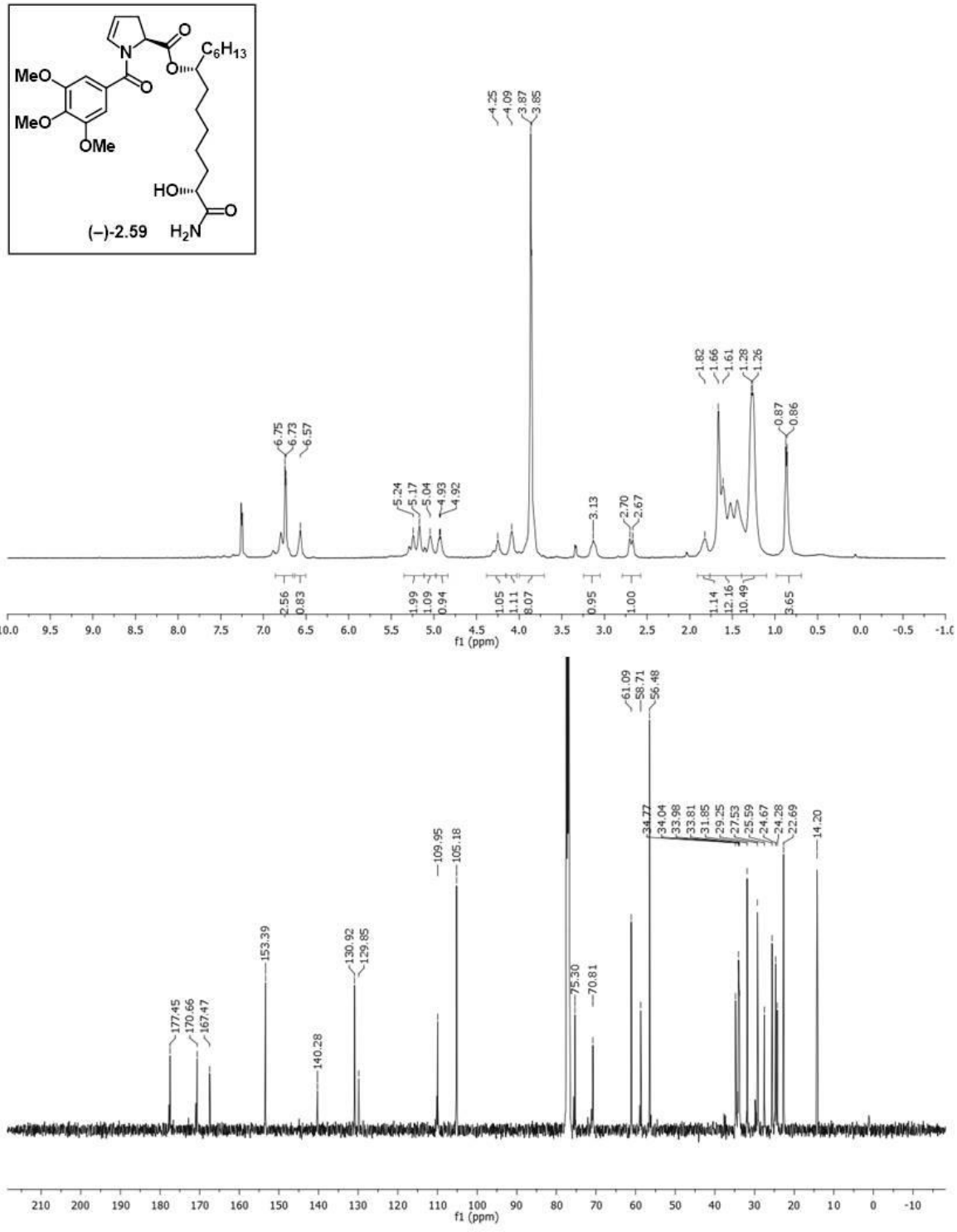
MeO
MeO
OMe
O
N
O
O
C6H13
HO
O
H2N
(–)-2.59
4.25
4.09
3.87
3.85
6.75
6.73
6.57
5.24
5.17
5.04
4.93
4.92
3.13
2.70
2.67
1.82
1.66
1.61
1.28
1.26
0.87
0.86
2.56
0.83
1.99
1.09
0.94
1.05
1.11
8.07
0.95
1.00
1.14
12.16
10.49
3.65
f1 (ppm)
61.09
58.71
56.48
34.77
34.04
33.98
33.81
31.85
29.25
27.53
25.59
24.67
24.28
22.69
14.20
109.95
105.18
153.39
130.92
129.85
177.45
170.66
167.47
140.28
75.30
70.81
f1 (ppm)

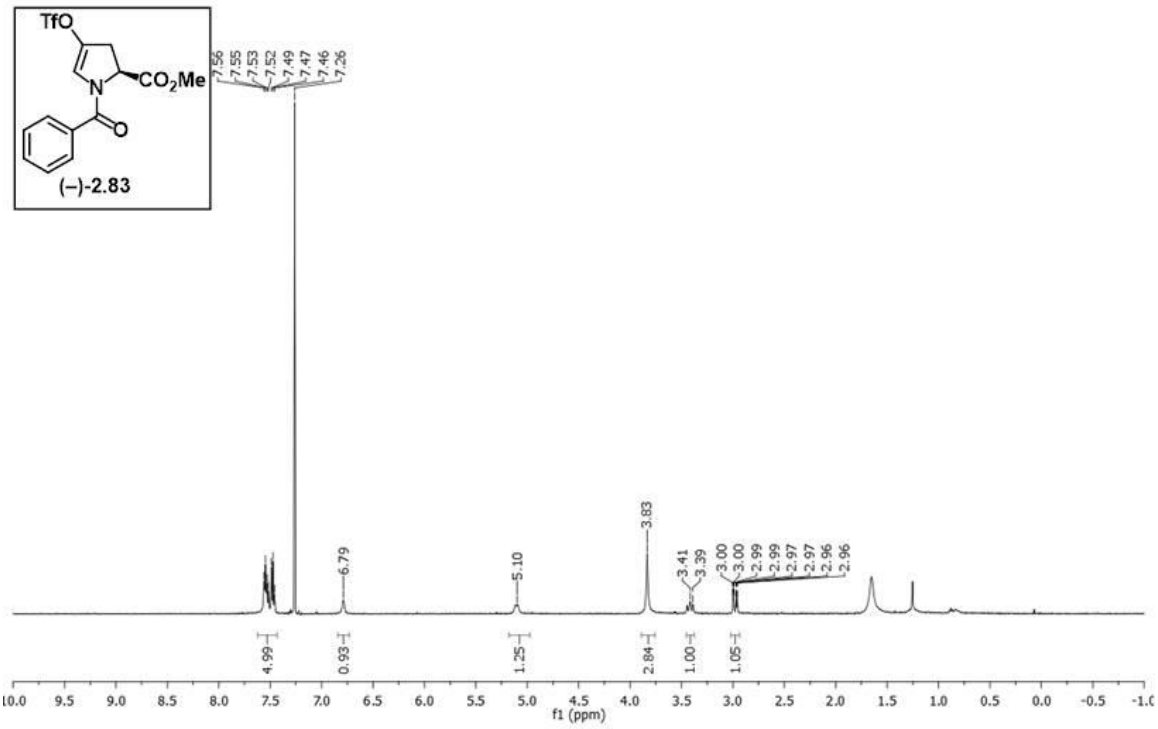
TfO
CO2Me
N
O
(–)-2.83
7.56
7.55
7.53
7.52
7.49
7.47
7.46
7.26
6.79
5.10
3.83
3.41
3.39
3.00
3.00
2.99
2.99
2.97
2.97
2.96
2.96
4.99
0.93
1.25
2.84
1.00
1.05
f1 (ppm)

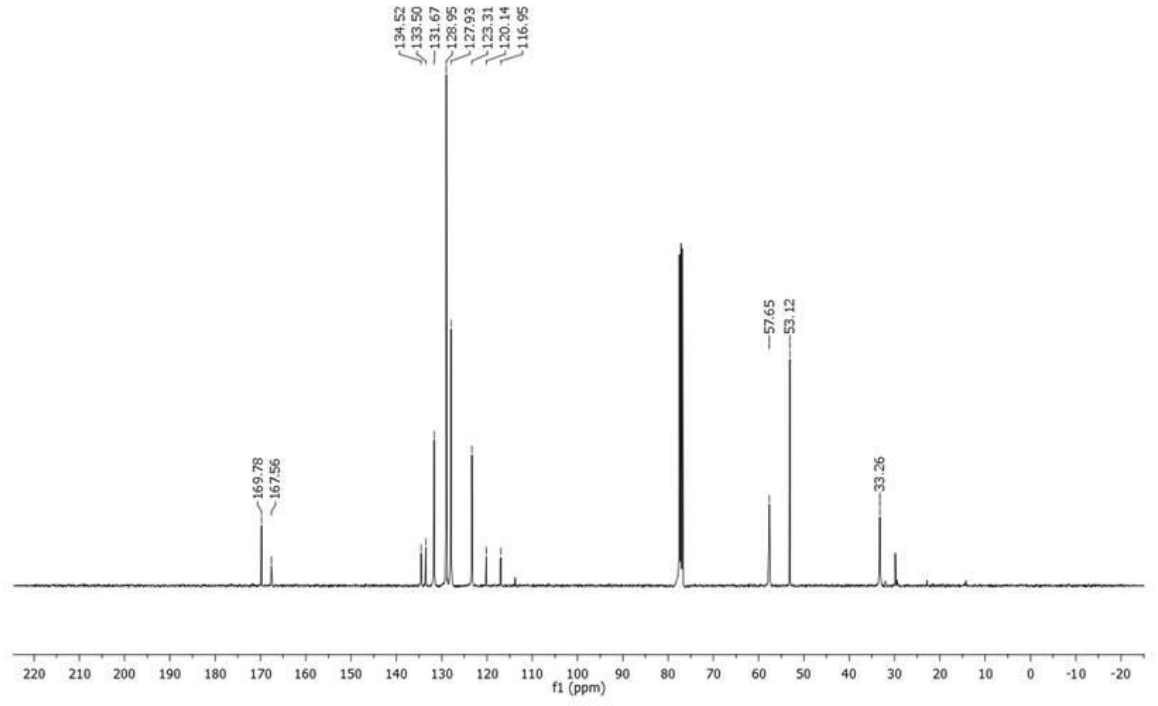
134.52
133.50
131.67
128.95
127.93
123.31
120.14
116.95
57.65
53.12
169.78
167.56
33.26
f1 (ppm)

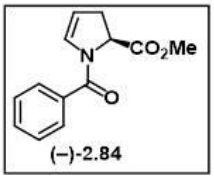
CO2Me
N
O

(–)-2.84

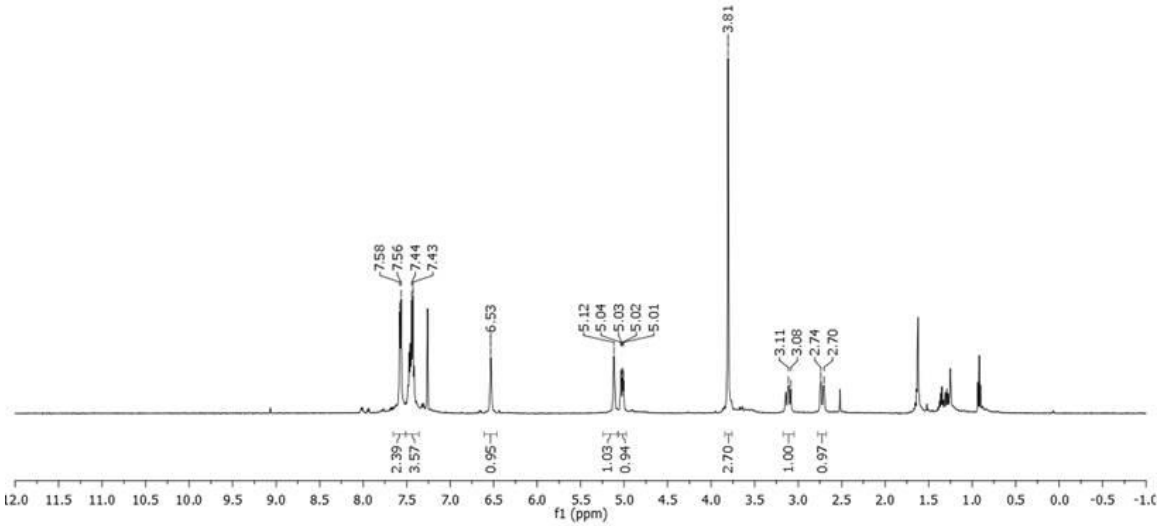
7.58
7.56
7.44
7.43
6.53
5.12
5.04
5.03
5.02
5.01
3.81
3.11
3.08
2.74
2.70
2.39
3.57
0.95
1.03
0.94
2.70
1.00
0.97
f1 (ppm)

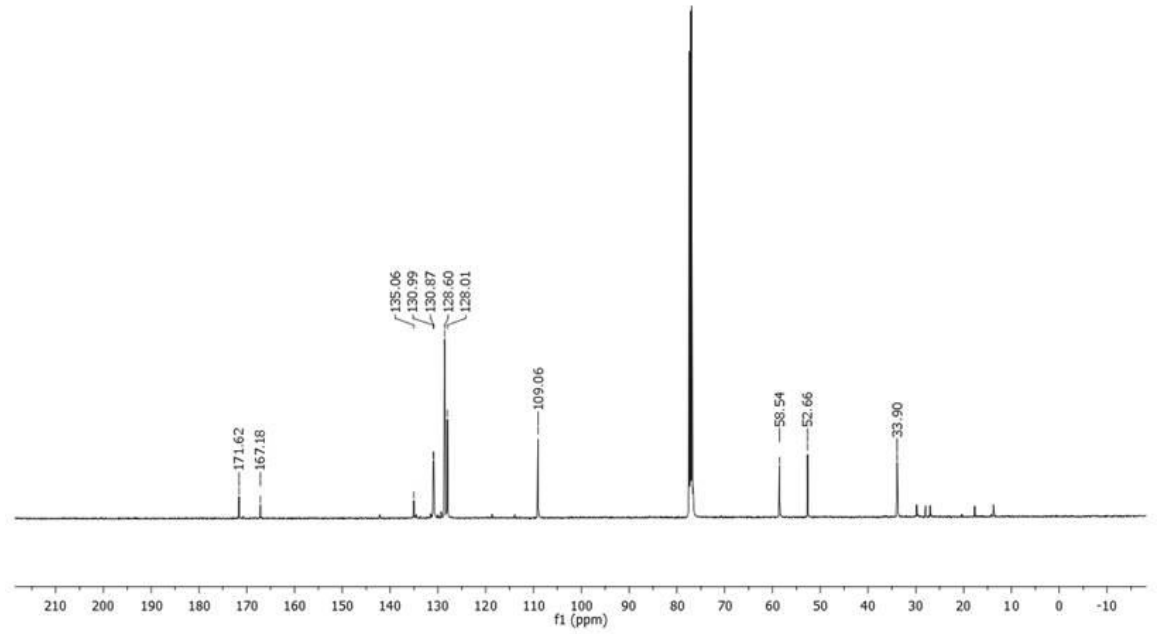
135.06
130.99
130.87
128.60
128.01
171.62
167.18
109.06
58.54
52.66
33.90
f1 (ppm)

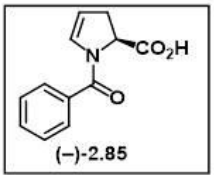
CO2H
N
O

(–)-2.85

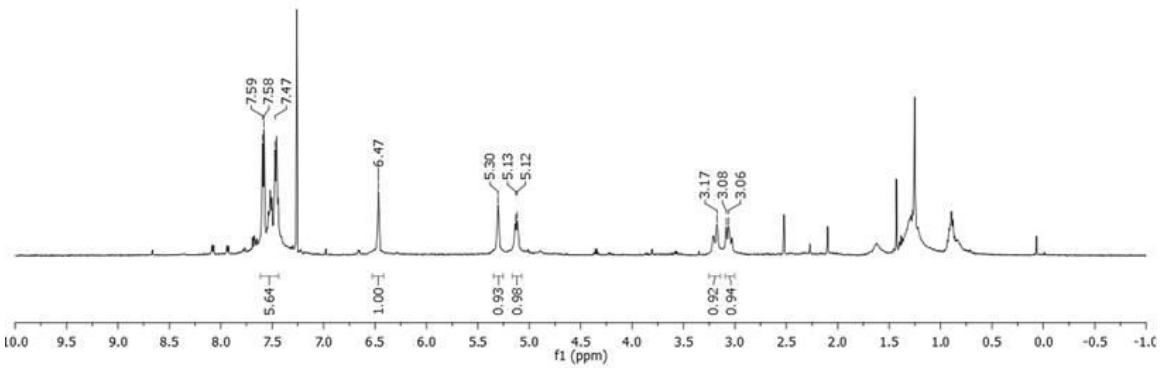
7.59
7.58
7.47
6.47
5.30
5.13
5.12
3.17
3.08
3.06
5.64
1.00
0.93
0.98
0.92
0.94
f1 (ppm)

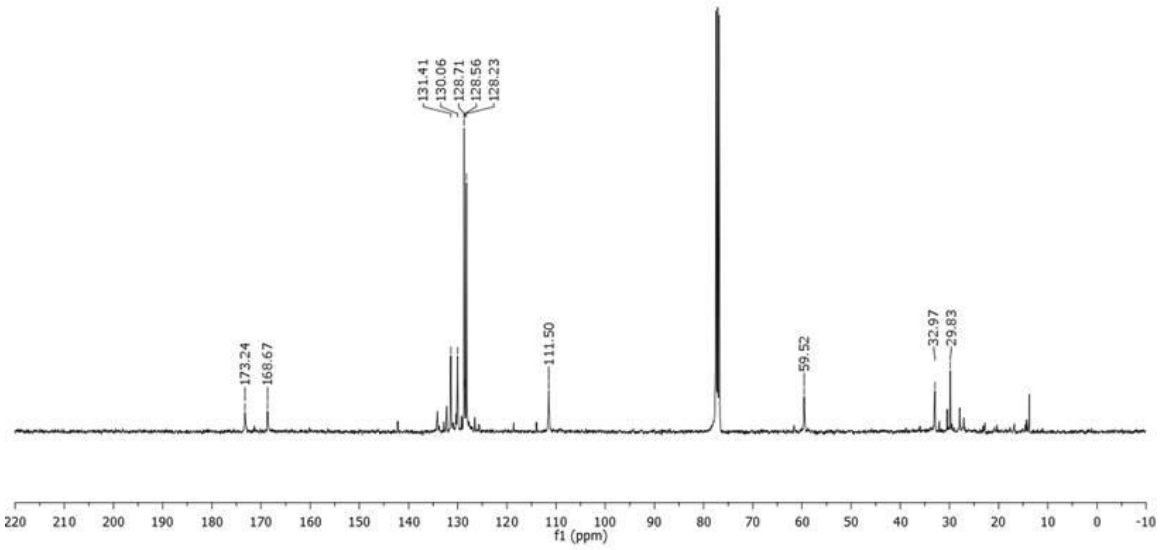
131.41
130.06
128.71
128.56
128.23
173.24
168.67
111.50
59.52
32.97
29.83
f1 (ppm)

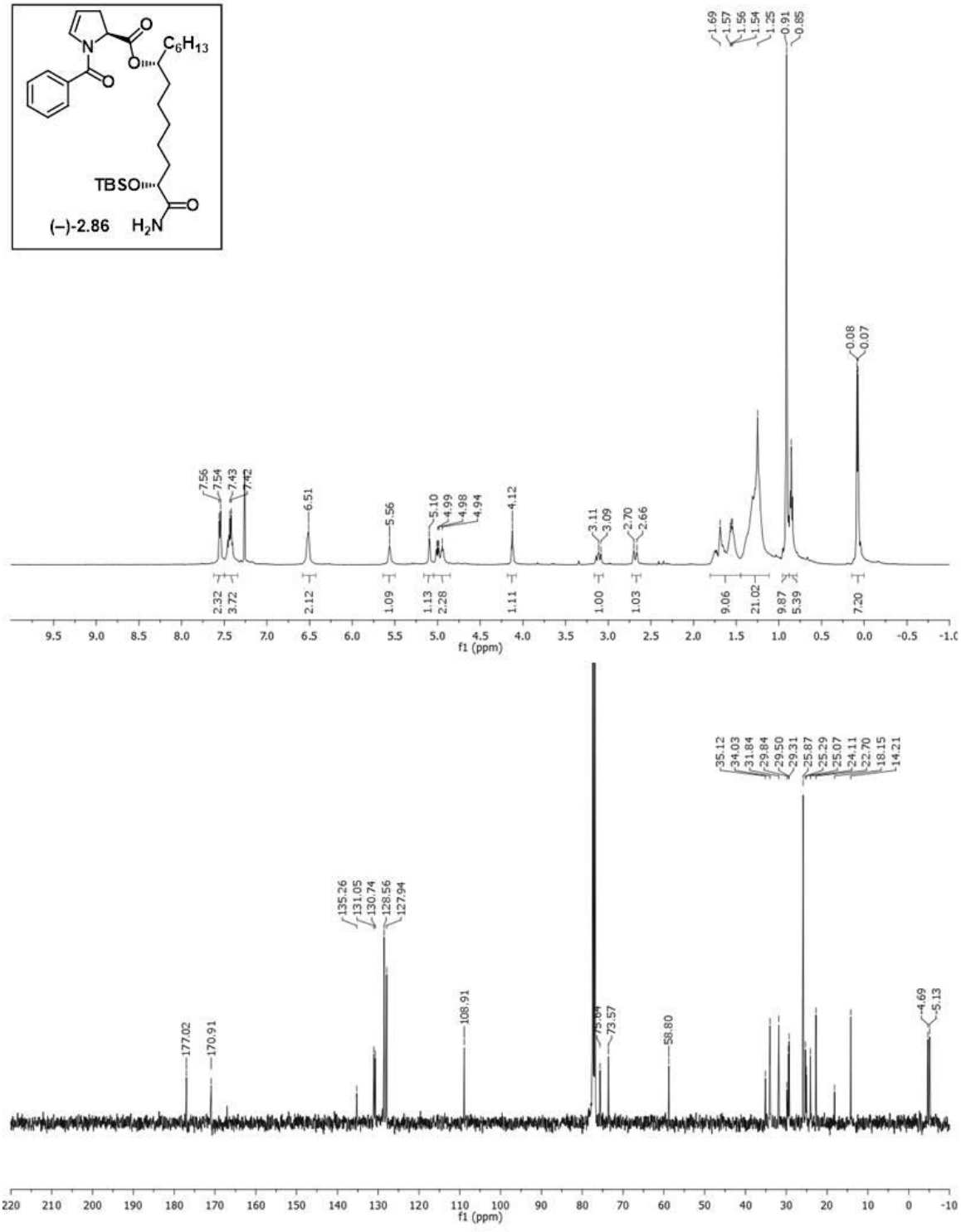
(–)-2.86
TBSO
C_6H_{13}
H_2N
f1 (ppm)
f1 (ppm)

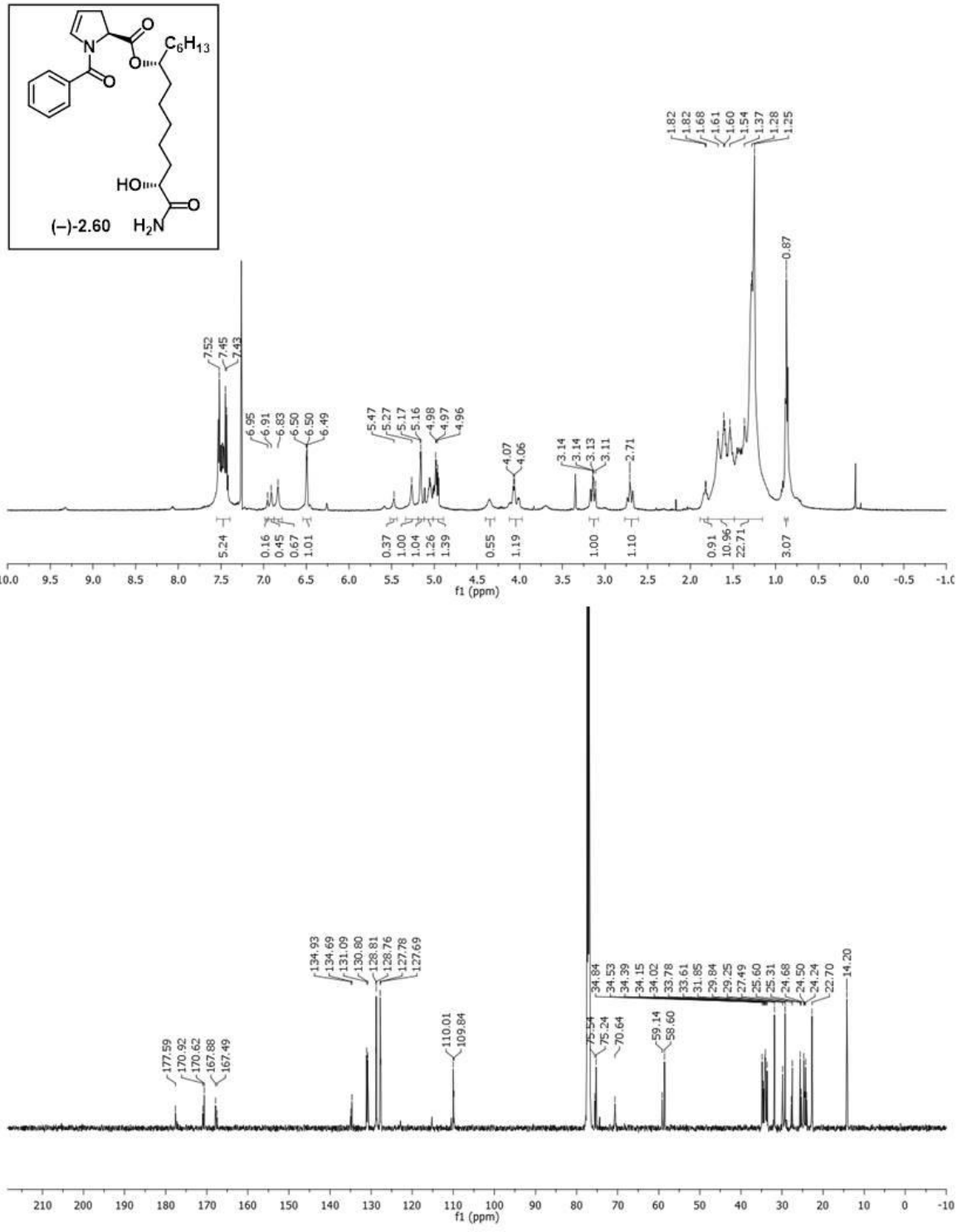
(–)-2.60
f1 (ppm)
f1 (ppm)

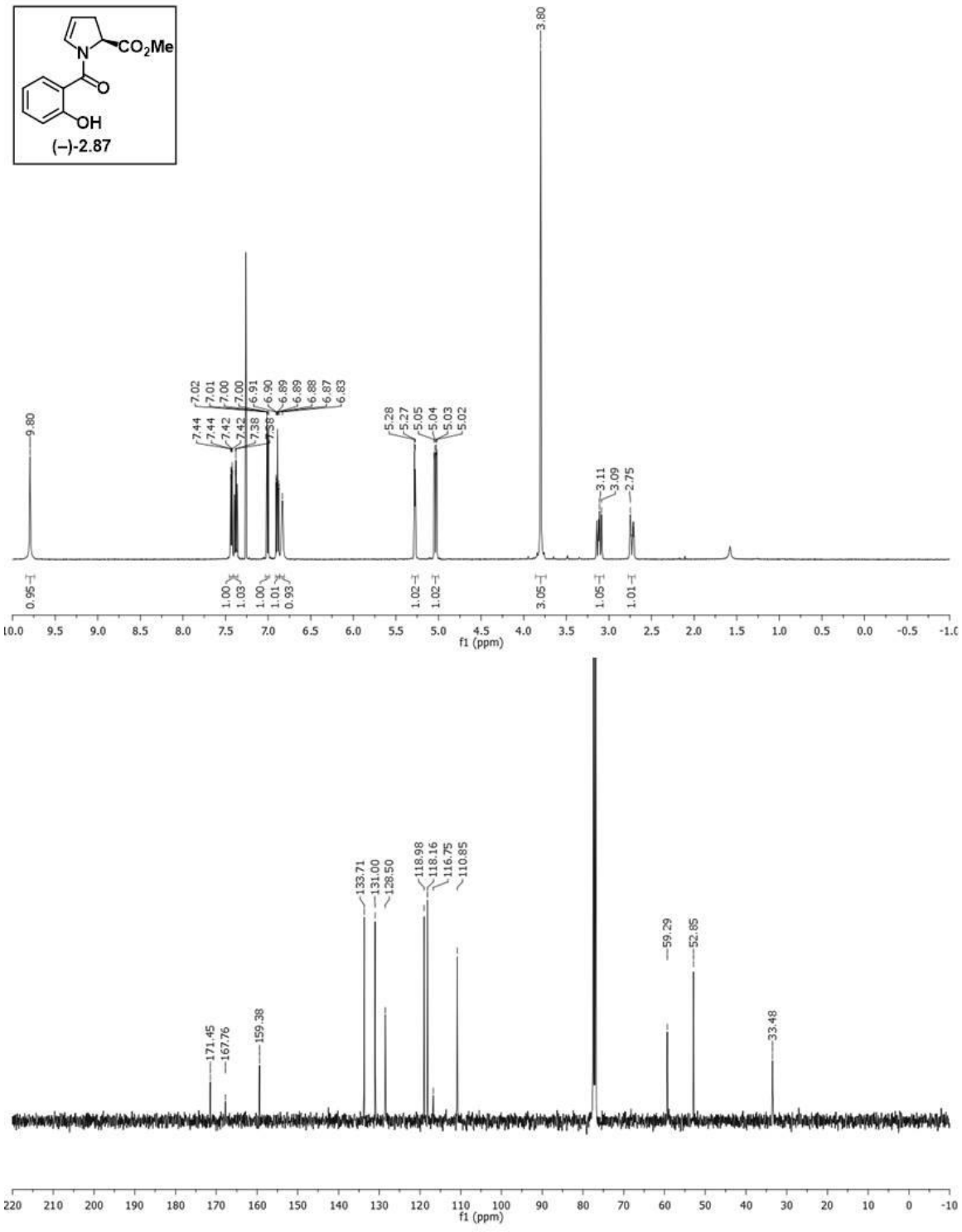
CO2Me
N
O
OH
(–)-2.87
f1 (ppm)
f1 (ppm)

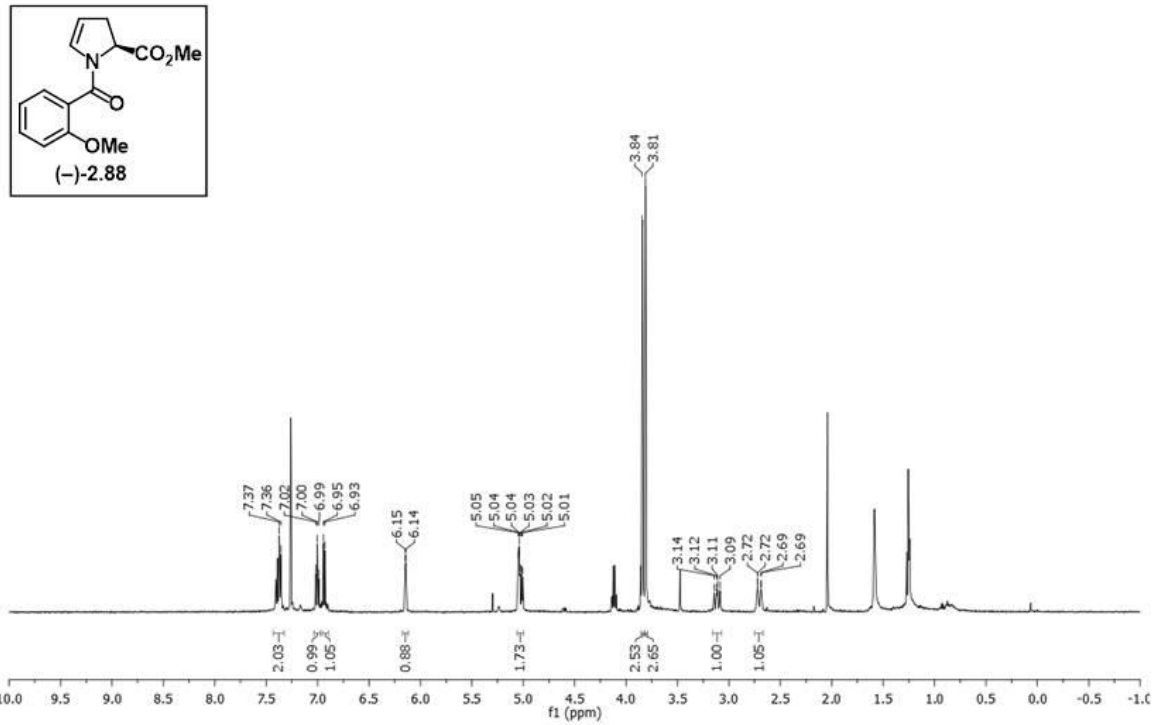
CO2Me
N
O
OMe
(–)-2.88
3.84
3.81
7.37
7.36
7.02
7.00
6.99
6.95
6.93
6.15
6.14
5.05
5.04
5.04
5.03
5.02
5.01
3.14
3.12
3.11
3.09
2.72
2.72
2.69
2.69
2.03
0.99
1.05
0.88
1.73
2.53
2.65
1.00
1.05
f1 (ppm)

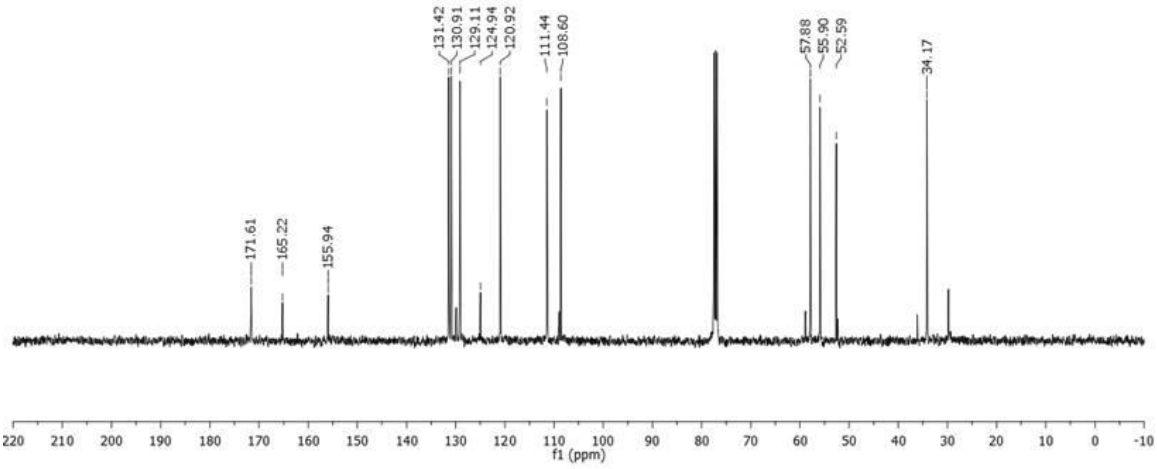
131.42
130.91
129.11
124.94
120.92
111.44
108.60
57.88
55.90
52.59
34.17
171.61
165.22
155.94
f1 (ppm)

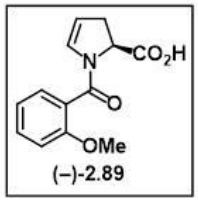
CO2H
N
O
OMe

(–)-2.89

3.84
8.03
7.44
7.38
7.37
7.03
6.96
6.95
6.06
5.23
5.22
5.14
5.13
5.12
5.11
3.21
3.17
3.07
3.05
3.03
3.01
0.12
1.37
1.12
1.28
1.36
1.00
0.95
0.93
3.42
1.11
1.14
f1 (ppm)

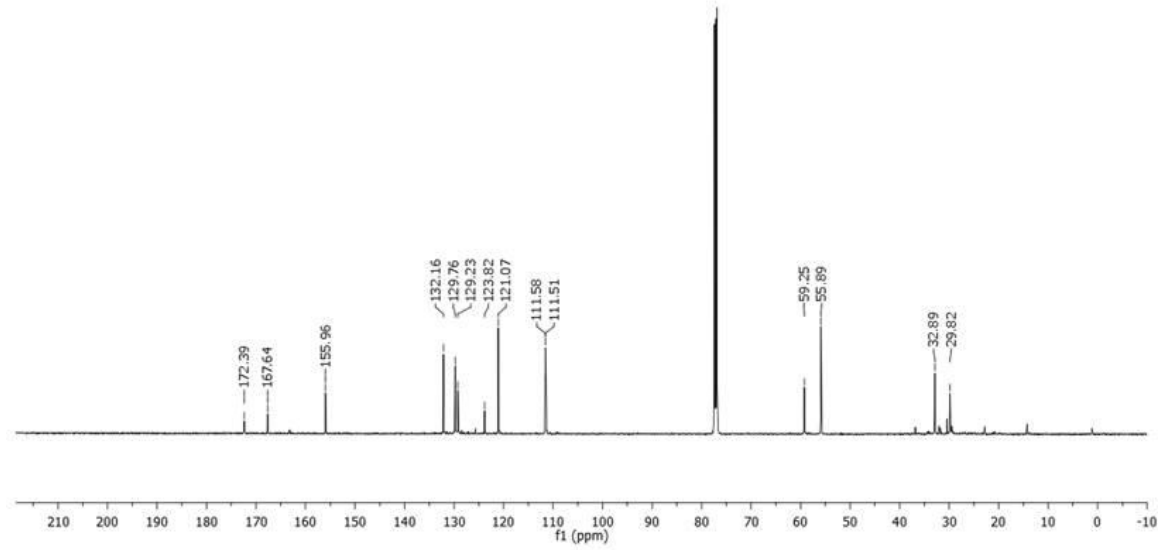
172.39
167.64
155.96
132.16
129.76
129.23
123.82
121.07
111.58
111.51
59.25
55.89
32.89
29.82
f1 (ppm)

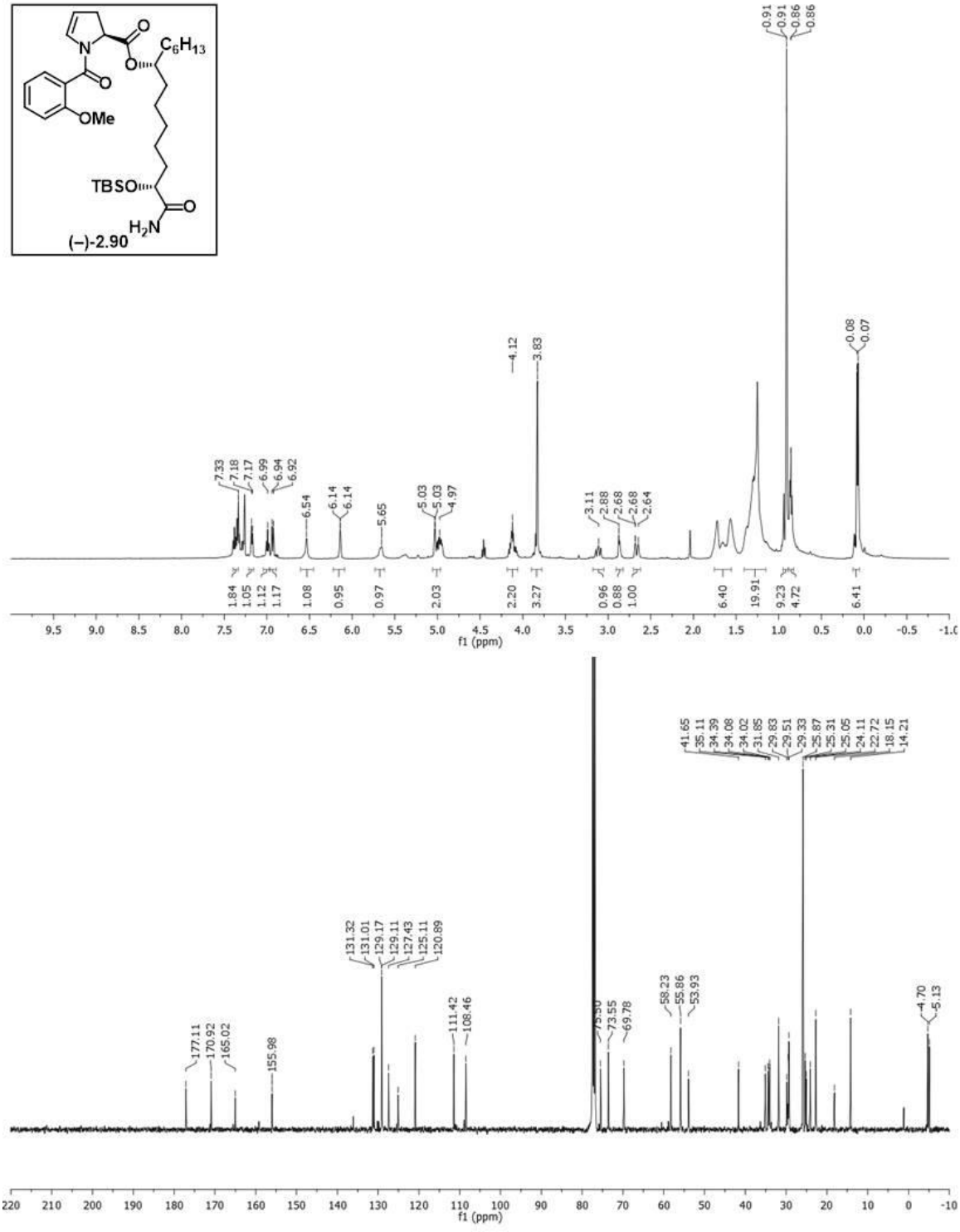
(–)-2.90
f1 (ppm)
f1 (ppm)

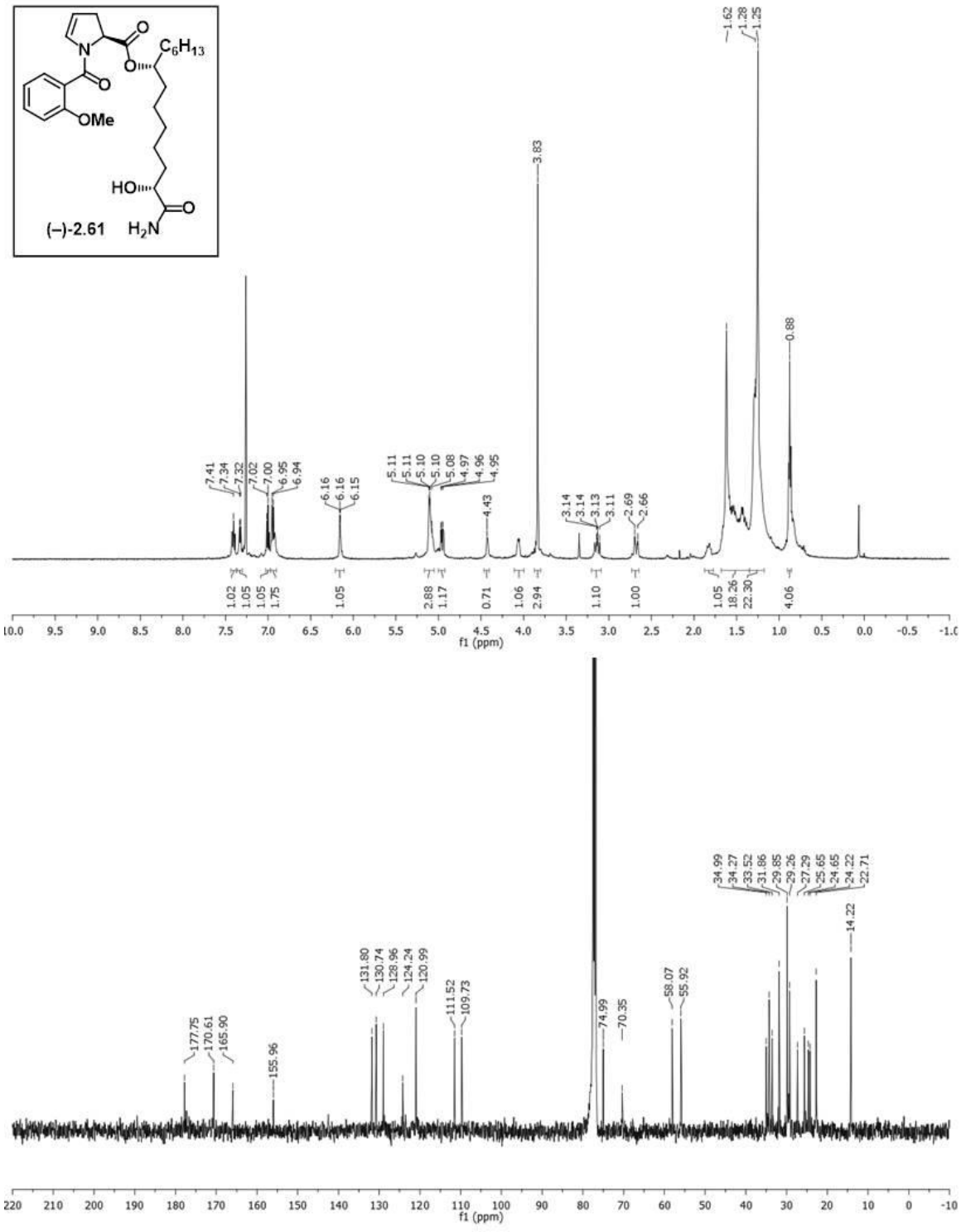
(–)-2.61
f1 (ppm)
f1 (ppm)

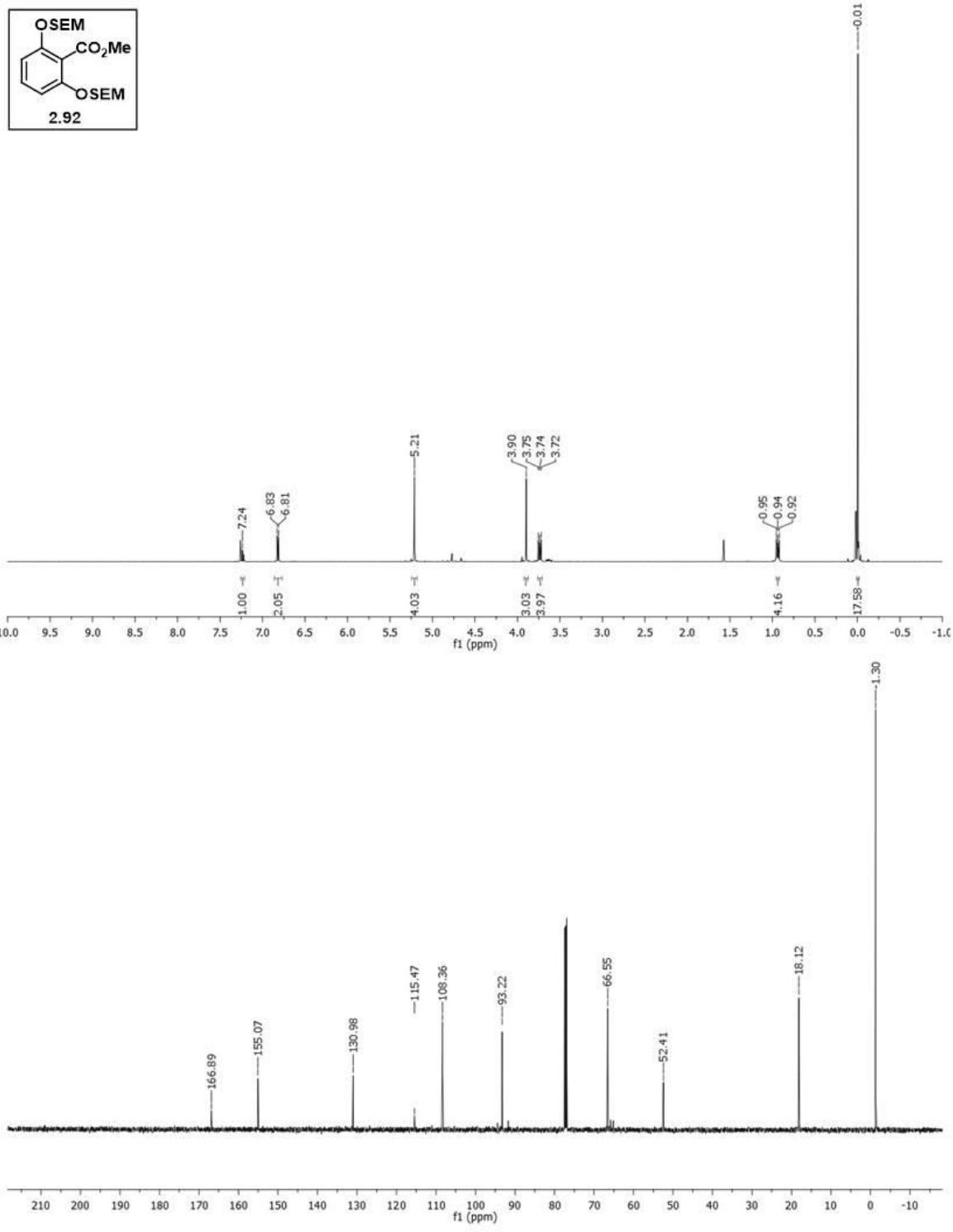
OSEM
CO2Me
OSEM
2.92
0.01
5.21
3.90
3.75
3.74
3.72
7.24
6.83
6.81
0.95
0.94
0.92
1.00
2.05
4.03
3.03
3.97
4.16
17.58
f1 (ppm)
1.30
166.89
155.07
130.98
115.47
108.36
93.22
66.55
52.41
18.12
f1 (ppm)

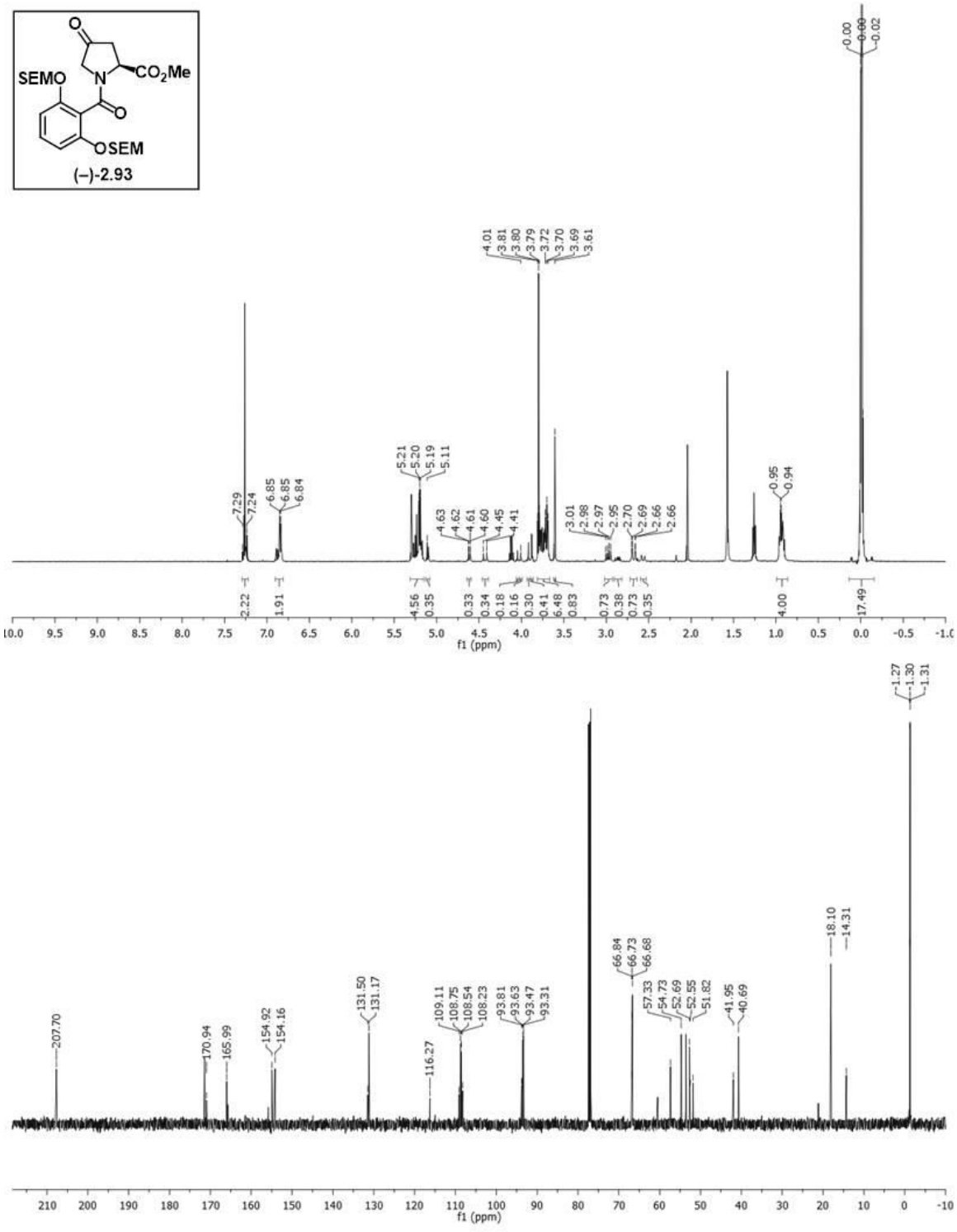
SEMO
N
CO2Me
O
OSEM
(–)-2.93
f1 (ppm)
f1 (ppm)

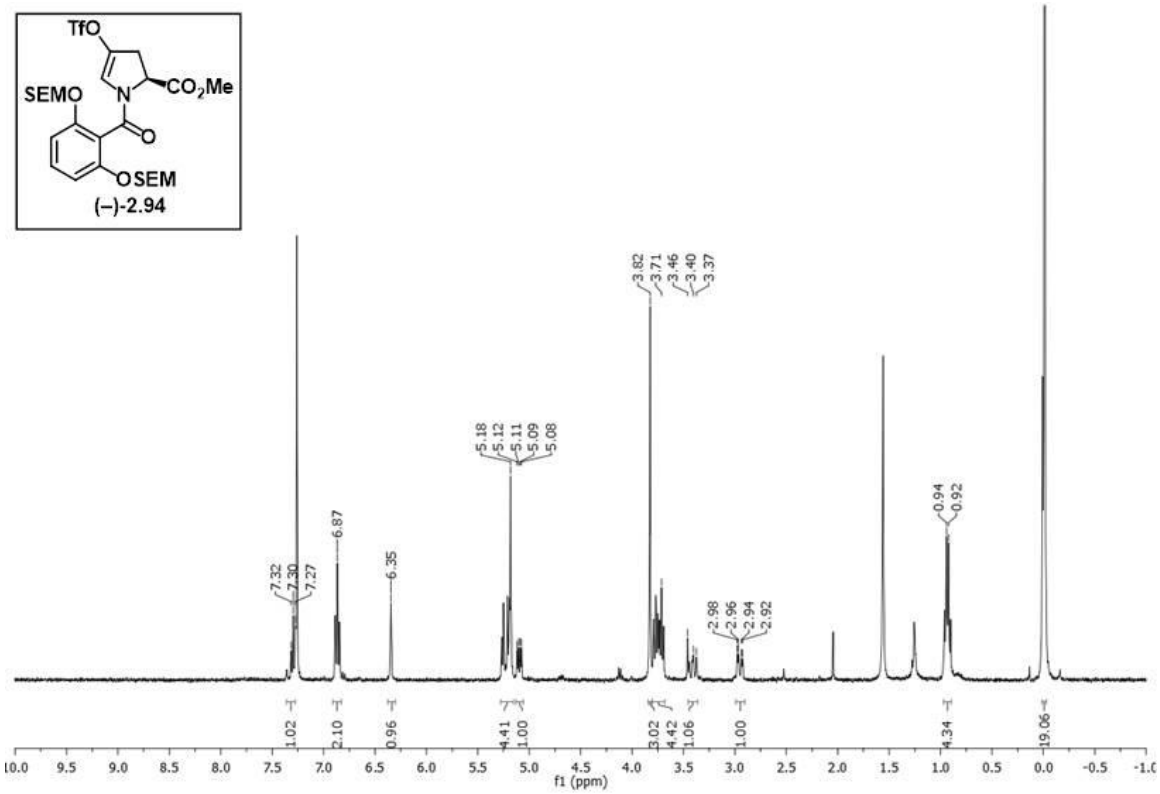
TfO
SEMO
N
CO2Me
O
OSEM
(–)-2.94
7.32
7.30
7.27
6.87
6.35
5.18
5.12
5.11
5.09
5.08
3.82
3.71
3.46
3.40
3.37
2.98
2.96
2.94
2.92
0.94
0.92
1.02
2.10
0.96
4.41
1.00
3.02
4.42
1.06
1.00
4.34
19.06
f1 (ppm)

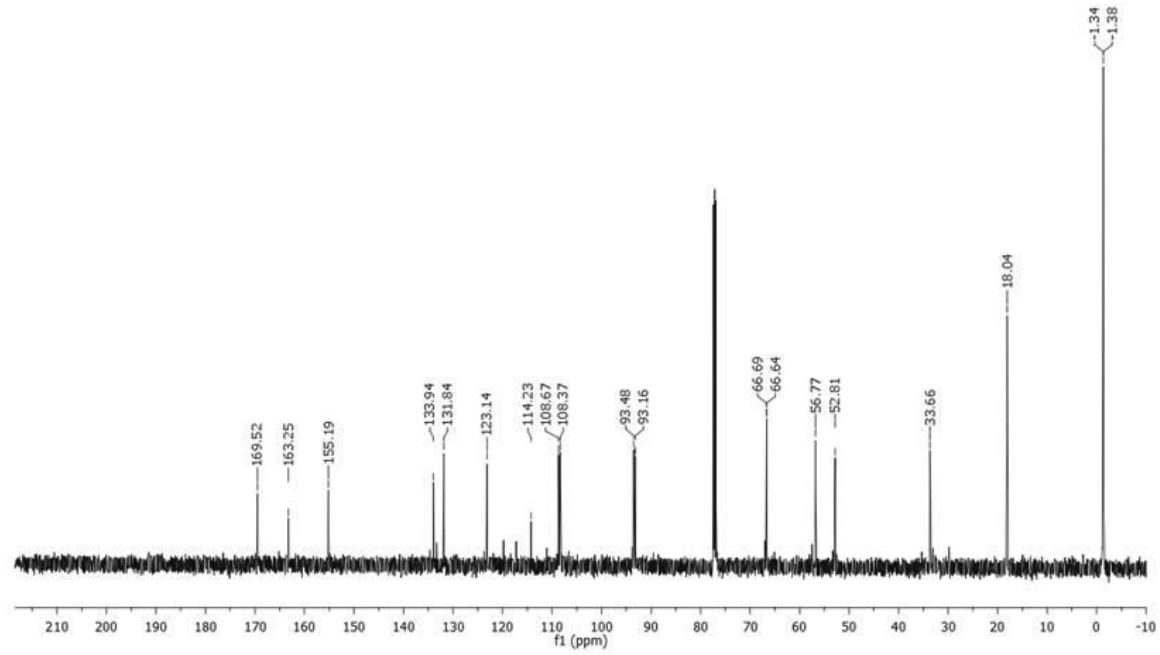
169.52
163.25
155.19
133.94
131.84
123.14
114.23
108.67
108.37
93.48
93.16
66.69
66.64
56.77
52.81
33.66
18.04
1.34
1.38
f1 (ppm)

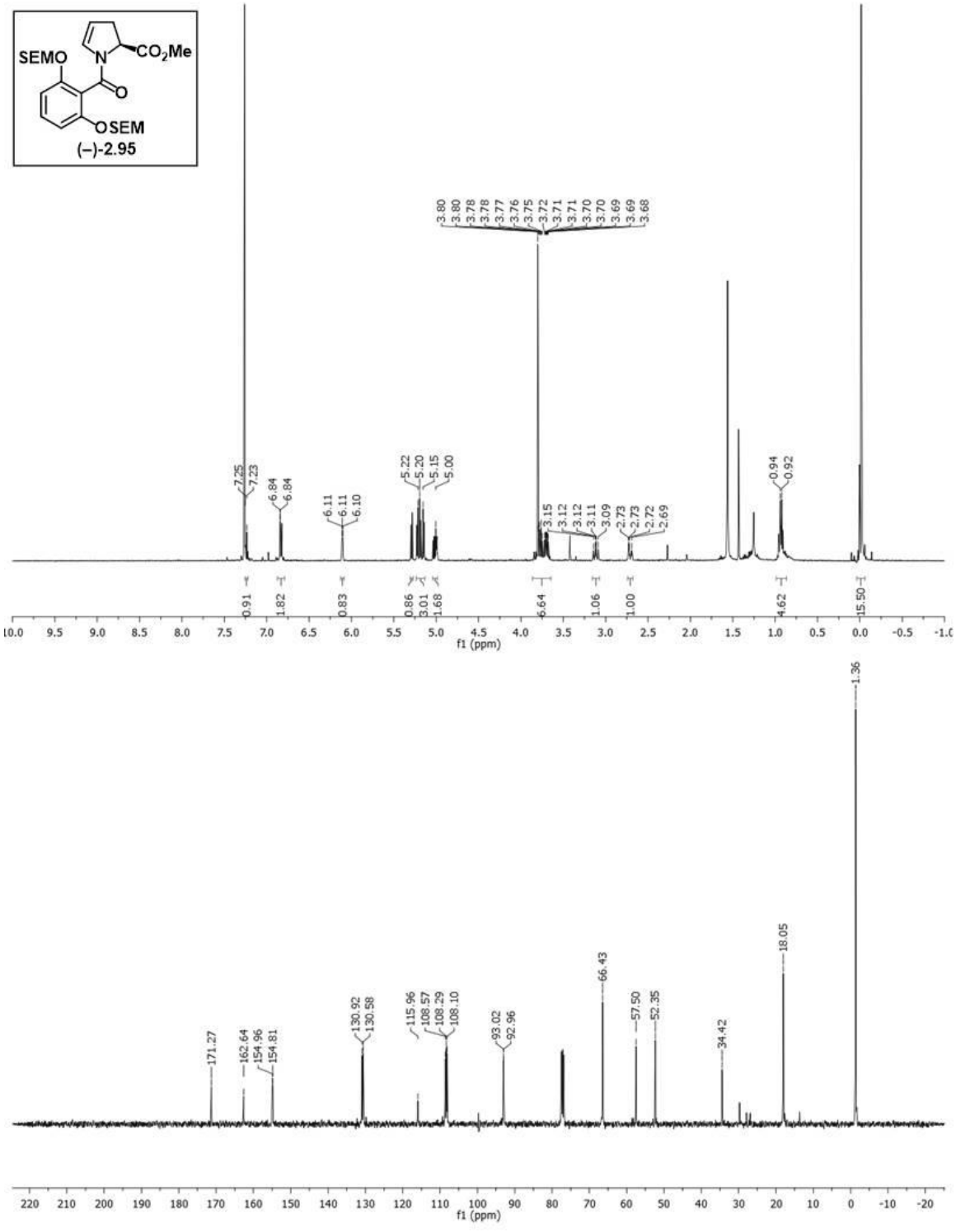
SEMO
N
CO2Me
O
OSEM
(–)-2.95
f1 (ppm)
f1 (ppm)

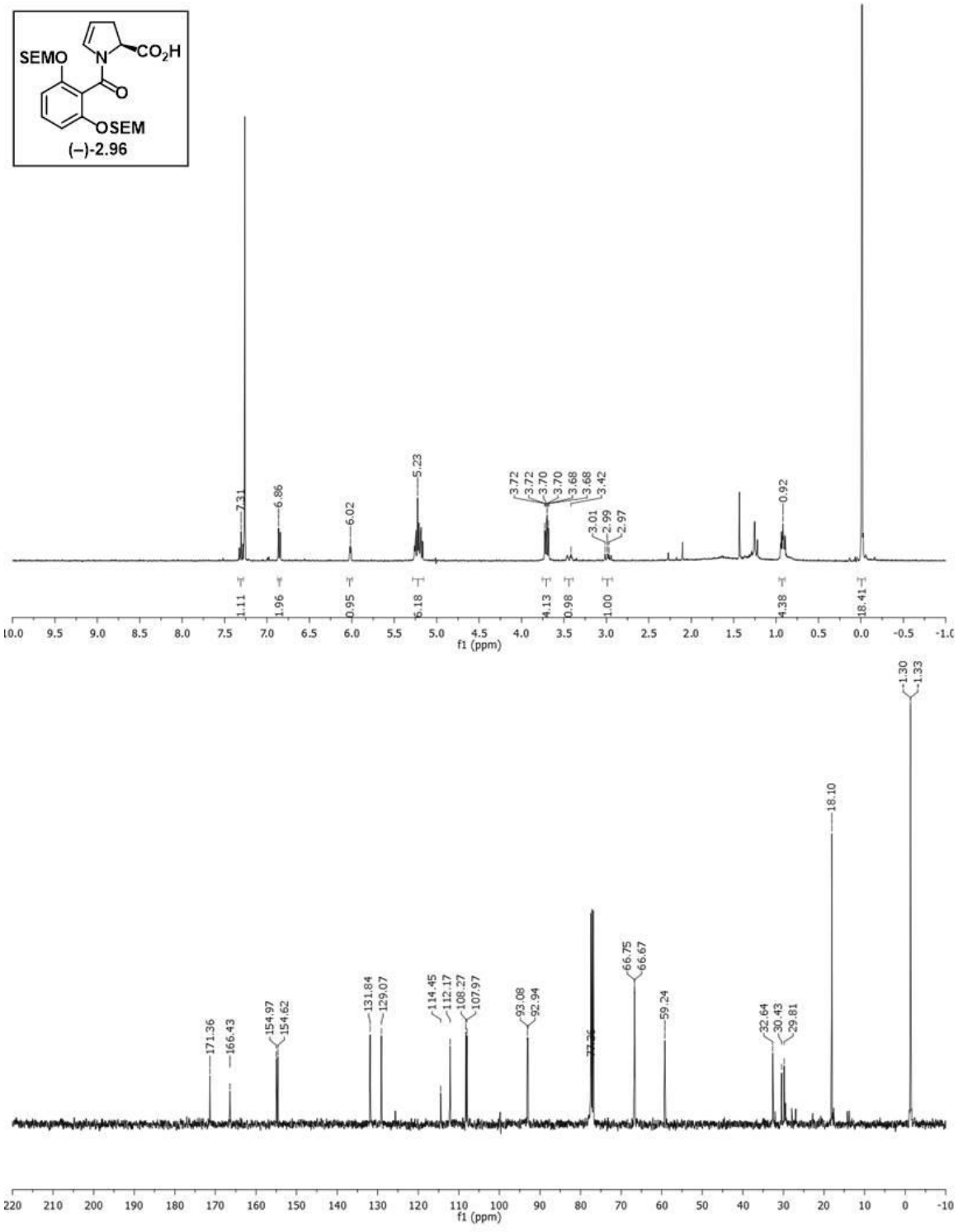
SEMO
N
CO2H
O
OSEM
(–)-2.96
7.31
6.86
6.02
5.23
3.72
3.72
3.70
3.70
3.68
3.68
3.42
3.01
2.99
2.97
0.92
1.11
1.96
0.95
6.18
4.13
0.98
1.00
4.38
18.41
f1 (ppm)
171.36
166.43
154.97
154.62
131.84
129.07
114.45
112.17
108.27
107.97
93.08
92.94
77.26
66.75
66.67
59.24
32.64
30.43
29.81
18.10
1.30
1.33
f1 (ppm)

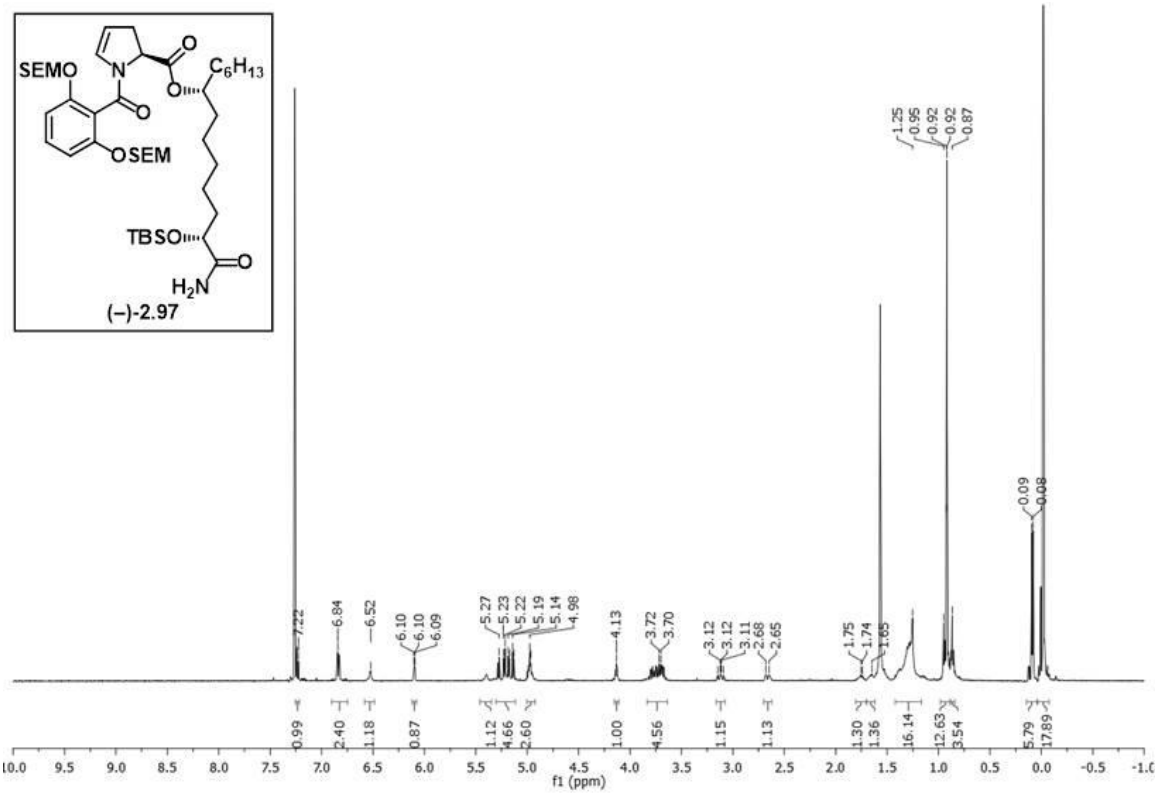
SEMO
OSEM
C_6H_{13}
TBSO
H_2N
(–)-2.97
f1 (ppm)

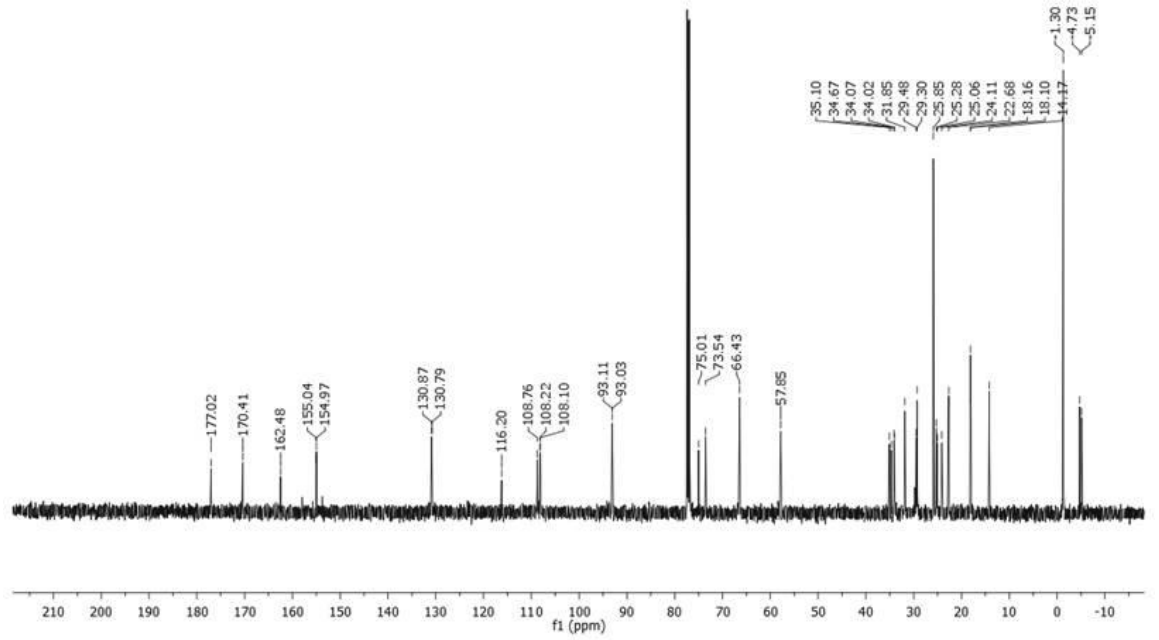
f1 (ppm)

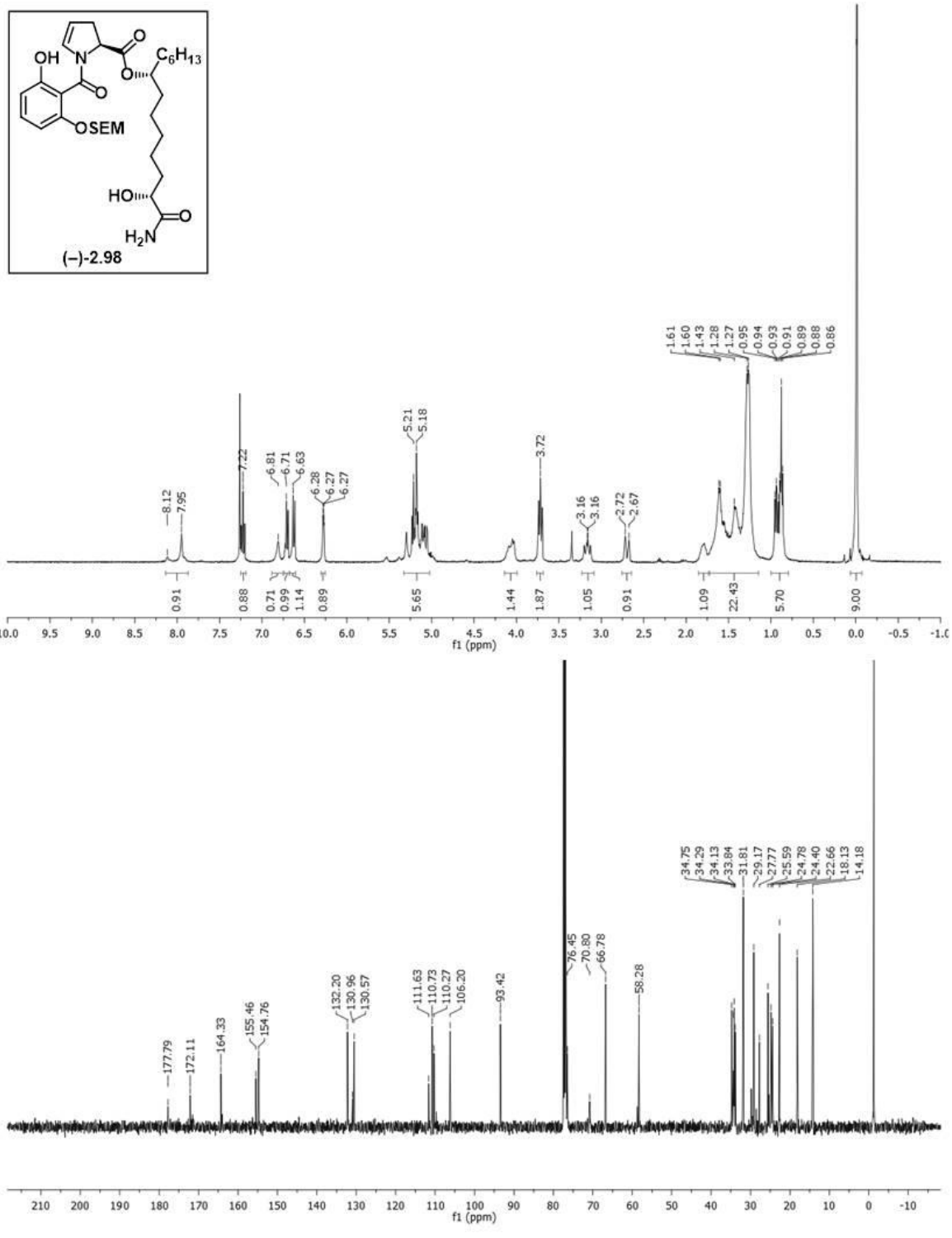
OH
N
O
O
C_6H_{13}
OSEM
HO
O
H_2N
(–)-2.98
8.12
7.95
7.22
6.81
6.71
6.63
6.28
6.27
6.27
5.21
5.18
3.72
3.16
3.16
2.72
2.67
1.61
1.60
1.43
1.28
1.27
0.95
0.94
0.93
0.91
0.89
0.88
0.86
0.91
0.88
0.71
0.99
1.14
0.89
5.65
1.44
1.87
1.05
0.91
1.09
22.43
5.70
9.00
f1 (ppm)
177.79
172.11
164.33
155.46
154.76
132.20
130.96
130.57
111.63
110.73
110.27
106.20
93.42
76.45
70.80
66.78
58.28
34.75
34.29
34.13
33.84
31.81
29.17
27.77
25.59
24.78
24.40
22.66
18.13
14.18
f1 (ppm)

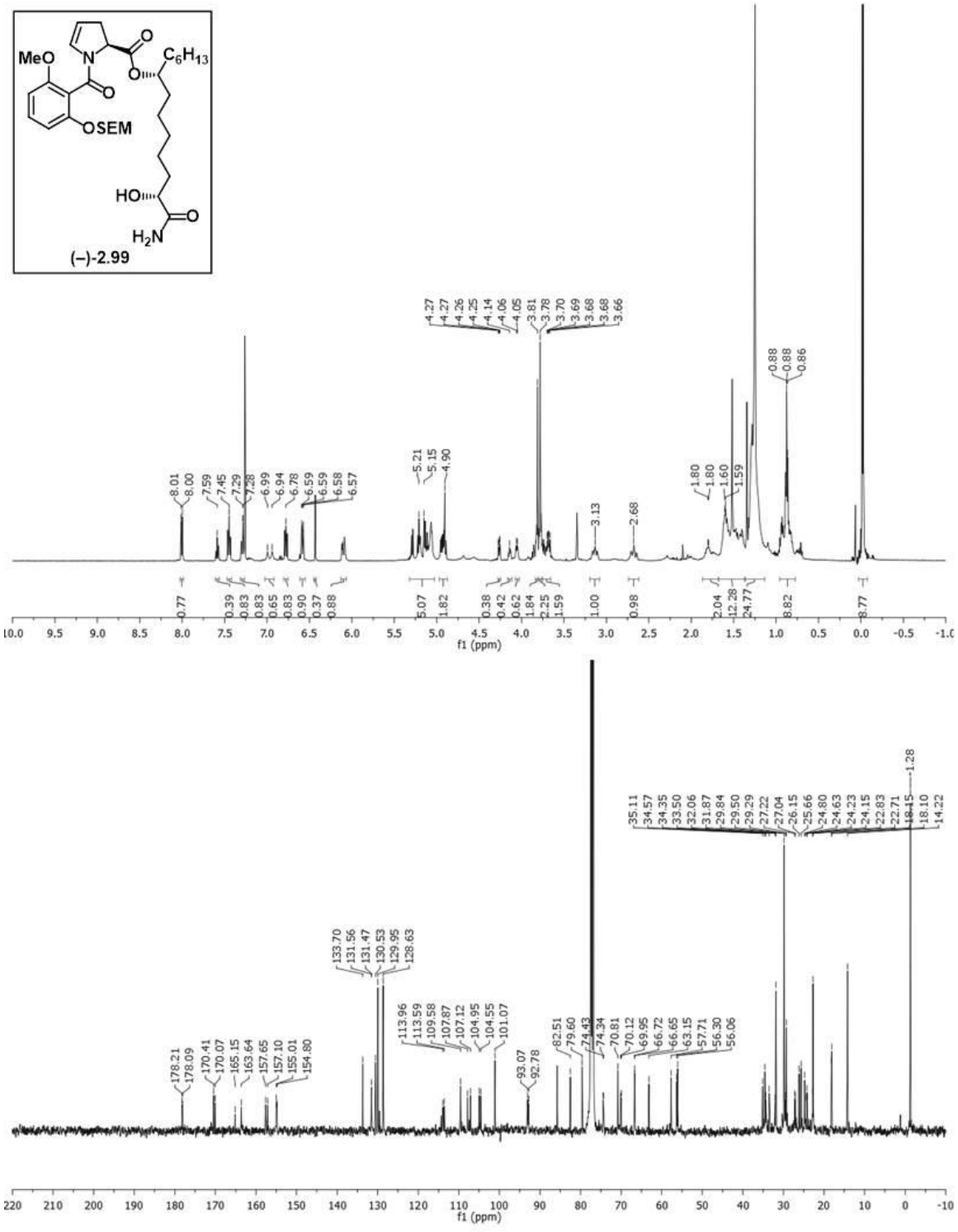
MeO
OSEM
HO
H_2N
C_6H_{13}
(–)-2.99
f1 (ppm)
f1 (ppm)

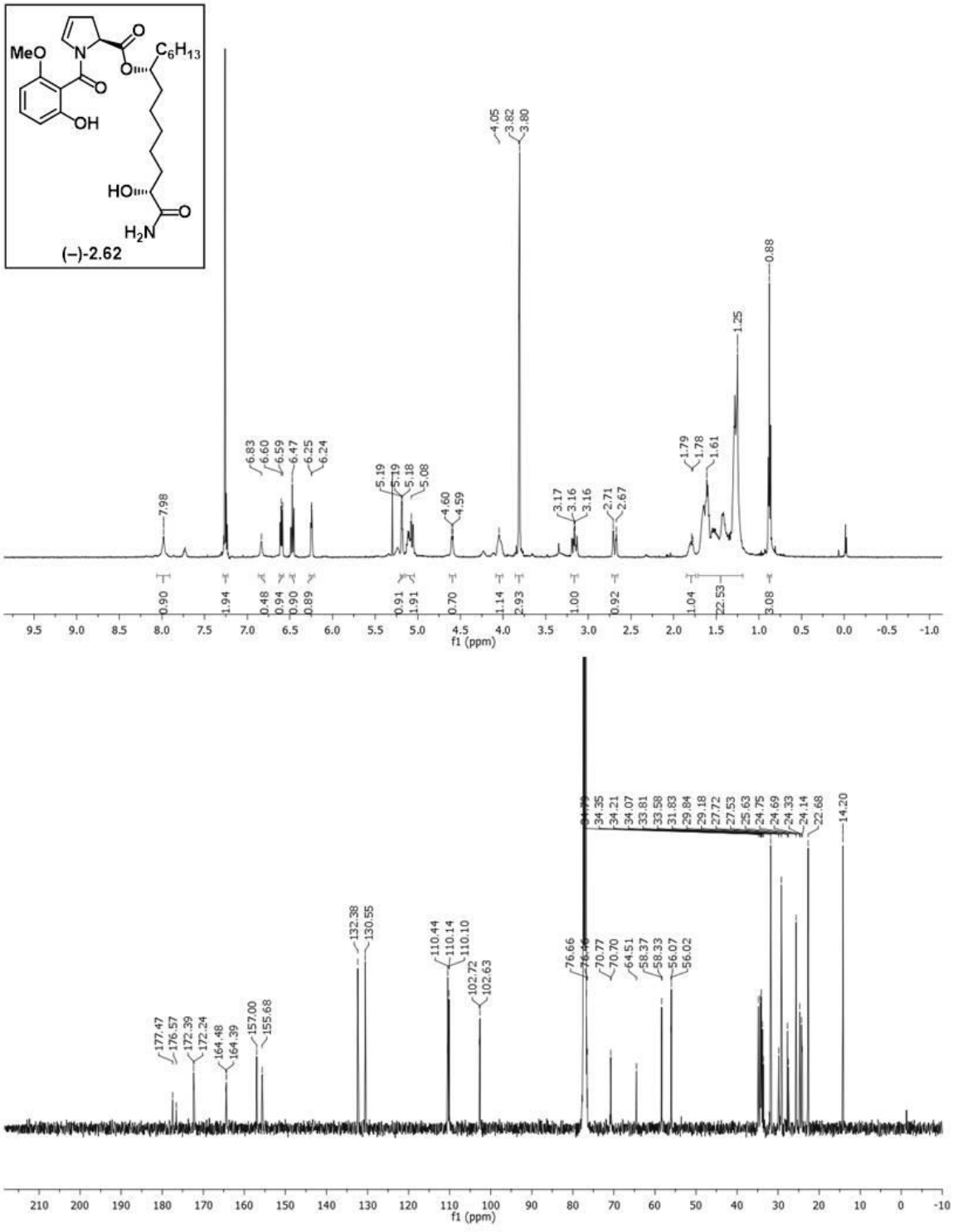
MeO
OH
HO
H_2N
C_6H_{13}
(–)-2.62
f1 (ppm)
f1 (ppm)

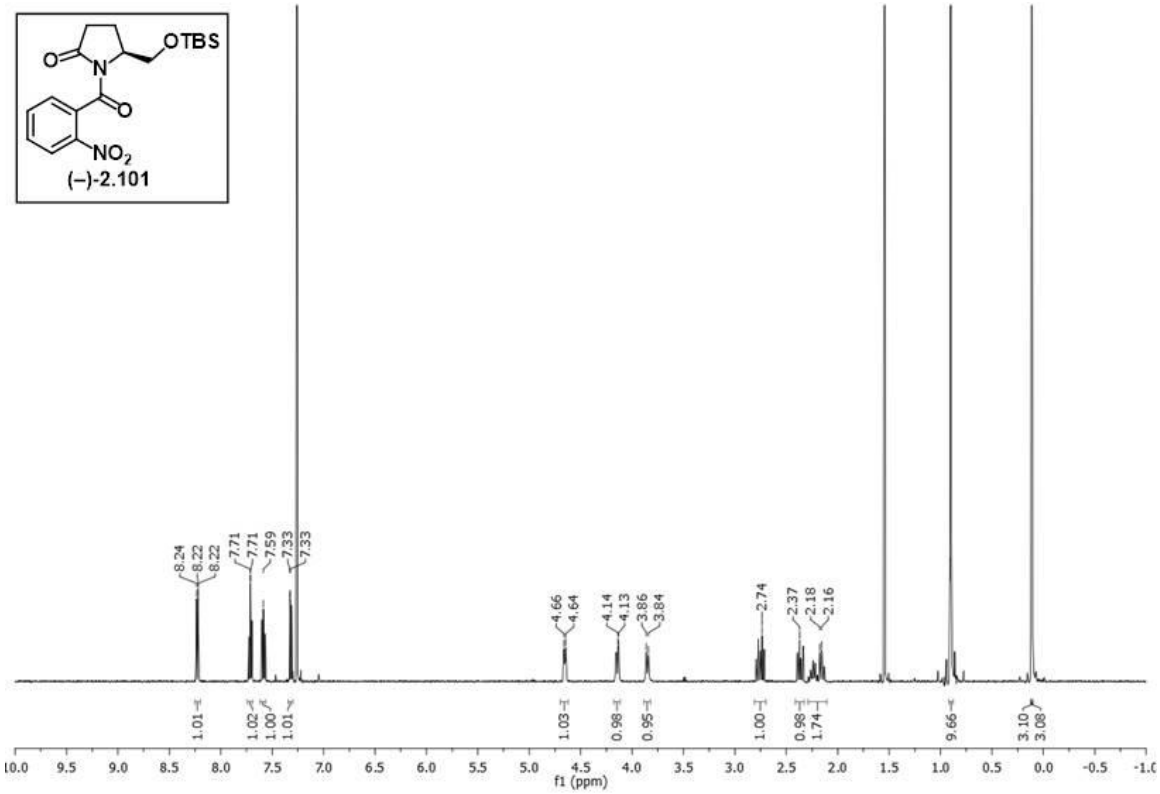
OTBS
O
N
O
NO2
(–)-2.101
8.24
8.22
8.22
7.71
7.71
7.59
7.33
7.33
4.66
4.64
4.14
4.13
3.86
3.84
2.74
2.37
2.18
2.16
1.01
1.02
1.00
1.01
1.03
0.98
0.95
1.00
0.98
1.74
9.66
3.10
3.08
f1 (ppm)

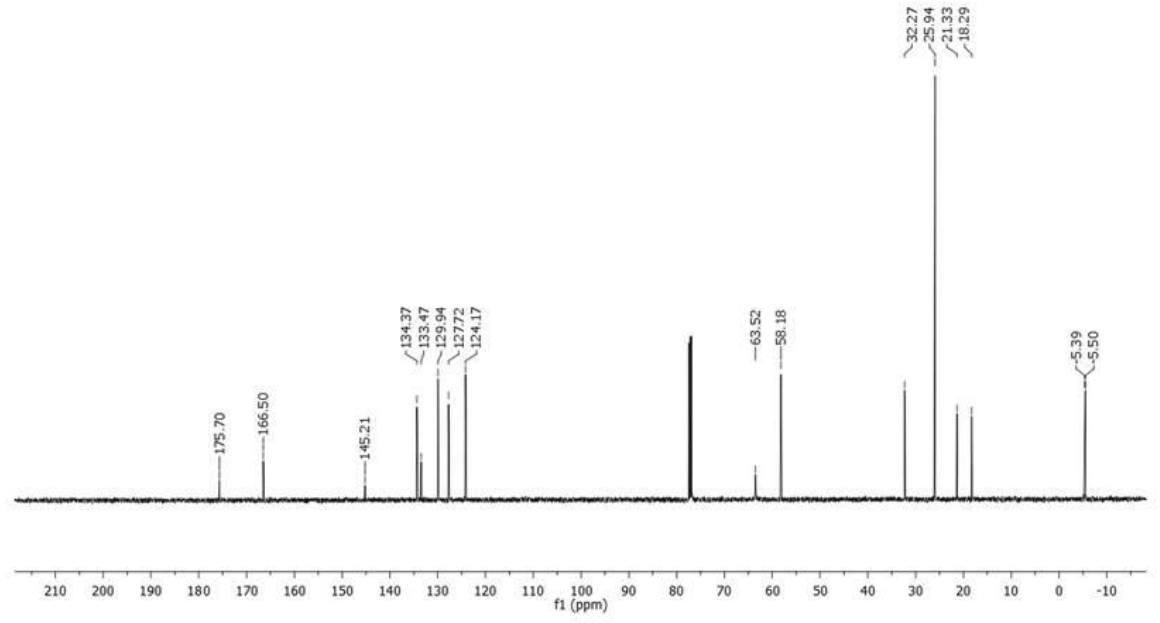
32.27
25.94
21.33
18.29
134.37
133.47
129.94
127.72
124.17
63.52
58.18
5.39
-5.50
175.70
166.50
145.21
f1 (ppm)

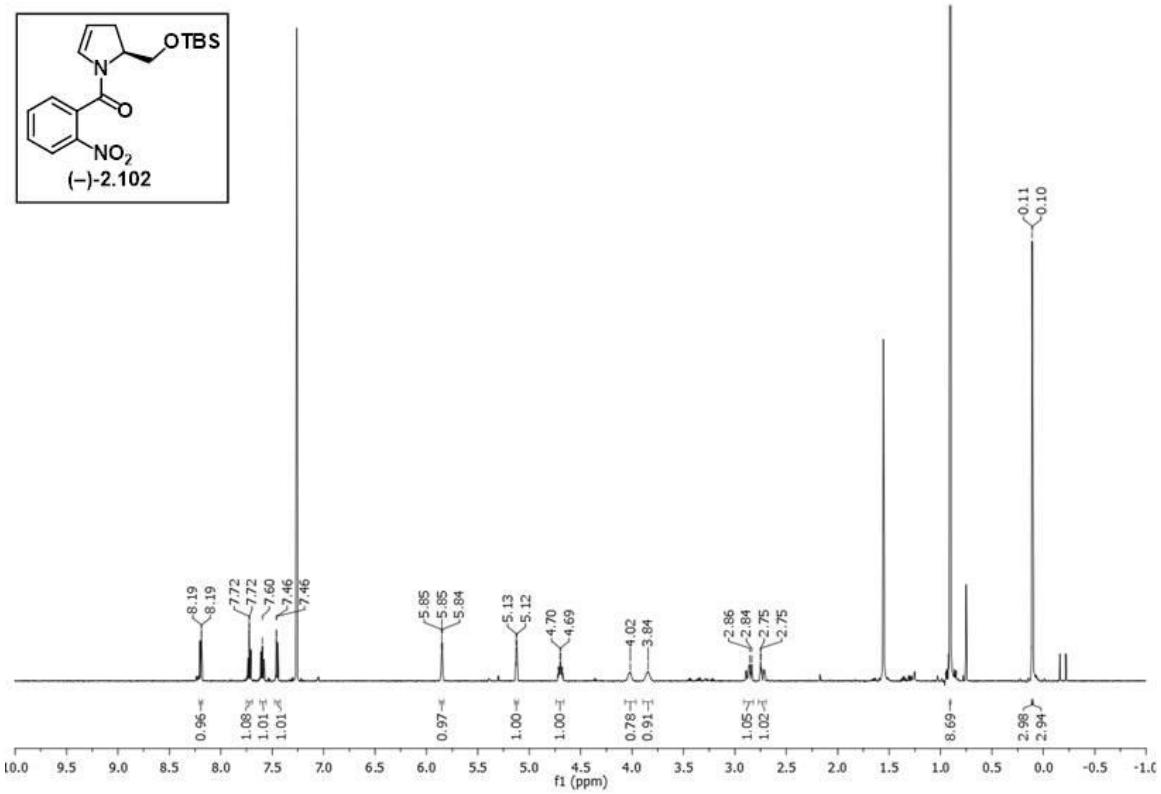
OTBS
N
O
NO2
(–)-2.102
8.19
8.19
7.72
7.72
7.60
7.46
7.46
5.85
5.85
5.84
5.13
5.12
4.70
4.69
4.02
3.84
2.86
2.84
2.75
2.75
0.11
0.10
0.96
1.08
1.01
1.01
0.97
1.00
1.00
0.78
0.91
1.05
1.02
8.69
2.98
2.94
f1 (ppm)

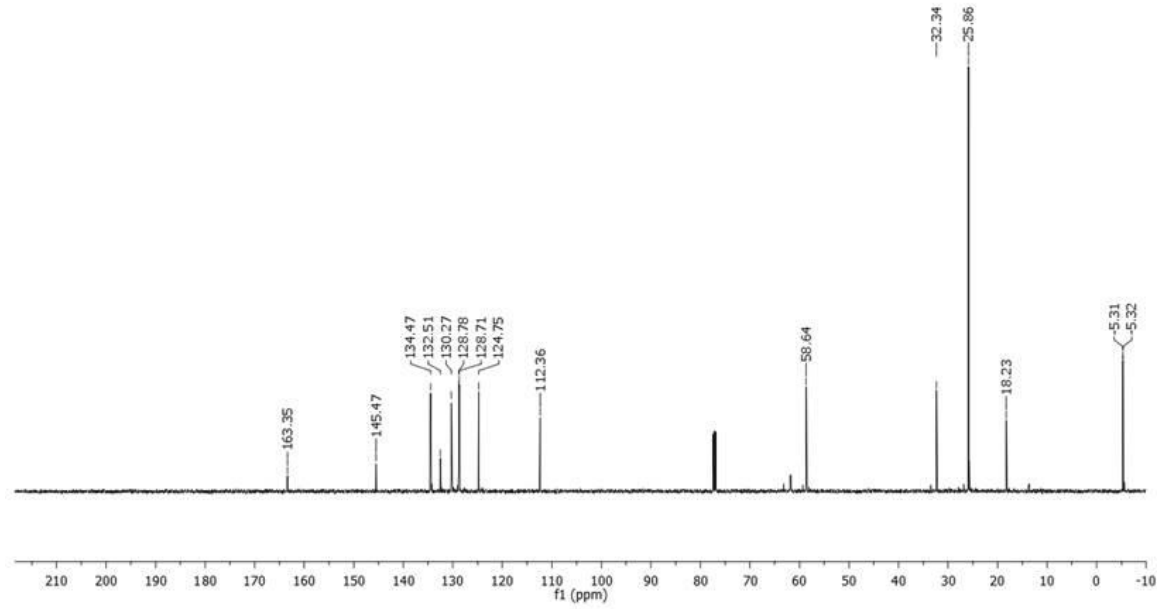
32.34
25.86
134.47
132.51
130.27
128.78
128.71
124.75
112.36
58.64
18.23
5.31
5.32
163.35
145.47
f1 (ppm)

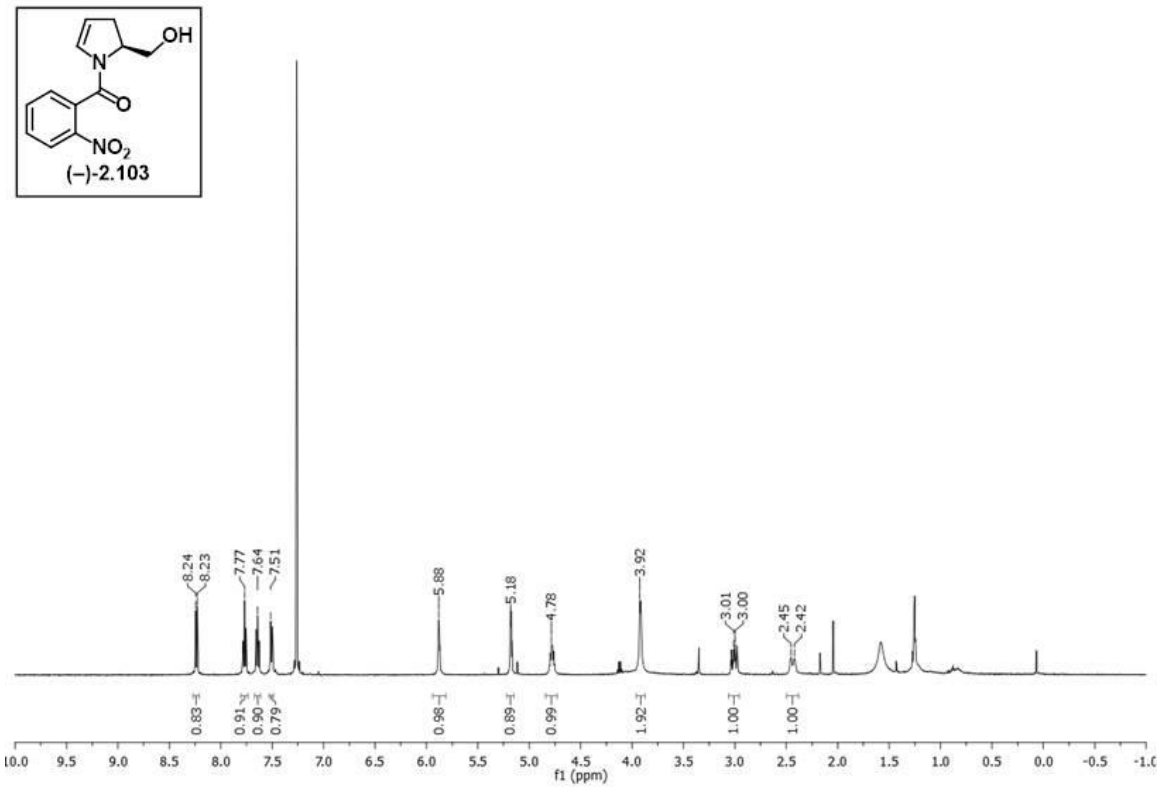
OH
N
O
NO2
(–)-2.103
8.24
8.23
7.77
7.64
7.51
5.88
5.18
4.78
3.92
3.01
3.00
2.45
2.42
0.83
0.91
0.90
0.79
0.98
0.89
0.99
1.92
1.00
1.00
f1 (ppm)

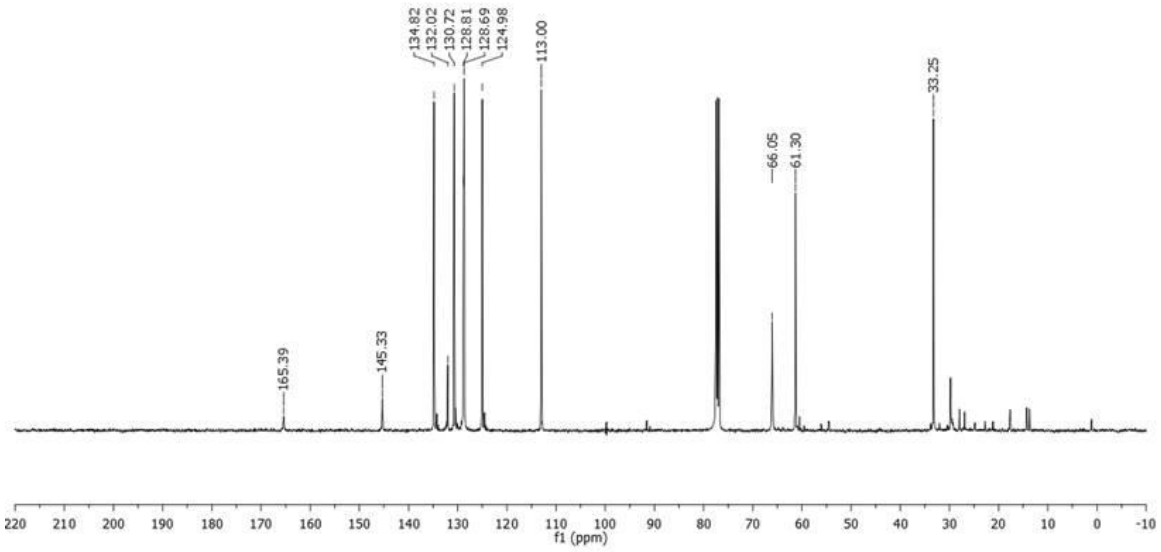
134.82
132.02
130.72
128.81
128.69
124.98
113.00
66.05
61.30
33.25
165.39
145.33
f1 (ppm)

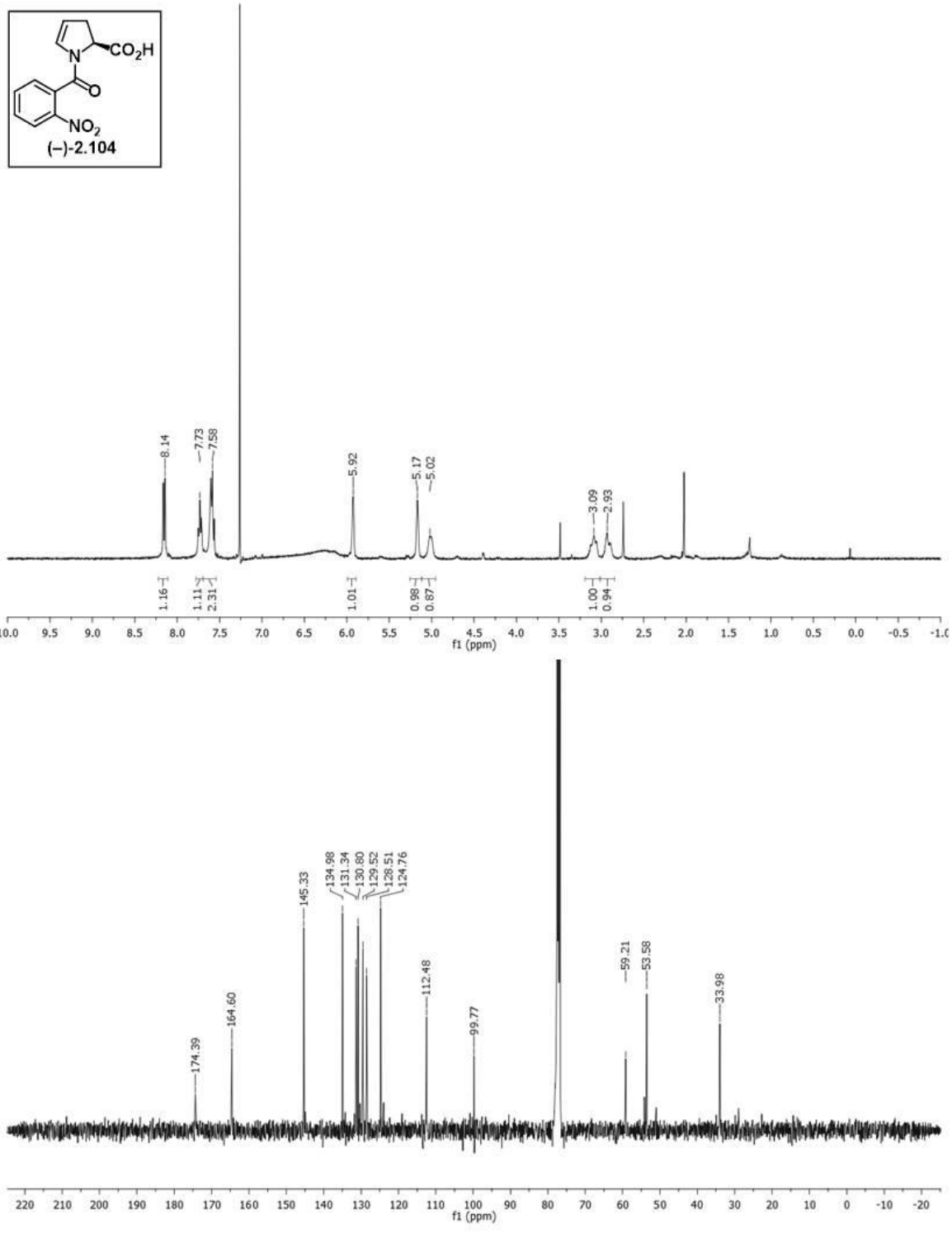
CO2H
N
O
NO2
(–)-2.104
8.14
7.73
7.58
5.92
5.17
5.02
3.09
2.93
1.16
1.11
2.31
1.01
0.98
0.87
1.00
0.94
f1 (ppm)
145.33
134.98
131.34
130.80
129.52
128.51
124.76
112.48
99.77
59.21
53.58
33.98
174.39
164.60
f1 (ppm)

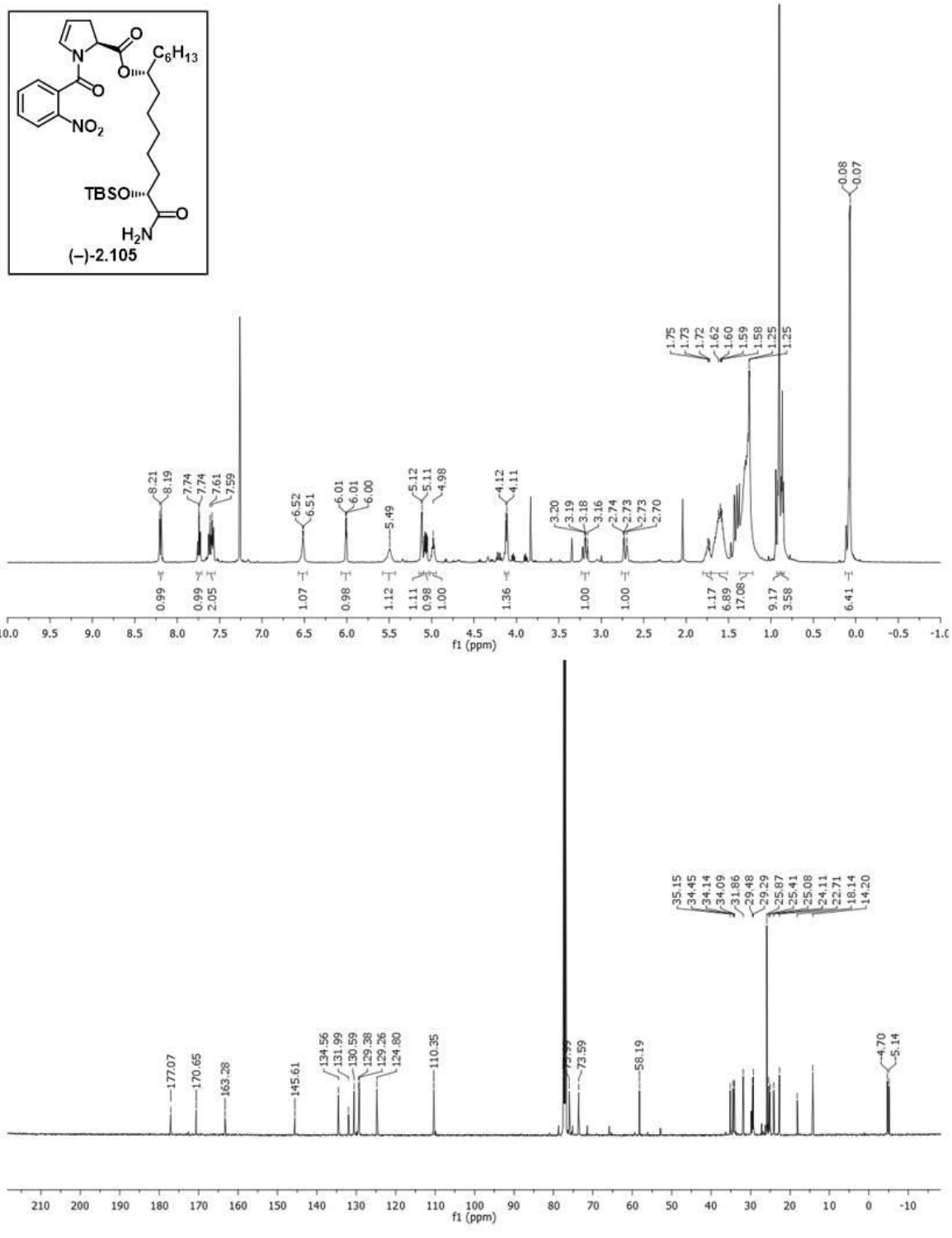
(–)-2.105
f1 (ppm)
f1 (ppm)

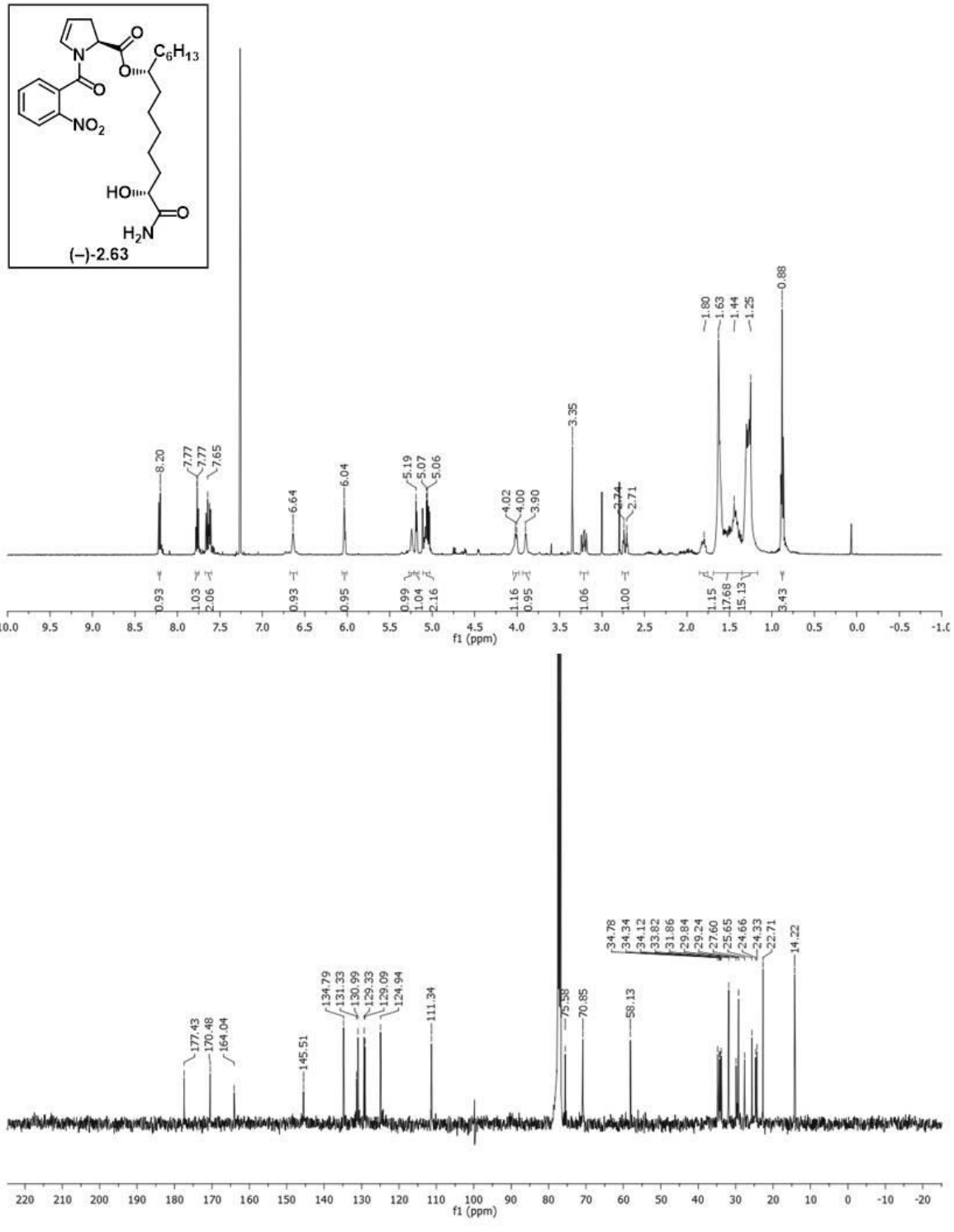
(–)-2.63
f1 (ppm)
f1 (ppm)

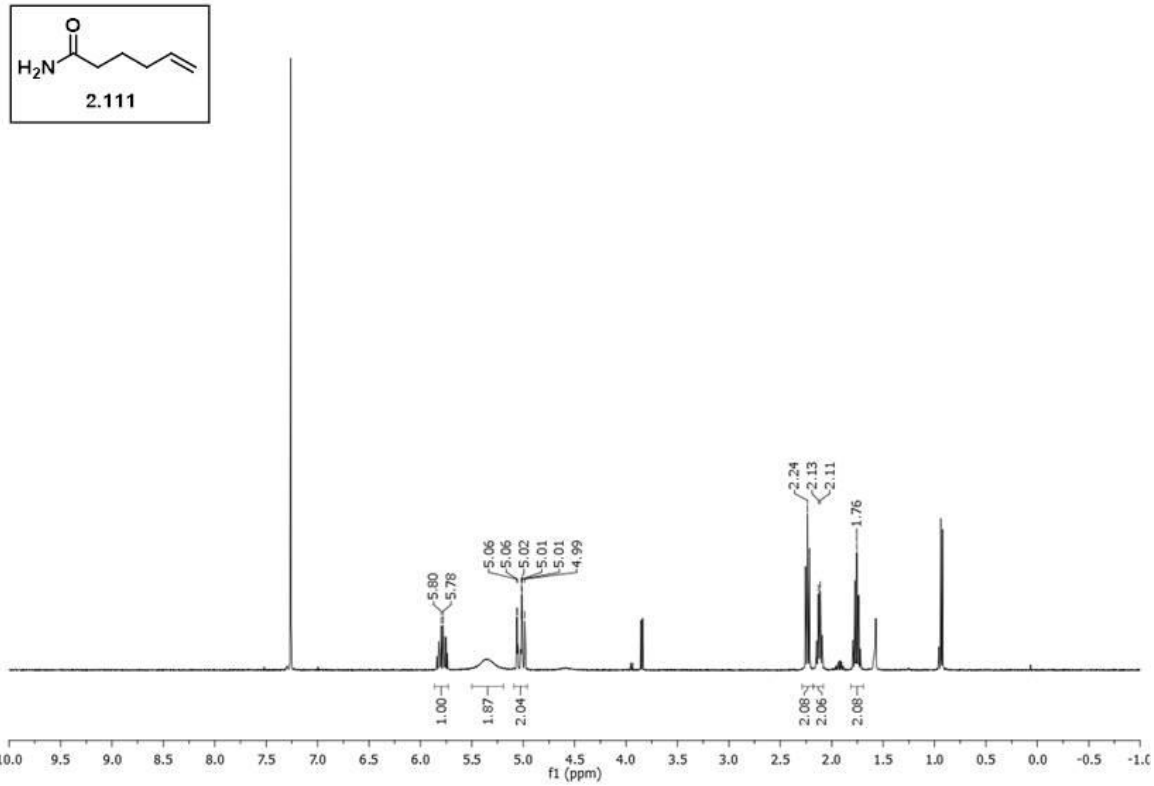
O
H2N
2.111
5.80
5.78
5.06
5.06
5.02
5.01
5.01
4.99
2.24
2.13
2.11
1.76
1.00
1.87
2.04
2.08
2.06
2.08
f1 (ppm)

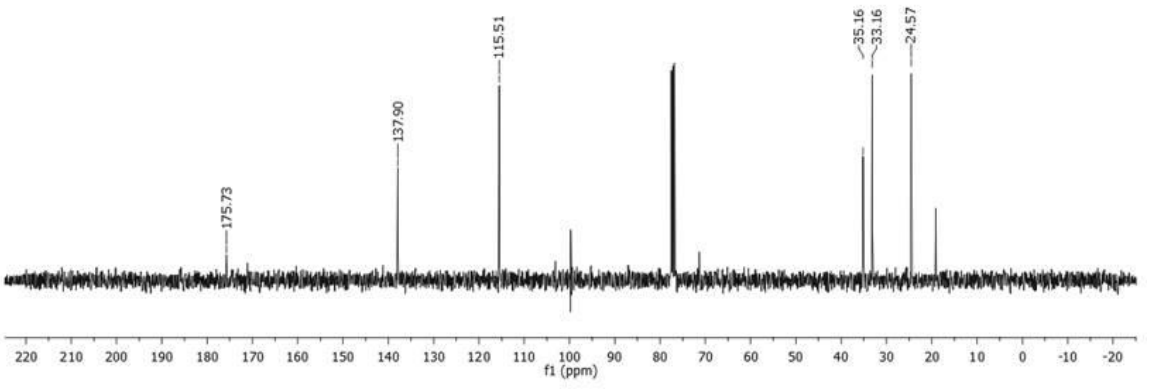
175.73
137.90
115.51
35.16
33.16
24.57
f1 (ppm)

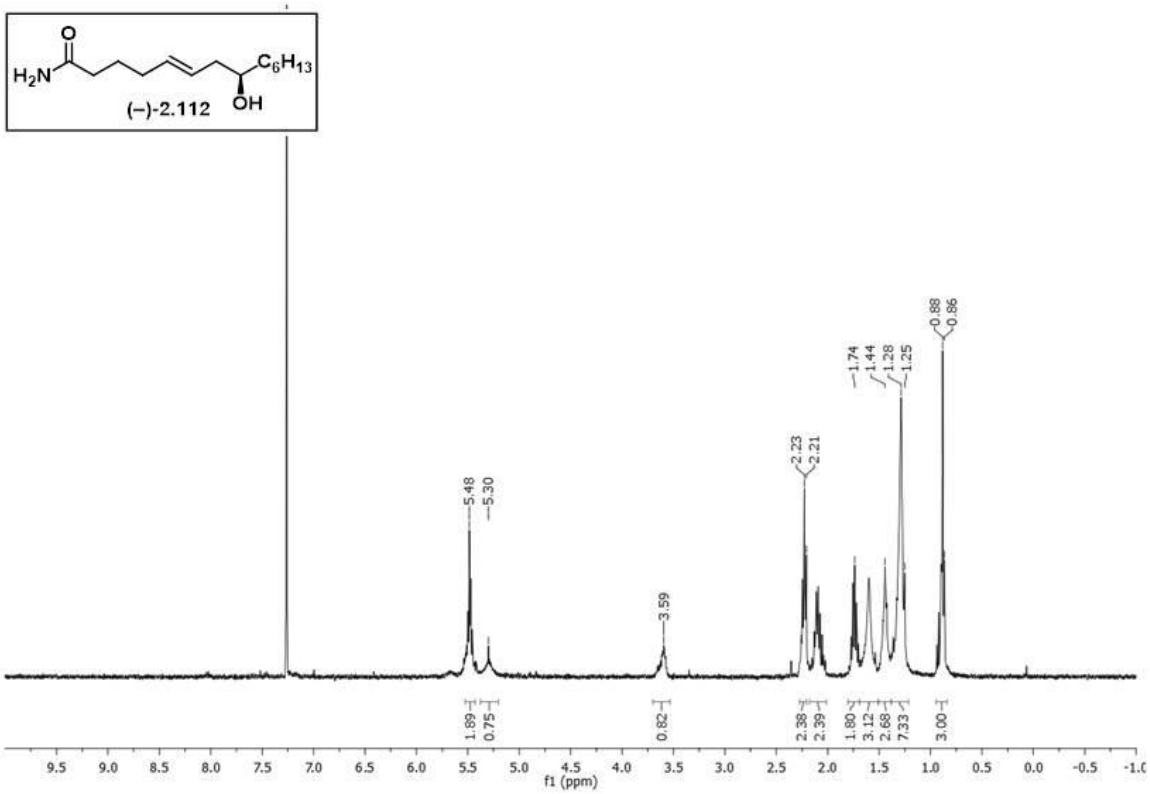
O
H2N
C6H13
OH
(–)-2.112
5.48
5.30
3.59
2.23
2.21
1.74
1.44
1.28
1.25
0.88
0.86
1.89
0.75
0.82
2.38
2.39
1.80
3.12
2.68
7.33
3.00
f1 (ppm)

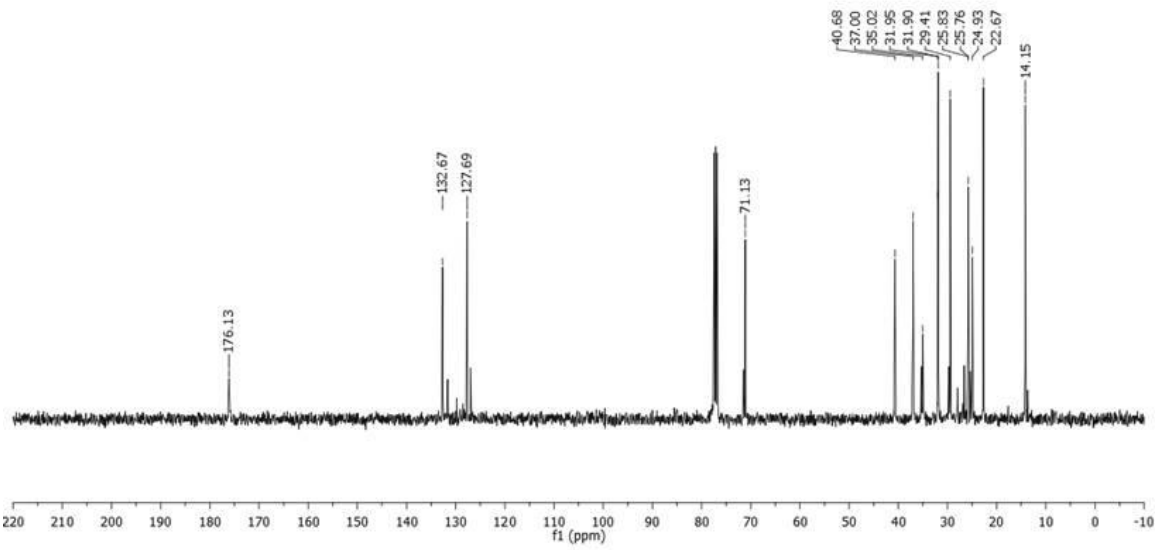
176.13
132.67
127.69
71.13
40.68
37.00
35.02
31.95
31.90
29.41
25.83
25.76
24.93
22.67
14.15
f1 (ppm)

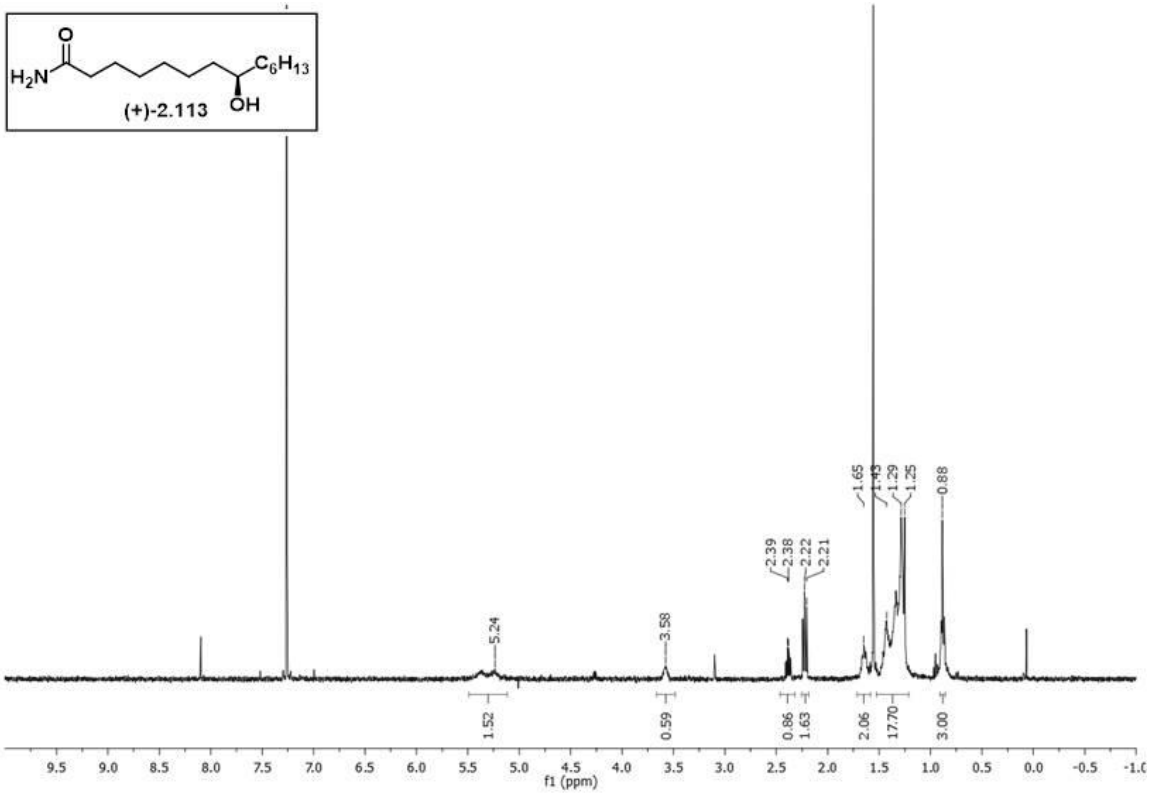
(+)-2.113
5.24
3.58
2.39
2.38
2.22
2.21
1.65
1.43
1.29
1.25
0.88
1.52
0.59
0.86
1.63
2.06
17.70
3.00
f1 (ppm)

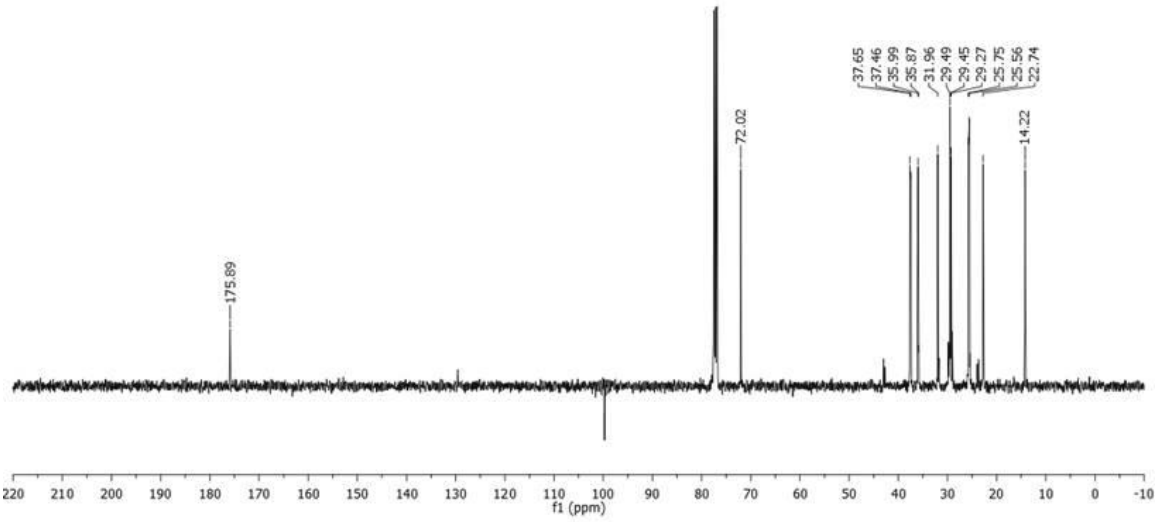
175.89
72.02
37.65
37.46
35.99
35.87
31.96
29.49
29.45
29.27
25.75
25.56
22.74
14.22
f1 (ppm)

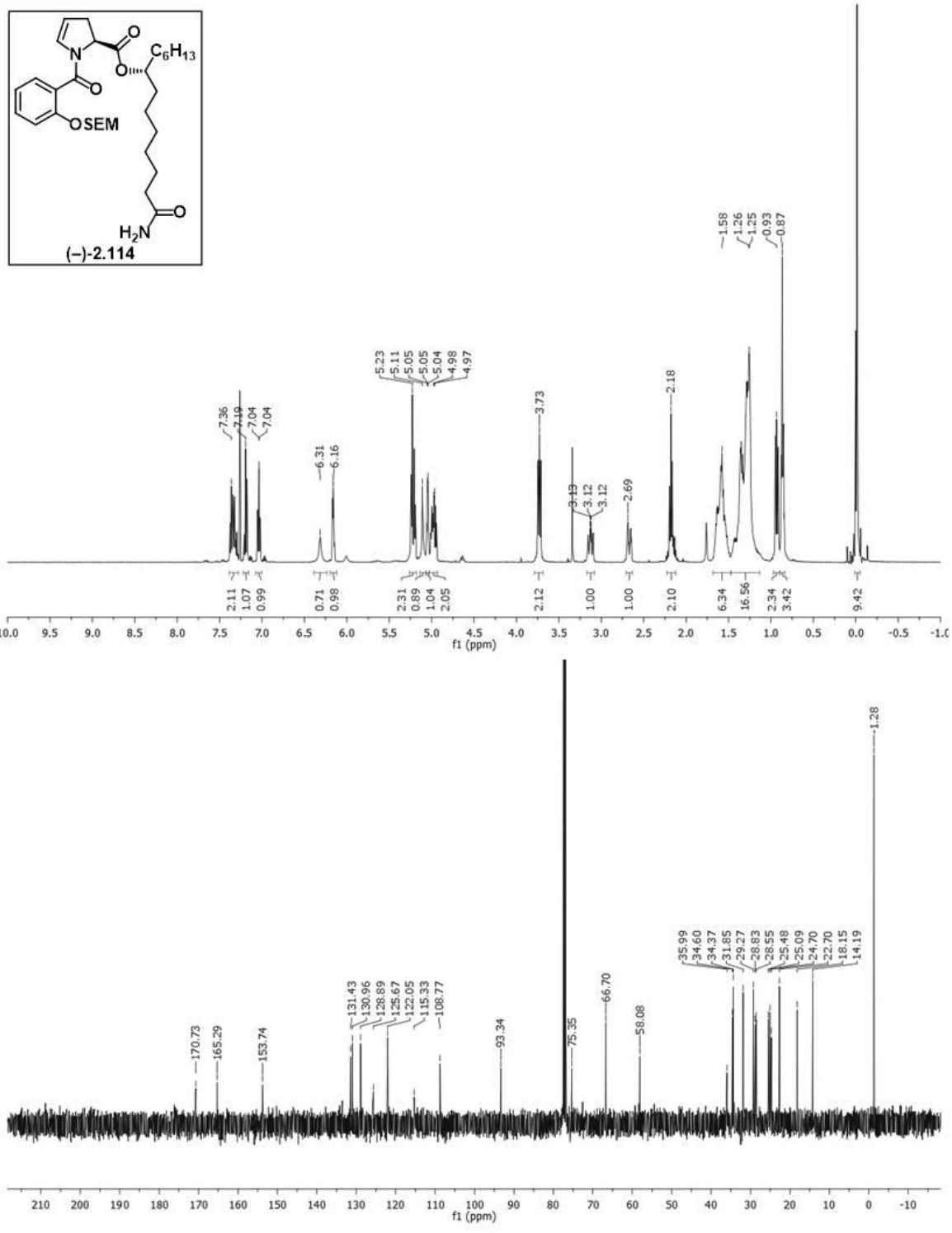
(–)-2.114
f1 (ppm)
f1 (ppm)

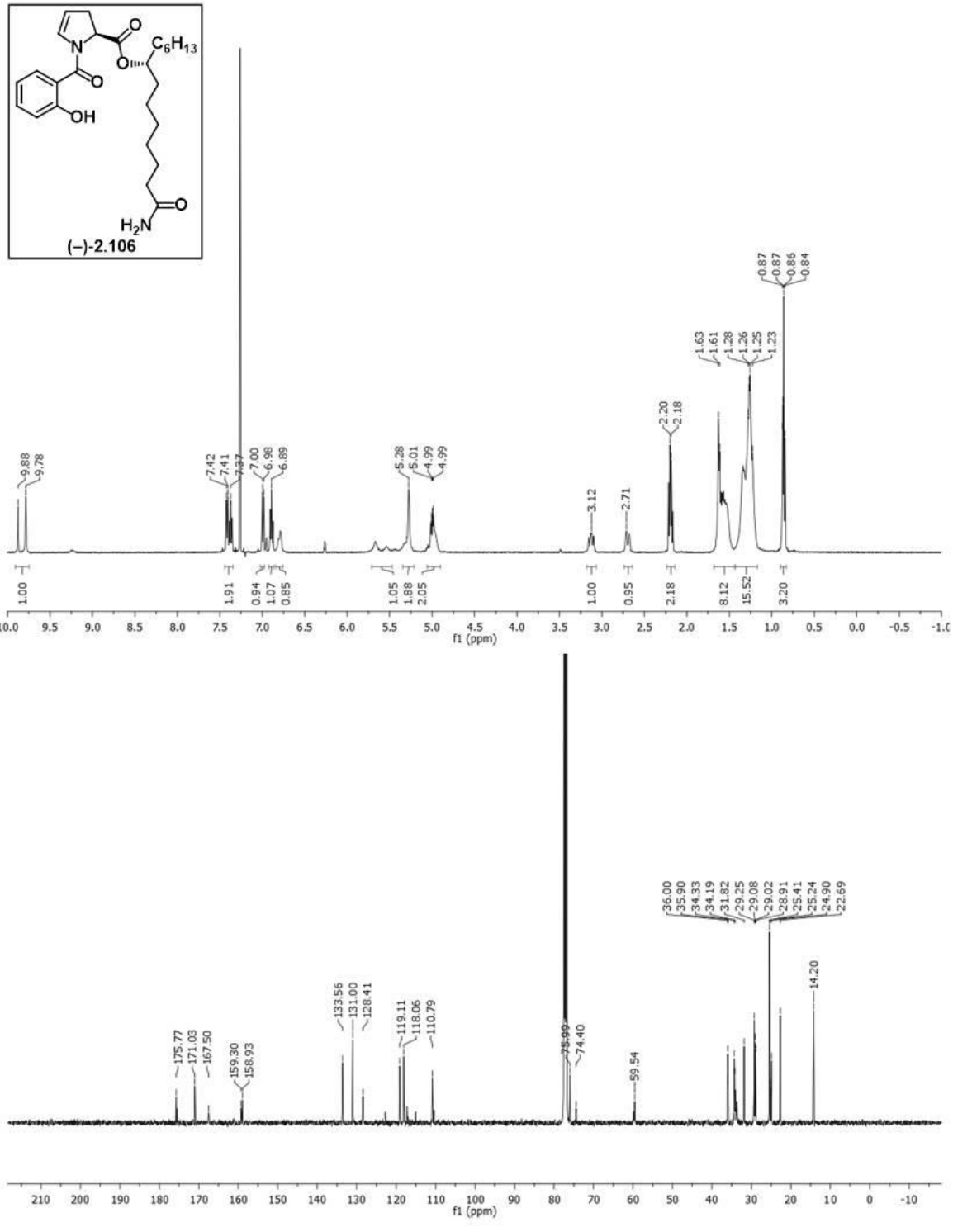
(–)-2.106
f1 (ppm)
f1 (ppm)

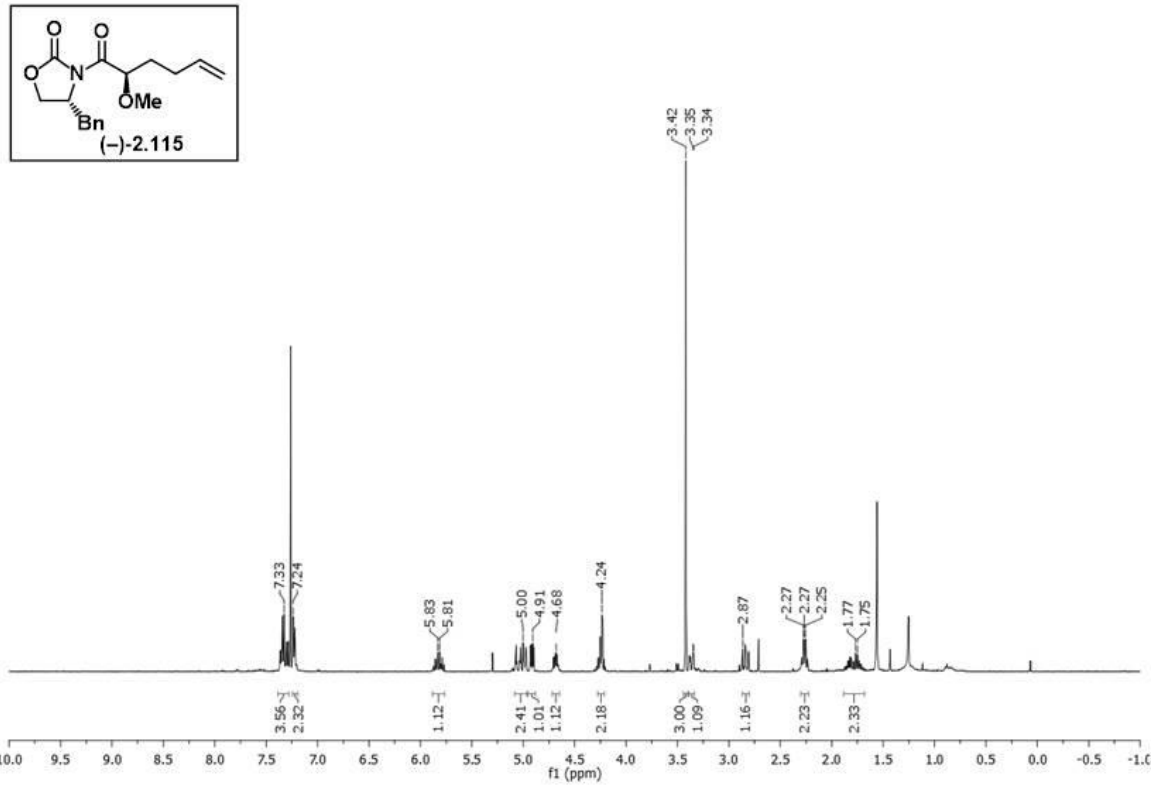
OMe
Bn
(–)-2.115
3.42
3.35
3.34
7.33
7.24
5.83
5.81
5.00
4.91
4.68
4.24
2.87
2.27
2.27
2.25
1.77
1.75
3.56
2.32
1.12
2.41
1.01
1.12
2.18
3.00
1.09
1.16
2.23
2.33
f1 (ppm)

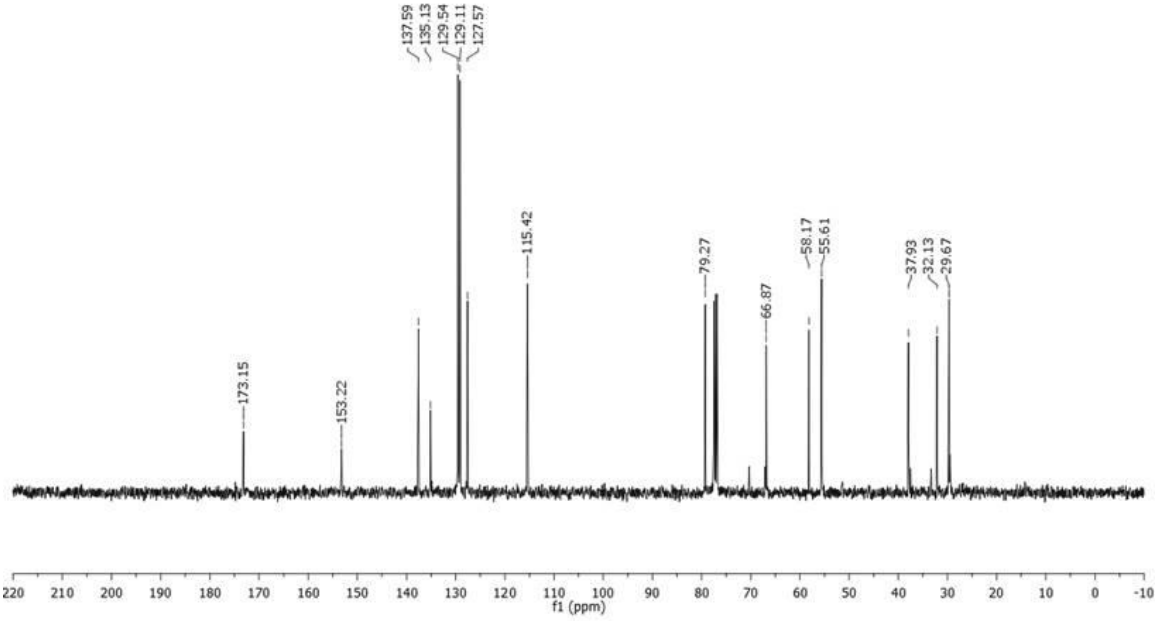
137.59
135.13
129.54
129.11
127.57
115.42
79.27
66.87
58.17
55.61
37.93
32.13
29.67
173.15
153.22
f1 (ppm)

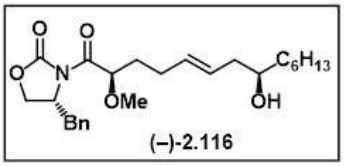
O
O
O
N
C_6H_{13}
OMe
OH
Bn

(–)-2.116

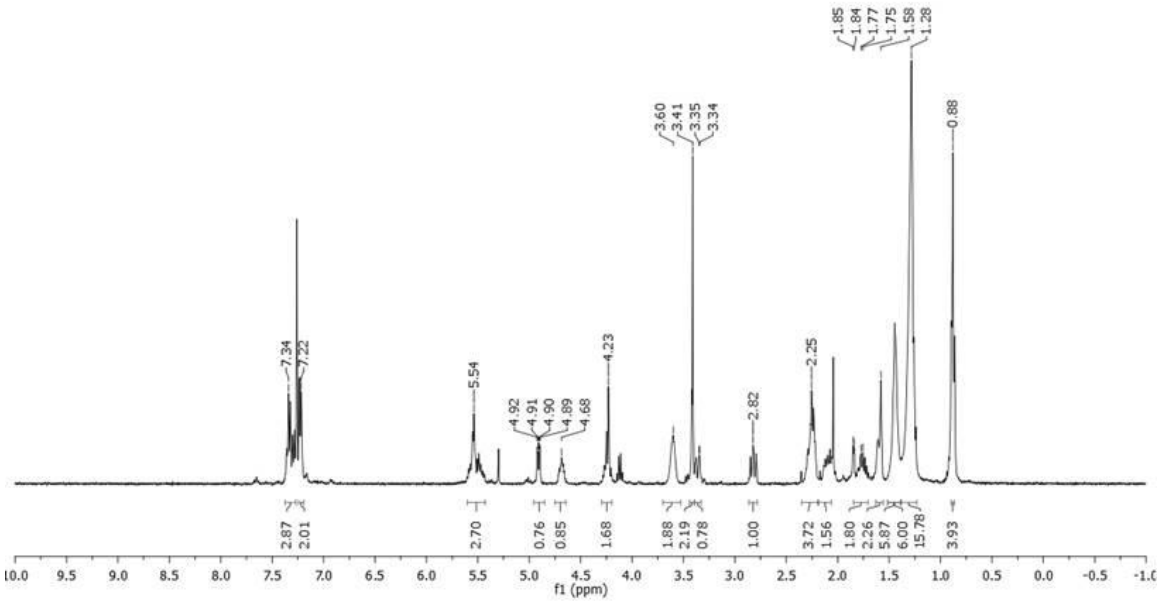
1.85
1.84
1.77
1.75
1.58
1.28
3.60
3.41
3.35
3.34
0.88
7.34
7.22
5.54
4.92
4.91
4.90
4.89
4.68
4.23
2.82
2.25
2.87
2.01
2.70
0.76
0.85
1.68
1.88
2.19
0.78
1.00
3.72
1.56
1.80
2.26
5.87
6.00
15.78
3.93
f1 (ppm)

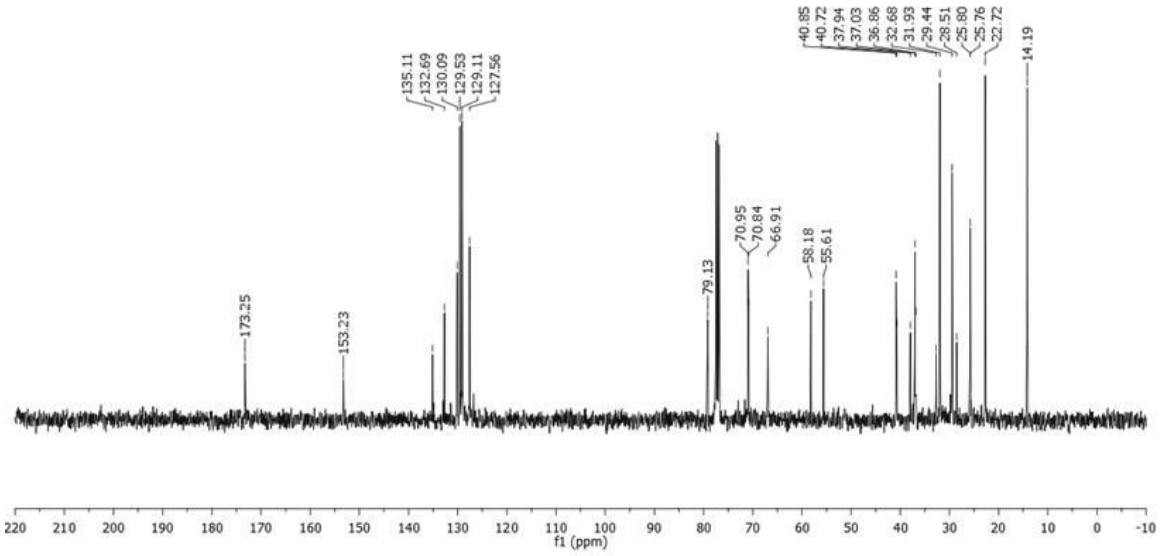
40.85
40.72
37.94
37.03
36.86
32.68
31.93
29.44
28.51
25.80
25.76
22.72
14.19
135.11
132.69
130.09
129.53
129.11
127.56
70.95
70.84
66.91
58.18
55.61
79.13
173.25
153.23
f1 (ppm)

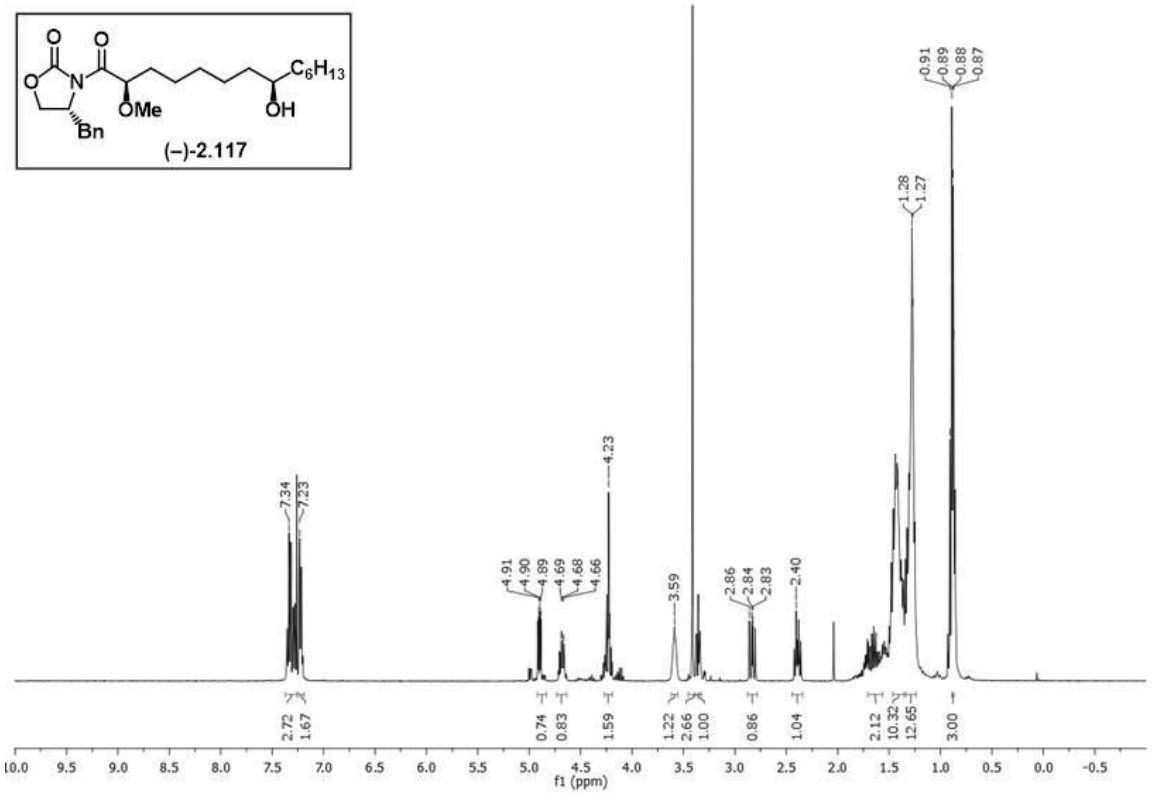
(–)-2.117
f1 (ppm)

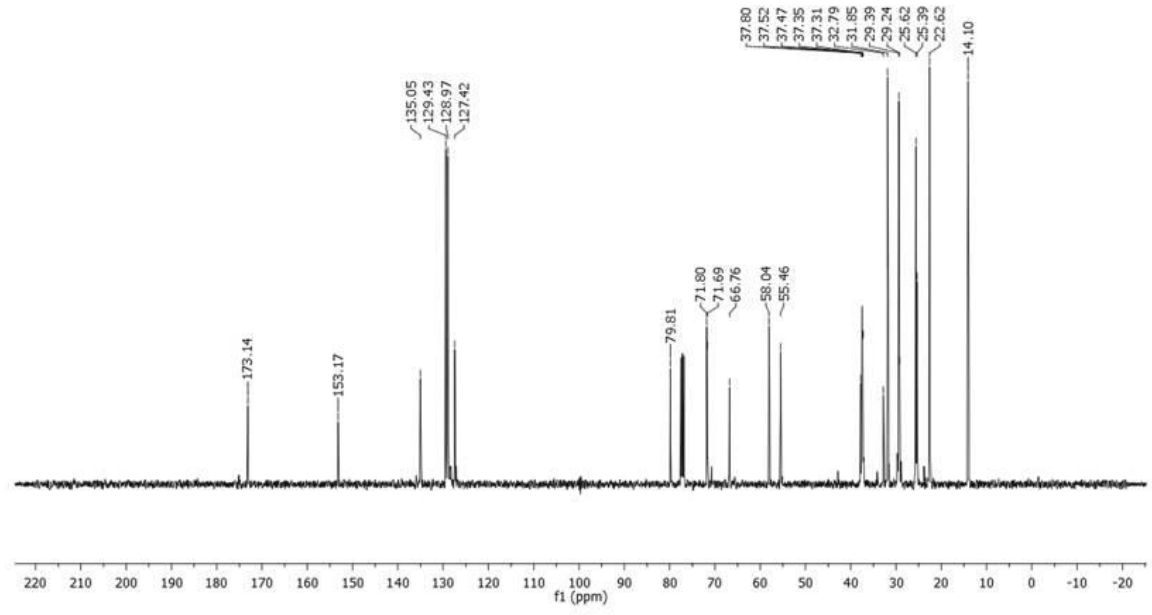
f1 (ppm)

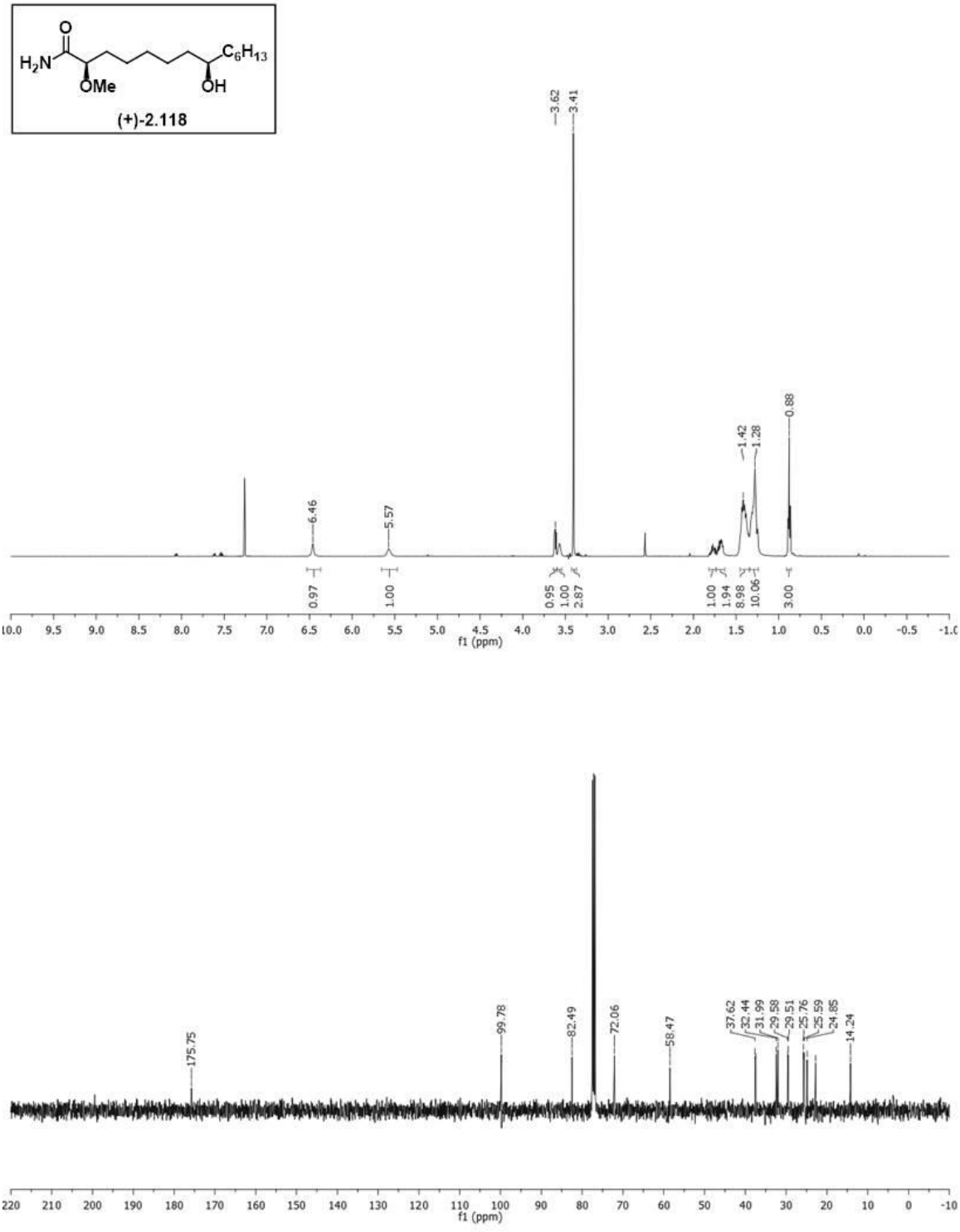
O
H2N
C6H13
OMe
OH
(+)-2.118
3.62
3.41
1.42
1.28
0.88
6.46
5.57
0.97
1.00
0.95
1.00
2.87
1.00
1.94
8.98
10.06
3.00
f1 (ppm)
175.75
99.78
82.49
72.06
58.47
37.62
32.44
31.99
29.58
29.51
25.76
25.59
24.85
14.24
f1 (ppm)

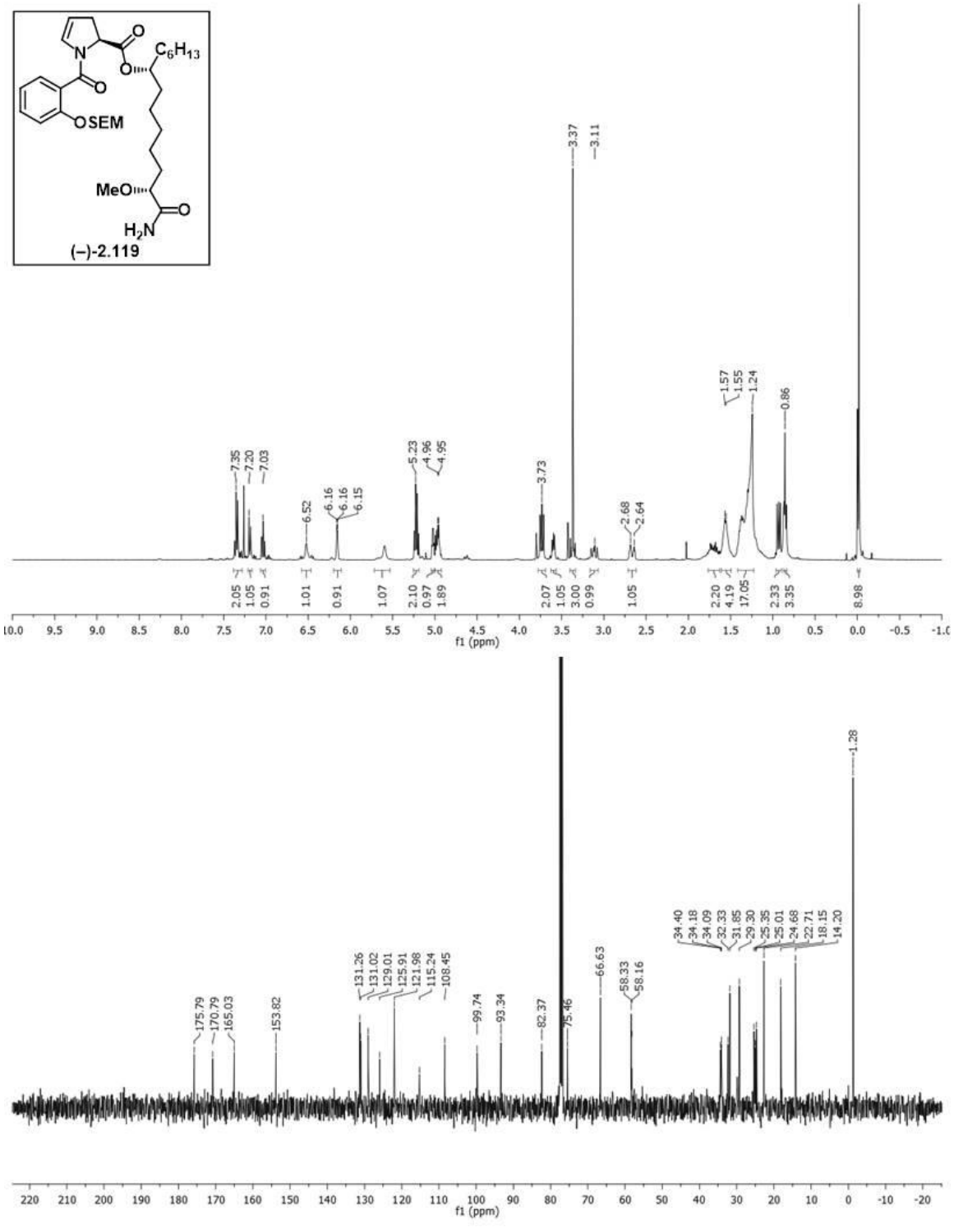
OSEM
MeO
C_6H_{13}
H_2N
(–)-2.119
f1 (ppm)
f1 (ppm)

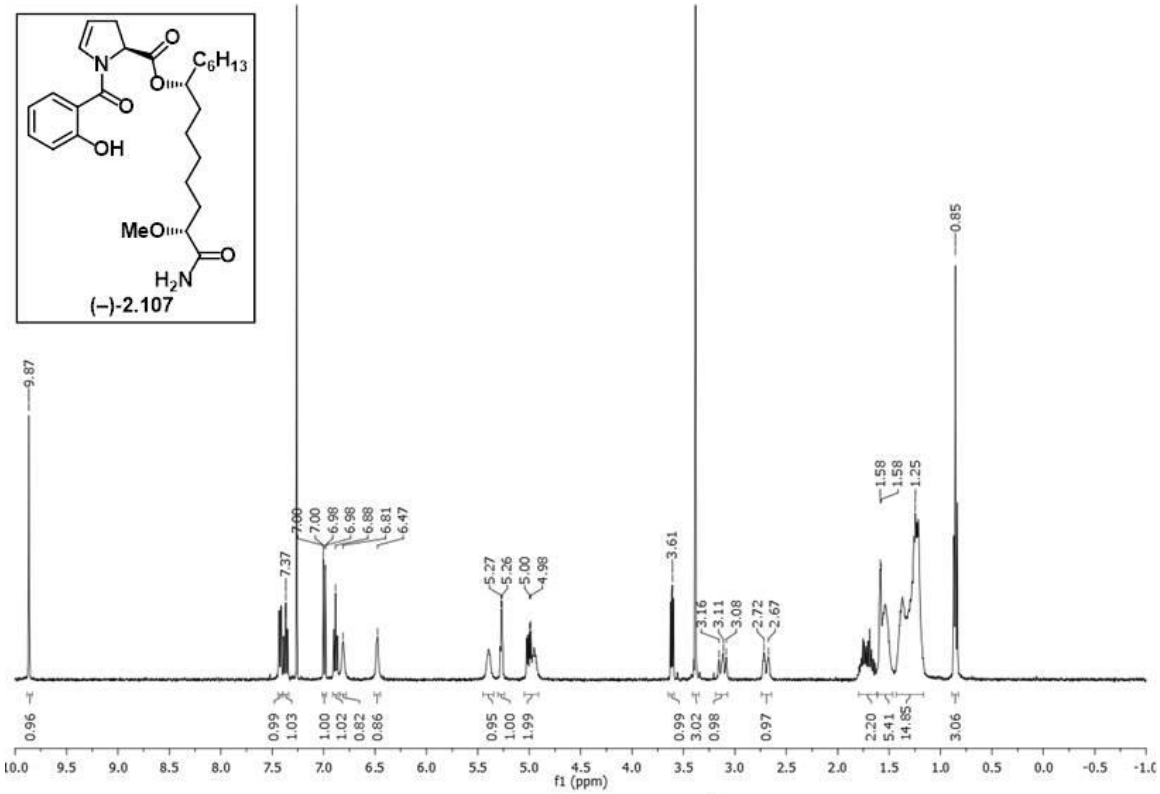
(–)-2.107
f1 (ppm)

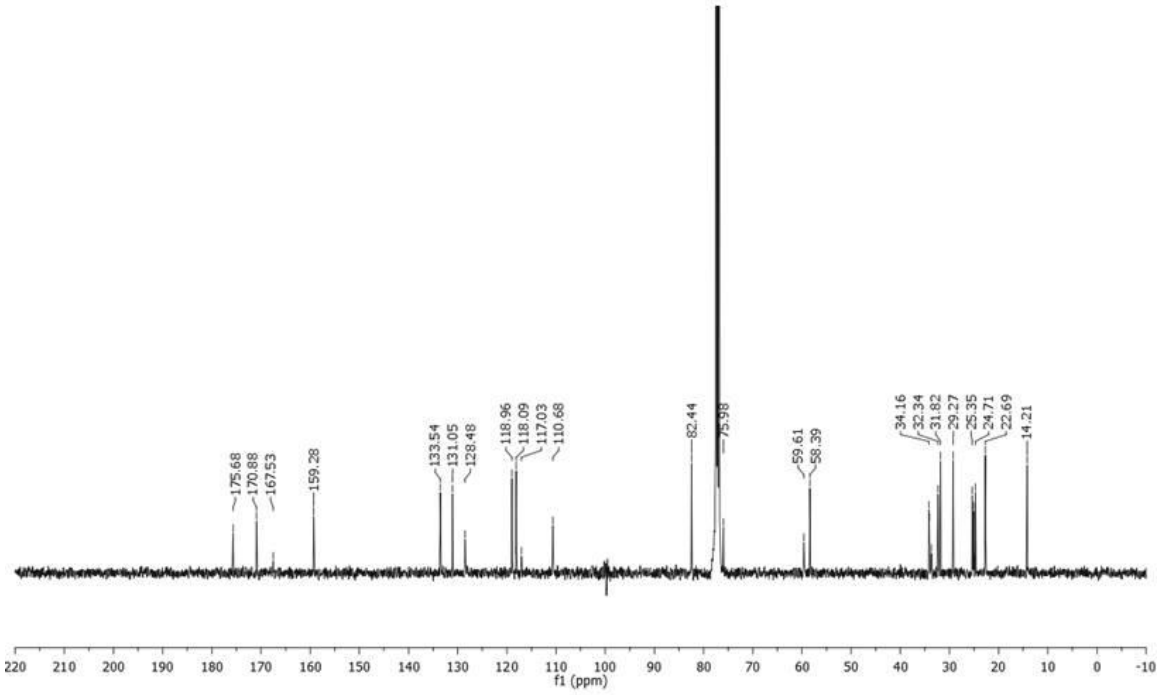
f1 (ppm)

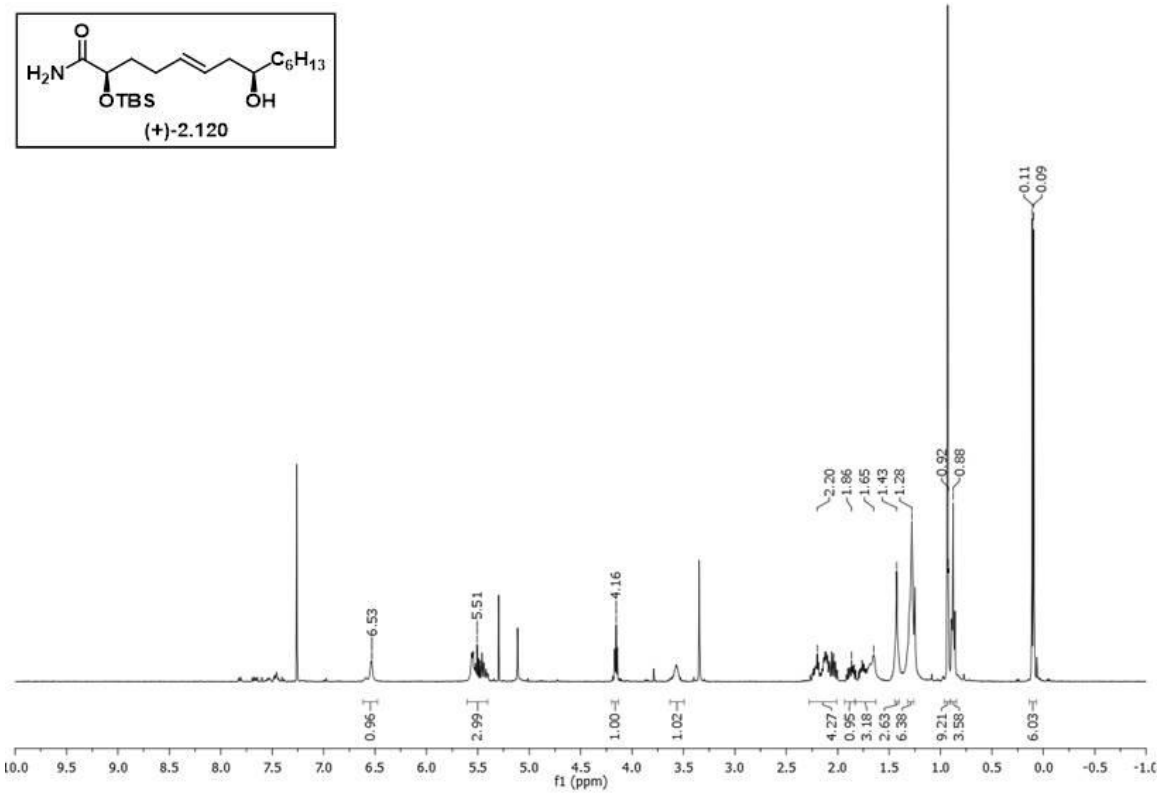
O
H2N
C6H13
OTBS
OH
(+)-2.120
0.11
0.09
2.20
1.86
1.65
1.43
1.28
0.92
0.88
6.53
5.51
4.16
0.96
2.99
1.00
1.02
4.27
0.95
3.18
2.63
6.38
9.21
3.58
6.03
f1 (ppm)

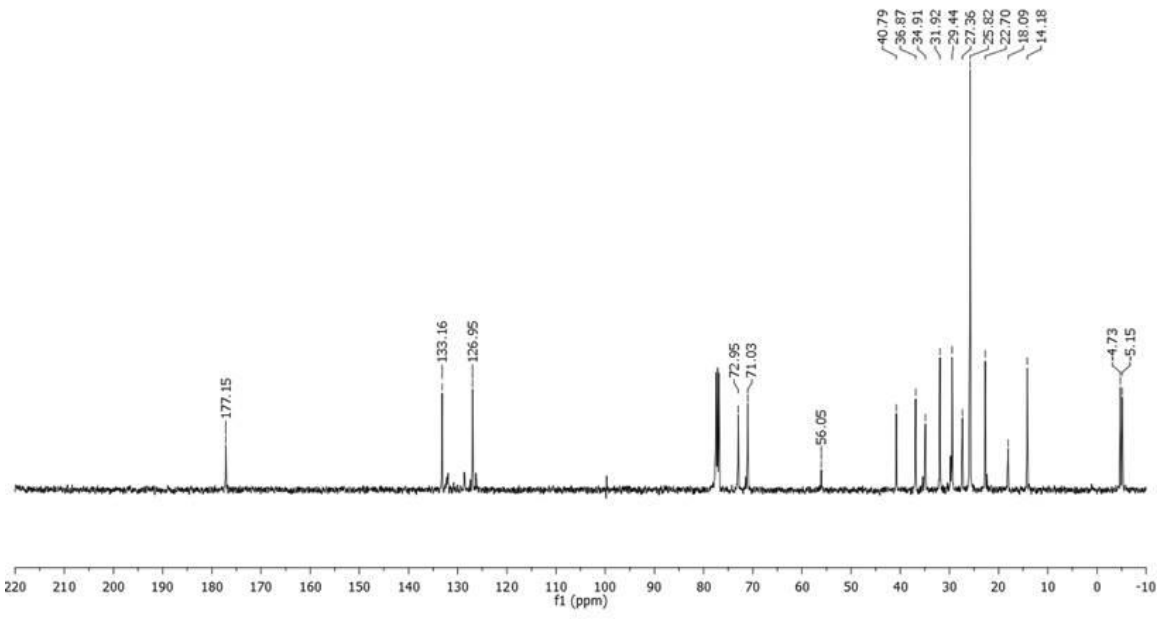
40.79
36.87
34.91
31.92
29.44
27.36
25.82
22.70
18.09
14.18
177.15
133.16
126.95
72.95
71.03
56.05
-4.73
-5.15
f1 (ppm)

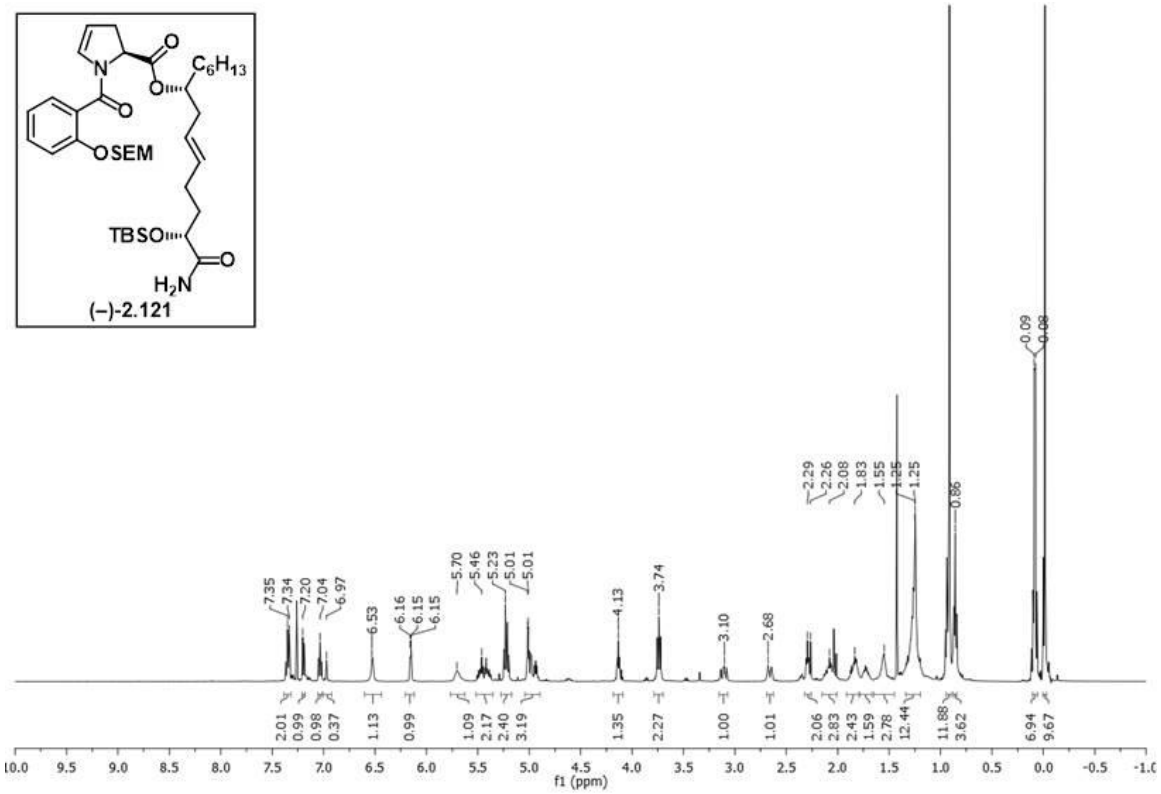
OSEM
TBSO
H_2N
C_6H_{13}
(−)-2.121
f1 (ppm)

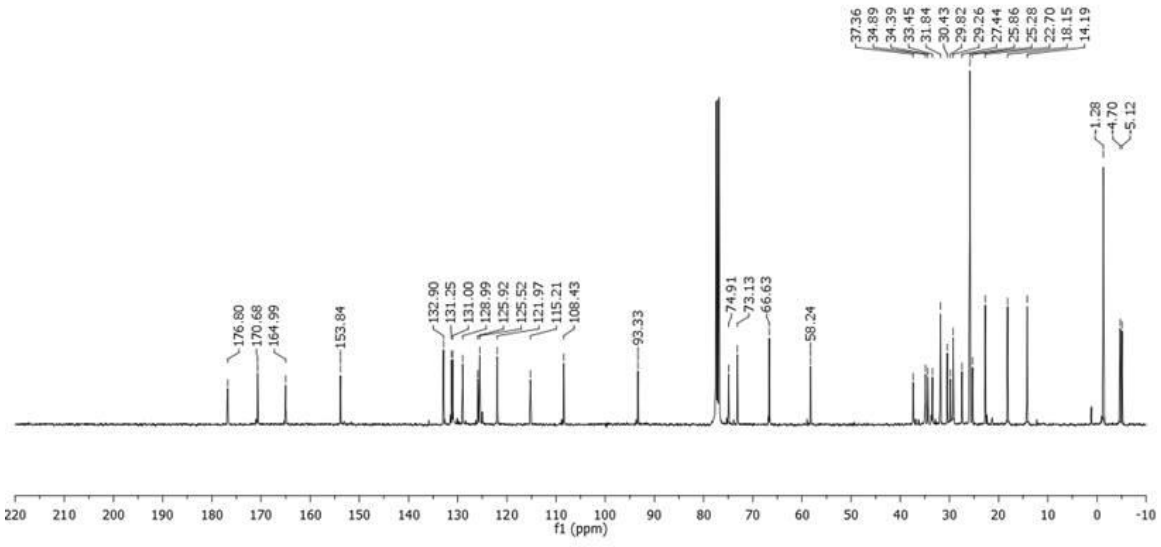
f1 (ppm)

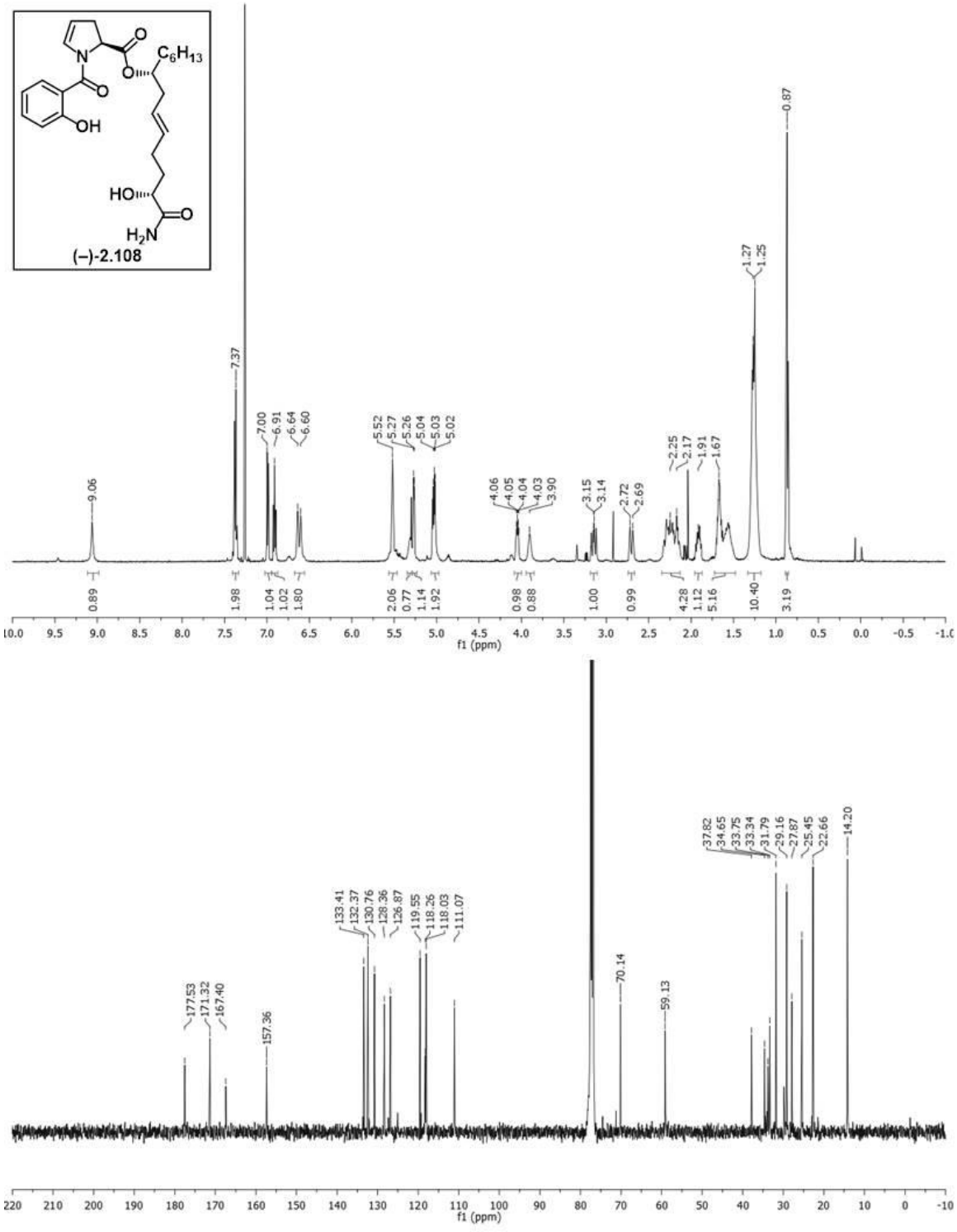
(–)-2.108
f1 (ppm)
f1 (ppm)

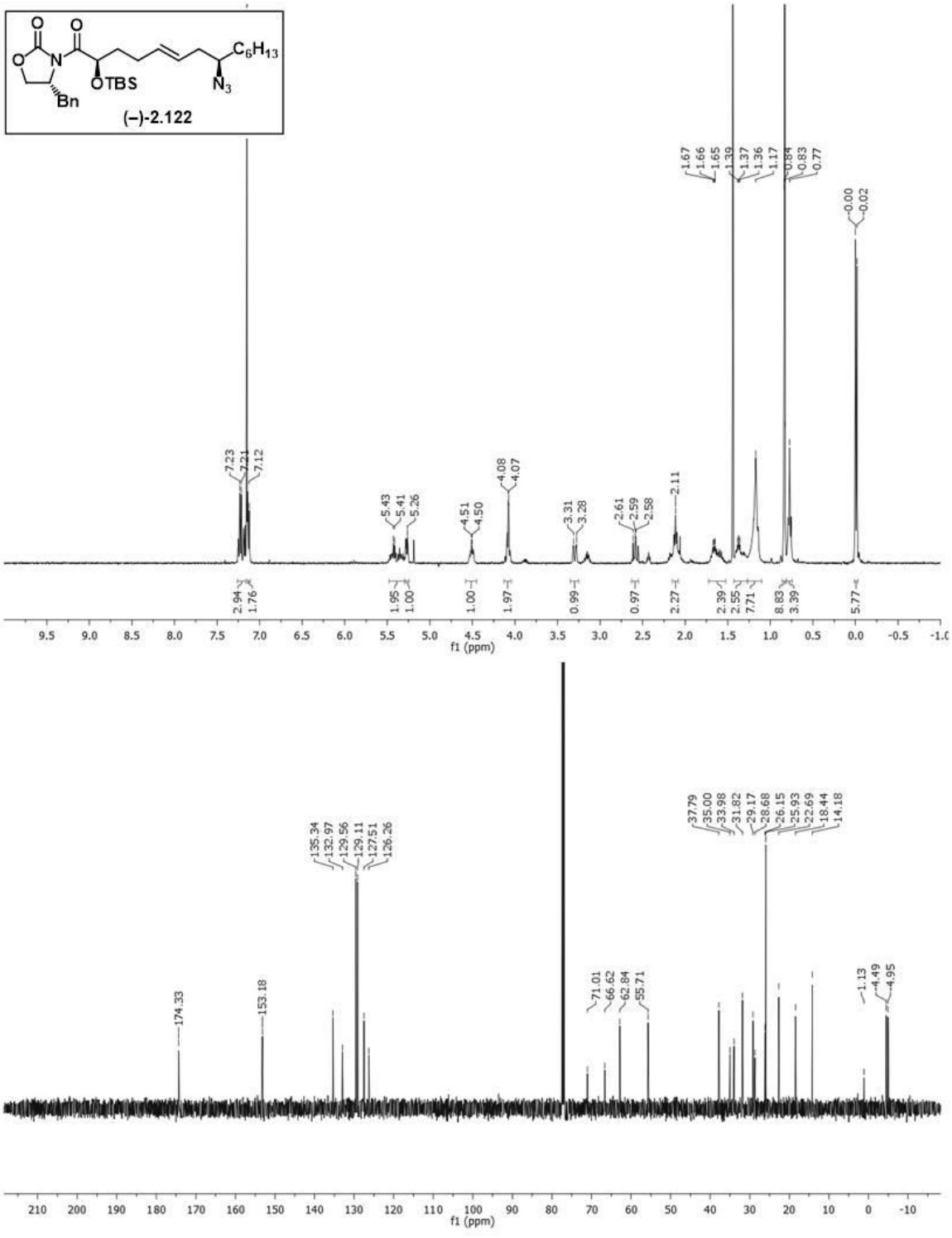
(–)-2.122
f1 (ppm)
f1 (ppm)

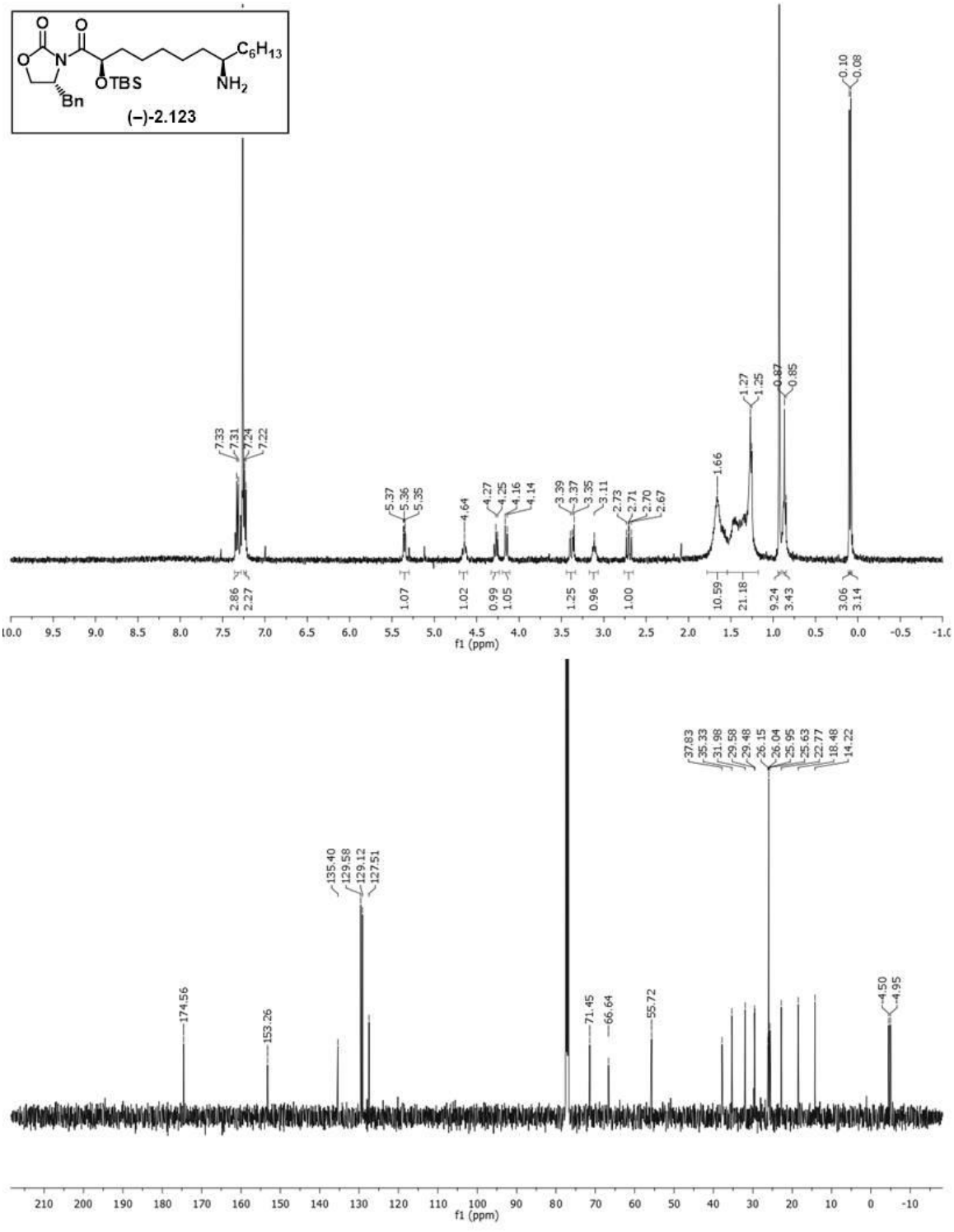
(–)-2.123
f1 (ppm)
f1 (ppm)

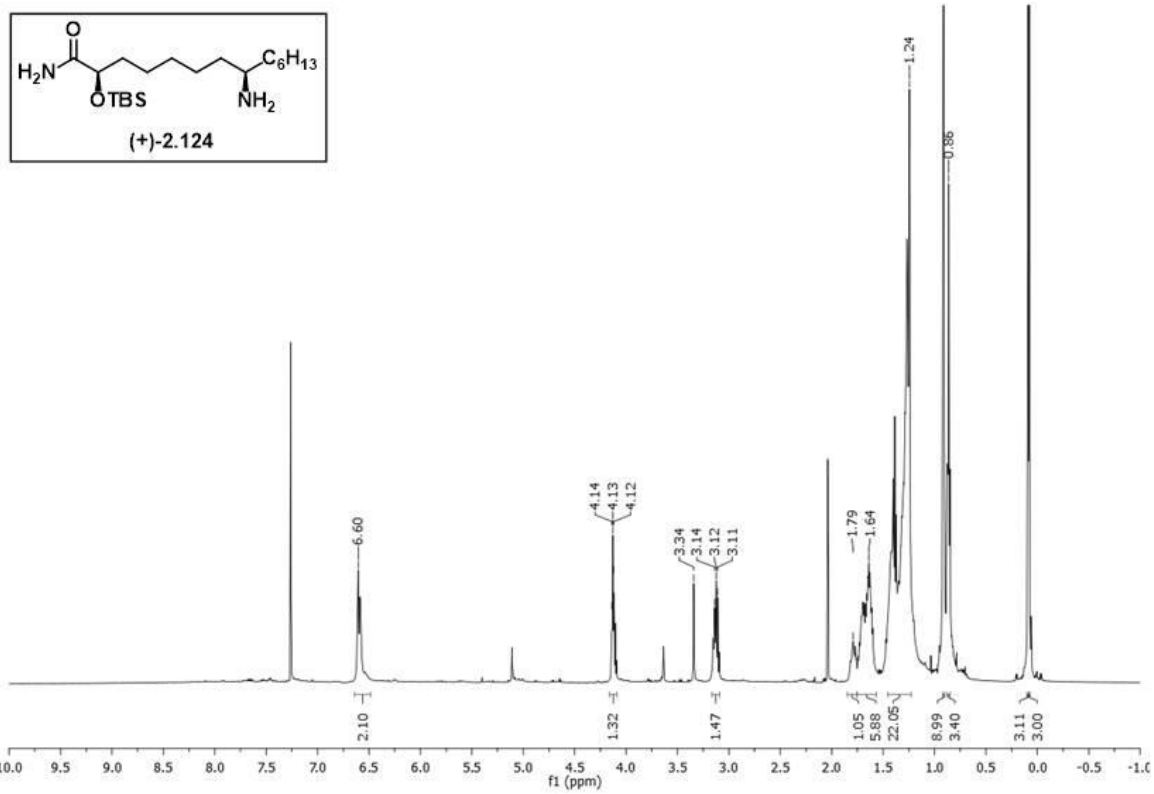
O
H2N
C6H13
OTBS
NH2
(+)-2.124
6.60
4.14
4.13
4.12
3.34
3.14
3.12
3.11
1.79
1.64
1.24
0.86
2.10
1.32
1.47
1.05
5.88
22.05
8.99
3.40
3.11
3.00
f1 (ppm)

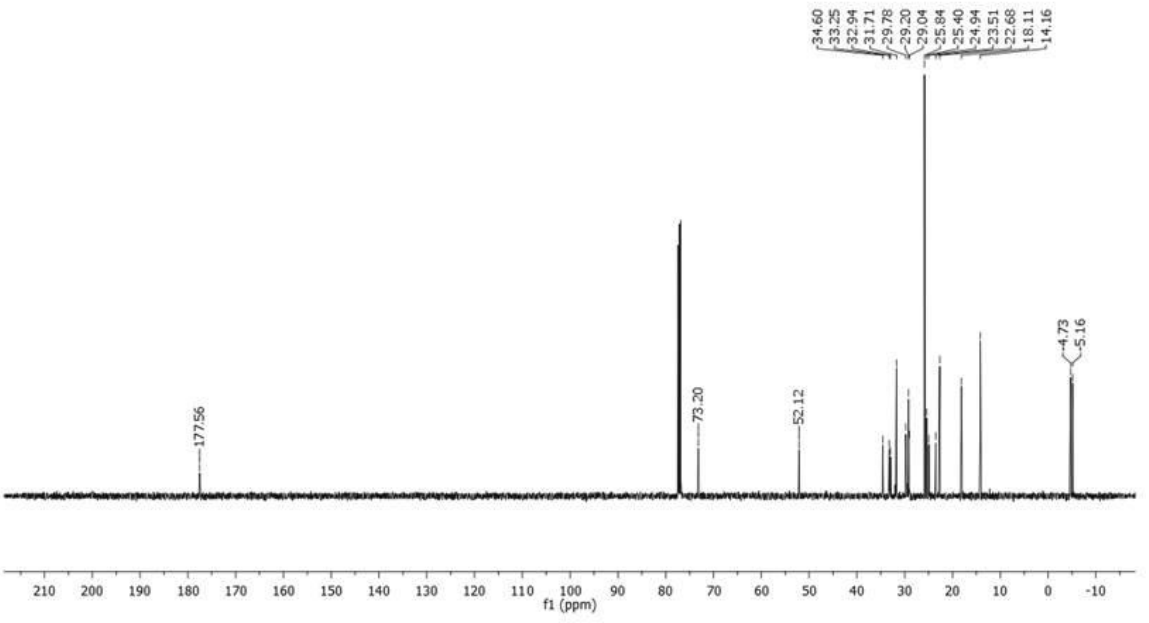
34.60
33.25
32.94
31.71
29.78
29.20
29.04
25.84
25.40
24.94
23.51
22.68
18.11
14.16
177.56
73.20
52.12
4.73
5.16
f1 (ppm)

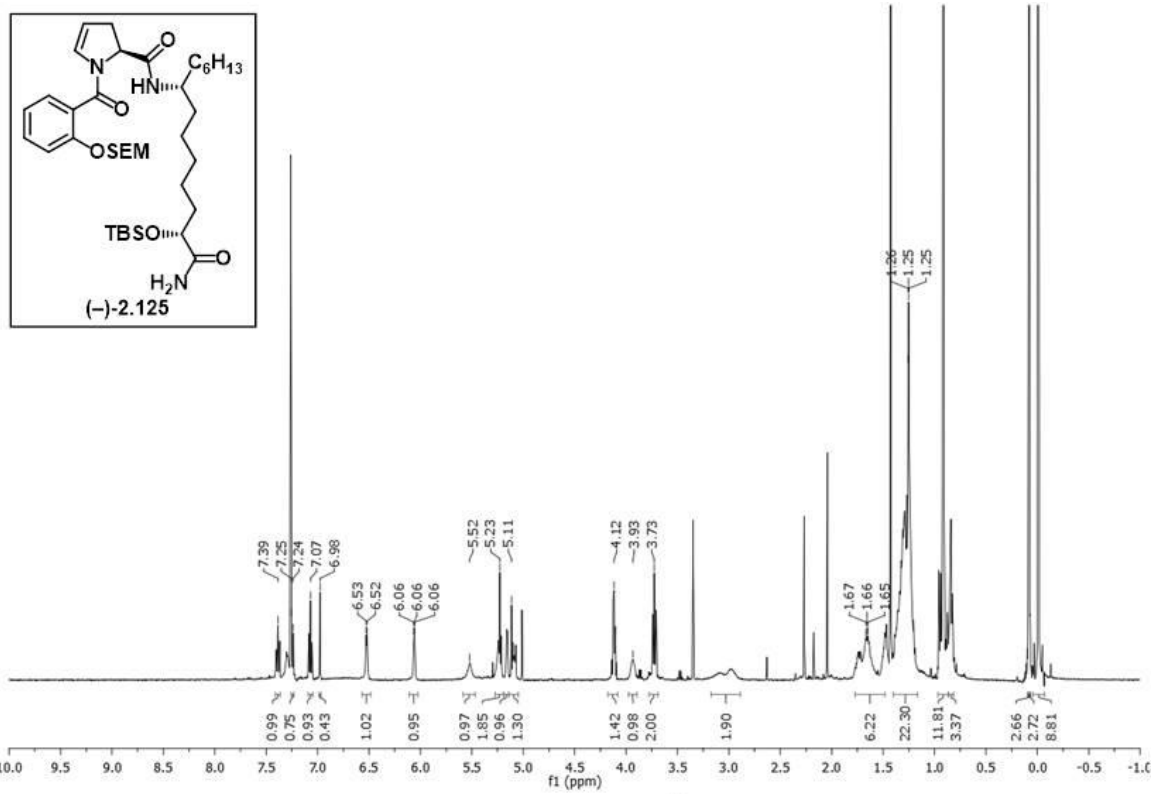
OSEM
TBSO
HN
C6H13
H2N
(–)-2.125
7.39
7.25
7.24
7.07
6.98
6.53
6.52
6.06
6.06
6.06
5.52
5.23
5.11
4.12
3.93
3.73
1.67
1.66
1.65
1.26
1.25
1.25
0.99
0.75
0.93
0.43
1.02
0.95
0.97
1.85
0.96
1.30
1.42
0.98
2.00
1.90
6.22
22.30
11.81
3.37
2.66
2.72
8.81
f1 (ppm)

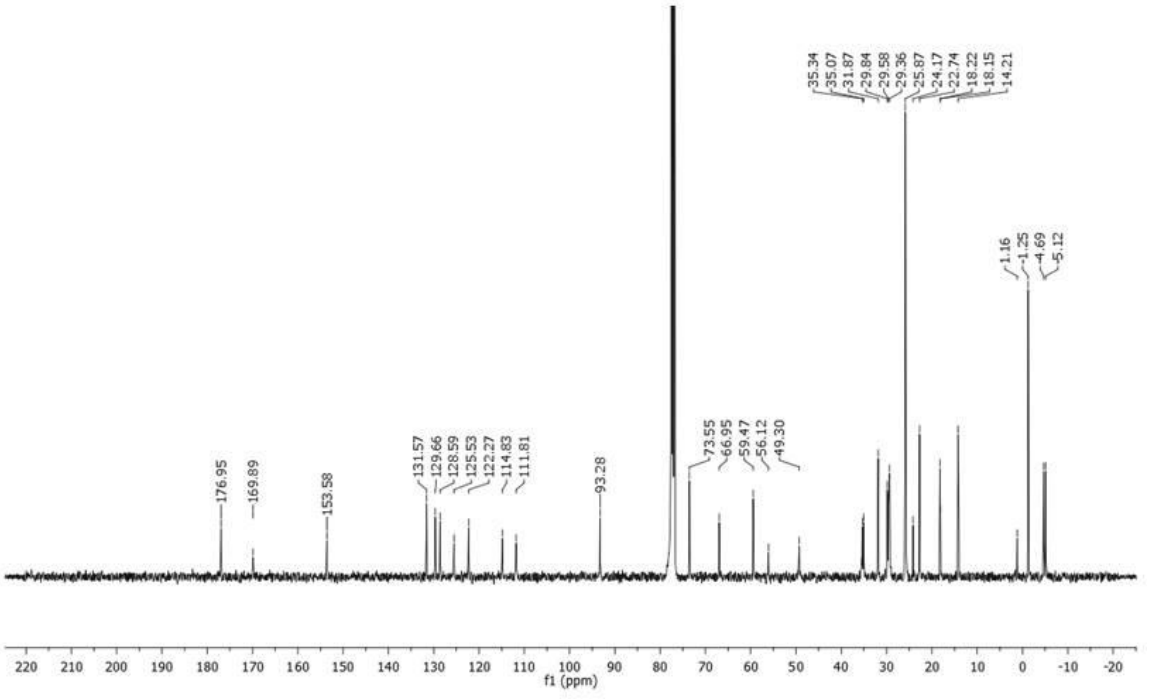
176.95
169.89
153.58
131.57
129.66
128.59
125.53
122.27
114.83
111.81
93.28
73.55
66.95
59.47
56.12
49.30
35.34
35.07
31.87
29.84
29.58
29.36
25.87
24.17
22.74
18.22
18.15
14.21
1.16
1.25
4.69
5.12
f1 (ppm)

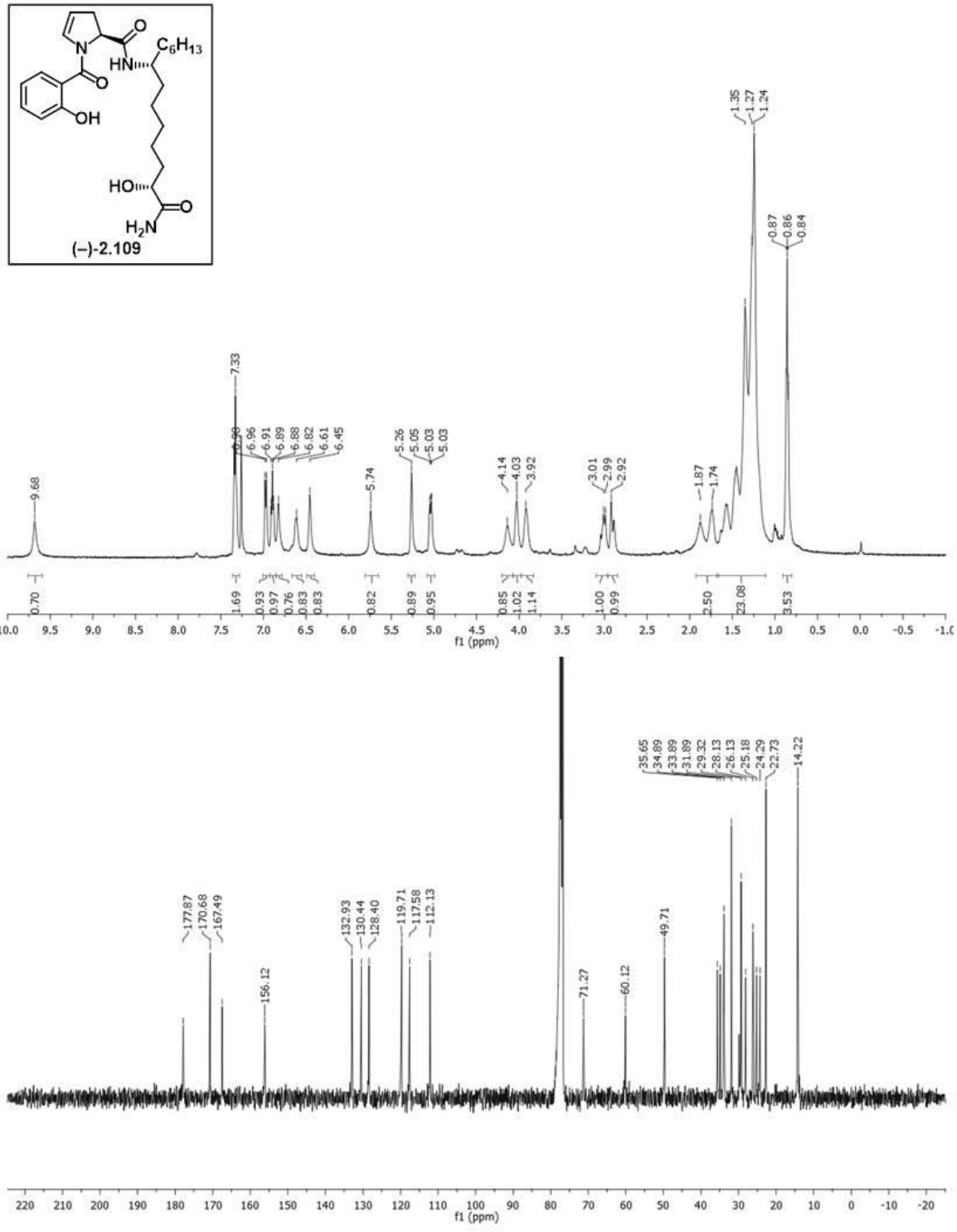
(–)-2.109
f1 (ppm)
f1 (ppm)

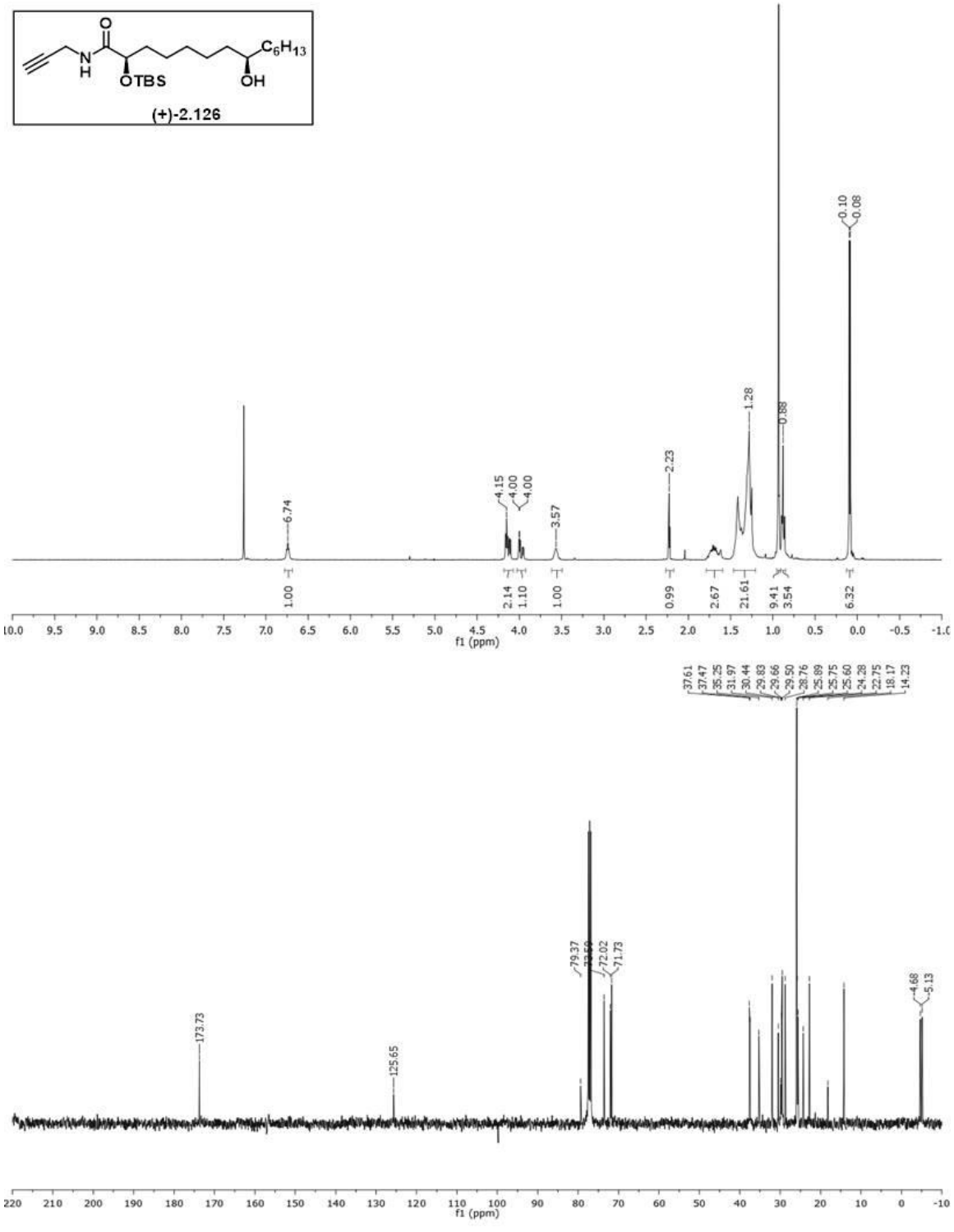
(+)-2.126
f1 (ppm)
f1 (ppm)

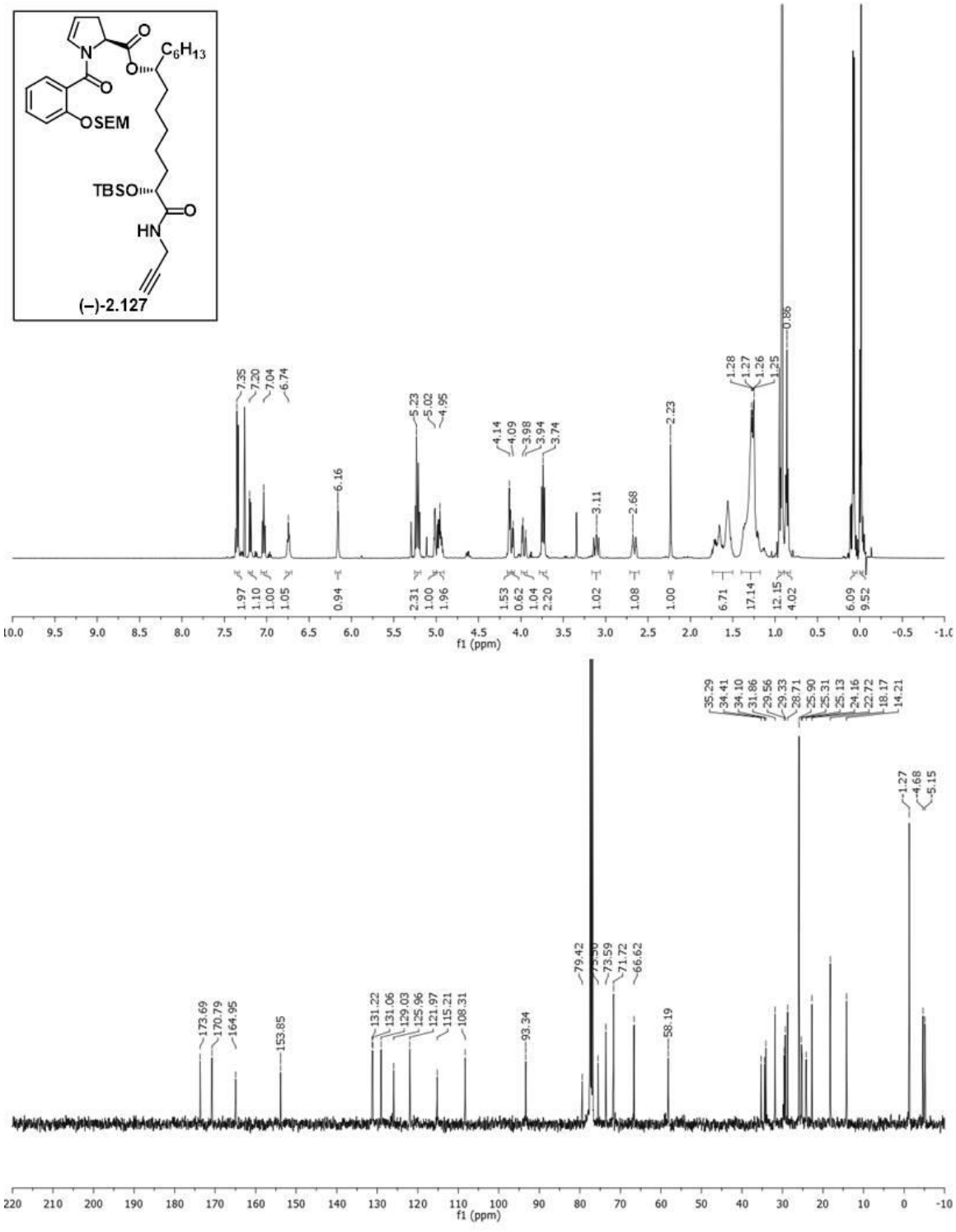
(–)-2.127
f1 (ppm)
f1 (ppm)

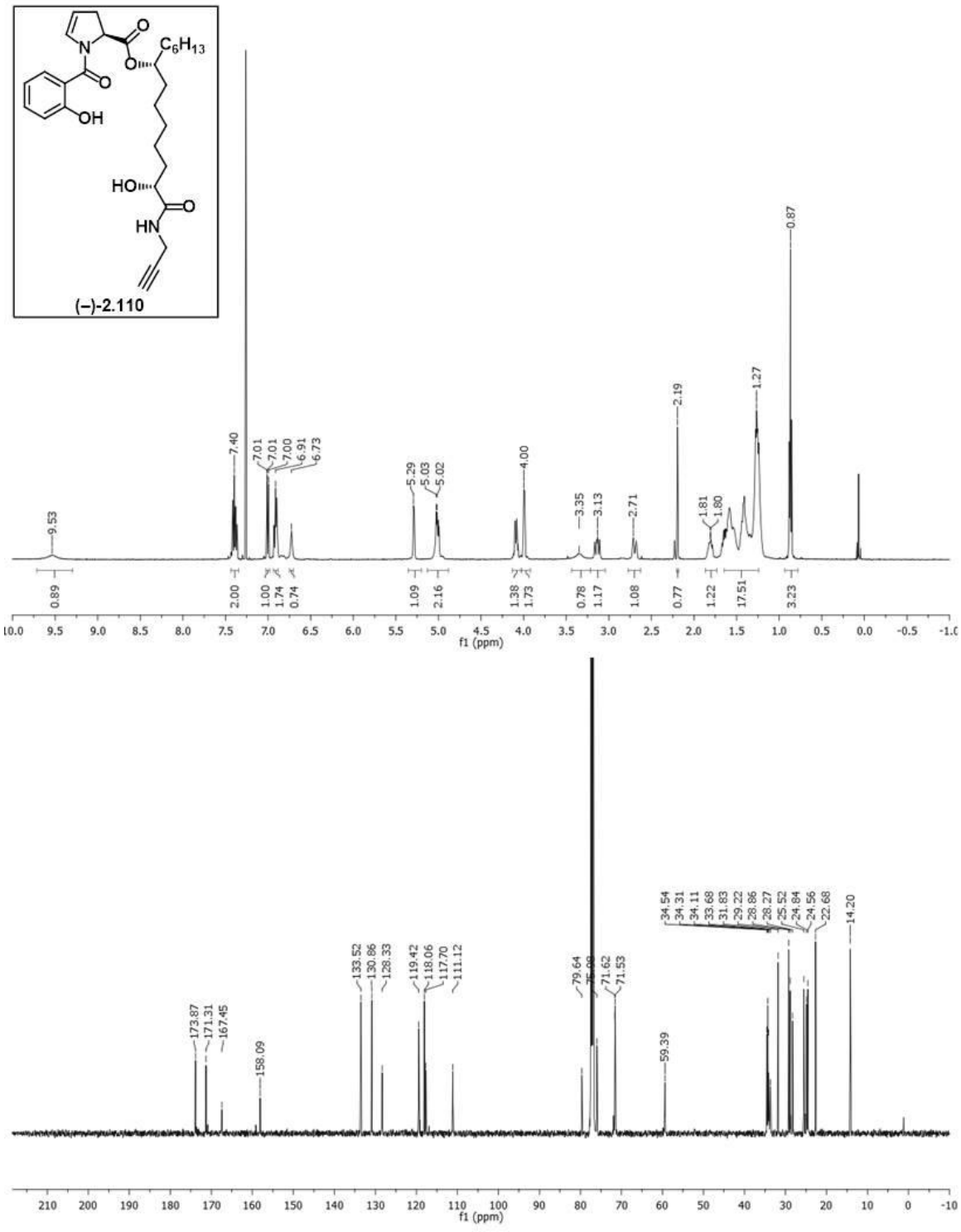
(–)-2.110
f1 (ppm)
f1 (ppm)

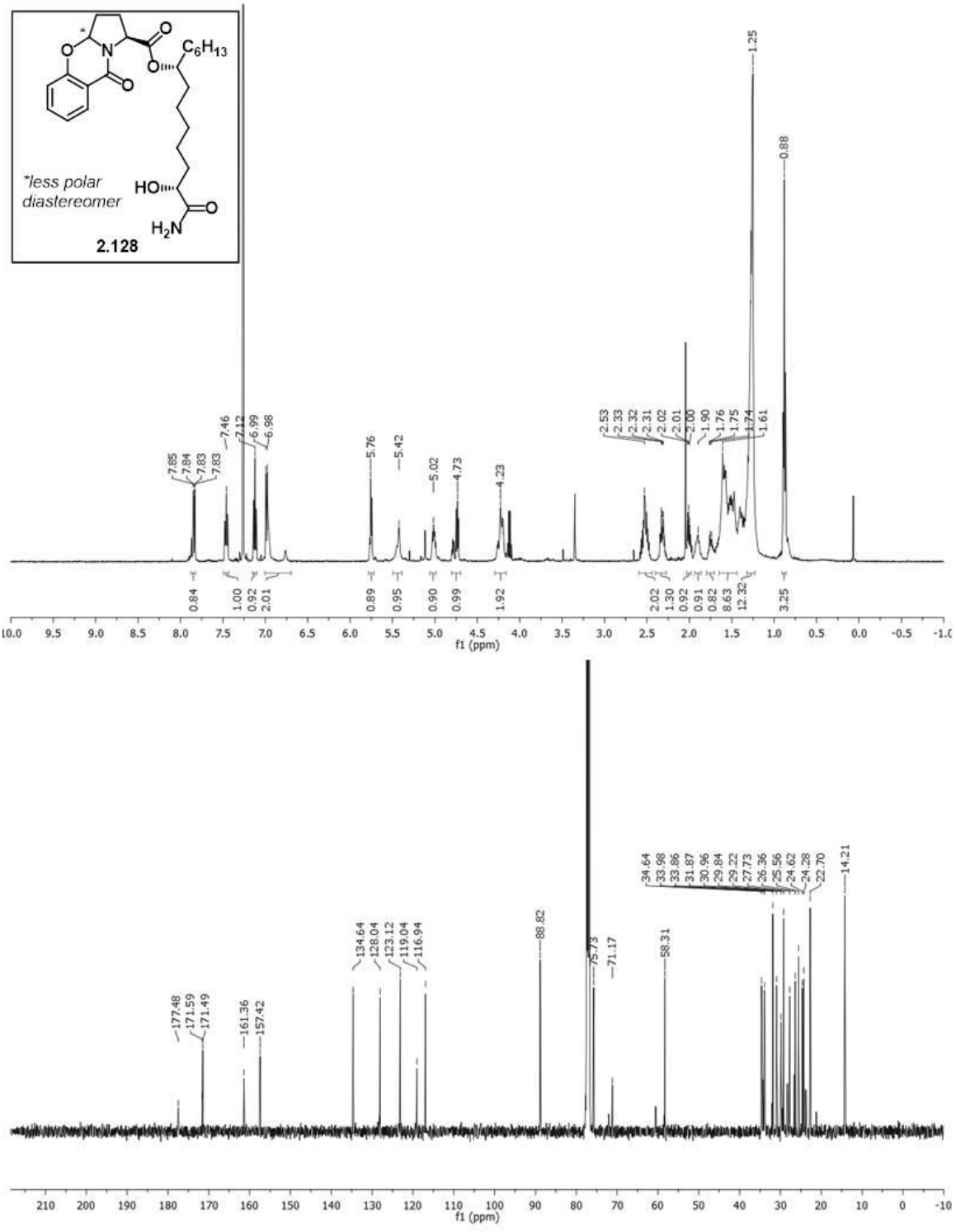
*less polar
diastereomer
2.128
f1 (ppm)
f1 (ppm)

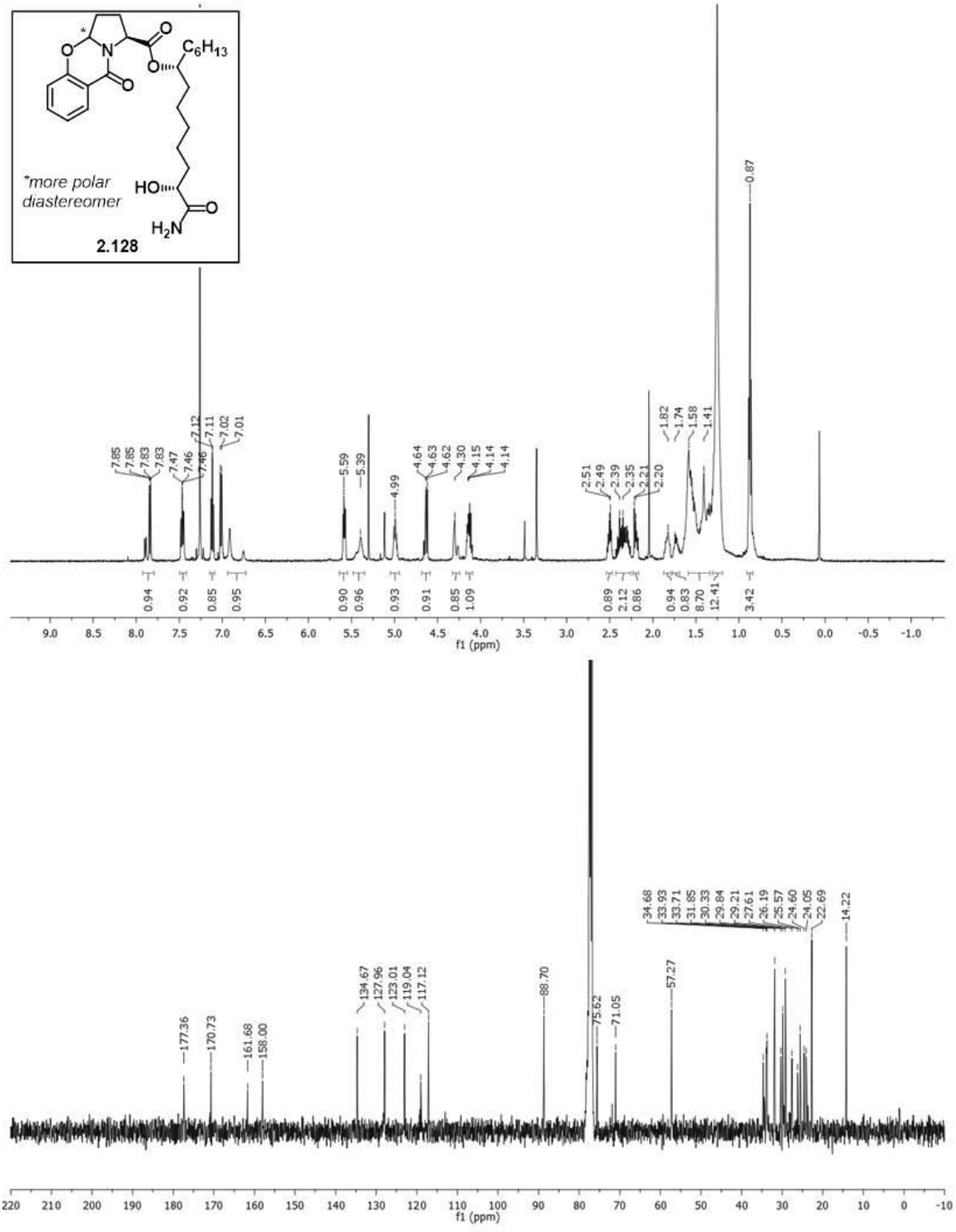
*more polar
diastereomer
2.128
f1 (ppm)
f1 (ppm)

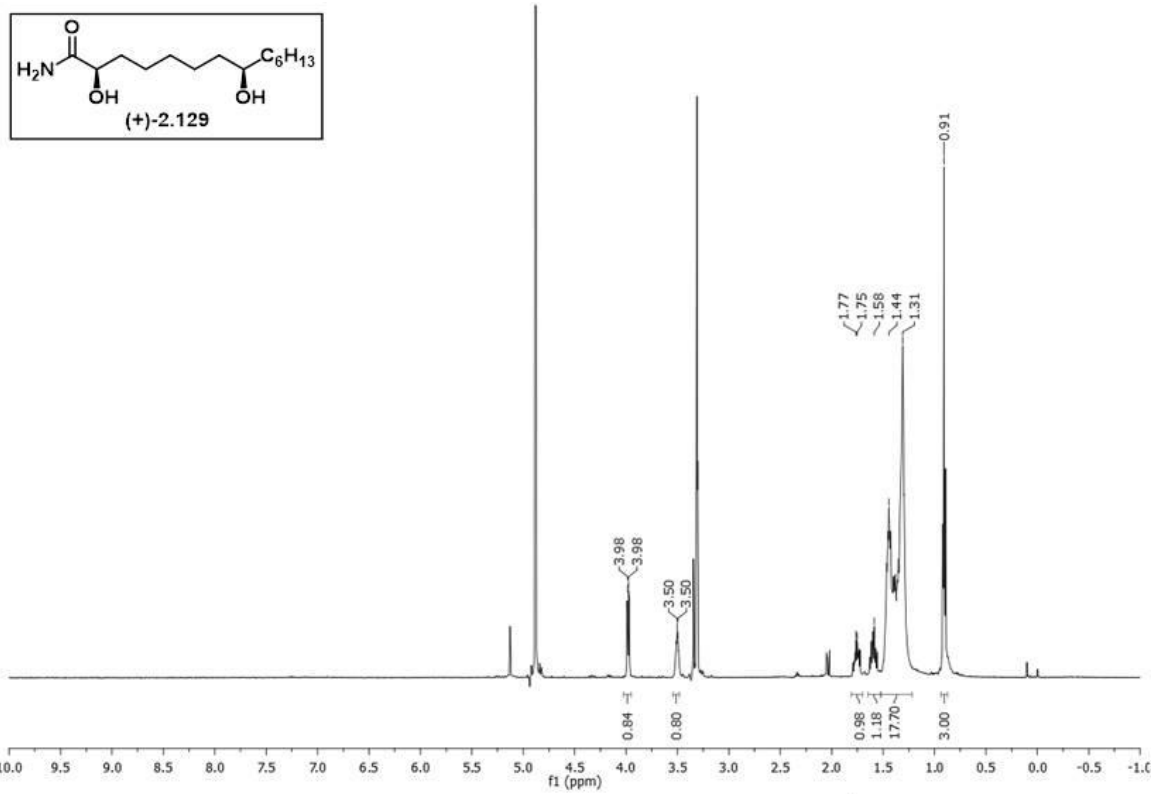
O
H2N
C6H13
OH
OH
(+)-2.129
3.98
3.98
3.50
3.50
1.77
1.75
1.58
1.44
1.31
0.91
0.84
0.80
0.98
1.18
17.70
3.00
f1 (ppm)

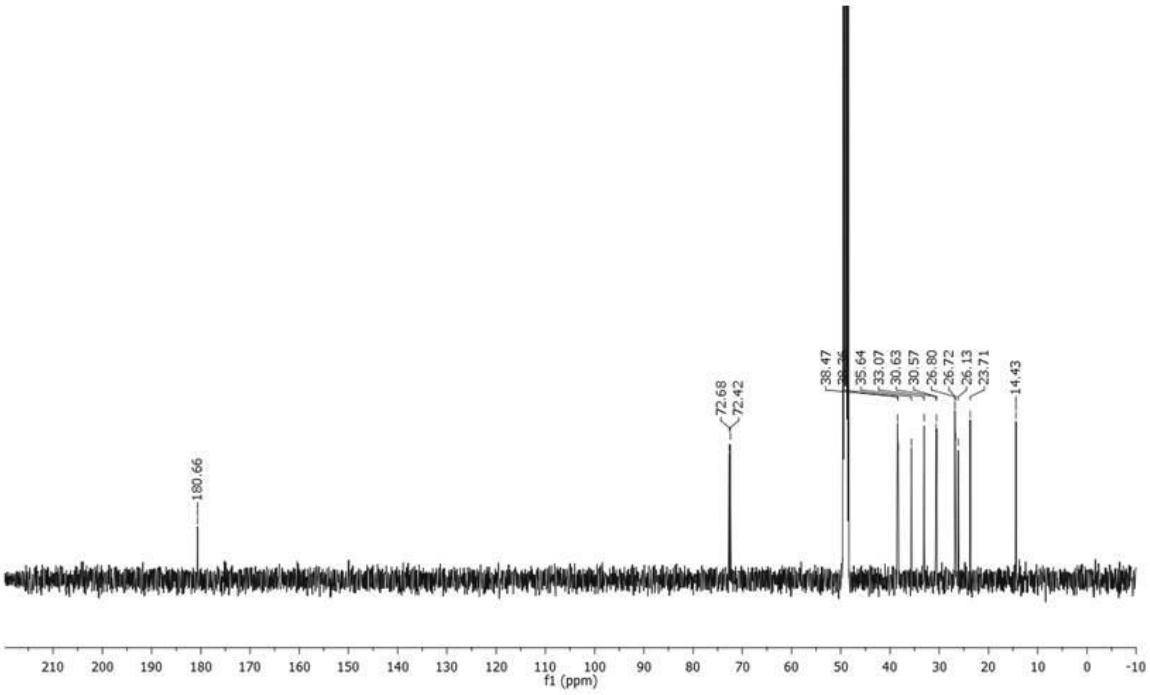
180.66
72.68
72.42
38.47
35.64
33.07
30.63
30.57
26.80
26.72
26.13
23.71
14.43
f1 (ppm)

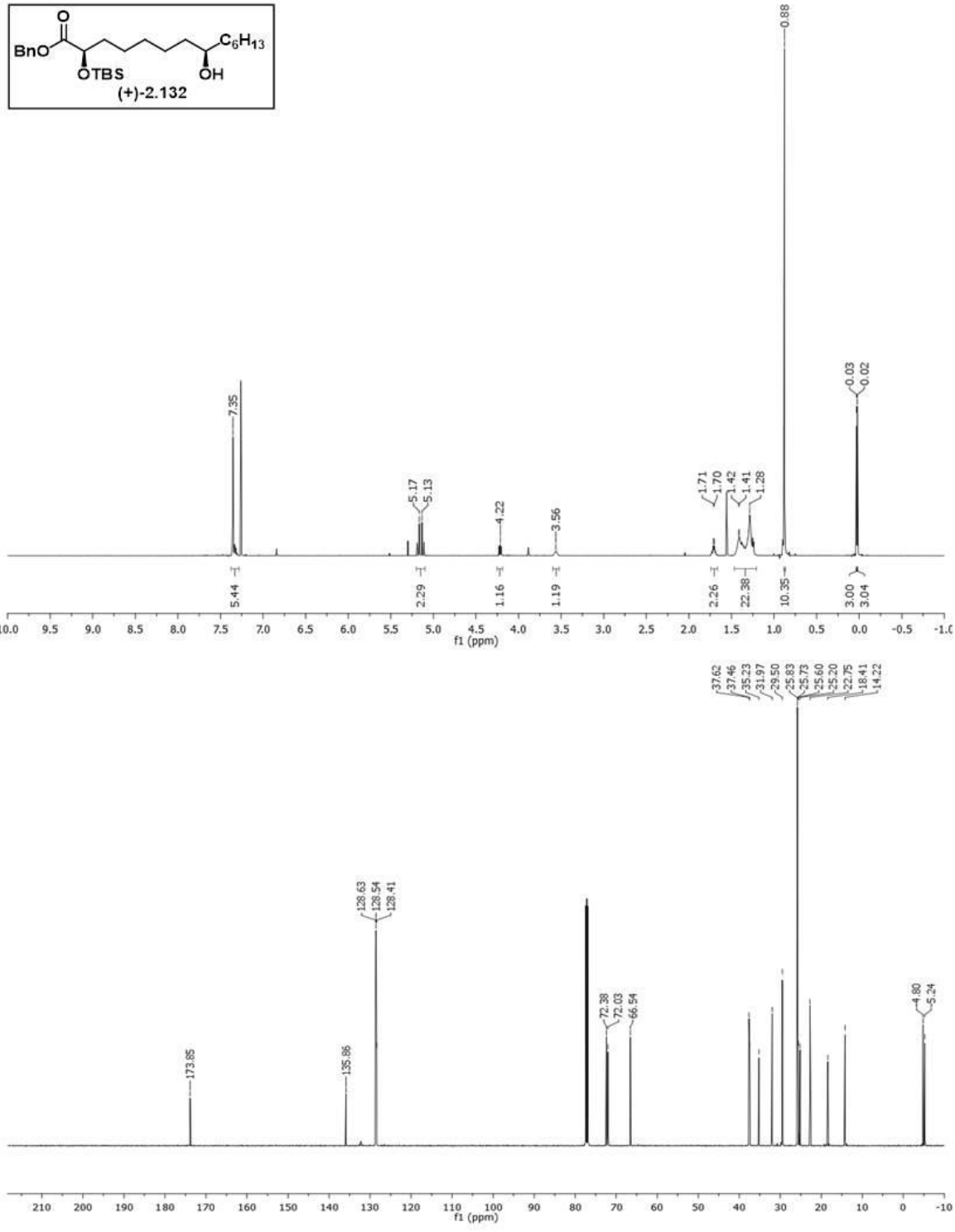
BnO
O
OTBS
OH
C6H13
(+)-2.132
0.88
7.35
5.17
5.13
4.22
3.56
1.71
1.70
1.42
1.41
1.28
0.03
0.02
5.44
2.29
1.16
1.19
2.26
22.38
10.35
3.00
3.04
f1 (ppm)
37.62
37.46
35.23
31.97
29.50
25.83
25.73
25.60
25.20
22.75
18.41
14.22
128.63
128.54
128.41
173.85
135.86
72.38
72.03
66.54
14.80
5.24
f1 (ppm)

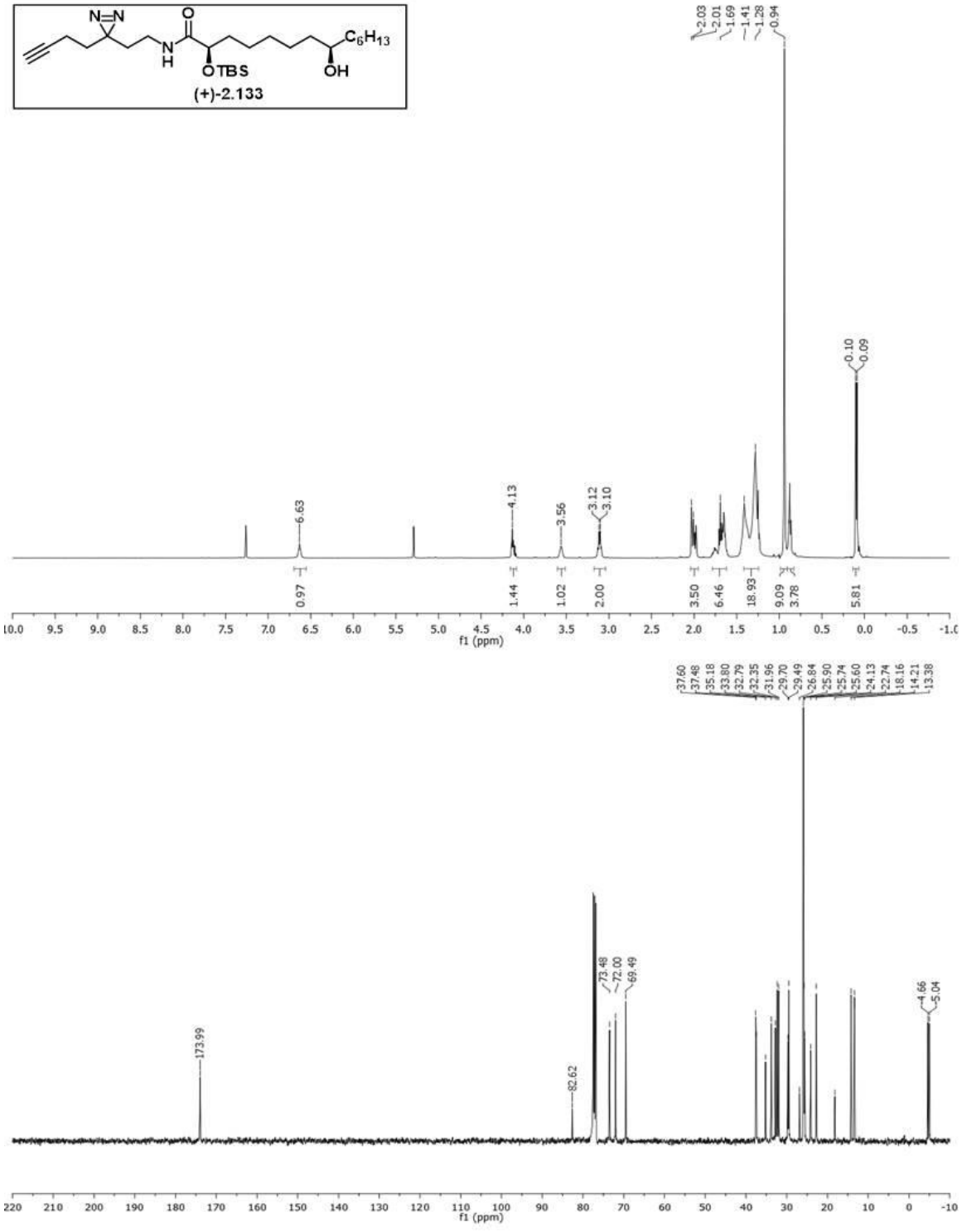
(+)-2.133
f1 (ppm)
f1 (ppm)

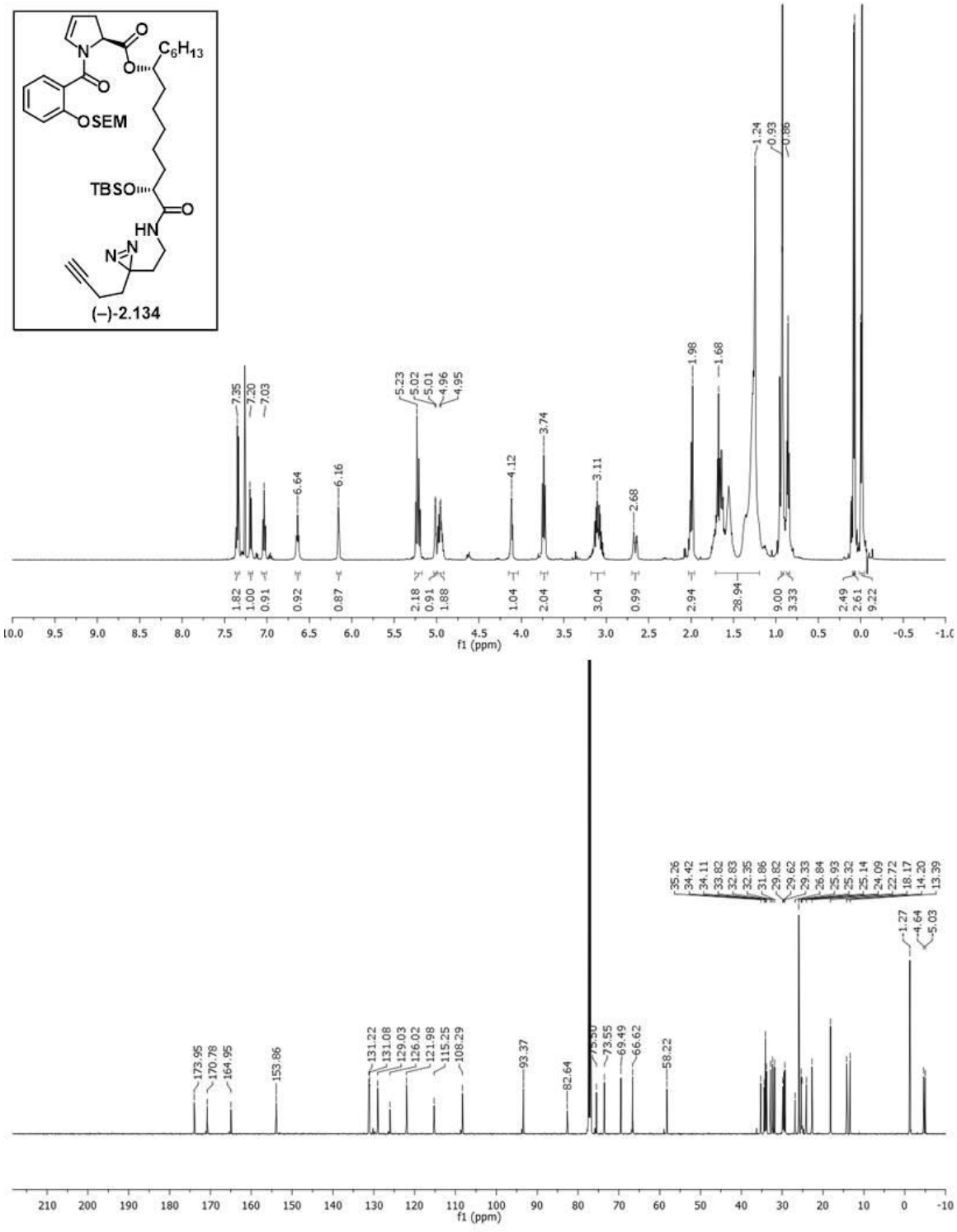
OSEM
TBSO
HN
N
C6H13
(–)-2.134
7.35
7.20
7.03
6.64
6.16
5.23
5.02
5.01
4.96
4.95
4.12
3.74
3.11
2.68
1.98
1.68
1.24
0.93
0.86
1.82
1.00
0.91
0.92
0.87
2.18
0.91
1.88
1.04
2.04
3.04
0.99
2.94
28.94
9.00
3.33
2.49
2.61
9.22
f1 (ppm)
173.95
170.78
164.95
153.86
131.22
131.08
129.03
126.02
121.98
115.25
108.29
93.37
82.64
73.55
69.49
66.62
58.22
35.26
34.42
34.11
33.82
32.83
32.35
31.86
29.82
29.62
29.33
26.84
25.93
25.32
25.14
24.09
22.72
18.17
14.20
13.39
-1.27
-4.64
-5.03
f1 (ppm)

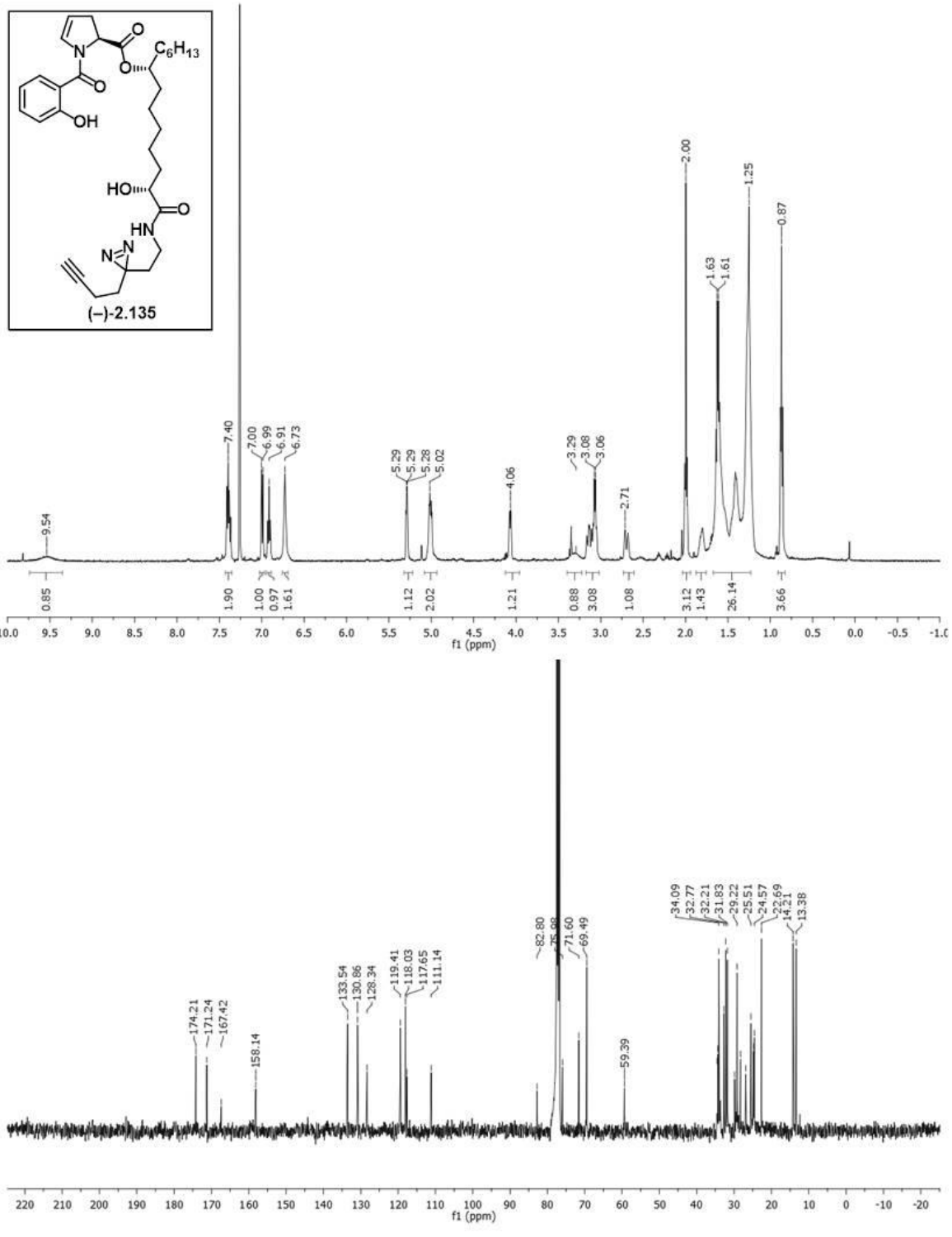
(–)-2.135
f1 (ppm)
f1 (ppm)

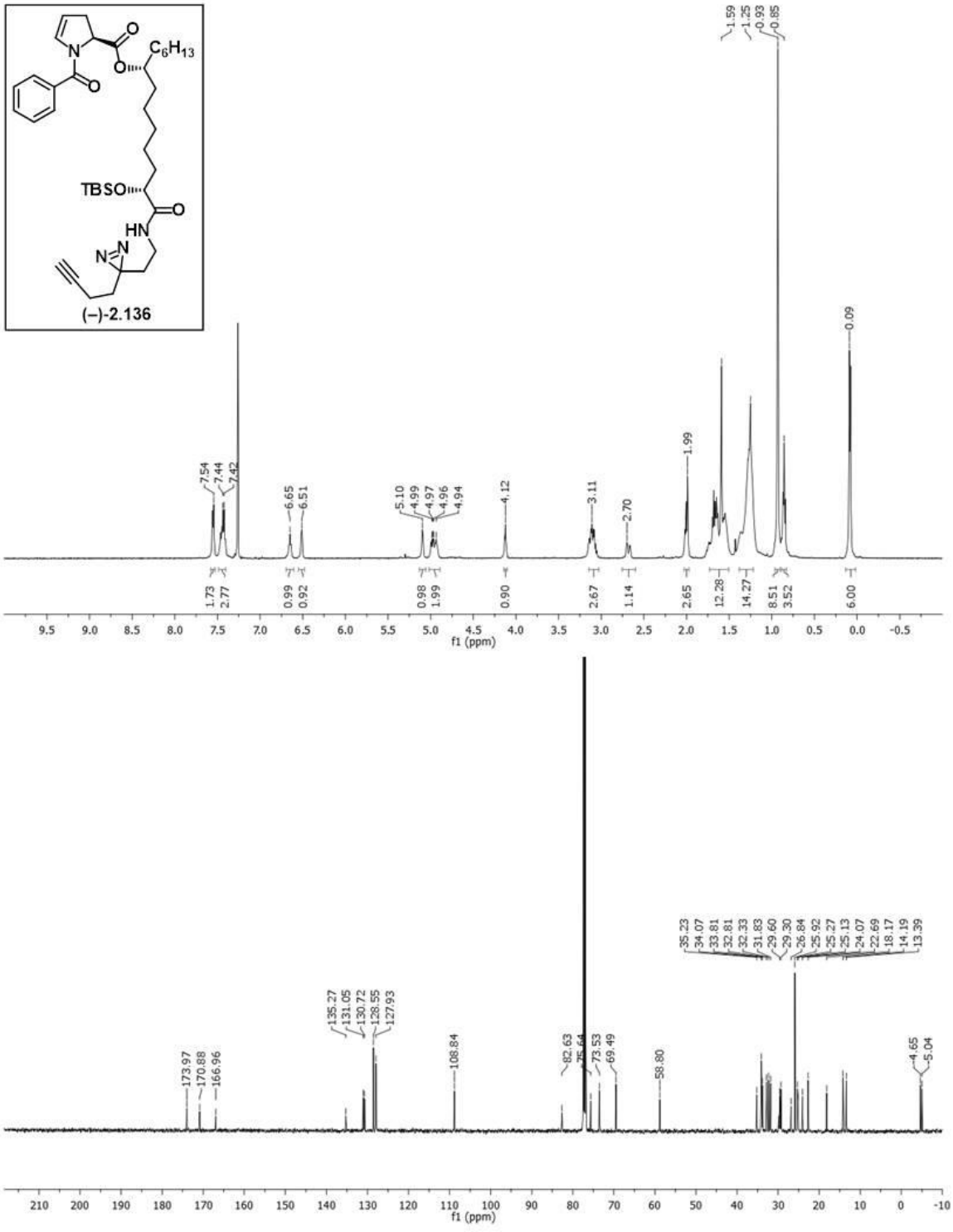
(–)-2.136
f1 (ppm)
f1 (ppm)

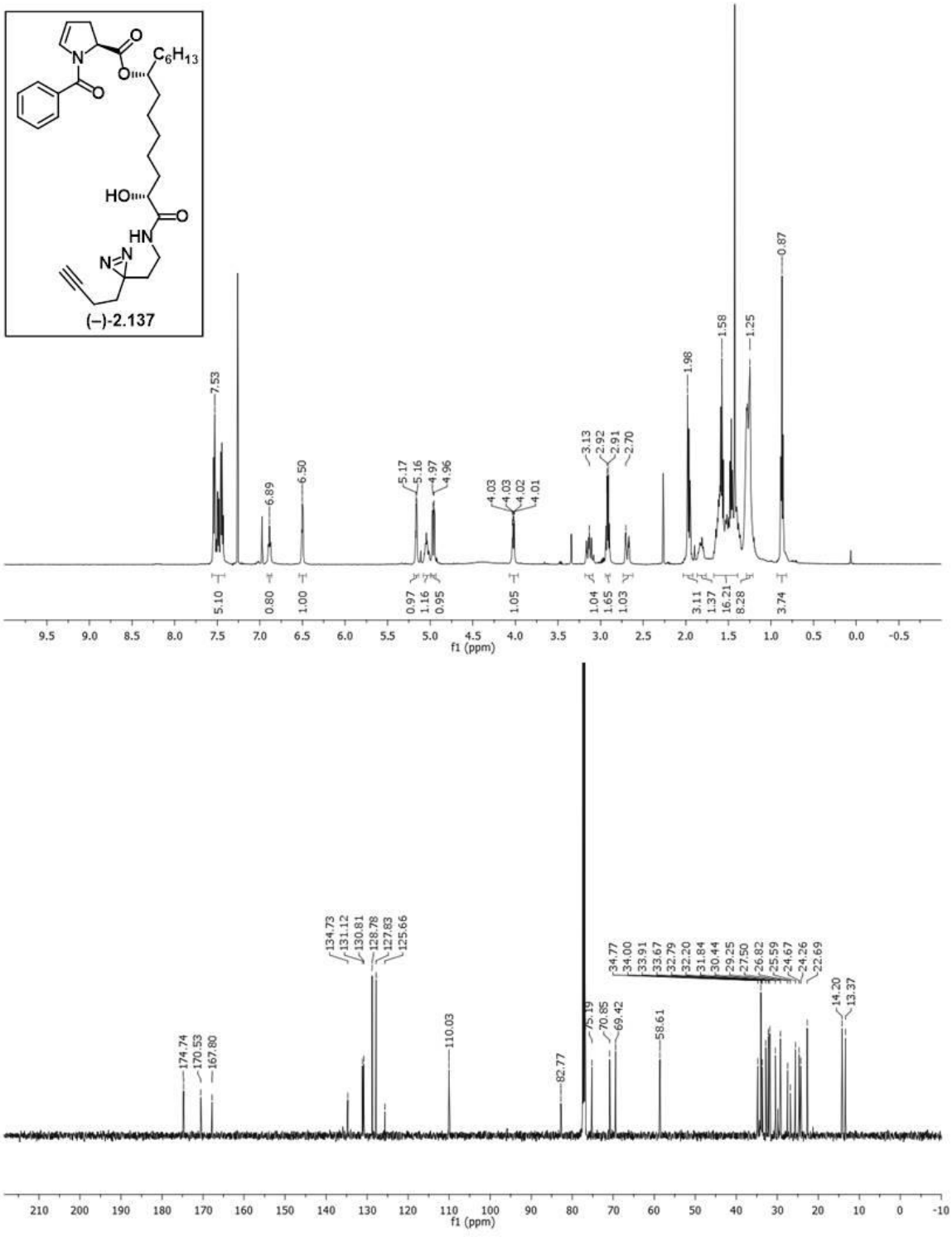
(–)-2.137
7.53
6.89
6.50
5.17
5.16
4.97
4.96
4.03
4.03
4.02
4.01
3.13
2.92
2.91
2.70
1.98
1.58
1.25
0.87
5.10
0.80
1.00
0.97
1.16
0.95
1.05
1.04
1.65
1.03
3.11
1.37
16.21
8.28
3.74
f1 (ppm)
174.74
170.53
167.80
134.73
131.12
130.81
128.78
127.83
125.66
110.03
82.77
75.19
70.85
69.42
58.61
34.77
34.00
33.91
33.67
32.79
32.20
31.84
30.44
29.25
27.50
26.82
25.59
24.67
24.26
22.69
14.20
13.37
f1 (ppm)

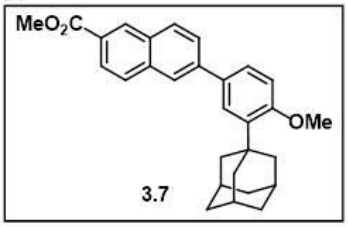
MeO2C
OMe
3.7

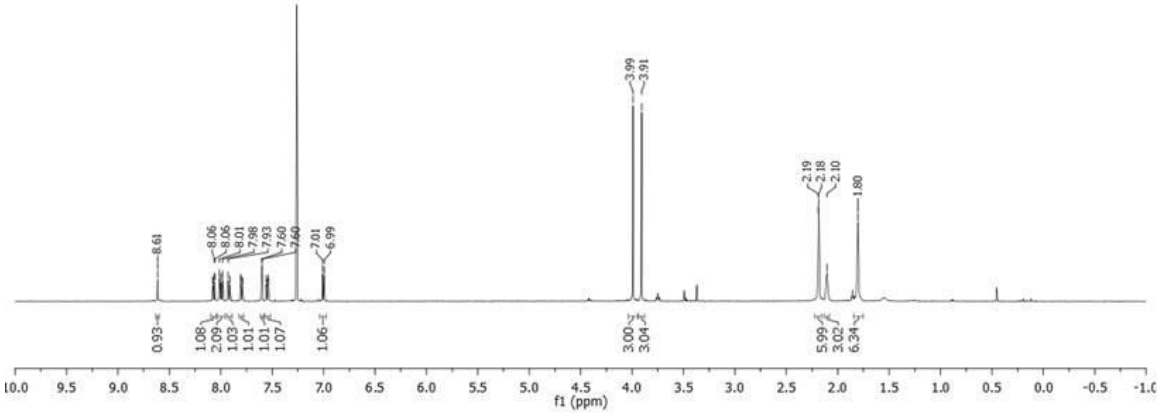
8.61
8.06
8.06
8.01
7.98
7.93
7.60
7.60
7.01
6.99
3.99
3.91
2.19
2.18
2.10
1.80
0.93
1.08
2.09
1.03
1.01
1.01
1.07
1.06
3.00
3.04
5.99
3.02
6.34
f1 (ppm)

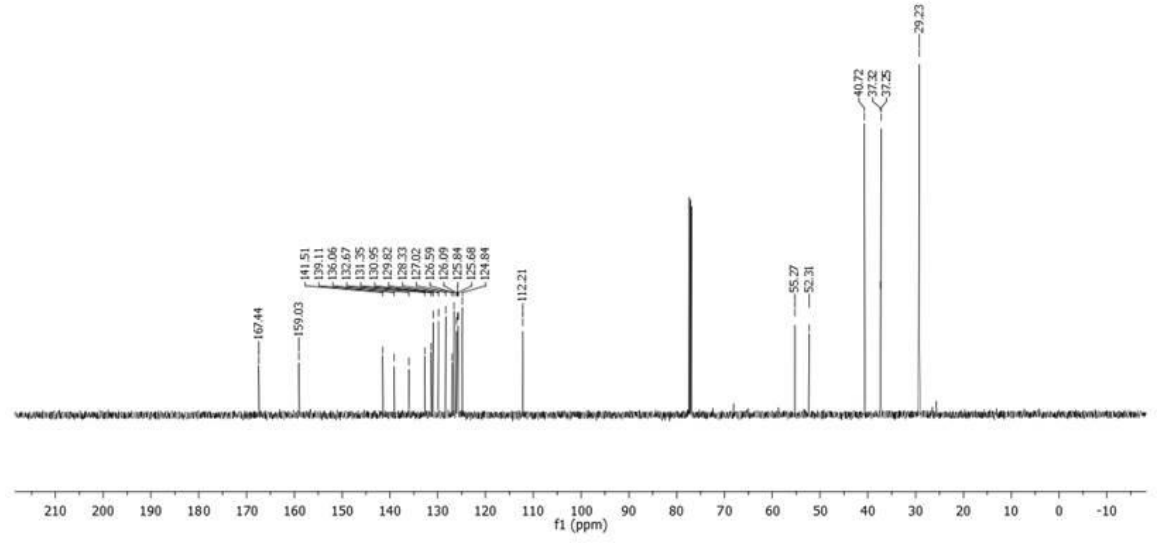
167.44
159.03
141.51
139.11
136.06
132.67
131.35
130.95
129.82
128.33
127.02
126.59
126.09
125.84
125.68
124.84
112.21
55.27
52.31
40.72
37.32
37.25
29.23
f1 (ppm)

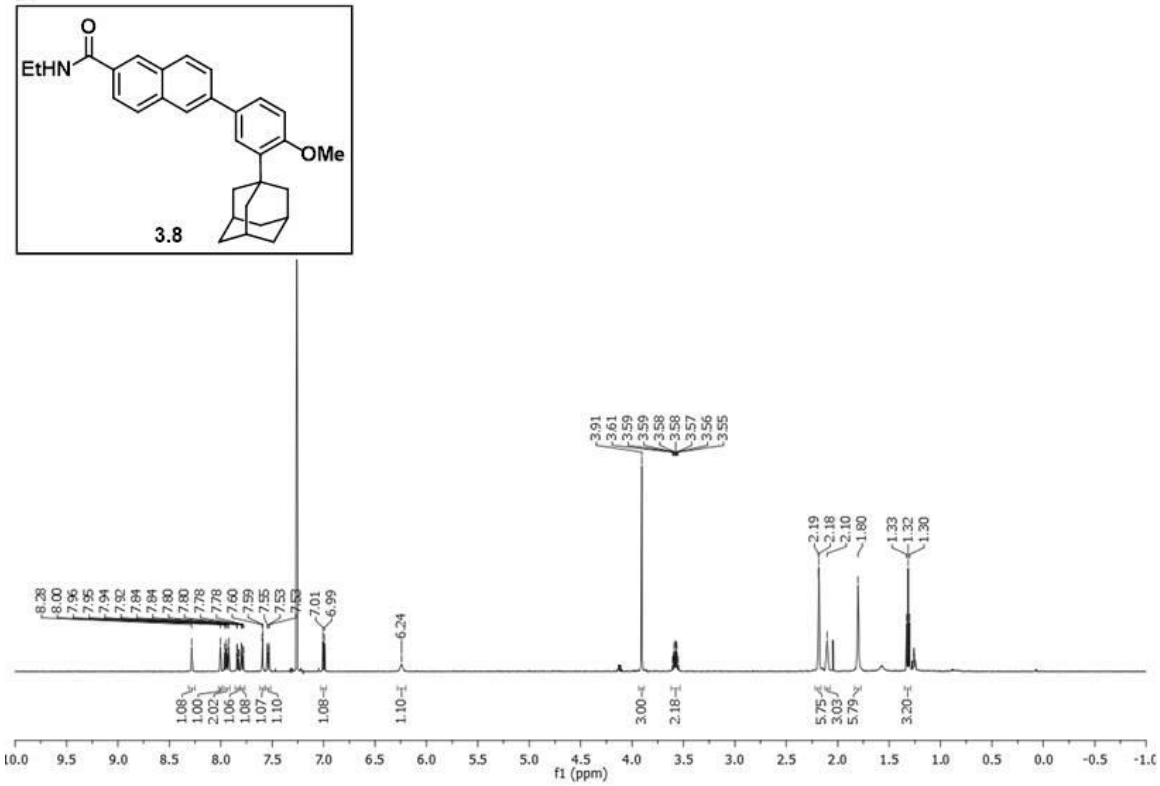
EtHN
O
OMe
3.8
8.28
8.00
7.96
7.95
7.94
7.92
7.84
7.84
7.80
7.80
7.78
7.78
7.60
7.59
7.55
7.53
7.01
6.99
6.24
3.91
3.61
3.59
3.59
3.58
3.58
3.57
3.56
3.55
2.19
2.18
2.10
1.80
1.33
1.32
1.30
1.08
1.00
2.02
1.06
1.08
1.07
1.10
1.08
1.10
3.00
2.18
5.75
3.03
5.79
3.20
f1 (ppm)

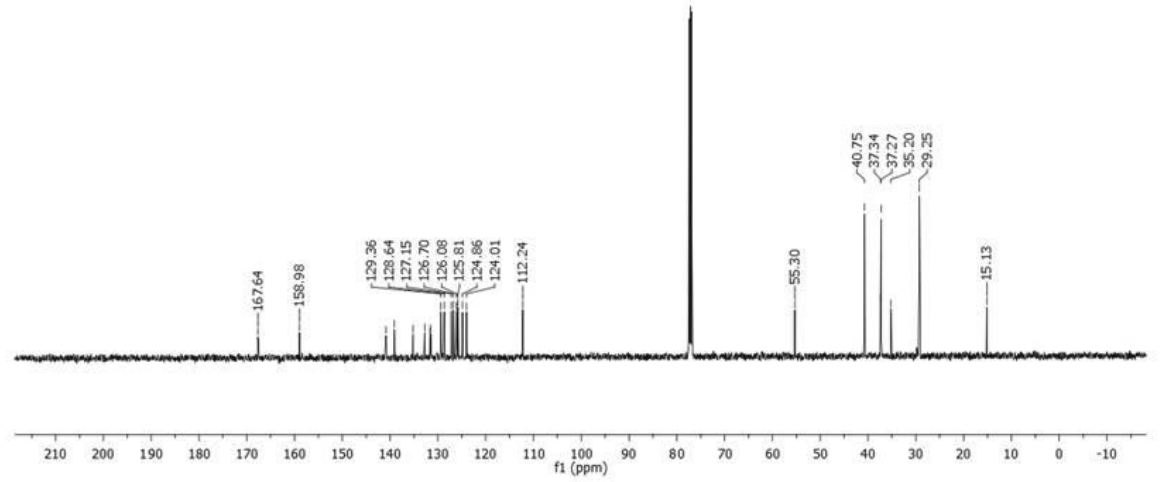
167.64
158.98
129.36
128.64
127.15
126.70
126.08
125.81
124.86
124.01
112.24
55.30
40.75
37.34
37.27
35.20
29.25
15.13
f1 (ppm)

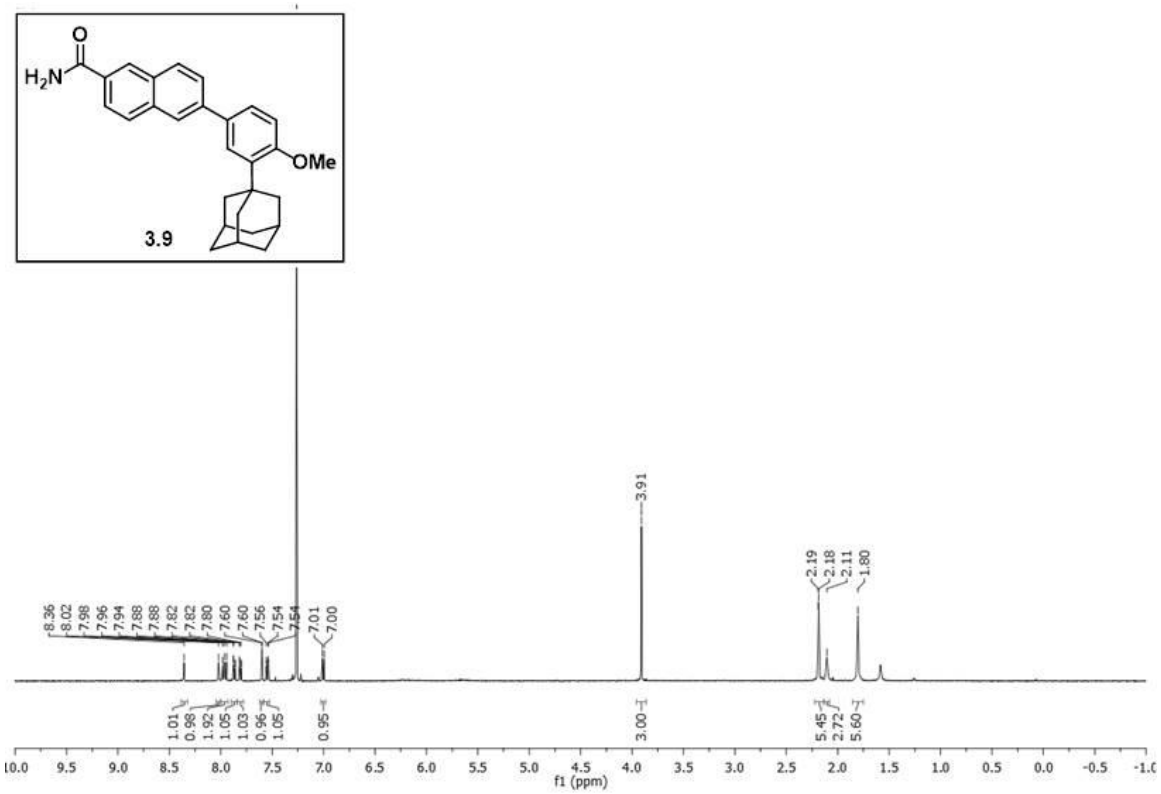
O
H2N
OMe
3.9
8.36
8.02
7.98
7.96
7.94
7.88
7.88
7.82
7.82
7.80
7.60
7.60
7.56
7.54
7.54
7.01
7.00
3.91
2.19
2.18
2.11
1.80
1.01
0.98
1.92
1.05
1.03
0.96
1.05
0.95
3.00
5.45
2.72
5.60
f1 (ppm)

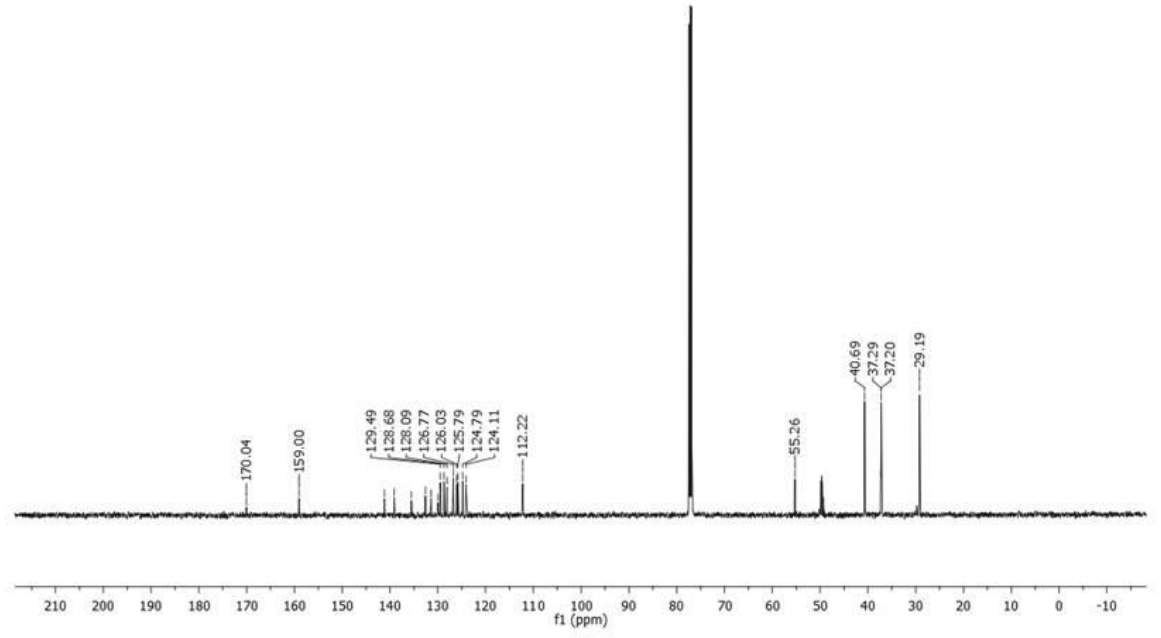
170.04
159.00
129.49
128.68
128.09
126.77
126.03
125.79
124.79
124.11
112.22
55.26
40.69
37.29
37.20
29.19
f1 (ppm)

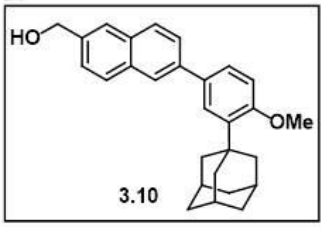
HO
OMe
3.10

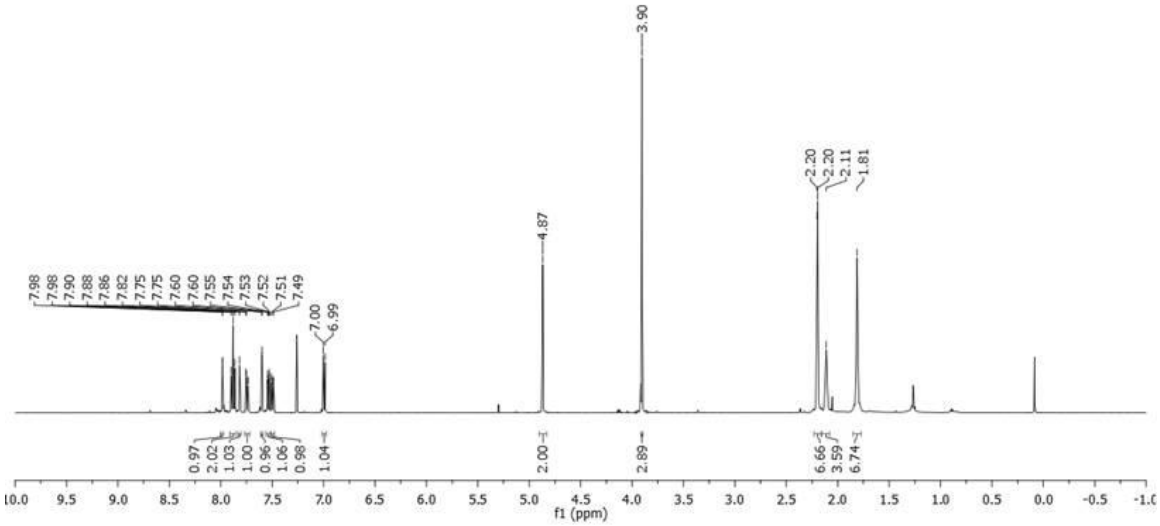
7.98
7.98
7.90
7.88
7.86
7.82
7.75
7.75
7.60
7.60
7.55
7.54
7.53
7.52
7.51
7.49
7.00
6.99
4.87
3.90
2.20
2.20
2.11
1.81
0.97
2.02
1.03
1.00
0.96
1.06
0.98
1.04
2.00
2.89
6.66
3.59
6.74
f1 (ppm)

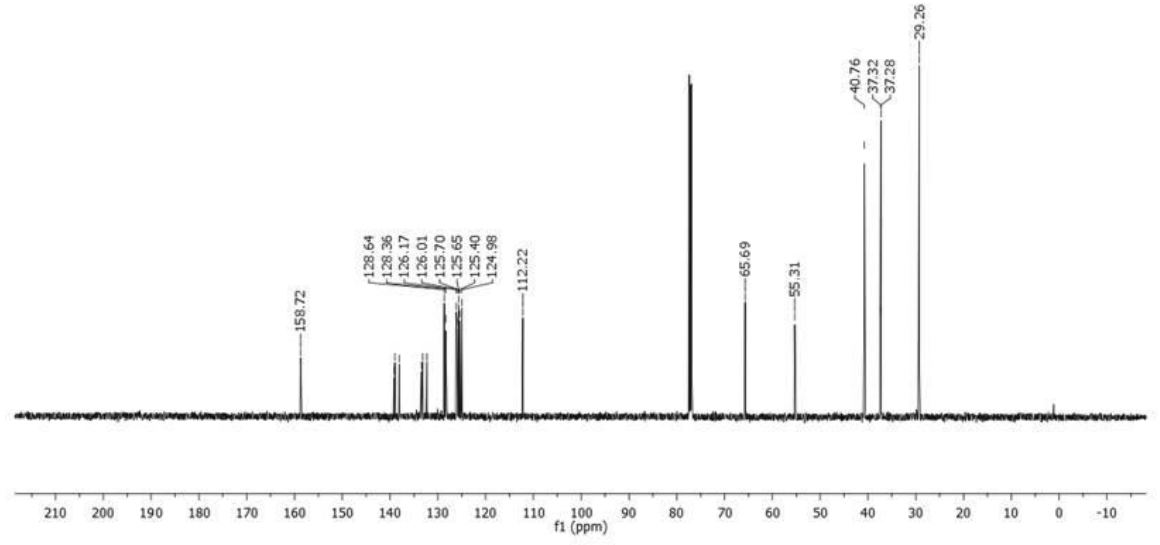
158.72
128.64
128.36
126.17
126.01
125.70
125.65
125.40
124.98
112.22
65.69
55.31
40.76
37.32
37.28
29.26
f1 (ppm)

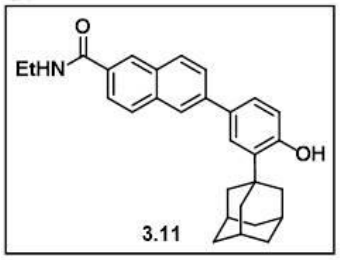
O
EtHN
OH
3.11

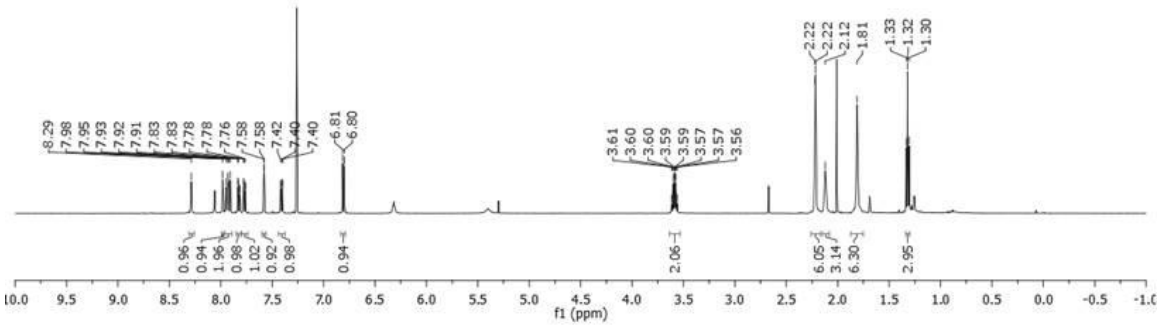
8.29
7.98
7.95
7.93
7.92
7.91
7.83
7.78
7.78
7.76
7.58
7.58
7.42
7.40
7.40
6.81
6.80
3.61
3.60
3.60
3.59
3.59
3.57
3.57
3.56
2.22
2.22
2.12
1.81
1.33
1.32
1.30
0.96
0.94
1.96
0.98
1.02
0.92
0.98
0.94
2.06
6.05
3.14
6.30
2.95
f1 (ppm)

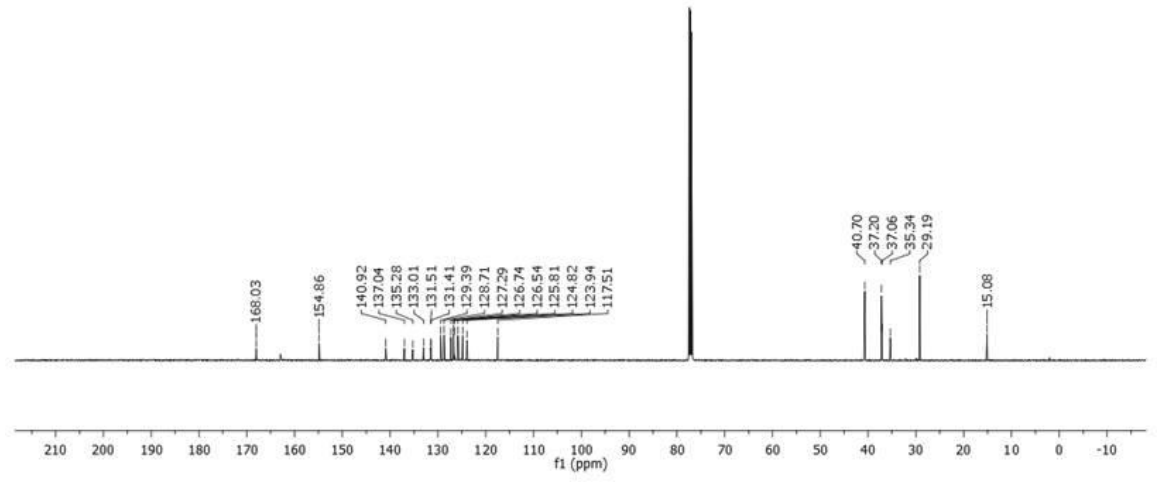
168.03
154.86
140.92
137.04
135.28
133.01
131.51
131.41
129.39
128.71
127.29
126.74
126.54
125.81
124.82
123.94
117.51
40.70
37.20
37.06
35.34
29.19
15.08
f1 (ppm)

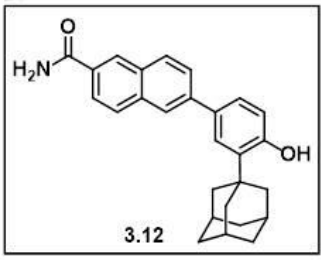
O
H2N
OH
3.12

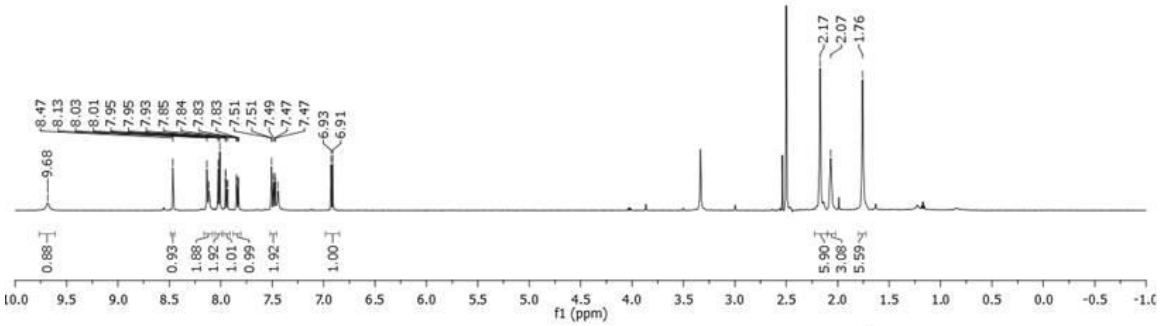
8.47
8.13
8.03
8.01
7.95
7.95
7.93
7.85
7.84
7.83
7.83
7.51
7.51
7.49
7.47
7.47
6.93
6.91
9.68
2.17
2.07
1.76
0.88
0.93
1.88
1.92
1.01
0.99
1.92
1.00
5.90
3.08
5.59
f1 (ppm)

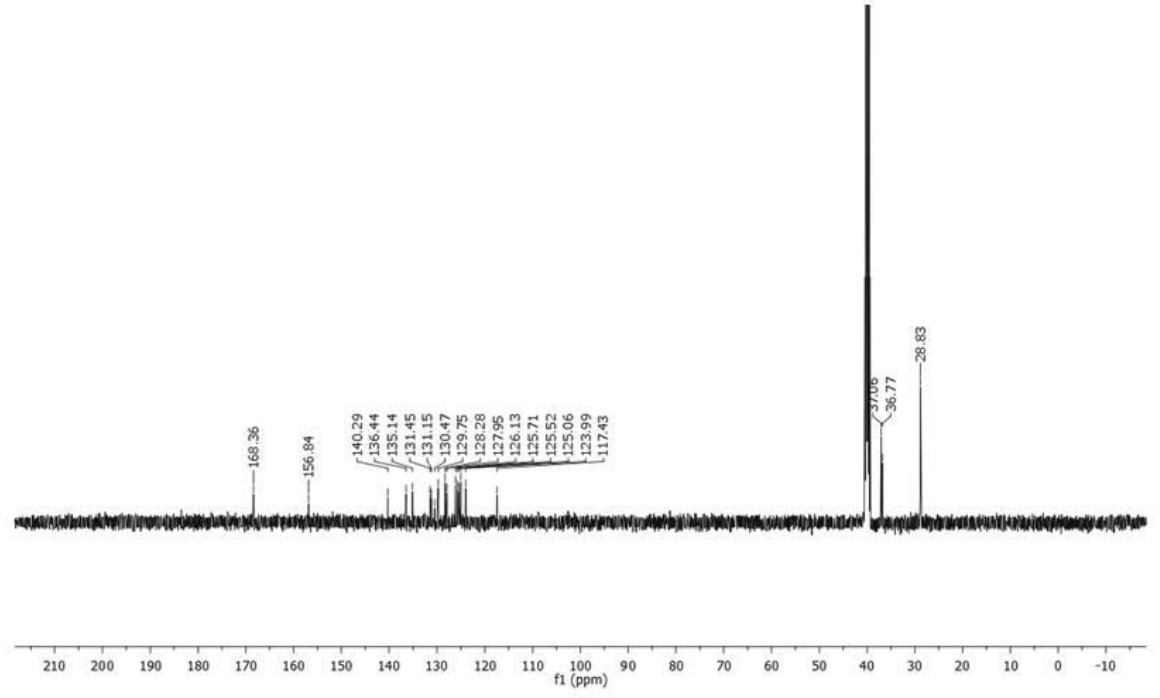
168.36
156.84
140.29
136.44
135.14
131.45
131.15
130.47
129.75
128.28
127.95
126.13
125.71
125.52
125.06
123.99
117.43
37.06
36.77
28.83
f1 (ppm)

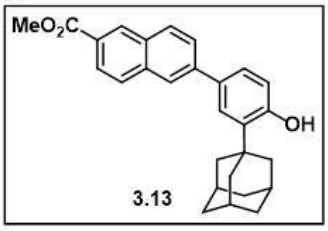
MeO2C
OH

3.13

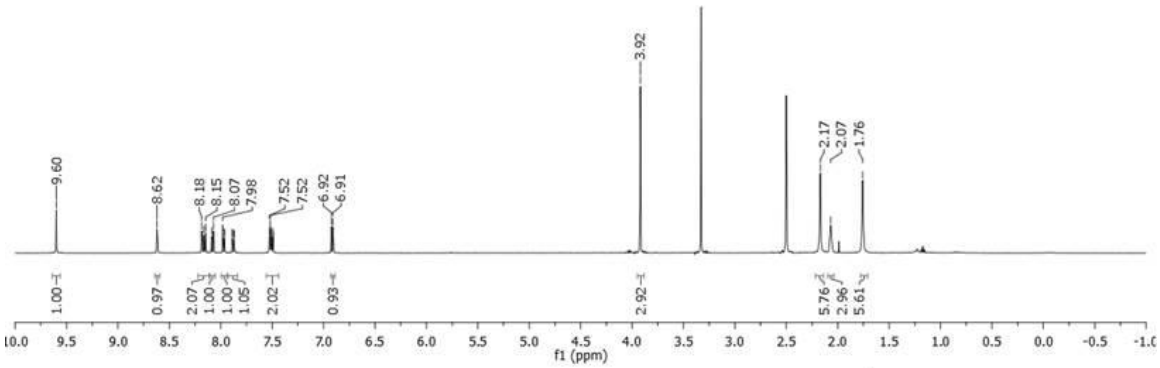
9.60
8.62
8.18
8.15
8.07
7.98
7.52
7.52
6.92
6.91
3.92
2.17
2.07
1.76
1.00
0.97
2.07
1.00
1.00
1.05
2.02
0.93
2.92
5.76
2.96
5.61
f1 (ppm)

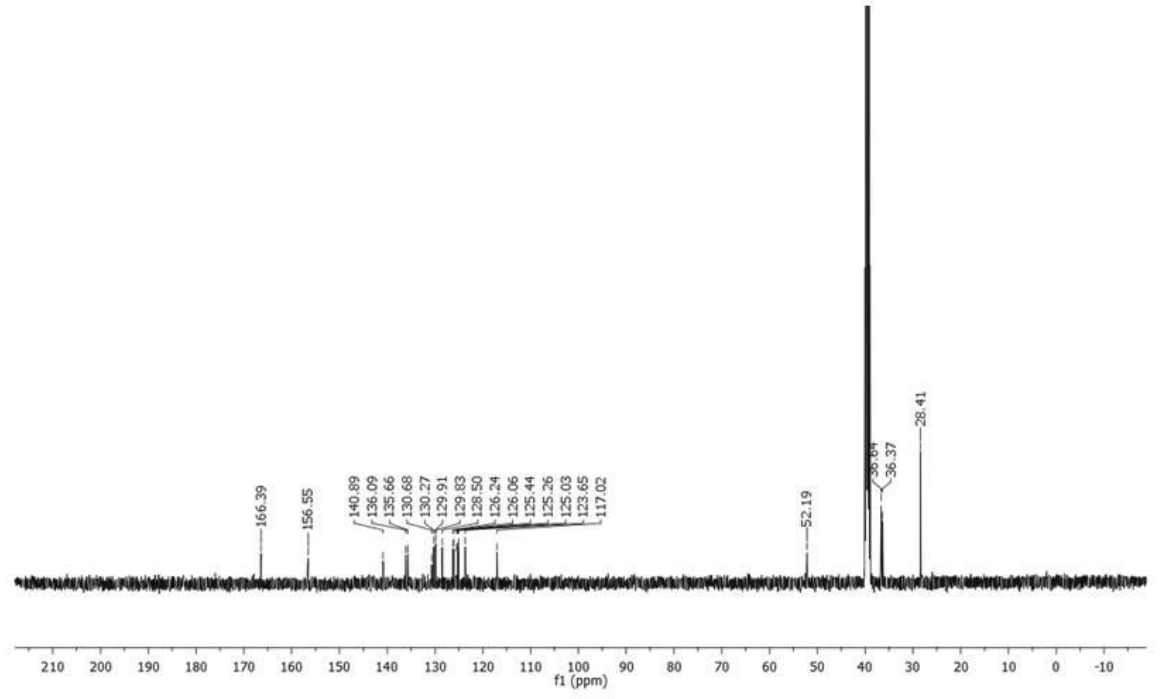
166.39
156.55
140.89
136.09
135.66
130.68
130.27
129.91
129.83
128.50
126.24
126.06
125.44
125.26
125.03
123.65
117.02
52.19
36.84
36.37
28.41
f1 (ppm)

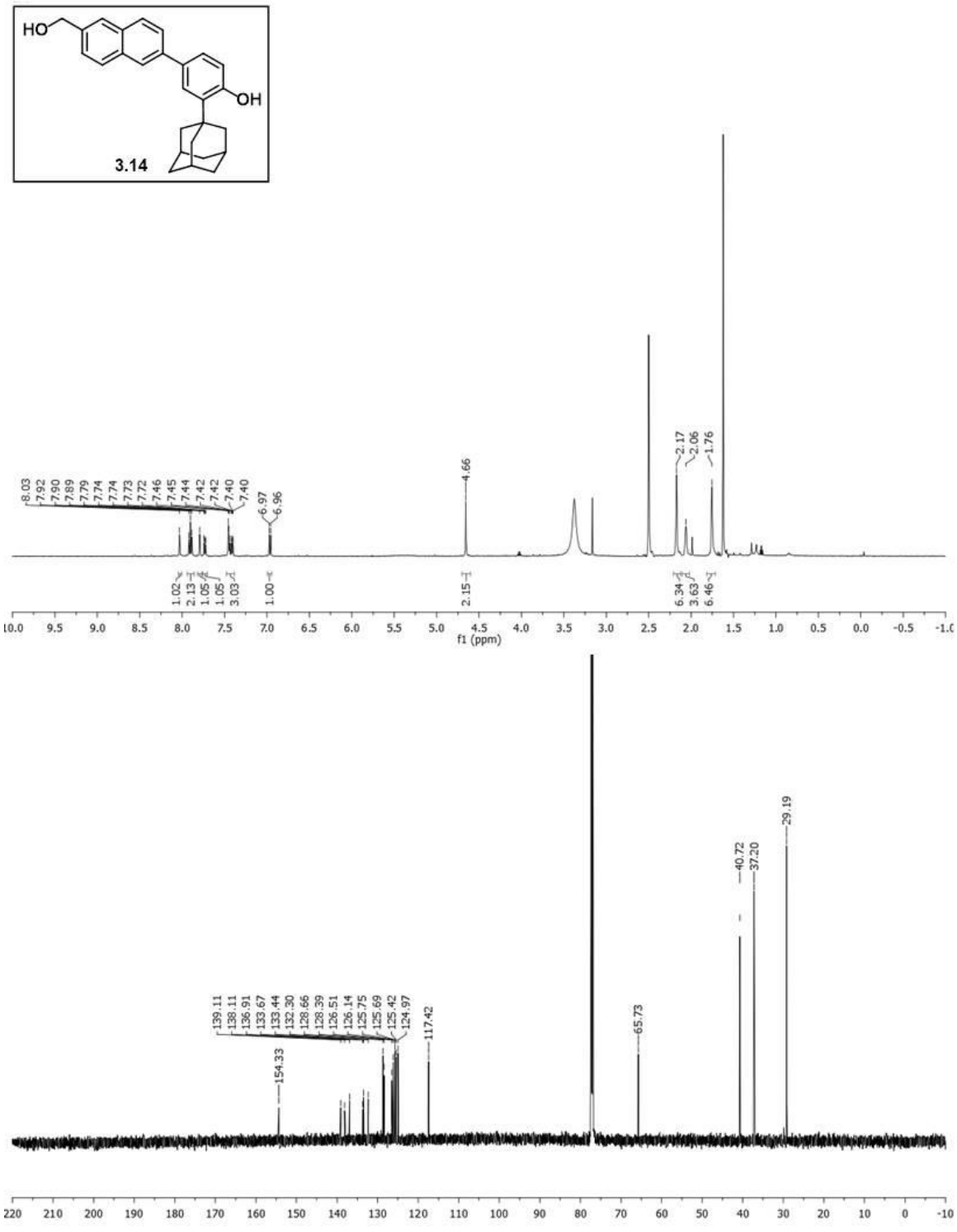
HO
OH
3.14
8.03
7.92
7.90
7.89
7.79
7.74
7.74
7.73
7.72
7.46
7.45
7.44
7.42
7.42
7.40
7.40
6.97
6.96
4.66
2.17
2.06
1.76
1.02
2.13
1.05
1.05
3.03
1.00
2.15
6.34
3.63
6.46
f1 (ppm)
139.11
138.11
136.91
133.67
133.44
132.30
128.66
128.39
126.51
126.14
125.75
125.69
125.42
124.97
117.42
154.33
65.73
40.72
37.20
29.19

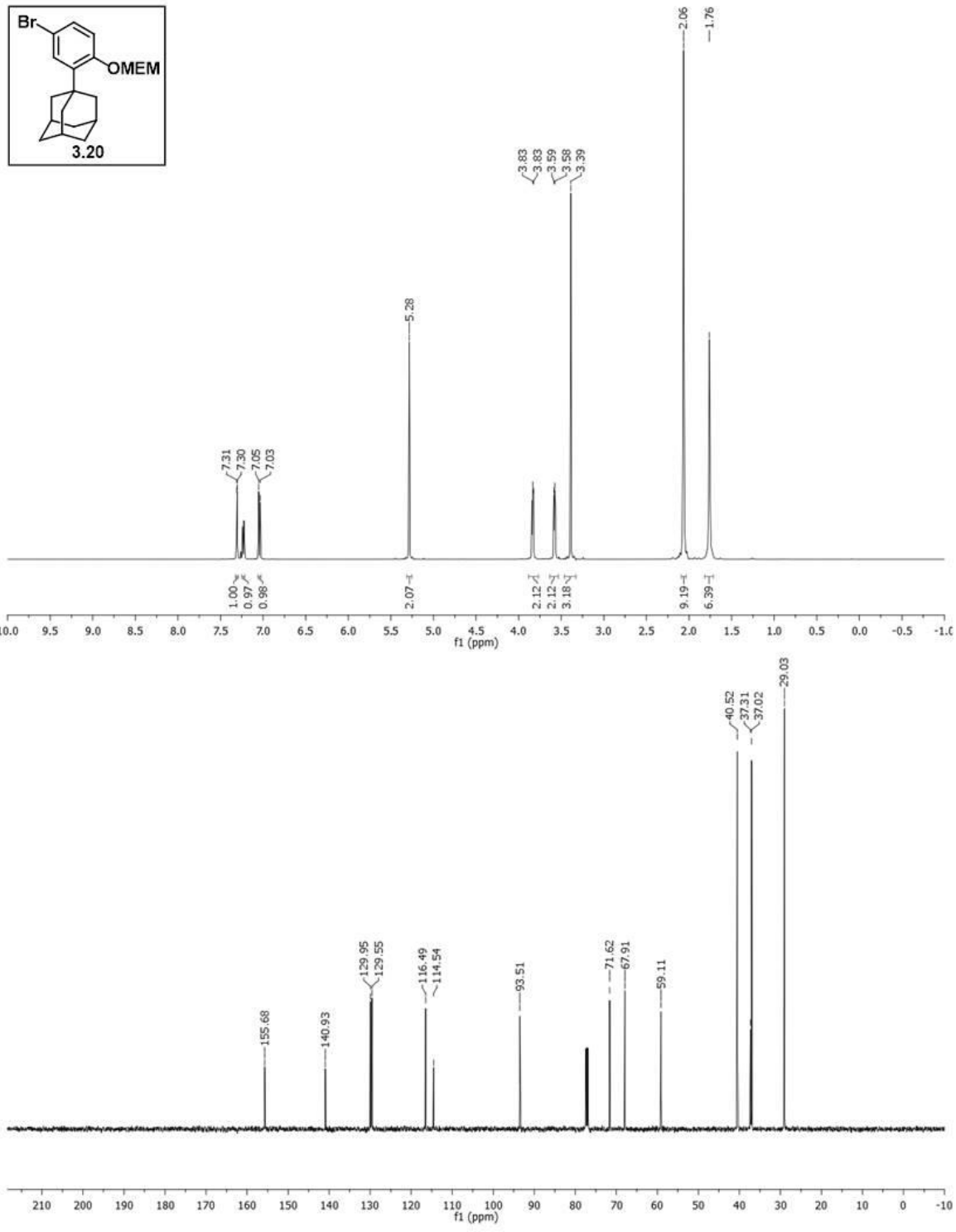
Br
OMEM
3.20
2.06
1.76
3.83
3.83
3.59
3.58
3.39
5.28
7.31
7.30
7.05
7.03
1.00
0.97
0.98
2.07
2.12
2.12
3.18
9.19
6.39
f1 (ppm)
40.52
37.31
37.02
29.03
155.68
140.93
129.95
129.55
116.49
114.54
93.51
71.62
67.91
59.11
f1 (ppm)

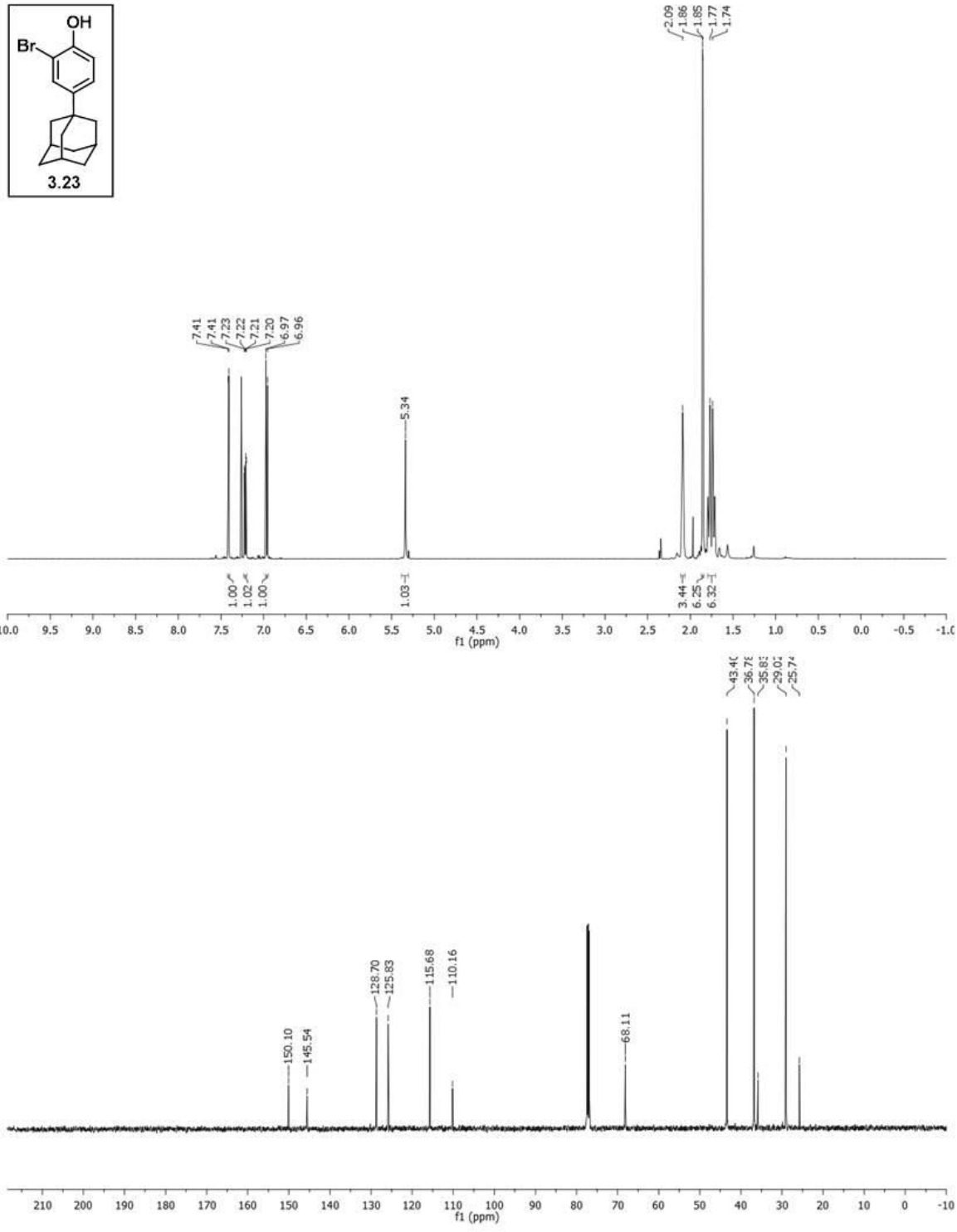
OH
Br
3.23
7.41
7.41
7.23
7.22
7.21
7.20
6.97
6.96
5.34
2.09
1.86
1.85
1.77
1.74
1.00
1.02
1.00
1.03
3.44
6.25
6.32
f1 (ppm)
150.10
145.54
128.70
125.83
115.68
110.16
68.11
43.4
36.7
35.8
29.0
25.7
f1 (ppm)

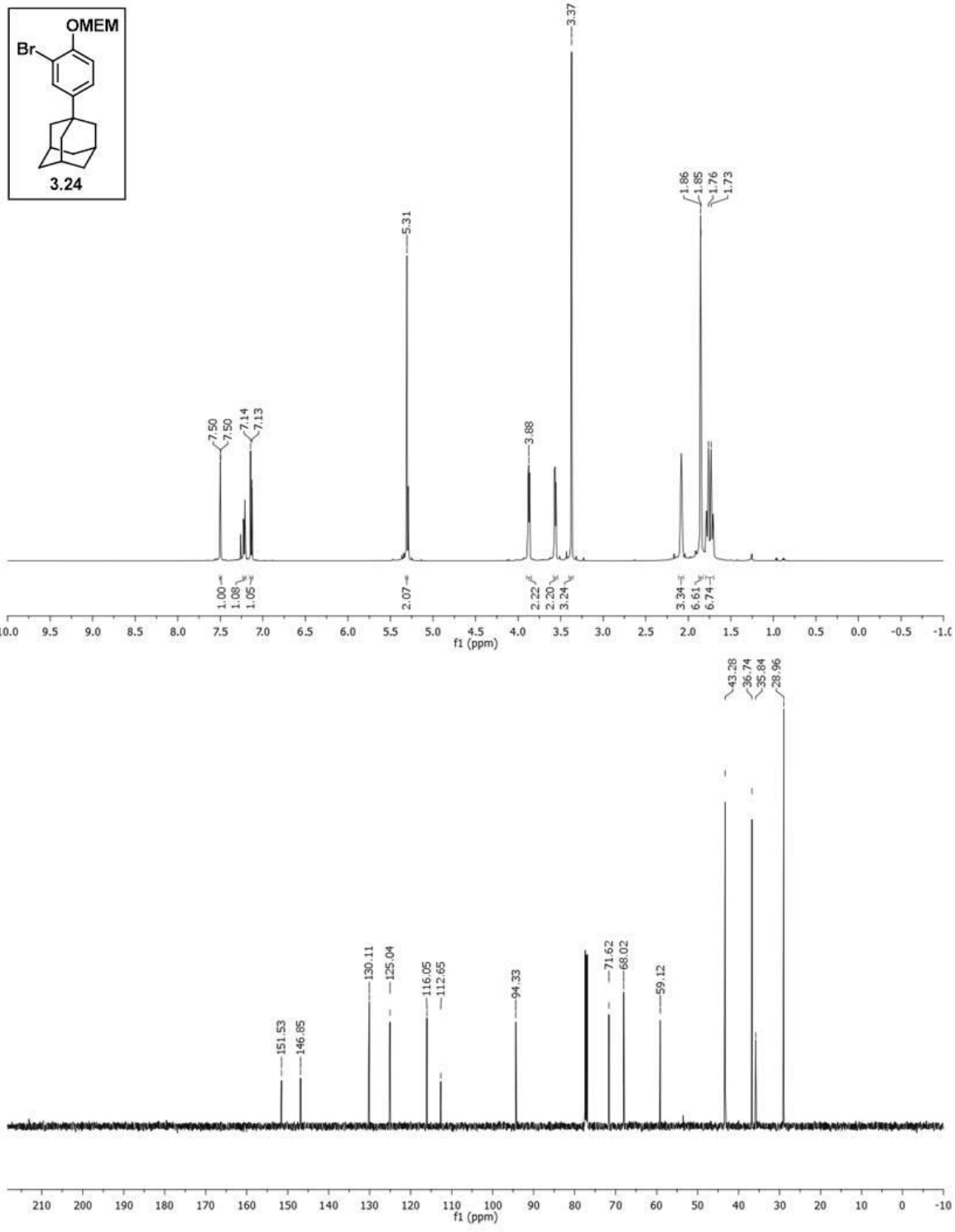
OMEM
Br
3.24
7.50
7.50
7.14
7.13
5.31
3.88
3.37
1.86
1.85
1.76
1.73
1.00
1.08
1.05
2.07
2.22
2.20
3.24
3.34
6.61
6.74
f1 (ppm)
43.28
36.74
35.84
28.96
151.53
146.85
130.11
125.04
116.05
112.65
94.33
71.62
68.02
59.12
f1 (ppm)

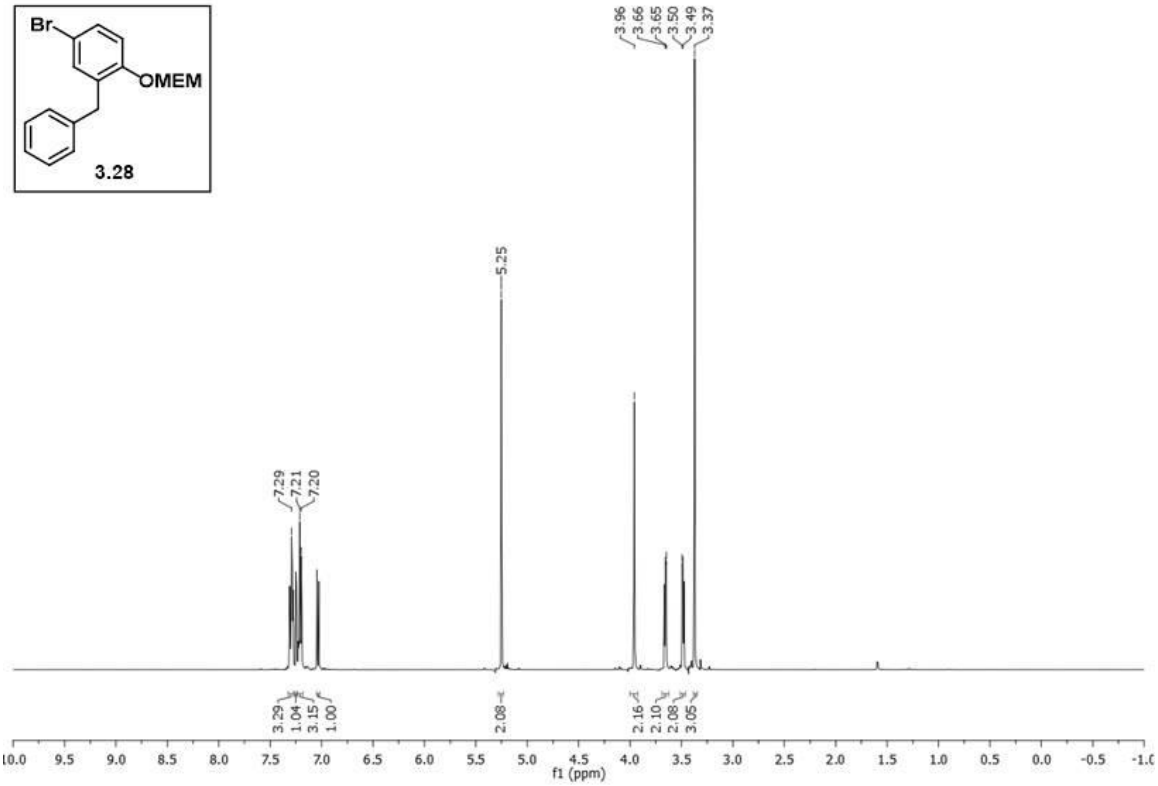
Br
OMEM
3.28
3.96
3.66
3.65
3.50
3.49
3.37
5.25
7.29
7.21
7.20
3.29
1.04
3.15
1.00
2.08
2.16
2.10
2.08
3.05
f1 (ppm)

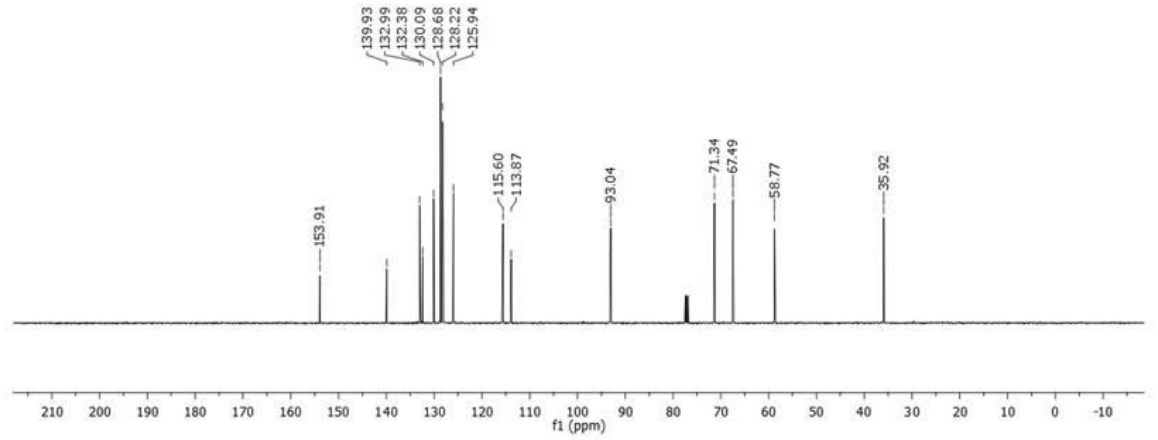
139.93
132.99
132.38
130.09
128.68
128.22
125.94
153.91
115.60
113.87
93.04
71.34
67.49
58.77
35.92
f1 (ppm)

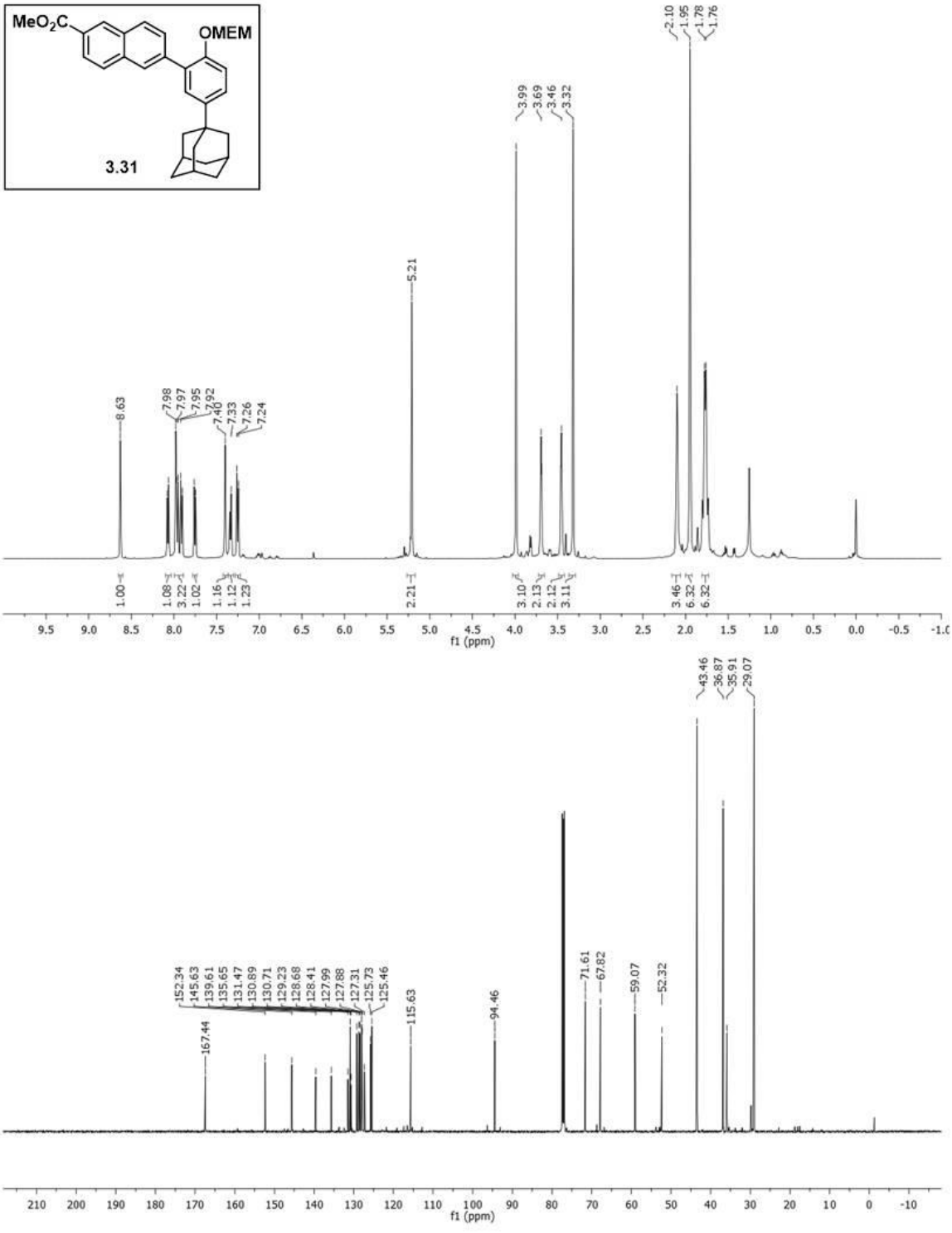
MeO2C
OMEM
3.31
8.63
7.98
7.97
7.95
7.92
7.40
7.33
7.26
7.24
5.21
3.99
3.69
3.46
3.32
2.10
1.95
1.78
1.76
1.00
1.08
3.22
1.02
1.16
1.12
1.23
2.21
3.10
2.13
2.12
3.11
3.46
6.32
6.32
f1 (ppm)
152.34
145.63
139.61
135.65
131.47
130.89
130.71
129.23
128.68
128.41
127.99
127.88
127.31
125.73
125.46
115.63
94.46
71.61
67.82
59.07
52.32
43.46
36.87
35.91
29.07
167.44
f1 (ppm)

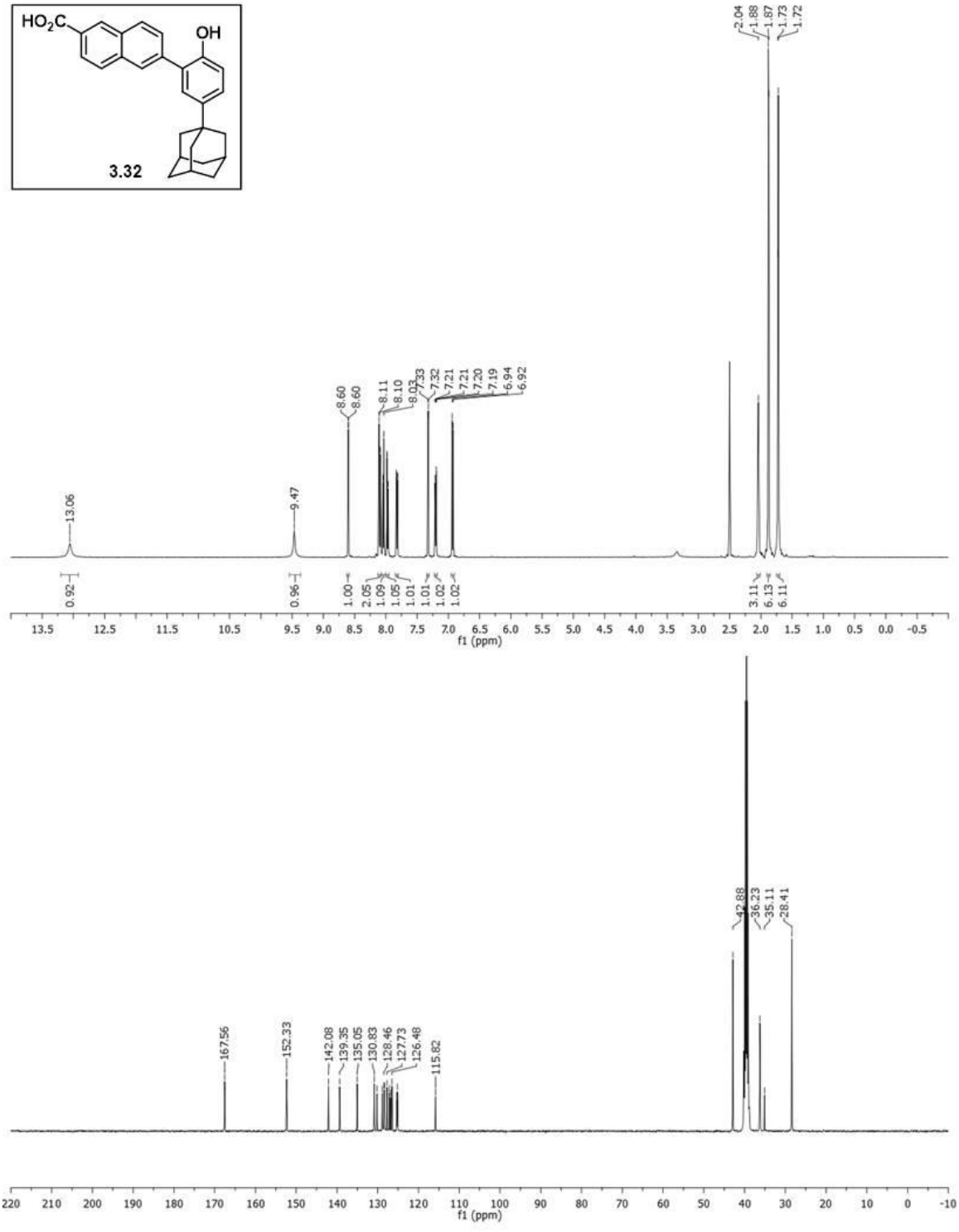
HO2C
OH
3.32
13.06
9.47
8.60
8.60
8.11
8.10
8.03
7.33
7.32
7.21
7.21
7.20
7.19
6.94
6.92
2.04
1.88
1.87
1.73
1.72
0.92
0.96
1.00
2.05
1.09
1.05
1.01
1.01
1.02
1.02
3.11
6.13
6.11
f1 (ppm)
167.56
152.33
142.08
139.35
135.05
130.83
128.46
127.73
126.48
115.82
42.88
36.23
35.11
28.41
f1 (ppm)

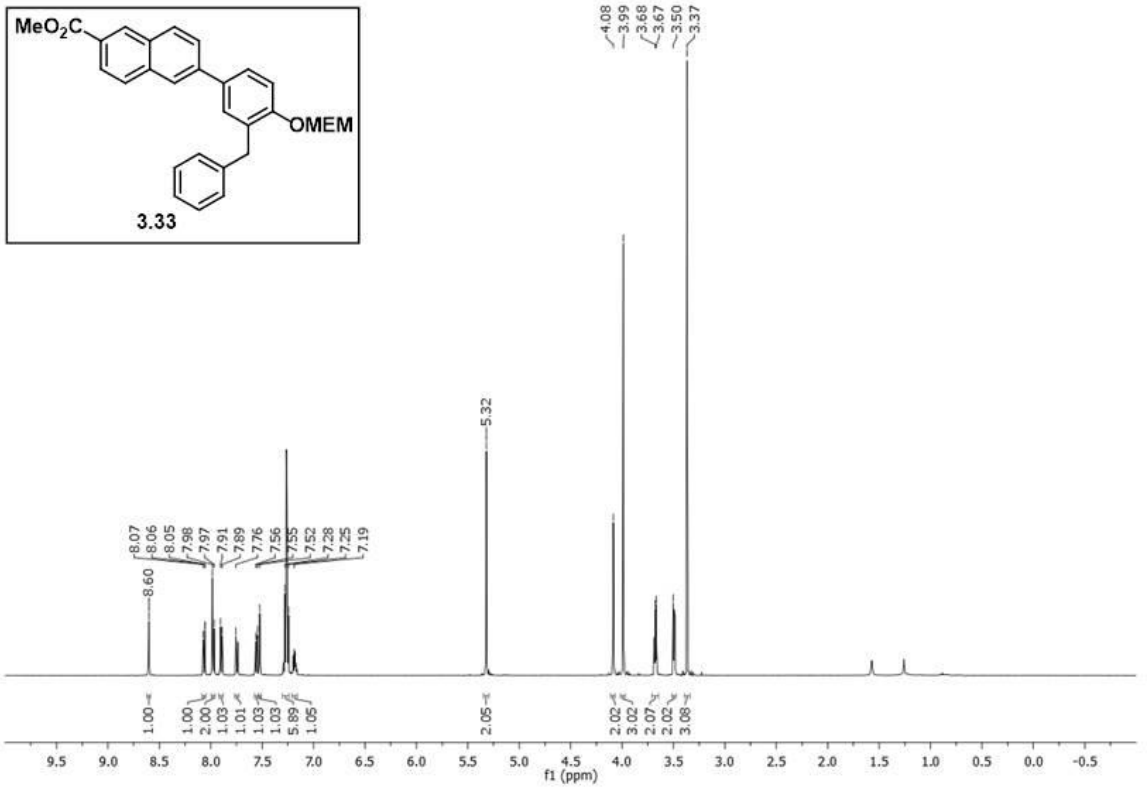
MeO2C
OMEM
3.33
4.08
3.99
3.68
3.67
3.50
3.37
5.32
8.07
8.06
8.05
7.98
7.97
7.91
7.89
7.76
7.56
7.55
7.52
7.28
7.25
7.19
8.60
1.00
1.00
2.00
1.03
1.01
1.03
1.03
5.89
1.05
2.05
2.02
3.02
2.07
2.02
3.08
f1 (ppm)

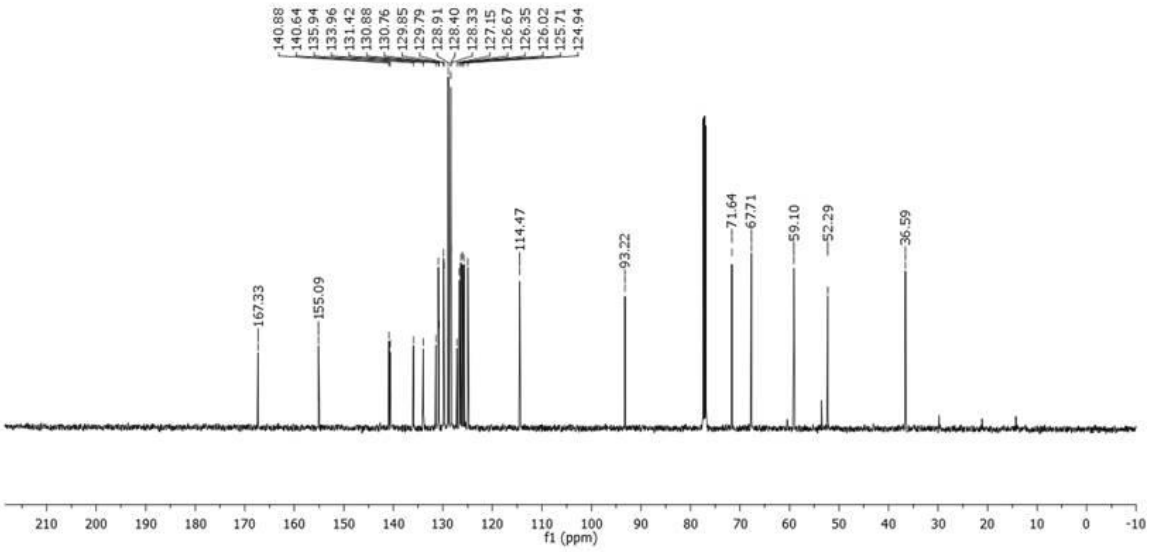
140.88
140.64
135.94
133.96
131.42
130.88
130.76
129.85
129.79
128.91
128.40
128.33
127.15
126.67
126.35
126.02
125.71
124.94
167.33
155.09
114.47
93.22
71.64
67.71
59.10
52.29
36.59
f1 (ppm)

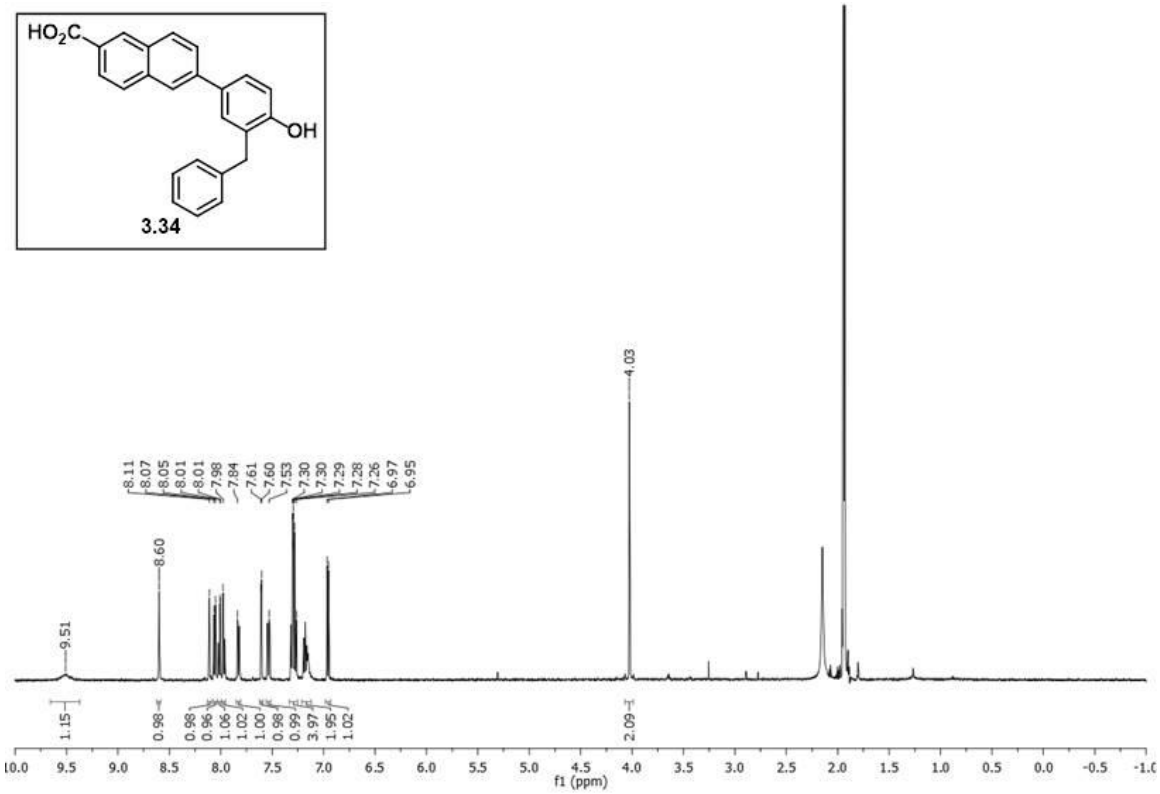
HO2C
OH
3.34
9.51
8.60
8.11
8.07
8.05
8.01
8.01
7.98
7.84
7.61
7.60
7.53
7.30
7.30
7.29
7.28
7.26
6.97
6.95
4.03
1.15
0.98
0.98
0.96
1.06
1.02
1.00
0.98
0.99
3.97
1.95
1.02
2.09
f1 (ppm)

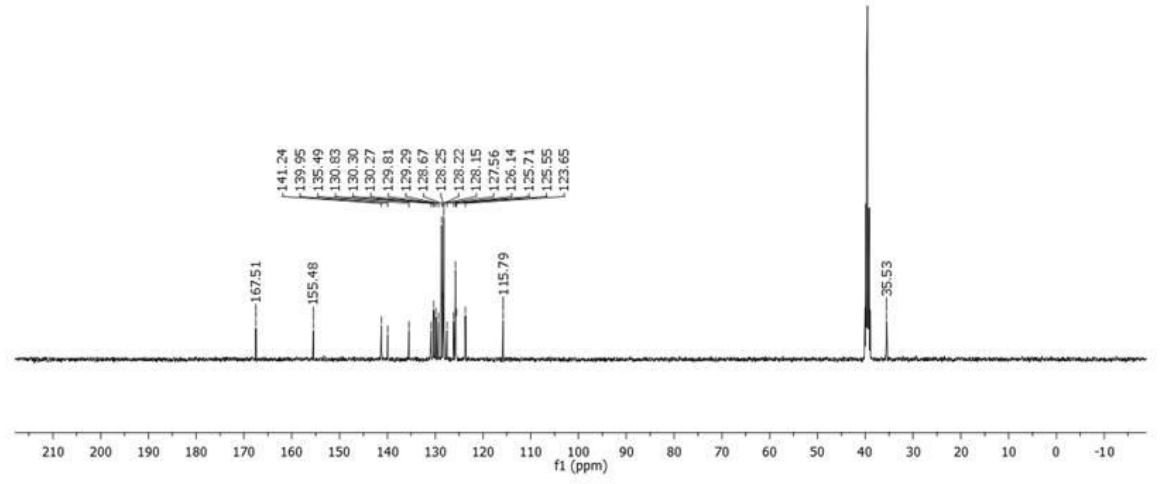
141.24
139.95
135.49
130.83
130.30
130.27
129.81
129.29
128.67
128.25
128.22
128.15
127.56
126.14
125.71
125.55
123.65
167.51
155.48
115.79
35.53
f1 (ppm)

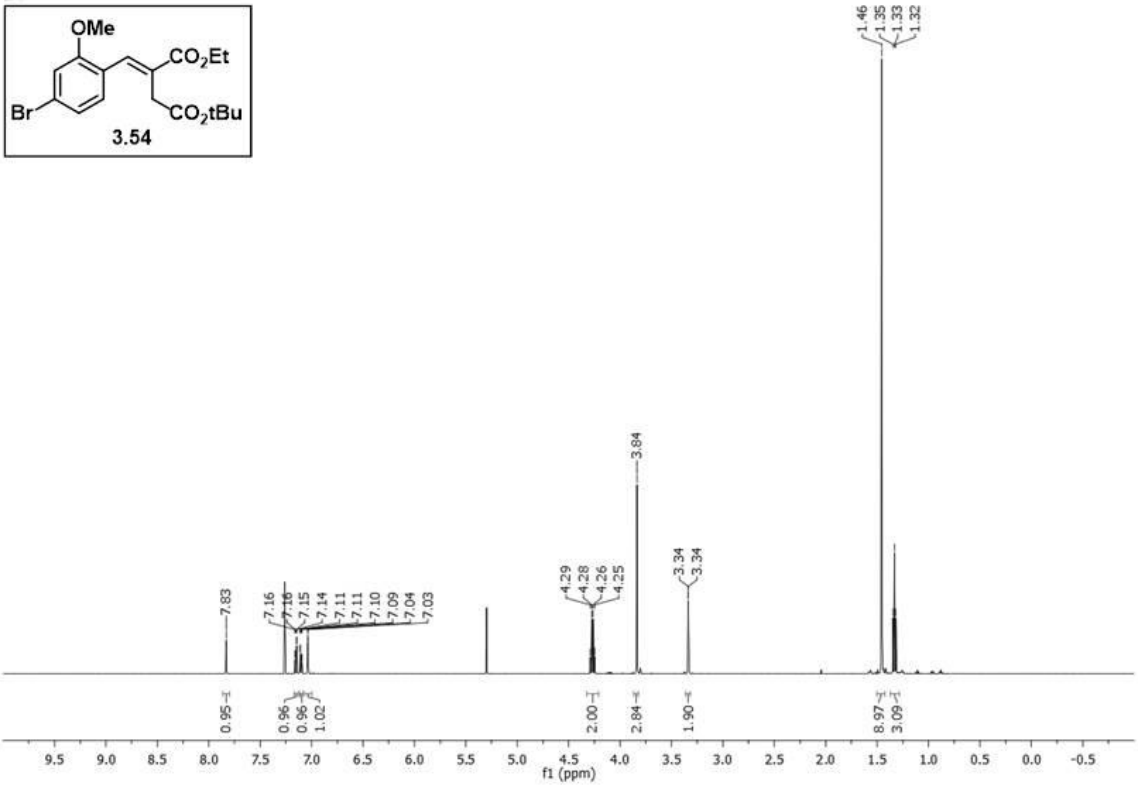
OMe
CO2Et
Br
CO2tBu
3.54
1.46
1.35
1.33
1.32
3.84
3.34
3.34
4.29
4.28
4.26
4.25
7.83
7.16
7.16
7.15
7.14
7.11
7.11
7.10
7.09
7.04
7.03
0.95
0.96
0.96
1.02
2.00
2.84
1.90
8.97
3.09
f1 (ppm)

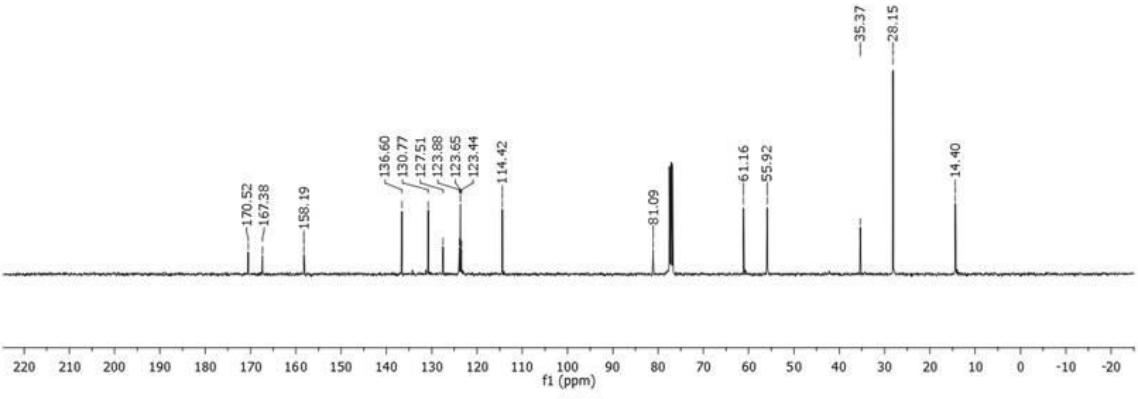
35.37
28.15
136.60
130.77
127.51
123.88
123.65
123.44
114.42
61.16
55.92
14.40
170.52
167.38
158.19
81.09
f1 (ppm)

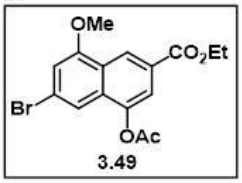
OMe
CO2Et
Br
OAc

3.49

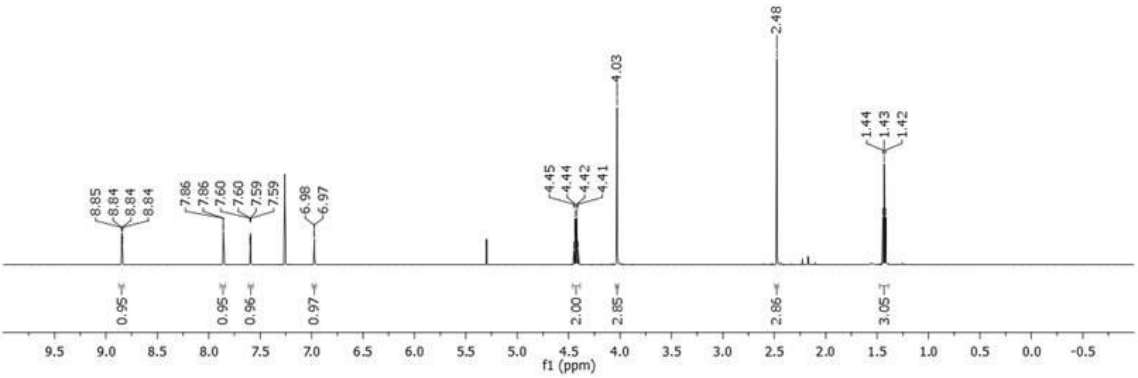
8.85
8.84
8.84
8.84
7.86
7.86
7.60
7.60
7.59
7.59
6.98
6.97
4.45
4.44
4.42
4.41
4.03
2.48
1.44
1.43
1.42
0.95
0.95
0.96
0.97
2.00
2.85
2.86
3.05
f1 (ppm)

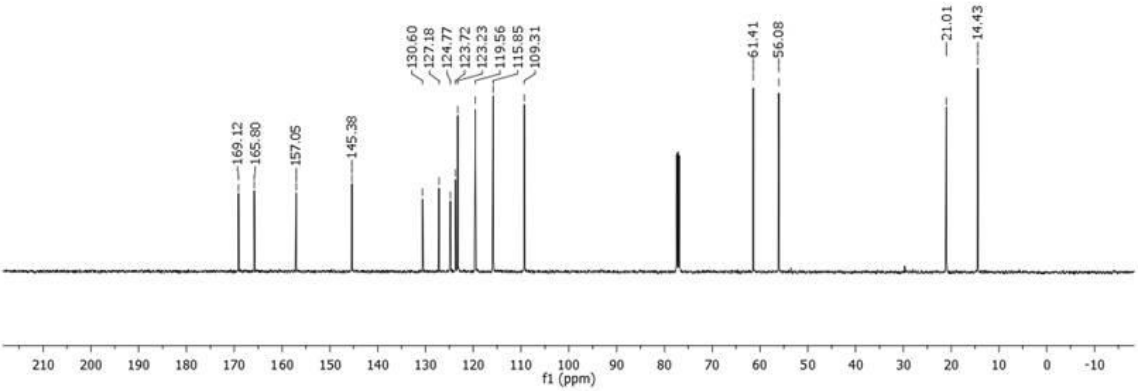
169.12
165.80
157.05
145.38
130.60
127.18
124.77
123.72
123.23
119.56
115.85
109.31
61.41
56.08
21.01
14.43
f1 (ppm)

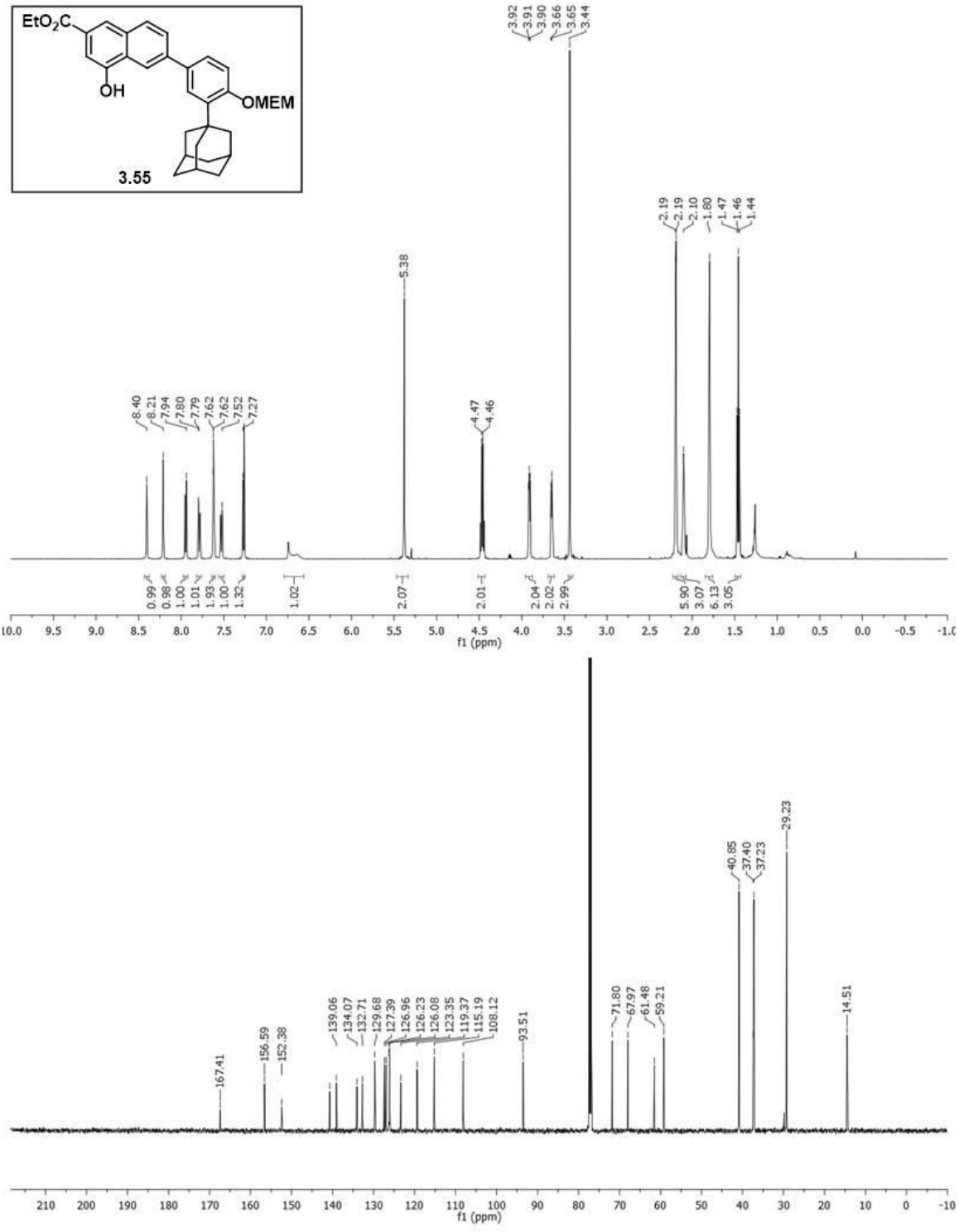
EtO2C
OH
OMEM
3.55
f1 (ppm)
f1 (ppm)

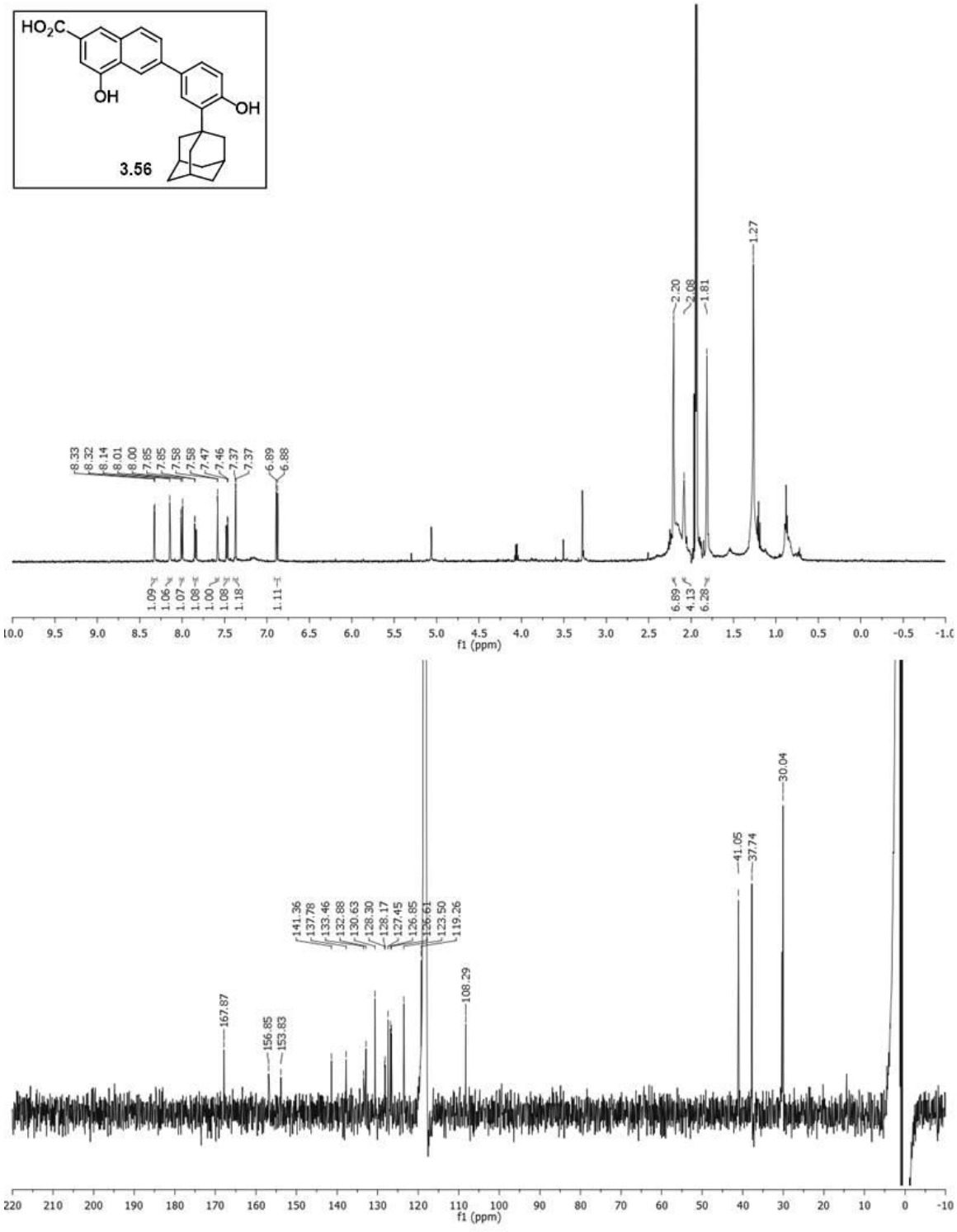
HO2C
OH
OH
3.56
8.33
8.32
8.14
8.01
8.00
7.85
7.85
7.58
7.58
7.47
7.46
7.37
7.37
6.89
6.88
2.20
2.08
1.81
1.27
1.09
1.06
1.07
1.08
1.00
1.08
1.18
1.11
6.89
4.13
6.28
f1 (ppm)
141.36
137.78
133.46
132.88
130.63
128.30
128.17
127.45
126.85
126.61
123.50
119.26
167.87
156.85
153.83
108.29
41.05
37.74
30.04
f1 (ppm)

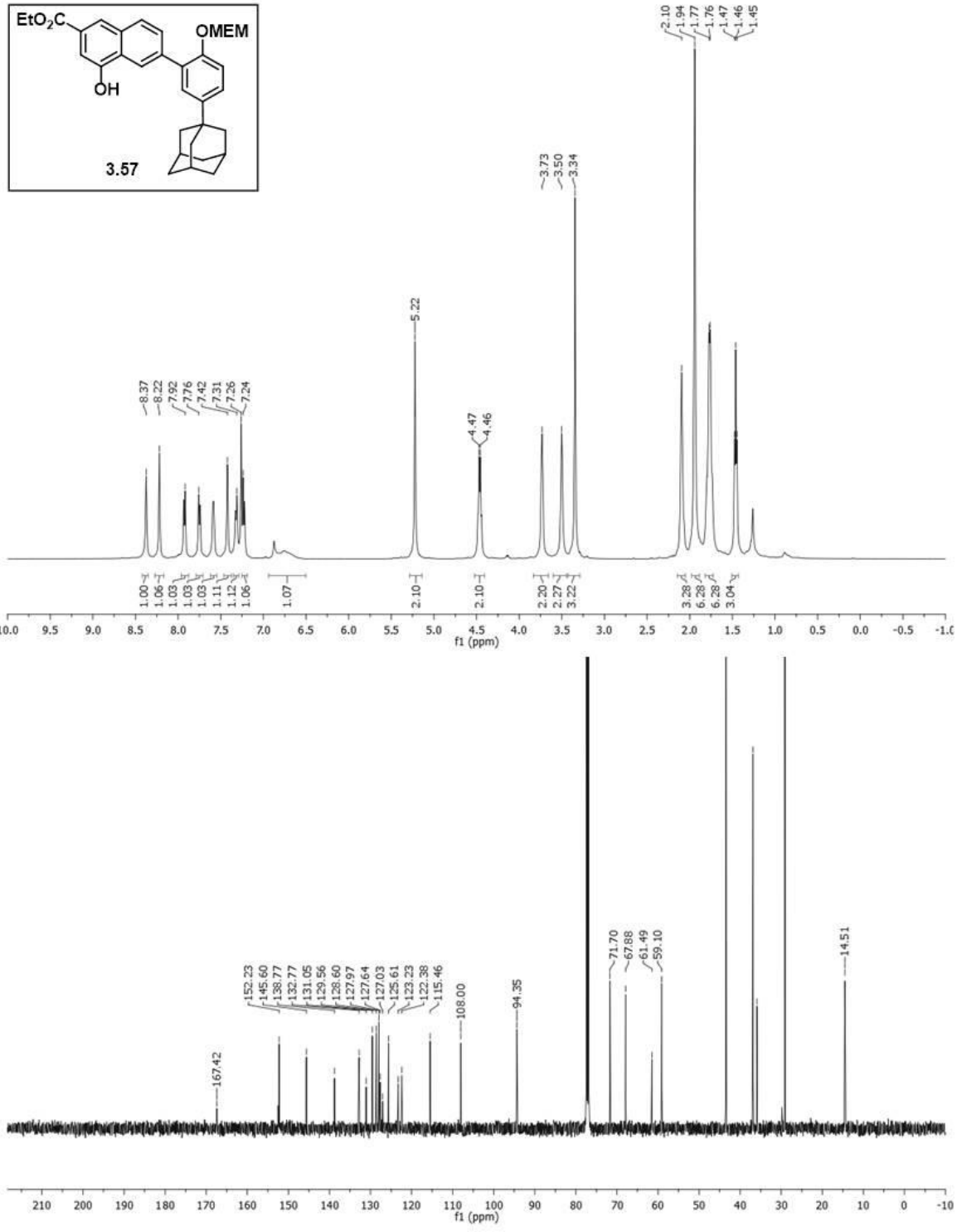
EtO2C
OMEM
OH
3.57
f1 (ppm)
f1 (ppm)

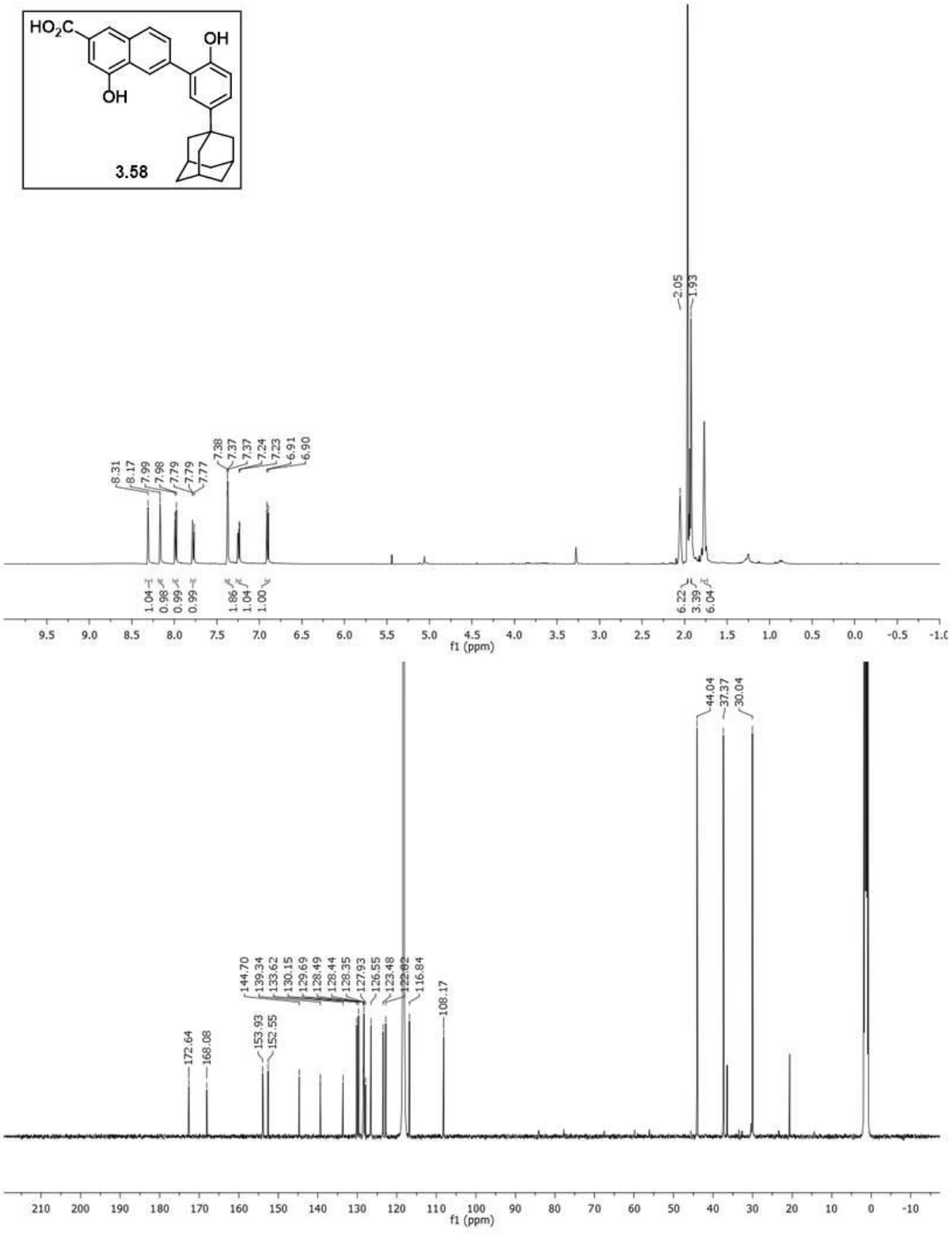
HO2C
OH
OH
3.58
8.31
8.17
7.99
7.98
7.79
7.79
7.77
7.38
7.37
7.37
7.24
7.23
6.91
6.90
2.05
1.93
1.04
0.98
0.99
0.99
1.86
1.04
1.00
6.22
3.39
6.04
f1 (ppm)
144.70
139.34
133.62
130.15
129.69
128.49
128.44
128.35
127.93
126.55
123.48
116.84
108.17
172.64
168.08
153.93
152.55
44.04
37.37
30.04
f1 (ppm)

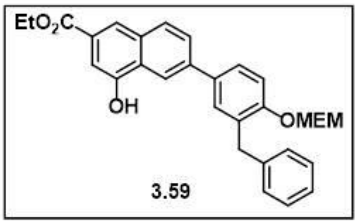
EtO2C
OH
OMEM

3.59

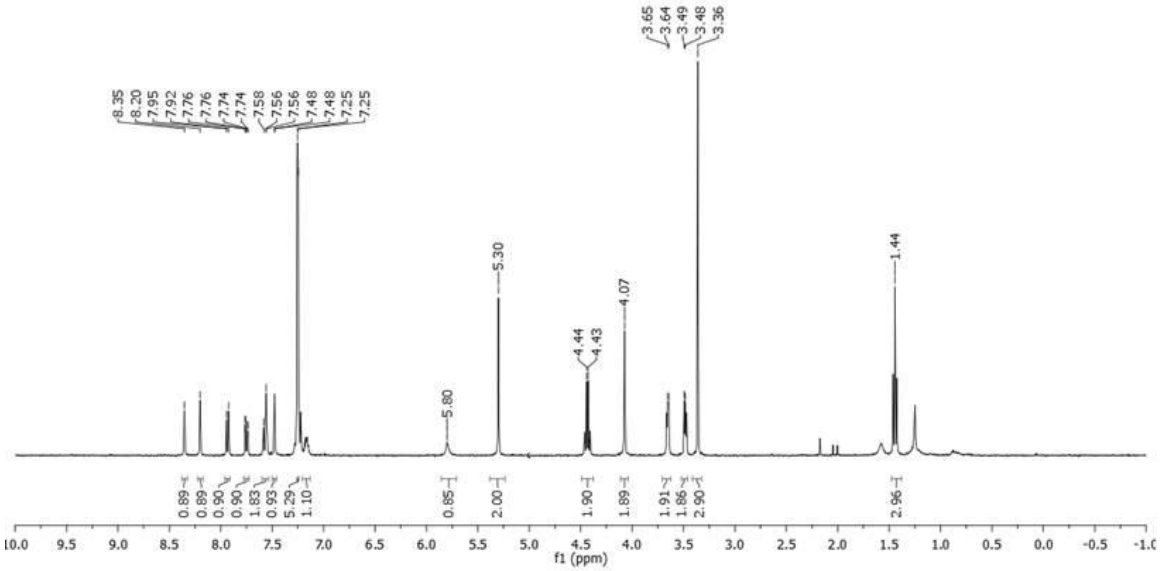
8.35
8.20
7.95
7.92
7.76
7.76
7.74
7.74
7.58
7.56
7.56
7.48
7.48
7.25
7.25
5.80
5.30
4.44
4.43
4.07
3.65
3.64
3.49
3.48
3.36
1.44
0.89
0.89
0.90
0.90
1.83
0.93
5.29
1.10
0.85
2.00
1.90
1.89
1.91
1.86
2.90
2.96
f1 (ppm)

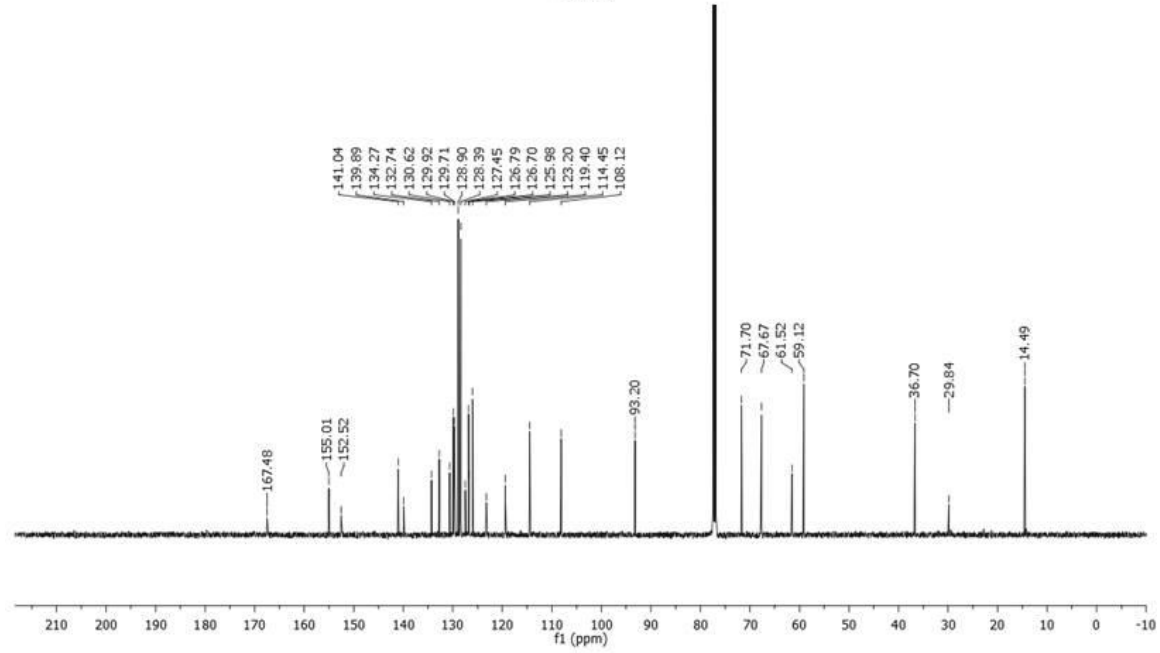
141.04
139.89
134.27
132.74
130.62
129.92
129.71
128.90
128.39
127.45
126.79
126.70
125.98
123.20
119.40
114.45
108.12
167.48
155.01
152.52
93.20
71.70
67.67
61.52
59.12
36.70
29.84
14.49
f1 (ppm)

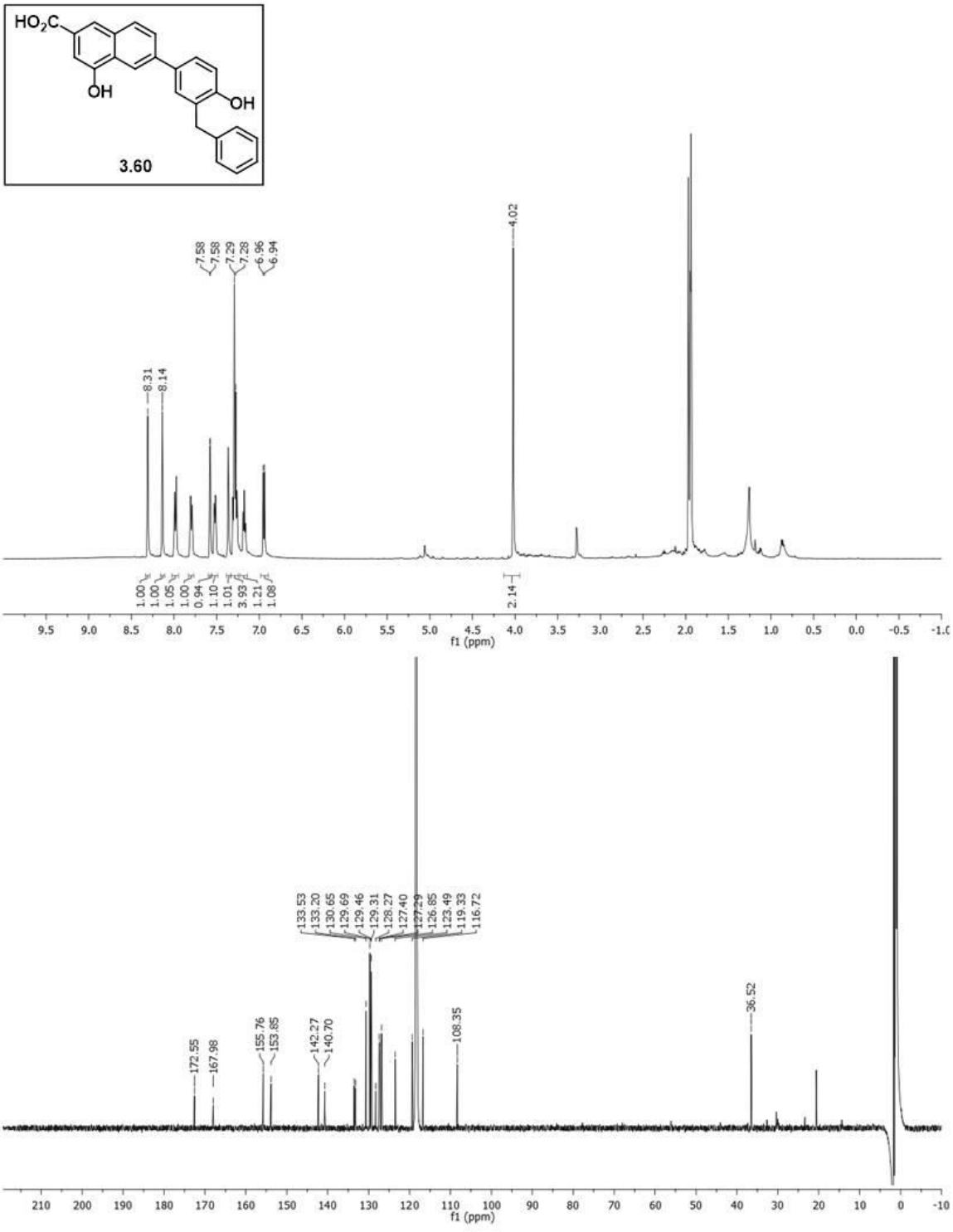
HO2C
OH
OH
3.60
8.31
8.14
7.58
7.58
7.29
7.28
6.96
6.94
4.02
1.00
1.00
1.05
1.00
0.94
1.10
1.01
3.93
1.21
1.08
2.14
f1 (ppm)
133.53
133.20
130.65
129.69
129.46
129.31
128.27
127.40
127.29
126.85
123.49
119.33
116.72
172.55
167.98
155.76
153.85
142.27
140.70
108.35
36.52
f1 (ppm)

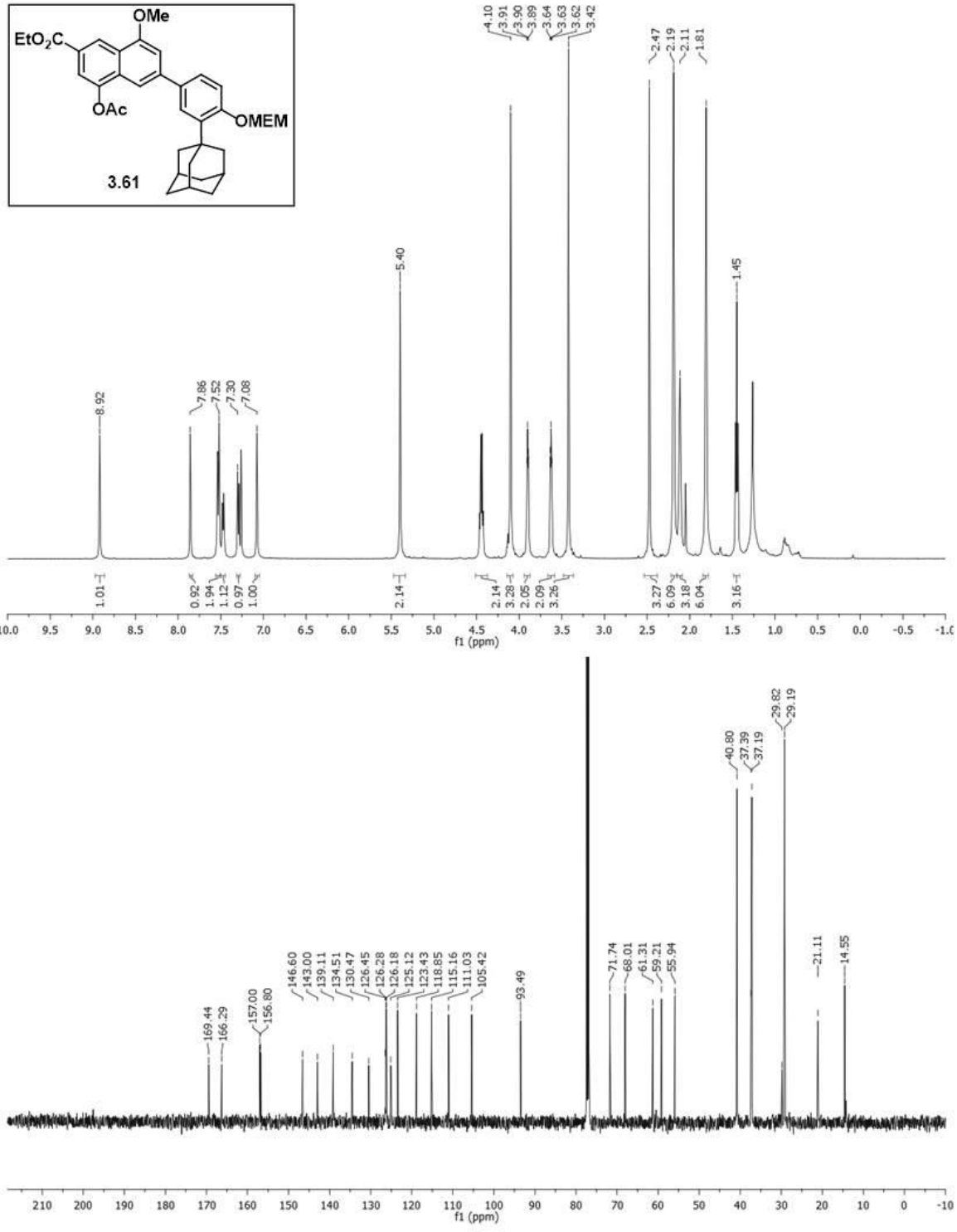
OMe
EtO2C
OAc
OMEM
3.61
f1 (ppm)
f1 (ppm)

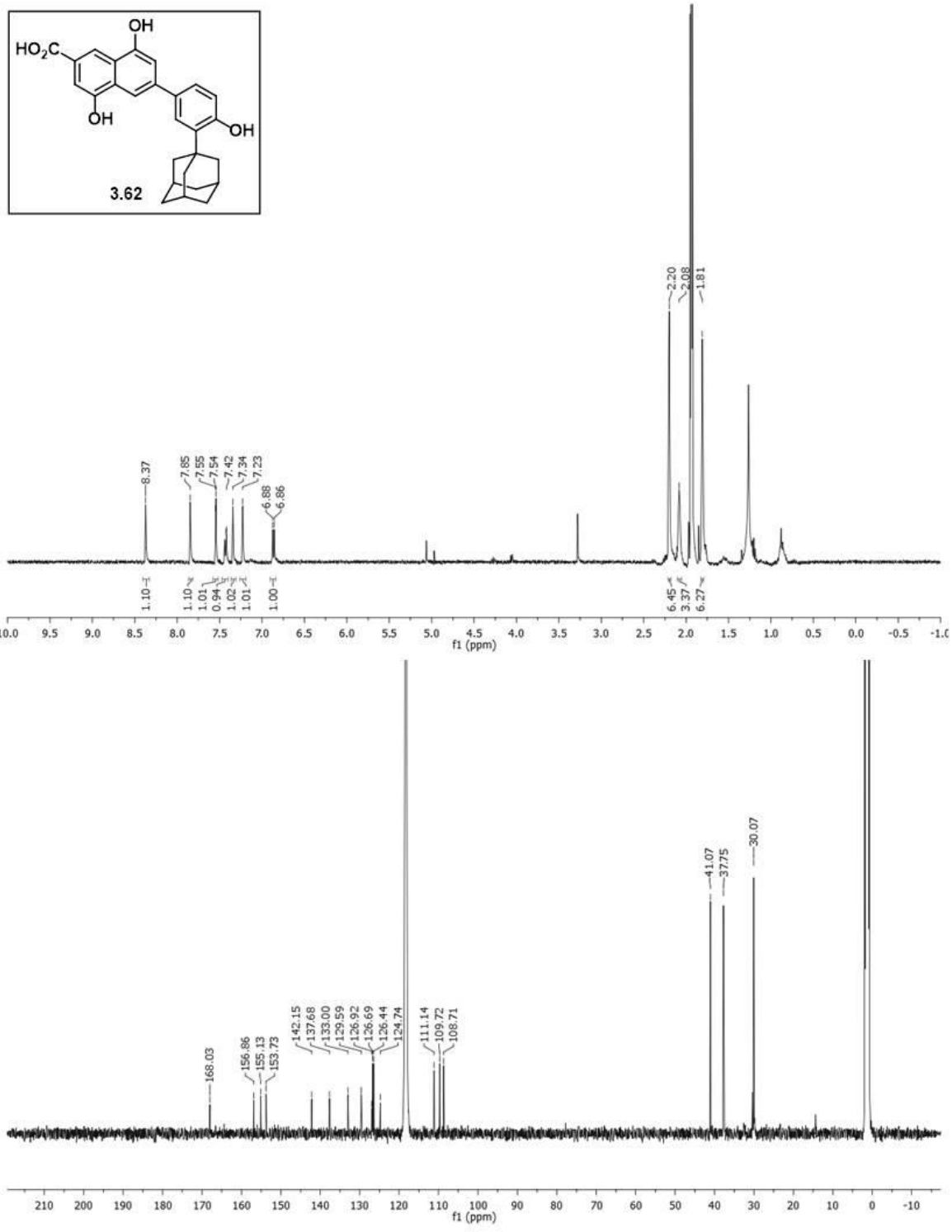
OH
HO2C
OH
OH
3.62
8.37
7.85
7.55
7.54
7.42
7.34
7.23
6.88
6.86
2.20
2.08
1.81
1.10
1.10
1.01
0.94
1.02
1.01
1.00
6.45
3.37
6.27
f1 (ppm)
168.03
156.86
155.13
153.73
142.15
137.68
133.00
129.59
126.92
126.69
126.44
124.74
111.14
109.72
108.71
41.07
37.75
30.07
f1 (ppm)

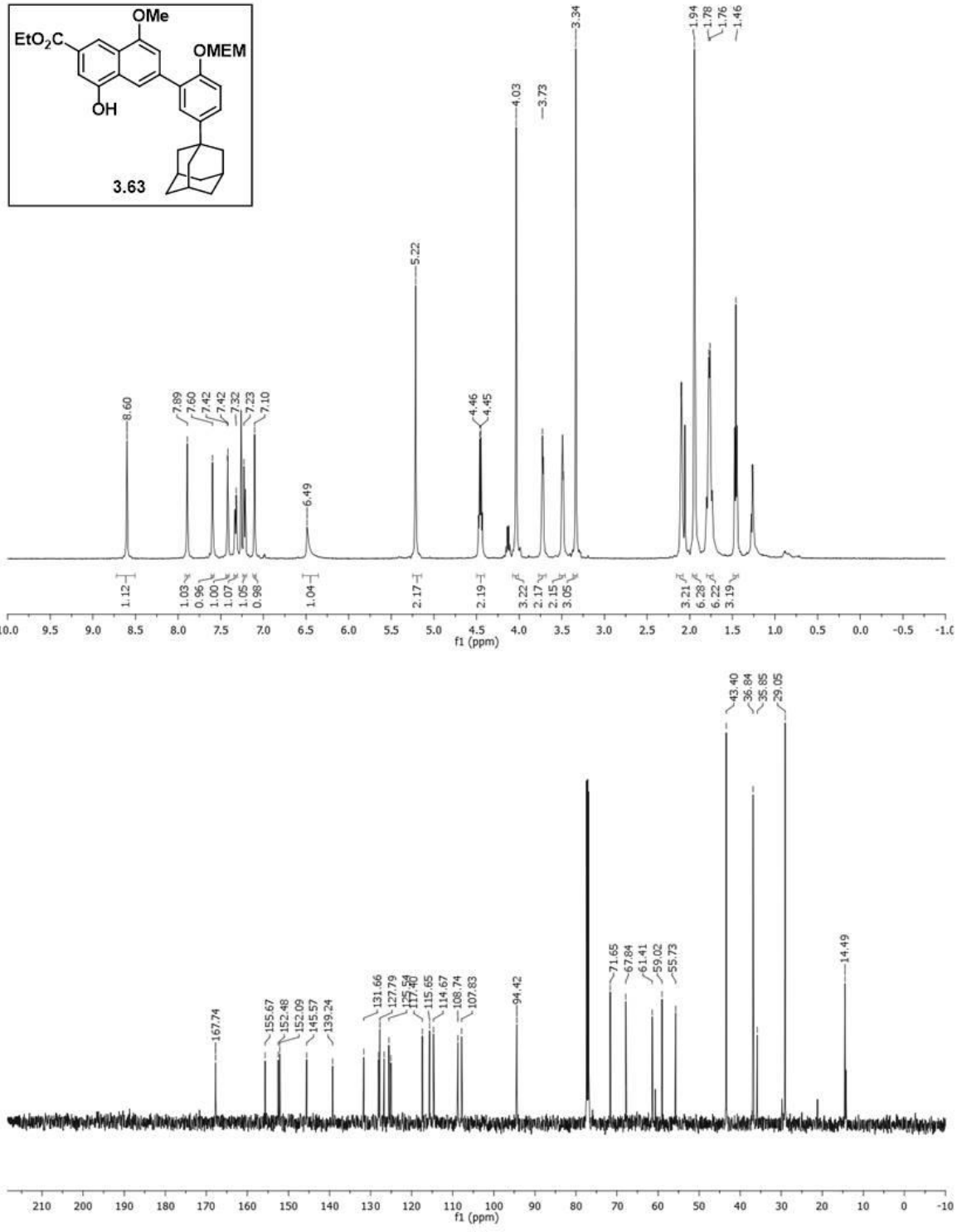
OMe
EtO2C
OMEM
OH
3.63
8.60
7.89
7.60
7.42
7.42
7.32
7.23
7.10
6.49
5.22
4.46
4.45
4.03
3.73
3.34
1.94
1.78
1.76
1.46
1.12
1.03
0.96
1.00
1.07
1.05
0.98
1.04
2.17
2.19
3.22
2.17
2.15
3.05
3.21
6.28
6.22
3.19
f1 (ppm)
167.74
155.67
152.48
152.09
145.57
139.24
131.66
127.79
125.54
117.40
115.65
114.67
108.74
107.83
94.42
71.65
67.84
61.41
59.02
55.73
43.40
36.84
35.85
29.05
14.49
f1 (ppm)

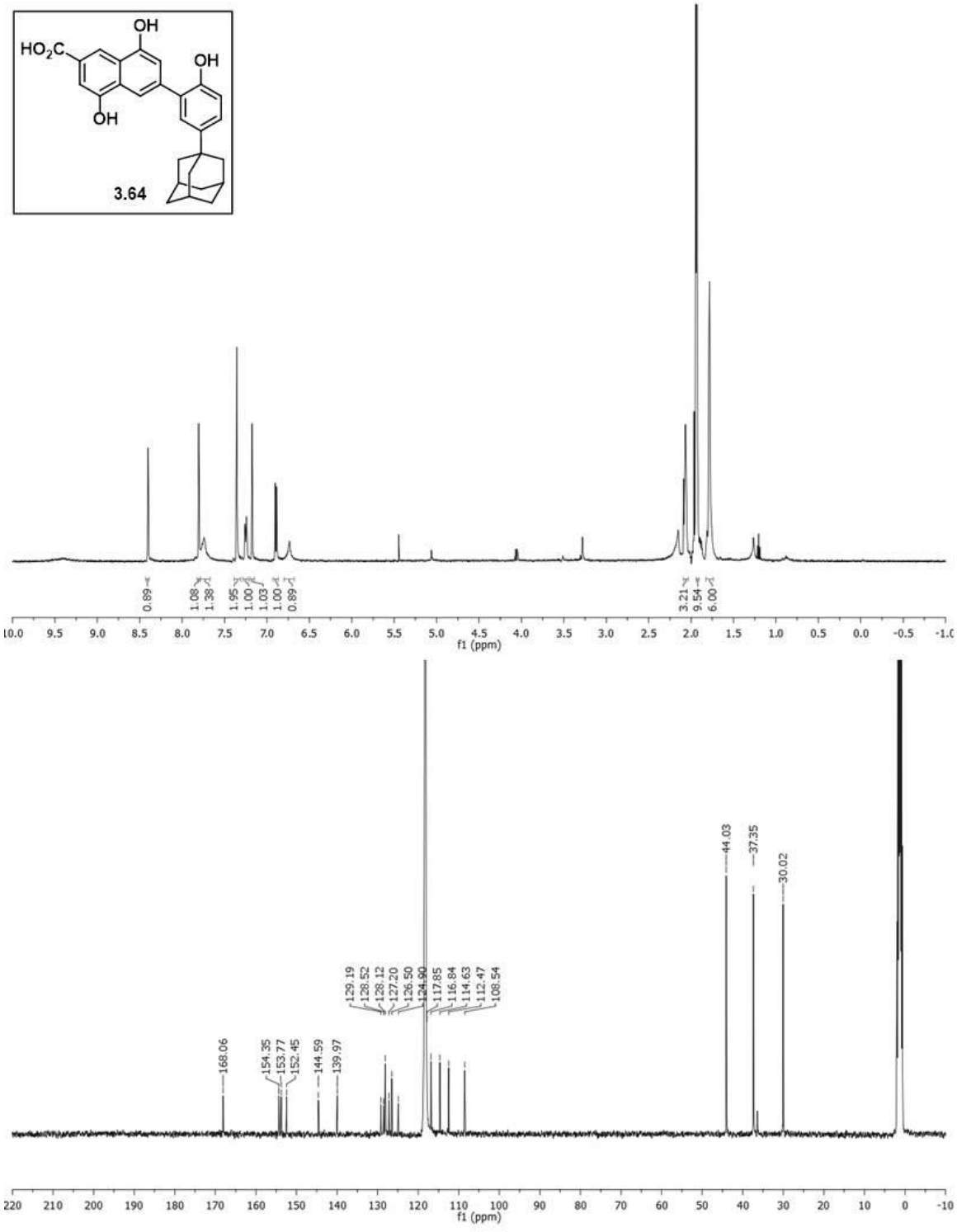
OH
HO2C
OH
OH
3.64
0.89
1.08
1.38
1.95
1.00
1.03
1.00
0.89
3.21
9.54
6.00
f1 (ppm)
168.06
154.35
153.77
152.45
144.59
139.97
129.19
128.52
128.12
127.20
126.50
124.80
117.85
116.84
114.63
112.47
108.54
44.03
37.35
30.02
f1 (ppm)

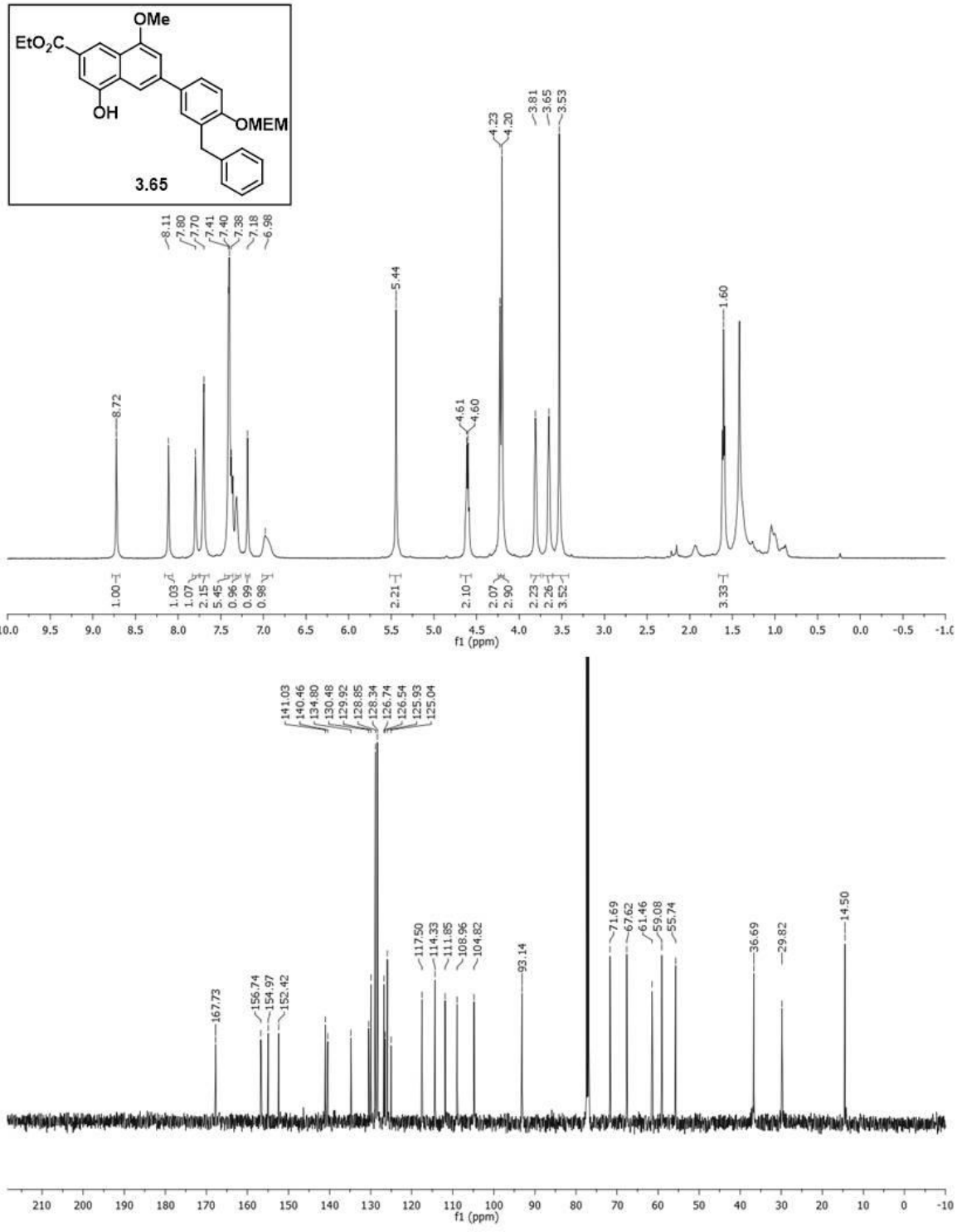
OMe
EtO2C
OH
OMEM
3.65
8.72
8.11
7.80
7.70
7.41
7.40
7.38
7.18
6.98
5.44
4.61
4.60
4.23
4.20
3.81
3.65
3.53
1.60
1.00
1.03
1.07
2.15
5.45
0.96
0.99
0.98
2.21
2.10
2.07
2.90
2.23
2.26
3.52
3.33
f1 (ppm)
141.03
140.46
134.80
130.48
129.92
128.85
128.34
126.74
126.54
125.93
125.04
167.73
156.74
154.97
152.42
117.50
114.33
111.85
108.96
104.82
93.14
71.69
67.62
61.46
59.08
55.74
36.69
29.82
14.50
f1 (ppm)

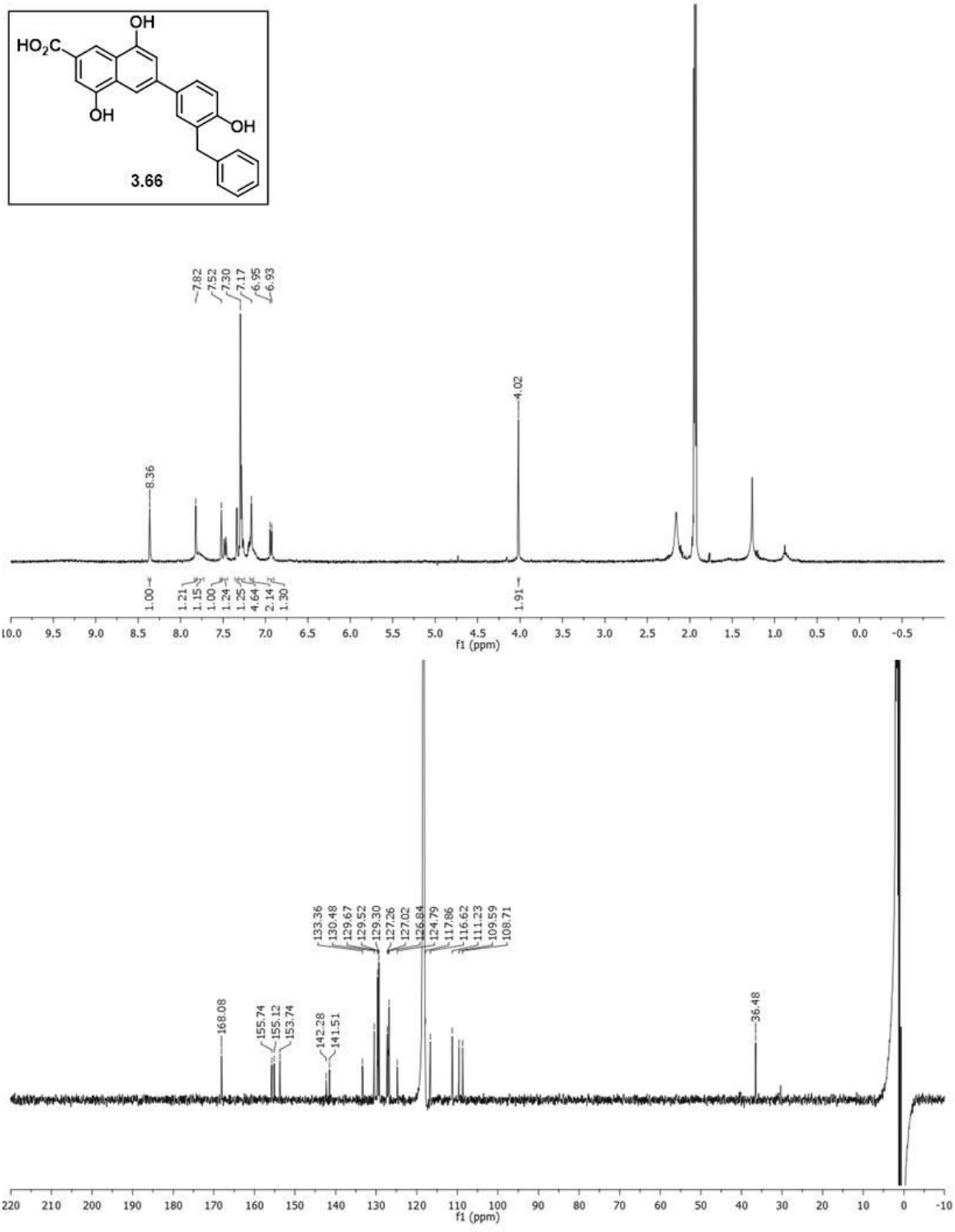
OH
HO2C
OH
OH
3.66
7.82
7.52
7.30
7.17
6.95
6.93
8.36
4.02
1.00
1.21
1.15
1.00
1.24
1.25
4.64
2.14
1.30
1.91
f1 (ppm)
133.36
130.48
129.67
129.52
129.30
127.26
127.02
126.84
124.79
117.86
116.62
111.23
109.59
108.71
168.08
155.74
155.12
153.74
142.28
141.51
36.48
f1 (ppm)

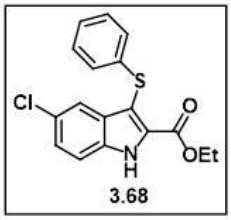
Cl
S
O
OEt
N
H

3.68

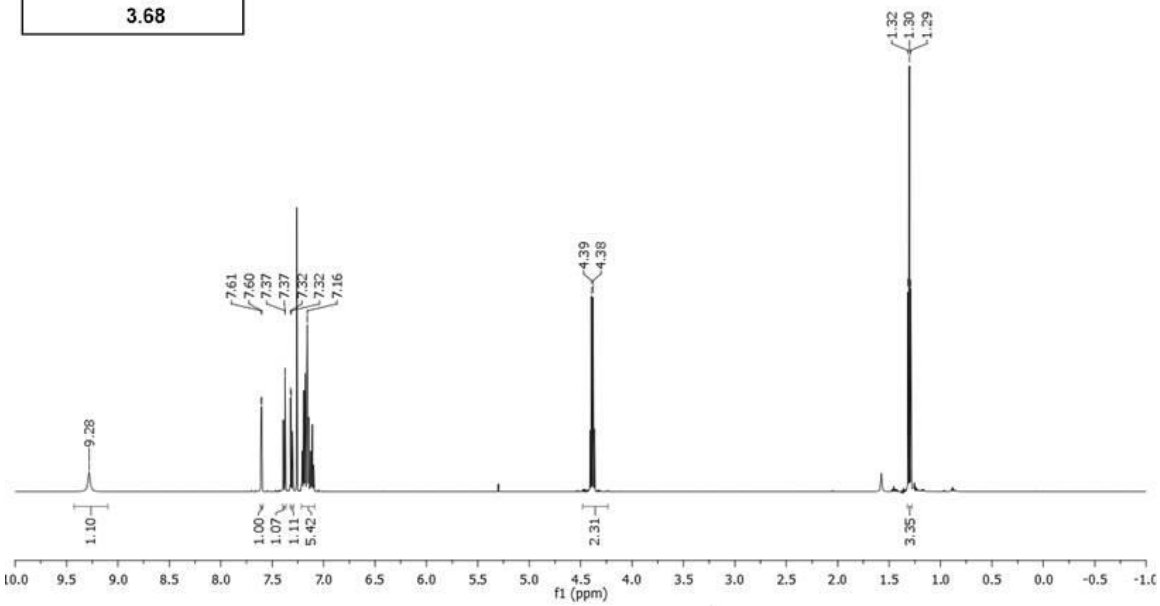
9.28
7.61
7.60
7.37
7.37
7.32
7.32
7.16
4.39
4.38
1.32
1.30
1.29
1.10
1.00
1.07
1.11
5.42
2.31
3.35
f1 (ppm)

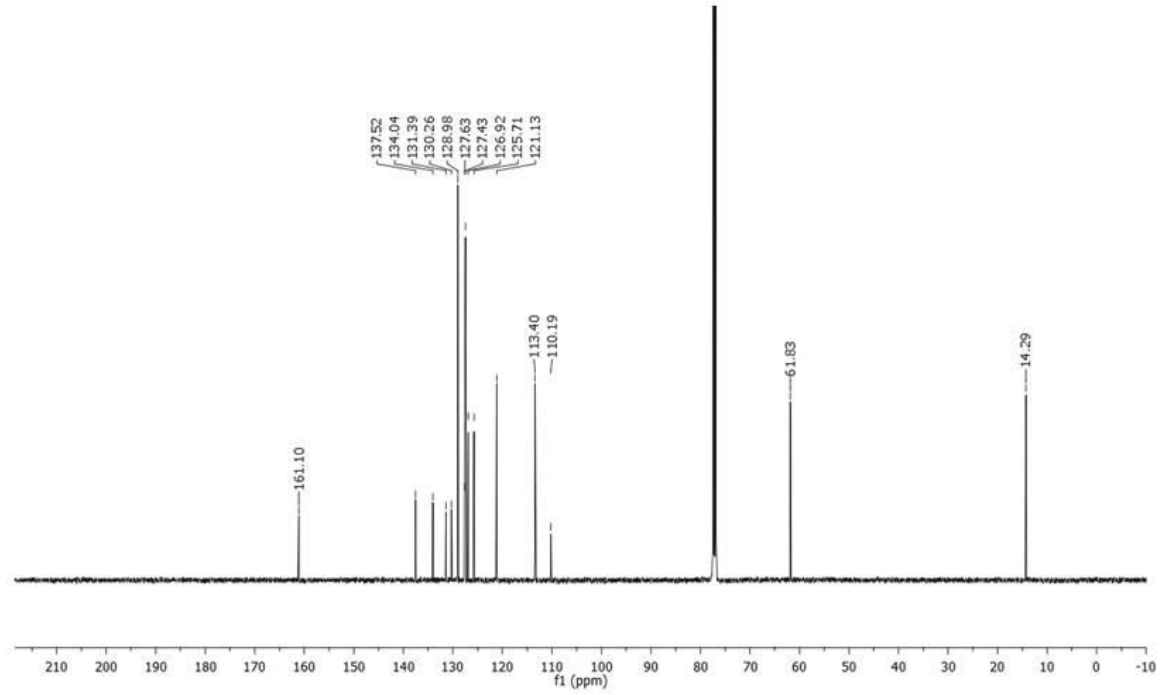
137.52
134.04
131.39
130.26
128.98
127.63
127.43
126.92
125.71
121.13
113.40
110.19
161.10
61.83
14.29
f1 (ppm)

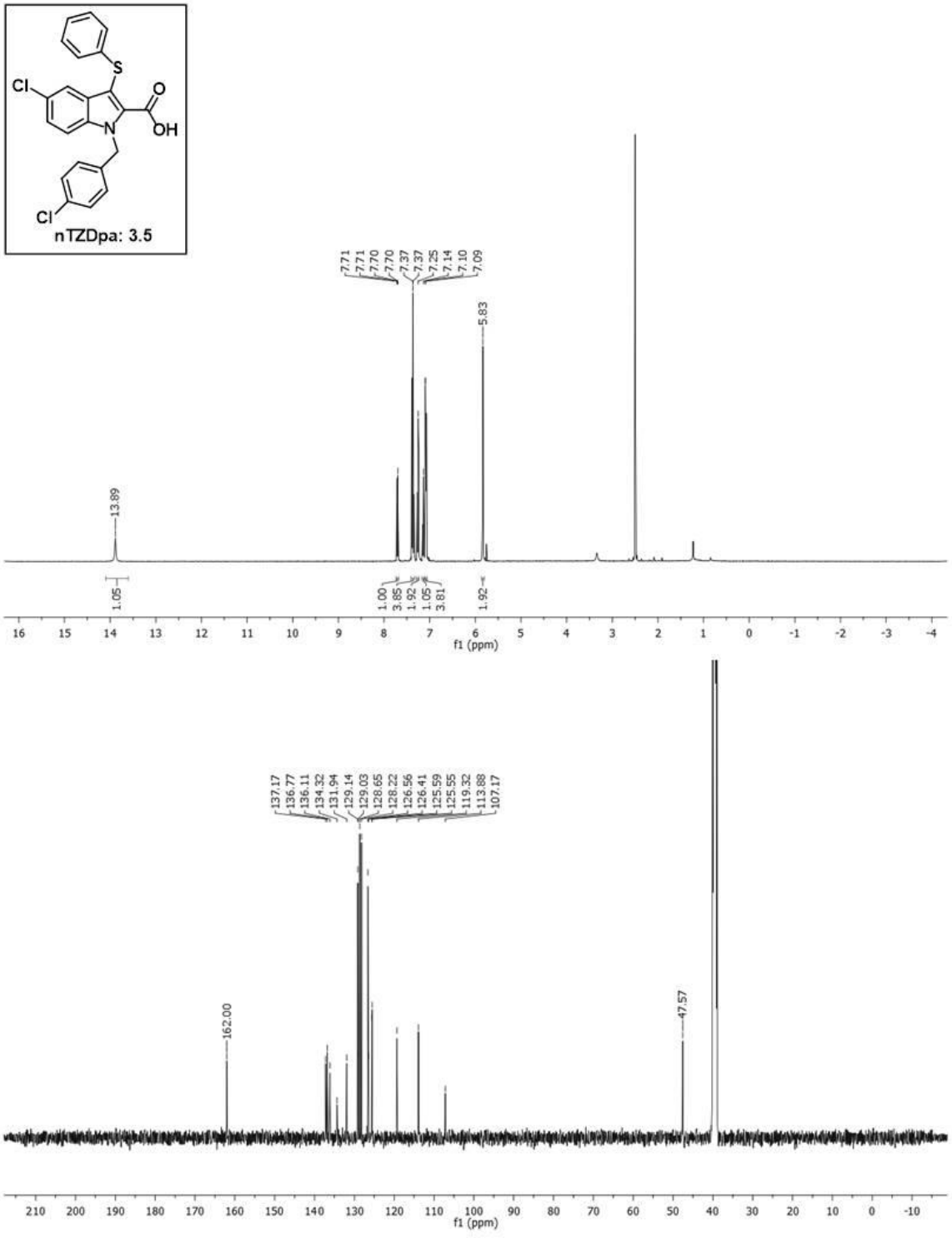
nTZDpa: 3.5
7.71
7.71
7.70
7.70
7.37
7.37
7.25
7.14
7.10
7.09
5.83
13.89
1.05
1.00
3.85
1.92
1.05
3.81
1.92
f1 (ppm)
137.17
136.77
136.11
134.32
131.94
129.14
129.03
128.65
128.22
126.56
126.41
125.59
125.55
119.32
113.88
107.17
162.00
47.57
f1 (ppm)

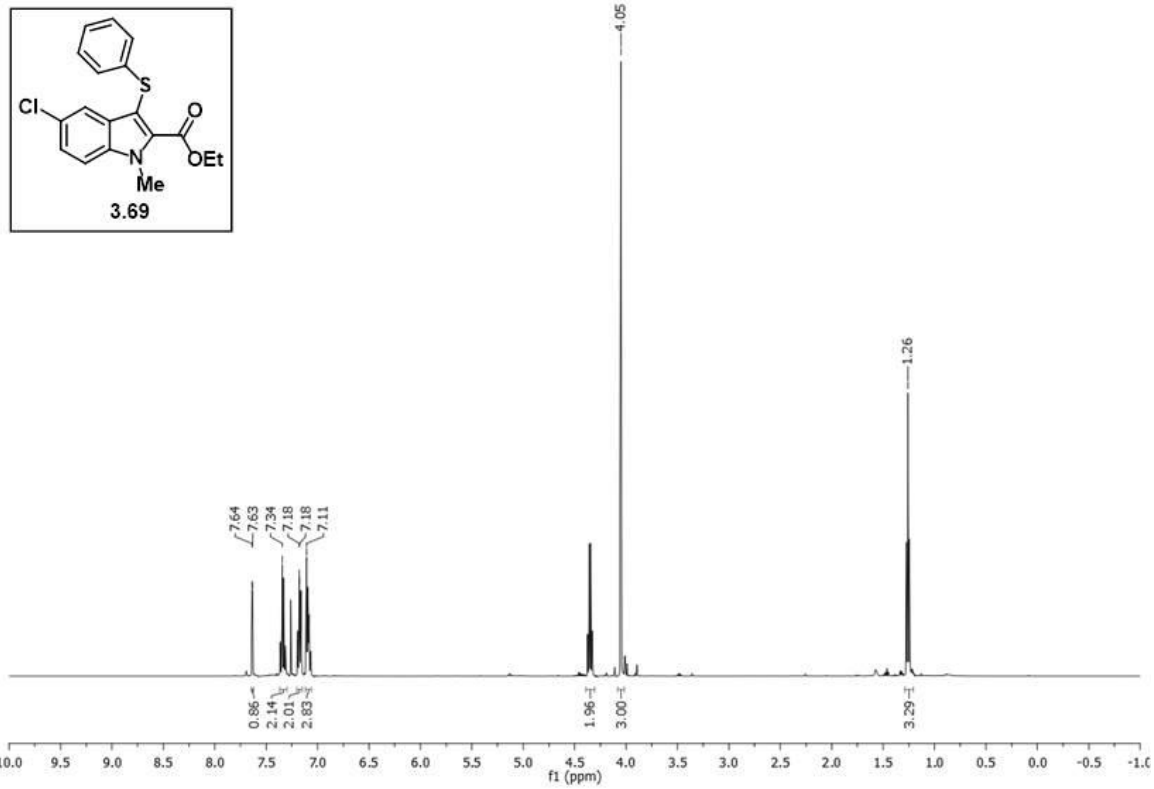
Cl
S
O
OEt
N
Me
3.69
4.05
1.26
7.64
7.63
7.34
7.18
7.18
7.11
0.86
2.14
2.01
2.83
1.96
3.00
3.29
f1 (ppm)

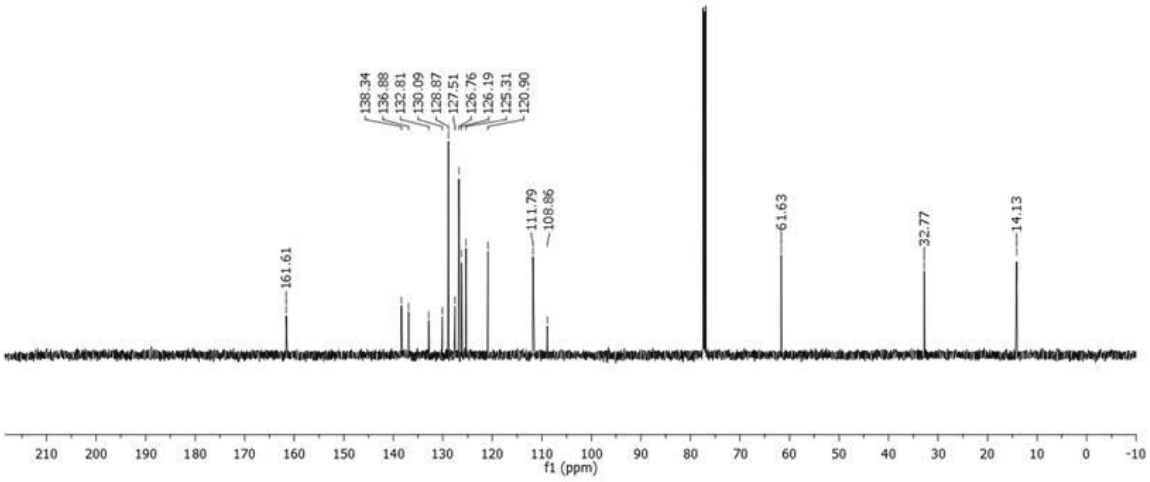
138.34
136.88
132.81
130.09
128.87
127.51
126.76
126.19
125.31
120.90
111.79
108.86
161.61
61.63
32.77
14.13
f1 (ppm)

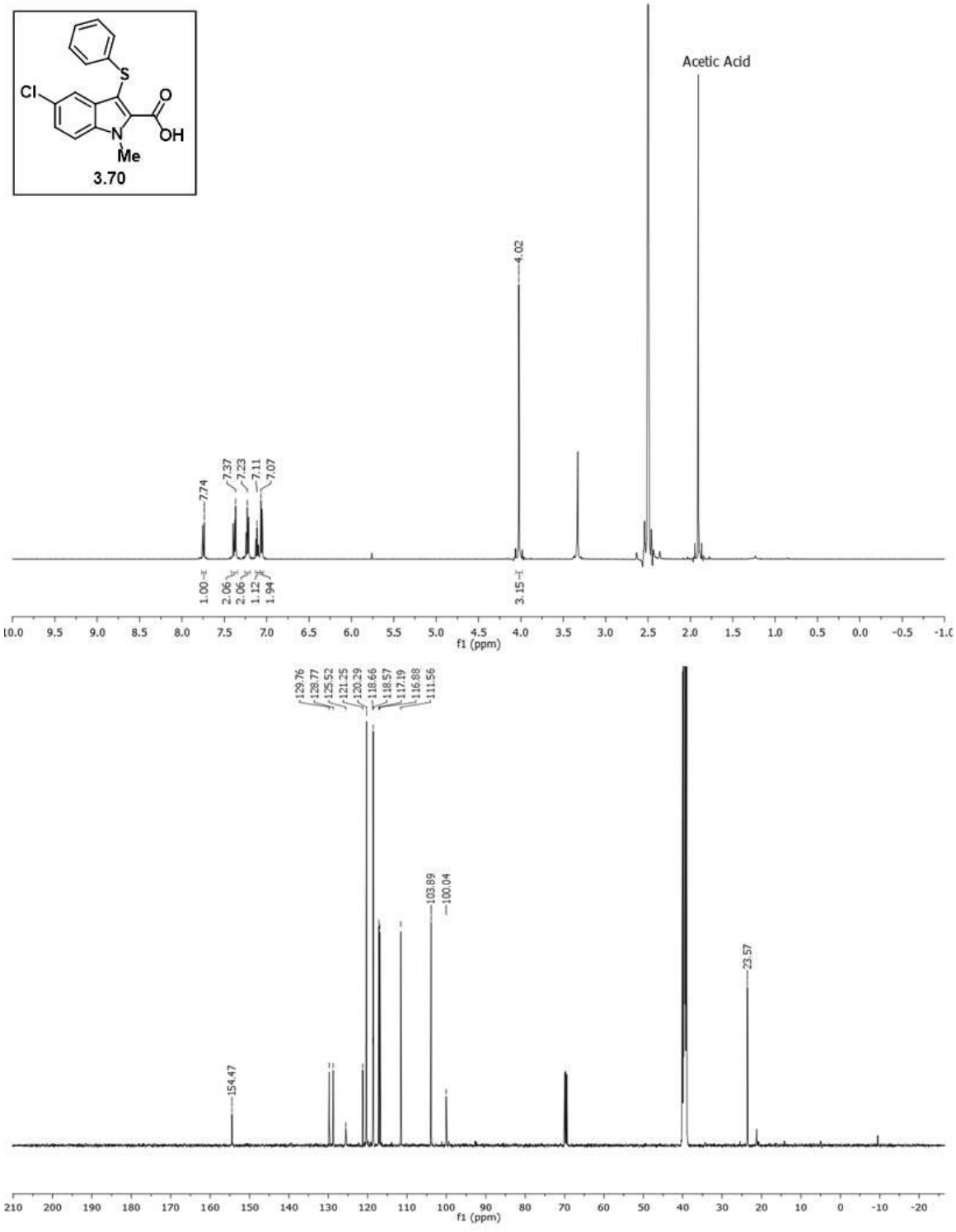
Cl
S
O
OH
N
Me
3.70
Acetic Acid
4.02
7.74
7.37
7.23
7.11
7.07
1.00
2.06
2.06
1.12
1.94
3.15
f1 (ppm)
129.76
128.77
125.52
121.25
120.29
118.66
118.57
117.19
116.88
111.56
103.89
100.04
23.57
154.47
f1 (ppm)

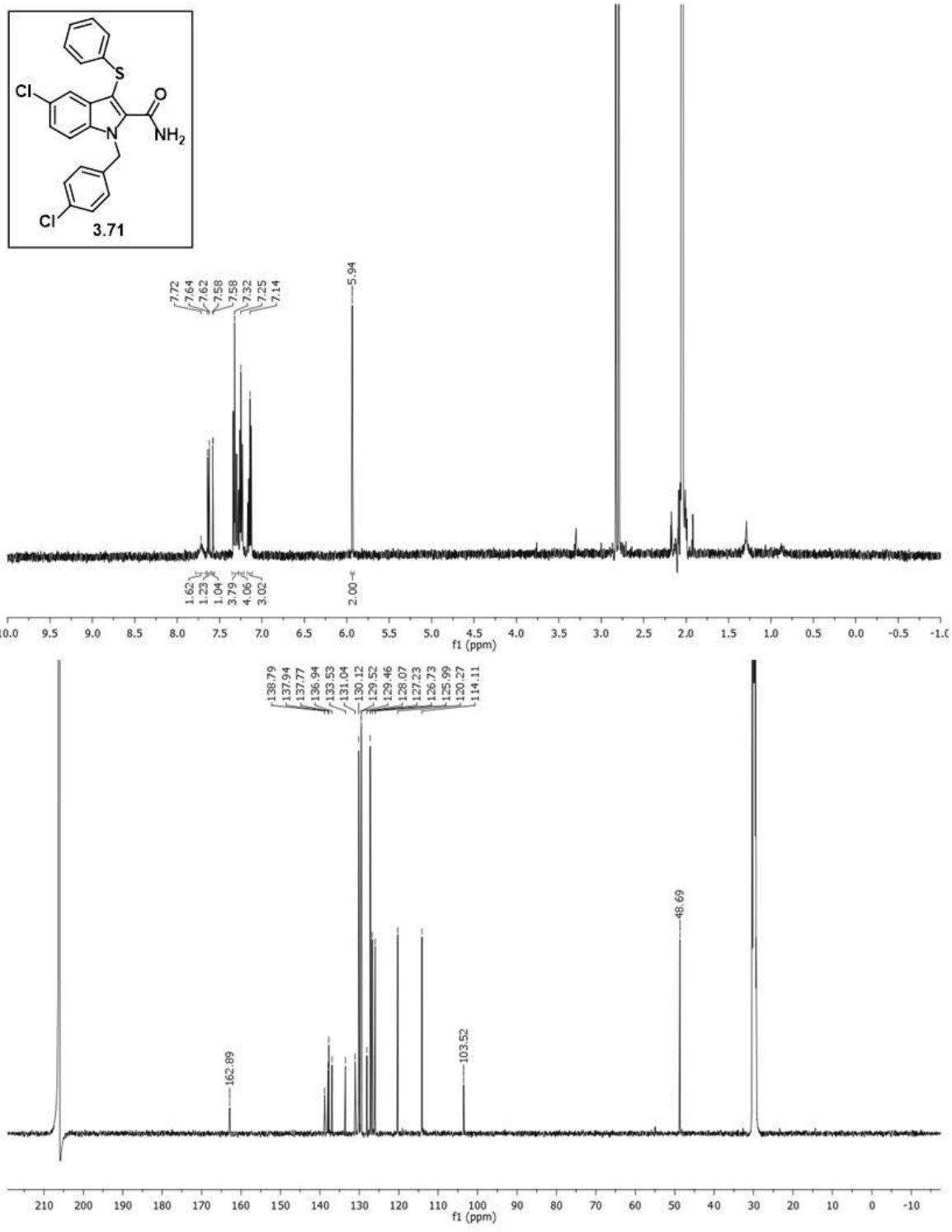
Cl
S
O
N
NH2
Cl
3.71
7.72
7.64
7.62
7.58
7.58
7.32
7.25
7.14
5.94
1.62
1.23
1.04
3.79
4.06
3.02
2.00
f1 (ppm)
138.79
137.94
137.77
136.94
133.53
131.04
130.12
129.52
129.46
128.07
127.23
126.73
125.99
120.27
114.11
48.69
162.89
103.52
f1 (ppm)

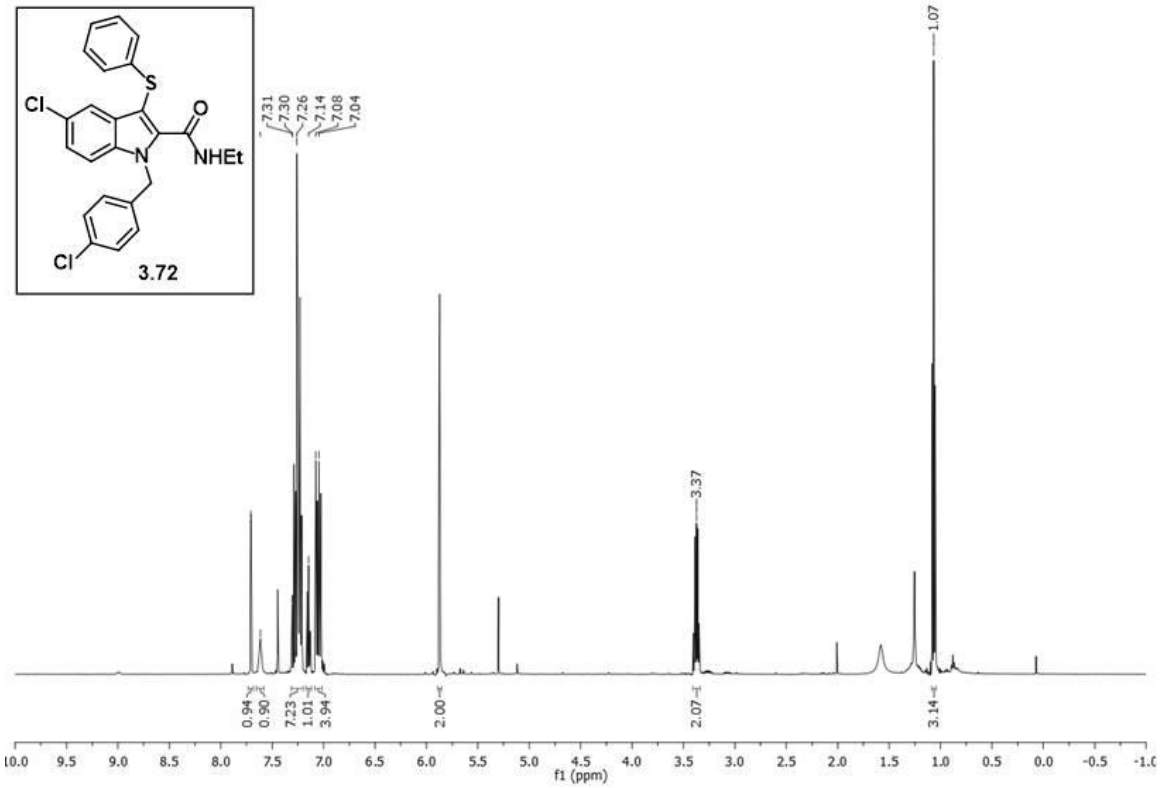
Cl
S
O
N
NHEt
Cl
3.72
7.31
7.30
7.26
7.14
7.08
7.04
1.07
3.37
0.94
0.90
7.23
1.01
3.94
2.00
2.07
3.14
f1 (ppm)

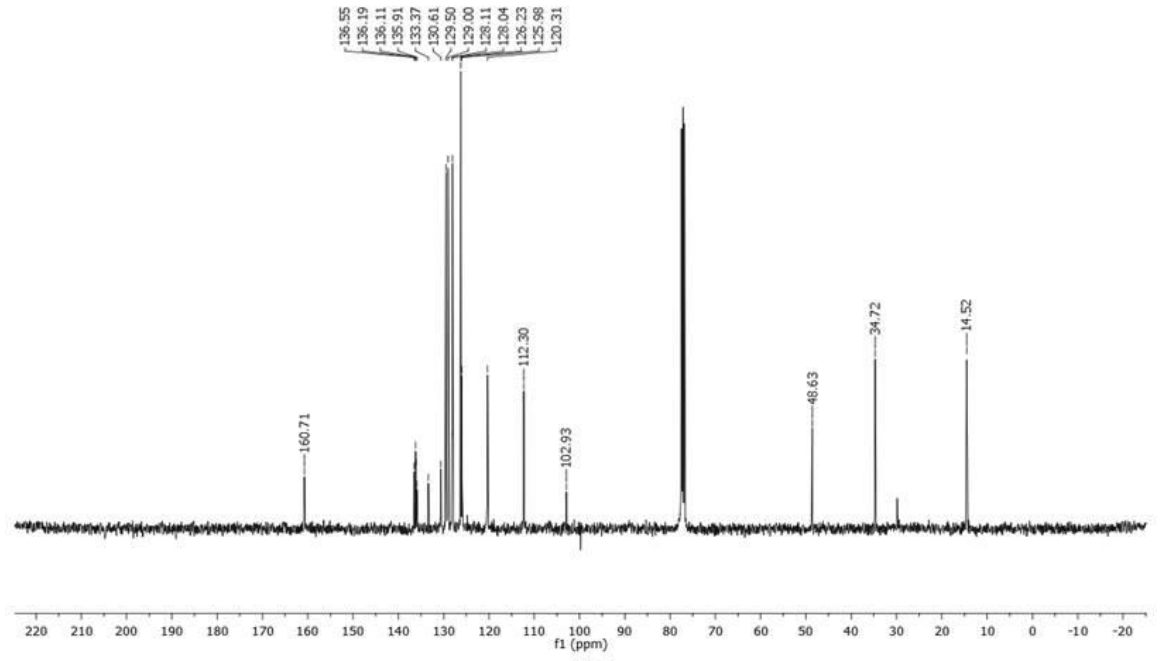
136.55
136.19
136.11
135.91
133.37
130.61
129.50
129.00
128.11
128.04
126.23
125.98
120.31
160.71
112.30
102.93
48.63
34.72
14.52
f1 (ppm)

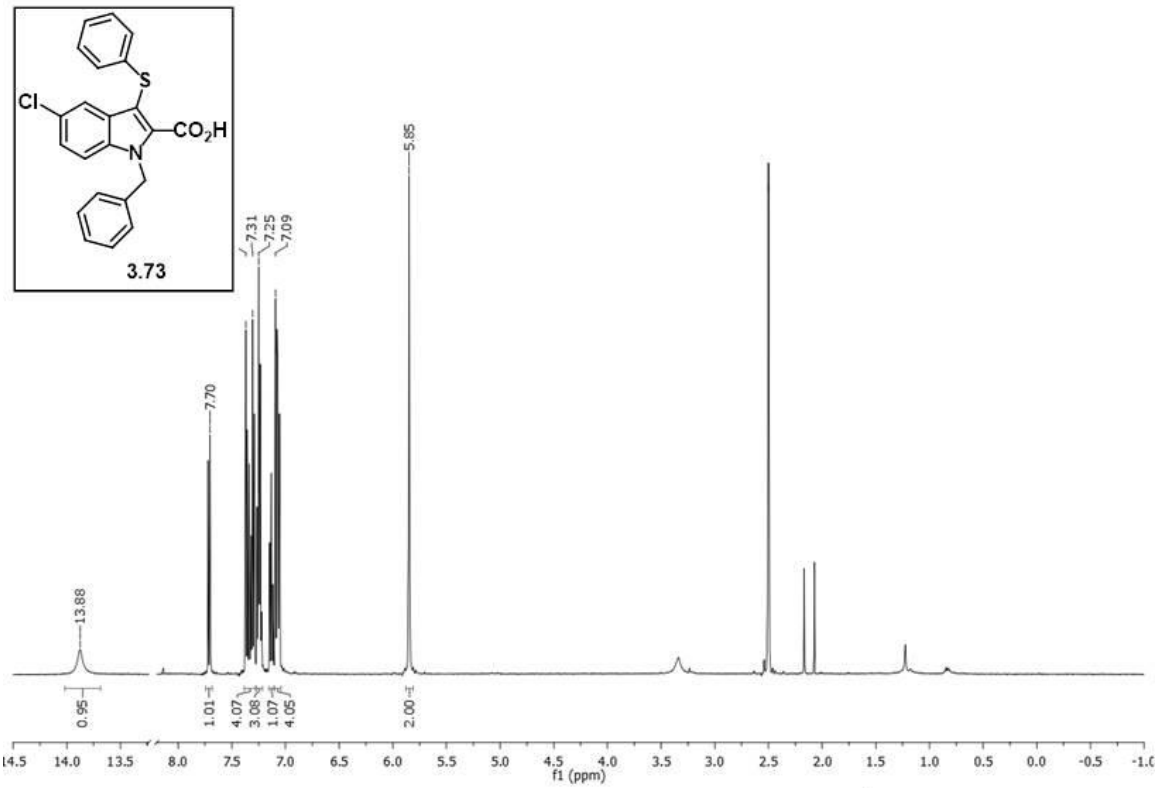
Cl
S
CO2H
N
3.73
13.88
7.70
7.31
7.25
7.09
5.85
0.95
1.01
4.07
3.08
1.07
4.05
2.00
f1 (ppm)

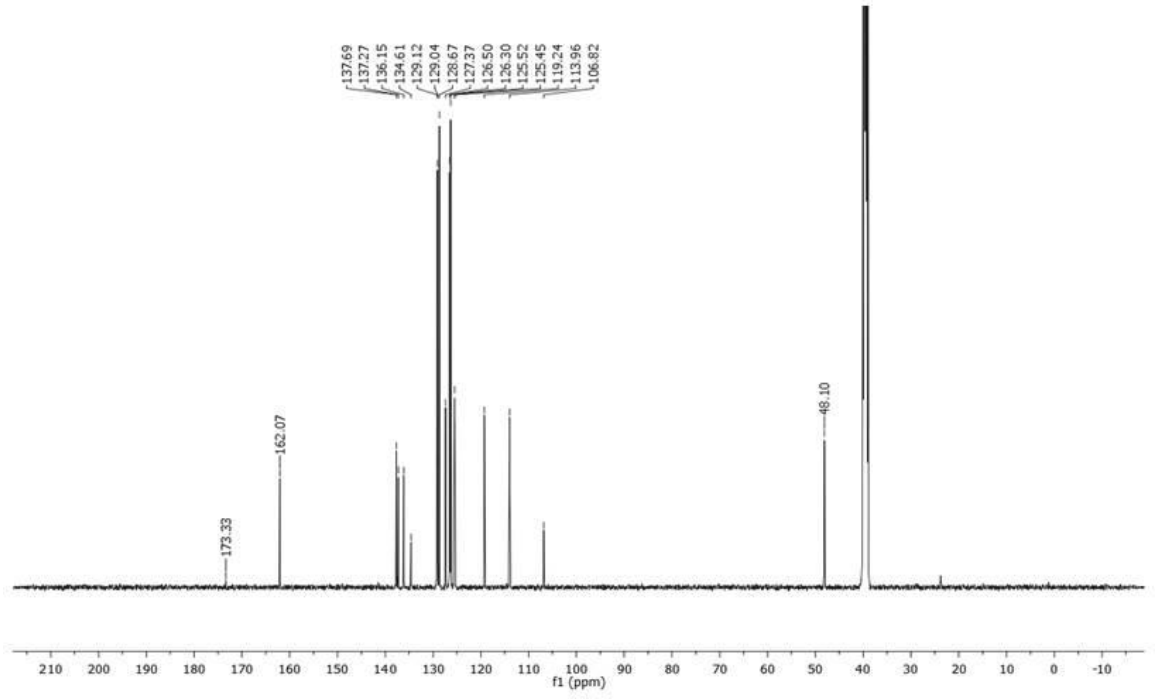
137.69
137.27
136.15
134.61
129.12
129.04
128.67
127.37
126.50
126.30
125.52
125.45
119.24
113.96
106.82
173.33
162.07
48.10
f1 (ppm)

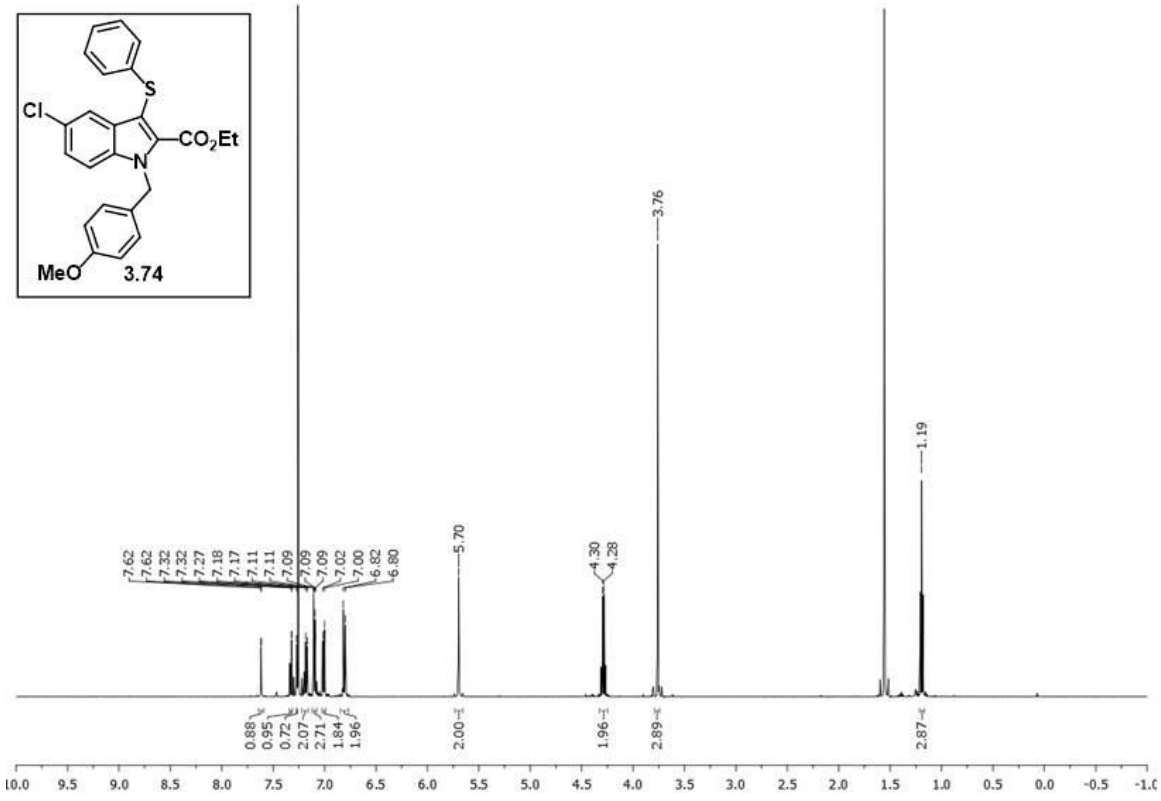
Cl
S
CO2Et
N
MeO
3.74
7.62
7.62
7.32
7.32
7.27
7.18
7.17
7.11
7.11
7.09
7.09
7.09
7.09
7.02
7.00
6.82
6.80
5.70
4.30
4.28
3.76
1.19
0.88
0.95
0.72
2.07
2.71
1.84
1.96
2.00
1.96
2.89
2.87

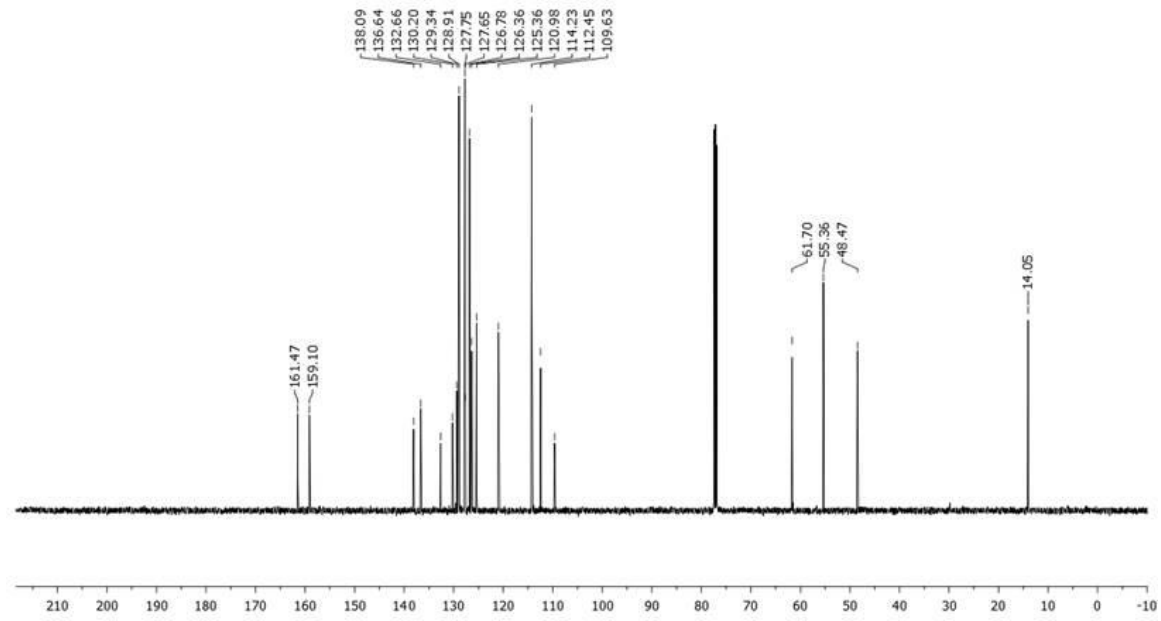
138.09
136.64
132.66
130.20
129.34
128.91
127.75
127.65
126.78
126.36
125.36
120.98
114.23
112.45
109.63
161.47
159.10
61.70
55.36
48.47
14.05

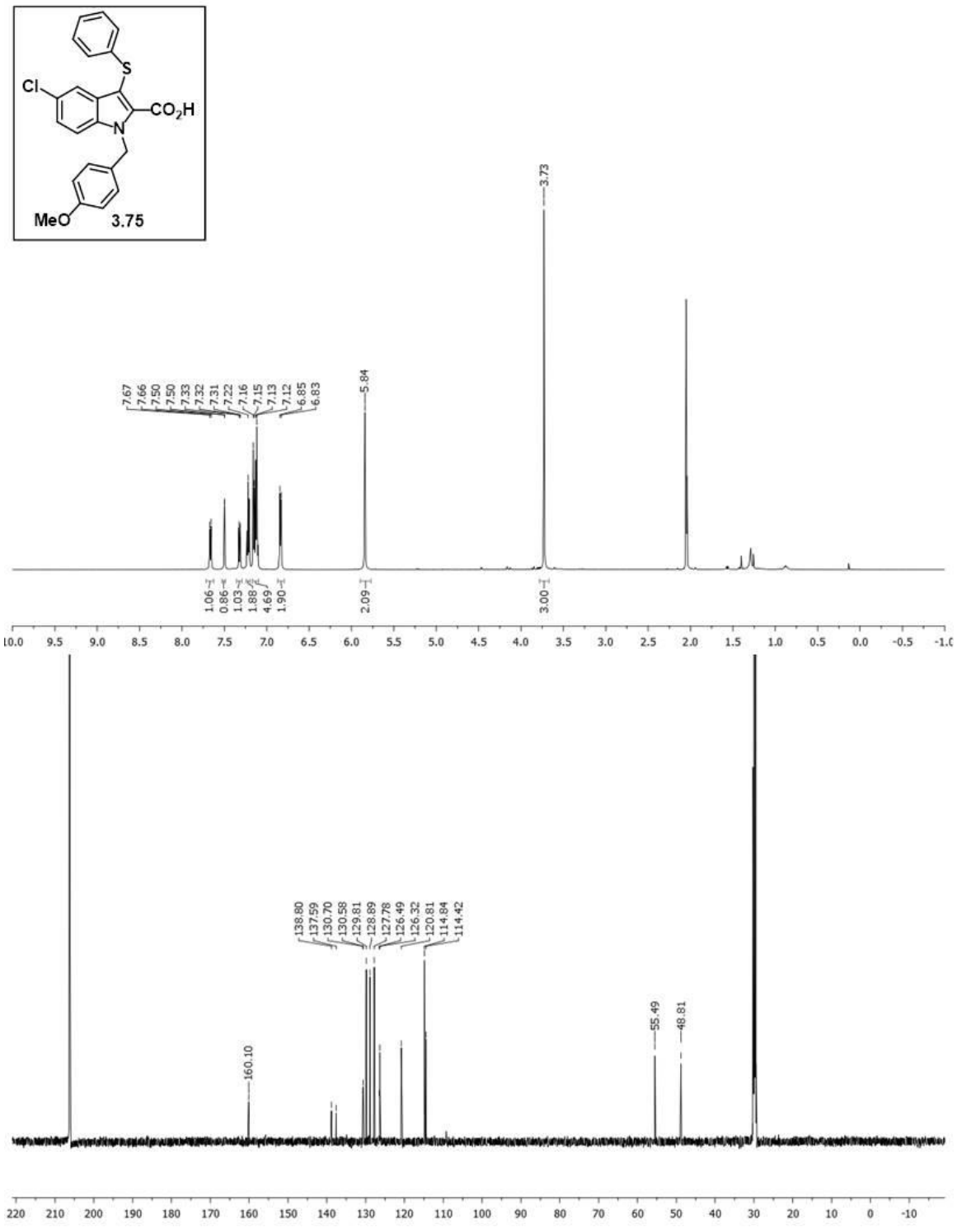
Cl
S
CO2H
N
MeO
3.75
7.67
7.66
7.50
7.50
7.33
7.32
7.31
7.22
7.16
7.15
7.13
7.12
6.85
6.83
5.84
3.73
1.06
0.86
1.03
1.88
4.69
1.90
2.09
3.00
138.80
137.59
130.70
130.58
129.81
128.89
127.78
126.49
126.32
120.81
114.84
114.42
160.10
55.49
48.81

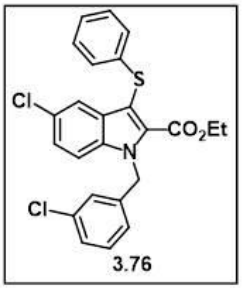
S
Cl
CO2Et
N
Cl

3.76

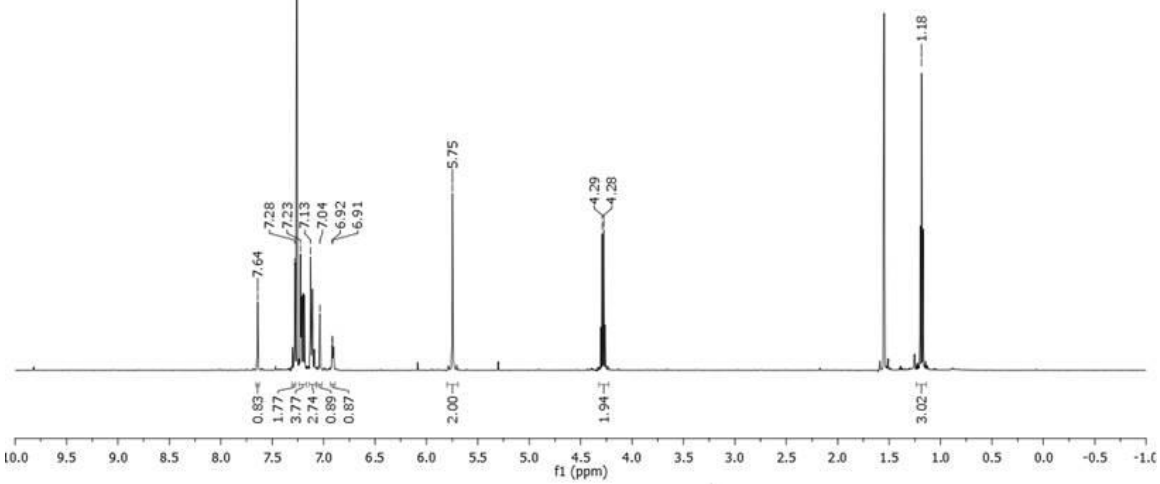
7.64
7.28
7.23
7.13
7.04
6.92
6.91
5.75
4.29
4.28
1.18
0.83
1.77
3.77
2.74
0.89
0.87
2.00
1.94
3.02
f1 (ppm)

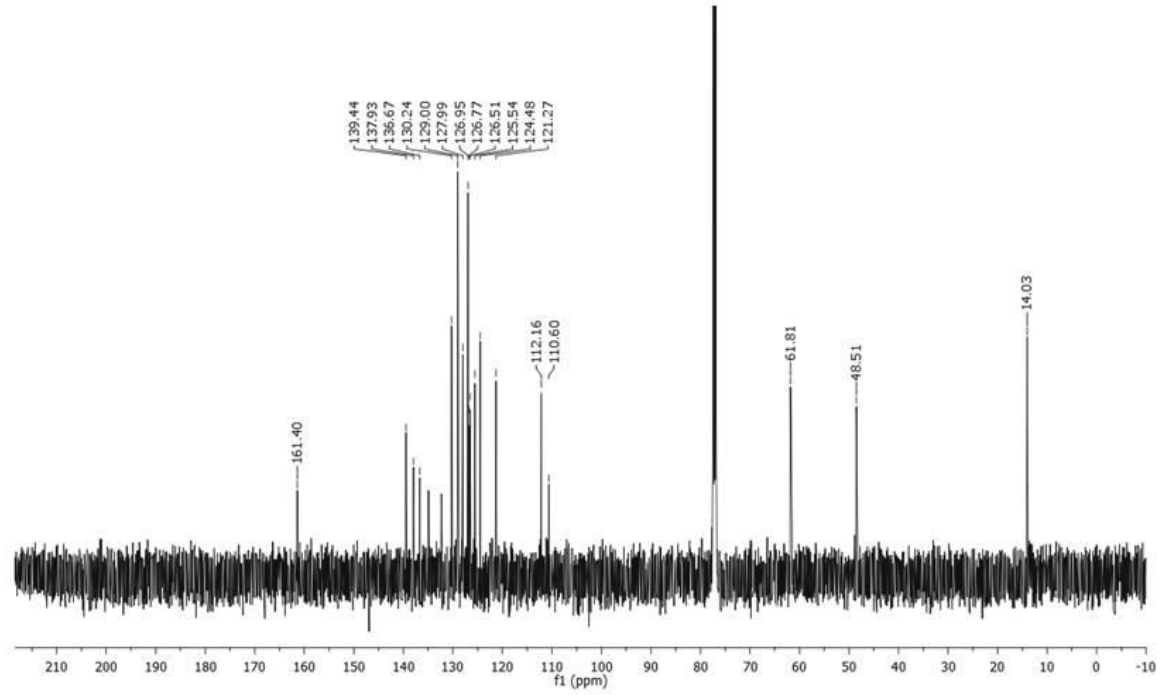
139.44
137.93
136.67
130.24
129.00
127.99
126.95
126.77
126.51
125.54
124.48
121.27
112.16
110.60
161.40
61.81
48.51
14.03
f1 (ppm)

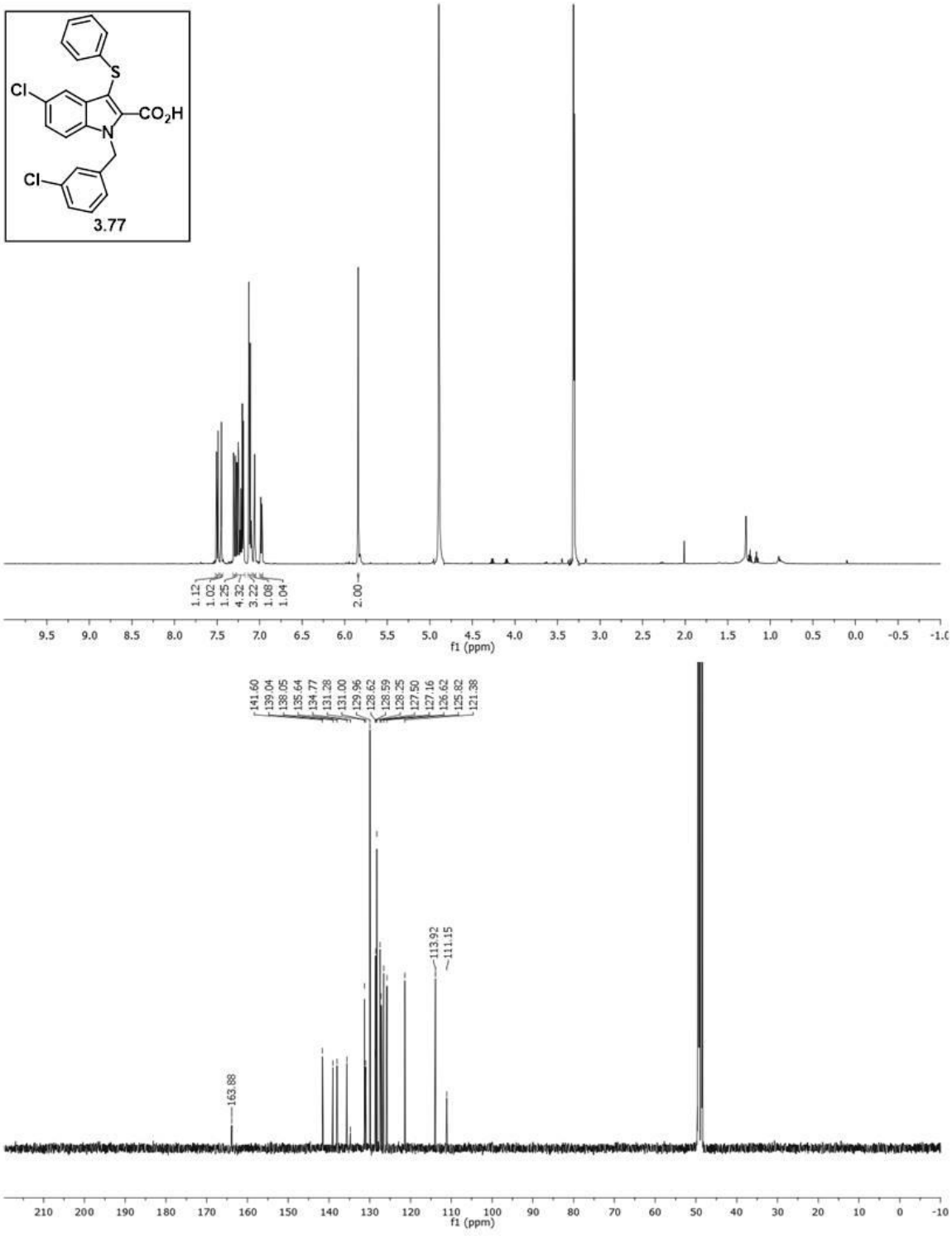
Cl
S
CO2H
N
Cl
3.77
1.12
1.02
1.25
4.32
3.22
1.08
1.04
2.00
f1 (ppm)
141.60
139.04
138.05
135.64
134.77
131.28
131.00
129.96
128.62
128.59
128.25
127.50
127.16
126.62
125.82
121.38
113.92
111.15
163.88
f1 (ppm)

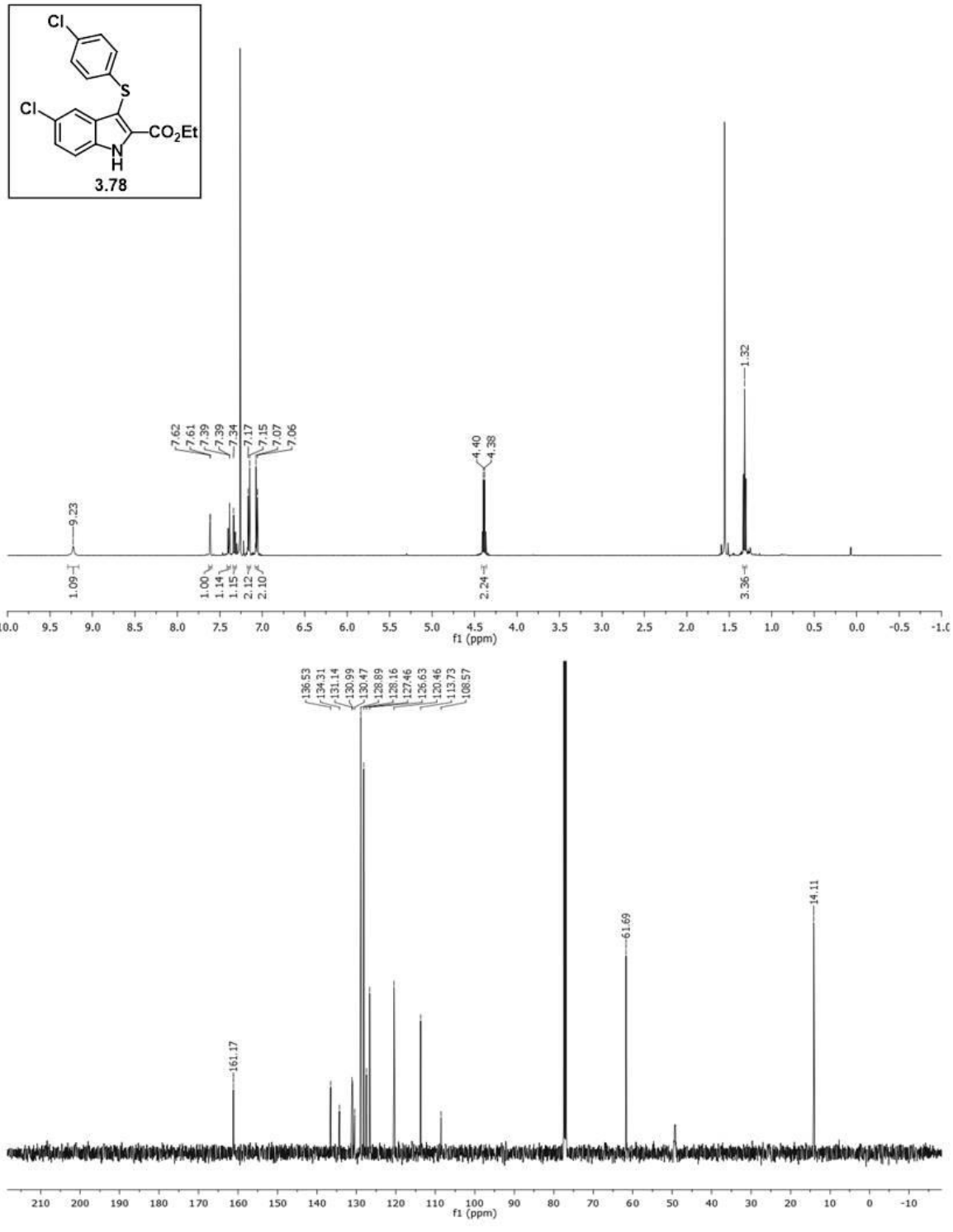
Cl
S
Cl
CO2Et
N
H
3.78
9.23
7.62
7.61
7.39
7.39
7.34
7.17
7.15
7.07
7.06
4.40
4.38
1.32
1.09
1.00
1.14
1.15
2.12
2.10
2.24
3.36
f1 (ppm)
136.53
134.31
131.14
130.99
130.47
128.89
128.16
127.46
126.63
120.46
113.73
108.57
161.17
61.69
14.11
f1 (ppm)

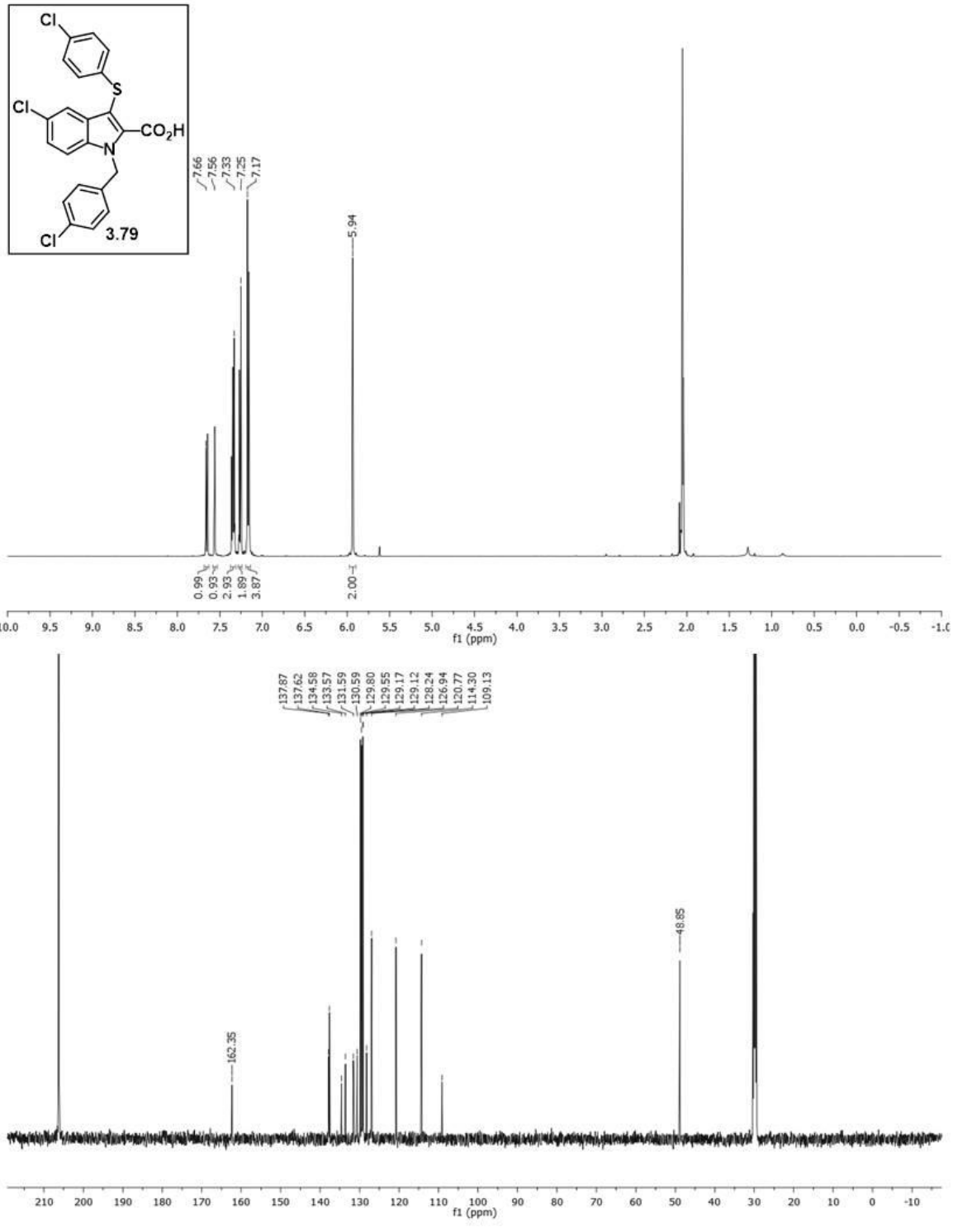
Cl
S
Cl
CO2H
N
Cl
3.79
7.66
7.56
7.33
7.25
7.17
5.94
0.99
0.93
2.93
1.89
3.87
2.00
f1 (ppm)
137.87
137.62
134.58
133.57
131.59
130.59
129.80
129.55
129.17
129.12
128.24
126.94
120.77
114.30
109.13
162.35
48.85
f1 (ppm)

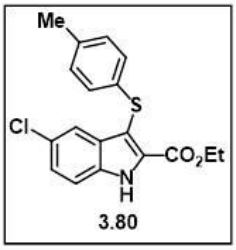
Me
S
Cl
CO2Et
N
H

3.80

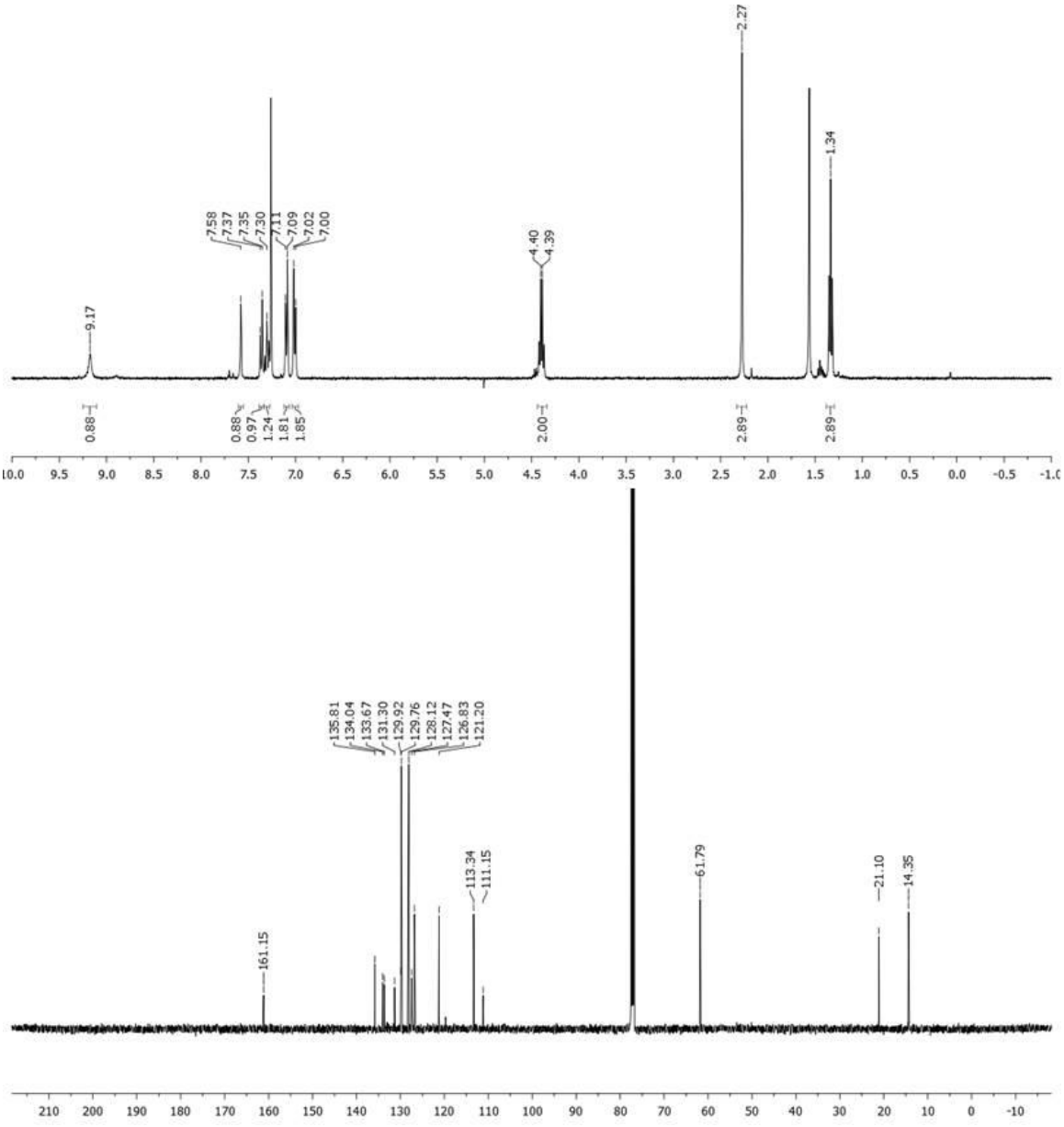
9.17
7.58
7.37
7.35
7.30
7.11
7.09
7.02
7.00
4.40
4.39
2.27
1.34
0.88
0.88
0.97
1.24
1.81
1.85
2.00
2.89
2.89
135.81
134.04
133.67
131.30
129.92
129.76
128.12
127.47
126.83
121.20
113.34
111.15
161.15
61.79
21.10
14.35

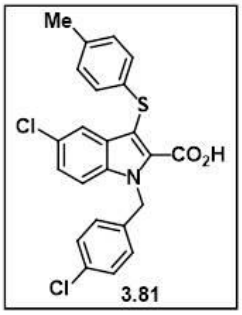
Me
S
Cl
CO2H
N
Cl
3.81

7.63
7.63
7.61
7.61
7.52
7.52
7.51
7.51
7.32
7.16
7.14
7.12
7.10
7.06
7.05
5.91
2.24
1.06
1.02
3.14
2.09
2.14
2.05
2.00
3.00

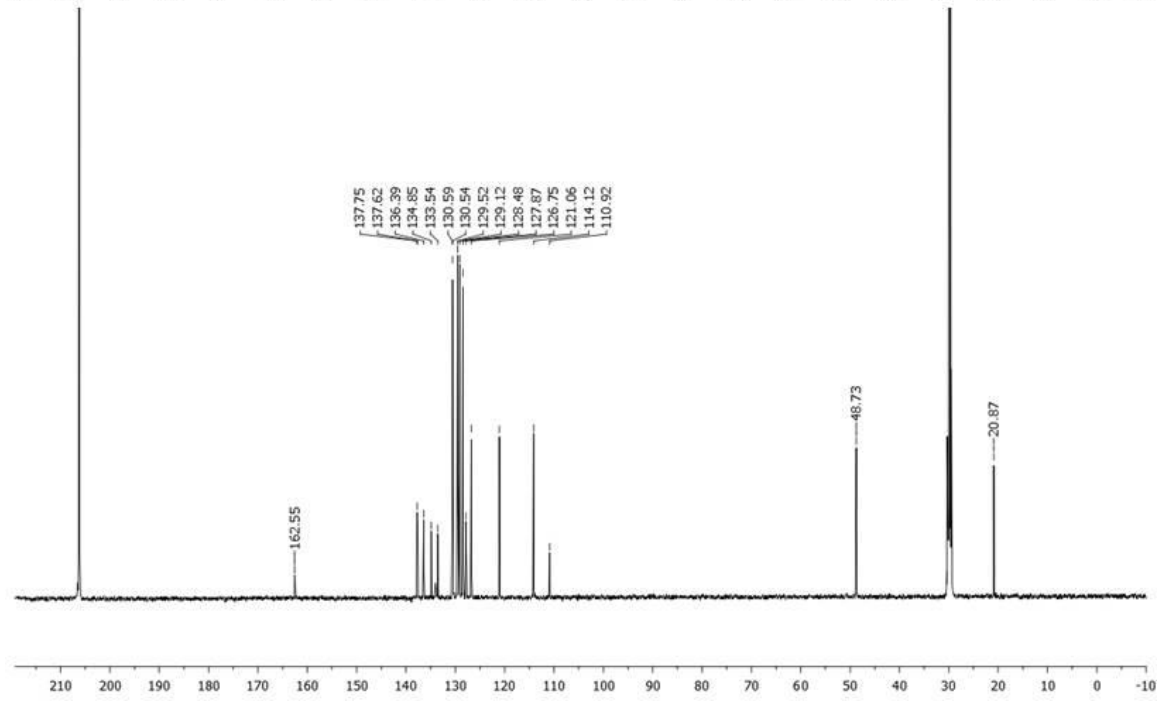
137.75
137.62
136.39
134.85
133.54
130.59
130.54
129.52
129.12
128.48
127.87
126.75
121.06
114.12
110.92
162.55
48.73
20.87

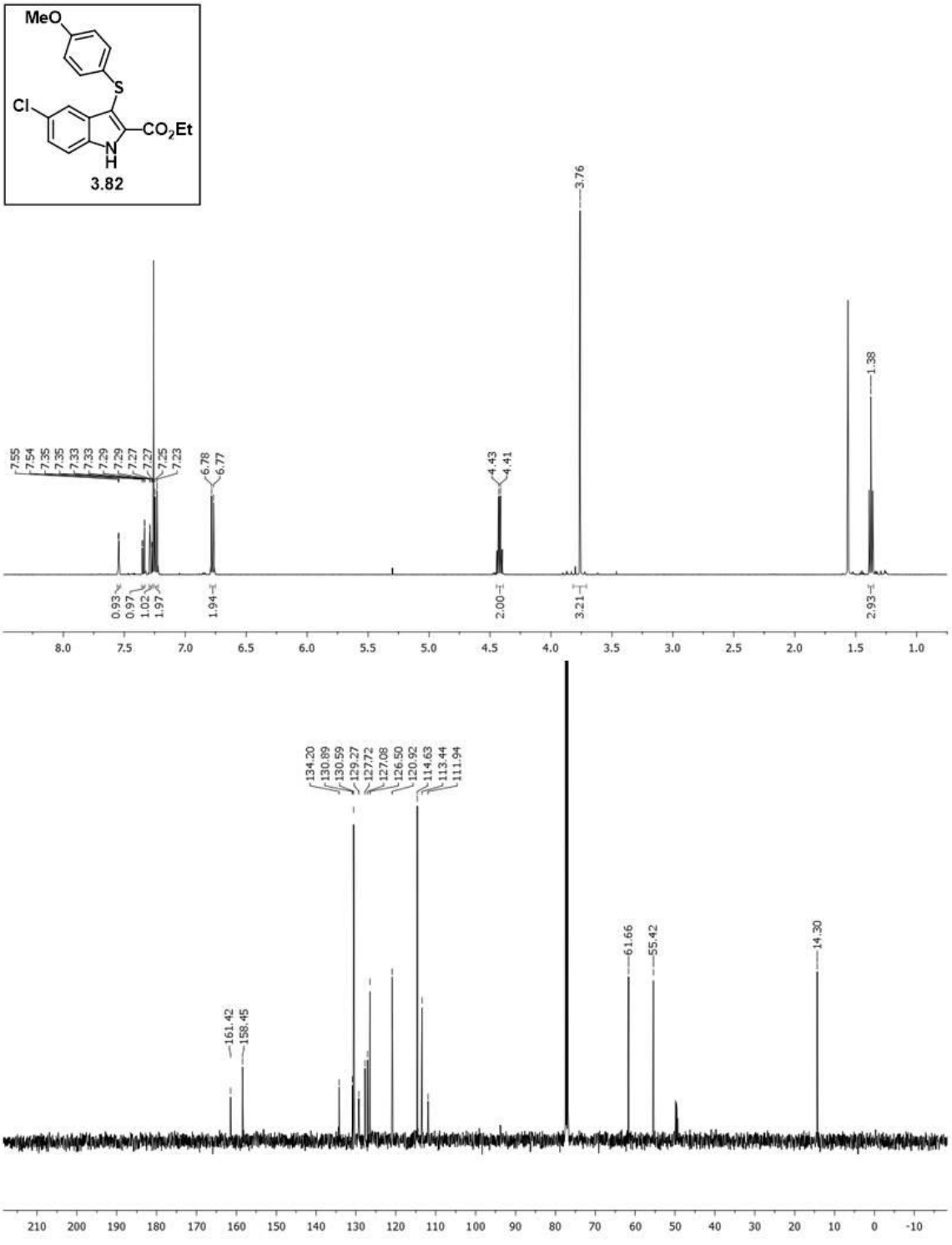
MeO
S
Cl
CO2Et
N
H
3.82
7.55
7.54
7.35
7.35
7.33
7.33
7.29
7.29
7.27
7.27
7.25
7.23
6.78
6.77
4.43
4.41
3.76
1.38
0.93
0.97
1.02
1.97
1.94
2.00
3.21
2.93
134.20
130.89
130.59
129.27
127.72
127.08
126.50
120.92
114.63
113.44
111.94
161.42
158.45
61.66
55.42
14.30

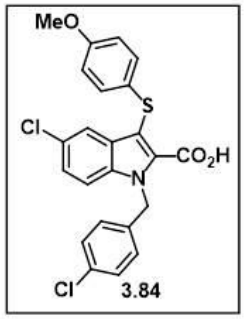
MeO
S
Cl
CO2H
N
Cl
3.84

7.66
7.64
7.38
7.36
7.33
7.33
7.19
7.17
7.07
7.05
6.88
6.86
5.79
3.70
0.99
1.99
1.91
1.98
1.98
1.97
2.00
3.07

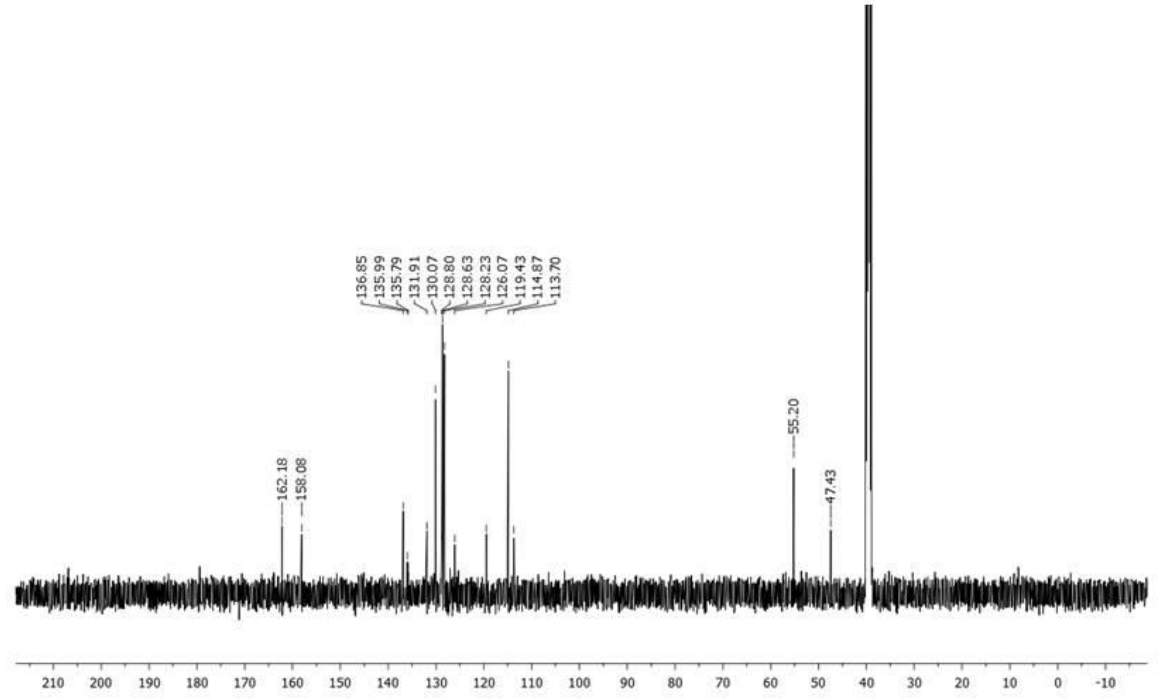
136.85
135.99
135.79
131.91
130.07
128.80
128.63
128.23
126.07
119.43
114.87
113.70
162.18
158.08
55.20
47.43

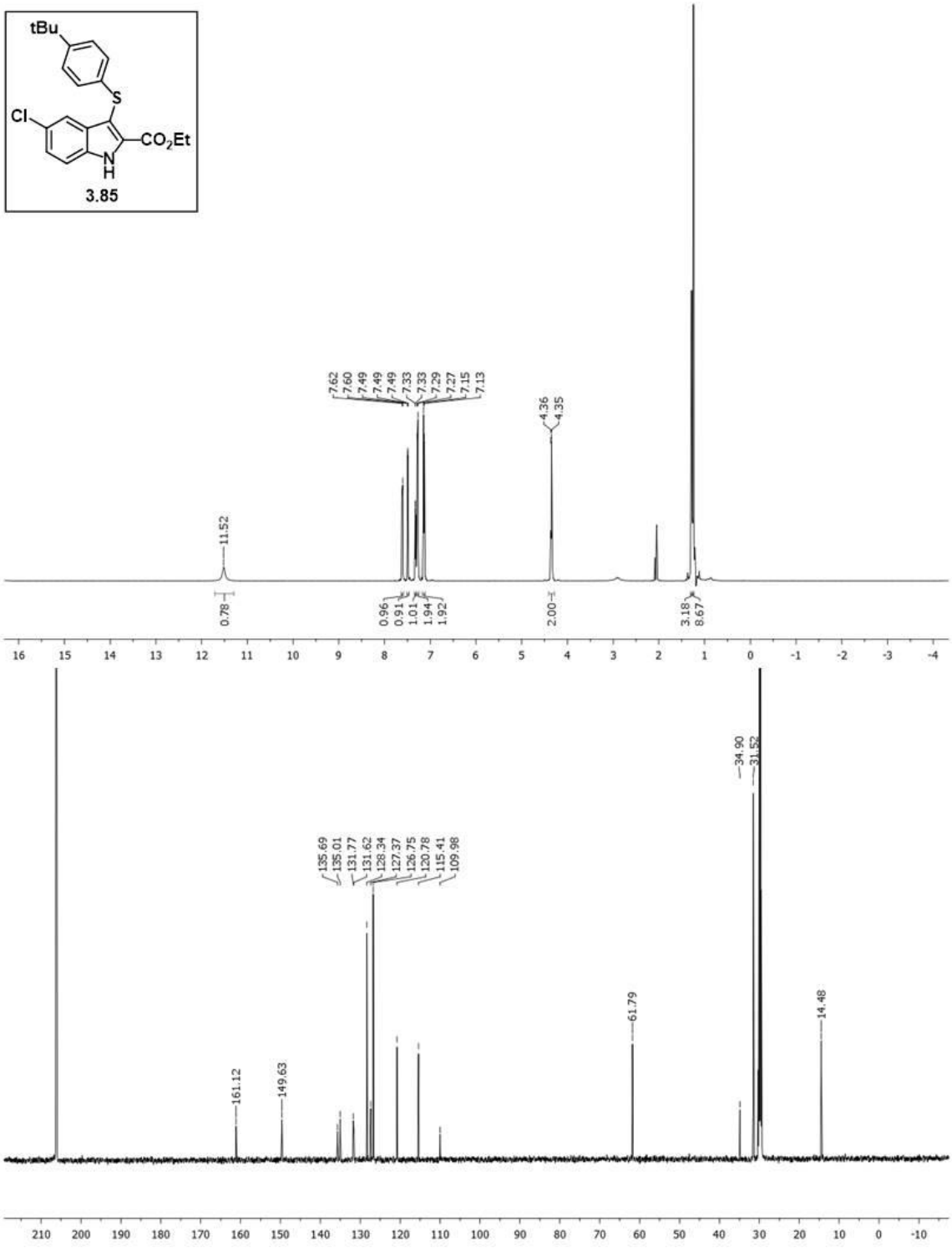
tBu
S
Cl
CO2Et
N
H
3.85
11.52
7.62
7.60
7.49
7.49
7.49
7.33
7.33
7.29
7.27
7.15
7.13
4.36
4.35
0.78
0.96
0.91
1.01
1.94
1.92
2.00
3.18
8.67
34.90
31.52
135.69
135.01
131.77
131.62
128.34
127.37
126.75
120.78
115.41
109.98
161.12
149.63
61.79
14.48

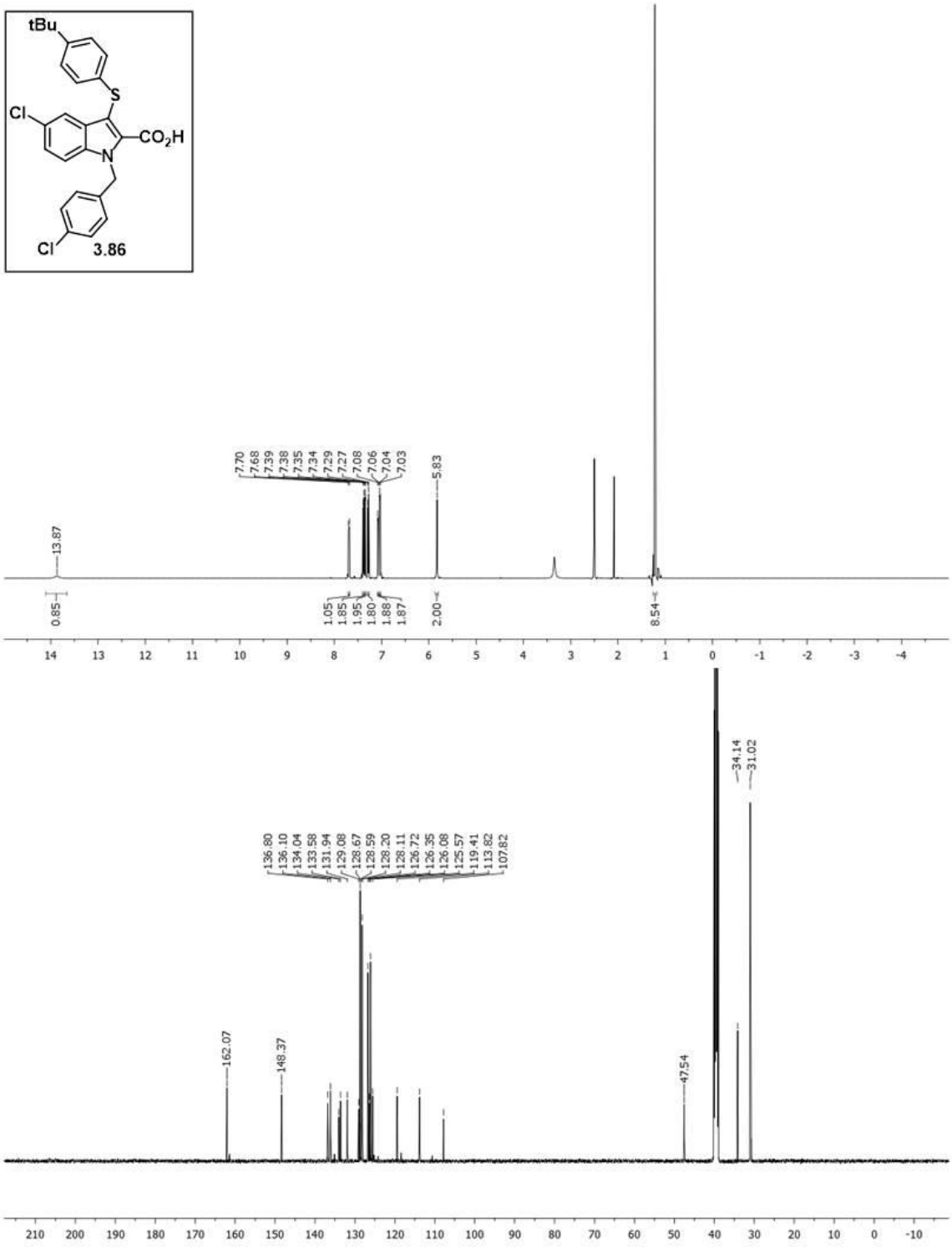
tBu
S
Cl
CO2H
N
Cl
3.86
7.70
7.68
7.39
7.38
7.35
7.34
7.29
7.27
7.08
7.06
7.04
7.03
5.83
13.87
0.85
1.05
1.85
1.95
1.80
1.88
1.87
2.00
8.54
14 13 12 11 10 9 8 7 6 5 4 3 2 1 0 -1 -2 -3 -4
34.14
31.02
136.80
136.10
134.04
133.58
131.94
129.08
128.67
128.59
128.20
128.11
126.72
126.35
126.08
125.57
119.41
113.82
107.82
162.07
148.37
47.54
210 200 190 180 170 160 150 140 130 120 110 100 90 80 70 60 50 40 30 20 10 0 -10

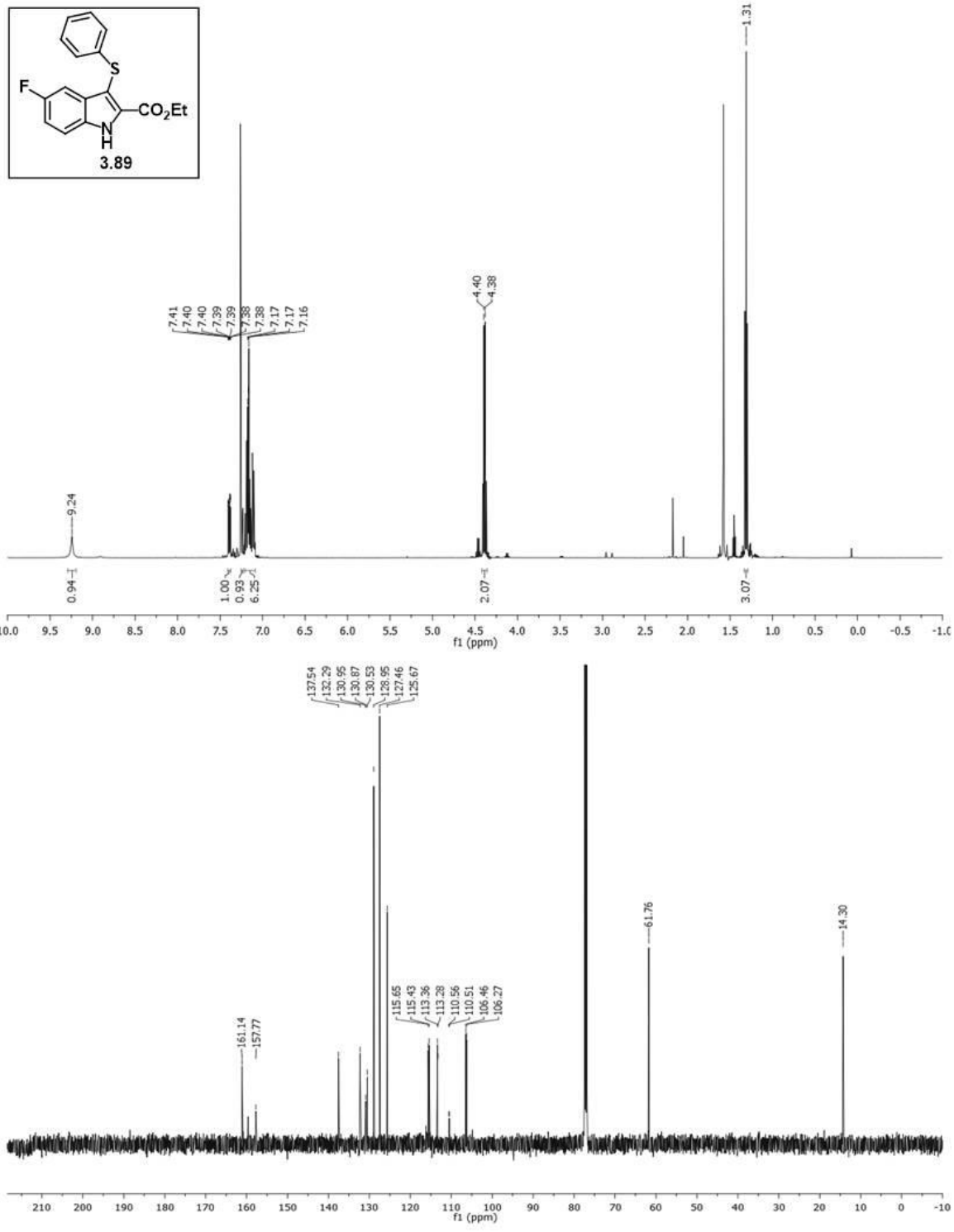
F
S
CO2Et
N
H
3.89
9.24
7.41
7.40
7.40
7.39
7.39
7.38
7.38
7.17
7.17
7.16
4.40
4.38
1.31
0.94
1.00
0.93
6.25
2.07
3.07
f1 (ppm)
137.54
132.29
130.95
130.87
130.53
128.95
127.46
125.67
115.65
115.43
113.36
113.28
110.56
110.51
106.46
106.27
161.14
157.77
61.76
14.30
f1 (ppm)

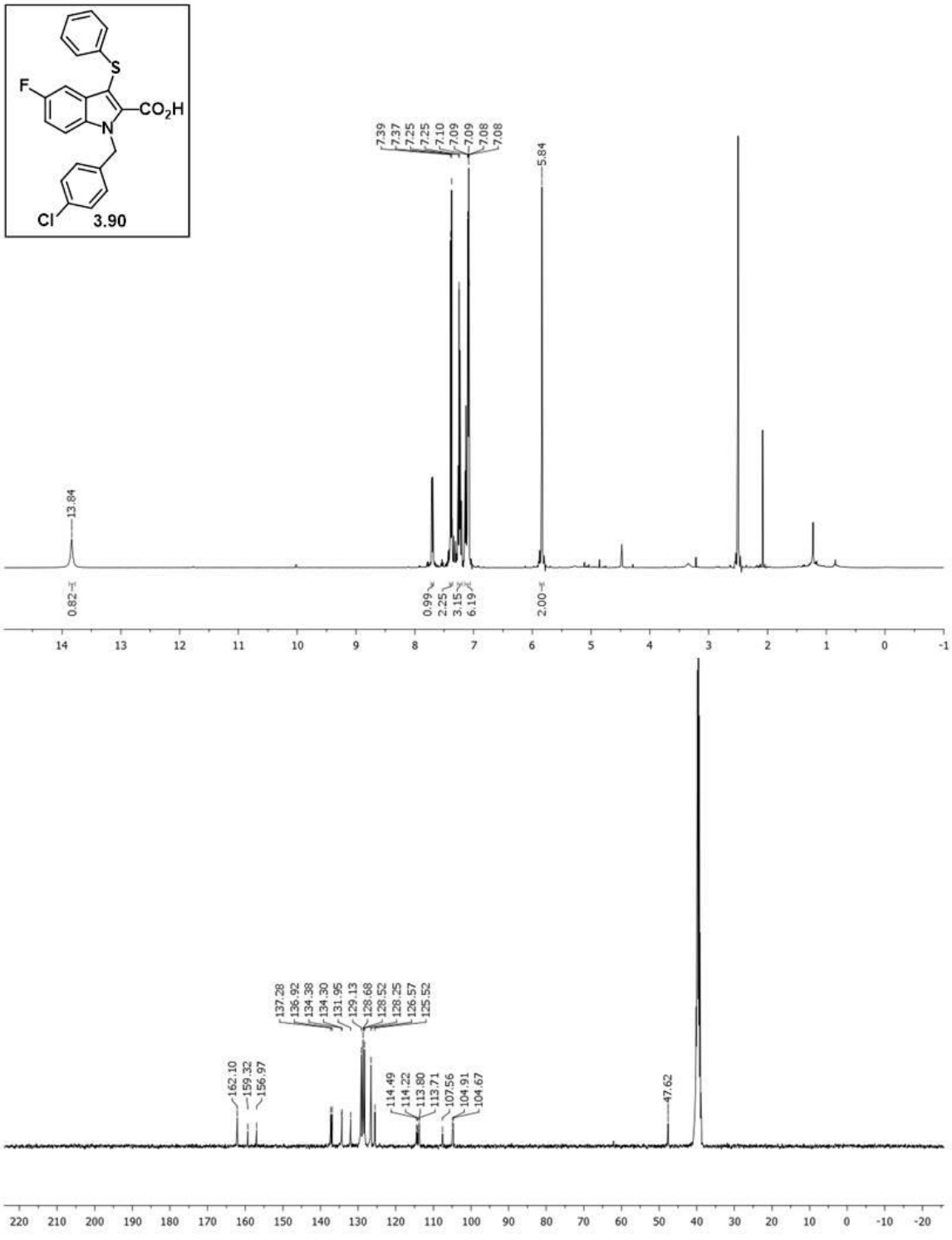
F
S
CO2H
N
Cl
3.90
7.39
7.37
7.25
7.25
7.10
7.09
7.09
7.08
7.08
5.84
13.84
0.82
0.99
2.25
3.15
6.19
2.00
14 13 12 11 10 9 8 7 6 5 4 3 2 1 0 -1
137.28
136.92
134.38
134.30
131.95
129.13
128.68
128.52
128.25
126.57
125.52
162.10
159.32
156.97
114.49
114.22
113.80
113.71
107.56
104.91
104.67
47.62
220 210 200 190 180 170 160 150 140 130 120 110 100 90 80 70 60 50 40 30 20 10 0 -10 -20

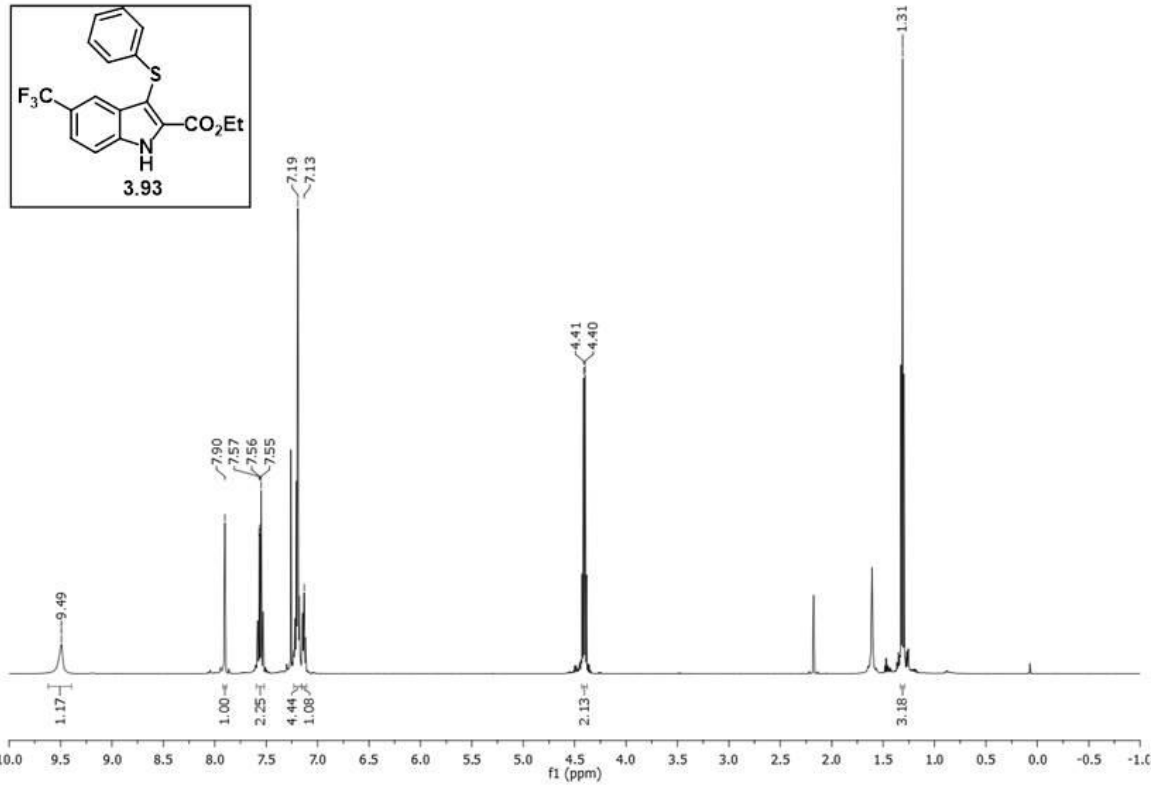
S
F3C
CO2Et
N
H
3.93
9.49
7.90
7.57
7.56
7.55
7.19
7.13
4.41
4.40
1.31
1.17
1.00
2.25
4.44
1.08
2.13
3.18
f1 (ppm)

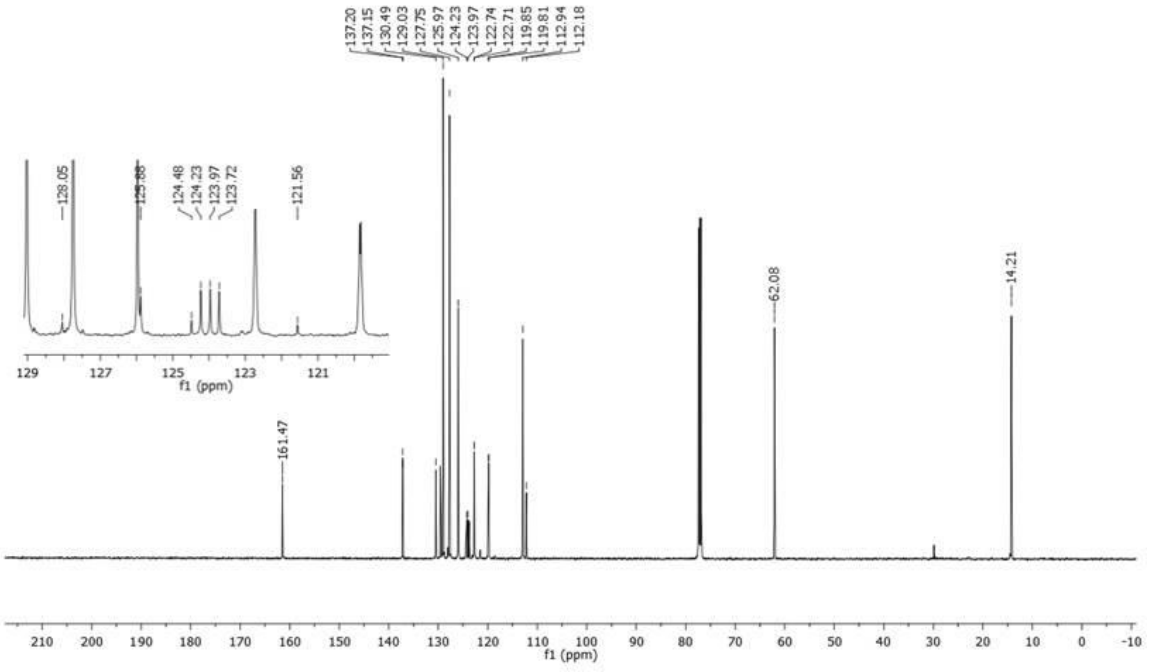
137.20
137.15
130.49
129.03
127.75
125.97
124.23
123.97
122.74
122.71
119.85
119.81
112.94
112.18
128.05
124.48
124.23
123.97
123.72
121.56
62.08
14.21
161.47
f1 (ppm)

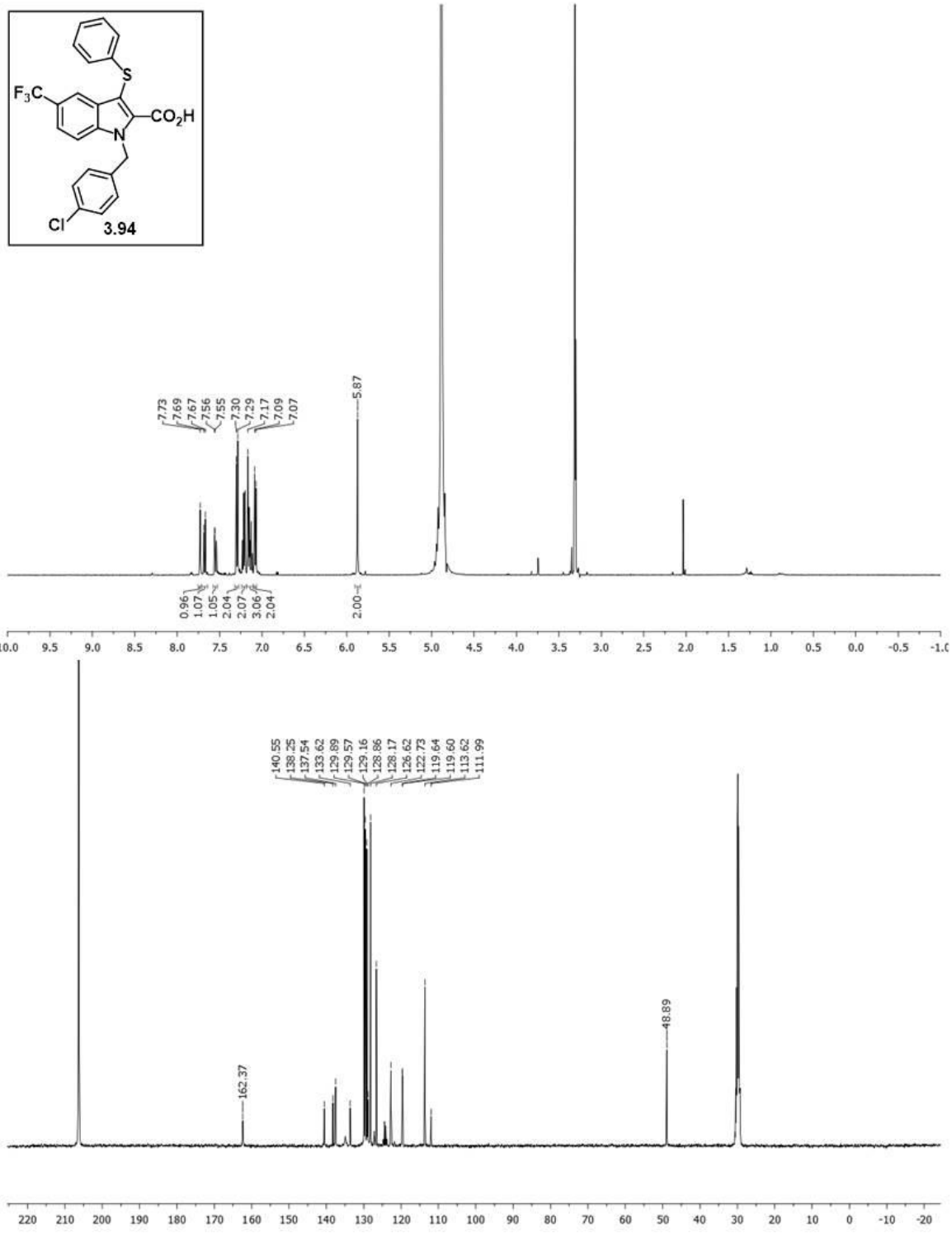
F3C
S
CO2H
N
Cl
3.94
7.73
7.69
7.67
7.56
7.55
7.30
7.29
7.17
7.09
7.07
5.87
0.96
1.07
1.05
2.04
2.07
3.06
2.04
2.00
140.55
138.25
137.54
133.62
129.89
129.57
129.16
128.86
128.17
126.62
122.73
119.64
119.60
113.62
111.99
162.37
48.89

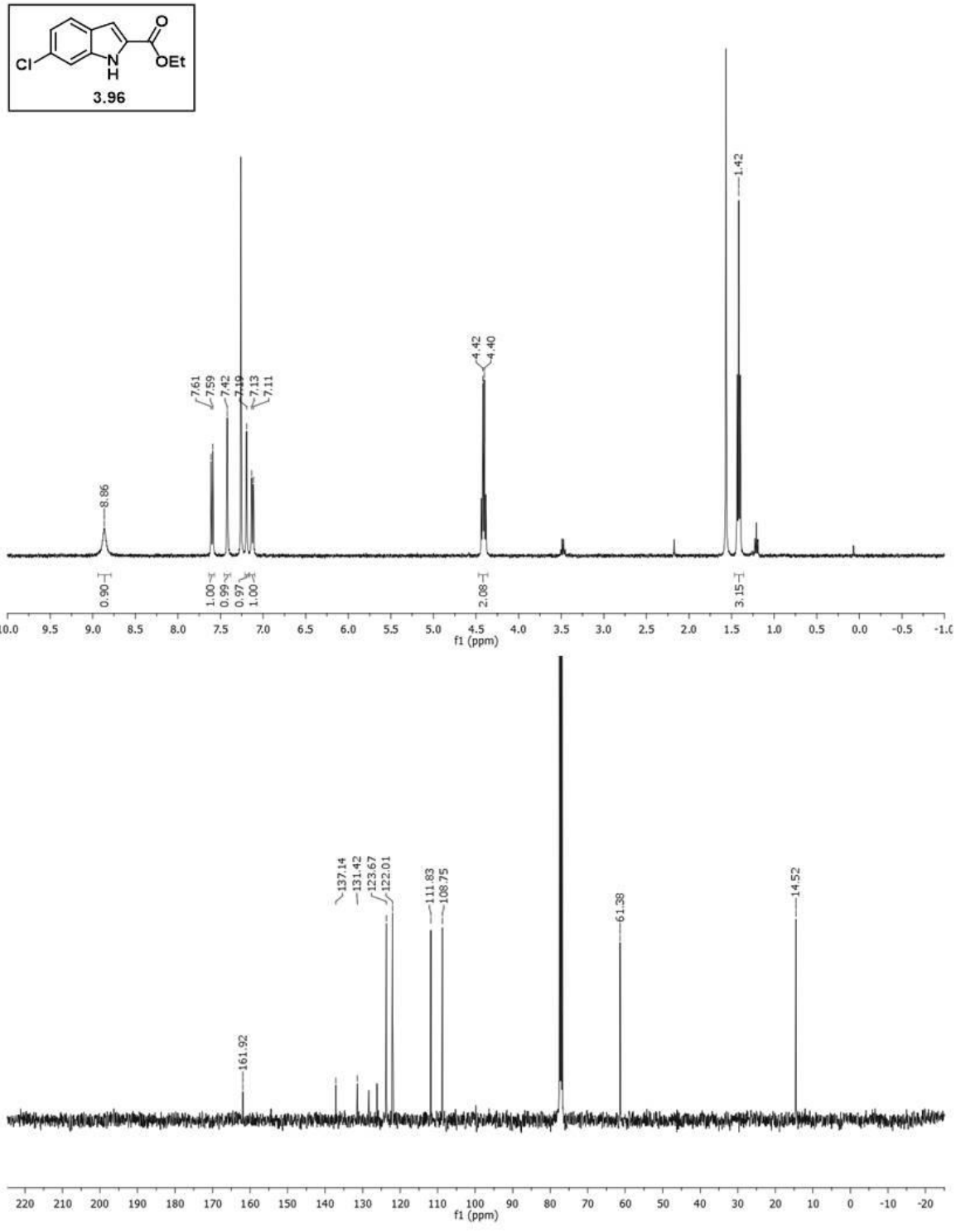
Cl
N
H
O
OEt
3.96
8.86
7.61
7.59
7.42
7.19
7.13
7.11
4.42
4.40
1.42
0.90
1.00
0.99
0.97
1.00
2.08
3.15
f1 (ppm)
161.92
137.14
131.42
123.67
122.01
111.83
108.75
61.38
14.52
f1 (ppm)

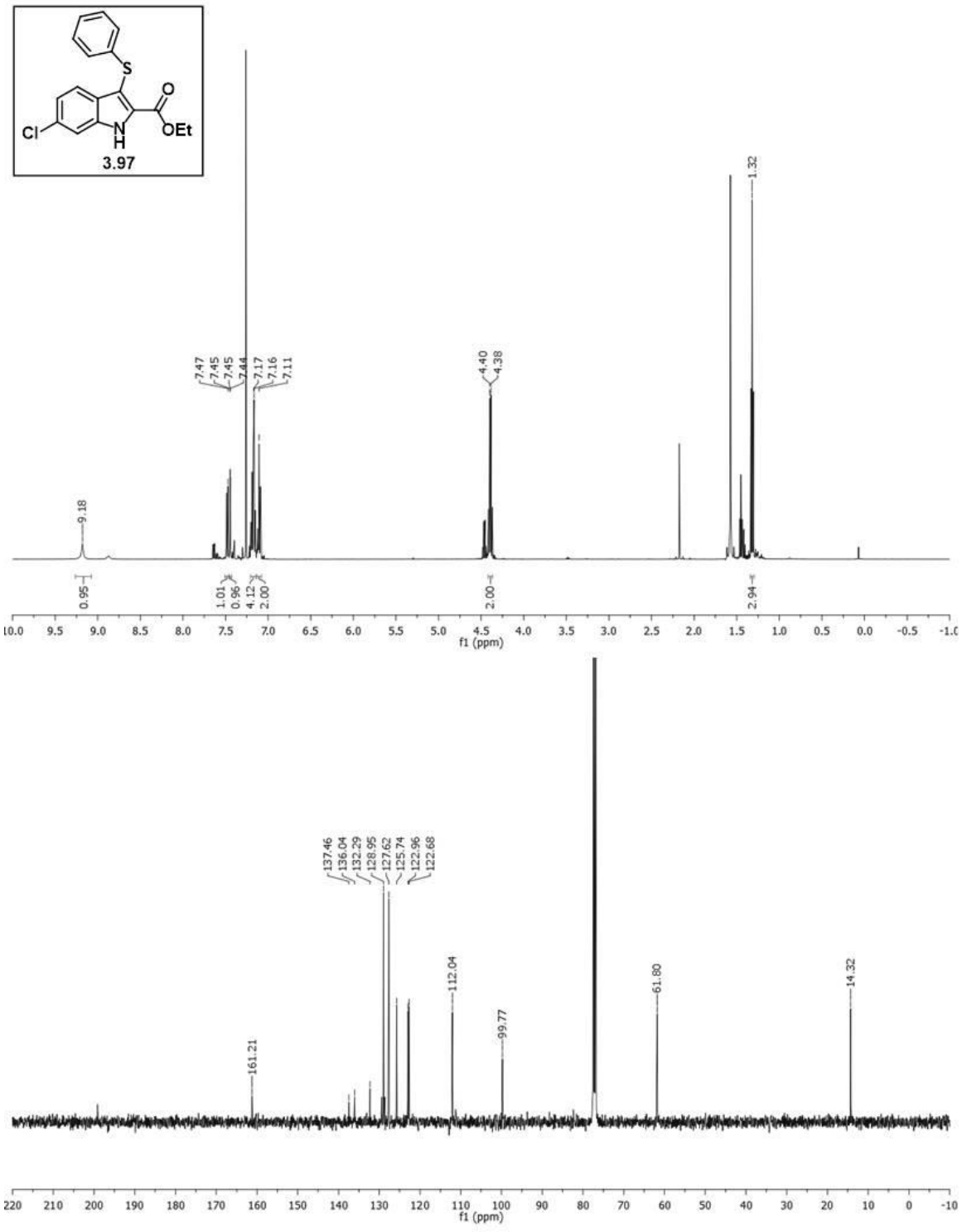
S
O
OEt
Cl
N
H
3.97
9.18
7.47
7.45
7.45
7.44
7.17
7.16
7.11
4.40
4.38
1.32
0.95
1.01
0.96
4.12
2.00
2.00
2.94
f1 (ppm)
137.46
136.04
132.29
128.95
127.62
125.74
122.96
122.68
112.04
99.77
61.80
14.32
161.21
f1 (ppm)

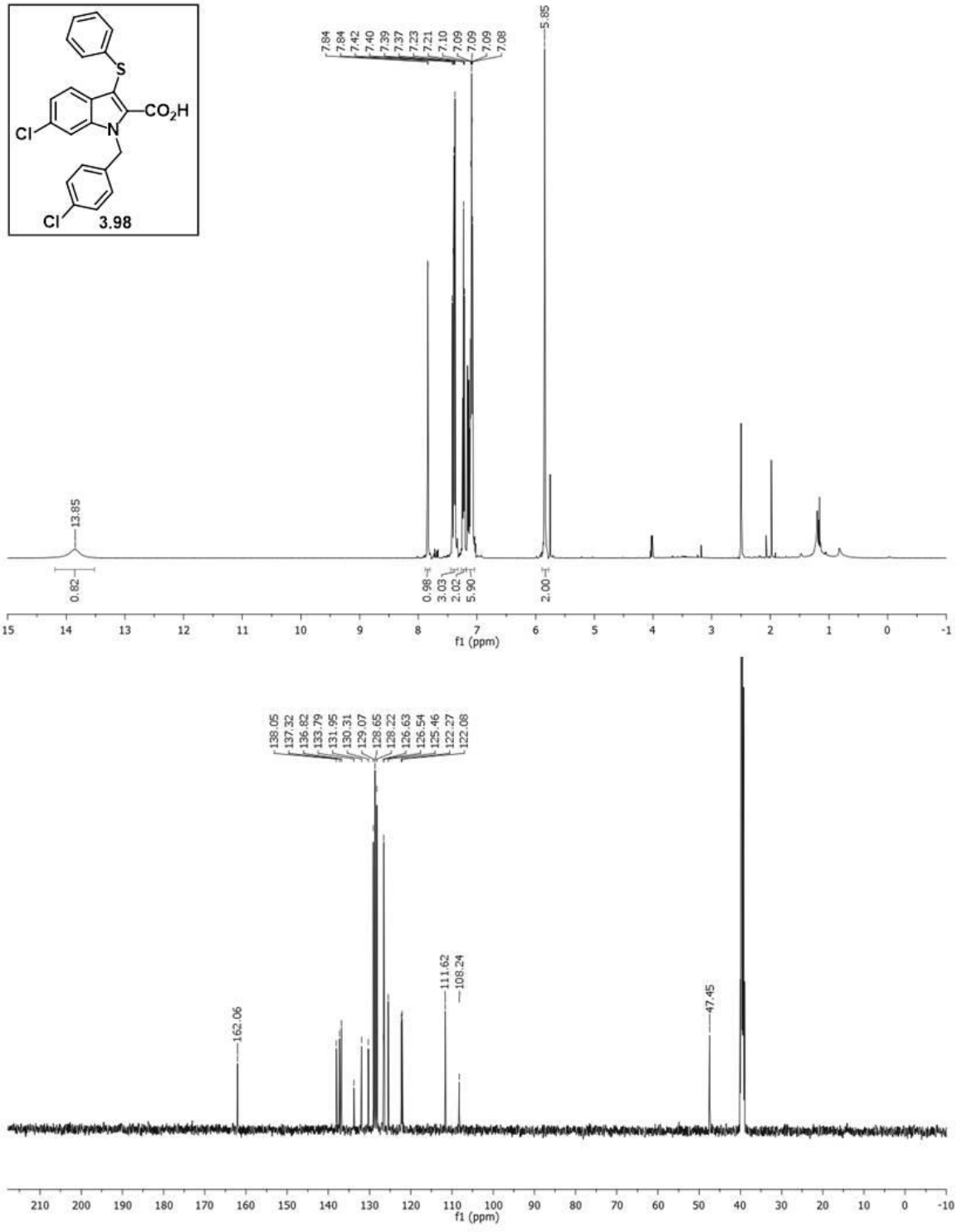
S
CO2H
Cl
N
Cl
3.98
7.84
7.84
7.42
7.40
7.39
7.37
7.23
7.21
7.10
7.09
7.09
7.09
7.08
5.85
13.85
0.82
0.98
3.03
2.02
5.90
2.00
f1 (ppm)
138.05
137.32
136.82
133.79
131.95
130.31
129.07
128.65
128.22
126.63
126.54
125.46
122.27
122.08
162.06
111.62
108.24
47.45
f1 (ppm)

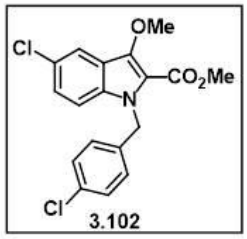
OMe
Cl
CO2Me
N
Cl

3.102

4.05
3.90
7.76
7.19
6.94
5.65
1.00
4.29
2.10
2.23
3.16
3.22
f1 (ppm)

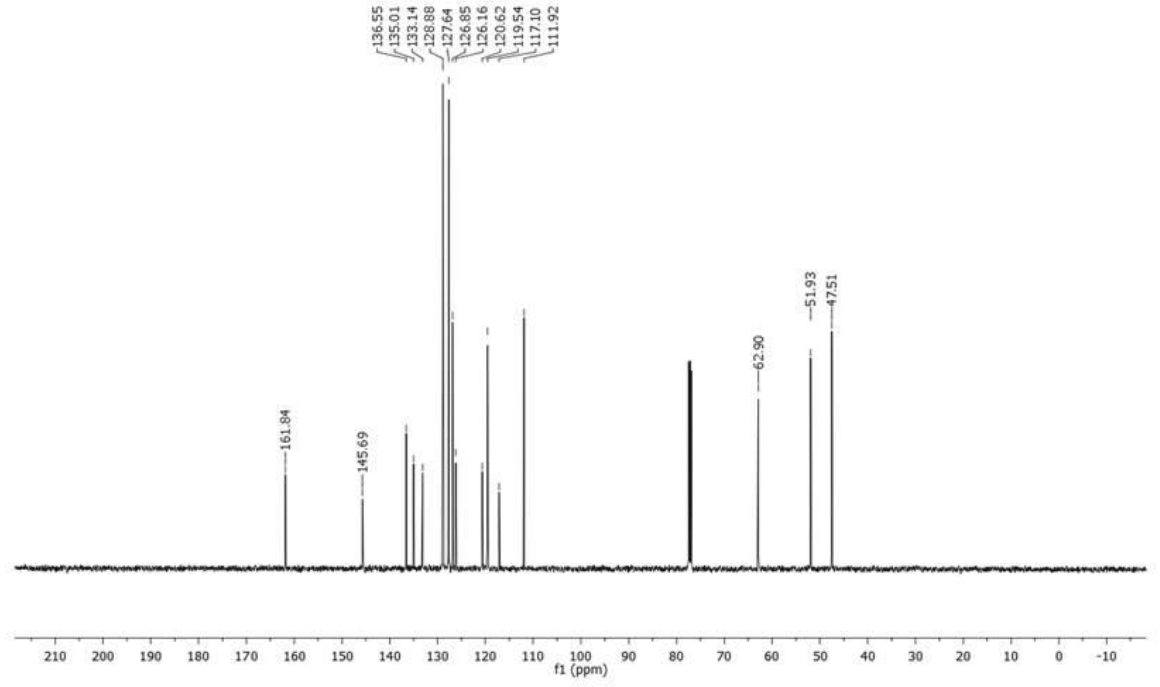
136.55
135.01
133.14
128.88
127.64
126.85
126.16
120.62
119.54
117.10
111.92
161.84
145.69
62.90
51.93
47.51
f1 (ppm)

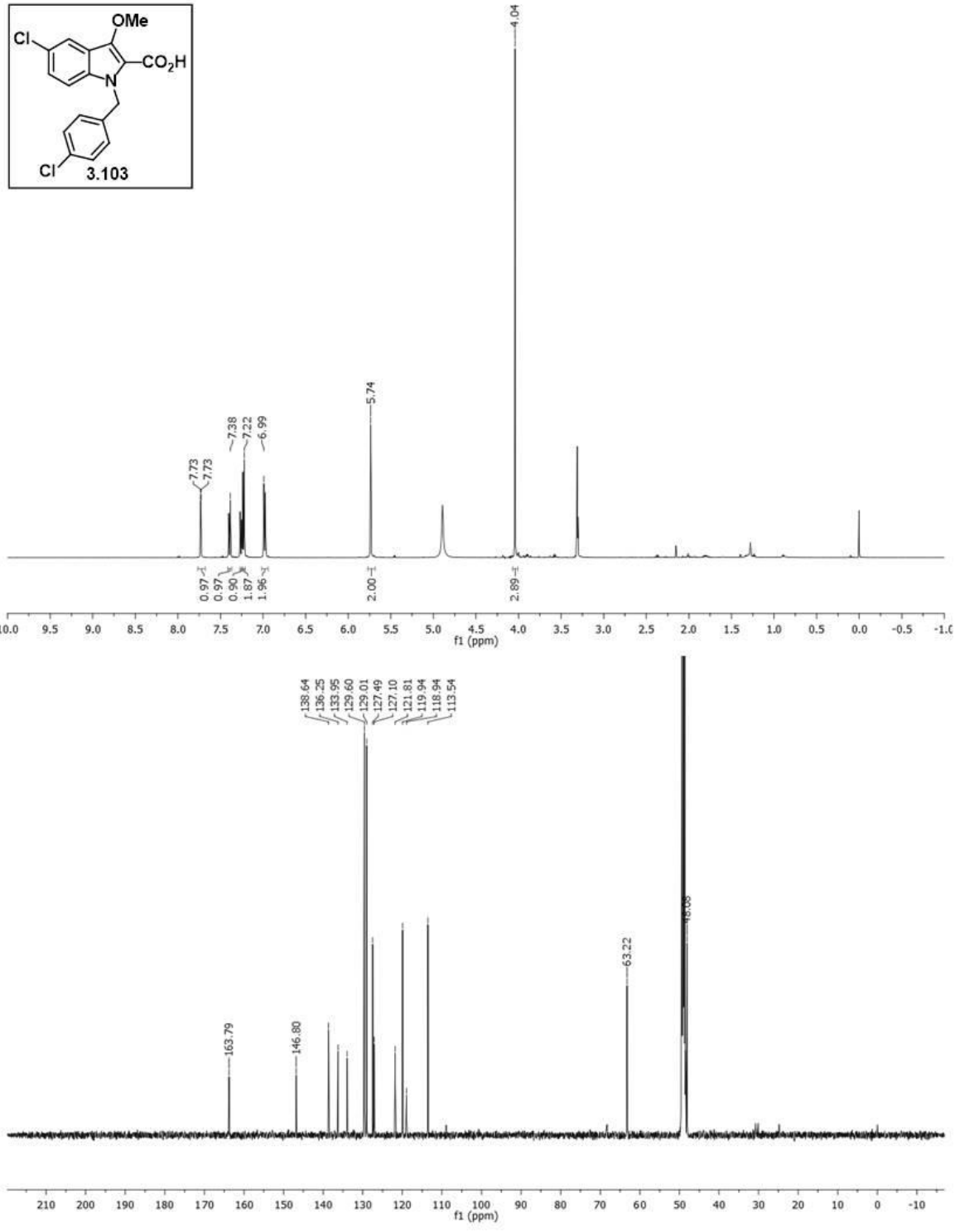
OMe
Cl
CO2H
N
Cl
3.103
4.04
5.74
7.38
7.22
6.99
7.73
7.73
0.97
0.97
0.90
1.87
1.96
2.00
2.89
f1 (ppm)
138.64
136.25
133.95
129.60
129.01
127.49
127.10
121.81
119.94
118.94
113.54
63.22
163.79
146.80
f1 (ppm)

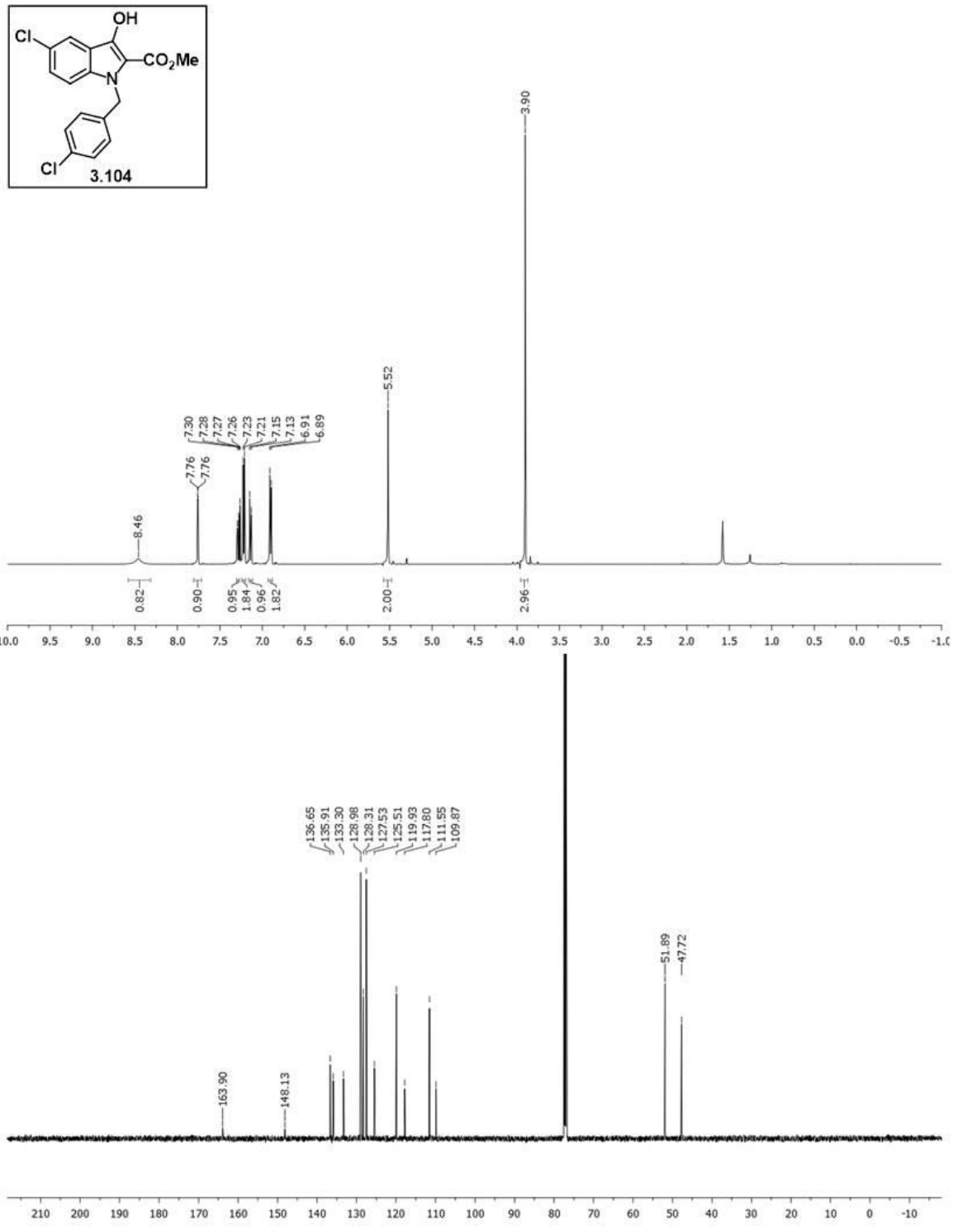
OH
Cl
CO2Me
N
Cl
3.104
3.90
5.52
7.30
7.28
7.27
7.26
7.23
7.21
7.15
7.13
6.91
6.89
7.76
7.76
8.46
0.82
0.90
0.95
1.84
0.96
1.82
2.00
2.96
136.65
135.91
133.30
128.98
128.31
127.53
125.51
119.93
117.80
111.55
109.87
51.89
47.72
163.90
148.13

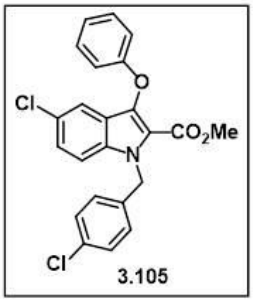
Cl
O
CO2Me
N
Cl

3.105

7.42
7.28
7.27
7.26
6.99
6.98
6.96
6.94
6.94
5.76
3.71
0.92
6.62
0.99
3.89
2.00
2.94

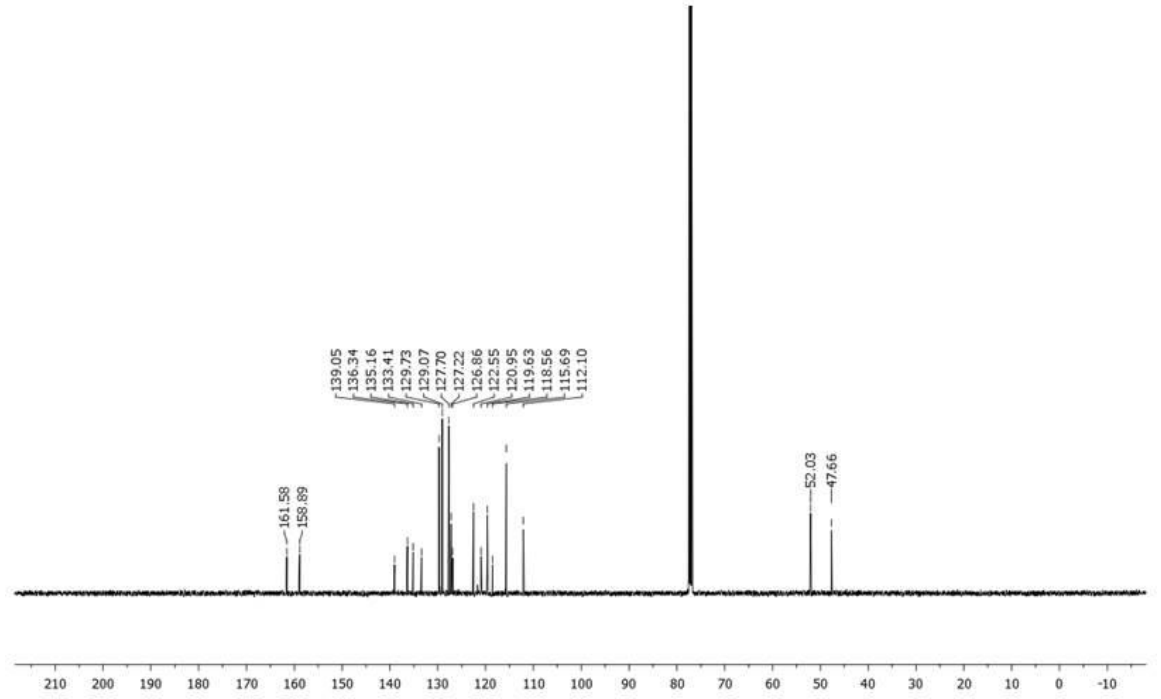
139.05
136.34
135.16
133.41
129.73
129.07
127.70
127.22
126.86
122.55
120.95
119.63
118.56
115.69
112.10
161.58
158.89
52.03
47.66

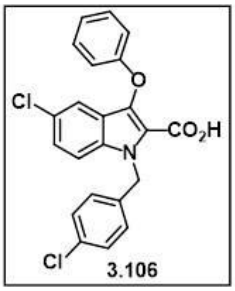
Cl
O
CO2H
N
Cl
3.106

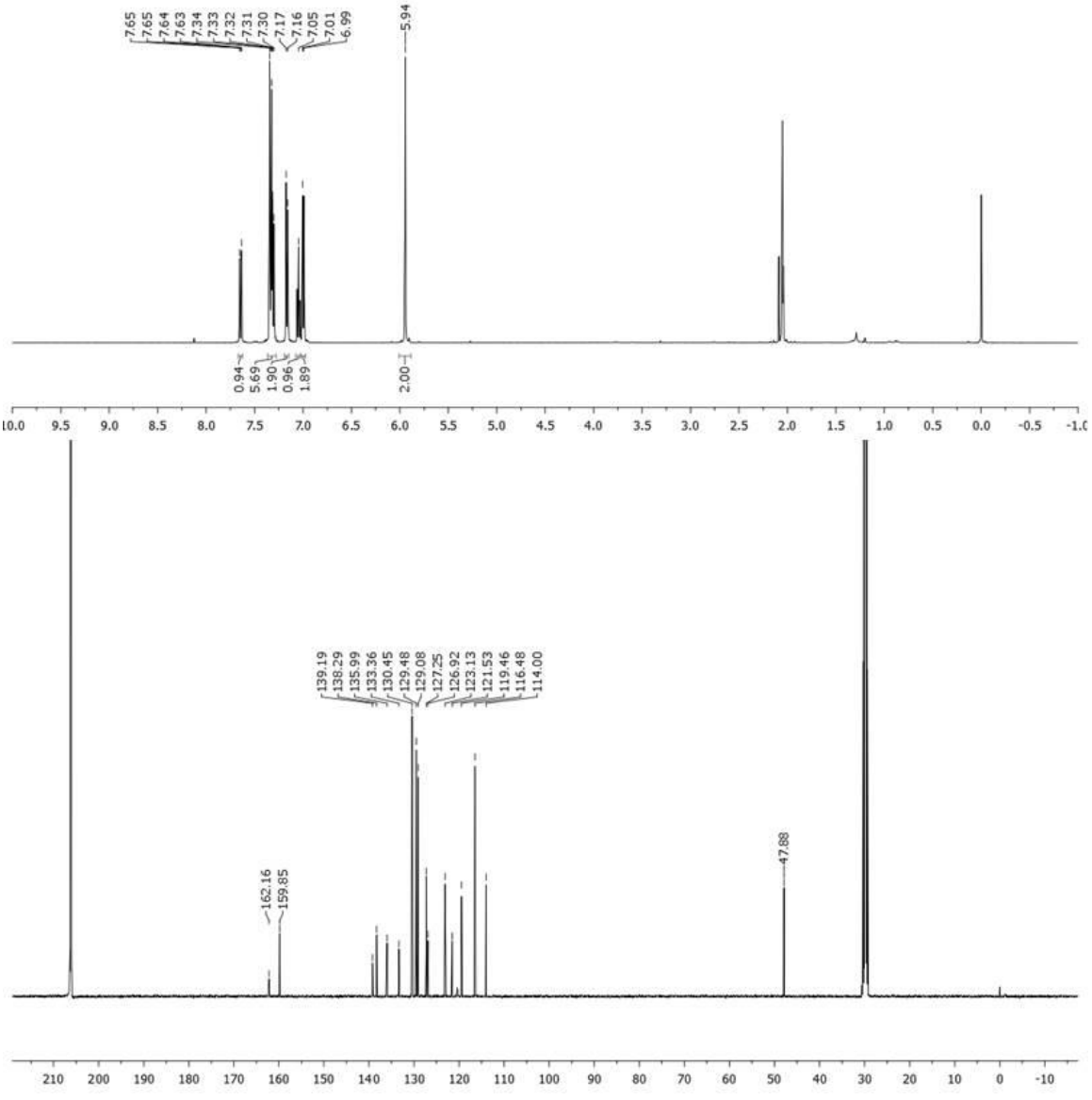
7.65
7.65
7.64
7.63
7.34
7.33
7.32
7.31
7.30
7.17
7.16
7.05
7.01
6.99
5.94
0.94
5.69
1.90
0.96
1.89
2.00
139.19
138.29
135.99
133.36
130.45
129.48
129.08
127.25
126.92
123.13
121.53
119.46
116.48
114.00
162.16
159.85
47.88

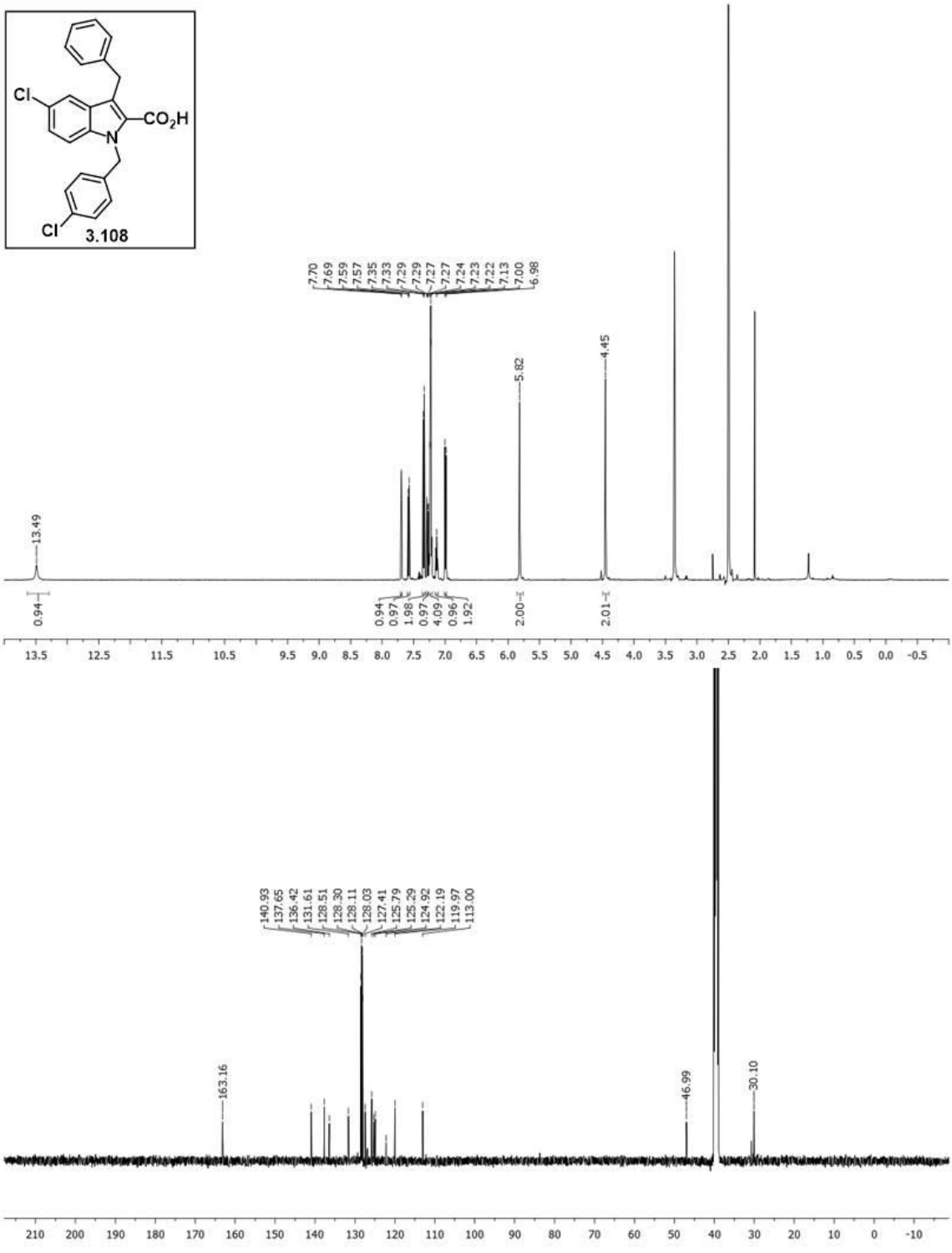
Cl
CO2H
N
Cl
3.108
7.70
7.69
7.59
7.57
7.35
7.33
7.29
7.29
7.27
7.27
7.24
7.23
7.22
7.13
7.00
6.98
5.82
4.45
13.49
0.94
0.94
0.97
1.98
0.97
4.09
0.96
1.92
2.00
2.01
13.5 12.5 11.5 10.5 9.5 9.0 8.5 8.0 7.5 7.0 6.5 6.0 5.5 5.0 4.5 4.0 3.5 3.0 2.5 2.0 1.5 1.0 0.5 0.0 -0.5
140.93
137.65
136.42
131.61
128.51
128.30
128.11
128.03
127.41
125.79
125.29
124.92
122.19
119.97
113.00
163.16
46.99
30.10
210 200 190 180 170 160 150 140 130 120 110 100 90 80 70 60 50 40 30 20 10 0 -10

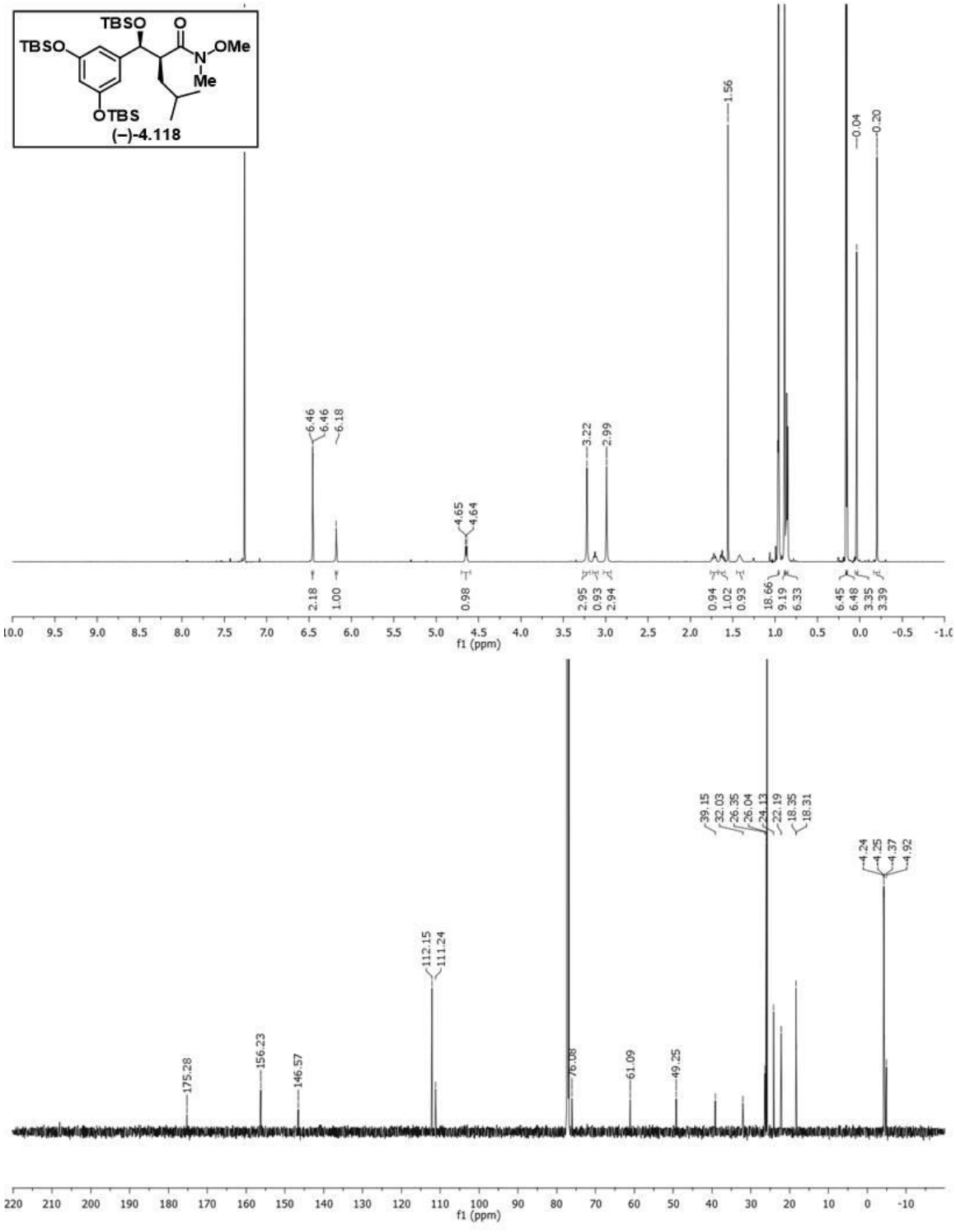
TBSO
TBSO
O
N
OMe
Me
OTBS
(–)-4.118
6.46
6.46
6.18
4.65
4.64
3.22
2.99
1.56
0.04
0.20
2.18
1.00
0.98
2.95
0.93
2.94
0.94
1.02
0.93
18.66
9.19
6.33
6.45
6.48
3.35
3.39
f1 (ppm)
39.15
32.03
26.35
26.04
24.13
22.19
18.35
18.31
4.24
4.25
4.37
4.92
112.15
111.24
175.28
156.23
146.57
77.08
61.09
49.25
f1 (ppm)

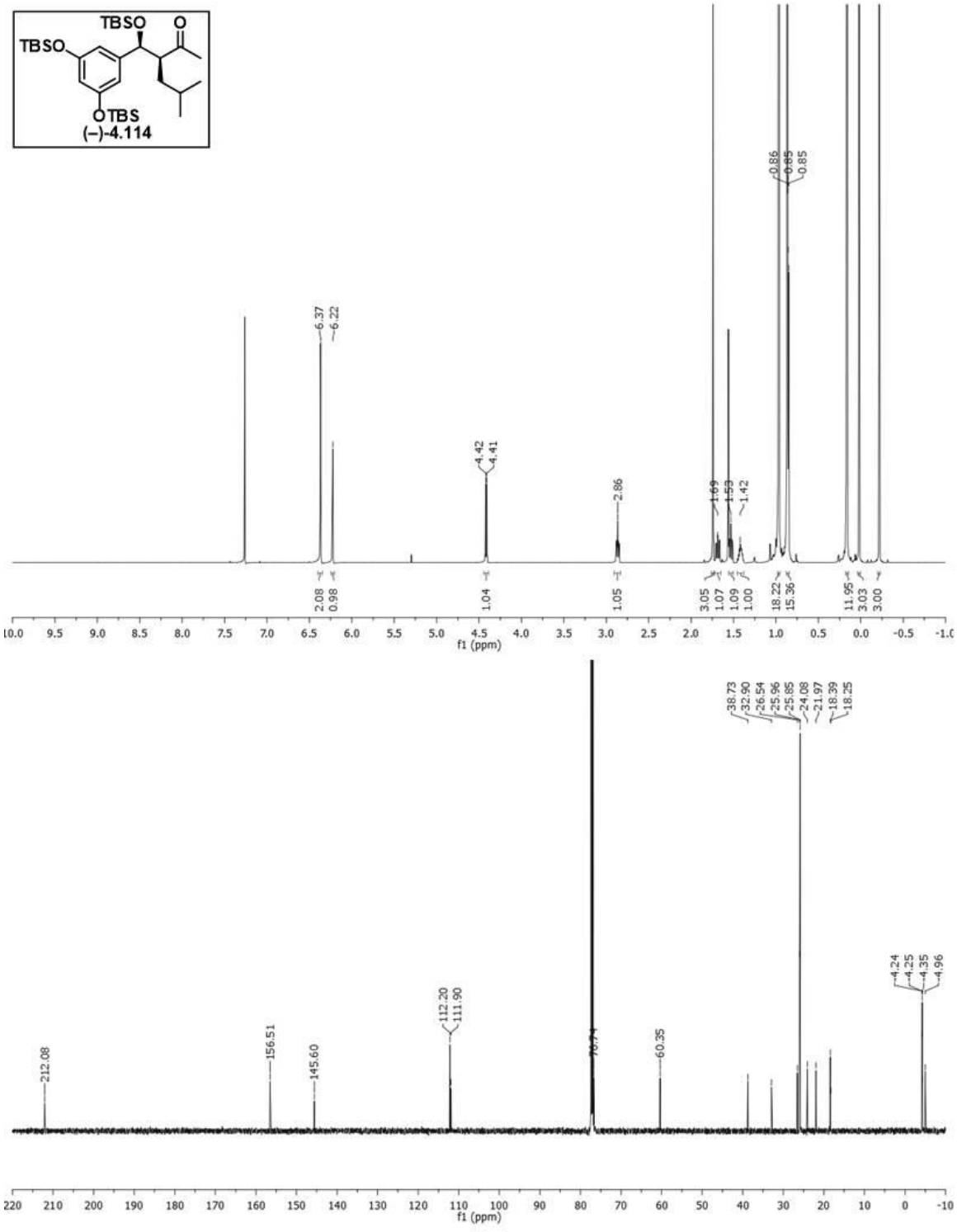
TBSO
O
TBSO
OTBS
(–)-4.114
6.37
6.22
4.42
4.41
2.86
1.69
1.53
1.42
0.86
0.85
0.85
2.08
0.98
1.04
1.05
3.05
1.07
1.09
1.00
18.22
15.36
11.95
3.03
3.00
f1 (ppm)
38.73
32.90
26.54
25.96
25.85
24.08
21.97
18.39
18.25
4.24
4.25
4.35
4.96
212.08
156.51
145.60
112.20
111.90
76.71
60.35
f1 (ppm)

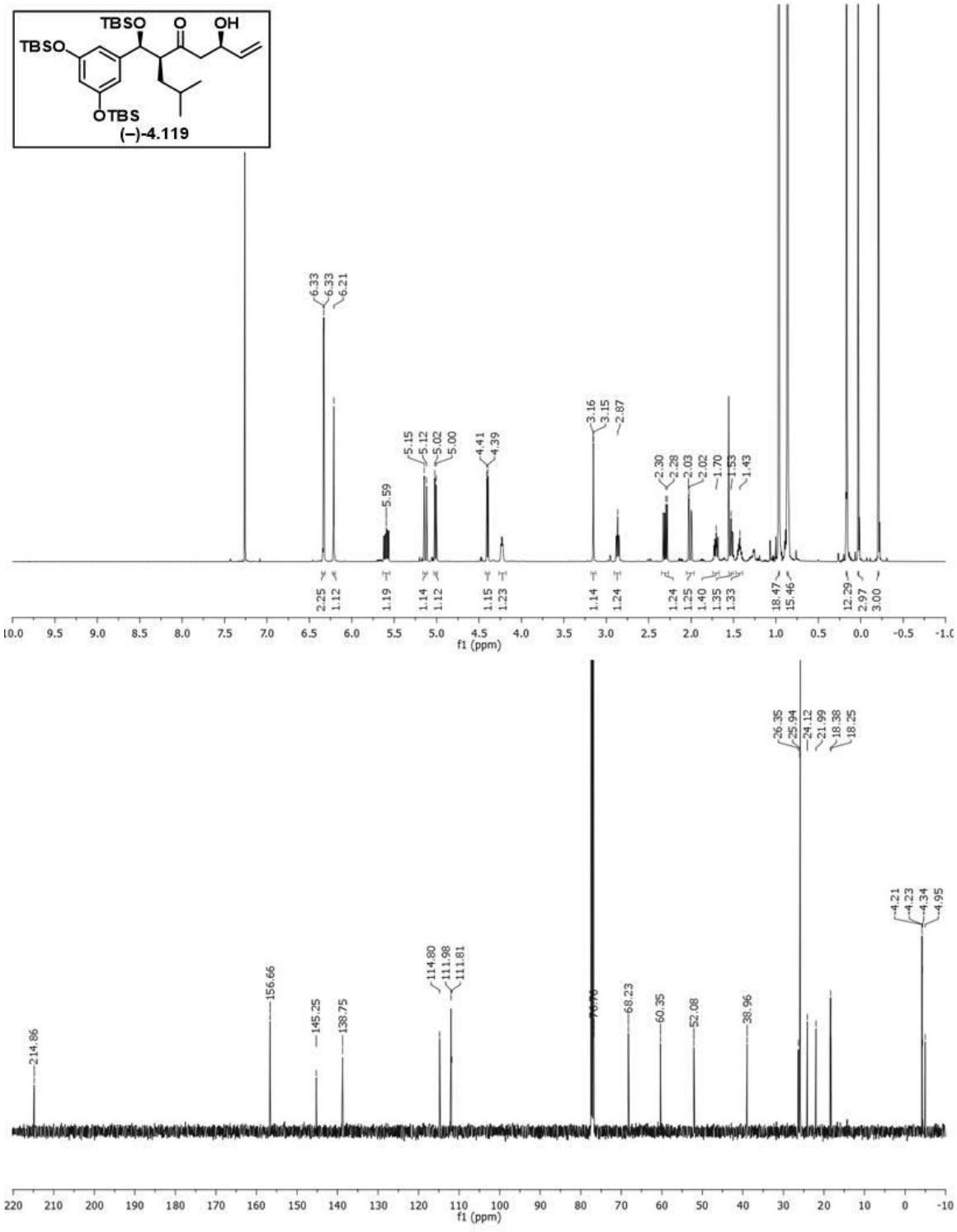
TBSO
O
OH
TBSO
OTBS
(–)-4.119
f1 (ppm)
f1 (ppm)

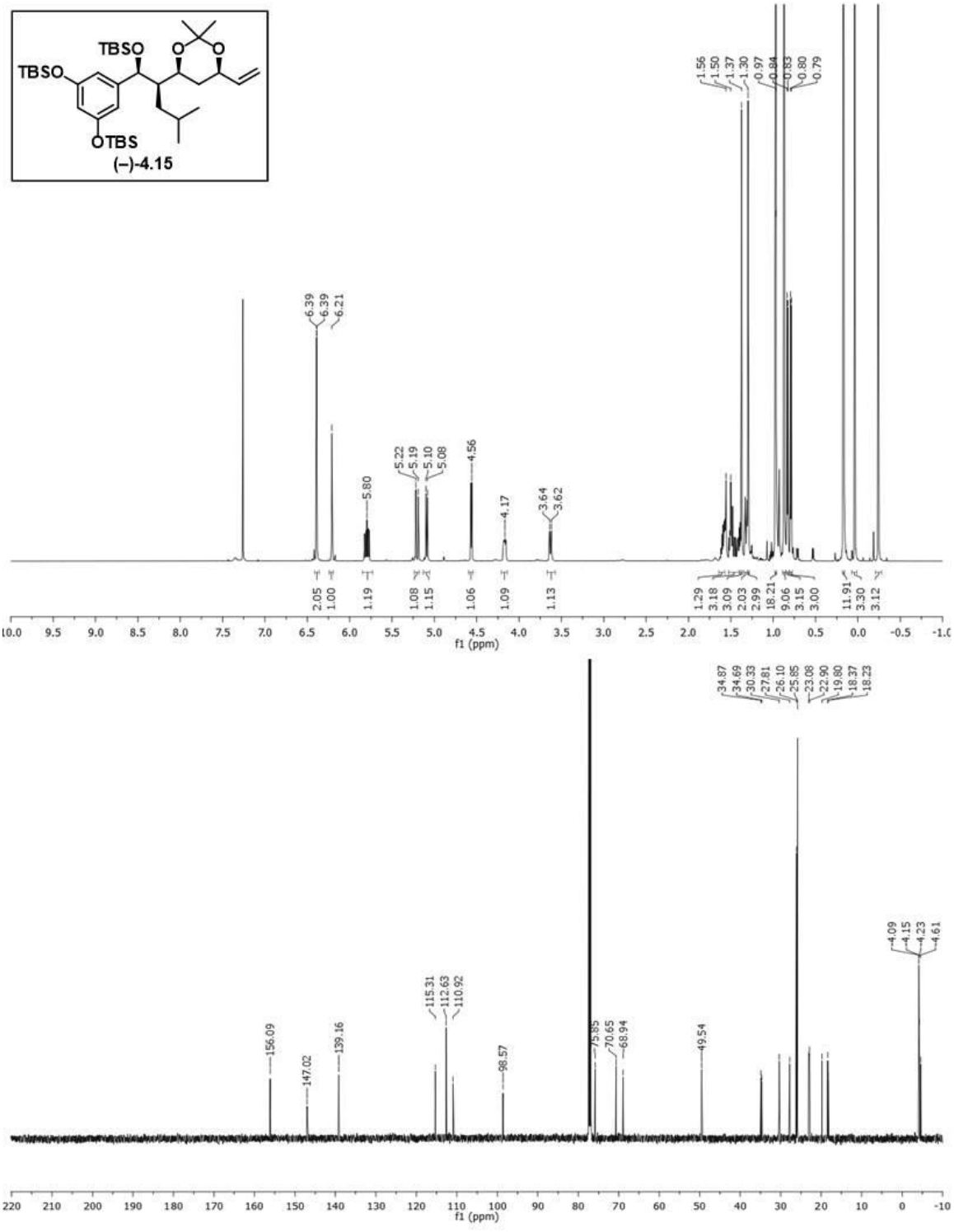
TBSO
TBSO
OTBS
(–)-4.15
f1 (ppm)
f1 (ppm)

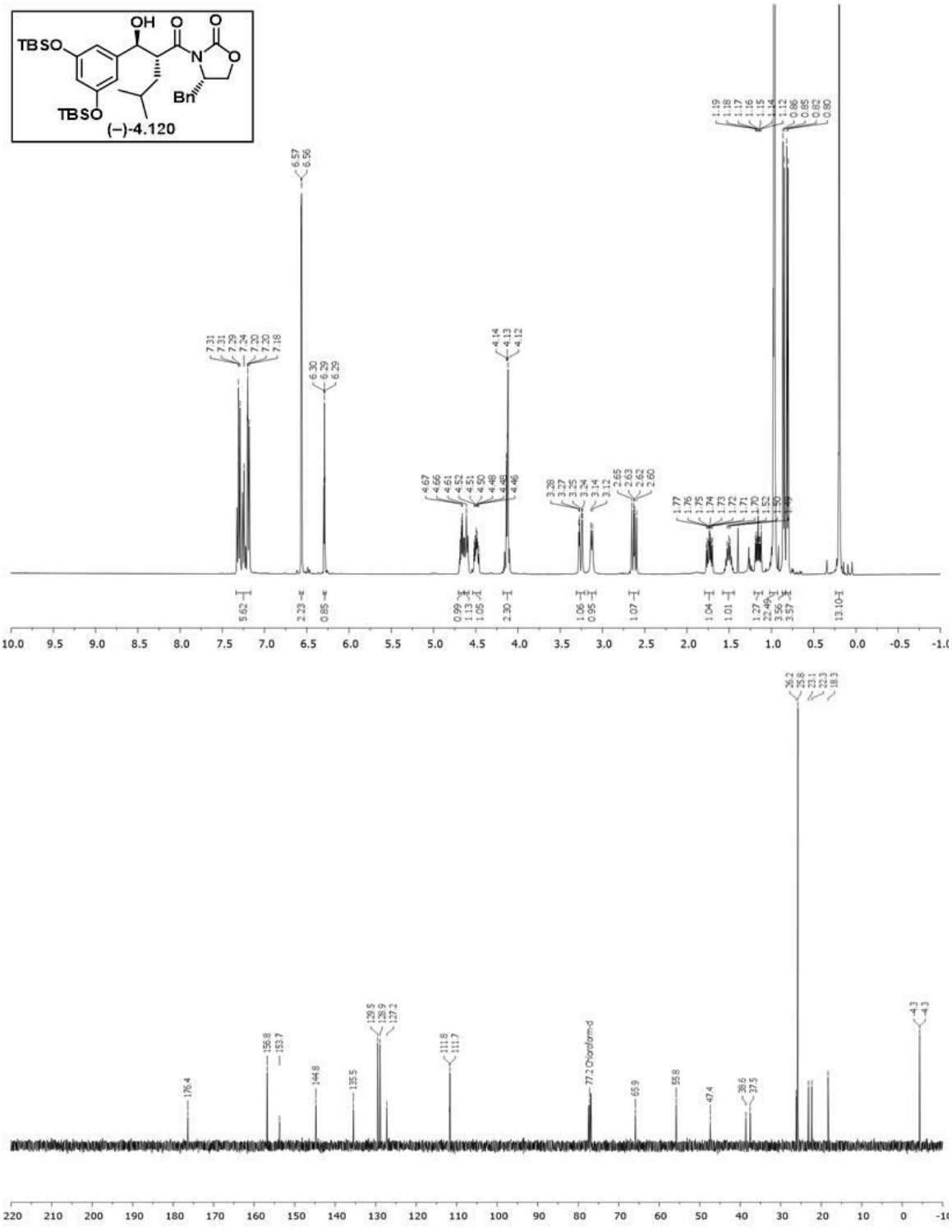
TBSO
OH
O
O
N
O
Bn
TBSO
(−)-4.120

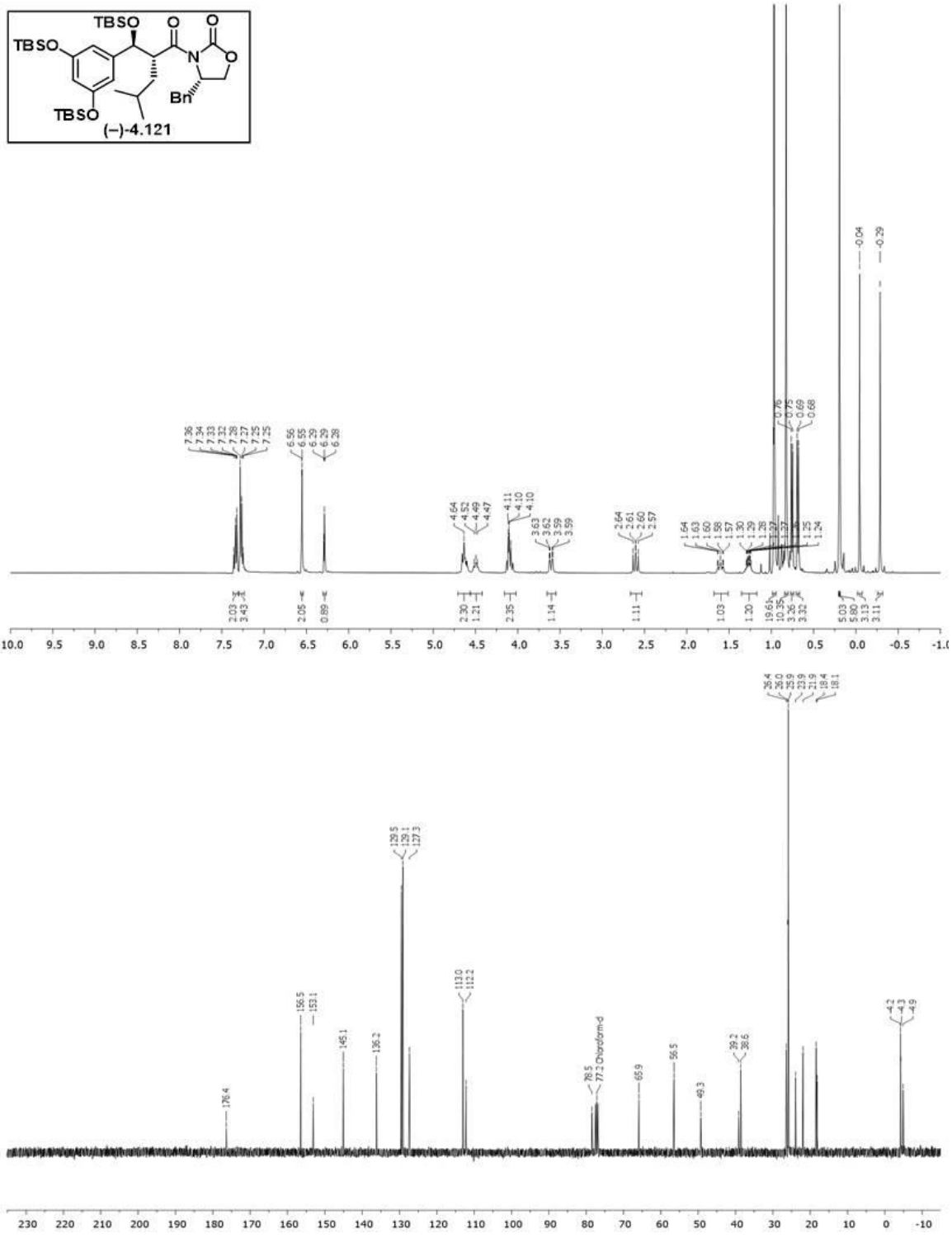
TBSO
TBSO
TBSO
O
O
N
O
Bn
(−)-4.121
7.36
7.34
7.33
7.32
7.29
7.27
7.25
7.25
6.56
6.55
6.29
6.29
6.28
4.64
4.51
4.49
4.47
4.11
4.10
4.10
3.63
3.62
3.59
3.59
2.64
2.61
2.60
2.57
1.64
1.63
1.60
1.59
1.57
1.30
1.29
1.28
1.27
1.25
1.24
0.76
0.75
0.69
0.68
-0.04
-0.29
2.03
3.43
2.05
0.89
2.30
1.21
2.35
1.14
1.11
1.03
1.20
19.65
10.35
3.26
3.32
5.03
5.80
3.13
3.11
10.0 9.5 9.0 8.5 8.0 7.5 7.0 6.5 6.0 5.5 5.0 4.5 4.0 3.5 3.0 2.5 2.0 1.5 1.0 0.5 0.0 -0.5
26.4
26.0
25.9
25.9
25.9
21.9
18.4
18.1
129.5
129.1
127.3
113.0
112.2
156.5
153.1
145.1
136.2
176.4
78.5
77.2 Chloroform-d
65.9
56.5
49.3
39.2
38.6
14.2
14.3
14.9
230 220 210 200 190 180 170 160 150 140 130 120 110 100 90 80 70 60 50 40 30 20 10 0 -10

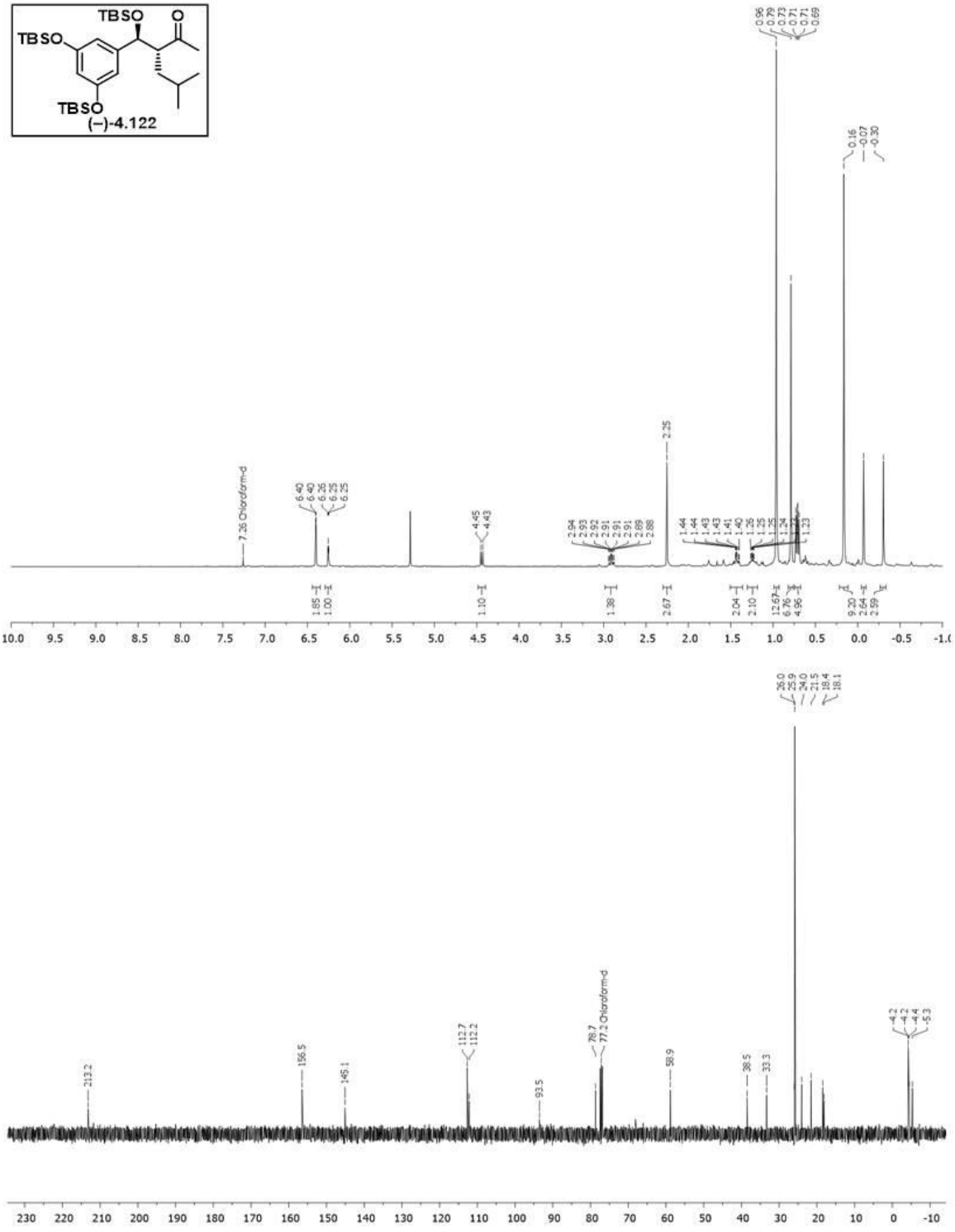
TBSO
O
TBSO
TBSO
(−)-4.122
7.26 Chloroform-d
6.40
6.40
6.26
6.25
6.25
4.45
4.43
2.94
2.93
2.92
2.91
2.91
2.91
2.89
2.88
2.25
1.44
1.44
1.43
1.43
1.41
1.40
1.26
1.25
1.24
1.23
0.96
0.79
0.73
0.71
0.71
0.69
0.16
-0.07
-0.30
1.85
1.00
1.10
1.38
2.67
2.04
2.10
12.67
6.76
4.96
9.20
2.64
2.59
10.0 9.5 9.0 8.5 8.0 7.5 7.0 6.5 6.0 5.5 5.0 4.5 4.0 3.5 3.0 2.5 2.0 1.5 1.0 0.5 0.0 -0.5
213.2
156.5
145.1
112.7
112.2
93.5
78.7
77.2 Chloroform-d
58.9
38.5
33.3
26.0
25.9
24.0
21.5
18.4
18.1
-4.2
-4.2
-4.4
-5.3
230 220 210 200 190 180 170 160 150 140 130 120 110 100 90 80 70 60 50 40 30 20 10 0 -10

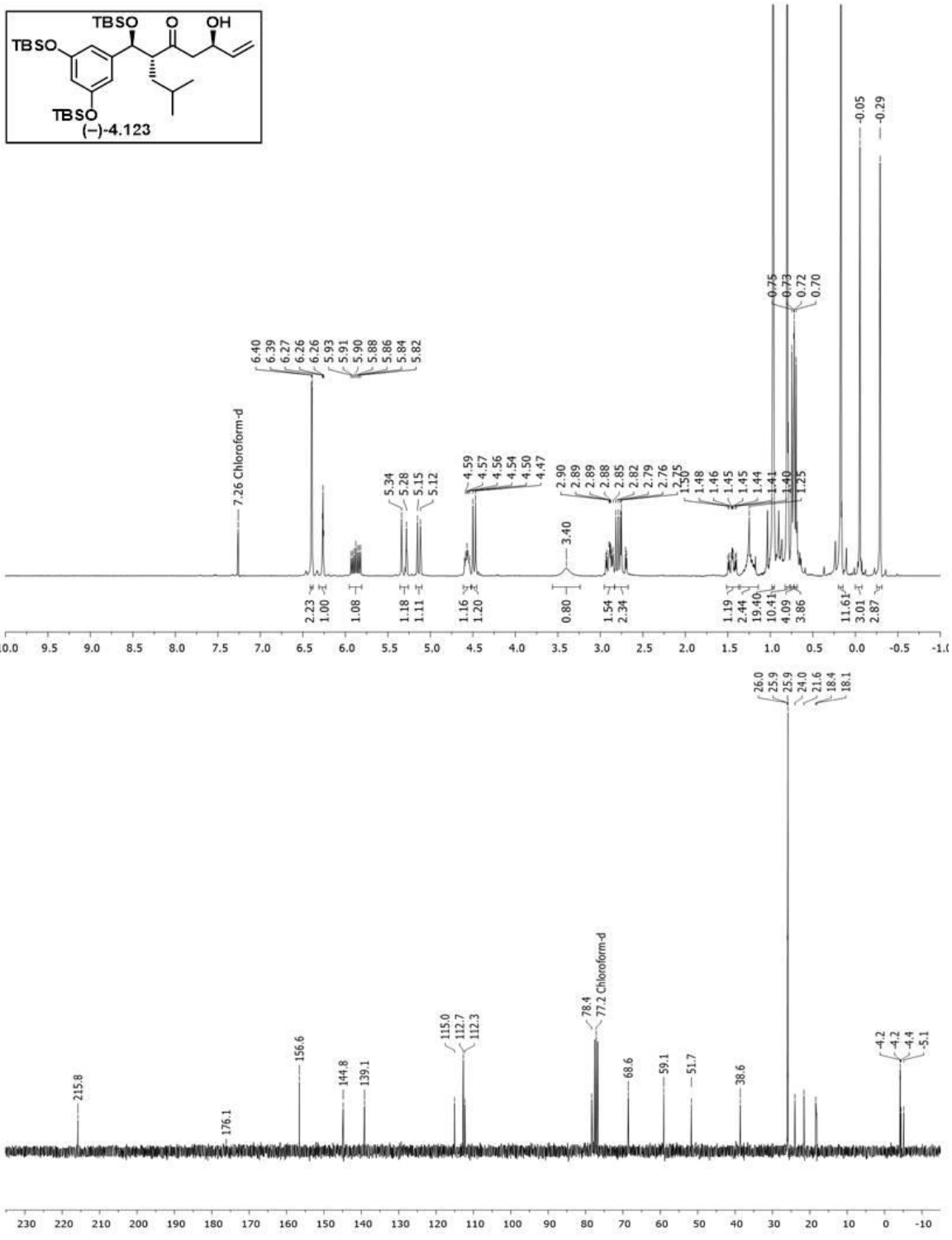
TBSO
O
OH
TBSO
TBSO
(−)-4.123
7.26 Chloroform-d
6.40
6.39
6.27
6.26
6.26
5.93
5.91
5.90
5.88
5.86
5.84
5.82
5.34
5.28
5.15
5.12
4.59
4.57
4.56
4.54
4.50
4.47
3.40
2.90
2.89
2.89
2.88
2.85
2.82
2.79
2.76
2.75
1.50
1.48
1.46
1.45
1.45
1.44
1.41
1.40
1.25
0.75
0.73
0.72
0.70
-0.05
-0.29
2.23
1.00
1.08
1.18
1.11
1.16
1.20
0.80
1.54
2.34
1.19
2.44
19.40
10.41
4.09
3.86
11.61
3.01
2.87
10.0 9.5 9.0 8.5 8.0 7.5 7.0 6.5 6.0 5.5 5.0 4.5 4.0 3.5 3.0 2.5 2.0 1.5 1.0 0.5 0.0 -0.5
215.8
176.1
156.6
144.8
139.1
115.0
112.7
112.3
78.4
77.2 Chloroform-d
68.6
59.1
51.7
38.6
26.0
25.9
25.9
24.0
21.6
18.4
18.1
-4.2
-4.2
-4.4
-5.1
230 220 210 200 190 180 170 160 150 140 130 120 110 100 90 80 70 60 50 40 30 20 10 0 -10

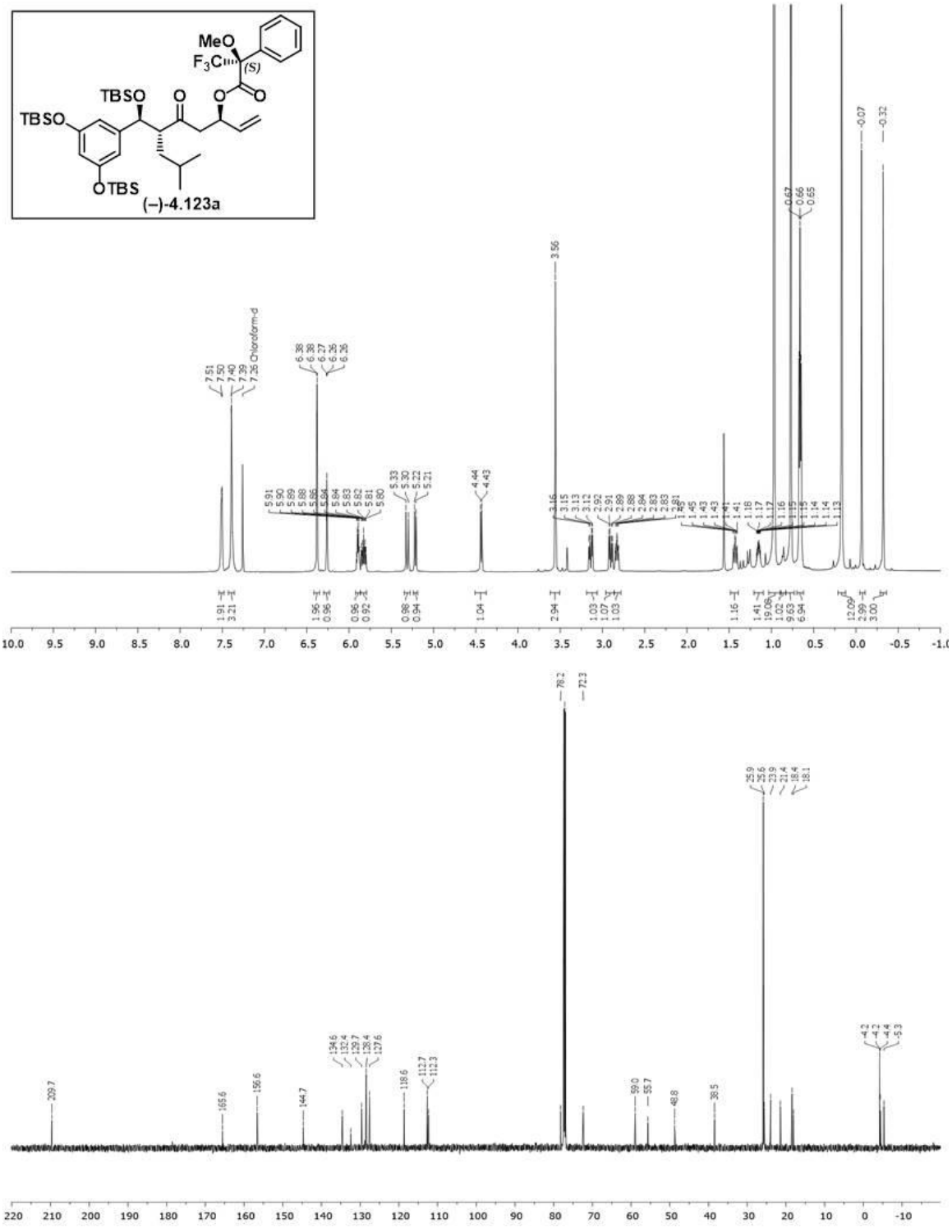
MeO
F3C
(S)
TBSO
TBSO
OTBS
(–)-4.123a
Chloroform-d

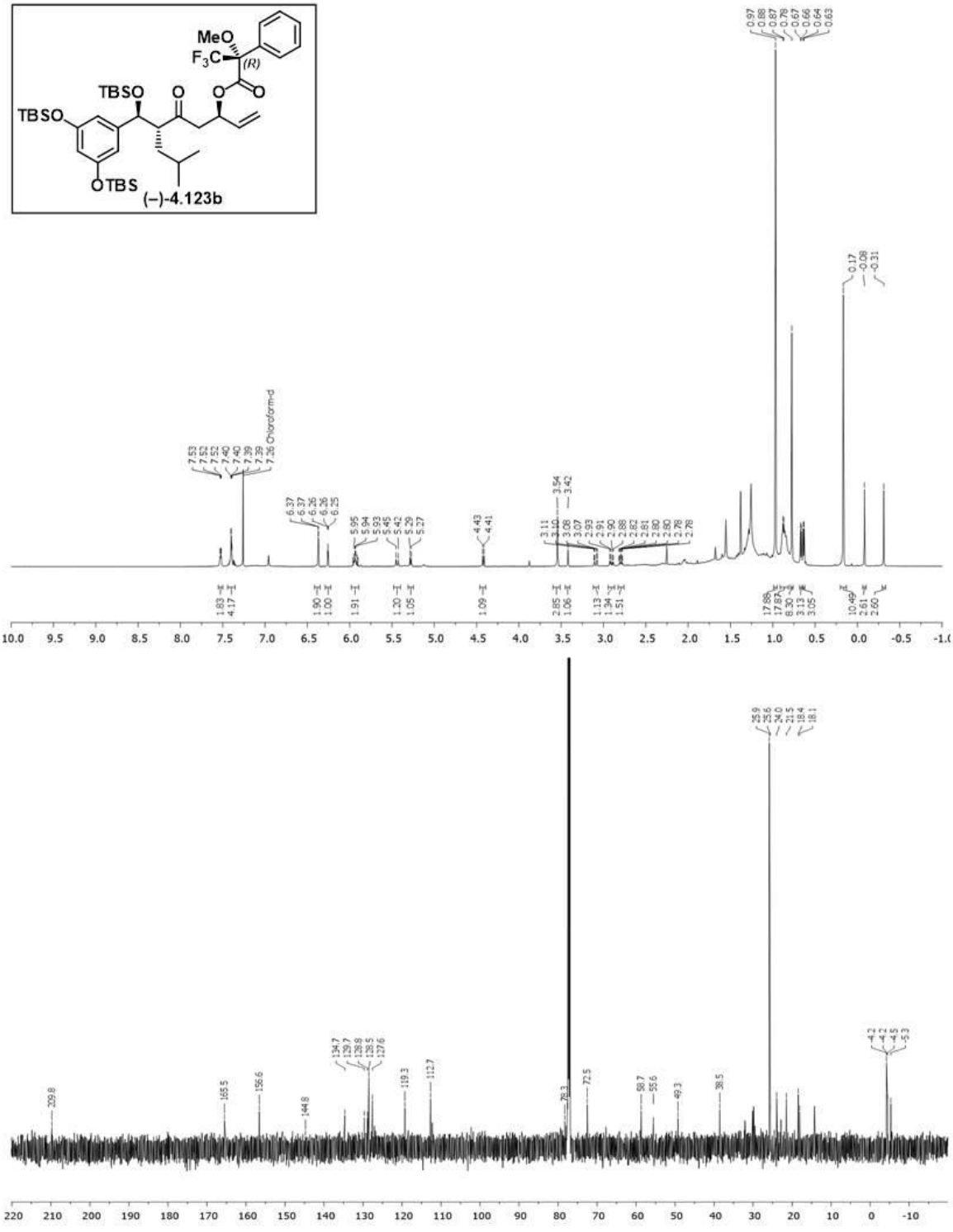
MeO
F3C
(R)
TBSO
TBSO
OTBS
(–)-4.123b
Chloroform-d

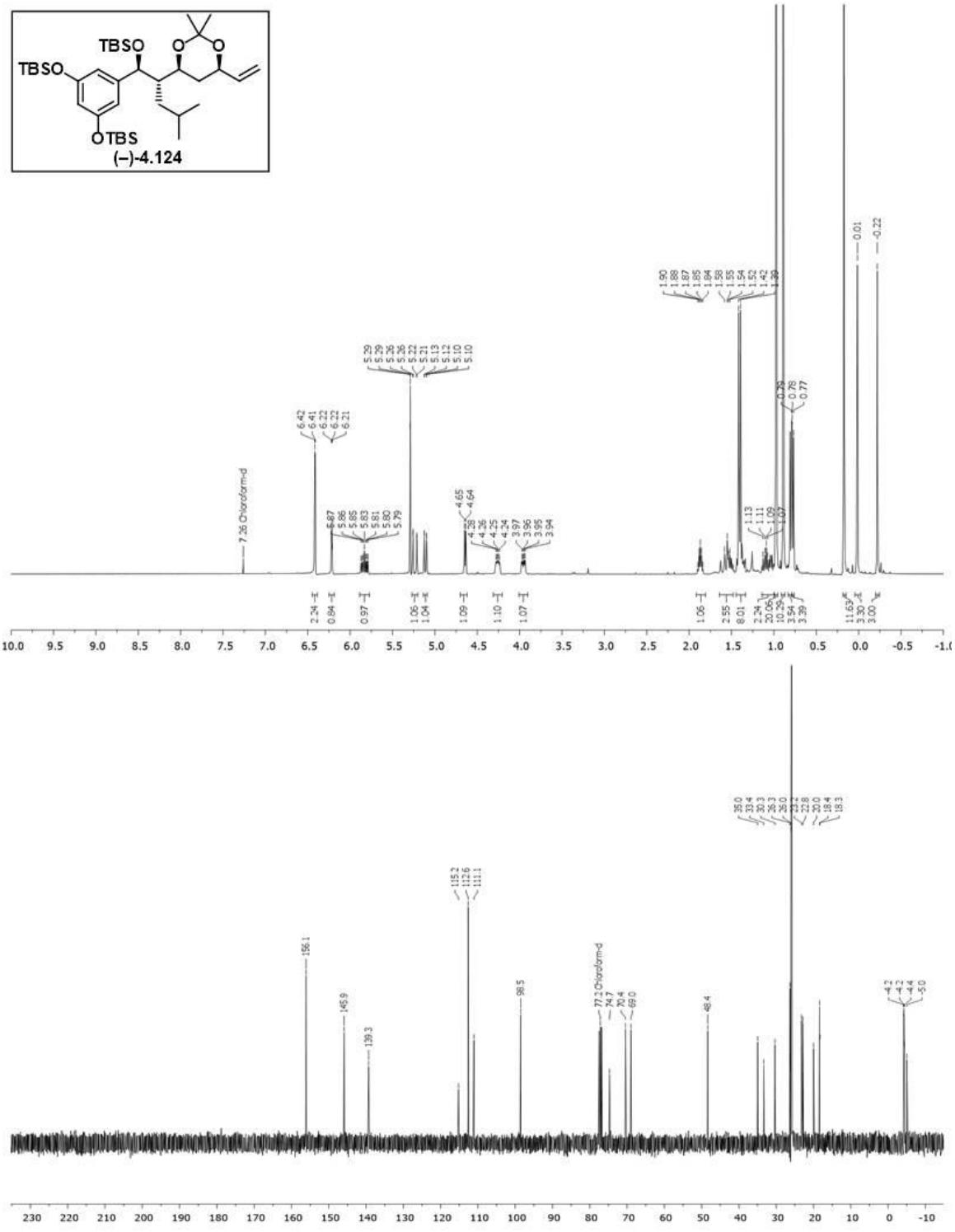
TBSO
TBSO
OTBS
(–)-4.124
7.26 Chloroform-d
77.2 Chloroform-d

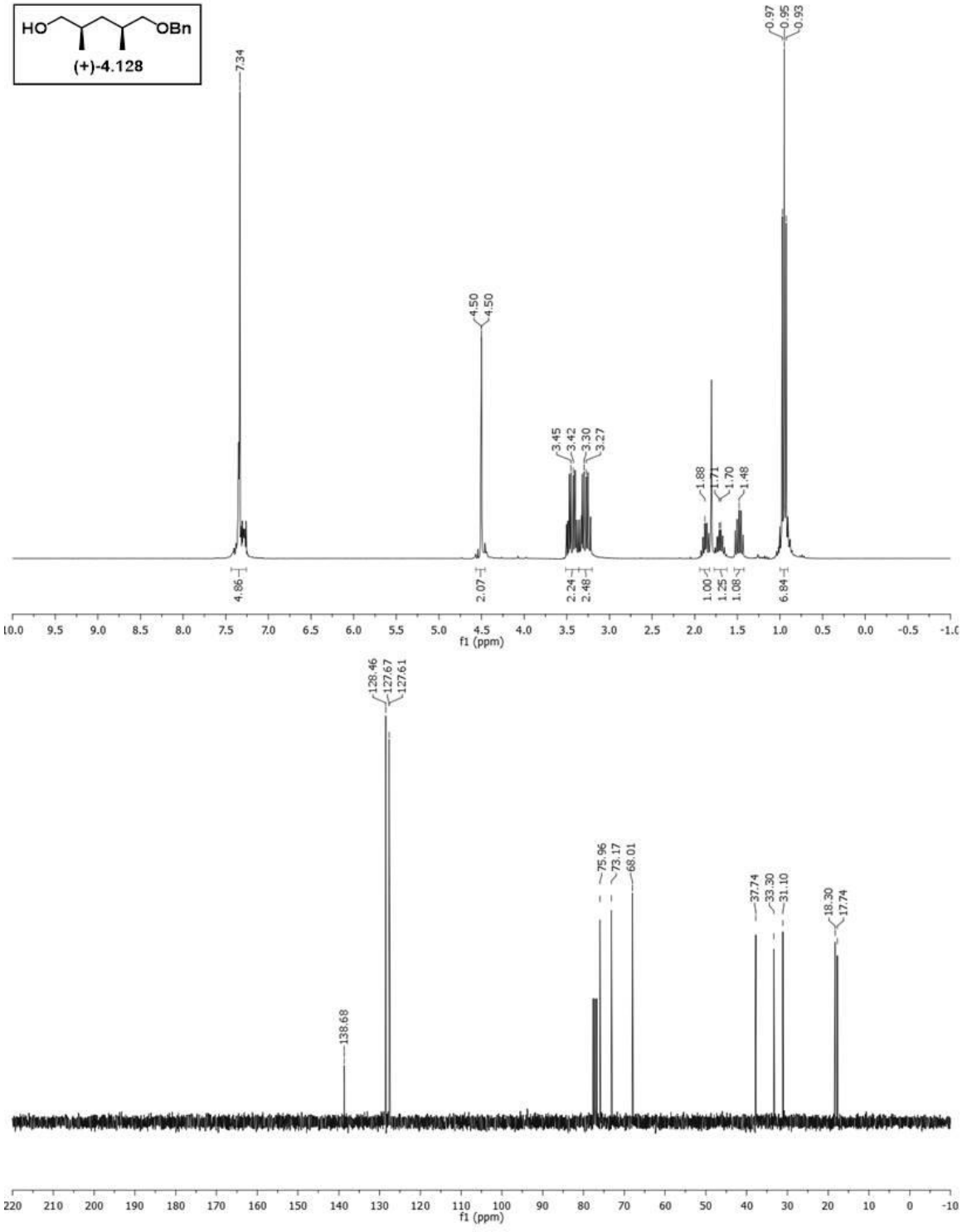
HO
OBn
(+)-4.128
7.34
4.50
4.50
3.45
3.42
3.30
3.27
1.88
1.71
1.70
1.48
0.97
0.95
0.93
4.86
2.07
2.24
2.48
1.00
1.25
1.08
6.84
f1 (ppm)
128.46
127.67
127.61
138.68
75.96
73.17
68.01
37.74
33.30
31.10
18.30
17.74
f1 (ppm)

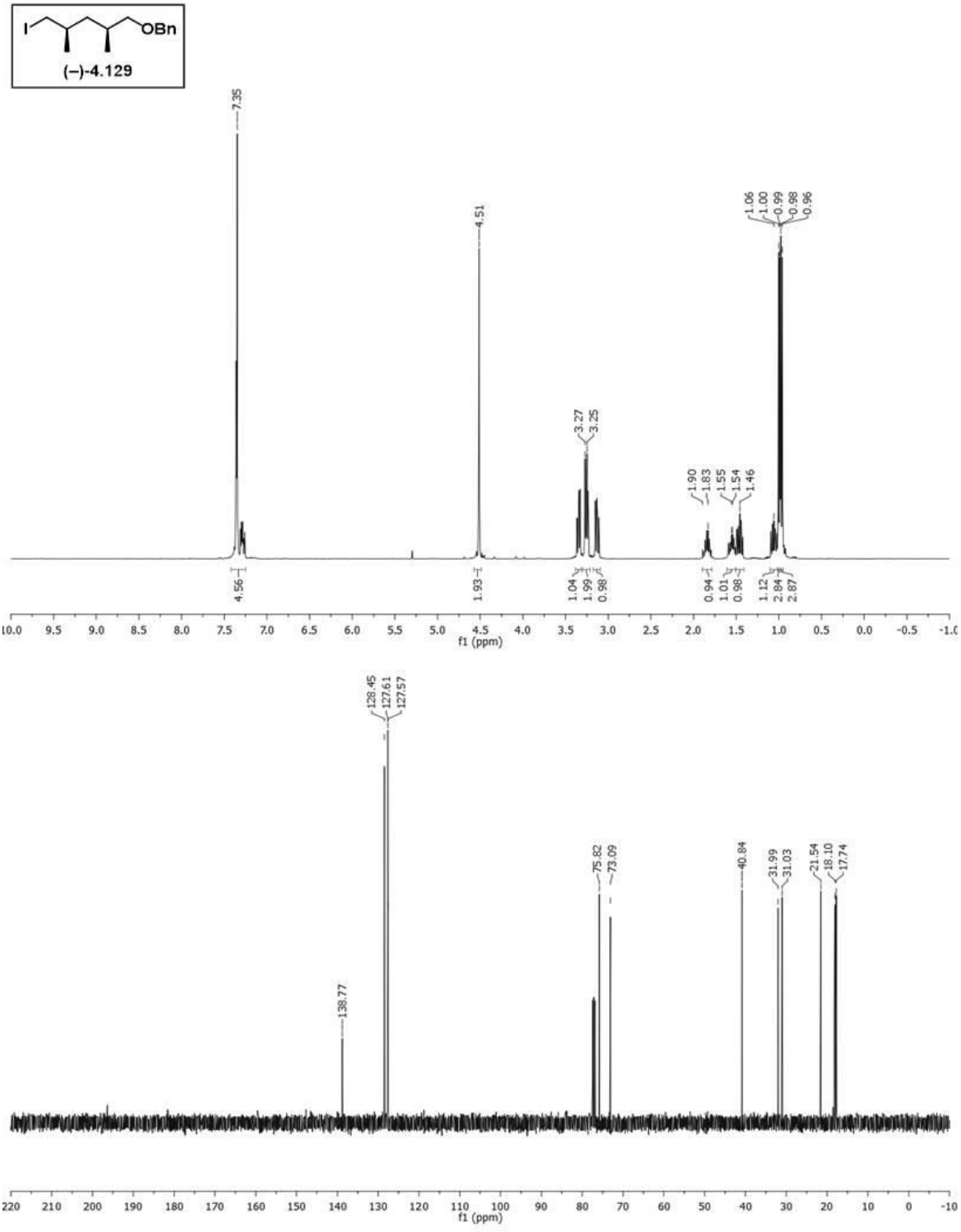
I
OBn
(–)-4.129
7.35
4.51
3.27
3.25
1.90
1.83
1.55
1.54
1.46
1.06
1.00
0.99
0.98
0.96
4.56
1.93
1.04
1.99
0.98
0.94
1.01
0.98
1.12
2.84
2.87
f1 (ppm)
128.45
127.61
127.57
138.77
75.82
73.09
40.84
31.99
31.03
21.54
18.10
17.74
f1 (ppm)

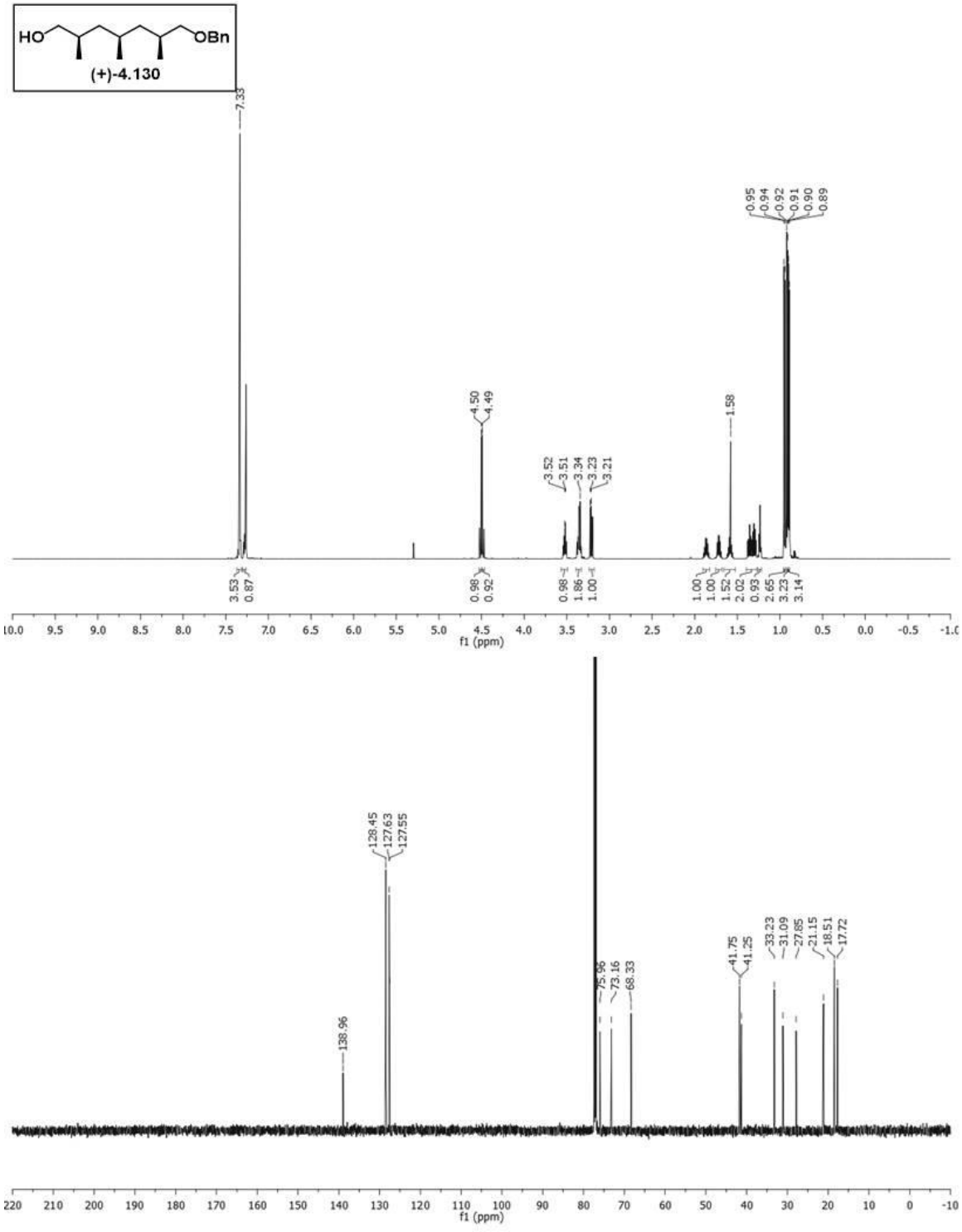
HO
OBn
(+)-4.130
7.33
4.50
4.49
3.52
3.51
3.34
3.23
3.21
1.58
0.95
0.94
0.92
0.91
0.90
0.89
3.53
0.87
0.98
0.92
0.98
1.86
1.00
1.00
1.00
1.52
2.02
0.93
2.65
3.23
3.14
f1 (ppm)
138.96
128.45
127.63
127.55
75.96
73.16
68.33
41.75
41.25
33.23
31.09
27.85
21.15
18.51
17.72
f1 (ppm)

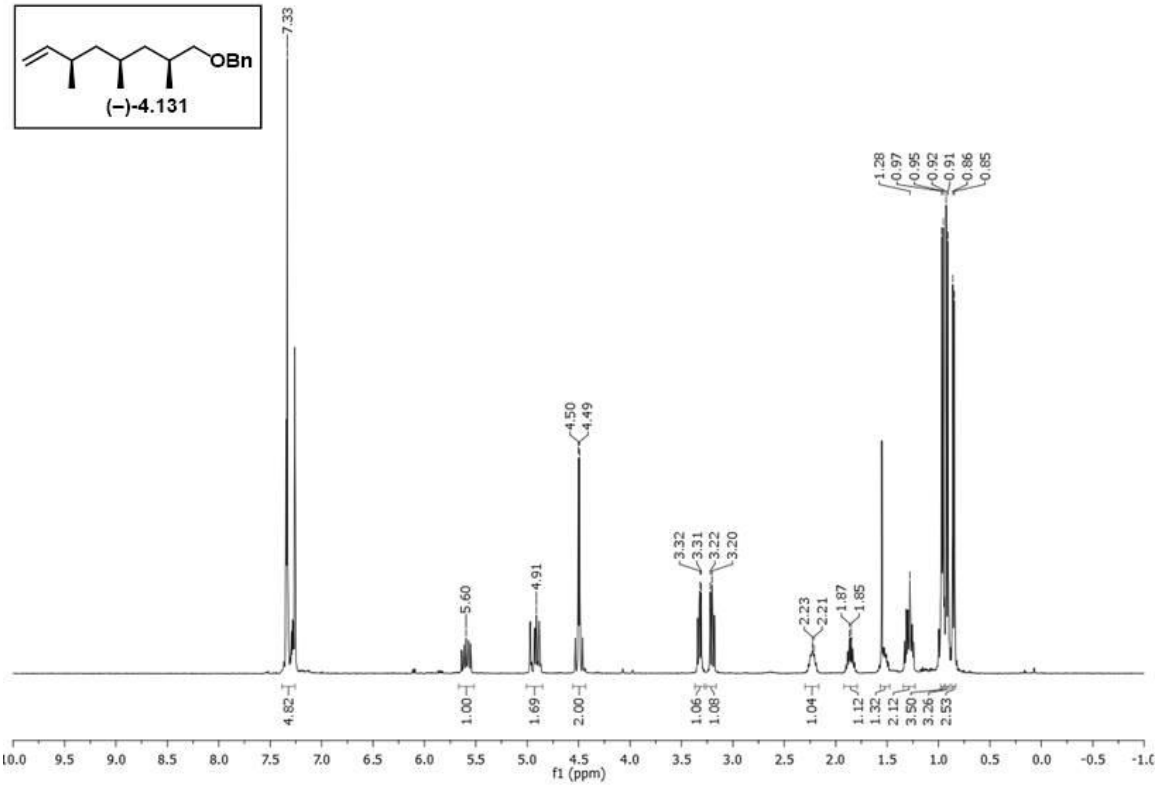
OBn
(–)-4.131
7.33
5.60
4.91
4.50
4.49
3.32
3.31
3.22
3.20
2.23
2.21
1.87
1.85
1.28
0.97
0.95
0.92
0.91
0.86
0.85
4.82
1.00
1.69
2.00
1.06
1.08
1.04
1.12
1.32
2.12
3.50
3.26
2.53
f1 (ppm)

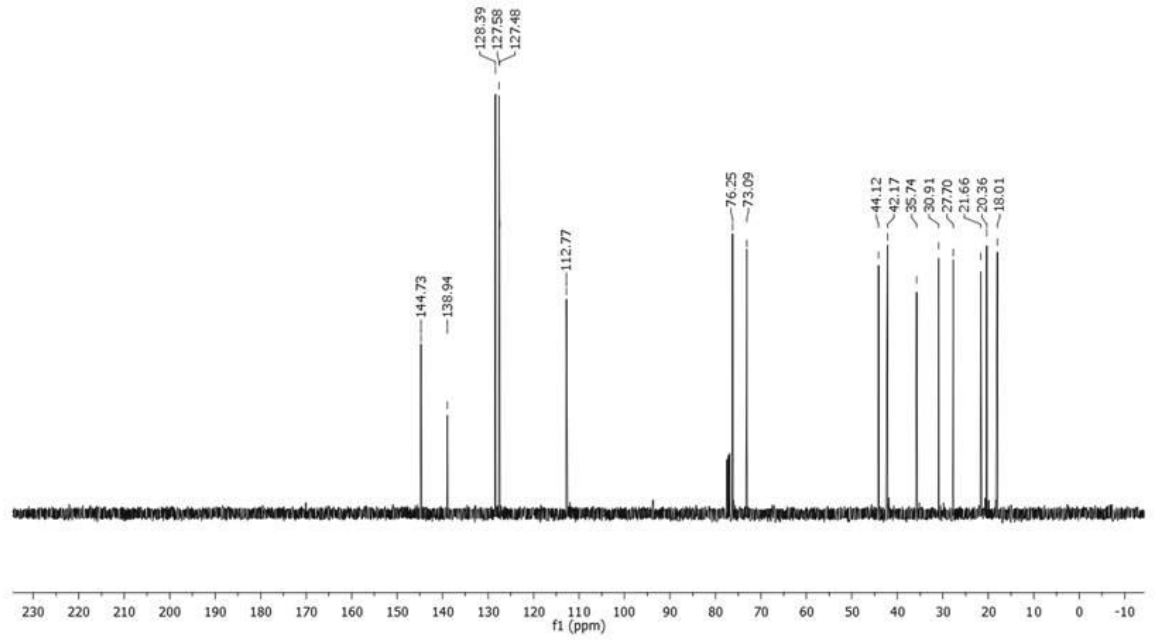
128.39
127.58
127.48
144.73
138.94
112.77
76.25
73.09
44.12
42.17
35.74
30.91
27.70
21.66
20.36
18.01
f1 (ppm)

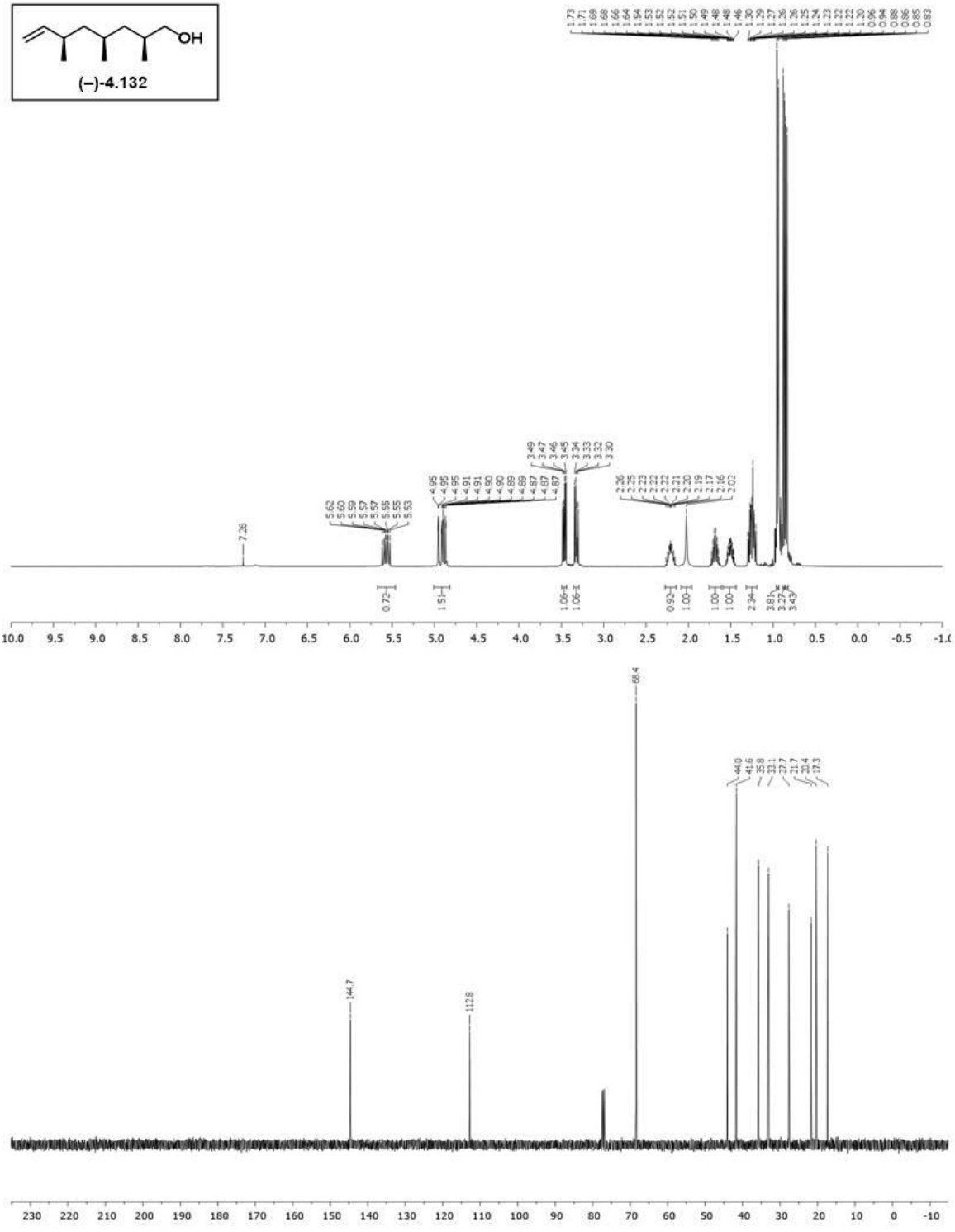
OH
(–)-4.132

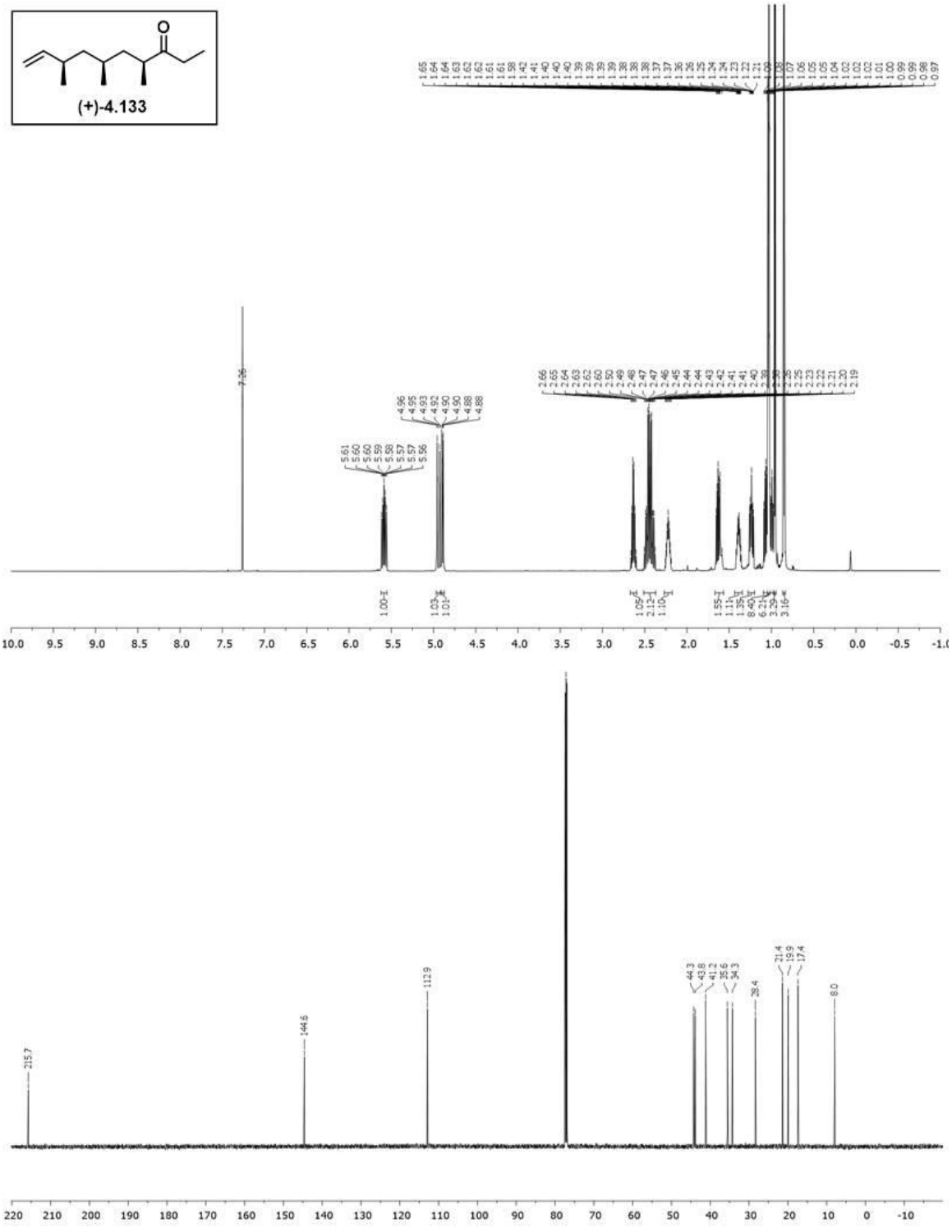
(+)-4.133
7.26
5.61
5.60
5.60
5.59
5.58
5.57
5.57
5.56
4.96
4.95
4.93
4.92
4.90
4.90
4.88
4.88
2.66
2.65
2.64
2.63
2.62
2.60
2.50
2.49
2.48
2.47
2.47
2.46
2.45
2.44
2.44
2.43
2.42
2.41
2.41
2.40
2.39
2.38
2.26
2.25
2.23
2.22
2.21
2.20
2.19
1.65
1.64
1.64
1.63
1.62
1.62
1.61
1.61
1.58
1.42
1.41
1.40
1.40
1.40
1.39
1.39
1.39
1.39
1.38
1.38
1.38
1.37
1.37
1.36
1.26
1.25
1.24
1.24
1.23
1.22
1.21
1.08
1.07
1.06
1.05
1.04
1.02
1.02
1.02
1.01
1.00
0.99
0.99
0.98
0.97
1.00
1.03
1.01
1.05
2.12
1.16
1.55
1.11
1.35
8.40
6.21
3.29
3.16
10.0 9.5 9.0 8.5 8.0 7.5 7.0 6.5 6.0 5.5 5.0 4.5 4.0 3.5 3.0 2.5 2.0 1.5 1.0 0.5 0.0 -0.5
215.7
144.6
112.9
44.3
43.8
41.2
35.6
34.3
28.4
21.4
19.9
17.4
8.0
220 210 200 190 180 170 160 150 140 130 120 110 100 90 80 70 60 50 40 30 20 10 0 -10

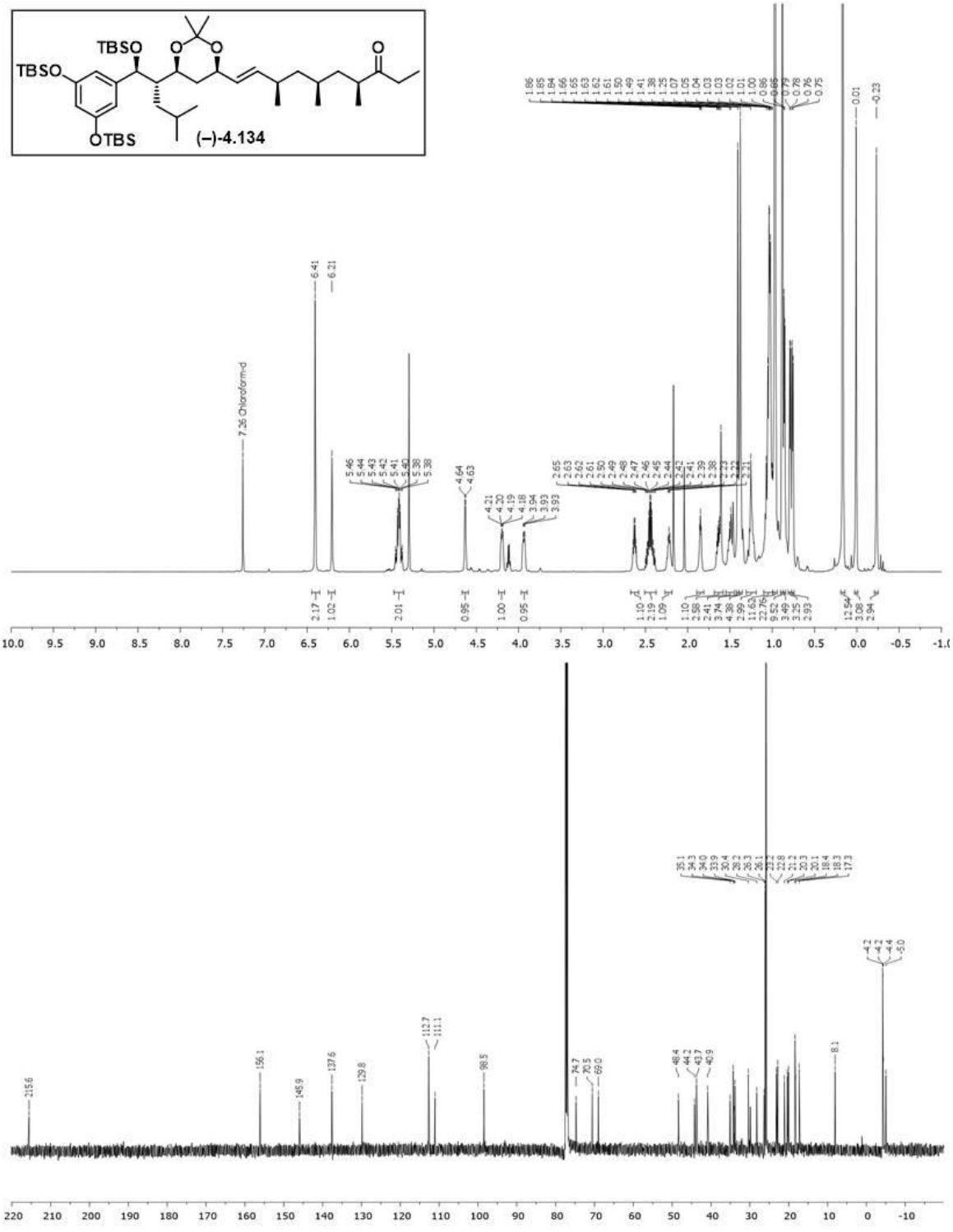
TBSO
TBSO
OTBS
(–)-4.134
7.26 Chloroform-d

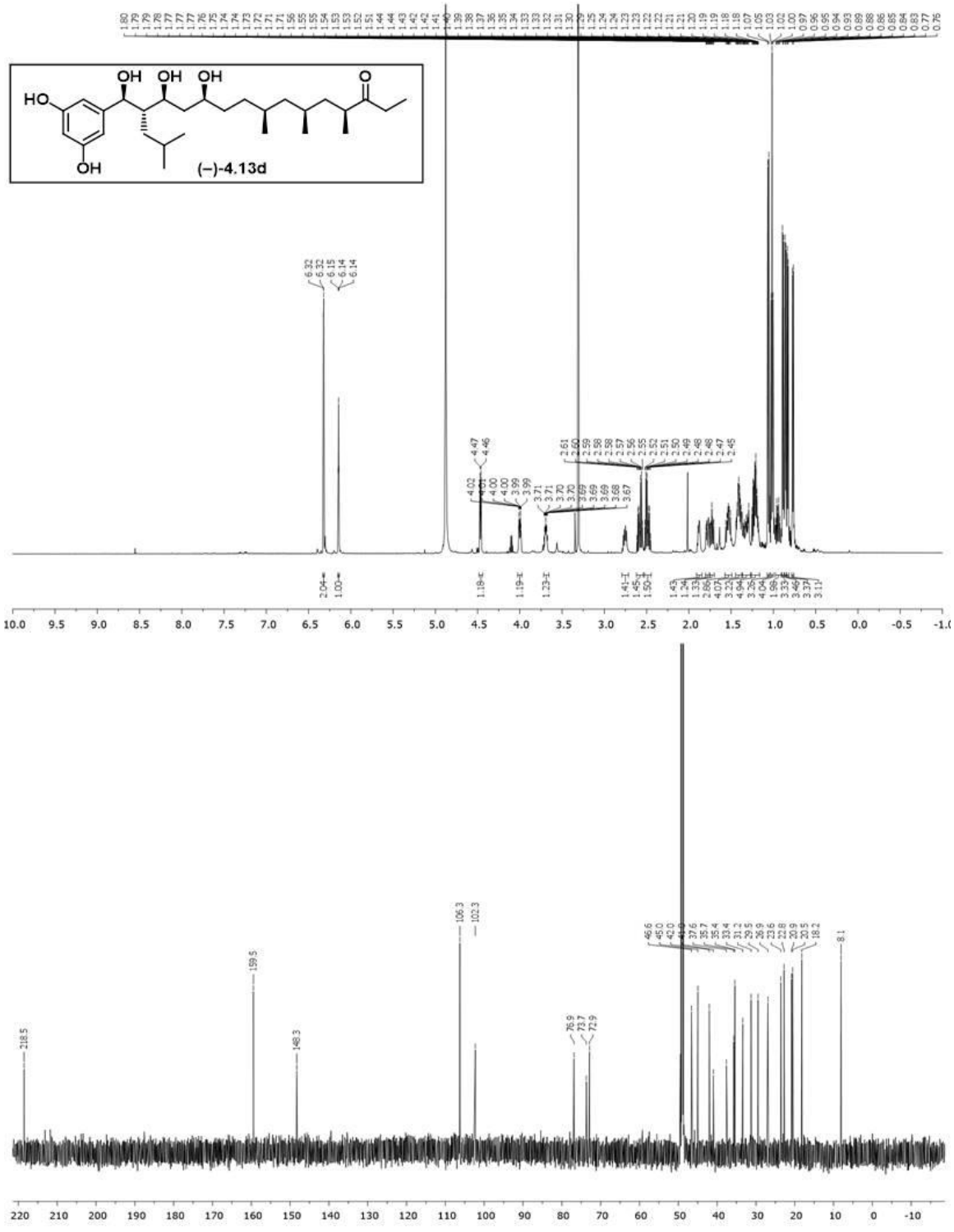
OH
OH
OH
O
HO
OH
(–)-4.13d

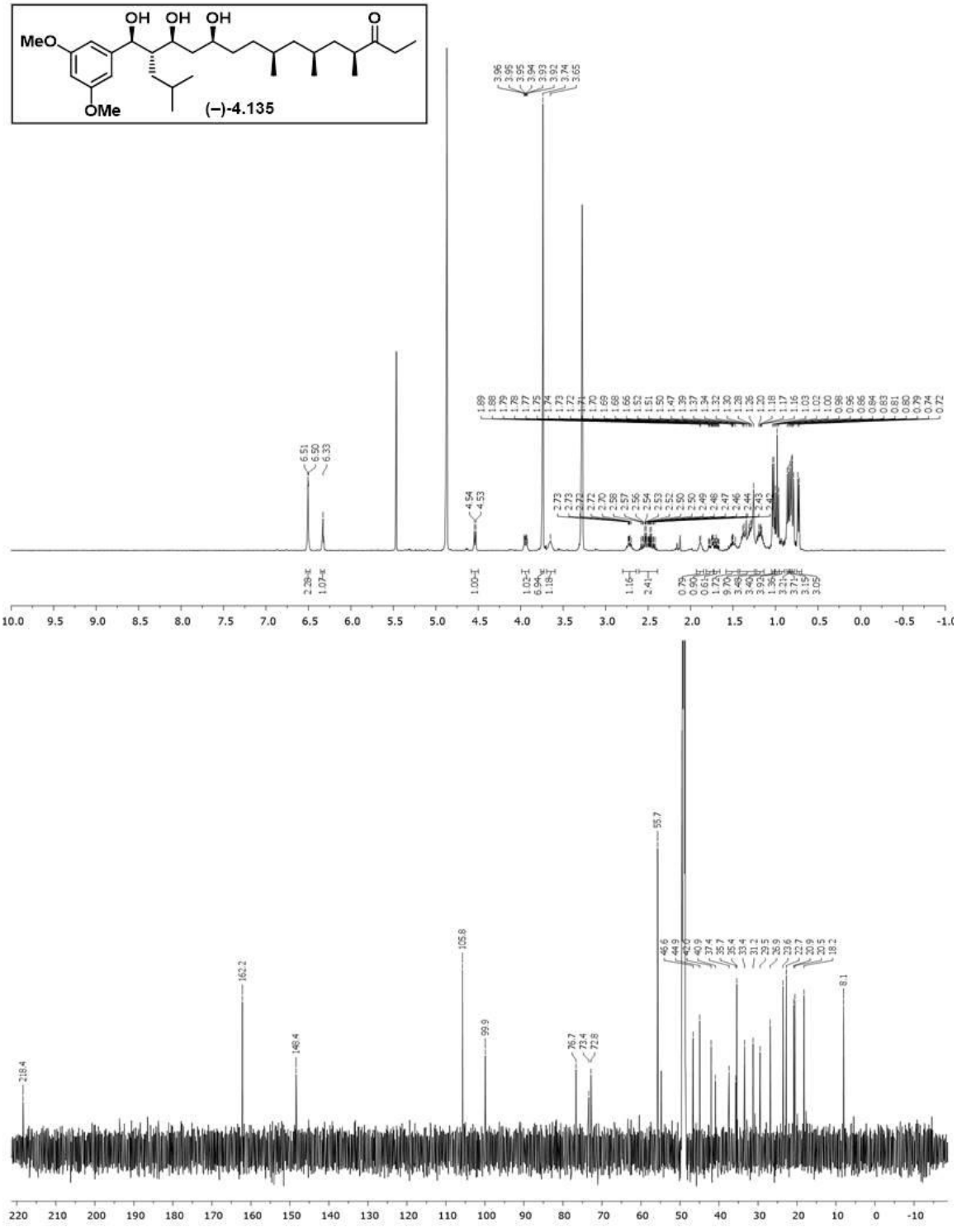
OH
OH
OH
O
MeO
OMe
(–)-4.135

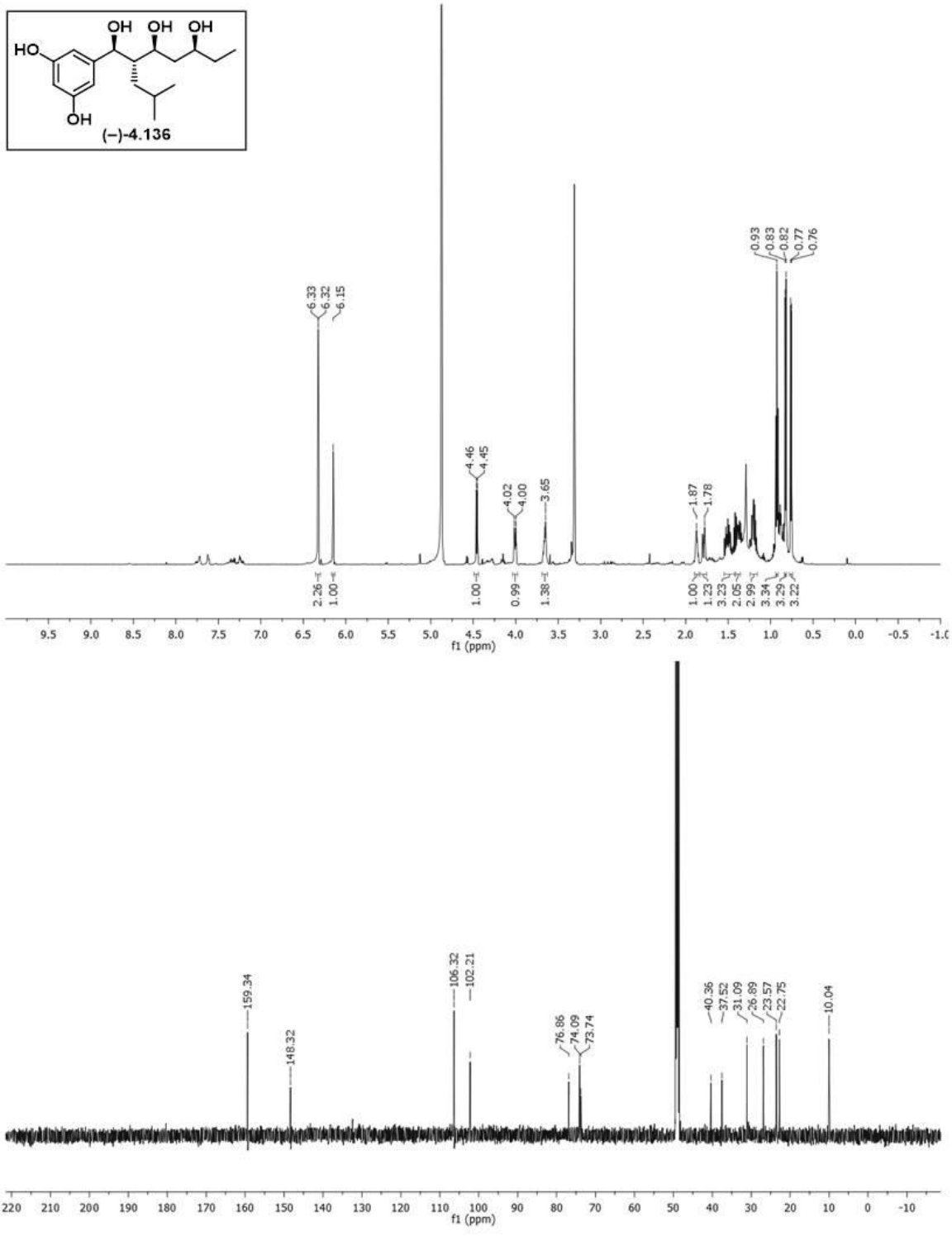
OH
OH
OH
HO
OH
(–)-4.136
6.33
6.32
6.15
4.46
4.45
4.02
4.00
3.65
1.87
1.78
0.93
0.83
0.82
0.77
0.76
2.26
1.00
1.00
0.99
1.38
1.00
1.23
3.23
2.05
2.99
3.34
3.29
3.22
f1 (ppm)
159.34
148.32
106.32
102.21
76.86
74.09
73.74
40.36
37.52
31.09
26.89
23.57
22.75
10.04
f1 (ppm)

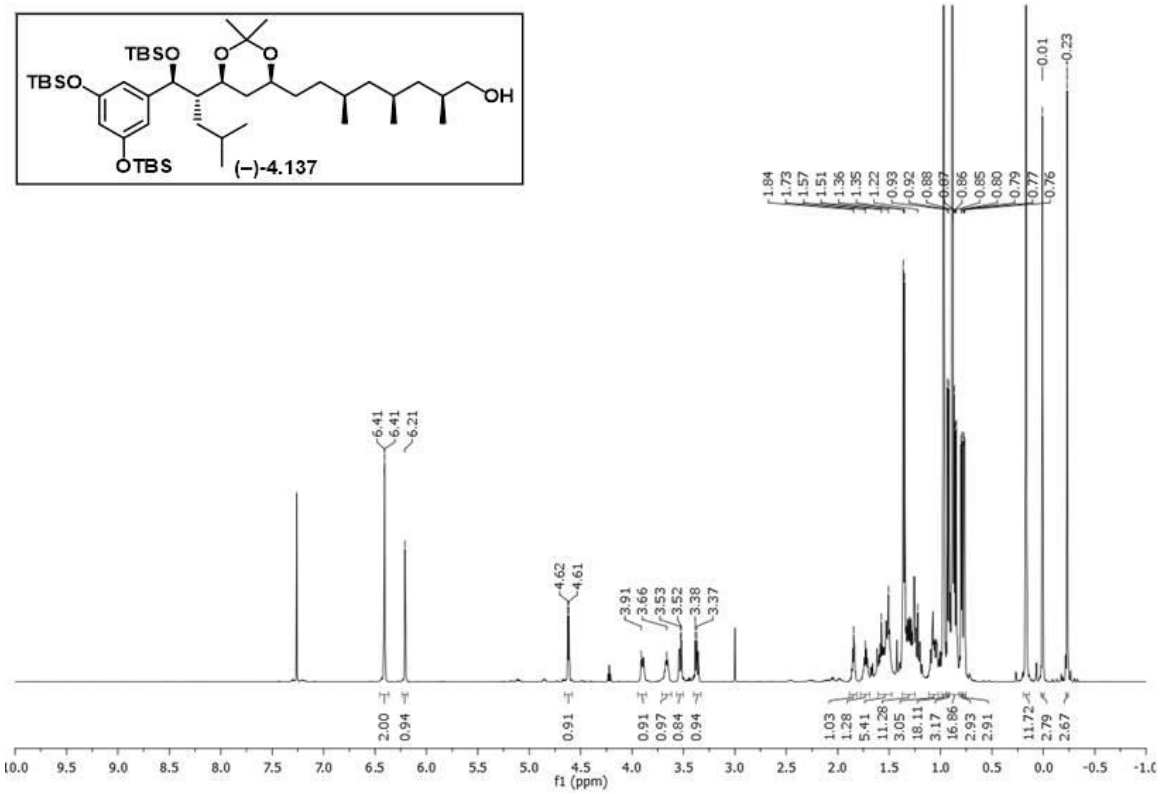
TBSO
TBSO
OH
OTBS
(–)-4.137
f1 (ppm)

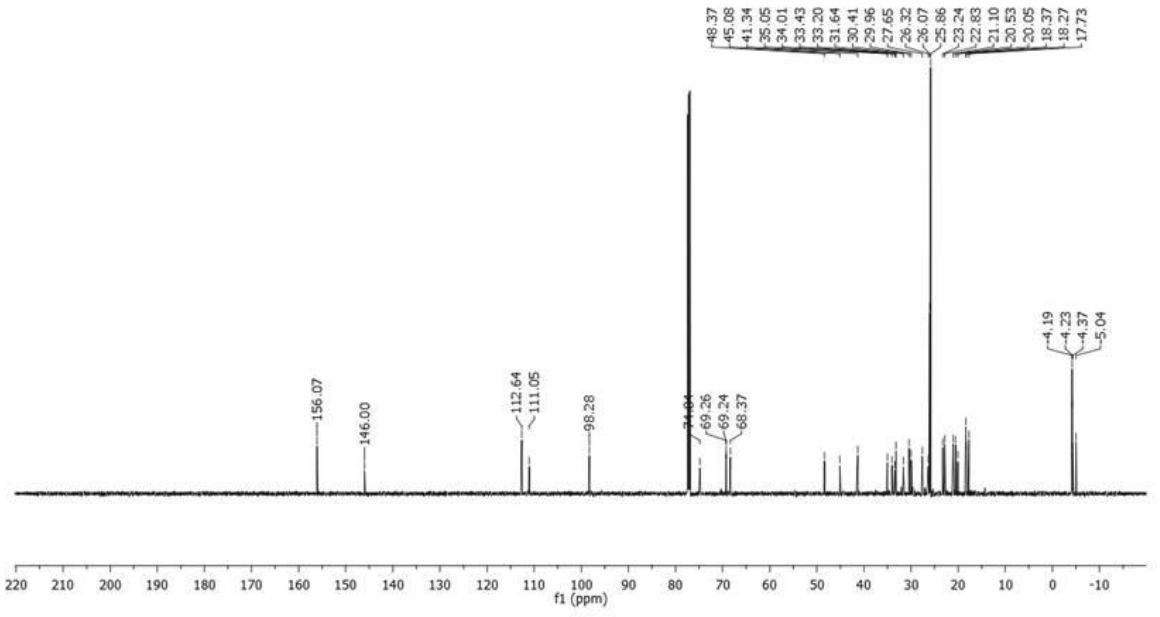
f1 (ppm)

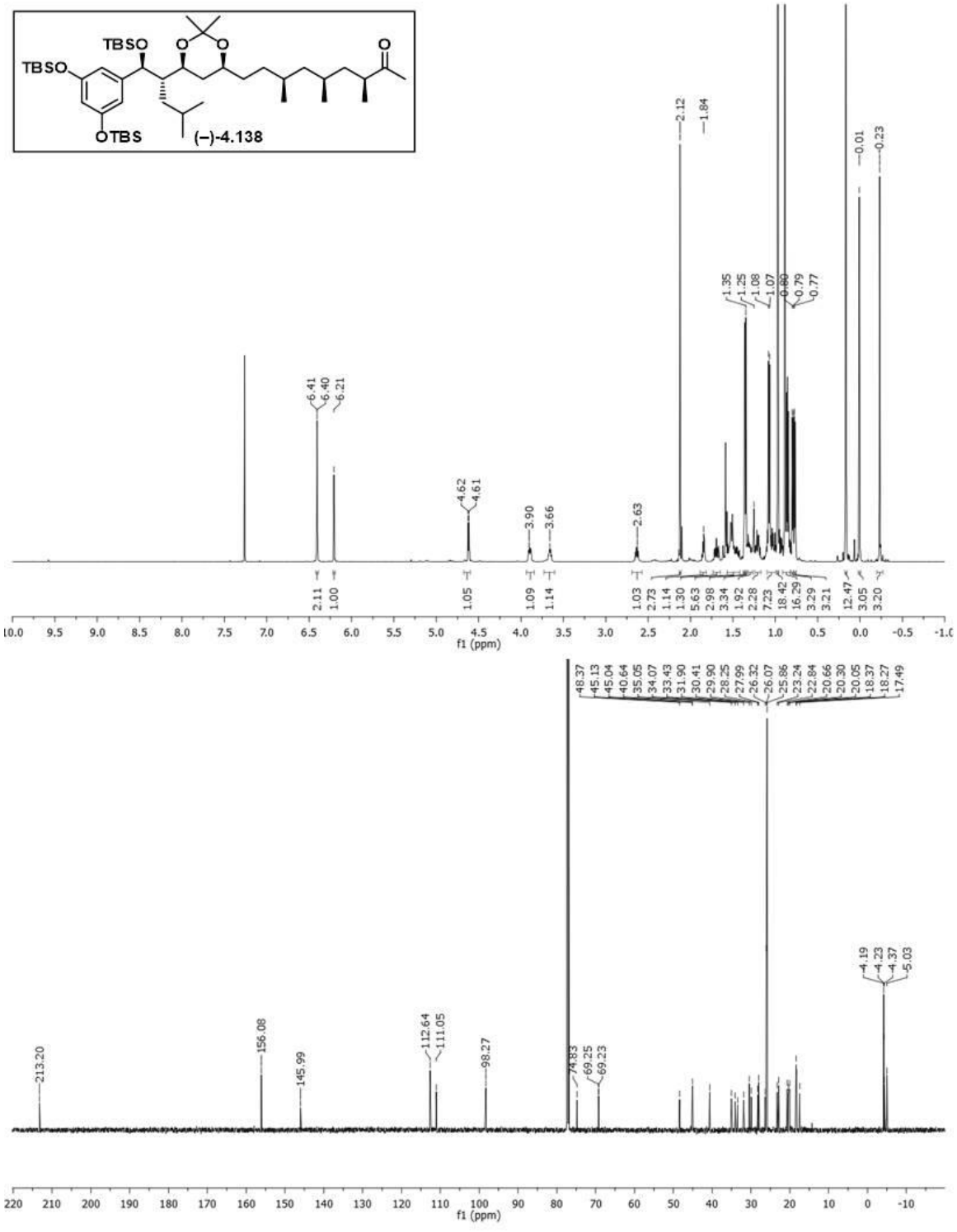
TBSO
TBSO
OTBS
(–)-4.138
f1 (ppm)
f1 (ppm)

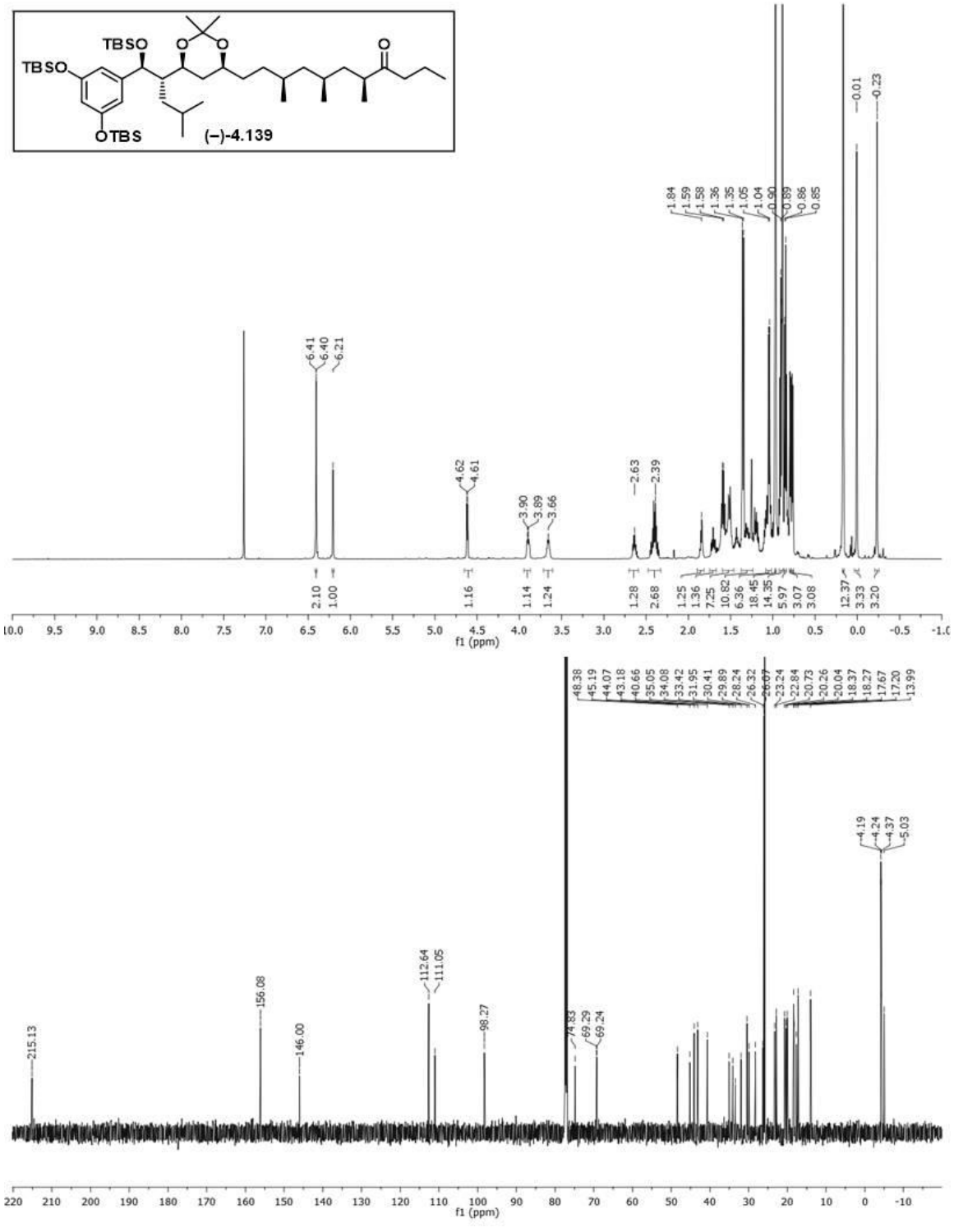
TBSO
TBSO
OTBS
(–)-4.139
f1 (ppm)
f1 (ppm)

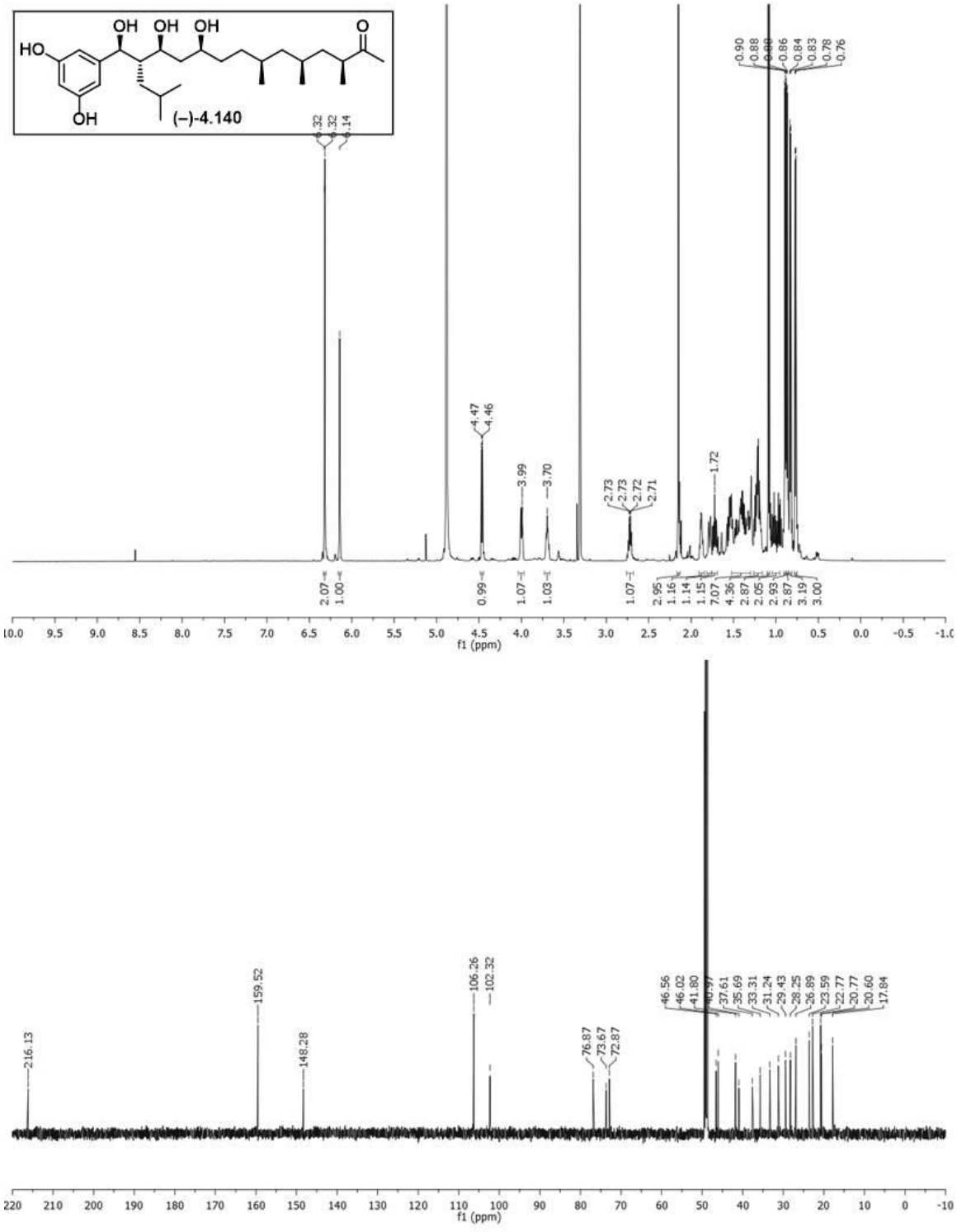
OH
OH
OH
HO
O
OH
(–)-4.140
6.32
6.32
6.14
4.47
4.46
3.99
3.70
2.73
2.73
2.72
2.71
1.72
0.90
0.88
0.86
0.84
0.83
0.78
0.76
2.07
1.00
0.99
1.07
1.03
1.07
2.95
1.16
1.14
1.15
7.07
4.36
2.87
2.05
2.93
2.87
3.19
3.00
f1 (ppm)
216.13
159.52
148.28
106.26
102.32
76.87
73.67
72.87
46.56
46.02
41.80
40.97
37.61
35.69
33.31
31.24
29.43
28.25
26.89
23.59
22.77
20.77
20.60
17.84
f1 (ppm)

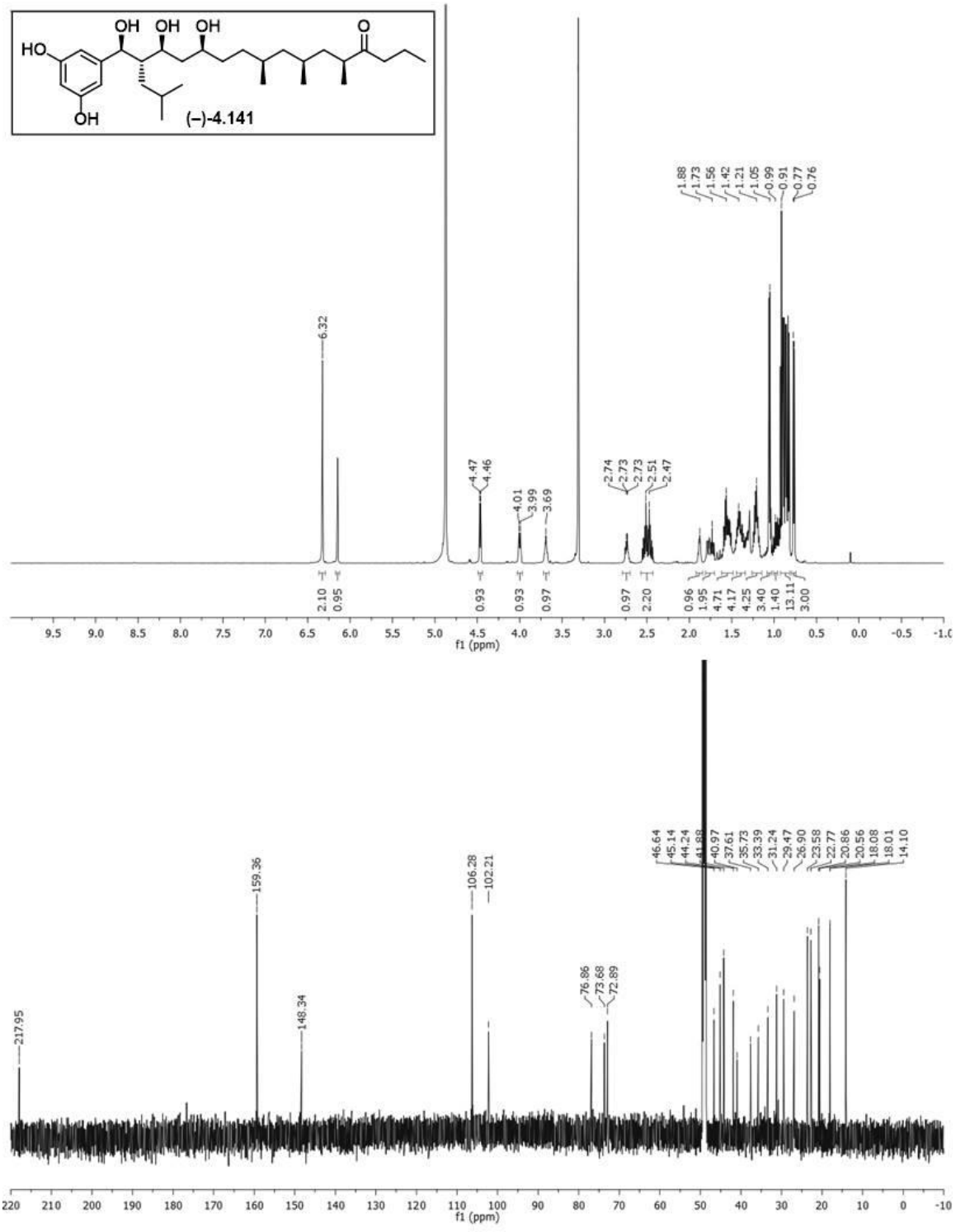
OH
OH
OH
O
HO
OH
(–)-4.141
6.32
4.47
4.46
4.01
3.99
3.69
2.74
2.73
2.73
2.51
2.47
1.88
1.73
1.56
1.42
1.21
1.05
0.99
0.91
0.77
0.76
2.10
0.95
0.93
0.93
0.97
0.97
2.20
0.96
1.95
4.71
4.17
4.25
3.40
1.40
13.11
3.00
f1 (ppm)
217.95
159.36
148.34
106.28
102.21
76.86
73.68
72.89
46.64
45.14
44.24
40.97
37.61
35.73
33.39
31.24
29.47
26.90
23.58
22.77
20.86
20.56
18.08
18.01
14.10
f1 (ppm)

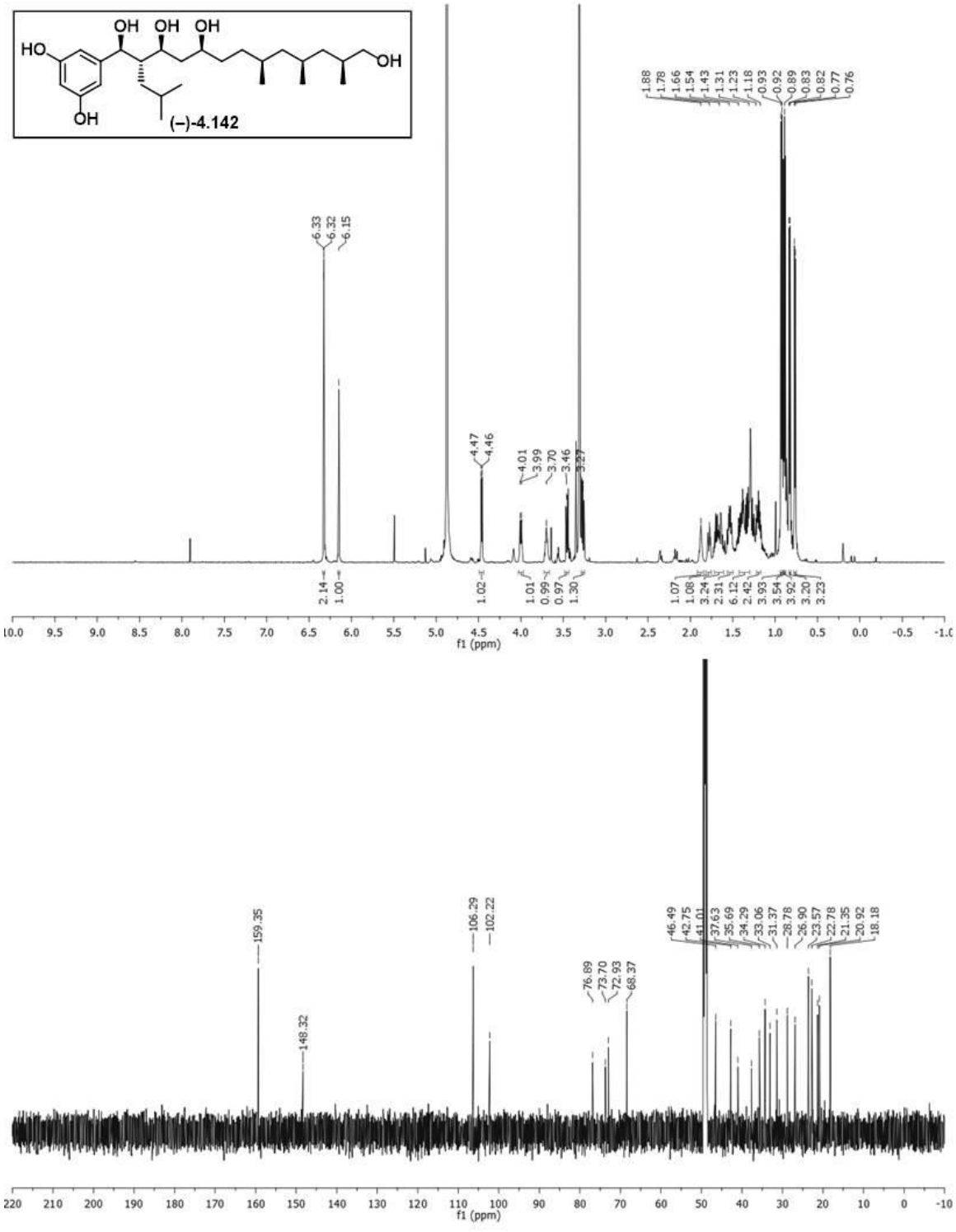
OH
OH
OH
HO
OH
OH
(–)-4.142
f1 (ppm)
f1 (ppm)

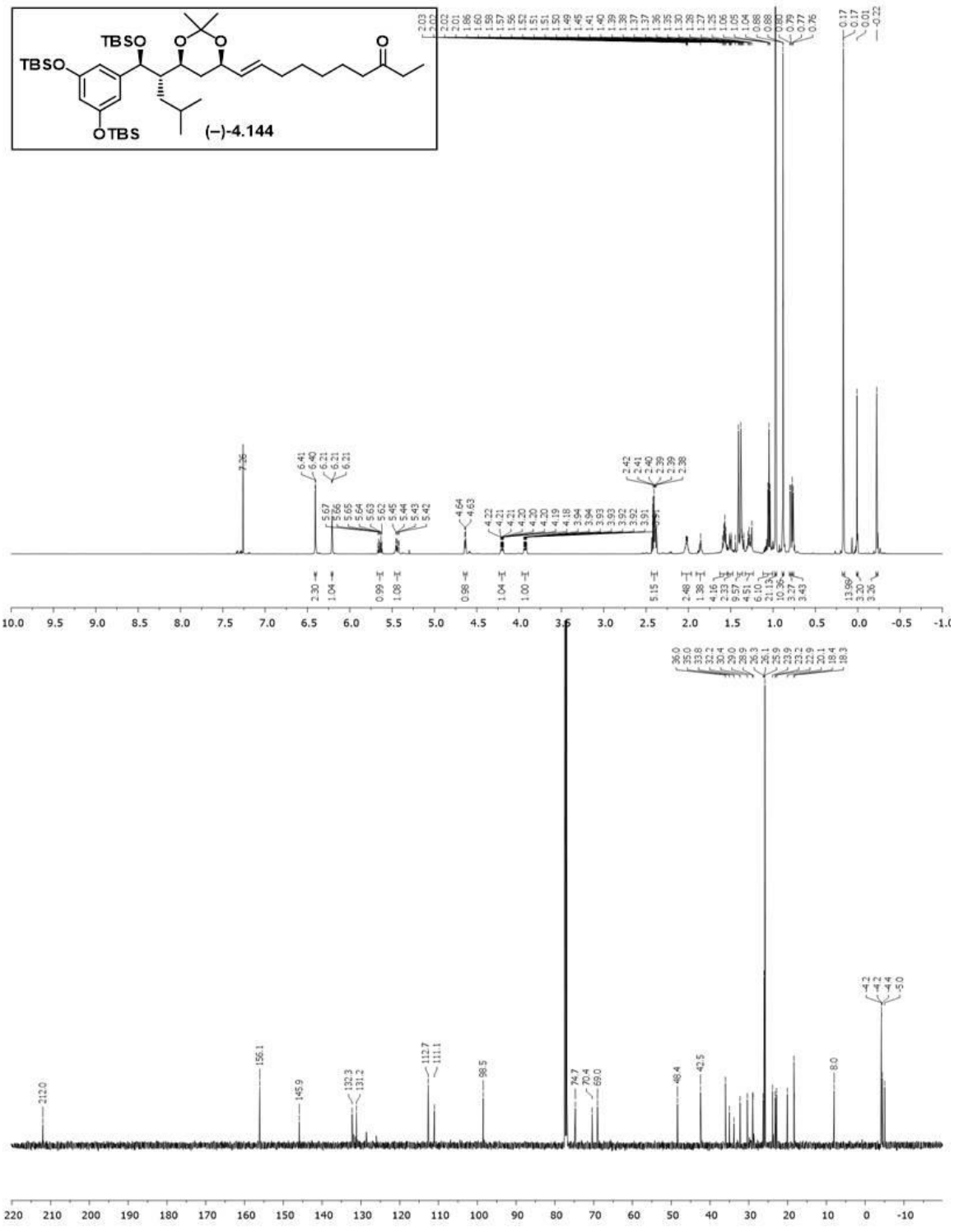
TBSO
TBSO
OTBS
O
O
O
(–)-4.144

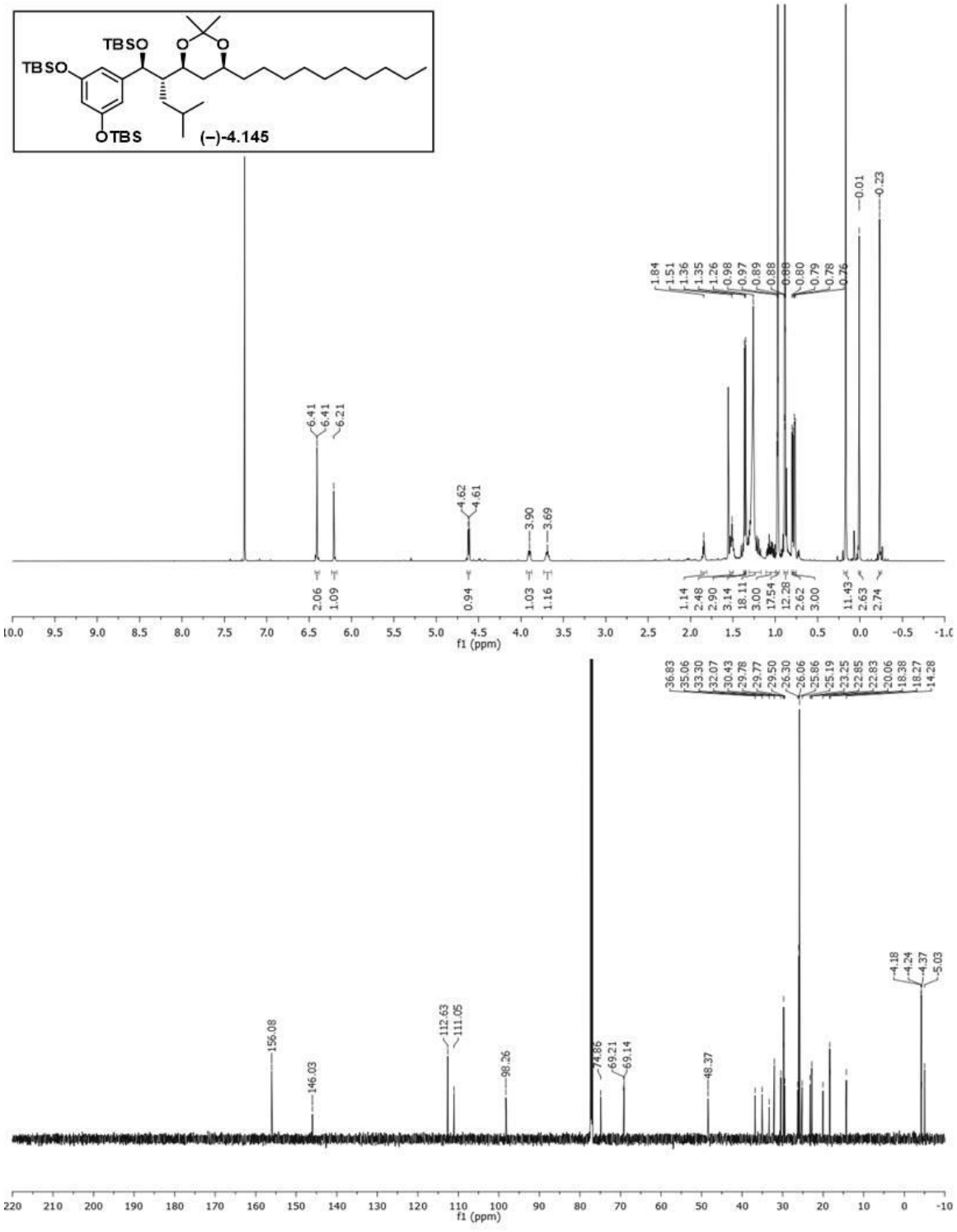
TBSO
TBSO
OTBS
(–)-4.145
f1 (ppm)
f1 (ppm)

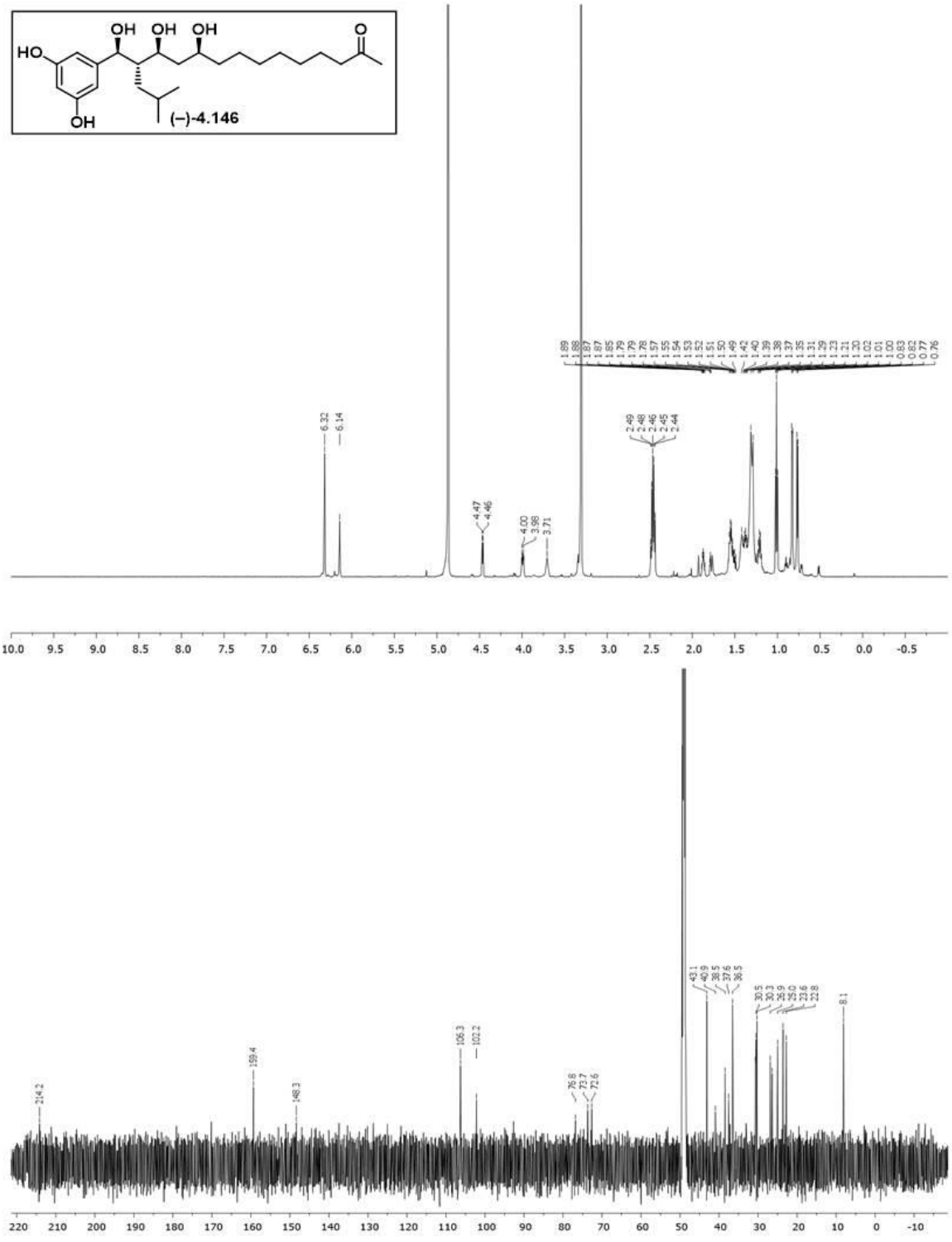
OH
OH
OH
O
HO
OH
(−)-4.146
6.32
6.14
4.47
4.46
4.00
3.98
3.71
2.49
2.48
2.46
2.45
2.44
10.0 9.5 9.0 8.5 8.0 7.5 7.0 6.5 6.0 5.5 5.0 4.5 4.0 3.5 3.0 2.5 2.0 1.5 1.0 0.5 0.0 -0.5
214.2
159.4
148.3
106.3
102.2
76.8
73.7
73.6
43.1
40.9
38.5
37.6
36.5
30.5
30.3
26.9
25.0
23.6
22.8
8.1
220 210 200 190 180 170 160 150 140 130 120 110 100 90 80 70 60 50 40 30 20 10 0 -10

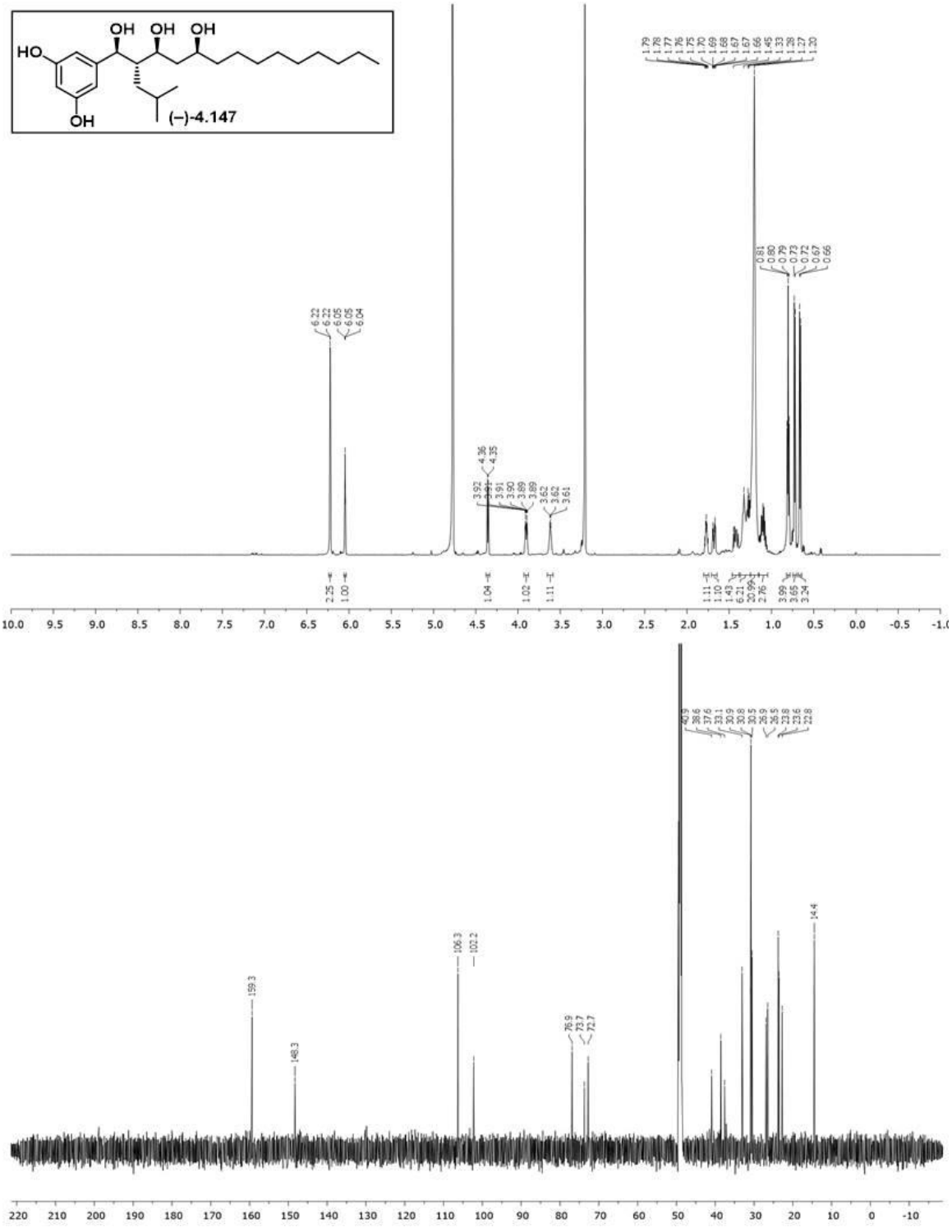
OH
OH
OH
HO
OH
(–)-4.147

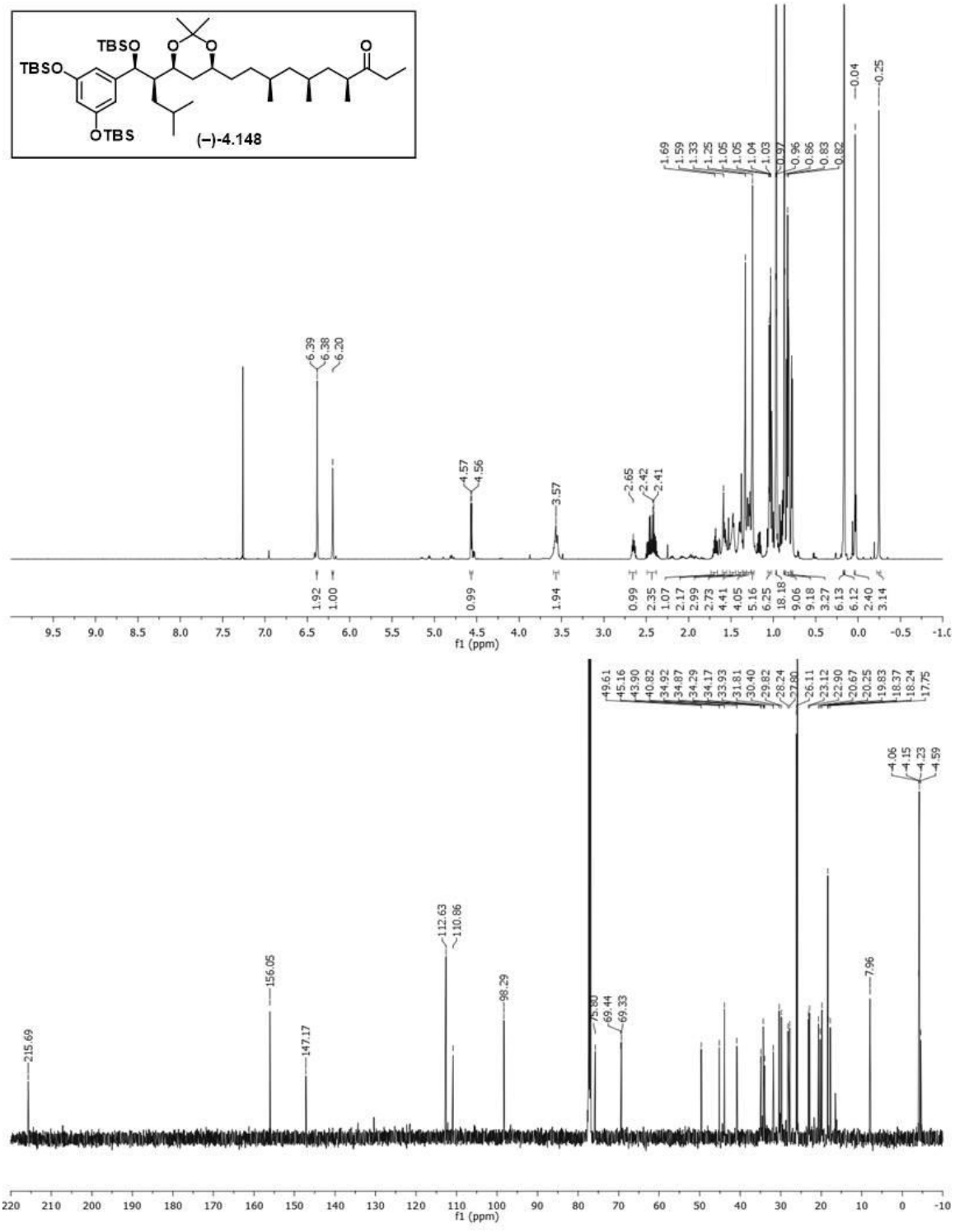
TBSO
TBSO
OTBS
(–)-4.148
f1 (ppm)
f1 (ppm)

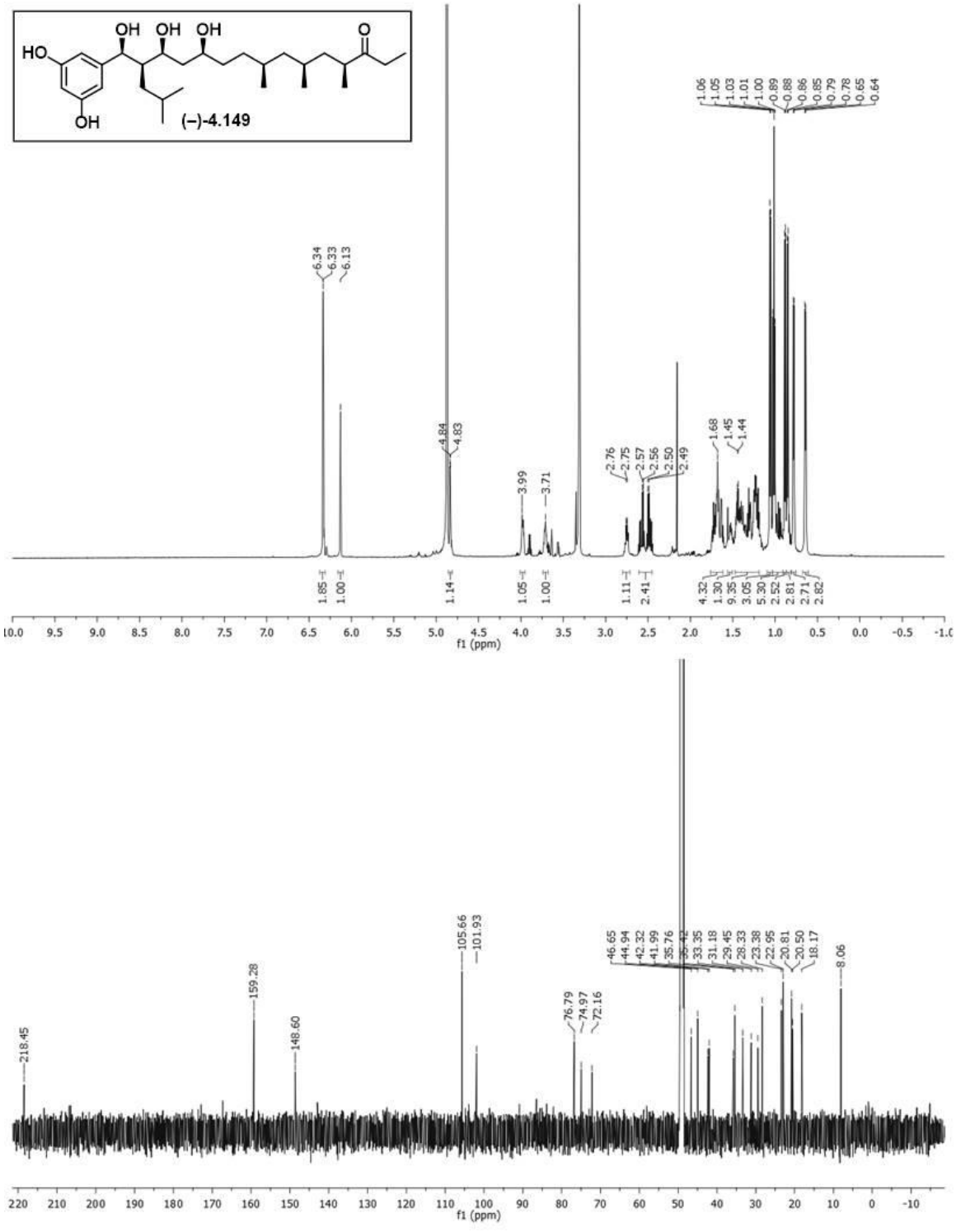
HO
OH
OH
OH
OH
O
(–)-4.149
f1 (ppm)
f1 (ppm)

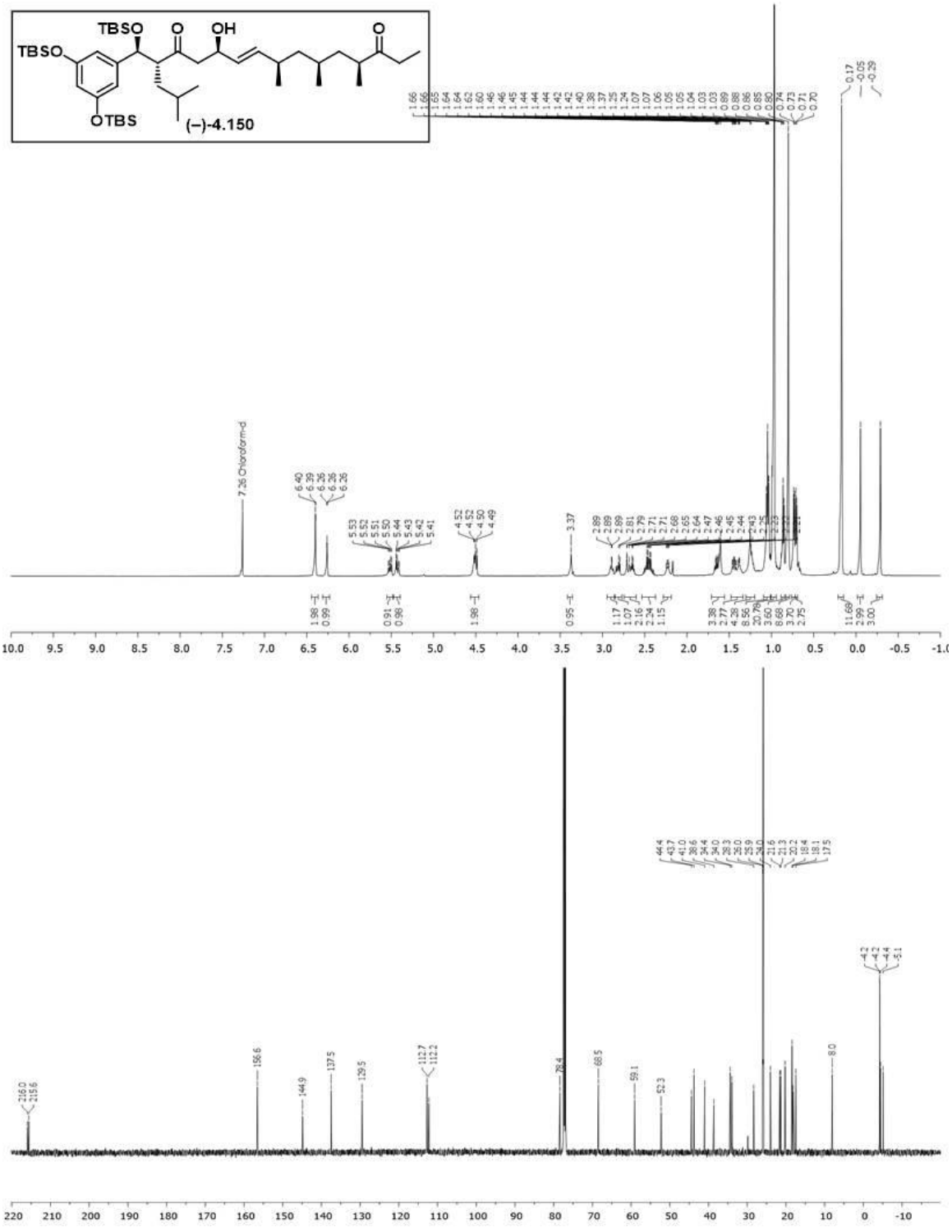
TBSO
O
OH
O
TBSO
OTBS
(–)-4.150
7.26 Chloroform-d

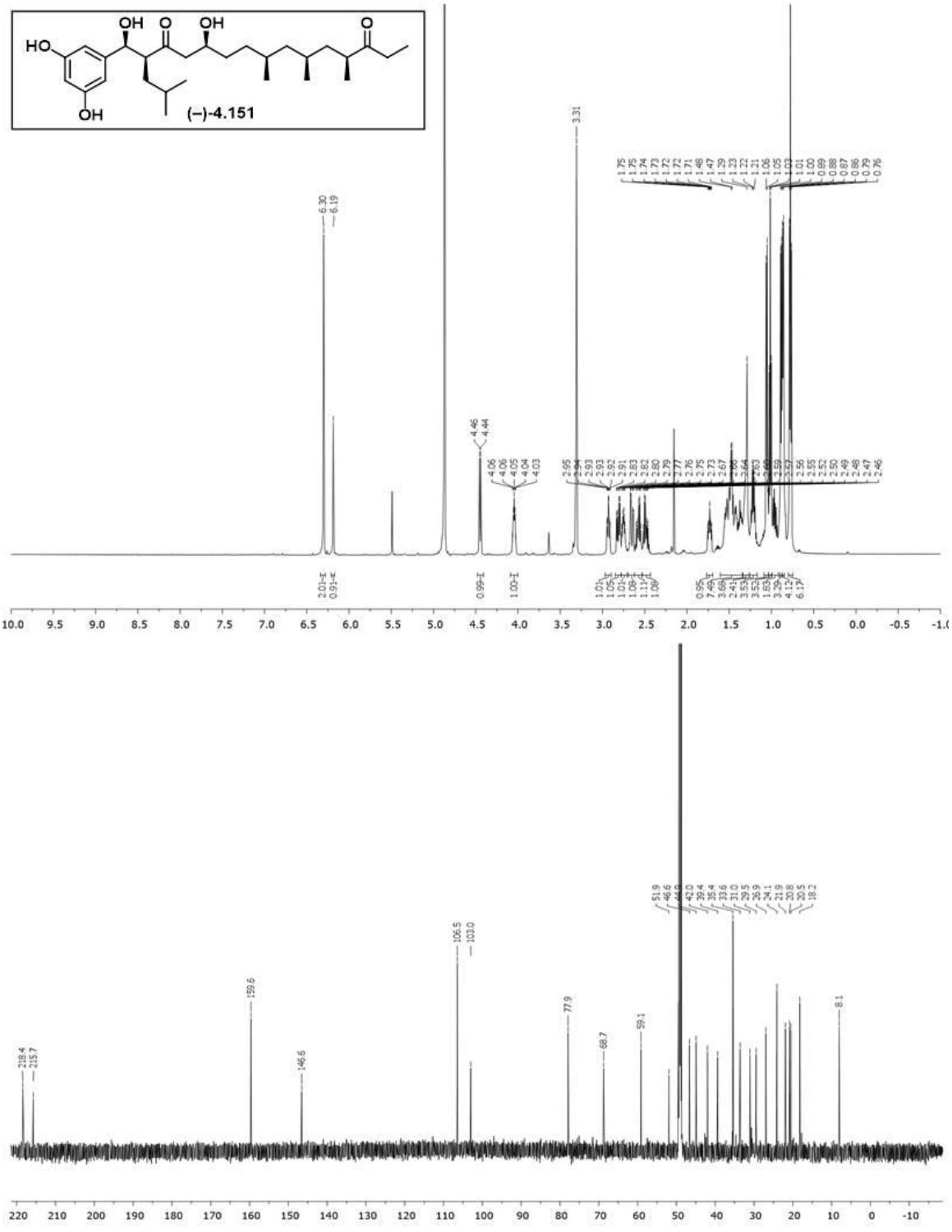
OH
O
OH
O
HO
OH
(–)-4.151